



University of Belgrade  
Technical Faculty in Bor

EcoTEK

31<sup>st</sup> International conference

# Ecological Truth & Environmental Research

Editor

Prof. Dr Snežana Šerbula

## PROCEEDINGS

Hotel Sunce, Sokobanja, Serbia  
18–21 June 2024

## PROCEEDINGS

### 31<sup>st</sup> INTERNATIONAL CONFERENCE

### ECOLOGICAL TRUTH & ENVIRONMENTAL RESEARCH – EcoTER'24

**Editor:**

Prof. Dr Snežana Šerbula, University of Belgrade, Technical Faculty in Bor

**Technical editors of the Proceedings:**

Dr Tanja Kalinović, University of Belgrade, Technical Faculty in Bor

Dr Jelena Kalinović, University of Belgrade, Technical Faculty in Bor

Prof. Dr Ana Radojević, University of Belgrade, Technical Faculty in Bor

Dr Jelena Jordanović, University of Belgrade, Technical Faculty in Bor

Sonja Stanković, MSc, University of Belgrade, Technical Faculty in Bor

**Editor of the 6<sup>th</sup> Student Section:**

Prof. Dr Maja Nujkić, University of Belgrade, Technical Faculty in Bor

**Technical editor of the 6<sup>th</sup> Student Section:**

Vladan Nedelkovski, MSc, University of Belgrade, Technical Faculty in Bor

**Cover design:**

Aleksandar Cvetković, BSc, University of Belgrade, Technical Faculty in Bor

**Publisher:** University of Belgrade, Technical Faculty in Bor

**For the publisher:** Prof. Dr Dejan Tanikić, Dean

**Printed:** University of Belgrade, Technical Faculty in Bor, 100 copies, electronic edition

**Year of publication:** 2024



This work is available under the Creative Commons Attribution-Non-commercial-NoDerivs licence (CC BY-NC-ND)

CIP - Katalogizacija u publikaciji  
Narodna biblioteka Srbije, Beograd

502/504(082)(0.034.2)

574(082)(0.034.2)

**INTERNATIONAL Conference Ecological Truth & Environmental Research (31 ; 2024 ; Sokobanja)**

Proceedings [Elektronski izvor] / 31st International conference Ecological Truth & Environmental Research - EcoTER'24, Sokobanja, Serbia, 18-21 June 2024 ; [organized by] University of Belgrade, Technical faculty in Bor (Serbia) ; [co-organizers University of Banja Luka, Faculty of Technology – Banja Luka (B&H) ... [et al.]] ; [editor Snežana Šerbula]. - Bor : University of Belgrade, Technical faculty, 2024 (Bor : University of Belgrade, Technical faculty). - 1 elektronski optički disk (CD-ROM) ; 12 cm

Sistemski zahtevi: Nisu navedeni. - Nasl. sa naslovne strane dokumenta. - Preface / Snežana Šerbula. - Tiraž 100. - Bibliografija uz svaki rad.

ISBN 978-86-6305-152-2

a) Животна средина -- Зборници б) Екологија – Зборници

COBISS.SR-ID 147002889



**The 31<sup>st</sup> International Conference  
Ecological Truth & Environmental Research – EcoTER'24**

*is organized by:*

UNIVERSITY OF BELGRADE  
TECHNICAL FACULTY IN BOR (SERBIA)

*Co-organizers of the conference:*

University of Banja Luka, Faculty of Technology,  
Banja Luka (B&H)

University of Montenegro, Faculty of Metallurgy and Technology, Podgorica  
(Montenegro)

University of Zagreb, Faculty of Metallurgy, Sisak (Croatia)

University of Pristina, Faculty of Technical Sciences, Kosovska Mitrovica  
(Serbia)

Society of Young Researchers – Bor (Serbia)



**The EcoTER'24 conference is financially supported  
by  
the Ministry of Science, Technological Development and  
Innovation  
of the Republic of Serbia**



**Republic of Serbia**

---

**MINISTRY OF SCIENCE,  
TECHNOLOGICAL DEVELOPMENT AND INNOVATION**



**Platinum donor of the EcoTER'24 conference**



**Platinum donor of the EcoTER'24 conference**

**HBIS SERBIA**

**Gold donor of the EcoTER'24 conference**



**Silver donor of the EcoTER'24 conference**



**ИНЖЕЊЕРСКА  
КОМОРА  
СРБИЈЕ**

## SCIENTIFIC COMMITTEE

### **Prof. Dr Snežana Šerbula, *President***

Prof. Dr Alok Mittal (India)	Prof. Dr Milutin Milosavljević (Serbia)
Prof. Dr Jan Bogaert (Belgium)	Prof. Dr Nenad Stavretović (Serbia)
Prof. Dr A. Nadgórska-Socha (Poland)	Prof. Dr Ivan Mihajlović (Serbia)
Prof. Dr Luis A. Cisternas (Chile)	Prof. Dr Milovan Vuković (Serbia)
Prof. Dr Wenhong Fan (China)	Prof. Dr Nada Blagojević (Montenegro)
Prof. Dr Martin Brtnický (Czech Republic)	Prof. Dr Darko Vuksanović (Montenegro)
Prof. Dr I.M. De Oliveira Abrantes (Portugal)	Prof. Dr Irena Nikolić (Montenegro)
Prof. Dr Shengguo Xue (China)	Prof. Dr Šefket Goletić (B&H)
Prof. Dr Tomáš Lošák (Czech Republic)	Prof. Dr Džafer Dautbegović (B&H)
Prof. Dr Maurice Millet (France)	Prof. Dr Borislav Malinović (B&H)
Prof. Dr Murray T. Brown (New Zealand)	Prof. Dr Slavica Sladojević (B&H)
Prof. Dr Xiaosan Luo (China)	Prof. Dr Nada Šumatić (B&H)
Prof. Dr Daniel J. Bain (USA)	Prof. Dr Snežana Milić (Serbia)
Prof. Dr Che Fauziah Binti Ishak (Malaysia)	Prof. Dr Dejan Tanikić (Serbia)
Prof. Dr Richard Thornton Baker (UK)	Prof. Dr Milan Trumić (Serbia)
Prof. Dr Mohamed Damak (Tunisia)	Dr Jasmina Stevanović (Serbia)
Prof. Dr Jyoti Mittal (India)	Dr Dragana Randelović (Serbia)
Prof. Dr Miriam Balaban (USA)	Dr Viša Tasić (Serbia)
Prof. Dr Fernando Carrillo-Navarrete (Spain)	Dr Ljiljana Avramović (Serbia)
Prof. Dr Pablo L. Higuera (Spain)	Dr Stefan Đorđievski (Serbia)
Prof. Dr Mustafa Cetin (Turkey)	Prof. Dr Branimir Jovančičević (Serbia)
Prof. Dr Mauro Masiol (Italy)	Dr Mirjana Marković (Serbia)
Prof. Dr George Z. Kyzas (Greece)	Dr Lidija Mančić (Serbia)
Prof. Dr Mustafa Imamoğlu (Turkey)	Dr Tanja Brdarić (Serbia)
Prof. Dr Petr Solzhenkin (Russia)	Prof. Dr Tatjana Anđelković (Serbia)
Prof. Dr Yeomin Yoon (USA)	Prof. Dr Milan D. Antonijević (UK)
Prof. Dr Chang-min Park (South Korea)	Prof. Dr Jelena Mitrović (Serbia)
Prof. Dr Faramarz Doulati Ardejani (Iran)	Prof. Dr Polonca Trebše (Slovenia)
Prof. Dr Natalija Dolić (Croatia)	Prof. Dr Popescu Francisc (Romania)
Prof. Dr Adrian Eugen Cioablă (Romania)	

## HONORARY COMMITTEE

**Dr. Petar Paunović**

(Zaječar, Serbia)

**Prof. Dr Zvonimir Stanković**

(Bor, Serbia)

**Prof. Dr Velizar Stanković**

(Bor, Serbia)

**Prof. Dr Milan M. Antonijević**

(Bor, Serbia)

**Prof. Dr Ladislav Lazić**

(Sisak, Croatia)

**Dragan Randelović, Society of Young Researchers – Bor**

(Bor, Serbia)

**Toplica Marjanović, Society of Young Researchers – Bor**

(Bor, Serbia)

**Mihajlo Stanković, Special Nature Reserve of Zasavica**

(Sremska Mitrovica, Serbia)

## ORGANIZING COMMITTEE

**Prof. Dr Snežana Šerbula, *President***

**Prof. Dr Snežana Milić, *Vice President***

**Prof. Dr Đorđe Nikolić, *Vice President***

**Prof. Dr Ana Radojević, *Vice President***

**Dr Tanja Kalinović, *Vice President***

Prof. Dr Marija Petrović Mihajlović

Prof. Dr Milan Radovanović

Prof. Dr Milica Veličković

Prof. Dr Danijela Voza

Prof. Dr Maja Nujkić

Prof. Dr Ana Simonović

Dr Jelena Kalinović

Dr Jelena Jordanović

Dr Dragana Medić

Sonja Stanković, MSc

Vladan Nedelkovski, MSc

Aleksandar Cvetković, BSc

Dragan Milenković, IT service



## **PREFACE**

*The 31<sup>st</sup> international conference Ecological Truth & Environmental Research – EcoTER'24 focuses on showing the latest research findings and innovations in the field of ecology, environmental protection and sustainable development. The conference will be held in Sokobanja (Serbia) in hotel Sunce in the period of 18–21 June 2024.*

*The aim of the conference is to connect the experts in various fields in order to transform attitudes and behaviors in everyday practices, as well as in the industry and economy sector which is essential for achieving the desired changes that our society must undergo.*

*The 31<sup>st</sup> international conference Ecological Truth & Environmental Research – EcoTER'24 is organized by the University of Belgrade, Technical Faculty in Bor, and co-organized by the University of Banja Luka, Faculty of Technology; the University of Montenegro, Faculty of Metallurgy and Technology – Podgorica; the University of Zagreb, Faculty of Metallurgy – Sisak; the University of Pristina, Faculty of Technical Sciences – Kosovska Mitrovica and the Society of Young Researchers – Bor.*

*These Proceedings encompass 119 papers from the authors coming from the universities, research institutes and industries in 15 countries: Brazil, Norway, USA, Spain, Austria, Libya, Italy, Israel, Slovenia, Croatia, Romania, Bulgaria, Montenegro, Bosnia and Herzegovina, North Macedonia, and Serbia. It is a great honor and pleasure to cordially wish a warm welcome to all the participants of the conference.*

*As a part of this year's conference, the 6<sup>th</sup> Student Section – EcoTERS'24 will be held. We appreciate the contribution of the students and their mentors who have also participated in the conference and hope that students will continue to explore and to be curious, since education is a never-ending process, and knowledge is continuously growing.*

*The organization of the EcoTER'24 conference has been financially supported by the Ministry of Science, Technological Development and Innovation of the Republic of Serbia.*

*The support of the Donors and their willingness and ability to cooperate has been of great importance for the success of the EcoTER'24 conference. The organizing committee would like to extend their appreciation and gratitude to the Platinum donors of the conference – Serbia ZiJin Copper doo Bor and HBIS SERBIA, to the Gold donor of the conference – Elixir Group, as well as to the Silver donor of the conference – Serbian Chamber of Engineers.*

*We would like to express our sincere appreciation to all the authors who have contributed to the Proceedings. We would also like to express our gratitude to the members of the scientific, organizing and honorary committees, reviewers, speakers, chairpersons and all the conference participants for their support of the EcoTER'24. Sincere thanks go to all the people who have contributed to the successful organization of the EcoTER'24.*

*Prof. Snežana Šerbula,*

*President of the scientific and organizing committee*



## TABLE OF CONTENTS

### Plenary Lectures

**Branko Bugarski**

ELECTROSTATIC DISPERSION OF POLYMER SOLUTIONS IN THE PRODUCTION OF MICROGEL BEADS CONTAINING BIOCATALYST 1

**Anupama Ghosh, M. R. Del Grande, L. T. Teixeira, S. Letichevsky, C. A. Senna, M. D. Carbajal Ccoyllo, J. F. Chaves e Silva, V. C. Gois de Oliveira, R. N. Correia de Siqueira**

HEAT TREATMENT OF IRON-ADSORBED FUNCTIONALIZED NANOCELLULOSE FIBERS IN ORDER TO SYNTHESIZE HYBRID INORGANIC-CARBON MATERIAL 8

**Alena Bartonova**

ENVIRONMENTAL PROTECTION: WHY IS EUROPE'S AIR (MOSTLY) SO CLEAN? 14

### Invited Lectures

**Nevenka Rajić, J. Pavlović**

APPLICATION OF NATURAL ZEOLITE – CLINOPTILOLITE IN WATER TREATMENT BY ADSORPTION AND PHOTOCATALYSIS 17

**Dušan Nikolić, A. Tasić**

THE EUROPEAN PERCH (*Perca fluviatilis*) AS AN INDICATOR OF OCPs POLLUTION IN DIFFERENT TYPES OF RESERVOIRS IN SERBIA 24

**Jelena Korać Jačić, M. R. Milenković, D. Bartolić**

DEGRADATION OF TETRACYCLINE ANTIBIOTICS IN AQUATIC ENVIRONMENT BY UV IRRADIATION AND FERRIC ION PHOTOLYSIS 30

### Conference Papers

#### Environmental monitoring and impact assessment

**Aleksandra Papludis, S. Alagić, S. Milić, J. Nikolić, I. Zlatanović, S. Jevtović, V. Stankov Jovanović**

NAPHTALENE SCREENING IN BOR'S MUNICIPALITY BASED ON ITS CONCENTRATIONS IN LEAVES AND STEMS OF *Hedera helix* L. 38

**Darko Anđelković, M. Branković**

APPLE PEEL AS A BARRIER TO PESTICIDES MIGRATION INTO DEEPER FRUIT PARTS 43

<b>Darko Anđelković, M. Branković</b>	PERFORMANCES OF QuEChERS BASED GC-MS AND LC-MS/MS METHODS FOR PESTICIDES ANALYSIS IN APPLES	49
<b>Darko Anđelković, M. Branković</b>	COMPARISON OF PESTICIDES STABILITY STORED IN TWO SOLVENTS OF DIFFERENT VISCOSITY	55
<b>Milena Tadić, I. Nikolić, D. Đurović, N. Cupara, J. Vuković</b>	TRIHALOMETHANES CONTENT IN HOTEL'S SWIMMING POOLS WATER IN A SOUTH OF MONTENEGRO	61
<b>Jelena Vranković, K. Jovičić, V. Đikanović</b>	FIRST LINE DEFENCE ANTIOXIDANT ENZYMES IN <i>Blicca bjoerkna</i> (LINNAEUS, 1758) FROM THE BELGRADE SECTION OF THE DANUBE RIVER	66
<b>Miomir Mikić, R. Marković, V. Marjanović, R. Rajković, M. Jovanović</b>	RECUltIVATION OF RTH FLOTATION TAILINGS IN BOR, SERBIA	71
<b>Miomir Mikić, V. Marjanović, R. Marković, M. Jovanović, R. Rajković</b>	MINING AND THE ENVIRONMENT, ENVIRONMENTAL IMPACT MONITORING PROGRAM FOR FLOTATION TAILING RTH-BOR, SERBIA	77
<b>Vesna Obradović, M. Perović, T. Vučković</b>	EVALUATING CORROSION AND BIOFOULING POTENTIAL BASED ON GROUNDWATER MICROBIOLOGICAL COMPOSITION	83
<b>Vesna Obradović, M. Perović, J. Lekić</b>	EVALUATION OF CORROSION POTENTIAL USING PHYSICO-CHEMICAL WATER QUALITY ASSESSMENT	89
<b>Jelena Čanak Atlagić, A. Marić, K. Jovičić, J. Stanković, V. Đikanović, T. Mitić, M. Raković</b>	QUESTIONING THE RESILIENCE OF THE DANUBE FISH FAUNA UNDER THE PRESSURE OF BELGRADE WASTEWATERS	95
<b>Vladan Marinković, M. Maksimović, M. Jovanović, S. Trujić</b>	MONITORING OF THE STATE OF THE ENVIRONMENT IN THE BOR DISTRICT, GIVEN THROUGH THE EXAMPLE OF THE DISTRIBUTION OF Pb IN THE SOIL LOCATED IN THE IMMEDIATE VICINITY OF THE BOR RIVER	101
<b>Mirjana Ocokoljić, Dj. Petrov, N. Galečić, D. Skočajić, D. Vujičić, J. Čukanović, I. Simović</b>	EFFECTIVENESS OF <i>Photinia × Fraseri</i> 'RED ROBIN' IN THE URBAN LANDSCAPE: TOWARDS OF CLIMATE CHANGE	106
<b>Mirjana Ocokoljić, Dj. Petrov, N. Galečić, D. Skočajić, D. Vujičić, J. Čukanović, I. Simović</b>	<i>Chaenomeles japonica</i> (Thunb.) Lindl. ex Spach IN THE DESIGN OF URBAN PARKS: LEARNING FROM NATURE	113

<b>Mirjana Ocokoljić, J. Čukanović, Dj. Petrov, N. Galečić, D. Skočajić, D. Vujičić, I. Simović</b> <i>Parthenocissus quinquefolia</i> L.: PHENOMONITORING IN BLUE-GREEN INFRASTRUCTURE OF BELGRADE AND NOVI SAD	119
<b>Bojana Tubić, J. Đuknić, K. Zorić, N. Popović, N. Marinković, M. Paunović, M. Raković</b> EFFECTS OF THE IRON GATE DAMS ON THE BENTHIC MACROINVERTEBRATE COMMUNITY	126
<b>Danica Bogdanović, T. Anđelković, I. Kostić Kokić, M. Milovanović</b> GC-MS QUANTITATIVE DETERMINATION OF PHTHALATES IN PVC ARTICLES INTENDED FOR CHILDREN'S USE	132
<b>Danica Bogdanović, T. Anđelković, I. Kostić Kokić, M. Milovanović</b> OPTIMIZATION OF LIQUID-LIQUID PHTHALATES EXTRACTION FROM ARTIFICIAL SALIVA	138
<b>Danica Bogdanović, T. Anđelković, I. Kostić Kokić, M. Milovanović</b> MIGRATION OF DI-2-ETHYLHEXYL PHTHALATE AND DI-N-OCTYL PHTHALATE FROM PVC ARTICLES TO ARTIFICIAL SALIVA	144
<b>Daliborka Stanković, D. Z. Rajković, M. Raković, S. Skorić</b> HAEMOSPORIDIAN PARASITES IN LONG-EARED OWLS WINTERING IN BANAT, SERBIA	150
<b>Nenad Zarić, I. Hotea, A. Lato, M. Zarić, F. Crista</b> UNVEILING PESTICIDE CONTAMINATION IN TRANSBOUNDARY WATERS: A CASE STUDY OF SERBIA AND ROMANIA	156
<b>Nenad Zarić, F. Crista, A. Berbecea, I. Hotea, L. Crista, M. Zarić</b> COMPARATIVE ANALYSIS OF PESTICIDE RESIDUES IN AGRICULTURAL SOILS OF SERBIA AND ROMANIA	160
<b>Milica Veličković, D. Voza</b> THE RELATIONSHIP BETWEEN PM <sub>10</sub> AND METEOROLOGICAL PARAMETERS CLOSE TO THE MINING AREA	164
<b>Biljana Budzakoska Gjoreska, S. Trajanovski</b> MACROZOOBENTHOS COMMUNITY AND ECOLOGICAL STATUS IN PRESVA LAKE (OTESHEVO, STENJE AND EZERANI) IN SPRING 2022	169
<b>Suzana Patcheva, J. Leshoski, E. Veljanoska Sarafiloska</b> PHYTOPLANKTON COMMUNITY AS BIOINDICATOR OF WATER TROPHIC STATE IN LAKE PRESVA	176
<b>Boris Novaković, M. Raković</b> EARLY, LATE AND OUT-BREEDING SEASON BIRD SINGING – EFFECTS OF CLIMATE CHANGE?	183
<b>Boris Novaković, M. Raković</b> THE USE OF HOA (HEMIPTERA-ORTHOPTERA-AVES) INDICATORS TO FORMULATE THE SERBIAN CLIMATE CHANGE INDEX (S <sub>CCI</sub> )	189

<i>Ana Marić, V. Nikolić, D. Škraba Jurlina, V. Sokolović, D. Miličić, T. Karan Žnidaršič, T. Kanjuh, P. Simonović</i>	ASSESSMENT OF NON-NATIVE SPECIES IMPACT ON FISH DIVERSITY IN THE ČELIJE RESERVOIR: IMPLICATIONS FOR CONSERVATION AND MANAGEMENT	194
<i>Ivana Jelić, A. Savić, T. Miljojčić, M. Rajković, M. Janković, N. Sarap, S. Dimović, M. Čurčić, V. Stanić, D. Antonijević, M. Šljivić-Ivanović</i>	THE IMPACTS OF WASTE MATERIALS UTILIZATION IN LIQUID RADIOACTIVE WASTE SOLIDIFICATION BY MORTAR MATRIX	200
<i>Stefan Đorđievski, M. Đukić, A. Petrović, D. Adamović, J. Petrović, Lj. Lekić</i>	INSIGHTS FROM THE DAILY MONITORING OF WATER QUALITY PARAMETERS IN CEROVO RIVER NEAR BOR CITY IN OCTOBER 2023	206
<i>Nataša Kojadinović, S. Đuretanović, A. Milošković, M. Radenković, M. Jakovljević, T. Veličković, M. Nikolić, V. Simić</i>	FISH DIVERSITY ASSESSMENT OF THE IBAR RIVER: A 20-YEAR PERSPECTIVE	212
<i>Milanka Negovanović, L. Kričak, S. Milanović, N. Simić, J. Majstorović</i>	APPLICATION OF EXPANSIVE MORTARS FOR THE FORMATION OF ARTIFICIAL SCREENS DURING BLASTING IN URBAN AREAS	216
<i>Snežana Šerbula, T. Kalinović, A. Radojević, J. Kalinović, J. Jordanović</i>	AIR POLLUTION IN THE BOR REGION FROM 1994 TO 2023	225
<i>Irena Blagajac, I. Samardžić</i>	CAUSES OF FLOODING AND MEASURES TO MITIGATE THE CONSEQUENCES – CASE STUDY OF RAKOVICA MUNICIPALITY (BELGRADE, SERBIA)	231
<b>Urban and industrial ecology</b>		
<i>Žarko Radović, N. Tadić</i>	SIMULATION OF THE EAF DUST RECYCLING	240
<i>Mirko Gojić, S. Kožuh, I. Ivanić, D. Dumenčić</i>	DEVELOPMENT OF METALLURGY AND ENVIRONMENTAL PROTECTION IN THE REPUBLIC OF CROATIA IN THE PERIOD FROM 1900 TO 2020	246
<b>Air, water and soil pollution, prevention and control</b>		
<i>Viša Tasić, T. Apostolovski-Trujić, V. Kamenović, B. Radović, I. Zlatković, N. Ristić, Z. Damnjanović</i>	APPLICATION OF LOW-COST NETWORK FOR URBAN MICROCLIMATE AND AIR QUALITY MONITORING	251

<i>Nebojša Tadić, Ž. Radović, A. Knežević</i> ANALYSIS OF THE INFLUENCE OF NATURAL GAS COMPOSITION AND EXCESS AIR COEFFICIENT ON COMBUSTION PRODUCTS	258
<i>Aleksandar Jovanović, N. Knežević, M. Bugarčić, J. Petrović, M. Sokić, M. Stevanović, A. Marinković</i> INVESTIGATION OF MULTI-CYCLE USAGE OF NANOPHOTOCATALYSTS IN DEGRADATION OF THIOPHANATE- METHYL	265
<i>Vesna Obradović, M. Perović, P. Pajić</i> PHYSICO-CHEMICAL AND MICROBIAL ANALYSIS IN SELECTED GROUNDWATER IN SERBIA	270
<i>Silvia Dimova, K. Zaharieva, O. Dimitrov, P. D. Petrov, H. Penchev</i> METHATHESIS SYNTHESIZED OLIGOMERIC POLYPHENYLACETYLENE AS STERIC STABILIZER OF CARBON NANOTUBES/PLANT EXTRACT SYNTHESIZED ZINC OXIDE HYBRIDS	276
<i>Miljan Marković, M. Gorgievski, N. Štrbac, V. Grekulović, M. Marković, K. Božinović, D. Jovanović</i> EQUILIBRIUM ANALYSIS OF COPPER IONS BIOSORPTION ONTO HAZELNUT SHELLS	282
<i>Vesna M. Marjanović, R. Marković, D. Božić</i> CALCULATION OF CALCIUM OXIDE CONSUMPTION IN THE MINE WASTEWATER TREATMENT FROM INACTIVE OPEN PITS OF THE COPPER MINE	287
<i>Marina Marković, M. Gorgievski, N. Štrbac, V. Grekulović, M. Marković, M. Zdravković, D. Jovanović</i> THERMODYNAMIC ANALYSIS AND INFLUENCE OF THE pH VALUE ON THE BIOSORPTION OF COPPER IONS ONTO HAZELNUT SHELLS	294
<i>Jelena Korać Jačić, D. Bartolić, M.R. Milenković</i> THE IMPACT OF FERROUS AND FERRIC IONS ON DEGRADATION OF ANTIHYPERTENSIVE DRUG DIHYDRALAZINE IN IRON-BASED FLOCCULATION AND COAGULATION METHODS FOR WASTE WATER TREATMENT	299
<i>Berina Sejdinović</i> OILY WASTEWATER	305
<i>Vesela Radović, S. Krnjajić, S. Stanković, V. Tomić, G. Knežević</i> ENVIRONMENTAL RISKS CAUSED BY THE POLLUTION FROM AGRICULTURAL PLASTICS – A BRIEF STATE OF ART	311
<i>Marija Koprivica, J. Dimitrijević, J. Petrović, M. Ercegović, M. Simić</i> COMPARISON BETWEEN HYDROCHAR AND ITS ALKALI MODIFIED FORM IN THE REMOVAL OF Cd(II) IONS FROM AQUEOUS SOLUTION	317

<b>Milena Pijović Radovanović, M. Seović, I. Perović, N. Zdolšek, J. Georgijević, P. Laušević, S. Brković</b>	EFFICIENT REMOVAL OF RHODAMINE B FROM AQUEOUS SOLUTIONS USING CARBONIZED WASTE CAR TIRES: CHARACTERIZATION AND ADSORPTION STUDIES	323
<b>Svetlana Butulija, J. Maletaškić, B. Todorović, G. Branković, A. Krstić, R. Mihailović, B. Matović</b>	SYNTHESIS, CHARACTERIZATION AND ADSORPTION POTENTIAL OF CORN COB-DERIVED ACTIVATED CARBON	329
<b>Vladan Nedelkovski, S. Stanković, D. Medić, D. Buzdugan, I. Hulka, S. Milić, M. Radovanović</b>	PHOTOCATALYTIC PROPERTIES OF C-ZnO NANOPARTICLES SYNTHESIZED <i>via</i> MECHANOCHEMICAL METHOD	335
<b>Aleksandar Zdravković, M. Nikolić, D. Marković Nikolić, D. Stojadinović, G. Petković, T. Nikolić</b>	EQUILIBRIUM AND THERMODYNAMICS OF NITRATE SORPTION BY MODIFIED ZEOLITE FROM AQUEOUS SOLUTION	341
<b>Aleksandar Zdravković, M. Nikolić, D. Marković Nikolić, D. Stojadinović, I. Ristić, T. Nikolić</b>	POTENTIAL USAGE OF OAT STRAW FOR ANIONS REMOVAL FROM WATER: A KINETIC STUDY	348
<b>Aleksandar Zdravković, M. Nikolić, A. Pavlović, D. Marković Nikolić, G. Petković, T. Nikolić</b>	ULTRASOUND-ASSISTED EXTRACTION OF ACETAMIPRID FROM POLLUTED SOIL	354
<b>Katerina Zaharieva, B. Barbov</b>	PLANT-MEDIATED SYNTHESIS AND PHOTOCATALYTIC INVESTIGATIONS OF CeO <sub>2</sub> -ZnO COMPOSITES	358
<b>Milena Milošević, M. Abdualatif Abduarahman, M. M. Vuksanović, Z. Veličković, N. Knežević, B. Najdanović, A. Marinković</b>	CELLULOSE BASED MEMBRANE FOR CATIONIC POLLUTANTS REMOVAL FROM WATER	363
<b>Milena Milošević, A. Marinković, M. M. Vuksanović, Z. Veličković, I. Đuričković, B. Najdanović, N. Knežević</b>	HEMP MODIFIED WITH BETAINE AS A GREEN AND EFFICIENT ADSORBENT FOR REMOVAL OF ANIONIC DYES FROM WATER	369
<b>Nevena Surudžić, M. Spasojević, M. Crnoglavac Popović, M. Stanišić, R. Prodanović, O. Prodanović</b>	PHENOL REMOVAL FROM WASTEWATER WITH HORSERADISH PEROXIDASE IMMOBILIZED BY PERIODATE METHOD ONTO NOVEL MACROPOROUS POLY(GMA-CO-EGDMA) CARRIERS	375



<b>Miljana Radović Vučić, N. Velinov, J. Mitrović, S. Najdanović, M. Petrović, M. Kostić, A. Bojić</b>	MODIFIED ACTIVATED WOOD SAWDUST AS GREEN ENVIRONMENTAL-FRIENDLY CATALYST FOR TREATMENT OF PHARMACEUTICAL EFFLUENT	381
<b>Jelena Mitrović, M. Radović Vučić, N. Velinov, S. Najdanović, M. Kostić, M. Petrović, A. Bojić</b>	ADVANCE OXIDATION OF TEXTILE DYE BY ACTIVATED HYDROGEN PEROXIDE WITH UV-C LIGHT	387
<b>Protection and preservation of natural resources</b>		
<b>Gordana Šekularac, M. Aksić, T. Dimitrijević, M. Ratknić, N. Gudžić</b>	QUANTIFYING SOIL EROSION OF THE TOM'S BROOK CATCHMENT (WESTERN SERBIA)	393
<b>Gordana Šekularac, M. Aksić, T. Dimitrijević, S. Gudžić, N. Gudžić, D. Gračak, M. Grčak, M. Ratknić</b>	EFFECT OF IRRIGATION RATE ON THE ONSET INTENSITY OF GREY MOULD AND LATE BLIGHT IN GREEN HOUSE TOMATOES	399
<b>Tatjana Dimitrijević, M. Ratknić, G. Šekularac, M. Aksić</b>	INFLUENCE OF SOIL TYPE ON MEAN TREE HEIGHTS OF FIR TREES IN A 40-YEAR PROVENANCE TRIAL	406
<b>Dragana Božić, Lj. Avramović, V. Trifunović, R. Marković, Z. Stevanović, V. Marjanović, E. Požega</b>	AGITATION LEACHING OF FLOTATION TAILINGS AT THE PILOT PLANT	412
<b>Ivana Kerkez Janković, D. Vilić, M. Nonić, J. Devetaković, M. Šijačić-Nikolić</b>	FOREST FRUIT SPECIES OF URBAN FOREST "KOŠUTNJAK" (SERBIA) – GENEPOOL ASSESSMENT AND CONSERVATION	418
<b>Boris Novaković, N. Paskaš, M. Raković</b>	NEW DATA ON THE DISTRIBUTION OF AQUATIC BEETLES IN SERBIA	424
<b>Matej Fike, M. Pezdevšek, A. Roger</b>	COMPARING FROST PROTECTION STRATEGIES FOR SUSTAINABLE AGRICULTURE IN SLOVENIA	430
<b>Filip Maksimović, M. Nonić, D. Vilotić, I. Kerkez Janković, M. Šijačić-Nikolić</b>	GENE POOL OF FOREST FRUIT TREES IN THE PROTECTED AREA OF THE NATURAL MONUMENT "KOŠUTNJAK FOREST" – THEN AND NOW	435
<b>Dragana Medić, S. Milić, N. Milošević, M. Nujkić, M. Pešić, V. Nedelkovski, S. Stanković</b>	APPLICATION OF THE SHRINKING CORE MODEL IN THE LEACHING PROCESS OF $\text{LiNiMnCoO}_2$	441

## Ecotoxicology and environmental safety

<b>Branko Matovic, J. Maletaskic, S. Butulija, S. Petrovic, B. Todorovic</b> IMMOBILIZATION OF LEAD USING CERIA CRYSTAL STRUCTURE	448
<b>Dragana Medić, S. Milić, N. Milošević, M. Nujkić, S. Alagić, A. Cvetković, A. Papludis</b> CAUSES AND POSSIBLE CONSEQUENCES OF THERMAL RUNAWAY IN LITHIUM-ION BATTERIES	454
<b>Nena Velinov, M. Radović Vučić, J. Mitrović, M. Petrović, S. Najdanović, D. Bojić, A. Bojić</b> KINETIC AND EQUILIBRIUM STUDIES OF CHROMIUM SORPTION USING ULTRASONICALLY MODIFIED WOOD SAWDUST BY ALUMINA	460
<b>Hazardous materials and green technologies</b>	
<b>Uroš Stamenković, I. Marković, V. Čosović, B. Markoli</b> THE INFLUENCE OF AGEING PARAMETERS ON MICROHARDNESS, ELECTRICAL CONDUCTIVITY AND MICROSTRUCTURE OF SOME Al-Mg-Si ALLOYS	466
<b>Marija Simić, D. Aćimović, B. Savić Rosić, M. Ječmenica Dučić, K. Stojanović, D. Maksin, T. Brdarić</b> KINETIC STUDY OF DEGRADATION BISPHENOL A BY FENTON PROCESS	472
<b>Danka Aćimović, K. Stojanović, M. Simić, B. Savić Rosić, Z. Vranješ, M. Ječmenica Dučić, T. Brdarić</b> DETECTION OF BISPHENOL A INTERMEDIATES DURING FENTON PROCESS AND PREDICTION OF REACTION PATHWAYS	476
<b>Tanja Brdarić, D. Aćimović, B. Savić Rosić, K. Stojanović, M. Simić, Z. Vranješ, M. Ječmenica Dučić</b> ADVANCED OXIDATION PROCESSES (AOPs) FOR WASTEWATER TREATMENT: BIBLIOMETRIC STUDY	480
<b>Vanja Trifunović, S. Milić, Lj. Avramović</b> POSSIBILITY OF ZINC AND CADMIUM RECOVERY FROM HAZARDOUS INDUSTRIAL WASTE – EAF DUST	486
<b>Sandra Bulatović, N. Nedić, T. Tadić, B. Marković, A. Nastasović</b> MAGNETIC BIOSORBENT BASED ON THE <i>Ambrosia arthemisiifolia</i> FOR ADSORPTION OF MALACHITE GREEN FROM WATER	491
<b>Milan Nedeljković, S. Mladenović, J. Petrović, M. Mitrović</b> STUDIES OF THE INFLUENCE OF GRAPHENE NANOSHEETS ON THE WETTABILITY OF ECO-FRIENDLY SOLDER ALLOYS	497

<i>Ana Simonović, M. Petrović Mihajlović, M. Radovanović, Ž. Tasić, M. Antonijević</i> ELECTROCHEMICAL SENSORS FOR DETERMINATION OF ANTIBIOTICS	502
<i>Sonja Stanković, V. Nedelkovski, D. Buzdugan, I. Hulka, M. Gorgievski, S. Milić, M. Radovanović</i> INFLUENCE OF CALCINATION TEMPERATURE ON THE MORPHOLOGY, CHEMICAL COMPOSITION, AND STRUCTURE OF ZnO NANOPARTICLES	508
<b>Human and ecological risk assessment</b>	
<i>Milena Tadić, I. Nikolić, D. Đurović, J. Vuković, N. Cupara</i> CHILDREN HEALTH RISK ASSESSMENT OF TRIHALOMETHANES CONTENT IN HOTEL'S SWIMMING POOL WATER IN MONTENEGRO	515
<i>Miljan Bigović, D. Đurović, Lj. Ivanović, M. Blagojević, A. Orahovac</i> HEALTH RISK ASSESSMENT OF ACRYLAMIDE IN POTATO CHIPS FROM MONTENEGRIN MARKET	520
<i>Vesna Djikanović, K. Jovičić, J. S. Vranković, M. Dimitrijević, S. Kovačević, N. Pankov, B. Miljanović</i> ACCUMULATION OF HEAVY METALS AND HUMAN HEALTH RISK ASSESSMENT <i>via</i> THE CONSUMPTION OF FRESHWATER FISH <i>Esox lucius</i>	524
<b>Agriculture: nutrition, organic food and health impacts</b>	
<i>Vitaly Erukhimovitch, M. Huleihel</i> OPTIMIZATION OF PREPARATION PROCEDURES FOR FUNGAL INFECTED PLANTS BY FTIR ANALYSES	531
<i>Mahmoud Huleihel, V. Erukhimovitch</i> POSSIBLE USE OF FOURIER–TRANSFORM INFRARED (FTIR) MICROSCOPY FOR IDENTIFICATION OF FUNGAL PHYTO–PATHOGENS	536
<i>Ana Čučulović, J. Stanojković, R. Čučulović</i> RADIOACTIVITY IN SAMPLES OF IMPORTED MINERAL FERTILIZER ANALYZED IN THE PERIOD 2020–2022	541
<i>Nenad Zarić, M. Zarić</i> METAL CONTENTS IN VEGETABLES ORIGINATING FROM COAL FIRED THERMAL POWER PLANTS REGION	547
<b>Alternative energy: efficiency and environmental policy</b>	
<i>Snežana Brković, N. Zdolšek, I. Perović, M. Seović, P. Laušević, J. Georgijević, M. Čebela</i> ENHANCING OXYGEN EVOLUTION: THE ELECTROCATALYTIC POWER OF Ag-DOPED BISMUTH FERRITE	552

<i>Nebojša Potkonjak, Đ. Čokeša, M. Marković</i>	NONLINERA PHENOMENA DURING VOLTAMMETRIC MEASUREMENT OF COPPER CORROSION	558
<i>Mirjana Marković, Đ. Čokeša, N. Potkonjak</i>	EVALUATION OF THE HYDROGEN DIFFUSION COEFFICIENT IN METAL HYDRIDE BATTERIES	562
<b>Greenhouse effect and global climate change</b>		
<i>Slobodan Milutinović, T. Radenović, S. Živković</i>	FORESTS UNDER THREAT: IMPLICATIONS OF CLIMATE CHANGE ON SERBIAN WOODLANDS	566
<i>Danijela Nikolić, S. Jovanović, Z. Đorđević, D. Končalović, V. Vukašinić</i>	GLOBAL WARMING – TREND ANALYSIS IN THE REPUBLIC OF SERBIA	574
<b>Sustainable development and green economy</b>		
<i>Dragana Randelović, A. Jovanović, B. Marković, M. Sokić</i>	CONTRIBUTION OF THE INSTITUTE FOR TECHNOLOGY OF NUCLEAR AND OTHER MINERAL RAW MATERIALS TO THE SDGs – TOWARDS INTERNATIONAL DECADE OF SCIENCE FOR SUSTAINABLE DEVELOPMENT	580
<i>Veljko V. Savić, J. D. Nikolić, V. Topalović, M. S. Djošić, M. Marković, S. Matijašević, S. Grujić</i>	CHEMICAL DURABILITY EVALUATION OF SINTERED FLY ASH BASED GLASS	586
<i>Stefan Mitrović, S. Brković, M. Seović, N. Zdolšek, P. Laušević, J. Georgijević, I. Perović</i>	RECYCLING ELECTRONIC WASTE CPUs FOR ENHANCED HYDROGEN AND OXYGEN EVOLUTION: AN ECO-FRIENDLY LEACHING APPROACH	593
<i>Adrijana Jevtić, D. Riznić, M. Vuković</i>	BRAND MANAGEMENT AND SOCIO-ECONOMIC ASPECTS OF ADAPTATION TO CLIMATE CHANGES	598
<i>Ana Radojević, J. Jordanović, T. Kalinović, J. Kalinović, S. Šerbula</i>	PROSPECTS OF SUSTAINABLE UTILIZATION OF FOOD WASTE	606
<i>Maja Bogdanović, I. Blagajac</i>	DECENTRALIZATION OF THE URBAN TOURIST ZONE OF ZLATIBOR	613

## Environmental biology

- Sladana Popović, N. Nikolić, Ž. Savković, M. Stupar, D. Predojević, A. Anđelković, O. Jakovljević**  
ISOLATION AND CULTIVATION OF CHROOCOCCUS (CYANOBACTERIA) FROM AEROPHYTIC BIOFILM IN STOPIĆ CAVE 621
- Tamara Mitić, J. Čanak Atlagić, J. Tomović, J. Stanković, D. Mrdak, D. Škraba Jurlina, A. Marić**  
MORPHOMETRIC STUDY OF EUROPEAN BULLHEAD *Cottus gobio* FROM DIFFERENT DRAINAGE POPULATIONS 626
- Jelena Đuknić, N. Popović, B. Vasiljević, B. Tubić, S. Andjus, M. Ilić, M. Paunović**  
ECOLOGICAL POTENTIAL OF THE DANUBE RIVER THROUGH SERBIA BASED ON BIOLOGICAL QUALITY ELEMENTS 632
- Sladana Popović, G. Subakov Simić, S. Stanković, D. Lazić**  
*Chlorella vulgaris* GROWTH IN SMALL OPEN CULTIVATION SYSTEMS 638
- Olga Jakovljević, S. Popović, D. Predojević**  
EPIPHYTIC DIATOMS AS TOOL IN BIOINDICATION OF LAKE PALIĆ 643
- Mihailo Jovanović, J. Paunković**  
IMPROVING PALEOENVIRONMENTAL RECONSTRUCTIONS BASED ON SMALL VERTEBRATES IN THE BALKANS 648
- Jovana Damjanović, M. Milković, A. Mišćević, M. Šćiban, V. Lakušić, M. Stanković**  
SUPPLEMENT TO THE LIST OF ENTOMOFAUNA FROM THE RESEARCH ACTIONS AND CAMPS OF SRSBE “JOSIF PANČIĆ” AT SRN ZASAVICA 654
- Mihajlo Stanković**  
“LIVING FOSSILS” IN THE CRASH FAUNA OF THE ZASAVICA SPECIAL NATURE RESERVE 662

## Environmental and material flow management

- Nataša Knežević, A. Jovanović, M. Vuksanović, M. Savić, M. Milošević, A. Marinković**  
DEGRADATION OF DYE CRYSTAL VIOLET RELEASED FROM THE TEXTILE INDUSTRY 669
- Milenko Jovanović, D. Kržanović, E. Požega, V. Marinković, M. Mikić**  
APPLICATION AND ENVIRONMENTAL SUITABILITY OF HYBRID GEOGRIDS 674
- Miroslav Drljača**  
MODERN APPROACH TO SUPPLY CHAIN BASED ON CIRCULAR ECONOMY PRINCIPLES 681

<i>Isidora Berežni, T. Marinković, N. Stanisavljević, M. Muhadinović, B. Batinić</i> ASSESSMENT OF THE MUNICIPAL SOLID WASTE MANAGEMENT – CASE STUDY: NOVI SAD (SERBIA)	687
---	-----

<i>Ljubiša Balanović, D. Manasijević, I. Marković, U. Stamenković, K. Božinović</i> CALCULATION OF THERMODYNAMIC PROPERTIES Al-Ga-Sn TERNARY ALLOY USING GENERAL SOLUTION MODEL	693
---	-----

### Life-Cycle-Analysis (LCA)

<i>Danijela Nikolić, S. Jovanović, D. Mikić, Z. Đorđević</i> LIFE CYCLE ASSESMENT OF THE HAIR DRYER WITH ECO-it SOFTWARE	701
--	-----

## Student Section – EcoTERS'24

<i>Students: Sofija Kostić, Aleksa Marjanović (Serbia)</i> <i>Mentor: Maja Nujkić (Serbia)</i> SOME ASPECTS OF THE APPLICATION OF METAL-ORGANIC FRAMEWORKS	709
---	-----

<i>Student: Jelena Janković (Serbia)</i> <i>Mentor: Maja Nujkić (Serbia)</i> MECHANISMS OF CADMIUM UPTAKE INTO THE PLANT	711
--	-----

<i>Student: Jovana Kumbrijanović (Serbia)</i> <i>Mentors: Maja Nujkić, Sonja Stanković (Serbia)</i> COAGULATION PROCESS AND APPLICATION OF NEW ECOLOGICAL COAGULANTS	713
---	-----

<i>Student: Lazar Cvetković (Serbia)</i> <i>Mentors: Maja Nujkić, Tanja Kalinović, Jelena Kalinović (Serbia)</i> SOME APPLICATION ASPECTS OF THE MATERIALS BASED ON THE GREEN MAGNESIUM OXIDE ECOLOGICAL COAGULANTS	715
--	-----

<i>Students: Milena Radivojević, Kristina Konstadinović (Serbia)</i> <i>Mentors: Maja Nujkić, Dragana Medić (Serbia)</i> RECYCLING OF USED LITHIUM-ION BATTERIES	717
--	-----

<i>Student: Milica Denić (Serbia)</i> <i>Mentor: Ana Radojević (Serbia)</i> MEDICAL WASTE ISSUES RELATED TO COVID-19 PANDEMIC	719
---	-----

<i>Student: Sara M. Pantović (Serbia)</i> <i>Mentor: Enisa S. Selimović (Serbia)</i> PRESENCE OF TOXIC AND POTENTIALLY TOXIC ELEMENTS IN SOME DOMESTIC FRUIT FROM THE PEŠTER PLATEAU, SJENICA, SERBIA	721
---	-----

<i>Student: Milena Stanković (Serbia)</i> <i>Mentor: Ljiljana Stanojević (Serbia)</i>	CHEMICAL COMPOSITION OF ESSENTIAL OIL ISOLATED FROM FRESH AND DRY LEAVES OF <i>Geranium robertianum</i> L.	723
<i>Student: Nikola Petrović (Serbia)</i> <i>Mentor: Ana Simonović (Serbia)</i>	TOXIC EFFECTS OF PETROLEUM DERIVATIVES ON LIVING ORGANISMS FROM CONTAMINATED SOILS	725
<i>Students: Anja Antanasković, Nevena Ilić (Serbia)</i> <i>Mentors: Milan Miliwojević, Suzana Dimitrijević-Branković, Zorica Lopičić, Nikola Vuković (Serbia)</i>	ENZYME IMMOBILIZATION ON MODIFIED BIOMASS: OPTIMIZATION AND CHARACTERIZATION	727
<i>Student: Milena Balabanović (Serbia)</i> <i>Mentor: Ana Radojević (Serbia)</i>	BIOLOGICAL TREATMENT OF THE BIODEGRADABLE WASTE	729
<i>Student: Natalija Stojanović (Serbia)</i> <i>Mentors: Maja Nujkić, Vladan Nedelkovski (Serbia)</i>	ADSORPTION MATERIALS BASED ON NANOPARTICLES FOR THE REMOVAL OF ARSENIC FROM WASTEWATER	731
<i>Student: Jelena Vesković (Serbia)</i> <i>Mentor: Antonije Onjia (Serbia)</i>	HEALTH RISK ASSESSMENT OF RARE EARTH ELEMENTS IN GROUNDWATER NEAR A THERMAL POWER PLANT	733
<i>Students: Vladimir Topalović, Anja Antanasković, Veljko Savić (Serbia)</i> <i>Mentors: Marija Djošić, Zorica Lopičić, Ana Vujošević, Jelena Nikolić (Serbia)</i>	EFFECT OF PHOSPHATE GLASS AND BIOCHAR ON ROSE GROWTH	735
<i>Student: Aleksandra Milenković (Serbia)</i> <i>Mentor: Ljiljana Stanojević (Serbia)</i>	THE REDUCING POWER OF BLACK PEPPER ( <i>Piper nigrum</i> L.) ESSENTIAL OIL HYDRODISTILLATION FRACTIONS	737
<i>Student: Marija Tasić (Serbia)</i> <i>Mentor: Dragan Cvetković (Serbia)</i>	ENVIRONMENTAL METHOD OF GOLD NANOPARTICLES SYNTHESIS AND THEIR CHARACTERIZATION	739
<i>Student: Marija Stanković (Serbia)</i> <i>Mentor: Jelena Kalinović (Serbia)</i>	PURIFICATION METHODS FOR POLLUTED AIR	741
<i>Student: Marija Stanković (Serbia)</i> <i>Mentor: Jelena Kalinović (Serbia)</i>	PURIFICATION OF INDUSTRIAL WASTEWATER	743



<i>Students: Željka Nikolić, Nebojša Radović (Serbia)</i> <i>Mentor: Olga Tešović (Serbia)</i>	
RISKS OF CHLORINE EXPOSURE IN HOUSEHOLD CLEANING: A CALL FOR AWARENESS AND PREVENTION	745
<i>Students: Željka Nikolić, Nebojša Radović (Serbia)</i> <i>Mentor: Olga Tešović (Serbia)</i>	
IS THERE A NEED TO INFORM CITIZENS MORE DIRECTLY ABOUT THE HANDLING OF HOUSEHOLD HAZARDOUS WASTE?	747
<i>Students: Nataša Simonović, Tamara Milosavljević (Serbia)</i> <i>Mentors: Jelena Stanojević, Ljiljana Stanojević, Jelena Zvezdanović, Dragan Cvetković (Serbia)</i>	
SOLID WASTE FROM HYDRODISTILLATION OF HERNIARIAE HERBA ( <i>Herniaria glabra</i> L.) AS A POTENTIAL SOURCE OF ANTIOXIDANTS	749
<i>Students: Aleksa Vizi, Nebojša Radović, Željka Nikolić, Stefan Lekić (Serbia)</i> <i>Mentors: Goran Roglić, Ksenija Stojanović, Vele Tešević (Serbia)</i>	
SUSTAINABLE SOLUTIONS IN ANALYTICAL CHEMISTRY: COMBINING OF INSTRUMENTAL TECHNIQUES AND ENVIRONMENTAL-FRIENDLY NATURAL INDICATORS FOR CLASSICAL VOLUMETRY	751
<i>Students: Aleksa Vizi, Nebojša Radović, Željka Nikolić (Serbia)</i> <i>Mentors: Ivan Kojić, Ksenija Stojanović (Serbia)</i>	
EFFICIENT DETERMINATION OF UNDECYLENIC ACID CONTENT IN PHARMACEUTICAL PRODUCTS: A NOVEL SIMPLE APPROACH	753
<i>Student: Andrijana Miletić (Serbia)</i> <i>Mentor: Antonije Onjia (Serbia)</i>	
HEALTH RISK ASSESSMENT OF POTENTIALLY TOXIC ELEMENTS IN AGRICULTURAL SOIL OF BRANIČEVO DISTRICT	755
<i>Student: Jelena Obradovic (Serbia)</i> <i>Mentor: Antonije Onjia (Serbia)</i>	
DISTRIBUTION OF PM <sub>2.5</sub> , CO <sub>2</sub> , HCHO, AND TVOC IN AIR IN A HIGH SCHOOL CLASSROOM	757
<i>Student: Gordan Mišić (Serbia)</i> <i>Mentors: Ana Radojević, Jelena Jordanović (Serbia)</i>	
TOXICOLOGICAL EFFECTS OF MICRO- AND NANO-PLASTICS ON HUMAN HEALTH	759
<i>Student: Anđela Bogdanović (Serbia)</i> <i>Mentor: Marija Petrović Mihajlović (Serbia)</i>	
MAGNESIUM AND ITS ALLOYS	761
<b>Author index</b>	<b>763</b>

# **Plenary Lectures**



## ELECTROSTATIC DISPERSION OF POLYMER SOLUTIONS IN THE PRODUCTION OF MICROGEL BEADS CONTAINING BIOCATALYST

**Branko Bugarski<sup>1\*</sup>**

<sup>1</sup>University of Belgrade, Faculty of Technology and Metallurgy, Karnegieva 4,  
11000 Belgrade, SERBIA

\*branko@tmf.bg.ac.rs

### **Abstract**

*Encapsulation strategy has emerged as a mean to protect sensitive cells, enzymes and bioactive compounds, to improve their stability and to deliver their active forms to the targeted place. A number of bio entities can be encapsulated – cells, enzymes, vitamins, minerals, aromas and antioxidants. Over the years various encapsulation technologies were employed in encapsulation of bioactive compounds. A short overview of commonly used technologies for the encapsulation of cells, enzymes and bioactive substances will be presented. Applications of encapsulation, include, enzymes as biocatalysts, pre-and pro-bacteria, as well as targeted drug delivery. It is also emerging in the agricultural sector, particular in seeds, as well as in the development of more environmentally friendly bio pesticides Encapsulation, therefore, offers a unique tool for resolving a variety of problems in sectors as diverse as food, nutrition, agriculture and water treatment.*

**Keywords:** dispersion techniques, electrostatic extrusion, cell, encapsulation technology.

### **INTRODUCTION**

Many biological systems, in their natural state, are immobilized. Furthermore, the majority of functions of living systems are based on the confinement of reactions in a limited space. In such models, the membrane insures the protection of the internal, bioactive, substance. The concept of immobilization is based on a natural, and effective, analogy, and is applied both in products and processes. Immobilised systems were widely investigated and used in different fields such as pharmacy, biomedicine, food and environmental technologies. Immobilised cell technology is successfully established at the industrial scale in wastewater treatment and production of biopharmaceuticals and fermented beverages. Cell immobilisation provides several advantages over the conventional free cell systems including higher cell concentrations, higher volumetric productivities, cell protection required for shear sensitive cells, and easy separation of cells and products. In addition, immobilised cell systems can be operated in continuous mode at higher dilution rates without the risk of cell washout. Especially attractive are the options for co-immobilisation of different cell types for the simultaneous implementation of consecutive reactions. Selections of immobilisation methods are function of active substance and material used in this process. In that respect, various actives isolates from natural sources can be employed, such as plant polyphenols, probiotic bacteria, omega-3-fatty acids, vitamins, minerals [1,2]. These compounds usually face the problem of low stability against the light, moisture, changes of pH or temperature; all this negatively affects the biological activity of bioactive compounds, and in long term lowers

their bioavailability and reduce the shelf-life of products. To overcome these limitations, encapsulation technology implies the entrapment of bioactive substances within the bead or capsule – e.g. polymeric carrier material, where the particles of desired diameters are produced therefore protecting interior of the microcapsule [3]. Among different encapsulation technologies we will focus on short overview of electrostatic encapsulation technology.

## MATERIALS AND METHODS

Solution of 1.5% sodium alginate was prepared by dissolving sodium alginate powder (Keltone LV, Kelco, Chicago, IL, USA) in WFI water. Spherical droplets were formed by a syringe pump using electrostatic droplet generator which extruded the alginate solution with cells through a 26 gauge blunt end needle. As the liquid was forced out of the end of the needle, droplets were pulled off by the action of gravitational and electrostatic forces forming gelled beads with diameter of 200–400 microns in  $\text{CaCl}_2$  solution. Droplet formation under the influence of electrostatic forces was examined with a video/image analysis system (Jandel Scientific, CA, USA) under strobe light.

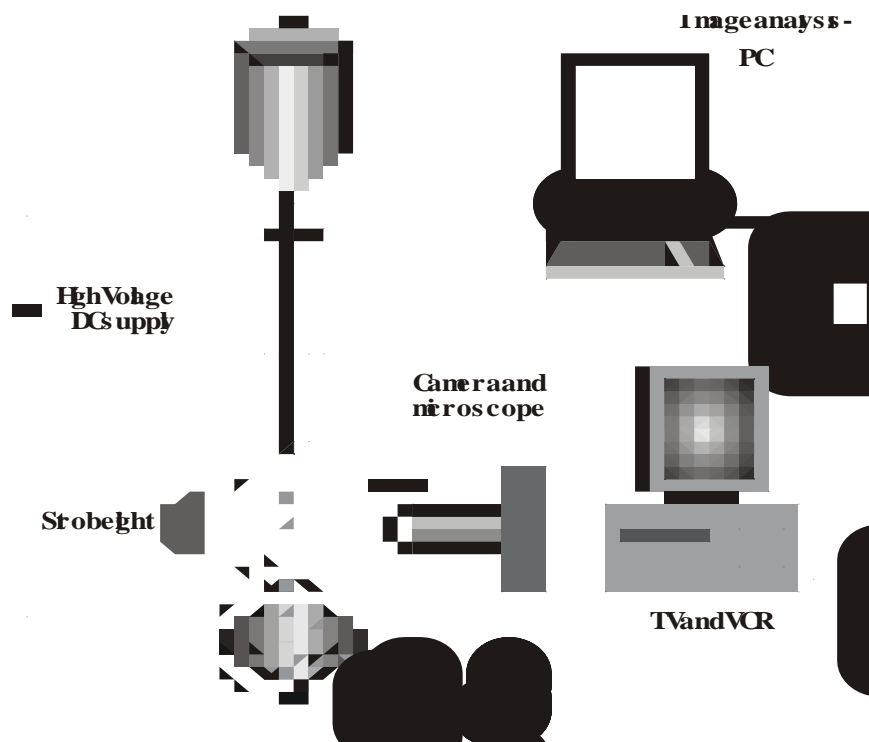
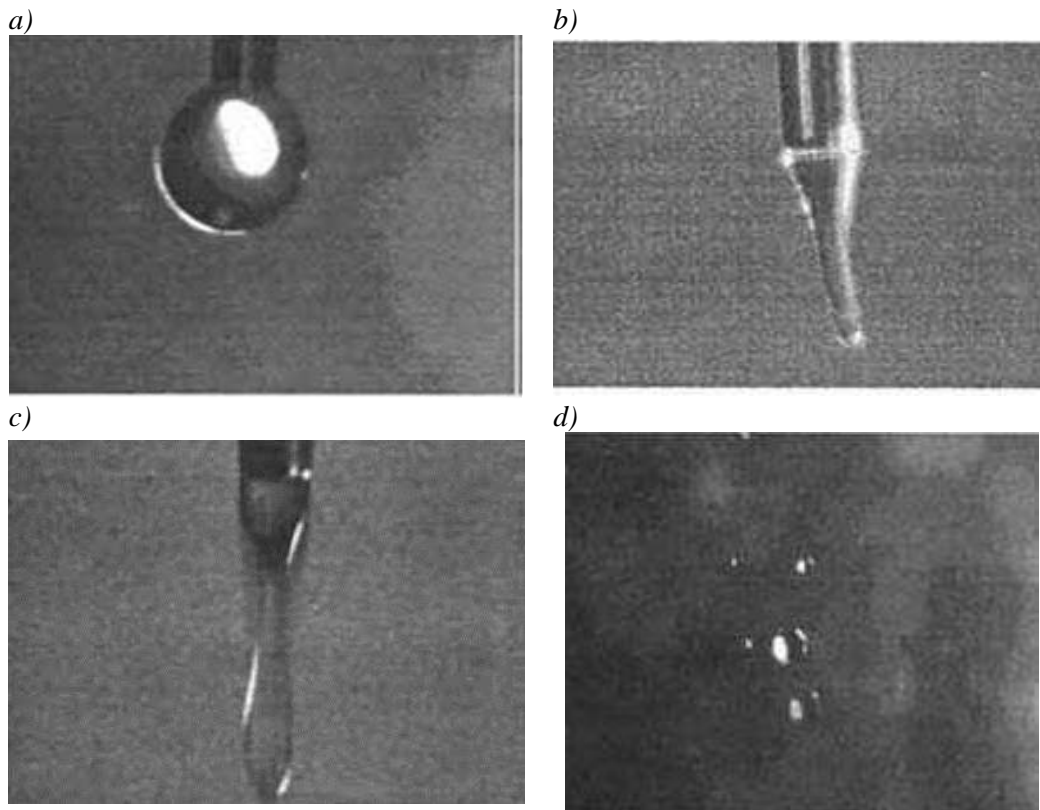


Figure 1 Schematic diagram of experimental set-up

## RESULTS AND DISCUSSION

In the absence of an electrostatic field with gravitational force acting alone, the mean bead diameter was about 2500 microns at a constant alginate flow rate using a 26 gauge needle. In this case, a droplet was produced every 1 to 2 s. Each drop grew at the tip of the needle until its weight overcame the net vertical component of the surface tension force (Figure 2a). Examination of the formation of droplets under the influence of electrostatic forces revealed that an elongated cone formed as the droplet meniscus advanced (Figure 2b). The forming

droplet was drawn out into a long, slender filament (4–7 kV). A high charge density at the tip of the inverted cone reduced the surface tension of the alginate solution resulting in neck formation (Figure 2c) where the neck elongated further before detachment [4]. While the main part of the liquid neck quickly coalesced into a new drop, the long linking filament broke up into a large number of smaller drops (Figure 3d). It was also observed that small (satellite) droplet formation usually accompanied higher voltages (above 7 kV), because the elongation of the liquid neck rupture was much more pronounced [5].



**Figure 2** Image analysis of polymer behavior sequences under influence of electric field phenomena

Formation of droplets with a charged needle arrangement in a defined electric field was examined. As the voltage applied to the needle (through which the semiconducting alginate solution flowed) increased from 4 to 7 kV, a rise in droplet emission frequency and a reduction in droplet diameter from 1000 microns to 150 microns was observed. The minimum diameter that could be obtained in this electric field range is often called the dripping mode with the average bead diameter of 200 microns and applied potential of 4.5 KV (Figure 3a). As the voltage increased beyond a certain point (i.e. critical voltage) a sudden transition from dripping mode to the high frequency spraying mode was observed [6]. The size distribution curves, obtained by plotting relative frequencies versus bead diameter, typically resulted in a continuous function symmetrical about the mean value. At 6 kV, the mean bead distribution was found to vary about the mean of 150 microns (Figure 3b). The microbeads produced with the electrostatic droplet generator operating with an applied voltage of 6 kV appearing as regular spheres with unimodal distribution [7]. At 7 kV, for example, the main drop develops into a cone with a fine stable stream of droplets issuing from the needle tip, due to the high

applied electrostatic force (Figure 3c) resulting in bimodal distribution ranging from 50 to 200 microns [8]. However the bimodal results are not favorable since the cell growth in different particle diameters are not the same neither the repeatability of process [9]. The proper choice of geometric parameters allows to avoid the formation of the undesirable satellite fraction of the very small microbeads.

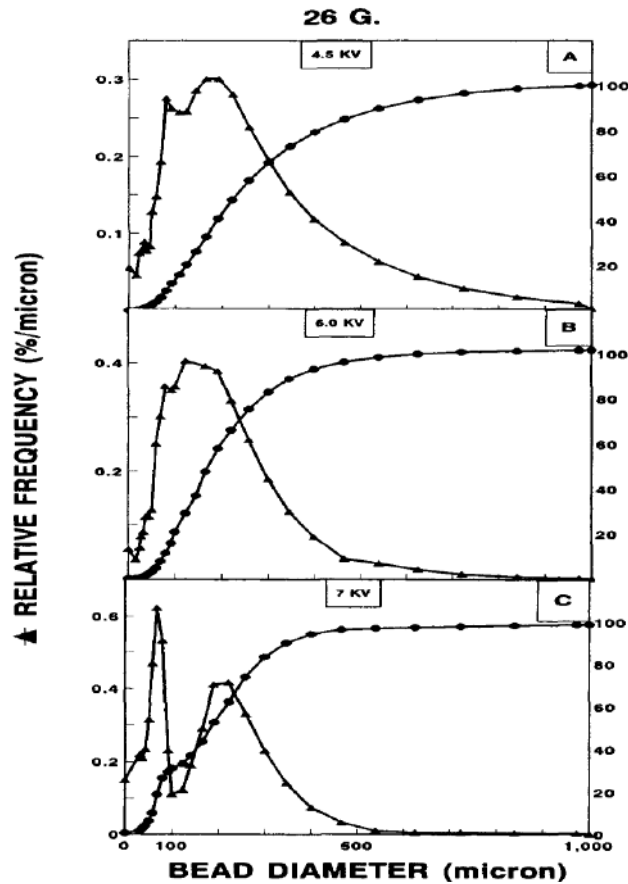


*Figure 3* Diagram of droplet diameter ( $d$ , micron) as a function of electric potential  $U$  (kV), and the needle diameter [4]

In the case of the positively charged needle setup, the effect of electrode spacing on alginate bead size, produced with a 22-gauge needle, is shown in Figure 4A. The electrode spacing was not found to be significant over the range investigated. For example, at an applied voltage of 6 kV, the mean bead size decreased from 530 to 450 microns, as the electrode spacing decreased from 4.8 to 2.5 cm, respectively, with a standard deviation of approximately 100 microns. When the applied voltage to the alginate solution was increased to 12 kV, at a distance between the needle tip and collecting solution of 4.8 cm, the average bead diameter decreased to 340 microns. Keeping the applied potential constant at 12 kV, but reducing the electrode distance to 2.5 cm, resulted in only a slightly smaller bead size. The relationship between the applied voltage, alginate concentration, and droplet diameter was also investigated (Figures 4B and 4C). When the alginate concentration was decreased from 1.5 to 0.8% the average bead diameter decreased from 10 to 20%. The standard deviation also decreased at the lower polymer concentration due to a more uniform bead size distribution.

For example, at an applied voltage of 5 kV, the mean bead diameter decreased from 440 to 380 microns with standard deviations of 200 and 80 microns for microbeads prepared with alginate concentrations of 1.5 and 0.8%, respectively.

While the alginate concentration was not found to be significant, bead diameter could be readily controlled by needle size and applied voltage (Figures 4B and 4C). For example, at an applied voltage of 4 kV, the mean bead diameter was reduced by a factor of 3 from approximately 1,700 to 600 pm when the needle size was reduced from 22 to 26 gauge. In the case of the 26-gauge needle, as the voltage increased above 6 kV resulted in formation of microbeads with bimodal size distribution with the large fraction of 50 microns in diameter which was not favorable as described previously [9].

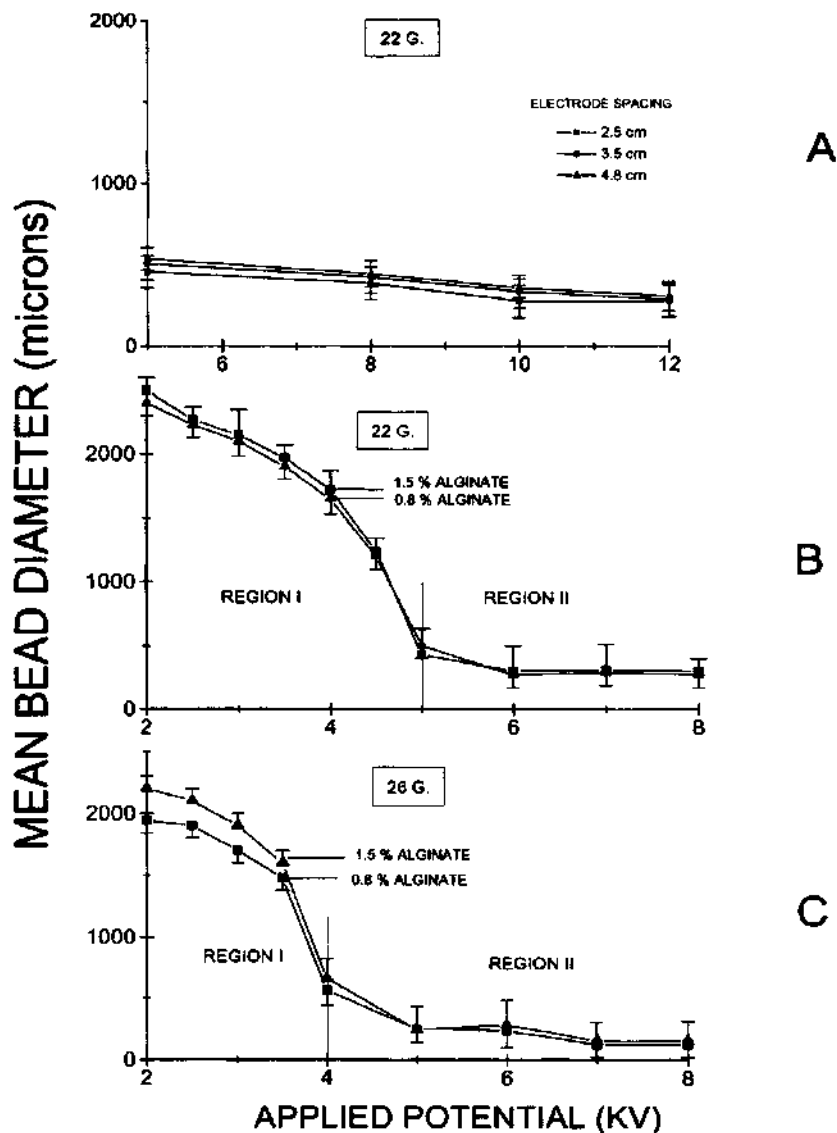


**Figure 4** Effect on microbeads size: A) applied potential and electrode spacing; B) alginate concentration; and C) small needle size with the positively charged needle setup [6] (22-gauge needle was used in A) and B) and a 26-gauge needle in C))



To assess the effect of an electrostatic field on cell viability, an insect cells suspension was extruded using the electrostatic droplet generator. No detectable change in cell viability was observed after extrusion. The initial cell density,  $4 \cdot 10^5$  cell/mL remained essentially unchanged at  $3.85 \cdot 10^5$  and  $3.78 \cdot 10^5$  immediately after passing through the generator needle at applied potential difference of 6 and 8 kV, respectively. Prolonged cultivation of these cells did not show any loss of cell density and viability.

## **CONCLUSION**

The formation of droplets with a charged needle arrangement in a defined electric field was examined. Reducing the electrode distance and increasing the applied voltage resulted in smaller beads, suggesting a strong influence of distance and applied potential on bead diameter. Further reduction in bead size was achieved by decreasing the needle size. Electrode spacing between the electrodes was important parameter for bead size with the positively charged needle arrangement. The microbeads produced with the electrostatic droplet generator operating optimally with an applied voltage of 6 kV were  $150 \pm 20$  microns in diameter, appearing as regular spheres of a uniform size. Electrostatic extrusion is an effective technique for producing micro beds of desired size. Finally, there was no detectable loss in viability after passing different types of cells through the electrostatic droplet generator. This is a promising result as it proves the technique amenable for cell immobilization. The liquid droplet electrostatic formation technique provides preparation of core/shell microbeads, where all the cells are immobilized deeply inside the matrix and no cell protrusion out of the bed/capsule occurs. Applied electric field is safe for the encapsulated cells and does not cause any cell dysfunctions. It is easy to use, fully controlled and reproducible technique.

Electrostatic droplet formation utilizes a special type of physical process taking advantage of electrostatic effects occurring in flowing conductive liquids after introduction of an electric field. When an electrostatic field is applied to the metal needle and an electric charge is induced in the liquid flowing out of the needle, the size of droplet detaching from the needle tip decreases as a function of applied electrostatic field. It has been shown that few parameters affect microbeads size: applied voltage, electrode geometry, needle size, polarity arrangement and polymer concentration. The electrostatic droplet formation is one of the most precise methods, which enables one to produce spherical and uniform particles ranging from 100 up to 1000 microns [10].

Low efficiency of electrostatic process can be significantly improved by multiplication of the nozzles, without any loss of the microbeads quality. The electrostatic technique using an impulse voltage droplet generator seems to be a simple and very useful method of cells encapsulation.

The development of potential industrial applications requires considering the optimization of these processes in terms of costs and environmental impacts. Both aspects are closely related because an environmental-friendly technology is generally more efficient and less costly at medium and long term.

## ACKNOWLEDGEMENT

The authors are grateful to this research which was supported by the Science Fund of the Republic of Serbia, #GRANT No 7751519, MultiPromis.

## REFERENCES

- [1] Lević S., Nedović V., Bugarski B. (Editors), Encapsulation in food processing and fermentation, CRC Press Taylor&Francis Group, Boca Raton, USA (2022), p.368, ISBN: 978-0-367-25831-3.
- [2] Đorđević V., Balanč B., Belščak-Cvitanović A., *et al.*, Food Eng. Rev. 7 (2015) 452–490.
- [3] Nedovic V., Kalusevic A., Manojlovic V., *et al.*, Procedia Food Sci. 1 (2011) 1806–1815.
- [4] Bugarski B., Li Q., Goosen M.F.A., *et al.*, AIChE J. 40 (1994) 1026–1031.
- [5] Nedović V.A., Obradović B., Poncelet D., *et al.*, Landbauforsch. Volkenrode Vol b (2002) 11–17.
- [6] Poncelet D., Neufeld R.J., Goosen M.F.A, *et al.*, AIChE J. 45 (1999) 2018–2023.
- [7] Poncelet D., Bugarski B., Amsdem B.G., *et al.*, Appl. Microbiol. Biotechnol. 42 (1994) 251–255.
- [8] Ken Giap L., Soh Fong L., J. Appl. Sci. Process Eng. 1 (2014) 9–26.
- [9] Marison I.W., J. Microencapsulation 28 (2011) 669–688.
- [10] Bošković S. and Bugarski B. Two-phase electro-magneto-fluid dynamics model and its computational fluid dynamics implementation. Physics of Fluids 36, (2024), Available on the following link: <https://doi.org/10.1063/5.0190651>.



## HEAT TREATMENT OF IRON-ADSORBED FUNCTIONALIZED NANOCELLULOSE FIBERS IN ORDER TO SYNTHESIZE HYBRID INORGANIC-CARBON MATERIAL

Anupama Ghosh<sup>1\*</sup>, Mariana Rodrigues Del Grande<sup>2</sup>, Lucas Tonette Teixeira<sup>1</sup>,  
Sonia Letichevsky<sup>1</sup>, Carlos Alberto Senna<sup>2</sup>, Mario Dayvid Carbajal Ccoyllo<sup>1</sup>,  
João Felipe Chaves e Silva<sup>2</sup>, Victor Carôzo Gois de Oliveira<sup>2</sup>,  
Rogério Navarro Correia de Siqueira<sup>1</sup>

<sup>1</sup>Chemical and Material Engineering Department, Pontifical Catholic University of Rio de Janeiro, Rua Marquês de São Vicente, 225, Gávea, Rio de Janeiro, RJ 22451-900 (Post box: 38097), BRASIL

<sup>2</sup>Physics Department, Pontifical Catholic University of Rio de Janeiro, Rua Marquês de São Vicente, 225, Gávea, Rio de Janeiro, RJ 22451-900 (Post box: 38097), BRASIL

\*anupama@puc-rio.br

### Abstract

*In the light of waste management and sustainable synthesis, chemically modified and oxidized cellulose nanofibers (TCN), after iron ion adsorption from aqueous solution, was thermally treated at 500°C, 600°C and 750°C under inert atmosphere to generate hybrid inorganic-carbonaceous nanohybrids, named TCN@Fe 500°C, TCN@Fe 600°C and TCN@Fe 750°C, respectively. These nanocomposites were characterized by X-ray and electron diffraction (XRD and ED), Raman spectroscopy, scanning and transmission electron microscopy (SEM and TEM) and Energy Dispersive Spectroscopy (EDS). All of these samples showed hybrid structure with mixed iron oxide (hematite and magnetite) particles dispersed in the amorphous carbon matrix. However, with increasing temperature, both the inorganic and carbon phase shows substantial changes, especially in hematite/magnetite ratio in the inorganic phase and crystallinity as well as chemical composition (oxygen/carbon ratio) of the carbonaceous phase. Also, with temperature, the dispersion of the iron oxide nanoparticle in the carbonaceous matrix becomes uniform whereas HRTEM analysis of the sample TCN@Fe 750°C shows the average diameter of the iron oxide nanoparticle to be of 6.26 nm, making this material a true inorganic-carbonaceous nanohybrid with possibility of various applications, mainly as an electrode material for supercapacitor application.*

**Keywords:** inorganic-carbonaceous hybrid material, cellulose nanofiber, iron oxide nanoparticle, amorphous carbon matrix, electron microscopy.

### INTRODUCTION

In the mission of mitigation of environmental damage as well as solving the increasing global demand of renewable energy, advanced functional carbon materials, obtained from renewable sources, like biomass, has drawn enormous attention not only because of their rich chemistry and interesting surface properties [1], which makes them susceptible towards further modification and functionalization, opening up the possibility of anchoring other functional systems, thus leading to a multifunctional hybrid material, targeted to various

energy and environment-related applications [2]. Ever-increasing demand for environment-friendly, high-performance and renewable energy storage devices gave rise to supercapacitors, which is an electrical energy storage device with high specific capacitance, long life cycle and high-power density [3]. It can store energy either through formation of an electrical double layer (mainly in case of electrodes based on carbon nanostructures) [4] or through redox reactions taking place on the surface of the electrode (electrodes based on transition metal oxides) [5]. Asymmetric or hybrid supercapacitor can be prepared by combining biomass-derived carbon material with transition metal oxide nanostructures, where the charge can be stored both by Faradaic (redox reactions) and non-Faradaic processes (electrochemical double layer formation) showing a better capacitance as well as improved charge-discharge process [6]. For example, Glucose or other cellulose-rich biomass-derived carbon material, after Fe<sub>3</sub>O<sub>4</sub> nanoparticle loading, showed enhanced specific capacitance [7]. Cellulose is certainly among the most abundant naturally occurring polymers in the planet, extracted from natural sources like plants and have variable applications [8]. It is possible to obtain nanocellulose fibres from cellulose and possible to apply adequate surface functionalization so that the resultant material can be a very good adsorbent of metal ions from their aqueous solutions [9]. After the completion of such an adsorption process, the precipitate (metal ion adsorbed onto functionalized nanocellulose fibers) can be filtered and it can be submitted to heat treatment in a tubular furnace under different atmosphere varying temperature and time of the thermal treatments [10]. Therefore, in the current work,  $\alpha$ -cellulose had been treated chemically in order to generate oxidized cellulose nanofibers, it was allowed to adsorb high quantity of iron from aqueous solution, and then washed and dried in order to generate iron loaded oxidized cellulose nanofibers. Then heat treatment was applied to this metal-carbon precursor in a tubular furnace under argon atmosphere, varying the temperature. After the calcination, resultant hybrid materials (metal/metal oxide nanoparticle embedded in a carbonaceous matrix) were characterized through X-ray and electron diffraction (XRD and ED) to identify the phases, Raman spectroscopy to understand the electronic structure, scanning and transmission electron microscopy (SEM and TEM) to understand the morphology and Energy Dispersive Spectroscopy (EDS) for elemental analysis. These materials can be a good candidate for supercapacitor application as it contains nanoparticles of metal/metal oxides of varying composition and stoichiometry, in a porous carbon matrix, thereby allowing both Faradaic and non-Faradaic processes in the electrochemical evaluation.

## **MATERIALS AND METHODS**

### **Synthesis of hybrid inorganic-carbon material**

All the chemicals were purchased from Sigma-aldrich. To prepare the functionalized cellulose nanofiber (TCN), 1 g of  $\alpha$ -cellulose is added to 100 mL of deionized water, along with 100 mg of NaBr, 6.1 mL of NaClO and 16 mg of N-oxy1-2,2,6,6- tetramethylpiperidine (TEMPO) as catalyst in a beaker and stirred for 150 min maintaining the pH at 10, followed by washing and centrifuging. 1 g of TCN is suspended in 100 mL of FeSO<sub>4</sub> solution in an Erlenmeyer flask and stirred for 120 min. TCN has a high capacity of iron adsorption ( $q_{eq}=5677$  mg/g at room temperature) and the resultant material, named TCN@Fe is washed

and centrifuged. TCN@Fe was submitted to heat treatment in a tubular furnace under inert atmosphere (argon, 100 sccm) at temperatures 500°C, 600°C and 750°C for 2 hours in order to generate samples named as TCN@Fe 500°C, TCN@Fe 600°C and TCN@Fe 750°C respectively.

### **Characterization of materials**

PXRD was done by a Bruker D8 Discover (Cu source, Ni filter, Lynxeye detector) in the  $2\theta$  range of  $5^\circ$  to  $95^\circ$ ,  $0.02^\circ$  step size. The Rietveld refinement method was performed by Topas 5.0 program. Raman spectra were recorded by Xplora Horiba, with 532 nm laser, in the range of  $200\text{--}4000\text{ cm}^{-1}$  and gratings of 1200 and 1800 grooves  $\text{mm}^{-1}$ . The laser was focused with a 100x magnification objective lens. The SEM images were obtained using a SCIOS 2, the samples were fixed on copper tape attached to aluminium sample holders. For elemental mapping, energy dispersive X-ray spectroscopy (EDS) was recorded using X-ray detector and Pathfinder software version 2.11. TEM images were obtained with a JEOL 2100F microscope, the samples were dispersed in isopropyl alcohol and drop-casted onto carbon coated 400 mesh copper grids.

## **RESULTS AND DISCUSSION**

Figures 1 (a–c) show the XRD patterns of the pyrolyzed TCN@Fe samples and Table 1 displays the Rietveld refinement results. The inorganic, crystalline phase of iron oxide presented hematite ( $\text{Fe}_2\text{O}_3$ ) and magnetite ( $\text{Fe}_3\text{O}_4$ ) crystalline phases that were fitted using ICSD (Inorganic Crystal Structure Database) CIF # 82902 and 85806, respectively. It can be noted that there is a modification in the hematite/magnetite composition that varies with the pyrolysis temperature, ensuring the presence of both  $\text{Fe}^{+2}$  and  $\text{Fe}^{+3}$  ions. Both hematite and magnetite phases had mean crystallite sizes that increased with temperature raising that is expected due to a sintering process. Also, the samples pyrolyzed at relatively higher temperature (TCN@Fe 750°C, Figure 1c) showed presence of amorphous material detected by a large halo from  $2\theta = 5^\circ$  to  $15^\circ$  and a very broad one over the other  $2\theta$  range. This amorphous material is probably the partially graphitized carbonaceous phase, named as turbostatic carbon [11]. To understand better the nature of the carbonaceous phase of the sample TCN@Fe 750°C, spatial Raman spectroscopy was performed. A representative optical microscopic image of the sample (inset of Figure 1d) shows a clear color contrast: the black part is mainly due to the carbonaceous part, the reddish hue is due to the inorganic hematite phase, found from XRD measurements. Raman measurements were done intentionally on these two spots of separate color contrast (the black part, marked with a white circle and the red part, marked with a yellow circle) and are shown in Figures 1d and 1e respectively. The carbonaceous phase (Figure 1d) shows characteristic first order (one-phonon process) and second order (two phonon process) Raman bands in the range of  $200\text{--}4000\text{ cm}^{-1}$  [12]. The first order region ( $1000\text{--}2000\text{ cm}^{-1}$ ) can be deconvoluted using a mixed Lorentzian-Gaussian function (Voigt) in six bands centered around  $1170\text{ cm}^{-1}$ ,  $1271\text{ cm}^{-1}$ ,  $1334\text{ cm}^{-1}$ ,  $1471\text{ cm}^{-1}$ ,  $1575\text{ cm}^{-1}$  and  $1611\text{ cm}^{-1}$ , which can be designated as  $D''$ , A1, D, A2, G and  $D'$  bands respectively. The  $D''$ , D, G and  $D'$  are related to graphitic carbon, whereas A1 and A2 are two broad peaks relating to the amorphous carbon present [13]. In the second order region, the peaks around  $2449\text{ cm}^{-1}$ ,  $2682\text{ cm}^{-1}$ ,  $2922\text{ cm}^{-1}$  and  $3213\text{ cm}^{-1}$  can be designated as  $D+D''$ ,

2D, D+G and 2D' bands respectively of graphitic carbon. The typical spectra of inorganic phase, obtained in the range of 250–2800  $\text{cm}^{-1}$ , shown in the Figure 1e. The principal peaks were registered at around 284  $\text{cm}^{-1}$ , 403  $\text{cm}^{-1}$ , 494  $\text{cm}^{-1}$ , 604  $\text{cm}^{-1}$ , 655  $\text{cm}^{-1}$ , 804  $\text{cm}^{-1}$ , 1033  $\text{cm}^{-1}$ , 1086  $\text{cm}^{-1}$  and 1309  $\text{cm}^{-1}$ . The bands centered around 494  $\text{cm}^{-1}$  can be assigned to the  $A_{1g}$  mode and the bands centered around 284, 403 and 604  $\text{cm}^{-1}$  can be assigned as the  $E_g$  modes of the hematite phase [14]. Raman spectra were collected from other parts of the sample in the range of 200–1700  $\text{cm}^{-1}$ , where all the signature Raman bands corresponding to the iron oxide phase as well as the first order spectra of carbonaceous phase can be seen, although the relative intensity of bands originated from carbonaceous and inorganic phases may differ depending on the composition of the carbonaceous/inorganic phase in that spatial location. Such a typical spectra is shown in Figure 1f), which gives an idea of the hybrid nature of the sample.

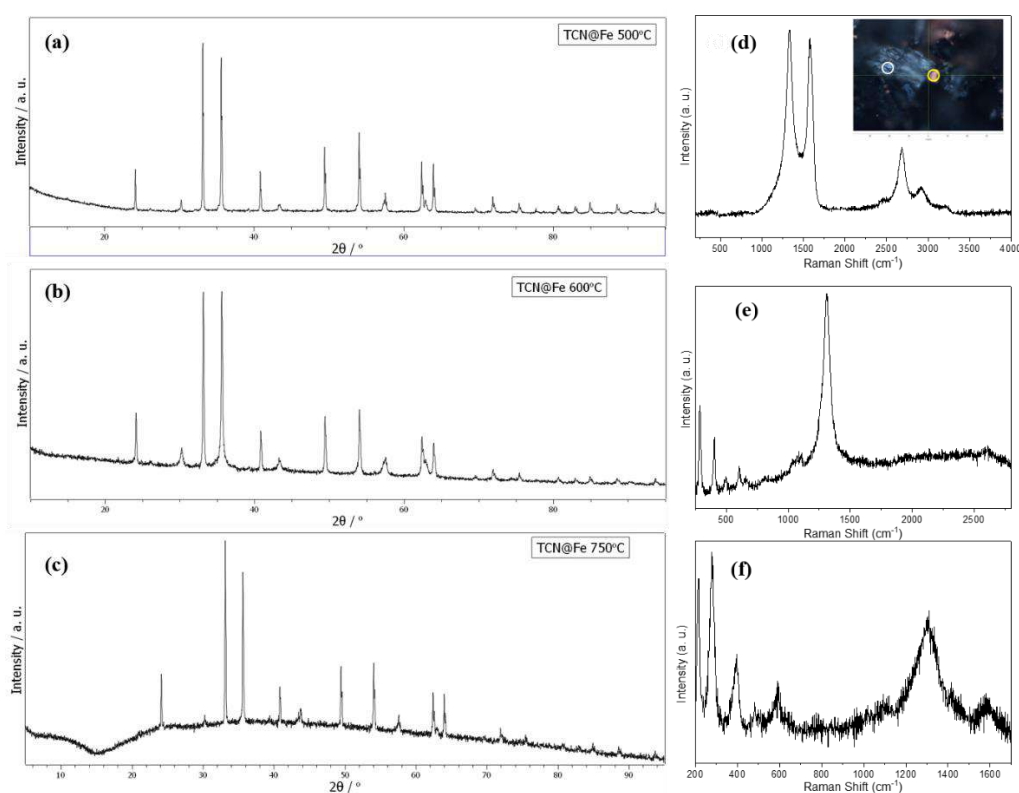


**Figure 1** PXRD profile of a) TCN@Fe 500°C; b) TCN@Fe 600°C; c) TCN@Fe 750°C; Raman spectra of TCN@Fe 750°C, in d) only carbonaceous; e) only inorganic; f) mixed phase, inset showing an optical microscopic image of the sample

**Table 1** Crystalline phases, mean crystallite size obtained by the Rietveld refinement of PXRD data and elemental analysis from EDS data

Sample	% phase		Crystallite size (nm)		Elemental composition		
	Hematite	Magnetite	Hematite	Magnetite	C (At%)	O (At%)	Fe (At%)
TCN@Fe-500	84.5	15.5	244	44	62.46	27.38	9.35
TCN@Fe-600	71.2	28.8	98	12	65.33	26.44	7.35
TCN@Fe-750	90.2	9.8	159	36	82.84	11.70	4.71



To look into the morphological features of these samples SEM was performed and are illustrated in Figure 2.

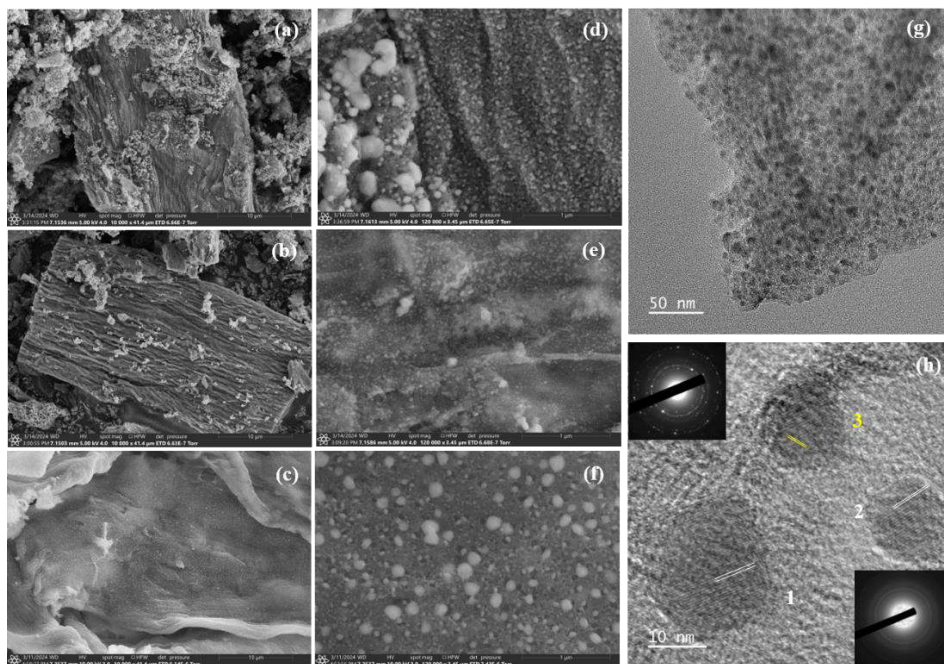


**Figure 2** Low-magnification (10000x) SEM micrograph of a) TCN@Fe 500°C; b) TCN@Fe 600°C; c) TCN@Fe 750°C; high-magnification (120000x) SEM micrograph of d) TCN@Fe 500°C; e) TCN@Fe 600°C; f) TCN@Fe 750°C; g) TEM; h) HRTEM of TCN@Fe 750°C

All the samples show the fibrous morphology of the carbonaceous matrix, corroborating with the precursor material as cellulose nanofibers. The inorganic phase, iron oxide particles, are distributed over the whole carbonaceous matrix. However, with increasing pyrolysis temperature, the aggregation of the particles decreases and the dispersity increases. For example, the sample TCN@Fe 750°C shows a very uniform distribution of iron oxide nanoparticle with the diameter of most the spherical nanoparticle ranging from 3–8 nm, with some larger nanoparticles, with diameter 10–20 nm. Elemental analysis was performed by EDS and was presented in the Table 1. It showed that with increasing the pyrolysis temperature, the % C content increases and the % O attributing to the fact that with higher temperature, more oxygen functional groups are volatilized from the cellulose structure, exposing more the carbon skeleton. Also, the % Fe content decreased with increasing the temperature because of a more uniform distribution of these nanoparticles in the carbon matrix as seen from the SEM images. TEM was performed with the sample TCN@Fe-750°C, TEM and shown in Figure 2g. A diameter distribution of almost 60 nanoparticles were done on this sample, which revealed the average diameter of these nanoparticles is 6.26 nm. High resolution TEM was performed in the selected region with some nanoparticles in the matrix and shown in the Figure 2h. The lattice planes were clearly observed in the nanoparticles, whereas, even with higher resolution, the matrix carbonaceous phase continued to be seen as amorphous, corroborating with the turbostratic nature of the carbon matrix found in XRD results. The interplanar distance between the crystal planes were measured and shown in the figure, as consecutive pair of parallel straight lines of white and yellow color. The

nanoparticles, #1 and 2 showed interplanar distance of around 0.37 nm (shown as white pair of parallel lines), which can be designated as the (012) plane whereas nanoparticle #3, shows interplanar distance of around 0.27 nm (shown as yellow pair of parallel lines), which can be designated as (104) plane of hematite lattice calculated from Bragg's law [15]. This data corroborates with XRD data presented before. The inset (above) of the Figure 2h shows a selected area electron diffraction (SAED) pattern of the region with inorganic nanoparticles, which showed distinct polycrystalline nature of this phase, whereas, the inset (below) shows the SAED pattern of the region with matrix, without nanoparticles, which clearly shows an amorphous nature.

## CONCLUSION

In this work, iron-adsorbed chemically oxidized nanocellulose fibres were pyrolyzed in different temperatures under argon atmosphere to generate iron oxide-carbon nanocomposites and characterized. XRD recognized crystalline inorganic phase is composed of hematite and magnetite phase, and an amorphous carbonaceous phase. Raman spectra shows signature of the hematite phase as well as turbostratic carbon. Microscopy revealed the sheet like morphology of the carbonaceous phase with hematite nanoparticles with a mean diameter of 6.26 nm distributed in the matrix. The synthesis scheme described in this work has successfully integrated more than one application related to the environment and energy with the possibility of changing reaction parameters in order to bring in subtle changes in the carbon skeleton, as well as structure and electronic behaviours of the inorganic phases.

## REFERENCES

- [1] Lima P.N.S., Ghosh A., Nascimento A., *et al*, J. Phys. Chem. Solids, 176 (2023) 111188.
- [2] Vieira L.H.S., Sabino C.M.S., Júnior F.H.S., *et al*, Carbon 161 (2020) 758.
- [3] Sharma K., Arora A., Tripathi S.K., J. Energy Storage, 21 (2019) 801–825.
- [4] Ghosh A., Razzino C.A., Dasgupta A., *et al*, Carbon 145 (2019) 175.
- [5] Mensah-Darkwa K., Zequine C., Kahol P.K., Sustainability 11 (2019) 414.
- [6] Zhi M., Xiang C., Li J., Nanoscale 5 (2013) 72–88.
- [7] Ozpinar P., Dogan C. Demiral H., *et al*, Renew. Energy 189 (2022) 535–548.
- [8] Eichhorn S., Dufresne A., Aranguren M., *et al*, J. Mater. Sci. 45 (2010) 1–33.
- [9] Teixeira L., Braz W., Siqueira R., *et al*, JMST 15 (2021) 434–447.
- [10] Teixeira L., Lima S., Rosado T., *et al*, Int. J. Mol. Sci. 24 (2023) 1–18.
- [11] Toth P., Carbon 178 (2021) 688–707.
- [12] Beyssac O., Lanzaeriemu M., Notes in Mineralogy 12 (2012) 415–454.
- [13] Ghosh A., Santos A., Cunha J., *et al*, Vib. Spectrosc. 98 (2018) 111.
- [14] Ma J., Zhu Z., Chen B., *et al*, J. Mater. Chem. A. 1 (2013) 4662–4666.
- [15] Wahab R., Khan F., Al-Khedhairya A., RSC Adv. 8 (2018) 24750–24759.





## ENVIRONMENTAL PROTECTION: WHY IS EUROPE'S AIR (MOSTLY) SO CLEAN?

Alena Bartonova<sup>1\*</sup>

<sup>1</sup>NILU, Instituttveien 18, N-2007 Kjeller, NORWAY

\*[aba@nilu.no](mailto:aba@nilu.no)

### Abstract

*Air pollution is one of the leading causes of noncommunicable disease globally [1], and in Europe [2]. The London Smog of 1952 [3] was a major wake-up call, but European legislation as we know it today started to develop only in the late 1950's [4] with the recognition of acid rain and the transboundary pollution contributing to it. European legislation developed in collaboration with the UN ECE Convention on Long Range Transboundary Air Pollution (CLRTAP) of 1977 [5]. The approach to air pollution is three-pronged [6]: through limiting emissions to air on national and source level, by setting limit values for air pollutants, and through product regulations (such as, eco-stoves). This approach has been supported by knowledge base development: monitoring and measurement systems and technologies are constantly developing, effects on man-related and natural systems are better understood, and elaborate governance systems are put in place. This has been a successful effort [7], even if at times, high pollution levels still occur – both due to man-made and natural causes. Emissions of most criteria pollutants decreased, as has the exposure of the European population. Future developments in legislation will reflect the significant new knowledge on the nature of air pollution, on health effects and on benefits of pollution-free environments [8,9]. This will lead to lowering the limit values for air pollution. Recognizing the efforts on climate change mitigation, more emphasis will likely be given to co-benefits of mitigation measures for air pollution and for climate, and to the complex interrelations between the two issues.*

**Keywords:** air emissions, air pollution, health, governance, mitigation.

### REFERENCES

- [1] GBD 2021 Risk Factors Collaborators, *Lancet* 2024; 403: 2162–203, DOI: [https://doi.org/10.1016/S0140-6736\(24\)00933-4](https://doi.org/10.1016/S0140-6736(24)00933-4).
- [2] Soares J., Plass D., Kienzler S., *et al.*, (2023). Health Risk Assessment of Air Pollution: assessing the environmental burden of disease in Europe in 2021 (Eionet Report – ETC HE 2023/7). European Topic Centre on Human Health and the Environment, *Available on the following link:* <https://www.eionet.europa.eu/etcs/etc-he/products/etc-he-products/etc-he-reports/etc-he-report-2023-7-health-risk-assessment-of-air-pollution-assessing-the-environmental-burden-of-disease-in-europe-in-2021>.
- [3] Bell M.L., Davis D.L., Fletcher T. (2008). A Retrospective Assessment of Mortality from the London Smog Episode of 1952: The Role of Influenza and Pollution. In: Marzluff, J.M., *et al.* *Urban Ecology*. Springer, Boston, MA. *Available on the following link:* [https://doi.org/10.1007/978-0-387-73412-5\\_15](https://doi.org/10.1007/978-0-387-73412-5_15)

- [4] Brooks H., Cooper C.L., (2013) Science for public policy, pp. 164–195. Elsevier. ISBN 1483286606, 9781483286600.
- [5] United Nations Convention on long-range transboundary air pollution. Available on the following link:  
[https://treaties.un.org/Pages/ViewDetails.aspx?src=TREATY&mtdsg\\_no=XXVII-1&chapter=27&clang=\\_en](https://treaties.un.org/Pages/ViewDetails.aspx?src=TREATY&mtdsg_no=XXVII-1&chapter=27&clang=_en).
- [6] EEA (2018) Air quality in Europe -2018 report. Figure 1.1. *Available on the following link:* <https://www.eea.europa.eu/publications/air-quality-in-europe-2018>.
- [7] EEA (2024) Europe's air quality status 2024. EEA briefing. *Available on the following link:* <https://www.eea.europa.eu/publications/europes-air-quality-status-2024>.
- [8] European Commission (2020) Fitness Check of the EU ambient air quality directives. *Available on the following link:* [https://commission.europa.eu/publications/fitness-check-eu-ambient-air-quality-directives\\_en](https://commission.europa.eu/publications/fitness-check-eu-ambient-air-quality-directives_en).
- [9] European Commisison (2022) Proposal for the revision of the Amnient Air Quality Directives. *Available on the following link:* [https://environment.ec.europa.eu/publications/revision-eu-ambient-air-quality-legislation\\_en](https://environment.ec.europa.eu/publications/revision-eu-ambient-air-quality-legislation_en).

**Invited lectures**



## APPLICATION OF NATURAL ZEOLITE – CLINOPTILOLITE IN WATER TREATMENT BY ADSORPTION AND PHOTOCATALYSIS

Nevenka Rajić<sup>1\*</sup>, Jelena Pavlović<sup>2</sup>

<sup>1</sup>Faculty of Ecology and Environmental Protection, University Union – Nikola Tesla,  
Cara Dušana 62–64, 11158 Belgrade, SERBIA

<sup>2</sup>Institute of Soil Science, Teodora Drajzera 7, 11000 Belgrade, SERBIA

\*nrajic@unionnikolatesla.edu.rs

### Abstract

*The adsorptive and photocatalytic performance of the Serbian clinoptilolite-rich zeolitic tuff (ZT) is reported. Mg<sup>2+</sup>, Pb<sup>2+</sup>, Mn<sup>2+</sup>, Ni<sup>2+</sup>, Cu<sup>2+</sup>, and Zn<sup>2+</sup> adsorption studies, as well as kinetics and thermodynamics, were conducted by ZT under carefully controlled temperature, pH, grain size, and solid/liquid weight ratio conditions. ZT has a good adsorption capacity for the metal cations under study. By converting ZT to Fe-containing ZT (Fe-ZT and Fe<sub>3</sub>O<sub>4</sub>-ZT), the ZT becomes effective at eliminating phosphate and nitrate ions, which are typically found in surface and groundwater, as well as the antibiotic ciprofloxacin, which is one of the most used antibiotics and is present in wastewater as an organic micropollutant. It was also found that ZT exhibits photocatalytic activity in the decomposition of common organic dyes such as methylene blue (MB). The photocatalytic activity was ascribed to trace amounts of the Fe species as a minor satellite phase in the tuff. Sn-containing ZT (Sn-ZT) also shows catalytic activity in the MB degradation. The ZT decomposes MB in an eco-friendly manner at room temperature, atmospheric pressure, and visible light irradiation.*

**Keywords:** zeolite, clinoptilolite, toxic metal cations, adsorption, photocatalysis.

### INTRODUCTION

Zeolites are crystalline porous minerals with a three-dimensional lattice structure composed of a network of corner-sharing tetrahedra, TO<sub>4</sub> (T=Si, Al), which have Si and Al atoms in the center of the tetrahedra. Because the crystal structure contains geometrically precise structured channels and cages, only species of the appropriate size can diffuse through the lattice. Zeolites can, therefore, be used in ion exchange, adsorption, separation procedures, and molecular sieves. Zeolites can also be employed as heterogeneous catalysts by being transformed into strong solid acids [1,2].

Clinoptilolite is the most prevalent kind of natural zeolite. With a pore diameter of up to 0.7 nm, eight- and ten-member ring channels show an open reticular structure readily accessible [3,4]. Two channels (A and B) are parallel to the *c*-axis. The ten-membered rings in the A channels have a tightly compressed aperture of 0.31 x 0.75 nm, while the eight-membered rings in the B channels have an aperture of 0.36 x 0.46 nm. The C channels comprise eight-membered rings parallel to the *a*-axis with an aperture of 0.28 x 0.47 nm. Water molecules occupy extra-framework sites specific to crystallography, as do

exchangeable alkali and alkali earth cations. Due to differences in the Si/Al ratio, clinoptilolite samples from various regions have varying ion-exchange capacities.

We have studied the adsorption and photocatalytic properties of clinoptilolite from the Slanci deposit in Serbia. The clinoptilolite's ability to exchange cations with different heavy metal cations frequently present in wastewater and its ability to adsorb certain anions and exhibit photocatalytic activity have all been thoroughly examined.

## **MATERIALS AND METHODS**

Zeolitic tuff (ZT) from the Serbian deposit Slanci (Veliko selo, Belgrade) was used in experiments. Clinoptilolite content determined by a semiquantitative X-ray diffraction analysis (using the Rietveld refinement method Topas-Academic v.4) was 80 wt.%, feldspar – 16 wt.% and quartz – 4 wt.%. The cation exchange capacity (CEC), measured by standard procedure [5] was 162 mmol M<sup>+</sup>/100 g. For all the experiments, the grain size was chosen in the range 0.063–0.125 mm, for which preliminary tests proved that it is an optimal range for experimental work and achieving high capacity [6,7]. Before the experiments, the samples were sieved, washed with deionized water to remove impurities, and dried in an oven at 105°C overnight to a constant mass. All samples were converted into Na-rich form (Na-ZT) by treatment with 2 mol dm<sup>-3</sup> of NaCl for 24 h at 70°C to achieve the best possible exchange capacity.

### **Conversion of ZT into Fe-ZT, Fe<sub>3</sub>O<sub>4</sub>-ZT, and Sn-ZT**

The ZT was converted into Fe-containing ZT (Fe-ZT) using a two-step procedure: 1) treatment of ZT with a water solution of Fe(NO<sub>3</sub>)<sub>3</sub> in an acetate buffer (pH=3.6) followed by the addition of 0.1M NaOH until pH~7, and 2) heating of the product at 80°C until a constant mass. The ZT was also converted to Fe<sub>3</sub>O<sub>4</sub>-ZT by alkaline co-precipitation of FeCl<sub>3</sub>·6H<sub>2</sub>O and FeSO<sub>4</sub> water solution in a molar ratio of 2:1, and to avoid the formation of non-magnetic iron oxide particles, the synthesis was performed under N<sub>2</sub> atmosphere. The obtained product was heated at 80°C until a constant mass. Conversion of ZT into Sn-ZT included: 1) treatment of ZT with 1 mol dm<sup>-3</sup> HCl at 100°C for 4 h followed by treatment with 0.2 mol dm<sup>-3</sup> NH<sub>4</sub>OH at 65°C for 0.5 h to obtain H-form of clinoptilolite (H-ZT), and 2) treatment of H-ZT with the ethanolic solution of SnCl<sub>2</sub> (8.8 mmol dm<sup>-3</sup>) and NH<sub>4</sub>OH followed by calcination at 400°C for 2h.

Fe-ZT surface was examined by transmission electron microscopy (TEM) by using a 200-kV TEM microscope (JEM-2100 UHR, Jeol Inc., Tokyo, Japan) equipped with an ultra-high-resolution, objective-lens pole-piece having a point-to-point resolution of 0.19 nm. Electron diffraction patterns (EDPs) and TEM images were recorded by 2k charge-coupled device camera using Digital Micrograph™ (Gatan Inc., USA) as a user interface. Elemental compositions of samples were obtained by a Carl Zeiss Supra™ 3VP (Zeiss, Jena, Germany) field-emission gun scanning electron microscope (FEG-SEM) equipped with an EDS detector (Oxford Analysis) with the INCA Energy system for quantification of elements. The specific surface area of samples was determined by the nitrogen sorption method using an automatic sorption analyzer (Micrometrics ASAP 2020, Norcross, GA, USA).

### Adsorption studies of M(II) ions onto ZT

The M(II) sorption (M – Mg, Mn, Ni, Cu, Zn, Pb) was studied at 25–55°C. The suspensions of Na-ZT and the chosen M(II) solution (100–400 mg M dm<sup>-3</sup>) were shaken at about 100 rpm for 24 h in a thermostated water bath (Memmert WPE 45, Germany). M(II) solutions were prepared by dissolving M(NO<sub>3</sub>)<sub>2</sub> (Fluka, p.a.) in deionized water. The M(II) concentrations were measured by AAS (Varian SpectrAA 55B atomic absorption spectrophotometer, SpectraLab inc., Markham, ON, Canada).

### Adsorption studies of nitrate, phosphate, and ciprofloxacin onto Fe-ZT and Fe<sub>3</sub>O<sub>4</sub>-ZT

Solutions of KNO<sub>3</sub> and KH<sub>2</sub>PO<sub>4</sub> (1–6 mmol dm<sup>-3</sup>) were used for nitrate and phosphate adsorption. Adsorption of ciprofloxacin (CIP) was studied for the initial CIP concentrations from 0.04 to 0.2 mmol dm<sup>-3</sup>. The adsorption experiments were carried out at pH~5, for which CIP is present as a cation. KNO<sub>3</sub>, KH<sub>2</sub>PO<sub>4</sub>, and CIP (supplied by Aldrich) were dissolved in deionized water. The concentration of adsorbates was measured using a UV-Vis spectrometer (Lambda 365 spectrophotometer, Perkin Elmer Inc., Waltham, MA, USA).

All adsorption experiments were carried out by a batch method under controlled conditions: the thermostated bath temperature was maintained constant to within ± 0.1°C, the zeolite samples were weighted to four-digit accuracy, and the solution concentrations were determined with four-digit accuracy. All chemicals used were analytical-grade reagents. The adsorbate concentration was measured in filtrate after solid/liquid separation.

The concentration of adsorbate on adsorbents was calculated using the following formula:

$$q_t = \frac{C_0 - C_i}{m} \cdot V \quad (1)$$

where  $C_0$  and  $C_i$  are concentrations of the adsorbate in aqueous solution (mg dm<sup>-3</sup>) before and after the contact with ZT (Fe-ZT or Fe<sub>3</sub>O<sub>4</sub>-ZT), respectively;  $V$  is the solution volume in dm<sup>3</sup>, and  $m$  is the mass of the ZT (Fe-ZT or Fe<sub>3</sub>O<sub>4</sub>-ZT) in g.

### Photocatalytic test

Photocatalytic tests were carried out using a batch reactor system equipped with a 50 cm<sup>3</sup> Pyrex glass cell and a circulating water jacket to keep the temperature constant at 25°C during the reaction (Figure 1).

Suspension contained water solution of MB ( $C_0 = 10$  mg dm<sup>-3</sup>) and ZT or Sn-ZT in the concentration of 0.2 g dm<sup>-3</sup> at different pH (pH = 3, 6, or 9), was continuously stirred by magnetic stirrer for 30 min to achieve an adsorption/desorption equilibrium and then irradiated for 300 min by using Osram Ultra Vitalux lamp/300 W, served as the visible light source and positioned 10 cm above the photocatalytic reactor. The concentration of MB was followed colorimetrically at  $\lambda=664$  nm by UV/VIS spectroscopy (Lambda 365 spectrophotometer, Perkin Elmer).

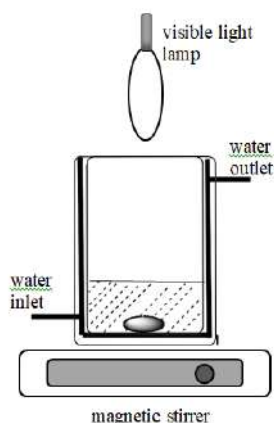


**Figure 1** The schematic presentation of the reactor system used in photocatalytic tests

## RESULTS AND DISCUSSION

Conversion to Fe-ZT, Fe<sub>3</sub>O<sub>4</sub>-ZT, and Sn-ZT resulted in the production of novel phases that covered the ZT surface. An EDS analysis revealed that there was a significant decrease in exchangeable cation content for Fe-ZT, Fe<sub>3</sub>O<sub>4</sub>-ZT, and Sn-ZT when compared to ZT and that the decrease in exchangeable cation content for Fe (as well as Sn) content was significantly greater than that for ZT. This indicates that 1) an ion exchange reaction happened, and 2) precipitation of the Fe (or Sn species) at the ZT surface occurred during the conversion of ZT to Fe-ZT/Fe<sub>3</sub>O<sub>4</sub>-ZT/Sn-ZT. The Fe content in Fe-ZT rose from 0.21 (ZT) to 18.1 wt.%, Fe<sub>3</sub>O<sub>4</sub>-ZT from 0.40 (ZT) to 5.63 wt.%, while the Sn content was 14.9 wt.%. Figure 2 depicts the Fe-ZT surface as a representative example of cover at the ZT surface.

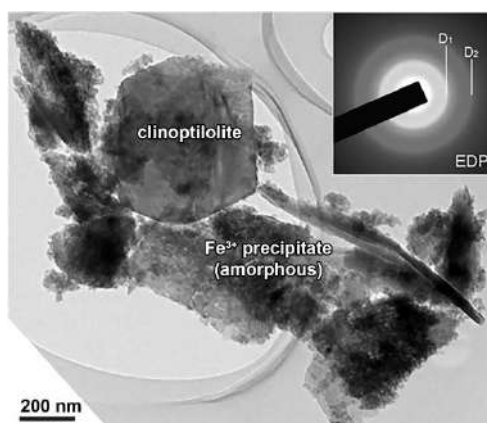


**Figure 2** TEM image of Fe-ZT: bright-field image of clinoptilolite sheets coated with a precipitate rich in Fe(III). The amorphous nature of the Fe(III) precipitate is confirmed by its electron diffraction pattern (EDP) in the upper right corner

Accumulation of the Fe- and Sn-containing precipitates increases the specific surface area of ZT from 28.6 to 140.3 m<sup>2</sup> g<sup>-1</sup> for Fe-ZT, to 45.2 m<sup>2</sup> g<sup>-1</sup> for Fe<sub>3</sub>O<sub>4</sub>-ZT and to 78.0 m<sup>2</sup> g<sup>-1</sup> for Sn-ZT. It seems likely that the increase in the specific surface can be attributed to forming a second porous system at the ZT surface. Powder XRD analysis showed that the conversion did not affect the crystallinity of ZT. TEM analysis showed amorphous Fe(III) precipitates on



Fe-ZT, and an abundant coverage of the ZT plates by rounded magnetite nanocrystals on Fe<sub>3</sub>O<sub>4</sub>-ZT, and X-ray photoelectron spectroscopy (XPS) exhibited the presence of SnO<sub>2</sub> on Sn-ZT. According to the XPS depth profiles, the Fe and Sn concentrations decrease from the samples' top to bottom.

Adsorption experiments showed that Na-ZT can capture the investigated cations from water media through an endothermic ion exchange reaction. Specifically, metal ions from an aqueous solution that come into contact with the Na-ZT replace Na<sup>+</sup> ions from the clinoptilolite lattice. Even though all the metal ions under study have hydrated radii that are noticeably larger than the clinoptilolite's lattice aperture, the ion exchange process does not seem to be restricted by intra-particle diffusion. One offered explanation is that the cations' coordination sphere changes as the reaction progresses [8]. Table 1 displays the Na-ZT's removal efficiency and ionic radii [9] of the removed cations.

**Table 1** Removal efficiency (%) of Na-ZT towards M(II) at the initial concentration of 1.5 mmol M(II) dm<sup>-3</sup> at 25°C

M(II)	Removal, %	Ionic radius, pm
Mg	60	66
Mn	47	82
Ni	15	70
Cu	84	73
Zn	50	74
Pb	100	119

The removal efficiency increases with temperature for all of the cations under study. Thus, when the temperature rose from 25 to 45°C, the removal efficiency towards Cu(II) increased by about 14%. Furthermore, the pseudo-second-order rate model provides the most accurate description of the cations' adsorption kinetics. However, only for Mn<sup>2+</sup> and Ni<sup>2+</sup> does the rate of adsorption increase with temperature, and only for Mn<sup>2+</sup> does the increase become statistically significant. This may be because the hydrolysis of metal ions affects the adsorption kinetics [10,11].

The adsorption kinetics for nitrate and phosphate anions agrees reasonably well with the Lagergren pseudo-second-order model. The maximum affinity for the phosphate ions Fe-ZT was found at pH~6.5. The <sup>31</sup>P NMR analysis, according to Kaplanec *et al.* [12], showed the intricacy of the phosphate adsorption mechanism, which consists of a more substantial covalent bonding between the phosphate ion and Fe(III) and also electrostatic interactions. The phosphate is bound as a bidentate ligand most of the time. Temperature increases the removal efficiency of both phosphate and nitrate ions. The Langmuir isotherm, which produces the Langmuir constant ( $R_L$ ) values in the range of 0–1, suggests favourable adsorption. As part of their adsorption mechanism, nitrate ions partially bind by ion exchange, replacing hydroxyl ions [13].

Adsorption of CIP onto Fe<sub>3</sub>O<sub>4</sub>-ZT is very fast [14]. Over 80% of the maximum adsorption capacity is reached within the first ten minutes. The Langmuir isotherm model explains the equilibrium adsorption data, while the Lagergren pseudo-second-order equation describes the



adsorption kinetics. The adsorption mechanism most likely involves strong electrostatic interactions between the cationic form of CIP and the negatively charged Fe<sub>3</sub>O<sub>4</sub>-ZT surface.

Sn-ZT showed a high photocatalytic activity in the degradation of methylene blue, which could mainly be ascribed to the presence of photocatalytically active SnO<sub>2</sub> at the surface of ZT [15]. However, the clinoptilolite lattice and SnO<sub>2</sub> particles work together synergistically. ZT's adsorption affinity for cationic organic dyes draws more molecules to the surface, which produces hydroxyl radicals that open up many active sites for the adsorption of intermediates. Moreover, the lattice prevents the SnO<sub>2</sub> particles from aggregating, which usually reduces their activity. Electron-hole recombination accompanying photocatalysis is possible because oxide particles are attached to specific crystallographic sites in the lattice.

ZT demonstrates remarkable photocatalytic activity in the degradation of MB as well [16]. The total degradation of MB is affected by pH, which peaks at pH=6 (70% for C<sub>0</sub>=10 mg MB dm<sup>-3</sup> for 300 min). The photodegradation process follows the Langmuir–Hinshelwood kinetic model. The entire dye degradation process is caused by the combined action of the Fe(III) species, which are generally present as impurities in zeolitic tuffs. When MB is exposed to visible light, these species also impact its initial adsorption and degradation. Comparable results are obtained from zeolitic tuffs in other regions [17]. Fe impurities play a role in photocatalysis, as evidenced by the fact that photocatalytic activity rises with increasing Fe content.

## CONCLUSION

One of the most common natural zeolites, clinoptilolite, is a mineral resource in R. Serbia. This study's results suggest that clinoptilolite is a valuable adsorbent for various contaminants and can be applied to wastewater treatment in environmentally friendly processes. It exhibits photocatalytic activity, which is currently one of the most promising ways to eliminate organic micropollutants such as organic dyes.

## ACKNOWLEDGEMENT

*The authors are grateful to the Faculty of Ecology and Environmental Protection (University "Union - Nikola Tesla" Belgrade, Serbia) and the Ministry of Science, Technological Development and Innovation of the Republic of Serbia for financial support (Project number: 451-03-66/2024-03/200011).*

## REFERENCES

- [1] Yilmaz B., Müller U., Top. Catal. 52 (2009) 888–895.
- [2] Garcia-Basabe Y., Rodriguez-Iznaga I., de Menorval L.-C., *et al.*, Micropor. Mesopor. Mat. 135 (2010) 187–196.
- [3] Godelitsas A., Armbruster T., Micropor. Mesopor. Mat. 61 (2003) 3–24.
- [4] Dzedzicka A., Sulikowski B., Ruggiero-Mikolajczyk M., Catal. Today 259 (2016) 50–58.
- [5] Ming D.W., Dixon J.B., Clay Clay Miner. 35 (1987) 463–468.
- [6] Rajić N., Stojaković D., Jovanović M., *et al.*, Appl. Surf. Sci. 257 (2010) 1524–1532.
- [7] Stojaković D., Milenković J., Danu N., *et al.*, Clay Clay Miner. 59 (2012) 277–285.

- [8] Shibata W., Steff K., *Zeolites* 19 (1997) 87–89.
- [9] Marcus Y., *Chem. Rev.* 88(8) (1988) 1475–1498.
- [10] Stojaković Đ., Milenković J., Daneu N., *et al.*, *Clays Clay Miner.* 59 (2011) 277–285.
- [11] Rajić N., Stojaković Đ., Jevtić S., *et al.*, *J. Hazard. Mater.* 172 (2009) 1450–1457.
- [12] Kaplanec I., Rečnik A., Mali G., *et al.*, *Desalin. Water Treat.* 78 (2017) 231–240.
- [13] Pavlović J., Milenković J., Rajić, N., *J. Serb. Chem. Soc.* 79 (2014) 1309–1322.
- [14] Kalebić B., Pavlović J., Dikić J., *et al.*, *Minerals* 11 (2021) 518.
- [15] Šuligoj A., Pavlović, J., Arčon I., *et al.*, *Catalysts* 10 (2020) 253.
- [16] Pavlović J., Šuligoj A., Opresnik M., *et al.*, *Catalysts* 12 (2022) 224.
- [17] Sydoruk V., Vasylechko V., Khyzhun O., *et al.*, *Appl. Catal. A Gen.* 610 (2021) 117930.



## THE EUROPEAN PERCH (*Perca fluviatilis*) AS AN INDICATOR OF OCPs POLLUTION IN DIFFERENT TYPES OF RESERVOIRS IN SERBIA

Dušan Nikolić<sup>1\*</sup>, Aleksandra Tasić<sup>2</sup>

<sup>1</sup>University of Belgrade, Institute for Multidisciplinary Research, Department of Inland Water Biology and Protection, Kneza Višeslava 1, 11030 Belgrade, SERBIA

<sup>2</sup>Scientific Institute of Veterinary Medicine of Serbia, Janisa Janulisa 14,  
11107 Belgrade, SERBIA

\*[dusan@imsi.rs](mailto:dusan@imsi.rs)

### Abstract

*The aim of this study was to determine the concentrations of 17 organochlorine pesticides (OCPs) in muscle tissue of the European perch from six reservoirs in Serbia with different properties and used for different purposes: electricity generation (Vlasina, Zaovine, and Perućac), recreation (Lake Sava), and water supply (Garaši). A gas chromatography with mass spectrometric detection (GC-MS) was used for OCPs detections. The concentrations of aldrin, dieldrin, endrin, endrin aldehyde,  $\alpha$ -HCH,  $\beta$ -HCH,  $\gamma$ -HCH,  $\delta$ -HCH, endosulfan I, endosulfan II, endosulfan sulfate, 4,4'-DDT, heptachlor epoxide, and metoxychlor were not detected at any studied reservoir. On the other hand, we detected concentrations of 4,4'-DDE in one individual ( $17 \mu\text{g kg}^{-1}$ ) from Garaši, 4,4'-DDD in one individual ( $15 \mu\text{g kg}^{-1}$ ) from Garaši and two individuals ( $15 \mu\text{g kg}^{-1}$ ,  $17 \mu\text{g kg}^{-1}$ ) from Zaovine, as well as heptachlor in two individuals ( $12 \mu\text{g kg}^{-1}$ ,  $15 \mu\text{g kg}^{-1}$ ) from Zaovine and three individuals ( $9 \mu\text{g kg}^{-1}$ ,  $11 \mu\text{g kg}^{-1}$ ,  $12 \mu\text{g kg}^{-1}$ ) from Lake Sava. Concentrations of analyzed OCPs did not exceed the proscribed maximum residue levels (MRLs). Therefore, we can conclude that meat of European perch from all investigated reservoirs is safe for human consumption regarding these pesticides.*

**Keywords:** fish, organochlorine pesticides, QuEChERS, GC-MS.

### INTRODUCTION

Since the World War II, the organochlorine pesticides (OCPs) were widely used in agriculture and public health as insecticides and biocides [1]. It soon became apparent that these components represent a major environmental problem regarding their persistence, toxicity, high potential to enter, bioaccumulate and biomagnify in food chains causing adverse effect on wildlife and humans [2]. Human exposure to OCPs may lead to the development of cancer, genotoxicity, neurotoxicity, and/or cause endocrine, cardiovascular, urinary, growth, and reproductive abnormalities [1,3]. Therefore, the use of the majority of OCPs was banned in most countries, but their metabolic forms and residues can be still detected in aquatic ecosystems due to their environmental persistence [1].

Aquatic environments are particularly sensitive to pollution, since reservoirs and lakes serve as collectors of persistent pollutants [2,4]. Fish are recognized as important indicators of aquatic pollution as they are highly positioned in food chains, are easy to sample and well investigated group of organisms, have potential to accumulate pollutants over time, and are

important part of the human diet [5]. The European perch (*Perca fluviatilis* Linnaeus, 1758) a significant bioindicator in environmental studies, because it is an opportunistic predator, widely distributed in Eurasia and a frequently abundant species in different types of habitats, and important species in commercial and sport fishing [5].

The aim of this study was to determine the concentrations of 17 OCPs in muscle tissue of European perch from six reservoirs in Serbia, built for drinking water supply (Garaši), recreation (Lake Sava), and electricity generation (Vlasina, Perućac, Zaovine, and Međuvršje), and in different stages of eutrophication.

## MATERIALS AND METHODS

### Fish sampling and sample preparation

Sampling was conducted from reservoirs that serve for electricity generation (Vlasina, Zaovine, and Perućac), recreation (Lake Sava), and water supply (Garaši) (Figure 1). Ten individuals from each reservoir were sampled during summer of 2017 using standing gillnets (30 m × 2 m, 30–50 mm mesh size).

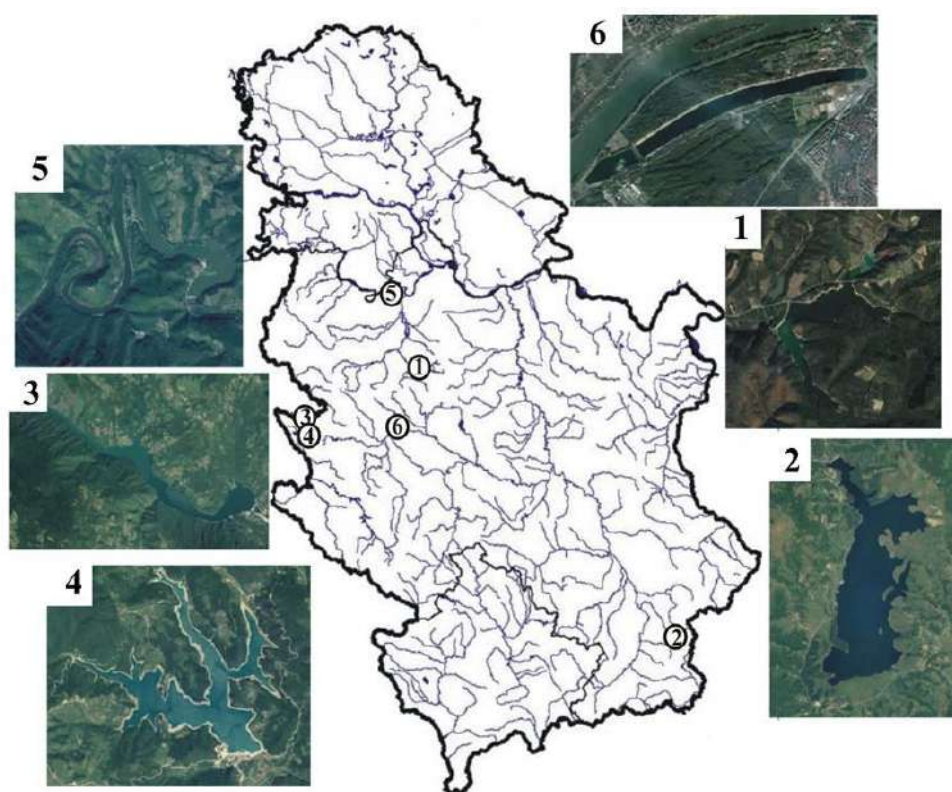


**Figure 1** Map of the sampling sites (Serbia): 1 – Garaši; 2 – Vlasina; 3 – Perućac; 4 – Zaovine; 5 – Međuvršje; 6 – Lake Sava

The extraction of OCPs was performed using the modified QuEChERS procedure. Analytical-grade acetone, acetonitrile and hexane were purchased from J.T. Baker (Deventer, The Netherlands). The samples were kept in a freezer (at -20°C) before analysis, thawed at room temperature and homogenized. A 10 g portion of homogenized sample was weighed

into a 50 mL centrifuge tube. Then, 5 mL of cold purified water was added into the tube, which was then shaken by hand for a 20 seconds to hydrate the samples and allowed to stand for 10 min. Next, 100  $\mu\text{L}$  of internal standard (concentration of 10  $\mu\text{g mL}^{-1}$ ) and 10 mL acetonitrile were added. The sample was shaken for 2 min, after which anhydrous magnesium sulphate (4 g) and sodium chloride (1 g) were added, which was shaken vigorously by hand for 1 min, mixed on a vortex (Labbox Labware, S.L. Barcelona, Spain) for 2 min, and finally the tube was centrifuged (Hettich EBA 280, US) for 5 min. Then, the centrifuge tube was placed in a  $-20^{\circ}\text{C}$  freezer for 30 min. And in the next step, the dispersive solid-phase composed of C18 (0.08 g), primary secondary amine (0.08 g), and  $\text{MgSO}_4$  (0.15 g) was applied to clean up the obtained upper layer. An aliquot of 2 mL was transferred into a vial, evaporated to dryness and reconstituted in 1 ml of mixture of hexane and acetone for GC/MS analysis.

### **Analysis of organochlorine pesticides residues (OCPs)**

A gas chromatography with mass spectrometric detection (GC-MS) was used to determine the concentrations of 17 OCPs (aldrin, dieldrin, endrin, endrin aldehyde,  $\alpha$ -HCH,  $\beta$ -HCH,  $\gamma$ -HCH,  $\delta$ -HCH, endosulfan I, endosulfan II, endosulfan sulfate, 4,4'-DDD, 4,4' -DDE, 4,4'-DDT, heptachlor, heptachlor epoxide, metoxychlor) in fish muscle tissue (fillet). We used a GC Clarus 680 PerkinElmer system comprising an autosampler and a gas chromatograph interfaced with an MS Clarus SQ8T instrument under the following conditions: capillary column Elite-5MS (30  $\times$  0.25 mm ID  $\times$  0.25  $\mu\text{m}$  df, composed of 95% dimethyl polysiloxane and 5% Phenyl), operating in the electron impact mode at 70 eV. The recorded ion source temperature was  $280^{\circ}\text{C}$ . The carrier gas was helium (99.999%; 22.5 psi constant pressure) and an injection volume of 2  $\mu\text{L}$  (a split ratio of 50:1) was used at  $250^{\circ}\text{C}$  injector temperature. The oven temperature was raising from  $70^{\circ}\text{C}$  for 3 min, through  $150^{\circ}\text{C}$  at a rate of  $25^{\circ}\text{C min}^{-1}$  and  $200^{\circ}\text{C}$  at  $3^{\circ}\text{C min}^{-1}$ , and all the way to  $280^{\circ}\text{C}$  at  $8^{\circ}\text{C min}^{-1}$ , and held for 10 min. Mass spectra were taken at 70 eV. The scan interval was set to 0.2 s and for the detection of fragmented ions, ion masses in the range of 50 to 400 Da were monitored. The software analyzes were performed in Turbo Mass Ver 6.1.0.

Stock standard solutions (AccuStandard Inc., New Haven, USA) with a concentration of 10  $\mu\text{g mL}^{-1}$  and working solutions by appropriate dilutions with hexane were used. A blank sample of European perch (10 g) was used for preparation matrix calibration curves by addition calibration standard of 10, 20, 30, 50 and 100  $\mu\text{g kg}^{-1}$  in European perch before extraction. Triphenyl phosphate (TPP) was used as an internal standard. The SANTE 11312/2021 validation guidelines was used for validations of linearity, limits of detection (LOD), limits of quantification (LOQ), specificity, recovery, and precision of the applied method. A six replicates were done in order to obtain mean recovery values after a spike of 10 and 20  $\mu\text{g kg}^{-1}$  (Table 1). Initially, the blank fish sample was mixed with spike and a preparation procedure was performed. The average recoveries of the OCPs in European perch muscle ranged from 88.4% to 99.4%, for fortification level of 10  $\mu\text{g kg}^{-1}$  and 20  $\mu\text{g kg}^{-1}$ .

Concentrations of analyzed OCPs are expressed as  $\mu\text{g kg}^{-1}$ . Concentrations of heptachlor, heptachlor epoxide, 4,4'-DDD, 4,4'-DDE, and 4,4'-DDT in fish muscle tissue were compared with the maximum residue levels (MRLs) in fish meat set by the national legislation of Serbia



[6]. The MRL for sum heptachlor and heptachlor epoxide is  $0.1 \text{ mg kg}^{-1}$  (i.e.  $100 \text{ } \mu\text{g kg}^{-1}$ ), as well as  $1.0 \text{ mg kg}^{-1}$  (i.e.  $1000 \text{ } \mu\text{g kg}^{-1}$ ) for DDT and derivatives.

## RESULTS AND DISCUSSION

The linearity of the analytical response across the studied range of concentrations, correlation coefficient ( $R^2$ ), limits of detection (LOD), and limits of quantification (LOQ) are given in the Table 1.

**Table 1** Linear regression parameters of the calibration curve of OCPs, correlation coefficient ( $R^2$ ), limits of detection (LOD), limits of quantification (LOQ), recovery for the spiked levels of  $10 \text{ } \mu\text{g/kg}$  and  $20 \text{ } \mu\text{g/kg}$

Pesticide residue	Calibration curve	$R^2$	LOD ( $\mu\text{g/kg}$ )	LOQ ( $\mu\text{g/kg}$ )	Recovery (%)	
					10 $\mu\text{g/kg}$	20 $\mu\text{g/kg}$
Aldrin	$y=0.9883x + (-36.981)$	0.99622	1.8	6.1	95.2	98.1
Dieldrin	$y=1.2682x + (-27.282)$	0.99911	2.0	6.7	96.2	99.4
Endrin	$y=0.1490x + (-7.337)$	0.99998	0.8	2.8	97.6	99.0
Endrin aldehyde	$y=0.8009x + (-30.728)$	0.99461	0.6	2.0	89.1	97.6
$\alpha$ -HCH	$y=0.7790x + (-16.126)$	0.99906	0.8	2.5	88.9	94.2
$\beta$ -HCH	$y=1.2947x + (-30.965)$	0.99886	0.7	2.3	90.1	90.4
$\gamma$ -HCH	$y=1.1845x + (-12.415)$	0.99697	2.0	6.7	98.0	90.3
$\delta$ -HCH	$y=0.5890x + (-12.466)$	0.99782	0.9	2.9	95.1	99.1
Endosulfan I	$y=0.1205x + (-2.387)$	0.99977	2.4	7.9	89.6	89.9
Endosulfan II	$y=0.1766x + (-3.906)$	0.99993	2.0	6.7	97.8	97.9
Endosulfan sulfate	$y=0.3969x + (-14.492)$	0.99342	1.1	3.6	90.1	92.6
4,4'-DDD	$y=2.8343x + (-127.38)$	0.99373	1.7	5.6	99.0	99.2
4,4'-DDE	$y=1.9067x + (-82.059)$	0.99445	1.0	3.3	99.0	99.3
4,4'-DDT	$y=2.1650x + (-105.75)$	0.99604	1.0	3.3	98.7	99.1
Heptachlor	$y=0.2500x + (-8.818)$	0.99621	1.6	5.4	98.7	99.1
Heptachlor epoxide	$y=0.9883x + (-36.988)$	0.99839	1.0	3.2	95.1	97.5
Metoxychlor	$y=4.2590x + (-194.09)$	0.99333	0.3	1.0	96.1	97.4

The concentrations of aldrin, dieldrin, endrin, endrin aldehyde,  $\alpha$ -HCH,  $\beta$ -HCH,  $\gamma$ -HCH,  $\delta$ -HCH, endosulfan I, endosulfan II, endosulfan sulfate, 4,4'-DDT, heptachlor epoxide, and metoxychlor were not detected at any studied reservoir. On the other hand, we detected concentrations of 4,4'-DDE in one individual ( $17 \text{ } \mu\text{g kg}^{-1}$ ) from Garaši, 4,4'-DDD in one individual ( $15 \text{ } \mu\text{g kg}^{-1}$ ) from Garaši and two individuals ( $15 \text{ } \mu\text{g kg}^{-1}$ ,  $17 \text{ } \mu\text{g kg}^{-1}$ ) from Zaovine, as well as heptachlor in two individuals ( $12 \text{ } \mu\text{g kg}^{-1}$ ,  $15 \text{ } \mu\text{g kg}^{-1}$ ) from Zaovine and three individuals ( $9 \text{ } \mu\text{g kg}^{-1}$ ,  $11 \text{ } \mu\text{g kg}^{-1}$ ,  $12 \text{ } \mu\text{g kg}^{-1}$ ) from Lake Sava. Interestingly to mention, two individuals from Zaovine in which heptachlor was detected also accumulated 4,4'-DDD in their muscle tissues.

$\alpha$ -HCH,  $\beta$ -HCH,  $\gamma$ -HCH, and 4,4'-DDT were also under the detection limits in edible tissue of European perch from five location along the tributaries of the Moselle River at Lorraine Region (France) [7]. The concentrations of 4,4'-DDE ranged from  $0.12$  to  $0.85 \text{ } \mu\text{g kg}^{-1}$  (4,4'-DDD and 4,4'-DDT were not detected), and sum of total DDTs were below safety values of  $1.0 \text{ } \mu\text{g kg}^{-1}$  indicating no health risk due to consumption of this species [7]. In Latvia,

$\alpha$ -HCH and  $\gamma$ -HCH [8] as well as dieldrin [9] were detected in European perch from four lakes (Kishezers, Siksalas, Engures, and Burtnieks) and three locations along the coast (Daugavgriva, Kurmrag, and Lielirbe), respectively. In all the mentioned locations, concentrations of DDT and its derivatives (DDTs) were in line with our results. Compared to our study, a higher concentrations of HCH isomers ( $\alpha$ -HCH,  $\beta$ -HCH, and  $\gamma$ -HCH) and DDTs (4,4'-DDD, 4,4'-DDE, 4,4'-DDT) were recorded in muscle tissue of European perch from Odra river estuary [10]. Similar findings are recorded for European perch from Caraorman at the Danube Delta (Romania) [11] and Sulejowski Reservoir (Central Poland) [12]. Aldrin, endrin,  $\delta$ -HCH, heptachlor, heptachlor epoxide, and  $\alpha$ -endosulfan were below detection limits in European perch sampled at three lakes of Latinum (Bolsena, Bracciano, and Salto) in Italy [13]. On contrary, dieldrin,  $\alpha$ -HCH,  $\gamma$ -HCH, and 4,4'-DDT were detected in all studied lakes [13]. In all perch samples from Italy, concentrations of 4,4'-DDE were lower compared to Garaši and 4,4'-DDD compared to Zaovine and Garaši.

Concentrations of analyzed OCPs did not exceed the proscribed MRLs, indicating the absence of health risk due to consumption of fish meat regarding the analyzed pesticides. The absence or low concentrations of the analyzed OCPs in European perch from Garaši, Lake Sava, Vlasina, Perućac, Zaovine, and Međuvršje was probably due to the absence of recent application of these pesticides. These was also noted for European chub (*Squalius cephalus*), pikeperch (*Sander lucioperca*), and common nase (*Chondrostoma nasus*) sampled at mentioned reservoirs in Serbia [2,4,14].

## CONCLUSION

Of 17 OCPs analyzed in this study, only three were recorded – 4,4'-DDE in one individual from Garaši, 4,4'-DDD in one individual from Garaši and two individuals from Zaovine, and heptachlor in two individuals from Zaovine and three individuals from Lake Sava. Concentrations of all detected pesticides were low and did not exceed the proscribed MRLs. Therefore, we can conclude that meat of European perch from all investigated reservoirs is safe for human consumption regarding these pesticides.

## ACKNOWLEDGEMENT

*This study was supported by the Ministry of Science, Technological Development and Innovation of the Republic of Serbia (Grant numbers: 451-03-66/2024-03/200053 and 451-03-66/2024-03/200030).*

*The authors wish to express their gratitude to Dr. Gorčin Cvijanović, Dr. Stefan Skorić, Dr. Katarina Jovičić and Mr. Stojan Janjić, who helped with the fish sampling. Also, we are grateful for the help and hospitality of our hosts from NP Tara, PIO Vlasina and PIO Međuvršje.*

## REFERENCES

- [1] Varol M., Sünbül M.R., Environ. Pollut. 230 (2017) 311–319.
- [2] Nikolić D., Poleksić V., Skorić S., *et al.*, Environ. Pollut. 310 (2022) 119871.
- [3] WHO, World Health Organization, Persistent organic pollutants (POPs). Available on the following link: [www.who.int/foodsafety/areas\\_work/chemical-risks/pops/en/](http://www.who.int/foodsafety/areas_work/chemical-risks/pops/en/).

- [4] Nikolić D., Poleksić V., Tasić A., *et al.*, Sustainability 15 (2023) 11321.
- [5] Nikolić D., Skorić S., Rašković B., *et al.*, Chemosphere 244 (2020) 125503.
- [6] Official Gazette of the Republic of Serbia Nos, 2002. 25/2010 & 28/2011, Pravilnik o količinama pesticida, metala i metaloida i drugih otrovnih supstancija, hemioterapeutika, anabolika i drugih supstancija koje se mogu nalaziti u namirnicama. Available on the following link: <https://www.pravno-informacioni-sistem.rs/SlGlasnikPortal/eli/rep/slsrj/ministarstva/pravilnik/1992/5/1/reg>.
- [7] Thomas M., Lazartigues A., Banas D., *et al.*, Ecotoxicol. Environ. Saf. 77 (2012) 35–44.
- [8] Valters K., Olsson A., Asplund L., *et al.*, Chemosphere 38 (9) (1999) 2053–206.
- [9] Olsson A., Vitinsh M., Plikshs M., *et al.*, Sci. Total Environ. 239 (1999) 19–30.
- [10] Falandysz J., Wyrzykowska B., Warzocha J., *et al.*, Food Chem. 87 (2004) 17–23.
- [11] Covaci A., Gheorghe A., Hulea O., *et al.*, Environ. Pollut. 140 (2006) 136–149.
- [12] Waszak I., Dabrowska H., Chemosphere 75 (2009) 1135–1143.
- [13] Orban E., Navigato T., Masci M., *et al.*, Food Chem. 100 (2007) 482–490.
- [14] Nikolić D., Skorić S., Subotić S., Environ. Sci. Pollut. Res. 31 (2024) 1050–1063.





## DEGRADATION OF TETRACYCLINE ANTIBIOTICS IN AQUATIC ENVIRONMENT BY UV IRRADIATION AND FERRIC ION PHOTOLYSIS

Jelena Korać Jačić<sup>1\*</sup>, Milica R. Milenković<sup>2</sup>, Dragana Bartolić<sup>1</sup>

<sup>1</sup>University of Belgrade, Institute for Multidisciplinary Research,  
Kneza Višeslava 1, 11030 Belgrade, SERBIA

<sup>2</sup>University of Belgrade, Faculty of Chemistry, Studentski trg 12–16, 11000 Belgrade,  
SERBIA

\*jskorac@gmail.com

### Abstract

*Tetracyclines are largely used antibiotics in human and veterinary medicine due to their wide spectrum of antibacterial activity. Besides the benefits of their use in defense from pathogenic microorganisms their presence in surface water, groundwater, wastewater treatment plant, effluent and influents, and sludge is a growing problem for the environment. Understanding of interactions between tetracyclines and metal ions in aqueous ecosystems are of special importance for development of methods for their removal, especially advanced oxidation processes initiated or enhanced by UV irradiation. The influence of pH and the presence of ferric ions on photosensitivity of tetracycline antibiotics tetracycline and doxycycline to UV A and UV B irradiation were investigated by UV-Vis, Raman and EPR spectroscopy, MS, HPLC, and cyclic voltammetry. The formation of Fe<sup>3+</sup>-tetracycline complexes is pH dependent. UV-Vis and Raman spectra showed Fe<sup>3+</sup> binding with both tetracycline antibiotics through amide and OH groups in tricarbonylamide moiety of A ring and phenolic diketone oxygen atoms of BCD system at acidic solutions pH≤5. MS showed 1:1 stoichiometry of Fe<sup>3+</sup>-tetracycline antibiotic complexes. Coordination interactions between Fe<sup>3+</sup> and tetracyclines are reversible. Tetracyclines are released unchanged from their Fe<sup>3+</sup> complexes by pH increase. The effect of UV irradiation on tetracyclines, their Fe<sup>3+</sup> complexes and tetracyclines in the presence of Fe<sup>3+</sup> prior the formation of the complexes was investigated at pH 5. The results showed that coordination of tetracyclines with Fe<sup>3+</sup> makes them less susceptible to oxidation with hydroxyl radical generated by UV-induced photolysis of Fe<sup>3+</sup>-OH complexes. The exposure of tetracyclines to UV-A and UV-B irradiation led to their photodegradation at neutral and basic pH, while acidic pH preserved tetracyclines from photodegradation. Redox properties of tetracyclines are pH dependent and related to deprotonation of phenolic diketone moiety of BCD system which makes them more susceptible to oxidation at higher pH.*

**Keywords:** advanced oxidation process, tetracycline, ferric ion, complexes, photo-degradation.

### INTRODUCTION

Tetracyclines (TCs) are commonly used antibiotics in the human health care and animal husbandry sector. They possess a tetracyclic ring system substituted with various hydroxyl, methyl, keto, and dimethylamino functional groups as a common structural motif and exhibit a broad spectrum of antibacterial activity [1]. TCs are excreted out almost unchanged due to

their high resistance to metabolic degradation in human and animal organisms and reached the aquatic environment [2]. Hospitals, pharmaceutical industries, and livestock additionally contribute to the presence of TCs in waste (industrial and municipal), surface, underground, and drinking water [1]. The slow degradation rates of TCs in water led to their long-term detrimental effects on ecosystems manifested as a high toxicity to aquatic organisms, development of antimicrobial resistance, and their accumulation and transmission through the food chain [3]. Several strategies for removal and degradation of TCs from aquatic and terrestrial environment are developed that can be categorized as biological, chemical, physical methods and their combinations [4–6]. Conventional methods for drinking and wastewater treatment (coagulation/flocculation, clarification, filtration and wastewater treatment plants) are not able to sufficiently remove pharmaceuticals. UV irradiation of wastewater can be used for both disinfection and degradation of pharmaceuticals. TCs are very sensitive to photodegradation by UV irradiation, but the photoproducts are toxic [7]. Photodegradation of pharmaceuticals in aqueous systems can be enhanced in the presence of ferric iron by photolysis of Fe(III) hydroxo complexes that led to the production of HO<sup>•</sup> radical [8,9]. Chelation of pharmaceuticals with metal ions may affect their redox properties, i.e. susceptibility to oxidation and reduction [10]. TCs possess several ionisable functional groups which are available for coordination with metal ions. The impact of pH on interactions between Fe<sup>3+</sup> and TCs and photodegradation of TCs by ferric iron photolysis is not fully investigated. In this study, we investigated the structures and redox properties of TC complexes with Fe<sup>3+</sup>, the pH dependence of their formation, and the impact of Fe<sup>3+</sup> ions on susceptibility of TCs to photodegradation in aqueous systems.

## **MATERIALS AND METHODS**

### **UV irradiation**

Samples were prepared in 1 mL of water with specific pH, placed in a quartz cuvette (1×1×5 cm), exposed to UV up to 10 min using a lamp with filter for visible light (Carl Roth GmbH, Karlsruhe, Germany; H469.1) and UV tubes (Sankyo Denki, Tokyo, Japan). The irradiation was initiated immediately or following 15 min incubation. UV-B and UV-A lamps had maximal emissions at 312 nm and 352 nm, respectively. Irradiation was conducted in a temperature-regulated chamber. Irradiance was 17 J m<sup>-2</sup>s<sup>-1</sup> for UV-A and 7.7 J m<sup>-2</sup>s<sup>-1</sup> for UV-B.

### **UV–Vis spectroscopy**

UV–Vis spectra were recorded using 2501 PC Shimadzu spectrophotometer (Kyoto, Japan).

### **Cyclic voltammetry**

The voltammetric measurements were performed using a potentiostat/galvanostat CHI 760b (CH Instruments, Inc, Austin, TX, USA). The electrochemical cell (10 mL) was equipped with: a glassy carbon working electrode (inner diameter of 3 mm; Metrohm, Herisau, Switzerland); Ag/AgCl (3M KCl) (reference electrode); and Pt wire (counter electrode).

### Raman spectroscopy

The Raman spectra of 5  $\mu\text{L}$  solution placed on calcium fluoride glass were recorded using a DXR Raman microscope (Thermo Fisher Scientific, Waltham, MA, USA) with the 532 nm laser excitation line, and a constant power illumination of 8.0 mW. The exposure time was 10 s, with 10 exposures. The laser spot diameter was 2.1  $\mu\text{m}$ . The scattered light was analyzed by the spectrograph equipped with a 900 lines  $\text{mm}^{-1}$  grating using 50  $\mu\text{m}$  slit as spectrograph aperture. The automatic fluorescence correction was performed using the OMNIC software (Thermo Fisher Scientific).

### EPR spectroscopy

Systems were exposed to UV for 10 min and recorded using X-band EPR spectrometer Bruker EMX Nano and following settings: power, 10 mW; modulation amplitude, 0.1 mT; sweep width, 12 mT; scan time, 60 s; number of scans, 4. The production of  $\text{HO}^\bullet$  and the impact of TC were evaluated using EPR spin-trapping and BMPO spin trap, which reacts with  $\text{HO}^\bullet$  to produce BMPO/ $\text{HO}^\bullet$  paramagnetic adduct. Spectral simulation of BMPO/ $\text{HO}^\bullet$  adduct spectrum was performed in WINEPRSimFonia (Bruker Analytische Messtechnik GmbH, Darmstadt, Germany), with following parameters: BMPO/ $\text{HO}^\bullet$  adduct: isomer I (81.6%):  $a\text{N}=1.356$  mT,  $a\text{H}\beta=1.230$  mT,  $a\text{H}\gamma=0.066$  mT; isomer II (18.4%):  $a\text{N}=1.347$  mT,  $a\text{H}\beta=1.531$  mT,  $a\text{H}\gamma=0.062$  mT.

## RESULTS AND DISCUSSION

The impact of pH on interactions between  $\text{Fe}^{3+}$  and TC antibiotics, tetracycline (TC) and doxycycline (DOX), was monitored by UV-Vis spectroscopy (Figure 1). The observed changes in UV-Vis spectra of TC and DOX in the presence of  $\text{Fe}^{3+}$  imply that both antibiotics interact with ferric ions in acidic conditions particularly at pH 5. At  $\text{pH}\geq 7$  the presence of ferric ion did not induce changes in UV-Vis spectra of antibiotics. In neutral and basic solutions deprotonation of the phenolic-diketone moiety of TCs enhances their coordination ability, but the poor solubility of  $\text{Fe}^{3+}$  at this pH limits formation of complexes. The formation of  $\text{Fe}^{3+}$  complexes with antibiotics at acidic pH was confirmed by HESI-MS showing their 1:1 stoichiometry. The highest amount of TCs complexes with ferric ion was observed for  $[\text{Fe}^{3+}]/[\text{TCs}]=6$  molar ratio.

The results of Raman spectroscopy indicate  $\text{Fe}^{3+}$ -binding with tricarbonylamide group of ring A and phenolic-diketone oxygens of BCD rings of antibiotics (data not shown). The interactions of TC and DOX with  $\text{Fe}^{3+}$  are reversible without hydrolysis or oxidation of antibiotics. TC and DOX are sensitive to UV-A and UV-B irradiation at  $\text{pH}\geq 7$  (Figure 2). In acidic solutions both antibiotics are not affected by UV irradiation.

The impact of complex formation on TCs photodegradation in acidic solutions can be elucidated only in the case of TC for which slower kinetic of complex formation was observed ( $\sim 15$  min after mixing of  $\text{Fe}^{3+}$  and TC solutions formation of complex reaches equilibrium) (Figure 3a and 3b). The kinetic of DOX- $\text{Fe}^{3+}$  complex formation is faster, reaching equilibrium almost immediately after mixing of  $\text{Fe}^{3+}$  and DOX solutions (Figure 3d). UV-Vis spectra of  $\text{Fe}^{3+}/\text{TC}$  system irradiated immediately (most of TC was free), and after 15 min of incubation (when all TC was bound in the complex) showed  $\text{Fe}^{3+}$  promoted photo-

degradation, which is evidenced by the decrease of characteristic TC absorption (Figure 3a and Figure 3b). However, the decrease TC absorption peaks was modest and twofold less pronounced for TC in the complex than for free TC. The process of photodegradation involves the photolysis of Fe(III) hydroxo complex with reduction of  $\text{Fe}^{3+}$  by  $\text{OH}^-$  to give  $\text{Fe}^{2+}$  and a very strong oxidizing agent  $\text{HO}\cdot$  (standard reduction potential is  $\sim 2$  V). The photolysis of Fe(III) hydroxo complex was confirmed as a drop of  $\text{Fe}^{3+}$  solution absorption after UV irradiation. A significant drop of efficiency of photodegradation of TC in its  $\text{Fe}^{3+}$  complex could not be attributed to the low concentration of “free”  $\text{Fe}^{3+}$ , since only  $30\ \mu\text{M}$  of the total  $\text{Fe}^{3+}$  concentration of  $180\ \mu\text{M}$  was bound to TC. The possible explanation is that TC in the complex is less susceptible to oxidation by  $\text{HO}\cdot$ . Similar as in the case of TC, the presence of  $\text{Fe}^{3+}$  ions in acidic solutions of DOX led to its photodegradation after UV irradiation (Figure 3e and Figure 3f).

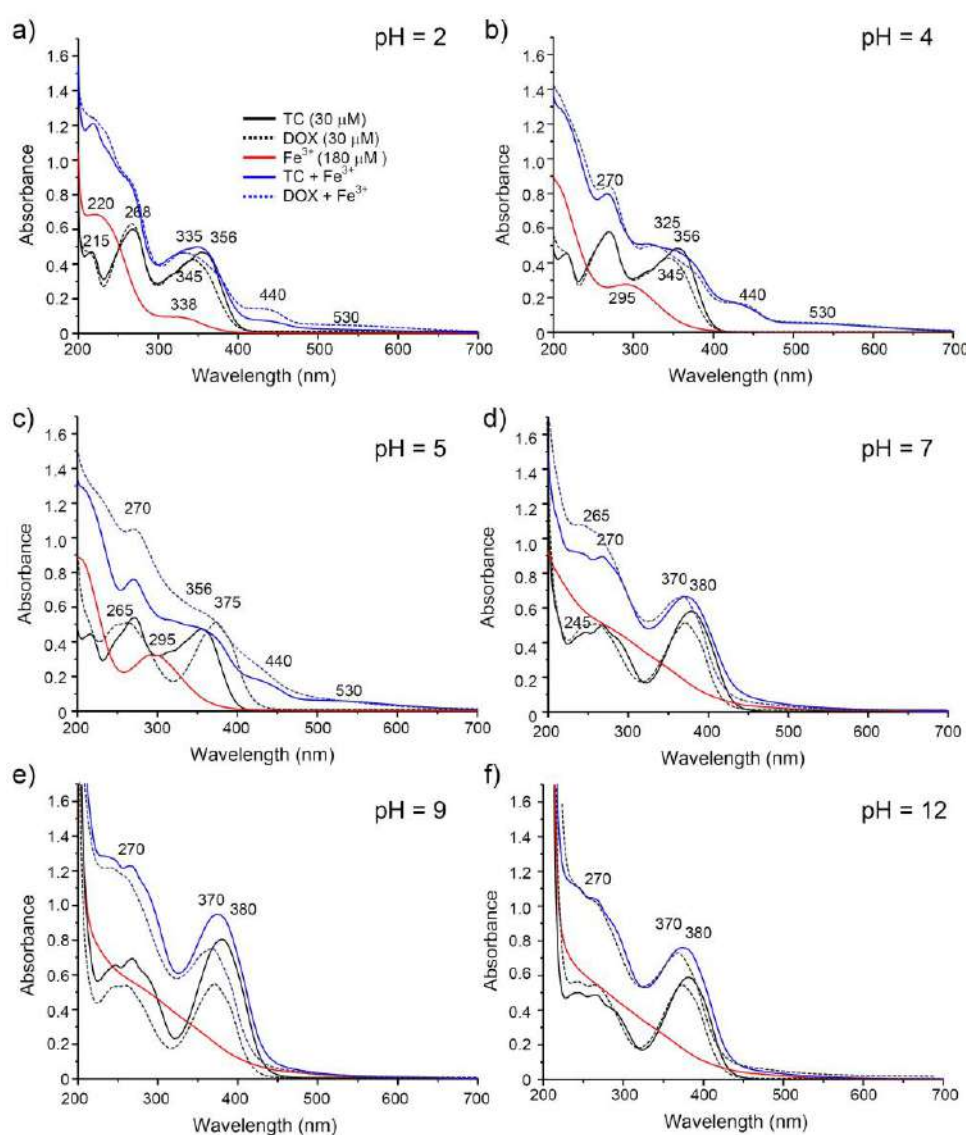


**Figure 1** UV-Vis spectra of TCs in the presence and absence of  $\text{Fe}^{3+}$  at different pH. Sums of spectra of TCs and  $\text{Fe}^{3+}$  are presented for pH values 7, 9 and 12: a) pH 2; b) pH 4; c) pH 5; d) pH 7; e) pH 9; f) pH 12

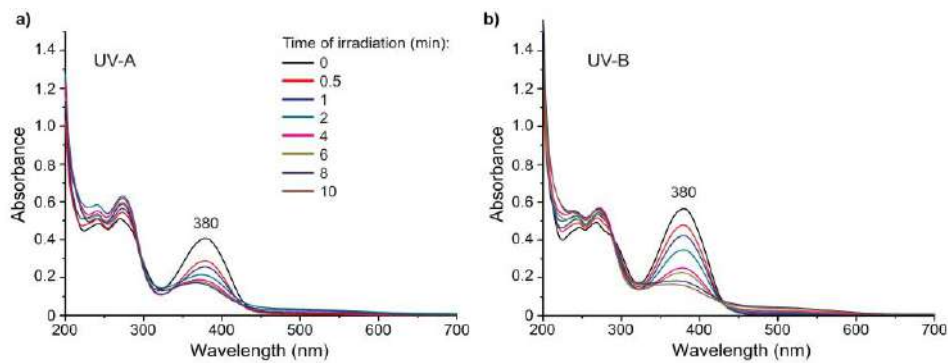


**Figure 2** UV-induced degradation of TC (TC; 30  $\mu\text{M}$  initial concentration) at pH 7, that was monitored by UV-Vis spectroscopy: a) UV-A irradiation; b) UV-B irradiation

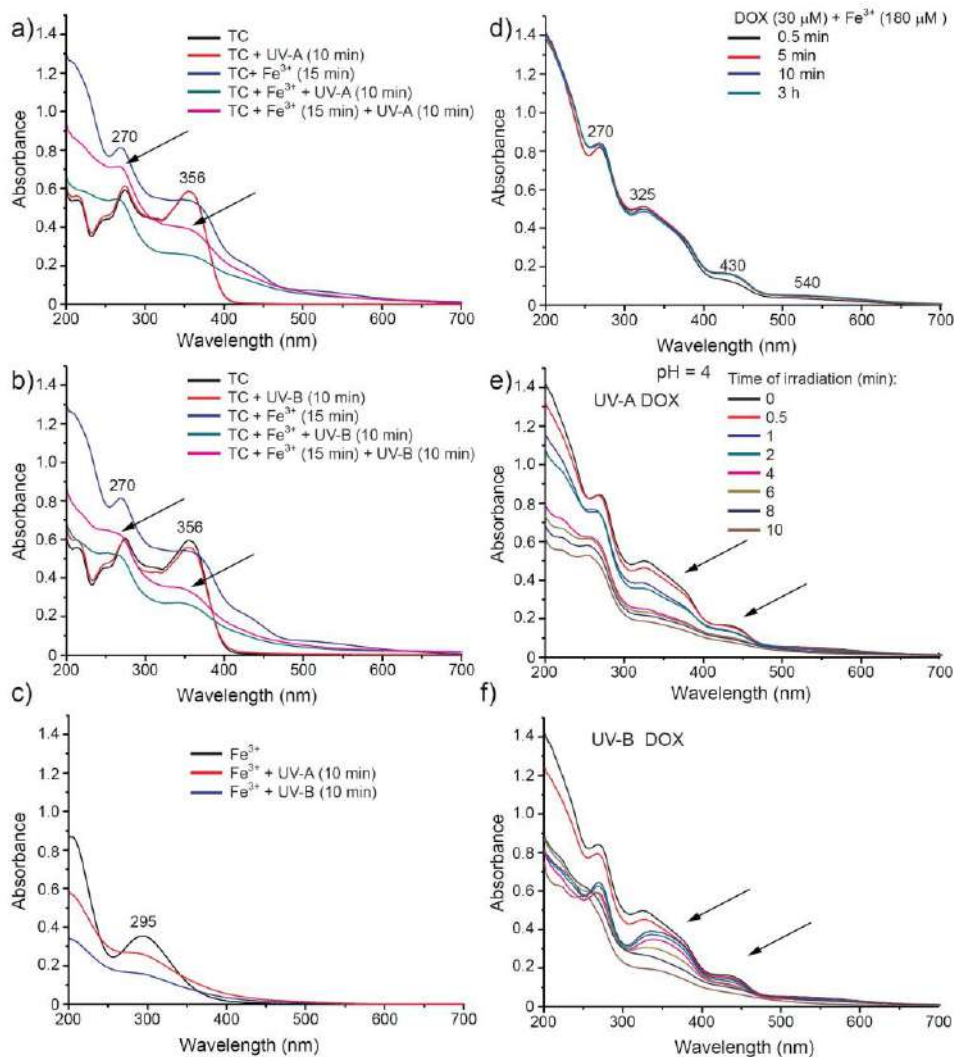


**Figure 3** TCs and  $\text{Fe}^{3+}$  exposed to UV: a) UV-A; b) UV-B; TC and  $\text{Fe}^{3+}$  were exposed immediately or after 15 min of incubation which allowed the formation of  $\text{Fe}^{3+}$ -TC complex; c) Photo-reduction of  $\text{Fe}^{3+}$  results in the loss of  $\text{Fe}^{3+}$  absorption line. [ $\text{Fe}^{3+}$ ]=180  $\mu\text{M}$ ; [TC]=30  $\mu\text{M}$ ; pH=5; period of irradiation: 10 min. Irradiance was 17  $\text{J m}^{-2} \text{s}^{-1}$  for UV-A and 7.7  $\text{J m}^{-2} \text{s}^{-1}$  for UV-B; d) formation and stability of  $\text{Fe}^{3+}$ -DOX complex in time; e) DOX and  $\text{Fe}^{3+}$  exposed to UV-A after 15 min of incubation; f) DOX and  $\text{Fe}^{3+}$  exposed to UV-B after 15 min of incubation



The capacity of TC and TC in its ferric complex to remove HO• radical produced by photolysis of Fe(III) hydroxo complex was analyzed by EPR spin-trapping (Figure 4a). It can be observed that non-coordinated TC removes HO• efficiently confirming involvement of HO• in photodegradation. On the other hand, the coordination of TC with Fe<sup>3+</sup> prevented HO• scavenging. These results imply that coordination of TC with Fe<sup>3+</sup> makes it less susceptible towards oxidation. Redox properties of free TC and TC in its ferric complex were investigated by cyclic voltammetry. At acidic pH the strong oxidation peak of free TC at E<sub>pa</sub>=1060 mV was not observed for Fe<sup>3+</sup>-TC complex, which means that TC is less susceptible to oxidation in the complex. The reduction peak of Fe<sup>3+</sup> at E<sub>pc</sub>=174 mV was shifted to E<sub>p</sub>=140 mV, showing that Fe<sup>3+</sup> was less susceptible to reduction (Figure 4b). The increase of pH led to significant shift of E<sub>pa</sub> of TC to lower potentials from 1090 mV (at pH=5) to 820 mV (pH=7) to 730 mV (pH=9) (Figure 4c), showing its pronounced susceptibility to oxidation at high pH which is related to deprotonation of phenolic diketone moiety in resonant BCD system.

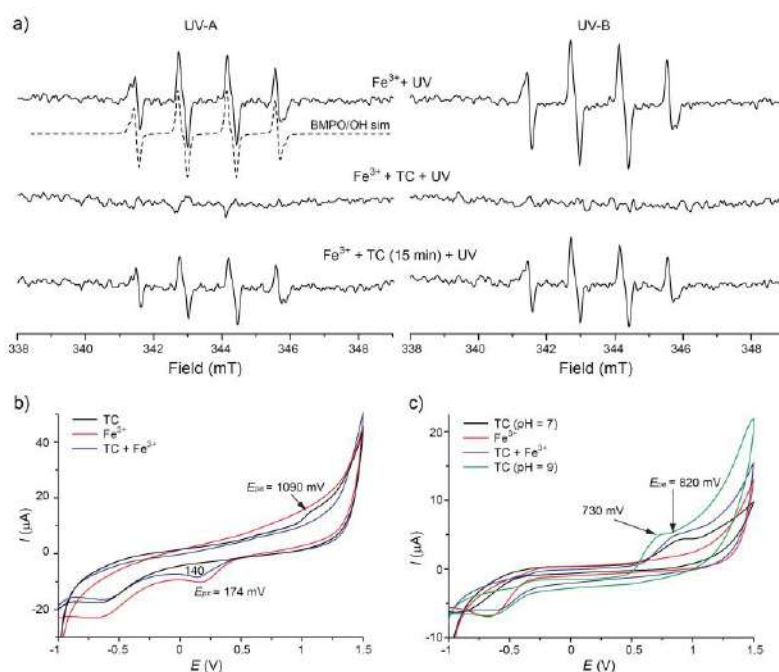


**Figure 4** Redox properties of TC in the complex with Fe<sup>3+</sup>: a) EPR spin-trapping analysis of HO• scavenging capacity of TC; b) Cyclic voltammograms of TC, Fe<sup>3+</sup>, and Fe<sup>3+</sup>-TC complex in water at pH=5 at glassy carbon electrode (scan rate 0.05 V s<sup>-1</sup>); c) Cyclic voltammograms of TC, Fe<sup>3+</sup>, and Fe<sup>3+</sup>-TC complex in water at pH=7 at glassy carbon electrode

## CONCLUSION

The present study simulates conditions present in real environmental aqueous systems containing ferric ions which originate from sediments or ferric chloride used for coagulation as a conventional method for drinking and wastewater treatment. Such aqueous systems can be exposed to UV irradiation emitted by sun or ultraviolet germicidal irradiation as disinfection technique. The obtained results showed that the binding of ferric ion to TCs depends on pH. Ferric complexes of TCs with 1:1 stoichiometry are formed in acidic solution.

TCs are resistant to photodegradation in acidic solutions. UV irradiation induced degradation of TC in the absence of iron at neutral/alkaline pH. In acidic conditions the presence of  $\text{Fe}^{3+}$  ions promotes photodegradation of TCs. Coordination of TCs with  $\text{Fe}^{3+}$  makes them less susceptible to oxidation with  $\text{HO}^\bullet$  generated by UV-induced photolysis of  $\text{Fe}^{3+}\text{-OH}^-$  complexes. In future development of advanced oxidation processes for water treatment it should be taken into account that formation of ferric complexes with organic pollutants at acidic solutions influence their redox properties possibly making it less susceptible to oxidation with  $\text{HO}^\bullet$  radicals produced by ferric ion photolysis.

### ACKNOWLEDGEMENT

*The authors are grateful to the Ministry of Science, Technological development and Innovation of the Republic of Serbia for financial support according to the contract with the registration number (e.g. e.g. 451-03-66/2024-03/200053, 451-03-66/2024-03/200168).*

### REFERENCES

- [1] Ahmad F., Zhu D., Sun J., Environ. Sci. Eur. 33 (64) (2021) 1–17.
- [2] Agwuh K.N., MacGowan A., J. Antimicrob. Chemother. 58 (2) (2006) 25–65.
- [3] Kumar M., Jaiswal S., Sodhi K.K, Environ. Int. 124 (2019) 448–461.
- [4] Yang Q., Gao Y., Ke J., *et al.*, Bioengineered 12 (2021) 7376–7416.
- [5] Lu Z.-Y., Ma Y.-L., Zhang J.-T., *et al.*, J. Water Process Eng. 38 (2020) 101681.
- [6] Singh S., Faraz M., Khare N., ACS Omega 5 (2020) 11874–11882.
- [7] Patel M., Kumar R., Kishor K, Chem. Rev. 119 (2019) 3510–3673.
- [8] Milić Komić S., Bogdanović Pristov J., Popović-Bijelić A., *et al.*, Appl. Catal. B 185 (2016) 174–180.
- [9] Thomas N., Dionysiou D.D., Pillai S.C., J. Hazard. Mat. 404 (2021) 124082.
- [10] Korać J., Stanković D.M., Stanić M., *et al.*, Sci. Rep. 8 (2018) 3530.

# **Conference Papers**





## NAPHTHALENE SCREENING IN BOR'S MUNICIPALITY BASED ON ITS CONCENTRATIONS IN LEAVES AND STEMS OF *Hedera helix* L.

Aleksandra Papludis<sup>1\*</sup>, Slađana Alagić<sup>1</sup>, Snežana Milić<sup>1</sup>, Jelena Nikolić<sup>2</sup>,  
Ivana Zlatanović<sup>2</sup>, Snežana Jevtović<sup>2</sup>, Vesna Stankov Jovanović<sup>2</sup>

<sup>1</sup>University of Belgrade, Technical Faculty in Bor, V.J. 12, 19210 Bor, SERBIA

<sup>2</sup>University of Nis, Faculty of Sciences and Mathematics, Department of Chemistry,  
Višegradska 33, 18000 Niš, SERBIA

\*[apapludis@tfbor.bg.ac.rs](mailto:apapludis@tfbor.bg.ac.rs)

### Abstract

*Naphthalene (Nap) belongs to the group of polycyclic aromatic hydrocarbons, and is considered as the simplest compound (it consists of two benzene rings). The aim of this work was to determine the content of Nap in the unwashed leaves and stems of poison ivy (PI). The samples were collected from nine locations in the area of Bor municipality, situated at different distances from the main source of pollution, i.e. from the metallurgical complex in the city of Bor, containing also the city heating plant. The highest concentration of Nap was found in stems of PI at the site S (66.63 µg/kg), while in the leaves was at site BN (45.89 µg/kg). Obtained results for the concentration of Nap in PI samples from each location were processed using factor R. Based on the calculated values for factor R, it can be concluded that at the sites FJ (2.05) and BN (1.39) closest to the metallurgical complex, and at rural sites SN (1.28), and O (1.70), the pollution of atmospheric origin was the greatest; also, it can be supposed that the proximity of the city heating plant and smelter was responsible for the increased R values ( $R>1$ ) at the sites from the urban/industrial zone, while increased R values in the rural zone were the result of domestic heating. In both zones, the traffic was also one of the possible sources of Nap. There is a possibility that plants absorbed Nap not only from the atmosphere but also from the soil.*

**Keywords:** naphthalene, *Hedera helix*, PAHs, factor R.

### INTRODUCTION

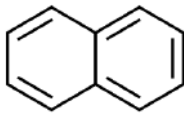
Polycyclic aromatic hydrocarbons (PAHs) are highly persistent in the environment, toxic and represent significant health risk to humans [1]. In recent years, there has been increasing concern about the negative impact of PAHs on terrestrial and marine ecosystems, because for several of them are known to exhibit toxic, carcinogenic, and mutagenic effects [1].

The behavior of PAHs in the environment is greatly influenced by the physical and chemical properties of the individual compounds, such as their molecular weight, water solubility, vapor pressure etc. [2]. They are chiefly defined by the number of benzene rings [2]. The simplest PAHs compound is naphthalene (Nap) [3], comprised of two fused benzene rings [4,5], with molecular weight of 128.2 g/mol [6]. In Table 1 are given physical and chemical properties of Nap. Based on the value for water solubility, Nap can be considered as very low soluble [3,7].

Because of its tendency to biodegrade and volatilize/evaporate relatively easily, Nap has a short half-life in soil. The estimated half-life of Nap in soils with 0.2–0.6% organic carbon and 92–94% sand was 11–18 days [8]. The half-life of a three-ring phenanthrene molecule in soil can be from 16 to 126 days, while the half-life of a five-ring benz(a)pyrene is 229–1400 days [3]. In the atmosphere Nap has a relatively short half-life of 3–8 hours [9]. Therefore, comparing with other PAH compounds, Nap has a relatively low tendency to accumulate in the environment. Outdoor concentrations of Nap are low in Europe, typically ranging from 1 to 4  $\mu\text{g}/\text{m}^3$ . Generally, concentrations of Nap in the air are lower in rural than in urban areas [9].

The pollution sources responsible for the presence of PAHs in the environment are numerous. The origin of Nap is associated with fossil fuels; it is naturally found in petroleum and coal tar [7,10]. The indirect source responsible for releasing Nap into the environment is vehicle emissions [7]. Naphthalene is released into the environment via the incomplete combustion (pyrolysis) of organic compounds, oil spills, oil processing, household waste disposal, and use of fumigants and deodorants [3].

**Table 1** Physical and chemical properties of Nap [4,7]

Property	Value
Molecular formula <sup>[4]</sup>	$\text{C}_{10}\text{H}_8$
Structural formula <sup>[7]</sup>	
Molecular weight <sup>[4]</sup>	128.19 g/mol
Melting point <sup>[7]</sup>	80.0–80.3°C
Boiling point <sup>[7]</sup>	217.9–218°C
Density <sup>[7]</sup>	1.175 g/cm <sup>3</sup>
Henry's Law Constant <sup>[4]</sup>	$4.83 \cdot 10^{-4}$ atm m <sup>3</sup> /mol
Vapor pressure <sup>[4]</sup>	0.0087 mm Hg
Water solubility <sup>[4]</sup>	31.69 $\mu\text{g}/\text{L}$
Log $K_{ow}$ <sup>[4]</sup>	3.36
Log $K_{oc}$ <sup>[4]</sup>	2.97

Naphthalene is classified and listed among the sixteen priority pollutants by the United States Environmental Protection Agency (USEPA) [2,5,6]. According to the International Agency for Research on Cancer (IARC), Nap can be considered as possible carcinogenic to humans and animals [5,6].

In humans, exposure to Nap through dermal contact, inhalation and ingestion can lead to toxic manifestations such as: liver and lung damage, eye sensitivity, and neurological damage in infants. In the human body, high concentrations of Nap can destroy red blood cells, causing hemolytic anemia [5,6].

In this paper, the concentrations of Nap were determined in the unwashed stems and leaves of *Hedera helix* L., i.e., poison ivy (PI), as a way to monitor the level of this hazardous compound in the municipality of Bor (East Serbia). Given that Nap represents one of rare low

molecular weight (LMW) PAHs that can be absorbed through leaves but also through root and transported into the aboveground parts [4], the focus of this paper was on the estimation of atmospheric pollution, using the unwashed stems and leaves and calculating the so-called factor R [11].

## MATERIALS AND METHODS

Sampling of PI plant material (stems and leaves) was carried out at nine locations in the area of the city of Bor and its surroundings. Sampling sites (four urban and five rural sites) were chosen at different distances from the primary source of pollution – smelter and the heating city plant in the centre of metallurgical complex in the Bor town. The urban zone included the following locations: Flotacijsko jalovište (FJ) – at a distance of 0.7 km from the main pollution source, Bolničko naselje (BN) at a distance of 1.3 km, Slatinsko naselje (SN) at a distance of 3.2 km and Naselje Sunce (NS) at a distance of from 3.6 km. The rural zone included: Oštrej (O) at a distance of 4.5 km, Slatina (S) at a distance of 6.5 km, Borsko jezero (BJ) at a distance of 7.0 km, Krivelj (K) at a distance of 8.0 km and Gornjane (G) at a distance of 19 km.

PI material was collected as described in detail in Papludis *et al.* [12], as well as the manner of its preparation and analysis (using gas chromatographic-mass spectrometric, GC/MS method); exception was that stems and leaves were analyzed as unwashed.

Obtained results for the concentrations of Nap in PI samples from each location were processed using the factor R, i.e., the ratio of Nap concentrations in the unwashed leaves and stems:  $R_{\text{leaf/stem}} = C_{\text{leaf}}/C_{\text{stem}}$  ( $C_{\text{leaf}}$ , and  $C_{\text{stem}}$  are the concentrations of Nap in the equivalent plant organ). Factor R bigger than 1 indicates the sites where the atmospheric pollution had the greatest influence [11].

## RESULTS AND DISCUSSION

The concentration of Nap in the leaf and stem samples of PI are given in Table 2.

*Table 2* The content of Nap ( $\mu\text{g}/\text{kg}$ , *dw*) in the leaf and stem samples of PI

Location	Leaf	Stem
FJ	24.14	11.79
BN	<b>45.89</b>	33.06
SN	<b>45.20</b>	35.42
NS	25.44	43.45
O	<b>44.84</b>	26.35
S	<b>42.47</b>	<b>66.63</b>
BJ	4.57	25.72
K	8.89	40.98
G	6.38	23.99

Bold values indicate Nap highest concentrations

The highest concentration of Nap was in stem of PI at the site S (66.63  $\mu\text{g}/\text{kg}$ ), while in the leaves, the highest, and very similar Nap concentrations were found at several sites: BN (45.89  $\mu\text{g}/\text{kg}$ ), SN (45.20  $\mu\text{g}/\text{kg}$ ), O (44.84  $\mu\text{g}/\text{kg}$ ) and S (42.47  $\mu\text{g}/\text{kg}$ ).

The lowest concentration of Nap in ivy leaves was at one of the farthest locations from the industrial complex, namely, BJ (4.57  $\mu\text{g}/\text{kg}$ ), while the lowest concentration in stems was at the site FJ (11.79  $\mu\text{g}/\text{kg}$ ), which is the closest to the industrial complex. These discrepancies were the first signals that the main source of pollution in the complete municipality (metallurgical and the heating plant) cannot be considered as the only source of Nap pollution in the investigated area.

At 4 out of 9 locations the values for factor R were greater than 1: FJ (2.05), BN (1.39), SN (1.28), and O (1.70) (Figure 1). In the case of phenanthrene, in the study of Papludis *et al.* [11] at the same locations, R factor was also elevated at the sites SN and O, which confirms the greatest atmospheric influence of both compounds at depicted sites. Other sites had very low values for the calculated R factor. All these facts further point that PI from the investigated area may assimilated Nap from different spheres – from the atmosphere, but also from the soil. Further, pollution of atmospheric origin can be ascribed (in different extents) not only to the metallurgical and heating plants but also to domestic heating in rural sites, as well as to the traffic, which is in constant increasing in recent years.

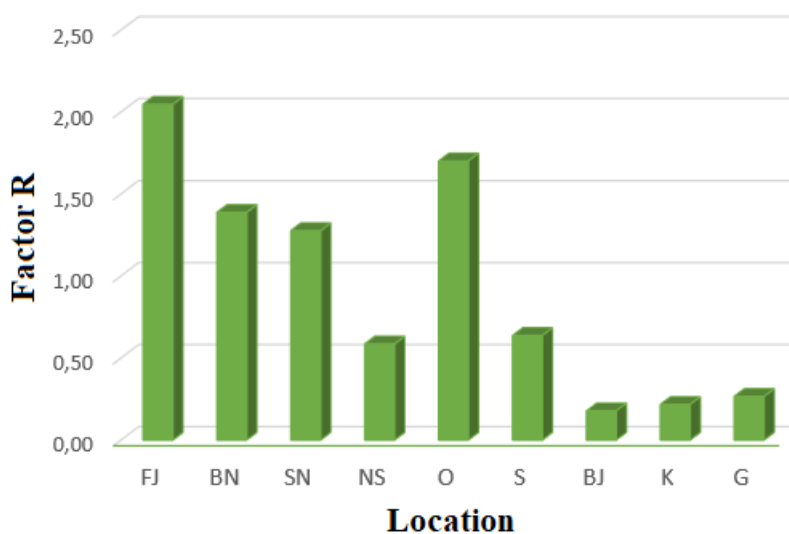


Figure 1 The calculated values for factor R at examined sites

## CONCLUSION

The most important conclusions of this work are as follows:

1) Based on the obtained values for the factor R, it can be said with certainty that Nap content in the investigated plant parts came not only from the atmosphere but also from the soil. The biggest atmospheric contribution was confirmed in the case of sites such as: FJ (R=2.05), BN (R=1.39), SN (R=1.28), and O (R=1.70).

2) The mining and metallurgical complex (smelter and city heating plant) cannot be considered as the only source of pollution in the area of the town of Bor and its surroundings; other sources are most likely: domestic heating and traffic.

## ACKNOWLEDGEMENTS

*The research presented in this paper was done with the financial support of the Ministry of Science, Technological Development and Innovation of the Republic of Serbia, within the funding of the scientific research work at the University of Belgrade, Technical Faculty in Bor (contract number 451-03-65/2024-03/200131), and at the University of Nis, Faculty of Science and Mathematics in Nis (contracts numbers 451-03-66/2024-03/200124, and 451-03-65/2024-03/200124).*

## REFERENCES

- [1] Tuhuloula A., Altway A., Juliastuti, S.R., *et al.*, Earth Environ. Sci. 175 (2018) 012014.
- [2] Paraíba L.C., Queiroz S.C.N., Maia A., *et al.*, Sci. Total Environ. 408(16) (2010) 3270–3276.
- [3] Travkin V.M., Solyanikova I.P., Processes 9(11) (2021) 1862.
- [4] Alagić S.Č., Maluckov B.S., Radojičić V.B., Clean Technol. Environ. Policy 17(3) (2015) 597–614.
- [5] Agoun-Bahar S., Djebbar R., Nait Achour T., *et al.*, Environ. Technol. 40(28) (2019) 3713–3723.
- [6] Mendes G.P., Magalhães V.M.A., Soares, L.C.R., *et al.*, J. Environ. Sci. 90 (2020) 67–77.
- [7] ECB, 2003. European Chemicals Bureau, “Naphthalene, Summary Risk Assessment Report” Institute for Health and Consumer Protection, European Communities (2003).
- [8] Available on the following link: <https://www.atsdr.cdc.gov/ToxProfiles/tp67-c6.pdf>.
- [9] Buckpitt A., Kephelopoulos S., Koistinen K., *et al.*, WHO Guidelines for Indoor Air Quality: Selected Pollutants, World Health Organization, Geneva (2010), p.157, ISBN: 978 92 890 0213 4.
- [10] Yost E.E., Galizia A., Kapraun D.F., *et al.*, Environ. Health Perspect. 129(7) (2021) 76002.
- [11] Papludis A.D., Alagić S.Č., Milić S.M., *et al.*, 11<sup>th</sup> International Conference on Renewable Electrical Power Sources, November 2–3. 2023, Belgrade, Serbia (2023) 239–243.
- [12] Papludis A., Alagić S., Milić S., *et al.*, Zaštita materijala 64(1) (2023) 13–21.



## APPLE PEEL AS A BARRIER TO PESTICIDES MIGRATION INTO DEEPER FRUIT PARTS

Darko Anđelković<sup>1</sup>, Milica Branković<sup>2\*</sup>

<sup>1</sup>University of Niš, Faculty of Agriculture, Kosančićeva 4, 37000 Kruševac, SERBIA

<sup>2</sup>University of Niš, Faculty of Sciences and Mathematics, Department of Chemistry,  
Višegradska 33, 18000 Niš, SERBIA

\*milica.chem@outlook.com

### Abstract

*Apple fruit is frequently exposed to pesticide treatment, especially in the latest stages of apples production. When a pesticide gets the fruit, its interaction with the cuticle and the cuticular waxes starts via absorption mechanisms. Sorption behavior, that ultimately depends on the pesticide and the peel waxes characteristics, tends to affect the fate of the pesticide as well as its persistence in the fruit. This laboratory scaled study was designed to determine the residue levels of four fungicides and one insecticide in apple fruit's part after pesticides application by immersion in solution of commercial pesticides and fruits 3-day storage. The results showed that pesticides migrated in the deeper fruit parts to some extent, but peel has retained most of them.*

**Keywords:** fruit, sorption, fungicides, insecticides.

### INTRODUCTION

A specific morphology defines fruit peel as a natural barrier to xenobiotics, limiting the degree of their migration into deeper sections of the fruit. Main contributors to such features are peel waxes, however the expression of antimigration properties depends on fruit type, pesticides application conditions or pesticides chemical structure. Satisfying antimigration properties of apple and grape peel were observed for chlorpyrifos-methyl migration, where significant amounts of the pesticide remained in peel [1]. Such outcome was observed for apple and grape, but not for strawberry peel, confirming the dependence of peel antimigration properties on the fruit type. Another study showed partial restriction of grape peel towards the migration of 8 pesticides from different chemical classes, meaning that some pesticides amounts were detected in grape pulp, however the majority was found in the peel [2]. The same study revealed the migration degree depends on pesticides migration tendencies (systemics/non-systemics) and on the application solution (pesticides mixture vs single solutions).

Pesticides migration into apple fruit can be explained via following major stages [3]: The migration starts when pesticide formulation reaches peel layer consisted of epicuticular waxes. The waxes have role of reducing fruit surface wettability and consequently the degree of pesticides formulation retention and contact time with the fruit. In this stage main factors affecting cuticular permeability are abiotic factors such as air moisture and temperature or pesticides formulation additives. Pesticides dissolution and diffusion primarily takes place in



the amorph regions of the cuticula, then in the layers made of intracuticular waxes and cutin. The last stage of the migration is pesticides molecules desorption from the inner cuticula and sorption to the epiderm cells.

The objective of this study was to evaluate apple peel retention properties towards five pesticides regularly used in apple crops protection. Pesticides were applied to apple fruit from commercial formulations in laboratory scaled experiments.

## MATERIALS AND METHODS

### Chemicals

High purity pesticide standards of trifloxystrobin, bifenthrin and boscalid were obtained from Sigma-Aldrich<sup>®</sup> (Germany). High purity pesticide standards of pyrimethanil and cyprodinil were obtained from AccuStandard<sup>®</sup> (USA). High purity dibutyl adipate (DBA) used as internal standard (IS) was purchased from Sigma-Aldrich Chemie<sup>®</sup> (Germany). HPLC grade ethanol, HPLC grade hexane and HPLC grade methanol were purchased from Fisher Scientific (USA). SELECTRA<sup>®</sup> (octadecyl, bulk form) was purchased from UCT (USA). Florisil<sup>®</sup> (60–100 mesh) was purchased from LGC Promochem (Germany).

The following commercial formulations of pesticides were used: *Botrystock*<sup>®</sup> - pyrimethanil (Stockton Crop Protection AG, Swizerland), *Cormax*<sup>®</sup> – cyprodinil (Shanghai Mio, China), *Bosco*<sup>®</sup> – boscalid (Ningbo Synagrochem, China), *Zato 50 WG*<sup>®</sup> – trifloxystrobin (Bayer AG, Germany) and *Talstar 10 EC*<sup>®</sup> – bifenthrin (FMC Corporation, USA).

### Appliances

In sample preparation procedure, following appliances were used: balance KERN KB 2000-2N, Germany (acc.  $\pm 0.01$  g); food processor TEFAL 0.9L BL142A; Manifold SPE system Waters<sup>®</sup>, USA; centrifuge Thermo Scientific Jouan C4i and TurboVap<sup>®</sup> LV evaporator, Zymark USA.

### Experimental setup

Apples of the *Granny Smith* variety, similar in shape, mass and maturity stage, were chosen at the open-air market (JP “Tržnica”, city of Niš, Serbia). The average mass of 15 apple units used in this study was  $153.64 \pm 8.89$  g. Apples were cleaned from any visible dirtiness by wiping. Pesticides sorption was studied by soaking each apple unit in 300 mL of aqueous solution fortified with five pesticides with final concentration of  $150 \text{ mg L}^{-1}$  in a 500 mL glass beaker. The submersion period was 2.00 minutes. Each submersion was performed in triplicates. Immediately after submersion has finished, the excess of immersion solution was removed from apple surface by 2–3 times short immersion in tap water and wiping, after which apples were peeled. Pesticides in-peel starting concentration was determined right after the submersion, without any fruit storage. Pesticides migration was tested after 1 h, 3 h, 24 h i 72 h of fruit storage at room temperature in open air. The first 3 and another 3 layers of pulp were peeled along with the peel and analyzed after each storing period.



### Sample preparation

The complete peel mass obtained from apple unit was homogenized by blending after which a 10 g-sub portion was weighted for analysis. Each portion was mixed with 20 mL of water and additionally blended. The resulting mixture was transferred to a glass container and subjected to liquid-liquid extraction with two 10 mL-portions of hexane. Four millilitres of the obtained hexane extract were subjected to the SC, SE/LTP procedure to remove waxes, as detailed in Andelković *et al.* [4]. Afterwards, partially cleaned-up extract was subjected to a SPE procedure to remove pigments. The SPE cartridge was filled with 500 mg of C<sub>18</sub>, then with 500 mg of Florisil<sup>®</sup> and at last with another 500 mg of C<sub>18</sub>, thus creating a three-layered form. Prior to sample extract loading, the column was conditioned with 3 mL of methanol. Then, 1 mL of previously obtained methanol extract was loaded. The elution of analytes was performed with 2 mL of methanol, while the pigmentation was retained on the C<sub>18</sub> part of the column. The obtained eluate was evaporated to dryness, re-dissolved in 0.50 mL of DBA hexane solution (1 µg mL<sup>-1</sup>), and subjected to GC-MS analysis.

### Instruments and instrumental parameters

Instrumental analysis was performed on Agilent 6890 gas chromatograph equipped with 5973 Mass Selective Detector (MSD) and 7683 autosampler and SGE 25QC2/BPX5 0.25 capillary column (25 m × 0.22 mm × 0.25 µm, non-polar). The mass spectra were recorded under an electron ionization (EI) voltage of 70 eV. The gas chromatograph was operated in the splitless injection mode (purge time 1 min). The oven temperature was programmed from 90°C (hold time 0 min) to 280°C (4 min) at 20°C min<sup>-1</sup> rate; post run: 300°C (2 min). Helium was the carrier gas with constant flow rate of 1.0 mL min<sup>-1</sup>. The target compounds were identified and confirmed at scan mode (*m/z* 50–400) and analyzed at selected ion monitoring (SIM) mode. Both data acquisition and processing were accomplished by Agilent MSD ChemStation<sup>®</sup> D.02.00.275 software. Samples quantification was performed with pesticides calibration standards in the concentration range 2.00–10.00 mg kg<sup>-1</sup>.

## RESULTS AND DISCUSSION

Pesticides mass applied by fruit soaking, calculated by multiplying in-peel determined pesticide amount and peel mass, was presumed as the starting in-fruit pesticides mass (100%). Two-minutes soaking period resulted in applied pesticides amount ranging from 12.710 mg kg<sup>-1</sup> (trifloxystrobin) to 118.628 mg kg<sup>-1</sup> (bifenthrin); none of pesticides was detected in pulp fractions (Table 1). Fruit storage resulted in decreased in-peel pesticides amount. After 72 h of storage in-peel pesticides amount ranged from 5.891 mg kg<sup>-1</sup> (pyrimethanil) to 23.594 mg kg<sup>-1</sup> (bifenthrin). Storage has also resulted in pesticides detection in pulp layers (first 3 layers; 3–4 mm of depth) (Table 1). Over 72 h the amount of pyrimethanil in pulp increased from 0.425 mg kg<sup>-1</sup> to 1.847 mg kg<sup>-1</sup>. Other analytes did not show any obvious trend in in-pulp amount, but the amounts were measurable, except from trifloxystrobin, with in-pulp amount reaching methods limits of quantification after 72 h.

Bearing in mind that soaking procedure was performed with highly concentrated pesticides solution, pesticides were expected to be also detected in deeper pulp layers. Therefore another 3 pulp layers were peeled and analysed, contributing to the total tested depth of 7–8 mm. In

these layers, pesticides become detectable after 24 h of storage (Table 1). Pyrimethanil and cyprodinil amounts were 0.222 and 0.104 mg kg<sup>-1</sup>, respectively. Other pesticides amounts ranged between methods limits of detection and limits of quantification. After 72 h of storage the amounts of pyrimethanil and cyprodinil raised to 0.834 and 0.129 mg kg<sup>-1</sup>, respectively. Trifloxystrobin was not detected and the amounts of bifenthrin and boscalid ranged between methods limits of detection and limits of quantification for pulp matrix.

**Table 1** Pesticide amount in peel and in the first 3 layers of pulp, right after fruit soaking for 2 min in 150 mg L<sup>-1</sup> pesticides mixture solution and after different storage periods

Storage period, h	Amount	Pyrimethanil	Cyprodinil	Trifloxystrobin	Bifenthrin	Boscalid
<b>Peel</b>						
0	mg kg <sup>-1</sup> (RSD, %)	19.027 (29.68)	15.224 (35.06)	12.710 (29.35)	118.628 (34.60)	21.513 (40.11)
1	mg kg <sup>-1</sup> (RSD, %)	16.306 (35.71)	11.234 (32.32)	9.907 (37.27)	29.154 (40.85)	17.781 (29.46)
3	mg kg <sup>-1</sup> (RSD, %)	16.339 (8.37)	12.302 (25.24)	10.700 (22.81)	25.397 (36.56)	21.637 (8.10)
24	mg kg <sup>-1</sup> (RSD, %)	13.150 (38.92)	13.355 (32.86)	11.334 (24.43)	32.654 (37.06)	20.928 (39.12)
72	mg kg <sup>-1</sup> (RSD, %)	5.891 (27.52)	8.903 (27.96)	9.247 (17.41)	23.594 (21.30)	19.094 (4.95)
<b>Pulp</b>						
0	mg kg <sup>-1</sup> (RSD, %)	n.d.	n.d.	n.d.	n.d.	n.d.
1	mg kg <sup>-1</sup> (RSD, %)	0.425 (22.66)	0.344 (15.01)	0.061 (17.57)	0.226 (14.77)	0.097 (2.16)
3	mg kg <sup>-1</sup> (RSD, %)	0.386 (25.42)	0.397 (15.63)	0.116 (25.40)	0.280 (46.48)	0.197 (38.69)
24	mg kg <sup>-1</sup> (RSD, %)	0.645 (30.60)	0.340 (37.00)	0.090 (17.12)	0.351 (24.44)	0.138 (29.70)
72	mg kg <sup>-1</sup> (RSD, %)	1.847 (5.47)	0.552 (20.56)	0.044 (26.81)	0.129 (13.81)	0.151 (11.09)

Percentage of pyrimethanil retained in peel, decreases from starting 100% to 78% after 1 h and to 28% after 72 h of storage (Figure 1), due to pesticide migration into pulp layers and evaporation from the fruit surface. After 72 h the percentage of pyrimethanil mass in the first 3 mm of pulp is close to that in peel and reaches 26%. The percentage of pyrimethanil assumed to be lost via the evaporation ranged from 20 to 30%. Distribution of cyprodinil mass after 1 h and 3 h of storage is similar to that of pyrimethanil (Figure 1). After 24 h and 72 h of storage the percentage of cyprodinil mass retained in peel is 80 and 55, respectively. The percentage of mass found in the first 3 mm of pulp is 6 and 10, respectively. It can be assumed that over 72 h of storage cyprodinil mass distribution is uniform, that is it primarily takes place between peel and pesticide loss via the evaporation. Trifloxystrobin and boscalid were majorly retained in peel, with the percentages of 70 and 60, respectively. Since these pesticides were practically not detected in pulp fractions, it was assumed that the rest of the amount was lost via the evaporation (Figure 1). Bifenthrin stand out, with the highest applied mass. Then, the percentage of bifenthrin mass retained in peel was the lowest among masses of other pesticides; it was around 20% over the entire storage period. Bifenthrin percentage in

the first 3 mm of pulp ranged from 0.5 to 0.8, suggesting that the majority of the pesticide had been evaporated from the fruit surface prior to any penetration (Figure 1).

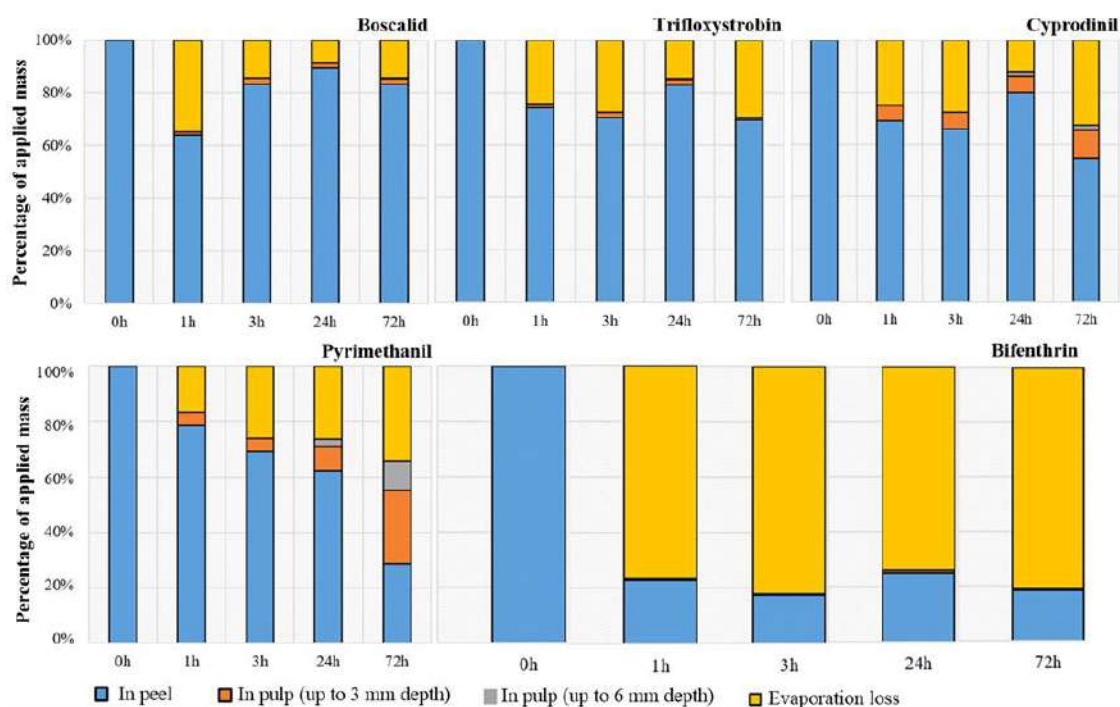


**Figure 1** Percentages of total applied pesticides masses in fruit parts and assumed to be evaporated from fruit surface

## CONCLUSION

Apple peel retained most of the applied pesticides. The percentage of total applied pesticides mass in peel after 72 h of fruit storage was higher than 60% for trifloxystrobin and boscalid, higher than 50% for cyprodinil and around 30% for pyrimethanil. The in-peel mass of bifenthrin was around 20% of the total mass. However, the rest of 80% did not penetrate into the pulp, but evaporated from fruit surface. The highest penetration ability had pyrimethanil, reaching ~30% of the total mass in pulp fractions after 72 h.

## ACKNOWLEDGEMENT

*This work was supported by the Ministry of Education, Science and Technological Development of the Republic of Serbia (contract numbers 451-03-66/2024-03/200124 and 451-03-65/2024-03/200383).*

## REFERENCES

- [1] Riccio R., Trevisan M., Capri E., Food Addit. Contam. 23(7) (2006) 683–692.
- [2] Lagunas-Allué L., Sanz-Asensio J., Martínez-Soria M.T., Food Control 51 (2015) 85–93.
- [3] Giacinti G., Raynaud C., Simon V., Pesticide Interactions with Foodstuffs: Case study of Apple *in* Pesticides in Crop Production: Physiological and Biochemical Action, Editors:

Srivastava P.K., Pratap Singh V., Singh A., Singh S., Prasad S.M., Tripathi D.K., John Wiley & Sons Canada, Limited (2020) p.195–214, ISBN: 9781119432197.

[4] Andelkovic D., Brankovic M., Kocic G., *et al.*, Biomed. Chrom 34(1) (2020) e4720.



## PERFORMANCES OF QuEChERS BASED GC-MS AND LC-MS/MS METHODS FOR PESTICIDES ANALYSIS IN APPLES

Darko Anđelković<sup>1</sup>, Milica Branković<sup>2\*</sup>

<sup>1</sup>University of Niš, Faculty of Agriculture, Kosančićeva 4, 37000 Kruševac, SERBIA

<sup>2</sup>University of Niš, Faculty of Sciences and Mathematics, Department of Chemistry,  
Višegradska 33, 18000 Niš, SERBIA

\*milica.chem@outlook.com

### Abstract

*The diversity and complexity of fruits and vegetables content remains the main challenge in pesticides monitoring in these matrices. At this point, the established sample preparation method is QuEChERS and its two modifications - the acetate-buffered version or AOAC 2007.01 certified method and the citrate-buffered version or EN 15662 certified method. The aim of the study was to evaluate the performances of both QuEChERS modifications, followed by the two most common analytical techniques in pesticides analysis in complex matrices, GC-MS and LC-MS/MS. A review of methods validation parameters confirms that mass spectrometry-based methods combined with the two established QuEChERS sample preparation procedure modifications have satisfactory selectivity and sensitivity for the analysis of pesticides in complex samples.*

**Keywords:** AOAC 2007.1, EN 15662.

### INTRODUCTION

The diversity and complexity of fruits and vegetables content remains the main challenge in pesticides monitoring in these matrices. Consequently, various sample preparation methods have been developed, each one with the same goal, to generate consistent high-quality results of multiresidue analysis in many plant matrices at lowest possible pesticides concentration. At this point, the established sample preparation method is QuEChERS. Owing to the simple steps, QuEChERS is time effective and less prone to errors, thus it represents a streamlined approach to assess pesticides residues in food. The original version was developed in 2003 [1]. Organic phase separation was performed by the addition of MgSO<sub>4</sub> and NaCl. In later attempts, the method has been modified to expand both analytes and commodity range by introducing buffers, which led to better recovery of some pH-sensitive analytes. Consequently, two buffered versions have been established, the acetate-buffered version or AOAC 2007.01 certified method and the citrate-buffered version or EN 15662 certified method. The last step of the QuEChERS is the dispersive solid phase extraction (d-SPE), originally performed with primary-secondary amine (PSA) as a sorbent for impurities collection. Nowadays, there are numerous combinations of PSA and other sorbents.

The aim of the study was to evaluate the performances of both buffered QuEChERS versions, followed by GC-MS and LC-MS/MS analysis. Targeted analytes were five pesticides mostly used in apple production in Serbia - pyrimethanil, cyprodinil (fungicides,

anilino-pyrimidines), boscalid (fungicide, pyridine-carboxamides), trifloxystrobin (fungicide, strobilurin) and bifenthrin (insecticide, pyrethroids).

## MATERIALS AND METHODS

### Chemicals and appliances

High purity standards of pyrimethanil and cyprodinil were purchased from AccuStandard<sup>®</sup>, USA. Formic acid (98%), acetic acid (99.8%) and high purity standards of boscalid, trifloxystrobin and bifenthrin were purchased from Sigma-Aldrich<sup>®</sup>, Germany. HPLC grade methanol and acetonitrile were produced by J.T. Baker, USA; ammonium-formate (98%), HPLC grade deionized water, ethanol and hexane were produced by Carlo Erba, Italy. Prepacked QuEChERS extraction pouches (*Package 1*: 0.5 g of anhydrous sodium acetate and 2 g of anhydrous MgSO<sub>4</sub>; *Package 3*: 1 g of NaCl, 4 g of MgSO<sub>4</sub>, 1 g of trisodium citrate dihydrate and 0.5 g disodium hydrogen citrate) and dispersion kits (*Package 2*: 50 mg PSA, 50 mg C<sub>18</sub> and 150 mg MgSO<sub>4</sub>); *Package 4*: 25 mg PSA and 150 mg MgSO<sub>4</sub>) were produced by Hillium, USA. Syringe microfilters (Nylon Hydrophilic 0.22 μm) were produced by Membrane Solutions, USA.

For high purity standards weighing procedures analytical balance Sartorius BP110S (Germany) was used. In sample preparation procedure following appliances were used: peeler and slicer (China), balance (acc. ±0.01 g) KB 2000-2N KERN (Germany), kitchen blender 0.9L BL142A TEFAL (France), centrifuge Jouan C4i Thermo Scientific (USA), syringe microfilter Nylon Hydrophilic 0.22 μm, Membrane Solutions (USA). Apples of Granny Smith variety were purchased in a local supermarket.

### Sample preparation

One-kilogram batch of Granny Smith apple variety was chopped and additionally homogenized by blending.

MET-GC-Q: Acidified acetonitrile (5 mL) and *Package 1* were added to the representative sample subportion of 5 g and extraction by shaking was performed (1 min). The mixture was centrifuged (3500 rpm, 1 min). *Package 2* was added to 1 mL of the supernatant. The mixture was shaken and centrifuged (3500 rpm, 1 min). The supernatant was concentrated 5 times by evaporation. Solid residue was dissolved in hexane, microfiltered (Nylon 0.22 μm) and analyzed.

MET-LC-Q: Acetonitrile (10 mL) was added to the representative sample subportion of 10 g and extraction by shaking was performed (1 min). *Package 3* was added, after which strong shaking was performed to prevent lumps formation. The mixture was additionally shaken for 1 min and centrifuged (3000 rpm, 5 min). *Package 4* was added to 1 mL of the supernatant. The mixture was shaken and centrifuged (3500 rpm, 1 min). The supernatant was microfiltered (Nylon 0.22 μm) and analyzed.

### Validation

Validation procedure included the evaluation of the matrix effect (ME), methods trueness and precision and limits of detection (<sub>m</sub>LOD). The ME was evaluated by calculating the slopes of calibration curves developed by the standards prepared in matrix extract and in solvent and combining them into the formula:  $S_m/S_s \times 100\%$ , ( $S_m$  – the slope in matrix;



$S_s$  – the slope in solvent). Trueness and precision were determined by analyzing procedural standards (in 5 replicates), with spiking levels equal to 0.10; 1.00 and 5.00 mg kg<sup>-1</sup>. Limits of detection were evaluated by analyzing procedural standards in concentration range adjusted to each analyte (MET-GC-Q) and in range 0.005 – 0.075 mg kg<sup>-1</sup> for each analyte (MET-LC-Q). The obtained linear regression parameters were combined into the formula:  $3 \times A/S$  ( $A$  – the standard deviation of the intercept;  $S$  – the slope of the calibration function).

### Instruments and instrumental parameters

**MET-GC-Q:** Analysis was performed on Agilent 6890 gas chromatograph equipped with 5973 Mass Selective Detector (MSD) and 7683 autosampler and SGE 25QC2/BPX5 0.25 capillary column (25 m × 0.22 mm × 0.25 μm, non-polar). The mass spectra were recorded under an electron ionization (EI) voltage of 70 eV. The gas chromatograph was operated in the splitless injection mode (purge time 1 min). The oven temperature was programmed from 90°C (hold time 0 min) to 280°C (4 min) at 20°C min<sup>-1</sup> rate; post run: 300°C (2 min). Helium was the carrier gas with constant flow rate of 1.0 mL min<sup>-1</sup>. The target compounds were identified and confirmed at scan mode ( $m/z$  50–400) and analyzed at selected ion monitoring (SIM) mode. Both data acquisition and processing were accomplished by Agilent MSD ChemStation® D.02.00.275 software.

**LC-MS/MS analysis:** Analysis was performed on instrumental configuration comprising autosampler Surveyor (Thermo Finnigan, USA), MS pump Accela 1250 (Thermo Scientific, USA) and LTQ XL mass spectrometer equipped with ESI probe and linear ion trap analyzer. Ten μL of the sample was loaded on column (Hypersil GOLD™, 3 μm, 175 Å, 150 mm × 2.1 mm, Thermo Fisher Scientific, USA) in a partial loop injection mode and eluted with a mixture of: eluent A (solution of 0.30% of FA and 0.01% of AMF in water) and eluent B (MeOH) following the gradient: 0 min (50% B), 0–13 min (50–75% B), 13–15 min (75% B), 15–16 min (75–100% B), 16–19 min (100% B), 19–20 min (100–50% B), 20–25 min (50% B) with flow equal to 300 μL min<sup>-1</sup>. Mass analysis was performed in multiple reaction monitoring (MRM) mode including qualitative and quantitative transition, under optimized parameters of ion source, ion optic and ion detection system of the mass spectrometer.

**Table 1** Overview of the main features of methods MET-GC-Q and MET-LC-Q

Method	Sample preparation	Instrumental configuration	Mass analysis (ionization/analyzer/mode)
MET-GC-Q	Acetate buffered QuEChERS (αSPE: PSA + C <sub>18</sub> )	Autosampler HP 7683 (Hewlett-Packard, USA), Gas chromatograph HP 6890 (Hewlett-Packard, USA), Mass spectrometer HP 5973 (Hewlett-Packard, USA)	EI / Single quadrupole / SIM mode (MS <sup>1</sup> analysis)
MET-LC-Q	Citrate buffered QuEChERS (αSPE: PSA)	Autosampler Surveyor (Thermo Finnigan, USA), MS pump Accela 1250 (Thermo Scientific, USA), Mass spectrometer LTQ XL/LTQ Orbitrap (Thermo Electron Corporation, USA) with (Heated) ESI probe (HESI)	ESI / Linear ion trap / MRM mode (MS <sup>2</sup> or MS <sup>3</sup> analysis)



## RESULTS AND DISCUSSION

The selected variants of QuEChERS method (AOAC 2007.1 and EN 15662 with PSA in the dSPE step) are applicable to the analysis of fruits and vegetables with high acid and wax content. Figure 1 illustrates the steps of the both procedures applied for the preparation of Granny Smith apple samples. After the step of solid-liquid extraction with acetonitrile, the addition of salt packages facilitates phases separation (Figures 1 A2, B2). Acetonitrile extract freezing (AOAC 2007.1 procedure, Figure 1 B4) shows the presence of significant amount of water even after  $\text{MgSO}_4$  was used, suggesting the need for the extract carrier exchange to hexane prior to GC/MS analysis. The d-SPE step of both procedures leads to a partial pigmentation removal (Figures 1 A4, B5).

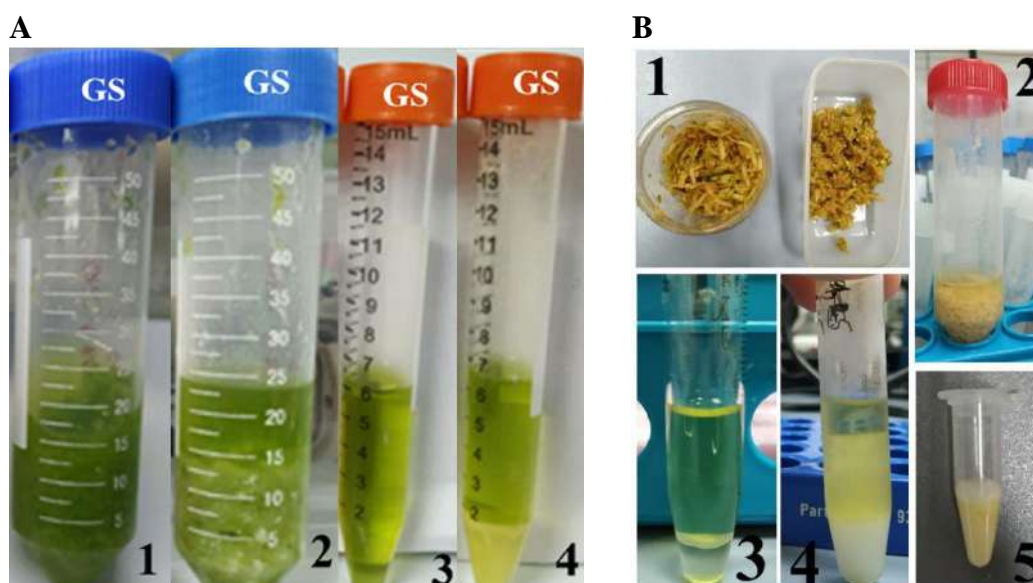


**Figure 1** Illustration of citrate buffered A) and acetate buffered QuEChERS procedure B) through steps: A) 1. after the extraction with AcN; 2. after mixing with citrate salts; 3. after centrifugation; 4. extracts after the dSPE; B) 1. homogenized sample; 2. after the extraction with AcN; 3. after centrifugation; 4. after the freezing step; 5. after the dSPE step

**The matrix effect.** Acetate buffered QuEChERS followed by GC-MS analysis results in significant positive ME for each tested analyte, reaching up to 450% (pyrimethanil, cyprodinil). Citrate buffered QuEChERS followed by LC-MS/MS analysis results in moderate negative ME for 4 analytes (-10 to -30%) and in significant negative ME for bifenthrin (-70 %). The opposite ME in ESI/MS from that in GC-MS analyses is expected due to the different mechanism of the ME manifestation. Such significant ME meaning altered analytes response, if not taken into account, can cause uncertainty in pesticides analysis. In practice that means analytes quantification should be performed in blank matrix extract rather than in solvent.

**Trueness and precision.** Methods trueness and precision were assessed by spiking apple peel with known concentration of analytes in the earliest sample preparation phase, then by sample treatment and analytes quantification, considering the ME. Calculated trueness was compared to the trueness criteria of the SANTE validation guidelines [2]. Methods trueness is

satisfactory if analytes recovery ranges from 70–120% with the relative standard deviation (RSD) less than 20%. If a method meets the criteria, quantification results do not need to be corrected for the calculated trueness. According to the SANTE guidelines, satisfactory trueness can be broadened to the range 30–140% if the RSD is still less than 20%.

MET-GC-Q trueness (Table 2) ranges from 18% (bifenthrin) to 87% (pyrimethanil). Coefficients of variation (average precision) suggest there is not any dependance of method trueness on pyrimethanil, trifloxystrobin and bifenthrin concentration. However, RSD is higher than 60% for cyprodinil and boscalid. The cause of this variation is much lower pesticides recovery for 0.10 mg kg<sup>-1</sup> spiking level when compared to the recovery for other two levels. MET-LC-Q trueness (Table 2) ranges from 84% (bifenthrin) to 96% (trifloxystrobin). Coefficients of variation (average precision) suggest there is not any dependance of method trueness on analytes concentration. Somewhat higher RSD was observed for pyrimethanil. Pyrimethanil trueness ranged from 69% (0.10 mg kg<sup>-1</sup>) to 128% (1.00 mg kg<sup>-1</sup>).

**Limits of detection.** To compare LODs to pesticides MRLs, calculated LODs (mg kg<sup>-1</sup> of peel) were re-calculated to the mass of fruit, considering a 10% peel contribution to the mass of fruit. LOD of each tested analyte is below set MRLs. MET-GC-Q and MET-LC-Q LODs are 3 to 10 000 and 10 to 37 500 times lower than the set MRLs.

*Table 2 Methods validation parameters overview*

Method	Analyte	1. mLOD, mg kg <sup>-1</sup>	2. MRL, mg kg <sup>-1</sup>	Ratio 2./1.	Average trueness, %	Average precision, %
MET-GC-Q	Pyrimethanil	0.0015	15.00	10000	87.31	19.71
	Cyprodinil	0.0013	2.00	1538	43.71	67.26
	Trifloxystrobin	0.0027	0.70	260	60.86	16.70
	Bifenthrin	0.0030	0.01	3.33	18.12	34.33
	Boscalid	0.012	2.00	166	41.09	75.74
MET-LC-Q	Pyrimethanil	0.0004	15.00	37500	94.65	31.94
	Cyprodinil	0.0004	2.00	5000	93.17	19.97
	Trifloxystrobin	0.0004	2.00	5000	95.80	20.41
	Bifenthrin	0.0005	0.70	1400	84.28	3.09
	Boscalid	0.0010	0.01	10	93.73	5.93

## CONSLUSION

A review of methods validation parameters confirms that mass spectrometry-based methods combined with the two established QuEChERS sample preparation procedure variations have satisfactory selectivity and sensitivity for the analysis of pesticides in complex samples such as fruits. Pre-defined amounts of the d-SPE sorbents, widely used for fruits sample clean-up, did not completely remove the co-extractives (pigments, acids). This has probably affected pesticides response in sample extracts, since significant alterations have been observed – positive and negative matrix effect in GC-MS and LC-MS/MS analysis, respectively. Additionally, acetate buffered QuEChERS resulted in half-aqueous extract, requiring an additional step of extract carrier exchange prior to GC-MS analysis. Both methods have limits of detection lower than the established MRLs, but MET-LC-Q method, combining citrate buffered QuEChERS and LC-MS/MS analysis resulted in higher analytes recovery and better repeatability than MET-GC-Q method, suggesting the superior accuracy.

## **ACKNOWLEDGEMENT**

*This work was supported by the Ministry of Education, Science and Technological Development of the Republic of Serbia (contract numbers 451-03-66/2024-03/200124 and 451-03-65/2024-03/200383).*

## **REFERENCES**

- [1] Anastassiades M., Lehotay S.J., Štajnbaher D., *et al.*, J. AOAC Int. 86(2) (2003) 412–431.
- [2] European Commission. Analytical Quality Control and Method Validation Procedures for Pesticide Residues Analysis in Food and Feed: SANTE/12682/2019. *Available on the following link:* [https://www.eurl-pesticides.eu/docs/public/tmpl\\_article.asp?CntID=727](https://www.eurl-pesticides.eu/docs/public/tmpl_article.asp?CntID=727).



## COMPARISON OF PESTICIDES STABILITY STORED IN TWO SOLVENTS OF DIFFERENT VISCOSITY

Darko Anđelković<sup>1</sup>, Milica Branković<sup>2\*</sup>

<sup>1</sup>University of Niš, Faculty of Agriculture, Kosančićeva 4, 37000 Kruševac, SERBIA

<sup>2</sup>University of Niš, Faculty of Sciences and Mathematics, Department of Chemistry,  
Višegradska 33, 18000 Niš, SERBIA

\*milica.chem@outlook.com

### Abstract

*Stability of pesticide stock solutions used in pesticide residue analysis is crucial for accomplishing reliable data on pesticide presence and quantification in actual samples. This study was conducted to determine pesticides solution stability during a chosen storage period. The investigation included nine pesticides (fluazifop-p-butyl, S-metolachlor, chlorpyrifos, alpha-cypermethrin, bifenthrin, difenoconazole, pyriproxyfen, buprofezin and dimethoate) and two storage solvents of different density, kept for 34 days in refrigerator at 4°C. During this period, a decline in pesticide response is observed. For most pesticides, visible decline was observed after the first 6 or 12 days of storage, after which the decline was less pronounced or not observed at all in the solvent of higher viscosity. Although the stability of pesticide stock solutions is affected during storage, high density solvents can moderate the degradation rate.*

**Keywords:** ethanol, cyclohexanol, storage.

### INTRODUCTION

Pesticide residue analysis is essential in the evaluation of human and environmental exposure to pesticides. To accomplish reliable data on pesticide presence in the sample and their quantification, laboratories should regularly check the stability of stock standard solutions and replace them which is time-consuming. Factors that can affect pesticide storage stability include storage temperature, storage period, pesticides physical and chemical properties and in particular matrix properties [1]. The aim of the study was to evaluate pesticides degradation rate stored in ethanol and in cyclohexanol. Cyclohexanol has about 40 times higher viscosity than ethanol and a melting point at 26°C. When stored at low temperatures, cyclohexanol reaches a solid gel-alike state. Consequently, it was assumed that pesticides should degrade less when stored in such solvent, due to a limited mobility of molecules. The study was investigated with nine pesticides of different chemical classes.

### MATERIALS AND METHODS

#### Chemicals

Cyclohexanol (99% purity) and analytical standards of nine pesticides i.e., fluazifop-p-butyl, S-metolachlor, chlorpyrifos, alpha-cypermethrin, bifenthrin, difenoconazole, pyriproxyfen, buprofezin and dimethoate were produced by Sigma-Aldrich,

USA. Formic acid (FA) (98%) and quinoline (98%) were produced by Sigma-Aldrich®, Germany. Ammonium-formate (AMF) (98%) and deionized water were produced by Carlo Erba, Italy. HPLC grade ethanol and methanol (MeOH) were produced by J.T. Baker, USA.

### **Samples preparation**

Pesticides analytical standards were dissolved in ethanol to a final concentration of 100 µg mL<sup>-1</sup>. Two types of single pesticide working solutions were prepared; one type was ethanol, and another was cyclohexanol solution. Each solution type was prepared in 10 replicates with final concentration of each pesticide equal to 10 µg mL<sup>-1</sup>. Each standard also contained 1 µg mL<sup>-1</sup> of internal standard (quinoline) used for the correction of any instrument variation.

### **Appliances**

For high purity standards weighing procedures analytical balance Sartorius BP110S, Germany was used. Nitrogen (99%) was supplied by nitrogen generator PEAK N32 Scientific, Scotland, UK.

### **Instruments and instrumental parameters**

Instrumental analysis was performed on LC/MS system comprising of Accela autosampler and Accela MS pump (Thermo Fisher Scientific, USA) and TSQ Quantum Ultra mass spectrometer (Thermo Finnigan, USA) with ESI ionization source and triple quadrupole analyzer. Analytes were separated on a Hypersil GOLD column (C<sub>18</sub>, 150 mm × 2.1 mm, particle size 3 µm), ionized in ESI+ ionization mode and monitored in MS<sup>1</sup> full scan mode (scan range *m/z* 150–600, 3 micro scans, scan time 1s). Data was acquired and analyzed by Quantum Tune Master software, version 1.4.1.

Ten microliters of sample were loaded on column in partial loop injection mode and eluted with a mixture of: eluent A (buffer solution - 0.1% of FA and 0.03% of AMF in water) and eluent B (MeOH) following the gradient: 0 min (50% A), 0–12 min (35% A), 12–13 min (20% A), 13–15 min (20% A), 15–16 min (0% A), 16–19 min (0% A), 19–20 min (50% A), 20–25 min (50% A) with flow equal to 200 µL min<sup>-1</sup>. Ion optic parameters were optimized according to each pesticide pseudo-molecular ion. Tuned ion source parameters that meet good detectability for all pesticides, selected for the analysis were as follows: spray voltage was 4000 V, sheath/auxiliary gas pressures were 30/10. The capillary temperature and offset voltage were set at 270°C and 35 V, respectively. Tube lens offset voltage was 140 V.

### **Methodology**

Solutions were analyzed freshly prepared (0 days of storage) and in regular intervals – after 2, 6, 12, 19, 26 and 34 days of storage. Chromatographic peak areas of pesticides, normalized to that of quinoline, were measured each time; any variability (decrease) in chromatographic peak area was assumed to be related with pesticide loss during storage and thus to the decrease in pesticide amount in the solution.



**Figure 1** Ethanol (left) and cyclohexanol (right) standard pesticide solution after being stored at low temperature (4°C)

## RESULTS AND DISCUSSION

Each type of pesticide standard experienced analyte loss during storage. For 5 of 9 analytes the amount decreased exponentially, for the other 4 it decreased linearly (Table 1). Over 34 days of storage amount of **fluazifop-p-butyl**, **bifenthrin**, **pyriproxyfen**, **buprofezin** and **dimethoate** decreased exponentially in both ethanol and cyclohexanol solution (Table 1). Continual moderate decline over the total period was observed for **fluazifop-p-butyl**, **bifenthrin** and **pyriproxyfen** in both types of the solution. Continual loss of **buprofezin** was observed over the total period only in ethanol, while the loss in cyclohexanol was observed in the first 6 days of storage, after which there was no change in pesticide amount. **Dimethoate** loss was more pronounced in the first 12 days of storage in both types of the solution, after which the decline rate dropped in ethanol and stopped in cyclohexanol solution. Fluazifop-p-butyl, bifenthrin, pyriproxyfen, buprofezin and dimethoate amount decline rate was always higher in cyclohexanol than in ethanol. The percentage of the total pesticide loss after 34 days of storage in cyclohexanol ranged from ~30% (buprofezin) to ~85% (dimethoate) (Figure 2). The percentage of the total pesticide loss after the same storage period in ethanol ranged from ~30% (fluazifop-p-butyl) to ~65% (dimethoate) (Figure 2).

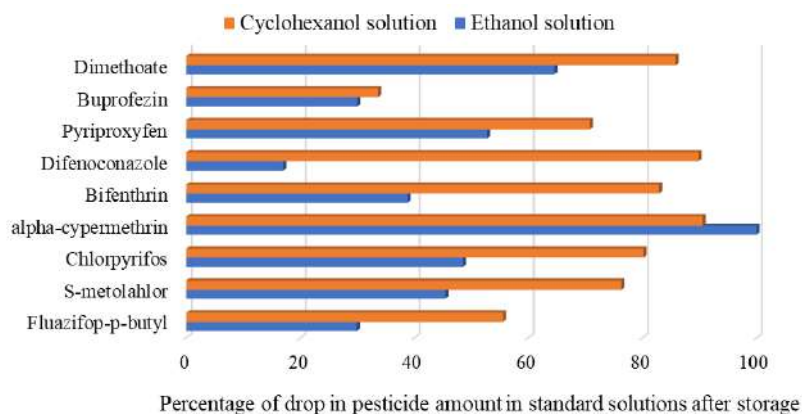


**Figure 2** Percentage of drop in pesticides amount in single pesticide solutions prepared in ethanol and cyclohexanol stored for 34 days



Over 34 days of storage amount of **S-metolachlor**, **chlorpyrifos**, **alpha-cypermethrin** and **difenoconazole** decreased linearly in both ethanol and cyclohexanol solution (Table 1). **S-metolachlor** and **chlorpyrifos** amount declined faster in the first 12 and 6 days of storage, respectively in both solution types. Over that period, the decline rate was about 3 times (**S-metolachlor**) and 7.5 times higher (**chlorpyrifos**) in ethanol than in cyclohexanol solution, respectively. The decline rate of **alpha-cypermethrin** was slightly higher in ethanol solution, leading to a complete pesticide loss after 19 days of storage. In cyclohexanol solution pesticide amount continued to decline with lower rate than in the first 19 days. **Difenoconazole** amount in cyclohexanol solution declined continually at the same rate. In ethanol solution, however, the decline rate was the highest in the first 6 days of storage. In the period between 6<sup>th</sup> and 19<sup>th</sup> day, it dropped by half. In the last days of the tested period (19<sup>th</sup>–34<sup>th</sup> day) the decline rate was ~7 times lower than in the first days of storage. S-metolachlor, chlorpyrifos, alpha-cypermethrin and difenoconazole amount decline rate was always higher in ethanol than in cyclohexanol. However, the total pesticide loss was always higher in cyclohexanol than in ethanol solution, except for alpha-cypermethrin. The percentage of the total pesticide loss after 34 days of storage in ethanol ranged from 17% (difenoconazole) to 100% (alpha-cypermethrin) (Figure 2). The percentage of the total pesticide loss after the same storage period in cyclohexanol ranged from ~75% (S-metolachlor) to ~90% (difenoconazole and alpha-cypermethrin) (Figure 2).



**Table 1** Correlation between pesticides amount and instrumental response measured after the storage

Analyte	Ethanol			Cyclohexanol		
	Type of correlation	Correlation function	The trend	Type of correlation	Correlation function	The trend
Fluazifop-p-butyl	exponential	$y=2\times 10^9 e^{-0.011x}$ , $R^2=0.9094$ (0–34 d)	Continual moderate decline over the entire period	exponential	$y=5\times 10^8 e^{-0.024x}$ , $R^2=0.9496$ (0–34 d)	Continual moderate decline over the entire period
S-metolachlor	linear	$y=-6\times 10^8 x+2\times 10^{10}$ (0–12 d), $R^2=0.9818$ $y=-2\times 10^7 x+1\times 10^{10}$ (12–34 d), $R^2=0.9899$	Continual decline, higher decline rate in the first 12 days	linear	$y=-2\times 10^8 x+4\times 10^9$ (0–12 d), $R^2=0.9650$ $y=-3\times 10^7 x+2\times 10^9$ (12–34 d), $R^2=0.9962$	Continual decline, higher decline rate in the first 12 days
Chlorpyrifos	linear	$y=-3\times 10^7 x+5\times 10^8$ (0–6 d), $R^2=0.9530$ $y=-2\times 10^6 x+3\times 10^8$ (6–34 d), $R^2=0.9536$	Continual decline, higher decline rate in the first 6 days	linear	$y=-4\times 10^6 x+5\times 10^7$ (0–6 d), $R^2=0.9352$ $y=-7.2\times 10^5 x+3\times 10^7$ (6–34 d), $R^2=0.9918$	Continual decline, higher decline rate in the first 6 days
Alpha-cypermethrin	linear	$y=-7\times 10^6 x+2\times 10^8$ (0–19 d), $R^2=0.9558$ n.d. (19–34 d)	Continual decline reaching zero after 19 days of storage	linear	$y=-5\times 10^6 x+1\times 10^8$ (0–19 d), $R^2=0.9827$ $y=-3\times 10^5 x+2\times 10^7$ (19–34 d), $R^2=0.9760$	Continual decline, higher decline rate in the first 19 days
Bifenthrin	exponential	$y=2\times 10^8 e^{-0.015x}$ , $R^2=0.9932$ (0–34 d)	Continual moderate decline over the entire period	exponential	$y=1\times 10^8 e^{-0.051x}$ , $R^2=0.9551$ (0–34 d)	Continual moderate decline over the entire period
Difenoconazole	linear	$y=-1\times 10^7 x+8\times 10^8$ , (0–6 d) $R^2=0.9973$ $y=-5\times 10^6 x+8\times 10^8$ , (6–19 d) $R^2=0.9814$ $y=-7\times 10^5 x+7\times 10^8$ , (19–34 d) $R^2=0.9997$	Continual decline over the total period, with decreasing rates;	linear	$y=-7\times 10^6 x+3\times 10^8$ , $R^2=0.9675$ (0–34 d)	Continual decline over the total period with the same rate
Pyriproxyfen	exponential	$y=1\times 10^9 e^{-0.02x}$ , $R^2=0.9121$ (0–34 d)	Continual moderate decline over the entire period	exponential	$y=5\times 10^8 e^{-0.033x}$ , $R^2=0.9750$ (0–34 d)	Continual moderate decline over the entire period
Buprofezin	exponential	$y=3\times 10^9 e^{-0.01x}$ , $R^2=0.9536$ (0–34 d)	Continual moderate decline over the entire period	exponential	$y=8\times 10^8 e^{-0.052x}$ (0–6 d), $R^2=0.9946$ (0–34 d)	Continual moderate decline in the first 6 days, no change afterwards
Dimethoate	exponential	$y=1\times 10^9 e^{-0.076x}$ (0–12 d), $R^2=0.9952$ $y=5\times 10^8 e^{-0.007x}$ (12–34 d), $R^2=0.9828$	Continual decline, higher decline rate in the first 12 days	exponential	$y=7\times 10^9 e^{-0.146x}$ (0–12 d), $R^2=0.9581$	Continual decline in the first 12 days, no change afterwards

## **CONCLUSION**

In ethanol solution most stable pesticide was difenoconazole with % of loss equal to 17. Fluazifop-p-butyl, bifenthrin and buprofezin experienced moderate loss in amount, with percentage of loss ranging from 30–40%. The other 5 pesticides experienced significant loss in amount ranging from approx. 45% (S-metolachlor) to 100% (alpha-cypermethrin). In cyclohexanol solution the most stable pesticide was buprofezin with % of loss equal to 33. Other pesticides experienced significant loss in amount ranging from 55% (fluazifop-p-butyl) to 90% (alpha-cypermethrin). Similar storage stability was observed in both solvents, however, for several analytes the storage in higher viscosity solvent moderated the degradation rate.

## **ACKNOWLEDGEMENT**

*This work was supported by the Ministry of Education, Science and Technological Development of the Republic of Serbia (contract numbers 451-03-66/2024-03/200124 and 451-03-65/2024-03/200383).*

## **REFERENCES**

[1] Bian Y., Liu F., Chen F., *et al.*, Food Chem. 250 (2018) 230–235.



## TRIHALOMETHANES CONTENT IN HOTEL'S SWIMMING POOLS WATER IN A SOUTH OF MONTENEGRO

Milena Tadić<sup>1</sup>, Irena Nikolić<sup>1</sup>, Dijana Đurović<sup>2,3\*</sup>, Nevena Cupara<sup>2</sup>, Jelka Vuković<sup>2</sup>

<sup>1</sup>University of Montenegro, Faculty of Metallurgy and Technology, Džordža Vašingtona bb,  
81000 Podgorica, MONTENEGRO

<sup>2</sup>Institute of Public Health of Montenegro, Džona Džeksona bb,  
81000 Podgorica, MONTENEGRO

<sup>3</sup>Faculty of Food Technology, Food Safety and Ecology, University Donja Gorica, Oktoih 1,  
81000 Podgorica, MONTENEGRO

\*[dijana.djurovic@ijzcg.me](mailto:dijana.djurovic@ijzcg.me)

### Abstract

*This paper aimed to investigate the content of trihalomethanes (THMs) in swimming pool waters in coastal area of Montenegro since THMs content is one of the main indicators of pool water quality. The both, indoor and outdoor swimming pools were considered. The content of total THMs in all water samples of indoor pools was below the maximum allowed concentration of 100 µg/L prescribed by Montenegrin legislation while content of total THMs in the waters of outdoor pools exceeded the maximum allowed concentration in 27% of the tested water samples. Chloroform, mainly contributed to the total THMs content in waters of swimming pool waters followed by BDCM and DBCM.*

**Keywords:** trihalomethanes, chloroform, bromodichloromethane, dibromochloromethane.

### INTRODUCTION

Disinfection by-products are toxic and carcinogenic compounds, and their formation occurs through the reaction between the disinfectant and organic compounds present in the water. Trihalomethanes (THMs) are the most common disinfection by-products that can be found in drinking water, but also in swimming pool water as chloroform, bromodichloromethane (BDCM), dibromochloromethane (DBCM) and tribromomethane (bromoform) [1]. The formation of disinfection by-products depends on a number of factors, such as: temperature, pH, contact time, inorganic and organic compounds present in the water, the type of organic matters and the concentration and type of added disinfectant [2]. Of course, it is quite clear, when the pools have more users, THMs concentration is higher, due to a increased burden of organic compounds. This indicates that the user's organic matter contributes to the formation of THMs. Value of pH is also very important factor that influencing the THMs content in pools water. It has been reported that the formation of THMs increases in pools with a pH>7.2 [3]. In most countries, THMs are the only disinfection by-products that are included in the list of substances whose presence in drinking water must be controlled and for whose concentrations maximum allowed concentrations are prescribed. The World Health Organization (WHO) [4] recommends maximum permissible values of 100 µg/l for total THMs, which is also transposed in Montenegrin legislation [5], and also for

each THMs compound, namely, 80 µg/l for chloroform, 60 µg/l for BDCM and 100 µg/l for DBCM.

## **MATERIALS AND METHODS**

### **Sampling and analysis**

For the purposes of this work, a total of 23 water samples from indoor and 74 water samples from outdoor hotel pools from 6 municipalities in the southern part of Montenegro (Herceg Novi, Kotor, Tivat, Budva, Bar and Ulcinj) were examined in the period from June to September 2022.

Sampling of pool water was done using glass bottles with a capacity of 1 L, and for total THMs content glass vessels with a cap (Winkler bottles/vessels) with a capacity of 100 to 150 ml, were used. For the purposes of sampling, the Winkler vessel was immersed in a pool to a depth of about 30 cm. The vessel was filled to the top, then removed from the pool and closed tightly with a stopper, so that the water was forced out to remove air bubbles. The samples were stored at room temperature. THM in water samples were analysed by GC/ECD with Head Space (Agilent 7890).

## **RESULTS AND DISCUSSION**

The concentrations of the four analysed THMs: chloroform, bromodichloromethane (BDCM), dibromochloromethane (DBCM) and bromoform, detected in the samples of indoor and outdoor swimming pools of hotel complexes from six municipalities in the Montenegrin coast, are given in Figure 1 and 2. The concentrations of total THMs were in the range of 0.91 to 93.80 µg/L in indoor swimming pools and from 2.19 to 237.18 µg/L in outdoor swimming pools. The average values of THMs content in indoor and outdoor swimming pools were 39.31 µg/L and 67.96 µg/L, respectively. It is evident that the values of total THMs in indoor swimming pools water (Figure 1a) did not exceed the maximum allowed concentration of 100 µg/L prescribed by Montenegrin legislative [5], while in the samples of outdoor pools water total THMs content exceeded values of the maximum allowed concentration in 20 of 74 tested samples (Figure 2a). Evaluation of individual THMs content in swimming pools water indicated the highest content of chloroform, followed by DBCM, BDCM and bromoform for both, outdoor and indoor swimming pools water which is in accordance with the literature data [6]. Bromoform was detected in negligible concentrations only in 2 water samples from indoor and 9 water samples from outdoor pools, while in other samples it was below the detection limit, so the content of bromoform was not considered in this paper.

Chloroform contributes to total THMs content with 87% in the indoor pools (Figure 3) and 86% in the outdoor pools water (Figure 4). Chloroform concentration in indoor pools water ranged from 0.44–87.35 µg/L (Figure 1b) with a mean value of 34.18 µg/L, while in outdoor pools water the chloroform content ranged from 1.13–217.16 µg/L (Figure 2b), with a mean value of 58.69 µg/L. The values of chloroform that exceeded the value of 80 µg/L prescribed by WHO [4] value was detected in several water samples (1 samples of indoor pool waters and 19 samples of outdoor pool water) (Figures 1 and 2). As for the content of BDCM and DBCM, they contribute to the total THMs content with 10% and 3 %, respectively for indoor

pools water (Figure 1) and 10 and 4%, respectively for outdoor pools water. The average content of BDCM and DBCM in indoor pool water samples were 3.93  $\mu\text{g/L}$  and DBCM 1.10  $\mu\text{g/L}$ , respectively and 6.95  $\mu\text{g/L}$  and 2.40  $\mu\text{g/L}$ , respectively for outdoor pools water. The concentrations of these two THMs were below the maximum permissible concentrations recommended by the WHO, of 60  $\mu\text{g/L}$  for BDCM and 100  $\mu\text{g/L}$  for DBCM [4].

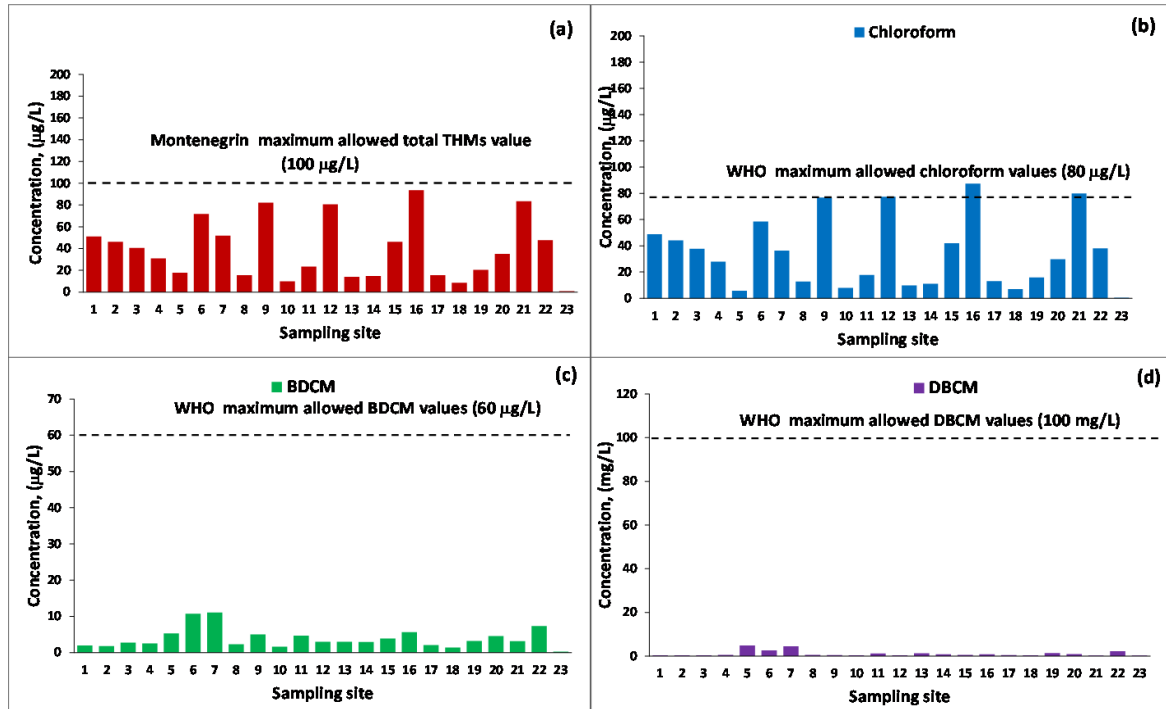


Figure 1 Content of total and individual THMs in indoor pool waters

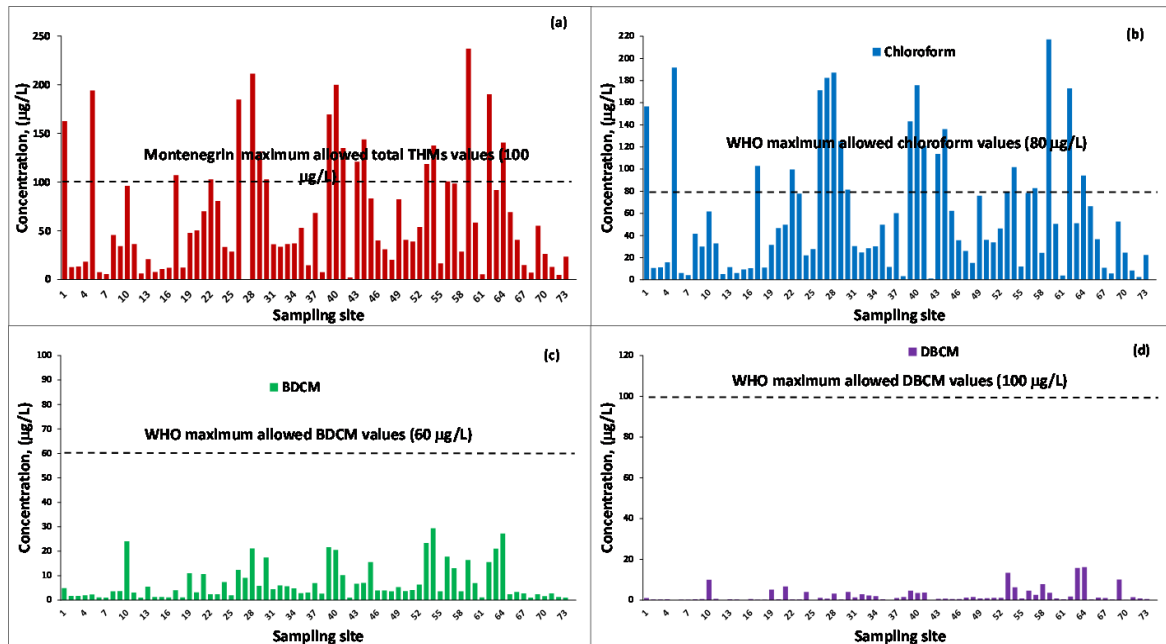
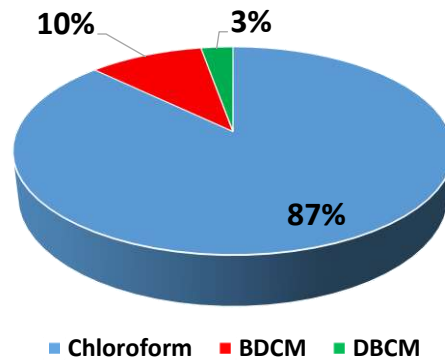
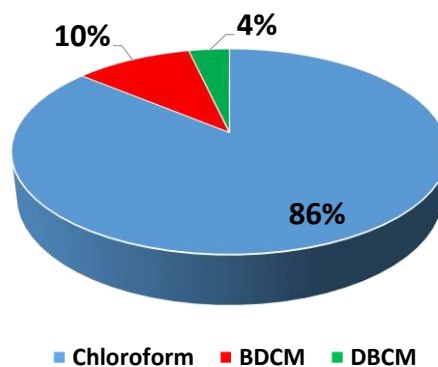


Figure 2 Content of total and individual THMs in outdoor pool waters



**Figure 3** Contribution of individual THMs to total content of THMS for indoor pool waters



**Figure 4** Contribution of individual THMs to total content of THMS for outdoor pool waters

## CONCLUSION

The content of total THMs in all samples of indoor swimming pools water was below the maximum allowed concentration of 100 µg/L prescribed by Montenegrin legislation. On the other hand, the content of total THMs in outdoor swimming pool waters exceeded the maximum allowed concentration in 20 of 74 tested samples. This data is not unexpected, because the sampling was carried out in a summer touristic period, when number of swimmers in outdoor pools is increased, and therefore the concentration of undesirable organic substances that serve as precursors for the formation of THMs, increased as well. Chloroform was the most abundant in total THMs content in both, indoor (87%) and outdoor swimming pools water (86%), followed by BDCM and DBCM.

## REFERENCES

- [1] Lara P., Ramírez, V., Castrillón, *et al.*, Colombia. *Int. J. Environ. Res. Public. Health*. 28 (2020) 4659.
- [2] Teo T.L.L., Coleman H.M., Khan, S.J., *Environ. Int.* 76 (2015) 16–31.
- [3] Carter R.A.A., Joll C.A., *J. Environ. Sci.* 58 (2017) 19–50.
- [4] WHO. World Health Organization, guidelines for drinking-water quality, 4<sup>th</sup> edn. Geneva: WHO; 2021.

- [5] Pravilnik o sanitarno-tehničkim i higijenskim uslovima, kao i uslovima za zdravstvenu ispravnost vode za rekreativne potrebe i druge vode od javnozdravstvenog interesa, SL.Crne Gore, br. 57/2018 i 112/2020.
- [6] Kanan A., Selbes M., Karanfil T., Occurrence and Formation of Disinfection By-Products in Indoor U.S. Swimming Pools *in* Recent Advances in Disinfection By-Products, Editors: Karanfil T., Mitch B., Westerhoff P., Xie Y., ACS Publications p.405–430, ISBN-10: 9780841230767.





## FIRST LINE DEFENCE ANTIOXIDANT ENZYMES IN *Blicca bjoerkna* (LINNAEUS, 1758) FROM THE BELGRADE SECTION OF THE DANUBE RIVER

Jelena S. Vranković<sup>1\*</sup>, Katarina Jovičić<sup>1</sup>, Vesna Đikanović<sup>1</sup>

<sup>1</sup>Department of Hydroecology and Water Protection, Institute for Biological Research  
“Siniša Stanković”, National Institute of Republic of Serbia, University of Belgrade,  
Despot Stefan Blvd 142, 11108 Belgrade, SERBIA

\*jeca.s@ibiss.bg.ac.rs

### Abstract

*The white bream (*Blicca bjoerkna*) is a common fish species in the Danube and is therefore suitable for biomonitoring studies. In this study, the activity of superoxide dismutase and catalase is investigated to evaluate the response of these two biomarkers in the liver of white bream. The fish were collected in the Danube River (Serbia) at two sites with different levels of anthropogenic pollution. The average values of the measured enzymes with a statistical significance of  $p < 0.05$  were higher at the Višnjica site than in the protected area “Veliko Ratno ostrvo”. The results indicate that a certain level of oxidative stress occurred in the fish from Višnjica, suggesting the presence of xenobiotics at this site that stimulate antioxidant enzymes.*

**Keywords:** white bream, liver, antioxidant enzyme.

### INTRODUCTION

Rapid urbanization and industrialization produce numerous pollutants and their derivatives that are released into the environment. Both organic and inorganic substances are found in wastewater and threaten the aquatic environment and the communities living in it [1].

Fish are at the top of the aquatic food chain and are important bioindicators for monitoring the aquatic environment [2]. The effects of fish exposure to sub-lethal levels of pollutants can be measured by their biochemical, physiological or histological responses. Environmental pollutants that accumulate in fish tissue can lead to reactions in the body that generate free radicals. When the formation and accumulation of free radicals exceeds the ability of the organism to remove the excess, oxidative stress occurs [3].

Organisms have an antioxidant protection system consisting of enzymatic and non-enzymatic components. This system keeps the level of free radicals at a physiological level and mitigates the harmful effects of their high concentration. Fluctuations in the activity of protective antioxidant enzymes have been proposed as biomarkers of oxidative stress caused by the presence of environmental pollutants. Since the response to oxidative stress is directly related to cell function, biomarkers can indicate the state of environmental pollution [4].

The fish liver is the main detoxification organ and the effects of prolonged exposure to pollutants can be seen at the cellular and tissue level. It is also one of the most affected organs in contaminated waters, but also plays an important role in the physiology of fish [5].

The aim of this study was to investigate whether untreated wastewater from the city of Belgrade can cause oxidative stress and damage in fish from the Danube. To assess the effects of pollution, the activities of the enzymes superoxide dismutase (SOD) and catalase (CAT) in the liver of white bream (*Blicca bjoerkna*) from the two sites Veliko Ratno ostrvo (VRO) and Višnjica (VIS) were analyzed.

## MATERIALS AND METHODS

### Sampling sites

The white bream was caught at two sites in the Belgrade section of the Danube in April 2021. The first site, VRO, is a protected area with no visible sources of pollution and the second site, VIS, is a polluted area with a marina for recreational boats. During the fish collection, some physico-chemical parameters of the water were measured at two sampling sites (Table 1).

**Table 1** Values of some physicochemical parameters in Veliko Ratno ostrvo (VRO) and Višnjica (VIS) on the day of fish collection in situ

Physicochemical parameter	VRO	VIS
Temperature (°C)	9.3	10
pH	8.1	8.3
Dissolved O <sub>2</sub> (mg <sup>-1</sup> )	9.7	9.8

The adult fish (n=7 per sampling point) were transported to the laboratory on the same day in ice-cold containers (0–4°C). The fish were dissected and the livers were quickly removed (Figure 1) and stored at -80°C until enzyme measurement.



**Figure 1** The whole body of the white bream (*Blicca bjoerkna*) and its excised liver

### Antioxidant enzyme measurement

Liver tissue from each fish (100 mg from each liver, n=7) was minced and homogenized in 5 volumes of 25 mmol L<sup>-1</sup> sucrose with 10 mmol L<sup>-1</sup> Tris-HCl, pH 7.5, using an IKA-Werk

Ultra-Turrax homogenizer from Janke & Kunkel (Staufen, Germany) [6] and sonicated for 15 s at 10 kHz on ice [7]. Sonicates were centrifuged at  $100,000 \times g$  for 90 min at  $4^{\circ}\text{C}$ . Protein content and enzyme assays were performed on the supernatant fraction.

Protein content was determined using the Folin–phenol reaction as described by Lowry *et al.* [8], using bovine serum albumin as a standard. The activity of SOD was determined by the epinephrine method [9]. One unit of SOD activity was defined as the amount of protein causing 50% inhibition of the autoxidation of epinephrine and was expressed as U/mg protein. Catalase activity was assessed by the rate of degradation of hydrogen peroxide ( $\text{H}_2\text{O}_2$ ) [10]. The method is based on  $\text{H}_2\text{O}_2$  degradation by the action of CAT contained in the samples tested. In this method, 50 mM phosphate buffer (pH 7.0) and 30 mM  $\text{H}_2\text{O}_2$  were used as substrate. The activity was expressed as  $\mu\text{mol H}_2\text{O}_2/\text{min}/\text{mg protein}$ .

### Statistical analyses

The Kolmogorov-Smirnov test and the Levene test were used to determine the normality of the data and the homogeneity of the variances. Significant differences were analysed using one-way ANOVA and the Tukey HSD comparison test, with  $p < 0.05$  considered significant. All analyses were performed using SAS 9.1.3 software (SAS Institute, Cary, NC, USA).

## RESULTS AND DISCUSSION

The physico-chemical parameters of the water samples from two sites (Table 1) varied within narrow ranges. The specific activities of the investigated antioxidant enzymes in the liver of *B. bjoerkna* from the Danube are shown in Figure 2.

The superoxide dismutase and CAT activities were statistically significantly higher in the VIS fish than in the VRO fish. A more pronounced significant difference ( $p < 0.001$ ) between the two groups was observed in liver SOD activity (Figure 1a) relative to liver CAT activity (Figure 1b). Superoxide dismutase and CAT represent the first line of defence in the process of neutralizing free radicals. Superoxide dismutase catalyses the conversion of the superoxide anion to  $\text{O}_2$  and  $\text{H}_2\text{O}_2$ . The effectiveness of SOD as an antioxidant is based on its cooperation with other enzymes: CAT, glutathione peroxidase and glutathione reductase. Catalase is often one of the first antioxidant enzymes to be activated. It breaks down  $\text{H}_2\text{O}_2$  into  $\text{O}_2$  and water. It has already been shown that an induced increase in CAT and SOD activity leads to a reduction in both free radicals and oxidative damage [11]. Alternatively, the relatively high CAT activity in the liver (~30-fold higher than SOD activity) in the VRO individuals could indicate a durable protection against the cytotoxic effect of  $\text{H}_2\text{O}_2$ .

In the present study, the significant increase in the activities of SOD and CAT enzymes in fish from the VIS area could be related to pollutants that increase the production of free radicals, leading to oxidative stress. Normally, a simultaneous induction of SOD and CAT activities is observed when exposed to pollutants [12]. Since the VIS site is exposed to the discharge of the largest wastewater collector in the city of Belgrade [13], higher activity levels of SOD and CAT were observed at this site, suggesting a “cooperative” mechanism of the two enzymes. However, this relationship is not always observed and is known to be species-dependent [14].

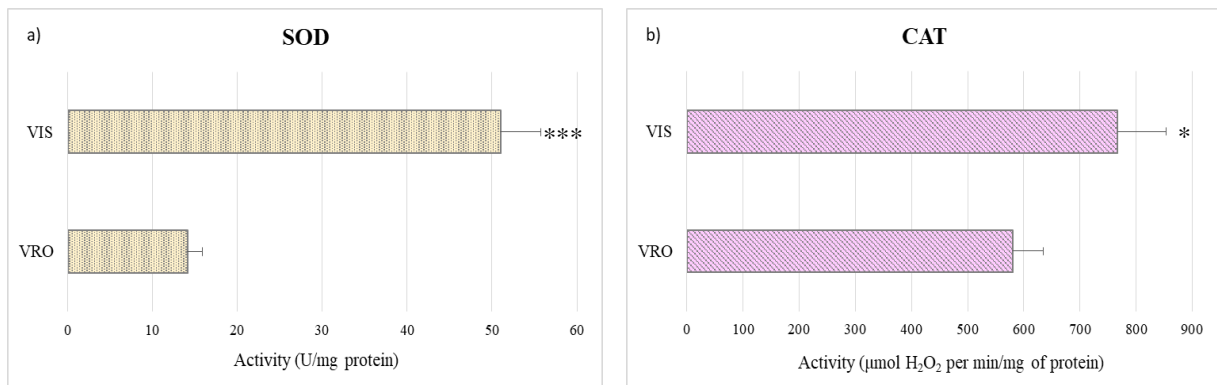


**Figure 2** a) Activity of superoxide dismutase – SOD; b) catalase - CAT in the liver of white bream (*Blicca bjoerkna*) from Veliko Ratno ostrvo (VRO) and Višnjica (VIS). Data are presented as mean + SD (n=7 for each site). Significant differences between the VRO and VIS samples were calculated by one-way ANOVA and marked with an asterisk, \* $p < 0.05$ ; \*\*\* $p < 0.001$

As the changes in the cell antioxidant defenses reflect the exposure to contaminants and/or their toxicity, all of them may be useful biomarkers in monitoring aquatic ecosystems [15]. Various xenobiotics which are discharged daily into water bodies can induce free radicals production in fish, consequently, a response of antioxidative defenses [16]. When the free radicals production exceeds the basal cell levels and surpassed the defense capacity of the cell the oxidative stress occurs [17]. Several classes of pollutants are capable of enhancing the formation of free radicals and thereby provoke oxidative stress. Some of these pollutants include polychlorinated biphenyls, polycyclic aromatic hydrocarbons, phenols and heavy metals [18].

## CONCLUSION

The results of this work show that pollution of the aquatic environment leads to a change in the physiological response of fish. This is reflected in the increase in SOD and CAT activities at the VIS site and confirms that this site is under anthropogenic pressure. The presence of certain pro-oxidant pollutants that may lead to oxidative stress in the fish at the VIS point and the biomarkers of oxidative stress may be important to evaluate the impact of untreated waste on living organisms in the Danube.

## ACKNOWLEDGEMENT

The authors are grateful to the Ministry of Science, Technological development and Innovation of the Republic of Serbia for financial support according to the contract with the registration number 451-03-66/2024-03/200007.

## REFERENCES

- [1] Bashir I., Lone F.A., Bhat R.A., *et al.*, Bioremed. Biotechnol. 27 (2020) 1–26.
- [2] Meng H., Lin Y., Zhong W., *et al.*, Water. 15 (2023) 399.
- [3] Livingstone D.R., Rev. Med. Vet. 154 (2003) 427–430.
- [4] Jena K.B., Verlecar X.N., Chainy G.B.N., Mar. Pollut. Bull. 58 (2009) 107–113.

- [5] Stoyanova S., Georgieva E., Velcheva I., *et al.*, *Water* 12 (2020) 1837.
- [6] Rossi M.A., Cecchini G., Dianzani M.U., *Med. Sci-Biochem.* 11 (1983) 805–806.
- [7] Takada Y., Noguchi T., Okabe T., *et al.*, *Cancer Res.* 42 (1982) 4233–4235.
- [8] Lowry O.H., Rosebrough N.J., Farr A.L., *et al.*, *J. Biol. Chem.* 193 (1951) 265–275.
- [9] Misra H.P., Fridovich I., *J. Biol. Chem.* 247 (1972) 3170–3175.
- [10] Claiborne A., *CRC Handbook of Methods for Oxygen Radical Research*, CRC Press, Boca Raton, (1985), pp. 283–284.
- [11] Carvalho C.S., Bernusso V., Araújo H.S.S., *et al.*, *Chemosphere* 89 (2012) 60–99.
- [12] Peixoto F.P., Carrola J., Coimbra AM., *et al.*, *Rev. Int. Contam. Ambient.* 29 (2013) 29–38.
- [13] Kostić-Vuković J., Kolarević S., Kračun-Kolarević M., *et al.*, *Environ. Monit. Assess.* 193 (2021) 465.
- [14] Ferreira M., Moradas-Ferreira P., Reis-Henriques M.A., *Aquat. Toxicol.* 71 (2005) 39–48.
- [15] Monteiro D.A., Rantin F.T., Kalinin A.L., *Ecotoxicol.* 19 (2010) 105–123.
- [16] Ruas C.B.G., Carvalho C.S., Araújo H.S.S., *et al.*, *Ecotoxicol. Environ. Safe.* 71 (2008) 86–93.
- [17] Tagliari K.C., Vargas V.M.F., Zimiani K., *et al.*, *Environ. Toxicol. Phar.* 17 (2004) 149–157.
- [18] Van der Oost R., Beyer J., Vermeulen N.P.E., *Environ. Toxicol. Phar.* 13 (2003) 57–149.





## RECUITIVATION OF RTH FLOTATION TAILINGS IN BOR, SERBIA

Miomir Mikić<sup>1\*</sup>, Radmila Marković<sup>1</sup>, Vesna Marjanović<sup>1</sup>, Radmilo Rajković<sup>1</sup>,  
Milenko Jovanović<sup>1</sup>

<sup>1</sup>Mining and Metallurgy Institute Bor, Albert Ajnštajn 1, 19210 Bor, SERBIA

\*miomir.mikic@irmbor.co.rs

### Abstract

*Degraded areas were formed by depositing flotation tailings at the location of RTH near Bor, in Serbia. The final contour of the flotation tailings was projected, and it is at the elevation K +390 m above sea level. In order to protect the environment, protection measures are taken at the flotation tailings by recultivation of all degraded areas. For this purpose, an analysis will be performed to determine the optimal method of recultivation. In order to prevent air pollution and erosion of tailings material through torrents and its transport to the surrounding land, special attention is paid to the possibility of afforestation and greening of degraded areas by deciduous and coniferous species. In this way, i.e. by applying biological reclamation, seedlings of birch, and juniper, are planned. The alternating combination of these plant species enables the binding of the substrate and gives a beautiful aesthetic appearance to the environment.*

**Keywords:** recultivation, degraded areas, afforestation and greening.

### INTRODUCTION

The RTH (Mine body H – Rudno Telo H) flotation tailings pond (Figure 1) was formed southeast of the Bor flotation in the excavation area of the RTH open pit. After the excavation, space of the open pit RTH was filled, and due to the need to increase the volume of the storage area, the flotation disposal site was expanded to the northwest and southeast in the former valley of the Bor river. The river valley in the northwest towards the smelter slag disposal site and the abandoned open pit Bor was blocked by Dam 1 (Figure 1). Downstream, the valley of the Bor river is blocked by dam 2 (Figure 1). On the eastern side, the flotation tailings pit abuts the Eastern landfill of open pit Bor, and on the western side of the flotation tailings, a perimeter embankment has been erected.

The general characteristics of the soil of the flotation tailings in the area of Bor are lighter mechanical composition, degraded structure, high porosity and water permeability, mostly low humus content, dominance of fulvic acids over humic acids, low pH, high hydrolytic and exchangeable acidity of the soil and lower cation exchange capacity, high concentrations of arsenic (As) and copper (Cu) and low microbiological activity.

Compared to natural soils, the characteristic of flotation tailings soils is that they have a significantly lower content of the clay fraction, worse structural characteristics, lower cation exchange capacity values, lower humus content and less favorable humus absorption (dominance of fulvic acids over humic acids).

Based on the analysis of the flotation tailings, several conclusions were reached [1]:

- At dams 1 (one) and 2 (two) and the perimeter embankment of the RTH flotation tailings, uniform technogenic material prevails. Morphologically, this material consists of fine sand. This type of substrate conditions a poor water-air regime for plant development.
- In certain places on the dam where the sulfur sulfide oxidation processes have not progressed, the flotation tailings have a pH value of around 6. This flotation material has a neutral reaction with high values of active phosphorus and a complete lack of potassium.
- In the places where the oxidation of sulphur to sulphide took place the pH value of the substrate is about 3.
- The lack of clay particles with organic matter in the flotation tailings makes the substrate unfavorable for self-renewal and the development of plants on it. Particles of clay and humus in the flotation tailings serve to activate the work of the soil microflora and initiate the pedological processes of creating humus and accessible elements of plant nutrition. For these reasons, soil material rich in humus is added to the substrate.
- By introducing organic matter into the substrate in the form of humus, the microbiological process is accelerated and a continuous flow of plant assimilates is enabled for the development of grass cover and bushy types of plants foreseen by biological recultivation.



*Figure 1* Spacial representation of the location of the flotation tailing RTH

## DEGRADED AREA

The new project addresses the elevation of the dam from elevation K+378 to elevation K+390. Based on the projected state of the flotation tailings, with an elevation up to K+390, the surface area of the flotation tailings RTH, which will be treated by recultivation, was measured (Table 1). Total degraded area projected for recultivation is 551.200 m<sup>2</sup>.



**Table 1** Degraded areas

Area object	Area, m <sup>2</sup>	
	Flat	Slope
K+385 – beach	414.000	
K+390/385 – internal slope		25.700
K+390 – kruna brane	16.800	
K+390/378 – spoljašnja kosina brane		94.700
Total	<b>430.800</b>	<b>120.400</b>
	<b>551.200</b>	

## CHOICE OF RECULTIVATION METHODS

Due to the condition of the surfaces after the disposal of the flotation tailings and the specific pedological, microclimatic and climatic conditions, for the recultivation of the RTH flotation tailings, optimal recultivation with grassing is foreseen.

Based on the physical and chemical properties of the flotation deposit, the shape of the surfaces of the hydrotechnical facilities at the RTH flotation tailings pond and the preparation of the surfaces using the technical phase of reclamation, the biological phase of reclamation comes into consideration, namely:

- Weeding on the outer slopes of the dam;
- On the crown of the dam, afforestation and grassing;
- On the inner slopes of the dam, alternating belts of grass and shrub vegetation;
- Weeding and afforestation on dried areas of the storage area (beaches);

Reclamation works consist of two phases:

1. Technical phase of reclamation,
2. Biological phase of recultivation.

The phase of technical reclamation consists of the planning of soil material on damaged surfaces. The purpose of this layer - soil, is to cover the plateau, crown and slope of the flotation tailings dam. Agrotechnical works include all works on the preparation of the applied layer of soil for weeding.

The biological phase includes a complex of biotechnical and phytoremediation measures on prepared surfaces in order to restore the phyto-ecosystem. The biological phase will include grassing and afforestation of degraded areas.

## SELECTION OF CULTURES FOR RECULTIVATION IN RELATION TO NATURAL AND ECONOMIC CONDITIONS

Taking into account the factors that influence biological recultivation, and above all the quality of the substrate (substrate), i.e. physico-chemical properties, habitat conditions and exposure of the tailings to the south, then the continental climate and the high proportion of winds from the WNW and NW, a combined method of afforestation was chosen and weeding of the flotation tailings pond. The choice of plant species was also limited.

Based on the above, the project seeks to favor the ecological functions of future forest-meadow ecosystems through biological recultivation. The mentioned future anthropogenically created ecosystems should provide a relatively healthy environment with healthy air, aesthetic impressions of landscape units with a rich color of grouped mixed different types of deciduous trees.

The characteristics of flotation tailings-flotisol are such that it has unfavorable chemical properties because it lacks clay particles and organic matter, which would activate the work of soil microflora and initiate pedological processes and the initial creation of humus, as well as providing accessible nutritional elements.

Acidic soil increases the mobility of heavy metal ions and their accumulation in plants in an amount greater than allowed. For a  $\text{pH} < 6.5$  in the soil, the mobility of Cd ions increases [2]. For  $\text{pH} < 5.5$ , the mobility of Ni, Mn, Zn, Co and Al ions increases, while for  $\text{pH} < 4$ , the mobility of Cu and Pb ions increases [2].

For these reasons, high-quality soil humus material is necessary on the degraded surfaces of the flotation tailings, i.e. the application of the technical and agrotechnical recultivation phase, which has the task of forming a layer by applying a cover (soil material) at a height of 0.5 m.

### **TECHNICAL RECULTIVATION**

As part of the technical reclamation, in order to ensure the execution of the works, several operations will be carried out, namely:

1. leveling degraded surfaces,
2. planning of soil material according to projected areas,
3. agrotechnical works.

### **BIOLOGICAL RECULTIVATION**

The biological phase of optimal recultivation is the application of phytomelioration measures on the previously prepared soil substrate (degraded surface) in order to establish and survive vegetation for the later formation of a stable ecosystem. The greening of the degraded area has primarily the role of environmental protection, and at the same time contributes to a better appearance of the environment and a better microclimate of the area.

A biological method of recultivation will be applied for the greening of degraded areas at the site in question, namely:

1. Sowing a mixture of grasses 49 kg/ha: Red fennel (50%), English rye (35%), Yellow star (10%), White clover (5%)
2. Woody plants: *Betula alba* L. (birch) – a total of 47,974 seedlings, *Acer campestre* L. (juniper) – a total of 4787 seedlings.

On the outer slope of the flotation tailings pond, only grass is planned. It will be done using hydroseeding. The other areas will be grassed using agricultural machinery. After weeding, the next phase is afforestation.

The planting of trees, chub, on the internal slopes of the dam will be done according to a triangular scheme at a distance of 3 m between the seedlings. This means that about 1100 seedlings can be planted on one hectare. The planting of trees on the crown of the dam will be done in two rows, with a space of 4 m wide for the road, 6 m between these rows. Birch seedlings are planted at a distance of 3 m. The total number of seedlings per hectare is about 1100.

For the beach of the flotation tailings, afforestation was designed according to a mosaic layout. At the same time, birch and chub are planted according to a square pattern at a distance of 3 m between the seedlings. In this way, about 96% of the area will be forested, while the rest will be the space reserved for the road (4%) for the passage of machinery.

Works on the formation, i.e. the raising of green areas on the beach consists of the formation of individual mosaics that will consist of shrubby and woody plants. Woody plants (birch) will be used within one mosaic. Planting will be done two meters from the edge at a distance of 3 m between seedlings (square scheme). In this way, about 1100 seedlings will be planted per hectare. Seedlings aged 2+1 will be used for planting.

Bushy vegetation (clump) will be used for roundabouts. Planting will be done two meters from the edge at a distance of 3 m between seedlings (square scheme). In this way, about 1100 seedlings will be planted per hectare. Seedlings aged 2+1 will be used for planting.

## **CONCLUSION**

The goal of recultivation of flotation tailings is to restore the ecological integrity of disturbed areas. Revegetation is the most widely accepted and useful way of recultivating mining facilities in order to reduce material erosion and protect the soil from degradation.

The same must be done with plants selected based on their ability to survive and regenerate in the local environment, and on their ability to stabilize the soil structure.

The success, efficiency, and recultivation of flotation tailings are conditioned by the correct determination of the chemical, physical and biological properties of the soil.

Compaction, low water holding capacity, bulk density, lack of micro and macro nutrients and associated rooting limitations are the main factors limiting tailings productivity. Also, a high level of potential acidity (low pH) severely limits the productivity of the tailings pond. The acidity of tailings requires the planting of metal-resistant plants, which can grow in nutrient-deficient soils with elevated metal content. Planting different types of grasses, trees, which are rotated with legumes and indigenous species due to their adaptation to the lack of nutrients and fast-growing properties, will allow soil fertility to be restored and ecological succession to be accelerated.

The specificity of man-made soils is the irregular distribution of some characteristics by soil depth (porosity, humus content and microbiological activity), which is a consequence of their man-made origin.

The recultivation of degraded areas at the RTH flotation tailings is aimed at preserving the environment, and with the application of the foreseen technical and biological measures, good results can be expected despite the unfavorable basic substrate. In this case, no economic

profit is expected from the plantations, but only the protection of damaged soil from erosion and the improvement of the microclimate. In addition, the root system of seedlings and leaves that fall and rot on degraded surfaces will initiate pedological processes in the direction of humus creation.

### **ACKNOWLEDGEMENT**

*The authors are grateful to the Ministry of Science, Technological development and Innovation of the Republic of Serbia for financial support according to the contract with the registration number 451-03-66/2024-03/200052.*

### **REFERENCES**

- [1] Dopunski rudarski projekat nadvišenja flotacijskog jalovišta RTH. Institut za rudarstvo i metalurgiju Bor, 2022.
- [2] M. Miljković, Uticaj površinske eksploatacije rude metala na ekološke faktore životne okoline, Technical Faculty in Bor, Bor (1998), ISBN: 86-80987-03-4.



## MINING AND THE ENVIRONMENT, ENVIRONMENTAL IMPACT MONITORING PROGRAM FOR FLOTATION TAILING RTH-BOR, SERBIA

**Miomir Mikić<sup>1\*</sup>, Vesna Marjanović<sup>1</sup>, Radmila Marković<sup>1</sup>, Milenko Jovanović<sup>1</sup>,  
Radmilo Rajković<sup>1</sup>**

<sup>1</sup>Mining and Metallurgy Institute Bor, Albert Ajnštajn 1, 19210 Bor, SERBIA

\*miomir.mikic@irmbor.co.rs

### Abstract

*Because mining, dumping, and tailings can generate waste and radioactive consequences, society must develop methods for successfully treating mining waste from mine dumps, tailings, and abandoned mines. Several characteristics, including background contamination from natural sources related to mineral deposits, contamination from industrial activities in three-dimensional subsurface space, a problem with long-term remediation following mine closure, a problem with secondary contaminated areas near mine sites, land use conflicts, and abandoned mines, distinguish it. The paper study on RTH Bor flotation tailings, which is acquiring waste from near by flotation Bor. Considering great potential of RTH Bor on environmental impact it is necessary to establish adequate monitoring program for monitoring the quality of air, water and surrounding land, in order to monitor the quality of the living environment.*

**Keywords:** monitoring, flotation tailing, environmental.

### INTRODUCTION

Mineral resources can serve as critical parts of socioeconomic development and innovative technological materials. Meanwhile, mining has been highlighted as an effective way to eradicate global poverty especially for the remote mountain areas [1]. However, with increasing demand for mineral deposits, the negative impact on the eco-environment is also quickly growing, such as deforestation, habitat and biodiversity loss, forest fragmentation, disruption of food chains, air and water pollution [2]. To quantify mining's impact on the eco-environment, a large number of studies have documented the evaluation of negative impacts during mining, such as the mine environment monitoring, which integrates remote sensing ecological index (RSEI) and ecological index (EI) to investigate mine land use, surface subsidence and vegetation [3–5]. In addition, mine ecological restoration, mainly including environmental pollution and geological disasters control, has also been intensely applied. More recently, the mine eco-environmental survey is also playing a significant role, utilizing multiple methods, including GIS and RS analytical tools, to comprehensively evaluate a series of mine soil, surface water, and underground water problems caused by mining processes [6]. Although these studies have provided important insights for mine eco-environmental evaluation, they commonly only emphasized the current ecological and environmental disturbance caused by mining.

The primary purpose of the monitoring plan is to define the criteria and details for the environmental monitoring plan and implementation in order to quantify the environmental impact of the facility and provide a basis for the decision-making process.

The monitoring plan and the results obtained from its implementation should lead to the achievement of the following specific goals:

- evaluations of compliance of the operator's emissions with the emission limit values defined by the respective laws and by-laws;
- assessments of the implementation of the best available techniques;
- provision of data confirming the implementation of the measures required by the permit;
- provision of data necessary for assessing the impact of the operator's activities on the environment;
- provision of preventive measures to prevent possible environmental pollution that may occur as a result of the operator's activities.

## MINING AND THE ENVIRONMENT

Concerns were raised among the general public regarding the impact that the mining industry may have impact on the environment due to its operations (Figure 1) [7]. This is because people are becoming increasingly aware of the potential adverse effects that these operations may have [8]. The government and the mining sector have collaborated on a number of pieces of legislation aimed at reducing the negative impacts of mining on the surrounding environment before, during, and after mining operations to study environmental impact assessment (EIA) [9]. The effects of mining and its environmental impact is illustrated in Figure 2 where we explored the impact of excessive mining and their effects.

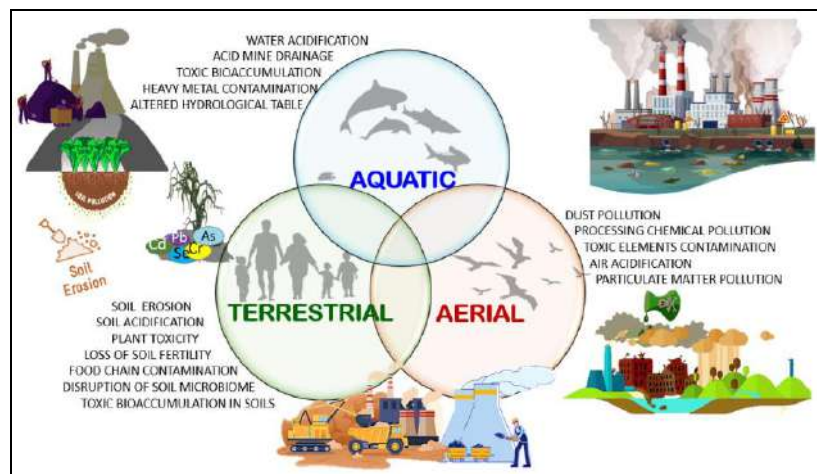


Figure 1 Potential effects of mining and imbalance in different environments [10]

Depending on a number of elements unique to each mine, the extent and character of the repercussions could range from negligible to severe [11]. Some of these include the nature of the ore body, the mining equipment and extraction methods employed, whether or not minerals are processed onsite, and how fragile the local ecosystem is [12]. The negative consequences of mining on the environment are widespread, yet they are often only felt in



small places [13]. In addition to the readily apparent physiological effects that extractive activities have, there is also the potential for air, land, and water contamination. Mining may not be the primary land use that disrupts biological systems [14]. This is because the effects on the environment are cumulative by their varying nature, and other activities or events that occurred in the past may have contributed to these consequences [15].

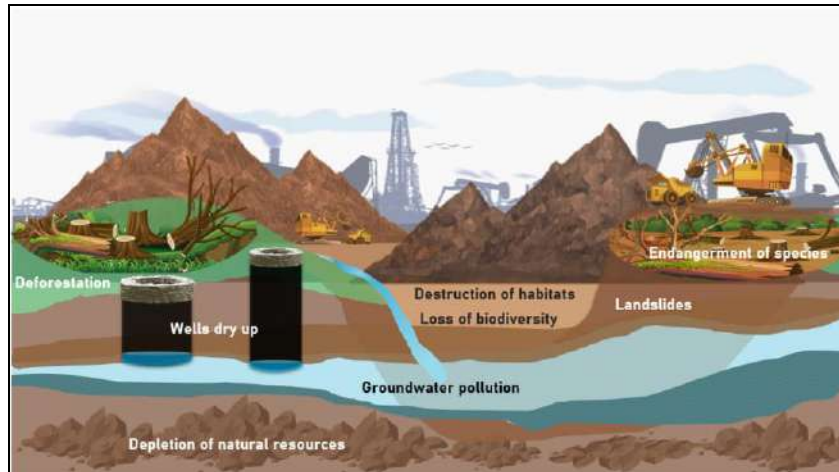


Figure 2 Impact of excessive mining and their consequences in the environment [10]

### STUDY CASE – FLOTATION TAILING RTH BOR

The RTH (Mine body H (**Rudno Telo H**)) flotation tailings pond (Figure 3) was formed southeast of the Bor flotation in the excavation area of the RTH open pit. After the excavation, space of the open pit RTH was filled, and due to the need to increase the volume of the storage area, the flotation disposal site was expanded to the northwest and southeast in the former valley of the Bor river. The river valley in the northwest towards the smelter slag disposal site and the abandoned open pit Bor was blocked by Dam 1 (Figure 3). Downstream, the valley of the Bor river is blocked by dam 2 (Figure 3). On the eastern side, the flotation tailings pit abuts the Eastern landfill of open pit Bor, and on the western side of the flotation tailings, a peripheral embankment has been erected.



Figure 3 Spatial representation of the location of the flotation tailing RTH



## PARAMETERS ON THE BASIS OF WHICH HARMFUL EFFECTS ON THE ENVIRONMENT CAN BE DETERMINED

Study of this paper includes all activities at the RTH flotation tailings pond. Considering the characteristics of the facilities themselves, it can be stated that the active surfaces of the flotation tailings (beach, dams) are the largest emitters of polluting substances at the location in question.

Surface water, as the largest transport medium, should be monitored diligently, in terms of monitoring the water quality of nearby watercourses. Taking into account the location of the flotation tailings and its structural characteristics, it can be concluded that there is a possibility of influence on underground water. Monitoring soil quality will mean monitoring the distribution of heavy metals in the soil in accordance with the wind rose. The flotation tailings pond is a facility where there are no machines and devices that would have a significant impact on increasing the noise level. Apart from the mining machinery that periodically works at this location, there are no other sources of noise.

The measurement of noise emissions into the environment will be monitored, with an emphasis on the area where the concentration of the surrounding population is closest to the mining facilities. The parameters to be monitored on the mentioned entities are shown in Table 1. Disposition of measuring points are shown on Figure 4.

*Table 1 Monitoring parameters*

Location	Frequency of monitoring	Parameters
<b>Waters:</b> <b>Underground piezometer</b> <ul style="list-style-type: none"> <li>(3 referent)</li> </ul>	2 times per year	<ul style="list-style-type: none"> <li>Water temperature, colour, smell, pH, electrical conductivity, sedimentary matter, suspended matter, HPK, BPK5, soluble oxygen, oxygen saturation;</li> <li>Metals, metalloids and their compounds: Cr, As, Cd, Pb, Zn, Hg, Ni, Fe, Cu, Mn</li> <li>Sulfates; Cyanides; Nitrates, nitrites; Mineral oils and hydrocarbons; Total fats and oils.</li> </ul>
<b>Air</b> <ul style="list-style-type: none"> <li>Measuring points are placed near private houses in the south, east, southwest of the proposed location</li> </ul>	<ul style="list-style-type: none"> <li>Sedimentation matter - monthly</li> <li>Suspended particles - daily samples, twice a year (summer and winter period, 30 days each);</li> </ul>	<ul style="list-style-type: none"> <li>Total sediments: amount of sediments,</li> <li>Suspended particles: PM10, PM2.5</li> <li>content of heavy metals (Cr, As, Cd, Pb, Zn, Hg, Ni, Fe, Cu, Mn)</li> </ul>
<b>Noise:</b> Measuring points in the vicinity of the nearest private buildings (northeast and east)	1 per year	<ul style="list-style-type: none"> <li>Equivalent intensity level, daily measurements</li> <li>Equivalent level-intensity, night measurements</li> </ul>
<b>Soil:</b> <ul style="list-style-type: none"> <li>The measuring points are located on the surrounding areas to the southeast, northeast and east of the subject location</li> </ul>	1 per year	<ul style="list-style-type: none"> <li>Humus content</li> <li>Soil pH</li> <li>calcium carbonate, nitrogen, electrical conductivity; phosphorus;</li> <li>Metals: As, Cd, Pb, Zn, Hg, Ni, Fe, Cu</li> <li>Sulfates; Fluorides; Chlorides; Nitrites, nitrates, Cyanides. Aromatic organic compounds.</li> </ul>



Figure 4 Disposition of measuring points

## CONCLUSION

Mining activity has increased significantly due to significant population growth and worldwide demand for mineral resources [16]. This increase coincides with a new awareness in which environmental issues have become an increasing challenge for all actors in the sector [17,18]. There is an increased social demand for sustainable development of all activities related to mining, especially adequate management of waste products during each phase of the mining process, including prospecting and research, development, extraction, transportation and treatment of the obtained products, *etc.* [19]. Energy requirements, environmental and human health risks, water resource requirements and required technology must be taken into account [20].

Taking these arguments into account, the monitoring system gains great importance. The monitoring system collects and interprets the information necessary to determine whether the environmental protection management plan and related systems have been effectively implemented, and whether the environmental goals set by the company, the authorities and the community have been properly met.

The monitoring system should consist of: identification of pollution sources and parameters, selection of environmental parameters for which measurements are made, determination of critical areas and data collection, analysis and assessment. The goal of the environmental monitoring system is to analyze the sources of pollution while considering the effectiveness of the applied environmental protection measures.

## ACKNOWLEDGEMENT

The authors are grateful to the Ministry of Science, Technological development and Innovation of the Republic of Serbia for financial support according to the contract with the registration number 451-03-66/2024-03/ 200052.

## REFERENCES

- [1] Yang H., Yang W., Zhang J., *et al.*, *Sci. Adv.* 4 (3) (2018) eaao6652.
- [2] Sovacool B.K., Ali S.H., Bazilian M., *et al.*, *Science* 367(6473) (2020) 30–33.
- [3] Enshe D., Hongsheng Z., *Re. Sci.* 03 (2008) 440–445.
- [4] Islam K., Vilaysouk X., Murakami S., *Resour. Conserv. Recycl.* 154 (2020) 104630.
- [5] Mengjing L.I., Xiaoqin, W., Aifang, X., *et al.*, *J. Fuzhou Univ. Nat. Sci. Ed.* 48(02) (2020) 230–235.
- [6] Majzlan, J., Plášsil, J., Škoda, R., *et al.*, *Environ. Sci. Tech.* 48 (23) (2014) 13685–13693.
- [7] Xu Y., Bi R., Li Y., *Ecotoxicol. Environ. Saf.* 249 (2023) 114436.
- [8] Wang P., Sun Z., Hu Y., *et al.*, *Sci. Total Environ.* 695 (2019) 133893.
- [9] Petersen S., Krätschell A., Augustin N., *et al.*, *Mar. Pol.* 70 (2016) 175–187.
- [10] Vinayagam S., Sathishkumar K., Ayyamperumal R., *et al.*, *Environmental Research* 240 117473 (2024) 1–13.
- [11] Hein J.R., Mizell K., Koschinsky A., *et al.*, *Ore Geol. Rev.* 51 (2013) 1–14.
- [12] Aktürk G., *Environ. Sci. Pol.* 136 (2022) 19–32.
- [13] Levin L.A., Amon D.J., Lily H., *Nat. Sustain.* 3 (2020) 784–794.
- [14] Genisoglu M., Ergi-Kaymaz C., Sofuoglu, S.C., *J. Environ. Manag.* 233 (2019) 823–831.
- [15] Rajaram R., Ganeshkumar A., Emmanuel Charles P., *Chemosphere* 310 (2022) 136737.
- [16] Reichl C., Schatz M., Zsak G. *World-Mining-Data in Minerals Production*, International Organizing Committee for the World Mining Congresses, Vienna (2016), vol. 31.
- [17] Dold B., *Rev. Environ. Sci. Bio/Technol.* 7 (2008) 275–285.
- [18] Gómez Ros J.M., García G., Peña, J.M., *Ecol. Eng.* 57 (2013) 393–402.
- [19] Bakken G.M. *Historian* 69 (2007) 36–48.
- [20] Durucan S., Korre A., Muñoz-Melendez G., *J. Clean. Prod.* 14 (2006) 1057–1070.



## EVALUATING CORROSION AND BIOFOULING POTENTIAL BASED ON GROUNDWATER MICROBIOLOGICAL COMPOSITION

Vesna Obradović<sup>1</sup>, Marija Perović<sup>1\*</sup>, Tanja Vučković<sup>1</sup>

<sup>1</sup>Jaroslav Černi Water Institute, Belgrade, Jaroslava Černog 80, 11226 Belgrade, SERBIA

\*marija.perovic@jcerni.rs

### Abstract

*Microbiologically influenced corrosion was recognized in the mid-20<sup>th</sup> century, but the study of corrosion influenced by microorganisms (prokaryotes) is relatively new compared to other research. Microbiologically induced corrosion (MIC) can manifest in diverse environments, extending beyond aqueous conditions to thrive even in humid atmospheres. Biofouling pertains to the adhering of biological matter (including bacteria, algae, and various microorganisms) on surfaces submerged in water. In groundwater settings, biofouling manifests when these organisms attach to well screens, pipes, and other infrastructure components. This buildup can restrict water flow, reduce well efficiency, and deteriorate water quality, affecting overall groundwater utilization. By simultaneously applying a system of six types of bioactivity reaction tests (BART biotests), the biochemical diversity and estimated population size of ecological groups of bacteria participating in the transformation of organic matter and redox-sensitive species were determined. These bacteria predominantly form biofilms at the water-matrix interface, water-metal interfaces, and other surfaces. The goal was to comprehensively assess the microbiological status of groundwater and detect the biochemical activity of bacteria primarily posing risks for corrosion and biofouling processes on hydraulic structures, which could also pose risks to public health. Conducted research indicated the existence of potential for possible intensive and highly aggressive biofouling processes. The forecasted risk was in the range of high risks for the development of corrosion processes.*

**Keywords:** biofouling, groundwater, BART tests, wells.

### INTRODUCTION

Corrosion is an electrochemical process consisting of an anodic reaction involving the ionization (oxidation) of the metal (corrosion reaction) and cathodic reactions based on the reduction of chemical species. These reactions can be influenced by microbial activities, especially when organisms are in close contact with the metal surface and form a biofilm. The result of microbial biochemical activity is the degradation of metal known as Microbiologically Influenced Corrosion (MIC). Microorganisms involved in the biocorrosion of metals such as iron, copper, and aluminium, and their alloys, are physiologically diverse. Biocorrosion processes on metal surfaces are associated with the colonization of microorganisms and the products of their metabolic activities, including enzymes, exopolymers (slime), organic and inorganic acids, as well as volatile compounds such as ammonia or hydrogen sulfide. Bacteria, with their activity and metabolic by-products, can influence cathodic and/or anodic reactions, thus altering the electrochemistry at the biofilm/metal interface. Various mechanisms of biocorrosion have been identified and

recognized, reflecting the diversity of physiological activities performed by different types of microorganisms [1–6]. Many contemporary studies focus on the corrosion of copper and copper alloys under the influence of microbes, with particular attention given to sulfate-reducing bacteria and metal-oxidizing bacteria that deposit metals (especially iron and manganese) [2]. Based on numerous environmental and laboratory studies, the importance of microbial consortia (community-associations) and the role of extracellular polymeric substances (slime) in biocorrosion and biofouling have been emphasized [1–6]. It has been noted that microbiological growth in the form of biofilm promotes biofouling. The presence of biofilm can promote physicochemical reactions that are not typical for the given physicochemical conditions. In both natural and artificial environments, corrosion occurs when materials made of pure metals and/or their mixtures (alloys) undergo a chemical change from the neutral-basic state to an ionic form.

The metabolic activity of analysed bacterial groups can cause biofouling and corrosion, as well as turbidity, changes in taste, odor, and color, deteriorating the overall quality of raw water. Through their biochemical-physiological capabilities, these bacterial groups participate in the self-purification of groundwater and in biofouling processes on filters and in the filter zone. The examined bacterial groups can also be the cause of corrosion on hydraulic elements and structures beside leading to changes in overall water quality.

## MATERIALS AND METHODS

In a one sampling campaign conducted in 2023, microbiological quality testing was performed using a system comprising six types of bioactivity reaction tests (BART analysis) on three groundwater samples: Bn1, Bn4, Bn6, all obtained from the Bn well zone. Sampling of groundwater for microbiological analysis was carried out in accordance with the standard SRPS EN ISO 19458:2009, Water Quality - Sampling for Microbiological Analysis. Prior to sampling, the piezometers were flushed with at least three water column changes using a pump and an aggregate. Following the flushing of the piezometers and upon return to static level, in situ measurements of temperature, dissolved oxygen content, oxygen saturation, redox potential, specific electrolytic conductivity, and pH values were conducted using a HACH probe. Samples were collected in sterile 500 mL bottles using a sterile metal sampler with a cord.

By simultaneously applying a system of six types of BART biotests, the biochemical diversity and estimated population size of ecological groups of bacteria participating in the transformation of organic matter and redox-sensitive species were determined. These bacteria predominantly form biofilms at the water-matrix interface, water-metal interfaces, and other surfaces. The following BART tests were employed to detect the presence of: Iron-Related Bacteria (IRB BART) for detecting iron-associated bacteria and certain enteric species capable of iron deposition; Slime Forming Bacteria (SLYME BART) for detecting a wide range of bacteria producing extracellular polymeric substances, predominantly biofilm-forming, including enteric and opportunistic fluorescent *Pseudomonas* species; Sulfate Reducing Bacteria (SRB BART) for detecting sulfate-reducing bacteria that generate biogenic H<sub>2</sub>S and cause localized corrosion; Total Aerobic Bacteria (TAB) or Heterotrophic Aerobic Bacteria (HAB BART) for detecting a broad range of heterotrophic aerobic and facultatively



anaerobic bacteria, which contribute to biofilm formation and biofouling processes. An excessive abundance of these bacteria may compromise water quality by causing turbidity, changes in raw water organoleptic properties, and may pose risks to public health. Denitrifying Bacteria (DN BART) for detecting denitrifying bacteria and assessing the aquifer's potential for denitrification (nitrate removal), indicating organic pollution and potential presence of pesticides and pathogenic species.

Results of the BART analyses were processed using BART-SOFT V.6 software designed for this type of testing. The appearance and patterns of observed signature reactions and metabolism products (turbidity, color, gases, fluorescence, precipitates) in each individual biotest were entered into the software application. The size of the population for each tested bacterial group, aggressiveness, and calculated risks for corrosion, biofouling, and health risks were assessed. During the lag period of sample incubation, lasting ten to fifteen days, the analysis progress and reactions in biotests were observed daily, photographed, and archived as photo documentation. The scale of estimated risks of corrosion and biofouling is presented as numerical values ranging from 0 (no risk) to 9 (maximum risk).

## RESULTS AND DISCUSSION

According to the results of BART biotesting, the biochemical diversity in groundwater in the Bn zone included metabolic activity of iron-oxidizing, sulfate-reducing, heterotrophic aerobic, and facultative anaerobic bacteria, fluorescent *Pseudomonas* species (*Pseudomonas aeruginosa*), and aerobic and facultative anaerobic bacteria capable of producing extracellular polymeric substances. Denitrification activity in groundwater in the Bn zone was not detected, likely due to the suppression of nitrate reductase activity by sulfate-reducing bacteria (Figure 2).

The highest abundance and biochemical activity (aggressiveness) of bacteria were observed in SLYM and HAB BART biotests (8810000 and 454000 pac/ml, equivalent to the number capable of forming colonies). Specifically, a very high abundance of aerobic and facultative anaerobic heterotrophic bacteria capable of synthesizing and secreting extracellular polymeric substances (EPS) was detected compared to other tested groups, indicating a high risk (potential) for biofilm development and somewhat lower than corrosion, both in the aquifer matrix and on all metal surfaces (Figure 2). These bacterial groups also perform biomineralization of organic matter and participate in its removal from groundwater, whereby resulting degradation products can alter the primary water quality (e.g., changes in water pH, CO<sub>2</sub> content, and HCO<sub>3</sub>). The abundance of heterotrophic bacteria and bacteria excreting extracellular polymers (mostly polysaccharides) is also important because opportunistic and pathogenic species, protected within these groups of biofilms from predation and within cooperative metabolism consortia of biofilm, persist longer in the environment.

The abundance of fermentation bacteria detected within the IRB BART system was also high, with an average of 9000 presumed active cells per 1 ml. Fermentation bacteria can participate in the transformation of iron (oxidation-reduction), and during incomplete degradation of organic matter, they generate acidic products (e.g., organic acids and alcohols), H<sup>+</sup>, and CO<sub>2</sub>, which can contribute to both iron deposition processes and accelerate corrosive

processes on well metal structures and pipelines. Due to signature reactions indicating possible presence of enteric and pathogenic species (e.g., appearance of blackening along the entire length of the IRB BART detector reaction tube), it is necessary to conduct an analysis of the sanitary-hygienic suitability of groundwater in the Bn zone.

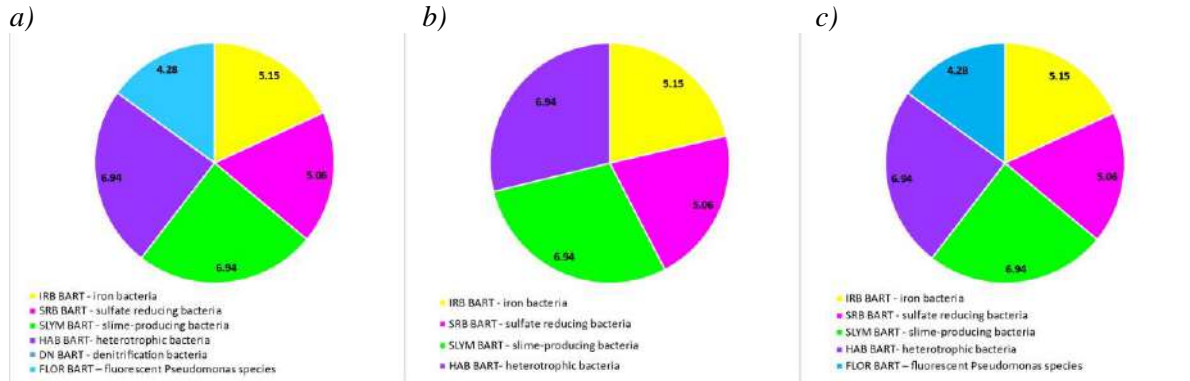


Figure 1 Abundance of tested bacterial groups, as log pac/ml a) Bn1; b) Bn4; c) Bn6

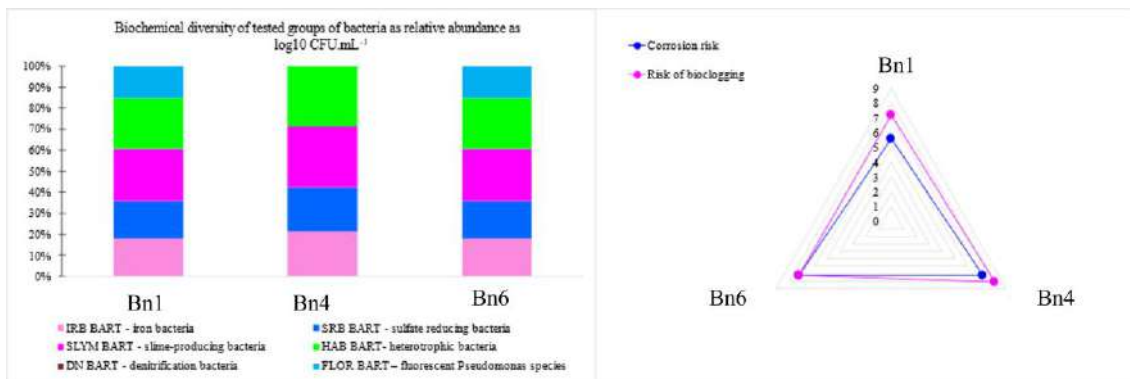


Figure 2 Relative abundance of tested bacterial groups (community structure based on abundance and manifestation of biochemical capabilities) and terminal reactions in bart biodetectors in the Bn zone

Sulfate-reducing bacteria were detected in all groundwater samples from observational piezometers with a constant count of 115,000 presumed active cells per ml, indicating a possible development of localized corrosion on well metal surfaces, equipment, and pipelines. Sulfate-reducing bacteria, strict anaerobes, utilize sulfates as primary electron acceptors in the degradation of organic matter, resulting in the production of H<sub>2</sub>S and thus contributing to the unpleasant odour of groundwater. The metabolic versatility of sulfate-reducing bacteria in the degradation of organic matter is important because they can perform fermentation and use other electron acceptors besides sulfates. In the case they use nitrate, the product of this transformation is ammonium ion. They can also use trivalent iron as an electron acceptor, thus contributing to the increase in reduced iron content in groundwater. The activity of hydrogenase enzymes in sulfate-reducing species *Desulfovibrio vulgaris* (Hildenl) is regulated by the availability of Fe<sup>2+</sup>, offering another mechanism under which corrosion could occur. Thus, the influence of dissolved iron on the development of corrosion processes under the influence of SRB is a complex phenomenon. SRB can lead to corrosion of zinc and zinc-



based alloys with sphalerite as a product, while the activity of SRB with lead carbonates leads to the formation of galena (PbS). Biogenically produced sulfides pose health and safety issues, are hazardous to the environment, and result in significant economic losses due to equipment corrosion. These organisms can coexist in natural biofilms, often forming synergistic communities (consortia) capable of influencing electrochemical processes through cooperative metabolism not observed in individual species.

During microbiological analyses, within the SRB BART biotesting, subsequent generation of substrate blackening along the tester was observed, indicating the activity of some proteolytic species in H<sub>2</sub>S generation. The primary appearance of reactions around the flotation ball in the SRB system, in groundwater samples in the Bn zone, indicates that sulfate-reducing bacteria are active in the community with primarily aerobic heterotrophs and producers of extracellular polymers and can cause sudden and dramatic drops in production of extraction wells, primarily caused by corrosion and pump failure.

Based on observed signature biochemical reactions and the time of their occurrence in each individual tester, using software BART Softv6, the population abundance of bacterial groups was estimated, and predicted risks for biofouling and corrosion were provided (Figure 2 and Table 1).

The software-calculated risk in the forecast of biofouling (biofilm formation) on a scale of 0–9 (from no risk to maximum risk) was >5 in all samples, suggesting possible intensive and highly aggressive biofouling processes. The forecasted risk for corrosive processes was >7, ranking in the range of high risks for the development of corrosion processes (Table 1).

**Table 1** Software-predicted risks for corrosion and biofouling for each sample from the Bn zone

Piezometer	Bn1	Bn4	Bn6
The risk of corrosion	5.6	7.2	7.2
The risk of fouling	7.2	8.1	7.2

Several signature reactions within all applied tests may indicate the potential presence of opportunistically pathogenic and enteric-type bacteria. Based on these identified reactions or the absence thereof, the predicted health risk and the potential presence of pathogenic species in the groundwater in the zone of the examined observational piezometers were moderately high to high, ranging from 6.3 to 8.1 (HRaver-6.9).

## CONCLUSION

The main groups of bacteria associated with the corrosion of cast iron and stainless-steel structures are sulfate-reducing bacteria (SRB), sulfur-oxidizing bacteria, iron-oxidizing/reducing bacteria, and manganese-oxidizing/reducing bacteria (IRB - iron and manganese associated bacteria), bacteria emitting organic acids and exopolymers or slime (EPS or slime-producing). It is known that some bacteria primarily adhere to corrosive products and can be present in large numbers, even when they do not play any role in primary corrosion processes, and some among them belong to the group of pathogenic bacteria.

The conducted analysis of fouling and corrosion risk revealed a significant risk of intensive and highly aggressive biofouling, with all samples indicating a risk level surpassing 5 on a scale of 0–9. Moreover, the forecasted risk for corrosive processes exceeded 7, indicating a substantial likelihood of corrosion development in the studied samples. These findings underscore the importance of proactive measures to mitigate both biofouling and corrosion in relevant systems.

## **REFERENCES**

- [1] Cullimore R., *Water Well Biofouling, Diagnosis in Microbiology of Well Biofouling*, CRC Press, Boca Raton (1999), eBook ISBN9780203747247.
- [2] Kosec T., Qin, J. Chen Z., *et al.*, *Corros. Sci.* 90 (2015) 248–258.
- [3] Mohammadi A., Corbett T., French A., *et al.*, *ACS ES T Water* 2 (4) (2022) 518–526.
- [4] Singh K.S., Keevill B. *Using The Well Fouling Index (WFI) in Microbiology of Well Biofouling*. CRC Press. (1999) eBook ISBN9780203747247.
- [5] Wang R, Jones K.C., Zhang H., *Environ. Sci. Technol.* 54 (13) (2020) 7961–7969.
- [6] Šaraba V., Nikodinović-Runić J., Obradović V., *et al.*, *Proceedings of the 2<sup>nd</sup> International Conference on Chemo and Bioinformatics Kragujevac: Institute for Information Technologies, September 28–29, Kragujevac, Serbia (2023)* 186–190.



## EVALUATION OF CORROSION POTENTIAL USING PHYSICOCHEMICAL WATER QUALITY ASSESSMENT

Vesna Obradović<sup>1</sup>, Marija Perović<sup>1\*</sup>, Jelena Lekić<sup>1</sup>

<sup>1</sup>Jaroslav Černi Water Institute, Belgrade, Jaroslava Černog 80, 11226 Belgrade, SERBIA

\*marija.perovic@jcerni.rs

### Abstract

*To select an appropriate location for well installation, and to decide on its construction, materials, operational regime, and the necessity for additional infrastructure such as drains, a comprehensive assessment of water quality at the site of interest is imperative. Moreover, forecasting the water quality under the anticipated operational conditions of the well holds even greater significance. Water quality assessment including calcium saturation provides insights into the mineral content of groundwater, which is essential for assessing water quality and optimizing treatment processes. By understanding calcium saturation levels, appropriate corrosion control measures can be implemented to mitigate these risks. Excessive calcium saturation and scale formation can impact aquatic ecosystems by altering water chemistry and habitat conditions. Overall, understanding calcium saturation in groundwater is very important for maintaining water quality, preventing infrastructure corrosion, minimizing environmental impacts, and optimizing water treatment processes. Subsequently, this discussion delves into an analysis of the findings derived from water quality testing conducted at eight observation piezometers. With the aim of assessing the corrosivity of water and its potential to form calcium carbonate scale the Langelier Saturation Index and Ryznar Stability Index were calculated.*

**Keywords:** Langelier Saturation Index, Ryznar Stability Index.

### INTRODUCTION

As a part of the groundwork for various studies conducted by the Jaroslav Černi Water Institute and projects of the Ministry of Science, Technological Development and Innovation, physico-chemical analyses of groundwater quality in the Wn well zone, between 2007 and 2012, were conducted. In-situ measurements of redox potential, oxygen content, pH values, electrolytic conductivity, and temperature were also conducted. Laboratory analyses included heavy metal content, organic matter, and other relevant micro and macro components of groundwater significant for assessing drinking water quality. Additionally, key physico-chemical parameters and indicators necessary for assessing the transformation processes of organic matter, iron, manganese, sulfur, and nitrogen components, as well as the potential for mechanical and chemical corrosion, were analysed in hydro-technical facilities and their key elements. The last sampling campaign was conducted in July 2023, when eight piezometers (from Wn1 through Wn8) in the vicinity of Ranney well Wn were analysed. Considering that Ryznar and Langelier classifications for determination of the corrosion and incrustation potential, are crucial for groundwater development and exploitation, these indices have been calculated. Numerous studies have been conducted with the aim of determining the potential

for well corrosion by calculating these indices, illustrating the importance of their application [1–7].

## MATERIALS AND METHODS

### Langelier index

To assess the stability of groundwater under natural conditions, based on the results of chemical analysis, the pH<sub>s</sub> value is calculated, which corresponds to the equilibrium state in the solution of carbonate compounds. The pH<sub>s</sub> value represents the index of hydrogen ions corresponding to the equilibrium saturation of groundwater with carbonic acid compounds. The pH value represents the actual concentration of hydrogen ions in groundwater (measured on-site). The pH value measured in the laboratory will always be higher than the actual pH value measured on-site. The calculation procedure involves water temperature, pH, total dissolved solids, calcium concentration, and total alkalinity. Based on the analysis and interpretation of available literature data, the following Eq. (1) is proposed for the practical calculation of the pH<sub>s</sub> value:

$$\text{pH}_S = 9,92 - \frac{t \left[ ^\circ\text{C} \right]}{40} - \log \left[ \text{Ca}^{++} \text{ (mg/l)} \right] - \log \left[ \text{HCO}_3^- \text{ (mg/ekv/l)} \right] + 0,2 \log \left[ \text{S.O. (mg/l)} \right] \quad (1)$$

t – groundwater temperature (°C)

s.o. – total dissolved solid (mg/l)

The Langelier index (Li) of saturation represents a parameter indicating conditions for the deposition of a calcium carbonate layer that can prevent corrosive processes, Eq. (2):

$$\text{Li} = \text{pH} - \text{pH}_S \quad (2)$$

If the value of the index is positive (>0.3): water is saturated and tends to deposit calcium carbonate. If this value is negative (<-0.3): water is undersaturated and tends to dissolve calcium carbonate, i.e., water has a corrosive effect. In practice, water is in equilibrium if the index values range from -0.3 to 0.3.

### Ryznar Stability Index

Ryznar index (RSI) indicates the stability of carbonate systems in water and can be calculated using Eq. 3:

$$\text{RSI} = 2\text{pH}_S - \text{pH} \quad (3)$$

RSI has only positive values, and the higher the values, the more corrosive the water is based on the obtained values, the tendency of groundwater according to this index is described as follows: when RSI is greater than 9.0, it indicates very strong corrosion; For RSI values between 7.5 and 9.0, the groundwater is characterized by severe corrosion; when RSI

falls between 7.0 and 7.5, significant corrosion is observed. RSI values ranging from 6.0 to 7.0 suggest little carbonate formation or corrosion. If RSI lies between 5.0 and 6.0, it indicates easy carbonate formation. When RSI falls between 4.0 and 5.0, severe carbonate formation is expected.

## **RESULTS AND DISCUSSION**

### **Groundwater quality**

The groundwater quality from the well Wn was analysed in the period 2007–2012. Based on a total of six pH measurements, a range from 7.1 to 8.4 and a mean value of 7.5 were determined, indicating slightly alkaline conditions in the groundwater environment of the tested site. The measured redox potential of the Wn ranged from 125 to 244 mV, with a mean value of 146 mV for the period from 2007 to 2012. Redox potential values <135 mV and oxygen levels <0.5 mg/l indicate that microbial processes likely dominate over chemical oxidations in iron transformation. Experiences from the Belgrade aquifer have shown that wells with redox potentials <130 mV and total iron values >1.2 mg/l are usually associated with flow rates ( $Q_{\text{average}}$ ) of 40 L/sec [2–4]. The electrical conductivity varied over time and was measured within a range of values from a minimum of 491 to a maximum of 650  $\mu\text{Scm}^{-1}$ . The difference between the maximum and minimum measured values was 159  $\mu\text{Scm}^{-1}$ . The mean electrical conductivity value measured between 2007 and 2012 was 561  $\mu\text{Scm}^{-1}$ , placing examined groundwater at the upper limit of the group of low-mineralized freshwater bodies (with oligosalinity), characterized by conductivity ranging from 20 to 650  $\mu\text{Scm}^{-1}$ . The dominant cationic species in terms of concentration were arranged as follows:  $\text{Ca}^{2+} > \text{Mg}^{2+} > \text{Na}^+ > \text{K}^+$ , while the anionic species followed the order  $\text{HCO}_3^- > \text{SO}_4^{2-} > \text{Cl}^- > \text{PO}_4^{3-} > \text{NO}_3^-$ . The dominant anion was bicarbonate (consistent with the measured pH values), with a maximum value of 360.51 mg/l. Among the cationic species, calcium ions predominated (max. 90.59 mg/l) followed by magnesium ions (max. 24 mg/l). According to the dominant ions and the classification by Alekin, the groundwater from well Wn belonged to the type I hydrocarbonate (calcium-magnesium) water, which is in accordance with a general characteristic of Sava alluvium ( $\text{HCO}_3^- > (\text{Ca}^{2+} + \text{Mg}^{2+})$ ). Out of 8 measurements of dissolved oxygen concentration in groundwater, the maximum recorded value was 0.1 mg/l, while the minimum was below quantification limit of the applied method. Considering the multi-year period, in the degradation of organic matter (originating from infiltration through the unsaturated zone and/or infiltration of Sava water), oxygen was not dominating electron acceptor, but rather other redox-sensitive species, which is a general characteristic of Sava alluvium. The maximum concentration of total iron was 2.55 mg/l. The ratio of the maximum observed values of divalent iron to total iron ( $\text{Fe}^{2+}/\text{Fe}_{\text{tot}}$ ) was 0.46, indicating anaerobic and occasionally aerobic conditions in the zone of this well. Based on the concentrations of sulfates, which varied in a relatively wide range (28.96–94 mg/l), with a mean value of 51 mg/l, higher than the average values for the Sava River, it can be assumed that iron sulfide oxidation was likely one of the processes in the genesis of divalent and trivalent iron and sulfate in the examined groundwater (Wn well zone). The manganese content was measured in the range of 0.290–0.547 mg/l. After the consumption of organic matter or if its concentration is below the usability threshold for microorganisms (<1 mg/l),

the groundwater microbiome may be dominated by species that can utilize inorganic carbon sources as donors ( $\text{CO}_2$  and  $\text{HCO}_3^-$ ) or reduced sulfur and  $\text{H}^+$ , and as acceptors ferrous ions, manganese, nitrates, sulfates,  $\text{CO}_2$ , which can affect the chemical quality of water. The concentration of ammonium ions varied to a maximum of 0.31 mgN/l. Oxidized forms of nitrogen, nitrates, were detected with a maximum value of 0.4 mgN/l, and nitrites were detected only in one sampling campaign (0.005 mgN/l).

### Groundwater quality of the piezometers

Selected piezometers: Wn1, Wn2, Wn3, Wn4, Wn5, Wn6, Wn7, Wn8 are sampled and analysed in a campaign conducted in July 2023 (Table 1). The maximum dissolved oxygen value was measured in the Wn6 (1.50 mg/l), while the minimum was recorded in Wn7 (0.36 mg/l). The average oxygen content for groundwater in the Wn zone was 0.7 mg/l, significantly higher than the values measured between 2007 and 2012 in the Wn. The *in-situ* pH value was measured within the range of slightly alkaline values, from 7.27 to 7.76. The redox potential values in the Wn zone were unusually high for the Belgrade aquifer, with significant spatial variations. The maximum value of 511.96 mV was measured in the Wn1, while the minimum value of -252.47 mV was observed in Wn3. The average redox potential value (294.10 mV) was significantly higher compared to the average values measured in Belgrade aquifer. Observed range suggests that groundwater in the Wn zone is not in redox equilibrium and that processes in the groundwater of this well include reduction processes (e.g., sulfate reduction) and complementary oxidation processes, involving electron transfer between chemical species. Variable redox potential values also indicate mixing of different hydrochemical zones and a trace of organic pollution in the recent past. The electrolytic conductivity was not uniform across space. The measured range varied from 444.6  $\mu\text{Scm}^{-1}$  in Wn3 to a maximum of 672  $\mu\text{Scm}^{-1}$  in Wn4. The dominant cationic species, follow the order:  $\text{Ca}^{2+} > \text{Mg}^{2+} > \text{Na}^+ > \text{K}^+$ , while the anionic species follow the order:  $\text{HCO}_3^- > \text{SO}_4^{2-} > \text{Cl}^- > \text{PO}_4^{3-} > \text{NO}_3^-$ . According to the ionic species and classification by Alekin, the groundwater in the Wn zone can be categorized as Type I hydrocarbonate calcium-magnesium soft water with low salt and potassium content ( $(\text{HCO}_3^- > (\text{Ca}^{2+} + \text{Mg}^{2+}))$ ), which is a general characteristic of the Sava alluvium. The total organic carbon content (TOC) was measured in the range of values from a minimum of 0.94 mg/l in the Wn2 to a maximum of 1.63 mg/l in the Wn3, where significantly negative redox potential values were observed. The content of readily oxidizable organic matter, estimated through  $\text{KMnO}_4$  consumption, was maximum 5.06 mg/l, which was accompanied by low boron concentrations in all examined water samples in the Wn zone ( $< 100 \mu\text{g/l}$ ). In eight samples, the concentration of ferrous iron was in the range of 0.10 to 0.21 mg/l, with a mean value of 0.14 mg/l, significantly lower than the average value for the Belgrade aquifer and the Sava alluvium. Similarly, the average total iron content was also lower compared to the average measured in the water from the Belgrade aquifer wells (0.33 mg/l). The measured concentrations of manganese exhibited a wide range of values, ranging from a minimum of 0.16 to a maximum of 0.68 mg/l. The minimum measured concentration of sulfates of 14.44 mg/l (Wn1), while the maximum of 25.25 mg/l (Wn4), on average, lower than the average sulfate concentrations in the Sava River (26.60 mg/l). The average concentration of ammonium ions, (eight groundwater samples in the Wn zone), was 0.27 mgN/l, and for nitrites, it was 0.33 mgN/l, with nitrites being more



frequently detected (in three samples) compared to nitrates. Nitrates were only detected in the groundwater sample Wn6, with a maximum oxygen concentration of 1.5 mg/l. The average oxygen concentration for groundwater in the Wn zone was 0.7 mg/l, suggesting that the oxygen concentration in the groundwater in the Wn zone likely limits nitrification processes and favours denitrification. The first intermediate of denitrification is represented by nitrites (possible DNRA transformation of nitrates).

**Table 1** Selected parameters of groundwater quality

Sample	Unit	Wn1	Wn2	Wn3	Wn4	Wn5	Wn6	Wn7	Wn8
Date		2023	2023	2023	2023	2023	2023	2023	2023
pH		7.59	7.58	7.67	7.26	7.76	7.62	7.47	7.7
E. Conductivity	μS/cm	498	489	445	672	472	503	464	458
DO	mg/l	0.48	0.5	0.56	0.51	0.54	1.50	0.36	0.49
Turbidity	NTU	0.8	1	1.2	1.1	1.2	3.3	5.3	3
Alkalinity	mg/l	235	230	195	315	205	220	205	200
Bicarbonates	mg/l	286.7	280.6	237.9	384.3	250.1	268.4	250.1	244
CO <sub>2</sub>	mg/l	12.1	12.1	8.3	33.8	7.1	10.6	13.9	8
Chlorides	mg/l	14.64	13.57	23.21	18.85	23.92	27.13	20.35	22.13
Sulfates	mg/l	14.44	16.24	14.88	25.25	19.06	18.67	20.87	18.7
TP	mg/l	0.021	0.042	0.022	0.368	0.046	0.083	0.06	0.13
TDS	mg/l	248	250	221	412	257	280	259	246
TOC	mg/l	1.36	0.94	1.63	1.39	1.05	1.39	1.19	1.45

According to earlier calculations, water from all wells in the Belgrade water source had Lsi values ranging from -0.98 to 0.88 [2,3,5]. At some point, Li values were >0, and at another, they were <0, indicating that the groundwater from the source was somewhere around the carbonate equilibrium. At one point, it tended to form calcium carbonate, and at another, it tended to dissolve it [2]. In practice, it has been shown that values in the range of ±0.3 to ±0.5 cannot reliably indicate water properties, as small changes in temperature, pH, or calcium and bicarbonate content in the water can change the sign of Li. The Ryznar Stability Index in the groundwater from piezometers Wn1 to Wn8 ranged between 7.5<RSI<9.0, suggesting that the groundwater in the Wn zone was aggressive with the potential for severe corrosion (Table 2).

**Table 2** Values of calculated Langelier saturation index and Ryznar stability index in groundwater in zone Wn

	Wn1	Wn2	Wn3	Wn4	Wn5	Wn6	Wn7	Wn8
Langelier saturation index	-0.02	-0.07	-0.17	-0.05	-0.03	0.13	-0.03	-0.09
Ryznar stability index	7.62	7.72	8.00	7.37	7.82	7.78	7.81	7.88

## CONCLUSION

Based on the values of LI obtained from the calculated parameters for the examined piezometers (LI ranging from -0.02 to 0.13), groundwater in zone Wn is generally undersaturated and tends to dissolve calcium carbonate, except in the case of sample Wn6 where the water showed a tendency for carbonate deposition. Based on the values of the

calculated parameters LI, carbonate deposition in groundwater in zone Wn is unlikely to dominate. The Ryznar Stability Index calculated for the groundwater sampled from piezometers indicated the aggressive nature of the groundwater in the Wn zone and its potential for severe corrosion. The Langelier Index serves as an approximation rather than a direct measure of water corrosiveness. Nevertheless, it presents a valuable tool for assessing this tendency. The LI value is subject to variation, influenced by factors such as temperature and ionic strength. Understanding the LI's significance is crucial for implementing appropriate control strategies. In oversaturated conditions, excessive calcium carbonate precipitates, forming scales that can obstruct pipes and impair water flow. Conversely, in undersaturated conditions, the relationship between calcium carbonate and alkalinity may heighten water corrosiveness. Therefore, water operators must take proactive measures to ensure water equilibrium, minimizing both corrosive and scale-forming tendencies. It's important to recognize that these indices, such as LSI, and RSI do not directly forecast the corrosion of steel and other metals. Corrosion of metals typically depends on factors like pH, concentration of anions (such as sulfates and chlorides), and oxidants, which must also be considered.

## **REFERENCES**

- [1] Derakhshannia M., Dalvand S., Asakereh B., *et al.*, IJHST 10 (4) (2020).
- [2] Dimkić M., Pušić M., Civil Engineering Calendar (40) (2008) 430–496.
- [3] Dimkić M., Pušić M., Obradović V., *et al.*, Water Sci. Technol. 63 (11) (2011) 2567–2574.
- [4] Hussien M.B., Rabeeea M.A., Mukhlif H.N., Environ. Nanotechnol. Monit. 14 (2020) 100334.
- [5] Dimkić M., Pušić M., Obradović V., *et al.*, IWA Specialist Groundwater Conference, 08–10 September 2011, Belgrade, Serbia (2011) 225–230.
- [6] Houben G., Treskatis CH., Water Well Rehabilitation and Reconstruction. McGraw Hill, New York (2007). p.391, ISBN-13: 978-0-07-148651-4.
- [7] Lodha R., Sharma Y., Surecha O.P., *et al.*, IARJSET ISSN (O) 2393-8021, ISSN (P) 2394-1588 (2023).



## QUESTIONING THE RESILIENCE OF THE DANUBE FISH FAUNA UNDER THE PRESSURE OF BELGRADE WASTEWATERS

Jelena Čanak Atlagić<sup>1\*</sup>, Ana Marić<sup>2</sup>, Katarina Jovičić<sup>1</sup>, Jelena Stanković<sup>1</sup>,  
Vesna Đikanović<sup>1</sup>, Tamara Mitić<sup>1</sup>, Maja Raković<sup>1</sup>

<sup>1</sup>Department of Hydroecology and Water Protection, Institute for Biological Research  
“Siniša Stanković”, National Institute of the Republic of Serbia, University of Belgrade,  
Bulevar despota Stefana, 142, 11108 Belgrade, SERBIA

<sup>2</sup>University of Belgrade, Faculty of Biology, Studentski trg 16, 11000 Belgrade, SERBIA  
\*jelena.canak@ibiss.bg.ac.rs

### Abstract

*Two large rivers, the Sava and the Danube, meet in the heart of Belgrade, the capital of the Republic of Serbia. This still growing city has no communal waste water treatment and the two rivers are the main recipients of wastewater pollution. Previous studies have shown that a high diversity of fish fauna can be expected in the broader Belgrade area. The present study examines whether municipal wastewater pollution affects the diversity of fish species, their overall structure and well-being in the Višnjica - Pančevačke ade locality, which continuously has bad water quality. Most of the fish species in the studied community are under some form of protection (Bern Convention, IUCN, Habitats Directive and/or national legislation), so the assessment of biodiversity is of great importance. The analysis of diversity, evenness, saprobity and abundance biomass comparison (ABC) curve has shown that this community is under moderate stress, which is reflected in the lower number of present species. The Danube is known to have a high self-purification capacity, and an improvement in wastewater management would certainly lead to a rapid recovery of the diversity of this resilient local fish community.*

**Keywords:** fish assemblage, communal wastewaters, diversity, urban ecology.

### INTRODUCTION

The Danube is the second largest river in Europe, it flows into Serbia on the border with Hungary (1433 rkm), flows 588 km through Serbia, has two hydropower dams (Đerdap I and II) and leaves Serbia at the mouth of the Timok on the border with Bulgaria (845 rkm). The most important and navigable watercourses on the territory of the city of Belgrade, belong to the lowland sections of the Danube and its right tributary the Sava River. Belgrade is a rapidly growing city with more than 1.5 million inhabitants, whose untreated municipal wastewater is discharged directly into these rivers. The water quality downstream of the Belgrade center is consistently classified as class V due to the high levels of *E. coli* and enterococci as well as the concentration of ammonium ions ( $\text{NH}_4^+$ ) [1,2]. The recreational and commercial fishing is also present in the urban area. Joint Danube Survey 4 report [1] says that river Danube has total of 72 recorded species, where the highest number at one locality was 33 species at Ilok – Bačka Palanka [1]. According to the literature, the fish fauna of the broader Belgrade area includes about 40 or even more fish species, with an increasing number and abundance

of allochthonous species. This is no surprise, as the Danube and its navigable watercourse is one of the four main routes for the introduction of alien freshwater species in Europe, as it connects the watersheds of the Black Sea and the North Sea [3,4]. The present study on the biodiversity of the fish fauna of the Danube in the Belgrade urban area was conducted to determine whether the expected fish species, especially the protected and strictly protected ones, still inhabit this area under strong anthropogenic pressure.

## MATERIALS AND METHODS

In August and September of 2023, field surveys were carried out at the Višnjica site to obtain a representative sample of the Danube fish fauna in the urban area downstream of the most affected section of the Sava and Danube rivers. Višnjica is known as a commercial fishing site and is located 10 rkm downstream of the mouth of the Sava River. The sampling was carried out using standard equipment for reversible stunning, electric generator type ELT62II GI HONDA GCV160, 230/400 V, power 11.9/7.4A DC and frequency 360 Hz. Sampling was carried out by electrofishing on eight transects, each 1000 m long in the stretch from Paradajz Island near Višnjica, along the Danube to Pančevačke ade islands, around and between the river islands of Čakljanac and Forkontumac (Figure 1).

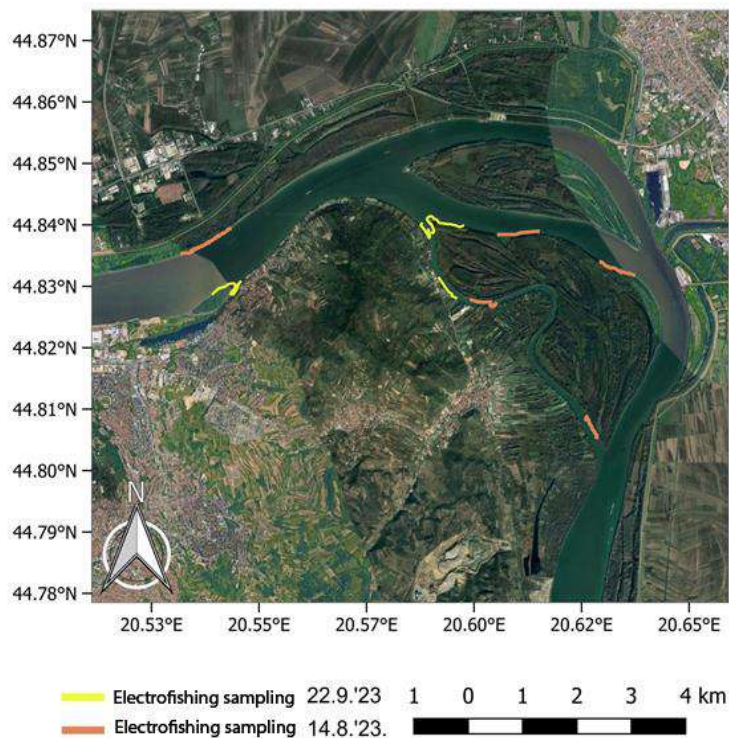


**Figure 1** Map of the researched area, Danube Višnjica – Pančevačke Ade islands, Belgrade

Individuals were identified in the field to the species level and released after taking measurements. Each fish was measured for standard length (SL (cm)) and weight (W (g)). The mean condition factor (CF) was calculated for each individual ( $CF = W (g) / SL (cm)^3 \cdot 100$ ), and mean CF for each species [5]. Based on the obtained data on the species presence and abundance in the sample, the Shannon and Simpson diversity, and

evenness of the community were determined [6–8]. Saprobity, based on the fish assemblage, was determined using the Sládeček indicator list [9]. As only 13 of 25 recorded species are included in this list, the results would not give a realistic assessment of the saprobity. This problem was overcome to a certain extent by setting the values for some species based on their frequency of occurrence in different types of water bodies according to Hofrat and Ottendorfer [10] and experience with local fish communities. The abundance biomass comparison (ABC) curve analysis was carried out to examine the effects of the pollution load on the fish community based on the abundance and weight of the fish species [11]. Ecological index (EI) was also calculated [12]. For each species recorded, the protection status was checked in accordance with national and European legislation and recommendations.

## RESULTS AND DISCUSSION

During the surveys conducted in August and September of 2023, a total of 25 fish species were recorded in the Danube downstream from Višnjica to the Pančevačke ade islands. In total, 466 specimens were sampled and 25 species identified. In order to assess the biodiversity, Shannon, Simpson and Evenness indices were determined, with the values of 1.86, 0.67 and 0.579, respectively. The results correspond to III class or moderate status [13]. The body size and condition factor of the species are given in Table 1. The saprobity was 1.71 which is considered  $\beta$ -mesosaprobic or class II water quality, while the assemblage was potamon type according to the EI. Cyprinid species *Carassius gibelio*, *Blicca bjoerkna*, *Cyprinus carpio*, and *Rutilus rutilus* had the highest CF values ( $CF > 2$ ), with the highest value recorded for *C. gibelio* (3.38). The lowest CF of the cyprinid species had *Ballerus ballerus* (0.98), and the lowest of all species *Babka gymnotrachelus* (0.46). The abundance biomass curves overlapped showing the moderate stress effect on the fish community (Figure 2).

The conservation status of the recorded species was checked according to the IUCN Red List, the EU Red List, EU 27 [14], the Bern Convention [15], the Habitats Directive [16] and national legislation for protected species [17]. Out of a total of 25 species, 10 are listed in the Bern Convention [15] (*Aspius aspius*, *Ballerus ballerus*, *Ballerus sapa*, *Chondrostoma nasus*, *Rutilus pigus*, *Vimba vimba*, *Neogobius fluviatilis*, *Ponticola kessleri*, *Gymnocephalus schraetser* and *Silurus glanis*) and 4 species in the Habitats Directive [16] (*Aspius aspius*, *Barbus barbus*, *Rutilus pigus* and *Gymnocephalus schraetser*). Based on national legislation, strictly protected species were not recorded, while 15 out of 25 identified species are protected [17]. Six species are considered non-native to this part of the Danube (*Carassius gibelio*, *Hypophthalmichthys molitrix*, *Babka gymnotrachelus*, *Neogobius fluviatilis*, *Neogobius melanostomus* and *Ponticola kessleri*), while four species are not under any protection (*Alburnus alburnus*, *Blicca bjoerkna*, *Rutilus rutilus* and *Gobio gobio*). Some strictly protected species that were expected based on the previous data were not recorded in this field work.



**Table 1** List of identified species, number of caught individuals, percentage, mean standard body length in cm (SL), body weight in g (W), condition factor (CF) and standard deviation (SD)

Family	Species	Individuals	%	SL AVG	SD	W AVG	SD	CF	SD
Cyprinidae	<i>Alburnus alburnus</i>	259	55.58	7.28	1.58	4.75	2.99	1.11	0.19
	<i>Ballerus sapa</i>	31	6.65	12.08	2.62	34.90	21.09	1.69	0.29
	<i>Abramis brama</i>	29	6.22	10.81	5.81	70.59	275.89	1.54	0.59
	<i>Rutilus rutilus</i>	24	5.15	11.69	5.55	62.42	75.37	2.11	0.43
	<i>Aspius aspius</i>	15	3.22	11.87	5.10	37.93	49.24	1.26	0.26
	<i>Blicca bjoerkna</i>	12	2.58	16.96	3.42	158.50	136.13	2.66	0.56
	<i>Hypophthalmichthys molitrix</i>	5	1.07	51.20	1.60	2441	460.28	1.83	0.41
	<i>Carassius gibelio</i>	4	0.86	23.25	3.90	462.75	204.53	3.38	0.27
	<i>Barbus barbus</i>	3	0.64	7.83	3.01	8.67	8.01	1.55	0.74
	<i>Rutilus pigus</i>	3	0.64	14.00	3.94	60.00	48.93	1.76	0.04
	<i>Cyprinus carpio</i>	2	0.43	28.00	10.00	490.00	282.00	2.49	1.53
	<i>Chondrostoma nasus</i>	2	0.43	8.00	0.50	7.00	1.00	1.36	0.08
	<i>Ballerus ballerus</i>	1	0.21	8.50	0.00	6.00	0.00	0.98	0.00
	<i>Leuciscus idus</i>	1	0.21	6.00	0.00	4.00	0.00	1.22	0.00
	<i>Vimba vimba</i>	1	0.21	12.00	0.00	34.00	0.00	1.97	0.00
Esocidae	<i>Esox lucius</i>	7	1.50	25.86	6.72	194.86	134.11	0.96	0.08
Gobiidae	<i>Neogobius fluviatilis</i>	9	1.93	5.39	1.51	1.94	1.44	115	0.57
	<i>Neogobius melanostomus</i>	5	1.07	6.20	0.68	2.80	1.60	1.05	0.43
	<i>Babka gymnotrachellus</i>	2	0.43	6.00	0.00	1.00	0.00	0.46	0.00
	<i>Ponticola kessleri</i>	2	0.43	5.25	0.25	2.00	1.00	1.30	0.71
Gobionidae	<i>Gobio gobio</i>	4	0.86	8.38	0.96	6.50	2.60	1.06	0.10
Percidae	<i>Sander lucioperca</i>	22	4.72	19.61	11.66	203.64	417.89	1.16	0.13
	<i>Perca fluviatilis</i>	21	4.51	9.21	4.13	29.62	50.50	1.77	0.66
	<i>Gymnocephalus schraetser</i>	1	0.21	14.00	0.00	36.00	0.00	1.31	0.00
Siluridae	<i>Silurus glanis</i>	1	0.21	80.00	0.00	3700	0.00	0.72	0.00

Considering the sampling effort and the 466 individuals of 25 species caught, the diversity of the fish fauna of the Danube in Belgrade near Višnjica can be assessed as moderate at the time of sampling. The fish assemblage is stable with moderate evenness, as expected, dominated by cyprinid species (84%). Cyprinids are known to be able to tolerate considerable pollution. The ecological index shows the potamon type of assemblage, which is adequate to this section of the Danube. The highest abundance was found for *Alburnus alburnus* (55.58%), as this is a typical swarm fish, which prefers the upper parts close to the water surface, sensitive to electrofishing sampling method. Similar abundance was reported in JDS4 – 52.28% [1]. Other species that are abundant and make up the majority of the assemblage



were *Ballerus sapa*, *Abramis brama*, *Rutilus rutilus*, *Aspius aspius*, and *Blicca bjoerkna*. Although it is known that this site continuously has a high load of microorganisms, which are indicators of fecal pollution (class V water quality - very poor) and the presence of hazardous compounds [1], based on this study, the water saprobity is assessed as  $\beta$ -mesosaprobic, which is a considerably better result. The pressure that pollution exerts on the fish community is, perhaps, best reflected in the number of species and community structure. It can be reflected in reduced numbers or potential absence of rare and protected species that we know should be present. The highest CF was found for a cyprinid, the allochthonous *C. gibelio*, which raises concerns that pollution may favor non-native species at the expense of native species. The following strictly protected species were not recorded in this survey, although it is assumed they should be present based on the previous studies: *Cobitis elongatoides*, *Carassius carassius*, *Tinca tinca*, *Gymnocephalus baloni*, *Pelecus cultratus*, *Rhodeus amarus*, *Scardinius erythrophthalmus*, *Lota lota*, *Misgurnus fossilis*, *Zingel zingel*, *Zingel streber*, protected species *Acipenser rhutenus*, *Squalius cephalus*, *Lota lota*, *Sander volgensis*, as well as some non-native species: *Ameiurus nebulosus/melas*, *Ctenopharyngodon idella*, *Hypophthalmichthys nobilis*, *Lepomis gibbosus*, *Perccottus glenii*, and *Pseudorasbora parva*.

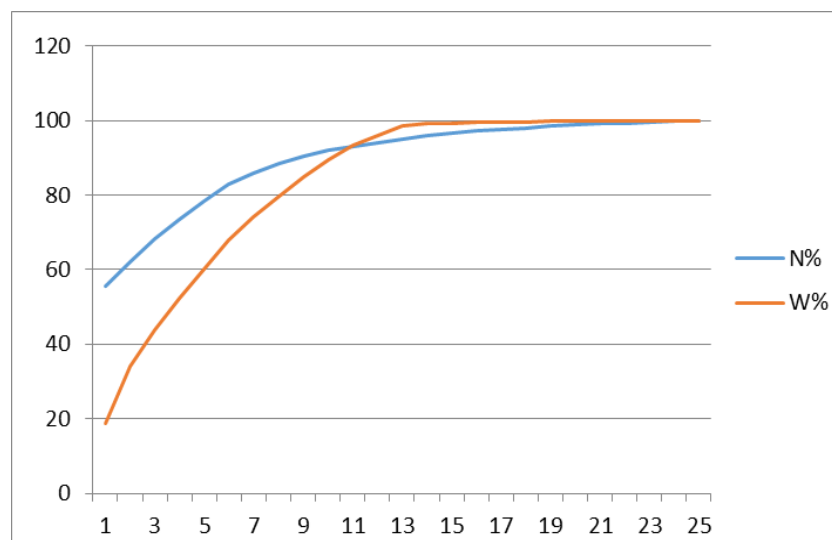


**Figure 2** ABC curve for the fish assemblage at Višnjica locality in Belgrade, where N% is abundance curve and W% represents biomass curve

## CONCLUSION

As Belgrade is a large city that has a significant impact on the ecology of the Danube, the results point to the need for better wastewater management, which, together with the natural self-purification capacity of the Danube, would probably be sufficient to restore the diversity of fish fauna at this sector of Danube.

## AKNOWLEDGEMENT

This research was funded by the Ministry of Science, Technological Development and Innovation (451-03-66/2024-03/200007) and the Jaroslav Černi Water Institute through Project No. 32/20/49-104-08/09.

## REFERENCES

- [1] JDS4, 2019. Scientific Report: A Shared Analysis of the Danube River. Joint Danube Survey 4, ICPDR, editors: Liška, I., Wagner, F., Sengl, M., *et al.*, Available on the following link: [www.danubesurvey.org](http://www.danubesurvey.org).
- [2] Kolarević S., Micsinai A., Szántó-Egész R., *et al.*, *Sci. Total Environ.* 783 (146967) (2021).
- [3] Copp G.H., Garthwaite R., Gozlan R.E., *J. Appl. Ichthyol.* 21(4) (2005) 371–373.
- [4] Panov V.E., Alexandrov B., Arbačiauskas K., *et al.*, 5 (1) (2009) 110–126.
- [5] Ricker W.E., Computation and interpretation of biological statistics of fish populations, Fisheries Research Board of Canada, Ottawa (1975), p.382, ISBN: 0662014405.
- [6] Shannon C.E., Weaver W., *The Mathematical Theory of Communication*, University of Illinois Press, Chicago & Urbana (1949), p.125, ISBN: 0252725484.
- [7] Simpson E.H., *Nature* 163 (4148) (1949) 688.
- [8] Pielou E.C., *J. Theor. Biol.* 13 (1966) 131–144.
- [9] Sládeček V., *Arch. Hydrobiol.* 58 (1) (1961) 103–121.
- [10] Hofrat W., Ottendorfer J. *Wien-Kaisermuhlen: Bundesanstalt für Wasserergute* 26 (1983) 175.
- [11] Clarke K.R., Warwick R.M., *Change in marine communities: an approach to statistical analysis and interpretation*, Natural Environment Research Council UK, Plymouth (1994), p.114, ISBN: 9781855311404.
- [12] Šorić V.M., *Ichthyologia* 30 (1998) 51–70.
- [13] Năstase A., Iani M., Honț Ș., *et al.*, *Scientific Annals of the Danube Delta Institute* 26 (2021) 47–68.
- [14] IUCN, 2023. *The IUCN Red List of Threatened Species. Version 2023-1. Available on the following link: [www.iucnredlist.org](http://www.iucnredlist.org), Accessed on [04.03.2024].*
- [15] Bern Convention (Appendix/Annexe III). *Convention on the Conservation of European Wildlife and Natural Habitats.* (1979) ETS/STE 104.
- [16] Directive, Habitats. “Council Directive 92/43/EEC of 21 May 1992 on the conservation of natural habitats and of wild fauna and flora” *Official Journal of the European Union* 206.7 (1992): 50.
- [17] „Službeni glasnik” RS 5/2010, 47/2011, 32/2016 i 98/2016, Pravilnik o proglašenju i zaštiti strogo zaštićenih i zaštićenih divljih vrsta biljaka, životinja i gljiva.



## MONITORING OF THE STATE OF THE ENVIRONMENT IN THE BOR DISTRICT, GIVEN THROUGH THE EXAMPLE OF THE DISTRIBUTION OF Pb IN THE SOIL LOCATED IN THE IMMEDIATE VICINITY OF THE BOR RIVER

Vladan Marinković<sup>1\*</sup>, Miroslava Maksimović<sup>1</sup>, Milenko Jovanović<sup>1</sup>, Stefan Trujić<sup>1</sup>

<sup>1</sup>Mining and metallurgy institute Bor, Albert Einstein 1, 19210 Bor, SERBIA

\*vladan.marinkovic@irmbor.co.rs

### Abstract

*Geochemical mapping provides a means of visualizing spatial variations in the chemical composition of the Earth's surface.*

*Mapping of coastal profiles in the catchment area of the Bor river was performed in order to make geochemical maps of soil pollution in the valley of the mentioned river. The Bor river is one of the most polluted rivers in the Republic of Serbia. The sampling network at selected locations of coastal profiles is adapted to the morphological and hydrographic characteristics of the terrain. Samples from A horizon with five sampling points were collected on each profile. In the analytical procedure, the content of pollutant elements was determined: Pb, Zn, Cu, Cr and As.*

**Keywords:** geochemical mapping, coastal profiles, soil pollution.

### INTRODUCTION

Monitoring of the state of the environment in Bor was carried out over a two-year period by collecting and then analysing samples of surface and underground water, river sediments and soil. Based on the results obtained from the laboratory analysis of the collected samples, geochemical maps were created that visually show the state of the environment in Bor and its surroundings.

Surface water samples were taken from the following watercourses: Industrial wastewater, Bor river, Krivelj river, Ravna river, Bela river, Timok river, Danube and Robule lake. Surface water samples were collected from a total of 30 sampling points. Geochemical maps of the distribution of harmful (polluting) elements in surface water were created for: As, Cd, Cu, Fe, Mn, Ni, Pb, Zn and pH.

Groundwater samples (water from wells), were collected in the village of Slatina, and only from those wells that are closest to the banks of the Bor river. Groundwater samples were collected from a total of 22 sampling points. Geochemical maps of the distribution of harmful (polluting) elements in groundwater were created for: As, Mn and pH.

Sediment samples were collected from the beds of the following rivers: Bor river, Krivelj river, Bela river, Timok river and from the Danube. Sediment samples were collected from a total of 12 sampling sites. Geochemical maps of the distribution of harmful (polluting) elements in sediments were created for: As, Cr, Cu, Pb and Zn.

Soil samples were collected from the location of the Bor river, one of the most polluted rivers in the Republic of Serbia. The samples were taken according to the cross-sections that were placed perpendicular to the Bor River. The sampling network at the selected locations of coastal profiles was adapted to the morphological and hydro graphic characteristics of the terrain, there were a total of 14 of these cross-sections, while each cross-section had 5 sampling points. Geochemical maps of the distribution of harmful (polluting) elements in sediments were created for: As, Cr, Cu, Pb and Zn.

## **GEOCHEMICAL MAP CREATION**

Geochemical mapping is a tool for visualizing spatial variations in the chemical composition of the Earth's surface. Geochemical mapping is a technique based on the exploration of mineral deposits, but in the modern age it has found application in the study of urban environments. Such studies, involving multidisciplinary teams, including geochemists, must present their results in a way that non-geochemists can understand. Demands for urban geochemical data driven by legislation regarding the need to identify contaminated soil and watercourses and subsequent health risk assessments have led to greater global interest in the urban geochemical environment.

The procedure for creating geochemical maps will be explained in the following text using the example of a geochemical map of Pb distribution in the soil in the Bor river valley.

In the first step of creating a geochemical map, limit values for Pb in the soil are determined, on the basis of which the geochemical map is created. These values are as follows:

1. Class I of soil quality (recommended value that is less than 85 mg/kg), if the Pb content in the soil is lower than the recommended value, the soil is considered uncontaminated;
2. Class II of soil quality (MAX value ranges between 85 mg/kg and 310 mg/kg) if the Pb content is within these values, it is assumed that the soil has a certain degree of pollution, but it is not yet dangerous for the environment because it does not exceed the maximum allowed value.
3. Class III of soil quality (remediation value ranges between 310 mg/kg and 530 mg/kg) if the Pb content is within these values, it is assumed that the soil is polluted and its remediation is recommended.
4. Class IV of soil quality (values above remediation, higher than 530 mg/kg) if the Pb content is higher than this value, the soil is considered to be highly polluted and as such represents a danger to the environment.

In the second step, the points from which the samples were collected are painted with colours (for better visual monitoring) that correspond to certain quality classes, Figure 1.

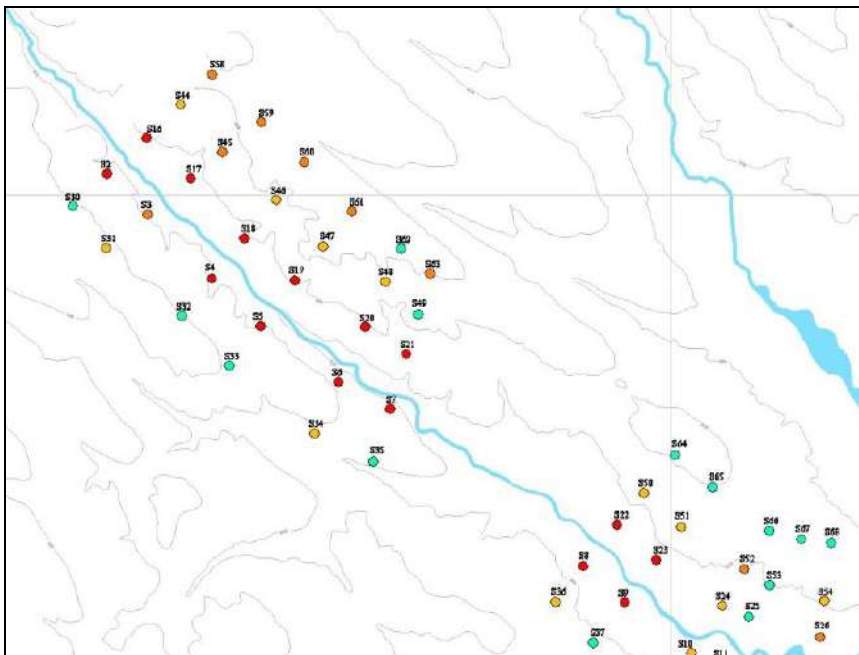


*Figure 1* Schedule of points from which soil samples were collected

In the third step of creating a geochemical map, the separated soil quality classes are outlined so that each class represents a closed polygon line of an irregular shape, where special care should be taken not to cross or intersect different quality classes, Figure 2.

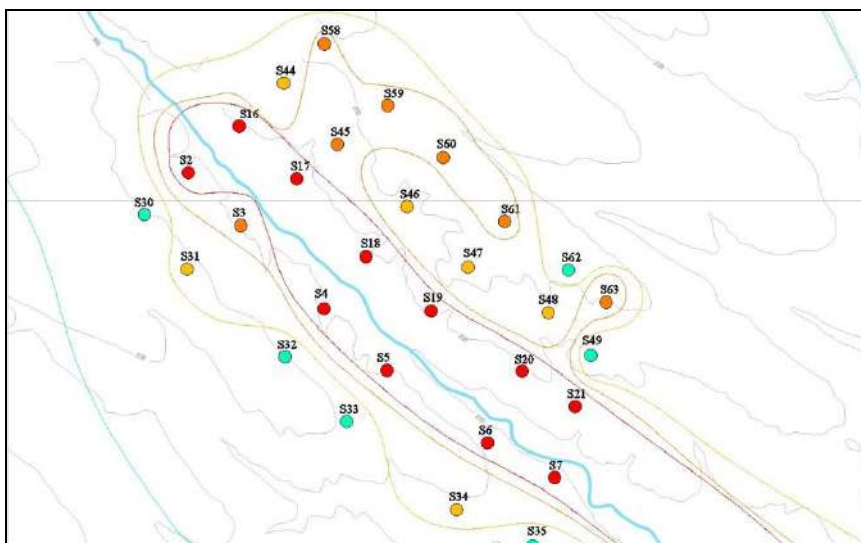


*Figure 2* Layout of selected quality classes

In the last step, the quality classes are colored in colours that correspond to certain quality classes, thus obtaining visually well-reviewed and easy-to-understand separate data sets that represent the distribution of pollution by a certain element in a separate area, Figure 3.

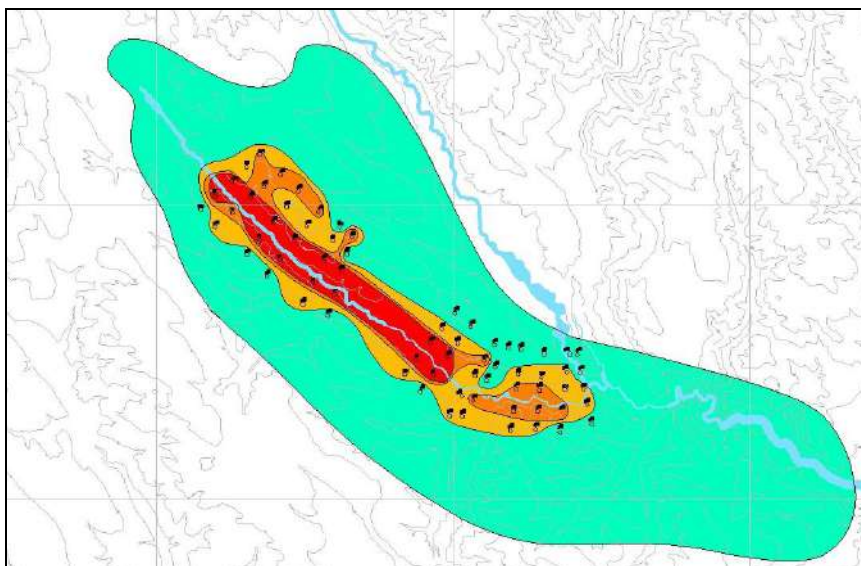


**Figure 3** Geochemical map of Pb distribution in soil

## CONCLUSION

As already mentioned, the Bor river is one of the most polluted river courses in the Republic of Serbia. Based on the results collected during the two-year monitoring of soil quality in the valley of the Bor river, the following can be concluded:

The soil in the immediate vicinity of the river is of the IV quality class, it is highly polluted and as such represents a danger both to the environment and to the life and health of people living in near the Bor river;

The more we move away from the river, the less polluted the land becomes. At a distance of more than 200 m, the land already passes into quality class III, where it is possible to successfully carry out remediation;

The pollution of the river itself can be closely related to decades of mining activities in the surrounding mining facilities, as well as the preparation, processing and smelting of the ore that has been exploited;

The solution to this situation is also the only possible one, which is the installation of a plant for the purification of all waste water that is discharged into the Bor river, and then the remediation of the surrounding land.

## ACKNOWLEDGEMENT

*This work was financially supported by the Ministry of Science, Technological Development and Innovation of the Republic of Serbia, Contract on realization and financing of the scientific research work of the Mining and Metallurgy Institute Bor in 2024, contract number: 451-03-66/2024-03/ 200052.*

*Also, this work was financially supported by the EU under Interreg – IPA CBC Romania-Serbia Programme and co-financed by the partner states in the Programme.*

*Project Romania Serbia NETwork for assessing and disseminating the impact of copper mining activities on water quality in the cross-border area (RoS-NET2) eMS code RORS - 337.*



*Also, this work was financially supported by the EU under Program 2nd EIT-HEI call: Building Ecosystem Integration Labs at HEI to foster Smart Specialization and Innovation on Sustainable Raw Materials - HEI4S3-RM.*

## **REFERENCES**

- [1] The law on land protection (Official Gazette of RS, No. 112/2015).
- [2] Regulation on the limit values of pollutant, harmful and dangerous substances in the soil (Official Gazette of RS, no. 30/2018 and 64/2019).
- [3] Mrvić V., Petrović V., Jakovljević M., *et al.*, Soil and plant 59 (2010) 83–98.
- [4] Novaković V., Tomić A., Nikolić N., *et al.*, Pollution and protection of soil and groundwater, Feljton DOO, Novi Sad (2018), p.500, ISBN: 978-86-84863-38-8.
- [5] Available on the following link: <http://indicator.sepa.gov.rs/pretrazivanje-indikatora/indikatorilat/allfindp/bb8be41cab544c05b965cd2d5b45aee3>.



## EFFECTIVENESS OF *Photinia × fraseri* 'RED ROBIN' IN THE URBAN LANDSCAPE: TOWARDS OF CLIMATE CHANGE

Mirjana Ocokoljić<sup>1</sup>, Djurdja Petrov<sup>1\*</sup>, Nevenka Galečić<sup>1</sup>, Dejan Skočajić<sup>1</sup>,  
Dragan Vujičić<sup>1</sup>, Jelena Čukanović<sup>2</sup>, Isidora Simović<sup>3</sup>

<sup>1</sup>University of Belgrade – Faculty of Forestry, Kneza Višeslava 1, 11030 Belgrade, SERBIA

<sup>2</sup>University of Novi Sad – Faculty of Agriculture, Dositeja Obradovića Square 8,  
21000 Novi Sad, SERBIA

<sup>3</sup>BioSense Institute, University of Novi Sad, Dr Zorana Djindjića 1,  
21000 Novi Sad, SERBIA

\*[djurdja.stojicic@fb.bg.ac.rs](mailto:djurdja.stojicic@fb.bg.ac.rs)

### Abstract

*The paper explores the effectiveness of *Photinia × fraseri* 'Red Robin' in the urban environment of Belgrade, particularly in light of a modified temperate-continental climate. The research focuses on assessing how urban design and climate change affect the phenological events of Red Robin Christmas Berry across four locations in Belgrade. By analyzing climatic variables such as accumulated cold hours and their correlations with phenological patterns of flowering, the study unveils the substantial impact of insolation, air temperature, and urban layout on these phenophases. The findings underscore the significance of site selection in optimizing the delivery of ecosystem services.*

**Keywords:** Red Robin Christmas Berry, landscape urban design, air temperature, insolation, phenological observations.

### INTRODUCTION

Rapid urbanization disrupts the balance in the urban environment [1]. For landscape urban design, plants hold paramount importance for both visual appeal and practical functionality because they affect ecosystem services with seasonal, aesthetic, economic and functional characteristics [2], and they have a pivotal role in human health [1]. The utilization of non-native woody plants enhances the urban landscape's value but poses a significant challenge due to the impacts of climate change. Therefore, it is very important that plants in the urban landscape can adapt to climatic conditions, and taxa with high climatic plasticity, such as *Photinia × fraseri* 'Red Robin', stand out in particular [3]. Red Robin Christmas Berry, an impressive evergreen cultivar with striking red young leaves transitioning to green mature leaves, serves as an attraction for bees during flowering phenophase and for birds (such as woodpeckers and thrushes) during fruiting phenophase, as its fruits persist until the subsequent vegetation period. Furthermore, all stages of its phenology contribute to its ornamental value [4]. This highlights the significance of phenological patterns in evaluating the efficacy of aligning Red Robin Christmas Berry's phenological events with landscape urban design objectives.

The objective of this study is to investigate how the urban environment and climate fluctuations impact the phenological patterns and growth of *Photinia × fraseri* 'Red Robin' in the context of operationalizing landscape design. The research aims to address the following inquiries: 1) What is the influence of climate change on *Photinia × fraseri* 'Red Robin' in Belgrade? 2) How do air temperature, insolation, and urban layout affect the four selected locations? 3) Future prospects: Assessing the readiness of Red Robin Christmas Berry to cope with climate change for optimal site selection, enhancing visual aesthetics, ecosystem services, and optimizing maintenance costs.

## MATERIALS AND METHODS

The research area is an urban zone of the Belgrade municipalities of Stari grad (Location 1 and part of Location 2) and Savski venac (part of Location 2 and Locations 3 and 4) where the presence of *Photinia × fraseri* 'Red Robin' (Red Robin Christmas Berry) is noted. In three locations, there are trees in pots in the streets, and in the fourth one, it is on a cascade designed slope in the park “Lep izgled” on anthropogenized soil of haplic fluvisol type [5]. The description of the research locations is shown in Table 1.

*Table 1* Description of the research area

Location	Latitude $\phi$ Longitude $\lambda$	Altitude H (m)	Number of individuals	Aspect	Slope*
1. Čika Ljubina street	44° 48' 59.61" N 20° 27' 33.98" Er	113	4	E	0–1°
2. Balkanska street	44° 48' 35.34" N 20° 27' 33.08" Er	83–97	11	SW	5–8°
3. Kneza Miloša street	44° 48' 05.83" N 20° 27' 18.82" Er	97	9	NW	0–1°
4. Park “Lep izgled”	44° 47' 58.02" N 20° 27' 08.52" Er	89–95	3	W	5–8°

\*Slope: 0–1° (flat terrain) and 5–8° (steep terrain)

In the research, elements of phenological patterns were monitored using the BBCH (Biologische Bundesanstalt, Bundessortenamt and Chemical industry) scale [6], from November 1, 2022 to March 15, 2024 to determine the impact of climate change and the urban layout on the key events of the Red Robin Christmas berry (flowering, fruiting, but also leaves color change). Phenological observations were made visually every other day, at all locations, by recording the dates: budbreaking - BB (the day when the bud opening began), beginning of flowering - BF (the day when more than 10% of the flowers were open), full flowering - FF (the day when more than 50% of the flowers were open), end of flowering - EF (the day when more than 80% of the flowers had opened), the appearance of red leaves (RL), the transition of leaves to green color (GL) and the decline of ripe fruits (RF). The determined dates used for phenological events were summed up to the mean value for each location. The recorded dates were automatically converted into days of the year by the software (e.g. January 1 = 1 DOY). According to the method and formula of Cosmulescu and Ionescu [7], the accumulated cold hours ( $CHt$ ) were determined from November 1, 2022 and November 1, 2023 until the date when the BB was recorded in 2023 and 2024, respectively.

Before November 1, due to high temperatures, there is no accumulation of cold hours for moderate-continental climate conditions [8], which is characteristic of the research area [9]. The sum of growing degree days (*GDD*) was determined according to Lalić *et al.* [8] and Ocokoljic *et al.* [10], using a temperature threshold of 5°C. *GDD* were determined by summing the active temperature sums for each location, and then presented as the mean value for each research location. Fruit yield was evaluated by quantifying phenological observations on a five-point scale, where 0 is a tree without fruit (0% of branches bearing fruit); 1 – is a small number of fruits ( $\leq 20\%$ ); 2 – is a low number of fruits ( $>20\text{--}\leq 40\%$ ); 3 – is a moderate number of fruits ( $>40\text{--}\leq 60\%$ ); 4 – abundant fruits ( $>60\text{--}\leq 90\%$ ) and 5 – maximum number of fruits ( $>90\%$ ).

Pearson's correlation coefficient and one-factor ANOVA determined the relationship between phenological events and accumulated *CHt*. Climatological data were taken from the Main Meteorological Station (GMS) Belgrade (44°47'54.44" N; 20°27'53.35" E; altitude: 132m) [9]. The program package Excel 2016 was used for data processing. Photographic material was collected during the field research.

## RESULTS AND DISCUSSION

The number of accumulated cold hours from November 1, 2022 to BB 2023 varied from 936h (location 1), over 1602h (locations 2 and 3) to 1762 (location 4). The mean value of *CHt* for the beginning of the vegetation period in 2023 was 1475.5h; while the same value of *CHt* for the beginning of the vegetation period in 2024 was 1165h (310.5h less), which confirms that air temperatures influenced the vegetation period in 2024 to start on average 53 days earlier. This is in accordance with the fact that climate change is intensifying and with the data of RHMZ [11] that states 2023 to be the warmest year in Belgrade since 1888 with a deviation from 1.7°C compared to average temperatures. In January 2024 [9], the mean daily air temperature during most of the first decade and in the middle of the month was in the extremely warm category. Very warm in the middle of the last decade of the month. February 2024 in Belgrade was the warmest since the beginning of the measurements, with the average daily temperature at the beginning of the month in the category of normal values, and then during the first and half of the second decade, as well as during most of the last decade of the month, it was in the categories of very warm and extremely warm. In the middle of the month it was in the warm category. In January 2024,  $T_{\text{mean}}$  was higher by 1.5°C, and the number of sunny hours by 27.6h; while in February the temperature was higher by 6.4°C with fewer sunny hours by 12.4h compared to 2023 (Figures 1 and 2). The results of the study confirm the necessity of individual research, as well as that each taxon has certain requirements regarding *CHt* and that only after accumulating the required *CHt* do different phenophases begin [12].

We determined Pearson's correlation coefficients, with a probability threshold of  $p < 0.05$ , resulting in: a) very strong positive correlations for the following - (1.00) *GDD* BF and - *GDD* FF, BF DOY and FF DOY; *GDD* FF and – BF DOY and FF DOY; *GDD* EF and EF DOY and BF DOY and FF DOY, as well as b) strong positive correlations (0.878 to 0.974) *CHt* and all *GDD* and DOY. Correlation analysis confirmed the direct correlation of the decrease in the number of *CHt* with higher air temperatures from November 1 to BB, that

*GDD* BF affects the beginning but also the duration of full flowering as well as the *GDD* of full flowering, but also that a greater number of days from FF to EF affects the length of the flowering period. The above results confirm the significant impact of climate change on phenological patterns, which is in line with the previous findings of Oćokoljić *et al.* [9]. Statistical significance was confirmed by one-way ANOVA tests, with  $p < 0.0001$ , with *F* of 39.07 (between *CHt* and BF DOY) and 37.55 (*CHt* and EF DOY), which confirmed that *CHt* significantly influences both the beginning of flowering and the end of flowering. Also, with *F* values from 91,6 to 105, 81 it is confirmed that *GDD* BF affects all DOY flowering phenophases (BF, FF i EF), and that *GDD* EF has a significant effect only on EF DOY (end of flowering) with *F* of 152.64.

Figure 3 shows the phenological observations for Christmas Berry at the 4 research locations. The trees in the park “Lep izgled” stand out, where the end of flowering was recorded the latest (30.05.2023). The length of the flowering phenophase was 28 days. In the other two locations, the length of the flowering phenophase was similar, 27 days (Kneza Miloša Street) and 25 days (Balkanska Street), but in the same locations flowering ended 9 days earlier (Kneza Miloša Street) and 12 days earlier (Balkanska Street). In Čika Ljubina Street, the trees did not bloom.

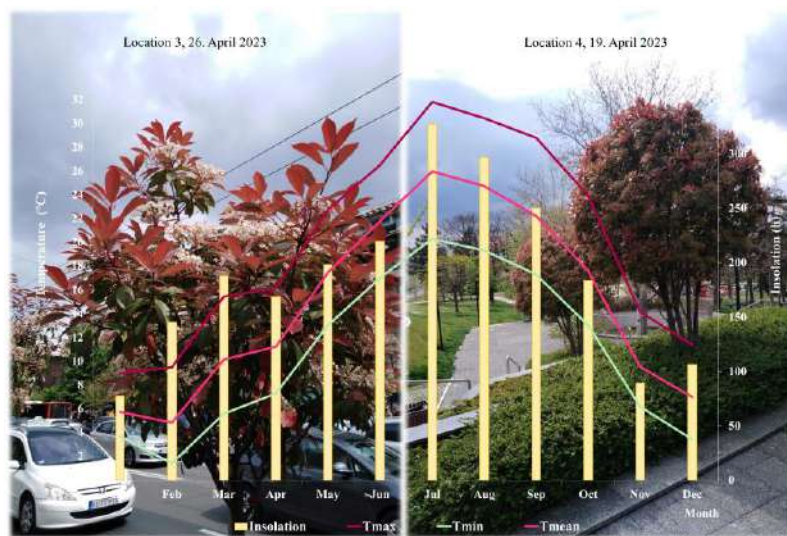


**Figure 1** Minimum, maximum, and average monthly air temperatures and insolation (sum of monthly hours of sunshine) during 2023, according to RHMZ [9]

The results confirm that Red Robin Christmas Berry is visually attractive at the beginning of the growing season when the leaves are red, in the phenophase of flowering and later while fruiting [13] but also that the urban layout affects phenological events. The trees are overshadowed by tall buildings surrounding them. In densely built-up areas of the city, street trees have limited access to light throughout the day. Reduced insolation as a result of shading by tall buildings caused changes in phenological patterns [14]. Location 1 (Čika Ljubina Street - the first one-way street in Belgrade) stands out, where no leaf color changes were recorded in 2023, and no flowering phenophases were recorded (Figure 3).



The street's width is approximately 9 meters, bordered by tall buildings ranging from four to six floors, which obstruct sunlight from reaching the tree crowns. Location 2, Balkanska Street, historically significant for Belgrade, has seen a decline in craft shops and small family-owned businesses. Its width fluctuates between 10 to 13 meters, lined with several-story buildings, predominantly five to six floors high, not only along Balkanska Street but also in adjacent streets. Only three trees, positioned at the corners of Lomina Street and Kraljica Natalija Street, displayed the characteristic red hue of spring foliage and bore fruit, while the remaining eight trees maintained a green color and completed their flowering phase during the growing season. Along Kneza Miloša Street (location 3), two out of nine trees exhibited a red coloration, attributed to their positioning amidst high-rise buildings, with all trees fully flowering and fruiting. In the park “Lep izgled” during 2023, three trees situated in the Sava amphitheater area displayed all expected phenological events.

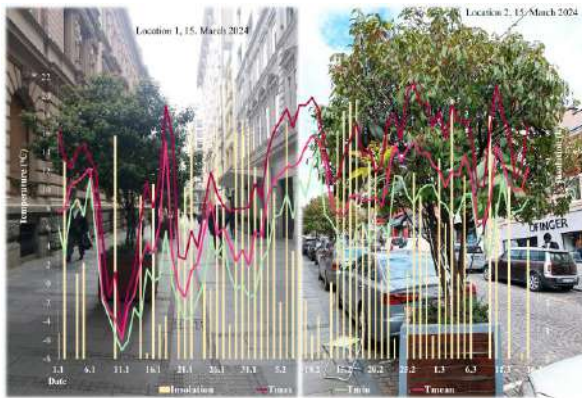


**Figure 2** Minimum, maximum and average daily air temperatures and insolation (h) in the period January 1, 2024 to March 15, 2024

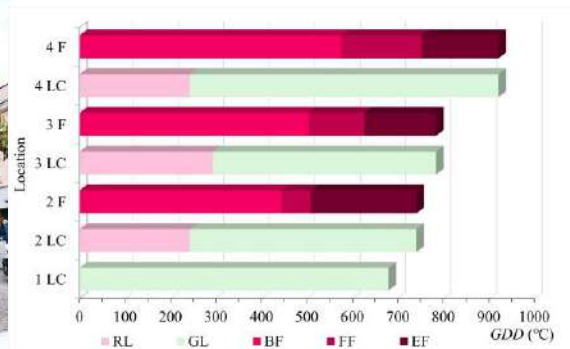


**Figure 3** Phenological observations: GDD - temperature sums (°C), for the BF, FF, EF, RL and GL during 2023 for Christmas Berry at four researched locations in Belgrade

However, despite this, fruiting was rated as minimal in all trees and locations, with the fruits persisting until March 15, 2024, when this research was concluded. This outcome can be attributed to the climatic conditions during the flowering period of April-May 2023, characterized by cold to extremely cold temperatures during the first decade, followed by very cold conditions towards the end of the month. Similarly, May 2023 experienced cold to very cold temperatures, particularly towards the beginning, middle, and end of the month. In 2024, inflorescences differentiation and the emergence of green leaves were observed across all locations and trees (totaling 27), with the beginning of flowering not occurring until March 15. These findings underscore the influence of urban layout, particularly the lack of sunlight in certain locations, and climate change, primarily the insufficient accumulation of cold hours ( $CH_t$ ), on the productivity and ecosystem services provided by Red Robin Christmas Berry in Belgrade.



## CONCLUSION

Based on research conducted across four locations in the urban area of Belgrade, it has been confirmed that the timing and duration of phenophases, along with ecosystem services, are influenced by climatic factors, urban layout, and microenvironmental conditions. This study enhances understanding of the interactions between Red Robin Christmas Berry and the urban environment, shedding light on its impact on ecosystem services. Given the challenges posed by climate change, this taxon faces new stressors, emphasizing the importance of comprehending long-term trends for effective management and mitigation of climate change effects. The research serves as a foundation for operationalizing urban design, which plays a pivotal role in promoting environmental sustainability through design interventions. An innovative aspect of this study lies in correlating the findings with urban design and their subsequent management.

Recommendations are contextually appropriate and specific to benefit the implementation of Red Robin Christmas berry in the urban landscape.

## ACKNOWLEDGEMENT

*The authors are grateful to the Ministry of Ministry of Science, Technological Development and Innovation of the Republic of Serbia for financial support of the University of Belgrade - Faculty of Forestry the scientific research work in 2024, the registration number 451-03-65/2024-03/200169.*

## REFERENCES

- [1] Yücedag C., Asik Y., Urban Ecosyst. 26 (2023) 1071–1080.
- [2] Wang C., Xiao H., Liu J., *et al.*, J. For. Res. 28 (2016) 473–479.
- [3] Laaribya S., Alaoui A., Ayan S., *et al.*, Forestist 74 (3) (2023) 1–10.
- [4] Cetiner S., Zencirkıran M., Journal of Bartın Faculty of Forestry, 22 (2) (2020) 294–306.
- [5] Škorić A., Filipovski G., Ćirić M., Posebna izdanja knjiga LXXVIII, Sarajevo (1985).
- [6] Meier U., Growth Stages of Plants, Wiley-Blackwell, Wissenschafts-Verla: Berlin, (1997) 622. ISBN: 3 8263 3152 4.
- [7] Cosmulescu S., Ionescu M., Int. J. Biometeorol. 62 (11) (2018) 2007–2013.
- [8] Lalić B., Ejcinger J., Dalamarta A., *i sar.*, Meteorologija i klimatologija za agronome. Univerzitet u Novom Sadu-Poljoprivredni fakultet, Novi Sad, Srbija, (2021) p.219, ISBN: 978-86-7520-520-3.
- [9] RHMZ Republic Hydrometeorological Service of Serbia, *Available on the following link:* <https://www.hidmet.gov.rs/index.php>.
- [10] Ocokoljić M., Petrov Dj., Galečić N., *et al.*, Land 12 (2023) 706.
- [11] RHMZ Republic Hydrometeorological Service of Serbia, *Available on the following link:* <https://www.hidmet.gov.rs/data/klimatologija/ciril/2023.pdf>.
- [12] Coutts A.M., White E.C., Tapper N.J., *et al.*, Theor. Appl. Climatol. 124 (2015) 55–68.

- [13] POWO (2024). Plants of the World Online. Facilitated by the Royal Botanic Gardens, Kew, *Available on the following link: <http://www.plantsoftheworldonline.org/>*, Assessed on 10 February 2024.
- [14] Takebayashi H., Kasahara M., Tanabe S., *et al.*, Sustainability 9 (2017) 1398.



## ***Chaenomeles japonica* (Thunb.) Lindl. ex Spach IN THE DESIGN OF URBAN PARKS: LEARNING FROM NATURE**

**Mirjana Ocokoljić<sup>1</sup>, Djurdja Petrov<sup>1\*</sup>, Nevenka Galečić<sup>1</sup>, Dejan Skočajić<sup>1</sup>,  
Dragan Vujičić<sup>1</sup>, Jelena Čukanović<sup>2</sup>, Isidora Simović<sup>3</sup>**

<sup>1</sup>University of Belgrade - Faculty of Forestry, 1 Kneza Višeslava Street, 11030 Belgrade,  
SERBIA

<sup>2</sup>University of Novi Sad - Faculty of Agriculture, 8 Dositeja Obradovića Square,  
21000 Novi Sad, SERBIA

<sup>3</sup>BioSense Institute, University of Novi Sad, 1 Dr Zorana Djindjića Street,  
21000 Novi Sad, SERBIA

\*[djurdja.stojicic@sfb.bg.ac.rs](mailto:djurdja.stojicic@sfb.bg.ac.rs)

### **Abstract**

*The research investigates the changes in the phenological dynamics of *Chaenomeles japonica* (Thunb.) Lindl. ex Spach under the influence of climate factors in Karadjordje's Park, Belgrade. Our findings affirm the significant impact of air temperature and precipitation on phenological phases and their duration. The year emerges as a significant factor; notably, in 2024, the growing season commenced with leafing in January, followed by flowering 29 days later. The duration of flowering in 2024 was reduced by 54 days compared to 2023, resulting in a diminished visual appeal. Male genotypes were identified, with male flowers observed across all specimens. The study underscores key phenological events to highlight climate's impact on the urban phenology of Japanese Quince, with the aim of design operationalisation or urban park reconstruction.*

**Keywords:** Japanese Quince, urban environments, phenological duration, landscape design, climate change.

### **INTRODUCTION**

Urban shrubbery holds aesthetic, socio-cultural, ecological, and economic values crucial for enhancing sustainability and quality of life in urban environments [1–4]. Within this context, urban parks and green spaces with woody plants play a pivotal role in cities' adaptation to climate change [5]. However, to fulfill their intended ecosystem services, shrubs must be healthy, vigorous, and in good condition. The average lifespan of urban shrubs is brief, sometimes as short as a mere decade [6]. Ocokoljić *et al.* [7] attribute this shortened lifespan to differences in environmental conditions between urban settings and natural habitats. The 21<sup>st</sup>-century cities have been significantly altered by the effects of phenomena such as urban heat islands (UHI), restricted space for root system expansion, impervious surfaces, and poor soil quality. Thus, fostering conditions suitable for the growth and sustainable development of urban dendroflora emerges as a pressing imperative [7]. An initial step involves identifying suitable species and genotypes tailored to European urban parks, particularly in anticipation of projected rises in air temperatures and prolonged drought periods as forecasted by the World Meteorological Organization (WMO) [8]. In the face of

climate change, China stands out as a potential source of woody plants suitable for European environments [9].

Given the vital role of shrubs in urban parks and the observed decline in their presence during park reconstructions in Belgrade over the past two decades, this research focuses on Japanese Quince, introduced from China to European gardens at the end of the eighteenth century [6]. The primary aim of this study was to assess how urban environmental conditions affect the growth, phenological patterns, and key events of *Chaenomeles japonica* (Thunb.) Lindl. ex Spach (Japanese Quince) within the urban park setting. The application of phenological data in urban park design offers opportunities to: a) optimise maintenance costs, b) guide the appropriate selection of plants based on location and purpose, and c) contribute to achieving a high-quality, sustainable, and diverse design.

## MATERIALS AND METHODS

The study was conducted in Karadjordje' Park (*Ser. Karadžorđev park*), Belgrade, where field surveys revealed a group planting of *Ch. japonica* near Nebojšina Street and Boulevard of Liberation (*Ser. Bulevar Oslobođenja*). Situated on historically significant grounds, the park housed a camp and military cemetery for Belgrade liberators under Karadjordje in 1806. The monument to Karadjordje (1848) was the first public monument in Belgrade erected to commemorate a historical event [10]. Subsequent to the monument's installation, black locust and horse chestnut trees were planted, and significant park expansion occurred at the turn of the 20th century, spanning the slope from the Temple of Saint Sava to Autokomanda [10].

Presently, the park covers an area of 28,132 m<sup>2</sup>, which is of great importance as it is located in the territory of the Vračar municipality, where the degree of urbanization amounts to 95.33% [11]. The park's area under trees and shrubs covers 18,947 m<sup>2</sup>, while the Japanese Quince occupies 68 m<sup>2</sup>, consisting of three groups of four individuals on anthropogenised Haplic Cambisol (Eutric) soil [12], on gently sloping terrain (4.1°) with a southwest (SW) aspect. To underscore the impact of climatic parameters on the phenological patterns and key events of the Japanese Quince, climate data from the Main Meteorological Station (MMS) in Belgrade, located at coordinates 44°47'54.44"N and 20°27'53.35"E, with an altitude of 132 m, were employed [13], situated at a distance ranging from 307.97 to 472.81 m from the research area.

Over two consecutive years (2023–2024), phenophases were documented every other day by recording dates, which were subsequently converted into days of the year (DOY) using software and following the BBCH scale [14]. These phases included bud breaking (BB), marking the onset of bud opening; beginning of flowering (BF), denoting when more than 10% of flowers had bloomed; full flowering (FF), indicating when over 50% of flowers were in bloom; end of flowering (EF), signifying when over 80% of flowers had withered; and ripening phase (RP), identifying the day when fruits displayed the characteristic colour of ripeness. Chilling hours accumulated (CHt) from 1 November 2022 and 1 November 2023 to the date of BB recorded in 2023 and 2024 were determined using the method by Cosmulescu and Ionescu [15]. Heat sum accumulation (GDD) was calculated by summing mean daily air temperatures until the onset of a specific phenophase, according to Lalić *et al.* [16], to determine the necessary GDD for Japanese Quince and the occurrence of particular

phenophases (in our study, flowering during two consecutive years and fruiting in 2023). Yield abundance was evaluated on a scale ranging from 0 to 5, with 0 indicating no fruiting and 5 denoting maximum fruiting. Morphometric analysis of flowers was conducted on a sample of 400 flowers (50 flowers from each monoecious individual in FF from the southern portion of the crown). The analysis, facilitated by the UTHSCSA Image Tool Program, encompassed measurements of calyx length, petal length, flower diameter, and number of petals, stamens, and pistils.

Quantitative data underwent statistical analysis employing descriptive statistics, ANOVA, and the Spearman Rank test for inter-variable comparisons, utilising the XLSTAT 2020 software package.

## RESULTS AND DISCUSSION

The phenological patterns and key events of Japanese Quince within the urban park setting are influenced by a range of ecological factors. Among these, air temperature and precipitation emerge as critical factors that shape plant development and, implicitly, phenology [7,15]. These factors imply that phenophases have optimal timing, which varies across different taxa [8]. The primary response of Japanese Quince to climate change was an extended growing season in 2023, marked by an early onset of flowering and delayed autumnal phenophases. Fruit retention persisted until 358 DOY and beyond, while the growing season of 2024 began with Japanese Quince leafing out as early as January (DOY 24) and the beginning of flowering (BF) commencing after full leaf emergence, approximately 29 days later. The duration of flowering in 2024 was 54 days shorter compared to 2023 and exhibited lower visual appeal (Figure 1a).

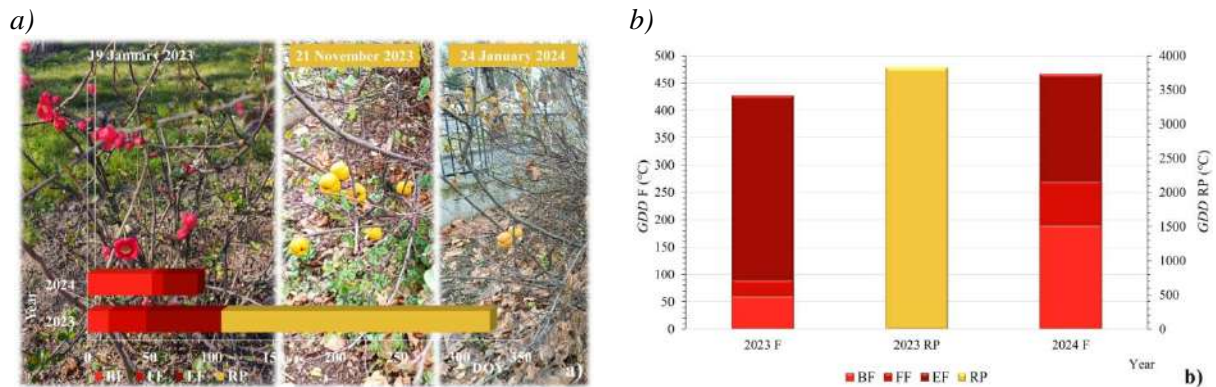


**Figure 1** Phenological observations: BF, FF, EF and RP of Japanese Quince in Karadjordje's Park in Belgrade during the research period: a) DOY; and b) GDD

The cumulative CHt required for the onset of the flowering phenophase from 1 November 2022 to BB 2023 was 634 h, whereas from 1 November 2023 to BB 2024, it amounted to 960 h. Our finding aligns with the conclusion drawn by Cosmulescu and Ionescu [15] that it is necessary to conduct multi-year research at the individual level. The observed difference stems from the influence of climatic parameters (Figure 2). Observations of the flowering phenophase for Japanese Quince over two consecutive years are presented in Figures 1a and b. BF was recorded 35 days earlier in 2023 (BF DOY=17) compared to 2024 (BF DOY=52),



with an accumulation of GDD required for BF amounting to 60.8 in 2023 and 190.0 in 2024. The delayed onset of flowering in 2024 can be attributed to freezing days at the beginning of the second decade of January, while the higher accumulation of heat can be attributed to the fact that, according to the percentile method, the daily mean air temperature was within the extremely warm category during the first and middle decades of the month, and warm in the third decade. In February 2024 (Figure 2), temperatures reached historic highs, with a monthly mean temperature of 11.2°C, marking an increase of 7.4°C compared to the 1991–2020 period (RHMS). The GDD values for EF followed almost the same trend, with flowering concluding at a GDD value of 426.9 (2023) and 466.2 (2024), confirming that GDD, rather than DOY, is crucial for phenological events. The duration of the flowering phenophase in 2024 spanned 37 days, which was 54 days shorter compared to the 91 days observed in 2023. This finding is in direct alignment with climatic parameters and reports of RHMS, indicating that the winter of 2023/2024 was the warmest and driest on record, with notably higher mean seasonal air temperatures and below-average precipitation levels compared to the 1991–2020 period. Figure 2 provides a comparative analysis of the relationship between air temperature and precipitation for January, February, and March of the research years, highlighting significant fluctuations in these variables.

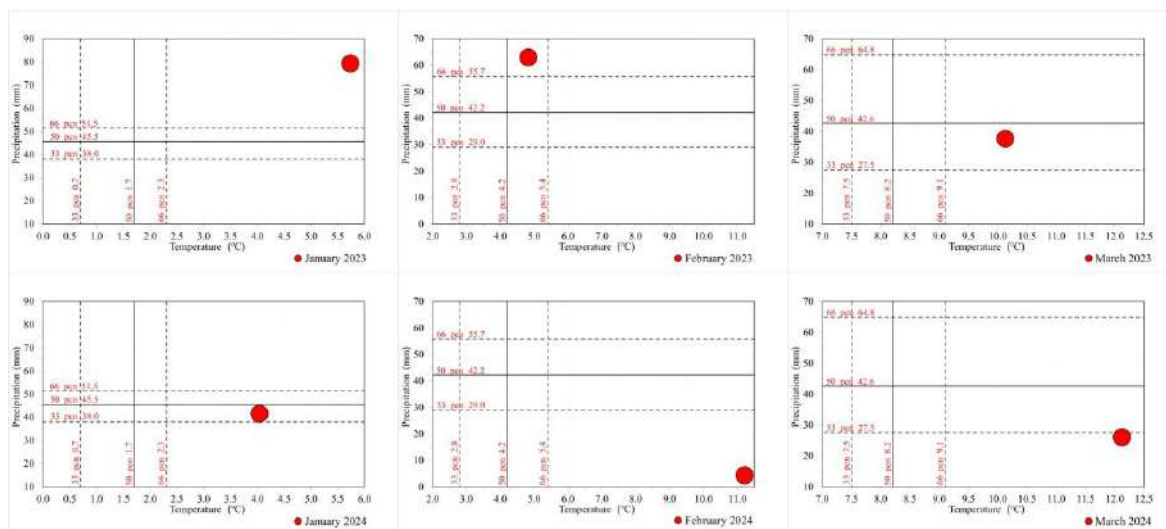


**Figure 2** Mean monthly air temperatures and monthly precipitation sums with their corresponding terciles for MMS in Belgrade for the reference period 1991–2020

During 2023, RP spanned 305 DOY, with a GDD value of 3822.9. The fruits persisted until January 2024. Figure 2 illustrates that March 2023, with air temperatures surpassing the upper tercile threshold and precipitation within average values, can be characterised as warm and moderately rainy according to the percentile and tercile method (RHMS). In contrast, April 2023 was notably cold and ranked as the sixth rainiest month (RHMS). Air temperatures fell significantly below the lower tercile, while precipitation exceeded the upper tercile (Figure 2). A sudden temperature drop and snowfall on the 98<sup>th</sup> DOY (Figure 3), in early April, resulted in surpassing the maximum snow cover height for that day since measurements began in Belgrade. Nevertheless, this event did not cause snow damage or



canopy deformities, and the flowering phenophase continued, affirming the resilience of Japanese Quince.



**Figure 3** Mean monthly air temperature and monthly precipitation sum for April 2023 with their corresponding terciles for the MMS in Belgrade (1991–2020)

The impact of climate change was evident in maximum temperatures, which fell below the normal range for minimum temperatures during the period from 3 to 7 April 2023 compared to the specified dates in the reference period 1991–2020 (RHMs). However, these conditions did not affect the fruiting of Japanese Quince, as indicated by the highest yield rating of 5.

Spearman's correlation coefficients ( $\rho$ ) were calculated, with a significance level of  $p < 0.05$ , confirming statistically significant values for GDD for end of flowering in the study years. Conversely, correlations between years for climatic variables were found to be insignificant, suggesting ongoing climate change. Moreover, it was established that there was not continuously increasing or decreasing association between GDD and DOY, and that the days of the year are not significant for the phenological patterns of flowering. The significance of the year factor was affirmed by the F value (137) obtained from the ANOVA test. Additionally, the study provides crucial insights into the morphological characteristics of flowers from monoecious individuals, contributing to our understanding of the species' acclimatisation.

The ANOVA test did not confirm statistically significant differences in the morphological elements of flowers between two consecutive years, with  $p < 0.0001$  and F values ranging from 60.779 to 141.523. Male genotypes were identified, with male flowers present in all individuals, constituting 4.7% of the total. This led to the absence of fruiting in 4 out of 12 individuals.

## CONCLUSIONS

By identifying ecological strategies, and characteristics of Japanese Quince and its genotypes within the urban park, we have determined the adaptability and potential of the species. Apart from meeting general functionality and formal, technical, and conceptual requirements, urban park design must consider emerging trends driven by addressing

ecological concerns. Consequently, ecology becomes both a functional and a designing dimension of landscape architecture.

Our research indicates certain trends based on the ecological requirements of Japanese Quince: the vital necessity of its presence in the shrub layer for spatial insulation, noise and dust reduction, and biodiversity preservation (serving as bird shelters). We propose that there should be all “layers” within urban parks to maximise ecosystem benefits and enhance ecological effectiveness and sustainability.

## ACKNOWLEDGEMENT

*The authors are grateful to the Ministry of Minister of Science, Technological Development and Innovation of the Republic of Serbia for financial support of the University of Belgrade - Faculty of Forestry the scientific research work in 2024, the registration number 451-03-65/2024-03/200169.*

## REFERENCES

- [1] Tyrväinen L., Mäkinen L., Schipperijn, J., *Landsc. Urban Plan.* 79 (2005) 5–19.
- [2] Forrest M., *Landscape trees and shrubs – selection, use and management.* Athenaeum Press, Gateshead (2006), p.179, ISBN: 978-1-84593-054-7.
- [3] Harris V., Kendal D., Hahs A.K., Threlfall C.G., *Landsc. Res.* 43 (1) (2018) 150–162.
- [4] Lis A., Pardela Ł., Iwankowski P., *Sustainability* 11 (22) (2019) 6324.
- [5] Gill S.E., Handley J.F., Ennos A.R., Pauleit S., *Built Environ.* 33 (1) (2007) 115–133.
- [6] Ocokoljić M., Petrov Dj. *Decorative Dendrology*, University of Belgrade – Faculty of Forestry, Belgrade (2022), p.409, ISBN: 978-86-7299-339-4.
- [7] Ocokoljić M., Petrov Dj., Galečić N., *et al.*, *Land* 12 (2023) 706.
- [8] World Meteorological Organization (WMO), *State of the Global Climate 2021: WMO Provisional Report.* No. 1290, *Available on the following link:* [https://library.wmo.int/doc\\_num.php?explnum\\_id=10859](https://library.wmo.int/doc_num.php?explnum_id=10859).
- [9] Sjöman H., Richnau G., *J. Plant Dev.* 16 (2009) 37–46.
- [10] Timotijević M., *Nasleđe* 5 (2004) 9–34.
- [11] Copernicus, *Land Monitoring Service*, *Available on the following link:* <https://land.copernicus.eu/local/urban-atlas/urban-atlas-2018>.
- [12] Škorić A., Filipovski G., Ćirić M., *Klasifikacija zemljišta Jugoslavije.* Akademije nauka i umjetnosti Bosne i Hercegovine. Posebna izdanja knjiga LXXVIII. Sarajevo (1985), p.72, ISBN: (Broš.). COBISS.SR-ID 84018956.
- [13] RHMZ Republic Hydrometeorological Service of Serbia, *Available on the following link:* [www.hidmet.gov.rs/ciril/meteorologija/klimatologija\\_godisnjaci.php](http://www.hidmet.gov.rs/ciril/meteorologija/klimatologija_godisnjaci.php) and [www.ogimet.com/synopsc.phtml.en](http://www.ogimet.com/synopsc.phtml.en).
- [14] Meier U., *Growth Stages of Plants*, Wiley-Blackwell, Wissenschafts-Verla: Berlin, (1997) 622. ISBN: 3 8263 3152 4.
- [15] Cosmulescu S., Ionescu M.B., *Int. J. Biometeorol.* 62 (2018) 2007–2013.
- [16] Lalić B., Ejcinger J., Dalamarta A., *et al.*, *Meteorologija i klimatologija za agronome.* Univerzitet u Novom Sadu-Poljoprivredni fakultet. Novi Sad, Srbija (2021) p.219, ISBN: 978-86-7520-520-3.



## ***Parthenocissus Quinqefolia* L.: PHENOMONITORING IN BLUE-GREEN INFRASTRUCTURE OF BELGRADE AND NOVI SAD**

**Mirjana Ocoljčić<sup>1</sup>, Jelena Čukanović<sup>2</sup>, Djurdja Petrov<sup>1\*</sup>, Nevenka Galečić<sup>1</sup>,  
Dejan Skočajić<sup>1</sup>, Dragan Vujičić<sup>1</sup>, Isidora Simović<sup>3</sup>**

<sup>1</sup>University of Belgrade, Faculty of Forestry, Kneza Višeslava 1, 11030 Belgrade, SERBIA

<sup>2</sup>University of Novi Sad, Faculty of Agriculture, 8 Dositeja Obradovića Square,  
21000 Novi Sad, SERBIA

<sup>3</sup>BioSense Institute, University of Novi Sad, 1 Dr Zorana Djindjića Street,  
21000 Novi Sad, SERBIA

\*[djurdja.stojicic@sfb.bg.ac.rs](mailto:djurdja.stojicic@sfb.bg.ac.rs)

### **Abstract**

*The study examines the proposition that variations in climatic factors impact the phenological patterns of Virginia creeper within blue-green infrastructure (BGI) situated in urban areas adjacent to major rivers. Key events of phenophases were documented alongside climatic variables as part of the phenological observations. The findings of the investigation validate the species' suitability for innovative strategies, suggesting that, with appropriate maintenance measures, it can contribute to the preservation of vertical greening systems within the urban landscape. Research analyses show that *Parthenocissus quinquefolia* L. demonstrates adaptability in the BGI of Belgrade and Novi Sad, even amidst the conditions of climate change. Recommendations have been formulated to strengthen BGI by the introduction of novel natural solutions involving Virginia creeper to mitigate climate-related risks while revitalizing ecosystems. The integration of nature-inspired elements such as rain gardens, green roofs, and permeable pavements is proposed as part of a solution.*

**Keywords:** blue-green infrastructure, Virginia Creeper, urban environment, landscape design, adaptability.

### **INTRODUCTION**

Blue-green infrastructure (BGI) integrates various measures aimed at enhancing water management and urban landscapes to improve the resilience against climate change. BGI plays a pivotal role in reinstating natural water balance structures within cities by capturing rainwater and expanding permeable surfaces. The infrastructure where plants and water interact is crucial for provision of ecosystem services in urban environments. Namely, plant function is dependent on the water resources, with vegetation exerting a significant influence on local hydrological processes [1]. A comprehensive review of literature [2,3] identifies rain gardens, green roofs, permeable sidewalks, and vertical greening systems as highly effective components of BGI. According to the European Commission [4], tailored solutions designed to mitigate stressors are most effective. Given the unique technical composition of each BGI element, there is no universal BGI solution. Therefore, this study focuses on recording the phenological patterns and key events of Virginia Creeper within the BGI of Belgrade and Novi Sad under the influence of climate change. The objectives are: 1) to assess the condition

and potential utilization of *Parthenocissus quinquefolia* L. in BGI, 2) to revitalize vertical greening systems in BGI areas near major river courses within compact urban centers through innovative approaches, 3) to delineate environmental protection measures and conserve selected elements by relating phenomonitoring data with climate factors, and 4) to implement nature-based solutions.

## MATERIAL AND METHODS

The research was conducted in BGI of Belgrade (location 1 - L1) and Novi Sad (location 2 - L2). At both locations, elements of public green areas near large rivers were selected (Figure 1), where *Parthenocissus quinquefolia* L. (Virginia Creeper), a native species from North America, was identified [5].

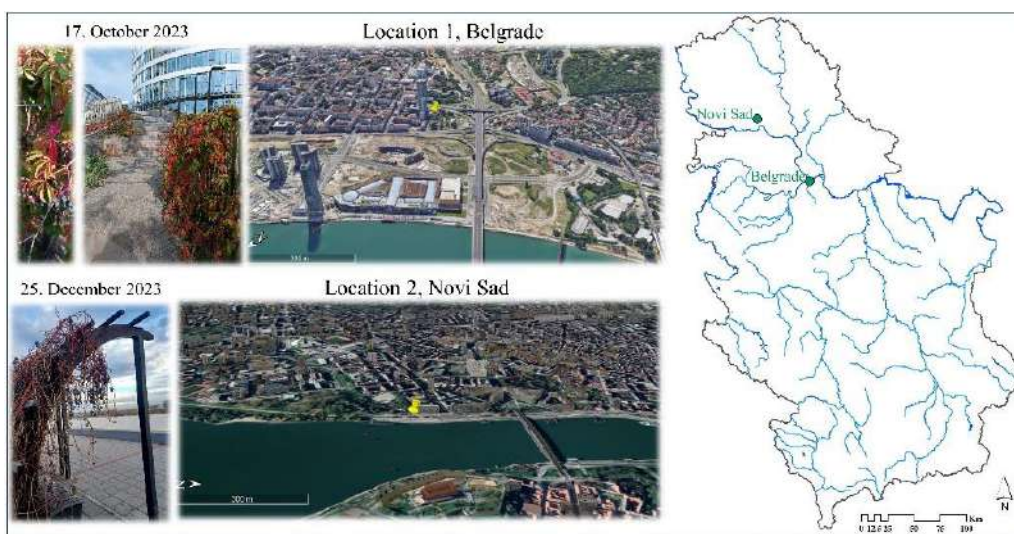


**Figure 1** Locations of the study areas

At Location 1 Virginia Creeper is part of the cascading designed entrance to the Skyline business and residential buildings in the Sava amphitheater. The coordinates are 44°47'58.02" N and 20°27'08.52" E, the altitude is 84–95 m, placed in the terrain with a slope of 4.2° western exposure. The soil is anthropogenic haplic fluvisol [6], and the distance from the right bank of the Sava River is 752.03m. In Location 2, Virginia Creeper is on the pergola, in the „Belgrade Quay“ in the Bač part of Novi Sad. The coordinates are 45°15' 04.78" N and 19°51' 21.16" E, the altitude is 77 m on the exposed terrain. The soil is anthropogenic alluvial sand [7], and the distance from the left bank of the Danube is 24.17 m.

Phenological data are the results of monitoring during the period November 2022 to December 2023. Observations were made visually twice a week, on the same day at both locations using the extended BBCH scale according to Meier [8]. Application of the mentioned scale included the following dates: bud breaking - BB (the day when the buds began to spread), beginning of flowering - BF (the day when more than 10% of the flowers were open), full flowering - FF (the day when more than 50% of flowers), end of flowering - EF (day when more than 80% of flowers have bloomed), secondary flowering - SF (days when flowering repeated), full leaf discolouration - FLD (day when 80% of the leaf mass



acquired autumn color), end of discolouration and leaf-fall - EDL (the day when there were no more leaves on the plants) and ripening of the fruits - RF (the day when the fruits were ripe). Recorded dates are converted by software to days of the year, assuming that DOY 1 – is the first of January. Accumulated cold hours (CHt) from November 1, 2022 to the date when the BB was recorded in 2023 were determined by the Cosmulescu & Ionescu [9] method. Growing degree days (GDD) were determined for flowering phenophases according to the method of Lalić *et al.* [10] (2021). The abundance of the crop is evaluated on a scale where 0 is the absence of fruiting, and 5 is maximum fruiting (>90%). Hourly and daily climatological data were downloaded from RHMZ [11,12] for Location 1 from the Main Meteorological Station (GMS) Belgrade (44°47'54.44" N; 20°27'53.35" E; altitude: 132 m), and for Location 2 from GMS Rimski šančevi (45°19'19.97" N; 19°49'48.01" E; altitude: 86 m). Percentiles and terciles methods were used for air temperature and precipitation, with the  $n^{\text{th}}$  percentile being the value below which  $n$  percent of the data previously arranged in ascending order is located. Quantitative parameters were processed using the XLSTAT2020 software package. Photographic material was collected during the field research.

## RESULTS AND DISCUSSION

At Location 1, *P. quinquefolia* is 4 years old, while at Location 2 it is 16 years old. The number of required CHt for the beginning of the vegetation period from November 1<sup>st</sup>, 2022 to BB 2023 was 1411 h (at Location 1) and 1658 h (at Location 2). The result is consistent with the research of Coutts *et al.* [13]. Differences in CHt between the analyzed locations may be the result of different ages of plants and the influence of climatic parameters, primarily the influence of the urban heat island (UHI) in Location 1 (Table 1).

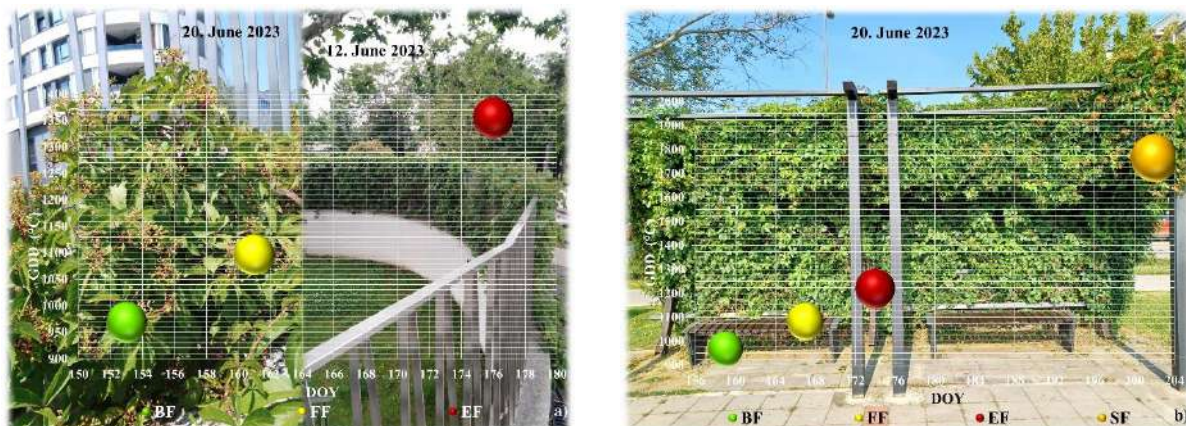


**Figure 2** Phenological observations: GDD and DOY for the flowering phenophase during 2023 (BF, FF, EF) and secondary flowering (SF) in a) Belgrade (L1); and b) Novi Sad (L2)

Figure 2 shows observations of the flowering phenophase for Virginia Creeper at the 2 research locations. BF was recorded 6 days earlier at Location 1 (BF DOY=153), but GDD accumulation requirements for both location was 968.3 (L1) and 967.7 (L2), which confirms that DOY is not crucial for phenological events but rather GDD. The GDD values for FF and EF have the same trend. The earlier BF in Location 1 is explained by the influence of UHI,

and the secondary flowering in Location 2, lasting 5 days in July 2023, by the influence of climatic parameters (tables 1 and 2) as previously shown in the research of Ocokoljić et al. [14]. According to the percentile and tercile method, July in Location 2 was very warm and dry, and in Location 1 very warm and rainy with a deviation of 159 mm of precipitation compared to the reference period 1991–2020, which is why no secondary flowering was recorded in Location 1. Our findings in Location 1 showed that the length of autumnal colorful ornamental effect lasted 71 days similarly to the research of Petrov *et al.* [15] where it lasted 70 days, with an almost identical beginning (DOY 290) and the same ending (DOY 361), as well as the typical coloration reported for the species [4] during this period. At Location 2, the length of autumnal color was 49 days (DOY 303 - DOY 359), and the presence of red and red-purple color was short, after which the leaves changed to shades of brown (Figure 3).

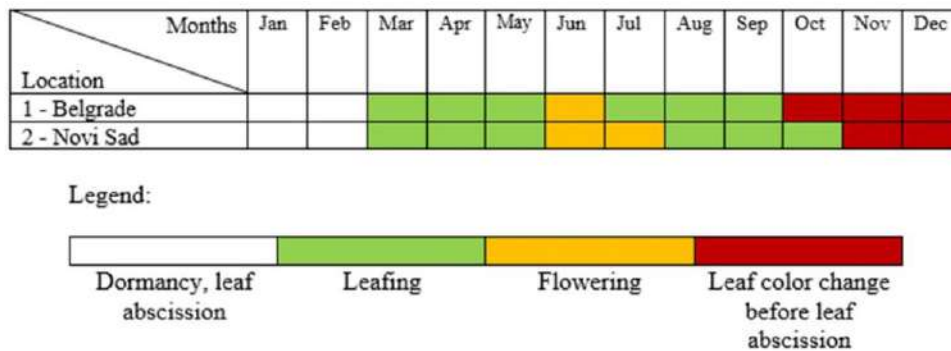


Figure 3 Phenogram of Virginia Creeper for 2023 in Belgrade and Novi Sad

The obtained results correlate with the percentiles and terciles for October and November, which for Location 1 were in the category of very hot and dry in October, and in November in the category of normal and very rainy; while for Location 2 they were in the categories of very warm and dry in October, and warm and rainy in November (Tables 1 and 2). The duration of autumnal color change observed during the autumn and early winter of 2023/24 in both Location 1 and Location 2 correlates directly with climatic factors. These results are consistent with Andersen and Jordheim's [16] observations, which suggest that the alteration in leaf color during autumn is driven by shifts in the metabolic activity of temperate woody plants, as well as that the combination of warm, sunny days and cold and mild nights stimulates the production of anthocyanin pigments that affect the autumn red, purple and crimson color. According to the same authors, the altitude also affects the pace of the autumnal color change, however, this factor is irrelevant in our study since both locations share similar elevations. In both locations, the yield was maximum with a grade of 5. These attractive blue-black fruits are toxic to humans and mammals but serve as a food source for various bird species, including woodpeckers and thrushes.



**Table 1** Mean monthly air temperatures and associated percentiles and terciles and their deviations in Location 1 and Location 2 in relation to the reference period 1991–2020

L	T <sub>mean</sub> (°C)	Perc. Cat.*	T <sub>mean</sub> (°C)	Deviation (°C)	1991–	1991–	1991–	Terciles**
		1991– 2020	1991– 2020		2020	2020	2020	
33.-Perc.								
50.-Perc.								
66.-Perc.								
<b>March</b>								
1	10.1	W	8.3	1.8	7.5	8.2	9.1	1
2	9.0	W	7.0	2.0	5.9	6.8	7.9	1
<b>April</b>								
1	11.2	EC	13.6	-2.4	12.8	13.5	14.2	-1
2	10.4	EC	12.4	-2.0	11.8	12.6	13.1	-1
<b>May</b>								
1	17.4	N	18.2	-0.8	17.5	18.2	19.1	-1
2	17.2	N	17.3	-0.1	16.9	17.3	17.8	0
<b>Jun</b>								
1	21.8	N	21.9	-0.1	21.1	21.8	22.4	0
2	21.5	N	20.9	0.6	20.1	20.6	21.5	0
<b>July</b>								
1	26.0	VW	23.8	2.2	23.1	23.7	24.3	1
2	24.7	VW	22.5	2.2	21.9	22.2	22.9	1
<b>August</b>								
1	24.7	N	23.8	0.9	22.6	24.1	24.8	0
2	23.7	N	22.4	1.3	21.5	22.3	23.0	1
<b>September</b>								
1	22.2	EW	18.5	3.7	17.6	18.3	19.3	1
2	21.4	EW	17.2	4.2	16.3	17.2	18.0	1
<b>October</b>								
1	17.6	EW	13.3	4.3	12.6	13.3	14.4	1
2	16.6	EW	12.0	4.6	11.6	12.1	13.0	1
<b>November</b>								
1	9.5	N	8.1	1.4	7.6	8.3	9.2	1
2	8.4	W	6.8	1.6	6.5	7.1	7.9	1

\* Extremely warm (EW), Very warm (VW), Warm (W), Normal (N), Very cold (VC), Extremely cold (EC)

\*\* Warm (1), Normal (0), Cold (-1), categorization RHMZ

Based on the analysis of species phenomonitoring at two locations, the following recommendations are formulated: a) Continuous, multi-year monitoring of phenological patterns is imperative; b) Greater integration of vertical greening systems within urban landscapes of blue-green infrastructure (BGI) is advised; c) Utilization of the species in novel BGI elements is encouraged, given our research confirms its adaptability in adverse conditions. Furthermore, the implementation of innovative nature-inspired solutions is suggested to mitigate climate risks and foster ecosystem regeneration. Our research validates the resilience of *Parthenocissus quinquefolia* L. in environments characterized by low nutrient levels, drought, urban heat island (UHI) effects, and varying temperature and radiation levels.

**Table 2** Monthly precipitation sums and associated percentiles and terciles and their deviations in Location 1 and Location 2 in relation to the reference period 1991–2020

L	Sum (mm)	Perc. Cat.*	Sum (mm) 1991–2020	Deviation (mm)	1991–2020		1991–2020	Terciles**
		1991–2020			33.-Perc.	50.-Perc.		66.-Perc.
<b>March</b>								
1	37.6	H	48.7	-11.1	27.5	42.6	64.8	-1
2	25.3	H	38.7	-13.4	30.3	36.7	47.8	0
<b>April</b>								
1	79.0	K.	51.5	27.5	38.1	52.1	59.5	1
2	63.9	K.	46.6	17.3	30.3	43.2	54.0	1
<b>May</b>								
1	92.8	K.	72.3	20.5	50.2	62.1	79.6	1
2	124.8	BK.	78.2	46.6	59.4	74.0	84.8	1
<b>Jun</b>								
1	75.6	H	95.6	-20.0	55.7	83.0	127.0	0
2	35.4	C	93.0	-57.6	65.0	94.2	107.0	-1
<b>July</b>								
1	46.8	H	66.6	-19.8	35.3	43.4	58.2	0
2	58.2	H	69.5	-11.3	39.9	59.8	78.3	0
<b>August</b>								
1	87.7	K.	55.1	32.6	42.8	47.6	64.5	1
2	39.9	H	59.7	-19.8	30.1	46.6	78.8	0
<b>September</b>								
1	71.2	H	58.6	12.6	40.2	51.7	61.9	1
2	63.5	H	58.9	4.6	35.0	51.4	76.9	0
<b>October</b>								
1	13.0	BC	54.8	-41.8	35.0	50.4	73.5	-1
2	11.4	C	58.6	-47.2	34.0	61.3	80.0	-1
<b>November</b>								
1	110.3	BK.	49.6	60.7	33.8	48.1	60.2	1
2	83.8	K.	51.5	32.3	32.7	43.8	64.2	1

## CONCLUSION

The analysis of Virginia Creeper phenological monitoring in Belgrade and Novi Sad reaffirmed the species' exceptional adaptability. This characteristic highlights its potential application in innovative strategies aimed at revitalizing and conserving elements of blue-green infrastructure (BGI) through the implementation of appropriate maintenance practices. Beyond its role as a lush green covering, the species serves as a biomeliorator, aiding in soil erosion control, dust retention, and mitigating air pollution. It holds significance as an ornamental plant, contributing to the management of urban BGI environments situated near major river courses.

## ACKNOWLEDGEMENT

The authors are grateful to the Ministry of Education, Science and Technological development of the Republic of Serbia for financial support of the University of Belgrade - Faculty of Forestry the scientific research work in 2024, the registration number 451-03-65/2024-03/200169.

## REFERENCES

- [1] Dreiseitl H., Wanschura B., Strengthening Blue-Green Infrastructure in our Cities: Enhancing Blue-Green Infrastructure & Social Performance in High-Density Urban Environments. Ramboll Foundation. (2016), *Available on the following link:* <https://ramboll.com/-/media/38fc23d12a5d47dcb7b3821716d69270.pdf>.
- [2] Andrew R.F., *Water* 9 (12) (2017) 953.
- [3] Ahmed S., Meenar M., Alam A., *Land* (2019) 138.
- [4] European Commission Towards an EU Research and Innovation Policy Agenda for Nature-Based Solutions and Re-Naturing Cities; European Commission: Brussels, Belgium. (2015), *Available on the following link:* <https://ec.europa.eu/programmes/horizon2020/en/news/towards-eu-research-and-innovationpolicy-agenda-nature-based-solutions-renaturing-cities>.
- [5] Ocokoljić M., Petrov Đ., *Decorative Dendrology*, University of Belgrade – Faculty of Forestry, Belgrade (2022), 409, ISBN: 978-86-7299-339-4.
- [6] Škorić A., Filipovski G., Ćirić M., *Klasifikacija zemljišta Jugoslavije. Akademije nauka i umjetnosti Bosne i Hercegovine. Posebna izdanja knjiga LXXVIII. Sarajevo (1985), p.72, ISBN: (Broš.). COBISS.SR-ID 84018956.*
- [7] Živković B., Nejgerbauer V., Tanasijević Đ., *et al.*, *Zemljišta Vojvodine [Kartografska građa]*. Institut za poljoprivredna istraživanja, Novi Sad (1972), p.5, ISBN (Broš.) COBISS.SR-ID 145833479.
- [8] Meier U., *Growth Stages of Plants*, Wiley-Blackwell, Wissenschafts-Verla: Berlin, (1997) 622. ISBN: 3 8263 3152 4.
- [9] Cosmulescu S., Ionescu M.B., *Int. J. Biometeorol.* (2018) 2007–2013.
- [10] Lalić B., Ejcinger J., Dalamarta A., *et al.*, *Meteorologija i klimatologija za agronome. Univerzitet u Novom Sadu-Poljoprivredni fakultet, Novi Sad, Srbija (2021), p.219, ISBN: 978-86-7520-520-3.*
- [11] RHMZ Republic Hydrometeorological Service of Serbia, *Available on the following link:* [https://www.hidmet.gov.rs/ciril/meteorologija/klimatologija\\_godisnjaci.php](https://www.hidmet.gov.rs/ciril/meteorologija/klimatologija_godisnjaci.php).
- [12] OGIMET Weather Information Service, *Available on the following link:* <https://www.ogimet.com/synopsc.phtml.en>.
- [13] Coutts A., White E., Tapper N., *et al.*, *Theor. Appl. Climatol.* 124 (2015) 55–68.
- [14] Ocokoljić M., Petrov Dj., Galečić N., *et al.*, *Land* 12 (2023) 706.
- [15] Petrov Đ., Ocokoljić M., Galečić N., *et al.*, *Proceedings of EcoTER'23. 20–23.06.2023, Stara planina, Serbia (2023) 210–215.*
- [16] Andersen Ø.M., Jordheim M., *Anthocyanins in Encyclopedia of Life Sciences (ELS)*. Editor Andersen Ø.M., Jordheim M., Publisher Wiley-Blackwell, John Wiley & Sons, Ltd; Chichester: (2010) p.12, ISBN: 9780470015902. 10.1002/9780470015902.a0001909.pub2.



## EFFECTS OF THE IRON GATE DAMS ON THE BENTHIC MACROINVERTEBRATE COMMUNITY

**Bojana Tubić<sup>1\*</sup>, Jelena Đuknić<sup>1</sup>, Katarina Zorić<sup>1</sup>, Nataša Popović<sup>1</sup>, Nikola Marinković<sup>1</sup>,  
Momir Paunović<sup>1</sup>, Maja Raković<sup>1</sup>**

<sup>1</sup>Department for Hydroecology and Water protection, Institute for Biological Research  
“Siniša Stanković”, National Institute of the Republic of Serbia, University of Belgrade,  
Bulevar despota Stefana 142, 11108 Belgrade, SERBIA

\*[bojana@ibiss.bg.ac.rs](mailto:bojana@ibiss.bg.ac.rs)

### Abstract

*The most important factors that influence the condition of the Lower Danube (Serbian stretch) are regulation, damming of the river and the potential influence of structures used as temporary dumping sites for ship debris and equipment. The aim of this paper was to determine the state of the benthic macroinvertebrate community in the area under these influences. A total of 110 taxa in 14 taxonomic-ecological groups were recorded at three surveyed sites. The recorded benthic macroinvertebrate fauna was typical for large lowland rivers and was dominated by Diptera (Chironomidae), Oligochaeta, followed by Gastropoda and Crustacea. Allochthonous invasive species were found to have colonized Serbian aquatic ecosystems, originating from the Ponto-Caspian region, East Asia and North America. Theodoxus transversalis (C. Pfeiffer, 1828), an endangered species in Serbia, was also found. The identified impacts can be assessed as locally significant and the negative impacts are of negligible significance.*

**Keywords:** benthic macroinvertebrate, the Danube River, damms, invasive species, protected species.

### INTRODUCTION

At around 800,000 km<sup>2</sup>, the Danube catchment area is the second largest river basin in Europe. The catchment area extends across 17 countries and the total length of the river is 2,857 km. The Serbian section of the Danube has a length of 588 km. The catchment area covers 178,000 km<sup>2</sup> within the borders of our country. The largest part of the Danube through Serbia (358 km) belongs to the Pannonian plain. In this section, the Danube is a typical lowland river. The construction of the dam at 943 rkm (Iron Gate I, 1970) created a large, 100 km long reservoir. After the Danube was dammed, the flow velocity upstream to Slankamen (1,215 km) was slowed down. In 1984, another dam (Iron Gate II, 863 rkm) was built. The Iron Gate sector is a transitional area (between the middle - Panonian and the lower part of the Danube) and in many aspects (geomorphology, hydromorphology, etc.) this river sector is specific. The long-term harmful effects result mainly from the increase in untreated industrial and municipal wastewater from the rapidly growing cities along the riverbanks and from the changes in the hydrological regime caused by the damming of the Danube and the construction of the Iron Gate hydropower plants [1]. In addition, this sector is an important

target for monitoring, as the river section is under considerable human pressure on the territory of Serbia and neighboring countries.

The aim of this study was to analyze the benthic macroinvertebrate communities in this river sector that is under the influence of the dams on the Danube (HPP “Iron Gate 1” and “Iron Gate 2”).

## MATERIALS AND METHODS

The study area includes investigations of the Danube in the section from Kuskjak (863 rkm), Prahovo (861 rkm) to Radujevac (851 rkm) at a total of 3 investigation sites. Kuskjak is an international border crossing and is also the last port of departure on the territory of Serbia on the Danube River. Prahovo is an industrial settlement northeast of Negotin. The port of Prahovo is located 4 km downstream Iron Gate 2 hydroelectric power plant. Radujevac is the settlement situated upstream the confluence of the Timok and the Danube.

Sampling at the above-mentioned locations was part of the research that was carried out every year during spring and autumn in cooperation with the Institute of Water Management “Jaroslav Černi” to monitor and analyze the effects of the reduction in flow velocity on water quality and the environment in the Đerdap area. In addition to the data from the databases, the lists were supplemented with results collected during field research at the Prahovo site in 2023 (Figure 1).

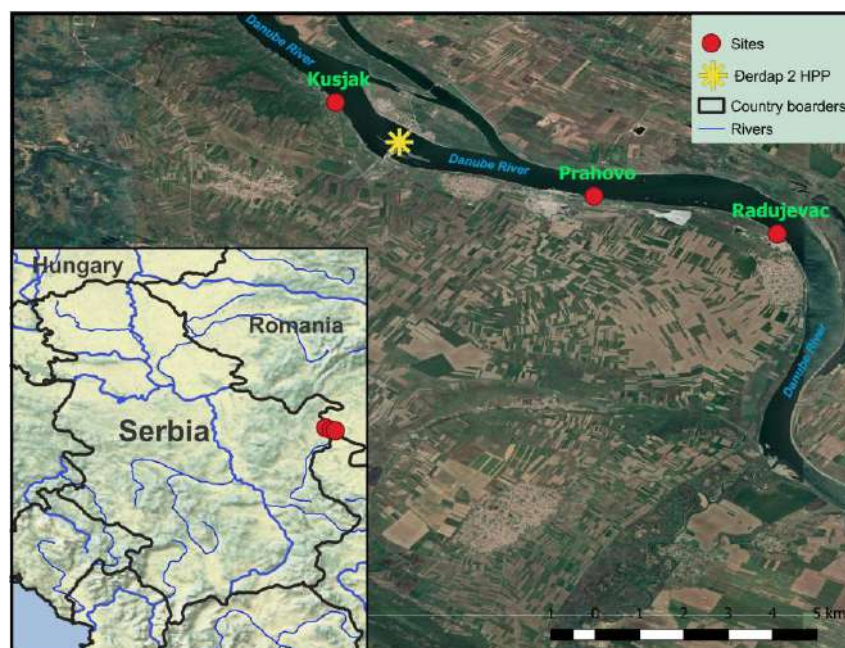


*Figure 1* Map of sampling localities

Sampling was carried out using different techniques adapted to the characteristics of the habitat along the large lowland rivers. Samples of aquatic macroinvertebrates were collected with a benthological handnet with a mesh diameter of 250  $\mu\text{m}$  in the coastal zone (up to 1.5 m depth) from all available microhabitats, using the Multi-Habitat Sampling (MHS technique) [2], and in zones with greater depth samples were collected with a benthological dredge and a



Van Veen grab with a catchment area of 270 cm<sup>2</sup> [3]. Samples were collected with a dredge by dragging it across the river bottom over a length of approximately 10 m with 3 transects along the river cross-section. Where possible, the samples were also collected by diving.

The organisms were sorted and identified using a Nikon SMZ800N stereomicroscope (magnification 10–80x) and ZEISS Axio Lab.A1 microscope (magnification 1000x). Organisms were identified to the lowest possible taxonomic level using appropriate identification keys. All community parameters calculations, based on a macroinvertebrate taxa list, were performed using ASTERICS 4.04 software package.

## RESULTS AND DISCUSSION

A total of 110 taxa in 14 taxonomic-ecological groups were recorded at the Danube studied sites. The most diverse benthic groups are Diptera with 30 recorded taxa, 25 of which belong to the family Chironomidae, and Oligochaeta with 27 recorded taxa. In addition to these groups, a great diversity was also found in the groups of Crustacea and Gastropoda with 15 and 14 recorded taxa respectively. The diversity of other macroinvertebrate groups was lower: 8 taxa were recorded in the Trichoptera group, 2 taxa in the Ephemeroptera and Polychaeta groups. Three groups of macroinvertebrates were represented by only one species: Nematoda, Coleoptera and Coelenterata.

The highest number of taxa (78) was recorded at the Radujevac site. A significant taxa richness was also found at the Kusjak site (58), while the lowest number of taxa (26) was recorded at the Prahovo site. The number of recorded taxa per site is shown in the Figure 2.

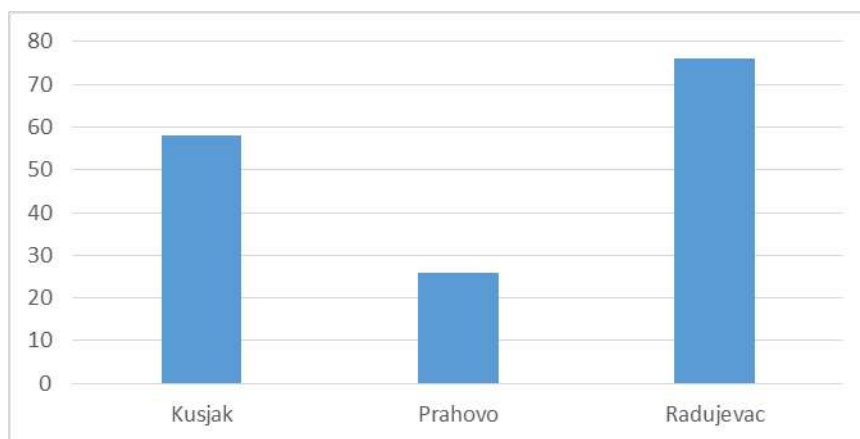


**Figure 2** Number of taxa per sampling sites

The most dominant group in the community in terms of percentage contribution was the Oligochaeta (29.44%), while the rest of the community consisted of Diptera (28.43% - almost 80% of the Diptera belonged to the family Chironomidae), Gastropoda (18.25%) and Crustacea (14.1%). Other taxa groups had a lower percentage participation in the benthic community (Figure 3). The groups Trichoptera and Bivalvia formed the community with 5.07% and 3.58% percentage participation, respectively, while the rest of the community had a percentage participation of less than 1% of the total community.



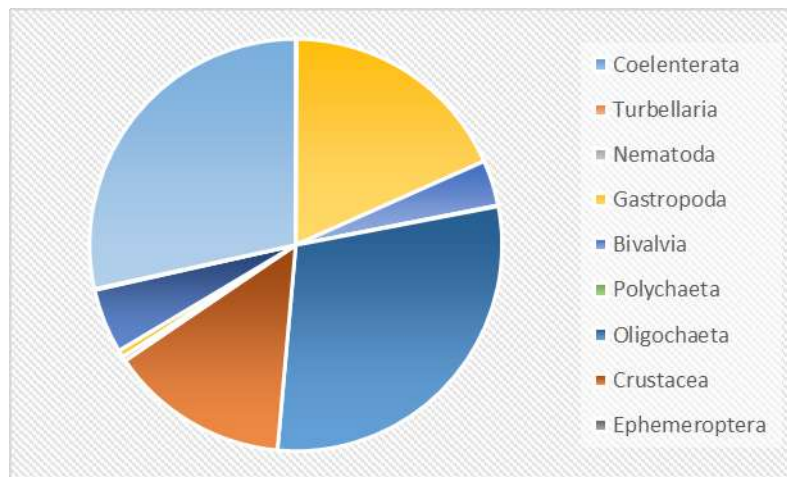


**Figure 3** Percentage of benthic macroinvertebrate taxa in the community

The most abundant species in the community were representatives of the family Chironomidae: *Cricotopus bicinctus* (Meigen 1818), *Polypedilum* gr. *scalaenum* and *Cricotopus* gr. *sylvestris*. All three species were found at the Radujevac site. The number of the Oligochaeta species *Limnodrilus hoffmeisteri* Claparede 1862, was significant, especially at the Kusjak site.

According to the ecological classification of taxa in terms of saprobic valence [4],  $\beta$ -mesosaprobic taxa are the most represented with a percentage of 32.6% and 20.97% of the taxa could be characterized as  $\alpha$ -mesosaprobic (tolerant to high loads of organic material). The oligosaprobic group (tolerant to low levels of organic matter pollution) participated with 12.39% in the community, while polysaprobic organisms were recorded with 10.93%. Only 0.04% of the recorded taxa belong to the xenosaprobic group (tolerant to the lowest levels of organic matter pollution). For 23.07% of the community, there is no data to classify them in terms of saprobic tolerance. A high percentage of  $\alpha$ - and  $\beta$ -mesosaprobic organisms in the entire community indicates moderate organic pollution.

The community was observed according to zonation preferences within the river continuum (longitudinal zonation). Most of the recorded species (42.86%) were typical of the lower reaches of a river (the potamal type: epi-, metha- and hypopotamal). A smaller proportion (18.32%) belonged to the taxa typical of the upper river sections (the rhithral – epi, metha-, hyporhithral), while 15.71% of the recorded taxa belong to organisms that occur in the littoral zone. As expected, the percentage of taxa favoring the headwaters of the river was very low. A similar distribution pattern was observed for each site.

As far as flow preference is concerned, the recorded community is characterized by the dominance of rheo-limnophilous taxa, which prefer slow-flowing streams and lentic zones and also occur in stagnant waters (Type RL–21.49%). The rheophilous type of taxa (Type RP), which occurs in streams and favors zones with moderate to high flow velocity, was recorded with 16.16% of recorded taxa. 8.03% was indifferent taxa (Type IN), which have no preference for a particular current velocity. The next type was limnophilous (Type LR) with 8.82% taxa characterized as preferring stagnant waters but regularly occurring in slow-flowing streams. Limnophilous taxa, which prefer stagnant waters, avoid currents and

are rarely found in slow-flowing streams (Type LP), accounted for 4.47% of the community. 40.73% of the taxa could not be classified in regard to current velocity preference.

The structure of the community in terms of its adaptation to different habitat types shows that organisms favoring fine to medium-sized grains, mud, silt and sand (pelal, argilal and psammal) were recorded with 23.98% of the total community, followed by lithophilous taxa, favoring coarse gravel, stones and boulders (grain size >2 cm) (16.39%). Phytophyllous taxa, which favor algae, mosses and macrophytes, including living parts of terrestrial plants as a specific microhabitat, were recorded with 10.3% of the total community. 4.78% of the recorded taxa belong to Type POM, which favor particulate organic material such as woody debris. For the 42.37% of taxa, there is insufficient data on microhabitat preference.

Among the main feeding types, the collectors were the dominant group, making up 41.01% of the community. Grazers and scrapers (26.66%) and active and passive filter feeders (almost 15%) were also abundant. The predators and shredders were detected with a lower percentage (3.51% and 2.07%, respectively). A smaller number of taxa belonged to other feeding types.

The Danube as a part of the southern invasive corridor in Europe [5] represents one of the most interesting areas for the monitoring and spread of non-native aquatic species. The dispersal routes in Serbia continue along the main tributaries, the Sava, Tisa and Morava Rivers. The natural habitats of alien species that have colonized Serbian aquatic ecosystems are the Ponto-Caspian region, East Asia and North America [6]. Allochthonous invasive species were found in the groups of Oligochaeta (*Branchiura sowerbyi* Beddard, 1892), Polychaeta (*Hypania invalida* (Grube, 1860) and *Manayunkia caspica* Annenkova, 1929), Gastropoda (*Clathrocaspia knipowitschii* (Makarov, 1938)), Bivalvia (*Corbicula fluminea* Müller, 1774, *Dreissena bugensis* Andrusov, 1897 and *Dreissena polymorpha* Pallas, 1771) and Crustacea (*Chelicorophium robustum* (G.O. Sars, 1895), *Corophium curvispinum* Sars, 1895, *Corophium robustum* G.O. Sars, 1895, *Corophium sowinskyi* Martynov, 1924, *Dikerogammarus haemobaphes* (Eichwald, 1841), *Dikerogammarus villosus* Sowinsky, 1894, *Echinogammarus ischnus* Stebbing, 1899, *Faxonius limosus* (Rafinesque, 1817), *Limnomysis benedeni* Czerniavsky, 1882, *Jaera istri* Veuille, 1979 and *Paramysis (Serrapalpis) lacustris* (Czerniavsky, 1882)). In addition to the non-native species, species of great importance for protection and conservation were also found in the study area. At the Prahovo site, a considerable relative abundance of *Theodoxus danubialis* (Pfeiffer, 1828) and *Theodoxus fluviatilis* Linnaeus, 1758, were found. These species are characteristic for the Đerdap sector of the Danube. The species *Theodoxus transversalis* (C. Pfeiffer, 1828), an endangered species in Serbia, which will be included in the first edition of the Red Book for the territory of Serbia (unpublished data), was also found.

## CONCLUSION

The construction of Iron Gate dams lead to the changes in the quantity of suspended particles due to disturbance of sediment at the river bottom, changes in water quality due to mobilization of pollutants from sediment and morphological changes to the riverbed. These changes of the environment influence structure of macroinvertebrate communities. Thus, the recorded benthic macroinvertebrate fauna was typical for large lowland rivers, with

predominance of fine and medium substratum (akal, psammal/psammopelal, argyllal). The recorded communities were dominated by Diptera (especially Chironomidae), Oligochaeta, followed by Gastropoda and Crustacea groups.

The mentioned changes may affect the entire macroinvertebrate community, mainly the relation of native and alien species, especially invasive ones. The populations of the endangered species *T. transversalis* present at Prahovo are significant and should be protected.

Even though the negative impacts of the Iron Gate dams are of negligible importance, the identified impacts can be assessed as locally significant.

### ACKNOWLEDGEMENT

*This research was funded by Ministry of science, technological development and innovation of the Republic of Serbia, contract No. 451-03-66/2024-03/200007.*

### REFERENCES

- [1] Marković V., Atanacković A., Tubić B., *et al.*, Water Research and Management 2 (2012) 41–46.
- [2] AQEM. Manual for the Application of the AQEM System. A Comprehensive Method to Assess European Streams Using Benthic Macroinvertebrates, Developed for the Purpose of the Water Framework Directive, Version 1; The AQEM Consortium: Duisburg-Essen, Germany, (2002).
- [3] Liška I., Wagner F., Sengl M., *et al.*, Joint Danube Survey 4 Scientific Report: A Shared Analysis of the Danube River. Int. Comm. Prot. Danube River, Vienna, (2021).
- [4] Moog O., Fauna Aquatica Austriaca – a comprehensive species inventory of Austrian aquatic organisms with ecological notes. Federal ministry for agriculture and forestry, Wasserwirtschaftskataster Vienna: loose-leaf binder (2002).
- [5] Essl F., Rabitsch W., Austrian action plan of invasive alien species. Federal ministry of agricultural, forestry, environment and water management. Vienna, Austria, (2004) p.15.
- [6] Zorić K., Atanacković A., Tomović J., *et al.*, Water 12(12) (2020) 3521.



## GC-MS QUANTITATIVE DETERMINATION OF PHTHALATES IN PVC ARTICLES INTENDED FOR CHILDREN'S USE

Danica Bogdanović<sup>1\*</sup>, Tatjana Anđelković<sup>1</sup>, Ivana Kostić Kokić<sup>1</sup>, Marina Milovanović<sup>1</sup>

<sup>1</sup>University of Niš, Faculty of Science and Mathematics, Department of Chemistry,  
Višegradska 33, 18000 Niš, SERBIA

\*danica.milojkovic@pmf.edu.rs

### Abstract

*The aim of this work was qualitative and quantitative determination of five phthalates: dimethyl phthalate (DMP), di-n-butyl phthalate (DBP), benzyl butyl phthalate (BBP), di(2-ethylhexyl)phthalate (DEHP) and di-n-octyl phthalate (DOP) in 13 plastic articles intended for children's use using the GC-MS technique. The testing by dissolving plastic articles in tetrahydrofuran (THF) resulted that all 13 examined plastic items were made of polyvinyl chloride (PVC) plastic. By further gas chromatography-mass spectrometry analysis (GC-MS), it was determined that 6 PVC articles contain DEHP in mass percent 17.20 to 20.28%, while the remaining 7 PVC articles contain DOP in the following mass percentages 7.82 to 11.92%. PVC articles that contain DEHP originate from Chinese market. PVC articles that contains DOP originate from the European market. The obtained results are in accordance with the legislation, which gives a limit for the tolerable daily intake for DEHP in Europe, while there is no limit for DOP. Certainly, the values for both DEHP and DOP are extremely higher compared to the values provided for by European regulative, which concern assembled toys intended for children's use.*

**Keywords:** di(2-ethylhexyl) phthalate, di-n-octyl phthalate, PVC, GC-MS.

### INTRODUCTION

Because of the benefits it provides, plastic is a widespread material that is used in almost all spheres of life: medicine, pharmaceuticals, household, food and beverage packaging, for clothing production, etc. Due to its widespread use, people are exposed to plastic daily, and thus are also exposed to additives in plastic, of which phthalates are the most abundant [1]. Phthalates are a series of chemical compounds, which are most often used as plasticizers added to polyvinyl chloride (PVC) plastics. Plastics that contain phthalates are flexible, soft, and convenient to use for various purposes. Because of their physico-chemical properties, phthalates are easily leached from plastic into the environment, in which people are exposed to the harmful effects of phthalates on health. Phthalates have been identified as endocrine-disrupting chemicals which interfere with normal hormonal actions and harmful influence on growth and reproductive system. Children are particularly sensitive to the exposure to endocrine disruptors during early growth [2]. Given that children often encounter plastic toys while growing up, the European Commission has restricted the use of some phthalates. According to directive 1907/2006/EC, products containing more than 0.1% of di(2-ethylhexyl)phthalate (DEHP), di-n-butyl phthalate (DBP) and benzyl butyl phthalate (BBP) (individually or together) in relation to the weight of the plastic product may not be

placed on the market. Also, this directive prohibits the placing on the market of plastic products that children can put in their mouths, which contain DINP, DIDP and di-*n*-octyl phthalate (DOP) in a concentration above 0.1% by mass [3]. European Food Safety Authority (EFSA) had set the tolerable daily intakes (TDI) for these phthalates: 0.01, 0.05, 0.5 mg/kg body weight per day for DBP, DEHP and BBP, respectively [4]. Although there are clear regulations and laws related to phthalates, the amount of phthalates in certain articles, the amount of phthalates that can be introduced into the body during the day (TDI), there are manufacturers who, due to the properties that phthalates provide to plastic, as well as the cost of production, still use phthalates in the production of articles in which the presence of phthalates is strictly prohibited. Such is the case with toys that are intended for children and are made of PVC. That is why it is necessary monitoring of phthalate concentration in PVC articles, for which different techniques are applied. The chromatographic methods frequently used for phthalates determination because of their high sensitivity and selectivity. Technique based on gas chromatography (GC) are GC with Mass Detector (GC-MS), GC with flame ionization detector (GC-FID), solid phase microextraction coupled with GC (SPME-GC-FID), single drop microextraction coupled to GC (SDME-GC-FID), etc. Technique based on high-performance liquid chromatography (HPLC) are solid phase microextraction HPLC (SPME-HPLC), solid phase extraction-HPLC (SPE-HPLC), liquid chromatography coupled with MS (LC-MS), etc.

In this paper thirteen plastic toys are analysed for phthalate content. The qualitative and quantitative determination of five phthalates: DMP, DBP, BBP, DEHP and DOP in thirteen plastic toys, was performed by GC-MS analysis.

## **MATERIALS AND METHODS**

### **Reagents and materials**

#### *Chemical reagents*

The tetrahydrofuran (THF, HPLC grade) was purchased from Fischer scientific (USA). The *n*-hexane (HPLC grade) was purchased from Carlo Erba (France). The DMP, DBP, BBP, DEHP and DOP were purchased, in the highest available purity, from Sigma-Aldrich (USA). Dibutyl adipate (DBA) was purchased from Fluka (Switzerland) and used as an internal standard.

#### *Plastic articles*

Thirteen plastic toys were bought in three different stores in Serbia, although there was composition declaration for only four toys. The declarations of remaining nine analysed toys did not provide information regarding manufacturer or composition. There was only indication of the country of origin of the product. Plastic toys (no. 1–6) were bought in a Chinese store in Serbia, and there was no declaration (country of origin is China). Plastic toys (no. 7–13) were bought in store in Serbia (country of origin is Poland). First three toys (no. 7–9) were marked as plastic only, while other toys from this group (no. 10–13) were marked as being made of PVC plastic.



### *Preparation of calibration standards*

All stock, intermediate and working solutions were prepared in *n*-hexane. The stock solutions of five phthalates separately and DBA were prepared at a concentration about 1000 µg mL<sup>-1</sup>. The stock standard was diluted stepwise with *n*-hexane to prepare working solutions of five phthalates. The calibration standard series was obtained with five phthalates at concentration range 0.25, 0.50, 1.00, 1.50 and 2.50 µg mL<sup>-1</sup> with DBA at a concentration of 1 µg mL<sup>-1</sup>.

### **Apparatus and equipment**

Gas chromatographic analysis was performed by Gas Chromatograph 6890 (Hewlett-Packard, USA) equipped with a mass selective detector (MSD) 5973 (Hewlett-Packard, USA), Auto sampler 7683 (Agilent, USA) and SGE 25QC2/BPX5 0.25 capillary column (25 m×0.22 mm×0.25 µm, non-polar). The gas chromatograph was operated in the split less injection mode. The oven temperature was programmed from initial temperature 90°C (hold time 0 min) to 280°C at a rate of 20°C min<sup>-1</sup> with hold time of 4 min, and post run 300°C (2 min). Helium was the carrier gas (flow rate of 1.0 mL min<sup>-1</sup>). The operating temperature of the MSD was 280°C with the electron impact ionization (EI) voltage of 70 eV. The dwell time was 100 ms. The MSD was used in the single ion-monitoring mode (SIM), the quantification ion is *m/z* 149 for DBP, BBP, DEHP, DOP, *m/z* 163 for DMP and ion *m/z* 185 was chosen as representative ion of DBA. Analyte response was normalized to DBA as internal standard. The identification and quantification of target compound was based on the relative retention time, the presence of target ions and its relative abundance. Both data acquisition and processing were accomplished by Agilent MSD ChemStation<sup>®</sup> D.02.00.275 software.

The centrifuge Jouan C4I Benchtop (Termo Fisher) was used for separation and the analytical balance (Kern, CA) with accuracy of ±0.00001 g for gravimetric measurements.

### **Sample preparation**

To confirm that these plastic articles are PVC, the mentioned articles were dissolved in THF. Dissolution was accelerated using an ultrasonic bath with gentle heating. Bearing in mind that PVC plastics are dissolved in THF, it was considered that all investigated articles which were dissolved in THF, were made of this kind of plastic material.

The noted 13 plastic articles were weighted and dissolved in 4 mL THF. To obtain solutions of phthalates without plastic polymer, after dissolving of PVC articles in THF, 10 mL of *n*-hexane was added to each sample with the aim of polymer precipitation. Obtained turbid solutions were centrifuged at 3500 rpm and filtered through the 0.45 µm PTFE filter. A certain volume of THF-*n*-hexane solutions (10 µL) were diluted with *n*-hexane and after adding DBA as internal standard, samples were analysed by GC-MS technique.

## **RESULTS AND DISCUSSION**

### **GC-MS analysis**

The SIM GC-MS chromatogram of a standard solution of five investigated phthalates and DBA is given in Figure 1. The given chromatogram shows good separation of phthalates and



DBA occurred within a running time of 13.5 min with retention times for DMP, DBA, DBP, BBP, DEHP and DOP 4.78, 6.38, 7.41, 9.23, 9.83, 10.88 min, respectively.

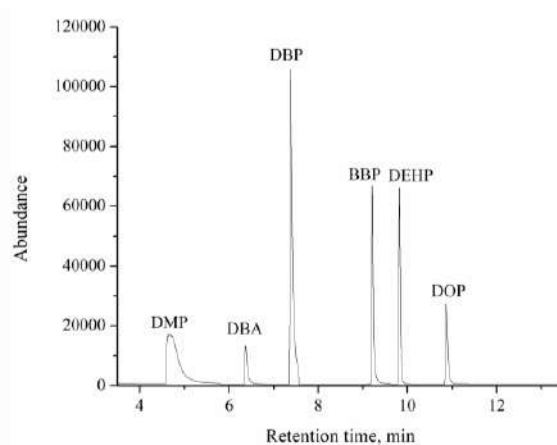


**Figure 1** SIM GC-MS chromatogram of the standard solution of phthalates in concentrations of  $2.5 \mu\text{g mL}^{-1}$  and DBA in concentration  $1.0 \mu\text{g mL}^{-1}$

The calibration curves were linear in the range from  $0.25$  to  $2.5 \mu\text{g mL}^{-1}$  with correlation coefficients of calibration curves higher than  $0.990$ . A calibration curves are presented in Figure 2. The limit of determination (LOD) and limit of quantification (LOQ) were calculated from the signal/noise ratios which were multiplied with the factor 3 and 10 respectively [5]. The LOD values for DMP, DBP, BBP, DEHP are  $0.03$  for each and for DOP is  $0.06 \mu\text{g mL}^{-1}$ ; the LOQ values for DMP, DBP, BBP, DEHP are  $0.10$  for each, and for DOP is  $0.20 \mu\text{g mL}^{-1}$ ; The relative standard deviation (RSD) values for DMP, DBP, BBP, DEHP, DOP are  $7.14$ ,  $10.00$ ,  $6.67$ ,  $6.67$ ,  $12.50$  % ( $n=3$ ), respectively.

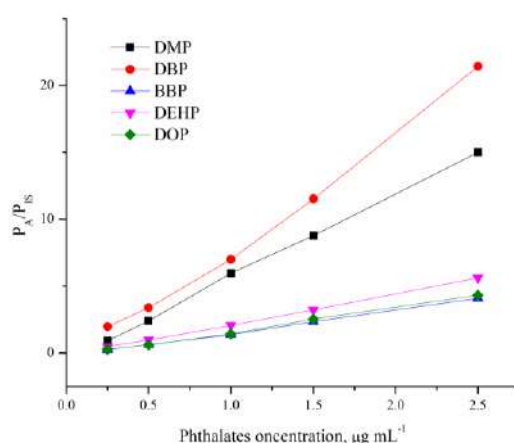


**Figure 2** Calibration curves for DMP, DBP, BBP, DEHP and DOP ( $P_A$  and  $P_{IS}$  represent the chromatographic peak areas of analyte and internal standard, respectively)

### Determination of phthalates in plastic articles

All thirteen investigated plastic articles were dissolved in THF, which showed that they are PVC plastic. These PVC articles were further analyzed for phthalate content by GC-MS

technique after above described preparation. Results obtained after GC-MS analysis showed the presence of DEHP and/or DOP in each investigated article, while DMP, DBP and BBP were not detected. SIM GC-MS chromatograms of two PVC articles are shown in Figure 3.

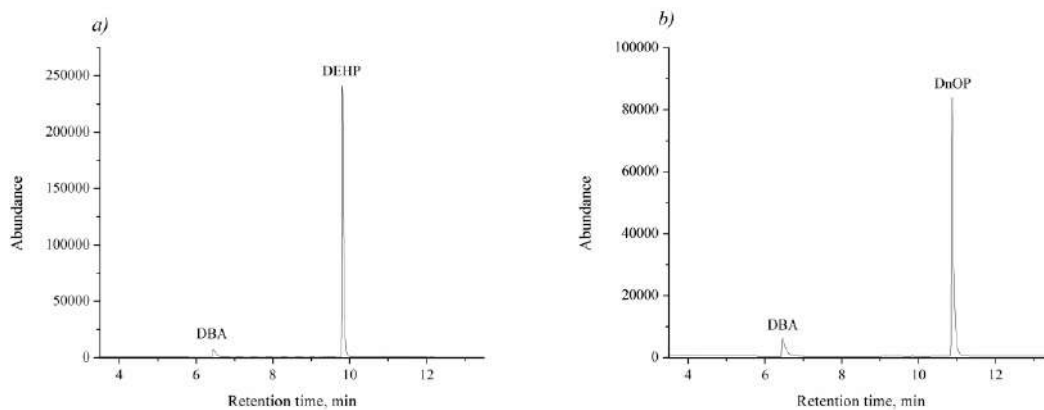


**Figure 3** SIM GC-MS chromatogram of a) PVC article no. 2; b) PVC article no. 13

The percentage of DEHP and DOP in PVC toys obtained using GC-MS analysis are given in Table 1. The results show that PVC toys bought in a Chinese store (no. 1–6) contain DEHP in a mass percentage of 17.20 to 20.28%, the DOP mass percentage in these toys is negligible and amounts of 0.04 to 1.03%. The toys (no. 7–13) made in Poland contain DOP in higher amount than DEHP, with a mass percentage of 7.82 to 11.92%. The DEHP mass percentage in these toys amounts to 0.00 to 0.44%.

**Table 1** Mass percentage of DEHP and DOP in PVC articles

No.	Phthalates in PVC toys (%)	
	DEHP	DOP
1	17.20 ± 0.23	0.14 ± 0.07
2	20.28 ± 1.48	0.04 ± 0.03
3	19.06 ± 0.47	0.30 ± 0.02
4	17.94 ± 0.65	0.09 ± 0.00
5	17.83 ± 1.12	0.11 ± 0.00
6	19.43 ± 1.19	1.03 ± 0.25
7	0.44 ± 0.16	9.91 ± 0.93
8	0.17 ± 0.08	7.82 ± 0.20
9	0.05 ± 0.04	9.69 ± 0.64
10	0.05 ± 0.04	11.80 ± 0.19
11	0.05 ± 0.02	11.20 ± 1.66
12	0.10 ± 0.00	10.29 ± 0.20
13	0.0 ± 0.0	11.92 ± 0.58

## CONCLUSION

By comparing the obtained results, toys of Chinese origin contain a large percentage of DEHP, while toys of Polish origin contain a large percentage of DOP. These results can connect with the fact that the EFSA set a TDI limit for DEHP of 0.05 mg/kg body weight, while EFSA did not set a limit for TDI for DOP. In this regard, toys produced in Europe only contain DOP. However, bearing in mind that there is legislation related to children's toys where both DEHP and DOP are limited to 0.1% of the toy's mass, it concludes that the obtained values for mass concentration of DEHP and DOP by performed GC-MS analysis are significantly increased compared to the permitted ones, as much as 200 times for DEHP and 100 times for DOP. These results are worrying, considering the impact of phthalates on children's health.

## ACKNOWLEDGEMENT

*This study was performed within the research program – Contract No. 451-03-66/2024-03/200124.*

## REFERENCES

- [1] Murphy J., Additives for Plastics Handbook, Second ed., Elsevier Science Ltd, New York, (2001), p.5–11, ISBN: 978-1-85617-370-4.
- [2] Wang Y., Qian H., Healthcare-Basel. 9 (5) (2021) 603–611.
- [3] European Union, Official Journal of the European Union, 50(L247) (2007) 21–55.
- [4] Silano V., Baviera J.M.B., Bolognesu C., *et al.*, Efsa J. 17 (12) (2019) 5838–5923.
- [5] Wisconsin Department of Natural Resources Laboratory Certification Program (1996) Analytical Detection Limit Guidance & Laboratory Guide for Determining Method Detection Limits. Available on the following link: <http://dnr.wi.gov/regulations/labcert/documents/guidance/-lodguide.pdf>.
- [6] Qureshi M.S., Yusoff A.R. bin M., Wirzal M.D.H., *et al.*, Crit. Rev. Anal. Chem. 46 (2) (2016) 146–159.



## OPTIMIZATION OF LIQUID-LIQUID PHTHALATES EXTRACTION FROM ARTIFICIAL SALIVA

Danica Bogdanović<sup>1\*</sup>, Tatjana Anđelković<sup>1</sup>, Ivana Kostić Kokić<sup>1</sup>, Marina Milovanović<sup>1</sup>

<sup>1</sup>University of Niš, Faculty of Science and Mathematics, Department of Chemistry,  
Višegradska 33, 18000 Niš, SERBIA

\*danica.milojkovic@pmf.edu.rs

### Abstract

Children often come into contact with toys made of polyvinyl chloride (PVC) in their earliest years, during the period when they put toys into mouth. For this reason, the aim of this work was optimization the liquid-liquid extraction of phthalates from artificial saliva, in order to determine the most favourable conditions under which the maximum migration of phthalates into the appropriate extraction agent occurs. The analyzed phthalates were dimethyl phthalate (DMP), di-*n*-butyl phthalate (DBP), benzylbutyl phthalate (BBP), di-2-ethylhexyl phthalate (DEHP) and di-*n*-octyl phthalate (DOP). The gas-chromatography coupled with mass-spectrometry (GC-MS) technique for the phthalates quantitative determination were used. The applied parameters of extraction were different extraction agent, agitation time, agitation type, application of reextraction, evaporation of the extract to dryness and evaporation to about 1 mL. The parameters that gave the best recovery values for all investigated phthalates are the application of *n*-hexane, manual shaking, shaking in an ultrasonic bath, evaporation of the extract to a volume of about 1 mL.

**Keywords:** phthalates extraction, artificial saliva, GC-MS.

### INTRODUCTION

Phthalates, or diesters of phthalic acid (1,2-benzenedicarboxylic acid), represent a large group of chemical compounds that are widely used as plasticizers. By adding phthalates to the polymer, the plastic material gains softness and flexibility. Usually, phthalates are added to polyvinyl chloride (PVC) [1]. Such PVC is widely used in various industries, for the production of medical equipment, cosmetics and pharmaceuticals materials, food packaging products, household equipment, childcare articles, including plastic toys, *etc.* [2]. Since phthalates are not covalently bound to the polymer, they can be leached from the plastic under appropriate conditions. The conditions under which the level of migrated phthalates increases are UV radiation, elevated temperature, unsuitable storage conditions, contact with fatty foods, *etc.* [3]. In this way, people are exposed to phthalates and their effects, where phthalates are known as endocrine disruptors. As such, they have a harmful effect on the work of hormones and affect the irregular development of the organism, leading to various malformations and diseases [4]. Because of this, there are laws that prohibit or limit the use of certain phthalates. Since phthalates can enter the body from various sources, but most often through ingestion, through food and drink, the European Food Safety Authority (EFSA) introduced values for the tolerable daily intakes (TDI) for certain phthalates, so for DEHP is 0.05 mg/kg, for DBP is 0.01 mg/kg and for BBP is 0.5 mg/kg body weight per day [5].

Bearing in mind the large use of plastic children's toys that are made of PVC, which contain certain phthalates in their composition, although there are prohibitions for this, it is important to constantly control and monitoring of the composition of such articles. Given that children can put the mentioned PVC article in their mouths, this way children's saliva can be contaminated with phthalates from toys. Children, due to their development, are more sensitive to the effects of endocrine disruptors, such as phthalates, and this is precisely why it is important to constantly monitor the migration of phthalates from these articles into the surrounding environment, in this case saliva. The most commonly used techniques for determining phthalates are techniques based on gas or liquid chromatography: gas chromatography coupled with mass spectrometry (GC-MS), liquid chromatography coupled with MS (LC-MS), solid phase micro extraction high-performance liquid chromatography (SPME-HPLC), *etc.* [6].

The aim of this work was to optimize the liquid-liquid extraction of phthalates from artificial saliva, which implies obtaining the most favourable conditions for phthalate extraction, including the choice of extraction solvent, extraction time, repetition of extraction and method of agitation. Optimisation parameters were investigated for five different phthalates: DMP, DBP, BBP, DEHP, DOP and determination was done using GC-MS technique.

## **MATERIALS AND METHODS**

### **Reagents and materials**

#### *Chemical reagents*

The *n*-hexane (HPLC grade) was purchased from Carlo Erba (France), the chloroform (HPLC grade) and ethyl acetate (HPLC grade) were purchased from J.T. Baker (UK). DMP, DBP, BBP, DEHP and DOP were purchased (99.7% purity) from Sigma–Aldrich (USA). Dibutyl adipate (DBA) was purchased from Fluka (Switzerland) and used as an internal standard.

#### *Preparation of calibration standards*

The standard solutions of five phthalates at a concentration range 0.25, 0.50, 1.00, 1.50 and 2.50  $\mu\text{g mL}^{-1}$  with DBA at a concentration of 1  $\mu\text{g mL}^{-1}$  were prepared in *n*-hexane by diluted of their working solutions of 100  $\mu\text{g mL}^{-1}$  of each.

#### *Artificial saliva*

For optimization of liquid-liquid phthalates extraction from artificial saliva, artificial saliva was prepared according to the standard procedure of the European Commission [7]. The amounts of chemicals given in Table 1 were dissolved in 1 L of distilled water, the pH was adjusted to 6.8 with hydrochloric acid and the artificial saliva prepared by mentioned way was stored in the dark.

**Table 1** Salts used in the preparation of artificial saliva

Chemical compound	Molecular formula	Concentration (mmol L <sup>-1</sup> )
Magnesium chloride	MgCl <sub>2</sub>	0.82
Calcium chloride	CaCl <sub>2</sub>	1.00
Dipotassium hydrogen phosphate	K <sub>2</sub> HPO <sub>4</sub>	3.30
Potassium carbonate	K <sub>2</sub> CO <sub>3</sub>	3.80
Sodium chloride	NaCl	5.60
Potassium chloride	KCl	10.00

### Apparatus and equipment

Gas chromatographic analysis was performed by Gas Chromatograph 6890 (Hewlett-Packard, USA) equipped with a mass selective detector (MSD) 5973 (Hewlett-Packard, USA), Auto sampler 7683 (Agilent, USA) and SGE 25QC2/BPX5 0.25 capillary column (25 m × 0.22 mm × 0.25 μm, non-polar).

The analytical balance (Kern, CA) with accuracy of ±0.00001 g for gravimetric measurements was used.

The Vortex Genie (Scientific industries, USA) was used for vigorous shaking solution of artificial saliva.

The ultrasonic bath was used for shaking solutions of artificial saliva.

### GC-MS technique

The gas chromatograph was operated in the splitless injection mode. The oven temperature was programmed from initial temperature 90°C (hold time 0 min) to 280°C at a rate of 20°C per min with hold time of 4 min, and post run 300°C (2 min.). Helium was the carrier gas (flow rate of 1.0 mL min<sup>-1</sup>). The operating temperature of the MSD was 280°C with the electron impact ionization (EI) voltage of 70 eV.

### The liquid-liquid phthalates extraction procedures

In order to optimize the liquid-liquid extraction of phthalates from artificial saliva, 25 mL of the prepared artificial saliva was first spiked with phthalates so that the phthalates concentration in the artificial saliva samples was accurately known: 0.1, 0.2, 0.3, 0.4 and 0.5 μg mL<sup>-1</sup>. The set conditions and parameters of 5 different procedure of liquid-liquid extraction are as follows:

- 1) Extraction agent is 5 mL *n*-hexane, extraction time is 5 min and type of agitation is manual shaking, following with 5 min agitation in an ultrasonic bath with ultrasonic waves. After the applied type of agitation and after clarification of the layers, the *n*-hexane layer was pipetted. Then, another 5 mL of *n*-hexane to the same artificial saliva was added, and repetition of the agitation procedure was done. After clarification of the layers, the pipetted *n*-hexane layer evaporated to dryness, after which reconstitution of dry residue in 900 μL of *n*-hexane and 100 μL of DBA (10 μg mL<sup>-1</sup>) was performed. The phthalate concentration in the extract thus prepared was determined using the GC-MS technique.
- 2) The procedure is the same as the previous one, the difference is only in the extraction solvent. The chloroform was used as the extraction solvent.



- 3) The procedure is the same as the previous one, the difference is only in the extraction solvent. The ethyl acetate was used as the extraction solvent.
- 4) The extraction agent is 5 mL *n*-hexane, extraction time and method of agitation – 10 min of manual shaking, 30 min of agitation in an ultrasonic bath with ultrasonic waves. Reextraction with 5 mL *n*-hexane was performed, after which evaporation of *n*-hexane clear layer was carried out to a volume of about 1 mL. After addition of DBA, the phthalates determination was performed by GC-MS technique.
- 5) The procedure is the same as the previous one, the difference is that re-extraction was not applied in this extraction procedure, already one extraction with 10 mL of *n*-hexane was performed.

## RESULTS AND DISCUSSION

### GC-MS analysis

The mass spectrometry detector used in the single ion-monitoring mode (SIM). The obtained SIM GC-MS chromatogram of a standard solution of DMP, DBP, BBP, DEHP, DOP and DBA, as internal standard, shows good separation of investigated phthalates and DBA occurred within a running time of 13.5 min. The quantification ion is  $m/z$  149 for DBP, BBP, DEHP and DOP,  $m/z$  163 for DMP and ion  $m/z$  185 was chosen as representative ion of DBA. Analyte response was normalized to DBA as internal standard. The identification and quantification of target compound was based on the relative retention time, the presence of target ions and its relative abundance.

The obtained calibration curves are linear in this concentration range with calibration coefficients higher than 0.990 for each phthalate and are given in Figure 1.

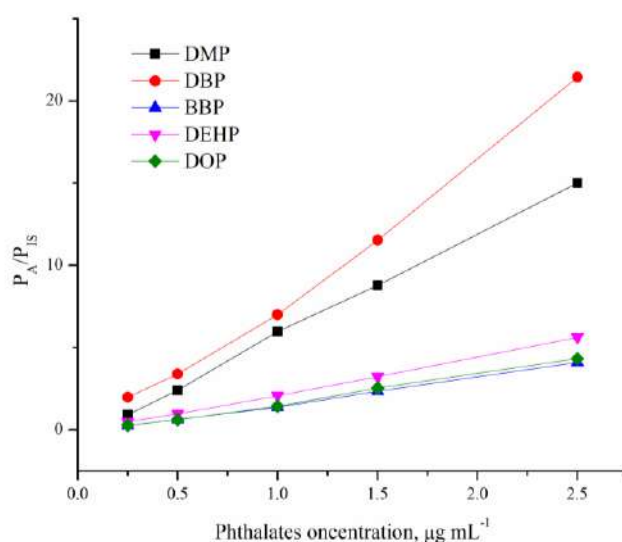


**Figure 1** GC-MS calibration curves in the concentration range 0.25–2.5 µg mL<sup>-1</sup> for: DMP, DBP, BBP, DEHP and DOP. PA and PIS represent the chromatographic peak areas of analyte and internal standard, respectively

### GC-MS phthalates determination after liquid-liquid extraction

After preparing and spiking artificial saliva with 5 analysed phthalates, and applying 5 types of liquid-liquid extraction, where the extraction conditions were changed: type of solvent, type of agitation, agitation time, application of re-extraction, evaporation of extract to dryness and evaporation of extract to about 1 mL, the GC-MS analysis of thus prepared samples was performed.

Based on the obtained calibration curves for phthalates and obtained chromatograms for extracts after appropriate extraction preparation, the phthalates quantification was done. The recovery values for all 5 types of liquid-liquid phthalates extraction were obtained based on the relationship between the phthalate concentration obtained by GC-MS analysis after the applied liquid-liquid phthalates extraction and the phthalates spike concentration. The recovery values for first four type of liquid-liquid phthalates extraction were not satisfactory, but the recovery values for phthalates extraction for fifth type of liquid-liquid phthalates extraction procedure were within satisfactory limits. The results of this analysis are shown in Table 2. The recovery values for DMP is from 0.66 to 1.07 for different spike concentration, for DBP is from 0.64 to 0.81, for BBP is from 0.46 to 0.72, for DEHP is from 0.50 to 0.73, for DOP is from 0.79 to 1.16.

**Table 2** Recovery values (%) of phthalate extraction from artificial saliva using type 5 of LLE

Phthalates concentration (ppm)	Recovery				
	DMP	DBP	BBP	DEHP	DOP
0.1	1.07±0.08	0.75±0.10	0.55±0.13	0.60±0.06	0.89±0.17
0.2	0.82±0.09	0.81±0.08	0.46±0.04	0.62±0.07	0.79±0.02
0.3	0.86±0.06	0.81±0.03	0.50±0.03	0.50±0.03	0.91±0.08
0.4	0.75±0.11	0.70±0.07	0.63±0.15	0.64±0.16	1.16±0.17
0.5	0.66±0.04	0.64±0.12	0.72±0.11	0.73±0.12	1.10±0.11

### CONCLUSION

After optimization of liquid-liquid extraction of phthalates (DMP, DBP, BBP, DEHP, DOP) – setting different extraction conditions and after phthalates quantification in the extracts by GC-MS analysis, the following conclusion is reached. The most favourable parameters for the liquid-liquid extraction of phthalates from artificial saliva are the following: *n*-hexane as an extraction agent, method of agitation and time of agitation – 10 min of manual shaking, 30 min of agitation in an ultrasonic bath with ultrasonic waves, evaporation the volume of the extract to about 1 mL, without the re-extraction procedure. The mean recovery value for DMP with standard deviation is 0.83±0.15, for DBP 0.74±0.07, for BBP 0.57±0.10, for DEHP 0.62±0.08, for DOP 0.97±0.15. These recovery values have reached a satisfactory level and for this reason the conditions applied during the noted liquid-liquid extraction process are considered suitable.

### ACKNOWLEDGEMENT

*This study was performed within the research program – Contract No. 451-03-66/2024-03/200124.*

## **REFERENCES**

- [1] Andrady A., Neal M., *Philos. T. R. Soc. B* 364 (2009) 1977–1984.
- [2] Özer E.T., Gücer S., *Talanta* 84 (2011) 362–367.
- [3] Staples C.A., Peterson D.R., Parkerton T.F., *et al.*, *Chemosphere* 35 (1997) 667–749.
- [4] Wang Y., Qian H., *Healthcare-Basel*. 9 (5) (2021) 603–611.
- [5] Silano V., Baviera J.M.B., Bolognesu C., *et al.*, *Efsa J.* 17 (12) (2019) 5838–5923.
- [6] Al-Natsheha M., Alawi M., Manar M., *et al.*, *J. Chromatogr. B.* 985 (2015) 103–109.
- [7] Standard operation procedure for Determination of release of phthalate plasticizers in saliva simulant, Appendix 1 of report V3932, Ref. Ares 4242543 (2015).



## MIGRATION OF DI-2-ETHYLHEXYL PHTHALATE AND DI-N-OCTYL PHTHALATE FROM PVC ARTICLES TO ARTIFICIAL SALIVA

Danica Bogdanović<sup>1\*</sup>, Tatjana Anđelković<sup>1</sup>, Ivana Kostić Kokić<sup>1</sup>, Marina Milovanović<sup>1</sup>

<sup>1</sup>University of Niš, Faculty of Science and Mathematics, Department of Chemistry,  
Višegradska 33, 18000 Niš, SERBIA

\*danica.milojkovic@pmf.edu.rs

### Abstract

*The aim of this work was to monitor the migration of di-2-ethylhexyl phthalate (DEHP) and di-n-octyl phthalate (DOP) from polyvinyl chloride (PVC) toys into artificial saliva under conditions that mimic the chewing of a toy by a child when he puts the toy in his mouth - temperature 37°C and shaking in an ultrasonic bath. The obtained results show an insignificant percentage of the migration of the mentioned phthalates in artificial saliva, the values of the percentage of DEHP migration are from 0.0025 to 0.0051%, while for DOP the mass percentage are from 0.0003 to 0.0009%. These results are due to the fact that DEHP and DOP are non-polar compounds, voluminous structures, and as such do not tend to transfer to a polar environment such as artificial saliva. However, one should be concerned, because this research determined migration only in a certain period of time, while in real conditions, the child repeatedly puts the same toy in the mouth, and is contaminated with phthalates every day during early childhood, which certainly has a negative effect on his development.*

**Keywords:** DEHP, DOP, artificial saliva, migration, GC-MS.

### INTRODUCTION

The properties of plastic, polymeric material, such as capability to being moulded, low density, transparency and toughness, allows plastics to be made into a great variety of products. To achieve even greater elasticity and softness, plasticizers are added to polymers, among which phthalates are the most famous. Plastic from polyvinyl chloride (PVC), which is otherwise curt and rigid, with the addition of phthalates becomes easy to shape, so the following products can be made from it: medical and pharmaceutical equipment, children's products including toys, products intended for home use, etc.

Phthalates are synthetic compounds, non-polar, and as such poorly soluble in a polar environment, and easily soluble in a non-polar environment. Usually, phthalates are added to a plastic made of PVC, and the most commonly used phthalates are: di-2-ethylhexyl phthalate (DEHP), di-n-butyl phthalate (DBP), di-n-octyl phthalate (DOP), benzyl butyl phthalate (BBP), etc. [1]. Of the listed phthalates, DEHP is the most commonly used plasticizer due to its market price. Although DEHP production is decreasing over time, DEHP is still one of the "biggest" pollutants, as plastics can contain from 1 to 40% of toxic DEHP [2]. Phthalates are not chemically bound to the polymer, but are incorporated into polymer, and by leaching, they easily reach the surrounding environment, which has a harmful effect on human health. Exposure to phthalates can cause various endocrinological and metabolic disorders because

phthalates negatively affect the work of glands that secrete hormones. Phthalates as such belong to endocrine disruptors and contribute to various outcomes when it comes to human health: negatively affect the reproductive health of adolescents, affect the endocrine disorder that leads to the appearance of breast cancer, affect kidney function and the appearance of cysts [3–5]. Bearing in mind adverse effects on human health, legislation established a tolerable daily intake (TDI) value of  $0.05 \text{ mg kg}^{-1}$  body weight for DEHP [6]. Due to the high exposure of children to phthalates from the PVC toys, the rapid metabolism, low body weight and insufficient physiological maturity of children, children are exposed to the effect of phthalates from plastic toys in the earliest stage of their development, laws which prohibiting the use of certain phthalates, as well as limiting the use of other phthalates have been passed. The European Commission has restricted the use of DEHP, DBP and BBP as plasticizers in children's toys and childcare products, while the restriction on the use of DINP, DIDP and DOP only applies to toys that children can put in their mouths. According to directive 1907/2006/EC, products containing more than 0.1% of DEHP, DBP and BBP (individually or together) in relation to the weight of the plastic product may not be placed on the market. Also, this directive prohibits the placing on the market of plastic products that children can put in their mouths, which contain DINP, DIDP and DOP in a concentration above 0.1% by mass [7]. Despite these bans, PVC toys containing phthalates, in mass percentages greater than 10%, can be found in markets [8].

The goal of this research was to determine the amount of DEHP and DOP migrated from PVC toys into artificial saliva, while simulating real conditions under which saliva contamination may occur when a child puts the toy in the mouth. Determination of the phthalate concentration in contaminated artificial saliva was performed using the GC-MS technique. Plastic toys that are designed to be put in the mouth were analysed and as such represent a potential source of phthalates, whose previous analysis determined the presence of DEHP and DOP.

## **MATERIALS AND METHODS**

### **Reagents and materials**

#### *Chemical reagents*

The *n*-hexane (HPLC grade) was purchased from Carlo Erba (France). DEHP and DOP were purchased (99.7% purity) from Sigma–Aldrich (USA). Dibutyl adipate (DBA) was purchased from Fluka (Switzerland) and used as an internal standard. Magnesium chloride, calcium chloride, dipotassium hydrogen phosphate, potassium carbonate, sodium chloride and potassium chloride (*p.a.*) were purchased from Thermo Fisher Scientific (USA).

#### *Preparation of calibration standards*

The standard solutions of DEHP and DOP at a concentration range 0.25, 0.50, 1.00, 1.50 and  $2.50 \mu\text{g mL}^{-1}$  with DBA at a concentration of  $1 \mu\text{g mL}^{-1}$  were prepared in *n*-hexane by diluted of their working solutions of  $100 \mu\text{g mL}^{-1}$  of each.

#### *Artificial saliva*

The artificial saliva was prepared according to the standard procedure of the European Commission: 0.82 mmol magnesium chloride, 1.00 mmol calcium chloride, 3.30 mmol

dipotassium hydrogen phosphate, 3.80 mmol potassium carbonate, 5.60 mmol sodium chloride, 10.00 mmol potassium chloride were dissolved in 1 L of distilled water, and the pH was adjusted to 6.8 with hydrochloric acid [9]. The artificial saliva prepared in this way was stored in the dark.

#### *PVC toys*

The phthalates migration from 13 different plastic toys was analysed, where the previous analysis determined that these plastic toys were made from PVC, as well as which phthalates are included in the composition of these toys. The first 6 analysed PVC toys contain DEHP in their composition, and were bought in a Chinese store. The following 7 PVC toys, produced in Poland, have DOP in their composition. These toys were cut into pieces with an area of 1 cm<sup>2</sup>, after which the mass of each sample was measured on an analytical balance (with ±0.00001 g accuracy).

#### **Apparatus and equipment**

Gas chromatographic analysis was performed by Gas Chromatograph 6890 (Hewlett-Packard, USA) equipped with a mass selective detector (MSD) 5973 (Hewlett-Packard, USA), Auto sampler 7683 (Agilent, USA) and SGE 25QC2/BPX5 0.25 capillary column (25 m × 0.22 mm × 0.25 μm, non-polar). The analytical balance (Kern, CA) with accuracy of ± 0.00001 g for gravimetric measurements was used. The ultrasonic bath was used for shaking solutions of artificial saliva.

#### **Phthalates migration test from PVC toys into artificial saliva**

This test simulates the real conditions in which a child chews on a PVC toy, where there is a potential migration of phthalates from the PVC toy into the child's saliva, which may expose the child to phthalates.

Each PVC toy, about 1 cm<sup>2</sup> in area, was covered with artificial saliva (12.5 mL). Ultrasonic agitation for 30 minutes at a temperature of 37°C was performed. Then the same piece of PVC toy was covered with a new volume of artificial saliva (12.5 mL), after which it was necessary to repeat the ultrasonic agitation for 30 minutes at a temperature of 37°C. The potential phthalate contaminated artificial saliva (25 mL) was collected, which was further used for phthalate determination using optimized liquid-liquid extraction.

The optimized liquid-liquid extraction involved the following steps: the extraction agent was 5 mL *n*-hexane, extraction time and method of agitation – 10 min of manual shaking, 30 min of agitation in an ultrasonic bath with ultrasonic waves. Reextraction with 5 mL *n*-hexane was performed, after which evaporation of *n*-hexane clear layer was carried out to a volume of about 1 mL. After addition of DBA, the phthalates determination was performed by GC-MS technique.

#### **GC-MS technique**

The gas chromatograph was operated in the split less injection mode. The oven temperature was programmed from initial temperature 90°C (hold time 0 min) to 280°C at a rate of 20°C per min with hold time of 4 min, and post run 300°C (2 min). Helium was the carrier gas (flow rate of 1.0 mL min<sup>-1</sup>). The operating temperature of the MSD was 280°C with the electron impact ionization (EI) voltage of 70 eV.



## RESULTS AND DISCUSSION

### GC-MS analysis

Identification and quantification of the mentioned phthalates were carried out based on quantitative, qualitative and target ions for DEHP, DOP and DBA, and their retention times, are given in Table 1.

**Table 1** The quantitative, qualitative and target ions and retention times for DEHP, DOP and DBA

Phthalat	Molecular weight (g/mol)	Ion (m/z)	Retention times (min)
DEHP	390	149*, 167, 279	9.83
DOP	390	149*, 167, 261, 279	10.88
DBA	258	185*, 129, 111	6.38

\* Target ions, quantification ions.

The calibration curves for DEHP and DOP were linear in the range of calibration standards concentration (0.25–2.50  $\mu\text{g mL}^{-1}$ ) with correlation coefficients of calibration curves higher than 0.99. The linear equations of these curves are given in Table 2.

**Table 2** The linear equations of calibration curves for DEHP and DOP

Phthalat	Equations	$r^2$
DEHP	$y = (2.29256 \pm 0.03991) \cdot x - (0.15477 \pm 0.05592)$	0.999
DOP	$y = (1.82695 \pm 0.05616) \cdot x - (0.26043 \pm 0.07867)$	0.996

### GC-MS phthalate determination

After appropriate preparation of the samples, where phthalates migrated from the PVC toys into artificial saliva, and after liquid-liquid phthalates extraction from artificial saliva into *n*-hexane as an extraction agent, GC-MS analysis was performed. Figure 1 shows the chromatograms of the sample extracts of PVC toy no. 1 and PVC toy no. 7. Obtained chromatograms show that DEHP migrated from PVC toy no. 1 to artificial saliva, because it is a toy that only contains DEHP from phthalates, which also applies to toys from no. 2 to no. 6, while only DOP migrated from toy no. 7, which was determined by earlier analysis to be part of the composition of toys no. 7 to no. 13.

The quantitative GC-MS analysis determined the concentration of DEHP and DOP in the extract. This determined the amount of this phthalates that migrated from the PVC toys into the artificial saliva after the migration test was set. The results in the form of the percentage of migrated phthalates in relation to the weight of the PVC toy are shown in Table 3.

The results show that only 0.0025–0.0051% of DEHP from the PVC toy composition migrates into artificial saliva, while only 0.0003–0.0013% of DOP from the PVC toy composition migrates into artificial saliva. The reason for this is that DEHP and DOP are non-polar, voluminous molecules, while artificial saliva is a polar environment, into which phthalates, being non-polar, do not tend to move under these conditions.

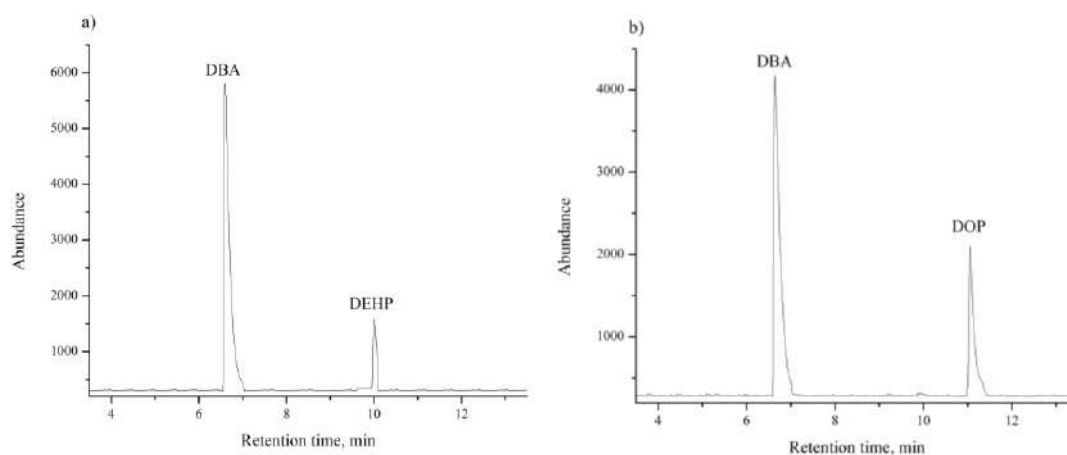


Figure 1 SIM GC-MS chromatogram of a) sample no. 1; b) sample no. 7

Table 3 Percentage of DEHP and DOP migration from PVC toys

PVC article	Percentage of DEHP migration
1	0.0051±0.0014
2	0.0030±0.0003
3	0.0036±0.0005
4	0.0028±0.0003
5	0.0031±0.0007
6	0.0025±0.0003
PVC article	Percentage of DOP migration
7	0.0003±7,83·10 <sup>-5</sup>
8	0.0004±5,90·10 <sup>-5</sup>
9	0.0008±4,26·10 <sup>-4</sup>
10	0.0009±4,92·10 <sup>-4</sup>
11	0.0004±1,77·10 <sup>-4</sup>
12	0.0008±3,26·10 <sup>-4</sup>
13	0.0013±1.06·10 <sup>-4</sup>

## CONCLUSION

The results obtained by this research show data no indicating that plastic toys are a significant source of phthalate exposure in children. However, bearing in mind, that phthalates are additive, *i.e.* that phthalates in combination with other phthalates and other chemicals can produce negative “cocktail” consequences, care should be taken when it comes to children and setting safety standards for phthalates boundaries. Therefore, when setting safety standards for phthalates, it is necessary to consider their mutual interaction and the cumulative effect of phthalates in a given product or several products that are used simultaneously, in order not to underestimate the real risk of using products contaminated with phthalates for human health. For this reason, polyethylene and polypropylene, plastics that do not contain phthalates and do not release other harmful substances into their environment, are recommended for the production of children's toys.

## ACKNOWLEDGEMENT

This study was performed within the research program – Contract No. 451-03-66/2024-03/200124.

## REFERENCES

- [1] Net S., Sempere R., Delmont A., *et al.*, *Environ. Sci. Technol.* 49 (7) (2015) 4019–4035.
- [2] Rudel R., Perovich L., *Atmos. Environ.* 43(1) (2008) 170–81.
- [3] Axelsson J., Rylander L., Rignell-Hydbom A., *et al.*, *Environ. Res.* 138 (2011) 264–270.
- [4] Waring R.H., Harris R.M., *Maturitas.* 68 (2011) 111–115.
- [5] Rowdhwal S.S.S., Chen J., *Biomed. Res. Int.* 2018 (2018) 1–10.
- [6] Silano V., Baviera J.M.B., Bolognesu C., *et al.*, *The Efsa Journal* 17(12) (2019) 5838–5923.
- [7] European Union, *Official J. of the European Union* (2006) 49(L396) (2006) 1–849.
- [8] Anđelković T., Bogdanović D., Kostić Kokić I., *et al.*, *J. Serb. Chem. Soc.* 87 (1) (2022) 145–156.
- [9] Standard operation procedure for Determination of release of phthalate plasticizers in saliva simulant, Appendix 1 of report V3932, Ref. Ares 4242543 (2015).



## HAEMOSPORIDIAN PARASITES IN LONG-EARED OWLS WINTERING IN BANAT, SERBIA

Daliborka Stanković<sup>1\*</sup>, Draženko Z. Rajković<sup>1</sup>, Marko Raković<sup>1</sup>, Stefan Skorić<sup>1</sup>

<sup>1</sup>University in Belgrade-Institute for Multidisciplinary Research, Kneza Višeslava 1,  
11000 Belgrade, SERBIA

\*daliborka@imsi.bg.ac.rs

### Abstract

*Parasites from the Phylum Apicomplexa (genera Haemoproteus, Plasmodium and Leucocytozoon) are the vector-born blood parasites distributed worldwide. This group of parasites has been the subject of extensive study in passerines, but less so in other groups of birds, such as owls. Four haemosporidian species have been discovered in the Long-eared Owl *Asio otus* so far. As there are only a few records of haemosporidian infection in wintering Long-eared Owls, in our pilot project we studied the prevalence, parasitemia, and diversity of the blood parasites of owl mentioned above in Banat, Serbia. We found the presence of all three genera, of which Leucocytozoon was the most abundant. The total prevalence was 52.2%, while the average parasitemia in winter was low, only 0.16%. We also observed two cases of co-infection. Interestingly, the presence of parasites did not affect the SMI (scaled mass index) and the health status of the birds.*

**Keywords:** haemosporidians, prevalence, long-eared owls, *Asio otus*.

### INTRODUCTION

Haemosporidian parasites from the Phylum Apicomplexa (genera *Haemoproteus*, *Plasmodium* and *Leucocytozoon*) are spread across all zoogeographical regions, excluding the Antarctic [1]. This group of vector-born parasites and their avian hosts is a very dynamic and complex system [2]. While some haemosporidian parasites are capable of infecting multiple host species [3–5], others are highly host-specialised [6–8]. Although parasites and their hosts have a long co-evolution history and adaptation, the clinical signs of infection caused by haemosporidians vary among individuals. In general, they can negatively affect feather growth, cause anemia, weight loss, negative body condition, or may even lead to detrimental effects [9–11].

Most haemosporidian studies have been conducted on passerines, while owls have been widely neglected [12,13] despite their important role in ecosystems [14]. So far, eight species of avian Haemosporidia have been discovered and described in order Strigiformes [1] with more than 298 unique lineages worldwide [15]. In the Long-eared Owl *Asio otus*, four haemosporidian species were detected, including seven *Haemoproteus*, one *Plasmodium* and 12 *Leucocytozoon* lineages [15]. The prevalence of the Long-eared Owl varies between 40% and 75% in Germany [12,16] up to 82% in the USA [13]. While in the most research *Leucocytozoon* tended to be the most common genus, Martín-Maldonado *et al.* [17] in Spain found *Haemoproteus* to be the only parasite infecting the Long-eared Owl with parasitemia

up to 12.8%. In Vojvodina (Serbia), Minichová *et al.* [18] detected all three haemosporidian genera in Long-eared Owl, with *Leucocytozoon* being the most abundant.

The Long-eared owl is a well-known, widespread, medium-sized owl. It breeds throughout northwest Africa, Europe, Asia and North America, except in the far north and south. Four subspecies have been recognised, of which the nominal inhabits mainland Europe [19]. It is a regular breeder in Serbia, mainly in Vojvodina [20], but also in the mountain regions [21]. It breeds mostly in old Corvid nests [20]. The national breeding population is estimated at 19,000–28,000 breeding pairs [22]. The presence of a large number of Long-eared Owls wintering in the Province of Vojvodina (Serbia) [23], allows us to sample a significant number of owls in the roost sites and to easily study haemosporidian parasites. However, no study on Long-eared Owl haemosporidian parasitemia has been conducted so far.

The aim of the present study was to assess the diversity, prevalence and parasitemia of blood parasites in Long-eared Owls wintering in Banat, Serbia. Additionally, we explore the potential impact of these parasites on the SMI (scaled mass index).

## **MATERIALS AND METHODS**

### **Study sites and sample collection**

The study was conducted in December 2023 at four localities (Taraš, Mokrin, Padinska skela and Opovo) in Banat, in Vojvodina region. Birds were captured while leaving the roosting trees using ornithological mist nets (mesh size 70 mm). They were ringed, aged, and measured with standard protocols [24]. To assess the physical condition of the birds we used the scaled mass index (SMI), as it appears to be a reliable predictor [25]. SMI is based on the scaling relationship between mass and wing/tarsus length, which was measured and then used for further calculation the SMI. We also collected a small amount of blood from each bird by puncturing the brachial vein. A small drop of blood was used to prepare a thin blood smear, air dried and later fixed in 96% ethanol for 5 minutes according to Valkiūnas [1]. After bleeding was stopped the owls were safely released.

### **Slides examination**

In the laboratory, blood smears were stained with Giemsa solution as recommended by Valkiūnas [1]. Slides were examined by LEICA DMLS light microscope [26] in order to estimate the prevalence and intensity of infection (parasitaemia). As described, parasitemia was estimated as a percentage by counting the number of parasites per 1,000 or 10,000 examined red blood cells, depending on the level of parasitemia [1,27].

### **Statistical analysis**

To examine within-individual differences, Welch Two Sample t-test was used for fitted for infection status, and sex, using the R package version 4.2.2. [28]. The regression slope was 0.34 and the averaged wing length was 258.9 mm, from which using the equation of the linear regression a scaled mass index (SMI) was calculated [25].

## RESULTS AND DISCUSSION

In the present study, we screened 23 Long-eared Owls for haemosporidian parasites during the wintering season in 2023, in Banat, Serbia. Even the highest prevalence in owls was recorded during the spring and summer season [17] some study recorded infection in winter as well [18,29]. Indeed, in our study we found haemosporidian infection in Long-eared owls during the autumn-winter period.

To detect haemosporidian blood parasites, we used only the method based on examination of blood smears [1]. We were able to identify parasites morphologically only to the genus level. Previous studies in the Long-eared owls revealed very high prevalence of the blood parasites varying among 70% and 75% [13,16]. In the USA, the prevalence was even higher, up to 82 % [13], while we found that it was 52.2% (Table 1).

**Table 1** Birds infected with haemosporidan parasites, as indicated by blood smears

Sampling place	No. of birds sampled per site	No. of infected birds	<i>H</i>	<i>P</i>	<i>L</i>	<i>MI</i> *
Taraš	1	0	-	-	-	-
Mokrin	1	0	-	-	-	-
Padinska Skela	7	2	1	1	-	-
Opovo	14	10	(2)*	1 (1)*	7 (1)*	2
<b>Total</b>	<b>23</b>	<b>12</b>	<b>1</b>	<b>2</b>	<b>7</b>	<b>2</b>

\*MI - 2 mixed infections (*Haemoproteus/Plasmodium* and *Leucocytozoon/Haemoproteus*);  
H - *Haemoproteus*; P - *Plasmodium*; L - *Leucocytozoon*.

So far, in Long-eared owls all three haemosporidian genera with only 4 species have been discovered [1]. Genus *Leucocytozoon* was isolated in the non-captive owls [13,16,18,30], and described as *L. danilewskyi* [1]. In the present study, we found all three genera, with *Leucocytozoon* being the most abundant (Figure 1), while Martín-Maldonado *et al.* [17] detected just *Haemoproteus* infection. According to Valkiūnas [1] and MalAvi database [15], from Strigiformes were isolated two *Haemoproteus* species: *H. syrnii* and *H. noctuae* and one *Plasmodium*: *P. subpraecox*. In our study, *Plasmodium* and *Haemoproteus* participated equally with 13%.

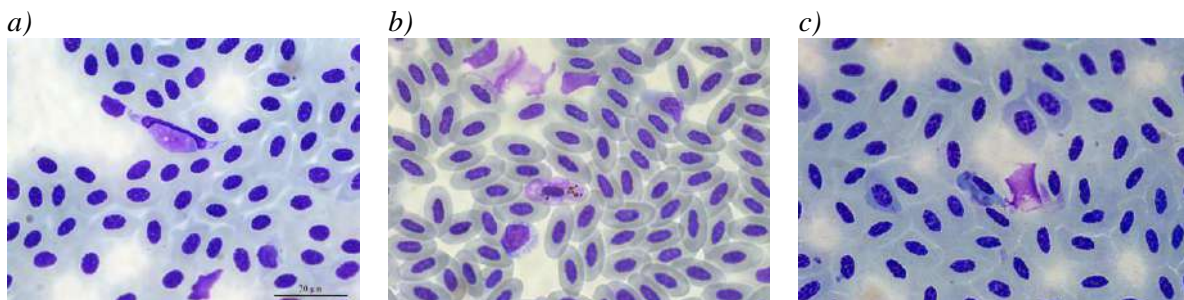


**Figure 1** Genera of Haemosporidian parasites found in the blood smears of the Long-eared Owl  
a) *Leucocytozoon*; b) *Haemoproteus*; c) *Plasmodium*



Since Martín-Maldonado *et al.* [17] conducted the study during the breeding season, when vectors are most active, recorded parasitemia in the Long-eared owls was very high, up to 12.8%. Average parasitemia in our study in winter was low, only 0.16%. Co-infections of two or more haemosporidian parasite species occur frequently in all avian species [1] including owls, with the most common combination *Leucocytozoon-Hemoproteus* [13,17]. We also recorded two mixed infections. One bird hosted *Haemoproteus* and *Plasmodium* parasites, while the other was infected with *Leucocytozoon* and *Haemoproteus* species.

Out of all Long-eared owls, 12 were females and 11 were males. There was no significant difference in parasitemia between sex (t-test = -0.97, p-value = 0.35) or age (t-test = 0.12, p-value = 0.9) of the birds, which agrees with Martín-Maldonado *et al.* [17] study. Additionally, as a reliable predictor of the physical condition of birds we used SMI [25]. In this sense, we compared the level of parasitemia with SMI to identify whether the presence of parasites affects the health status of the birds, because a low level of parasitemia depends on bird health, low stress levels and the absence of other pathogens. Therefore, parasitemia can be considered a reliable indicator of birds' health [31]. However, there was no significant difference (t-test = -1.48, p-value = 0.17) between infected and uninfected birds and their physical condition.

As PCR is a more sensitive method for detecting parasite *cytochrome b* gene [32], it will be a crucial tool in the next phase of our research. Moreover, we believe that designing more suitable primers for owl haemosporidian lineages will be necessary to delve deeper into the parasite fauna and gain a better understanding of their phylogenetic place as well as molecular differences, thereby contributing to the broader field of avian health and parasitology.

## CONCLUSION

We studied the diversity, prevalence and parasitemia of haemosporidian parasites in wintering population of Long-eared Owls from Banat, Serbia. Additionally, we compared the level of parasitemia with SMI to identify whether the presence of parasites affects the health status of the birds and their effect on SMI. The overall prevalence was 52.2% with the genus *Leucocytozoon* being the most abundant in the sampled birds. *Plasmodium* and *Haemoproteus* participated equally in the study. No significant difference was found between parasitised and non-parasitised birds and their physical condition. In order to gain a better insight into the parasite lineages in the next step of the study, we plan to expand the research to a wider area with more individuals. Additionally, we will use PCR to detect the parasite cytochrome b gene to achieve a better insight of the parasite lineages.

## ACKNOWLEDGEMENT

*The authors are grateful to the Ministry of Science, Technological Development and Innovation of the Republic of Serbia for financial support according to the contract with the registration number: 451-03-47/2023-01/200053. We also thank to Dr Gediminas Valkiūnas for helping us to clarify the doubts regarding some blood smears.*

*The samples involved in this study comply with the current legislation of the Ministry of Environmental Protection of the Republic of Serbia.*

## REFERENCES

- [1] Valkiūnas G., Avian Malaria Parasites and other Haemosporidia CRC Press, New York (2005), p.932, ISBN: 0-415-30097-5.
- [2] Ricklefs R.E., Fallon S.M., Bermingham E., Syst. Biol. 52 (2004) 111–119.
- [3] Bensch S., Pérez-Tris J., Waldenström J., *et al.*, Evolution 58 (2004) 1617–1621.
- [4] Križanauskienė A., Hellgren O., Kosarev V., *et al.*, J. Parasitol. 92 (2006) 1319–1324.
- [5] Huang X., Ellis V.A., Jönsson J., *et al.*, Mol. Ecol. 27 (2018) 4336–4346.
- [6] Shurulinkov P., Spasov L., Stoyanov G., *et al.*, Malar. J. 17 (1) (2018) 33–39.
- [7] Ellis V.A., Collins M.D., Medeiros M.C., *et al.*, PNAS (2015) 112 (36) 11294–9.
- [8] Doussang D., Sallaberry-Pincheira N., Cabanne G.S., *et al.*, Int. J. for Parasitol. 51 (11) (2021) 899–911.
- [9] Coon C.A.C., García-Longoria L., Martin L.B., *et al.*, J. Avi. Biol. 47 (2016) 779–787.
- [10] Jiménez-Peñuela J., Ferraguti M., Martínez-de la Puente J., *et al.*, Enviro. Res. 199 (2021) 111234.
- [11] Bichet C., Brischoux F., Ribout C., *et al.*, PLoS ONE 15 (8) (2020) e0237170.
- [12] Krone O., Priemer J., Streich J., *et al.*, Acta Protozool. 40 (2001) 281–289.
- [13] Ishak H.D., Dumbacher J.P., Anderson N.L., *et al.*, PLoS ONE 3 (35) (2008) e2304.
- [14] Mikkola H., T&A D Poyser Ltd, Staffordshire (1983), p.397, ISBN: 0 85661 034 8.
- [15] [MalAvi] A database for avian haemosporidian parasites, Available on the following link: [www.mbio-serv.mbioekol.lu.se/Malavi](http://www.mbio-serv.mbioekol.lu.se/Malavi).
- [16] Krone O., Waldenström J., Valkiūnas G., *et al.*, J. Parasitol. 94 (3) (2008) 709–715.
- [17] Martín-Maldonado B, Mencía-Gutiérrez A., Andreu-Vázquez C., *et al.*, Vet. Sci. 10 (54) (2023).
- [18] Minichová L., Ružić M., Rajković D., *et al.*, Zbornik z Konferencie III. Labudove dni, 24.-25.04.2013, Bratislava, Slovakia (2013) A123.
- [19] del Hoyo J., Collar N.J., Illustrated checklist of the Birds of the World, Volume 1: Non-passerines, Lynx Edicions (2014), p.903, ISBN: 978-84-96553-94-1.
- [20] Rajković D., Ciconia 18 (2009) 81–90.
- [21] Grubač B., Zaštita prirode (2004) 55 (1–2) 123–140.
- [22] Puzović S., Radišić D., Ružić M., *i sar.*, Društvo za zaštitu i proučavanje ptica Srbije i Prirodno-matematički fakultet, Departman za biologiju i ekologiju, Univerzitet u Novom Sadu, Novi Sad (2016) p.159, ISBN: 978-86-80728-00-1.
- [23] Jovanović B.T., Ciconia 13 (2004) 45–48.
- [24] Baker K., British Trust for Ornithology, Thetford, Norfolk, UK. (2016) p.336, ISBN: 0903793180.
- [25] Peig J., Green A.J., Oikos 118 (2009) 1883–1891.
- [26] Valkiūnas G., Iezhova T.A., Križanauskienė A., *et al.*, J. Parasitol. 94 (6) (2008) 1395–1401.

- [27] Godfrey R.D., Fedynich S.M., Pence D.B., *J. Wildlife Dis.* 23 (1987) 558–565.
- [28] R: A language and environment for statistical computing. R Foundation for Statistical Computing Vienna, Austria, *Available on the following link:* [www.r-project.org/index.html](http://www.r-project.org/index.html).
- [29] Giorgiadis M., Guillot J., Duval L., *et al.*, *Parasitol. Res.* 119 (2020) 2975–2981.
- [30] Ilgūnas M., Himmel T., Harl J., *et al.*, *Animals* 12 (2022) 2212.
- [31] Levin I., Parker G., Chapter 47 - Haemosporidian Parasites: Impacts on Avian Hosts, Editors: Miller R.E., Fowler M., *Fowler's Zoo and Wild Animal Medicine*, Amsterdam (2011), p.356–363, ISBN: 9781437719864.
- [32] Hellgren O., Waldenström J., Bensch S., *J. Parasitol.* 90 (4) (2004) 797–802.



## UNVEILING PESTICIDE CONTAMINATION IN TRANSBOUNDARY WATERS: A CASE STUDY OF SERBIA AND ROMANIA

Nenad Zarić<sup>1,2\*</sup>, Ionela Hotea<sup>3</sup>, Alina Lato<sup>3</sup>, Milana Zarić<sup>4</sup>, Florin Crista<sup>3</sup>

<sup>1</sup>Faculty of Biology, University of Belgrade, Studentski trg 12–16, 11000 Belgrade, SERBIA

<sup>2</sup>Department of Agrobiotechnology IFA-Tulln, Institute of Bioanalytics and Agro-Metabolomics, University of Natural Resources and Life Sciences Vienna (BOKU), Konrad-Lorenz-Straße 20, 3430 Tulln, AUSTRIA

<sup>3</sup>University of Life Sciences “King Michael I” from Timișoara, Calea Aradului 119, Timișoara 300645, ROMANIA

<sup>4</sup>Institute for chemistry, technology and metallurgy, University of Belgrade, Njegoševa 12, 11000 Belgrade, SERBIA

\*nenad.zaric@bio.bg.ac.rs

### Abstract

*The increasing use of pesticides in agriculture poses a significant environmental risk, especially to open water bodies such as rivers, lakes and canals. These chemicals, which include a variety of pesticides, enter aquatic ecosystems through various pathways and have detrimental effects on aquatic life, ecosystem health and human well-being. This study provides a comprehensive overview of pesticide pollution in open waters in the region between Serbia and Romania. We investigated the presence and spatial distribution of pesticides in water bodies in South Banat district in Serbia and Timiș County in Romania over a one-year period. Using high-resolution mass spectrometry, we identified and quantified a variety of pesticides to shed light on their occurrence and potential impact on the environment. Our results show that certain pesticides persisting despite legal bans. Spatial variability in pesticide concentrations highlights the influence of proximity to agricultural activities, while seasonal variations emphasize the dynamic nature of pesticide pollution. Furthermore, our comparative analysis between Romania and Serbia underlines the transboundary nature of pesticide pollution and highlights the need for joint regulatory efforts to mitigate environmental risks.*

**Keywords:** LCMSMS, water, pesticides, agriculture.

### INTRODUCTION

The increasing use of pesticides in agriculture and other sectors poses significant environmental risks, especially to open water bodies such as rivers, lakes and canals. Pesticides, which comprise a diverse group of pest control chemicals, inevitably enter aquatic ecosystems through various pathways, including surface runoff, leaching, atmospheric deposition and direct application [1]. These pollutants can have profound effects on aquatic life, ecosystem health and even human health through processes of bioaccumulation and biomagnification [2].

Research has shown that even low concentrations of pesticides can disrupt aquatic ecosystems. For example, certain herbicides and insecticides have been shown to affect the

reproductive and developmental processes of aquatic organisms, leading to a decline in biodiversity and a change in community structures [3]. In addition, the persistence of these chemicals in the environment is highly variable, with some having a long half-life that exacerbates their effects [4].

Recent advances in analytical techniques have improved our ability to detect and quantify pesticides in aquatic environments, showing that they are much more widespread than previously thought. Studies using high-resolution mass spectrometry have revealed the ubiquity of these pollutants, including those not normally monitored in environmental studies [5]. This highlights the need for comprehensive monitoring programs and more stringent regulatory frameworks to manage and mitigate the risks associated with pesticide contamination in the aquatic environment.

This paper aims to provide a comprehensive overview of the current state of knowledge on pesticide pollution in open waters in the region between Serbia and Romania.

## **MATERIALS AND METHODS**

### **Sampling locations and sampling**

All samples were taken in the South Banat district in the autonomous province of Vojvodina in Serbia and Timis County in Romania. South Banat is located in the south-eastern part of the province of Vojvodina. It borders Romania to the east. South Banat has a total population of just under 300,000 inhabitants. Timis County is located to the west of Romania, bordering Hungary and Serbia. Total population is just above 650,000. Water samples were taken every month for a period of one year at 25 locations in each country, 50 in total. Water was sampled from wells, standing waters (lakes and ponds) and running waters (rivers).

### **Sample preparation and analyses**

Water samples were taken every month for one year. In Serbia there were 25 sampling sites for water samples. At each sampling point 2 liters of water was taken into clean plastic bottles. The samples were frozen and kept in the freezer until analysis. Prior to analysis the water samples were defrosted at room temperature. Pesticides were extracted using Solid phase extraction (SPE). C18 disks were preconditioned with 10 mL of acetone, 10 mL of ethyl acetate, 10 mL of methanol and 10 mL of water. Before the disk were dry 500 mL of water samples were passed through the SPE disk using a vacuum manifold. Once the total sample is percolated, the disks were rinsed with  $2 \times 5$  mL of deionized water. The disks were dried under vacuum. The analytes were eluted with ethyl acetate / dichloromethane. Extracts were evaporated to dryness under a gentle stream of nitrogen. Before analysis the extracts were reconstituted with methanol/water (1:1). The analysis was performed on a TSQ Quantis™ Triple Quadrupole Mass Spectrometer.

We have analyzed water samples for 278 pesticides. A calibration curve was made in six points at different concentration levels between 1 ppb and 200 ppb.

## **RESULTS AND DISCUSSION**

The analysis of the water samples revealed a worrying but nuanced picture of pesticide contamination. Initially, fewer than 20 pesticides were detected, indicating a rather limited extent of contamination. The most commonly found pesticides included herbicides such as metolachlor and chlorotoluron and fungicides such as griseofulvin, fluopyram and azoxystrobin. Insecticides such as diflubenzuron and buprioferzin were also found. It is noteworthy that the neonicotinoid insecticide imidacloprid was sporadically detected, although it is banned in both the EU and Serbia. The detection of imidacloprid is worrying and indicates possible residues that remain in the environment despite legal measures.

Interestingly, the concentrations of these pesticides showed spatial variability, with smaller rivers and canals showing higher concentrations compared to the mighty Danube. The highest concentrations were found in an irrigation canal flowing through an agricultural area, highlighting the relationship between pesticide use and proximity to agricultural activities. In addition, an interesting pattern emerged in terms of the diversity and concentration of pesticides in relation to the timing of sampling. During the peak of agricultural activities, especially in spring (March and April), waters adjacent to agricultural areas showed a greater diversity of pesticides and concentrations peaked accordingly. In contrast, during the winter months (December, January, February), both the diversity and the concentrations of pesticides detected decreased, indicating seasonal variations in the use of pesticides and their persistence in the environment.

The comparative analysis between Romania and Serbia revealed a surprising similarity in the presence of pesticides, with all detected pesticides being ubiquitous in both countries. This finding points to a common environmental problem that transcends geopolitical boundaries and underlines the need for coordinated efforts in the management and regulation of pesticides at the regional level. Overall, the results underscore the multifaceted nature of pesticide contamination, which is influenced by factors such as agricultural practices, seasonal fluctuations and international regulatory frameworks.

## **CONCLUSION**

The analysis of the water samples reveals a complex picture of pesticide contamination in the region studied. Although fewer than 20 pesticides were initially detected, suggesting a reasonably limited extent of contamination, the presence of potent substances like imidacloprid raises significant concerns about persistence in the environment, despite legal bans. Spatially, concentrations varied, with smaller water bodies showing higher levels, particularly in agricultural areas, suggesting a direct link between pesticide use and proximity to agricultural activities. In addition, seasonal variations showed a distinct pattern, with the highest concentrations observed in spring, consistent with more intensive agricultural practices. The comparative analysis between Romania and Serbia also highlights the transboundary nature of pesticide pollution and underlines the need for joint regulatory action.



## **ACKNOWLEDGEMENT**

*We would like to acknowledge the support of the Interreg IPA CBC Romania – Serbia Programme, project RORS – 279 “Cross-border network for education and research of natural resources”. The authors are grateful to the Ministry of Science, Technological development and Innovation of the Republic of Serbia for financial support according to the contract with the registration number (451-03-66/2024-03/ 200178 and 451-03-66/2024-03/200026).*

## **REFERENCES**

- [1] Stehle S., Schulz R., Proc. Natl. Acad. Sci. 112 (2015) 5750–5755.
- [2] Chopra A.K., Sharma M.K., Chamoli S., Environ. Monit. Assess. 173 (2011) 905–916.
- [3] Liess M., Ohe P.C. Von Der, Environ. Toxicol. Chem. 24 (2005) 954–965.
- [4] Syafrudin M., Kristanti R.A., Yuniarto A., *et al.*, Int. J. Environ. Res. Public Health 18 (2021).
- [5] Song N.E., Jung Y.S., Choi J.Y., *et al.*, Separations. (2020) 7.



## COMPARATIVE ANALYSIS OF PESTICIDE RESIDUES IN AGRICULTURAL SOILS OF SERBIA AND ROMANIA

Nenad Zarić<sup>1,2\*</sup>, Florin Crista<sup>3</sup>, Adina Berbecea<sup>3</sup>, Ionela Hotea<sup>3</sup>, Laura Crista<sup>3</sup>,  
Milana Zarić<sup>4</sup>

<sup>1</sup>Faculty of Biology, University of Belgrade, Studentski trg 12–16, 11000 Belgrade, SERBIA

<sup>2</sup>Department of Agrobiotechnology IFA-Tulln, Institute of Bioanalytics and Agro-Metabolomics, University of Natural Resources and Life Sciences Vienna (BOKU), Konrad-Lorenz-Straße 20, 3430 Tulln, AUSTRIA

<sup>3</sup>University of Life Sciences “King Michael I” from Timișoara, Calea Aradului 119, Timișoara 300645, ROMANIA

<sup>4</sup>Institute for chemistry, technology and metallurgy, University of Belgrade, Njegoševa 12, 11000 Belgrade, SERBIA

\*nenad.zaric@bio.bg.ac.rs

### Abstract

*The widespread use of pesticides increased crop yields and improved food security. However, the use of pesticides has a negative impact for the environment, particularly for soil health and ecosystem sustainability. This study investigates the presence and distribution of pesticides in the border region between Serbia and Romania. Soil samples were collected in the South Banat district in Vojvodina, Serbia, and in the Romanian Timis district. Samples were taken during all four seasons of the year. The subsequent analysis included the extraction and identification of 278 pesticides using QuEChERS followed by a triple quadrupole mass spectrometer. Only two pesticides, atrazine and carbaryl, are regulated. Although atrazine was detected, it remained below the limit of quantification (LOQ), while carbaryl was completely absent. Of the approximately 20 pesticides detected, seven exceeded the LOQ, mainly herbicides such as metolachlor and terbuthylazine and the neonicotinoid insecticide imidacloprid. Spatial variability analysis revealed higher concentrations of pesticides in the upper soil layers, which decrease with depth, underlining the importance of soil stratification in monitoring strategies. While the comparative analysis between Serbia and Romania showed no statistical differences in the occurrence of pesticides, the soil from Romania showed a lower frequency of detection, possibly due to different agricultural practices or soil characteristics.*

**Keywords:** LCMSMS, soil, pesticides, agriculture, QuEChERS.

### INTRODUCTION

The widespread use of pesticides in modern agriculture has revolutionized crop protection, increased crop yields and ensured food security. However, this reliance on chemical pest control has had unintended negative consequences for the environment, particularly in terms of soil health and ecosystem sustainability [1]. Pesticides, which include a variety of chemicals designed to control pests, weeds and diseases, have become an integral part of agricultural practices worldwide. However, their indiscriminate use and persistence in the

environment have raised concerns regarding their impact on soil quality, microbial communities and long-term agricultural productivity [2].

Pesticides enter agricultural soils through a variety of pathways, including drift, leaching, surface runoff and direct application. They eventually accumulate in the soil matrix and have profound effects on soil biota and biogeochemical processes [3]. These chemicals can disrupt soil microbial communities, which are critical for nutrient cycling, organic matter decomposition and plant health, thus impairing soil fertility and ecosystem resilience [4]. In addition, pesticides can persist in the soil for long periods of time, undergoing complex transformations and potentially contaminating groundwater resources [5].

Research on the fate and behaviour of pesticides in agricultural soils has expanded in recent decades due to growing environmental concerns and advances in analytical techniques. Studies have elucidated the mechanisms of sorption, degradation and transport of pesticides in the soil matrix, providing information on their fate and persistence in the environment [6]. In addition, studies of the ecological effects of pesticides on soil organisms, including earthworms, microarthropods and soil-dwelling microorganisms, have revealed complex trophic interactions and ecosystem responses to pesticide exposure [7].

Despite the progress that has been made in understanding the dynamics of pesticides in agricultural soils, significant knowledge gaps remain, particularly regarding the long-term effects of chronic pesticide exposure on soil health and ecosystem functioning. In addition, the emergence of novel pesticide formulations and the increasing prevalence of pesticide-resistant pests pose new challenges for sustainable plant protection in agriculture.

The aim of this study was to assess the presence of pesticides in the cross-border region between Serbia and Romania.

## **MATERIALS AND METHODS**

### **Sampling locations and sampling**

Soil samples were gathered in the South Banat district in the autonomous province of Vojvodina in Serbia and Timis county in Romania. Samples of soil were taken once per season. In Autumn (October), Winter (February), Spring (April) and Summer (July). Fifty sampling locations were covered during the sampling campaign in each country, adding up to 100 samples in total. The samples were taken from the topsoil level, 20–40 cm depth and 40–60 cm depth. The samples were kept in the freezer until analysis.

### **Sample preparation and analyses**

Prior to sample preparation they were defrosted at room temperature and homogenized in an ultra-centrifugal mill with a final fineness size of <1 mm. Pesticides were extracted using QuEChERS method EN 15662. In short 10 g of homogenized soil sample was added to a 50 mL tubes. 10 mL of water was added to increase the sample moisture. Afterward 10 mL of acetonitrile was added as an extraction solvent and the sample was shaken for 1 minute. Following this, 4 g Anhydrous MgSO<sub>4</sub>, 1 g Trisodium Citrate, 0.5 g Disodium Citrate and 1 g NaCl were added to the tube and it was shaken as quick as possible. The samples were centrifuged for 5 minutes at 5000 rpm. Then, a clean-up dispersive solid phase extraction step was carried out by adding 10 mL of the supernatant to a 15-mL centrifuge tube that contained

150 mg PSA + 150 mg C18 + 900 mg MgSO<sub>4</sub>. The samples were again shaken and centrifuged for 5 minutes at 5000 rpm. An aliquot of 1 mL was transferred to an amber HPLC vial and evaporated to dryness. Before the analysis it was reconstituted with 1 mL of methanol / ultrapure water (50:50). The analysis of 278 pesticides was performed on a TSQ Quantis™ Triple Quadrupole Mass Spectrometer.

## **RESULTS AND DISCUSSION**

In our comprehensive analysis, which includes 278 pesticides, a clear regulatory gap becomes apparent, as only two pesticides, atrazine and carbaryl, fall under regulated status. Interestingly, although atrazine was detected, its concentration was below the limit of quantification (LOQ), making it practically negligible in our samples. Conversely, carbaryl was not present at all in our samples. This regulatory omission underscores the need for a more comprehensive approach to the management and monitoring of pesticides in agricultural soils.

Of the approximately 20 pesticides detected in our soil samples, only seven were above the LOQ, highlighting the prevalence of low-level contamination. In particular, herbicides such as metolachlor and terbuthylazine, along with the neonicotinoid insecticide imidacloprid, proved to be the most frequently detected pesticides in soils from Serbia. In addition, flutrioflor, tebuconazole, fenarimol and thiamethoxam were detected, with concentrations varying between 1 µg/kg (etoxazole) and 32 µg/kg (tebuconazole) [8,9]. These concentrations are in good agreement with the existing literature and confirm the consistency and reliability of our results.

The spatial variability of the pesticide distribution in the soil profiles shows intriguing patterns. Predominantly, pesticides showed higher concentrations in the upper soil layers, which gradually decreased with depth. At a depth of 20–30 cm, both the diversity and the concentrations of the detected pesticides decreased and reached their lowest values at a depth of 40–60 cm. This depth-dependent distribution emphasizes the importance of considering soil stratification in pesticide monitoring and management strategies.

Comparative analyzes between Serbia and Romania revealed no differences in the occurrence of pesticides. Although the comparison lacks statistical significance, it is noteworthy that pesticides were detected less frequently in Romanian samples. This discrepancy suggests possible differences in agricultural practices, soil characteristics or land management strategies between the two regions.

## **CONCLUSION**

Our study provides valuable insights into the presence and distribution of pesticides in agricultural soils in the cross-border region of Serbia and Romania. Through a comprehensive analysis covering 278 pesticides, 20 pesticides were detected, out of which only seven exceeded the limit of quantification (LOQ), indicating predominantly low levels of contamination. Herbicides such as metolachlor and terbuthylazine in particular proved to be the most frequently detected pesticides, along with the neonicotinoid insecticide imidacloprid.

In addition, flutrioflor, tebuconazole, fenarimol and thiamethoxam were detected in concentrations consistent with the existing literature.

Spatial variability analysis showed higher pesticide concentrations in the upper soil layers, which gradually decrease with depth. This depth-dependent distribution demonstrates the importance of considering soil stratification in pesticide monitoring and management strategies to effectively mitigate environmental risks. Furthermore, our comparative analysis between Serbia and Romania showed no statistically significant differences in the occurrence of pesticides, although pesticides were less frequently detected in Romanian samples. This discrepancy suggests possible differences in agricultural practices, soil characteristics or land management strategies between the two regions.

## ACKNOWLEDGEMENT

*We would like to acknowledge the support of the Interreg IPA CBC Romania – Serbia Programme, project RORS – 279 “Cross-border network for education and research of natural resources”. The authors are grateful to the Ministry of Science, Technological development and Innovation of the Republic of Serbia for financial support according to the contract with the registration number (451-03-66/2024-03/ 200178 and 451-03-66/2024-03/200026).*

## REFERENCES

- [1] Pethig R., *Agric. Econ.* 31 (2004) 17–32.
- [2] Lo C.-C., *J. Environ. Sci. Heal. Part B.* 45 (2010) 348–359.
- [3] Chaplain V., Mamy L., Vieuble-Gonod L., *et al.*, *Toward an Integrated Approach of Influential Factors in Pesticides in the Modern World - Risks and Benefits*, Editor Stoytcheva M., IntechOpen, London (2011), p.535, ISBN: 978-953-307-458-0.
- [4] Hussain S., Siddique T., Saleem M., *et al.*, *Impact of Pesticides on Soil Microbial Diversity, Enzymes, and Biochemical Reactions in Advances in Agronomy Book Series*, Academic Press, Cambridge (2009) Vol. 102, p.159, ISBN 0065-2113.
- [5] Pérez-Lucas G., Vela N., Aatik A. El., *et al.*, *Environmental Risk of Groundwater Pollution by Pesticide Leaching through the Soil Profile in Pesticides - Use and Misuse and Their Impact in the Environment*, Editors: Larramendy, M., Soloneski, S., IntechOpen, Rijeka (2018), Ch. 3, ISBN: 978-1-83880-047-5.
- [6] Vagi M.C., Petsas A.S., *Sorption/Desorption, Leaching, and Transport Behavior of Pesticides in Soils: A Review on Recent Advances and Published Scientific Research in Pesticides in Soils: Occurrence, Fate, Control and Remediation*, Editors: Rodríguez-Cruz M.S., Sánchez-Martín M.J., Springer International Publishing, Basel (2022) p.137, ISBN: 978-3-030-90546-0.
- [7] Pisa L.W., Amaral-Rogers V., Belzunces L.P., *et al.* *Environ. Sci. Pollut. Res.* 22 (2015) 68–102.
- [8] Mohapatra S., *Environ. Monit. Assess.* 187 (2015) 95.
- [9] Malhat F., Hassan A., *Environ. Contam. Toxicol.* 87 (2011) 190.



## THE RELATIONSHIP BETWEEN PM<sub>10</sub> AND METEOROLOGICAL PARAMETERS CLOSE TO THE MINING AREA

Milica Veličković<sup>1\*</sup>, Danijela Voza<sup>1</sup>

<sup>1</sup>University of Belgrade, Technical Faculty in Bor, V.J. 12, 19210 Bor, SERBIA

\*mvelickovic@tfbor.bg.ac.rs

### Abstract

*PM<sub>10</sub> is one of the most dangerous air pollutants and represents a serious environmental and health problem. Its concentration is influenced by many factors, among which meteorological parameters stand out as the most important. In this sense, this study aimed at exploring the relationship between PM<sub>10</sub> and meteorological variables (atmospheric temperature (AT), barometric pressure (BPR) and relative humidity (RH)) in rural area near copper mine. The data about meteorological parameters and PM<sub>10</sub> concentrations were collected for 2019–2022. The dataset was divided into two periods (cold and warm) to analyze potential seasonal variations. The correlation analysis was employed in order to investigate the relationship between the observed variables. The results have shown that coefficient of correlation is positive and statistically significant, but very low between PM<sub>10</sub> and AT and BPR, and negative between PM<sub>10</sub> and RH, for both periods.*

**Keywords:** PM<sub>10</sub>, meteorological parameters, correlation analysis.

### INTRODUCTION

Particulate matter (PM) presents a complex mixture of organic and inorganic substances and can have a different composition, depending on the emission. Sources of PM particles can be both natural and anthropogenic. Anthropogenic sources include industry, domestic fuel burning and traffic. On the other hand, natural sources include volcanoes, fires, dust storms, and aerosolized sea salt [1]. Previous studies have confirmed that fossil fuel combustion and industrial metallurgical processes are the most common anthropogenic sources of PM<sub>10</sub> [2]. PM particles in the air represent a serious environmental problem, primarily due to the content of toxic substances and heavy metals in them [3]. High concentrations of heavy metals in PM particles can cause serious respiratory and cardiovascular diseases [4]. Based on these facts, WHO recommended that the mean annual level of PM<sub>10</sub> should not exceed 15 µg/m<sup>3</sup> and mean 24-hour should not exceed 45 µg/m<sup>3</sup> [5] due to the protection of human health.

Apart from the pollution sources themselves, the level of particles in the air is influenced by other factors, among which meteorological parameters stand out as the most important. Meteorological conditions, such as wind speed, wind direction, temperature, relative humidity and atmospheric pressure, play an important role in the dispersion of suspended particles [6,7]. Research has shown that concentrations of suspended particles (PM<sub>10</sub>) correlate negatively with air temperature and wind speed but positively with air pressure and relative air humidity [8]. However, the relationship between the concentration of suspended particles



(PM<sub>10</sub>) and meteorological factors varies during different seasons. The study conducted by Chen et al., [9] found that the correlation between suspended particulate matter (PM<sub>10</sub>) and air temperature is negative during summer and autumn but positive during winter and spring. By observing the seasonal variation of PM<sub>10</sub>, it can be better understood, explained and predicted its future concentrations.

A large number of studies has proven that huge quantities of PM<sub>10</sub> are generated during mining operations, which include excavating machines, shovels, drilling machines and transportation by heavy-duty dumpers in the mining areas [10–12]. In general, when it comes to open pit mines the dispersion of PM depends on local meteorology. Wind flow is the prime mover of the PM from one place to the other [13], but other meteorological parameters also have their role. Hence, the main aim of this study was to analyse the relationship between meteorological factors and PM<sub>10</sub> near open pit mining area.

## **MATERIALS AND METHODS**

### **Study area**

For this study, the public datasets of PM<sub>10</sub> concentrations and meteorological conditions in Bor from January 2019 to December 2022 were obtained from the official website of Bor municipality. The concentration of suspended particles PM<sub>10</sub> is measured using the SRPS EN 12341 reference method and it was done by Institute for Mining and Metallurgy in Bor. The data were collected from the measuring station Krivelj, located in a rural area, at 425 m above sea level. The measuring point is positioned in the direction of the dominant southeast wind in the village of Krivelj. At this location, a large influence of the Velik Krivelj tailings pond was observed, and when the southeast wind blows, dust particles are blown in the direction of the village. In addition, due to very intensive industrial activities, there is also an increase in traffic in this area, which contributes to an increase in pollution.

The climate of study area is moderate to medium continental, with a transition to mild mountain in the higher mountain zones. The characteristics of this climate are warm and sunny summers and cold winters with a lot of snow. The seasons are recognizable, with autumn sometimes being warmer than spring, with more sunny days and less rainfall. Summers are characterized by stable weather conditions, with long sunny and shorter rainy periods. In winter, the weather is characterized by low temperatures and intense snowfall.

## **RESULTS AND DISCUSSION**

Data for study period were divided into cold (October–April) and warm (May–September) periods. The average daily content of PM<sub>10</sub> in the air in the period of 2019–2022 was measured at the measuring point Krivelj, and the obtained values (cold period, warm period, and an average values on annual level) are shown in Table 1.

**Table 1** Average concentration of  $PM_{10}$  particles in ambient air in the village Krivelj for period 2019–2022

Location		2019	2020	2021	2022
Measuring station Krivelj	Cold period	36.9	28.7	28.3	38.2
	Warm period	27.2	24.8	26.2	28
	Avg. Value	31.9	27.1	27.5	30.7
	Days above limit	29	10	3	24

Based on the results shown in Table 1, it can be concluded that somewhat higher values of  $PM_{10}$  were registered during the cold period over the entire study period, which is logical since this is also the heating period. The good thing is that the average daily limit was not exceeded more than 35 times [5], which confirms that air pollution in this area, very well known for high pollution [14], is improved.

In addition, correlation analysis was performed to investigate relationship between  $PM_{10}$  and meteorological parameters in different periods. For strong correlation, the value of the correlation coefficients must be near  $\pm 0.5$ , with the statistical significance of ( $p \leq 0.05$ ). The obtained results (Table 2) reveal that the coefficient of correlation is positive and statistically significant, but very low between  $PM_{10}$  and AT (atmospheric temperature) and BPR (barometric pressure), and negative between  $PM_{10}$  and RH (relative humidity), for both periods.

**Table 2** Correlation between  $PM_{10}$  and meteorological factors in different periods

	AT	RH	BPR
Cold	0.143**	-0.228**	0.095*
Warm	0.234**	-0.158**	0.105*

\*\*  $p < 0.000$ , \*  $p < 0.05$

The evaluation of the Pearson correlation coefficient between  $PM_{10}$  concentration and meteorological factors such as temperature, humidity and barometric pressure (Table 2) has indicated that  $PM_{10}$  is inversely correlated with relative humidity, both for warm and cold periods. Thus, when the humidity increases, the average  $PM_{10}$  concentration decreases and vice versa. It has been proven that humidity has different influences on particle size distribution, for small-size particles, the moisture content is usually negatively correlated, as shown by the evidence of the washing effect [15,16].

Atmospheric pressure and particulate matter concentrations were significantly positively correlated, but the correlation coefficient is about 0.1, which is very low. The same situation is regarding the correlation between  $PM_{10}$  and AT, which could be unexpected, since the obtained results (Table 1) have shown that the concentration of  $PM_{10}$  was higher during the cold period compared to the warm period.

Two important processes, atmospheric dispersion, which removes dust particles from air pollution through the process of dry and wet deposition by rain, and the second, aerosolization diffusion from the surface, which accounts for the air emission of particulate matter from street vehicles, industrial dust, and soil dust, can both explain the very low coefficients of

correlation. These linear connections have made it clear that human activity is the primary source of PM<sub>10</sub> in the study area [17].

## **CONCLUSION**

In this study, average concentrations of PM<sub>10</sub> for a four-year period are presented. Data were divided into cold and warm periods in order to analyse their possible seasonal variations. The results have shown that PM<sub>10</sub> concentrations were slightly higher during cold period. The correlation analysis revealed that PM<sub>10</sub> have positive correlation with AT and BPR but a negative with RH. However, although statistically significant, the coefficients of correlation are very low.

For future research, it is important to conduct further investigation on the influence of other meteorological factors (wind speed, precipitation) on PM<sub>10</sub> concentration in order to have more accurate assessments of the major causes of air pollution in this area.

## **ACKNOWLEDGEMENT**

*The authors are grateful to the Ministry of Science, Technological development and Innovation of the Republic of Serbia for financial support according to the contract with the registration number 451-03-65/2024-03/200131.*

## **REFERENCES**

- [1] Seinfeld J.H., Pandis S.N., Atmospheric Chemistry and Physics: From Air Pollution to Climate Change, 2nd ed., John Wiley and Sons, Inc, Hoboken, New Jersey (2006), ISBN: 978-0-471-72018-8.
- [2] Duan J., Tan J. Atmos Environ. 74 (2013).
- [3] Šerbula S.M., Antonijević M.M., Milosević N.M., *et al.*, J. Hazard. Mater. 181 (1–3) (2010) 43.
- [4] Ristić N., Veličković M., Živković Ž., *et al.*, Pol. J. Environ. Stud. 31(4) (2022) 3287–3296.
- [5] WHO. WHO global air quality guidelines. Particulate matter (PM<sub>2.5</sub> and PM<sub>10</sub>), ozone, nitrogen dioxide, sulfur dioxide and carbon monoxide. Geneva: World Health Organization; (2021).
- [6] Kermani M., Jafari A.J., Gholami M., *et al.*, Environ. Sci. Pollut. Res. 28 (2021) 16434–16446.
- [7] Xu J., Yan F., Xie Y., *et al.*, Particuology 20 (2015) 69–79.
- [8] Liu F., Tan Q. W. Jiang X., *et al.*, (2018). Huanjing Kexue, 39(4) (2018) 1466–1472.
- [9] Chen T., He J., Lu X., *et al.*, (2016). Int. J. Env. Res. Pu. 13(9) (2016) 921.
- [10] Pandey B., Agrawal M., Singh S. Atmos. Pollut. Res. 5 (2014) 79–86.
- [11] Yadav, S.K., Jain, M.K. Int. J. Environ. Sci. Technol. 17 (2020) 695–708.
- [12] Yadav S.K, Jain M.K, Patel D.K. Monitoring of air pollution in different region along road network, Jharia Coalfield, Dhanbad, India *in* Water Science and Technology Library.

Editor: Singh V., Yadav S., Yadava, R., Springer, Singapore (2018), ISBN: 978-981-10-5792-2.

[13] Patra A.K., Gautam S., Majumdar S. *et al.*, *Air Qual Atmos Health* 9 (2016) 697–711.

[14] Šerbula S.M., Milosavljević J.S., Kalinović J.V., *et al.*, *Sci Total Environ.* 777 (2021) 145981.

[15] Kozakova J., Pokorna P., Cernikova A., *et al.*, *Aerosol Air. Qual. Res.* 17 (2017) 1234–1243.

[16] Dung N., Son D., Hanh, N., *et al.*, *Geosci. Environ. Protect.* 7 (2019) 138–150.

[17] Giri D., Krishna M.V., Adhikary, P.R., *Int. J. Environ. Res.* 2 (2008) 49–60.



## MACROZOOBENTHOS COMMUNITY AND ECOLOGICAL STATUS IN PRESPA LAKE (OTESHEVO, STENJE AND EZERANI) IN SPRING 2022

**Biljana Budzakoska Gjoreska<sup>1\*</sup>, Sasho Trajanovski<sup>1</sup>**

<sup>1</sup>Department of benthic fauna, PSI Hydrobiological Institute Ohrid, Naum Ohridski 50,  
6000 Ohrid, REPUBLIC OF NORTH MACEDONIA

\*biljanab@hio.edu.mk

### Abstract

*This study represents the results for the invertebrate fauna carried out in the spring of 2022 at Prespa Lake (Republic of North Macedonia). The survey has covered three distinctive localities: Oteshevo, Stenje and Ezerani. Twelve species from six systematic groups have been registered from the above mentioned localities in Lake: Oligochaeta, Hirudinea, Gastropoda, Bivalvia, Amphipoda and Insecta. The results of the survey clearly showed that the structure of the invertebrate community along the littoral zone of the Lake varies from one locality to another. Thus, more than half of the total diversity was registered in the locality of Ezerani, while the community of invertebrates is almost half poorer in Stenje and Oteshevo, with 5 species on each locality. As for the density, similarly to biodiversity, the highest number of individuals per square meter was registered in the Ezerani locality - a total of 10,750 ind/m<sup>2</sup>. The second-highest density was recorded in the locality of Stenje with 4,225, while the lowest density was recorded in the locality of Oteshevo with 1,200 ind/m<sup>2</sup>. The highest population density of *Dreissena carinata* was recorded - 3,250 ind/m<sup>2</sup> in the Stenje locality at a depth of 5 m in the shell zone. The results of the research indicate that the biodiversity of the invertebrate fauna decreases with increasing depth, which is closely related to the increase in the uniformity of the sediments and the stability of the environmental factors along its depth. In contrast, there is no density dependence with depth.*

**Keywords:** macroinvertebrates, biodiversity, ecological status, Lake Prespa.

### INTRODUCTION

Benthic macroinvertebrates are common inhabitants of lakes and streams where they are important in moving energy through food webs. The term “benthic” means “bottom-living”, so these organisms usually inhabit bottom substrates for at least part of their life cycle; the prefix “macro” indicates that these organisms are retained by mesh sizes of ~200–500 mm [1]. In order to achieve and maintain the highest water quality in lakes, rivers, and streams, environmental researchers are using the resident organisms living in these waters as sensitive indicators of change. Biomonitoring is based on the straightforward premise that living organisms are the ultimate indicators of environmental quality. According to Annex V of the Water Framework Directive [2], the macrozoobenthos or organisms from the benthic fauna are one of the four most relevant indicators of the quality of aquatic ecosystems. The Prespa Lake's Basin is an area of rich biodiversity that has been subject to intense pressures from human activities over the past decades [3]. The main goals of the study were to ascertain the invertebrate community structure, the species abundances, as well as the general condition of

the benthic fauna from the Oteshevo, Stenje and Ezerani localities in Prespa Lake (Republic of North Macedonia) in the spring 2022.

## MATERIALS AND METHODS

The field research took place on three localities (Oteshevo, Stenje and Ezerani) which, according to previous research, are distinguished by the intensity of the anthropogenic pressure and changes in the ecological status. The research was done using standard limnological methods [4–6] and in accordance with the EU Directive. Samples were taken with a van Veen grab (225 cm<sup>2</sup>) from different depths (2, 5, 10 m) and habitats using the method of vertical transects to the extent of macrophytic vegetation in Lake Prespa. The density values refer to the average density of individuals from two samples on a unit surface - m<sup>2</sup>. Determination was done to the species level. The processed material was preserved in 96% ethyl alcohol, labeled and stored in plastic vials. The macrozoobenthos species were determined using keys by the following authors: [4,7–15].

To determine the ecological status of the structure of the macrozoobenthos community the following structural indices have been calculated: index of species richness - S, Shannon-Wiener Diversity Index - H' (diversity), Pielou's index of evenness J(e) and Simpson's index (c) in different habitats and localities. The Average Score Per Taxon (ASPT) represents the average tolerance score of all taxa within the community and is calculated by dividing the BMWP (Table-6 scores for pollution sensitivity grades for macroinvertebrates families) by the number of families represented in the sample [16].

## RESULTS AND DISCUSSION

During the field activities in June 2022, the qualitative and quantitative composition of the fauna at the bottom of the Oteshevo locality was analyzed. Consequently, five species from five classes of bottom fauna (Oligochaeta, Hirudinea, Gastropoda, Amphipoda, and Insecta) were recorded in the samples (Table 1). These species, representing the aforementioned five classes, serve as indicators of increased trophic levels in the water, signifying the presence of organic pollution. The highest biodiversity was observed at a depth of 2 meters, where all five species were registered. Regarding the density, the population of *Dreissena carinata* exhibited the highest density, with 400 ind/m<sup>2</sup>.

**Table 1** Composition and density of bottom fauna in Oteshevo (June 2022)

Locality Oteshevo				
Depth (m)	Bottom facies (ratio)	Class	Species	Density (ind/m <sup>2</sup> )
2	Muddy bottom with shells (50:50)	Oligochaeta	<i>Tubifex tubifex</i>	100
		Hirudinea	<i>Glossiphonia maculosa</i>	25
		Gastropoda	<i>Valvata piscinalis</i>	25
		Bivalvia	<i>Dreissena carinata</i>	125
		Insecta	<i>Chironomus plumosus</i>	50
5	Muddy with Dreissena shells	Oligochaeta	<i>Tubifex tubifex</i>	175
		Gastropoda	<i>Valvata piscinalis</i>	25
		Insecta	<i>Chironomus plumosus</i>	100
10	Muddy with Dreissena shells	Bivalvia	<i>Dreissena carinata</i>	400
		Insecta	<i>Chironomus plumosus</i>	175



The bottom fauna in the Stenje locality, as observed in the samples from the spring campaign, was represented by 5 taxa from 5 groups of organisms: Oligochaeta, Hirudinea, Amphipoda, Bivalvia and Insecta (Table 2). Despite the fair uniformity of the bottom profile along the transect (mud and shell facies), the distribution of species was not uniform. In this context, the highest density was observed at a depth of 5 meters, on a muddy facies with shells, where 5 species were registered, and the highest population of the species *Dreissena carinata* was recorded at 3250 ind/m<sup>2</sup>.

**Table 2** Composition and density of bottom fauna in Stenje (June 2022)

Locality Stenje				
Depth (m)	Bottom facies (ratio)	Class	Species	Density (ind/m <sup>2</sup> )
2	Muddy bottom with shells	Oligochaeta	<i>Tubifex tubifex</i>	50
		Hirudinea	<i>Erpobdella octoculata</i>	25
		Amphipoda	<i>Gammarus triacanthus prespensis</i>	25
		Insecta	<i>Chironomus plumosus</i>	250
5	Muddy bottom with shells	Oligochaeta	<i>Tubifex tubifex</i>	50
		Hirudinea	<i>Erpobdella octoculata</i>	25
		Bivalvia	<i>Dreissena carinata</i>	3250
		Amphipoda	<i>Gammarus triacanthus prespensis</i>	50
		Insecta	<i>Chironomus plumosus</i>	50
10	Muddy	Oligochaeta	<i>Tubifex tubifex</i>	375
		Insecta	<i>Chironomus plumosus</i>	75

During the spring period, the locality of Ezerani was characterized by greater biodiversity and density of organisms from the bottom fauna compared to other localities (Tables 3 and 4). In June, 9 taxa from 6 systematic groups (Oligochaeta, Hirudinea, Gastropoda, Amphipoda, Bivalvia and Insecta) were recorded in this locality. At a depth of 5 meters, distinguished by facies on the bottom with shells of snails and shells, the greatest biodiversity was observed, with 7 species from 6 systematic groups. The highest density was observed in the species *Limnodrilus hoffmeisteri* - 2000 ind/m<sup>2</sup>.

The results of the survey clearly showed that the structure of the invertebrate community along the littoral zone of the Lake varies from one locality to another (Figure 1). Thus, more than half of the total diversity is registered in the locality of Ezerani, while the community of invertebrates is almost half poorer in Stenje and Oteshevo by five species. Such status is strongly correlated with the intensity of anthropogenic pressure and changes in the quality of sediments resulting from fluctuations in the water level of the Lake.

According to the results of the research during April 2021 [17] greater biodiversity and density were found in the locality of Ezerani, while the lowest density and diversity were observed in Oteshevo. The most abundant species of the bottom fauna was *Dreissena carinata*. All physical-chemical parameters investigated indicate that Lake Prespa is undergoing eutrophication, and besides the increased phosphorus level, the water level has lowered as well [18,19]. The diversity and abundance of the benthic fauna, as one of the key components most affected by the constant fluctuation and withdrawal of the Lake's water, has already been drastically reduced based on the latest research (2020–2023) [20]. According to the authors, thus, global warming and changes in water trophy are considered the main triggers and

vectors that would facilitate the transmission and rapid acclimatization and adaptation of new species.

**Table 3** Composition and density of bottom fauna in Ezerani (June 2022)

Locality Ezerani				
Depth (m)	Bottom facies (ratio)	Class	Species	Density (ind/m <sup>2</sup> )
2	Muddy bottom with shells	Oligochaeta	<i>Eiseniella tetraedra</i>	100
		Gastropoda	<i>Pyrgohydrobia prespaensis</i>	25
		Insecta	<i>Baetis vernus</i>	25
			<i>Chironomus plumosus</i>	25
5	Shell zone	Oligochaeta	<i>Eiseniella tetraedra</i>	1500
			<i>Limnodrilus hoffmeisteri</i>	2000
		Hirudinea	<i>Glossiphonia complanata</i>	25
		Gastropoda	<i>Valvata piscinalis</i>	25
		Bivalvia	<i>Dreissena carinata</i>	1300
		Amphipoda	<i>Gammarus triacanthus prespensis</i>	150
		Insecta	<i>Chironomus plumosus</i>	1350
10	Muddy with shells (without vegetation)	Oligochaeta	<i>Eiseniella tetraedra</i>	1775
			<i>Limnodrilus hoffmeisteri</i>	1000
		Insecta	<i>Baetis vernus</i>	25
			<i>Chironomus plumosus</i>	1425

**Table 4** List of macrozoobenthos species composition in Prespa Lake in spring 2022

Class	Species	Otesevo	Stenje	Ezerani
Oligochaeta	<i>Tubifex tubifex</i>	+	+	
	<i>Eiseniella tetraedra</i>			+
	<i>Limnodrilus hoffmeisteri</i>			+
Hirudinea	<i>Glossiphonia maculosa</i>	+		
	<i>Glossiphonia complanata</i>			+
	<i>Erpobdella octoculata</i>		+	
Gastropoda	<i>Valvata piscinalis</i>	+		+
	<i>Pyrgohydrobia prespaensis</i>			+
Bivalvia	<i>Dreissena carinata</i>	+	+	+
Amphipoda	<i>Gammarus triacanthus prespensis</i>		+	+
Insecta	<i>Baetis vernus</i>			+
	<i>Chironomus plumosus</i>	+	+	+

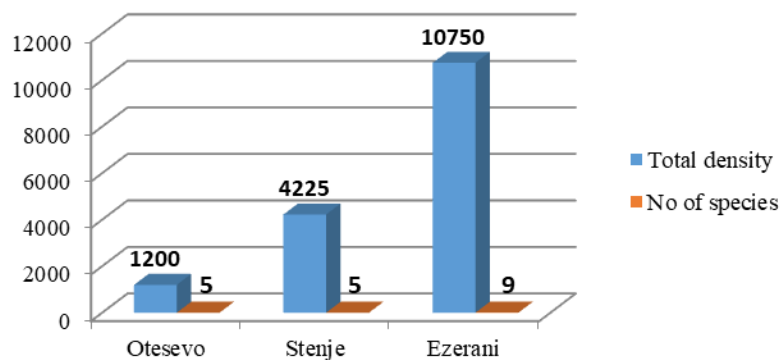


**Figure 1** Density and diversity in Otesevo, Stenje and Ezerani from Prespa Lake

Table 5 depicts the environmental status of the sampling sites according to traditional indices. The environmental status varied from poor to very good, based on the Pielou and Simpson indices. The values of H (Shannon & Wiener diversity index) and d (Margalef index) were closer reflections of the real picture of the ecological status of the sampling sites.

**Table 5** The ecological status of the localities according to the indexes in spring 2022

Indexes	Otesevo	Stenje	Ezerani
N (ind/m <sup>2</sup> )	1200	4225	10750
Number of species S	5	5	9
Shannon&Wiener H	2.82	1.38	3
Margalef d	2.92	2.76	3.47
Pielou e	0.85	0.4	0.77
Simpson c	0.18	0.6	0.14

\* red color-very heavily polluted waters; orange - heavily polluted waters; yellow -medium polluted waters; green-slightly polluted waters; blue -clean unpolluted waters.

None of the mentioned indices reflected the real condition of the Lake seen through the prism of the condition of the bottom fauna, which was generally either very poor in most of the localities in the Lake, or included representatives that were not indicative enough, or indicated an environmental status that did not meet the requirements for good environmental status according to the European Water Directive. Therefore, in this research, the ASPT index was also used, which proved to be sufficiently indicative and had been checked in past research. According to this index, no locality met the criteria for a good environmental condition. Specifically, the localities of Oteshevo and Stenje were categorized as having poor ecological status, while Ezerani had a moderate ecological status (Table 6).

**Table 6** The ecological status of localities according to the ASPT index in spring 2022

Indexes	Otesevo	Stenje	Ezerani
ASPT			

\*ASPT red color-bad ecological status; yellow color -moderate ecological status.

## CONCLUSION

In Prespa Lake, 12 species from 6 systematic groups of bottom fauna were registered: Oligochaeta, Hirudinea, Gastropoda, Bivalvia, Amphipoda, and Insecta. The richest diversity is observed in the groups Oligochaeta and Hirudinea, with 3 species each. Other groups are represented by two species each, with Bivalvia and Amphipoda being the least represented with one representative each. The results of the survey clearly showed that the structure of the invertebrate community varies from one site to another along the littoral Lake zone. More than half of the total diversity is registered in the Ezerani locality, while the invertebrate community is almost half poorer in Stenje and Oteshevo, with 5 species each. We found greater biodiversity and density in the locality of Ezerani, while the lowest density and diversity were observed in Oteshevo. The most abundant species of the bottom fauna was *Dreissena carinata*. According to the ASPT index, the localities of Oteshevo and Stenje were distinguished by a poor ecological status, while Ezerani by a moderate ecological status.

## **ACKNOWLEDGEMENT**

*The authors express their gratitude to PONT for the Grant: Identification of Anthropogenic Impacts on Prespa Lake (January 2021 - June 2024) and to the main researcher Dr. Elizabeta Veljanovska Sarafiloska by Grant Agreement Number (EA0180;03-155/1).*

## **REFERENCES**

- [1] Rosenberg D.M., Resh V.H., Freshwater Biomonitoring and Benthic Macroinvertebrates, Chapman & Hall, New York (1993), p.488, ISBN: 0-412-02251-6x.
- [2] EU 2000, Directive 2000/60/EC of the European Parliament and of the Council of 23 October 2000, establishing a framework for Community action in the field of water policy. Official Journal of the European Communities 327, p.73.
- [3] UNDP Project Final Report, Restoration of the Prespa Lake Ecosystem-Implementation of the Prespa Lake Watershed Management Plan (2012).
- [4] Lind O.T., Handbook of common methods in limnology. The C. V. Mosby Company, St. Luis-Toronto-London, (1985) p.199.
- [5] Wetzel R.G., Limnology, Saunders College Publishing, Philadelphia (1975) p.767.
- [6] Wetzel R.G., Likens G., Limnological Analyses, W.B. Saunders comp. Philadelphia, London, Toronto (1979), p.263–270.
- [7] Barnes R.D. Invertebrate Zoology, Saunders College, Philadelphia (1980), ISBN: 9780030567476/0030567475.
- [8] Brinkhurst R.O., Jamieson B.G., Aquatic Oligochaeta of the world. Oliver & Boyd, Edinburgh (1978), ISBN: 0050021559.
- [9] Hadžišće S., Zbor. I. Kongres biologa Jugoslavije, Zagreb (1953) 174–177.
- [10] Hadžišće S., Zbornik na rabotite, Hidrobioloski zavod, Ohrid. God.VI, Br. 16 (32) (1958) 1–6.
- [11] Hadžišće S., Zbornik na rabotite, Hidrobioloski zavod, Ohrid. God.VI, Br. 17 (33) (1958) 1–4.
- [12] Hrabe S., Zoo. Jhrb. Abt. Syst., Jena, 61 (1941) 1–62.
- [13] Lukin E.I., Fauna SSSR: Leeches (First part), Scientific Academy, Institute for Zoology, published by Nauka, Leningrad (1976).
- [14] Radoman P., Hydrobioidea, a superfamily of Prosobranchia (Gastropoda). I. Systematics. Monographs, Serb. Acad. Sci., Belgrade (1983), 1–256.
- [15] Šapkarev J. Sistematika i rasprostranjenje pijavica (Hirudinea) Makedonije (Taxonomy and distribution of leeches (Hirudinea) from Macedonia). Biosistematika I (1) (1975) 87–99.
- [16] Mandaville S.M., Benthic macroinvertebrates in freshwaters – taxa tolerance values, metric, and protocols, (Project H-1) Soil & Water Conservation Society of Metro Halifax, (2002), p.48.

- [17] Budzakoska-Gjoreska B., Trajanovski S., Veljanovska-Sarafiloska E., Book of Abstracts of International Conference “Kliment's Days 2023 - 60 years Faculty of Biology” Sofia, Bulgaria (2023), p.49.
- [18] ICR-Initial characterization of Lakes Prespa, Ohrid and Shkodra/Skadar Implementing the EU Water Framework Directive in South-Eastern Europe, Deutsche Gesellschaft für Internationale Zusammenarbeit (GIZ) GmbH, Bonn und Eschborn, 568 S. (2015), p.113.
- [19] Stojov V. Climate and anthropogenic impacts on the water reserves of the Prespa Lake (2020). Available on the following link: [https://www.moepp.gov.mk/wp-content/uploads/2020/12/prespa\\_klima\\_antropogeni\\_vlijanija\\_20201129.pdf](https://www.moepp.gov.mk/wp-content/uploads/2020/12/prespa_klima_antropogeni_vlijanija_20201129.pdf)
- [20] Trajanovski S., Budzakoska Gjoreska B., Trajanovska S., *et al.*, Book of Abstracts of Joint ESENIAS & DIAS Scientific Conference 2023 and 12<sup>th</sup> ESENIAS Workshop: Globalisation and invasive alien species in the Black Sea and Mediterranean regions- management challenges and regional cooperation, Varna, Bulgaria (2023), p.35.



## PHYTOPLANKTON COMMUNITY AS BIOINDICATOR OF WATER TROPHIC STATE IN LAKE PRESPA

Suzana Patcheva<sup>1\*</sup>, Jovica Leshoski<sup>1</sup>, Elizabeta Veljanoska Sarafiloska<sup>1</sup>

<sup>1</sup>Hydrobiological Institute - Ohrid, Naum Ohridski 50, 6000 Ohrid, NORTH MACEDONIA

\*spatceva@hio.edu.mk

### Abstract

*Lake Prespa is a very unique ecological and hydrological system shared by Macedonia, Greece and Albania that over the past years, has faced serious environmental challenges such as eutrophication and water level decline. Phytoplankton species represent the most sensitive biological components of water ecosystems that respond first to changes in nutrient concentrations. Regarding this fact, phytoplankton is a very good indicator of water trophic state in aquatic ecosystems. Phytoplankton samples were taken seasonally during 2023 at one pelagic and seven littoral sampling points in the Macedonian part of Lake Prespa. The phytoplankton community in the pelagic zone was dominated by diatoms and cyanophytes and rare occurrences of the groups dinoflagellates, chlorophytes and chrysophytes. The diatoms dominated in winter, spring and autumn periods while cyanophytes dominated in the summer. The total abundance of phytoplankton was considerably higher in summer than in other seasons which is characteristic for meso-eutrophic lakes. According to the trophic state index (TSI) based on chlorophyll a concentration two points of Lake Prespa are categorized as oligotrophic and all other points as mesotrophic.*

**Keywords:** Lake Prespa, phytoplankton community, trophic state.

### INTRODUCTION

The transboundary Lake Prespa basin, situated in the Balkan Peninsula is an ecosystem of global significance. This becomes even more important in the case of systems of great importance such as ancient world lakes (estimated age between 2 and 35 million years) which are about a dozen and have long been recognized as unique ecosystems in terms of their exceptional high biodiversity and levels of endemism [1].

In the past, periodical oscillations of the lake level were in the range of one to three metres, depending on the amount of rain in the season. After the mid 80's, a steady decrease of the water level has been recorded that disturbs the ecological balance of the lake and the watershed area resulting in serious consequences for the water trophic state, biodiversity and ecosystem health. A topographic map from the 1940s indicates that the present water level is 5–6 m lower than in the 1940s. As Lake Prespa is relatively shallow compared to its large surface area, wind and convective mixing lead to completed stratification of the entire water column from September to April/May and consequently all dissolved substances are homogenized annually [2]. In addition to this, the industrial activities as well as the over use of the herbicides in agriculture activities raised the problem of pollution of the water in Lake Prespa.



Phytoplankton is one of the most sensitive indicator of the water trophic state in lakes. Changes in environmental conditions related to anthropogenic load, climate change, nutrients, water depth and chemistry can affect the phytoplankton community structure and diversity. The EU Water Framework Directive [3] includes phytoplankton as one of four biological elements to be used in the assessment of the ecological status of surface waters.

In the last two decades, there were many investigations of the phytoplankton and trophic conditions that suggested process of eutrophication of Lake Prespa as result of anthropogenic pressure [4–10].

## MATERIALS AND METHODS

The surveys of the phytoplankton in the Macedonian part of Lake Prespa were carried out at seven sampling points in the littoral zone and one in the pelagic zone at three depths of 0 m, 7 m and 13 m. The phytoplankton samples were collected seasonality during four sampling campaigns. The samples were collected with a Niskin water sampler and preserved immediately at the sampling site by adding 4% formaldehyde. The identification of phytoplankton taxa and quantitative analyses (enumeration of individuals per volume of water) were done according to Utermöhl [11], using an inverted microscope LW101–2 trinocular, with epi-illumination module and camera OmniVID, 8.0 MP.

Chlorophyll *a* was analysed according to ISO 10260 [12], using a spectrophotometer UV–VIS SPECORD 10 (Zeiss) after an extraction with 90% ethanol. Total phosphorus (TP) was measured spectrophotometrically wavelength 885 nm, after digestion of the water sample with peroxodisulfate [13,14]. The Trophic State Index (TSI) was calculated based on values of chlorophyll *a* concentration and total phosphorus concentration [15].

## RESULTS AND DISCUSSION

A total number of 75 phytoplankton taxa were collected in Lake Prespa during the winter, spring, summer and autumn campaigns of 2023. The taxa belonged to eight divisions: Cyanophyta (Cyanobacteria), Bacillariophyta, Chlorophyta, Chrysophyta, Charophyta, Pyrrophyta, Cryptophyta and Euglenophyta. Most of the phytoplankton taxa identified belonged to Bacillariophyta (42 taxa), followed by Cyanophyta (12) and Chlorophyta (11). The other groups of algae are represented by a small number of taxa Chrysophyta (3) Charophyta (3) Pyrrophyta (2), Cryptophyta (1) and Euglenophyta (1).

The number of taxa at the littoral points was higher than in the pelagic zone because their phytoplankton communities contain species that usually live on the bottom and on macrophyte vegetation. The highest number of taxa (44) characterized littoral sampling point Krani, followed by Stenje (42) and the lowest number of taxa was recorded at Slivnica (29) and at the pelagic zone (31) (Table 1).

During the investigations it was determined that Cyanophyta was the dominant phytoplankton group in the summer period, and the species *Planktolyngbya limnetica* dominated in terms of its abundance. Other species of cyanobacteria that may be potentially toxic were represented with low or insignificant abundance or were not recorded at all in the phytoplankton. In the rest of the seasons, the pelagic zone was dominated by the diatom

*Cyclotella ocellata* and in the littoral points, in addition to this species, which was dominant in all seasons with high abundance, the species *Navicula sp.* was represented with significant abundance and in the autumn period the species *Aulacoseira sp.* was dominant species.

**Table 1** The number of phytoplankton species in each of the sampling points in Lake Prespa

	Pelagic zone	Stenje	Oteshevo	Pretot	Krani	Slivnica	Nakolec	Dolno Dupeni
<b>Cyanophyta</b>	7	7	5	4	5	5	2	3
<b>Bacillariophyta</b>	11	24	27	25	28	17	22	24
<b>Chlorophyta</b>	6	6	3	3	5	3	5	3
<b>Charophyta</b>	3	2	2	2	2	2	2	2
<b>Chrysophyta</b>	2		1		2	1	1	
<b>Pyrrophyta</b>	2	1	1	1	1	1	1	1
<b>Cryptophyta</b>		1	1	1	1			1
<b>Euglenophyta</b>		1						
<b>Total</b>	<b>31</b>	<b>42</b>	<b>40</b>	<b>36</b>	<b>44</b>	<b>29</b>	<b>33</b>	<b>34</b>

The total abundance of phytoplankton was considerably higher in summer than in other seasons and the lowest phytoplankton abundance was observed in autumn. In summer, the highest abundance of phytoplankton was recorded in Pretor with 7,720,000 ind/l, and the lowest density was in Slivnica (1,664,000 ind/l) and Nakolec, where it was 1,776,000 ind/l. In the other seasons, there were no significant differences in the abundance of phytoplankton between different points (Figure 1).

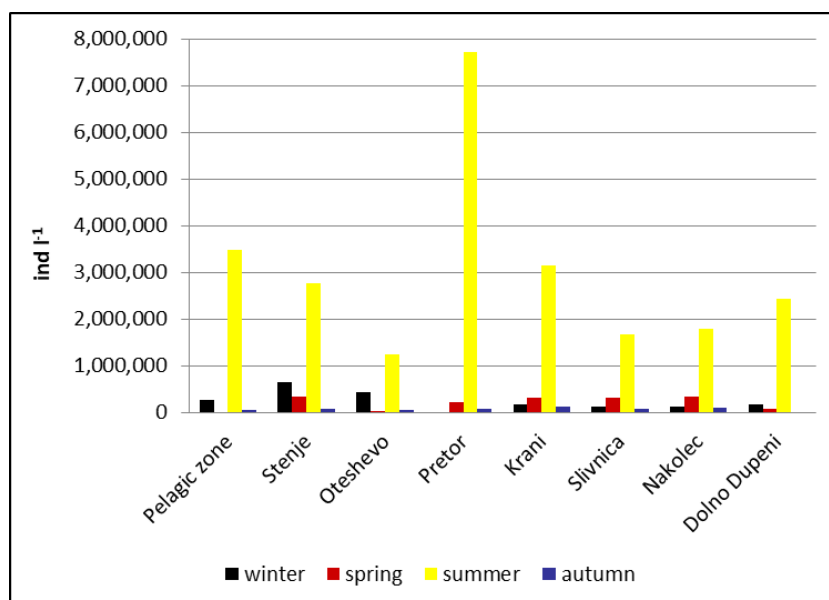


**Figure 1** Total phytoplankton abundance at sampling points of Lake Prespa

Chlorophyll *a* is a photosynthetic pigment that integrates all types of algae and serves as a measurable indicator for the entire phytoplankton production, that is, the phytoplankton

biomass, and therefore it is a very significant parameter for determining the trophic state of the lake water. The average annual values of chlorophyll *a* concentration at the all sampling points during 2023 were below 5.1  $\mu\text{g l}^{-1}$  and there were no significant differences in the values of different sampling points. The average value of chlorophyll *a* concentration in the pelagic zone was slightly lower than in the littoral zone and recorded 2.56  $\mu\text{g l}^{-1}$ , the highest values were observed in Pretor (5.04  $\mu\text{g l}^{-1}$ ) and Slivnica (4.78  $\mu\text{g l}^{-1}$ ) (Figure 2).

The average annual total phosphorus concentration in the pelagic zone was 28.87  $\mu\text{g l}^{-1}$ , while in the littoral zone the highest value of 57.74  $\mu\text{g l}^{-1}$  was recorded in Pretor, in Dolno Dupeni was 31.82  $\mu\text{g l}^{-1}$  and at all other points were below 30  $\mu\text{g l}^{-1}$  (Figure 3).

The obtained results showed that the anthropogenic impact, especially expressed in the littoral zone of the lake near the rivers inflows, agriculture areas and touristic complexes have significant influence on the water trophic state.

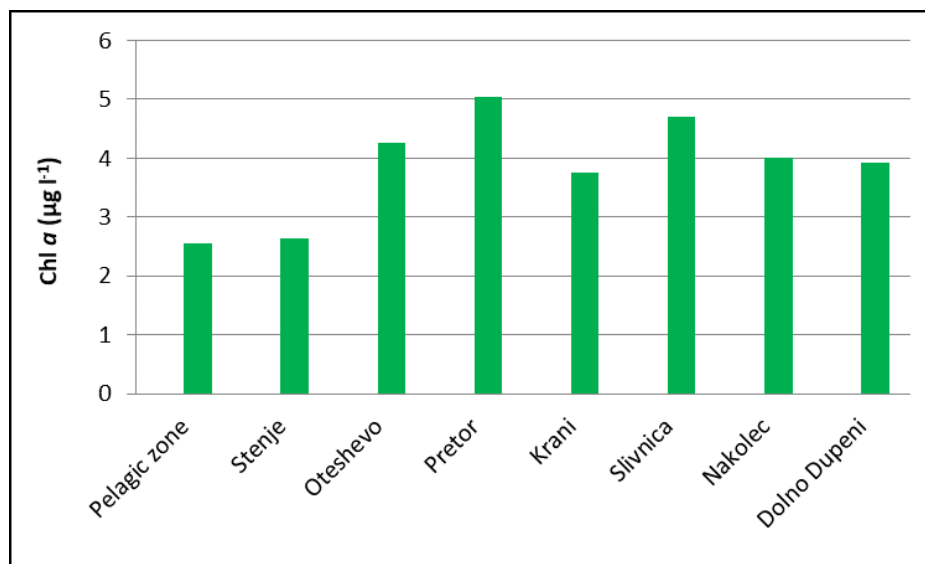


**Figure 2** Average annual chlorophyll *a* concentration at sampling point of Lake Prespa

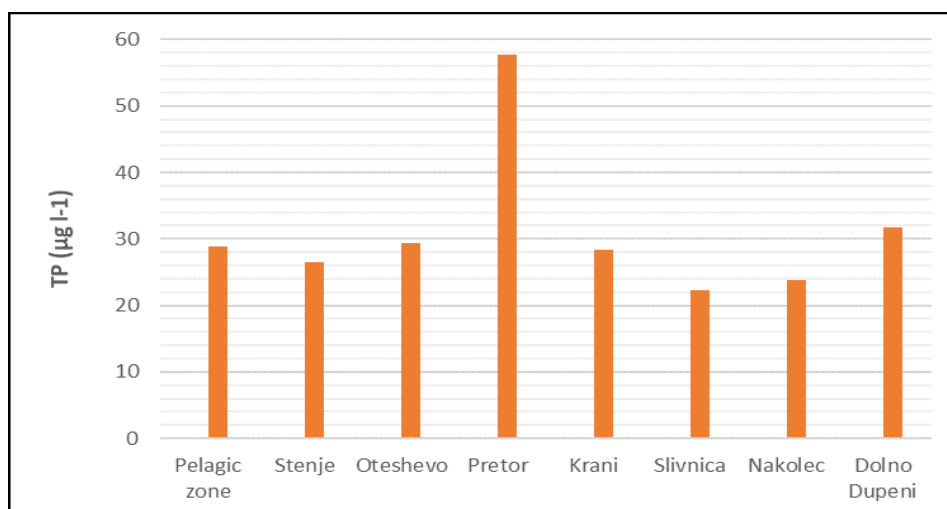


**Figure 3** Average annual total phosphorus concentration at sampling points of Lake Prespa

The trophic state index (TSI; Carlson, 1977) is an indicator of water trophic level and provides a basis for relating chlorophyll *a* levels and transparency to total phosphorus, which tends to promote algal production. According to the values of the trophic state index (TSI) based on the concentration of chlorophyll *a*, during 2023, the lake water at pelagic zone and Stenje was categorized as oligotrophic, and at all other points of littoral zone of Lake Prespa were categorized as mesotrophic (Figure 4).

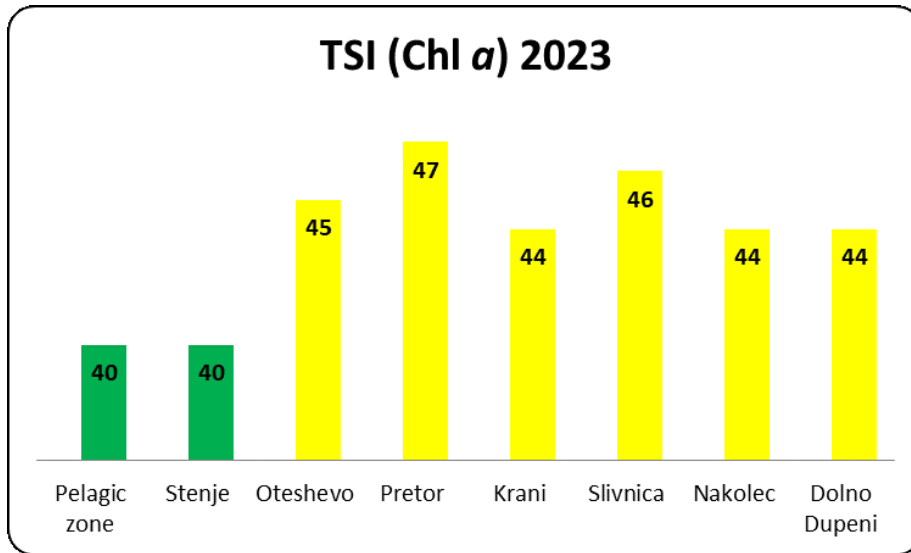


**Figure 4** Trophic state index based on chlorophyll *a* concentration

According to the values of the trophic state index (TSI) based on the concentration of total phosphorus, during 2023, the lake water at Stenje, Krani, Slivnica and Nakolec were categorized as mesotrophic, pelagic zone and Oteshevo was categorized as meso-eutrophic, Pretor and Dolno Dupeni as eutrophic (Figure 5).

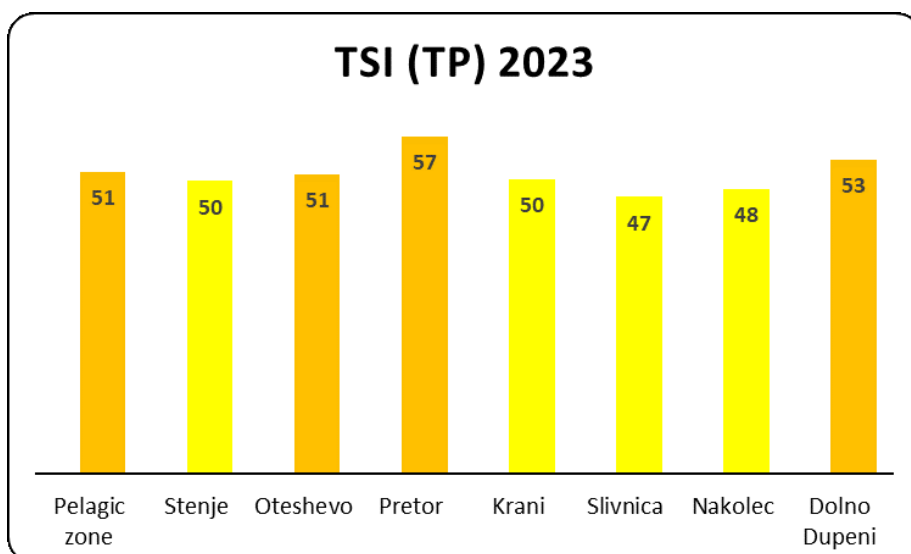


**Figure 5** Trophic state index based on total phosphorus concentration

## **CONCLUSION**

Phytoplankton diversity and abundance is a very important tool in the monitoring of the seasonal changes in Lake Prespa, showing process of eutrophication especially during the summer season. Most phytoplankton species identified belong to the Bacillariophyta. Investigations showed distinct seasonal differences in phytoplankton composition. Bacillariophyta were the dominant group in spring, autumn and winter. In summer Cyanophyta was the dominant algal group at all sampling points

Phytoplankton composition as well as spatial and temporal distribution of phytoplankton in Lake Prespa is typical for mesotrophic lakes.

The trophic state index based on chlorophyll *a* concentration and total phosphorus was the highest in littoral sampling point Pretor as a consequence of the negative influence of River Golema that flows into the lake at that point.

## **ACKNOWLEDGMENTS**

*The research presented in this paper was done with the grant support of PONT (Prespa-Ohrid Nature Trust) for the project section “Understanding anthropogenic pressures on Lake Prespa”.*

## **REFERENCES**

- [1] Martens W.H.J. Psychopathy and maturation, Shaker Publishing. MD-dissertation, Tilburg University, The Netherlands. Maastricht (1997).
- [2] Matzinger A., Jordanoski M., Veljanoska-Sarafiloska E., *et al.*, Hydrobiologia 553 (2006) 89–109.
- [3] Directive 2000/60/EC of the European Parliament and of the Council of 23 October 2000 establishing a framework for Community action in the field of water policy. Official Journal of the European Communities (2000), L 327: 1–72.
- [4] Patceva S., Mitic V., Phytoplankton composition of Lake Prespa and its response to eutrophication in the last fiftieth years. Collection of Papers Devoted to Academician KirilMicevski, (2006) 299–309.
- [5] Patceva S., Mitic V., Jordanoski M., *et al.*, Trophic state of Lake Prespa. Conference on water observation and information system for decision support “BALWOIS”, Ohrid, Republic of Macedonia (2006).
- [6] Petrova D., Patceva S., Mitic V., *et al.*, Journal JEPE 9 N3 (2008) 501–512.
- [7] Sarafiloska E.V., Patceva S., J. Int. Environmental Application & Science 7(1) (2012) 291–299.
- [8] Leshoski J., Sarafiloska-Veljanoska E., Vasilevska S., *et al.*, PSI Hydrobiological Institute, Ohrid, 43(1) (2015) 64–71.
- [9] Patceva S., Leshoski J., Acta zool. bulg., Suppl. 13 (2019) 51–56.
- [10] Veljanoska-Sarafiloska E., Lokoska L., Patceva S., Acta zool. bulg., Suppl. 13 (2019) 25–32.

- [11] Utermöhl H., *Mitteil. Int. Ver. Limnologie* (1958) 1–38.
- [12] ISO 10260. *Water quality - measurement of biochemical parameters - spectrometric determination of the chlorophyll *a* concentration*, ISO, Geneva (1992).
- [13] Strickland J.D.H., Parsons T.R., *A Practical Handbook of Seawater Analysis*. Fish. Res. Board Canada. *bull.* 167. Ottawa (1968). p.311.
- [14] APHA-AWWA-WPCF, *Standard methods for the examination of water and wastewater*. 21<sup>th</sup> ed – Washington DC (2005).
- [15] Carlson R.E., *Limnol. Oceanogr.* 22 (1977) 361–369.





## EARLY, LATE AND OUT-BREEDING SEASON BIRD SINGING – EFFECTS OF CLIMATE CHANGE?

**Boris Novaković<sup>1\*</sup>, Marko Raković<sup>2</sup>**

<sup>1</sup>Serbian Environmental Protection Agency, Ministry of Environmental Protection,  
Žabljačka 10A, 11160 Belgrade, SERBIA

<sup>2</sup>University of Belgrade-Institute for Multidisciplinary Research, Kneza Višeslava 1,  
11030 Belgrade, SERBIA

\*boris.novakovic@sepa.gov.rs

### Abstract

*The present study provides data on early, late and out-breeding season bird singing of the following songbird species: Eurasian Blackbird (*Turdus merula*), Eurasian Blackcap (*Sylvia atricapilla*) and Cirl Bunting (*Emberiza cirlus*). Untimely species' song was noted in the period 2013–2023 (one decade) at the total of 10 sites in Serbia. Also field notes on some other songbird species singing are given in the present study.*

**Keywords:** Blackbird, Eurasian Blackcap, Cirl Bunting, out-breeding song, Serbia.

### INTRODUCTION

The impacts of climate change on biodiversity are more intensive from year to year. Recently we could observe many consequences of climate change and global warming as well (e.g. in the temperate climate regions a growing season is prolonged; a winter season is shorter and less severe). Most bird species sing by day, with two distinct peaks of vocal activity - around sunrise and sunset. However, even typically diurnal birds also sing during at night what is for them an atypical part of the day. To date, the mechanism and function(s) of such behavior remain unclear across bird taxa [1].

Singing activities of birds in the early spring are mainly controlled by the photoperiod and other environmental factors such as temperature, food, and rainfall [2]. In spring, most adult males begin to sing for territorial defense and to attract mates for the coming breeding season [3,4]. Although spring singing of birds is mainly controlled by intrinsic mechanisms triggered by photoperiodic changes, fine-scale variations are mediated by other environmental factors such as temperature, food resources, and rainfall [5–9]. The environmental factor of temperature has been more often studied than other environmental factors. Also it was found a strong relationship between the overnight minimum temperature and singing activity the following morning in the Eurasian Wren (*Troglodytes troglodytes*) and Great Tit (*Parus major*) [10]. Also the vocal activity of the Song Thrush (*Turdus philomelos*) was significantly proportional to air temperature in the early morning [11]. These findings indicate that birds might reduce their singing activity in order to save energy during times of low temperature, because a considerable amount of energy and time is required for singing [12,13].

In the present study we noted the vocal activity of birds out of songbirds out of breeding season providing new data on early, late and out of breeding season bird singing of the following bird species in: Eurasian Blackbird *Turdus merula* Linnaeus, 1758, Eurasian Blackcap *Sylvia atricapilla* (Linnaeus, 1758), and Cirl Bunting *Emberiza cirlus* Linnaeus, 1758.

## MATERIALS AND METHODS

We evidenced accidentally the singing males in out-of-breeding season, of three songbird species: Eurasian Blackbird (*Turdus merula*), Eurasian Blackcap (*Sylvia atricapilla*) and Cirl Bunting (*Emberiza cirlus*) in Serbia. We set up a hypothesis related to analyzing of the correlation of air temperature with the species' vocal activity of the studied bird species. All the species have been acoustically identified based on singing in the field. We used an approach in which “target” species are linked to suitable breeding habitats. The observers walked around the investigated site and the surrounding area listening for males' singing. Considering these species are not highly territorial out of breeding period, the bird censuses were done with main goal to record infrequent and discontinuous species' singing.

## RESULTS AND DISCUSSION

The presented data refers to the singing out of the breeding season for three songbird species: *Turdus merula*, *Sylvia atricapilla* and *Emberiza cirlus*. In the period of 2013–2023 (one decade), the “untimely” song of the studied species was recorded at the total of 10 sites in Serbia. Additional information on species singing is provided in Table 1.

*Table 1* Relevant data on studied species singing

Species	Site	Date	Latitude	Longitude	Time	No. of singing ♂	Notes
<i>T. merula</i>	Zvezdara Forest	4-Feb-2018	44.7986111	20.509444	7:30 AM	1	
<i>T. merula</i>	Zvezdara Forest	25-Feb-2018	44.7986111	20.509444	8:20 AM	1	
<i>T. merula</i>	Zvezdara Forest	8-Feb-2019	44.7986111	20.509722	7:05 AM	1	
<i>T. merula</i>	Zvezdara Forest	16-Feb-2019	44.7986111	20.509722	5:15 PM	1	
<i>T. merula</i>	Zvezdara Forest	26-Feb-2019	44.7986111	20.509722	7:10 AM	1	
<i>T. merula</i>	Zvezdara Forest	28-Jan-2021	44.7986111	20.509722	7:41 AM	1	
<i>T. merula</i>	Zvezdara Forest	8-Feb-2021	44.7986111	20.509722	6:28 AM	1	
<i>T. merula</i>	Zvezdara Forest	24-Feb-2021	44.7986111	20.509722	6:36 AM	1	
<i>T. merula</i>	Zvezdara Forest	25-Feb-2021	44.7986111	20.509722	5:35 PM	1	
<i>T. merula</i>	Zvezdara Forest	14-Feb-2022	44.7986111	20.509444	5:05 PM	1	“silent” song
<i>T. merula</i>	Zvezdara Forest	18-Feb-2022	44.7986111	20.509444	5:18 PM	1	

Table 1 continued

<i>T. merula</i>	Zvezdara Forest	20-Feb-2022	44.7986111	20.509444	4:33 PM	1	intensive singing
<i>T. merula</i>	Zvezdara Forest	28-Feb-2022	44.7986111	20.509444	7:05 AM	1	rain and snow
<i>T. merula</i>	Zvezdara Forest	28-Feb-2022	44.7986111	20.509444	11:40 AM	1	
<i>T. merula</i>	Zvezdara Forest	13-Jan-2023	44.7986111	20.509444	6:05 AM	1	<i>E.rubecula</i> singing at same site
<i>T. merula</i>	Zvezdara Forest	15-Jan-2023	44.7986111	20.509444	3:47 PM	1	Very short song (1 minute) on sunny and windy day
<i>S. atricapilla</i>	Zvezdara Forest	26-Feb-2018	44.7986111	20.509444	8:36 AM	1	
<i>S. atricapilla</i>	Zvezdara Forest	28-Feb-2018	44.7986111	20.509444	3:40 PM	1	
<i>S. atricapilla</i>	Zvezdara Forest	24-Feb-2019	44.7986111	20.509444	7:12 AM	1	
<i>S. atricapilla</i>	Zvezdara Forest	4-Mar-2019	44.7986111	20.509722	7:40 AM		
<i>S. atricapilla</i>	Zvezdara Forest	8-Mar-2019	44.7986111	20.509722	7:50 AM	1	
<i>S. atricapilla</i>	Zvezdara Forest	11-Mar-2022	44.7986111	20.509444	8:56 AM	1	
<i>S. atricapilla</i>	Zvezdara Forest	21-Mar-2022	44.7986111	20.509444	7:15 AM	1	
<i>E. cirrus</i>	Brza Palanka	17-Oct-2013	44.465933	22.449896	2:50 PM	1	
<i>E. cirrus</i>	Prijepolje	3-Oct-2014	43.381002	19.638083	12:15 PM	1	
<i>E. cirrus</i>	Vrnjačka Banja	17-Oct-2014	43.618748	20.897502	11:12 AM	1	
<i>E. cirrus</i>	Vrnjačka Banja	17-Oct-2014	43.618748	20.897502	3:43 PM	1	
<i>E. cirrus</i>	Vrnjačka Banja	19-Oct-2014	43.618748	20.897502	9:33 AM	1	
<i>E. cirrus</i>	Vrnjačka Banja	20-Oct-2014	43.618748	20.897502	1:55 PM	1	
<i>E. cirrus</i>	Gradac River	26-Oct-2014	44.257637	19.889266	10:15 AM	1	
<i>E. cirrus</i>	Gradac River	26-Oct-2014	44.255797	19.888288	11:03 AM	1	
<i>E. cirrus</i>	Nemenikuće	20-Sep-2014	44.492503	20.574956	2:52 PM	1	
<i>E. cirrus</i>	Nemenikuće	4-Oct-2014	44.492503	20.574956	10:18 AM	1	
<i>E. cirrus</i>	Nemenikuće	12-Oct-2014	44.492503	20.574956	12:41 PM	1	
<i>E. cirrus</i>	Nemenikuće	4-Nov-2014	44.492503	20.574956	1:00 PM	1	
<i>E. cirrus</i>	Nemenikuće	11-Nov-2014	44.492503	20.574956	12:17 PM	1	
<i>E. cirrus</i>	Nemenikuće	11-Nov-2014	44.492503	20.574956	3:45 PM	1	
<i>E. cirrus</i>	Petnica	9-Nov-2014	44.252274	19.939166	10:05 AM	1	
<i>E. cirrus</i>	Petnica	9-Nov-2014	44.252274	19.939166	1:24 PM	1	
<i>E. cirrus</i>	Osanica River	22-Oct-2021	44.0675	21.155555	2:30 PM	1	

Many previous topic studies did not provide data on out-of-season singing for these three songbird species. For comparison, the breeding season of analysed species according to different literature sources is given in Table 2.

**Table 2** Breeding season of studied species according to different literature sources

Species	Common name	Makatsch (Vögel Mit Europe)	Switzerland (Vogelwarte)	(Rašajski, scribendarum)	Bird Protection and Study Society of Serbia (proposal)
<i>Turdus merula</i>	Eurasian Blackbird	Apr 01 <sup>st</sup> –July 10 <sup>st</sup>	March 10 <sup>st</sup> –Aug 10 <sup>st</sup>	March 20 <sup>st</sup> –June 10 <sup>st</sup>	March 15 <sup>st</sup> –July 20 <sup>st</sup>
<i>Sylvia atricapilla</i>	Eurasian Blackcap	May 15 <sup>st</sup> –July 30 <sup>st</sup>	Apr 20 <sup>st</sup> –Aug 10 <sup>st</sup>	Apr 20 <sup>st</sup> –July 15 <sup>st</sup>	Apr 15 <sup>st</sup> –July 10 <sup>st</sup>
<i>Emberiza cirius</i>	Cirl Bunting	Apr 20 <sup>st</sup> –Aug 01 <sup>st</sup>	Apr 20 <sup>st</sup> –Sep 08 <sup>st</sup>	May 1 <sup>st</sup> –July 01 <sup>st</sup>	Apr 10 <sup>st</sup> –Jul 20 <sup>st</sup>

Global warming is likely to initiate spring singing at an earlier date and thus advance the breeding cycle of birds [14,15].

Breeding males have to sing as early as possible in order to hold a territory [10] because the security of a territory will contribute greatly to their upcoming reproductive success. Temperature might play a crucial role in spring singing of birds and act as an important environmental factor in initiating the breeding process of birds [8].

Besides during this research the authors recorded singing of some other bird species, such as Icterine Warbler (*Hippolais icterina*) (Vieillot 1817) and Eastern Olivaceous Warbler (*Iduna pallida*) (Hemprich and Ehrenberg 1833) during late spring migration (May), out of breeding sites and typical habitats, and maybe close to them (for Icterine Warbler one observation from the the City of Kruševac, southern Serbia) which could be regarded as some “unterritorial” singing affected by air temperature, and maybe competitiveness of some other “territorial” and songbird species (predominantly tits and finches singing at the same time in their regular breeding habitats). We suppose if the singing birds are in suitable habitats, they can sing during migration. As contrary, we think if the temperature is high enough to initiate bird singing during migration, the birds could sing in other “non-breeding” habitats.

During the research the authors observed some type of “silent” song for Blackbird (early season song in February) and Blackcap (most recent observations in August 2022 on Maljen Mt, after breeding period, as well as early autumn (October) regular song for one more species, Mistle Thrush *Turdus viscivorus* L. 1758). “Silent” song consists of similar phrases, but faster and high-pitched, and very quiet. In general the authors recorded Blackbird often sings in sunny evenings after storm and rainfall, and in the early morning as well. Recently we recorded for Blackbird in the Zvezdara Forest, Belgrade, that specimens did not sing frequently (every day during breeding period), but 3-5 times weekly, often with vocal mimicry (some parts of the Blackbird song syllables of some phrases resembled Eurasian Golden Oriole (*Oriolus oriolus*), European Starling (*Sturnus vulgaris*) song, Eurasian Magpie (*Pica pica*) call and Eurasian Scops Owl (*Otus scops*) alarm call. These species breed in the surroundings supporting the Blackbird vocal mimicry. Also for Blackbird, we recorded forthcoming repetition of previous phrases or part of phrases in the song, particularly at the

dawn. In the Zvezdara forest and its suburbs, we recorded Common Redstart (*Phoenicurus phoenicurus*) song ending phrases resembled Lesser Whitethroat (*Curruca curruca*) song.

The authors also observed some other bird species were singing intensively during winter period compared to other seasons, even these species are not breed in winter, such as Eurasian Wren (*Troglodytes troglodytes*) (Linnaeus, 1758) - predominantly in sunny, cold mornings, and European Robin (*Erithacus rubecula*) (Linnaeus, 1758) - predominantly in dawn, late evening, and cold nights, also at foggy days without sunrays. Also, during September 2022 we record uncommon variation of the Black Redstart (*Phoenicurus ochruros*) (S. G. Gmelin 1774) song at the Zlatibor Mt. in early morning after night showers. During late winter and spring of 2023, night and dawn singing of the Great Tit (*Parus major*) Linnaeus, 1758 was recorded at three sites in Serbia: Belgrade City - Medaković II, Belgrade - Zvezdara Forest (Central Serbia), and Negotin - the town center (East Serbia). All sites are situated in urban area (city and town). The song is atypical, very loud, characterized by repeatable syllables with some variations. Often two males were singing at the same time.

## **CONCLUSION**

In the present study we assumed resident (sedentary) birds primarily sing with main goal to mark their territory as well as to attract mates for nesting. Female birds often choose their mates based on some blend of visual and vocal cues. Even male birds with beautiful breeding-season plumage can have trouble finding mates if their songs don't measure up. Each bird species typically has its own unique song. That allows an individual bird to hear a song and recognize whether the singer is from its own species [15].

We concluded early are late season singing of the studied songbird species could be primarily affected by air temperature (high air temperature affects singing). Also "silent" song we recorded could be explained by this fact.

Also we could confirm a hypothesis the average air temperature was highly correlated with the studied species' initiation to singing. Our results confirmed that air temperature can affect the vocal activity of birds as found in other studies corroborating the data obtained in our study. These results indicated that air temperature has a clear impact on bird vocal behavior at the community level. Previous studies, e. g. [10] reasoned that having spent much energy in maintaining the body temperature on cold nights, birds would show a greater demand to feed the following morning which would therefore lead to a decline in singing activity. Indeed, singing and foraging are mutually exclusive or close to being so, and thus a trade off might occur between the amount of time that a bird can spend on either behavior [7].

## **ACKNOWLEDGEMENT**

*The authors are grateful to Ms Katarina Zorić for providing some data on Great Tit singing.*

## **REFERENCES**

- [1] Kułaga K., Budka M., J. Ornithol. 161 (2020) 1143–1152.
- [2] Liao C.C., Shieh B.S., Chen C.C., Taiwan J. For. Sci. 33 (2018) 291–304.

- [3] Morse D.H., *Ecol. Monogr.* 40 (1970) 119–168.
- [4] Catchpole C.K., Slater P.J.B., *Bird Song: Biological Themes and Variations*, 2<sup>nd</sup> ed., Cambridge University Press, New York (2008), p.348, ISBN: 978-0521872423.
- [5] Slagsvold T., *Ornis. Scand.* 8 (1977) 197–222.
- [6] Ball G.F. The neuroendocrine basis of seasonal changes in vocal behaviour among songbirds *in* *The design of animal communication*, Editors: Hauser M.D., Konishi M., Cambridge MA: MIT Press, Cambridge (1999), p.213–253, ISBN: 0-262-08277-2.
- [7] Thomas R.J., *Anim. Behav.* 57 (2) (1999) 277–284.
- [8] Wingfield J.C., Hahn T.P., Maney D.L., *et al.*, *Gen. Comp. Endocrinol.* 131 (2) (2003) 143–158.
- [9] Dawson A., *Phil. Trans. of R. Soc. B.* 363 (1497) (2008) 1621–1633.
- [10] Garson P.J., Hunter M. L. Jr., *Ibis* 121 (4) (1979) 481–487.
- [11] Higgins R.M., *Ibis* 121 (3) (1979) 333–335.
- [12] Gil D., Gahr M., *TREE* 17(3) (2002) 133–141.
- [13] Dunn P.O., Winkle D.W., Effects of climate change on timing of breeding and reproductive success in birds *in* *Effects of climate change on birds*, Editors: Møller A. P., Fielder W., Berthold P., Oxford University Press, New York (2010), 113–128, ISBN: 978-0-19-956975-5.
- [14] Møller A. P., Flensted-Jensen E., Klarborg. K., *et al.*, *J. Ecol.* 79 (4) (2010) 777–784.
- [15] Steadman D., Why do birds sing?, *Available on the following link:* <https://theconversation.com/why-do-birds-sing-120266>.





## THE USE OF HOA (HEMIPTERA-ORTHOPTERA-AVES) INDICATORS TO FORMULATE THE SERBIAN CLIMATE CHANGE INDEX ( $S_{CCI}$ )

**Boris Novaković<sup>1\*</sup>, Marko Raković<sup>2</sup>**

<sup>1</sup>Serbian Environmental Protection Agency, Ministry of Environmental Protection,  
Žabljačka 10A, 11160 Belgrade, SERBIA

<sup>2</sup>University of Belgrade – Institute for Multidisciplinary Research, Kneza Višeslava 1,  
11030 Belgrade, SERBIA

\*boris.novakovic@sepa.gov.rs

### Abstract

*The study aimed to provide data on three faunistic groups (Hemiptera, Orthoptera and birds) used as indicators of climate change as well as to formulate area-specific climate change index (the Serbian Climate Change Index -  $S_{CCI}$ ). Based on the data obtained, a total of 56 indicator taxa (10 hemipteran, 21 orthopteran and 25 bird species) belong to 17 families were included from the entire territory of Serbia. The  $S_{CCI}$  is based on the statement that these species have expanded their distribution ranges and population density throughout Serbia during last decade (2012–2022) as well as predictions to inhabit still inhabitable habitats in the Peripannonian and Pannonian regions. Some of species, predominantly hemipteran and orthopteran, had acquired new habitat preference (e. g. expanded to urban areas) moving northwardly with their range and abundance expansion. On the other hand, as consequence of climate change and global warming, some species were found to be indicators of environmental degradation and habitat fragmentation.*

**Keywords:** bioindicators, climate change, Hemiptera, Orthoptera, birds, Serbia.

### INTRODUCTION

Republic of Serbia, which is in the South-East part of the Europe at Balkan Peninsula, is experiencing warming trend [1] with accelerated temperature increase, and evident signal in trend of increase since 1980-ties [2].

The study aimed to provide data on three groups (Hemiptera, Orthoptera and Aves) used as indicators of climate change as well as to formulate area-specific climate change index (the Serbian Climate Change Index -  $S_{CCI}$ ). Based on the data obtained, a total of 56 indicator taxa (10 hemipteran, 21 orthopteran and 25 bird species) belong to 17 families were included from the entire territory of Serbia. The  $S_{CCI}$  is based on the fact that these species have expanded their distribution ranges and population density throughout Serbia over a previous one decade (2012–2022) as well as predictions to inhabit still inhabitable habitats northwardly, situated in the Peripannonian and Pannonian regions. Some of the species, predominantly hemipteran and orthopteran, had acquired new habitat preference (e.g. expanded to urban areas).

## MATERIALS AND METHODS

The Serbian Climate Change Index (S<sub>CCI</sub>) was based on the statement these species expanded their distribution range, and population density as well, throughout Serbia during the last decade (2012–2022).

The indicators were selected using three main principles: 1) extending species' area to the previously known 2) increase species population density compared to earlier period, 3) adaptate to suburban in urban areas changing the species' native habitat preference.

## RESULTS AND DISCUSSION

The data on the selected Hemiptera-Orthoptera-Aves (HOA) indicator taxa which were used to develop the Serbian Climate Change Index (S<sub>CCI</sub>) are provided in Table 1.

*Table 1* Indicator taxa list and related data

Group/Species	Indicator weight	Urban area	Newly-colonized habitats (2012–2022) and ecological notes
<b>HEMIPTERA</b>			+
<i>Tettigetta dimissa</i> (Hagen, 1856)	5	+	+
<i>Pagiphora annulata</i> (Brullé, 1832)	5	+	+
<i>Tibicina haematodes</i> (Scopoli, 1763)	5	+	+
<i>Lyristes plebejus</i> (Scopoli, 1763)	4		+
<i>Cicada orni</i> Linnaeus, 1758	4	+	+
<i>Cicadatra hyalina</i> (Fabricius, 1798)	5	+	+
<i>Cicadatra atra</i> (Olivier, 1790)	5	+	
<i>Cicadetta concinna</i> Germar, 1821	4		
<i>Cicadetta montana</i> (Scopoli, 1772)	4		
<i>Cicadetta macedonica</i> Schedl, 1999	4		
<b>ORTHOPTERA</b>			
<i>Eumodicogryllus bordigalensis</i> (Latreille, 1804)	5	+	+
<i>Modicogryllus truncatus</i> (Tarbinsky, 1940)	4		
<i>Modicogryllus frontalis</i> (Fieber, 1844)	4		
<i>Melanogryllus desertus</i> (Pallas, 1771)	5		
<i>Oecanthus pellucens</i> (Scopoli, 1763)	4	+	+
<i>Pteronemobius heydenii</i> (Fischer, 1853)	5	+	+
<i>Acheta domesticus</i> (Linnaeus, 1758)	2	+	
<i>Acrida ungarica</i> (Herbst, 1786)	3		
<i>Empusa fasciata</i> Brullé, 1832	3		xerothermic species
<i>Saga pedo</i> (Pallas, 1771)	5		
<i>Phaneroptera nana</i> Fieber, 1853	5	+	+
<i>Phaneroptera falcata</i> (Poda, 1761)	5	+	+
<i>Conocephalus fuscus</i> (Fabricius, 1793)	3		
<i>Metrioptera brachyptera</i> (Linnaeus, 1761)	3	+	+
<i>Eupholidoptera chabrieri schmidtii</i> (Fieber, 1861)	4	+	+
<i>Pachytrachis gracilis</i> (Brunner von Wattenwyl, 1861)	4	+	+
<i>Ruspolia nitidula</i> (Scopoli, 1786)	5	+	stenotopic species
<i>Tettigonia viridissima</i> (Linnaeus, 1758)	2	+	+

Table 1 continued

<i>Tettigonia caudata</i> (Charpentier, 1845)	4		+
<i>Decticus albifrons</i> (Fabricius, 1775)	5	+	+
<i>Decticus verrucivorus</i> (Linnaeus, 1758)	2		predicted northward expansion in future
<b>AVES</b>			
<i>Accipiter brevipes</i> (Severtzov, 1850)	4		predicted northward expansion in future
<i>Falco naumanni</i> Fleischer, 1818	4		not breed in Serbia: predicted northward expansion in future
<i>Tachymarptis melba</i> (Linnaeus, 1758)	5	+	+
<i>Apus pallidus</i> (Shelley, 1870)	4	+	+
<i>Motacilla citreola</i> Pallas, 1776	3		
<i>Hirundo daurica</i> Linnaeus, 1771	2		
<i>Melanocorypha calandra</i> (Linnaeus, 1766)	5		predicted northward expansion in future
<i>Calandrella brachydactyla</i> (Leisler, 1814)	2		
<i>Sitta neumayer</i> Michachellis, 1830	5		predicted northward expansion in future
<i>Lanius senator</i> Linnaeus, 1758	4		predicted northward expansion in future
<i>Lanius nubicus</i> Lichtenstein, 1823	5		predicted northward expansion in future
<i>Oenanthe melanoleuca</i> (Güldenstädt, 1775)	5		predicted northward expansion in future
<i>Monticola solitarius</i> (Linnaeus, 1758)	5		predicted northward expansion in future
<i>Monticola saxatilis</i> (Linnaeus, 1758)	3		predicted northward expansion in future
<i>Cisticola juncidis</i> (Rafinesque, 1810)	5		predicted northward expansion in future
<i>Cettia cetti</i> (Temminck, 1820)	4		predicted northward expansion in future
<i>Sylvia crassirostris</i> (Cretzschmar, 1825)	5		predicted northward expansion in future
<i>Sylvia cantillans</i> (Pallas, 1764)	5		predicted northward expansion in future
<i>Sylvia melanocephala</i> (Gmelin, 1789)	5		not breed in Serbia: predicted northward expansion in future
<i>Hippolais olivetorum</i> (Strickland, 1837)	5		not breed in Serbia: predicted northward expansion in future
<i>Iduna pallida</i> Hemprich & Ehrenberg, 1833	4		
<i>Phylloscopus orientalis</i> (C. L. Brehm, 1855)	4		predicted northward expansion in future
<i>Petronia petronia</i> (Linnaeus, 1766)	4		predicted northward expansion in future
<i>Passer hispaniolensis</i> (Temminck, 1820)	4	+	
<i>Emberiza melanocephala</i> (Scopoli, 1769)	4		

### Serbian Climate Change Index (S<sub>CCI</sub>)

The Serbian Climate Change Index (S<sub>CCI</sub>) for the local area is calculated as follows:

$$S_{CCI} = \frac{\sum_{i=1}^n (a_i \times W_i)}{\sum_{i=1}^n a_i} \quad (1)$$

where:

n - number of indicator species in local area (i = 1, 2, 3...n)

a<sub>i</sub> - relative abundance of i<sup>th</sup>-species

W<sub>i</sub> - indicator weight of i<sup>th</sup>-species.

The species' indicator weight (W) is assessed as follows:

1 - very low

2 - low

3 - moderate

4 - high

5 - very high.

The species' relative abundance in local area (a) is estimated using the five-ranked abundance scale:

1 - very rare

2 - rare

3 - common

4 - frequent

5 - very frequent.

A degree of impact by climate change in local area was assessed based on the data obtained for the S<sub>CCI</sub>:

0.00–1.25 - not significantly affected area

1.26–2.50 - lowly-affected area

2.51–3.75 - moderately-affected area

3.76–5.00 - affected area.

### Species “thermal expansion”

The impacts of climate change on biodiversity are more intensive from year to year. Some species (particularly cicadas and crickets) have ability to relatively rapid dispersion and migration expanding their distribution range. Such expansion is primarily caused by temperature as a main factor (“thermal expansion“). Detectability of these species is very high due to, in some species, even continuous stridulation, particularly during prolonged heat waves with tropical nights. Heat retention and thermal radiation of urban infrastructure additionally affect species stridulation. The population of these cicada and cricket species in recent years has considerably increased in suburban and urban areas in Serbia. Furthermore the species have gradually selected new habitat types (previously different; natural and less degraded) broadening their ecological tolerance as well as becoming hemisynanthropes and synanthropes - is this could be considered as a climate change adaptation?

Urban heat island (UHI) effect, the ubiquitous consequence of urbanization, is considered to play a major role in population expansion of numerous insects. Effects of temperature on cicada densities have been discerned from other environmental factors, as cicada densities increased measurably in tandem with elevated temperature [3].

## **CONCLUSION**

Recent climate changes affect, predominantly, cicada and cricket species populations in suburban and urban areas of Serbia intensifying synanthropy of the species as a consequence of temperature-driven range expansion. Also some birds are good indicators of recent climate change, but it is more likely they need more time to colonize still inhabitable habitats northwardly, and simultaneously, to change their native habitat preference: it could be the long-term process. Nowadays we are aware of many consequences leaving climate change and global warming on biodiversity. Does such caused “synanthropization” include changing of habitat preference of these species and adaptation to the new habitats in urban in suburban areas with anthropogenic impact? Indeed, new findings could indicate synanthropy of the species as well as a wide range of the species habitat selection. Previously, the most of the species inhabit only less degraded habitats. Expansion of the species range, new records with higher species abundance in suburban and urban areas in Serbia could reflect consequences of recent climate changes and global warming (“prolonged” heat waves with tropical nights). Thus these species extending their range northwards could be used as good indicators of climate changes. Furthermore, the existing populations of the species are increased in the covered area (Serbia) following predicted future climate change scenarios.

## **REFERENCES**

- [1] Unkašević M., Tošić I., *Int. J. Climat.* 33 (15) (2013) 3152–3161.
- [2] Ruml M., Gregorić E., Vujadinović M., *et al.*, *Atmos. Res.* 183 (2017) 26–41.
- [3] Nguyen H., Kim Y., Yikweon J., *PeerJ Prepr.* 5 (2017) e3064v1.



## ASSESSMENT OF NON-NATIVE SPECIES IMPACT ON FISH DIVERSITY IN THE ĆELIJE RESERVOIR: IMPLICATIONS FOR CONSERVATION AND MANAGEMENT

Ana Marić<sup>1\*</sup>, Vera Nikolić<sup>1</sup>, Dubravka Škraba Jurlina<sup>1</sup>, Vojislav Sokolović<sup>1</sup>,  
Dragana Miličić<sup>1</sup>, Tamara Karan Žnidaršić<sup>1</sup>, Tamara Kanjuh<sup>1</sup>, Predrag Simonović<sup>1</sup>

<sup>1</sup>University of Belgrade, Faculty of Biology, Studentski trg 16, 11000 Belgrade, SERBIA

\*[anatosic@bio.bg.ac.rs](mailto:anatosic@bio.bg.ac.rs)

### Abstract

*The Ćelije reservoir was built to prevent flooding and sedimentation in the Đerdap reservoir, but now serves as an important water source for the Rasina district. Due to sediment deposits, its length has been reduced by about 1 km and is now about 31 km at normal water levels. The Lake Ćelije ichthyofauna has been monitored for over a decade. For this study, the ichthyocoenosis was analyzed in 2011, 2016 and 2023. Sampling was carried out using electrofishing and fishing nets with different mesh sizes. In 2011, eleven fish species were recorded, including strictly protected tench, Tinca tinca, and protected species, chub Squalius cephalus, which were only detected in that year. In 2016, nine fish species were found, with Wels catfish, Silurus glanis missing in 2023. The non-native species the pumpkinseed, Lepomis gibbosus and the Gibel carp Carassius gibelio were evenly represented each year. Even with the highest number of fish species in 2011, the Shannon diversity index was lowest at 1.33, likely due to the high abundance of freshwater bream, Abramis brama. In 2016, the Shannon index increased to 1.68, and in 2023 it increased further to 1.76. The ABC curve was also calculated. In 2011 and 2023, biomass exceeded abundance, indicating a stable biocoenosis with low fishing pressure. In 2016, the curves overlapped, indicating higher fishing pressure. Only two non-native species, the Gibel carp and the pumpkinseed, were detected in this ichthyocoenosis. Another invasive species spiny cheek crayfish Faxonius limosus has been recently detected and reported to be abundantly present by locals. While non-native species do not outnumber native species in Ćelije reservoir, the decrease in species diversity since the first year of sampling underscores the growing importance of conservation and monitoring efforts.*

**Keywords:** diversity index, accumulation, non-native species, fish fauna, ABC curve.

### INTRODUCTION

The The Ćelije reservoir, located in Central Serbia was originally established between 1972 and 1983 by damming the Rasina River, as part of flood prevention measures and sediment retention for the largest reservoir in Serbia, Đerdap gorge. Its purpose has since been changed to become a primary drinking water source of the Rasina district and now it serves as a main regional water source, supplying drinking water and catering to approximately 200,000 residents in this part of Serbia. Officially designated as a drinking water source for both utility and economic needs, the reservoir is regulated by the Law on the Use and Protection of Water Supply Sources. Reservoir Ćelije spans 12 kilometres in length and 450 meters in width, with a maximum depth of approximately 45 meters (average around



14 m). Water levels peak in late spring and dip in late summer and early autumn. Covering an area of about 598 square kilometres, its summer visibility averages four meters. Water levels fluctuate based on rainfall and usage. In winter, indirect thermal stratification occurs, but ice formation is rare in milder winters. The original purpose of the Čelije accumulation was to meet specific hydraulic engineering needs, resulting in a dam crest height of 28 meters above the water intake section's bottom. However, a significant challenge in managing the Čelije accumulation ecosystem is the presence of stagnant water, leading to increased organic load and water quality issues during periods of water inversion. This includes the proliferation of cyanobacteria *Microcystis aeruginosa*, which elevates water treatment costs. Among other challenges, the Čelije hydro-accumulation is surrounded by numerous point sources of pollution from rural households along its shores, making it highly susceptible to intense eutrophication and rapid aging processes [1]. Priority measures for protecting and sustainably utilizing the fish stock include controlled fishing and biomanipulative procedures based on the BOTTOM UP principle [2] aimed at regulating fish population size and structure while minimizing impacts on water quality. Improper fish stocking introduced the silver carp *Hypophthalmichthys molitrix*, a non-native species originating from Asia. Ichthyofauna of reservoir Čelije has been monitored for more than 10 years. For this study, the ichthyofauna and the dynamics between native and non-native species were analysed and compared in 2011, 2016 and 2023. Additionally, the presence of the invasive spiny cheek crayfish *Faxonius limosus* was confirmed last year [3], but the locals have reported abundant sightings of this invasive species. This species could pose a threat to native fauna due to its rapid reproduction and potential transmission of crayfish plague.

## MATERIALS AND METHODS

Sampling of ichthyofauna on reservoir Čelije (Figure 1) was carried out during summer of 2011, 2016 and 2023 using electrofishing gear and fishing nets with different mesh sizes. Electrofishing was done using Loncin apparatus motor power of 2.2. kW, with output current 220 V, max power 8A DC and frequency 10–60 Hz. Starting point for electrofishing was always the same: 43°23'22.4"N 21°09'48.2"E, 275 m with the surface covered approximately 1000 m<sup>2</sup> each year. Nets length of 150 m mesh size 6 mm, 5 mm and 4 mm were left for more than five hours in water each time. Crayfish sampling was done using plastic baited traps that were left in water for three hours. Species were determined on site using a determination key when needed [4] and each specimen were measured for standard length and mass. Abiotic parameters, temperature, pH, oxygen saturation and conductivity were also measured each year. Data were analysed in Excel 23, several diversity indices were measured: Shannon [5], Simpson [6] and Ecologic index [7], as well as saprobity index using the Sládeček indicator list [8]. Abundance biomass comparison (ABC) curves were calculated using both biomass and number of individuals per species [9]. Total biomass and number of non-native species were compared for each year, as well as biomass and number for native species. Repeated Measures ANOVA was used to assess the statistical significance of differences in both the percent number and biomass between non-native and native species across each year. For each species recorded, the protection status was checked in accordance with national and European legislation and recommendations.

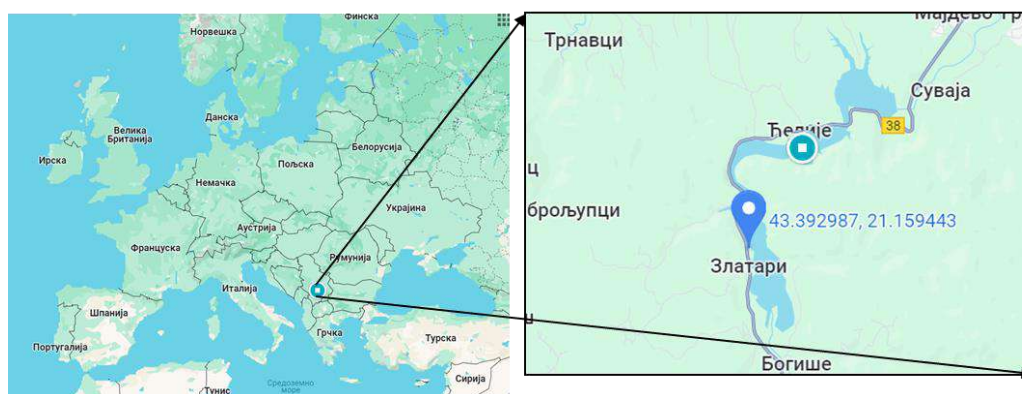


Figure 1 Position of reservoir Ćelije in central part of Serbia

## RESULTS AND DISCUSSION

During the monitoring of ichthyofauna of reservoir Ćelije, a maximum of eleven fish species were recorded in 2011 (Table 1).

Table 1 List of identified species, number of caught individuals ( $N$ ), percentage of number ( $N\%$ ), body weight in g ( $W$ ) and percentage of body weight ( $W\%$ ) in 2011, 2016 and 2023

Family	Species	2011				2016				2023			
		$N$	$\%N$	$W$ (g)	$\%W$	$N$	$\%N$	$W$ (g)	$\%W$	$N$	$\%N$	$W$ (g)	$\%W$
Cyprinidae	<i>Alburnus alburnus</i>	51	6,75	126	0,12	19	12,75	281	0,93	24	7,67	131	0,21
	<i>Carassius gibelio</i>	50	6,62	6764	6,26	1	0,67	519	1,71	11	2602	3,51	4,14
	<i>Cyprinus carpio</i>	1	0,13	3000	278	1	0,67	11000	36,24	13	9693	4,15	15,43
Leuciscidae	<i>Squalius cephalus</i>	3	0,40	60	0,06	0	0	0	0	0	0	0	0
	<i>Abramis brama</i>	465	61,58	73675	68,21	29	19,46	5062	16,68	21	6,71	2661	4,23
	<i>Rutilus rutilus</i>	62	8,21	1530	1,42	61	40,94	1770	5,83	95	30,35	1231	1,96
Tincidae	<i>Tinca tinca</i>	1	0,13	12	0,01	0	0	0	0	0	0	0	0
Percidae	<i>Sander lucioperca</i>	93	12,32	15374	14,23	13	8,72	7282	24	97	31	39889	63,49
	<i>Perca fluviatilis</i>	16	2,12	102	0,09	15	10,07	1289	4,25	33	6293	10,54	10,02
Siluridae	<i>Silurus glanis</i>	6	0,79	7238	6,70	3	2,01	3016	9,94	0	0	0	0
Centrarchidae	<i>Lepomis gibbosus</i>	7	0,93	127	0,12	7	4,70	129,5	0,43	19	6,07	330	0,53
Total		755	100	108008	100	149	100	30349	100	313	100	62830	100

On the basis of national legislation [10], one strictly protected species, tench (*Tinca tinca*) was detected but only in 2011. Six protected species: chub *Squalius cephalus*, pikeperch *Sander lucioperca*, Eurasian perch *Perca fluviatilis*, freshwater bream *Abramis brama*, Wels catfish *Silurus glanis* and common carp *Cyprinus carpio* were also detected of which chub was detected solely in 2011. Wels catfish is also listed as a protected species by Bern convention [11]. Beside those, two native species that are not under protection were sampled: bleak *Alburnus alburnus* and roach *Rutilus rutilus*. Non-native fish species that were detected through sampling were Gibel carp *Carassius gibelio* and pumpkinseed *Lepomis gibbosus*, both present every sampling year. No individuals of silver carp were caught during the investigation. In 2016, nine fish species were found, with *Silurus glanis* missing in 2023.

The abundance and biomass of non-native species *Lepomis gibbosus* and *Carassius gibelio* were evenly represented each year (Figure 2). The results of the Repeated Measures ANOVA indicated no statistically significant difference ( $P > 0.05$ ) between non-native fish abundance

and mass over the years. Another non-native species, spiny cheek crayfish, was caught in high abundance. While there are unofficial reports of its presence dating back about ten years, it was never in such large quantities, with 65 individuals caught in an area of 5 m<sup>2</sup>.

Even with the highest number of fish species in 2011, the Shannon diversity index was lowest at 1,33, likely due to the high abundance of *Abramis brama*. In 2016, the Shannon index increased to 1,68, and in 2023 it increased further to 1,76. Similar results were with the Simpson index: the lowest value 0,59 was detected in 2011, in 2016 it was 0,76 and in 2023 0,78. Ecological index ranged from 3,56–3,61 describing this biocoenosis as potamon. Saprobity index ranged from 1,95 to 1,98 classifying this water body within II class of water and  $\beta$ -mesosaprobic water quality.

In 2011 and 2023, biomass exceeded abundance, indicating a stable biocoenosis with low fishing pressure. In 2016, the curves overlapped, indicating higher fishing pressure.

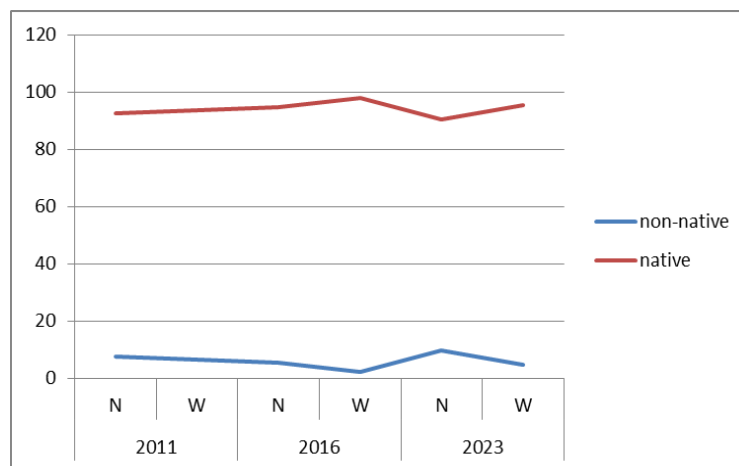


**Figure 2** Percentage distribution of biomass and abundance of native and non-native species for the years 2011, 2016, and 2023. The X axis represents abundance (N) and biomass (W) over the years and Y axis represents percentages

The temperature was highest in 2023 measuring 27.8°C while the pH was lowest 8.08 and conductivity 224  $\mu$ S/cm. In 2016 temperature was 25.3°C, conductivity 300  $\mu$ S/cm and pH 8.57. In 2011 the temperature was lowest at 21.4°C, conductivity 287  $\mu$ S/cm and pH 8.9.

Although diversity indices show an increase in diversity in 2016 and even more in 2023 year and a share of invasive species number and biomass is running low over the years, the qualitative composition of ichthyocoenosis is important as well. The presence of silver carp was not detected during these surveys but its presence is confirmed by local fishermen and management. Absence in tench and chub from samples in 2016 and 2023 indicates their lower abundance.

The introduction of silver carp and Gibel carp into new ecosystems has been cited as a significant factor contributing to the decline in populations of tench [12]. This decline is primarily attributed to intensified competition for food resources [13]. Moreover, empirical evidence underscores the considerable impact of Gibel carp, especially in their juvenile stage, on both the survival and growth rates of Crucian carp (*Carassius carassius*) and tench

populations [14]. Beyond their effects on Crucian carp and tench, Gibel carp have also been observed to influence the abundance of common carp [15]. This influence extends to competition for reproductive resources and food, further exacerbating the ecological pressure on native species.

Furthermore, the presence of pumpkinseed introduces yet another formidable competitor into the ecosystem. Feeding on bottom fauna and young fish alike, pumpkinseed competes vigorously for habitat and spawning sites. This multifaceted competition poses a significant threat to native species [16]. Recent findings [17] identify Gibel carp as one with the highest invasive score (39) indicating its high invasive potential.

Another competitor, the spiny cheek crayfish, presents a dual concern for native fauna. Its competitive edge lies in its robust ability to outcompete native species, coupled with the potential threat it poses due to its rapid reproduction and the risk of transmitting crayfish plague [1]. The species' introduction to the reservoir Čelije is likely attributed to human activities, particularly during the stocking of the reservoir with fish from ponds in the River Danube basin. With few natural predators or competitors to curb its proliferation, spiny cheek crayfish is believed to have already established itself within the River Danube basin in Serbia [4]. This establishment comes at the cost of adverse effects on native species and the restructuring of aquatic ecosystems, impacting both the biological and environmental dynamics of lowland aquatic ecosystems.

## **CONCLUSION**

While non-native species do not outnumber native species overall in Čelije reservoir and their biomass remains stable over the years, the decrease in species richness (number of species) since the first year of sampling underscores the growing importance of conservation and monitoring efforts. It is important to emphasize that non-native species present in reservoir Čelije are the ones of the highest invasive potential, and their stable population in 2011 outnumbers tench and chub that were long ago dominant species in this reservoir. In 2016 and 2023 those strictly protected and protected species were not even sampled in this lake. This indicates that presence of Gibel carp and pumpkinseed has certainly affects the ichthyofauna of Lake Čelije, and knowing that these species are significant competitors for food with tench and related species, they impact them in various other ways as well.

Consequently, the cumulative impact of these interactions underscores the complex ecological dynamics at play and emphasizes the urgent need for comprehensive management strategies to mitigate the adverse effects on native biodiversity.

## **ACKNOWLEDGEMENT**

*The authors are grateful to the Ministry of Science, Technological development and Innovation of the Republic of Serbia for financial support according to the contract with the registration number (451-03-65/2024-03/ 200178). We would like to thank executive director and members of Rasina Plus Company for their invaluable assistance in the field and with logistics.*

## REFERENCES

- [1] Simonović P., Nikolić V., Tošić A., *et al.*, Program upravljanja ribarskim područjem Rasina za period 2023–2032. godinu. Univerzitet u Beogradu, Biološki fakultet (2023).
- [2] Chase J., *Trends Ecol. Evol.* 15(10) (2000) 408–412.
- [3] Nikolić V., Roljić R., Nedić Z., *et al.*, Joint ESENIAS and DIAS Scientific Conference and 12th ESENIAS Workshop 11–14 October 2023, Varna, Bulgaria (2023) 114.
- [4] Simonović P. Ribe Srbije Biološki fakultet, Univerzitet u Beogradu, Beograd (2006), p.247, ISBN: 86-83635-60-0.
- [5] Shannon C., Weaver W., *The Mathematical Theory of Communication*, University of Illinois Press, Chicago & Urbana (1949), p.125, ISBN: 0252725484.
- [6] Simpson E., *Nature* 163(4148) (1949) 688–688.
- [7] Šorić V.M., *Ichthyologia* 30 (1998) 51–70.
- [8] Sládeček V., *Arch. Hydrobiol.* 58(1) (1961) 103–121.
- [9] Clarke K, Warwick R., *Change in marine communities: an approach to statistical analysis and interpretation*, Natural Environment Research Council UK, Plymouth (1994), p.114, ISBN: 9781855311404.
- [10] „Službeni glasnik” RS 5/2010, 47/2011, 32/2016 i 98/2016 Pravilnik o proglašenju i zaštiti strogo zaštićenih i zaštićenih divljih vrsta biljaka, životinja i gljiva.
- [11] Bern Convention (Appendix/Annexe III). *Convention on the Conservation of European Wildlife and Natural Habitats* (1979) ETS/STE 104.
- [12] Lenhardt M., Hegedis A., Cvijanović G. *et al.*, Non-native freshwater fishes in Serbia and their impacts to native fish species and ecosystems *Geoph. Res Abstracts, European Geosciences Union* 8, (2006) 07727.
- [13] Ćirković M., Marković G., Simić V., *et al.*, IV International conference fishery 27–29 May 2009, Belgrade, Serbia (2009) 132–137.
- [14] Demeny F., Sipos S., Ittzes I., *et al.*, IV International conference fishery Belgrade Serbia (2009) 138–144.
- [15] Maletin S., Djukic N., Miljanović B., Ivanc B. *Ekologija* 32 (1997) 87–98.
- [16] Marković G., Simović S. *The proceedings of symposium Ribarstvo Jugoslavije*, 21–25 September, Cetinje, SR Jugoslavija (1997) 123–128.
- [17] Radočaj T., Špelić I., Vilizzi L., *et al.*, *Glob. Ecol. Conserv.* (2021) 27.





## THE IMPACTS OF WASTE MATERIALS UTILIZATION IN LIQUID RADIOACTIVE WASTE SOLIDIFICATION BY MORTAR MATRIX

Ivana Jelić<sup>1\*</sup>, Aleksandar Savić<sup>2</sup>, Tatjana Miljojčić<sup>1</sup>, Maja Rajković<sup>1</sup>, Marija Janković<sup>1</sup>,  
Nataša Sarap<sup>1</sup>, Slavko Dimović<sup>1</sup>, Milica Ćurčić<sup>1</sup>, Vojislav Stanić<sup>1</sup>, Dragi Antonijević<sup>3</sup>,  
Marija Šljivić-Ivanović<sup>1</sup>

<sup>1</sup>University of Belgrade, Vinca Institute of Nuclear Sciences, M.P.A. 12–14, 11351 Belgrade,  
SERBIA

<sup>2</sup>University of Belgrade, Faculty of Civil Engineering, B.K.A. 73, 11000 Belgrade, SERBIA

<sup>3</sup>University of Belgrade, Innovation Center of Faculty of Mechanical Engineering, K.M. 16,  
11000 Belgrade, SERBIA

\*ivana.jelic@vin.bg.ac.rs

### Abstract

*The nuclear industry generates significant radioactive waste (RW) amounts, with its safe disposal being a primary safety and environmental issue. RW management involves solidification and disposal, often in deep underground facilities. Cement mortar is commonly used for liquid RW solidification due to its cost-effectiveness and simplicity. However, Portland cement concrete production raises environmental concerns, such as CO<sub>2</sub> emissions and natural resource depletion. Additionally, RW storage and disposal costs drive research into low-cost matrices, especially those made from final waste products. The main requirements for matrix materials for liquid RW immobilization, which accept the role of primary barrier, are compatibility with RW material, good mechanical properties, and resistance to chemical and biological agents. However, partially substituting cement with waste materials can reduce strength and durability, increase susceptibility to cracking, porosity, and corrosion, further leading to harmful substance release. The matrix material must demonstrate long-term stability under various environmental conditions, including changes in temperature, humidity, and exposure to radiation ensuring that RW remains stable and safe within the matrix for decades or centuries. In addition, factors such as groundwater infiltration and seismic activity should also be considered when evaluating the long-term effectiveness of a protective structure. To manage these hazards, the selection, treatment, and preparation of recycled waste are crucial, alongside with proper design and utilization of such concrete. Monitoring concrete performance over time and implementing maintenance measures are necessary to ensure the long-term durability and reliability of structures. This work aims to assess the overall impact of recycled materials utilized in liquid RW solidification matrix.*

**Keywords:** nuclear industry, radionuclide, disposal, recycling.

### INTRODUCTION

Nuclear energy is recognized as a significant aspect of the new energy landscape and the factor of energy stability, particularly amidst the current global energy crisis. Moreover, it is regarded as a substitute for fossil fuels, offering a potential solution to mitigate their adverse environmental effects. This is crucial for reducing greenhouse gas emissions, which would



help slow down global warming and climate change. However, the activity of the nuclear industry generates significant amounts of liquid and solid radioactive waste (RW) and the primary safety and environmental concerns related to nuclear power are its safe disposal. RW is created in the processes of the nuclear fuel cycle, the industry of exploitation, processing, and enrichment of uranium ore, the activities of the reactors of nuclear power plants and research centers, the use of radionuclides in research institutes, hospitals, and industry [1,2].

RW has to be processed to make it safe for storage, transportation, and final disposal. This process involves waste conditioning to immobilize it before storage and disposal. Immobilization of waste radionuclides in durable waste forms provides the most significant barrier to contribute to the overall performance of any storage and disposal system. RW immobilization is the conversion of waste into a waste form by solidification, embedding, or encapsulation that reduces the potential for migration or dispersion of radionuclides during the operational and disposal stages of the waste lifecycle. RW can be immobilized by chemical incorporation into the structure of a suitable matrix like cement, glass, or ceramic, which captures it and prevents it from escaping. The distinction between chemical and physical immobilization mechanisms is not always clearly defined. Chemical immobilization occurs at atomic distances, while physical immobilization occurs at larger distances, e.g. at the microscope level. High-level waste (HLW) is usually chemically immobilized, while physical immobilization (encapsulation) involves surrounding the waste with material, like bitumen or cement, to isolate the RW and retain the radionuclides.

Materials used to immobilize RW are essential for multibarrier systems that isolate waste from the environment, ensuring safe disposal in the long term. The volume of liquid RW is much larger than solid, and its processing increases the storage capacity and ensures the safe release of decontaminated liquid into the environment. Compared with the HLW liquid, the amount of the intermediate-level waste (ILW) and low-level waste (LLW) liquids is much larger, accounting for more than 90% of the total RW.

Very high costs of immobilization, temporary storage and final disposal of liquid RW stimulate research into the development of cost-effective, low-cost matrices, especially those that represent final waste during production or after their useful life. In particular, it is necessary to pay attention to the European legislation that encourages the development of the “circular economy”, which implies the efficient use of materials [3]. The aim of this study is to assess the impact of recycled materials used in liquid RW solidification matrix.

## **ASPECTS OF CEMENT USAGE IN RW SOLIDIFICATION**

Cement is the oldest and most extensively researched base material for solidifying and stabilizing various types of solid waste. Cement solidification is a well-established technology that relies on the hydration of cement and its gelatinizing effect to immobilize radioactive elements. This method is widely used for treating LLW and ILW liquids due to its cost-effectiveness and the simplicity of the process [2,4].

Cement is a porous material, with a wide range of pore sizes that are filled with liquid under normal conditions. Incomplete filling of the space between the clinker grains in the reaction of formation of hydration products creates mesopores, usually in the size range of

0.05–1  $\mu\text{m}$  [5]. Entrapped air or gas contributes to the creation of macropores larger than 1  $\mu\text{m}$ , filling 1–10 cubic meters. % hydrated cement. During solidification, the volume of the cement-waste mixture decreases and shrinks. As a result of shrinkage, based on gel drying or crystallization, gel pores are formed, with diameters in the range of 10 nm–0.0005 mm. Their volume fraction decreases with the time of hydration and reaches 20–30% of the hardened cement paste fraction. Gel pores are not significant from the point of view of leaching and corrosion. Capillary pores are also formed by evaporation of excess free water. Capillary pores reach a diameter of 1–10 nm. They increase with the water content in the mixture and with advancing hydration. If there are large particles in the cement paste, e.g. grains of sand or gravel, and due to the formation of zones of poor packing on the boundary surface of paste particles, the total mesoporosity increases. The total porosity of the cement paste is in the range of 16–24% [5]. As the curing time of the cement increases, the porosity decreases steadily in the first 6–12 months.

In the past few decades, the production of concrete has raised significant environmental concerns not only related to  $\text{CO}_2$  emissions but also regarding the depletion of natural resources. It is known that concrete consumes large amounts of natural resources, specifically gravel and sand. Environmental issues, in particular climate change caused by carbon dioxide emissions, have aroused huge attention across the world. The biggest contributor to the carbon footprint of the construction industry is the production of Portland cement [6]. Currently, approximately 4 to 6 GJ of energy are used per ton of cement clinker produced, with energy costs accounting for up to 40% of the total production cost. One ton of cement clinker production typically results in the release of around 0.8 tons of  $\text{CO}_2$  into the atmosphere and contributes to approximately 7% of total  $\text{CO}_2$  emissions, exacerbating the greenhouse effect and consuming around 5% of global industrial energy [6,7]. This inefficiency is a major environmental concern due to its contribution to global warming and climate change. Also, the energy-intensive manufacture of cement emits not only carbon dioxide but also other hazardous gases such as  $\text{NO}_x$  and  $\text{SO}_2$ .

## **PARTIAL SUBSTITUTION OF CEMENT WITH WASTE MATERIALS**

Each treatment of RW creates a specific concentrate. Depending on the treatment process, the concentrate will be solid (spent ion-exchange resins, filter cartridges, filter cakes, sludge, etc.) or liquid (evaporator concentrates, membrane process concentrates). To immobilize RW of low and medium activity levels, solidification of the concentrate is carried out by binding it into inactive matrices: cement, bitumen, polymer materials, and rarer glass. The processes available for treating liquid RW effluents can be divided into three main categories: ion exchange, chemical precipitation, and evaporation (evaporation) [8,9].

The primary requirements for matrix materials for liquid RW immobilization, which serve as the primary barrier, include the following [10]:

- **Compatibility with RW:** Matrix materials must be compatible with the RW itself. Ensures that the matrix material chemically and physically bonds well with the liquid RW, preventing separation or degradation over time. This means that they must not react with the radioactive material in a way that could compromise the stability or integrity of the container or structure that holds the waste.

- **Mechanical properties:** These materials should have good mechanical properties in order to withstand physical stresses and loads during the handling, transport, and long-term storage of RW. These include factors such as strength, flexibility, elasticity, resistance to cracking or breaking, and toughness.
- **Durability:** Ensures long-term stability under various environmental conditions such as temperature fluctuations, humidity, and radiation exposure.
- **Resistance to chemical and biological agents:** The material must resist degradation caused by chemical reactions with the waste or exposure to environmental conditions, including resistance to acids, alkalis, and microbial activity. Resistance to corrosion and degradation is critical to ensure the long-term stability and safety of RW containment systems.
- **Permeability:** The matrix should be impermeable to water and gases to prevent the leaching or release of radionuclides into the environment.
- **Processing Feasibility:** The material should be easy to process, handle, and apply using existing technologies and equipment.
- **Cost-effectiveness:** The use of the matrix material should be economically viable, considering the costs of production, application, and long-term maintenance.

The matrix material must demonstrate long-term stability under various environmental conditions, including changes in day temperatures, air humidity, and radiation exposure. This ensures that RW remains stable and safe within the matrix for decades or even centuries. Moreover, factors such as groundwater infiltration and seismic activity must be considered when evaluating the long-term effectiveness of a protective structure.

## **PARTIAL REPLACEMENT OF CEMENT WITH WASTE: IMPLICATIONS AND BENEFITS**

Partial replacement of cement with waste materials can reduce the strength and durability of concrete structures [11]. Utilizing scrap raw materials may lead to uneven material distribution, making it challenging to achieve consistent performance. This inconsistency can increase susceptibility to cracking, porosity, and corrosion. In homogeneous concrete, uneven distribution of waste particles can cause localized weakening or heightened corrosion susceptibility. Variations in the quality and characteristics of recycled materials can result in performance inconsistencies, complicating efforts to achieve predictable and reliable concrete structures.

Waste materials can affect the porosity of the concrete matrix, leading to increased absorption of water and chemical agents. Increased porosity reduces concrete's resistance to frost and aggressive chemicals, accelerating deterioration. This can allow the penetration of water, chemicals, and other harmful substances, further weakening the structure and potentially leading to the release of radionuclides.

Despite these challenges, it can be concluded that using recycled materials in the solidification of liquid RW offers significant environmental and economic benefits as follows:

### **Environmental Benefits**

- **Reduced Resource Depletion – Preservation of two types of natural raw materials:** Using recycled materials decreases the demand for virgin raw materials.

- **Energy Savings:** Reducing energy consumption associated with processing raw materials can lower greenhouse gas emissions.
- **Waste Reduction – Treatment of two types of waste:** Recycling helps to minimize waste going to landfills, reducing environmental pollution.
- **Lower Pollution Risks:** Properly managed recycling can reduce the risk of soil, air, and water pollution from waste materials.
- **Climate change and Global Warming Reduction.**

#### **Economic Benefits**

- **Cost Savings:** Using recycled materials can lower production costs by reducing the need for expensive raw materials.
- **Revenue Generation:** The recycling industry can generate revenue through the sale of recycled products.
- **Job Creation:** Establishing new markets for recycled materials can create jobs and stimulate economic growth at local and national levels.
- **Regulatory Compliance:** Companies can meet environmental regulations and standards more easily by incorporating sustainable practices.

Overall, the use of recycled materials in the solidification of liquid RW offers a balanced approach, providing environmental benefits by reducing resource consumption and waste generation, and economic benefits by lowering costs and creating new economic opportunities.

## **CONCLUSION**

Nuclear energy can substitute fossil fuels almost completely and significantly reduce greenhouse gas emissions, which is key to mitigating global warming and climate change. However, the nuclear industry generates large quantities of RW, and the safe disposal of this waste is a primary environmental and safety concern. Processing of RW is necessary for safe storage, transport, and final disposal. Immobilization of RW by converting waste into solid form via cement, glass, or ceramics provides a key barrier to waste storage and disposal. Immobilization materials must be compatible with RW, have good mechanical properties, and be resistant to chemical and biological agents.

The use of recycled materials in the solidification of liquid RW brings environmental and economic advantages. Environmental benefits include reduced resource depletion, energy savings, waste reduction, and lower risk of soil, air, and water pollution. Economic benefits comprise cost reduction, revenue generation, and the creation of new jobs and markets for recycled materials.

Despite challenges such as the reduction of strength and durability of concrete structures when partially replacing cement with waste materials, the benefits of recycled materials in the solidification of liquid RW are significant. They enable a more sustainable approach to RW management, reduce the environmental footprint, and contribute to sustainable economic development. This approach represents a balanced path to reducing resource consumption and waste generation, while at the same time bringing economic benefits through cost reduction and the creation of new economic opportunities.

## **ACKNOWLEDGEMENT**

*The research presented in this paper was completed with the financial support of the Ministry of Science, Technological Development and Innovation of the Republic of Serbia, with the funding of scientific research work at the University of Belgrade, Vinča Institute of Nuclear Sciences (Contract No. 451-03-66/2024-03/200017), the University of Belgrade, Faculty of Civil Engineering (Contract No. 200092), and the University of Belgrade, Innovation Centre of Faculty of Mechanical Engineering (Contract No. 451-03-66/2024-03/200213).*

## **REFERENCES**

- [1] IAEA, Treatment of Low and Intermediate-Level Liquid Radioactive Wastes, Technical Reports Series No.236, Vienna (1984), p.146, ISBN: N92-0-125184-X.
- [2] IAEA, The Principles of radioactive waste management: A Safety Fundamental, IAEA-Safety Series No. 111-F, Vienna (1995), p.24, ISBN: 92-0-110706-4.
- [3] Köster R., Kraemer R., Proceedings of an International Symposium of Management of Low and Intermediate Level Radioactive Wastes, Vienna, Austria (1995).
- [4] IAEA, Radioactive Waste Management Glossary, IAEA-TECDOC-264, Vienna (1989), p.44.
- [5] Glasser F.P., J. Hazard. Mater. 52 (1997) 151–170.
- [6] Jelić I., Savić A., Miljojčić T., *et al.*, Sci. of Sinter. 2024 OnLine-First (2024) 1–29.
- [7] Jiaying B., Jian-Xin L., Ligang P., *et al.*, Cem. Concr. Compos. 139 (2023) 105037.
- [8] IAEA, Advanced in Technologies for the Treatment of Low and Intermediate Level Radioactive Liquid Wastes, Technical Reports Series No. 370, Vienna (1994), p.103, ISBN: 92-0-104194-2.
- [9] IAEA, Combined methods for liquid radioactive waste treatment, IAEA-TECDOC-1336, Vienna (2003), p.250, ISBN: 92–0–100903–8.
- [10] IAEA, Improved Cement Solidification of Low and Intermediate Level Radioactive Wastes, Technical Reports Series No. 350, Vienna (1993), p.124, ISBN: 92-0-100493-1.
- [11] Bawab J., Khatib J., El-Hassan H., *et al.*, Sustainability 13 (2021) 11529.



## INSIGHTS FROM THE DAILY MONITORING OF WATER QUALITY PARAMETERS IN CEROVO RIVER NEAR BOR CITY IN OCTOBER 2023

Stefan Đordjević<sup>1\*</sup>, Miloš Đukić<sup>1</sup>, Ana Petrović<sup>1</sup>, Dragana Adamović<sup>1</sup>, Jelena Petrović<sup>1</sup>,  
Ljiljana Lekić<sup>2</sup>

<sup>1</sup>Mining and Metallurgy Institute Bor, Alberta Ajnštajna 1, 19210 Bor, SERBIA

<sup>2</sup>Bor City, Moše Pijade 3, 19210 Bor, SERBIA

\*stefan.djordjevski@irmbor.co.rs

### Abstract

*The aims of this paper are: 1) to assess the ecological status of Cerovo River after the Cerovo open pit based on limit values, and 2) to investigate daily variations in pH, conductivity, and concentrations of  $SO_4^{2-}$ , Fe, Cu, and Cd depending on the amount of rainfall. The water of Cerovo River had poor ecological status during the entire monitoring period from October 9 to November 5, 2023, due to very high average concentrations of  $SO_4^{2-}$  (1456 mg/L), Cu (25328 µg/L), and Cd (43 µg/L). The increase in the amount of rainfall during the sampling period caused the change of pH value from acidic to neutral, and the decrease in conductivity and concentrations of  $SO_4^{2-}$ , Fe, Cu, and Cd.*

**Keywords:** Cerovo River, acid mine drainage, monitoring.

### INTRODUCTION

Cerovo mine is a relatively small copper mine near the Bor City in Eastern Serbia. In October 2023, Cerovo mine consisted of two open pits, one of which was no longer in operation, and the other was recently opened. These two open pits and overburden deposits were located on the right side of the Cerovo River, which is also called Valja Lutarica River in its upper reach (Figure 1a). Acid mine drainage (AMD) from the Cerovo mine and overburden was flowing into the Cerovo River, causing its pollution (Figure 1b).

The water quality of Cerovo River was not studied as much as the water quality of the other rivers around copper mines near the Bor City, such as Bor River, Krivelj River, and Bela River [1–5]. The possible reasons for the underrepresentation of Cerovo River in the literature are its relatively small discharge (the watershed area and length of Cerovo River are 16 km<sup>2</sup> and 6 km, respectively) and remote location (Cerovo River is located in the mountains, far away from the main roads and inhabited areas). Nevertheless, the monitoring of Cerovo River is significant because it contributes to the contamination of the Krivelj River.

In this paper, the results of 28-day monitoring of pH, electrical conductivity, sulfate ( $SO_4^{2-}$ ), iron (Fe), copper (Cu), and cadmium (Cd) concentrations in Cerovo River after the Cerovo open pit are presented [6]. The monitoring period from October 9 to November 5, 2023, was chosen because it represents the transition from the dry summer season to the rainy autumn season. According to this, the aims of this paper are 1) to assess the ecological status of Cerovo River based on limit values from the Regulation [7], and 1) to investigate daily variations in water quality parameter values depending on the amount of rainfall.



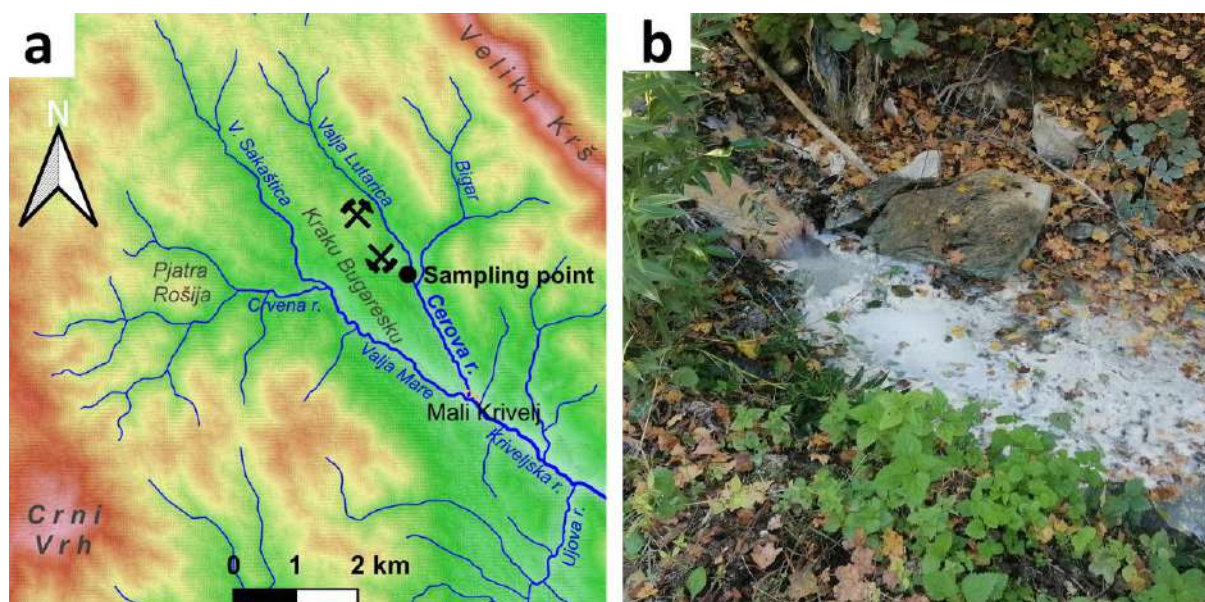


**Figure 1** a) Location of the sampling point; b) Photo of the sampling point taken on 11/10/2023

## MATERIALS AND METHODS

The location of sampling point on Cerovo River is downstream from the Cerovo mine, before the junction with the left unpolluted tributary with relatively higher discharge. The coordinates of the sampling point are 44.164599 N, 22.036550 E. Samples were collected in plastic bottles by using the telescope sampler. Measurements of pH and electrical conductivity were carried out in the field by using Thermo Scientific PC450 Meter.

The concentration of sulfate was determined by developing turbidity with barium chloride and measurement of turbidity using a turbidimeter model WTW Turb 550 IR.

For the determination of Fe, Cu, and Cd, the samples were filtered through the white spot filter paper in order to remove particulate matter, diluted 2 times, and acidified with concentrated  $\text{HNO}_3$  (Zorka Šabac, Serbia). The determination of Fe, Cu, and Cd was performed using an inductively coupled plasma mass spectrometer (ICP-MS), model NexION 1000 (PerkinElmer, USA). Syngistix software was used to collect and analyze the data. Multi-element standard solution containing Cd, Cu, and Fe (AccuStandard, USA) was used for calibration. Individual standard solutions of Re (Acros Organics, Belgium) and Rh (AccuStandard, USA) were used as internal standards. Quality control of the ICP-MS measurements was carried out by analyzing the Standard Reference Material WP Trace Metals VHGLABS-VHG-QWPTM-15 (VHGLABS, USA), and the obtained recoveries for Fe, Cu, and Cd were 92.9%, 102.5%, and 106.0%, respectively. Limits of quantitation for Fe, Cu, and Cd, obtained by analyzing sample blanks, were 3.7  $\mu\text{g/L}$ , 3.3  $\mu\text{g/L}$ , and 0.14  $\mu\text{g/L}$ , respectively.

The amount of rainfall during the sampling period was obtained from the Republic Hydrometeorological Service of Serbia. The meteorological station “Crni Vrh”, from which the data was collected, is located at the top of the Crni Vrh mountain (1043 m above the sea level), which is about 7 km far from the sampling point on Cerovo River (Figure 1a). The proximity of this meteorological station to the sampling point allowed the correlation of the amount of rainfall with the change in concentrations of contaminants.

## RESULTS AND DISCUSSION

The assessment of the ecological status of Cerovo River was carried out by comparing measured values of water quality parameters with the limit values from the Regulation on limit values of pollutants in surface water and groundwater and sediment and deadlines for their achievement (“Official Gazette of RS”, No. 50/2012) [7]. Five classes of surface water from the Regulation correspond to ecological status described as excellent for class I, good for class II, moderate for class III, weak for class IV, and poor for class V. Also, the measured values are compared with the limit values CP1 and CP2 obtained by the statistical analysis of 198 water samples in Eastern Serbia, using cumulative probability (CP) diagrams [5]. CP1 represents the limit value between background concentrations and moderately elevated concentrations, and CP2 represents the limit value between moderately and highly elevated concentrations. Limit values from the Regulation and CP diagrams are presented in Table 1.

*Table 1* Limit values from the Regulation [1] and cumulative probability (CP) diagram [2]

Parameter	Unit	I [1]	II [1]	III [1]	IV [1]	V [1]	CP1 [2]	CP2 [2]
pH	-	6.5–8.5	6.5–8.5	6.5–8.5	6.5–8.5	<6.5 or >8.5	-	-
EC	μS/cm	<1000	1000	1500	3000	>3000	-	-
SO <sub>4</sub> <sup>2-</sup>	mg/L	50	100	200	300	>300	200	-
Fe	μg/L	200	500	1000	2000	>2000	500	-
Cu	μg/L	112	112	500	1000	>1000	15	1000
Cd	μg/L	0.45	0.6	0.9	1.5	>1.5	0.1	3

Diagrams showing the change in pH value, conductivity, and concentrations of SO<sub>4</sub><sup>2-</sup>, Fe, Cu, and Cd during the sampling period are presented in Figure 2. Bars on the diagrams are colored in blue for class I, green for class II, yellow for class III, orange for class IV, and red for class V. Horizontal lines represent the limit values between the classes of surface water. Table 2 shows statistical values such as minimum (min.), maximum (max.), average (aver.), and median (med.) of measured parameters in Cerovo River, as well as the number of days in which the water of Cerovo River belonged to a certain class of surface water.

The water of the Cerovo River after the Cerovo open pit belonged to class V during the entire monitoring period of 28 days (from October 9, 2023, to November 5, 2023) because the measured concentrations of SO<sub>4</sub><sup>2-</sup>, Cu and Cd exceeded the limit concentrations from the Regulation, which corresponded to a poor ecological status. The average concentrations for sulfates, copper, and cadmium were 1456 mg/L SO<sub>4</sub><sup>2-</sup>, 25328 μg/L Cu, and 43 μg/L Cd, which exceeded the limit concentrations for class V about 5, 25 and 29 times, respectively. Also, the measured pH value in 24 out of 28 days and iron (Fe) concentration in 18 out of 28 days belonged to the class V of surface waters, which corresponded to poor ecological status.

Measured concentrations of Cu and Cd exceeded the statistical limit concentration CP2 during the entire sampling period. Average concentrations of Cu and Cd exceeded the statistical limit concentration CP2 about 25 and 14 times, respectively. This means that the concentrations of Cu and Cd in Cerovo River were very high compared to the background concentrations of these elements in Eastern Serbia.

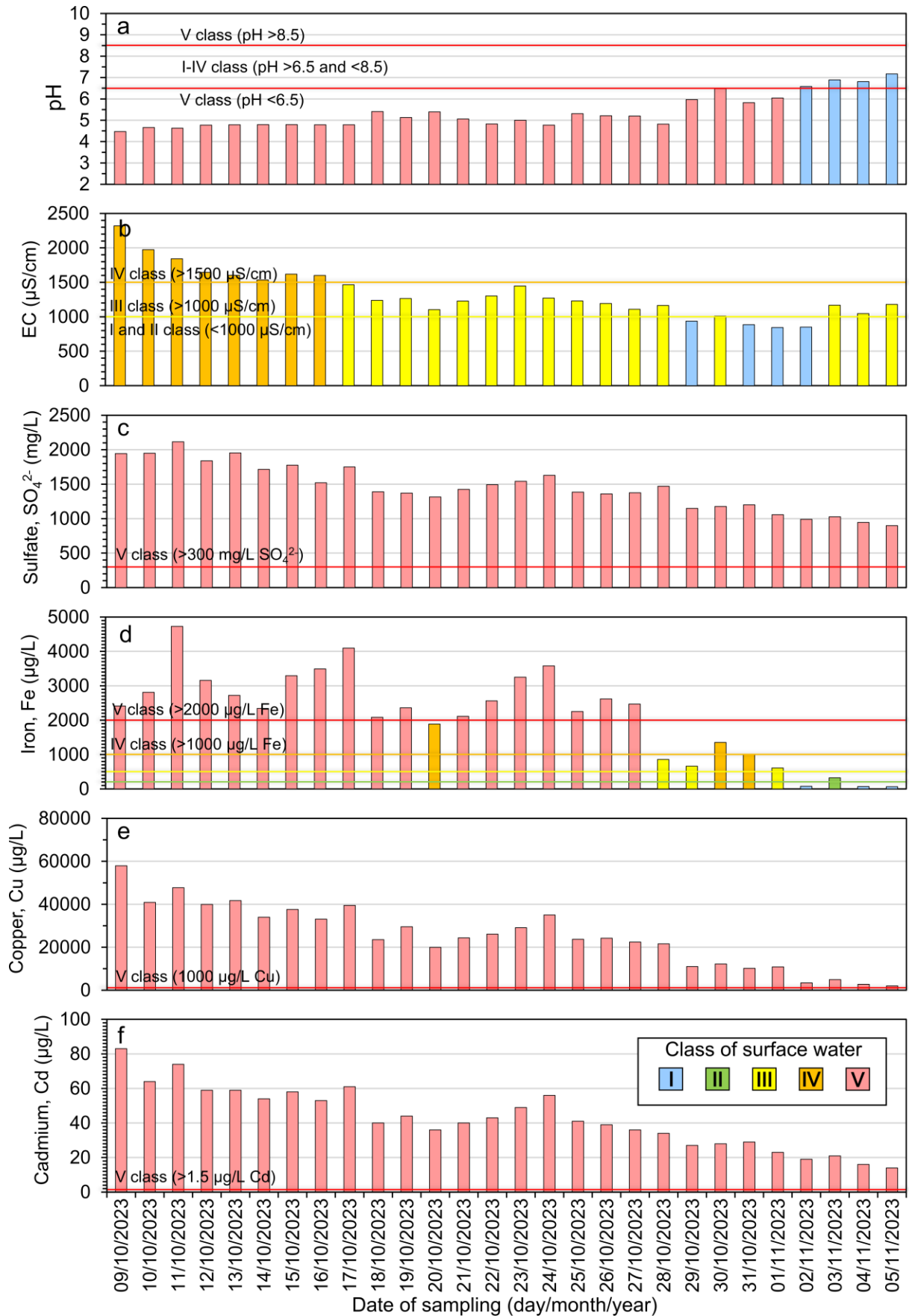
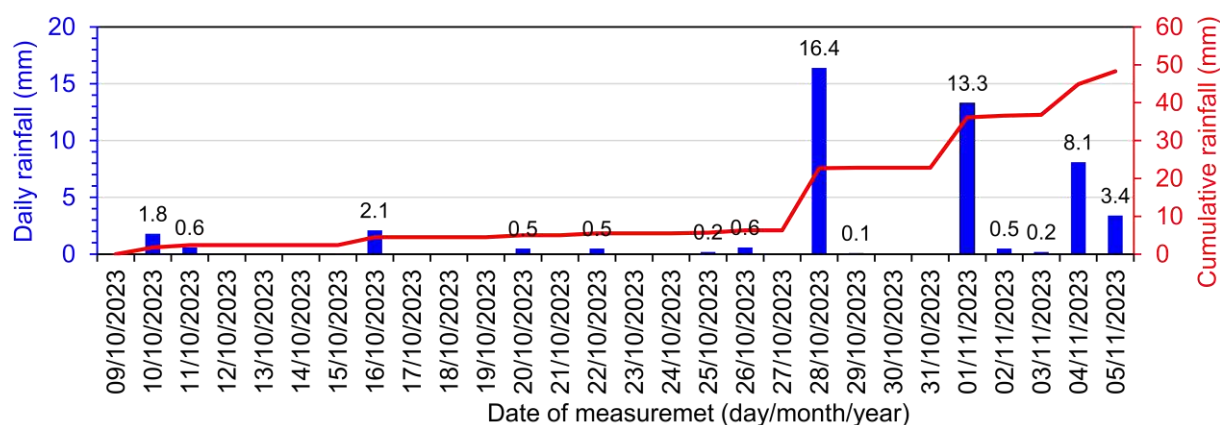


Figure 2 Change of a) pH; b) EC; c)  $\text{SO}_4^{2-}$ ; d) Fe; e) Cu; and f) Cd during the sampling period

**Table 2** Statistical summary of water quality parameters in Cerovo River

Parameter	Unit	statistical values				number of days belonging to a class				
		min.	max.	aver.	med.	I	II	III	IV	V
pH	-	4.47	7.17	5.37	5.10	4	-	-	-	24
EC	$\mu\text{S/cm}$	844	2320	1324	1234	4	-	8	16	0
$\text{SO}_4^{2-}$	$\text{mg/L}$	898	2115	1456	1407	0	0	0	0	28
Fe	$\mu\text{g/L}$	65	4730	2116	2352	3	1	3	3	18
Cu	$\mu\text{g/L}$	2037	57900	25328	24274	0	0	0	0	28
Cd	$\mu\text{g/L}$	14	83	43	41	0	0	0	0	28

The diagram of the daily and cumulative amount of rainfall during the sampling period is presented in Figure 3. In general, the amount of rainfall was higher in the second half of the sampling period compared to the first half. The increase in the amount of rainfall during the sampling period follows the increase of the pH value and the decrease in conductivity and concentrations of  $\text{SO}_4^{2-}$ , Fe, Cu, and Cd. The highest amount of rainfall in the sampling period was measured on 28/10/2023 when the largest increase in pH value and drop in Fe concentration was also measured. This correlation is explained by the dilution of Cerovo River water by the rainwater and the subsequent change in its chemical composition.

**Figure 3** Change of daily and cumulative amount of rainfall during the sampling period

The pH value in Cerovo River changed gradually during the sampling period from acidic (pH 4.47) to neutral (pH 7.17). When the pH value changed from 4.82 to 5.97 on 29/10/2023, a drastic decrease in Fe concentration was observed, while Cu and Cd did not decrease so drastically. This drastic decrease was attributed to the change in the chemical form of Fe from dissolved to particulate and the precipitation of particulate Fe on the river bed. Such behavior of Fe was also confirmed by Cánovas *et al.* [8] who suggested that Fe in river water containing AMD is mainly present in particulate form above pH 6, while from pH 3 to pH 6 the chemical form of Fe varies from dissolved to particulate depending on different factors.

The Cu concentration decreased from 57900  $\mu\text{g/L}$  to 2037  $\mu\text{g/L}$ , and the particulate matter in Cerovo River had a characteristic light-blue color (Figure 1b), which suggests that Cu concentration may have partly decreased due to precipitation. The decrease in  $\text{SO}_4^{2-}$  and Cd concentrations was less drastic since these species do not precipitate at neutral pH value [1].



## CONCLUSION

The water of the Cerovo River after the Cerovo open pit belonged to class V during the entire monitoring period, which corresponded to a poor ecological status. According to the Regulation [7], surface waters having a poor ecological status cannot be used for any purpose. The concentrations of Cu and Cd were very high compared to the background concentrations of these elements in Eastern Serbia. The increase in the amount of rainfall during the sampling period caused the change of pH value from acidic to neutral, and the decrease in conductivity and concentrations of  $\text{SO}_4^{2-}$ , Fe, Cu, and Cd. The concentrations of  $\text{SO}_4^{2-}$  and Cd decreased mainly due to dilution with rainwater, while the precipitation played a significant role along with the dilution in the decrease in concentrations of Fe and Cu.

## ACKNOWLEDGEMENT

*This paper was financially supported by the Ministry of Science, Technological Development and Innovation of the Republic of Serbia, Contract on realization and financing of the scientific research work of the Mining and Metallurgy Institute Bor in 2024, number: 451-03-66/2024-03/ 200052.*

*Results of chemical analysis of river water presented in this paper are obtained as part of the water monitoring project financed by the City of Bor, Serbia, contract number 404-951/2023-III/01.*

## REFERENCES

- [1] Đorđević S., Ishiyama D., Ogawa Y., *et al.*, Environ. Sci. Poll. Res. 25 (2018) 25005–25019.
- [2] Osenyeng O., Ishiyama D., Đorđević S., *et al.*, Resour. Geol. 73 (1) (2023) e12314.
- [3] Adamović D., Ishiyama D., Đorđević S., *et al.*, Resour. Geol. 71 (2) (2021) 123–143.
- [4] Stevanović Z., *et al.*, Mine Waste Water Management in the Bor Municipality in Order to Protect the Bor River Water *In Waste Water – Treatment Technologies and Recent Analytical Developments*, Editor: García E., InTech, (2013) 41–62. ISBN: 978-953-51-0882-5.
- [5] Đorđević S., (2018) PhD Thesis, Akita University, Japan, *Available on the following link*: <https://air.repo.nii.ac.jp/record/3301/files/kouhakukou1272.pdf>.
- [6] Đorđević S., Stanković S., Petrović J., (2023) Test report 4779/23, Mining and Metallurgy Institute Bor, *Available on the following link*: <https://bor.rs/wp-content/uploads/2023/12/4779-23-GU-Bor-vode-Mesecni-izvestaj-za-oktobar-.pdf>.
- [7] Regulation on limit values of polluting substances in surface water and groundwater and sediment and deadlines for their achievement (“Official Gazette of RS”, No. 50/2012), *Available on the following link*: <https://pravno-informacioni-sistem.rs/SIGlasnikPortal/eli/rep/sgrs/vlada/uredba/2012/50/1/reg>.
- [8] Cánovas C.R., Riera J., S. Carrero Olías M. (2018) Catena 165 414–424.



## FISH DIVERSITY ASSESSMENT OF THE IBAR RIVER: A 20-YEAR PERSPECTIVE

Nataša Kojadinović<sup>1\*</sup>, Simona Đuretanović<sup>1</sup>, Aleksandra Milošković<sup>2</sup>,  
Milena Radenković<sup>1</sup>, Marija Jakovljević<sup>1</sup>, Tijana Veličković<sup>1</sup>, Marijana Nikolić<sup>1</sup>,  
Vladica Simić<sup>1</sup>

<sup>1</sup>University of Kragujevac, Faculty of Science, Department of Biology and Ecology,  
Radoja Domanovića 12, 34000 Kragujevac, SERBIA

<sup>2</sup>University of Kragujevac, Institute for Information Technologies, Jovana Cvijića bb,  
34000 Kragujevac, SERBIA

\*[natasa.kojadinovic@pmf.kg.ac.rs](mailto:natasa.kojadinovic@pmf.kg.ac.rs)

### Abstract

*The aim of this study was to present the diversity of the fish communities of the upper and lower reaches of the Ibar River in the last 20 years. We calculated several species diversity indices, namely the Shannon Index (H), Reciprocal Simpson's Index (1/D), Fisher's Alpha Diversity Index (A), Margalef's Index, and Pielou's Evenness Index (J). We recorded 16 fish species from 7 families between the 2003 and 2023 investigation period. The highest value of Shannon's diversity index was recorded in the upper course of the river (0.691), while the lowest was in the lower course (0.314) in 2017 and 2019. The relatively low values of diversity indices are most likely the consequence of the dominance of a few species, but they also may be the result of strong anthropogenic influence. Evenness Index ranged from 0.226 to 0.424, indicating a low level of homogeneity of fish assemblages. This study has contributed to the knowledge of fish diversity in the Ibar River and could assist in carrying out future ecological studies in line with conservation, restoration, and management strategies.*

**Keywords:** fish diversity indices, fish assemblages, Ibar River, Serbia.

### INTRODUCTION

Freshwater ecosystems are known for their high diversity, but they are also considered the most threatened ecosystems in the world. Changes in the structure and quality of aquatic habitats are the result of a large number of different anthropogenic activities such as overexploitation, pollution, flow modification, degradation of habitat, and invasive species [1]. Freshwater fish play a significant role in the diversity and functioning of these ecosystems, particularly in lotic systems where they can provide valuable information about biological structure and ecological sustainability.

The Ibar River has a specific hydromorphology that was changed by the construction of the Gazivode reservoir. Plans for the construction of nine mini-hydroelectric power raise concerns about this specific river's ecosystem. Also, the Ibar River ranks among the most polluted rivers in Serbia due to increased pollution in recent decades (industrial and municipal



wastewater) [2] That's why in the present study we analyzed the 20-year temporal changes in the taxonomic diversity of the fish using fish diversity indices.

## MATERIALS AND METHODS

The Ibar River, the largest tributary of the West Morava, is a typical mountain river with a highly branched hydrographic basin (total length of 276 km). It springs on the north side of the Hajla mountain (1360 m above sea level) in Montenegro, flows into the West Morava near the town of Kraljevo [3], and belongs to the Black Sea basin. Due to high mountain flow, the great erosion in the basin, and river fall, the Ibar River exhibits a torrential character and causes frequent floods in periods of high waters. The Gazivode reservoir (total length of 22 km, volume of 380 million m<sup>3</sup>) was formed by damming the Ibar River at its upper course [4]. After 45 years the Pavlica mini-hydroelectric power plant was built (2021) near the town of Raška. There are plans for the construction of nine more similar plants.

The ichthyological research was conducted in the period 2003–2023, to develop fisheries management plans for protection and sustainable use of fish stocks. Fishes were sampled using the electrofishing equipment (Aquatech IG 1300) and samples were identified to species according to Kottelat and Freyhof [5] and Simonović [6]. We sampled at 12 localities shown in Table 1.

Species diversity was assessed using different indices: Shannon Diversity Index (H), Alpha Diversity Index (A), Margalef Diversity Index (M), and Evenness Index (J). The Shannon Diversity Index is the most commonly used diversity index in ecology and combines species richness (S) and evenness (E) [7]. The Simpson's Index (D) was used to measure the probability that two randomly chosen specimens from a sample will belong to different fish species. Due to the potential errors during the reverse interpretation of the obtained results, Simpson's Index was expressed as Reciprocal Simpson's Index (1/D) because its value increased with greater diversity [8]. Additionally, the link between the number of species and their abundances is determined with Fisher's Alpha Diversity Index (A) [9]. Margalef's index was used as a simple measure of species richness [10] and Pielou's evenness (J) was used to compare the actual diversity value (H index) to the maximum possible diversity value (lnS). It's constrained between 0 and 1 and the more variation in abundances between different fish species within the community, the J is lower [9]. All fish diversity indices were calculated using BioDiversityPro v. 2 software [11].

## RESULTS AND DISCUSSION

The obtained results of fish diversity and Evenness indices in investigated area were summarized and presented in Table 1.

During the study period, a total number of 16 fish species belonging to 7 families were recorded. The most represented families are Leuciscidae and Cyprinidae. Our results show a change in the composition of the fish community in accordance with longitudinal fish zonation concept. The upper course of the Ibar River represents the grayling zone with the only autochthonous populations of *Thymallus thymallus* (Linnaeus, 1758), for the Morava basin. Therefore, they are especially important in terms of conservation issues [12]. The lower

course belongs to the barbel zone, which is confirmed by the dominance of typical species for this zone, *Barbus barbus* (Linnaeus, 1758) and *Chondrostoma nasus* (Linnaeus, 1758). Interesting for this region is the appearance of *Zingel streber* (Siebold, 1863), which is rare in Serbia.

*Table 1 Diversity index of fish assemblages in the upper and lower reaches of the Ibar River*

Localities	year		Species richness	Shannon Index H	Reciprocal Simpson's Index 1/D	Alpha Index A	Margalef's Index M	Evenness Index J
<b>Crna Reka</b>	2003	upper course	7	0.632	3.607	2.161	8.699	0.325
<b>Above mauth in W.Morava</b>	2003	lower course	7	0.664	4.033	2.764	9.966	0.341
<b>Mehov krš</b>	2011	upper course	7	0.609	3.368	1.558	7.01	0.313
<b>Žičko polje</b>	2011	lower course	6	0.59	3.174	1.781	8.829	0.329
<b>Topoljak</b>	2016	lower course	6	0.444	2.051	1.386	7.437	0.248
<b>Miljina glava</b>	2017	upper course	8	0.691	3.742	2.342	8.157	0.332
<b>Topoljak</b>	2019	lower course	4	0.314	1.635	0.946	8.305	0.226
<b>Špiljani</b>	2020	upper course	5	0.406	1.986	1.541	9.495	0.252
<b>Mataruška banja</b>	2021	lower course	5	0.568	3.242	1.663	9.966	0.353
<b>Špiljani</b>	2023	upper course	7	0.668	3.774	3.066	10.48	0.343
<b>Miljina glava</b>	2023	upper course	4	0.333	1.83	0.925	8.157	0.24
<b>Topoljak</b>	2023	lower course	4	0.601	4.168	0.942	8.274	0.434

Fish as indicators of aquatic habitat health are widely used through biotic ichthyological indices [12]. Based on values of Shannon's Diversity Index (H) the highest diversity of fish species was observed in the upper course of the river (Miljina glava - 0.691 and Špiljani - 0.669) and the lowest in the lower course (Topoljak - 0.314) (Table 1).

The highest value of Margalef's Index was recorded in Špiljani in 2020, while the lowest value was recorded in Mehov krš in 2011 (Table 1). Relatively low values of diversity indices are most likely the consequence of the dominance of a few species, but they also may be the result of strong anthropogenic influence.

Evenness Index ranged from 0.226 to 0.424, and both values were recorded at the same locality, Topoljak, in 2019 and 2023. Evenness indices show how homogenous is the fish community, even an ecosystem, considering different fish species' abundances [9]. Our results indicated a relatively low level of homogeneity in terms of a well-balanced fish assemblage structure.

## **CONCLUSION**

Freshwater fish conservation efforts should be focused on knowledge of regional patterns of species richness. Our results provide important information about fish diversity and evenness in the investigated area under high anthropogenic threats, which is valuable for future conservation measures and management.

## **ACKNOWLEDGEMENT**

*This research is funded by the Ministry of Science, Technological Development and Innovation, Republic of Serbia, Grants: No.451-03-66/2024-03/ 200122.*

## **REFERENCES**

- [1] Dudgeon D., Arthington A., Gessner M., *et al.*, *Biol Rev* 81(2) (2006) 163–182.
- [2] Milošković A., Dojčinović B., Kovačević S., *et al.*, *Environ Sci Pollut Res Int* 23(10) (2016).
- [3] Gavrilović Lj., Dukić D. *Reke Srbije. Zavod za udžbenike i nastavna sredstva. Beograd* (2002), p.208, ISBN: 8617185597.
- [4] Obradović S., *Serbian Journal of Geosciences* 7 (2021) 15–23.
- [5] Kottelat M., Freyhof J., *Handbook of European freshwater fishes. Publications Kottelat, Cornol and Freyhof, Berlin* (2007), p.646, ISBN: 978-2-8399-0298-4.
- [6] Simonović P., *Uvod u ihtiologiju. Univerzitet u Beogradu, Biološki fakultet, Beograd* (2010), p.316.
- [7] Kathleen A., Callahan J., *Proceedings St. Francis College, Brooklyn, NY, USA, (2005),* 201.
- [8] Buj I., Pleše S., Onorato L., *et al.*, *Water* 15(2023) (2023) 311.
- [9] Ulfah M., Fajri S.N., Nasir M., *et al.*, *IOP Conf. Ser.: Earth Environ. Sci.* 19–20 June Banda Aceh, Indonesia (2019).
- [10] Margalef R., *General System* 3 (1958) 36–71.
- [11] McAleece N., Gage J., Lamshead P., *et al.*, *BioDiversity Professional statistics analysis software. Jointly developed by the Scottish Association for Marine Science and the Natural History Museum London. (1997).*
- [12] Simić V., Bănăduc D., Curtean-Bănăduc A., *et al.*, *Front. Environ. Sci.* 10 (2022) 952692.



## APPLICATION OF EXPANSIVE MORTARS FOR THE FORMATION OF ARTIFICIAL SCREENS DURING BLASTING IN URBAN AREAS

Milanka Negovanović<sup>1\*</sup>, Lazar Kričak<sup>1</sup>, Stefan Milanović<sup>1</sup>, Nikola Simić<sup>1</sup>,  
Jelena Majstorović<sup>1</sup>

<sup>1</sup>University of Belgrade - Faculty of Mining and Geology, Đušina 7, 11000 Belgrade,  
SERBIA

\*milanka.negovanovic@rgf.bg.ac.rs

### Abstract

*During construction of buildings in urban areas, sometimes there is a need to blast solid rock mass in the immediate vicinity of the surrounding buildings. In that case, the aim is not only to increase the efficiency of blasting, but also to reduce harmful effects of ground vibration induced by blasting. At the same time, it is very important to protect the buildings located in the safe zone from the blast site as well as remaining rock mass around the blast site. This can be achieved by the formation of artificial screens. Artificial screens represent discontinuities in the rock mass placed between the blasting site (source of seismic waves) and building to be protected. The formation of artificial screens using expansive mortars is presented in the paper. Expansive mortars are environmentally friendly products. They do not cause shock waves, ground vibrations, air blast, flyrock and do not release toxic fumes as side effects of blasting process which may occur. They do not cause excessive breakage to the surrounding rock mass.*

**Keywords:** expansive mortar, artificial screens, pressure, rock breaking, building foundation.

### INTRODUCTION

During construction of buildings in urban areas, the removal of rock mass for the purpose of making foundations is usually done by mechanization. However, in some cases there is a need to build the building in solid rock mass. In that case, to excavate foundations, it is necessary to break the large quantity of solid rock mass that cannot be broken by machinery. Then the special blasting techniques can be applied, using small-diameter holes with small amounts of explosive charges. Of particular importance is the choice of optimal delay time of initiation system and initiation pattern. Sometimes, despite the significant reduction of the quantity of explosives in blastholes and the selection of an adequate initiation pattern, it is necessary to additionally reduce the intensity of seismic waves caused by blasting, to protect the surrounding buildings [1]. One of the methods is the formation of artificial screens that represent a discontinuity in the rock mass located between the blast site and the building to be protected [1].

Artificial screens in our Country are mostly carried out in the form of a crack using the method of contour blasting during production blasting or road construction and other construction works. Contour blasting methods mean the use of small-diameter explosive charges or a detonating cord. Delay time of initiation system are very small and sometimes

explosive charges of contour blast holes are initiated simultaneously. The paper presents the first attempt of applying the expansive mortar to form a crack as the discontinuity in rock mass that has the function to protect buildings from seismic waves from blasting.

The tendency in the world today is to find new solutions that can be applied to break solid rock masses, and which will be an adequate replacement for commercial explosives in sensitive areas. The reason for this is the problems related to blasting in urban areas, in road and railroad construction, demolition works, secondary breaking, rock breakage for foundation, trenching, stabilization of slopes and similar civil construction operations especially in urban areas as well as quarrying of dimension stone. In all cases mentioned, there is a problem of removing solid rock mass or concrete structures in an efficient way, while protecting the environment.

One of these solutions are expansive mortars, which are increasingly used in mining and construction, especially in cases where there are buildings declared as cultural heritage, industrial and other objects that are very sensitive to ground vibration, when the use of explosives is prohibited.

### **EXPANSIVE MORTARS**

Expansive mortars have developed from a need to full fill the requirement in civil engineering works especially demolition works in urban areas where the explosives are not permitted [2]. Nowadays, expansive mortars have found a wide range of application in excavating foundations, levelling rocks for road works, trenching, underground excavations, marine and submarine excavations, removing boulders, demolition of concrete or reinforced concrete etc. They have quickly found the application in mining particularly in dimension stone mining for splitting the primary blocks from the rock massive or squaring the primary blocks into commercial ones.

Expansive mortars can be in the form of a cartridge - capsule type and in bulk - bulk type. The cartridges of expansive mortars must be immersed in water before loading the holes while the bulk type should be mixed with water before pouring into the holes (Figure 1). Expansive mortars in bulk are powdery materials which are mixed with water at a certain percentage, depending on the type of expansive mortars. The mixture is poured into previously drilled holes.

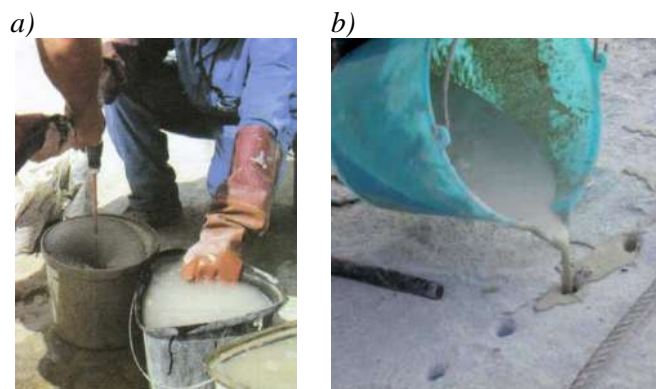


**Figure 1** Procedure of using the expansive mortar in bulk; a) mixing with water, b) pouring into the holes [2]

Depending on the reaction time, expansive mortars start to expand. Under confinement, this expansion can generate significant expansive pressure. When the resultant force exceeds the tensile strength of material, cracking occurs through the predetermined direction or pattern. During splitting process, the holes are drilled in the line - the predetermined direction of splitting. In processes of breaking the rock or concrete (demolition works, excavating foundations etc.) the holes are drilled in predefined pattern. The pressure of expansive mortars provides silent cracking and breaking the rock or concrete along this pattern. There are expansive mortars with slow and fast reaction. The reaction time of expansive mortars depending on temperature is given in Table 1.

**Table 1** Reaction time of expansive mortars depending on temperature [2]

Temperature (°C)	Reaction time (h)	
	Slow reaction	Fast reaction
50	8	3
40	12	4
30	15	5
20	20	10
10	30	15

Expansive mortars have the following advantages in relation to other technologies of rock breakage:

- rock breakage do not cause shock waves and explosion,
- rock breaking is carried out without noise and air blast,
- no smoke, dust or toxic fumes,
- no ground vibration and flyrock,
- the process of rock breakage do not cause excessive damage to the surrounding rock mass,
- ecological and environmentally friendly product,
- storage and transport are not hazardous to the environment,
- the use and preparation of expansive mortars is very simple and safe for operators.

Expansive mortars are highly alkaline products so the operator must wear safety goggles and rubber gloves,

- expansive mortars do not require special authorizations or licenses like explosives,
- there is no need for a highly skilled operator,
- there is no limit to the time period when expansive mortars can be used during the day.

The disadvantages of expansive mortars are:

- expansive mortars cannot be applied at very low temperatures,
- the earlier types of expansive mortars were related to a much higher price than commercial explosives, however, currently there are expansive mortars with more affordable prices,
- the application of expansive mortars in fractured rocks is limited.



Nowadays, there are various expansive mortars in market. In order to present the detail characteristics and fields of application in further part of the paper three expansive mortars are presented.

### Expansive mortar Dexpan

The expansive mortar Dexpan [3] is used for demolition and concrete breaking, excavating and rock breaking as well as stone quarrying. Dexpan is a powder which is mixed with water and poured into previously drilled holes (Figure 2a). The expansion within holes develops a pressure of 1241 bar providing silent cracking that breaks reinforced concrete and rock safely and quietly without noise, vibration, and dust. Dexpan provides controlled demolition according to drilling pattern breaking reinforced concrete or rocks [3].

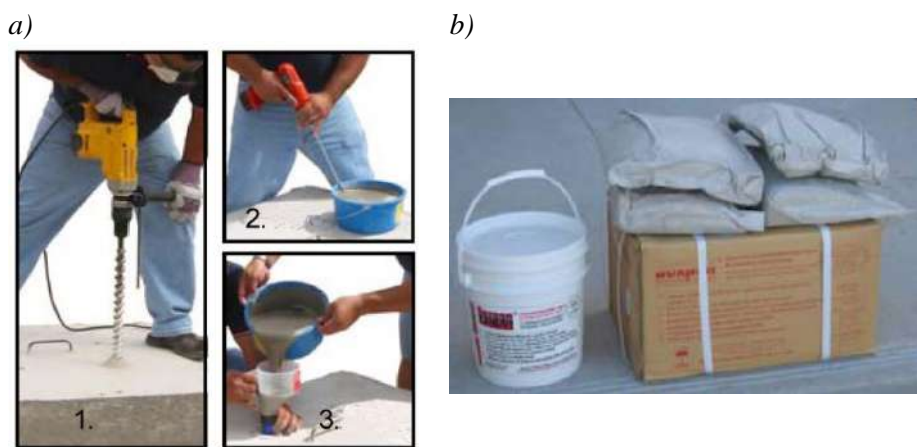


Figure 2 a) Phases of using Dexpan: 1 – drilling, 2 – mixing Dexpan with water, 3 – pouring the mixture into holes; b) Packages of Dexpan [3]

Packing of Dexpan may be plastic container or box with bags, (Figure 2b). There are three types of Dexpan depending on temperature [3]:

- Dexpan I for temperatures from 25 to 40°C,
- Dexpan II for temperatures from 10 to 25°C,
- Dexpan III for temperatures from -5 to 10°C .

Dexpan [3] can be used for:

- demolition and concrete breaking (demolition of mass reinforced concrete, foundations for machinery, partial demolition of various concrete structures, reinforced concrete cutting),
- excavating and rock breaking (excavation of rock, splitting the boulders, rock and slab breaking for road expansion, excavation associated with tunnelling, construction works),
- stone quarrying and dimension (limestone, onyx, marble, granite quarrying).

### Expansive mortar FRACT.AG

FRACT.AG [4] is a highly expansive mortar which expands when poured into a hole and develops a pressure higher than 8000 t/m<sup>2</sup> on the walls of holes. FRACT.AG is environmentally friendly. It releases no toxic fumes or harmful substances of any kind [4].

FRACT.AG can be used in any type of rock formation, concrete, reinforced concrete or tiled structure in [4]:

- excavating foundations,
- levelling rocks for road works,
- excavating trenches for pipe laying,
- underground excavations,
- marine and submarine excavations,
- removing boulders,
- demolition of concrete or reinforced concrete piers, towers, walls, wharves, etc.
- demolition of foundations.

FRACT.AG is a powder (Figure 3) that is mixed with clean water before use, in a ratio of 30% of the overall weight (1.5 liters of water for each 5 kg package) [4]. Water is poured first in a large container then gradually the powder is added to water stirring all the time to obtain a smooth, lumpfree mortar. After preparation time of 5 to 10 minutes the mortar is poured into holes.



Figure 3 Expansive mortar FRACT.AG [4]



Figure 4 Expansive mortar SPLITSTAR [5]

Four types of FRACT.AG are available in market [4]:

- RED – for temperatures near 5°C,
- GREEN – for temperatures from 5 to 20°C,
- YELLOW – for temperatures from 20 to 35°C,
- BLUE – (multipurpose) to use in demolition work with hole of diameter 40 mm (the temperature affects the reaction time).

#### Expansive mortar SPLITSTAR

Expansive mortar SPLITSTAR [5] is a non-toxic and cementations powder, which consisting of calcined oxides of calcium, silicon, and aluminium (Figure 4). Expansive mortar SPLITSTAR becomes a highly powered amazing expansive pressure of 11200 t/m<sup>2</sup> when mixed with water. Marble, granite, limestone, plain concrete, reinforced concrete, boulders, and ledge are fractured overnight without noise, vibration, or fly rock. Especially, used as environment constraints or when explosive is not permitted for use [5].

Expansive mortar SPLITSTAR [5] develops rise of highly expansive capabilities at the consistent volume exceeding 122 MPa (11200 t/m<sup>2</sup>) more than enough to break up any materials to be cut or demolished. The tensile strength for most rock is less than 5–25 MPa (500–2500 t/m<sup>2</sup>, 50–250 kg/cm<sup>2</sup>), reinforced concrete breaks at 3–5 MPa (30–50 kg/cm<sup>2</sup>, 300– 500 t/m<sup>2</sup>).

Expansive mortar SPLITSTAR [5] is used for:

- quarrying marble and granite, limestone, sandstone; cracking nature ground,
- breaking rock into pieces; deposition of falling rocks,
- demolishing concrete structure, chipping defective concrete piles, etc.
- in the field as a new method of demolition, expansive mortar SPLITSTAR can effectively be used in the construction and civil engineering fields as follows: bridges dams, ledge boulders, machinery bases concrete piers, slabs 6" thick and more marble and granite.

Types of expansive mortar SPLITSTAR [5] are:

- SCA-1 (25–40°C),
- SCA-2 (10–25°C),
- SCA-3 (-5–10°C).

### **ARTIFICIAL SCREENS**

One of the methods to reduce seismic effects during blasting involves the formation of artificial screens in the path of propagation of seismic wave (Figure 5). These screens can be made using machinery or blasting methods. Artificial screens can be continuous or discontinuous [6]. The last type involves the blasting of a row of boreholes with a certain intermediate space between the holes.

Artificial screens establish two zones [6]:

- the protected zone from ground vibration induced by blasting,
- the zone where the effect of blasting increases.

The artificial screens are divided into [6]:

- artificial screens in the form of cracks,
- artificial screens in the form of a layer of loose rock material.

Experiments carried out in the former USSR [6] led to the conclusion that the placement of artificial screens in most cases achieved its goal, i.e. there is a decrease in the intensity of ground vibration in the “protected zone” and the effect of blasting in the “blasting zone” increases. The experiments were conducted to establish the mathematical dependencies of changing the parameters of the screen (width, depth, length, filling...) that affect the ground vibration in the protected zone.

There are two methods of forming the artificial screen: 1) closer to the source of disturbance (blast site) and 2) directly in front of the object to be protected [6]. In the first method, the screen is temporary. During multiple blasting, and sometimes in individual blasting, it is recommended to create a screen directly in front of the object to be protected. In this case, the screen is made permanent and can be made using absorbent material. Regarding the shape, the artificial screen can be vertical or inclined with extensions in the upper or lower part [1].

The effectiveness of artificial screens in the form of rows of boreholes depends on the diameter of the holes, the distance of the boreholes in the row, the distance between the screen and the source of the seismic wave or the object to be protected [6].

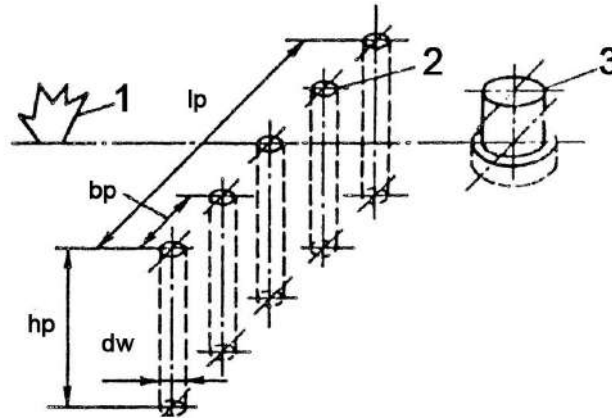


**Figure 5** The placement of the artificial screen: 1 – blast site; 2 – artificial screen; 3 – object to be protected;  $hp$  – screen depth,  $bp$  – distance between screen holes,  $dw$  – hole diameter / screen width,  $lp$  – screen length [6]

### The formation of artificial screen using expansive mortar

During the blasting of rock to excavate foundation for the future housing and business complex in an urban area, an attempt was made to form the artificial screen using expansive mortar. Holes with a diameter of 38 mm were drilled with spacing of 25 cm [7]. Drilling was carried out using a self-propelled drill rig FlexiROC T15 R [8] produced by Epiroc for percussive rotary drilling. FlexiROC T15 R (Figure 6) is a compact, self-propelled, four-wheel drive drill rig. It enables drilling the holes with maximum length up to 9 m. Technical data of the drill rig FlexiROC T15 R are shown in Table 2.



**Figure 6** FlexiROC T15 R [8]

Due to the uneven terrain, the lengths of boreholes varied (from 2.8 to 5.8 m). Boreholes were drilled in one row [7]. The row of drilled boreholes marked with blue spray is shown in Figure 7.

**Table 2** Technical data of Epiroc tophammer surface drill rig FlexiROC T15 R [8]

Technical data	FlexiROC T15 R
Hole diameter	27 mm – 51 mm
Feed force, max	4 kN
Rock drill/ DTH hammer size	COP 1022 ; COP 1028
Compressor	Atlas Copco C55 C106 GD, screw compressor
Compressor working pressure, max	8.5 bar
Air capacity (FAD) of compressor at normal working pressure	23 l/s
Engine	48 kW
Transport dimensions (height/ length/ width)	2250 mm/4950 mm/1770 mm

The SPLITSTAR expansive mortar was used to fill the boreholes. The mortar was mixed with water according to the manufacturer's recommendation and poured into the boreholes. After that, the mortar was left overnight to expand in boreholes. The mortar expands and presses the walls of the boreholes in all directions. When the resulting force overcomes the tensile strength of the rock, the rock cracks in a predisposed direction (line of drilled boreholes). Figure 8 shows a crack formed by the action of expansive mortar. The artificial screen formed in this way reduces the intensity of ground vibration induced by blasting in the protected zone, but also improves the effect of blasting in the blasting zone.



**Figure 7** The row of drilled boreholes marked with blue spray [7]



**Figure 8** Crack formed by the action of expansive mortar [7]

## CONCLUSION

The paper presents one of the possibilities of applying the expansive mortars for the formation of artificial screens. Expansive mortars are environmentally friendly products. Expansive mortars do not cause shock waves, ground vibration, air blast, flyrock and do not also release toxic fumes. Storage and transport are not hazardous to the environment. The use of expansive mortars is very simple and safe for operators if they follow the Instruction Manuel from the manufactures.

Artificial screens represent discontinuities placed between the blasting site (source of seismic waves) and the object to be protected. Screens have a dual function. One is to reduce the intensity of seismic waves caused by blasting in protected zone, and the second is to improve the effect of blasting in the blasting zone.

Extensive research on the effect of artificial screens on the intensity of seismic waves was carried out during the USSR, especially artificial screens that are made using mechanization.



In our Country, artificial screens have been applied only in the form of a crack made by contour blasting methods. The intensive application of expansive mortars will certainly lead to their greater application in the field of the formation of artificial screens, especially in sensitive areas. Even in the form of a crack, artificial screens prove to be useful for reducing the intensity of seismic waves in the protected zone.

### **ACKNOWLEDGEMENT**

*The authors of the Paper thank the Ministry of Science, Technological Development, and Innovation for providing the funds for the research based on the Agreement no. 451-03-65/2024-03/200126.*

### **REFERENCES**

- [1] Kričak L., Seismic from Blasting, Blasting Center, Faculty of Mining and Geology, Belgrade, (2006), p.214, ISBN: 86-7352-119-X, (*in Serbian*).
- [2] Maksimović M., Exploitation, Testing, Application of Dimension stone, Contractor d.o.o, Belgrade, (2006), p.174, ISBN: 9788690910908, (*in Serbian*).
- [3] Dexpan, Available on the following link: <https://www.dexpan.com/pages/what-is-dexpan-non-explosive-demolition-agent>.
- [4] FRACT.AG, Available on the following link: [http://www.chimicaedile.it/documenti/english\\_catalog.pdf](http://www.chimicaedile.it/documenti/english_catalog.pdf).
- [5] SPLITSTAR, Available on the following link: <https://www.stonecontact.com/products-c826099/split-ag-crack-max-splitstar-expansive-mortar>.
- [6] Kuzmenko A.A., Vorobev V.D., Denisyuk I.I., *et al.*, Seismic Effects of Blasting in Rock (Russian Translations Series Book 103), A.A.Balkema, Rotterdam/Brookfield (1993), p.97, ISBN: 9054102144.
- [7] The Project of removing the rock mass from the remaining rock massive at the location of the future housing and business complex “Skyline”, Belgrade, Faculty of Mining and Geology, Belgrade, (2018), (*in Serbian*).
- [8] FlexiROC T15 R, Epiroc, Available on the following link: <https://www.epiroc.com/en-sk/products/drill-rigs/surface-drill-rigs/flexiroc-t15r>.





## AIR POLLUTION IN THE BOR REGION FROM 1994 TO 2023

Snežana Šerbula<sup>1\*</sup>, Tanja Kalinović<sup>1</sup>, Ana Radojević<sup>1</sup>, Jelena Kalinović<sup>1</sup>,  
Jelena Jordanović<sup>1</sup>

<sup>1</sup>University of Belgrade, Technical Faculty in Bor, V.J. 12, 19210 Bor, SERBIA

\*ssherbula@tfbor.bg.ac.rs

### Abstract

*This study considered the historical air pollution data. Assessment of air quality in Bor was done for the period 1994–2023, namely since the installation of monitoring stations for measuring the concentrations of most common air pollutants such as SO<sub>2</sub>, PM<sub>10</sub> and toxic elements As, Cd and Pb in PM<sub>10</sub> samples, at several different locations in relation to the location of the copper smelter. Modernizations of the Flash smelting technology were carried out in 2015 and 2022, which partially affected the reduction of air pollution. The measured concentrations of SO<sub>2</sub>, PM<sub>10</sub>, As in PM<sub>10</sub> as well Pb and Cd indicated frequent exceedances of defined annual limit values, both at the national and European levels. The maximum average annual SO<sub>2</sub> concentration reached 372 µg/m<sup>3</sup> in 2012 and was 7.5 times higher than the legally prescribed values. Air quality regarding the levels of PM<sub>10</sub> and especially As in PM<sub>10</sub> was significantly worse after modernization. The annual concentration of As exceeded the annual target value defined by the European and Serbian regulations, at all monitoring sites, with a maximum exceedance of more than 90 times at the suburban location during 2019. Frequent exceedances of the respective annual target values were also noted for Pb and Cd in PM<sub>10</sub> samples. The analyzed data pointed out that the Bor region can still be characterized as an ecological hotspot in Serbia and beyond.*

**Keywords:** air pollution, SO<sub>2</sub>, PM<sub>10</sub>, As, Pb, Cd.

### INTRODUCTION

Industrial and urban-industrial environments suffer significantly more pollution than typical urban and rural environments, because the largest percentage of pollution comes from industrial activities, mining and metallurgy, combustion of fossil fuels and waste, as well as from traffic [1]. Concentrations of suspended particles in the atmosphere of urban areas range from 60–220 µg/m<sup>3</sup>. In highly polluted areas, these concentrations can reach up to 2,000 µg/m<sup>3</sup> [1].

The European Commission (EC) has determined the allowed limit values (LV) for PM<sub>10</sub> as follows: the annual LV is 40 µg/m<sup>3</sup>, and the daily LV is 50 µg/m<sup>3</sup>, whereby this value must not be exceeded more than 35 times during the year [2]. The US Environmental Protection Agency (USEPA) for PM<sub>10</sub>, on a daily basis, defines the LV of 150 µg/m<sup>3</sup> [3]. In Serbia, concentration of PM<sub>10</sub> defined for inhabited areas is 120 µg/m<sup>3</sup> on a daily basis, and 40 µg/m<sup>3</sup> on an annual level [4].

Numerous pollutants present in the environment, such as arsenic (As), lead (Pb), cadmium (Cd), chromium (Cr), nickel (Ni), antimony (Sb) and copper (Cu) are classified as PBT elements, i.e. persistent, bioaccumulative and toxic elements [1]. Based on epidemiological

evidence, the International organization for research in the field of cancer (IARC) classified As, Pb and Cd in the group of carcinogenic elements. Apart from being carcinogenic and the most dangerous poison, As is found in copper ore mainly as the mineral arsenopyrite [5]. When copper ore is processed, at all stages of processing, significant amounts of arsenic are emitted in the environment [6].

The aim of this paper is an environmental review of the air quality, which was affected by polluting substances released from the mining and metallurgical facilities for pyrometallurgical copper production, which started 120 years ago in Bor and the surroundings (Eastern Serbia).

## **MINING AND METALLURGICAL ACTIVITIES IN BOR AND ITS SURROUNDINGS**

Bor and its surroundings are known for deposits of copper ore, which are among the largest in Europe [6]. Mining production in Bor has existed for more than 120 years [7]. Mining in Bor began in 1902 with the discovery of copper-rich ore deposits, which were then exploited and processed. Natural hills were disappearing, and artificial hills of mine waste were formed. For years, the copper ore was exploited, so it became poorer over time. The poor copper ore was carried out in flotation, the copper concentrate was melted in the smelter and the flotation tailings formed new artificial lakes with fine sediment, like living mud.

Pyrometallurgical production of copper from sulphide ores (chalcopyrite –  $\text{CuFeS}_2$ , chalcosine –  $\text{Cu}_2\text{S}$ , coveline –  $\text{CuS}$ , arsenopyrite –  $\text{FeAsS}$ , etc.) was the main source of pollution with  $\text{SO}_2$  and PM particles, together with copper ore mining activities. The outdated technology was replaced by flash smelting technology (FST) as an advanced and energy-efficient production method during 2015 [8]. The monitoring of the level of air pollution in the city of Bor is carried out by the Mining and Metallurgical Institute Bor and the Serbian Environmental Protection Agency (SEPA). The measurement of air pollution started way back in 1994, and the levels of air pollution with sulfur dioxide ( $\text{SO}_2$ ), fine suspended particles up to  $10\ \mu\text{m}$  ( $\text{PM}_{10}$ ), as well as As, Pb, Cd and Ni in  $\text{PM}_{10}$ , were determined at several locations in the city of Bor and surrounding settlements, as part of the local and national air quality monitoring networks. The levels of pollutants in the air are accordingly published in the form of annual and monthly reports by the Mining and Metallurgy Institute Bor and are available for public [9].

## **AIR POLLUTION IN THE AREA OF BOR AND ITS SURROUNDINGS**

The area of Bor and its surroundings was under the influence of emissions of  $\text{SO}_2$ , sedimentary substances, and suspended particles with a high concentration of arsenic, for many years. Significant exceedances of LVs [4] proposed for these polluting substances have been recorded for many years. Figure 1 shows the average annual concentrations of  $\text{SO}_2$  at five measuring sites in the Bor area in the period 1994–2023. The limit value for  $\text{SO}_2$  at the annual level is set at  $50\ \mu\text{g}/\text{m}^3$  [4] and it is represented by the red horizontal line on the Figure 1. From 1994 to 2010, measurements were provided at three measuring site: Town Park, Institute and Jugopetrol, and later the measuring sites, such as Technical Faculty and

Slatina were also included. Since measurements of air pollution with sulfur dioxide have been carried out, there have always been exceedances of the average annual value of  $50 \mu\text{g}/\text{m}^3$ , implying that the daily and hourly values were also extremely high. During 2022, the average annual limit value for  $\text{SO}_2$  emissions was exceeded only at the measuring site Jugopetrol. The  $\text{SO}_2$  concentrations at other four measuring sites were within the defined limits. However, knowing that the reconstruction of the copper smelter, which is located in the very center of the city, was carried out during that year, being out of order for most of that year, then it is understandable that there was no air pollution with sulphur dioxide during 2022. With the reconstruction of the smelter and the introduction of the gas desulphurization process, the limit value of  $50 \mu\text{g}/\text{m}^3$  was not exceeded in 2023.

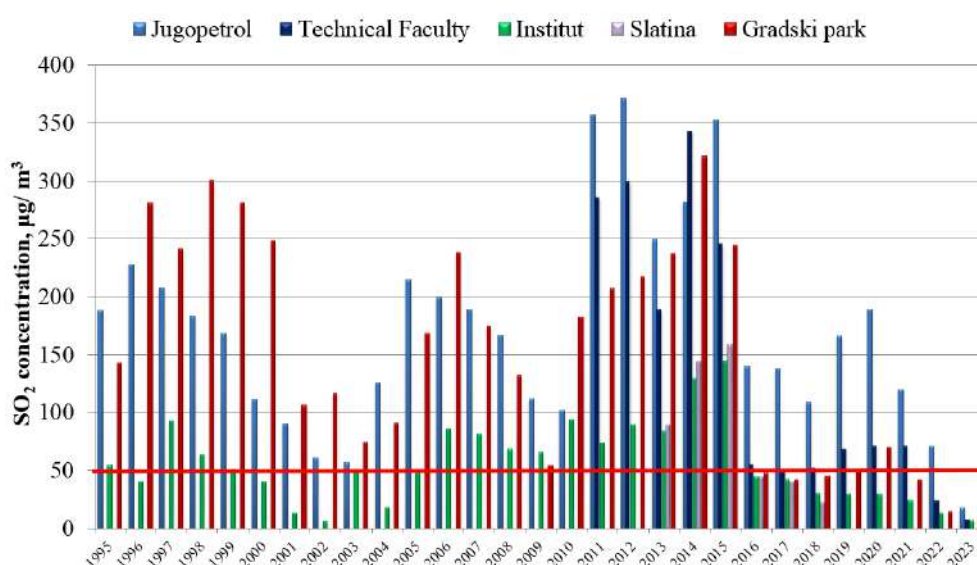


**Figure 1** Average annual concentrations of  $\text{SO}_2$  at five measuring sites in the Bor area in the period 1994–2023. The limit value (red horizontal line) is defined for  $\text{SO}_2$  at  $50 \mu\text{g}/\text{m}^3$

The average annual concentrations of total suspended particles (TSP) at all eight measurement sites in the Bor area were around the limit value [4]. The limit value for TSP was  $70 \mu\text{g}/\text{m}^3$  until 2013, and after that it was reduced to  $40 \mu\text{g}/\text{m}^3$  for  $\text{PM}_{10}$ , defined by the Regulation of the Republic of Serbia [4]. In both periods, before and after 2013, there were minor exceedances of the defined average TSP and  $\text{PM}_{10}$  annual values.

The average annual concentrations of As, in suspended particles  $\text{PM}_{10}$ , were determined at eight sites: Town Park, Jugopetrol, Technical Faculty, Krivelj, Institute, Brezonik, Slatina and Oštrelj during the period from 1994 to 2023, are shown in Figure 2. Over the years, the monitoring of pollutant concentrations was carried out at several other sites, but data for a whole period are not available. The measuring site Town Park is the closest to the copper smelter (0.5 km from the smelter), and is located in the direction of the dominant easterly winds. The measuring site Jugopetrol is located 3.3 km from the copper smelter, where westerly winds bring the pollution from the copper smelter.

During 28 years, the average annual concentrations of arsenic were largely above the LV target value (TV) of  $6 \text{ng}/\text{m}^3$  at all three measuring sites (Town Park, Institute and Jugopetrol)

[4]. The high content of As in the air represents a great risk for the entire environment and human health, because As is regarded as a carcinogenic substance [5].

The given concentrations of arsenic in Figure 2, indicate that the urban-industrial zone of Bor is among the most polluted regions in Serbia and in Europe.

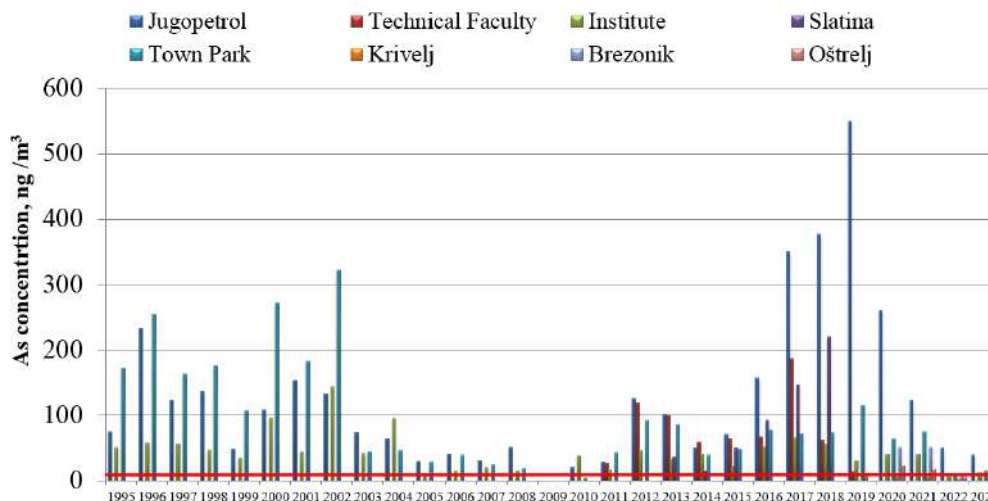


**Figure 2** Average annual concentrations of As in suspended  $PM_{10}$  particles at eight measuring sites in the Bor area in the period 1994–2023. The target value (red horizontal line) is defined for As at  $6 \text{ ng/m}^3$

The annual target value (TV) for Cd content in  $PM_{10}$  samples, defined by the Serbian [4], was exceeded at the sites Jugopetrol during the whole analyzed period and Town Park during 2019 (Figure 3). The measuring site Jugopetrol was characterized as the most polluted one with Cd in the Bor area, based on the annual concentrations in  $PM_{10}$  samples, during the period from 2010 to 2023. The data indicated that the FST implementation did not significantly contribute to the reduction of Cd emissions.

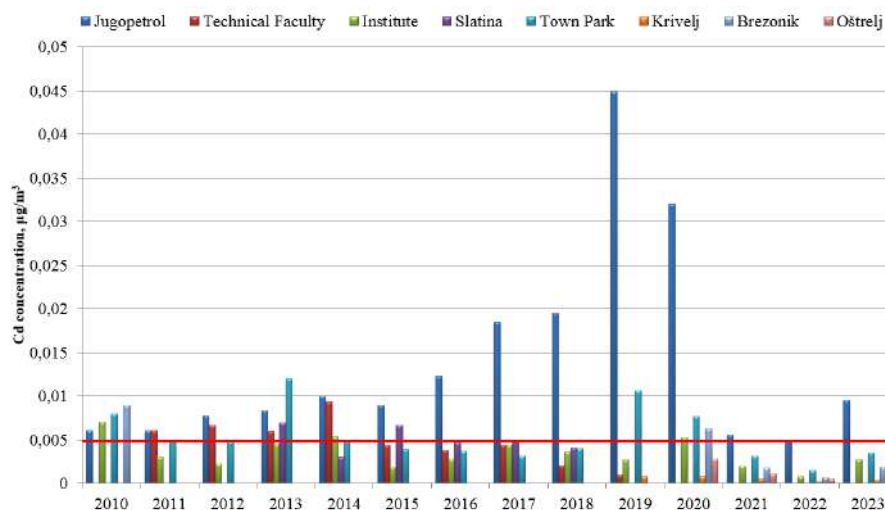


**Figure 3** Average annual concentrations of cadmium in suspended  $PM_{10}$  particles at eight measuring sites in the Bor area from 1994–2023. The target value (red horizontal line) is defined for Cd at  $5 \text{ ng/m}^3$

The annual Pb concentrations in PM<sub>10</sub> exceeded the annual LV of 0.5 µg/m<sup>3</sup> [4] during 2012 at the measuring sites Jugopetrol and Technical Faculty, during 2013 at the sites Jugopetrol and Town Park, during 2014 at the site Technical Faculty, and during 2016, 2017, 2019 and 2020 at the site Jugopetrol (Figure 4). In the period of the new smelter operation, until 2020, the annual limit values were exceeded at the measuring site Jugopetrol.

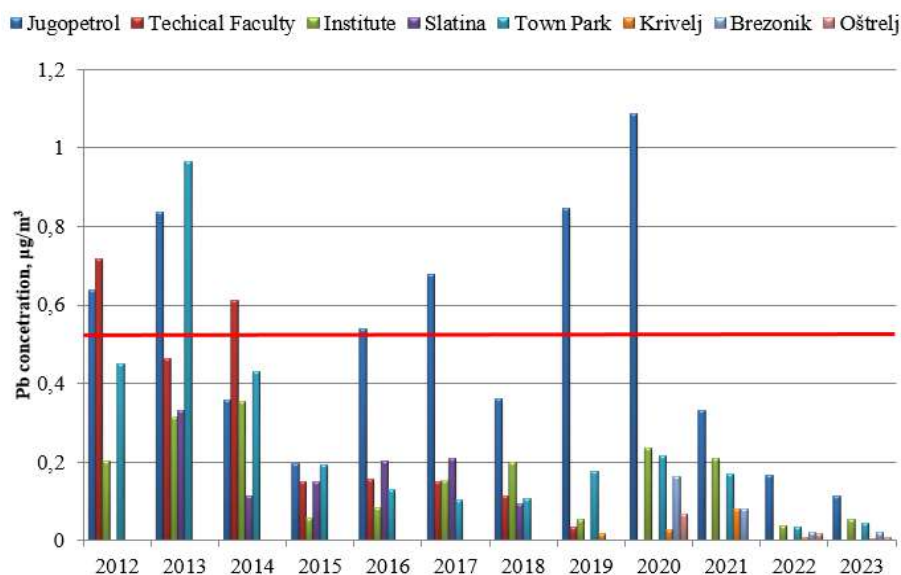


**Figure 4** Average annual concentrations of Pb in suspended PM<sub>10</sub> particles at eight measuring sites in the Bor area from 2012–2023. The limit value (red horizontal line) is defined for Pb at 0.5 µg/m<sup>3</sup>

## CONCLUSION

Over 120 years of mining and metallurgy in Bor and its surroundings have adversely affected the environment of this region. The natural relief of this area has been totally changed, large amounts of artificial tailings hills have contributed to air, water and soil pollution. The copper smelter located in the very center of the city of Bor, has been the source of increased emissions of sulfur dioxide and polluting particles of the smallest dimensions for decades. PM<sub>10</sub> particles, which contain some harmful and carcinogenic substances, such as As and heavy metals (lead, cadmium, nickel, etc.) can cause pollution of the remote areas due to their easy transport by the winds with the most frequently directions.

Since 1995, when air quality monitoring began, arsenic levels in the air have never been within the average annual concentration of 6 ng/m<sup>3</sup>.

## ACKNOWLEDGEMENT

The authors are grateful to the Ministry of Science, Technological Development and Innovation of the Republic of Serbia for financial support, within the funding of the scientific research at the University of Belgrade, Technical Faculty in Bor (No. 451-03-65/2024-03/200131). Our thanks go to Prof. Mara Ž. Manžalović from the University of Belgrade, Technical Faculty in Bor, for providing language assistance.

## REFERENCES

- [1] Šerbula S., Alagić S., Radojević A., *et al.*, Particulate Matter: Sources, Emission Rates and Health Effects, Chapter 4 *in* Particulate Matter Originated From Mining-Metallurgical Processes in Particulate Matter: Sources, Emission Rates and Health Effects, Editors: Knudsen H., Rasmunssen N., Nova Science Publishers US (2012), pp. 91–116, ISBN: 978-1-61470-948-0.
- [2] Council Directive 2008/50/EC of the European Parliament and of the council on ambient air quality and cleaner air for Europe. Off. J. Eur. Union L152 (31) (2008).
- [3] U.S. Environmental Protection Agency, NAAQS Table, *Available on the following link:* <https://www.epa.gov/criteria-air-pollutants/naaqs-table>.
- [4] Official Gazette of Republic of Serbia, Regulation on the conditions for monitoring and requirements of the air quality. No 11/10, 75/10, 63/13 (2013) (*in Serbian*).
- [5] International Agency for Research on Cancer (IARC), Monographs on the Evaluation of Carcinogenic Risks to Humans. Overall Evaluations of Carcinogenicity: An Updating of IARC Monographs volumes 1–42, Suppl. 7. Lyon (1987).
- [6] Šerbula S.M., Kalinovic T.S., Kalinovic J.V., *et al.*, Environ. Earth Sci. 68 (7) (2013) 1989–1998.
- [7] EIA Study-New Smelter and Sulphuric Acid Plant Project, University of Belgrade, Faculty of Metallurgy, SNC Lavalin (2010).
- [8] EIA Study-New Smelter and Sulphuric Acid Plant Project, University of Belgrade, Faculty of Metallurgy, SNC Lavalin (2010).
- [9] Milosavljević J., Šerbula S., Kalinović T., *et al.*, Proceedings of the International Scientific and Professional Conference POLITEHNIKA 2023, 15<sup>th</sup> December 2023, Belgrade, Serbia (2023) 156–161.





## CAUSES OF FLOODING AND MEASURES TO MITIGATE THE CONSEQUENCES - CASE STUDY OF RAKOVICA MUNICIPALITY (BELGRADE, SERBIA)

Irena Blagajac<sup>1\*</sup>, Ivan Samardžić<sup>1</sup>

<sup>1</sup>University of Belgrade, Faculty of Geography, Studentski trg 3/3, 11000 Belgrade, SERBIA

\*irena.blagajac@gef.bg.ac.rs

### Abstract

*The subject of research is the flood potential in the municipality of Rakovica, with emphasis on the Topcider river and its tributaries. The task of the research is to determine the flooding regime of the Topcider River and its tributaries through the analysis of natural and anthropogenic causes of flooding. The task is to analyze the monitoring results of the Topcider river due to poor water quality. The goal of the research is to offer proposals for anti-flooding measures. The features of the relief, terrain slope, hypsometry, hydrographic network, and spatial distribution of clay were analyzed. The paper covers the measures taken to regulate the flow of the Topcider River and its tributaries, which had an impact on the reduction of floods. However, additional scientific research and financial investment are necessary to ensure anti-flood measures. Based on hydrological yearbooks for the period 2010–2021, the flow at the measuring station Rakovica (Topcider Reka) is shown graphically. Using Geographical Information Systems (GIS), the data was analyzed and cartographically displayed. The paper includes the monitoring of the Topcider river from 2008 to 2022 with the aim of showing the poor state of water quality as a result of the lack of communal infrastructure and a large number of “wild” landfills, which increases the risk of soil pollution and the spread of infectious diseases during flooding.*

**Keywords:** flood, water monitoring, flow, mitigation measures, Rakovica.

### INTRODUCTION

The municipality of Rakovica is a Belgrade municipality that covers an area of 3,036 ha. Due to natural and anthropogenic conditions, it is susceptible to flash floods. Natural factors that contribute to the occurrence of floods: geological and pedological base, relief (terrain slope), amount of precipitation, specificity of microclimate, hydrological regime of torrential tributaries and land use. Anthropogenic factors are deforestation, agriculture, and unplanned construction. In the paper, the mentioned factors were analyzed with the aim of proposing anti-flood measures on the territory of the Municipality.

### MATERIALS AND METHODS

Methods of analysis and synthesis were used in the paper, with the aim of processing the collected and researched data on the flow, the potential of flooding and monitoring. Data available in strategic and planning documents, hydrological yearbooks and on the official website of the Municipality were analyzed. Using the analytical and synthesis method,

conclusions were drawn about the consequences that floods have on the population and their activities and on the environment. Using the comparative method, the previous situation on the Topcider River was compared with the current one, and conclusions were drawn about anti-flooding measures. Data from the hydrological yearbooks of the Republic Hydrometeorological Institute were used for the graphic presentation of the flow, data from the measuring station Rakovica (Topcider river) were processed, the research refers to the ten-year period 2010–2021 (apart from 2019 due to incomplete measurement data and 2020 because there is no flow measurement data). The research results are cartographically displayed using QGIS 3.16. [1–4].

## **RESULTS AND DISCUSSION**

### **Natural and geographical features**

The climate in the municipality of Rakovica is moderate continental. The most common soil types are alluvial soil, pseudogley and alluvial soil. Along the course of the Topcider river and its tributaries, there is an alluvial environment and lake clay sediment, which influence the soil in the eastern part to be susceptible to sliding. The karst characteristics of the terrain are also represented, which is important due to the hydrological regime that affects the intensity of floods [5–7].

The Topcider river is the right tributary of the Sava river and forms the largest river basin in the administrative territory of the city of Belgrade [8]. The municipality of Rakovica is in the downstream part of the Topcider river basin, which is characterized by a high degree of urbanization, which affects the change in the hydrological regime [9]. Illegal and unplanned construction of buildings, infrastructure, lack of communal infrastructure is represented in this area, which causes wastewater to flow directly, without purification, into waterways, and this leads to pollution of all environmental media.

The basin of the Topcider river is characterized by a pronounced dissection of the relief, with unevenness between the top of Avala (506 m above sea level, the highest point of the watershed) and the main stream, where, less than 2.5 km away, there is a relative height difference of 390 m and a terrain slope of 15.6%. The area of the basin that gravitates towards the Rakovica profile is 126.87 km<sup>2</sup> [7,10]. Such terrain conditions are a prerequisite for the occurrence of torrential floods. Slopes up to 35° are pronounced (Figure 1), and the highest peak is Orlovac, 217 m above sea level (Figure 2). The clay content is significant due to the occurrence of a water-bearing substrate, which is built of water-bearing sediments and causes landslides and floods. Clay is represented in the range of 22–32% in the territory of the municipality of Rakovica (Figure 3) [11].

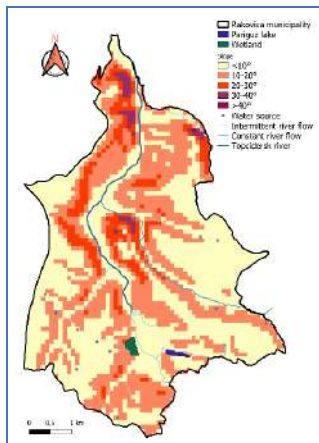


**Figure 1** Slope and hydrology [1–4]

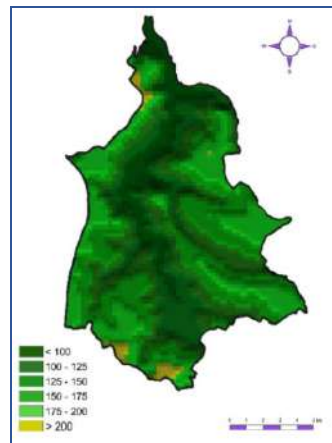


**Figure 2** Hypsometry [1–4]

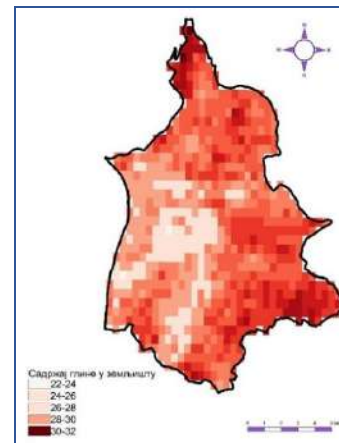


**Figure 3** Clay content in the soil (%) [1–4]

### Hydrographic characteristics of the Topcider river

Until 2014, 34 torrential flood events were recorded in the Topcider river basin, which also claimed human lives [7]. The municipality's hydrographic network (Figure 1) consists of the Topcider river (the right tributary of the Sava river) with its tributaries Rakovički potok, Jelezovac, Kaljavi potok, Manastirski and others. The length of the basin is 27 km, and the area is 146.6 km<sup>2</sup>. Topcider river is an epigeny [12,13]. At the end of the 1980s, the artificial reservoir “Pariguz” was built in the Municipality, on the stream of the same name, with the aim of flood protection, to preserve the biological minimum, to irrigate agricultural areas, for sports and recreation. The volume of the reservoir is 41,400 m<sup>3</sup>, and for receiving the flood wave it is 105,300 m<sup>3</sup>. The average sediment transfer on the barrier profile is 828 m<sup>3</sup>/y [14].

After the flood in 1985, two reservoirs were built on the Pariguz stream (Rakovica municipality) and on the Bela river (Voždovac municipality), with studies and plans for the construction of a larger number of reservoirs in the following period. The idea is to build the planned facilities as far upstream as possible, which would make the municipality of Rakovica safer from floods. The facilities that are planned resemble the two existing reservoirs, and the facility that stands out from the others is planned on the Rakovica stream and will have concrete dams that are placed centrally in the axis of the watercourse and that are combined with earthen blocks. The central concrete part has culverts for small and medium water [9]. According to research by Plavšić *et al.* the construction of all planned reservoirs will not have the effect of mitigating the maximum flows by more than 20% compared to the existing situation, so it is concluded that there is no cost-effectiveness for the construction of all facilities. The reason for the low profitability is the planning of the construction of facilities that should control large waters from small catchment areas. The unprofitability is also seen in the fact that the fastest runoff occurs in the most downstream urbanized parts of the watershed located in the municipality of Rakovica, where no measures are foreseen to control high water levels.

The average annual amount of precipitation in Belgrade is 684.3 mm [15]. According to research by Petrović [7] the absolute maximum daily precipitation amounts are expressed in the summer half of the year, and precipitation values range from 15 mm to over 100 mm in 24 h. This is the reason for the appearance of flood waves. Flow is one of the main factors that

increases the potential for flooding, so it is necessary to observe extreme flows, that is, absolute maximum and minimum flows [16]. Medium monthly and medium annual flows on the Topcider river at the hydrographic station Rakovica (Topcider Reka) were analyzed, with the aim of determining the change in flow according to the months, and for the sake of the precision of the research, the ten-year period 2010–2021 was observed. The maximum daily flow of  $109 \text{ m}^3/\text{s}$  was measured on May 15, 2014, while the average value for the month of May 2014 was  $1.19 \text{ m}^3/\text{s}$ , and 20 days of that month had a flow of less than  $1 \text{ m}^3/\text{s}$ . It was in May 2014 that the Topcider river and its tributaries flooded (Figure 4) [16]. In May 2013, the maximum daily value was  $1.4 \text{ m}^3/\text{s}$ .

As a result of melting snow and a large amount of precipitation, the largest flow in the territory of the Municipality is in spring, and a special problem is flash floods during spring showers when a large amount of rain falls in a short period of time (Figure 5). The average annual flow (for a ten-year period) varies from  $0.35 \text{ m}^3/\text{s}$  (measured in 2011 and 2017) to  $1.14 \text{ m}^3/\text{s}$  (measured in 2010) (Figure 6). In March and May, the flows are the most pronounced, while the lowest flow is in the summer months due to high temperatures. The results of the average maximum monthly flow (Figure 7) indicate that May is the month with the most pronounced extreme flow due to showers. Based on the standardized deviation of the median annual flows, it can be concluded that the biggest deviation was in 2010, 2014 and 2015 (Figure 8, the orange line indicates the size of the deviation, and the rectangles indicate how much the annual mean flow deviated from the mean value). May and March have the most pronounced deviations and extremes due to showers (Figure 9).

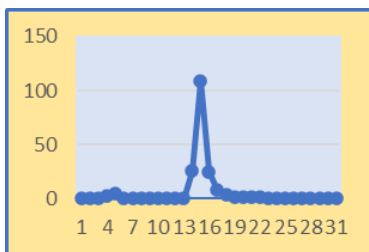


**Figure 4** Flow values in May 2014 [16]

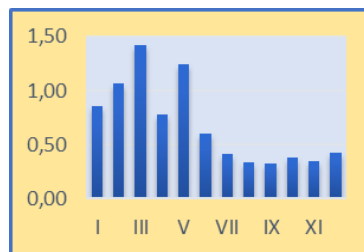


**Figure 5** Average monthly flow 2010–21 [16]

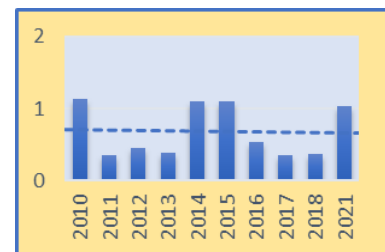


**Figure 6** Average annual flow 2010–21 [16]

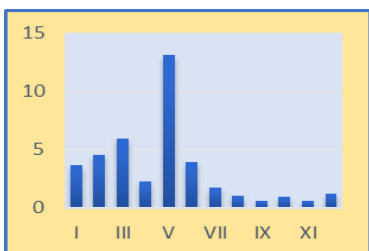


**Figure 7** Average max monthly flow 2010–21 [16]

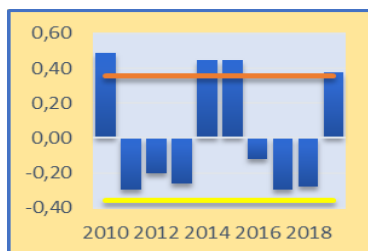


**Figure 8** Standardized deviation of mean annual flows [16]



**Figure 9** Deviation of min and max flows from the average [16]

### Monitoring of the Topcider river

Monitoring of the Topcider river in a fifteen-year period (2008–2022) indicates a catastrophic state of water quality. In the mentioned period, the most frequent sampling

involved one monthly sample from the measuring point of Tsareva ćuprija, i.e. near the bridge next to the hippodrome. However, there were exceptions, especially in the period 2012–2016 when fewer samples were taken for analysis. In 2018, during the analysis of the sample (September), the presence of Pb, PCB, Cu, Ni was determined. In May 2019 and 2020, during the analysis of samples (May), the presence of Ni and Hg was determined, and in September of the same year, the presence of Ni was determined. The presence of Ni was also determined in water samples from September 2021, then July and September 2022.

According to the Rulebook on parameters of the ecological and chemical status of surface waters and parameters of the chemical and quantitative status of underground waters [17] in the observed period, Topcider river has a poor ecological status, according to the Regulation on limit values of pollutants in surface and underground waters and sediment and deadlines for reaching them [18] Topcider River belongs to the V class of watercourses and is one of the most polluted rivers in the Republic of Serbia.

The former industrial zone is located along the course of the Topcider river, in the past the industry was the main source of watercourse pollution. Today, many companies are shut down, repurposed, under bankruptcy or have reduced production capacity, so they are no longer the main factor in pollution. However, there are increased areas under residential buildings and buildings with commercial content that pollute the flow of the Topcider river with municipal waste. A highway and a railway pass through the Topcider river valley, which are the transport routes for hazardous waste. The problem is the “wild” landfills on the Topcider River and its tributaries, as well as the discharge of untreated municipal wastewater into the recipient [19,20], and the health of the population and the environment is especially threatened when water overflows from the riverbed and floods the terrain with pollutants. Table 1 shows the monitoring results of the Topčider river.

*Table 1 Monitoring of the Topcider river [21]*

River	Year	Number of samples	II class		V class	
			River waters		Microbiological and physical-chemical	
			No	%	No	%
Topcider river (Bridge near the hippodrome)	2008	10	-	-	8	80
	2009	10	-	-	8	80
	2010	10	-	-	7	70
	2011	10	-	-	8	80
	2012–2015	23	-	-	23	100
	2016	6	-	-	6	100
	2017	12	-	-	12	100
	2018	12	-	-	12	100
	2019	12	-	-	12	100
	2020	10	-	-	10	100
	2021	10	-	-	10	100
	2022	12	-	-	12	100

### **Anti-flood measures**

It is necessary to explain to the local community the advantages they will have from afforestation and conversion of areas, as well as their role in the activities [22]. Since the municipality of Rakovica was industrially developed at the end of the last century, there are still “brownfield” locations that can represent the potential for reducing flooding processes. The revitalization of “brownfield” locations through reforestation would contribute to an increase in the percentage of greenery and a reduction in flood consequences. Limitations that can slow down the implementation of anti-flood measures are the financial difficulties of LGUs [23]. “Brownfield” locations are positioned along the course of the Topcider river and can be converted into facilities that will contribute to the purification of wastewater, which will have a higher percentage of greenery, or which will be a space for organizing educational workshops on the topic of fighting floods and reducing the pollution of watercourses.

To reduce the negative effects of flooding, it is necessary to consider the collection of rainfall from unplanned buildings and infrastructure [24]. It is necessary to carry out an inventory of illegally built buildings and infrastructure, and then prepare planning documentation that will include mitigation of rainwater runoff, with the aim of reducing pressure on sewage systems. Places where a large amount of precipitation accumulates, which are usually roads and intersections, should be monitored.

By establishing the Cadastre of Pollutants for the sources of pollution of the Topcider River, the coordinates of the outlets of untreated wastewater, descriptions, and photos of the outlets, monitoring results, monitoring of changes, with regular data updates and cartographic display would be determined. This system should be introduced due to the large number of illegal and unregistered discharges from households and from agriculture. The number of registered sources of pollution in the Topcider river basin is 219 [25]. To facilitate the monitoring and control of flash floods in the Topcider river basin, it is necessary to provide access to the Flash Flood Inventory to a larger number of users, regularly update the database, and categorize flash flood events according to intensity categories. It is necessary to integrate the Inventory into the national database on natural disasters, as well as into European databases on natural hazards [26]. To monitor the degree of risk of flooding, it is necessary to work on risk maps, and to assess the risk, it is necessary to know the characteristics of the flood wave, the topography of the terrain and the purpose of the surfaces. It is necessary to determine the potential damage, which is an expensive and complicated process [27]. The continuation of illegal construction in Rakovica affects the lack of space for flood risk management, but also increases the risk of human casualties and material damage in emergency situations. The proposal is to develop a comprehensive strategy for the integral management of catchment areas with the cooperation of water management, spatial planning, and environmental protection [9]. Preventive measures are a long-term process, they relate to reforestation, spatial planning of construction of buildings, streets and infrastructure, prohibition of construction on land prone to sliding and monitoring the trend of floods and high water throughout history. The construction of artificial reservoirs, such as the “Pariguz” lake, contributes to the reduction of floods. It is also possible to reduce the consequences of floods by strengthening the coastal fortifications and erecting ramparts. Educating the



population on how to act in an emergency and how to evacuate allows for an effective response to floods when they occur [28].

## **CONCLUSION**

In the municipality of Rakovica, the causes of floods are natural and anthropogenic. Many inhabitants and their activities influence the occurrence of floods. Lands that were most often used for agriculture and green areas, become places of construction of illegal and unplanned residential and commercial buildings and infrastructure. This affects the increase in the degree of erosion and the occurrence of flash floods, due to the lack of green areas and unfulfilled construction conditions. By increasing the number of untreated wastewater discharges, the degree of pollution of the Topčider river and its tributaries increases, which affects the fouling of the riverbed, and the increase in the number of “wild” landfills contributes to the burying of the riverbed with waste. In this way, the potential for flooding increases. That is why it is important to direct all available resources (people, knowledge, financial and technical-technological resources) to flood prevention measures.

## **ACKNOWLEDGEMENT**

*The study was supported by the Ministry of Science, Technological Development and Innovation of the Republic of Serbia (Contract number 451/03/65/2024-03/200091).*

## **REFERENCES**

- [1] Topographic map, Belgrade 1:100,000 sheet 429 Belgrade, Institute of Military Geography. Belgrade. Serbia (1985–1987).
- [2] Google Earth. *Available on the following link:* <https://earth.google.com/web/>
- [3] Open soil grids. *Available on the following link:* <https://soilgrids.org/>
- [4] USGS, USGS EROS Archive - Digital Elevation - SRTM. *Available on the following link:* <https://www.usgs.gov/centers/eros/science/usgs-eros-archive-digital-elevation-shuttle-radar-topography-mission-srtm-1>
- [5] City of Belgrade, Administration of the City of Belgrade. GUP Belgrade 2021 (“Official Gazette of the City of Belgrade”, no. 11/16). Belgrade, Serbia, (2021).
- [6] Pavlovic, M. Geography of Serbia. University of Belgrade - Faculty of Geography, Belgrade, Serbia (2019). ISBN: 978-86-6283-067-8.
- [7] Petrovic, A., Factors causing flash floods in Serbia - Doctoral dissertation. University of Belgrade - Faculty of Forestry. Belgrade, Serbia (2014).
- [8] Dragovic N. Study of the integral arrangement of the Topčider river basin in the function of sustainable management of natural resources. Faculty of Forestry, Faculty of Civil Engineering, Belgrade, Serbia (2008).
- [9] Plavsic, J., Jelusevic, D., Jevtic, D., Vodop.-Serbian Drain. and Irrigat. Com. 0350-0519, 50 (2018) No. 291–293 (2018) 47–58.

- [10] Dragicevic S., Ljesevic M., Kostadinov S., *et al.* Proceedings of the Faculty of Geography, University of Belgrade (68), Belgrade, Serbia (2018), 53–70.
- [11] Blagajac, I. Geospatial analysis of the municipality of Rakovica. University of Belgrade - Faculty of Geography. Belgrade, Serbia, (2021).
- [12] Milovanovic, I., Stefanovic, M., Gavrilovic, Z. Monitoring of torrential floods on the Topcider river in real time. Belgrade, Serbia, (2010).
- [13] Zermeski, M. Proceedings of the “Jovan Cvijic” Geographical Institute, 20, Belgrade. Serbia (1965).
- [14] RS, City Institute for Public Health. Report on the water quality of the under Avala reservoirs "Pariguz" in Resnik, "Bela reka" in Ripanj and “Duboki potok” in Barajevo during 2016 based on Contract V-01 no. 4011-51/2016, Belgrade, Serbia (2017).
- [15] Dukic D., Gavrilovic Lj., (2008): Hydrology, Textbook Institute, Belgrade. ISBN: 978-86-17-15346-3.
- [16] Republic Hydrometeorological Institute. Hydrological yearbook 1. Surface water for the period 2010-2021, *Available on the following link:*  
[http://www.hidmet.gov.rs/latin/hidrologija/povrsinske\\_godisnjaci.php](http://www.hidmet.gov.rs/latin/hidrologija/povrsinske_godisnjaci.php), 25.4.2023.
- [17] Official Gazette of the RS, Rulebook on parameters of the ecological and chemical status of surface waters and parameters of the chemical and quantitative status of groundwater (“Official Gazette of the RS”, no. 74/11), Belgrade, Srbia (2011).
- [18] Official Gazette of the Republic of Serbia, Regulation on limit values of pollutants in surface and underground waters and sediment and deadlines for reaching them (“Official Gazette of the Republic of Serbia”, No. 50/12), Belgrade, Srbia (2012).
- [19] Samardzic, I., Filipovic, D., Andjelkovic, G., *et al.*, Seventh scient. and profess. meeting with internat. particip. - Local govern. in plan. and arrang. of space and settle., Trebinje, Bosnia and Herzegovina (2018).
- [20] Samardzic, I., Radosavljevic, M., Bozic, M., *et al.*, Sixth scientific-expert meeting with internat. particip. - Local self-govern. in plan. and develop. of space and settle. Association of Spatial Planners of Serbia, University of Belgrade - Faculty of Geography. Vrsac. Serbia (2016).
- [21] City of Belgrade, City Administration, Secretariat for Environmental Protection. Environmental quality in Belgrade for the period 2008-2022, Belgrade, Serbia (2019).
- [22] Samardzic, I., Gazette of the Serbian Geograp. Soc., XCIV- no. 2, (2014) 15–30.
- [23] Samardzic I., Gazette of the Serbian Geograp. Soc., XCV-no. 4 (2015) 159–172.
- [24] Despotovic, J., Plavsic, J. Todorovic, A. Assoc. for Water Tech. and Sanit. Engin. XXXIX (4), Belgrade, Serbia (2009), 47–56.
- [25] Petric, I., Forestry 3-4. Belgrade, Serbia (2016) 155–162.
- [26] Petrovic A., Kostadinov S., Pol. J. Environ. Stud. 23, No. 3 (2013), 823–830.
- [27] Jovanovic, M., Todorovic, A., Rodic, M. Vodop.-Serbian Drain. and Irrig. Com. 0350-0519, 41, 237–239 Belgrade, Serbia (2009) 31–45.

- [28] Blagajac, I., Protec. and rescue tact. in emerg. situat.: Experi. from the field and less. lear. Scientific and Professional Society for Risk Management in Emergency Situations, International Institute for Disaster Research, Belgrade, Serbia, (2021) 53–64.



## SIMULATION OF THE EAF DUST RECYCLING

Žarko Radović<sup>1\*</sup>, Nebojša Tadić<sup>1</sup>

<sup>1</sup>University of Montenegro, Faculty of Metallurgy and Technology,  
Cetinjski put bb, 81000 Podgorica, MONTENEGRO

\*zarkor@ucg.ac.me

### Abstract

*For economic separation of Zn and Pb from electric arc furnace (EAF) dust its content should be greater than 25%. In this paper, it was calculatedly analyzed the effect of process parameters on dynamics of returned dust enrichment. Chemical analyzes of EAF dust from Niksic Steelworks and the mass balance of an 60 t EAF were used as a starting point. Simulation of changes in the Zn and Pb content during the return melting was carried out. Results of simulation show that in all analyzed variants, the total content Zn+Pb in slag does not exceed 0.1%.*

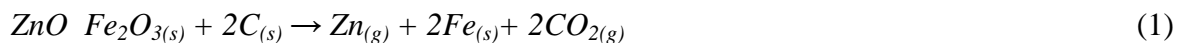
**Keywords:** EAF dust, melting, enrichment.

### INTRODUCTION

Electric arc furnace dust (EAFD) as a by-product of steel production can be deposited, which requires special conditions arising from the fact that EAF dust is classified as hazardous waste. If EAF dust is treated in this way, a large amount of important metals remains trapped in the dust, which would be an ineffective solution from the point of view of economics and metallurgy.

This type of dust is an form of spherical particles whose granulation is below 1 μm. In the production of carbon and alloyed steel EAF dust is richest in Zn and Pb, while in stainless steel production it is enriched with Cr and Ni. The chemical composition of EAF dust depends on the scrap quality and the technological parameters. Recycling of dust by injecting into EAF reduces the total amount of dust [1].

During pyrometallurgical treatment of dust in an electric are furnace, the reduction of components occurs according to the following reactions [2,3]:



### MATERIALS AND METHODS

The empirical data on the distribution of Zn and Pb at the metal-slag-gas boundary were used to derive the analytic expressions. For theoretical calculation EAF dust from steelworks Niksic was used (Figure 1). The average chemical composition of EAF dust is shown in Table 1.

The influence of two groups of parameters was carried out: those that are the results of circumstances which cannot be influenced during the process (mass and chemical composition of primary dust) as well as the influence of “sliding” parameters that can be changed (mass of returned dust).

**Table 1** The average chemical composition of EAFD from steelworks Niksic

Element	Fe	Si	C	Mn	Cr	Ni	Pb	Zn	Ca	Mg
Mass%	42–47	1.5–1.8	0.6–0.9	~4.5	~0.5	~0.4	~2.5	~8	~7	~4

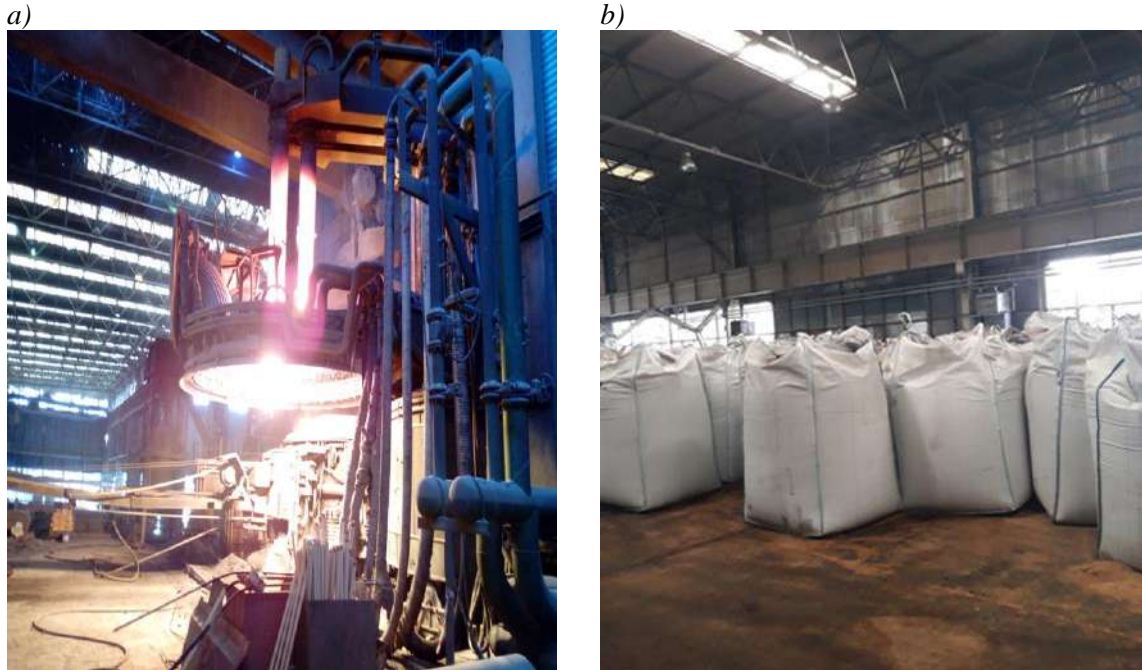


**Figure 1** Steel plant Niksic: a) electric arc furnace; b) EAF dust

The enrichment of EAF dust is a multiple return process, which is repeated in **-n-** steps. The content of analysed elements after each step can be calculated as:

$$X_{(n)}=X_{(0)}+a_1X_{(0)}+a_2X_1+\dots\dots+a_nX_{(n-1)} \quad (3)$$

where: -  $X_{(0)}$  – initial content of Zn and Pb in EAF dust,  
 - n- number of steps,  
 -  $a_n$  - empirical coefficients.

The following expression was used to define the correlation of Zn and Pb content [1]:

$$Pb=0.1169 (\%Zn)+0.5544 \quad (4)$$

Since it has been observed in practice that, depending on the initial raw materials, the mass of primary EAF dust ranges from 10–15 kg/t of steel, the average value of 12 kg/t was used

in the simulation [1,2,4]. In theoretical simulations, it is feasible for the mass of primary EAF dust to be less than that of the return dust, EAFD(r), and therefore, calculations were analyzed for values of 8 and 10 kg/t.

## RESULTS AND DISCUSSION

Although it is possible analytical dependencies for higher initial Zn percentages, in this case, the option with  $Zn_{(0)}=8\%$  was analyzed. This choice was made because chemical analyses of EAFD during the production of high-quality alloy steels showed values.

From the diagram (Figure 2), it can be observed that in both cases, the Zn content in EAF dust increases.

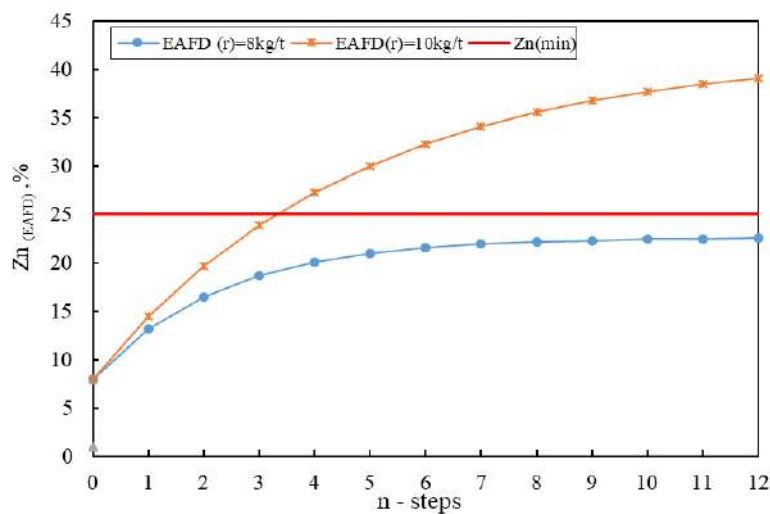


**Figure 2** The changes of %Zn in EAF dust

According to the empirical expression of the  $Pb=f(Zn)$  dependence, the change in %Pb during multiple return injections of EAF dust into the furnace was obtained (Figure 3).

From the diagram (Figure 2), it can be observed that in both cases, the Zn content in EAF dust increases. However, in the case where  $EAFD(r)=8$  kg/t, the rate of increase is notably lower, leading to failure in attaining the minimum Zn concentration (Zn min).

By increasing EAFD to 10 kg/t, the desired Zn content is reached within just 4 steps. Nevertheless, any increase in the number of EAFD return injections into the furnace would realistically impede the technological process.

From the diagram (Figure 3), it is observed that the trend of increasing %Pb is somewhat slower than that of Zn, so that at the end of the simulated process of 10 steps, a content of 4.5% is achieved.

Based on empirical data, the following distribution of Zn from primary dust was observed [1]:  $Zn_{(dust)}\sim 97\%$ ,  $Zn_{(metal)}\sim 1\%$  and  $Zn_{(slag)}\sim 2\%$ . Since both Zn and Pb are highly detrimental to the quality of steel, it is crucial that their content in the metal is negligibly small.

Taking into account practical experiences in the valorization of steel slag, the maximum allowable content of  $(Zn+Pb)_{slag}$  has been defined, amounting to 0.1%. According to the



stated distribution of Zn between metal, slag, and gas, with the interdependence of Zn and Pb, the simulation has demonstrated that in all considered variants, the (Zn+Pb) content is far below the critical value (Figure 4).

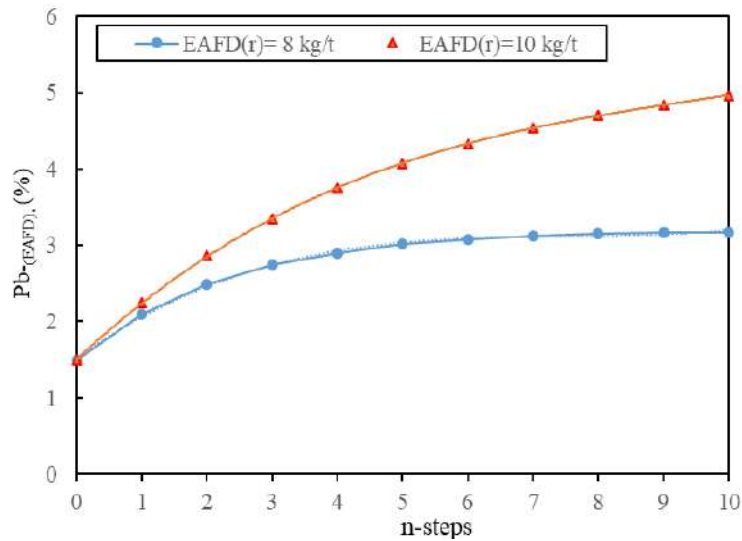


**Figure 3** The calculated changes of %Pb in EAF dust

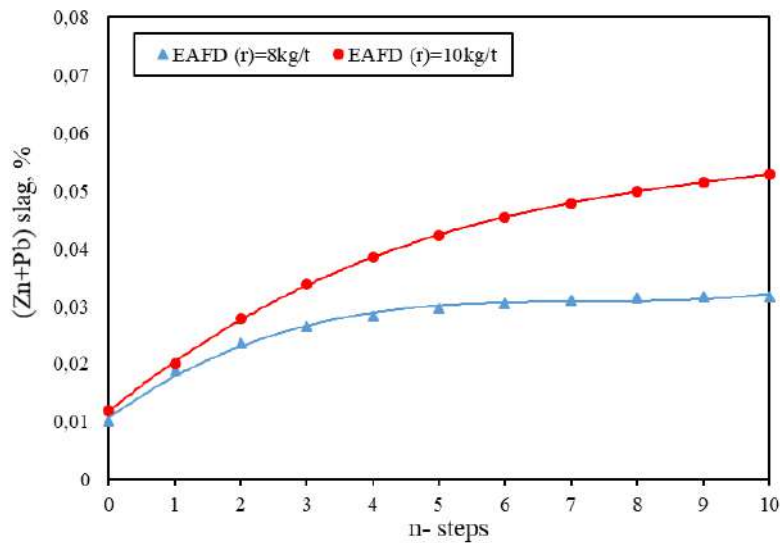


**Figure 4** Simulation of the values of  $(Zn+Pb)_{slag}$

In this case, the slag meets the criteria of the “leaching” test regarding the content of Zn and Pb, indicating the possibility of further treatment.

The simultaneous influence of two parameters: mass of primary and returned dust on its “enrichment” is simulated and shown in Figures 5 and 6. It can be seen on the graph (Figure 5) that in the case of  $m_{(EAFD)primary}=15$  kg/t, it is then practically impossible to reach  $Zn_{(min)}=25\%$  regardless of the increase in the mass of EAFD<sub>(r)</sub>.

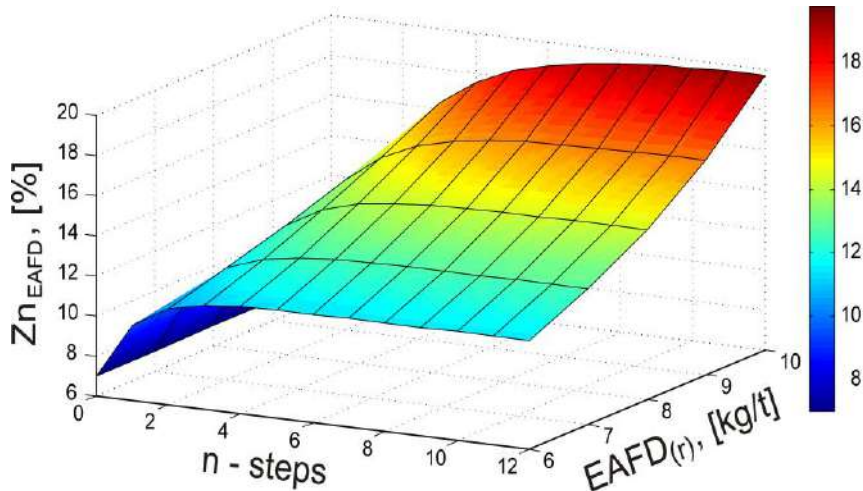


Figure 5  $Zn_{(EAFD)}$  as a function of  $EAFD_{(r)}$  ( $m_{EAFD_{primary}}=15$  kg/t)

In the case of  $m_{EAFD(primary)}=10$  kg/t, (Figure 6) the  $m_{(EAFD)(r)}=8$  kg/t is needed to reach the value of  $Zn_{(min)}$ .

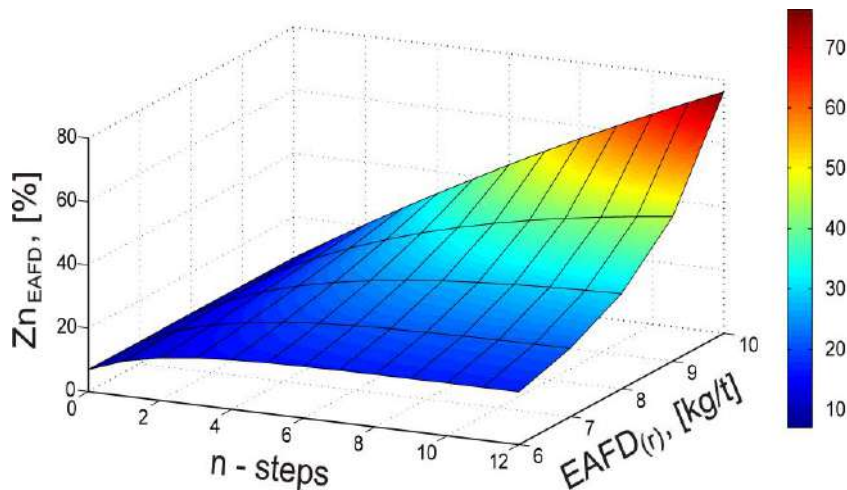


Figure 6  $Zn_{(EAFD)}$  as a function of  $EAFD_{(r)}$  ( $m_{EAFD_{primary}}=10$  kg/t)

## CONCLUSION

Based on analytical simulation it's noticeable that greatest effect of enriching “poor” EAF dust was achieved in the case of a small mass of primary dust by increasing the mass of the return EAF dust to the level technological justification. For higher values of primary EAFD ( $m=15$  kg/t) the influence of return dust is reduced due to its smaller relative share in the total mass. Simulation of changes in the %Zn and %Pb in the slag, during enrichment of EAFD show that in all analyzed variants the total content  $(Zn+Pb)_{slag}$  does not exceed the potentially problematic limit of 0.1%.

The presented analytical correlations give the possibility to theoretical predict the dynamics of enrichment of EAF dust.

## **REFERENCES**

- [1] Jensen J., Wolf K., MPT 3 (1997) 60–68.
- [2] Derda W., Metalurgija 48 (2009) 27–32.
- [3] Pickles C., J. Haz. Mat. 150 (2008) 265–278.
- [4] Malecki S., Gargul K., Warzecha M., Materials 14 (2021) 6061–6070.



## DEVELOPMENT OF METALLURGY AND ENVIRONMENTAL PROTECTION IN THE REPUBLIC OF CROATIA IN THE PERIOD FROM 1900 TO 2020

Mirko Gojić<sup>1,2\*</sup>, Stjepan Kožuh<sup>1</sup>, Ivana Ivanić<sup>1</sup>, Daniela Dumenčić<sup>1</sup>

<sup>1</sup>University of Zagreb, Faculty of Metallurgy, Aleja narodnih heroja 3, 44000 Sisak,  
CROATIA

<sup>2</sup>University North, Trg Dr. Žarka Dolinara 1, 48000 Koprivnica, CROATIA

\*gojic@simet.unizg.hr; mgojic@unin.hr

### Abstract

*Metallurgical activity on the territory of today's Republic of Croatia is more than 6000 years old. An important development of metallurgy is from 1945 and investments in environmental protection is from 1980s. Unfortunately, the current metallurgical production (steel from electric arc furnaces, aluminium products and castings) is 10 times lower than the production at the end of the 1980s. The current state of environmental protection in the Republic of Croatia is satisfactory, which is mainly due to lower industrial metallurgy (coke, pig iron, ferroalloys, etc. ceasing production) and the use of modern technologies for the production of semi-products and products, but also due to higher investments in environmental protection and energy efficiency.*

**Keywords:** metallurgy, environmental protection, ferroalloys, steel, castings.

### INTRODUCTION

The history of civilization is closely related with the development of materials, among which are metallic materials has primary role [1,2]. Metallurgy is of great importance for the development of industrial society. The activity of metallurgy on the territory of today's Republic of Croatia is more than 6000 years old [1]. Minting of coins began in the Roman Empire in the town of Siscia (262) and the area current Sisak-Moslavina County has a long mining and metallurgical tradition in the production of pig iron and castings.

The development of foundry began in the Copper Age. Castings were discovered in Slavonia during the Baden culture, the Vučedol culture, etc. In 15<sup>th</sup> century, the first foundries of guns, bells, etc. were opened. The first industry was founded in Rijeka (1853) for the casting of anchors.

In addition to the bell foundry, numerous foundries for other purposes were established in Zagreb (from 1874, etc.). Until the World War II, metallurgical activity in today's Republic of Croatia was based on the production of pig iron in old stone blast furnaces from 19th century and from 1939 in a new blast furnace in the Caprag smelter [3], the start of production of ferroalloys (1931) in Šibenik and Dugi Rat, the production of primary aluminium in Lozovac near Šibenik (1937) as well as castings in numerous foundries [1]. The World War II reduced or stopped metallurgical production.

## METALLURGICAL COMPANIES IN THE REPUBLIC OF CROATIA IN THE PERIOD FROM 1945 TO 2020

The development of metallurgy continued after the World War II until the end of the 1980s (Table 1). Restoration and modernization of existing companies and opening of new ones: Iron and Steel Works Sisak (1946), Factory light metals Šibenik, Iron and Steel Works Split (1971), numerous foundries, etc.

*Table 1 Metallurgical companies and products range semi-products and/or products in 1989 [1]*

Company	Products range	kt
Iron and Steel Sisak Works	Coke	780
	Pig iron	214
	Crude steel	365
	Steel tubes	357
Iron and Steel Works Split	Crude steel	120
	Rolled products from concrete steel	105
Factory light metals Šibenik	Al-blocks	50
	Rolled Al and Al-alloys	120
Factory of ferroalloys and electrodes (Šibenik, Dugi Rat)	Ferroalloys and electrodes	168
Mill steel Kumrovec	Civil engineering profiles	40
Armko Konjščina	Wire and reinforcement	
Mill of seam pipes Potpićan	Cold rolled seam pipes	12
Foundries	Ferrous and non-ferrous castings	127
	Total	2458.8

Iron and Steel Works Sisak was an integrated iron and steel works with production of seam and seamless pipes. This company produced SM and electro steel and was the only producer of seamless pipes in Yugoslavia [4]. Iron and Steel Works Split was established due to the rapid development of the construction industry for the reinforcement of reinforced concrete bars, wire, mesh, etc. [5].

The factory of light metal Šibenik (TLM) produces primary aluminium, Al-alloys from secondary aluminium and rolled products (strips, sheets, foils, etc.). The factory aluminium Lozovac was produced primary aluminium, Al-rolled products and Al-alloys from secondary aluminium. The Electrode and Ferroalloy Factory (TEF) in Šibenik and the Carbide and Ferroalloy Factory in Dugi Rat near Split have been producing ferroalloys, among other things, since 1931. Mill of steel Kumrovec has been producing civil engineering profiles since 1973. Armko Konjščina has been producing rolled and drawn wires and reinforcements for civil engineering since 1963. Potpićan seam pipe rolling mill from 1977 produced cold-formed seam pipes and galvanised pipes of various sections. The foundries produce castings from grey iron, ductile iron, etc., as well as castings from light metals.

Unfortunately, metallurgical production in the early 1990s is 10 times lower than in the late 1980s due to the consequences of the war, the wrong conversion and privatization, the lack of a decade-long industrial policy and industrialization by 2020 (Table 2). Many metallurgical companies are shutting down: the production of ferroalloys in Šibenik (1995) and Dugi Rat (1998), Iron and Steel Works Split (2018), numerous foundries, etc. Today,

metallurgical production has been reduced to the production of steel in electric arc furnaces, aluminum rolled products and castings (ferrous and non-ferrous castings), which are foreign-owned.

*Table 2 Production of metallurgical products during 2020 [1]*

<b>Metallurgical products</b>	<b>Production, kt</b>
Continuously casted steel	45
Al-products (rolled strips, sheets and folis)	111.8
Ferrous and non-ferrous castings	91.7
Total	248.5

Steel production takes place in a modern electric arc furnace with secondary metallurgical equipment (ladle-furnace, vacuum degasser, etc.) in the company ABS-Sisak Ltd. The production of Al-products takes place in the company Impol-TLM Ltd. The most important foundries in the Republic of Croatia today are: P.P.C Buzet Ltd., Ferro-Preis Ltd., Lipovica Ltd., LTH Metalni lijev Ltd., MIV Varaždin join-stock, Plamen Ltd., RS Metali Ltd., Almos Ltd., Dalekovod Oso Ltd., Saint Jean Industroies Ltd. and others [1].

## **ENVIRONMENTAL PROTECTION IN THE METALLURGY**

It is well known that metallurgical production generates by-products (red mud, slag, dust, etc.). From an environmental point of view, a very small or almost no investment at the end of the 1950s. In TEF Šibenik (until 1958) and in Dalmacija Dugi Rat (until 1962), practical open electric-arc furnaces for the production of ferroalloys were in operation. Serious investments in environmental protection began in the 1980s. In TEF Šibenik, a device for dust filters in the treatment of electrodes was installed (1987), etc. Unfortunately, the production facilities in TEF Šibenik were demolished without taking into account the restoration of land from the point of view of environmental protection. Slag, coal tar, phenolic compounds and remnants of graphite electrodes were left behind (Figure 1a). Later, the waste was excavated, ground and the slag transported. Unfortunately, the urban renewal area of the former TEF Šibenik is not fully planned [6]. A dust filtration system was installed near the electric-arc furnace for the production of ferroalloys in the Dalmacija Dugi Rat carbide and ferroalloy factory. At that time, it was the most modern system in Europe [7]. About 2/3 of the solid particles were collected in the filter system. The factory was demolished (2009), but the land is not restored (Figure 1b).

Slag delayed near the sea and in the sea (Figure 1b) contains primary metal oxides (Table 3). Industrial slag or the so-called “black mountain” with around 1.67 million m<sup>3</sup> of slag and other waste is still not recovered on sustainable manner.

The former Iron and Steel Works Sisak is to take environmental protection into account, particularly in the processing of iron ore, the construction of the Bakar coke plant, etc. [4]. The so-called new agglomeration plant (1987.) has maximum environmental protection using by electro-filter plants. Coke plant Bakar (1978) was built according to the most modern environmental protection technologies of the time, with a 252 m high chimney and a 360 m long underwater pipeline for coal transportation (the first of its kind in the world in



Yugoslavia). Today, ABS-Sisak Ltd. has made many investments in environmental protection and energy efficiency. From 1988 to 1990, TLM Šibenik invested heavily in the alumina electrolysis plant and 10 new, modern closed furnaces with dry filters. Today, Impol-TLM Ltd. in Šibenik is preparing to build a new foundry for aluminum ingots with the most modern equipment for environmental protection.

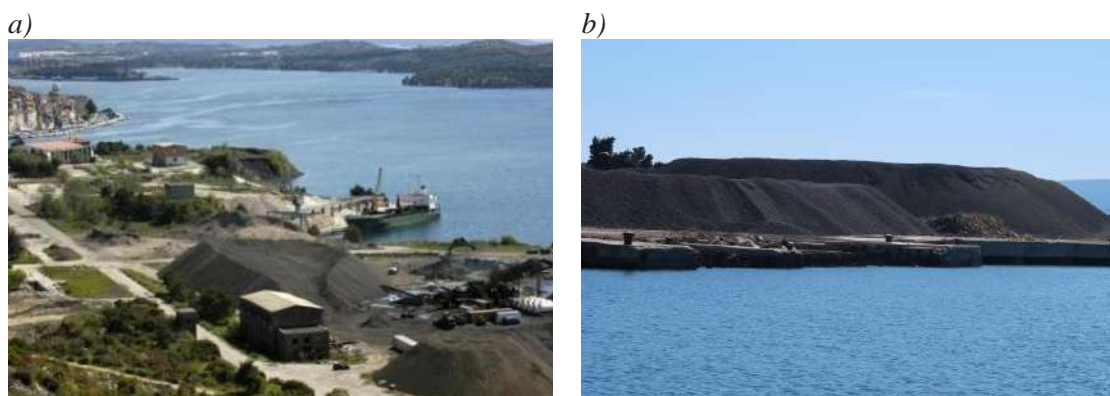


**Figure 1** Slag delayed a) from TEF Šibenik (2014); b) view of the sea (2023) on former factory carbides and ferroalloys Dalmacija – Dugi Rat [1]

**Table 3** Chemical composition of slag, mass. % [8]

Metal oxides	Slag ferrochrome	Slag silicamanganese
SiO <sub>2</sub>	33	41
Al <sub>2</sub> O <sub>3</sub>	20	12
MgO	36	-
MnO	-	16
CaO	-	25
Cr <sub>2</sub> O <sub>3</sub>	6	-
Others	5	6

The factory of alumina in Obrovac was only in operation for two years (1979 and 1980) and had a capacity of 46% in 1979. Residual red mud and waste alkali residues as by-products of alumina production are not utilised. Foundry production is automatized, especially moulding.

Teaching, science and professional activities in the field of environmental protection are introduced from 1980 [9]. Teaching activities started with the implementation of the Ecology course at the Faculty of Metallurgy, University of Zagreb in the academic year 1981/1982. Scientific research activities were carried out through the utilisation of by-products (red mud, slag, dust, etc.) [10–16].

## CONCLUSIONS

After the World War II until the end of the 1980s, much attention was paid to the development of metallurgy in the Republic of Croatia. Numerous metallurgical companies for the production of coke, pig iron, steel, aluminium, castings, etc. were established. The production of ferroalloys was modernised. From an environmental protection standpoint,

serious investments began in the 1980s. Today, the state of environmental protection in the Republic of Croatia is satisfactory. The main reason for this is the reduction in the production of metallurgical products, which is 10% compared to the end of the 1980s. Today, metallurgical companies (Impol-TLM Ltd., ABS Sisak, Ltd. and part of the foundries) invest a lot of money in environmental protection by using alternative energy sources.

## REFERENCES

- [1] Gojić M., Razvoj metalurgije i proizvodnje čelika u Republici Hrvatskoj, Hrvatsko društvo kemijskih inženjera i tehnologa, Sveučilište u Zagrebu Metalurški fakultet, Sveučilište Sjever, Zagreb-Sisak-Koprivnica (2024), ISBN: 978-953-6894-85-7.
- [2] Gojić M., Zavarivanje 65 (1–2) (2022) 25–33.
- [3] Gojić M., Kem. Ind. 70 (7–8) (2021) 411–418.
- [4] Gojić M., Kem. Ind. 70 (9–10) (2021) 563–598.
- [5] Gojić M., Kožuh S., Ivanić I., *et al.*, Kem. Ind. 72 (1–2) (2023) 87–93.
- [6] Poljičak I., Urbana obnova područja bivše tvornice elektroda i ferolegura (TEF) u Šibeniku, Godišnjak Titius 6–7 (2014) 437–450.
- [7] Zemunik V., Tin je bio prvi: hrvatski oklopni transporter, Udruga TVORNICA-Dugi Rat, Dugi Rat (2021), 1–157, ISBN: 978-953-8354-05-2.
- [8] Studija o utjecaju na okoliš ciljanog sadržaja za rušenje građevina i uklanjanje otpada na lokaciji bivše tvornice Dalmacija d.d. u Dugom Ratu, IPZ Uniprojekt d.o.o., Zagreb (2007).
- [9] Gojić M., 50 godina studija metalurgije (monografija 1960–2010.), Metalurški fakultet, Sisak (2010), 1–315, ISBN: 9789537082123.
- [10] Logomerac V., Primjena pirometalurškog i hidrometalurškog postupka, te solvent ekstrakcije u razradi kompleksnog postupka za preradu crvenog mulja, a u cilju dobivanja svih u njemu sadržanih korisnih sastojaka, disertacija, OOUR Metalurško inženjerstvo Tehnološkog fakulteta Sveučilišta u Zagrebu, Sisak (1976), 89–169.
- [11] Zelić J., Čelik 128 (1987) 23–26.
- [12] Črnko J., Metalurgija 33 (4) (1994) 167–169.
- [13] Rastovčan Mioč A., Sofilić T., Mioč B., Disposal of Metallurgical Waste and Research of its Potential Reuse, Proceedings Book included of the 14th International Foundrymen Conference: Development of Foundry Management and Technology, May 15–16, Faculty of Metallurgy, Opatija, Croatia (2014) 1–19.
- [14] Sofilić T., Unkić F., Dangerous substances in foundrymen, Proceedings Book of the 8<sup>th</sup> International Foundrymen Conference: Development and Optimization of the Castings, Production Processes, June 5–7, Faculty of Metallurgy, Opatija (2008) 1–6.
- [15] Rađenović A., Sofilić T., Ivančić A., Kem. Ind. 67 (7–8) (2018) 309–317.
- [16] Oreščanin V., Elez L., Sofilić T., Hrvatske vode 28 (112) (2020) 99–112.



## APPLICATION OF LOW-COST NETWORK FOR URBAN MICROCLIMATE AND AIR QUALITY MONITORING

Viša Tasić<sup>1\*</sup>, Tatjana Apostolovski-Trujić<sup>1</sup>, Vladan Kamenović<sup>1</sup>, Bojan Radović<sup>1</sup>,  
Ivan Zlatković<sup>1</sup>, Nevena Ristić<sup>1</sup>, Zvonko Damnjanović<sup>2</sup>

<sup>1</sup>Mining and Metallurgy Institute Bor, Albert Ajnštajn 1, 19210 Bor, SERBIA

<sup>2</sup>Kompjuter centar Bor, Trg Oslobođenja 8, 19210 Bor, SERBIA

\*visa.tasic@irmbor.co.rs

### Abstract

*In the last ten years, devices for monitoring gaseous air pollutants and meteorological parameters using low-cost sensors have been widely available. Such devices consist of several low-cost sensors, microcontrollers, communication, and power supply modules. Due to the need for a better understanding of urban microclimate parameters, the Mining and Metallurgy Institute Bor (Serbia) recently developed an automatic weather station based on low-cost sensors. The paper presents examples of the results of urban microclimate monitoring in the city of Bor using a network of automatic meteorological stations during the 2023. The measurement results show slight differences in the microclimatic parameters of individual measurement sites predominantly caused by changes in meteorological parameters and air pollution emissions from the local sources. The obtained results are very useful for understanding the spread of particulate matter pollution in urban areas in the city of Bor.*

**Keywords:** low-cost, sensor, air pollution, microclimate, weather station.

### INTRODUCTION

Automatic Meteorological Station (AMS) consist of sensors for measuring temperature, air humidity, air pressure, speed and direction of wind and precipitation, data collection and processing devices, communication, and power supply devices. The cost of a professional automatic weather station in complete configuration can be up to 10,000 euro's. In the national networks of automatic air quality monitoring, automatic meteorological stations of different types and manufacturers are used to measure meteorological parameters in the ambient air. In the Republic of Serbia, at more than 30 Air Quality Monitoring (AQM) stations, automatic monitoring of meteorological parameters is carried out using automatic weather stations LUFFT WS500 or WS600 [1]. The high cost of professional automatic weather stations is a limiting factor for their wider application. On the other hand, in order to better assess the impact of air pollution on human health, it is necessary to carry out continuous monitoring of air quality and meteorological parameters in real-time in different microenvironments (a part of a residential area, around schools, kindergartens, hospitals, factories).

In the last ten years, devices for monitoring meteorological parameters using low-cost sensors have been available. Such meteo stations consist of several low-cost sensors,

microcontrollers, communication, and power supply modules. However, the service life of low-cost sensors integrated into such meteo stations is significantly lower compared to professional ones, as well as the accuracy of measuring meteorological parameters (temperature  $\pm 1^\circ\text{C}$ , air humidity  $\pm 5\%$ , etc.). Due to the need for a better understanding of urban microclimate parameters, the Mining and Metallurgy Institute Bor (Serbia) recently developed an automatic weather station based on low-cost sensors [2,3].

For over a century, copper ore extraction and processing have been undertaken within the confines of the city of Bor in Serbia. These activities, encompassing the excavation and processing of copper ore, have given rise to various detrimental impacts on the local environment, affecting air, water, and soil. Concerns regarding the potential repercussions on human health have been articulated in multiple studies [4–6].

The city of Bor has been subject to systematic air quality monitoring since the seventies of the previous century. From 2005 onwards, automated techniques for measuring sulfur dioxide concentrations have been implemented at multiple locations within the city [7–9]. Notably, in 2016, significant alterations were made to the smelting technology at the copper smelter in Bor. Consequently, the recorded concentrations of sulfur dioxide have witnessed a notable decline compared to the era when the smelter operated with the previous technology.

Despite the technological modifications in copper smelting, certain measuring points within the city still register concentrations of carcinogenic elements, particularly arsenic, in suspended particles of the  $\text{PM}_{10}$  fraction that exceed legal limits [7–10].



**Figure 1** Distribution of measuring points in urban areas of Bor (1. TP, 2. TOP, 3. IRM, 4. ZOO, 5. JP)

In 2023, 4 automatic weather stations were installed in several places in the urban environment of the city of Bor to determine the microclimatic characteristics of the selected measuring points (as shown in Figure 1). This paper presents some of the measurement results



e.g. comparative measurements of deviation of the measured parameters from the results obtained at the reference measuring point in the Town Park in Bor.

## MATERIALS AND METHODS

During 2023, four meteorological stations were installed in the suburban areas of Bor to monitor the influence of meteorological parameters, primarily suspended particles' spread. The locations of these stations are shown in Figure 1. The air temperature, relative air humidity, air pressure, wind speed, direction, and concentrations of suspended particles ( $PM_{10}$  and  $PM_{2.5}$ ) were measured by these meteorological stations and recorded as 1-minute average values. The measurement results were then compared with the data obtained from the weather station at the Town Park location, which is part of the state air quality monitoring network (average daily values of measurement results were compared). The geographical data of measuring points is presented in Table 1. Figure 2 shows examples of meteorological stations installed at the measuring points of IRM and JP.

*Table 1* The geographical data about measuring points

Serial number	Measurement point	Abbreviated designation of measurement point	Geographical coordinates	Altitude (m)	Distance from the copper smelter (m)
1	Town park	TP	44°04'33" N 22°05'58" E	377	800
2	Toplifikacija	TOP	44°03'45" N 22°03'38" E	388	1300
3	Institut IRM Bor	IRM	43°57'24" N 22°08'19" E	384	2000
4	Zoološki vrt	ZOO	44°02'20" N 22°05'34" E	436	2400
5	Jugopetrol	JP	44°04'28" N 22°09'27" E	362	3100

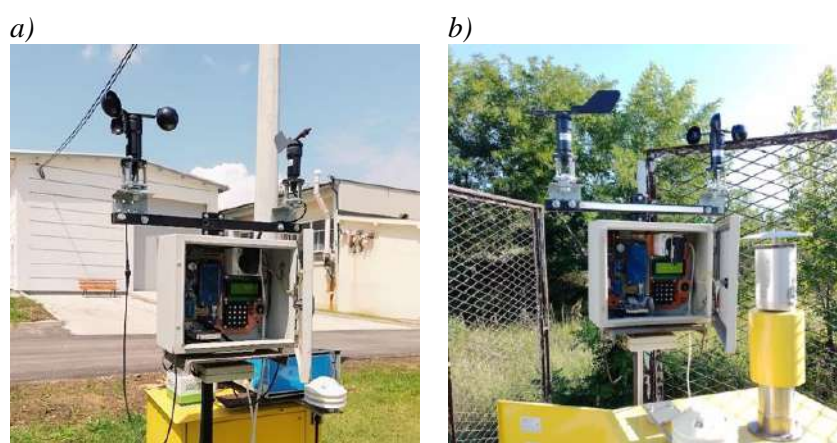


*Figure 2* Layout of the weather stations installed at the a) IRM; b) JP

## RESULTS AND DISCUSSION

In 2023, none of the measuring points detected concentrations of suspended particles  $PM_{10}$  that exceeded the mean annual limit value ( $40 \mu\text{g}/\text{m}^3$ ). Mean annual concentrations of  $PM_{10}$  were 18.3, 16.3, 18.9, 22.5, and  $23.3 \mu\text{g}/\text{m}^3$  at measurement sites 1–5 respectively. Additionally, no measuring point surpassed the allowed number of days (35) with

concentrations above the daily limit value for  $PM_{10}$ . The measuring point JP recorded the highest number of days (15) exceeding the daily limit value for  $PM_{10}$  concentration. In 2023, none of the measuring points detected concentrations of suspended particles  $PM_{2.5}$  that exceeded the mean annual limit value ( $25 \mu\text{g}/\text{m}^3$ ). Mean annual concentrations of  $PM_{2.5}$  were 12.3, 11.7, 12.1, 11.6, and  $13.3 \mu\text{g}/\text{m}^3$  at measurement sites 1–5 respectively. The measuring point JP recorded the highest number of days (23) exceeding the daily limit value for  $PM_{2.5}$  concentration. Figures 3 and 4 display the mean daily concentrations of suspended particles  $PM_{10}$  and  $PM_{2.5}$  measured throughout 2023.

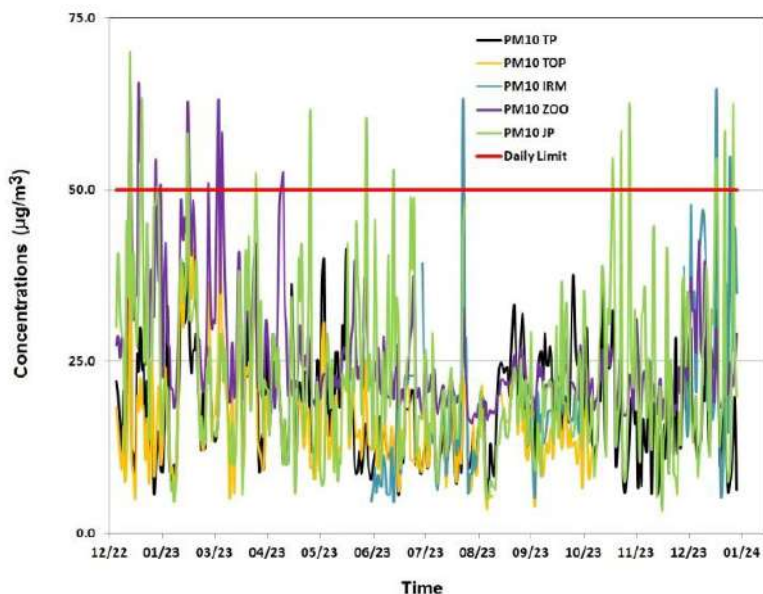


Figure 3 Mean daily concentrations of  $PM_{10}$  measured in Bor in 2023

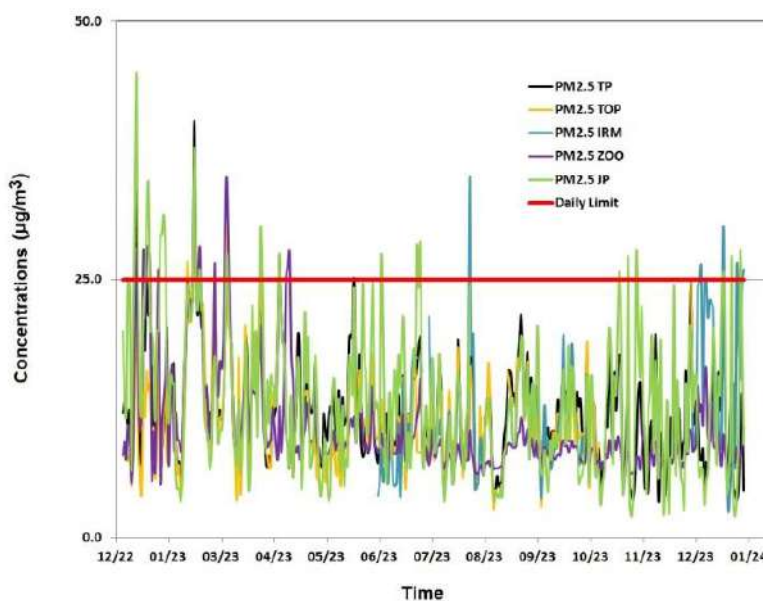


Figure 4 Mean daily concentrations of  $PM_{2.5}$  measured in Bor in 2023



**Table 2** Pearson correlation coefficient ( $r$ ) between the mean daily concentrations of  $PM_{10}$  and  $PM_{2.5}$  in 2023

$PM_{10}$ TOP	$PM_{10}$ IRM	$PM_{10}$ ZOO	$PM_{10}$ JP		$PM_{2.5}$ TOP	$PM_{2.5}$ IRM	$PM_{2.5}$ ZOO	$PM_{2.5}$ JP	
0.72	0.42	0.43	0.41	$PM_{10}$ TP	0.88	0.45	0.64	0.73	$PM_{2.5}$ TP
	0.58	0.66	0.45	$PM_{10}$ TOP		0.67	0.69	0.59	$PM_{2.5}$ TOP
		0.64	0.42	$PM_{10}$ IRM			0.66	0.44	$PM_{2.5}$ IRM
			0.43	$PM_{10}$ ZOO				0.51	$PM_{2.5}$ ZOO

Based on the value of the Pearson correlation coefficient of the mean daily concentrations of suspended particles  $PM_{10}$  and  $PM_{2.5}$  between measurement sites, it can be observed that there are mostly moderate ( $0.6 > r > 0.4$ ) and strong ( $0.8 > r > 0.6$ ) positive correlations between PM concentrations at different measurement sites. Correlations between  $PM_{2.5}$  concentrations are somewhat stronger than correlations between  $PM_{10}$  concentrations, which is a consequence of the different distribution of these particle fractions under the changes in microclimate conditions and influences of local sources of PM emissions. Figures 5 and 6 show the measured values of meteorological parameters. Mean annual values of air temperature were 13.2, 12.9, 13.3, 13.5, and 12.9°C at measurement sites 1–5 respectively. Mean annual values of relative humidity were 74.8, 72.1, 74.2, 71.6, and 72.4% at measurement sites 1–5 respectively. Mean annual values of wind speed were 1.3, 1.2, 0.9, 1.1, and 1.2 m/s at measurement sites 1–5 respectively. Mean annual values of air pressure were 971.7, 971.1, 971.2, 971.1, and 971.4 mbar at measurement sites 1–5 respectively.

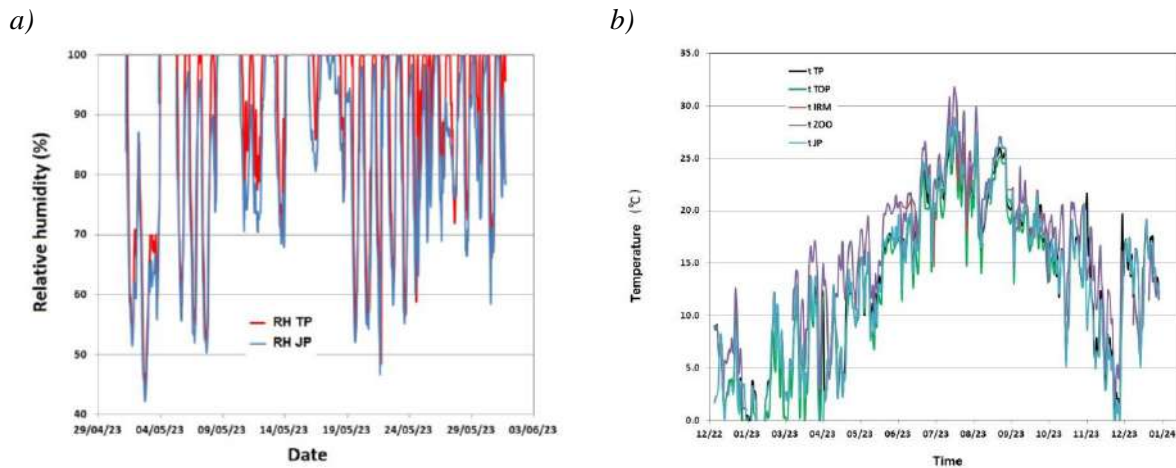


**Figure 5** Mean hourly values of a) RH and mean daily values b) Temperature in 2023

Based on the measured values of meteorological parameters at sites 1–5 in Bor, it can be concluded that they differ very little from each other, that is, they do not deviate from the average values of meteorological parameters measured in the last ten years at the measuring site Town Park in Bor.

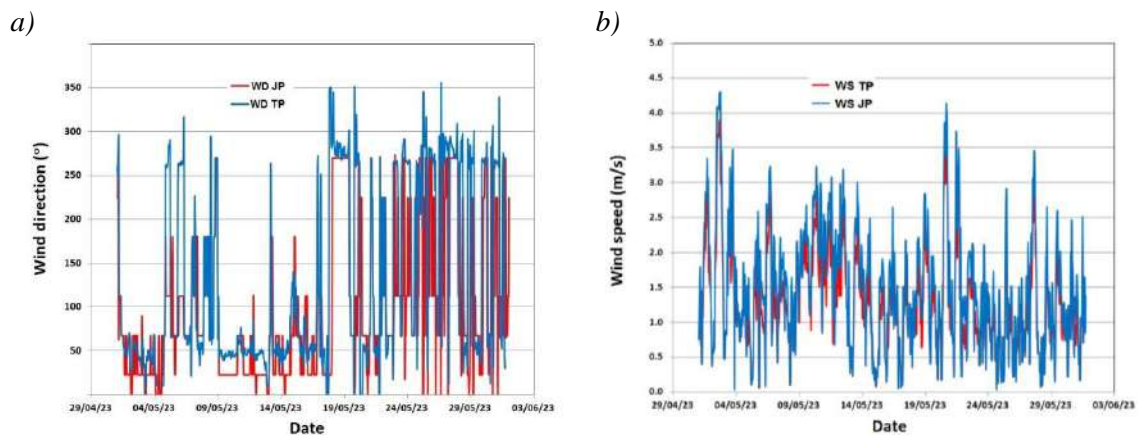


**Figure 6** Mean hourly values of a) WD; b) WS at TP and JP sites in 2023

## CONCLUSION

The paper presents examples of the results of urban microclimate monitoring in the city of Bor during 2023 using a network of automatic meteorological stations. The measurement results show slight differences in the microclimatic parameters of individual measurement sites predominantly caused by changes in meteorological parameters and air pollution emissions from the local sources. The obtained results are very useful for better understanding the principles of spreading air pollution in urban areas in the city of Bor.

## ACKNOWLEDGEMENT

*This work was financially supported by the Ministry of Science, Technological Development and Innovation of the Republic of Serbia, Contract on realization and financing of the scientific research work of the Mining and Metallurgy Institute Bor in 2024, contract number: 451-03-66/2024-03/200052.*

## REFERENCES

- [1] Available on the following link: <https://www.lufft.com/download/manual-lufft-wsxxx-weather-sensor-en/> (accessed on February 25, 2024).
- [2] Tasić V., Apostolovski-Trujić T., Lazović I., *et al.*, Automatic Meteorological Station (AMS/2022) Based on Low-Cost Sensors (part 1), Proceedings of the 53<sup>rd</sup> International October Conference on Mining and Metallurgy, 03.10.–05.10.2022, Hotel 'Albo', Bor, Serbia (2022) 221–224. ISBN: 978-867827-052-9.
- [3] Tasić V., Apostolovski-Trujić T., Lazović I., *et al.*, Automatic Meteorological Station (AMS/2022) Based on Low-Cost Sensors (part 2), Proceedings of the 53<sup>rd</sup> International October Conference on Mining and Metallurgy, 03.10.–05.10.2022, Hotel 'Albo', Bor, Serbia (2022) 225–228. ISBN: 978-867827-052-9.
- [4] Serbula S., Ilic A., Kalinovic J., *et al.*, Environ. Earth Sci. 71 (4) (2014) 1651–1661.
- [5] Serbula S., Kalinovic T., Kalinovic J., *et al.*, Environ. Earth Sci. 68 (7) (2013) 1989–1998.
- [6] Tasić V., Kovačević R., Maluckov B., *et al.*, Wat. Air and Soil Poll. 228 (2017) 230.

- [7] Annual Report on the State of Air Quality in the Republic of Serbia for 2019 (in Serbian), Available on the following link: [http://www.sepa.gov.rs/download/izv/Vazduh\\_2019.pdf](http://www.sepa.gov.rs/download/izv/Vazduh_2019.pdf) (accessed on February 25, 2024).
- [8] Annual Report on the State of Air Quality in the Republic of Serbia for 2020 (in Serbian), Available on the following link: [http://www.sepa.gov.rs/download/izv/Vazduh\\_2020.pdf](http://www.sepa.gov.rs/download/izv/Vazduh_2020.pdf) (accessed on February 25, 2024).
- [9] Serbula S., Milosavljevic J., Kalinovic J., *et al.*, *Sci. Total Environ.* 777 (2021) 145981.
- [10] Annual Report on the State of Air Quality in the Republic of Serbia for 2022 (in Serbian), Available on the following link: [http://www.sepa.gov.rs/download/Vazduh\\_2022.pdf](http://www.sepa.gov.rs/download/Vazduh_2022.pdf) (accessed on February 25, 2024).



## ANALYSIS OF THE INFLUENCE OF NATURAL GAS COMPOSITION AND EXCESS AIR COEFFICIENT ON COMBUSTION PRODUCTS

Nebojša Tadić<sup>1\*</sup>, Žarko Radović<sup>1</sup>, Anica Knežević<sup>1</sup>

<sup>1</sup>University of Montenegro, Faculty of Metallurgy and Technology, Cetinjski put bb,  
81000 Podgorica, MONTENEGRO

\*nebojsa@ucg.ac.me

### Abstract

*The paper presents a computation and analysis of the CO<sub>2</sub> emission factor, alongside the volume and composition of combustion products, contingent on the composition of high-quality natural gas and the excess air coefficient. The CO<sub>2</sub> emission factor values are within the range that natural gas of the selected composition is recommended for use from an ecological point of view. With an increase in the excess air coefficient, both the volume of combustion products and the concentrations of N<sub>2</sub> and O<sub>2</sub> within these products increase, whereas the concentrations of CO<sub>2</sub> and H<sub>2</sub>O decrease. The identified differences arise from variations in the composition of natural gas.*

**Keywords:** natural gas, excess air coefficient, combustion product.

### INTRODUCTION

Natural gas is a highly calorific fossil fuel widely used as an energy source in various thermal power plants and thermal engineering plants. It is a gaseous mixture primarily composed of hydrocarbons, with methane overwhelmingly predominant among them. As a result, the combustion of natural gas yields energy with the least carbon emissions compared to other fossil fuels [1,2]. The energy requirements of plants determine the fuel consumption and operating parameters of industrial furnaces, thereby influencing the quantity and composition of combustion products [3–6]. Although natural gas is the most environmentally friendly fossil fuel, its use necessitates the design of waste gas treatment procedures, primarily for the removal of carbon dioxide, nitrogen (nitrogen oxides), and soot particles. The initial step in these activities always involves the analysis of the quantity and composition of combustion products [4,6].

In this study, computation and analysis were conducted on the combustion products resulting from the combustion of natural gas of varying compositions under different excess air coefficient values, which represent one of the most significant operational parameters of the combustion process.

### MATERIALS AND METHODS

For the investigation, six different compositions of dry natural gas (without the presence of water vapor) were selected (Table 1). The gases are denoted as NG1÷NG6 and are arranged according to decreasing CH<sub>4</sub> content, which is the most dominant component in the

composition of natural gas. The gas compositions were cited from the literature and are characteristic of facilities for the preparation and utilization of natural gas in the European Union, Russia, and Serbia [7,8].

**Table 1** Selected compositions of natural gas

Natural gas	Composition of natural gas, [vol %]						
	CH <sub>4</sub>	C <sub>2</sub> H <sub>6</sub>	C <sub>3</sub> H <sub>8</sub>	C <sub>4</sub> H <sub>10</sub>	C <sub>5</sub> H <sub>12</sub>	CO <sub>2</sub>	N <sub>2</sub>
NG1	98.00	0.40	0.20	0.10	0.10	0.20	1.00
NG2	95.59	1.15	0.44	0.16	0.04	1.48	1.14
NG3	92.60	2.78	0.41	0.06	–	2.42	1.73
NG4	88.6	3.05	0.62	0.58	–	1.50	5.65
NG5	83.50	3.60	0.70	0.30	–	1.40	10.50
NG6	80.50	2.80	0.40	0.20	–	1.90	14.20

The combustion of gaseous fuels is conducted under excess air conditions of up to 10% compared to the theoretical air quantity [1,5]. As this is one of the most significant factors influencing fuel combustion conditions and the quantity and composition of resulting combustion products, six values of the excess air coefficient ( $\lambda = 1, 1.02, 1.04, 1.06, 1.08,$  and  $1.10$ ) were selected for computation and analysis.

The calculation was performed based on elementary stoichiometric ratios. It was carried out using the MATLAB software package and included the determination of: the heating value of natural gas ( $Q$ ); the elemental composition of natural gas (C, H, O and N); the CO<sub>2</sub> emission factor ( $K_{CO_2}$ ); the volume of combustion products ( $R$ ); and the composition of combustion products ( $r$ ).

## RESULTS AND DISCUSSION

Natural gas is classified as a high-quality gaseous fuel with a heating value ranging between 27 and 39 MJ/m<sup>3</sup>, depending on the gas composition [2]. The calculation of the heating value for the selected compositions of natural gas was based on the heating values of the components comprising natural gas and their volumetric contents. All selected compositions of natural gas have heating values from the middle part of this interval as shown in Table 2. The table illustrates the influence of the total content of combustible components ( $\Sigma(C_nH_m)$ ) on the heating value. These values are primarily influenced by the methane content in natural gas. Although other hydrocarbons have significantly higher heating values compared to methane, it is evident that the dominant content of methane in the gas is crucial for this distribution of values.

**Table 2** Influence of the total content of combustible components (CH<sub>4</sub>, C<sub>2</sub>H<sub>6</sub>, C<sub>3</sub>H<sub>8</sub>, C<sub>4</sub>H<sub>10</sub> and C<sub>5</sub>H<sub>12</sub>) on the heating value ( $Q$ ) of natural gas

Natural gas	NG1	NG2	NG3	NG4	NG5	NG6
$\Sigma(C_nH_m)$ , [vol %]	98.80	97.38	95.85	92.85	88.10	83.90
$Q$ , [MJ/m <sup>3</sup> ]	35.99	35.82	35.58	35.16	33.40	31.40

In Table 3, the results of the calculation of the elementary composition of natural gas are

presented. The trend of changes in the ratio of hydrogen to carbon content (H/C) among the selected compositions of natural gas aligns with the variation in methane content. This ratio ranges from 0.330 for NG1 to 0.318 for NG6. It is evident that the differences in this ratio are minimal regardless of significant variations in the composition of individual gases. Unlike other fossil fuels, natural gas exhibits higher values of the H/C ratio owing to its main component, CH<sub>4</sub>. Consequently, it also has the lowest CO<sub>2</sub> emission factor per unit of released heat energy (~56.1 kg/GJ) compared to other fossil fuels (63÷110 kg/GJ), which recommends it for use from an ecological perspective [9].

**Table 3** Results of the calculation of the elemental composition of natural gas (C, H, O and N)

Natural gas	NG1	NG2	NG3	NG4	NG5	NG6
$g_C$ , [kg/m <sup>3</sup> ]	0.5384	0.5439	0.5467	0.5377	0.5111	0.4821
$g_H$ , [kg/m <sup>3</sup> ]	0.1778	0.1763	0.1745	0.1712	0.1626	0.1533
$g_O$ , [kg/m <sup>3</sup> ]	0.0029	0.0211	0.0346	0.0214	0.0200	0.0271
$g_N$ , [kg/m <sup>3</sup> ]	0.0125	0.0142	0.0216	0.0706	0.1313	0.1775

The CO<sub>2</sub> emission factor was calculated using the equation (1). The calculation results presented in Table 4 indicate that the CO<sub>2</sub> emission factors for the selected compositions of natural gas are entirely consistent with the literature data [9].

$$K_{CO_2} = 3.67 \cdot (g_C / Q), \text{ [kg/GJ]}. \quad (1)$$

where: 3,67 – is the stoichiometric ratio;  $g_C$  – is the mass fraction of carbon in the natural gas [kg/m<sup>3</sup>];  $Q$  – is the heating value of the natural gas [GJ/m<sup>3</sup>].

**Table 4** CO<sub>2</sub> coefficient factor

Natural gas	NG1	NG2	NG3	NG4	NG5	NG6
$K_{CO_2}$ , [kg/GJ]	54.9	55.7	56.4	56.1	56.2	56.3

The total volume of combustion products depends on the excess air coefficient and the composition of natural gas (combustible and non-combustible components). An increase in the excess air coefficient ( $\lambda$ ) results in approximately linear growth in the volume of combustion products (R) (Figure 1). Moreover, as the content of combustible components in natural gas decreases, there is a corresponding reduction in the volume of combustion products. This difference is particularly noticeable between NG1 and NG6 gases, where it can reach up to a maximum of 13%. Figure 2 presents a 3D diagram demonstrating the change in the volume of combustion products as the function of the excess air coefficient and the total quantity of all elements (C, H, O, and N) per 1 m<sup>3</sup> of natural gas, which provides a more comprehensive understanding of how these parameters interact.

Carbon dioxide in combustion products is primarily present as a result of the combustion reactions of carbon-containing components, and to a lesser extent, due to its presence in natural gas itself. With an increase in the excess air coefficient, the CO<sub>2</sub> content ( $r_{(CO_2)}$ ) in



combustion products decreases (Figure 3). The lowest values are obtained for gas NG1, which has the highest total hydrocarbon content but also the lowest CO<sub>2</sub> content. Conversely, the second lowest values are obtained for gas NG6, which, conversely, has the lowest hydrocarbon content and the highest CO<sub>2</sub> content. It is evident that the CO<sub>2</sub> content in combustion products depends on the ratio of CO<sub>2</sub> to hydrocarbons in natural gas, as well as the structure of the hydrocarbons comprising the gas. Therefore, it is more reliable to analyze the volume fraction of CO<sub>2</sub> in combustion products as a function of the mass fraction of carbon in natural gas, as depicted in Figure 4.

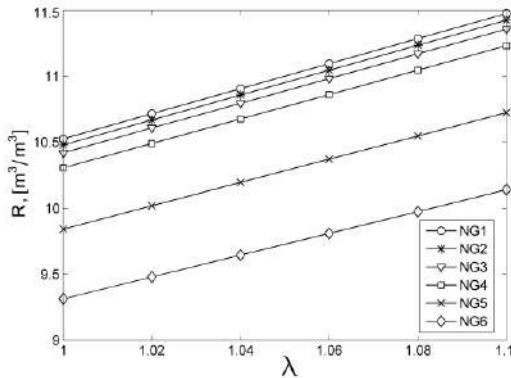


**Figure 1** Influence of the excess air coefficient on the volume of combustion products

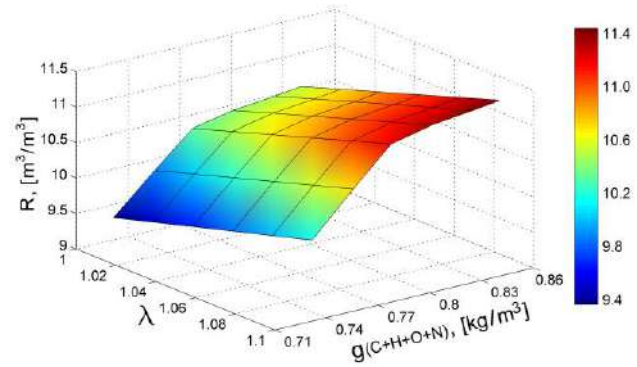


**Figure 2** Influence of the excess air coefficient and the total quantity of C, H, O, and N in the gas on the volume of combustion products

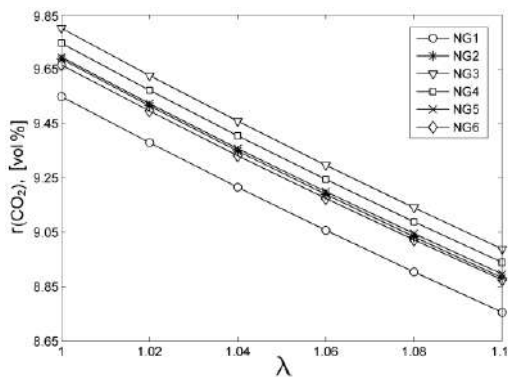


**Figure 3** Influence of the excess air coefficient on the CO<sub>2</sub> content in combustion products

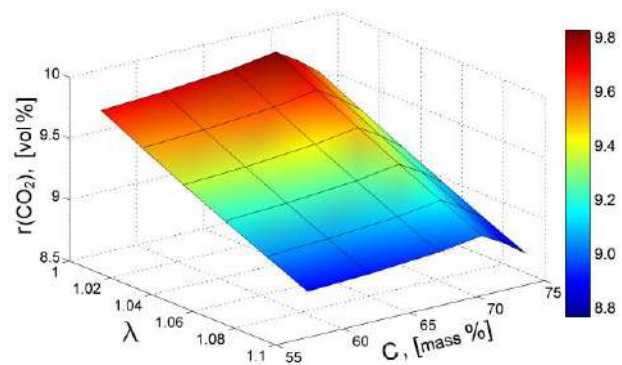


**Figure 4** Influence of the mass fraction of carbon in natural gas and the excess air coefficient on the CO<sub>2</sub> content in combustion products

The presence of water vapor in combustion products originates from the combustion of present hydrocarbons and hydrogen, as well as from the presence of moisture in the gas. Since H<sub>2</sub> and water vapor are not present in the selected compositions of natural gas, the presence of water vapor in combustion products is solely a consequence of the combustion of hydrocarbons. As the excess air coefficient increases, the water vapor content ( $r_{\text{H}_2\text{O}}$ ) in combustion products decreases (Figure 5). The obtained dependencies for individual gases are in a decreasing sequence from gas NG1 to gas NG6, in accordance with the decrease in the total hydrocarbon content in natural gas. This trend can be further analyzed by considering if

the mass fraction of elemental H<sub>2</sub> in natural gas is also taken into account (Figure 6).

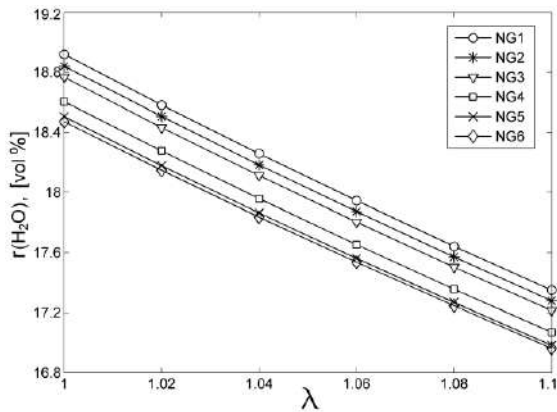


**Figure 5** Influence of the excess air coefficient on the H<sub>2</sub>O content in combustion products

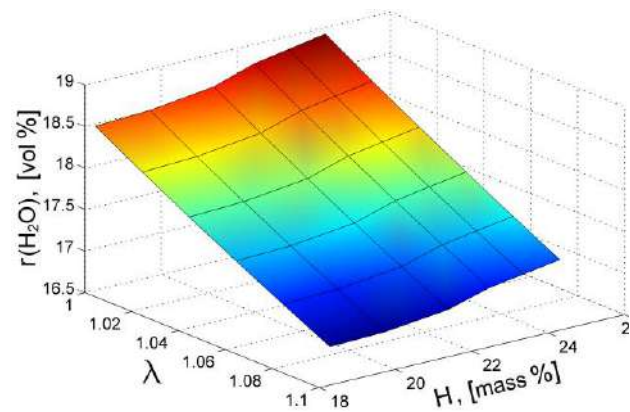


**Figure 6** Influence of the mass fraction of hydrogen in natural gas and the excess air coefficient on the H<sub>2</sub>O content in combustion products

The oxygen and nitrogen contents in combustion products increase with the increase in the excess air coefficient, as depicted in Figures 7 and 8. Since O<sub>2</sub> is not present in the selected compositions of natural gas, its presence in combustion products ( $r(\text{O}_2)$ ) is solely a result of excess air. The differences between individual gases are negligible (Figure 7).

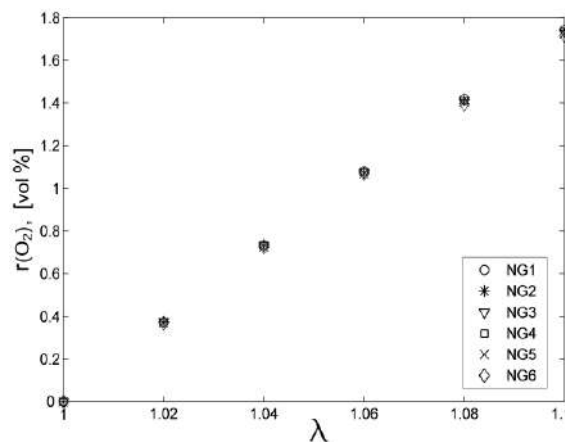


**Figure 7** Influence of the excess air coefficient on the O<sub>2</sub> content in combustion products

Nitrogen in combustion products originates partially from its presence in natural gas and partly from the required amount of air (actual quantity) for combustion. As expected the highest N<sub>2</sub> contents ( $r(\text{N}_2)$ ) in combustion products are obtained for gases NG6 and NG5 (Figure 8), due to its relatively high content in these gases of 14.2 vol% and 10.50 vol%, respectively. However, the distribution of values for the other gas compositions indicates that for impact analysis, the ratio of N<sub>2</sub> content to all other components entering the composition of natural gas must be taken into account. Therefore, it is justified to use a 3D diagram with the mass fraction of nitrogen in natural gas as the influencing parameter for analysis here (Figure 9).

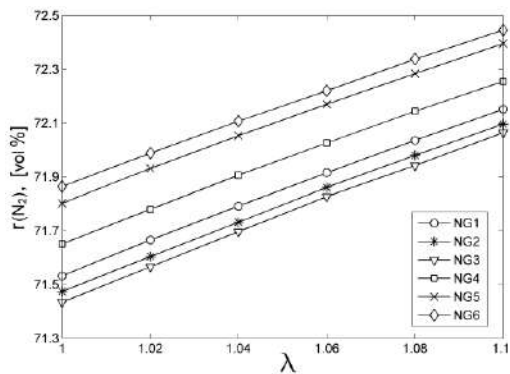


**Figure 8** Influence of the excess air coefficient on the  $N_2$  content in combustion products

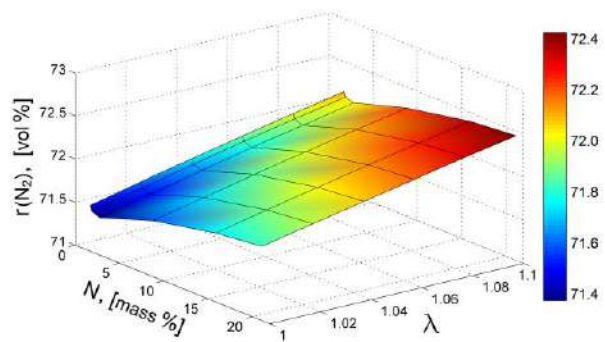


**Figure 9** Influence of the mass fraction of the  $N_2$  in natural gas and the excess air coefficient on the  $N_2$  content in combustion products

## CONCLUSION

Natural gas, for the selected six different compositions, falls within the category of quality gaseous fuels with a heating value exceeding  $31 \text{ MJ/m}^3$ .

The  $\text{CO}_2$  emission factor per unit of released thermal energy for the selected compositions of natural gas ranges from 54.9 to 56.4 kg/GJ, which recommends its use from an ecological perspective compared to all other fossil fuels.

With an increase in the excess air coefficient, the volume of combustion products increases, along with the concentrations of  $N_2$  and  $O_2$ , while the concentrations of  $\text{CO}_2$  and  $\text{H}_2\text{O}$  decrease, across all selected compositions of natural gas. Differences between individual gases are caused by the composition of these gases and the varying ratios of individual components' contents.

By selecting the optimal value of the excess air coefficient, it is necessary to meet the required process parameters while also reducing the volume of combustion products, especially  $\text{CO}_2$  and  $N_2$  ( $\text{NO}_x$ ), thus significantly mitigating negative environmental impacts.

## REFERENCES

- [1] Škrbić B., Technology of gas production and application, University of Novi Sad, Novi Sad (2002), p.1, 35, 333, ISBN: 86-499-0105-0.
- [2] Armstrong G.T., Jobe T.L., Heating values of natural gas and its components, U.S. National Bureau of Standards, Washington (1982), p.37, NBSIR: 82-2401.
- [3] Mullinger P., Jenkins B., Industrial and Process Furnaces, Elsevier, Oxford (2008), p.69, ISBN: 978-0-7506-8692-1.
- [4] Martinez F.R., Velázquez M.T., Polupan G., *et al.*, EPE 4(5) (2012) 353–357.
- [5] Huang M., Li R., Xu J., *et al.*, Fuel 302 (2021) p.121179.
- [6] Kayadelen H.K., J. Nat. Gas Sci. Eng. 45 (2017) 456–473.
- [7] Available on the following link: <https://www.gasruma.rs/index.php/prirodni-gas-m/specificnosti-prirodnog-gasa-m>.
- [8] Ivezić D., Čivković M., Danilović D., *et al.*, Energy Sources B: Econ. Plan. Policy 11(11)

(2016) 1061–1067.

- [9] Ivošev M, Proceedings of the 48<sup>th</sup> International HVAC&R Congress and Exhibition, 6–8.12.2017, Belgrade, Serbia (2017) 83–95.



## INVESTIGATION OF MULTI-CYCLE USAGE OF NANOPHOTOCATALYSTS IN DEGRADATION OF THIOPHANATE-METHYL

**Aleksandar Jovanović<sup>1\*</sup>, Nataša Knežević<sup>2</sup>, Mladen Bugarčić<sup>1</sup>, Jelena Petrović<sup>1</sup>,  
Miroslav Sokić<sup>1</sup>, Marija Stevanović<sup>3</sup>, Aleksandar Marinković<sup>4</sup>**

<sup>1</sup>Institute for Technology of Nuclear and Other Mineral Raw Material,  
Boulevard Franše d'Eperea 86, 11000 Belgrade, SERBIA

<sup>2</sup>University of Belgrade, “VINČA” Institute of Nuclear Sciences - National Institute  
of the Republic of Serbia, Mike Petrovića Alasa 12–14, 11351 Belgrade, SERBIA

<sup>3</sup>Institute of Pesticides and Environmental Protection, Banatska 31b,  
11080 Belgrade, SERBIA

<sup>4</sup>University of Belgrade, Faculty of Technology and Metallurgy, Karnegijeva 4,  
11060 Belgrade, SERBIA

\*a.jovanovic@itnms.ac.rs

### Abstract

*The presence of different organic pollutants in water leads to the need to apply different technologies and processes for their removal. Organic pollutants can cause several negative impacts on surrounding environment, inducing detrimental effects on living beings. Fungicides represent one of the biggest groups of crop protective agent with increased yearly consumption, frequently ending up in non-target organisms. Therefore, aim of this study was to determine the possibility of using two synthesized nanocatalysts Ag-P25 and Ce-P25 in several consecutive removal cycles of present pollutant in water. Catalysts were applied in process of photocatalytic degradation of fungicide thiophanate-methyl at atmospheric conditions. After each irradiation cycle, catalysts were collected, rinsed, dried, and applied in upcoming operational run. Fabricated catalysts were also likened to starter TiO<sub>2</sub> material. After fifth cycle, FTIR and XRD characterization techniques were used for proving stability of materials. Obtained results show that Ce-P25 possesses (98%) better stability than Ag-P25 (96%), but base TiO<sub>2</sub> (99%) has the best stability and efficiency after second cycle. Gathered findings can open a new way of employing photocatalysis as a process for treatment of polluted waters from various industries.*

**Keywords:** photodegradation, catalysts, stability, water treatment, environmental protection.

### INTRODUCTION

The main causes of contamination of water are natural disasters, industrialization, agriculture, inadequate sewage treatment systems, and inadequate supply water treatment plants. The initial factor contributing to water pollution is industry. In the course of industrial production, a variety of dangerous substances, both organic and inorganic, may be emitted into the environment. Water pollution will be outcome because of pollutants releasing into aquatic ecosystems without sufficient treatment [1], inducing negative impact on the

environment. In addition, intensive agricultural production led to the need for increased production of various preparations for crop protection.

One of the most abundant contaminants is pesticides. Pesticides can negatively affect an organism's health by contaminating water and entering food chain. When pesticide usage and health life expectancy data were compared, it was discovered that for every ten percent rise in consumption of pesticides, the medical disability index for people over 65 increased by 1% [2].

Different methods for pesticides elimination from water can be used [3]. However, the problem of pesticide removal from water is being initiated and clarified by the current treatment procedures, which combine physical, chemical, and biological processes. Every treatment method has "pros and cons" of its own, ranging from capital and operating expenses to environmental impact, operability, dependability, efficiency, pre-treatment needs, and the creation of hazardous byproducts and sludge [4].

Therefore, it is necessary to employ novel techniques so-called advanced oxidation processes (AOPs), where photocatalysis has a special place. Photocatalysis represents complex redox reactions, where pollutant in system is decomposed by interaction of different types of irradiation with the catalysts surface with generation of  $h^+/OH^-$  species [5].

The aim of this paper was to apply synthesized photocatalysts Ag-P25 and Ce-P25 in consecutive photocatalytic processes for degradation fungicide thiophanate-methyl under simulated sunlight radiation. The changes in concentrations with time were monitored with the aim to determine which catalyst has better performance after each operational cycle. Fabricated materials were structurally investigated by Fourier-transform infrared spectroscopy (FTIR) and X-ray powder diffraction (XRD) techniques to observe possible changes in the structures of fabricated materials and determine their stability.

## MATERIALS AND METHODS

Complete experimental procedures are shown in paper by Jovanovic *et al.* [6]. Shortly, photocatalytic tests were conducted under simulated sunlight by changing photocatalysts at an initial concentration of thiophanate-methyl  $5 \text{ mg/dm}^3$ . The amount of catalysts in reactions was  $70 \text{ mg/dm}^3$ , as it gets the best results in degradation. Fungicide standard of thiophanate-methyl (Figure 1) was obtained from Chemical Agrosava.

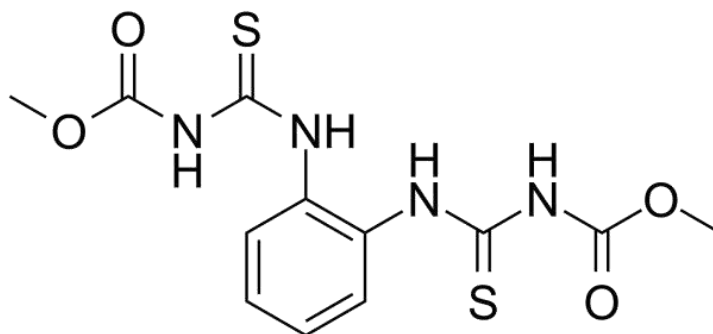


Figure 1 Thiophanate-methyl



Catalysts were gathered, washed 2 times with ethanol and two times with deionized water, dried at 80°C, and utilized for the next operating run following each irradiation cycle. Pollutant concentration was determined by UV spectrometry (Shimadzu UV-1800).

For determination of different nanomaterials present on the surface of base TiO<sub>2</sub>, X-ray diffractometer Philips 1050 with Ni-filtered Cu K $\alpha$  radiation and FTIR spectrophotometer Nicolet iS10 were applied.

## RESULTS AND DISCUSSION

The consistency and longevity of the synthesized catalysts were tested in five consecutive cycles at optimal operating conditions, and the results are visually presented in Figure 2. Fabricated materials were compared with starter TiO<sub>2</sub> P25 photocatalyst (P25 in further text).

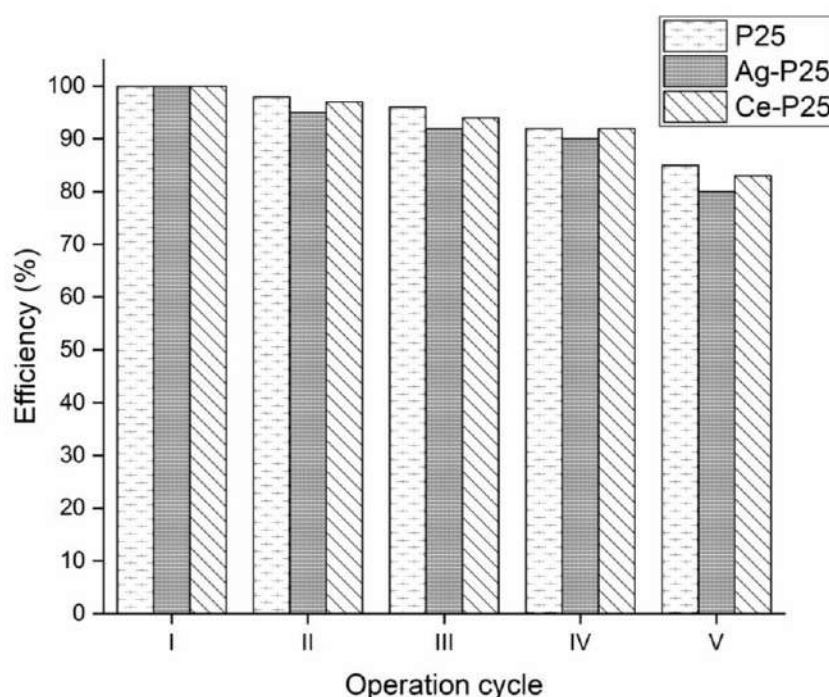


**Figure 2** Exploitation cycles of P25, Ag-P25 and Ce-P25 photocatalysts assuming ideal processing parameters (5 mg/dm<sup>3</sup> of TPM and mass of catalyst: 70 mg/dm<sup>3</sup>)

The degradation efficiency of the applied catalysts is shown to decrease slightly after the third reaction cycle, from 100% to 90%, which indicates an enhanced stability due to strong bonds between the P25 surface and Ag<sub>2</sub>O and CeO<sub>2</sub> deposits. No leaching of silver and cerium was detected in the washing solution. After the fifth cycle, the catalyst activity was reduced to 80%. The obtained result suggests that Ce-P25 has slightly better stability than Ag-P25, while P25 has greater stability than both. Figure 3 presents XRD (Figure 3a) and FTIR (Figure 3b) scans of the tested photocatalysts after the fifth cycle of employment. The applied characterization techniques showed that the prepared photocatalysts possess good mechanical resistance under experimental conditions enforced during photocatalytic assays.

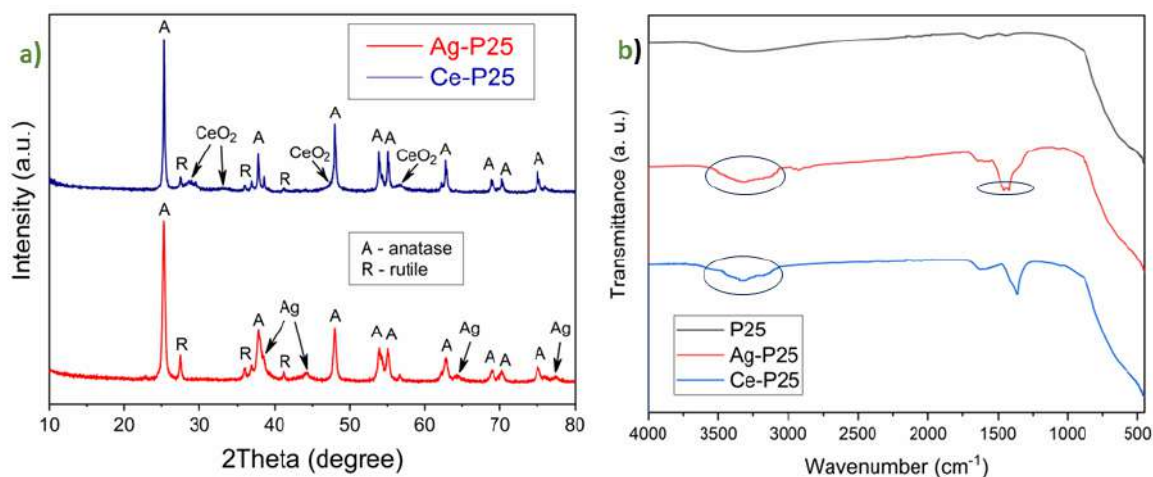


**Figure 3** Structural characterization of photocatalysts after the fifth employment cycle

The structural investigation of these materials after the fifth cycle of operation shows the stability and durability of the obtained photocatalysts. No phase changes were observed in Figure 3a. This result approves the firmness of prepared materials under operational conditions. In the FTIR spectrum, in Figure 3b, a broad bond vibration was observed at  $3000\text{--}3400\text{ cm}^{-1}$ , which is a consequence of the binding of water molecules. Another change was observed at  $1470\text{ cm}^{-1}$ , slightly decreased intensity of the peak originating from the Ag-TiO<sub>2</sub> interaction. This is the possible reason for the lower activity of the Ag-P25 photocatalyst in contrast to Ce-P25.

## CONCLUSION

Photocatalysis as a process for wastewater treatment is showing good results. Applied photocatalysts have shown great efficiency toward thiophanate-methyl degradation. Photocatalyst Ce-P25 shows the best results in the aim of degradation efficiency, while, base TiO<sub>2</sub> possesses the best stability. The stability of fabricated was reduced after each operational cycle, which is expected since the bonds within the materials weaken over time. Further improvements in this process should be reflected in the synthesis of cheaper catalysts.

## ACKNOWLEDGEMENT

*The authors are grateful to the Ministry of Science, Technological development and Innovation of the Republic of Serbia for financial support according to the contracts with the registration number 451-03-66/2024-03/200023; 451-03-66/2024-03/200017; 451-03-66/2024-03/2000214.*

## REFERENCES

- [1] Chowdhary P., Bharagava R. N., Mishra S., *et al.*, Role of industries in water scarcity and its adverse effects on environment and human health in Environmental Concerns and Sustainable Development, Editors: Shukla V., Kumar N., Springer, Singapore (2020), p.235–256, ISBN: 978-981-13-5889-0.
- [2] Lai W., J. Environ. Econ. Manag. 86 (2017) 93–120.

- [3] Saleh I.A., Zouari N., Al-Ghouti M.A., *Environ. Technol. Innov.* 19 (2020) 101026.
- [4] Marican A., Durán-Lara E.F., *Environ. Sci. Pollut. Res.* 25 (2018) 2051–2064.
- [5] Hassaan M.A., El-Nemr M.A., Elkatory M.R., *et al.*, *Top. Curr. Chem.* 381(6) (2023) 31.
- [6] Jovanović A., Stevanović M., Barudžija T., *et al.*, *Process Saf. Environ. Prot.* 178 (2023) 423–443.



## PHYSICO-CHEMICAL AND MICROBIAL ANALYSIS IN SELECTED GROUNDWATER IN SERBIA

Vesna Obradović<sup>1</sup>, Marija Perović<sup>1\*</sup>, Predrag Pajić<sup>1</sup>

<sup>1</sup>Jaroslav Černi Water Institute, Belgrade, Jaroslava Černog 80, 11226 Belgrade, SERBIA

\*marija.perovic@jcerni.rs

### Abstract

*The conducted research aims to explore the intricate relationship between the physicochemical properties of groundwater and its microbiological composition within the selected wells of the Danube alluvial zone. The study aimed to determine levels of physicochemical and microbiological composition, as well as their involvement in various transformation processes, allowing insights into the groundwater potential for specific transformations. Although groundwater is commonly viewed as a reliable water source, its slow flow in certain conditions allows pollutants to persist once they infiltrate, posing potential risks to its safety for consumption. Hence, conducting a comprehensive and meticulous analysis becomes crucial to evaluate its suitability for diverse purposes and to establish the necessary construction standards for sustainable utilization. The obtained results have shown that the Danube alluvium exhibits significant biochemical diversity, which, along with changes in the concentration of redox-sensitive species, suggests dynamic hydrochemical and microbiological oxidation-reduction processes that can affect the primary quality of infiltrated Danube water in various ways.*

**Keywords:** groundwater, BART tests, quality, wells.

### INTRODUCTION

Microorganisms play a crucial role in groundwater ecosystems by facilitating key biogeochemical processes such as carbon and nitrogen cycling, as well as the natural breakdown of contaminants [1]. Rather than acting independently, various functional groups of microorganisms interact synergistically to orchestrate these processes. Aquifers provide extensive and complex environments that host a wide array of microbial communities [2]. In this study, the current microbial biodiversity of analysed groundwater with known compositions in the Danube alluvium is evaluated. The potential of modern techniques to deepen our comprehension of microbial biodiversity patterns and their correlation with environmental conditions was also explored. In 2021, a sampling campaign was carried out for seven wells located within the Danube alluvium, specifically within the zones of hydro-technical facilities B-1, B-2, B-3, B-4 near settlement Vinci, and B-10, B-13, and B-15, near the settlement of Veliko Gradište in Serbia. Physico-chemical and microbiological analyses of the water quality were conducted using standard procedures and methods.

## MATERIALS AND METHODS

Sampling was performed in accordance with SRPS EN ISO 19458:2009, Water Quality - Sampling for Microbiological Analysis, and according to instructions on sampling methods and laboratory analysis based on the Standard Methods for The Examination of Water and Wastewater, 21<sup>st</sup> Edition (2005). Microbiological samples were collected in sterile 500 mL bottles using a sterile metal sampler equipped with a cord. They were transported in handheld refrigerators maintaining a controlled temperature of <10°C and processed within the standard prescribed timeframe. Determination of the microbiological status and quality of groundwater was carried out by simultaneous application of five types of biological activity reaction tests (BART tests). The purpose of these investigations was to determine the presence and biochemical diversity, aggressiveness, and population size, primarily of indigenous bacterial groups [1,5]. The following BART tests were applied: IRB BART tests, for the detection of iron-associated bacteria ("iron bacteria") and some enteric species that can deposit iron; SLYME BART bio-tests, for detecting a wide range of bacteria that produce extracellular polymeric substances and are mostly biofilm-forming, including enteric and opportunistic pathogenic fluorescent *Pseudomonas* species; SRB BART bio-tests, for the detection of sulfate-reducing bacteria that generate biogenic H<sub>2</sub>S and cause localized corrosion; HAB BART bio-tests, for detecting a wide range of heterotrophic aerobic and facultatively anaerobic bacteria that are integral parts of biofilms and contribute to biocorrosion and biofouling processes, whose excessive abundance can compromise water quality through turbidity, changes in the organoleptic properties of raw water, and may pose a risk to public health. DN BART bio-tests, for the detection of denitrifying bacteria and the aquifer's potential for denitrification (nitrate removal). The results of BART analyses were processed using BART-SOFT V.6 software [1]. Based on the type and timing of appearance of signature reactions it enabled a determination of consortia and estimation of the abundance and aggressiveness of detected bacterial groups.

## RESULTS AND DISCUSSION

### The results of physicochemical analyses

The gained results are presented in Table 1. The dissolved oxygen (DO) was determined by *in situ* measurements and ranged from 2.03 mg/l to a 3.91 mg/l. The dissolved oxygen levels suggest that the examined groundwater was oxidized at the time of measurement, indicating the potential for aerobic oxidation of organic matter and other reduced chemical species. This process can be mediated through both chemical and microbiological means. The values of the redox potential, ranging from 363 to a maximum of 459 mV, suggest that oxidative processes likely dominate in the zone of the investigated objects. Electrolytic conductivity varied within a slightly broader range of oligosalinity, from a minimum of 362 µS/cm in B-4 to a maximum of 583 µS/cm in B-3. pH values were measured within a range of slightly basic values from 7.16 to 8.49. The observed concentrations of ammonium ions were increased, up to 1.36 mgN/L. The presence of nitrites and nitrates can indicate unfolding of nitrification processes and oxidation of ammonium ions. The organic carbon levels were slightly elevated, suggesting potential impact from organic pollution. This may be attributed to the presence of high numbers of aerobic heterotrophic bacteria, which utilize

organic carbon as an electron donor. Consequently, there is a potential health risk due to the possible presence of pathogenic bacterial species. Additionally, determined certain content of divalent iron and oxygen at the same time of measurement suggests imbalance and disequilibrium of redox-sensitive species (redox states) due to artificially introduced oxygen, possibly because of lowering the static level or depression cone. A wide range of sulfate concentration values from a minimum of 3.33 mg/l in B-1 to a maximum of 30.03 mg/l, 33.45 mg/l and 34.30 mg/l in B-10, B-13 and B-15, respectively, suggests intensive microbial processes of sulfate reduction as well as oxidation of ferrous sulfide with nitrate reduction. Lack of sulfides may be attributed to rapid reaction with dissolved divalent iron (insoluble ferrous sulfides - black precipitates) and consequently precipitation from the water phase. The B-10 is characterised by the highest groundwater level and consequently highest redox potential.

**Table 1** Examined groundwater quality – selected parameters

Sampling site		B-1	B-2	B-3	B-4	B-10	B-13	B-15
Parameter	Unit							
pH		7.16	7.23	7.62	7.53	8.08	8.49	8.2
Ec	μS/cm	499	488	583	362	437	402	476
Eh	mV	371.5	394.2	363	389.9	458.7	414.3	406.6
DO	mgO <sub>2</sub> /l	2.5	3.59	3.75	2.96	2.03	3.91	2.49
The consumption of KMnO <sub>4</sub>	mg/l	8.89	9.05	8.51	16.84	6.71	4.52	5.93
NH <sub>4</sub>	mgN/l	1.36	0.72	1.02	0.14	0.97	0.06	0.14
NO <sub>2</sub>	mgN/l	0.006	0.054	0.038	0.028	0.01	<0.005	0.011
NO <sub>3</sub>	mgN/l	0.15	0.81	0.62	2.83	<0.05	0.63	<0.05
Cl	mg/l	17.6	17.44	17.49	11.07	16.85	16.48	16.69
SO <sub>4</sub>	mg/l	3.33	15.5	18.35	25.47	30.03	33.45	34.3
OP	mgP/l	0.218	0.34	0.08	0.262	0.068	0.019	0.009
H <sub>2</sub> S	mg/l	<0.04	<0.04	<0.04	<0.04	0.12	<0.04	<0.04
TDS	mg/l	322	302	360	243	233	213	241
Total hardness	mg CaCO <sub>3</sub> /l	222.4	233.4	275.4	151.3	218.8	202.9	189.1
TOC	mg/l	2.48	1.98	3.8	3.89	1.96	1.16	1.2
Iron (II)	mg/l	0.72	0.4	0.21	0.26	1.35	0.32	0.12
Iron	mg/l	2.77	5.42	0.72	0.3	30.44	7.26	0.46

Compared to the prescribed values set by the Regulation on the Hygienic Potability of Drinking Water (“Official Gazette of the FRY”, No. 42/98 and 44/99, and “Official Gazette of the Republic of Serbia”, No. 28/2019) [4], the concentrations of ammonium, nitrites, iron, and manganese exceeded the permissible limits. Figure 1 and Figure 2 present the values of selected parameters.



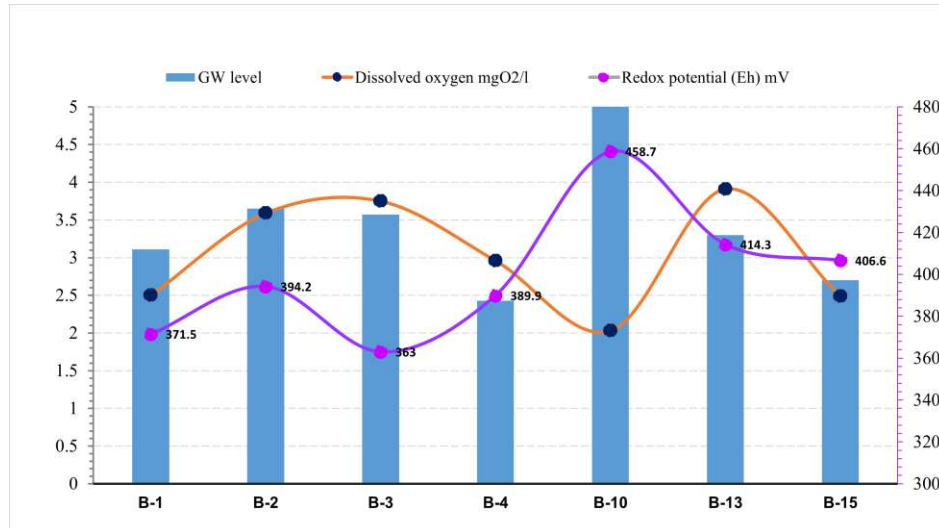


Figure 1 The measurement of oxygen levels and redox potential in groundwater

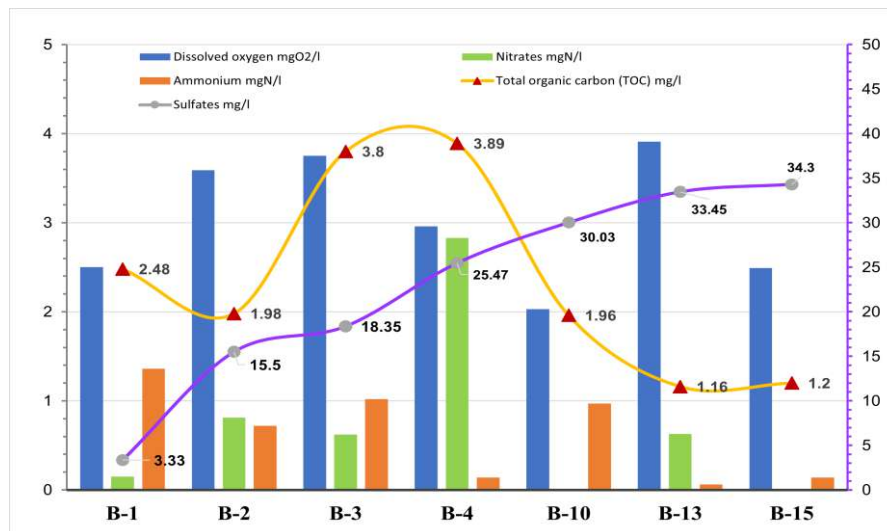
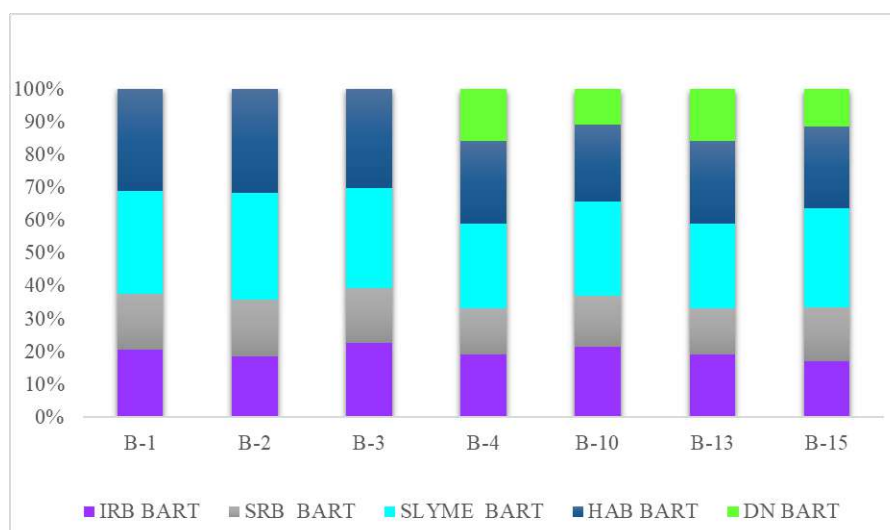


Figure 2 The content of redox-sensitive chemical species and total organic carbon in groundwater

### The results of the BART (Biological Activity Reaction Test) testing of groundwater

The community structure is depicted in Figure 3 as relative abundance, represented in percentages, with highlighted color-coded tested groups. Based on the obtained results, it can be concluded that the groundwater within examined objects exhibits similar biochemical diversity and very high abundance of aerobic and facultatively anaerobic, heterotrophic bacteria and bacteria producing extracellular polymers, i.e., biofilm-forming groups. In all samples, a uniform population of sulfate-reducing bacteria was observed, with their aggressiveness (biochemical activity) assessed as high as 6000 cfu/ml. Due to the detection of denitrifying bacteria in four examined objects, it is recommended to continuously monitor faecal indicator bacteria groups, particularly the presence of *Pseudomonas* species (*Pseudomonas aeruginosa*), at these sites.



**Figure 3** The structure of the bacterial community in examined groundwater

The determined biochemical diversity of the examined prokaryotic community in the groundwater alluvium of the Danube, besides the potential risk for the development of biofouling and biocorrosion processes on hydraulic elements, indicates a high potential for the removal of various pollutants. These pollutants are successfully degraded by aerobic and facultative anaerobic heterotrophic bacteria depending on prevailing conditions, as well as conditions of sulfate reduction, denitrification, and iron reduction.

For example, during the biodegradation of petroleum hydrocarbons, soil and groundwater microorganisms utilize oxygen ( $O_2$ ), nitrate ( $NO_3^-$ ), iron oxides [e.g.,  $Fe(OH)_3$ ], and sulfate ( $SO_4^{2-}$ ) as electron acceptors to degrade petroleum hydrocarbons to  $CO_2$  and  $H_2O$  through aerobic and anaerobic degradation [denitrification, iron (III) reduction, sulfate reduction, methanogenesis]. When these transformations occur, relevant geochemical indicators (e.g.,  $NO_3^-$ ,  $SO_4^{2-}$ ,  $CH_4$ ) will change accordingly, which can demonstrate the respective biodegradation mechanisms.

## CONCLUSION

Groundwater abstracted through hydraulic structures installed parallel to rivers, tapping adjacent aquifers for water production purposes, is widely utilized in a significant proportion in most European countries and certain regions of North America. The principle of bank filtration involves various physical, chemical, and biochemical processes and is particularly known for effectively reducing and/or removing suspended solids, organic pollutants, pathogenic microorganisms, heavy metals, nitrogen, toxic algae, as well as trace organic compounds (e.g., pharmaceuticals), compounds causing salinity, taste, and odor. Depending on hydrogeological conditions, redox status, and microbiome composition with their metabolic capabilities, the potential for the existence or biodegradation of various pollutants can be inferred based on biochemical indicators and chemical redox-sensitive species to protect and preserve the quality of groundwater in the vicinity of large rivers.

## **REFERENCES**

- [1] Cullimore R., *Water Well Biofouling, Diagnosis in Microbiology of Well Biofouling*, CRC Press, (1999), eBook ISBN9780203747247.
- [2] Fillinger L., Griebler C., Hellal J., *et al.*, *Microbial diversity and processes in groundwater in Groundwater Ecology and Evolution*, Academic Press, (2023), p.211–240, ISBN 9780128191194.
- [3] Griebler C., Lueders T., *Freshw. Biol.* 54 (2009) 649–677.
- [4] Regulation on the Hygienic Potability of Drinking Water (“Official Gazette of the Federal Republic of Yugoslavia”, No. 42/98 and 44/99, and “Official Gazette of the Republic of Serbia”, No. 28/2019).
- [5] Šaraba V., Nikodinović-Runić J., Obradović V., *et al.*, 2<sup>nd</sup> International Conference on Chemo and Bioinformatics Kragujevac: Institute for Information Technologies (2023) 186–190.



## METHATHESIS SYNTHESIZED OLIGOMERIC POLYPHENYLACETYLENE AS STERIC STABILIZER OF CARBON NANOTUBES/PLANT EXTRACT SYNTHESIZED ZINC OXIDE HYBRIDS

Silvia Dimova<sup>1\*</sup>, Katerina Zaharieva<sup>2</sup>, Ognian Dimitrov<sup>3</sup>, Petar D. Petrov<sup>1</sup>,  
Hristo Penchev<sup>1</sup>

<sup>1</sup>Institute of Polymers, Bulgarian Academy of Sciences, “Akad. G. Bonchev” St., Block 103A,  
1113 Sofia, BULGARIA

<sup>2</sup>Institute of Mineralogy and Crystallography “Akad. I. Kostov”, Bulgarian Academy of  
Sciences, Acad. G. Bonchev St., Block 107, 1113 Sofia, BULGARIA

<sup>3</sup>Institute of Electrochemistry and Energy Systems “Academician Evgeni Budevski”,  
Bulgarian Academy of Sciences, Acad. G. Bonchev St., Block 10, 1113, Sofia, BULGARIA

\*dimova@polymer.bas.bg

### Abstract

*Novel photocatalytically active polyphenylacetylene-stabilized multi-walled carbon nanotubes/zinc oxide (PPhA-MWCNTs/ZnO) hybrid dispersions in dimethylacetamide were prepared and then used for impregnation of cellulosic filter paper substrate. ZnO was prepared by plant extract – mediated synthesis. Attenuated Total Reflectance Fourier-transform Infrared (ATD FT-IR) Spectroscopy, Scanning Electron Microscopy (SEM) and Energy Dispersive Spectroscopy (EDS) analyses were used to establish the structure, morphology and composition of the hybrids. The potential of the prepared hybrid materials to degrade methylene blue (MB) dye as a model contaminant in aqueous solutions under UV illumination was studied. PPhA-MWCNTs/ZnO demonstrated a higher photocatalytic ability for MB degradation (59%) than PPhA-MWCNTs (53%).*

**Keywords:** polyphenylacetylene, carbon nanotubes, zinc oxide, green synthesis.

### INTRODUCTION

Multi-wall carbon nanotube - based composite materials have attracted attention due to the unique structural and electrical properties of carbon nanotubes and their specific interactions with different functional polymer matrixes. MWCNTs possess good electron conductivity, large surface areas, high adsorption capacities, and charge/size ratio, and can be relatively easy fabricated in an industrial scale. MWCNTs are widely used as effective support and as dopants in semiconductor nanocomposites for photoelectrochemical and photocatalytic applications [1,2]. Zinc oxide is environment-friendly and inexpensive n-type semiconductor having direct band gap of 3.3 eV as a pristine form [3]. Poly(phenylacetylene)s could be regarded as a special class of aromatic conjugated polymers. PPhA's and their hybrid materials show highly advanced functions toward sensors and actuators [4].

The present study aims at preparation, physicochemical characterization and photocatalytic investigations of novel polyphenylacetylene-stabilized multi-walled carbon

nanotubes/zinc oxide hybrid material for degradation of methylene blue dye (MB), as a contaminant in aqueous solutions, under UV irradiation.

## **MATERIALS AND METHODS**

### **Materials**

N,N-Dimethylacetamide (p.a.,  $\geq 99.5\%$  ((GC) as a solvent, Timestub<sup>TM</sup> -Graphitized Multi-walled Carbon nanotubes, TNGM3, Purity:  $>99\%$  OD: 10–20 nm Length: 5–30  $\mu\text{m}$  SSA: $>80\text{ m}^2/\text{g}$ , 1-phenyl-1-propyne (Alfa Aesar), isobutyraldehyde (Alfa Aesar), 1,2-dichloroethane,  $\text{Mg}_x\text{Fe}_{3-x}\text{O}_4$  ( $x=0.5$ ) catalyst,  $\text{Zn}(\text{NO}_3)_2 \cdot 6\text{H}_2\text{O}$  (Valerus Co.), NaOH (Valerus Co.) and *Vaccinium vitis-idaea* L (dried leaves).

### **Preparation of polyphenylacetylene-stabilized multi-walled carbon nanotubes/zinc oxide hybrid materials**

Oligomeric polyphenylacetylene was synthesized by carbonyl-olefin metathesis reaction described in our previous work [5]. Mixing dilute solution of conjugated PPhA and MWCNTs with or without ZnO nanoparticles in an appropriate organic solvent afforded polymer-wrapped MWCNTs and MWCNTs/ZnO dispersions. Two kinds of dispersions were prepared, namely: PPhA-MWCNTs and PPhA-MWCNTs/ZnO. In a typical synthetic procedure, 1 mg of PPhA was dissolved in 10 ml of dimethylacetamide and then 10 mg of MWCNTs were added and a 30 seconds ultrasonication treatment was applied till the stable dispersion was obtained. We assume that the stabilization was achieved through the spontaneous wrapping the conjugated PPhA chains round the MWCNT, which was driven by  $\pi$ - $\pi$  interactions of the PPhA skeleton.

Additionally, ZnO nanoparticle powders were prepared by green synthesis using plant extract of *Vaccinium vitis-idaea* L. and further used in the preparation of mixed hybrid dispersion PPhA-MWCNTs/ZnO (1:1 wt./wt.). The final concentration of both MWCNTs and ZnO was 1 mg/ml. Next, the obtained hybrid dispersions were used for surface impregnation of cellulosic filter paper substrate.

### **Physicochemical characterization**

The surface morphology of the samples was investigated with scanning electron microscopy using Zeiss Evo 10 microscope (Carl Zeiss Microscopy, Oberkochen, Germany). The photographs were taken in secondary electrons mode with accelerating voltage of 25 keV and no conductive coating on the samples. The chemical composition of the surface was studied with electron dispersive spectroscopy probe Oxford Ultim Max 40 (Oxford Instruments, Abingdon, United Kingdom). The results were compiled with AZtec software (version 6.1 HF4).

Attenuated total reflection Fourier transform infrared spectroscopic analysis was performed on an IR Affinity-1 spectrophotometer (Shimadzu, Kyoto, Japan) equipped with a MIRacle ATR accessory (diamond crystal, depth of penetration of the IR beam into the material is 2  $\mu\text{m}$ ).

## Photocatalytic tests

The photocatalytic degradation of aqueous solution of Methylene Blue dye with concentration of 5 ppm was studied in semi-batch slurry reactor using prepared PPhA-MWCNTs and PPhA-MWCNTs/ZnO as catalyst and 20 ml of dye solution under constant stirring and air flowing. The photocatalytic tests were carried out using UV–Vis spectrophotometer UV-1600PC in the wavelength range from 200 to 800 nm ( $\lambda_{\text{max}}=664$  nm) and a polychromatic UV-A lamp illumination (18W) with maximum of the emission at 365 nm and intensity of illumination was  $0.66 \text{ mW/cm}^2$ . The investigated systems were left in the dark for about 30 min to reach adsorption-desorption equilibrium state before switching on the UV irradiation for 3 hours. Periodically the sample aliquots were taken from the solution. The degree of dye degradation was calculated using the dependence:  $((C_0-C)/C_0) \cdot 100$ , where  $C_0$  and  $C$  were initial concentration before turning on the illumination and residual concentration of the dye solution after illumination for selected time interval.

## RESULTS AND DISCUSSION

FT-IR spectroscopy was performed to assess the quality of synthesized materials and the presence of functional groups. The FT-IR spectra were plotted in the range of  $650\text{--}4000 \text{ cm}^{-1}$  (Figure 1). The presence of aliphatic fragment is suggested by the aliphatic C-H stretching bands at  $2800\text{--}3000 \text{ cm}^{-1}$  accompanied by the aromatic C-H stretching band just above  $3000 \text{ cm}^{-1}$ . In the FT-IR spectra of PPhA-MWCNTs and PPhA-MWCNTs/ZnO were observed peaks at about  $1270 \text{ cm}^{-1}$  and  $1710 \text{ cm}^{-1}$  attributed to the carboxylic group (C-O and C=O). The peaks about  $1200 \text{ cm}^{-1}$  and  $1020 \text{ cm}^{-1}$  are related to the C-H and  $1550 \text{ cm}^{-1}$  to the C=C. These bands are characteristics of carbon nanotubes [6].

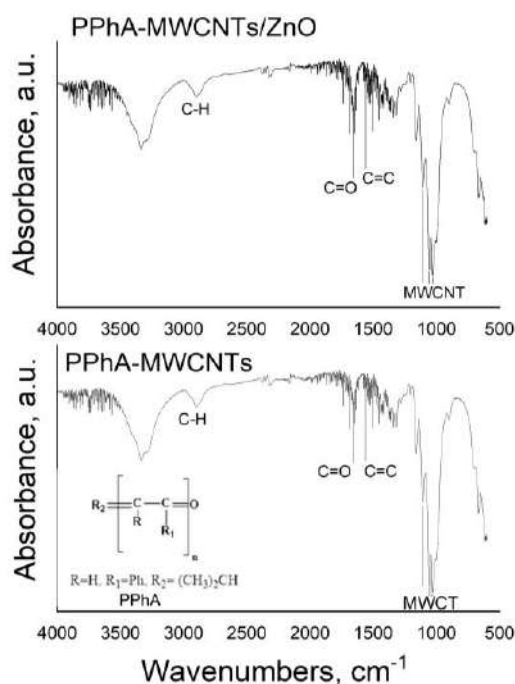


Figure 1 ATR FT-IR analysis of prepared PPhA-MWCNTs and PPhA-MWCNTs/ZnO hybrids



Figure 2 shows selected SEM images and EDS spectra of the synthesized PPhA-MWCNTs and PPhA-MWCNTs/ZnO hybrid materials. The EDS spectra show the presence of C and O for PPhA-MWCNTs and C, O and Zn peaks for PPhA-MWCNTs/ZnO, without other elemental contaminations. The EDS results of synthesized PPhA-MWCNTs and PPhA-MWCNTs/ZnO hybrid materials are presented in Tables 1 and 2. The SEM observation of cellulose substrate impregnated with PPhA-stabilized MWCNTs showed well-dispersed unbundled (individual) carbon nanotubes, as shown on Figure 2A. This is an indication of strong  $\pi$ - $\pi$  interactions of the surface wrapped PPhA macromolecules on the surface of the CNTs. The SEM image (Figure 2B) showed the presence of needle-like shaped ZnO nanoparticles which formed aggregates deposited onto the CNTs cellulose impregnated layer. A similar observation for pristine ZnO NPs obtained by phyto-mediated synthesis using *Berberis aristat* plant extract was reported by Chandra *et al.* [7].

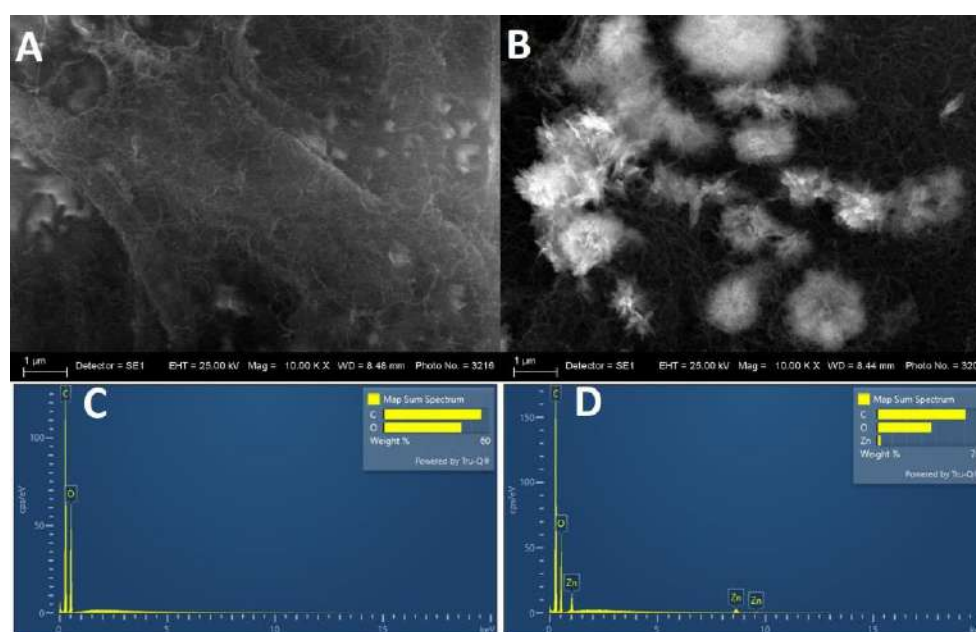


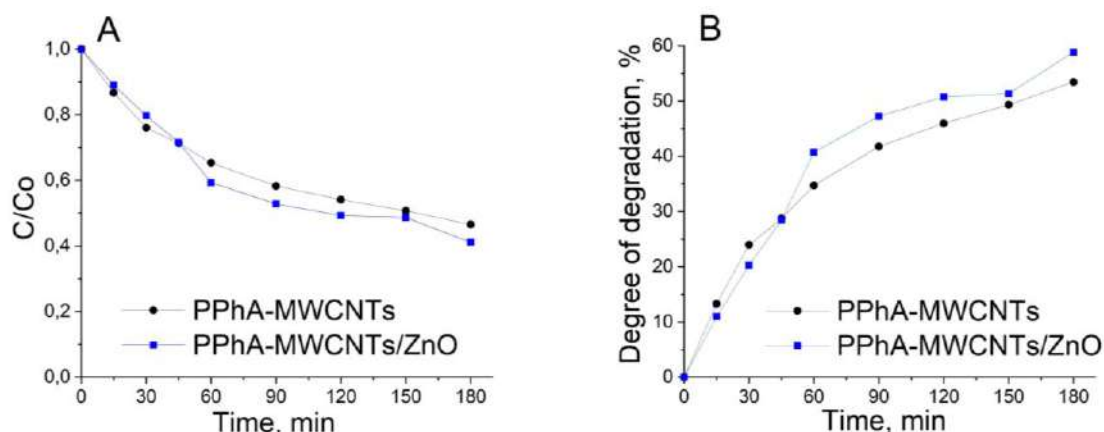
Figure 2 A) and B) SEM images; C) and D) EDS spectra of prepared PPhA-MWCNTs and PPhA-MWCNTs/ZnO hybrids

Table 1 EDS results of synthesized PPhA-MWCNTs hybrid materials

Element	Line	Wt.%	Atomic %
C	K series	55.72	62.63
O	K series	44.28	37.37
Total		100.00	100.00

Table 2 EDS results of synthesized PPhA-MWCNTs/ZnO hybrid materials

Element	Line	Wt.%	Atomic %
C	K series	60.60	68.19
O	K series	37.10	31.34
Zn	K series	2.30	0.48
Total		100.00	100.00



**Figure 3** A) The concentration ratio  $C/C_0$ ; B) Degree of degradation of Methylene Blue dye with time of UV illumination

The reaction of photocatalytic degradation of MB dye was carried out using synthesized PPhA-MWCNTs and PPhA-MWCNTs/ZnO hybrids as photocatalysts under UV light. Figure 3 A and B presents the concentration ratio  $C/C_0$  and degree of degradation of MB as a function of the UV irradiation time. The photocatalytic tests revealed that PPhA-MWCNTs/ZnO photocatalyst has higher photocatalytic ability for degradation of MB compared to PPhA-MWCNTs. The degree of degradation of MB after 180 minutes UV irradiation using PPhA-MWCNTs/ZnO and PPhA-MWCNTs hybrid materials were 59% and 53%, respectively. The enhanced photocatalytic activity of PPhA-MWCNTs/ZnO could be explained with interfacial connection between the ZnO and the conjugated polymer wrapped MWCNTs, the photo-generated electron of the conduction band of ZnO is transferred to good electron acceptor (MWCNTs) and the photo-generated holes remain on the surface of ZnO. Therefore the recombination rate of the photo-generated electron and holes slow down [8].

## CONCLUSION

New polymer hybrid photocatalysts, based on metathesis synthesized oligomeric polyphenylacetylene as steric stabilizer of multi-walled carbon nanotubes/plant extract synthesized zinc oxide, were successfully prepared and characterized. The PPhA-MWCNTs/ZnO demonstrated higher photocatalytic ability to degrade MB dye (59% degradation) in comparison with PPhA-MWCNTs hybrid materials (53%) after 180 min UV irradiation.

## ACKNOWLEDGEMENT

*The authors express their gratitude to the project with the Bulgarian National Science Fund, Bulgaria, KP-06-N69/8 (KII-06-H69/8), “Novel polymer-hybrid materials containing (bio)synthesized metal oxide particles with improved photocatalytic and antimicrobial potential” for the financial support. Research equipment of Distributed Research Infrastructure INFRAMAT, part of the Bulgarian National Roadmap for Research Infrastructures, supported by the Bulgarian Ministry of Education and Science, was used in this investigation.*

## **REFERENCES**

- [1] Alias M.F.A., Mouhamad Raghad S., Abd – Alsada A.S., *et al.*, AIP Conf. Proc. 2922 (2024) 120001-1–120001-10; 4th International Conference in Physical Science & Advanced Materials, 7–13 October, Antalya, Turkey (2022).
- [2] Wani A.A., Rather R.A., Shaari N., *et al.*, J. Environ. Chem. Eng. 12 (2) (2024) 112461.
- [3] Shakti N., Gupta P.S., Appl. Phys. Res. 2 (1) (2010) 19–28.
- [4] Jin Y.J., Kwak G., Polym. Rev. 57 (1) (2017) 175–199.
- [5] Dimova S., Zaharieva K., Sinigersky V., *et al.*, J. Int. Sci. Publ.: Mater. Methods Technol. 8 (2014) 233–240.
- [6] García-Hernández D.A., Manchado A., Gemmi M., *et al.*, Full. Nanotub. Car. N. 26 (10) (2018) 654–660.
- [7] Chandra H., Patel D., Kumari P., *et al.*, Mater. Sci. Eng. C. 102 (2019) 212–220.
- [8] Phin H.-Y., Ong Y.-T., Sin J.-C., J. Environ. Chem. Eng. 8 (2020) 103222.



## EQUILIBRIUM ANALYSIS OF COPPER IONS BIOSORPTION ONTO HAZELNUT SHELLS

Miljan Marković<sup>1\*</sup>, Milan Gorgievski<sup>1</sup>, Nada Štrbac<sup>1,2</sup>, Vesna Grekulović<sup>1</sup>,  
Marina Marković<sup>1</sup>, Kristina Božinović<sup>1</sup>, Dalibor Jovanović<sup>3</sup>

<sup>1</sup>University of Belgrade, Technical Faculty in Bor, V.J. 12, 19210 Bor, SERBIA

<sup>2</sup>Engineering Academy of Serbia, Kneza Miloša 9/IV, 11000 Belgrade, SERBIA

<sup>3</sup>Copper Mill Sevojno, Prvomajska bb, 31205 Sevojno, SERBIA

\*[mmarkovic@tfbor.bg.ac.rs](mailto:mmarkovic@tfbor.bg.ac.rs)

### Abstract

*The equilibrium analysis of the copper ions biosorption process using hazelnut shells as a biosorbent is presented in this paper. The experimental data were analyzed using the non-linear forms of three empirical isotherm models, namely the Langmuir isotherm model, the Freundlich isotherm model and the Temkin isotherm model. The performed analysis indicated that the Temkin isotherm model was the best fit for the analyzed data ( $R^2=0.9847$ ). The equilibrium analysis also showed a negligible difference between the experimentally obtained ( $q_{e,exp}$ ) and model calculated ( $q_{e,m}$ ) biosorption capacities, which indicates that the hazelnut shells are almost completely saturated with copper ions.*

**Keywords:** equilibrium analysis, biosorption, isotherm models, hazelnut shells, copper ions.

### INTRODUCTION

Some heavy metals are biologically significant as trace elements. However, their toxic effect on living organisms makes them an environmental problem. Years of scientific research indicates that these metals are released into the environment by natural and anthropogenic sources. The most common between them are mining and industrial activities, along with traffic exhaust fumes [1].

Water pollution is one of the biggest environmental problems today. Many industries, such as metallurgy processing plants, metal finishing plants, electronic industry, electroplating, phytopharmaceutical plants, and many others, release heavy metals along with their wastewaters, polluting the environment [2].

Wastewaters are being treated using the well known conventional technologies, in order to remove heavy metals. These treatments include: aeration, flotation, coagulation and flocculation, adsorption, ion-exchange, membrane processes, electrochemical methods, and others. However, these conventional methods come with certain disadvantages, including: high cost, continuous input of chemicals, incomplete metal removal, sludge generation, and others. Biosorption could be one of the possible alternatives to conventional methods for wastewater treatment, especially those with low heavy metal ions content [3,4].

Many biological waste materials, such as agricultural waste, fungi, algae, peat and yeasts have been tested as potential adsorbents for heavy metal ions adsorption from water solutions [5].

Adsorption isotherm models are mostly used in order to obtain information about the process mechanism, as well as the maximum biosorption capacity. Many empirical models can be used to describe the biosorption process [6].

In this work, the equilibrium of the biosorption of  $\text{Cu}^{2+}$  ions using hazelnut shells as a biosorbent was modelled using the non-linear Langmuir, Freundlich and Temkin adsorption isotherm model, as models most frequently used in literature.

## MATERIALS AND METHODS

Prior the biosorption experiments, hazelnut shells were ground and sieved on a set of laboratory sieves, and the fraction (-1+0.4) was used for the biosorption equilibrium experiments.

The equilibrium data was obtained by bringing into contact 0.5 g of hazelnut shells with 50 mL of synthetic solutions of different  $\text{Cu}^{2+}$  concentrations, ranging from 5 to 200  $\text{mg dm}^{-3}$ . The suspension was stirred on a magnetic stirrer for 60 minutes, considering this time long enough to reach the equilibrium between phases [4], then filtered, and the filtrate analysed for the remaining copper ions content.

## RESULTS AND DISCUSSION

### Biosorption isotherm for copper ions biosorption onto hazelnut shells

The obtained experimental equilibrium data is shown on Figure 1.

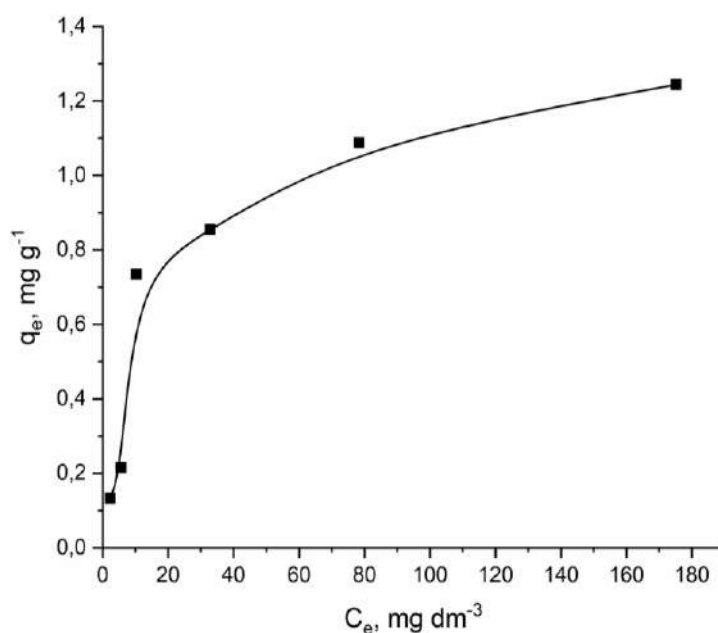


Figure 1 Biosorption isotherm for copper ions biosorption onto hazelnut shells

### Langmuir model

The Langmuir adsorption isotherm model is based on the assumption that the biosorption process occurs in a monolayer, at a finite number of definite localized sites [7].

This model can be expressed as:

$$q_e = \frac{q_m K_L C_e}{1 + K_L C_e} \quad (1)$$

where  $C_e$  is the equilibrium concentration of metal ions ( $\text{mg dm}^{-3}$ ),  $q_e$  is the equilibrium adsorption capacity ( $\text{mg g}^{-1}$ ),  $q_m$  is the maximum adsorption capacity ( $\text{mg g}^{-1}$ ) and  $K_L$  ( $\text{dm}^3 \text{g}^{-1}$ ) is the Langmuir equilibrium constant.

The non-linear Langmuir model analysis of copper ions biosorption onto hazelnut shells is shown on Figure 2. The obtained model parameters are given in Table 1.

### Freundlich model

The Freundlich isotherm model is used to describe adsorption on heterogeneous surfaces. This model can describe adsorption processes in a limited range of concentrations [7].

The Freundlich adsorption isotherm model can be expressed as:

$$q_e = K_f C_e^{1/n} \quad (2)$$

where  $C_e$  is the equilibrium concentration of copper ions in the solution ( $\text{mg dm}^{-3}$ );  $q_e$  is the adsorbent capacity defined as mass of the adsorbed metal per unit mass of the adsorbent ( $\text{mg g}^{-1}$ ) at equilibrium;  $K_f$  is the Freundlich equilibrium constant ( $(\text{mg g}^{-1}) (\text{dm}^3 \text{mg}^{-1})^{1/n}$ ), and  $1/n$  is the coefficient of heterogeneity in the Freundlich adsorption isotherm equation.

The non-linear Freundlich model analysis is shown on Figure 2. The obtained model parameters are given in Table 1.

### Temkin model

This model is based on the assumptions that the heat of sorption of all molecules linearly decreases with the coverage of the adsorbent, which is conditioned by adsorbent-adsorbate interactions, and (2) there is a uniform distribution of binding energies up to some maximum binding energy [8].

The Temkin model is given as:

$$q_e = B \ln(K_T C_e) \quad (3)$$

where  $B = RT/b$  is the Temkin constant, which refers to the adsorption heat ( $\text{J mol}^{-1}$ );  $b$  is the variation of adsorption energy ( $\text{J mol}^{-1}$ );  $R$  is the universal gas constant ( $\text{J mol}^{-1} \text{K}^{-1}$ );  $T$  is the temperature (K);  $K_T$  is the Temkin equilibrium constant ( $\text{dm}^3 \text{g}^{-1}$ );  $q_e$  is the adsorption



capacity defined as mass of the adsorbed metal per unit mass of the adsorbent ( $\text{mg g}^{-1}$ ) at equilibrium;  $C_e$  is the equilibrium concentration of copper ions in the solution ( $\text{mg dm}^{-3}$ ).

The analysis of the experimental data using the non-linear Temkin model is shown on Figure 2. The isotherm model parameters are given in Table 1.

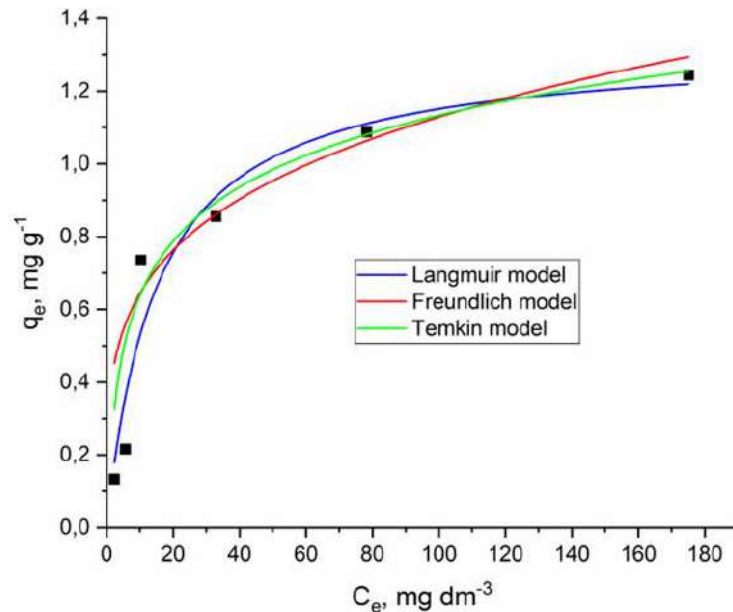


**Figure 2** Non-linear adsorption isotherm models for copper ions biosorption onto hazelnut shells

**Table 1** Obtained equilibrium parameters for the non-linear Langmuir, Freundlich and Temkin isotherm models for copper ions biosorption onto hazelnut shells

Langmuir		Freundlich			Temkin				
$K_L$ $\text{dm}^3 \text{mg}^{-1}$	$q_{\text{exp}}$ $\text{mg g}^{-1}$	$q_m$ $\text{mg g}^{-1}$	$R^2$	$K_F$	$1/n$	$R^2$	$B$ $\text{J mol}^{-1}$	$K_T$ $\text{dm}^3 \text{g}^{-1}$	$R^2$
0.067	1.244	1.324	0.935	0.367	0.244	0.916	0.215	1.936	0.985

Based on the results given in Table 1, it can be concluded that the Temkin adsorption isotherm model shows the best agreement with the experimental data ( $R^2=0.9487$ ), and is the best model for describing the equilibrium of the biosorption of  $\text{Cu}^{2+}$  ions onto hazelnut shells in the observed concentration range. This result indicates that the heat of sorption of all molecules linearly decreases with the coverage of the adsorbent, and that there is a uniform distribution of binding energies up to some maximum binding energy [8].

## CONCLUSION

Hazelnut shells were used as a biosorbent, in order to remove copper ions from synthetic aqueous solutions. The process equilibrium was analysed using three non-linear isotherm models, i.e. the Langmuir, the Freundlich and the Temkin adsorption isotherm model. The obtained results indicate that the Temkin adsorption isotherm model is the best fit for the analysed process, with the correlation coefficient  $R^2=0.9487$ . This model indicates that the

heat of sorption of all molecules linearly decreases with the coverage of the adsorbent, and that there is a uniform distribution of binding energies up to some maximum binding energy.

### **ACKNOWLEDGEMENT**

*The research presented in this paper was done with the financial support of the Ministry of Science, Technological Development and Innovation of the Republic of Serbia, within the funding of the scientific research work at the University of Belgrade, Technical Faculty in Bor, according to the contract with registration number 451-03-65/2024-03/200131.*

### **REFERENCES**

- [1] Mahurpawar M., Int. J. Res. Granthaalayah 3 (2015) 1–7.
- [2] Perez-Lopez R., Nieto J.M., Almodovar G.R., Appl. Geochem. 22 (2007) 1919–1935.
- [3] Šećerov Sokolović R., Sokolović S., Inženjerstvo u zaštiti okoline, Univerzitet u Novom Sadu Tehnološki fakultet, Novi Sad (2002), p.1–299. ISBN: 628.316.12(0.75).
- [4] Gorgievski M., Božić D., Stanković V., *et al.*, Ecol. Eng. 58 (2013) 113–122.
- [5] Nemes L.N., Bulgariu L., Open Chem. 14 (2016) 175–187.
- [6] Mohammed-Ridha M.J., Ahmed A.S., Raouf N.N., NJES 20 (2017) 298–310.
- [7] Chen X., Information 6 (2015) 14–22.
- [8] Hamdaoui O., Naffrechoux E., J. Hazard. Matter. 147 (2007) 381–394.



## CALCULATION OF CALCIUM OXIDE CONSUMPTION IN THE MINE WASTEWATER TREATMENT FROM INACTIVE OPEN PITS OF THE COPPER MINE

Vesna M. Marjanović<sup>1\*</sup>, Radmila Marković<sup>1</sup>, Dragana Božić<sup>1</sup>

<sup>1</sup>Mining and Metallurgy Institute, A. Ajštajna 1, 19210 Bor, SERBIA

\*vesna.marjanovic@irmbor.co.rs

### Abstract

*This paper presents the calculation of required amount of calcium oxide (CaO) for neutralization the mine water, accumulated in the abandoned open pits of the copper mine. This water represents a resource that can be reused in the mining activities after treatment. Calculation of calcium hydroxide consumption on a daily basis for converting the metal ions (Fe, Cu and Zn), dissolved in mine water into an insoluble hydroxide form and increasing the pH value, is given in relation to their flow and mass of CaO needed to neutralize 1 m<sup>3</sup> of water.*

**Keywords:** mine wastewater, neutralization, calcium oxide.

### INTRODUCTION

There is accumulation of large amounts of water at the inactive open pits of the copper mine, which most often come from atmospheric precipitation, underground water, water from the surrounding catchment areas and water from rock cracks [1]. The chemical composition of this water depends on the mineralogical and chemical composition of the ore deposit. Due to the long-term effect of accumulated water on this material, this water is characterized by the specific physical and chemical properties such as a low pH value between 2–3, a high content of dissolved iron, sulfates and heavy metals [2,3].

Acid mine water treatment technologies include the precipitation methods of metal hydroxide precipitation with lime milk, the process of precipitation the metal sulfides present in water, the return sludge method (HDS) and biological oxidation methods.

Probably the most conventional and widely used method of wastewater treatment is neutralization. By increasing the pH value of waste water by addition of lime milk, metals will settle in the form of metal hydroxides and form sludge [4,5].

The choice of wastewater treatment process is the key to designing a wastewater treatment system. It is directly related to the requirement for water quality after treatment, requirement for stable and reliable plant operation, adequately trained personnel and level of investment and operating costs.

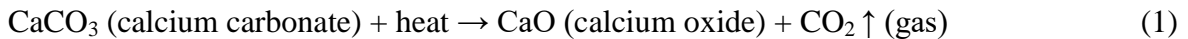
The wastewater treatment process should be carefully selected according to the wastewater quality, output water requirements, degree of treatment, local temperature, engineering geology, surrounding environment and other conditions, and at the same time the economic factors must be considered.

## MATERIALS AND METHODS

### Calculation of the CaO consumption for the mine water neutralization

For the process of chemical treatment the mine water, a process of neutralization with a 10% lime milk suspension is provided, which is prepared by mixing the calcium oxide (CaO, quicklime) and water in a certain ratio. In order to obtain the lime milk of a defined concentration, it is necessary to dissolve quicklime in water at a certain speed, defined by the procedure for preparation the lime milk and depends on the amount used for dissolution.

Quicklime consists primarily of calcium oxide and is produced from limestone in a process known as calcination:



During the preparation of lime milk, the following properties of CaO should be taken into account: type, purity, reactivity, particle size. The type of CaO affects the speed of its conversion into the form of  $\text{Ca(OH)}_2$ . Purity represents the amount of quicklime that is chemically available as calcium oxide (CaO) and it affects the reactivity and determines the purity of hydrated lime product. The purity of commercially available quicklime that will be used for calculation is with a calcium oxide content of approx. 70%. Reactivity describes the relative capacity of quicklime to react chemically with water. Reactivity is a function of purity, particle size, and other factors such as particle porosity. The quenching reaction of CaO is considered complete when the temperature of a given sample reaches a maximum. As the reactivity increases, so does the quenching rate, ultimate temperature rise, and specific surface area of hydrated lime. The mass concentration of 10% lime milk is defined as the ratio of the mass of water to the mass of quicklime. This ratio does not include dilution water or process water, which may be added to lime milk after its preparation.

The starting data used for calculation are:

- Mine water flow  $Q = 5000 \text{ m}^3/\text{day}$ ,
- Mass of CaO for mine water neutralization of  $1 \text{ m}^3$ : 1.5 kg,
- Mass of CaO for daily flow of  $5000 \text{ m}^3/\text{day}$  is 7.5 t/day,
- Coefficient of increased consumption: 1,
- Specific density  $\text{H}_2\text{O}$ ,  $\rho$ :  $1000 \text{ kg/m}^3$

Calculation of the required volume of water to prepare 10% lime milk:

$$V_{\text{H}_2\text{O}} = \frac{M_{\text{CaO}} \cdot 100}{10} - M_{\text{CaO}} = \frac{7.5 \cdot 100}{10} - 7.5 = 67.5 \frac{\text{m}^3}{\text{day}} \quad (1)$$

Calculation of lime consumption is based on real data on the quality of waste water that will be treated in the waste water treatment plant given in Table 1 and requirements for the output water quality given in Table 2. The concentrations of elements that are present in the mine water and are lower of 1 mg/L were not taken into account during the calculation.

**Table 1** An example of chemical composition of accumulated mine water in an inactive open pit

Element	Zn	Cd	Cr	Cu	Ni	Fe	Pb	As	Hg
mg/l	12.82	0.12	0.06	29.56	0.62	149.28	0.16	<0.020	<0.0005

**Table 2** pH value of accumulated mine water before and after neutralization

Water	Parameter	Value
Mine water before neutralization	pH	2.0–3.0
Water after neutralization	pH	6.0–9.0

## RESULTS AND DISCUSSION

The lime consumption to adjust the pH value from 2 to 9

The calculation was made on the basis of the following initial data:

- Flow of mine waste water on a daily basis,  $Q = 5000 \text{ m}^3/\text{day}$
- $\text{pH}_{\text{start}} = 2$ ;  $\text{pH}_{\text{end}} = 9$ ,
- Molar mass  $\text{Ca}(\text{OH})_2$ , 74 g/mol,
- Molar mass  $\text{CaO}$ , 56 g/mol,
- Activity  $\text{CaO}$ , 70%,
- Molar mass  $\text{CaSO}_4$ , 136 g/mol,
- Molar mass  $\text{H}_2\text{SO}_4$ , 98 g/mol,
- Concentration of calcium hydroxide, 10%  $C_{\text{Ca}(\text{OH})_2}$ .

Based on the pH value, the concentration of  $\text{H}^+$  ions at  $\text{pH}=2$  and  $\text{pH}=9$  were calculated and the same is:

- $\text{H}^+$  concentration at  $\text{pH} 2 = 0.01 \text{ mol/l}$ ,
- $\text{H}^+$  concentration at  $\text{pH} 9 = 0.000000001 \text{ mol/l}$ ,
- Number of  $\text{H}^+$  ions,  $n_{\text{H}^+}: 2$

The required mass of  $\text{Ca}(\text{OH})_2$  to change the pH value from pH 2 to pH 9 is:

$$M_{\text{Ca}(\text{OH})_2} = \frac{Q \cdot (C_{\text{pH}2} - C_{\text{pH}9}) \cdot 74}{n_{\text{H}^+} \cdot 10^6} = \frac{5000000 \cdot (0.01 - 0.000000001) \cdot 74}{2 \cdot 10^6} = 1.85 \frac{\text{t}}{\text{day}} \quad (2)$$

Consumption 10% calcium hydroxide  $M_{10\% \text{Ca}(\text{OH})_2}$ :

$$M_{10\% \text{Ca}(\text{OH})_2} = \frac{M_{\text{Ca}(\text{OH})_2}}{10} \cdot 100 = \frac{1.85}{10} \cdot 100 = 18.5 \frac{\text{t}}{\text{day}} \quad (3)$$

Consumption 100%  $\text{CaO}$ :

$$M_{100\% \text{CaO}} = \frac{M_{\text{Ca}(\text{OH})_2} \cdot 56}{74} = \frac{1.85 \cdot 56}{74} = 1.4 \frac{\text{t}}{\text{day}} \quad (4)$$

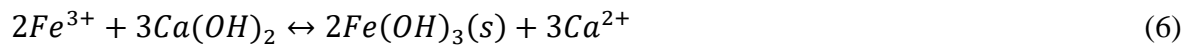
Consumption of  $\text{CaO}$  activity 70%:

$$M_{70\% CaO} = 1.4 / 0.7 = 2 \frac{t}{day} \quad (5)$$

After the lime is slaked, the slurry is added to the acid mine water, which leads to an increase in the pH value. Free (OH<sup>-</sup>) ions react with metal ions to form the metal hydroxides that precipitate at a certain pH value.

Calculation of lime consumption for precipitation of Fe<sup>3+</sup> ions at concentration of approx. 150 mg/l

Precipitation of Fe hydroxide is shown by the following reaction:



Calculation of CaO consumption was made on the basis of the following initial data:

- Concentration of Fe<sup>3+</sup> ion, cca 150 mg/l,
- Coefficient of increased consumption: 1,
- Atomic mass Fe, 56 g/mol,
- Molar mass Fe(OH)<sub>3</sub> 107 g/mol.

Consumption 10% Ca(OH)<sub>2</sub>:

$$M_{10\%Ca(OH)_2} = \frac{C_{Fe^{3+}} \cdot Q \cdot 74 \cdot 3}{56 \cdot 2 \cdot 10 \cdot 10^9} \cdot 100 = \frac{150 \cdot 5000000 \cdot 74 \cdot 3}{56 \cdot 2 \cdot 10 \cdot 10^9} \cdot 100 = 14.85 \frac{t}{day} \quad (7)$$

Consumption Ca(OH)<sub>2</sub>:  $M_{Ca(OH)_2} = 14.85 \cdot 0.1 = 1.485$  t/day.

Consumption 100% CaO:

$$M_{100\% CaO} = \frac{M_{Ca(OH)_2} \cdot 56}{74} = \frac{1.485 \cdot 56}{74} = 1.12 \frac{t}{day} \quad (8)$$

Consumption of CaO activity 70%:

$$M_{70\% CaO} = 1.12 / 0.7 = 1.6 \frac{t}{day} \quad (9)$$

Calculation of the water amount for chemical reaction with CaO, resulting in Ca(OH)<sub>2</sub>:

$$M_{H_2O} = \frac{18 \cdot M_{Ca(OH)_2}}{74} = \frac{18 \cdot 1.12}{74} = 0.27 \frac{t}{day} \quad (10)$$



Calculation of lime consumption for precipitation of  $\text{Cu}^{2+}$  ions at concentration of approx. 30 mg/l

Precipitation of Cu hydroxide is shown by the following reaction:



Calculation of lime consumption was made on the basis of the following initial data:

- Concentration of  $\text{Cu}^{2+}$  ions, cca 30 mg/l,
- Coefficient of increased consumption: 1.4,
- Atomic mass Cu, 64 g/mol,
- Molar mass  $\text{Cu}(\text{OH})_2$ , 98 g/mol.

Consumption 10%  $\text{Ca}(\text{OH})_2$ :

$$M_{10\% \text{Ca}(\text{OH})_2} = \frac{C_{\text{Cu}} \cdot Q \cdot 74}{A_{\text{rCu}} \cdot 0.1 \cdot 10^9} = \frac{30 \cdot 5000000 \cdot 74 \cdot 1.4}{64 \cdot 0.1 \cdot 10^9} = 2.40 \frac{\text{t}}{\text{day}} \quad (12)$$

Consumption of calcium hydroxide:  $M_{\text{Ca}(\text{OH})_2} = 2.40 \cdot 0.1 = 0.24 \text{ t/day}$ .

Consumption 100% CaO:

$$M_{100\% \text{CaO}} = \frac{M_{\text{Ca}(\text{OH})_2} \cdot 56}{74} = \frac{0.24 \cdot 56}{74} = 0.18 \frac{\text{t}}{\text{day}} \quad (13)$$

Consumption of CaO activity 70%:

$$M_{70\% \text{CaO}} = 0.18 / 0.7 = 0.26 \frac{\text{t}}{\text{day}} \quad (14)$$

Calculation of the required amount of water for chemical reaction of CaO and  $\text{H}_2\text{O}$  resulting in  $\text{Ca}(\text{OH})_2$  is:

$$M_{\text{H}_2\text{O}} = \frac{18 \cdot M_{\text{Ca}(\text{OH})_2}}{56} = \frac{18 \cdot 0.24}{56} = 0.08 \frac{\text{t}}{\text{day}} \quad (15)$$

Calculation of lime consumption for precipitation of  $\text{Zn}^{2+}$  ions at concentration of approx. 13 mg/l

Precipitation of Zn hydroxide is shown by the following reaction:



Calculation of lime consumption was made on the basis of the following initial data:

- Concentration of  $Zn^{2+}$  ions, cca 13 mg/l,
- Coefficient of increased consumption: 1
- Atomic mass of Zn, 65.5 g/mol,
- Molar mass of  $Zn(OH)_2$ , 99.5 g/mol.

Consumption 10%  $Ca(OH)_2$ :

$$M_{10\% Ca(OH)_2} = \frac{C_{Zn} \cdot Q \cdot 74}{A_{rZn} \cdot 0.1 \cdot 10^9} = \frac{13 \cdot 5000000 \cdot 74}{65.5 \cdot 0.1 \cdot 10^9} = 0.73 \frac{t}{day} \quad (17)$$

Consumption of calcium hydroxide:  $M_{Ca(OH)_2} = 0.73 \cdot 0.1 = 0.073$  t/day.

Consumption 100% CaO:

$$M_{100\% CaO} = \frac{M_{Ca(OH)_2} \cdot 56}{74} = \frac{0.073 \cdot 56}{74} = 0.055 \frac{t}{day} \quad (18)$$

Consumption of CaO activity 70%:

$$M_{70\% CaO} = 0.055 / 0.7 = 0.078 \frac{t}{day} \quad (19)$$

Calculation of the required amount of water for chemical reaction of CaO and  $H_2O$  resulting in  $Ca(OH)_2$  is:

$$M_{H_2O} = \frac{18 \cdot M_{Ca(OH)_2}}{56} = \frac{18 \cdot 0.073}{56} = 0.023 \frac{t}{day} \quad (20)$$

The total mass of CaO for treatment of 5000 m<sup>3</sup>/day of mine waste water obtained on the basis of previous calculations:

$$M_{70\% CaO} = 2 + 1.6 + 0.26 + 0.078 = 3.94 \frac{t}{day} \quad (21)$$

A 20% higher value is adopted (for other present elements):  $4.73 \frac{t}{day}$  CaO activity 70%.

## CONCLUSION

Large amounts of accumulated mine water in the abandoned open pits represent a resource that can be reused in the production processes after adequate treatment. Their treatment by the neutralization process of 10%  $Ca(OH)_2$ , during which the metal hydroxides are formed and pH value increases, is significant from the point of view of its reuse for the mining activities.

The calculation of calcium hydroxide consumption of known activity was made for elements that are present in water in a concentration higher than 1 mg/L. The calculated mass of CaO was increased by 20% due to the presence of other elements in accumulated water.

### **ACKNOWLEDGEMENT**

*The authors acknowledge the Ministry of Science, Technological Development and Innovation of the Republic of Serbia for the financial support of scientific research at the Mining and Metallurgy Institute Bor (contract no. 451-03-66/2024-03/200052).*

### **REFERENCES**

- [1] Stepanović S., Stanić N., Doderović A., *et al.*, Mining and Metallurgy Engineering Bor. (2) (2022) 51–58.
- [2] Dragišić V., Polomčić D., Hydrogeological Dictionary, University of Belgrade, Faculty of Mining and Geology, Belgrade (2009), p. 404. (In Serbian and English), ISBN 978-86-7352-189-3.
- [3] Stanković V., Božić D., Gorgievski M., *et al.*, J. Min. Metall. B. 57(1) (2021) 33–42.
- [4] Dimitrijević M. D. Copper. 37(1) (2012) 33–44. (In Serbian)
- [5] Dimitrijević M. D., Nujkić M. M., Milić S. M. Copper. 37(1) (2012) 45–55. (In Serbian)



## THERMODYNAMIC ANALYSIS AND INFLUENCE OF THE pH VALUE ON THE BIOSORPTION OF COPPER IONS ONTO HAZELNUT SHELLS

Marina Marković<sup>1\*</sup>, Milan Gorgievski<sup>1</sup>, Nada Štrbac<sup>1,2</sup>, Vesna Grekulović<sup>1</sup>,  
Miljan Marković<sup>1</sup>, Milica Zdravković<sup>1</sup>, Dalibor Jovanović<sup>3</sup>

<sup>1</sup>University of Belgrade, Technical Faculty in Bor, V.J. 12, 19210 Bor, SERBIA

<sup>2</sup>Engineering Academy of Serbia, Kneza Miloša 9/IV, 11000 Belgrade, SERBIA

<sup>3</sup>Copper Mill Sevojno, Prvomajska bb, 31205 Sevojno, SERBIA

\*marina.markovic@tfbor.bg.ac.rs

### Abstract

*The thermodynamic analysis of the copper ions biosorption process using hazelnut shells as a biosorbent, as well as the influence of the pH value on the biosorption capacity, are presented in this paper. The thermodynamic parameters that were analyzed are: activation energy ( $E_a$ ), change in Gibbs free energy ( $\Delta G^0$ ), enthalpy ( $\Delta H^0$ ), and entropy ( $\Delta S^0$ ), under standard conditions, at different temperatures (25°C, 35°C, and 45°C). The values of the calculated thermodynamic parameters indicate that the biosorption of copper ions onto hazelnut shells is favored at temperatures lower than the room temperature, that the process itself is endothermic and disordered, in which copper ions are bound to the surface of the hazelnut shell by chemisorption. The pH analysis showed that the pH value of the solution has a significant effect on the biosorption capacity, whereby the biosorption capacity increases proportionally with the increase in the pH value of the solution.*

**Keywords:** thermodynamic analysis, biosorption, copper ions, pH value, hazelnut shells.

### INTRODUCTION

Water, making up more than 70% of the Earth's surface, is our most valuable natural resource, without which life would not be possible [1]. However, as a result of continuous population growth, agricultural activities, industrialization and other geological, environmental and global changes, its pollution is increasing and in many parts of the world safe drinking water is not available [2].

Bearing in mind the development of mining, extractive and processing metallurgy, pollution by heavy metals, due to their non-degradable and persistent nature, leads to permanent contamination of the environment, and represents a serious environmental problem [3]. The solubility of heavy metals in the water environment is very high, which is why living organisms can absorb them. If they accumulate in the body beyond the permitted limits, they can cause serious health problems, which is why the treatment of wastewater contaminated with heavy metals, before their release into the environment, is necessary [4].

Removal of heavy metals from industrial wastewater can be achieved by various conventional methods. These treatment methods include: chemical precipitation, coagulation, complexation, adsorption with activated carbon, ion exchange, solvent extraction, electrodeposition, cementation, etc. [5]. The application of the mentioned methods does not

always give satisfactory results. Developing a new process – the biosorption process, which can become an alternative to conventional methods, certain advantages can be achieved when it comes to industrial wastewater treatment [6]. The main advantages of biosorption compared to conventional wastewater treatment technologies are its low cost, high efficiency, minimization of chemical or biological sludge, the ability to regenerate adsorbents, and the possibility of metal recovery after adsorption [7].

Adsorption of metal ions from aqueous solutions is a reversible process, which is why a change in temperature has an impact on its development. Thermodynamic parameters, such as Gibbs free energy ( $\Delta G^0$ ), enthalpy ( $\Delta H^0$ ) and entropy ( $\Delta S^0$ ), are evaluated to better understand the effect of temperature on the adsorption process [8].

In this work, the influence of the change in the pH value of the solution on the capacity of the biosorption process was investigated, along with the thermodynamic of the process.

## MATERIALS AND METHODS

Hazelnut shells were ground and sieved on a set of laboratory sieves, and the fraction (-1+0.4) was used for the experiments.

In order to examine the influence of the pH value of the solution on the biosorption capacity of copper ions, a series of experiments was performed using copper ions solutions of different pH values, ranging from 2–5. The pH value of the solution was adjusted by adding 0.1M HNO<sub>3</sub> and 0.1M KOH. The initial concentration of copper ions in the solution (0.2 g dm<sup>-3</sup>), as well as the stirring rate and adsorption time (60 minutes) were constant.

In order to determine the thermodynamic parameters, 1 g of biosorbent was brought into contact with 50 mL of a solution of copper ions with a concentration of 0.2 g dm<sup>-3</sup>, at temperatures of 25°C, 35°C and 45°C, for 90 minutes. The suspension was then filtered and the concentration of copper ions was determined in the obtained solution.

## RESULTS AND DISCUSSION

### Effect of pH value change on biosorption capacity

The experimental data obtained for the effect of the pH are shown in Figure 1.

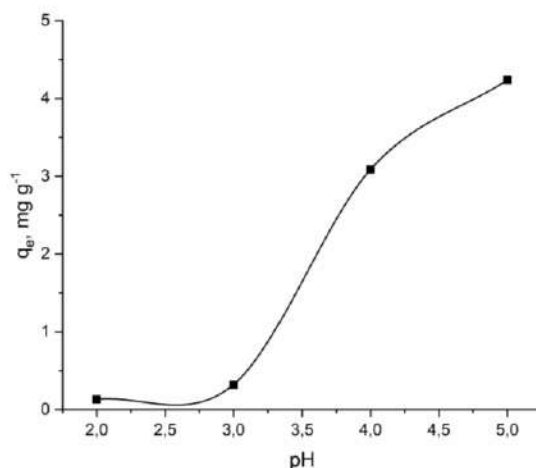


Figure 1 Change in biosorption capacity with change in the solution pH

It can be seen from Figure 1 that the removal of metal ions from an aqueous solution by biosorption is highly dependent on the pH value of the solution. At pH=2, the biosorption capacity was  $0.131 \text{ mg g}^{-1}$ , while it reached its maximum value of  $4.237 \text{ mg g}^{-1}$  at pH=5. Lower values of biosorption capacity at lower pH values are the result of higher concentration of  $\text{H}^+$  ions in the solution, which “compete” with copper ions for active sites in the structure of hazelnut shells [9].

### Thermodynamics of the biosorption process

The thermodynamic parameters of biosorption were calculated using the following equations [10]:

$$K_d = \frac{C_A}{C_S} \quad (1)$$

$$\Delta G^0 = -RT \ln K_d \quad (2)$$

$$\ln K_d = \left( \frac{\Delta S^0}{R} \right) - \left( \frac{\Delta H^0}{RT} \right) \quad (3)$$

$$\ln K_d = \left( \frac{-E_a}{RT} \right) + \ln A \quad (4)$$

where  $K_d$  is the equilibrium constant;  $C_A$ , the concentration of adsorbed substance at equilibrium ( $\text{mol dm}^{-3}$ );  $C_S$ , the equilibrium concentration of metal ions in solution ( $\text{mol dm}^{-3}$ );  $\Delta G^0$ , the Gibbs free energy ( $\text{kJ mol}^{-1}$ );  $R$ , the universal gas constant ( $\text{J mol}^{-1} \text{K}^{-1}$ );  $T$ , the operated temperature (K);  $\Delta H^0$ , the enthalpy change ( $\text{kJ mol}^{-1}$ );  $\Delta S^0$ , the entropy change ( $\text{J mol}^{-1} \text{K}^{-1}$ );  $E_a$ , the activation energy ( $\text{kJ mol}^{-1}$ );  $A$ , the Arrhenius factor.

Figure 2 shows the dependence of  $\ln K_d$  as a function of  $1/T$ . Based on the given dependence and experimental data, the thermodynamic parameters of the biosorption of copper ions onto hazelnut shells were calculated and are given in Table 1.

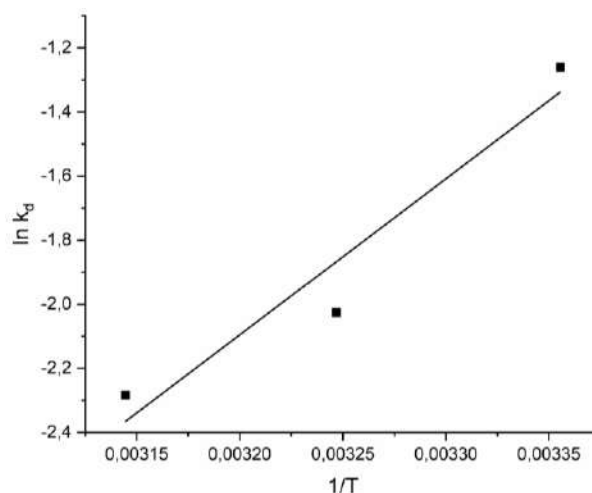


**Figure 2** Thermodynamic dependence ( $\ln K_d = f(1/T)$ ) for the biosorption of copper ions onto hazelnut shells



**Table 1** Thermodynamic parameters of copper ion biosorption process onto hazelnut shells

T (K)	$\Delta G^0$ (kJ mol <sup>-1</sup> )	$\Delta H^0$ (kJ mol <sup>-1</sup> )	$\Delta S^0$ (J mol <sup>-1</sup> K <sup>-1</sup> )	$E_a$ (kJ mol <sup>-1</sup> )
298	3.123			
308	5.188	4870.393	-17.681	40.492
318	6.037			

Based on the obtained values of the Gibbs free energy change, shown in Table 1, it can be concluded that the Gibbs free energy increases with an increase in temperature, as if the process itself is not feasible at room temperature, but is more favoured at lower temperatures. The obtained values of enthalpy and entropy indicate that the biosorption process of copper ions onto hazelnut shells is endothermic and disordered.

The obtained high value of activation energy ( $E_a$ ) indicates that the chemical binding of copper ions to active sites in the structure of the hazelnut shell is the dominant mechanism within the examined process.

## CONCLUSION

Hazelnut shells were used as a biosorbent for copper ions biosorption from synthetic solutions. The effect of changing the pH value of the solution on the capacity of the biosorption process was investigated and the thermodynamic parameters of the process were determined. Based on the performed experiments and the analysis of the obtained data, it can be concluded that the pH value of the solution has a significant influence on the biosorption capacity, whereby the biosorption capacity increases in proportion to the increase in the pH value of the solution. The values of the calculated thermodynamic parameters ( $\Delta G^0$ ,  $\Delta H^0$ ,  $\Delta S^0$  and  $E_a$ ) indicate that the biosorption of copper ions onto hazelnut shells is a more favoured process at lower temperatures than the room temperature, that the process itself is endothermic and disordered, in which copper ions bind to the surface of the hazelnut shell by chemisorption.

## ACKNOWLEDGEMENT

*The research presented in this paper was done with the financial support of the Ministry of Science, Technological Development and Innovation of the Republic of Serbia, within the funding of the scientific research work at the University of Belgrade, Technical Faculty in Bor, according to the contract with registration number 451-03-65/2024-03/200131.*

## REFERENCES

- [1] Vijayaraghavan K., Yun Y.S., *Biotechnol. Adv.*, 26 (2008) 266–291.
- [2] Ali I., Gupta V.K., *Nat. Protoc.* 1(6) (2007) 2661–2667.
- [3] Fu F., Xie L., Tang B., *et al.*, *CHEM ENG J* 189–190 (2012) 283–287.
- [4] Barakat M.A., *Arab. J. Chem.* 4 (2011) 361–377.
- [5] Gunatilake S.K., *JMESS* 1 (1) (2015) 2912–1309.

- [6] Rajčić-Vujasinović M., Grekulović V., Teorija hidro i elektrometalurških procesa, Univerzitet u Beogradu, Tehnički fakultet u Boru, Bor (2017), ISBN: 978-86-6305-070-9.
- [7] Park D., Yun Y.S., Park J.M., *Biotechnol. Bioprocess Eng.* 15 (2010) 86–102.
- [8] Olasehinde E.F., Adegunloye A.V., Adebayo M.A., *et al.*, *Anal. Lett.* (2018) 2710–2732.
- [9] Božić D., Stanković V., Gorgievski M., *et al.*, *J. Hazard. Mater.* 171 (2009) 684–692.
- [10] Ozcan A., Oncu E.M., Ozcan A.S., *Colloids Surf. A: Physicochem. Eng. Asp.* 277 (2006) 90–97.



## THE IMPACT OF FERROUS AND FERRIC IONS ON DEGRADATION OF ANTIHYPERTENSIVE DRUG DIHYDRALAZINE IN IRON-BASED FLOCCULATION AND COAGULATION METHODS FOR WASTE WATER TREATMENT

Jelena Korać Jačić<sup>1</sup>, Dragana Bartolić<sup>1</sup>, Milica R. Milenković<sup>2\*</sup>

<sup>1</sup>University of Belgrade, Institute for Multidisciplinary Research,  
Kneza Višeslava 1, 11030 Belgrade, SERBIA

<sup>2</sup>University of Belgrade, Faculty of Chemistry, Studentski trg 12–16, 11000 Belgrade,  
SERBIA

\*mrm@chem.bg.ac.rs

### Abstract

*Dihydralazine (dHZ) and hydralazine are hydrazine derivatives used as drugs in the treatment of hypertension. These drugs and their metabolites can be long-term pollutants in domestic and pharmaceutical industry waste water due to their high water solubility, low price and frequent use in the treatment of chronic disease. There are many methods for waste water treatment and some of them, such as flocculation, coagulation and advanced oxidation processes, involve the use of iron salts. In this study we investigated the effect of pH on dHZ degradation in the presence of ferrous and ferric ions in aqueous solutions using UV-Vis spectroscopy. It was found that in acidic solution dHZ forms stable complex with ferrous ions. The presence of ferric ions in acidic and neutral aqueous solutions of dHZ led to its degradation, which is faster at lower pH. EPR spectroscopy measurements showed that degradation of dHZ induced by ferric ions proceeds with the formation of OH<sup>•</sup> and carbon centered dHZ radical.*

**Keywords:** dihydralazine, complex, iron, degradation, wastewater.

### INTRODUCTION

Pharmaceuticals as biologically active compounds are used to improve health of human and animals. These compounds can be metabolized in body or excreted out unchanged in waste water. Some of them are toxic compounds which can be accumulated and transmitted through the food chain causing detrimental effect on ecosystem [1]. Dihydralazine (dHZ) and hydralazine are hydrazine derivatives of phthalazine widely used as drugs in the treatment of hypertension. Despite of their side effects such as: headache, loss of appetite, digestive problems and increased heart rate they are frequently used drugs due to their low price. Their intensive use and manufacturing contribute to their presence as pollutants in domestic and pharmaceutical industry waste water. Additionally, they are water soluble compounds resistant to hydrolysis [2]. Chemical coagulation based on iron coagulants is used for removal of some pharmaceuticals [3]. Ferrous sulfate and ferric chloride are commonly used iron coagulants due to their effectiveness as coagulants, ready availability and relatively low cost. They are able to form multi-charged mono- and polynuclear complexes with aqua and

hydroxo ligands which nature is pH dependent. Ferric coagulants are used over a wide range of pH from 4.0 to 11.0 [4]. Herein, we investigated the effect of pH on dHZ degradation in the presence of ferrous and ferric ions in aqueous solutions using UV-Vis spectroscopy. The mechanism of dHZ degradation induced by ferric ions was studied by EPR spectroscopy.

## **MATERIALS AND METHODS**

### **UV-Vis spectroscopy**

UV-Vis spectra of samples were recorded at wavelengths from 200 nm to 800 nm using 2501 PC Shimadzu spectrophotometer (Kyoto, Japan). Volume of sample was 1 mL with an optical path length of 10 mm. Scan time was 50 s.

### **EPR spectroscopy**

Free radicals formed in the reaction of dHZ and  $\text{Fe}^{3+}$  ions were identified by EPR spectroscopy measurements using DEPMPO (5-diethoxyphosphoryl-5-methyl-1-pyrroline-N-oxide) spin trap. All measurements were performed using Bruker EMX Nano (Billerica, SAD) at X-band frequency region (~9.65 GHz), under the following conditions: modulation amplitude 0.2 mT; modulation frequency 100 kHz; microwave power 5 mW; recording time 60 s; scanning field 20 mT. Eight spectra were accumulated. Simulations and processing of simulated EPR spectra were performed using Win EPR SimFonia program (Bruker Analytische Messtechnik GmbH, Karlsruhe, Germany). Simulation parameters were: for DEPMPO/OH adduct formed in the reaction with hydroxyl radical ( $\text{HO}^\bullet$ ):  $a_N=1.4$  mT,  $a_H=1.32$  mT,  $a_{H\gamma}(3) = 0.03$  mT,  $a_P=4.73$  mT [5]; for DEPMPO/OCR adduct formed in the reaction with oxidized dHZ:  $a_N=1.45$  mT,  $a_H=1.73$  mT,  $a_P=4.96$  mT [6].

## **RESULTS AND DISCUSSION**

Interactions of dHZ and  $\text{Fe}^{3+}$  ions in acidic (pH 4) and neutral solutions were investigated using UV-Vis spectroscopy. Absorption maxima in UV-Vis spectrum of dHZ at 272 nm and 305 nm originate from hydrazinyl substituents [7], and phthalazine ring [8], respectively. The addition of  $\text{Fe}^{3+}$  ions into acidic dHZ solution led to a decrease of dHZ absorption at 305 nm (Figure 1a).

This changes in dHZ UV-Vis spectra imply its degradation in acidic solution initiated by  $\text{Fe}^{3+}$  ions. Kinetic of dHZ degradation was studied by measurement of dHZ absorbance at 305 nm during 40 min (Figure 1b).

The absorption maxima of hydrazinyl substituents and phthalazine ring of dHZ are bathochromically shifted to 279 nm and 318 nm in neutral solution due to its deprotonation (Figure 2a). In neutral solution degradation of dHZ in the presence of  $\text{Fe}^{3+}$  is slower than in acidic solution. Such kinetic behaviour can be explained by lower solubility of ferrous ion at pH 7 (Figure 2b).

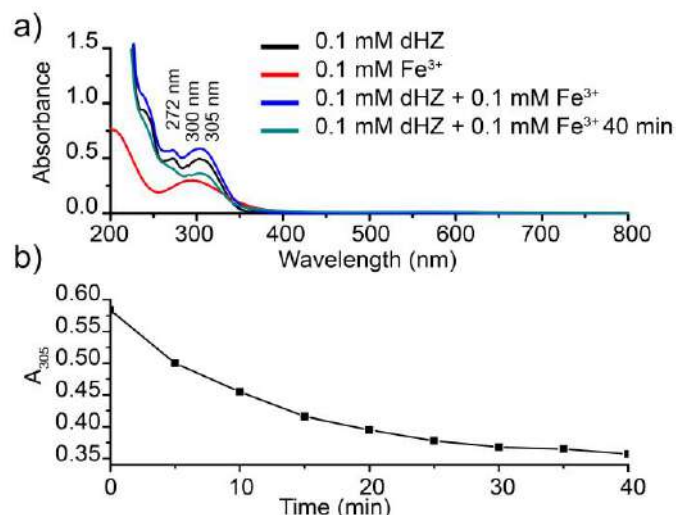


**Figure 1** a) UV-Vis spectra of 0.1 mM dHZ, 0.1 mM Fe<sup>3+</sup>, and 0.1 mM dHZ in the presence of 0.1 mM Fe<sup>3+</sup> at pH 4; b) Kinetic of dHZ degradation in the presence of Fe<sup>3+</sup> at pH 4

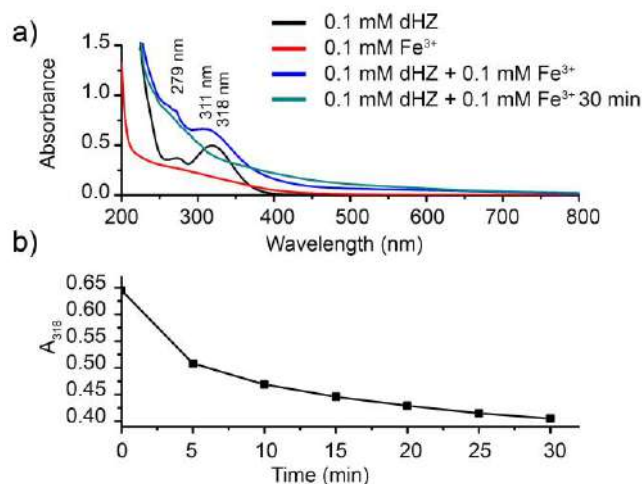


**Figure 2** a) UV-Vis spectra of 0.1 mM dHZ, 0.1 mM Fe<sup>3+</sup>, and 0.1 mM dHZ in the presence of 0.1 mM Fe<sup>3+</sup> at pH 7; b) Kinetic of dHZ degradation in the presence of Fe<sup>3+</sup> at pH 7

Interactions of dHZ and Fe<sup>2+</sup> were investigated at pH 4 (Figure 3). The hyperchromic shifts of absorption maxima of dHZ in the presence of Fe<sup>2+</sup> ions imply coordination of Fe<sup>2+</sup> with nitrogen donor atoms of dHZ. During 30 min after equilibrium of complex formation no changes of its UV-Vis spectrum were observed.

The stoichiometry of Fe<sup>2+</sup>-dHZ complex was studied by recording of dHZ UV-Vis spectra in the presence of various concentrations of Fe<sup>2+</sup> ion (Figure 4). The increasing of concentration of Fe<sup>2+</sup> ions led to increasing of absorption maxima until 1:1 molar ratio of dHZ/Fe<sup>2+</sup> was reached. According to these results it can be concluded that the stoichiometry of Fe<sup>2+</sup>-dHZ complex is 1:1. The proposed structure of Fe<sup>2+</sup>-dHZ complex is shown in Figure 5.

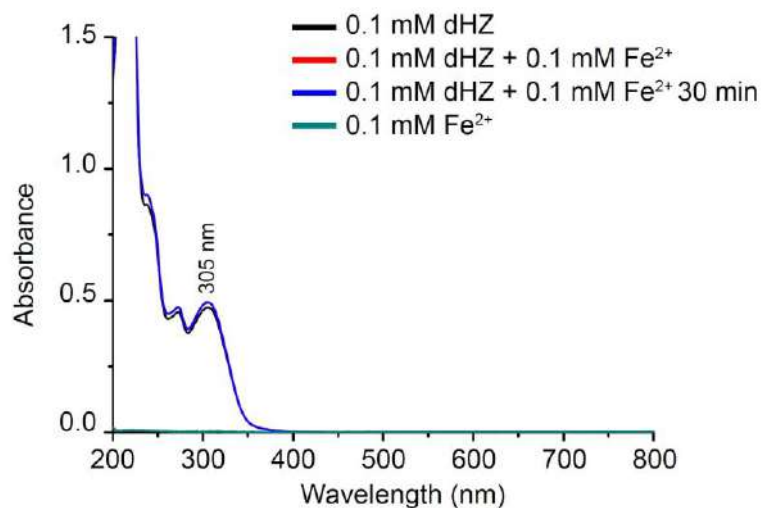


**Figure 3** UV-Vis spectra of 0.1 mM dHZ, 0.1 mM  $\text{Fe}^{2+}$ , and 0.1 mM dHZ in the presence of 0.1 mM  $\text{Fe}^{3+}$  at pH 4

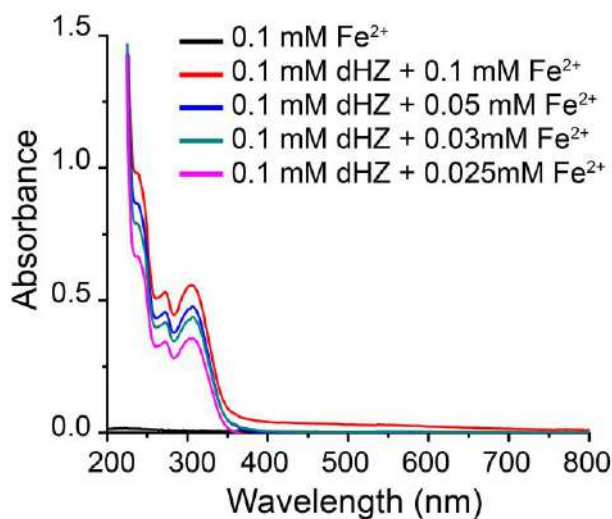


**Figure 4** UV-Vis spectra of 0.1 mM dHZ in the presence of different concentrations of  $\text{Fe}^{2+}$  ions at pH 4

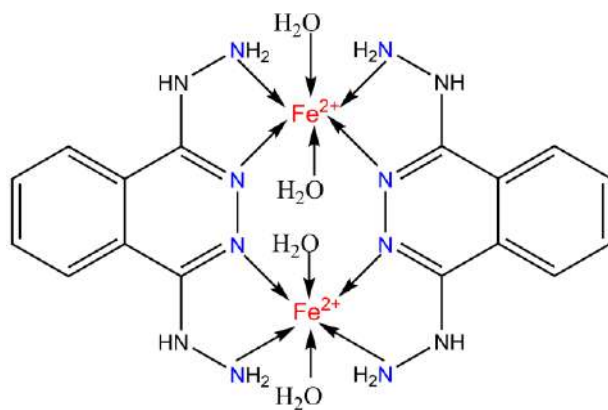


**Figure 5** The proposed structure of  $\text{Fe}^{2+}$ -dHZ complex



The addition of  $\text{Fe}^{2+}$  ions into the neutral solution of dHZ induces significant changes in its UV-Vis spectra which are manifested as a complete disappearance of absorption maximum at 318 nm. The observed degradation of dHZ in the presence of  $\text{Fe}^{2+}$  ions at pH 7 can be explained by fast oxidation of  $\text{Fe}^{2+}$  ions into  $\text{Fe}^{3+}$  ions (Figure 6). At pH 7 the degradation of dHZ after addition of  $\text{Fe}^{2+}$  ions is faster than its degradation in the presence of  $\text{Fe}^{3+}$  ions at the same pH. The faster kinetic of dHZ degradation at pH 7 after addition of  $\text{Fe}^{2+}$  ions can be related with initial better solubility of  $\text{Fe}^{2+}$  ions than  $\text{Fe}^{3+}$  ions at this pH and their very fast *in situ* oxidation by air oxygen into  $\text{Fe}^{3+}$ .

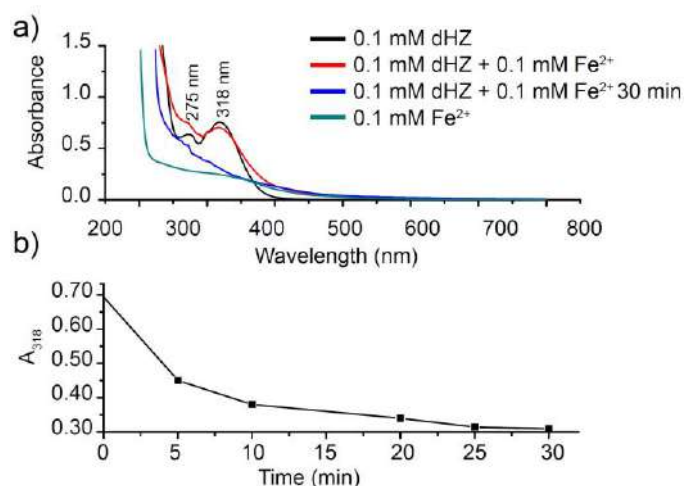


**Figure 6** a) UV-Vis spectra of 0.1 mM dHZ, 0.1 mM  $\text{Fe}^{2+}$ , and 0.1 mM dHZ in the presence of 0.1 mM  $\text{Fe}^{2+}$  at pH 7; b) Kinetic of dHZ degradation in the presence of  $\text{Fe}^{2+}$  at pH 7

The formation of free radicals in the oxidation reaction of dHZ in the presence of  $\text{Fe}^{3+}$  ions at pH 4 was investigated by EPR spectroscopy using spin trap DEPMPO (5-(diethoxyphosphoryl)-5-methyl-1-pyrroline-N-oxide). The results showed the formation of free radicals  $\text{OH}^{\cdot}$  and the carbon centered radical of dHZ in the reaction between dHZ and  $\text{Fe}^{3+}$  ions at pH 4 (Figure 7).

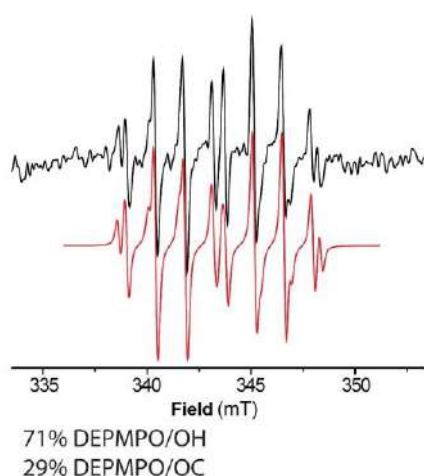


**Figure 7** EPR spectra of DEPMPO adduct formed in the system dHZ (1 mM) and  $\text{Fe}^{3+}$  (1 mM) in the presence of (10 mM) DEPMPO, Red—simulation of the spectra obtained by the combined signals DEPMPO/OH adduct (71%) and DEPMPO/OCR adduct (29%)

## CONCLUSION

dHZ is stable in acidic and neutral aqueous solutions. In acidic solution dHZ forms stable complex with  $\text{Fe}^{2+}$  ions with 1:1 stoichiometry. The presence of ferric ions in acidic and neutral aqueous solutions of dHZ led to its degradation, which is faster at lower pH due to better solubility of ferric ions. The addition of ferrous ions into neutral solution of dHZ and their *in situ* oxidation to ferric ions enhance degradation of dHZ in comparison with degradation process induced by ferric ions initially present at the same pH. EPR spectroscopy measurements showed that degradation of dHZ induced by ferric ions proceeds with the formation of  $\text{OH}^\bullet$  and carbon centered dHZ radical. The obtained results indicate that the application of chemical coagulation based on iron coagulants for the removal of pollutants from wastewater by adsorption would be accompanied by redox degradation of dHZ with the possible formation of toxic products.

## ACKNOWLEDGEMENT

*The authors are grateful to the Ministry of Science, Technological development and Innovation of the Republic of Serbia for financial support according to the contract with the registration number (e.g. 451-03-66/2024-03/200053, 451-03-66/2024-03/200168).*

## REFERENCES

- [1] Patel M., Kumar R., Kishor K, Chem. Rev. 119 (2019) 3510–3673.
- [2] Halasi S., Nairn J.G., J. Parenter Sci. Technol. 44(1) (1990) 30–4.
- [3] Kozub P., Kozub S., Mozaffari N., *et al.*, The Treatment schemes – conventional and dedicated for PhACs treatment in Pharmaceutical Wastewater Treatment Technologies: Concepts and Implementation Strategies, Editor: Khan A.N., Ahmed S., Vambol V., *et al.*, IWA Publishing, London (2021), p.123, ISBN: 9781789061338.
- [4] Bratby J., Coagulation and Flocculation in Water and Wastewater Treatment – Third Edition, IWA Publishing, London (2016), p.33, ISBN: 9781780407494.
- [5] Martinov J., Krstić M., Spasić S., *et al.*, Food Res. Int. 100(Pt 2) (2017) 132–136.
- [6] Khrantsov V., Berliner L.J., Clanton T.L., Magn. Reson. Med. 42(2) (1999) 228–34.
- [7] Naik D., Davis B., Minnet K., *et al.*, J. of Pharm. Sci. 65(2) (1976) 274–276.
- [8] Mason F.S., J. Chem. Soc. (1962) 493–498.



## OILY WASTEWATER

**Berina Sejdinović<sup>1\*</sup>**

<sup>1</sup>University of Zenica, Fakultetska 3, 72000 Zenica, BOSNIA & HERZEGOVINA

\*berina.sejdinovic.21@dl.unze.ba

### **Abstract**

*The introductory part of the paper lists the processes where oily wastewater is generated, as well as the places where it is mainly generated. Then, the conventional procedures for the treatment of oily wastewater and today's trends with newer procedures are listed. Legal regulations on water are presented through the Framework Directive on Water, the Law on Water and the Regulation on the Conditions of Discharge of Wastewater into the Environment and Public Sewerage Systems. The central part of the work describes the sources of danger and damage from the plant as well as the treatment of wastewater with an emphasis on sedimentation, and the monitoring of the quality and quantity of wastewater. In the end, it was stated that in the future, the integration of several systems or methods should be implemented in order to achieve the best possible scenario for the cleaning of oily wastewater.*

**Keywords:** oily wastewater, Water Framework Directive, primary, secondary and tertiary treatment systems.

### **INTRODUCTION**

#### **Oily wastewater**

For the needs of technological and energy processes in the industry, significant amounts of water are used, and significant amounts of wastewater are generated, including oily wastewater. With the increase in industrial production, the amount of generated oily wastewater is also increasing on a global level. Ecologically acceptable ways of their disposal while minimizing the costs of construction, operation and maintenance of facilities for their purification with final disposal in the environment or use as technological water represent a great challenge. That is why the efforts to find new technological solutions for purifying oily wastewater are becoming more and more pronounced.

Oily wastewater is produced mainly from oil processing, petrochemical, metallurgical and many other industries, maritime traffic and the collection of water from oil and grease separators from roads and parking areas. Oils and fats in these wastewaters, together with other contents such as heavy metals, cyanite, etc., are classified as hazardous waste and must be removed before discharge into the environment or the use of purified water as technological.

Conventional procedures for purifying oily wastewater (chemical coagulation, flotation, biological treatment, membrane procedures, etc.) often do not ensure satisfactory purification efficiency when applied independently, which, along with the additional fact that purification devices based on these technologies are characterized by increased construction costs,

operation and maintenance, makes it less acceptable in practice. From the above follows the need for the development of new technologies that will be more economically and environmentally acceptable with simpler operation and maintenance. Today's trends are aimed at researching the efficiency of purifying oily wastewater with ultrasonic and electrochemical procedures and combinations of different technologies (hybrid procedures) [1].

## **MATERIALS AND METHODS**

### **Legal regulation on water**

#### *Water Framework Directive*

The Water Framework Directive (2000/60/EC) was adopted by the Parliament and the Council of the European Union on October 23, 2000. This directive is the highest act related to water in the EU. The general goal of this directive from the aspect of environmental protection is to achieve “good water status” throughout the EU by 2015 and to maintain that status thereafter. The directive entered into force on December 22, 2000.

The key policy objectives of the European Union contained in the Water Framework Directive are: comprehensive protection of all waters, good status of all waters, integral river basin management, “combined approach”, pricing rule and public involvement [2].

#### *Water Law*

This Law regulates the manner of water management within the territory of the Federation of Bosnia and Herzegovina. Water management includes: protection of water, use of water, protection against harmful effects of water and arrangement of watercourses and other waters.

This Law regulates: water resources and public water resources, water facilities, legal entities and other institutions responsible for certain issues of water management and other issues related to water in the Federation [3].

#### *Regulation on conditions for discharge of wastewater into the environment and public sewage systems*

This regulation establishes: conditions for collection, purification and discharge of municipal wastewater, conditions for purification and discharge of technological wastewater into the environment or public sewage systems, limit values of wastewater emissions when discharged into the environment or public sewage systems, deadlines for reaching limit values, and wastewater monitoring and testing [4].

### **Sources of danger and harm**

Sources of danger and damage to the environment, which can threaten the environment, are divided into: sources of air pollution, sources of water pollution, sources of soil endangerment, sources of noise, causes of desecration of visual effects on the environment [5].

#### *Sources of water pollution*

Sanitary/fecal wastewater is discharged into the public sewage system. In this way, they are fully taken care of. Rainwater from traffic and manipulative surfaces is drained to a sedimentation tank through a drainage system and a system of underground canals, and is

then passed on to the public sewage system. Once a year, wastewater is sampled at the clarifiers, and regular monitoring is carried out [5].

## RESULTS AND DISCUSSION

### Wastewater treatments

#### *Primary treatment of wastewater*

The aim of primary treatment is to first remove coarse solid objects and other larger objects that can often be found in raw wastewater - pre-treatment. Removal of these materials is necessary to improve the operation and maintenance of the following components in the system. The operations of this wastewater treatment usually include coarse screening, gravel removal and, in some cases, comminution of large objects. In gravel chambers, the water velocity is kept high enough, or air is used, to prevent settling of most organic solids. Gravel removal is not treated as a pretreatment step in most small wastewater treatment plants. Sometimes shredders are additionally used as an addition to the coarse screening process, which reduce the size of the particulates in the wastewater, so that they can be removed as sludge in the subsequent wastewater treatment processes. One of the processes that can be used in the preliminary treatment of wastewater is chlorination.

A further process of primary treatment is deposition. For this stage of wastewater treatment, a device called a settling tank or primary settling tank is used, and its basic function is to separate clean water from biomass. If necessary, a screening device can be installed to prevent the entry of unwanted larger pieces of various materials [6].

A sedimentation tank is an underground tank with one partition wall. Within it, two main processes of wastewater treatment take place - the first is sedimentation or deposition and the second is stabilization and digestion of settled sludge through biological treatment. The volume space is usually enough for 18 to 36 months of operation, which is necessary for a stable process.

#### *Secondary treatment of wastewater*

Secondary treatment (biological treatment) of wastewater is the next treatment after the primary one, the aim of which is to remove residual organic matter and suspended solids. In most cases, secondary treatment follows primary treatment and involves the removal of dissolved biodegradable and colloidal organic matter using aerobic biological processes. Aerobic biological treatment is carried out in the presence of oxygen by aerobic microorganisms (mainly bacteria) that metabolize organic matter in wastewater, which produces more microorganisms and inorganic final products (mainly  $\text{CO}_2$ ,  $\text{NH}_3$  and  $\text{H}_2\text{O}$ ).

A simple system of septic tanks is the most well-known method of primary and secondary wastewater treatment “on-site” due to its great advantages. Septic tanks remove almost all solid suspended material and, in addition, function as anaerobic bioreactors in which partial digestion of organic matter takes place [7].

#### *Tertiary treatment of wastewater*

The purpose of tertiary wastewater treatment is to provide the final stage of wastewater treatment and thereby ensure its higher quality before it is released into the environment (sea,

river, lake, land, etc.). Several tertiary treatments can be used in wastewater treatment plants. If disinfection is carried out, it is always the final process, and it is also called “wastewater polishing”. Tertiary treatment is used in cases where wastewater contains specific pollutants that must be removed, and this is not achieved by secondary treatment. Therefore, special processes are used that are necessary for the removal of nitrogen, phosphorus, additional suspended substances, heavy metals, etc.

Nitrogen removal is carried out through its biological oxidation from ammonia to nitrates (nitrification), followed by denitrification, which converts nitrates into gaseous nitrogen, which is then released into the atmosphere. In this way, nitrogen is removed from wastewater during its treatment [8].

Phosphorus removal is important because it is a determining factor for algal growth and nutrients in many aquatic systems. Phosphorus can be removed by the so-called biological method. alternative biological processes for phosphorus removal. It can also be removed by chemical precipitation, usually with iron salts (e.g. iron chlorides), aluminum (alum) or lime. Chemical phosphorus removal requires significantly less equipment, is easier to perform and is often more reliable than the same biological treatment. Another method for phosphorus removal is the use of granular laterite. Once removed, the phosphorus, in the form of high-phosphate sludge, can be stored in a landfill or processed for use in mineral fertilizers [8].

### **Sedimentation**

Sedimentation is one of the important procedures of the first stage of purification. Sedimentation is the process of removing solids from liquids. The separation is done by the forces of gravity, and the course of the procedure depends on the density and size of the solid particles [9].

#### *Rectangular precipitator*

Precipitators are used on water purification devices to separate precipitable dispersed substances before the start of other purification processes or are used in the subsequent sedimentation process after biological and chemical purification processes [9]. The time required to separate dispersed substances from water by gravity depends on the size and type of particles.

The waste water that is fed to the previous clarifiers differs from the ideal liquid, so the dispersed substances are found in the form of grains, but also flakes. In waters that have been previously purified by biological or chemical processes, dispersed substances are mainly found in the form of flakes. Precipitators used for wastewater treatment, according to their position on the devices, are divided into: previous precipitators (primary) and subsequent precipitators (secondary) [9].

In some procedures of the second and third degree of purification, intermediate precipitators are also used. According to the shape of the clarifier floor plan, they are divided into: rectangular and round [9].

Furthermore, settling tanks differ according to the way water is introduced into the settling tanks, so they are: with horizontal (horizontal) flow and with vertical (vertical) flow [9].



Solids from wastewater settle under the influence of gravity, and collect at the bottom, from where they are separated as sludge (raw sludge). In the event that the sludge from the bottom is maintained in a floating state and water for clarification is introduced through such a layer, there will be a greater possibility of joining two or more particles, whereby the sedimentation effect will increase. In this way, deposition is performed through a "contact" layer, and therefore, according to the method of deposition, precipitators can be: static and contact or accelerated [9].

### **Monitoring of wastewater quality and quantity**

Monitoring of wastewater is carried out in accordance with the Regulation on conditions for the discharge of wastewater into the environment and public sewage systems, Official Gazette of FBiH no. 101/15 and the Decree amending the decree on the conditions for discharge of wastewater into the environment and public sewage systems, Official Gazette of the FBiH no. 01/16. Sampling of wastewater is carried out during the technological process, at the control point directly before the discharge of waste water into the environment or the public sewage system according to the applicable standards:

1. BAS EN ISO 5667 - 1 : Sampling — Part 1: Guidance for designing sampling programs and sampling techniques,
2. BAS EN ISO 5667 - 3: Sampling — Part 3: Guidelines for the storage and handling of water samples,
3. BAS EN ISO 5667 - 10: Sampling — Part 10: Guidelines for wastewater sampling,
4. BAS EN ISO 5667 - 16: Sampling — Part 16: Guidelines for the bioassay of samples.

Sampling is manual or automatic, samples are one-time or composite 8, 16 or 24-hour samples (depending on the duration of the technological process). The time interval for sampling and flow measurement is 60 min.

The measurement of the amount of technological wastewater as well as the taking of samples for testing their chemical composition will be performed at the connection points of the technological collectors to the public sewage system/at the point of discharge into the environment in order to be able to monitor the average and maximum values. In order to provide a simple inspection and measurement of the total quantities of wastewater as well as simple sampling of wastewater, every industrial and commercial user is obliged to make an audit shaft of appropriate dimensions at every connection of technological wastewater to the public sewage system/at the point of discharge into the environment.

In all samples, the following must be tested: relevant flow, temperature, pH, smell, color, dissolved oxygen content, BOD<sub>5</sub>, COD, suspended matter, sedimentable matter, electrical conductivity, total suspended matter, ammonia nitrogen NH<sub>4</sub>-N, total N, total P, toxicity test (bioassay with *Daphnia magna* Straus). Also, depending on the type of wastewater, specific parameters are made (highly volatile lipophilic substances — oils and fats, metals, etc.) [10].

### **CONCLUSION**

Oily industrial waste water originates mainly from oil processing, metallurgical and many other industries (milk processing and production of dairy products, meat processing, preservation of meat products, during exploitation, washing and separation of coal, etc.).

Oily wastewater most often appears in the form of an emulsion, which represents a major environmental problem.

The framework directive on water has a general goal of achieving “good water status”, while the Regulation on the conditions for the discharge of wastewater into the environment and public sewage systems establishes the conditions for the treatment and discharge of technological wastewater and the limit values of wastewater emissions when they are discharged into the environment or public sewage systems sewage.

Wastewater treatment includes: primary wastewater treatment, secondary wastewater treatment and tertiary wastewater treatment.

The latest treatments for oily wastewater are aimed at improving purification performance, eliminating secondary waste, and reducing costs for the implementation of oily wastewater treatment systems.

In the future, the integration of several systems or methods should be implemented in order to achieve the best possible scenarios for the cleaning of oily wastewater, thus fulfilling the aforementioned goals.

## **REFERENCES**

- [1] *Available on the following link:* <https://webgradnja.hr/clanci/prociscavanje-zauljenih-otpadnih-voda-elektrokemijskim-postupcima/4639> (15.11.2022.).
- [2] *Available on the following link:* [https://www.wikiwand.com/sh/2000/60/EC\\_\(15.12.2022.\)](https://www.wikiwand.com/sh/2000/60/EC_(15.12.2022.)).
- [3] Zakon o vodama „Službene novine Federacije BiH”, broj 70/06.
- [4] Uredba o uslovima ispuštanja otpadnih voda u okoliš i sisteme javne kanalizacije „Službene novine Federacije BiH”, broj 26/20.
- [5] *Available on the following link:*  
[https://mkipgo.ks.gov.ba/sites/mkipgo.ks.gov.ba/files/2021-03/zahtjev\\_za\\_okolinsku\\_dozvolu\\_cargo\\_beton\\_1\\_0.pdf](https://mkipgo.ks.gov.ba/sites/mkipgo.ks.gov.ba/files/2021-03/zahtjev_za_okolinsku_dozvolu_cargo_beton_1_0.pdf) (17.12.2022.).
- [6] Innocent N., Phys. Chem. Earth. 29 (15–18) (2004) 1265–1273.
- [7] Massoud M.A., Tarhini A., Nasr J.A., J. Environ. Manage. 90 (2009) 652–659.
- [8] Ljubisavljević D., Đukić A., Babić B., Prečišćavanje otpadnih voda, Građevinski fakultet, Beograd, 2004.
- [9] Goletić Š., Imamović N., Avdić N., Obrada otpadnih voda, Univerzitet u Zenici, Zenica, 2014.
- [10] *Available on the following link:*  
[https://mkipgo.ks.gov.ba/sites/mkipgo.ks.gov.ba/files/2021-03/izvjestaj\\_cargo\\_monitoring\\_otpadne\\_vode\\_4\\_0.pdf](https://mkipgo.ks.gov.ba/sites/mkipgo.ks.gov.ba/files/2021-03/izvjestaj_cargo_monitoring_otpadne_vode_4_0.pdf) (21.12.2022.)



## ENVIRONMENTAL RISKS CAUSED BY THE POLLUTION FROM AGRICULTURAL PLASTICS – A BRIEF STATE OF ART

Vesela M. Radović<sup>1\*</sup>, Slobodan B. Krnjajić<sup>1</sup>, Slađan R. Stanković<sup>2</sup>, Vedran M. Tomić<sup>2</sup>,  
Goran M. Knežević<sup>3</sup>

<sup>1</sup>University of Belgrade, Institute for Multidisciplinary Research, Kneza Višeslava 1,  
11030 Belgrade, P.O. Box 33, SERBIA

<sup>2</sup>Institute for Science Application in Agriculture, Bulevar despota Stefana 68,  
11000 Belgrade, SERBIA

<sup>3</sup>Faculty for Applied Ecology “Futura”, Metropolitan University, Požeška 83a,  
11000 Belgrade, SERBIA

\*vesela.radovic@imsi.bg.ac.rs

### Abstract

*Agriculture helps to sustain life by ensuring survival and contributing to the global economy. The revolution of plastics in agriculture from 1940 onwards led to a transformation of agricultural activity to rapidly increase productivity. Unfortunately, the use of plastics in agriculture is a double-edged sword. Plastic pollution has serious environmental, social, economic, and health consequences. Plastics of different sizes are found in ecosystems. Depending on their composition they are distributed in soil, water and air. Agriculture is one of the few sources of plastic that are the most frequently discussed. Therefore, the authors focus on the environmental risks – posed by evidence of plastic pollution and bad practice of waste management (WM) in agriculture. Those risks are briefly explained in this article. Using an appropriate social science methodology, the article presents the interdisciplinary work. The results presented in the form of recommendations are a basis for further research and societal discussion. At a time when landfills are frequently burning in the Republic of Serbia (Vinča in Belgrade, Duboko in Užice, etc.), the question arises: can we avoid the environmental consequences caused by inadequate management of agricultural plastic waste management? The main recommendation is that environmental impact assessment must be included in the overall process of risk management in agriculture, new recycling concepts must be accepted and an appropriate legal framework should be established.*

**Keywords:** agricultural plastic waste, APW, microplastics, risk management, sustainability.

### INTRODUCTION

From the dawn of humankind people strived to provide enough food for living, shifting from hunter gathering to an agrarian basis and that to urban living. Despite all efforts the hunger still is a concern of millions of people about the entire world. All governments, together with other interested parties, constantly striving to improve global crop yields to keep up with global population growth. Agriculture as unavoidable part of sustainable developments strategy in 21<sup>st</sup> century faces a major sustainable challenge: developing more towards a more sustainable method of production that is accepted and valued by society [1].

In a time when Information and Communication Technologies (ICTs) are constantly redefining industries, agriculture is no exception. Precision agriculture (“smart farming”) represent integration of artificial intelligence (AI) into farming techniques. Despite ongoing challenges, there is a belief that this concept-powered solution empowers farmers to optimize resource management and diminish environmental impact. Meanwhile, the applications of new technologies in agriculture, like everywhere else, brought unexpected environmental risks. In the modernization process of food production, the use of various agricultural plastics becomes inevitable. Agricultural plastic is a collective term that is generally used for products made from plastic in agricultural. China, South Korea, Spain and Turkey use significant amounts of agricultural plastic for greenhouses. Mainstream of urban growing food used a method of vertical farming, hydroponics, aquaponics, and small greenhouse increased the use of agricultural plastic. Hence, despite all benefits increasing use has raised concerns about the environmental impacts and sustainability. The United Nation Food and Agriculture Organization in 2021 launched a call for new action, assess of agricultural plastics and their sustainability [2].

Authors in the article investigate the newly recognized environmental risk of agricultural plastic waste (APW) pollution. Literature confirmed that till the end of 20<sup>th</sup> century, the term plastic pollution did not existed. The history of research around plastic pollution begins in the middle of the ocean basins, thousands of kilometers from land, when scientists discovered the Great Pacific Garbage Pitch in 1997 [3]. Global research community investigating plastic pollution and trying to understand how these diverse plastic particles interact with physical and biological environments, which has led to an expanded body of knowledge. The investigation of plastic pollution is very complex. Rochman [4] explained that “broad interactions of plastic waste and planetary cycles also bring up questions about how such processes may be affected by the combination of resource extraction, invasive species, climate change, eutrophication, chemical pollution, and plastic pollution, among others”. Over the last decade, the amount of research about and attention to the topic has elevated plastic pollution to the global stage, and set priorities for research and policy [4].

The transition from a linear to a circular economy in the European Union (UN) relating to agriculture is becoming more stringent in the area of APW management. Countries need to increase their efforts to be sustainable by imitating the nature where everything returns to the cycle [5]. The circular process has already been initiated in agriculture, but agricultural waste (especially plastic waste) has a significant potential to be utilized, which necessitates greater attention and research.

Serbian scientists are not an exception in those actions. The small consortium in 2020 applied on call IDEAS of the Science Fund of the Republic of Serbia. The Fund recognizes the importance of plastic pollution as an important scientific and social topics. Hence, the project titled: Evaluation of Microplastic in the Soils of Serbia (EMIPLAST-SoS) is approved for finance as one of the 105 projects in a period 2022–2024.

This article is a result of the theoretical research related to the environmental risk aspects of using agricultural plastic in the Republic of Serbia. Article after introduction in the first part explain the most important terms related to the APW, briefly explained the possible environmental risks caused by inadequate APW management, present conclusion and used

references. Since the last phase of the project is ongoing, the article ended with few recommendations related to the improvement risk management in agriculture and highlighted the need for creation adequate legislative framework which should prevent plastic pollution.

## **MATERIALS AND METHODS**

In a process of article preparation authors used appropriate social science methodology: analysis of documents, historical approach followed by with the field research in some specific areas where they detected the existence of agricultural plastics waste, and environmental risks related with use of agricultural plastics. Authors in the first phase of project investigated the available literature in the field of sustainable development, plastic pollution as an environmental risk, smart and sustainable agriculture, climate change and extreme weather events. Literature was searched from numerous libraries and trough different websites. The documents were also collected from electronic sources: Literature Resource Center like Go Gale Group EBSCOhost, Academic OneFile, e Library, and printing material (books, journals, official documents).

## **USE OF AGRICULTURAL PLASTICS – FROM SOLUTION FROM THE PAST TO THE CURRENT CHALLENGES**

From the creation of the first field greenhouse, covered from the new kind of plastic by a horticulture professor in the College of Agriculture at the University of Kentucky, Emery Emmert, plastic is tightly woven into the structure of agriculture. Wide range of plastics are used in agriculture, including polyolefins (PO), polyethylene (PE), polypropylene (PP), polyvinyl chloride (PVC), polycarbonate (PC), etc. [6]. Products from those materials are used in greenhouses, tunnels mulch, silage, reservoirs and irrigation and for many other purposes. Agricultural plastics provide multiple benefits, including weed and pest control, soil moisture conservation, a means to control soil and air temperatures, and enhanced nutrient uptake, which impacts several United Nations Sustainable Development Goals [7].

In 2022 global plastic production was estimated at 400.3 million metric tons, an annual increase of about 1.6 percent. The Global Agricultural Plastic Market reached USD 10.6 billion in 2022 and is expected to reach USD 17.1 billion by 2030 [8]. Unfortunately, after the use agricultural plastics became an agricultural waste. The durability of lifetime of an agricultural plastic depends on several factors. In general, the useful life of an agricultural plastic is estimated to be between two or three years. There is numerous evidence that APW abandon on field under the specific natural and anthropogenic factors can lead to unpredictable effect in the environment. The results of that processes are degradation/defragmentation of plastic waste. Plastic that ends up in the soil varies in size from macroplastics (>5 mm) to microplastics (<5 mm) and nanoplastics (<1  $\mu\text{m}$ ) [9].

Managing APW is a complex process. One of the most important reasons for its limitation, and the lack of needed data is the most difficult to effectively identify and measure plastic pollution in a standardized way. Although recycling initiatives are accelerating, the agricultural plastics sector faces challenges due to lacking WM policies and infrastructures. Most agricultural plastics after its use stay on site contaminated by pesticide, dirt, rocks, plant



residuals, etc. Impoverished farmers are unaware of possible consequences of APW and give up its recycling. The previously used concept of 3Rs of WM (reduce, reuse, and recycle) is now extended to address the new issues of plastic use in agriculture. Therefore, the 2021 FAO Assessment Report identified alternatives and interventions to improve the circularity and sound management of APW based on the 6Rs model (refuse, redesign, reduce, reuse, recycle and recover) [10]. Despite positive efforts of interested parties the management of APW is not a target in the European Union and Australia. A 2022 report by the United Nations Environment Program (UNEP) found that plastics are leaching into soil at an alarming rate, causing widespread contamination of agricultural soil and food supply [11].

### **AGRICULTURAL PLASTIC WASTE AS A NEW ENVIRONMENTAL RISK**

The inadequate agricultural waste disposal practice has become crucial in discussion on harmful effects of modern agriculture. Agricultural plastic waste is considered as industrial waste, from non-hazardous economic activities [12] which use led to an increase in environmental pollution. In the different kinds of those wastes, the risk of plastic waste in agriculture should be particularly addressed. Despite the fact that in the Republic of Serbia (RS), we witnessed bad practice related to the APW: abandonment, burring in fields, disposal in municipal landfills, etc. (Figure 1). This issue starts to be more serious in a case of emergencies, like extreme weather events (hail, heavy rain, floods, strong wind etc.) and forest fires. For example, in the RS in 2021, there were 15 thousand hectares flooded area by surface and ground water, of which 52.9% referred to utilized agricultural land. The area of eroded land in 2021 amounted to 3 912 km<sup>2</sup> [13]. In rural area APW mismanagement represents significant risk and could irreparably harm ecosystems. All environmental media are jeopardized, as well human health. Therefore, the question about the use of agricultural plastic becomes a hot topic for all interested parties in society. Are agricultural plastics a “curse” or a “blessing” for society? The empirical evidence suggests either outcome is possible.



*Figure 1 Different use of agroplastics in surrounding village Beška (private archive of authors)*

Although at the beginning most researchers investigate the influence of plastic in aquatic ecosystems [14], recently, the research topic of interest shifted to the occurrence of APW pollution in soil, air and biosphere. Soil environment greatly affected by the presence of microplastics (MPs) became an interesting field of study regarding source, potential toxicity, pathways and their sinks in the ecosystem [15]. The plastics degradation takes place very slowly and produces a host of secondary pollutants, which include a diversity of volatile



organics, representing a risk of groundwater contamination [16].

MPs are inherently toxic, which is mainly due to the use of plastic additives and some other substances, potentially more dangerous than the plastic itself. The recent report stated that currently around 24% of the additives used in plastic production are of potential concern [17]. Plastic additives in agricultural soil encompassing plasticizers, antioxidants and stabilizers pose a potential risk to farmworkers and nearby communities. Some of the health risks are related to the endocrine disruption, respiratory risks, skin irritation etc. The airborne MPs and their potential risk to human health and those through the food chain are documented as an additional risk, have not been fully realized and have not received the attention they deserve. Hence, environmental risk assessment (ERA) should become a necessary part of every future action related to the management of APW. To curb microplastic contamination, governments are encouraging the adoption of biodegradable alternatives and are exploring plastic usage bans in agriculture. Dr Andrew Forest recommended three big interventions helpful for mitigation of plastic waste pollution:

- Limit fossil fuel plastic production and consumption;
- Increase plastic products and materials that are designed for circularity and are circulated in practice, and
- Eliminate plastic leakage to the environment across the lifecycle through environmentally sound waste management [18].

Taking all of the above into consideration, it can be concluded that we already know the enormous benefits that agricultural plastics can provide, and now we have begun to prevent their environmental threats and risks.

## **CONCLUSION**

A growing role for agricultural plastics makes agricultural plastics an enormous environmental risk. More plastic means more plastic waste and more pollution. Before the full implementation of the smart agriculture concept, it is urgently necessary to improve environmental risk management in agriculture. It's important to point out that researchers should investigate both environmental risks that result in damage to agriculture and those caused by agriculture itself. Hence, an adequate APW plan is a key component of a farm risk management plan. However, there are many irrefutable facts that recycling is failing to scale fast enough and remains a marginal activity for the agriculture sector. Future research should focus on microplastics monitoring techniques along the supply chain and improved APW management, followed by needed legislation framework.

## **ACKNOWLEDGEMENT**

*The authors are grateful to the Science Fund of the Republic of Serbia, for financial support according to the contract #GRANT No 7742318, "Evaluation of the Microplastic in the Soils of Serbia - EMIPLAST - SoS".*

## **REFERENCES**

[1] Radović V., Pejanović R., Marinčić D., *Econ. Agric.* 62 (1) (2015) 181–191.

- [2] U.N. Food and Agriculture Organisation (2021), Assessment of agricultural plastics and their sustainability, *Available on the following link:* <https://www.fao.org/3/cb7856en/cb7856en.pdf>.
- [3] Moore C.J., Moore S.L., Leecaster M.K., *et al.*, *Marine Poll. B.* 42 (12) (2001) 1297–1300.
- [4] Rochman C.M., *Oceanography* 33 (3) (2020) 60–70.
- [5] European Commission (2020), A new Circular economy Action Plan for a cleaner and more competitive Europe, Brussels, Belgium.
- [6] Agriculture-Plastics Europe (2023). *Available on the following link:* <https://plasticseurope.org/sustainability/sustainable-use/sustainable-agriculture/>.
- [7] Hofmann T., Ghoshal S., Tufenkji N. *et al.*, *Commun. Earth Environ.* 4 (2023) 1–11.
- [8] Global Agricultural Plastic Market (2023–2030). *Available on the following link:* <https://www.marketresearch.com/DataM-Intelligence-4Market-Research-LLP-v4207/Global-Agricultural-Plastics-34371077/>
- [9] Kershawa P., Turrab A., Galganic F. (eds.) (2019), Guidelines for the Monitoring and Assessment of Plastic Litter in the Ocean. Nairobi: United Nations Environment Programme. *Available on the following link:* <http://www.gesamp.org/publications/guidelines-for-the-monitoring-and-assessment-of-plastic-litter-in-the-ocean>.
- [10] Food and Agriculture Organization of the United Nations (FAO) (2021), Assessment of agricultural plastics and their sustainability: A call for action. *Available on the following link:* <https://www.fao.org/3/cb7856en/cb7856en.pdf>
- [11] United Nations Environment Program (UNEP) (2022). Plastics in agriculture-An Environmental Challenge. *Available on the following link:* [https://wedocs.unep.org/bitstream/handle20.50011822/40403/Plastics\\_Agriculture.pdf](https://wedocs.unep.org/bitstream/handle20.50011822/40403/Plastics_Agriculture.pdf)
- [12] LeMoine B., Erälinna L., Trovati G., *et al.*, The agri-plastic end of life management, *Available on the following link:* [https://ec.europa.eu/eip/agriculture/sites/default/files/eip-agri\\_fg\\_plastic\\_footprint\\_minipaper\\_b\\_final.pdf](https://ec.europa.eu/eip/agriculture/sites/default/files/eip-agri_fg_plastic_footprint_minipaper_b_final.pdf)
- [13] Statistical Yearbook 2022, Statistical Office of the Republic of Serbia.
- [14] Rhodes C.J., *Sci. Progr.* 101 (3) (2018) 207–260.
- [15] Van den Berg P., Huerta Lwanga E., Corradini F., *et al.*, *Arch. Biol. Sci.* 64 (1) (2012) 97–105.
- [16] Webb H., Arnott J., Crawford J., *et al.*, *Polymers* 5 (1) (2013) 1–18.
- [17] Boucher J., Gallato M., Gomis M., *et al.*, Adding it Up. A global assessment of leakage from plastic additives. *Available on the following link:* [www.e-a.earth/adding-it-up/](http://www.e-a.earth/adding-it-up/)
- [18] Charles D., Kimman L., Plastic Waste Makers Index 2023. *Available on the following link:* <https://cdn.minderoo.org/content/uploads/2023/02/04205527/Plastic-Waste-Makers-Index-2023.pdf>.



## COMPARISON BETWEEN HYDROCHAR AND ITS ALKALI MODIFIED FORM IN THE REMOVAL OF Cd(II) IONS FROM AQUEOUS SOLUTION

Marija Koprivica<sup>1\*</sup>, Jelena Dimitrijević<sup>1</sup>, Jelena Petrović<sup>1</sup>, Marija Ercegović<sup>1</sup>,  
Marija Simić<sup>1</sup>

<sup>1</sup>Institute for Technology of Nuclear and Other Mineral Raw Materials,  
86 Franchet d'Esperey St., 11000 Belgrade, SERBIA

\**m.koprivica@itnms.ac.rs*

### Abstract

*The alkaline activation could be useful to improve the adsorption abilities of hydrochars. In this regard, the aim of this work was a comparison of the efficiency of non-modified (HPL) and modified hydrochar (MHPL) forms during the adsorption of cadmium (Cd) ions from aqueous media. It was found that MHPL had a higher capacity ( $q_m=19.60$  mg/g) and a different mechanism of bonding than HPL ( $q_m=11.76$  mg/g). The Langmuir isotherms model best described Cd(II) adsorption by HPL, while the Freundlich isotherm model better-described adsorption by alkali modified form. The SEM/EDS and the FTIR analysis confirmed that there is a structural difference between these two new adsorption materials, which might be attributed to the influence of the NaOH treatment. Also, the FTIR analysis showed that MHPL adsorbent most binds Cd ions using oxygen functional groups. It can be concluded that this paper also confirmed that alkaline modification improves the adsorption capacity of hydrochar.*

**Keywords:** alkali modified hydrochar, adsorption of Cd ions, isotherm studies, SEM/EDS, FTIR analysis.

### INTRODUCTION

The hydrothermal carbonization process (HTC) is a promising, low-cost cost, and simple method for the conversion of waste biomass with many benefits. Depending on chemical structures hydrochar might be useful for wastewater remediation, and adsorption of solute pollutants [1,2]. One of the advantages of hydrochar materials is the possibility of improving their potential with various modifications. There are physical and chemical ways of activation, which generally increase the efficiency of application [2]. Cadmium (Cd) is one of the most polluting heavy metals of wastewater because is a constituent of many industries' products (batteries, paint pigments, etc.) [3]. Unfortunately, due to industrial production, Cd is significantly available and transported to natural waters, ores, soils, and even food chains. Cadmium causes various health toxic effects for humans, animals, and plants [4]. Therefore, is necessary to develop low-cost and efficient products to remove Cd from the natural environment [3,4]. Among the all traditional technologies used for remediation, adsorption was recognized as a very suitable method for wastewater treatment. Efficiency, high selectivity, and cost-effectively are some of the benefits of used adsorbents [5].

The commercial cultivation of *Paulownia* tree trunks results in a significant amount of large leaves, often discarded as waste. The disposal problem can be solved by further utilization of leaves [2]. Comprehensively taken into account, this work aims to examine the possibility of *Paulownia* leaf hydrochar obtained at 220°C (HPL) and its alkali-modified form (MHPL) as potential and efficient cadmium (II) ions adsorbents from aqueous solutions. The hydrochars were characterized using SEM/EDS and FTIR for this purpose. For examination of the adsorption process, two isotherm models were used. We have analysed experimental data comparing the characterization and adsorption abilities of hydrochar and its alkali-activated form.

## MATERIALS AND METHODS

### Materials preparation

The waste biomass, the initial feedstock of obtained hydrochars, was leaves from the *Paulownia* tree (PL). It was gathered in a park in Belgrade after the leaf's growing period had ended. The leaves were washed with distilled water and air-dried for two weeks. The stems of the leaf were first cut into pieces about 1 cm in size, and then, together with the rest of the leaf, they were crushed with a grinder to obtain a more homogeneous and finer sample.

The 10 g of the tree leaf powder was used in the HTC process in a laboratory autoclave (Carl Roth, Model II) with 100 mL of ultrapure water at 220°C constant for 1 h. After completing HTC, the hydrochar (HPL) was filtrated, rinsed with ultrapure water, and dried at 105°C for constant mass.

Alkali-modified hydrochar (MHPL) was obtained from HPL. About 3 g of the HPL was stirred with 150 mL of 4 M NaOH solution for 2 h at room temperature (about 25°C). The obtained modified hydrochar was filtered, rinsed with ultrapure water to the neutral pH value, and dried at 105°C for 24 h.

### Adsorption test - Effect of initial metal concentration and isotherm studies

Adsorption isotherm studies were carried out by stirring 0.02 g of the HPL or the MHPL with 20 mL of Cd solutions at different initial concentrations (10, 25, 50, 75, 100 mg/L), for 6 hours and at room temperature. The solution was separated from the adsorbent by filtration and Cd(II) concentrations before and after adsorption were determined using atomic adsorption spectrophotometer (AAS, PerkinElmer, PinAAcle 900T).

The amount of Cd(II) ions adsorbed on the HPL and MHPL surface was calculated using the equation:

$$q = (C_0 - C_{eq})/m \cdot V \quad (1)$$

Where  $q$  [mg/g] was adsorbent capacity,  $C_0$  and  $C_{eq}$  [mg/L] were initial and after adsorption concentration of Cd ions,  $m$  [g] was amount of adsorbent and  $V$  [L] was volume of the Cd(II) solutions.

Isothermal modeling of the experimental results of the Cd (II) adsorption process on the HPL and MHPL surfaces was utilized using two different isotherms (Langmuir and Freundlich). The Langmuir isotherm model has been expressed by the following equation [6]:

$$q_e = q_m \cdot (K_L C_e) / (1 + K_L C_e) \quad (2)$$

This isotherm model considers monolayer adsorption onto homogeneous distinct sites with constant adsorption energy, where  $q_e$  and  $q_m$  [mg/g] represent the equilibrium and the maximum amount of the Cd ions adsorbed onto the HPL or MHPL surface,  $C_e$  [mg/L] is the equilibrium concentration, and  $K_L$  [L/mg] is the Langmuir constant related to the affinity of the binding sites.

On the other side, the Freundlich isotherm model is based on the multilayer binding process onto a heterogeneous adsorbate surface. This model could be expressed as [7]:

$$q_e = K_F \cdot C_e^{1/n} \quad (3)$$

in which  $q_e$  [mg/g],  $K_F$  [(mg/g) (L/mg)<sup>1/n</sup>],  $C_e$  [mg/L] and  $1/n$  are the adsorption capacity at equilibrium, the Freundlich constant related to the adsorption capacity, the Cd(II) concentration at equilibrium, and the adsorption intensity, respectively.

### **Characterisation of the adsorbents HPL and MHPL**

#### *SEM/EDS Analysis*

The surface morphology of the HPL before and after modification was observed using SEM analysis (JEOL JSM-6610LV SEM, JEOL Inc., USA). All samples were cathodic-coated with gold, placed on an adhesive carbon disc, and recorded in a vacuum under a voltage of 20 kV.

#### *FTIR Analysis*

The FTIR analysis was performed to determine organic functional groups from the surface of samples which are capable of adsorbing in the middle region of the IR spectrum (wavenumber 4000–400 cm<sup>-1</sup>). The Thermo Scientific Nicolet iS50 FT-IR spectrometer in transmission mode and with a resolution of 4 cm<sup>-1</sup> was used to obtain the FTIR spectra of the HPL and MHPL. The spectra were obtained from the potassium bromide (KBr) pastilles for each sample.

## **RESULTS AND DISCUSSION**

### **Effect of initial metal concentration and isotherm studies**

The adsorption test revealed that the hydrochar after alkaline activation with NaOH (MHPL) showed better adsorption capacity to remove Cd(II) ions from aqueous solution than before modification (HPL). Additionally, it can be noted that the difference in efficiency between these two adsorbents also increases with increasing amount of Cd(II) ions in solution (Figure 1a). To determine the maximum adsorption capacity and the influence of the Cd(II)

concentration on the removal efficiency, two isotherm models Langmuir and Freundlich, were applied to the experimental data (Equations 2 and 3). The results are shown in Table 1 and Figure 1b. The correlation coefficient  $R^2$  indicated that these two adsorbents have different ways of binding Cd ions at the surface (Table 1). Before modification with NaOH, the value of the  $R^2$  coefficient was highest for the Langmuir model, so it could be concluded that monolayer chemical sorption onto homogenous active sites of the HPL surface plays an important role in Cd(II) ions removal. However, after activation, the  $R^2$  value is higher for the Freundlich isotherm model, which provides insight into the nature of the interaction between the MHPL and Cd(II) ions. According to the Langmuir isotherms, the maximum adsorption capacity ( $q_m$ ) that could be achieved using HPL and MHPL was 11.76 and 19.60 mg/g, respectively (Table 1).

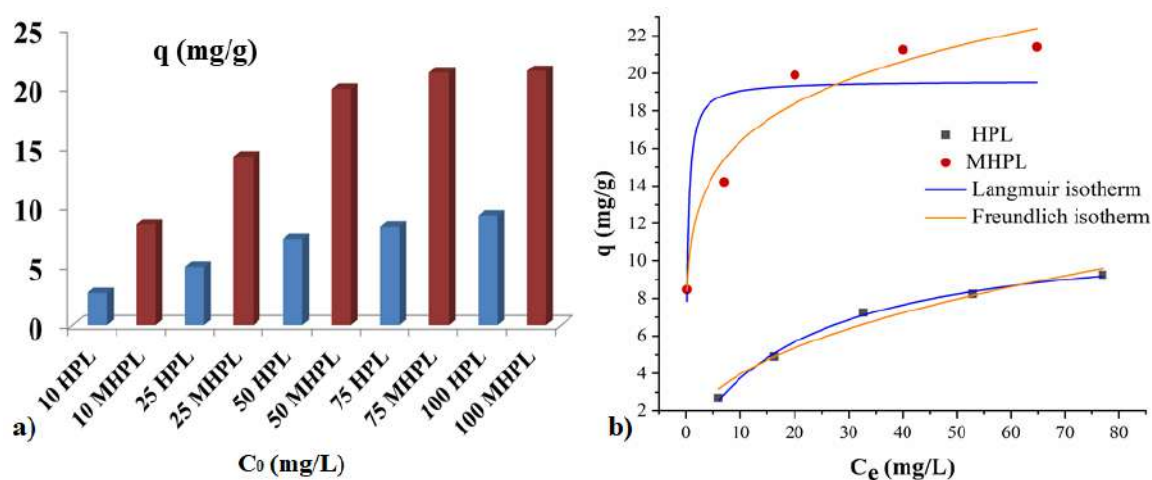


Figure 1 Adsorption capacity ( $q$ ) of HPL and MHPL during Cd (II) removal: a) effect of different Cd(II) concentration; b) isotherm studies

Table 1 Isotherm parameters for Cd(II) adsorption onto the HPL and MHPL surface

Adsorbent	HPL	MHPL
<b>Langmuir isotherm model</b>		
$q_m$ [mg/g]	$11.76 \pm 0.35$	$19.60 \pm 1.63$
$K_L$ [L/mg]	$0.047 \pm 0.004$	$3.52 \pm 0.422$
$\chi^2$	0.029	0.965
$R^2$	0.9969	0.7714
<b>Freundlich isotherm model</b>		
$K_F$ [(mg/g)(L/mg)]	$1.46 \pm 0.28$	$11.12 \pm 0.97$
$1/n$	$0.43 \pm 0.27$	$0.17 \pm 0.90$
$\chi^2$	0.25	0.69
$R^2$	0.9737	0.9599

### SEM/EDS Analysis

The SEM/EDS analysis was used in aim to provide the effect of alkaline modification on the HPL material surface. The external structure of the HPL displayed an irregular stacking structure with various pores (Figure 2). After treatment with NaOH, changes in the morphological structure of the material can be observed. The surface of the HPL was cracked into various dimension fragments with new channels, holes and pores. Some of the reasons



for this phenomenon may be polycondensation, rearrangement of the residual organics or discontinuity of carbon chains [8]. The EDS spectra of the HPL and MHPL showed that the main elements were carbon (C) and oxygen (O), with average values of C and O were about 55 and 40%, respectively. These results indicating that both samples had carbon-rich structures and organic functional groups on the surface.

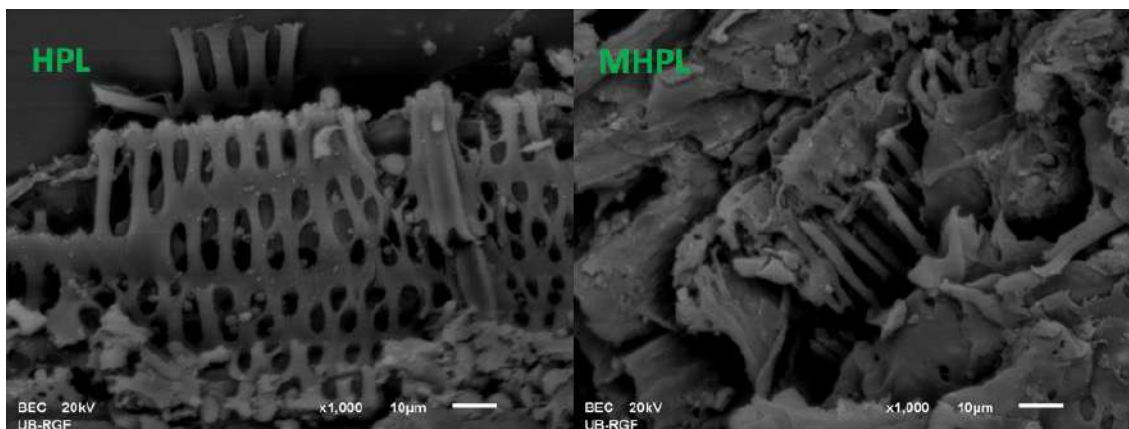


**Figure 2** The surface morphological structures of hydrochar sample before and after alkali modification

### FTIR Analysis

To determine the changes in the chemical structure of the HPL before and after NaOH activation, FTIR analysis was performed. According to the FTIR spectra (Figure 3), the surface functional groups of the HPL were changed fundamentally upon alkali activation. Peak reduction is highly noticeable for the peaks at 2851 and 2924  $\text{cm}^{-1}$ , which originated from asymmetric and symmetric -C-H valence vibration of  $\text{CH}_3$  and  $\text{CH}_2$  groups [2].

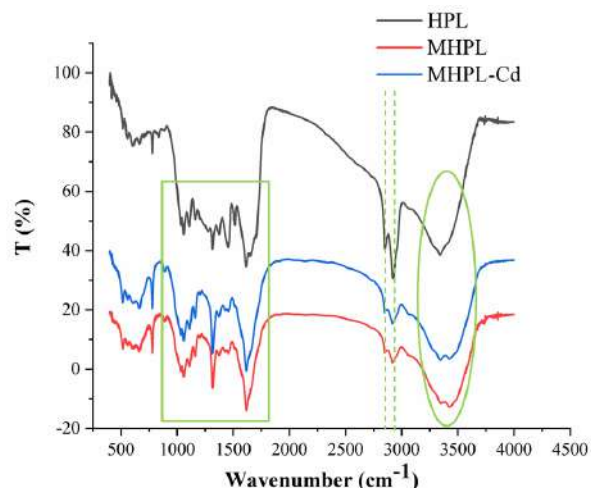


**Figure 3** The FTIR analysis of HPL and MHPL samples

Figure 3 also showed an additional change in the position and intensity of the FTIR peaks from the MHPL sample before and after Cd ions adsorption. The wide peak at about

3300 cm<sup>-1</sup> originated from the –OH groups [2]. This peak was changed after modification and additionally decreased after Cd (II) ions adsorption. Also, the peaks between 1000–1700 cm<sup>-1</sup> were changed by the effect of alkali and later the intensity decreased by sorption of Cd(II) ions. In most cases the peaks of these wavenumbers belong to lignocellulosic biomass, some oxygen functional groups such as -C-O, C-O-C, and –C=O groups [2].

## CONCLUSION

Based on the obtained results, it can be concluded that alkaline activation significantly changes the chemical structure and improves the ability of hydrochar to adsorb Cd(II) ions from aqueous solution. The SEM images showed new fragments at the surface of the modified hydrochar. Also, the differences in functional groups between these two hydrochars were shown by the FTIR analysis. The Langmuir isotherms model best describes metal adsorption by HPL. However, after activation, the R<sup>2</sup> value is higher for the Freundlich isotherm model, which shows that multilayer chemical sorption onto heterogeneous adsorbate sites of the MHPL surface plays an important role in Cd(II) ions removal. According to the Langmuir isotherms, the maximum adsorption capacity that could be achieved using HPL and MHPL was 11.76 and 19.60 mg/g, respectively.

## ACKNOWLEDGEMENT

*The authors are grateful to the Ministry of Science, Technological development and Innovation of the Republic of Serbia for financial support according to the contract with the registration number (e.g. 451-03-66/2024-03/200023).*

## REFERENCES

- [1] Petrović J., Ercegović M., Simić M., *et al.*, Processes (12) (2024) 207.
- [2] Koprivica M., Simić M., Petrović J., *et al.*, Processes (11) (2023) 1327.
- [3] Simić M., Petrović J., Šoštarić T., *et al.*, Processes 10 (10) (2022) 1957.
- [4] Rind I.K., Memon N., Khuhawar MY., *et al.*, Sci Rep. (12) (2022) 8001.
- [5] Dimitrijević J., Jevtić S., Marinković A., *et al.*, Processes (11) (2023) 1308.
- [6] Langmuir L., J. Am. Chem. Soc. (40) (1918) 1361–1368.
- [7] Freundlich H.M.F., J. Phys. Chem. (57) (1906) 384–470.
- [8] Tu W., Liu Y., Xie Z., *et al.*, Colloid Interface Sci. (593) (2021) 390–407.



## EFFICIENT REMOVAL OF RHODAMINE B FROM AQUEOUS SOLUTIONS USING CARBONIZED WASTE CAR TIRES: CHARACTERIZATION AND ADSORPTION STUDIES

Milena Pijović Radovanović<sup>1</sup>, Mina Seović<sup>1</sup>, Ivana Perović<sup>1\*</sup>, Nikola Zdolšek<sup>1</sup>,  
Jelena Georgijević<sup>1</sup>, Petar Laušević<sup>1</sup>, Snežana Brković<sup>1</sup>

<sup>1</sup>University of Belgrade, Vinča Institute of Nuclear Sciences, National Institute of the  
Republic of Serbia, Mike Petrovića Alasa 12–14, 11351 Vinča, SERBIA

\*ivanaperovic@vin.bg.ac.rs

### Abstract

*This study explores the potential of carbonized waste car tires (WCT800) produced at 800°C as an adsorbent for the removal of Rhodamine B (RhB) dye from aqueous solutions. Utilizing a waste-to-resource approach, waste car tires were transformed into a carbonaceous adsorbent, characterized by scanning electron microscopy (SEM) and Fourier-transform infrared spectroscopy (FTIR). The SEM analysis revealed a highly porous material with a heterogeneous grain distribution, while FTIR spectra indicated the presence of functional groups conducive to dye adsorption. The efficacy of the RhB dye adsorption material was monitored using UV-VIS spectroscopy. The effectiveness of removing RhB was highlighted, with 99% removal achieved with optimal amount (mass) of the adsorbent. The study confirms the efficacy of WCT800 in dye adsorption, underscoring its potential as a sustainable solution for environmental remediation of dye-contaminated waters.*

**Keywords:** waste tires, pyrolysis, Rhodamine B.

### INTRODUCTION

The natural decomposition process of discarded waste rubber is estimated to take about 150 years. According to today's level of road vehicle use, the number and size of landfills for discarded waste tires would grow very quickly, so systematic efforts are being made to solve the problem of waste tires in terms of sustainable development, respecting the doctrine: reuse, retraffic, recycling and renewable energy [1–4]. That is the reason why waste management is becoming increasingly important all over the world. Based on the growing need to remove waste tires from landfills and to treat them to obtain a new product that contains useable value, one of the solutions is a waste management plant and within it, the treatment of waste tires by technological process such as pyrolysis (carbonization) [5,6].

The challenges associated with removing organic dyes such as Rhodamine B (RhB) from aquatic environments due to their harmful effects on receiving water bodies. Rhodamine B (Figure 1) is categorized as a basic cationic dye, forming a colored cationic salt when dissolved in water, making it more toxic compared to anionic dyes.

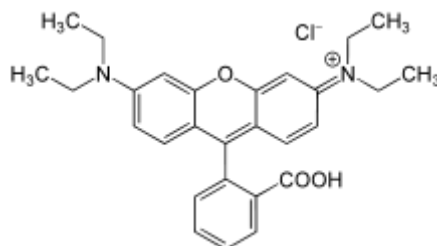


Figure 1 Rhodamine B (RhB) chemical structure

## MATERIALS AND METHODS

### Carbonization (pyrolysis) process

A sample of waste car tires (WCT) was sourced from a local car dealership, then cut into smaller pieces using a tire cutting machine, and subsequently granulated by an industrial rubber granulator to produce waste rubber granulate with particle sizes under 5 mm ( $r_p < 5000 \mu\text{m}$ ), consuming approximately  $0.23 \text{ kW kg}^{-1}$  of energy [7]. The sample was then taken to the lab for further preparation, adhering to the standard procedures outlined in ISO 21645:2021. In the lab, the sample was dried under controlled conditions to a constant mass, ground to a size under 0.25 mm ( $< 250 \mu\text{m}$ ), and sieved to ensure uniform particle size.

The carbonization process involves the use of a tube furnace (Protherm Electrical Tube Furnace (PTF 16/38/250)), to convert fine powdered WCT samples into carbon materials under specific operating conditions. This process requires heating the samples to  $800^\circ\text{C}$  in a  $\text{CO}_2$  atmosphere (with a continuous gas supply) with a heating step of  $5^\circ\text{C}$  per minute, and retention time of 1h at the reached temperature ( $800^\circ\text{C}$ ). After the carbonization process, the samples are cooled down to room temperature. The resulting black solid residue includes recovered carbon blacks, inorganic components, and carbonaceous deposits formed during the rubber conversion process. Obtained carbon materials are marked as WCT800.

### Surface characterization

The morphology of both the raw WCT and carbonized samples was examined using a scanning electron microscope (TESCAN MIRA 3 XMU) operating at current voltage of 10 keV. The instrument was equipped with a Polaron SC502 Sputter coater setup for carbon materials handling.

Fourier transform infrared (FTIR) spectroscopy was employed to identify the types of chemical bonds, functional groups, and potential oxygen-containing groups present. FTIR spectra of the raw WCT and carbonized samples were obtained using a PerkinElmer FTIR 180 spectrophotometer with KBr pellets over the range of  $4000 \text{ cm}^{-1}$ – $400 \text{ cm}^{-1}$ . Approximately 10 mg of each sample was encapsulated in 300 mg of KBr, maintaining a ratio of approximately 1:30, to prepare translucent sample disks for FTIR measurements.

### Analysis of adsorbate and removal efficiency

The evaluation of the WCT800 effectiveness was conducted by subjecting model dye solutions to adsorption reactivity tests employing Ultraviolet–Visible (UV–VIS) spectroscopy, utilizing a Lambda 35 UV–VIS Spectrometer, Perkin Elmer, Inc., Waltham, MA, USA. Adsorption experiments were carried out employing varying masses of the carbonized sample ranging from 0.005 g to 0.1 g, specifically 0.005, 0.01, 0.05, 0.07, and

0.1 g (comprising a series of five samples of the adsorbent with different masses), while maintaining a constant initial concentration of 1 ppm of Rhodamine B (RhB). The volume of the solution utilized in each experiment was fixed at 30 mL. The Rhodamine B used is a purity of at least 97.0% (Sigma Aldrich).

## RESULTS AND DISCUSSION

### Characterization

The SEM analysis of the raw waste tire sample (WCT) reveals significant surface roughness characterized by irregularly shaped particles, likely a result of the milling process to which the recycled rubber is subjected (Figure 2a). Conversely, in the case of the selected WCT800 obtained at a carbonization temperature of 800°C for a retention time of 1 hour, SEM images (Figure 2b–d) display numerous small particles, presumed to be amorphous carbon produced during carbonization. The particle diameters range from 100  $\mu\text{m}$  to 10  $\mu\text{m}$ , with the pore size distribution notably concentrated around 2–15 nm for the sample under consideration.

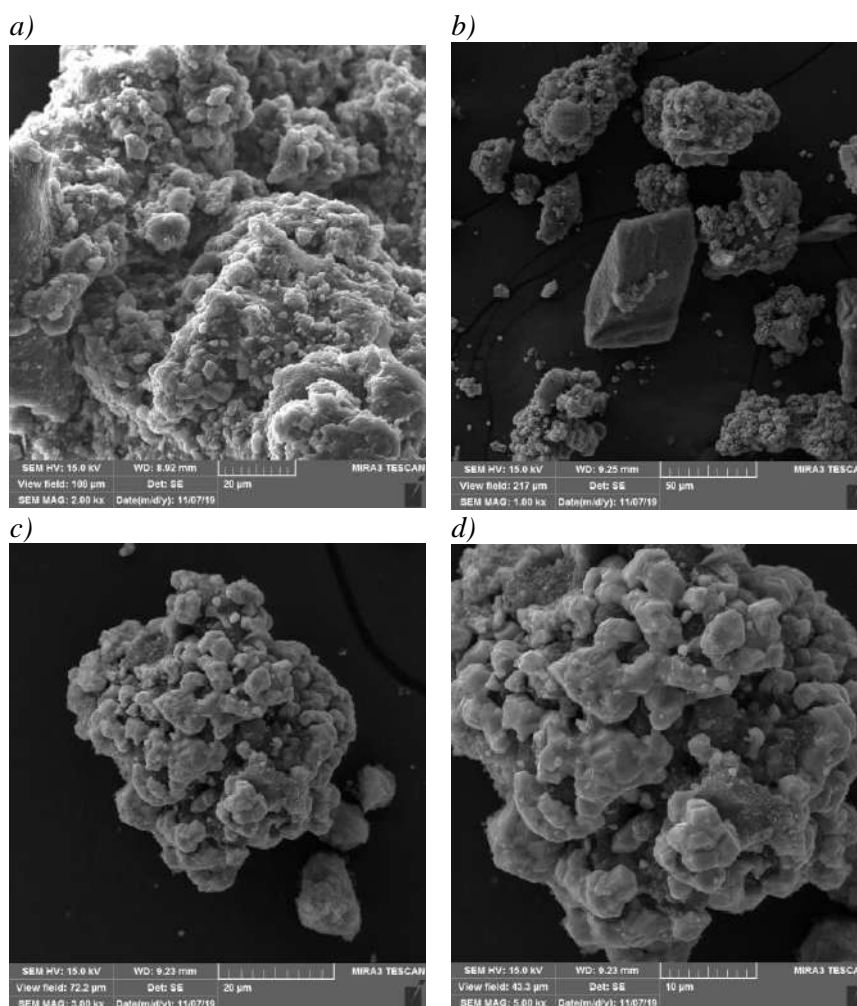


**Figure 2** SEM images of a) raw precursor (WCT) (2000 $\times$ ); b) WCT800 sample 1000 $\times$ ; c) WCT800 sample 3000 $\times$ ; d) WCT800 sample 5000 $\times$



In general, the SEM micrographs depict a heterogeneous distribution of grains and the presence of smaller-sized pores, indicative of a highly porous structure. Also, Figure 2 illustrates the existence of cavities and a rough texture, attributed to the release of organic compounds from the CO<sub>2</sub> reaction at elevated process temperatures.

The FTIR spectrum of carbon materials (Figure 3) showed several characteristic peaks for carbon materials. The peak at  $\sim 3441\text{ cm}^{-1}$  belongs to OH stretching vibrations. Next peak, located at  $\sim 2974\text{ cm}^{-1}$  correspond to the vibrations of the C-H group. Third peak in the FTIR spectrum located around  $1631\text{ cm}^{-1}$  indicate presence of C=O vibration bands. Additionally, these C=O functional groups, could be further attributed to carboxylic groups, carbonyl and lactone groups [8]. The last two peaks at  $1085\text{--}1040\text{ cm}^{-1}$  could be assigned to the C-O stretching vibration, from COOH functional group [9].

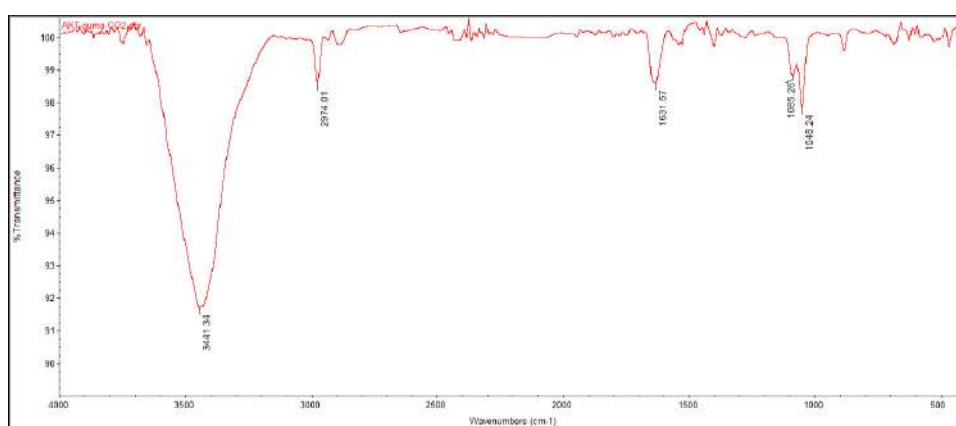


**Figure 3** FTIR spectrum of investigated carbon material

### Adsorption activity

The effect of adsorbent (WCT800) dosage on the adsorption, i.e. on the amount of RhB dye removed and the change in the concentration of residual dye in the solution are shown in Figure 4.

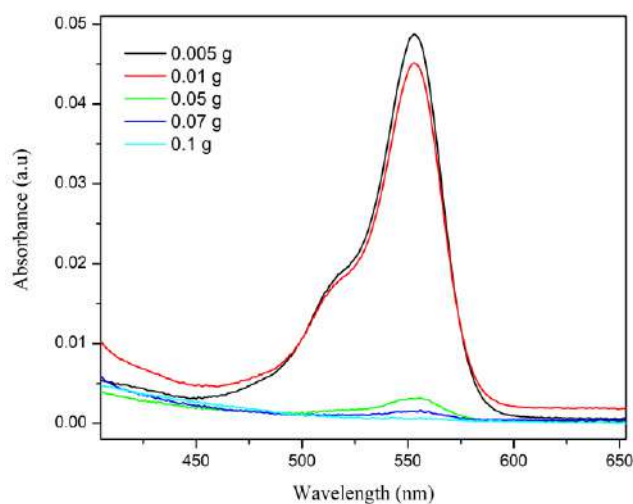


**Figure 4** UV-VIS absorption curves of RhB dye for different amounts of WCT800 sample



Based on the UV-VIS curves (Figure 4), it can be confirmed that larger amount of adsorbent allows a larger amount of dye to be adsorbed per unit mass of adsorbent. The increase in adsorption with the adsorbent dosage can be attributed to the availability of the greater surface area and a larger number of adsorption sites. As the optimal adsorbent dosage, the value of 0.05 g was taken which removes over 99% of the RhD dye from the aqueous solution. At doses higher from optimum dosage, the adsorbent surface becomes saturated with RhB, and the RhB concentration in the solution remains unchanged.

## CONCLUSION

This study demonstrates the effective utilization of carbonized waste car tires (WCT800) at 800°C for the adsorption of Rhodamine B (RhB) dye from aqueous solutions. The carbonization process not only contributes to waste tire management but also converts this environmental burden into a valuable adsorbent. The SEM analysis confirmed that WCT800 possesses a highly porous structure with a rough texture and a heterogeneous distribution of grain sizes, which are beneficial for adsorption processes. The FTIR spectra further revealed the presence of functional groups such as hydroxyl, carboxyl, and carbonyl, which are critical in the adsorption of RhB dye.

The adsorption experiments highlighted the capacity of WCT800 to remove up to 99% of RhB dye, with the optimal adsorbent dosage determined at 0.05 grams. This high efficiency is attributable to the increased surface area and the abundance of adsorption sites offered by the carbonized material. Moreover, the study indicated that beyond the optimal dosage, the adsorption capacity plateaus, suggesting the saturation of adsorption sites.

These findings underscore the dual benefits of this approach: addressing the environmental issue of waste tire accumulation and providing a sustainable solution to water pollution caused by synthetic dyes. Future studies could explore the regeneration and reuse of WCT800 and assess its applicability to other pollutants, potentially broadening its utility in environmental remediation.

## ACKNOWLEDGEMENT

*The authors are grateful to the Ministry of Science, Technological development and Innovation of the Republic of Serbia for financial support according to the contract with the registration number (e.g. 451-03-66/2024-03/200017).*

## REFERENCES

- [1] Cardona N., Campuzano F., *et al.*, IOP Conf. Ser. Mater. Sci. Eng. 437 (2018) 012012.
- [2] Mrad M., El-Samra R., J. Waste Manag. Dispos 3 (2020) 1–12.
- [3] Ryms M., Januszewicz K., *et al.*, Ecol. Chem. Eng. 20 (2013) 93–107
- [4] Sathiskumar C., Karthikeyan S., Sustain. Mater. Technol. 22 (2019) e00125.
- [5] Martínez J.D., Puy N., *et al.*, Renew. Sust. Energ. Rev. 23 (2013) 179–213.
- [6] Rodriguez I.M., Laresgoiti M.F., *et al.*, Fuel Process. Technol. 72 (2001) 9–22.
- [7] Pijovic M., Manic N., *et al.*, Diamond Relat. Mater. 121 (2022) 108768-97.

- [8] Figueiredo J.L., Pereira M.F.R., *et al.*, Carbon N. Y. 37 (1999) 1379–89.
- [9] Cymann-Sachajdak A., Graczyk-Zajac M., *et al.*, Electrochim. Acta 383 (2021)138356.



## SYNTHESIS, CHARACTERIZATION AND ADSORPTION POTENTIAL OF CORN COB-DERIVED ACTIVATED CARBON

Svetlana Butulija<sup>1\*</sup>, Jelena Maletaškić<sup>1</sup>, Bratislav Todorović<sup>2</sup>, Goran Branković<sup>3</sup>,  
Aleksandar Krstić<sup>1</sup>, Ružica Mihailović<sup>4</sup>, Branko Matović<sup>1</sup>

<sup>1</sup>Vinča Institute of Nuclear Sciences - National Institute of the Republic of Serbia,  
University of Belgrade, Mike Petrovića Alasa 12–14, 11351 Belgrade, SERBIA

<sup>2</sup>Faculty of Technology University of Nis, Bulevar Oslobođenja 124, 16000 Leskovac,  
SERBIA

<sup>3</sup>Institute for Multidisciplinary Research, University of Belgrade, Kneza Višeslava 1,  
11030 Belgrade, SERBIA

<sup>4</sup>Veterinary Specialist Institute “Kraljevo”, Žička 34, 36000 Kraljevo, SERBIA

\*svetlana8@vinca.rs

### Abstract

*This study investigates the production of activated carbon from corn cobs, an abundant agricultural waste, using physical activation. Corn cobs were carbonized at 900°C under nitrogen, followed by activation at 850°C with CO<sub>2</sub>. Morphological analysis showed a well-developed pore structure post-activation. Nitrogen adsorption isotherms classified both samples as type I, predominantly microporous, with the activated carbon exhibiting a higher specific surface area (883 m<sup>2</sup>/g) compared to the carbonized sample (207 m<sup>2</sup>/g). The adsorption capacity for methylene blue demonstrated superior performance of activated carbon, achieving 95% adsorption within 10 minutes. This research highlights the potential of corn cobs for sustainable activated carbon production, promoting waste minimization and environmental protection through effective biomass recycling for applications in water remediation and pollution control.*

**Keywords:** corn cob, activated carbon, biomass recycling, adsorption capacity.

### INTRODUCTION

Activated carbon is a highly porous material widely used in industrial processes for separation, purification, and recovery. Recent research has focused on utilizing biomass, including agricultural byproducts, for producing cost-effective activated carbon [1]. Corn cobs, abundant agricultural waste with high carbon content and low inorganic impurities, are promising candidates for this purpose.

Two primary methods, physical and chemical activation, are used to produce activated carbon. Chemical activation involves a single-step carbonization and activation process at lower temperatures, while physical activation includes carbonization followed by gasification at higher temperatures using oxidizing agents like CO<sub>2</sub> or steam [2].

This study explores the feasibility of employing physical activation to produce activated carbon from corn cobs. Utilizing corn cobs for activated carbon production offers a

sustainable and cleaner process for biomass recycling, yielding high-surface-area carbon products suitable for pollution control and other applications.

The growing interest in utilizing agricultural waste for activated carbon production aligns with efforts to minimize waste and reduce environmental impact. This research contributes to advancing biomass utilization by demonstrating corn cob-derived activated carbon's potential for water remediation and industrial applications, promoting a more sustainable approach to materials utilization.

## MATERIALS AND METHODS

The carbonaceous precursor used in the study is corn cob, a waste product from the production of 427ZP corn plant, collected from a local farm of Kraljevo, Serbia. Before the pyrolysis, corncob samples were washed from the impurities and dried in the oven at 100°C.

*Carbonization.* About 10 g of corn cob was put into a stainless steel crucible and heated at 1°C/min to a 900°C under a constant N<sub>2</sub> stream.

*Activation.* The char obtained from carbonization (CC) was followed by activation at the final carbonization temperature 850°C for 1 h. For obtaining of activated carbon (AC), CO<sub>2</sub> (purity of 99.99%), the flow rate was maintained at 200 cm<sup>3</sup>/min (measured at room temperature).

The crystal structure of samples was examined by X-ray diffraction (Rigaku Ultima IV, Japan). The X-ray beam was nickel-filtered CuK $\alpha$  radiation ( $\lambda=0.1540$  nm, operating at 40 kV and 40 mA). XRD data were collected over a range of 10° to 80° (2 $\theta$ ) at a scanning rate of 10°/min.

Before the FESEM analysis, samples were coated with Au alloy using a sputter coater. The morphologies of the CC and AC samples were studied by field emission scanning electron microscopy (FESEM) TESCAN Mira3 XMU at 20 kV.

FTIR spectra of raw, carbonated and activated corn cob were acquired at room temperature using a Bomem Michelson (Hartmann & Braun) MB-100 spectrometer set in absorbance mode. Spectra were obtained in the 3000–500 cm<sup>-1</sup> region with a resolution of 2 cm<sup>-1</sup>. Prior to analysis, samples were finely powdered, uniformly dispersed, vacuum-pressed into KBr pellets (1.5 mg sample/150 mg KBr at 200 MPa), and a pure KBr pellet served as the reference.

The specific surface areas (S<sub>BET</sub>) of the materials were analyzed by the low-temperature nitrogen adsorption according to Brunauer Emmet Teller (BET) method [3] using a Surfer porosimeter (Thermo Fisher Scientific, USA). Pore size distribution (PSD) was calculated by Barrett, Joyner, and Halenda (BJH) method [4], and the data was extrapolated from the desorption isotherm branch [3]. Prior to analysis, the samples were degassed for 8 hours at 200°C under vacuum.

In order to examine the application of the samples, methylene blue was used as a model analyte in adsorption kinetics experiments. The efficacy of adsorption was examined in the 5–1440 minute time interval. The initial concentration of the adsorbate solution was 20 ppm. The experiments were performed at 25° in duplicate. For the quantification of methylene blue

after adsorption, the LLG-uniSPEC 2 Spectrophotometer (LLG Labware) was used. The wavelength used for quantification is 668 nm.

## RESULTS AND DISCUSSION

Figure 1 presents FE-SEM micrographs of CC and AC samples. Following carbonization, the CC sample exhibited ordered and regularly shaped pores, with uniformly distributed cavities, small holes, and cracks, indicating the development of porosity. Notably, the morphology of the carbonized corn cob resembles that of carbonized wood [6].

Subsequent activation resulted in the development of a regular alveolar microstructure in the sample, characterized by thin-walled alveoli filled with air. Thinning the walls resulted in the formation of new pores, thereby increasing the total pore volume and surface area.

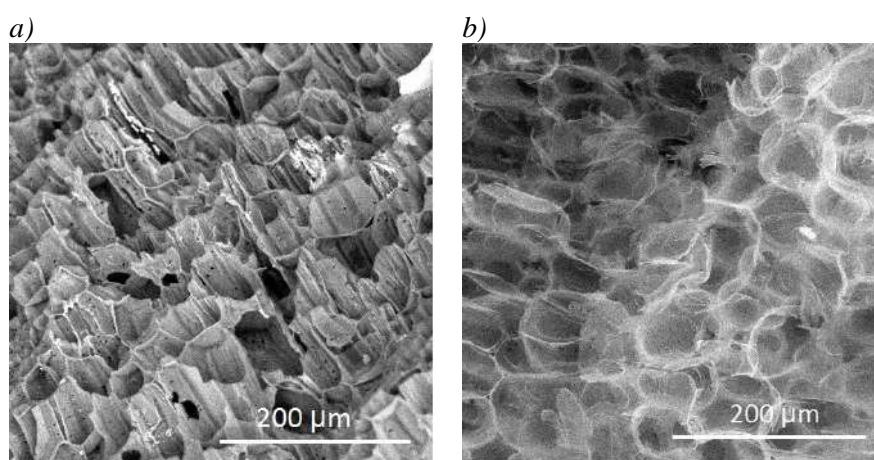


**Figure 1** FESEM micrographs of corn cob after carbonisation (a) and subsequent activation (b)

Figure 2a illustrates the XRD patterns of CC and AC samples. For both samples, the diffraction profiles exhibit two broad carbon peaks of at approximately  $24^\circ 2\theta$  and  $42^\circ 2\theta$  after activating with steam which are assigned to the reflection from (002) and (100) planes, respectively. Additionally, a sharp peaks at  $\sim 29, 31,$  and  $54^\circ 2\theta$  corresponds to  $\text{SiO}_2$  from the sample.

The FTIR spectra in the region of  $3000\text{--}500\text{ cm}^{-1}$  were analysed (Figure 2b). A broad band at  $3400\text{ cm}^{-1}$  is attributed to the stretching and deformation vibrations of the O-H bond. The O-H bending occurs at  $1423\text{ cm}^{-1}$ . The band at  $3400\text{ cm}^{-1}$  originates from physically associated water (O-H) molecules on the surface. The high intensity of this band is contributed by O-H bonds from carbohydrates and possibly other compounds with this functional group. In the region of  $3000\text{--}2850\text{ cm}^{-1}$ , the presence of aliphatic structures ( $\text{CH}_3$  and  $\text{CH}_2$  groups) can be observed. Peaks at  $2920$  and  $2851\text{ cm}^{-1}$  are attributed to  $\text{CH}_2$  groups, while the peak at  $2970\text{ cm}^{-1}$  is attributed to the presence of  $\text{CH}_3$  groups. The ratio of integrated absorbance areas in spectrum b)  $\text{CH}_3/\text{CH}_2=2955/2920\text{ cm}^{-1}$  peak is  $\geq 1$ . It is evident that during the pyrolysis process, alkyl chains from the initial sample (spectrum a) underwent degradation, leaving aliphatics bound in shorter chains to other macromolecules, mostly as  $\text{CH}_3$  groups. In contrast, activation of the investigated material led to the reestablishment of

longer alkyl chains. However, their length is not identical to the initial sample, as a slight presence of  $\text{CH}_3$  groups can be clearly observed. A small peak at  $1728\text{ cm}^{-1}$  originates from  $\text{C}=\text{O}$  stretching vibration. The peak at  $1642\text{ cm}^{-1}$  is attributed to a *cis*  $\text{C}=\text{C}$  bond. Activation of the pyrolyzed sample resulted in the disappearance of several small peaks in the  $1300\text{--}1000\text{ cm}^{-1}$  range and the formation of a broad band. Aromatic/polyaromatic structures were also formed in the sample during pyrolysis, indicated by a peak at  $879\text{ cm}^{-1}$ , showing isolated aromatic hydrogen atoms. The bending mode of polyaromatics is observed at  $618\text{ cm}^{-1}$ , which decreases during activation. These peaks are associated with  $\text{C}-\text{O}$  stretching vibrations, and the intensity of the peak at  $1383\text{ cm}^{-1}$  is related to the amount of cellulose [6].

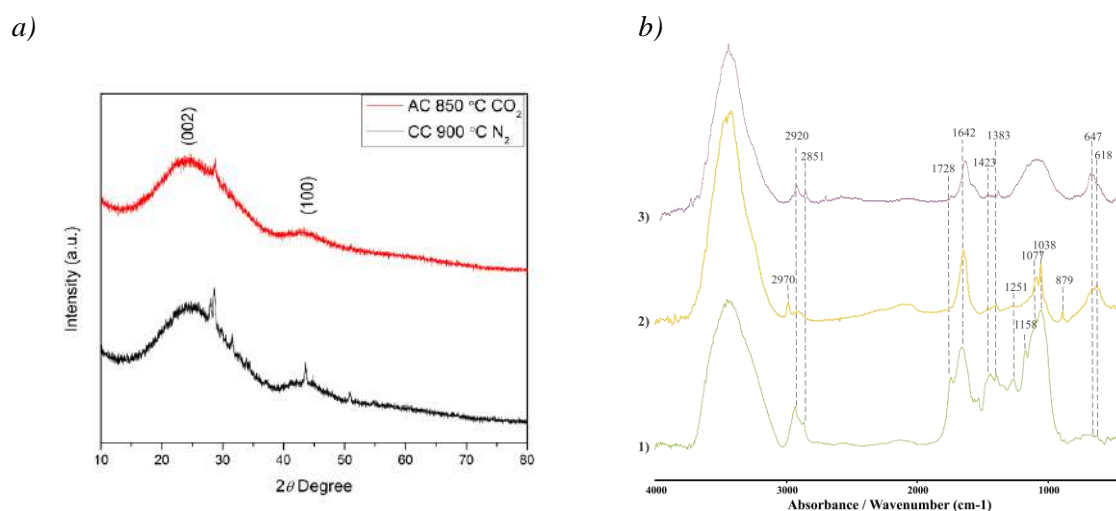


**Figure 2** a) XRD patterns of CC and AC; b) Comparison of FTIR Spectra for: 1) raw, 2) carbonated, and 3) activated corncob

Figure 3a presents nitrogen adsorption isotherms as the amount of  $\text{N}_2$  adsorbed as a function of relative pressure at  $196^\circ\text{C}$  for samples CC and AC. According to IUPAC classification [7], all the samples are type I isotherms. Both samples can absorb a large amount of nitrogen in a relative low pressure range. Hysteresis loops are of type H4, indicates that materials are predominantly microporous [7]. The specific surface areas of samples ( $S_{\text{BET}}$ ), calculated by the BET equation were  $207\text{ m}^3\text{g}^{-1}$  for CC sample and  $883\text{ m}^3\text{g}^{-1}$ . It is evident that after the activation, the specific surface of the sample increases together with the micropore region.

Pore size distribution (PSD) of samples is given in Figure 3b. For both samples, there is a sharp peak in the microporous region, and also a peak at  $\sim 2\text{ nm}$ —a limit between micro- and mesoporosity (micropores  $\leq 2\text{ nm}$ , mesopores  $2\text{--}50\text{ nm}$ , and macropores  $\geq 50\text{ nm}$ ). According to the PSD diagram, the increased intensity of the peaks confirms that activation has significantly increased the number of pores.

The adsorption of methylene blue results on investigated samples are shown in Figure 4. With the carbonized sample (Figure 4a), in the first two hours, an increase in adsorption up to 40% is observed, after which the adsorption slows down, and after 24 hours, about 70% of methylene blue is adsorbed, where a steady state is established. The activated sample shows a very fast and significantly better adsorption ability than the carbonized sample – in the first 10



minutes, about 95% of methylene blue is adsorbed (Figure 4b). This phenomenon can be explained by the higher specific surface area of the activated sample, i.e., the higher number of available active sites for the adsorption of methylene blue, which is a consequence of physical activation. A higher pore radius and higher amount of micropores also affect the adsorption abilities of the activated sample. The VIS spectrum of methylene blue (Figure 5) shows a significantly decreasing peak area of the activated sample than the carbonized sample and initial adsorbate concentration.

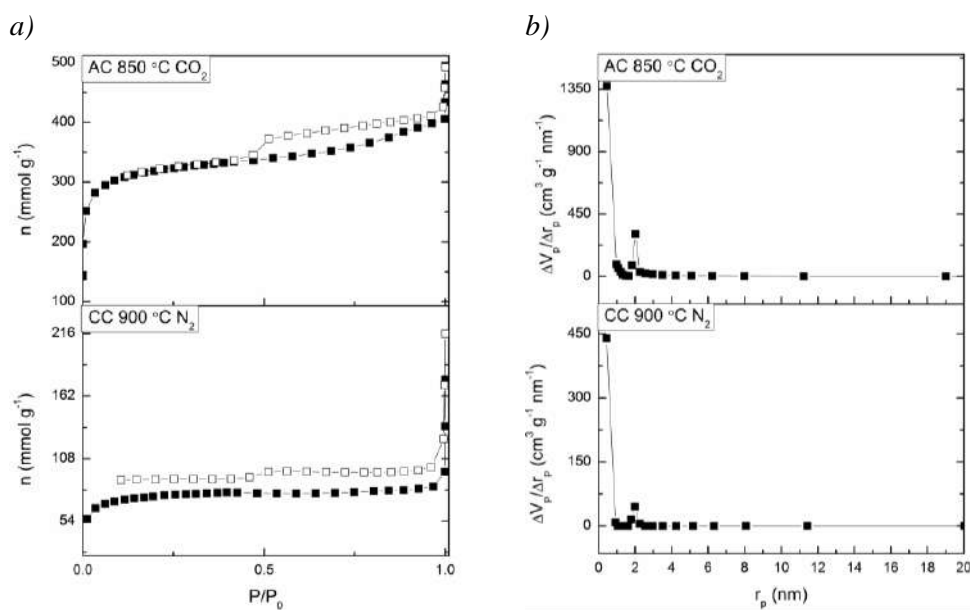


**Figure 3** Nitrogen adsorption isotherm plot for CC and AC. a) Solid symbols – adsorption, open symbols – desorption; b) Pore size distribution of CC and AC

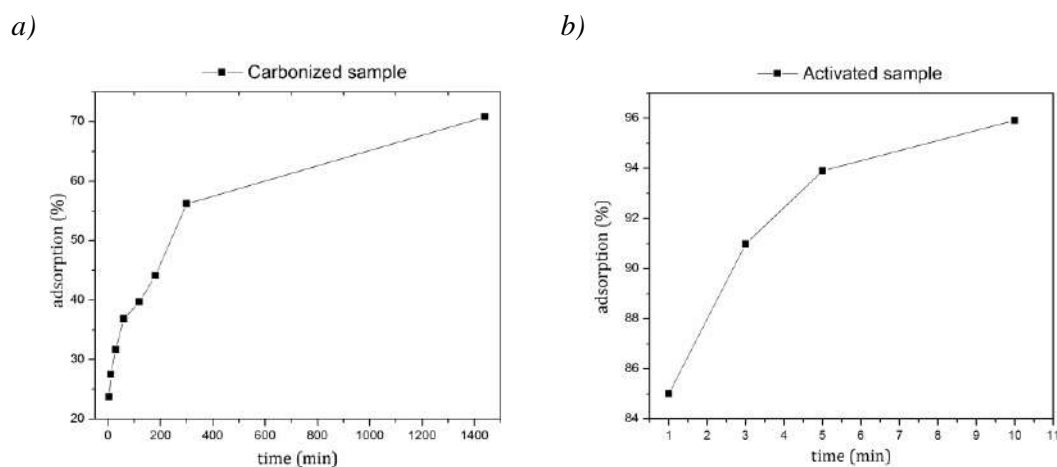


**Figure 4** The dependency of methylene blue adsorption from the time for a) CC; and b) AC

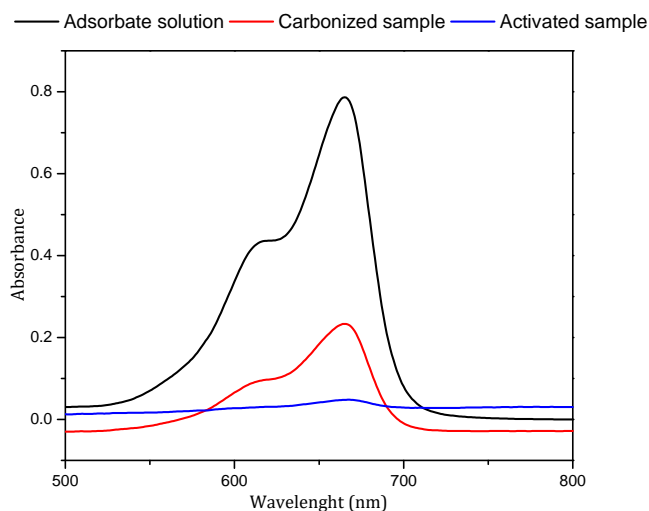


**Figure 5** VIS spectrum of initial adsorbate solution, CC and AC in steady state

## CONCLUSION

This study demonstrates that corn cobs can be effectively converted into high-performance activated carbon through physical activation. The resulting material exhibits enhanced porosity and surface area, significantly improving its adsorption capacity for pollutants like methylene blue. Utilizing corn cobs for activated carbon production offers a sustainable approach to waste management and environmental protection.

## ACKNOWLEDGEMENT

*The authors are grateful to the Ministry of Science, Technological development and Innovation of the Republic of Serbia for financial support according to the contract with the registration number (e.g. 451-03-68/2024-14/200017).*

## REFERENCES

- [1] Ukanwa K.S., Patchigolla K., Sakrabani R., *et al.*, Sustainability 11 (22) (2019) 6204.
- [2] Song M., Jin B., Xiao R., *et al.*, Biomass Bioenergy 48 (2013) 250–256.
- [3] Brunauer S., Emmett P.H., Teller E., J. Amer. Chem. Soc. 60 (1938) 309.
- [4] Barret E.P., Joyner L.G., Halenda P.P., J. Am. Chem. Soc. 73 (1951) 373–380.
- [5] Lippens B.C., Linsen B.G., de Boer J.H., J. Catalysis 3 (1964) 32–37.
- [6] Sevilla M., Macia-Agullo J. A., Fuertes A.B., Biomass Bioenergy 35 (2011) 3152.
- [7] Sing K.S.W., Everett D.H., Haul R.A.W., *et al.*, Pure Appl. Chem. 57 (1985) 603–619.
- [8] Lowell S., Shields J.E., Thomas M.A., *et al.*, Characterization of Porous Solids and Powders: Surface Area, Pore Size and Density, Ed. Kluwer Academic Publishers, Dordrecht Netherlands (2004), p.44, ISBN: 1-4020-2302-2.



## PHOTOCATALYTIC PROPERTIES OF C-ZnO NANOPARTICLES SYNTHESIZED via MECHANOCHEMICAL METHOD

Vladan Nedelkovski<sup>1\*</sup>, Sonja Stanković<sup>1</sup>, Dragana Medić<sup>1</sup>, Dragoş Buzdugan<sup>2</sup>,  
Iosif Hulka<sup>3</sup>, Snežana Milić<sup>1</sup>, Milan Radovanović<sup>1</sup>

<sup>1</sup>University of Belgrade, Technical Faculty in Bor, V.J. 12, 19210 Bor, SERBIA

<sup>2</sup>Politehnica University Timisoara, Faculty of Mechanics, M.V.S. 1,  
300222 Timisoara, ROMANIA

<sup>3</sup>Politehnica University Timisoara, Research Institute for Renewable Energies, G.M. 138,  
300501 Timișoara, ROMANIA

\*vnedelkovski@tfbor.bg.ac.rs

### Abstract

*Escalating water pollution necessitates the development of efficient and sustainable photocatalytic materials for the degradation of organic pollutants. In this work, the photocatalytic properties of carbon-doped zinc oxide (C-ZnO) nanoparticles synthesized by a novel mechanochemical method are investigated. The unique approach of doping ZnO nanoparticles with carbon not only increases the absorption of visible light but also improves the efficiency of charge separation, leading to a significant increase in photocatalytic activity. Experimental analytical methods such as X-ray diffraction (XRD), scanning electron microscopy (SEM), and UV-Vis spectroscopy are used to elucidate the structural, morphological, and photocatalytic properties of the synthesized C-ZnO nanoparticles. The photocatalytic performance of C-ZnO nanoparticles is evaluated by their ability to degrade methyl orange at a concentration of 5 ppm under UV light irradiation with and without mixing the solution for 60 minutes in the dark before exposure to UV light. The influence of the photocatalysis time on the degradation efficiency was investigated. The results show that the photocatalysis time has a strong influence on the degradation efficiency.*

**Keywords:** photocatalysis, nanomaterials, doping, mechanochemical, synthesis.

### INTRODUCTION

Zinc oxide nanoparticles (ZnO-NP) have attracted considerable attention in the field of photocatalysis due to their excellent optical properties, high electron mobility, and environmental friendliness. As a wide bandgap semiconductor (approximately 3.37 eV), ZnO inherently has strong absorption of ultraviolet (UV) light, but limited activity in visible light, which makes up the majority of the solar spectrum. This limitation has led to extensive research into the modification of ZnO to harness the broader spectrum of solar energy for photocatalytic applications, including the degradation of organic pollutants [1,2].

Among various strategies to extend the photocatalytic efficiency of ZnO NPs into the visible light range, doping with atoms of different elements has been identified as a particularly effective method. Doping introduces impurity levels within the bandgap of ZnO, which can facilitate the absorption of visible light by narrowing the bandgap or creating

mid-gap states that act as stepping stones for electron transition from the valence to the conduction band. In particular, carbon doping has proven to be a promising approach, as carbon can introduce p-type conductivity into ZnO, thereby improving charge separation and reducing the electron-hole recombination rate [3,4].

Carbon-doped ZnO nanoparticles (C-ZnO NP) exhibit significantly improved photocatalytic activity under visible light compared to their undoped counterparts. The incorporation of carbon into the ZnO lattice or the ZnO surface can lead to the formation of C-O-Zn bonds, which are believed to contribute to the generation of active sites for photocatalytic reactions. Furthermore, carbon doping can enhance the adsorption of pollutants on the catalyst surface, facilitating their subsequent degradation [4].

Recent studies have demonstrated the effectiveness of C-ZnO NPs in degrading various organic pollutants, under UV and/or visible light irradiation. For instance, the carbon doping of ZnO using natural precursors such as glucose or other similar chemicals offers an environmentally and cost-effective way to synthesize photocatalysts with enhanced activity and stability [5].

Despite the progress in the synthesis of C-ZnO NP, the challenge is to optimize the doping level, understand the exact mechanisms of photocatalytic enhancement and increase production for practical applications.

## **MATERIALS AND METHODS**

### **Sample preparation**

ZnO NPs, both undoped and carbon-doped, were produced using a mechanochemical method followed by a calcination process. The synthesis of undoped and carbon-doped ZnO nanoparticles involved mixing zinc acetate dihydrate (Sigma-Aldrich) with oxalic acid dihydrate (Sigma-Aldrich) and grinding them in an agate mortar for 10 minutes, resulting in a gel composed of zinc oxalate dihydrate and acetic acid. For the synthesis of C-ZnO NP, glucose (Merck) was additionally incorporated into the gel, with the grinding extended for another 10 minutes to form the precursor. The final undoped and C-ZnO NP were then produced by calcining this mixture at 500°C for 3 hours.

### **Characterization methods**

SEM photograph was obtained via QUANTA FEG 250 SEM microscope. The X-ray diffraction (XRD) patterns of the C-ZnO NP were recorded using an X'Pert<sup>3</sup> Powder X-ray diffractometer for a range of  $2\theta$  from 20–90°. The photocatalytic activity of synthesized nanomaterial was accessed via UV/VIS spectrometry.

## **RESULTS AND DISCUSSION**

SEM photograph is presented in Figure 1. The SEM image shows a closer look at the nanorods, which differ in shape, size, and surface roughness, which can be related to the growth conditions and carbon concentration during the synthesis process [6,7]. The diameter and length of the smallest nanorods are about 30 nm.

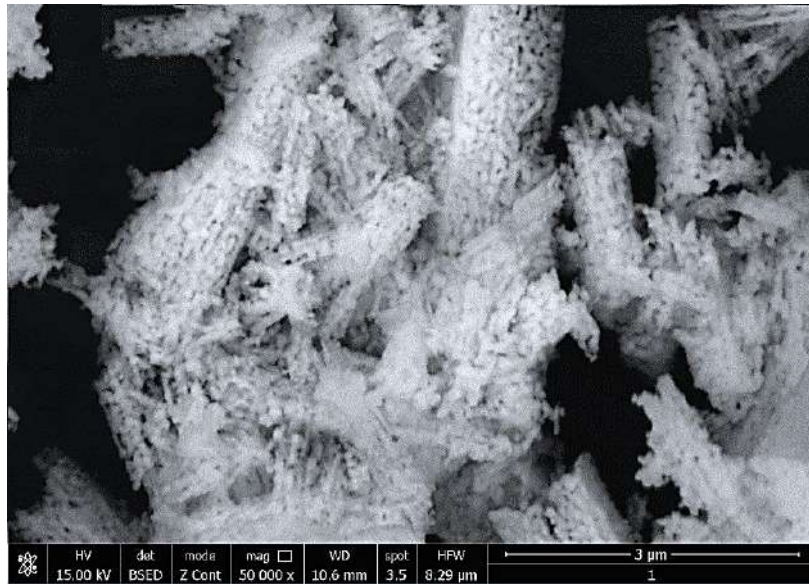


**Figure 1** SEM image of synthesized carbon-doped ZnO NP

The XRD pattern of the synthesized doped nanoparticles is presented in Figure 2. The X-ray diffraction pattern (XRD) image shows the crystalline structure of zinc oxide doped with 5% carbon compared to undoped ZnO as defined by the Joint Committee on Powder Diffraction Standards (JCPDS) [8]. The presence of distinct peaks at angles of  $33.48^\circ$ ,  $36.10^\circ$ ,  $37.92^\circ$  and  $58.07^\circ$ , which align with the undoped ZnO (JCPDS no. 36–1451), confirms the hexagonal wurtzite structure of ZnO without secondary phases. For the C-ZnO NP, there is an observed shift of the (002) peak towards higher angles compared to the ZnO NP JCPDS data. This indicates a decrease in the lattice constant “c” due to carbon doping, which is expected due to the incorporation of smaller carbon ions into the oxygen sites of the ZnO lattice [9].

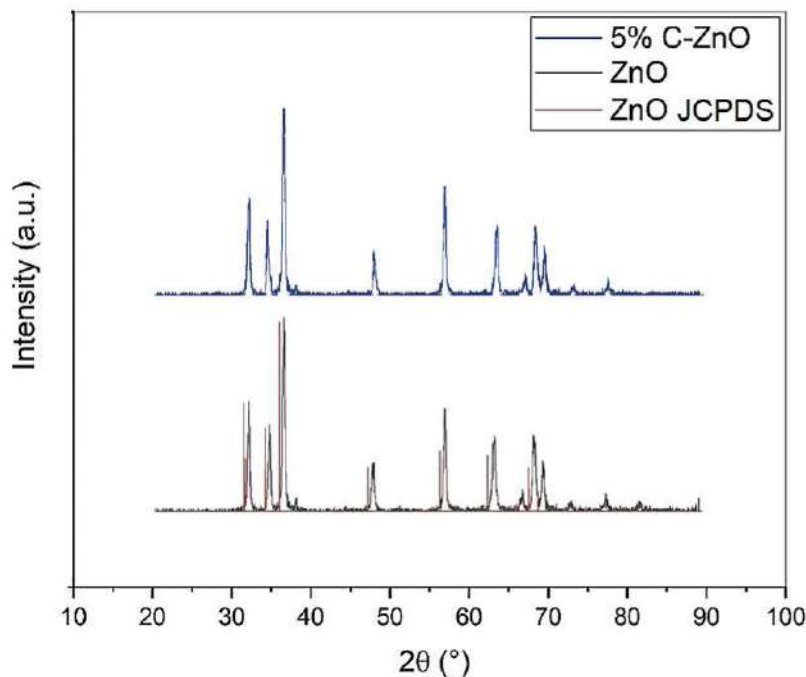


**Figure 2** XRD pattern of synthesized samples

Based on XRD analysis and calculations, data was obtained on crystallite parameters  $a$  and  $c$ ),  $c/a$  ratio, the crystallite size ( $D$ ), interplanar distance ( $d$ ), unit cell volume ( $V$ ), Atomic packing fraction (APF), dislocation density ( $\delta$ ), atomic displacements ( $u$ ), micro-strain ( $\epsilon$ ), number of unit cells contained in a grain ( $n$ ), stacking fault ( $\alpha^*$ ), stress ( $\sigma$ ), Young's modulus ( $Y$ ) and lattice volume ( $U$ ). Data is presented in Table 1.

**Table 1** Structural parameters of the analyzed NP samples

Sample	$a$ (Å)	$c$ (Å)	$c/a$	$D$ (nm)	$d$ (nm)	$V$ (Å <sup>3</sup> )	APF (%)	$\delta \cdot 10^{-3}$ (nm <sup>-2</sup> )
ZnO	3.24	5.2	1.47	68.05	0.27	55.92	0.59	0.21
5%C-ZnO	3.09	4.97	1.61	25.32	0.25	41.06	0.53	1.56
Sample	$u$	$\epsilon \cdot 10^{-3}$	$n \cdot 10^6$	$\alpha^*$	$\sigma \cdot 10^7$ (Pa)	$Y \cdot 10^{10}$ (Pa)	$U \cdot 10^4$ (J/m <sup>3</sup> )	
ZnO	0.4	1.2	31.6	0.0012	4.37	3.75	2.55	
5%C-ZnO	0.38	1.2	2.19	0.0011	4.37	3.75	2.55	

Table 1 presents the structural parameters of ZnO and 5% carbon-doped ZnO (5%C-ZnO) nanoparticle samples. Key differences between the samples highlight the impact of carbon doping on the structural and physical properties. Notably, doping reduces the crystallite size ( $D$ ) from 68.05 nm in pure ZnO to 25.32 nm in 5%C-ZnO, which can enhance surface area and reactivity. Moreover, the unit cell volume ( $V$ ) decreases from 55.92 Å<sup>3</sup> to 41.06 Å<sup>3</sup>, suggesting a more compact structure. The higher dislocation density ( $\delta$ ) in 5%C-ZnO ( $1.56 \cdot 10^{-3}$  nm<sup>-2</sup>) compared to pure ZnO ( $0.21 \cdot 10^{-3}$  nm<sup>-2</sup>) indicates increased lattice imperfections, which can facilitate charge separation and improve photocatalytic activity [10,11].

To gain insight into photocatalytic properties, model compound degradation experiments were conducted with the previously prepared 5 ppm methyl orange stock solution. Experiments were conducted with and without mixing in the dark for 60 minutes before exposing to UV light irradiation ( $\lambda=395$  nm), since it has been reported that in this step equilibrium for the adsorption and desorption of dye molecules is achieved. For the collected data, a pseudo-first-order model was employed and is expressed as [12,13]:

$$\ln\left(\frac{C_0}{C_t}\right) = kt \quad (1)$$

Where  $C_0$  and  $C_t$  represent model compound concentration values at zeroth and time “ $t$ ”, while “ $k$ ” represents the reaction rate constant. Figure 3a shows the degradation efficiency of synthesized nanoparticles, with and without mixing step in the dark for 60 minutes. The plot of  $\ln(C_0/C_t)$  vs irradiation time “ $t$ ” is depicted in Figure 3b and a linear relationship is observed. Reaction rate constants are evaluated from the slopes of  $\ln(C_0/C_t)$  vs time plot.

The degradation efficiency of undoped and carbon-doped ZnO NPs can reach 78.93% and 89.10% in 60 minutes, which is higher than the degradation efficiency values determined for experiments without mixing in the dark. Figure 3b shows the  $k$  values for degradation



experiments. The rate constants ( $k$ ) are highest for the 5%C-ZnO 500°C sample in an experiment with ( $k_4=0.0360 \text{ min}^{-1}$ ), and without mixing in the dark for 60 minutes before the ( $k_3=0.0316 \text{ min}^{-1}$ ). The pure ZnO samples have lower rate constants ( $k_1=0.0235 \text{ min}^{-1}$  and  $k_2=0.0243 \text{ min}^{-1}$  for experiments with and without mixing in the dark, respectively). This indicates faster degradation kinetics for the carbon-doped samples, corroborating their superior photocatalytic activity.

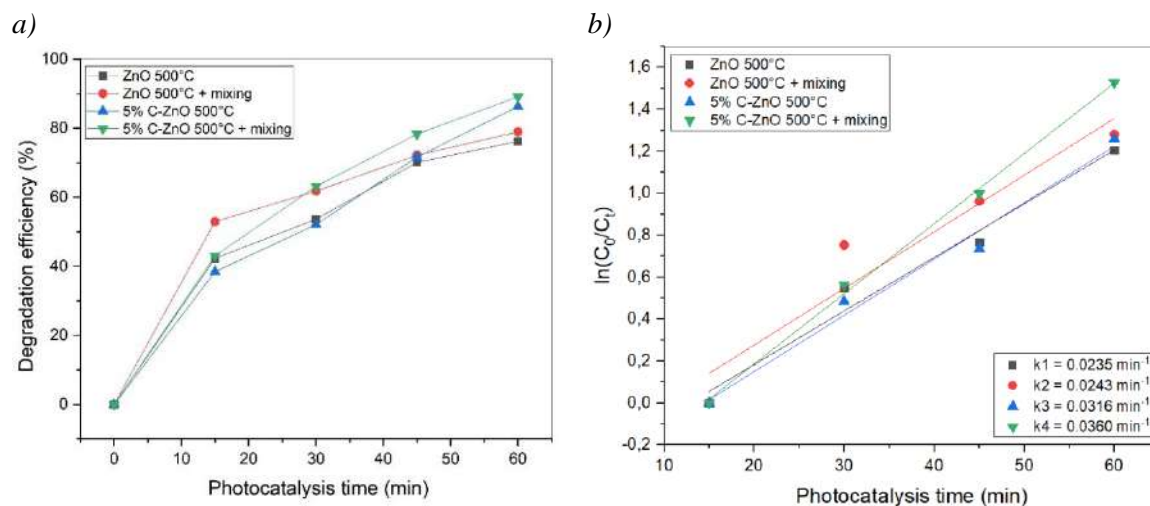


**Figure 3** a) Photocatalytic degradation efficiencies of synthesized nanoparticles; b) Kinetics curves of samples

Overall, the enhanced performance of 5%C-ZnO can be attributed to the structural modifications and increased surface area resulting from carbon doping, which improves the efficiency and rate of photocatalytic degradation.

## CONCLUSION

Facile and cost-effective mechanochemical synthesis of pure and C-doped ZnO nanoparticles was performed, and the prepared photocatalysts were used for photocatalytic degradation of methyl orange dye as a model pollutant. The results of the SEM and XRD studies were in agreement and showed that both samples were composed of nanoparticles. The XRD patterns illustrated that the C-ZnO-NP had a lower average crystallite size than the crystallite size of the pure ZnO-NPs, which indicates that the C-ZnO-NPs have a larger specific surface area as well as a larger number of defects, resulting in better overall photocatalytic properties. These alterations are more than just morphological; they confer enhanced photocatalytic efficiency to the C-ZnO-NP. Remarkably, a doping concentration of 5 wt% carbon enables the nanoparticles to achieve an 89.10% degradation rate of a 5 ppm methyl orange solution within the span of an hour, under neutral pH conditions. This efficiency not only underlines the potential for practical application in wastewater treatment but also makes the doped nanoparticles excellent candidates for environmental remediation.

## ACKNOWLEDGEMENT

*The authors are grateful to the Ministry of Science, Technological development and Innovation of the Republic of Serbia for financial support according to the contract with the registration number 451-03-65/2024-03/200131.*

## REFERENCES

- [1] Que M., Lin C., Sun J., *et al.*, *Sensors* 21 (16) (2021) 1–22.
- [2] Ansari S.A., Ansari S.G., Foad H., *et al.*, *New J. Chem.* 41 (17) (2017) 9314–9320.
- [3] Ayon S.A., Billah M.M., Nishat S.S., *et al.*, *J. Alloys Compd.* 856 (2021) 158217.
- [4] Zhang X., Qin J., Hao R., *et al.*, *J. Phys. Chem. C.* 119 (35) (2015) 20544–20554.
- [5] Wei D., Qi Y., Lv S., *et al.*, *Ceram. Int.* 45 (4) (2018) 4448–4454.
- [6] Ayeb K., Moussa N., Nsib M.F., *et al.*, *Mater. Sci. Eng. B.* 263 (2) (2021) 114870.
- [7] Majumder S., Chatterjee S., Basnet P., *et al.*, *J. Environ. Nanotechnol.* 14 (2020) 100386.
- [8] McMurdie H.F., Evans E.H., Morris M.C., *et al.*, *Powder Diffr.* 1(2) (1986) 64–77.
- [9] Heng T.S., Lau S.P., Wang L., *et al.*, *Appl. Phys. Lett.* 95 (1) (2009) 2007–10.
- [10] Nemiwal M., Zhang T.C., Kumar D., *Sci. Total Environ.* 767 (2021) 144896.
- [11] Qi K., Cheng B., Yu J., *et al.*, *J. Alloys Compd.* 727 (2017) 792–820.
- [12] Cho S., Jang J.W., Lee J.S., *et al.*, *Cryst. Eng. Comm.* 12(11) (2010) 3929–35.
- [13] Santos G.O.S., Eguluz K.I.B., Salazar-Banda G.R., *et al.*, *Chemosphere* 244 (2020) 125455.



## EQUILIBRIUM AND THERMODYNAMICS OF NITRATE SORPTION BY MODIFIED ZEOLITE FROM AQUEOUS SOLUTION

Aleksandar Zdravković<sup>1\*</sup>, Milena Nikolić<sup>1</sup>, Dragana Marković Nikolić<sup>1</sup>,  
Danijela Stojadinović<sup>1</sup>, Goran Petković<sup>1</sup>, Tanja Nikolić<sup>1</sup>

<sup>1</sup>Academy of Professional studies South Serbia, Department of Technology and Art studies,  
Vilema Pušmana 17, 16000 Leskovac, SERBIA

\*zdravkovic.aleksandar87@gmail.com

### Abstract

*The sorption performance of the modified zeolite-Fe(III) sorbent towards nitrate ions was investigated in batch conditions. The modified zeolite was characterized by Fourier transform infrared spectroscopy (FTIR). The analysis of equilibrium data indicates that the nitrates sorption process is the most adequately described by the Dubinin-Radushkevich isotherm. The main mechanism of binding of nitrate ions at sorption centers on the modified zeolite surface is physisorption. Thermodynamic parameters show the spontaneity and exothermicity of the nitrate removal process at the temperature range from 25 to 45°C. The maximum sorption capacity of the modified zeolite for nitrate ions under the tested thermodynamic and equilibrium experimental conditions is 12.068 mg/g. Modification achieved about three times greater ability to bind nitrate ions to the surface of the modified zeolite compared to raw zeolite,  $q_m=4.324$  mg/g. Chemically modified zeolite can serve as an alternative low-cost sorbent in removing nitrate ions from water to reduce the harmful effect on humans and the aquatic ecosystem (eutrophication).*

**Keywords:** sorption, zeolite, nitrate, equilibrium, thermodynamics.

### INTRODUCTION

In recent years, groundwater and surface water have been often polluted with inorganic ions such as nitrates ( $\text{NO}_3^-$ ), which have toxic effects on humans and aquatic ecosystems. They are naturally found in water, high concentrations of nitrites can cause methemoglobinemia, especially in infants, and potentially lead to the occurrence of cancer in humans [1,2]. Point and diffuse sources of nitrates that pollute groundwater and surface water are runoff from arable and urban areas, untreated industrial and sanitary waste, septic tanks, and animal manure [3]. It is known that higher nitrate concentrations in aquatic ecosystems, encourage the growth of plants and algae and cause eutrophication.

For all the above mentioned, it is necessary to remove excess nitrate ions from drinking water. For this purpose, can be used different sorbent materials such as zeolite, clay, activated carbon, etc. Natural zeolites are ecologically and economically acceptable hydrated aluminosilicate materials of three-dimensional structure with sorption and ion exchange properties. Primarily, raw and modified zeolites are used for the removal of cationic pollutants from the water environment [4,5].

This paper aims to determine the sorption performance of modified zeolite with Fe(III) ions for the removal of nitrate from aqueous medium and to characterize the process through equilibrium and thermodynamic parameters.

## MATERIALS AND METHODS

### Material

Raw zeolite with a particle size in the range of 200 to 800  $\mu\text{m}$  was purchased from the company ZeoKop from Brus (Serbia). Modification of raw zeolite was performed with 0.5 M  $\text{FeCl}_3$  solution (Centrochem, Serbia). 100 g of raw zeolite was treated with 250  $\text{cm}^3$  of  $\text{FeCl}_3$  solution under reflux for 6 h. After filtration, the filter cake was washed with distilled water to negative reaction to chlorides (test with  $\text{AgNO}_3$ ). The zeolite sample was dried for 12 h at 80°C in an oven (model ST-06, Instrumentaria, Zagreb, Croatia). Recordings of raw and modified zeolite by Fourier transform infrared spectroscopy (FTIR) have been performed on FTIR Bomen Hartmann & Braun MB-series spectrophotometer in the wavenumber range of 400–4000  $\text{cm}^{-1}$ . The samples were prepared by grounding of 1 mg of zeolite with 150 mg KBr (Merck, Darmstadt, Germany) into powder. Thin transparent pastille of powder sample was made under vacuum pressure of 200 MPa.

### Sorption experiments

Nitrate sorption was performed in Erlenmeyer flasks (250  $\text{cm}^3$ ) with a 50  $\text{cm}^3$  nitrate solution of pH 6 for a contact time of 1 h at 100 rpm on a magnetic stirrer (MSH-30A, Witeg, Germany). Equilibrium experiments were conducted in the sorbate concentration range of 10–50  $\text{mg}/\text{dm}^3$  with a sorbent dose of 2  $\text{g}/\text{dm}^3$ . The data obtained in the equilibrium experiments were analyzed using the Langmuir, Freundlich, Temkin, and Dubinin-Radushkevich isotherm. The thermodynamic parameters of nitrate removal by modified zeolite were determined based on sorption data obtained in a solution with an anion concentration of 50  $\text{mg}/\text{dm}^3$  and dose sorbate of 2  $\text{g}/\text{dm}^3$  at the following temperatures: 25, 35, and 45°C. The nitrate solution pH was adjusted using 0.1 M HCl or 0.1 M NaOH solution on a digital pH meter (HI-2209, Hanna, USA).

After the sorption process, an aliquot of the solution was taken and filtered through 0.45  $\mu\text{m}$  filters (Nylon Syringe filters, USA). In 2  $\text{cm}^3$  aliquots, 2  $\text{cm}^3$  of 1 M HCl solution was added and the absorbance was measured at 220 and 275 nm on a UniSpec 2 UV-VIS LLG spectrophotometer. The nitrate concentration in the solution was calculated based on calibration curve for  $\text{KNO}_3$ . The sorption capacity of zeolite towards nitrate anions over time,  $q_t$  (mg/g), was calculated according to the following equation:

$$q_t = \frac{(c_0 - c_t)V}{m} \quad (1)$$

where  $c_0$  and  $c_t$  represent the initial concentration and concentration of the nitrate solution in time  $t$  ( $\text{mg}/\text{dm}^3$ ), respectively,  $V$  volume of the nitrate solution ( $\text{dm}^3$ ), and  $m$  the mass of the zeolite (g).

## RESULTS AND DISCUSSION

On the FTIR spectrum of raw and modified zeolite (Figure 1), there are absorption bands from valence vibrations of the OH group ( $\nu_{\text{OH}}$ ) at  $3613\text{ cm}^{-1}$  (narrow band from isolated OH group) and  $3434\text{ cm}^{-1}$  (broad band from hydrogen-bonded OH group), as well as absorption band from deformation vibrations in the plane at  $1637\text{ cm}^{-1}$  ( $\delta_{\text{OH}}$ ) [4,5]. These absorption bands correspond to the vibration of intermolecular hydrogen bonds of OH groups on terminal silanol groups, OH groups on defect positions, and OH groups attached to cations in the zeolite structure [6]. Absorption with a maximum at  $1047\text{ cm}^{-1}$  on the FTIR spectrum of raw zeolite is assigned to the symmetrical stretching vibration of Si-O-T structure, where T is Si or Al. The stretching Si-O-T vibration of zeolite gives an absorption band at  $786\text{ cm}^{-1}$  [7]. Absorption bands in the area of wavenumbers from  $\approx 600\text{--}400\text{ cm}^{-1}$  are the consequence of deformation Si-O and Al-O vibrations [4].

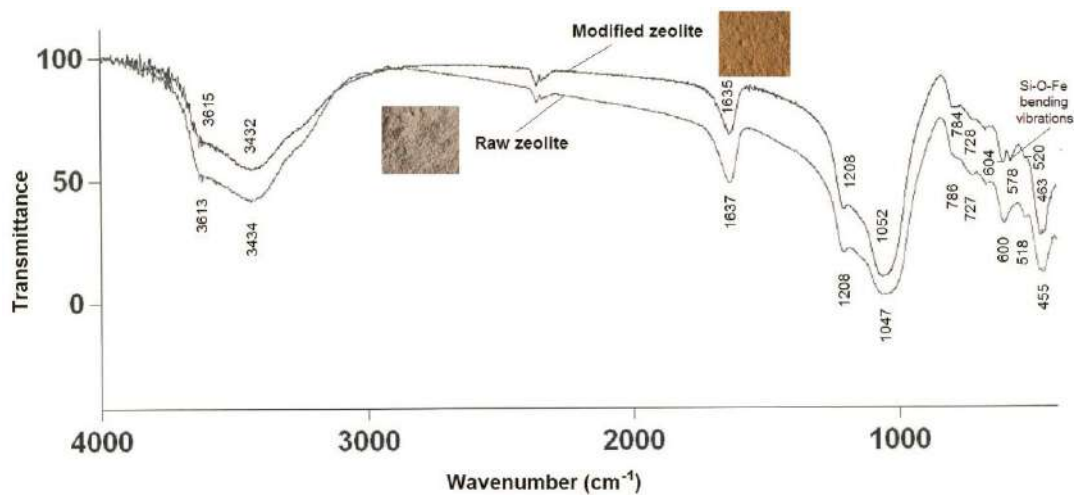


**Figure 1** FTIR spectra of raw and modified zeolite

On the FTIR spectrum of the modified zeolite, there are all absorption bands with small shifts compared to the same bands of the raw zeolite (Figure 1). The difference is reflected only in the presence of an absorption band of medium intensity with a maximum at  $578\text{ cm}^{-1}$  on the spectrum of modified zeolite. This absorption band is the result of Si-O-Fe bending vibrations [8]. From the photographs and the FTIR spectra shown in Figure 1, it is concluded that the  $\text{Fe}^{3+}$  ions are incorporated into the zeolite structure.

Sorption isotherms, i.e., sorption systems in equilibrium, defined the distribution of sorbate between the sorbent and the aqueous solution and gave data on the sorbent capacity, the nature of sorbent surface, and the type of bond between the sorbate and the sorbent [9,10]. The analysis of equilibrium experimental data was done with Origin Pro 8.0 software (OriginLab Corporation, USA) by the nonlinear regression method for Langmuir, Freundlich, Temkin, and Dubinin-Radushkevich (D-R) isotherm. The Langmuir model (Equation 2) implies the binding of sorbates to specific sorption centers on an energetically homogeneous sorbent surface. Sorbate binds in a monolayer on the sorbent surface, and there are no interactions between sorbate particles [11].

$$q_e = \frac{q_m K_L c_e}{1 + K_L c_e} \quad (2)$$

Where  $q_e$  (mg/g) represents the equilibrium sorption capacity of sorbent,  $q_m$  (mg/g) maximum sorption capacity of sorbent,  $c_e$  (mg/dm<sup>3</sup>) is the concentration of sorbate in the equilibrium state, and  $K_L$  (dm<sup>3</sup>/mg) is the Langmuir constant.

The Freundlich model (Equation 3) implies the existence of interactions between sorbed particles and multilayer sorption. Sorbat particles are bound on the energetically heterogeneous surface of the sorbent [12].

$$q_e = K_F c_e^{1/n} \quad (3)$$

The Freundlich constant  $K_F$  indicates the strength of adsorption, i.e., refers to the sorption capacity, while the exponent  $n$  refers to the energy heterogeneity of the sorbent surface.

According to the Temkin isotherm model (Equation 4), the sorption heat of molecules on the sorbent surface decreases linearly with the surface coverage, and there is no interaction between sorbed molecules [13].

$$q_e = B \ln(K_T c_e) \quad (4)$$

Where  $B$  (J/mol) is the constant that is related to sorption heat, and  $K_T$  (dm<sup>3</sup>/g) is the equilibrium constant corresponding to the maximum binding energy.

Dubinin-Radushkevich isotherm (Equation 5) determines the sorption mechanism of porous sorbents [14].

$$q_e = q_{DR} \exp(-K_{DR} \varepsilon^2) \quad (5)$$

Where  $q_{DR}$  (mg/g) is Dubinin-Radushkevich monolayer maximum sorption capacity,  $K_{DR}$  (mol<sup>2</sup>/J<sup>2</sup>) is the activity coefficient that is related to the mean free sorption energy  $E$  (J/mol),  $E = 1/(2K_{DR})^{1/2}$ , and  $\varepsilon$  is Polanyi potential.

The isotherm model curves obtained for nitrate sorption using non-linear regression are shown in Figure 2, and the isotherm parameters are given in Table 1. The best non-linear fitting with the experimental equilibrium data is shown by the Dubinin-Radushkevich isotherm and confirmed by high correlation coefficient of  $R^2=0.990$  in Table 1. The Freundlich, Langmuir, and Temkin models have lower correlation coefficients (Table 1), therefore, these models cannot be used to describe the nitrate sorption process.

The nature and mechanism of sorption define the mean free sorption energy. An  $E$  value of less than 8 kJ/mol indicates physical sorption as the dominant mechanism in the sorbate removal process, while  $E$  values in the range of 8-16 kJ/mol suggest that chemical sorption or ion exchange is the mechanism of bonding sorbate [15]. The physisorption mechanism ( $E= 326.651$  J/mol) can be involved in the removal of nitrates from aqueous solutions by modified zeolite.

The thermodynamic parameters of sorption were calculated by equations 6 and 7 [16,17], and the results are shown in Table 2.

$$\Delta G^\circ = -RT \ln K_c \quad (6)$$



$$\ln K_c = \frac{\Delta S^\circ}{R} - \frac{\Delta H^\circ}{RT} \quad (7)$$

Where:  $\Delta G^\circ$  (J) Gibbs free energy change,  $\Delta H^\circ$  (J/mol) enthalpy change,  $\Delta S^\circ$  (J/mol K) entropy change,  $K_c$  the equilibrium constant calculated from the ratio of the equilibrium concentration of sorbate on the sorbent ( $c_{ad}$ ) and in the solution ( $c_s$ ),  $K_c = c_{ad}/c_s$ . Via linear Plot of  $\ln K_c$  vs.  $1/T$  is determined  $\Delta H^\circ$  and  $\Delta S^\circ$  values (equation 7).

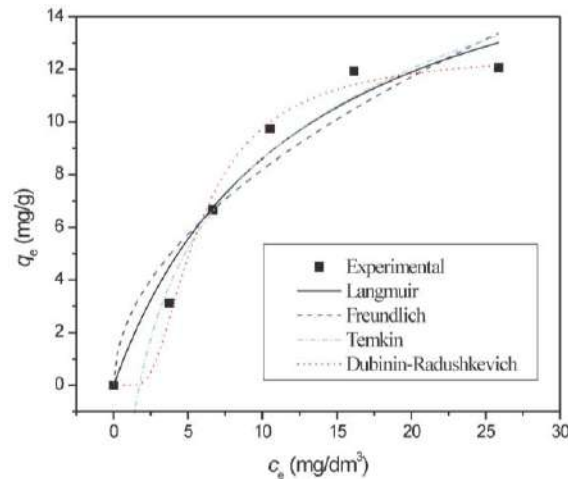


Figure 2 Isotherms of nitrate sorption onto modified zeolite

Table 1 Parameters of equilibrium isotherms for sorption of nitrates

Isotherm	Parameter	Sorbate
Langmuir	$K_L \times 10^2$ (dm <sup>3</sup> /mg)	8.128
	$q_m$ (mg/g)	19.209
	$R^2$	0.951
Freundlich	$K_F ((\text{mg/g}) (\text{dm}^3/\text{mg})^{1/n})$	2.496
	$n$ (g/dm <sup>3</sup> )	1.938
	$R^2$	0.908
Temkin	$K_T$ (dm <sup>3</sup> /g)	0.575
	$B$ (J/mol)	4.923
	$R^2$	0.962
Dubinin-Radushkevich	$q_{DR}$ (mg/g)	12.663
	$K_{DR} \times 10^6$ (mol <sup>2</sup> /J <sup>2</sup> )	4.686
	$E$ (J/mol)	326.651
	$R^2$	0.990

Table 2 Thermodynamic parameters of nitrate sorption by modified zeolite

$t$ (°C)	$T$ (K)	$\Delta G^\circ$ (kJ/mol)	$\Delta H^\circ$ (kJ/mol)	$\Delta S^\circ$ (kJ/mol K)	$R^2$
25	298.16	-1.900			
35	308.16	-1.787	-6.015	-0.014	0.989
45	318.16	-1.624			

The spontaneity process of the nitrate sorption onto modified zeolite decreases with increasing temperature from 25 to 45°C (Table 2). The removal of anions from an aqueous solution had a negative enthalpy change ( $\Delta H^\circ = -6.015$  kJ/mol), and therefore, sorption is exothermic. The enthalpy change value is in the range of 2–20 kJ/mol, which once again confirms that the mechanism of nitrate anion binding to zeolites is of physical nature (physisorption) [18]. The randomness at the sorbent/solution interface decreases by establishing the interaction of anions and sorption centres of zeolite ( $\Delta S^\circ = -0,014$ ).

The justification of the raw zeolite modification by  $\text{FeCl}_3$  is confirmed by the higher modified zeolite sorption capacity towards nitrate ( $q_m = 12.068$  mg/g), which is almost three times higher than the raw zeolite capacity ( $q_m = 4.324$  mg/g) under the following process conditions: dose 2 g/dm<sup>3</sup>, nitrate concentration of 25 mg/dm<sup>3</sup>, temperature 25°C, pH=6 and contact time of 1 h.

## CONCLUSION

The three-fold enhancement of the nitrate uptake was achieved by the modified zeolite compared to the raw one in a solution where pH, temperature, sorbent dose, sorbate concentration and contact time were varied. In general, modified zeolite has a potential application as a sorbent material for anions (nitrates, phosphates, etc). From the applied equilibrium isotherms, Dubinin-Radushkevich gives the best data correlation ( $R^2 = 0.990$ ) for the sorption and indicates that nitrate ions bind onto an energetically nonuniform surface of the modified zeolite. Thermodynamic and equilibrium investigations suggest that physisorption is involved in the interaction of zeolite and anions.

## REFERENCES

- [1] Yang C.Y., Wu D.C., Chang C.C., *Environ. Int.* 33 (5) (2007) 649–653.
- [2] Bryan N.S., van Grinsven H., *Adv. Agron.* 119 (2013) 153–182.
- [3] Bhatnagar A., Sillanpää M., *Chem. Eng. J.* 168 (2011) 493–504.
- [4] Kragović M., Pašalić S., Marković M., *et al.*, *Minerals*. 8 (1) (2018) 11.
- [5] Kašić V., Mihajlović S., Životić D., *et al.*, *Hem. Ind.* 72 (1) (2018) 29–37.
- [6] Alabbad E.A., *Arab. J. Chem.* 14 (4) (2021) 103041.
- [7] Firdaus M., Prameswari M.D., *Bull. Chem. React. Eng.* 14 (1) (2019) 9–16.
- [8] Ahangaran F., Hassanzadeh A., Nouri S., *Int. Nano Lett.* 3 (23) (2013).
- [9] Králik M., *Chem. Pap.* 68 (12) (2014) 1625–1638.
- [10] Worch E. *Adsorption Technology in Water Treatment: Fundamentals, Processes, and Modeling*. Berlin, Walter de Gruyter, Berlin (2012), p. 41, ISBN: 9783110240238.
- [11] Langmuir I., *J. Am. Chem. Soc.* 40 (9) (1918) 1361–1403.
- [12] Freundlich H.M.F., *J. Phys. Chem.* 57 (1906) 385–471.
- [13] Temkin M.I., Pyzhev V., *Acta Phys. Chim. USSR* 12 (1940) 327–356.
- [14] Dubinin, M.M., Radushkevich, L.V., *Proc. Acad. Sci. USSR Phys. Chem. Sect.* 55 (1947) 331–337.

- [15] Dang V. B. H., Doan H. D., Dang-Vu, T., *et al.*, *Bioresou. Technol.* 100 (2009) 211–219.
- [16] Ahmad R., Mirza A., *J. Mol. Liq.* 249 (2018) 805–814.
- [17] Aksu, Z., *Process Biochem.* 38 (1) (2002) 89–99.
- [18] Liu Y., Liu Y.J., *Sep. Purif. Technol.* 61 (3) (2008) 229–242.



## POTENTIAL USAGE OF OAT STRAW FOR ANIONS REMOVAL FROM WATER: A KINETIC STUDY

Aleksandar Zdravković<sup>1\*</sup>, Milena Nikolić<sup>1</sup>, Dragana Marković Nikolić<sup>1</sup>,  
Danijela Stojadinović<sup>1</sup>, Ivanka Ristić<sup>1</sup>, Tanja Nikolić<sup>1</sup>

<sup>1</sup>Academy of Professional studies South Serbia, Department of Technology and Art studies,  
Vilema Pušmana 17, 16000 Leskovac, SERBIA

\*zdravkovic.aleksandar87@gmail.com

### Abstract

*Potential usage of agricultural waste – oat straw was examined for anions removal from aqueous media. The point of zero charge of oat straw was found to be 6.57. Efficient removal of sulphates was achieved in acidic conditions (pH=4) with sorbent dose of 0.75 mg/dm<sup>3</sup>. The contact time had a significant influence on the sulphate removal up to 20 min of the process. Kinetic models were applied to describe the sorption mechanism. The sorption process was followed by pseudo-first order kinetics.*

**Keywords:** *Avena sativa*, oat straw, sulphates, Lagergren model, Weber-Morris model.

### INTRODUCTION

Due to the growth of the world population, development of industry and excessive use of natural resources, there is a constant growing pollution of surface and underground water. Techniques which could provide water reuse became a necessity. Although efficient, modern technologies such as electrolysis or chemical precipitation are expensive and energy and reagent-consuming. Biosorption provides satisfactory results in pollutants elimination from wastewaters [1]. Compared to conventional methods, biosorption has certain advantages: low-cost, efficient at low concentrations of pollutants and ecologically sustainable. A renewable source – biomass is used, which is often considered waste in the environment. It is possible to regenerate the used biomass, so metal concentrate and biomaterial ready for a new removal cycle are obtained. Biomass efficiency can be increased by modification by physical, chemical, thermal or combined treatments [2].

Oat (*Avena sativa*) is a cereal used for livestock feed, but also for human consumption. Health benefits of oat were emphasized since bioactive compounds in this cereal reduce the risk of cardiovascular disease and diabetes [3]. Since significant amount of oat straw is generated world-wide, this paper aimed to examine its possible application in water purification.

## MATERIALS AND METHOD

### Material

Oat straw was collected from local fields in the vicinity of Lebane. Oat straw was ground in a laboratory blender and sieved on a laboratory sieve of 1 mm diameter. It was then dried in the oven at 105°C to constant mass in order to determine moisture content.

### The point of zero charge

The pH at the point of zero charge ( $pH_{pzc}$ ) of sorbent surface is the pH at which this surface has a net neutral charge.  $pH_{PZC}$  for oat straw was determined by mixing 0.05 g of milled oat straw and 20 mL of 0.1 M KCl and varying the pH from 2 to 12 and measured by digital pH meter (HI-2209, Hanna, USA). The initial pH ( $pH_i$ ) was adjusted by adding HCl (0.1 M) or NaOH (0.1 M). The mixtures were left for 24 hours. The final pH ( $pH_f$ ) of the solution was measured and the  $\Delta pH = pH_f - pH_i$  was plotted against the pH of the initial solution.

### Sorption experiments

The sorption study was conducted in order to analyze the effect of sorbent dose (0.25 to 1 g/dm<sup>3</sup>), pH (2–10) and contact time (5–60 min) with sorbate concentration of 50 mg/dm<sup>3</sup>. All the experiments were performed at 25°C. Deionized water was used for preparation of all solutions.

The concentration of sulphates was measured spectrophotometrically at 420 nm, after reaction with BaCl<sub>2</sub>. The sorption capacity oat straw towards sulphates over time,  $q_t$  (mg/g), was calculated according to the following equation:

$$q_t = \frac{(c_0 - c_t)V}{m} \quad (1)$$

where  $c_0$  and  $c_t$  represent the initial concentration and concentration of the sulphates solution in time  $t$  (mg/dm<sup>3</sup>), respectively,  $V$  volume of the sulphates solution (dm<sup>3</sup>), and  $m$  the mass of the oat straw (g).

## RESULTS AND DISCUSSION

The moisture content in oat straw was found to be 5.64%. The influence of sorbent dose on sulphates sorption is presented in Figure 1.

The sorption capacity of the oat straw rises with an increase in the dose up to 0.75 g/dm<sup>3</sup> (Figure 1) because the available sorbent surface area and the number of active sites for binding sulphate anions are larger [4]. Further increasement of the dose to 1 g/dm<sup>3</sup> led to a slight change in the degree of sulphate removal by the oat straw.

Figure 2 shows the dependence of  $pH_f - pH_i$  on  $pH_i$ , based on which the  $pH_{pzc}$  of the sorbent was determined. The  $pH_f - pH_i$  dependence curve on  $pH_i$  intersected the x-axis at pH 6.57, i.e., sorbent  $pH_{pzc}$ . At a pH value lower than the  $pH_{pzc}$  value, the groups or sorption centres of oat straw are positively charged, while at a pH value higher than the  $pH_{pzc}$ , the functional groups are negatively charged [5,6].

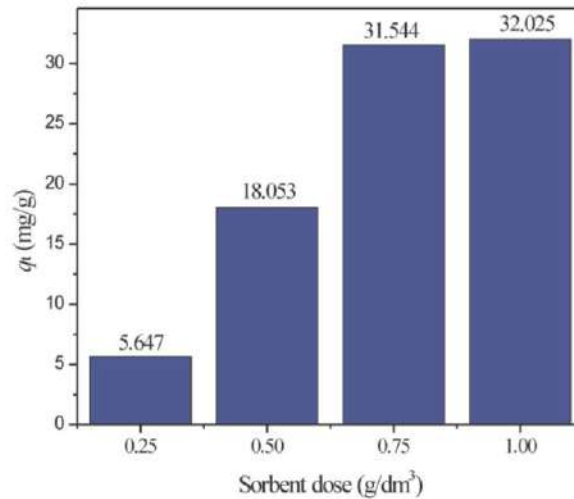


**Figure 1** The effect of sorbent dose on sulphates removal

At pH values of lower than 6.57, electrostatic interactions between the positively charged surface of the sorbent and sulphate anions are established.

The pH affects the sorption performance of the sorbent towards sorbates, either anionic or cationic. The ionization degree of the functional groups of the sorbent is a function of the acidity or basicity of the solution [4]. The results of the pH value effect on the sorption capacity of oat straw towards anions are shown in Figure 3.

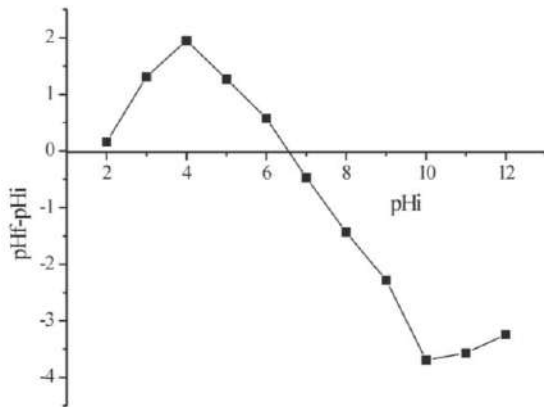


**Figure 2** Determination of zero point charge of oat straw

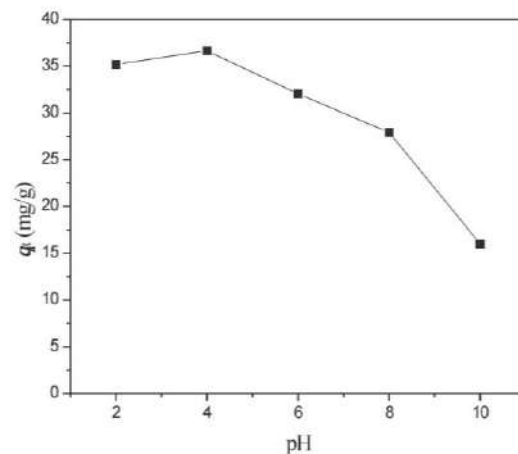


**Figure 3** Dependence of oat straw sorption capacity for sulphates on pH

Sulphate binding to the surface of oat straw is favored in acidic conditions (Figure 3) because the sorbent itself is positively charged below  $pH_{pzc}=6.57$ , which enables interaction with sulfate anions. At pH value 4, the highest removal capacity of sorbent towards sulphates ( $q_m=36.639$  mg/g) was achieved.

Kinetic models are applied to define the sorption mechanism, the stage that controls the sorption rate, and the surface reaction of the sorbent. Lagergren's pseudo-first-order model, Ho's pseudo-second-order model, and Weber-Morris intra-particle diffusion model have broad



applications in sorption processes [7–9]. The nonlinear forms of the pseudo-first and pseudo-second order models are shown by the following equations:

$$q_t = q_e(1 - e^{-k_1 t}) \quad (2)$$

$$q_t = \frac{q_e^2 k_2 t}{1 + q_e k_2 t} \quad (3)$$

where  $k_1$  (1/min) is the pseudo-first-order rate constant,  $k_2$  (g/mg min) is the pseudo-second-order rate constant,  $q_t$  (mg/g) is the sorbent capacity at time  $t$ , and  $q_e$  (mg/g) is the sorbent capacity in the equilibrium state.

According to Lagergren's pseudo-first-order model [10], one type of sorbate reacts with one sorbent center, and the model considers that the occupation degree of the sorbent surface is proportional to the unoccupied sorption centers. Ho's pseudo-second-order model [11] assumes that the sorption kinetics depends on the sorbate concentration in the solution and the number of free sorption centers on the surface of the sorbent.

Insight into the sorption mechanism and the rate-controlling step for porous sorbents is provided by the Weber-Morris intraparticle diffusion model [12]. The overall rate of sorption is determined by the slowest step or stage, which is diffusion through the boundary layer and diffusion within the pores. The linear Weber-Morris model is given by equation 4.

$$q_t = k_{id} t^{1/2} + C \quad (4)$$

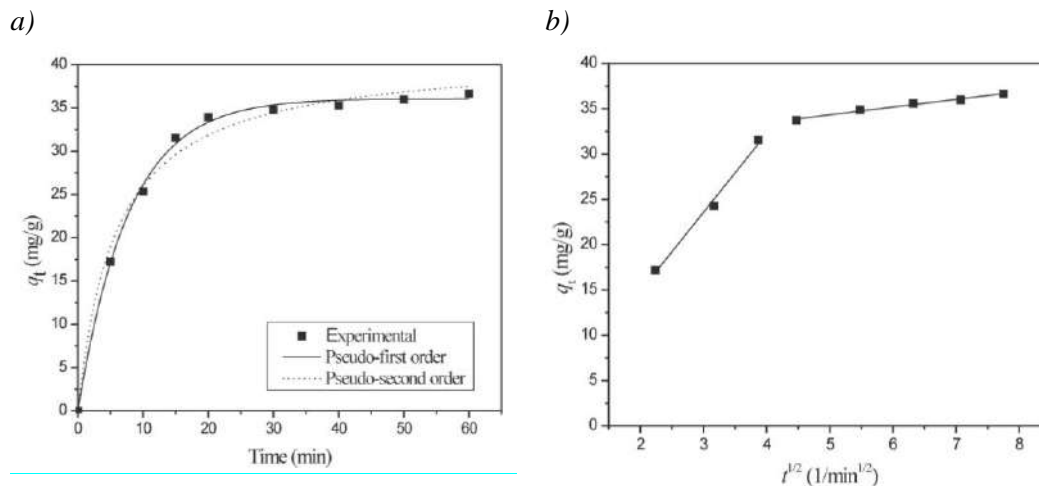
Where  $k_{id}$  is the intra-particle diffusion rate constant (mg/g min<sup>1/2</sup>), and  $C$  is a constant proportional to the thickness of the boundary layer.

The experimental data of sulphates sorption onto oat straw were fitted using the nonlinear regression method according to pseudo-first and pseudo-second order kinetic models. For this purpose, the software package Origin Pro 8.0 (OriginLab Corporation, USA) was applied. The kinetic parameter values are given in Table 1, while the nonlinear curves describing the sorption process are shown in Figure 4a.

The contact time has a significant influence on the sulphate removal up to 20 min. Oat straw sorption capacity does not change significantly afterwards (Figure 4a). It can be seen from the Figure 4a that the pseudo-first order model showed better agreement with the experimental data. This claim is supported by high correlation coefficient of the pseudo-first order ( $R^2=0.996$ ) model of the removal process of sulphate ions from aqueous solutions compared to the pseudo-second order model ( $R^2=0.986$ ) (Table 1). The calculated sorption capacity according to the pseudo-first-order model ( $q_e, \text{cal}=36.230$  mg/g) is closer to the obtained experimental value of sorption capacity ( $q_e, \text{exp}=36.639$  mg/g).

**Table 1** Kinetic parameters of models sorption of sulphates

Kinetic model	Parameter	Sulphate
Experimental	$q_{e, \text{exp}}$ (mg/g)	36.639
Pseudo-first order	$q_{e, \text{cal}}$ (mg/g)	36.230
	$k_1$ (1/min)	0.124
	$R^2$	0.996
Pseudo-second order	$q_{e, \text{cal}}$ (mg/g)	41.467
	$k_2 \times 10^3$ (g/mg min)	3.920
	$R^2$	0.986
Intra-particle diffusion	$k_{id1}$ (mg/g min <sup>1/2</sup> )	8.707
	$C_1$	-2.556
	$R^2$	0.985
	$k_{id2}$ (mg/g min <sup>1/2</sup> )	0.852
	$C_1$	30.072
	$R^2$	0.980

**Figure 4** a) Kinetic model of of pseudo-first and pseudo-second order; and b) intra-particle diffusion model of sulphate sorption

The linear straight line of the dependence of  $q_t$  on  $t^{1/2}$  does not pass through the coordinate origin, therefore, intra-particle diffusion is not the only rate-limiting step of sulphates removal from aqueous solutions. In the graph in Figure 4b, there is a multilinearity, which indicates two stages of the sorption process: external surface sorption and intra-particle diffusion. The first phase of the process lasts 10 minutes, during which the transport of sorbate occurs through the boundary layer to the outer surface of the sorbent. The second phase, intra-particle diffusion, significantly determines the rate of sulphate sorption. These steps determine the rate of the sorption process and high correlation coefficients were obtained by linear fitting (Table 1).

## CONCLUSION

Low-cost and non-toxic agricultural waste such as oat straw can be used for polluted water treatment. The sorption of sulphates is pH-dependent and favoured in acidic conditions since the sorbent itself is positively charged below  $\text{pH}_{\text{pzc}}=6.57$ , thus enables interaction with

sulphate anions. According to obtained data, the removal of sulphate anions by oat straw from aqueous solutions was very well described by the Lagergren pseudo-first order model. According to Weber-Morris intra-particle diffusion model, sorption of sulphates is a two-step process.

## **REFERENCES**

- [1] Pooja D.T., IJSETR 5 (2016) 3038–3040.
- [2] Amar M., Walha K., Salvado V., Adsorpt. Sci. Technol. (2021) 6678530.
- [3] Martinez-Villaluenga C., Penas E., Curr. Opin. Food Sci. 14 (2017) 26–31.
- [4] Bojić D., Nikolić G., Mitrović J., *et al.*, Chem. Ind. Chem. Eng. Q. 22 (2016) 235–247.
- [5] Ibrahim M.N., Norliyama M.S., J. Hazard. Mat. 182 (2010) 377–385.
- [6] Iqbal M., Saeed A., J. Hazard. Mater. 164 (2009) 161–171.
- [7] Su Y., Zhao B., Xiao W., *et al.*, Environ. Sci. Pollut. Res. 20 (2013) 5558–5568.
- [8] Xiong W., Tong J., Yang Z., *et al.*, J. Colloid Interface Sci. 493 (2017) 17–23.
- [9] Dang V.B.H., Doan H.D., Bioresour. Technol. 100 (2009) 211–219.
- [10] Lagergren S., Handlingar 24 (1898) 1–39.
- [11] Ho Y.S., McKay G., Chem. Eng. J. 70 (1998) 115–124.
- [12] Weber W.J., Morris J.C., J. Sanit. Eng. Div. 89 (1963) 31–60.



## ULTRASOUND-ASSISTED EXTRACTION OF ACETAMIPRID FROM POLLUTED SOIL

Aleksandar Zdravković<sup>1</sup>, Milena Nikolić<sup>1\*</sup>, Aleksandra Pavlović<sup>2</sup>,  
Dragana Marković Nikolić<sup>1</sup>, Goran Petković<sup>1</sup>, Tanja Nikolić<sup>1</sup>

<sup>1</sup>Academy of Professional Studies South Serbia, Department of Technology and Art,  
Vilema Pušmana 17, 16000 Leskovac, SERBIA

<sup>2</sup>University of Niš, Faculty of Science and Mathematics, Department of Chemistry,  
Višegradaska 33, 18000 Niš, SERBIA

\*[milenai.chem@gmail.com](mailto:milenai.chem@gmail.com)

### Abstract

*Ultrasound-assisted extraction was applied for acetamiprid extraction using non-toxic solvents of different polarity, which are recognized as “green” solvents. Soil with 1.87% of organic matter content was fortified and used as model of polluted soil. Acetamiprid was spectrophotometrically quantified at 240 nm. After 60 minutes of ultrasound-assisted extraction, the highest recovery was observed with methanol (82.45%), followed by 2-propanol. The lowest recovery was obtained with ethyl-acetate (54.23%).*

**Keywords:** acetamiprid, soil contamination, ultrasonic extraction, organic carbon, green solvents.

### INTRODUCTION

Soil represents the surface layer of the Earth's crust, where the most diverse processes of composition/decomposition of substances continuously occur. Soil is a biochemical complex of organic and inorganic compounds formed by synergistic effect of geological, chemical and biological factors. Fertile soil provides sufficient amount of essential nutrients for plant growth and reproduction, which are consequently used for livestock and human consumption.

However, due to constant human growth population, an intensive agricultural activity and food production leave far-reaching consequences on soil quality. Soil erosion, floods, landslides, salinization and organic matter decline contribute significantly to reduction of soil usability [1].

Also, an urging problem often represents unjustified, excessive application of different pesticides in agriculture, in order to increase yield of crops. Acetamiprid is a neonicotinoid, systemic, broad-spectrum insecticide used for crops, fruits, vegetables and ornamental plants protection against aphids, moths, leafhoppers. It is applied as an efficient alternative to more toxic organophosphates for suppression of potentially dangerous vectors such as mosquitos, but also flies and mites [2]. However, due to intensive use, residues of acetamiprid have been found in the environment and diverse tissues [3,4].

In this research, ultrasound-assisted extraction was applied to extract acetamiprid using solvents of different polarity from a model of polluted soil.

## **MATERIALS AND METHODS**

### **Soil sample**

Surface soil (0–20 cm in depth) was collected from the field in Jablanica district, west from Leskovac, with no agrotechnical procedures and agricultural production in the last five years. The soil was air-dried for 3 weeks, mixed daily, ground, sieved through a 2 mm mesh, and stored in plastic container until used.

### **Soil organic matter**

Soil organic matter was determined according to Turyin volumetric method [5]. Namely, 1 g of soil was mixed with 10 ml of  $0.167 \text{ mol/dm}^3 \text{ K}_2\text{Cr}_2\text{O}_7$  after which 20 ml of conc. sulphuric acid was added and the mixture was left for 60 minutes for complete oxidation and cooling. The mixture was diluted with 100 ml of deionized water. Standardized  $0.5 \text{ mol/dm}^3 \text{ FeSO}_4$  was used for titration, with freshly prepared ferroin indicator.

### **Soil fortification and extraction method**

The spectral recordings, performed in quartz cuvettes with path length 10 mm, showed peak at 240 nm for acetamiprid. Aquatic extract of soil showed no pronounced peaks at this wavelength, and therefore was considered non-treated. Amount of 500 g of soil was mixed with standard solution of acetamiprid in water, thoroughly stirred and left in a thin layer for 48 hours till completely dry. Acetamiprid was then extracted from the fortified soil samples using ethanol, 2-propanol and ethyl-acetate (Merck, Germany) in an ultrasonic bath (Vabsonic, Nis, Serbia) for 60 minutes. For blank, a sample of unpolluted soil was subjected to the same extraction procedure with previously mentioned solvents. Aliquots were taken after 10, 20, 30, 40, 50 and 60 minutes and centrifuged at 2000 rpm. Supernatants were passed through columns manually packed with 500 mg of silica gel, since humic substances can be absorbed on silica gel surface [6]. Deionized water was used conditioning (3x5 ml) and for acetamiprid elution (10 ml), due to high solubility of this insecticide in water. The absorbance was measured at 240 nm, on a UniSpec 2 UV-VIS LLG spectrophotometer.

Stock solution of acetamiprid ( $100 \text{ mg/dm}^3$ ) in water was appropriately diluted in order to prepare calibration set of samples with concentrations within the range  $0.05\text{--}20 \text{ mg/dm}^3$ .

## **RESULTS AND DISCUSSION**

Application of ultrasound-assisted extraction is of growing interest in scientific community due to its advantages: low consumption of solvents, shorter extraction time, few low-cost instrumental requirements, and low environmental impact. It is marked as “green chemistry” method [7].

UV spectrum of acetamiprid in water is given in the Figure 1a. Calibration curve (Figure 1b) was linear in the range  $0.05\text{--}20 \text{ mg/dm}^3$  ( $R^2=0.9985$ ). According to Turyin method, organic matter in analysed soil was 1.87%, which multiplied by 1.72 corresponds to 3.22% of humus in soil.

The results of some research indicated that humic-pesticide interactions can influence and alter the toxicity of agricultural chemicals, thus combined antagonistic and synergistic effects were manifested [8].

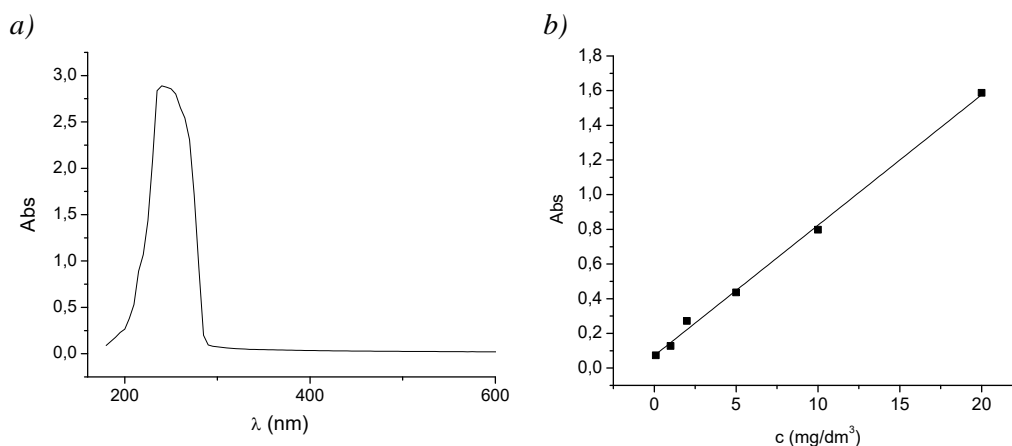


**Figure 1** a) UV/Vis spectrum; b) calibration curve of acetamiprid in water

Efficiency of ultrasound-assisted extraction using methanol, 2-propanol and ethyl acetate is represented in the Figure 2. The solvents were chosen based on the difference in polarity. As it can be seen, the most polar solvent in this group – methanol (relative polarity 0.762) provided the highest recoveries of acetamiprid content in soil over time: 30.04% after 10 minutes and reaching up to 82.45% after 60 minutes of extraction. In the case of 2-propanol (relative polarity 0.546), recoveries were 22.87% after 10 minutes, up to 72.89% after 60 minutes of ultrasound. In the case of the least polar ethyl acetate (relative polarity 0.228) recovery ranged from 19.21% to 54.23%, respectively. Solvents of higher polarity provided higher recoveries. However, it is noticeable that after 40 minutes, a balance is being established, and no significant increase of recovery is being noted with methanol, 2-propanol, nor ethyl acetate.

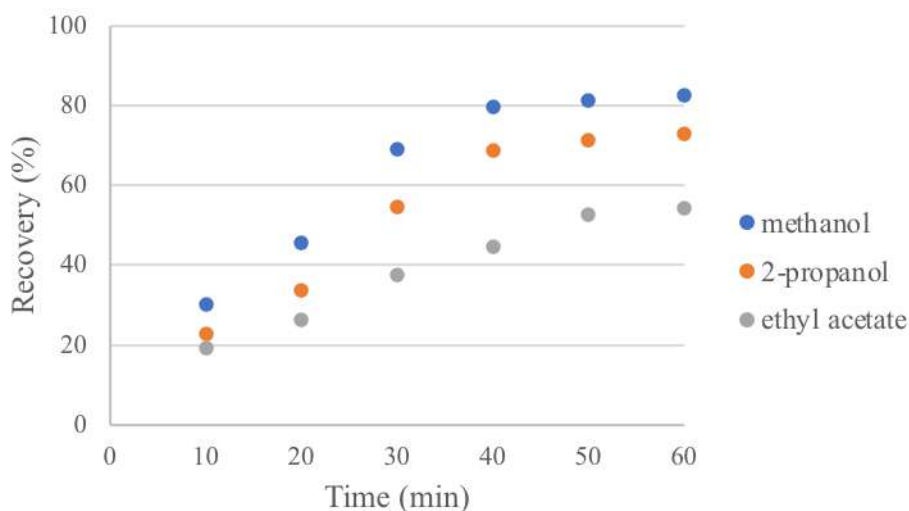


**Figure 2** Efficiency of ultrasound-assisted extraction of acetamiprid using solvents of different polarity



Acetamidrid had a strong negative influence on soil respiration and the enzymatic activities in soil [9]. Therefore, monitoring of its presence in the environment is of great importance.

## **CONCLUSION**

In order to decrease the growing exposure of human population to pollutants in the environment, there is a necessity for continuous screening of soil quality. The presence of all types of pesticides represents a great problem. Since through food chain, pesticides reach into humans, they pose a health risk, especially for vulnerable categories such as infants, children, elderly and chronic patients. Ultrasound-assisted extraction followed by spectrophotometric detection of acetamidrid provided satisfactory results, with low costs, non-demanding instrumentation and usage of ecologically friendly solvents, therefore can be used for fast, preliminary assessment of acetamidrid presence in agricultural soil.

## **REFERENCES**

- [1] Bunemann E., Bongiorno G., Bai Z., *et al.*, *Soil Biol. Biochem.* 120 (2018) 105–125.
- [2] Phogat A., Singh J., Kumar V., *et al.*, *Environ. Chem. Lett.* 20 (2022) 1453–1478.
- [3] Xu M., Huang H., Li N., *et al.*, *J. Ecotoxicol. Environ. Saf.* 175 (2019) 289–298.
- [4] Bonmatin J-M., Mitchel E, Glauser G., *et al.*, *Sci. Total Environ.* 757 (2021) 143822.
- [5] Tuyrin I., *Pochovovedenie* 26 (1931) 36–47.
- [6] Prado A., Miranda B., Dias J., *Colloids Surf. A: Physicochem. Eng. Asp.* 242 (2004) 137–143.
- [7] Carreira-Casais A., Otero P., Garcia-Perez P., *et al.*, *Int. J. Environ. Res. Public Health.* 18 (2021) 9153.
- [8] Benson W., Long S., *Ecotoxicol. Environ. Saf.* 21 (1991) 301–307.
- [9] Yao X.W., Min H., Lu Z., *et al.*, *Eur. J. Soil. Biol.* 42 (2006) 120–126.



## PLANT-MEDIATED SYNTHESIS AND PHOTOCATALYTIC INVESTIGATIONS OF CeO<sub>2</sub>-ZnO COMPOSITES

Katerina Zaharieva<sup>1\*</sup>, Borislav Barbov<sup>1</sup>

<sup>1</sup>Institute of Mineralogy and Crystallography “Akad. I. Kostov”,  
Bulgarian Academy of Sciences, Acad. G. Bonchev St., Block 107, 1113 Sofia, BULGARIA

\*zaharieva@imc.bas.bg

### Abstract

*In the present study the CeO<sub>2</sub>-ZnO composites were synthesized by plant extract – mediated synthesis combining hydrothermal treatment and/or calcination. The phase composition and structure of prepared CeO<sub>2</sub>-ZnO materials was determined by powder X-ray diffraction analysis (PXRD) and Fourier-transform Infrared (FT-IR) spectroscopy. The presence of ZnO and CeO<sub>2</sub> phases was established by PXRD and FT-IR analyses. The photocatalytic ability of prepared CeO<sub>2</sub>-ZnO was investigated in the reaction of degradation of Reactive Black 5 dye (RB5) as a model pollutant in aqueous solutions under UV illumination. Using thermally treated CeO<sub>2</sub>-ZnO material higher degree of degradation of RB5 dye (43%, 180 minutes UV irradiation) was achieved compared to CeO<sub>2</sub>-ZnO synthesized by hydrothermal treatment followed by calcination was used.*

**Keywords:** cerium dioxide-zinc oxide, green synthesis, photocatalytic ability, dye.

### INTRODUCTION

The contamination of aquatic systems with the textile and pharmaceutical wastes from industries is global problem for environmental. Photodegradation of industrial dyes and pharmaceutical wastes using metal oxide nanomaterials is often part of advanced oxidation processes [1]. Green synthesis has attracted the attention of researchers as a reliable, durable, and environmentally friendly method to obtain a wide range of nanomaterials, hybrid materials and biomaterials [2]. ZnO is a semiconductor that performs various functions due to its wide direct energy band gap of 3.37 eV and large exciton binding energy (about 60 meV) [3]. CeO<sub>2</sub> has been considered as an excellent semiconducting photocatalytic material due to its moderate band gap energy of 3.19 eV. By combining the properties of ZnO and CeO<sub>2</sub>, the composite material acts as an excellent photocatalyst because of the increasing charge carrier mobility [4]. The green approach using plant extracts from *Moringa oleifera* LE [1], *Hibiscus Sabdariffa* L. [3], *Glycosmis mauritiana* [5], Fruits of *Acacia Nilotica* [4], hydrothermal method [6,7] and precipitation [8] for preparation of CeO<sub>2</sub>-ZnO nanocomposites are discussed in the literature.

The current investigations deal the green synthesis using plant extract from *Vaccinium vitis-idaea* L., physicochemical characterization and comparative photocatalytic study of CeO<sub>2</sub>-ZnO composite materials for degradation of Reactive Black 5 dye (RB5), as a model pollutant in aqueous solutions, under UV illumination.

## MATERIALS AND METHODS

### Materials

Ce(NO<sub>3</sub>)<sub>3</sub>·6H<sub>2</sub>O (Alfa Aesar), Zn(NO<sub>3</sub>)<sub>2</sub>·6H<sub>2</sub>O (Valerus Co.), NaOH (Valerus Co.) and *Vaccinium vitis-idaea* L. (dried leaves).

### Plant-mediated synthesis of the CeO<sub>2</sub>-ZnO composites

The CeO<sub>2</sub>-ZnO materials were synthesized using 0.09M aqueous solutions of Ce(NO<sub>3</sub>)<sub>3</sub>·6H<sub>2</sub>O (Alfa Aesar) and Zn(NO<sub>3</sub>)<sub>2</sub>·6H<sub>2</sub>O (Valerus Co.) mixed in ratio 1:1 at constant stirring for 10 minutes. The prepared plant extract from *Vaccinium vitis-idaea* L. – 45 ml was added to the mixture of nitrate precursors. The obtained mixture from nitrate precursors and plant extract was stirred for 10 minutes. The precipitant 2M NaOH (Valerus Co.) was added drop by drop in the mixture of aqueous solutions of nitrate precursors and plant extract until pH reached 11 at continuous stirring. After co-precipitation the suspension was stirred for 30 minutes at room temperature and then sealed into autoclave at 180°C for 8 h, followed by natural cooling down to room temperature. The precipitates were filtered and washed with distilled water several times and dried at 50°C. The hydrothermally prepared sample was labelled CeO<sub>2</sub>-ZnO (CZH). After that the calcination at 500°C for 4 hours in air atmosphere was carried out and the obtained material was denoted CeO<sub>2</sub>-ZnO (CZHT). The other CeO<sub>2</sub>-ZnO sample was obtained using the above precipitation procedure and additionally sonicated. The precipitates were filtered and washed with distilled water several times and then dried at 50°C. After that the thermally treatment at 500°C for 4 hours in air media was performed. The prepared material was labelled CeO<sub>2</sub>-ZnO (CZT).

### Physicochemical characterization

The prepared CeO<sub>2</sub>-ZnO samples were characterized by Powder X-ray diffraction (PXRD) analysis and Fourier-transform Infrared spectroscopy (FT-IR). The PXRD analysis was performed on a X-ray powder diffractometer “Empyrean” within the range of 2θ values between 3° and 100° using Cu Kα radiation (λ=0.154060 nm) at 40 kV and 30 mA. The identification of phases was performed through X’pert High Score Plus software. FT-IR spectra were taken on a Bruker Tensor 37 spectrometer in the region 4000–400 cm<sup>-1</sup>, using KBr pellet technique.

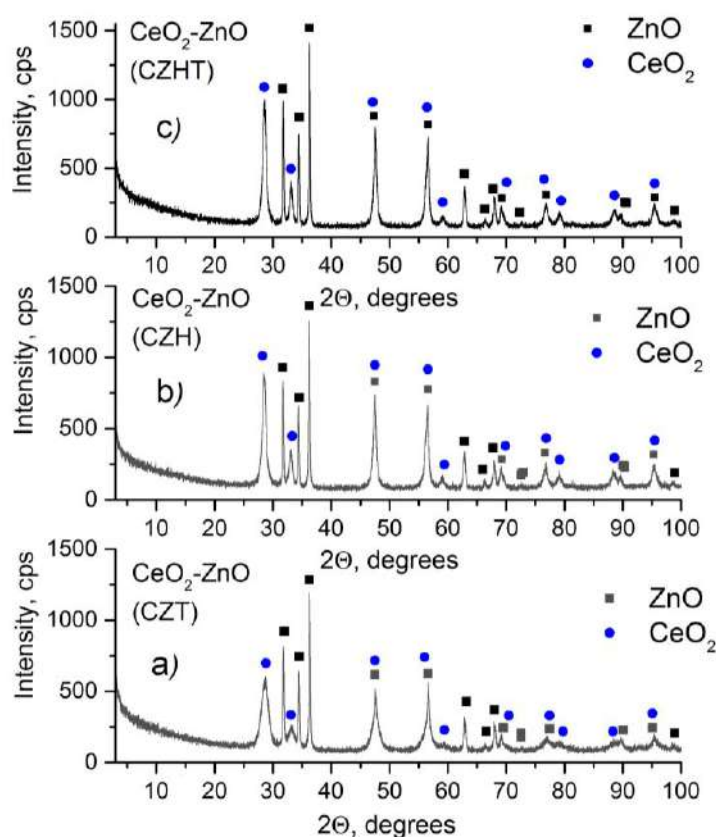
### Photocatalytic tests

The photocatalytic degradation of aqueous solution of Reactive Black 5 dye with concentration of 5 ppm was investigated in semi-batch slurry reactor using synthesized CeO<sub>2</sub>-ZnO composite materials as catalyst and 150 ml of dye solution under constant stirring and air flowing. The photocatalytic tests were carried out using UV–Vis spectrophotometer UV-1600PC in the wavelength range from 200 to 800 nm (λ<sub>max</sub>=599 nm) and a polychromatic UV-A lamp illumination (18 W) with maximum of the emission at 365 nm and intensity of illumination was 0.66 mW/cm<sup>2</sup>. The photocatalytic tests were performed in the presence of 1M HCl acid at pH=3.5. The investigated systems were left in the dark for about 30 min to reach adsorption-desorption equilibrium state before switching on the UV irradiation for 3 hours. The study of the photocatalytic ability of CeO<sub>2</sub>-ZnO samples was performed by taking aliquot parts of the suspension out of the reaction vessel after regular time intervals. The separation of the powder from the suspension was carried out by centrifugation before the

UV–Vis spectrophotometrical absorbance measurements. Thereafter, the separated amount is returned back to the sampling solution and further into the reaction vessel, which ensured operation under constant volume and constant catalyst amount.

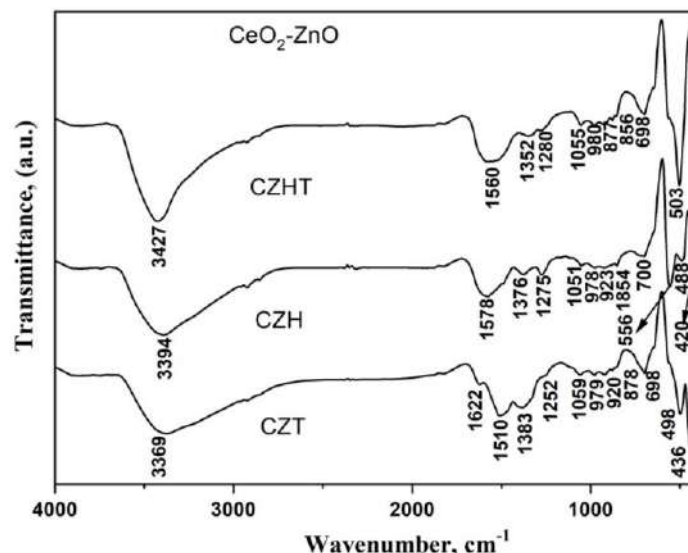
## RESULTS AND DISCUSSION

Figure 1 presents the X-ray diffractograms of prepared  $\text{CeO}_2$ -ZnO materials. The presence of  $\text{CeO}_2$  phase (Ref.Code 01-073-9516) and also ZnO phase (Ref.Code 01-083-6338) are registered in the obtained  $\text{CeO}_2$ -ZnO samples.



**Figure 1** PXR D patterns of green prepared a)  $\text{CeO}_2$ -ZnO (CZT); b)  $\text{CeO}_2$ -ZnO (CZH); c)  $\text{CeO}_2$ -ZnO (CZHT) composites using hydrothermal and/or thermal treatment

The FT-IR spectra of obtained  $\text{CeO}_2$ -ZnO materials in the range of  $4000\text{--}400\text{ cm}^{-1}$  are presented on the Figure 2. The peaks in range of  $556\text{ cm}^{-1}$  to  $420\text{ cm}^{-1}$  resulting from Zn–O and Ce–O bonds [1,3,5]. The other registered bands in the FT-IR spectra of prepared  $\text{CeO}_2$ -ZnO composites could be due to the plant extract used during the synthesis [2,3,5]. The results obtained from Fourier-transform Infrared spectroscopy (FT-IR) are in agreement with Powder X-ray diffraction (PXR D) analysis.



**Figure 2** FT-IR spectra of green synthesized  $\text{CeO}_2\text{-ZnO}$  materials using hydrothermal treatment and/or calcination

Reactive Black 5 is a toxic azo dye that has adverse effects on the health of peoples and the environmental ecosystems [9]. For this reason in the present work was investigated the reaction of photocatalytic degradation of Reactive Black 5 dye using green synthesized  $\text{CeO}_2\text{-ZnO}$  materials as photocatalysts under UV light. Figure 3 shows the concentration ratio  $C/C_0$  of Reactive Black 5 dye as a function of the UV irradiation time. The degree of dye degradation was calculated using the dependence:  $((C_0-C)/C_0) \cdot 100$ , where  $C_0$  and  $C$  were initial concentration before turning on the illumination and residual concentration of the dye solution after illumination for selected time interval.

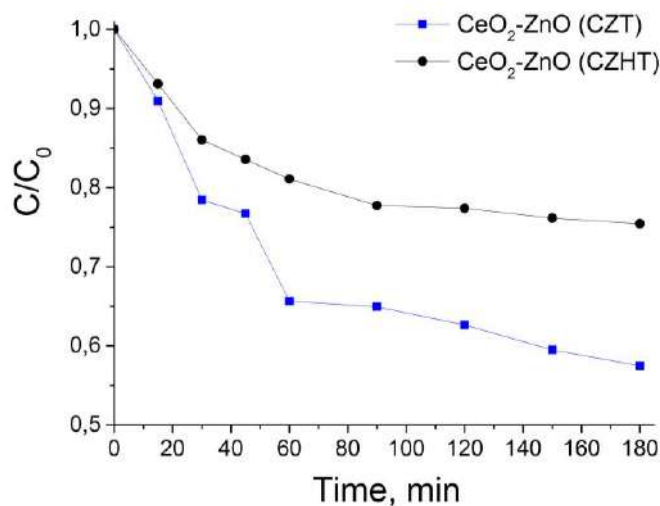


**Figure 3** The concentration ratio  $C/C_0$  of Reactive Black 5 dye with time of UV illumination

The photocatalytic tests determined that green synthesized  $\text{CeO}_2\text{-ZnO}$  material (CZT) demonstrates the higher photocatalytic ability for degradation of RB5 dye (43%) compared to  $\text{CeO}_2\text{-ZnO}$  (CZHT) (25%). The similar results about degradation of Reactive Black 5 dye in

acidic pH region using CeO<sub>2</sub>-ZnO photocatalyst obtained by chemical precipitation were established by Murugesan *et al.* [10]. According to the Pathak *et al.* [11] the photocatalytic efficiency of the CeO<sub>2</sub>-ZnO composites is influenced by the stability of both Ce<sup>3+</sup> and Ce<sup>4+</sup> states. Ce<sup>4+</sup> ions capture photoinduced electrons, transforming into Ce<sup>3+</sup> ions and reducing the recombination of charge carriers. The resulting holes left in the composite material generate highly reactive hydroxyl radicals [11].

## CONCLUSION

The CeO<sub>2</sub>-ZnO composites were successfully prepared by green synthesis in the presence of plant extract from *Vaccinium vitis-idaea* L. and combining hydrothermal and/or thermal treatment. The PXRD analysis and FT-IR spectroscopy confirmed the existence of ZnO and CeO<sub>2</sub> in the CeO<sub>2</sub>-ZnO composites. The thermally treated CeO<sub>2</sub>-ZnO material show higher photocatalytic efficiency to degrade RB5 dye (43% degradation) after 180 min UV illumination in comparison with CeO<sub>2</sub>-ZnO synthesized by hydrothermal treatment and then calcination.

## ACKNOWLEDGEMENT

*The authors express their gratitude to the project with the Bulgarian National Science Fund, Bulgaria, KP-06-N69/8 (KII-06-H69/8), “Novel polymer-hybrid materials containing (bio)synthesized metal oxide particles with improved photocatalytic and antimicrobial potential” for the financial support.*

## REFERENCES

- [1] Iqbal Y., Ahmed S., Hammad Aziz M., *et al.*, Mater. Chem. Phys. 318 (2024) 129299.
- [2] Alarfaj N.A., Alshehri E.M., Al-Tamimi S.A., *et al.*, Heliyon 10 (2024) e26164.
- [3] Shirzad Choubari M., Mazloom J., Esmaeili Ghodsi F., Ceram. Int. 48 (2022) 21344–21354.
- [4] Syed A., Sagar Reddy Yadav L., Bahkali A.H., *et al.*, Crystals 10 (2020) 0817.
- [5] Rosi H., Janci M., Preethi M., Mater. Today Proc. 48 (2022) 561–567.
- [6] Pujar M.S., Hunagund S.M., Khanapure, S., *et al.*, J Sol-Gel Sci Technol 101 (2022) 356–369.
- [7] Simović B., Radovanović Ž., Branković G., *et al.*, Mater. Sci. Semicond. Process. 162 (2023) 107542.
- [8] Lv Z., Zhong Q., Ou M., Appl. Surf. Sci. 376 (2016) 91–96.
- [9] Jalali Sarvestani M.R., Doroudi Z., J. Water Environ. Nanotechnol. 5(2) (2020) 180–190.
- [10] Murugesan S., Sasibabu V., Jegadeesan G.B., *et al.*, Environ. Sci. Pollut. Res. 30 (2023) 42713–42727.
- [11] Pathak V., Lad P., Thakkar A.B., *et al.*, Inorg. Chem. Commun. 159 (2024) 111738.





## CELLULOSE BASED MEMBRANE FOR CATIONIC POLLUTANTS REMOVAL FROM WATER

Milena Milošević<sup>1\*</sup>, Muna Abdualatif Abduarahman<sup>2,3</sup>, Marija M. Vuksanović<sup>4</sup>, Zlate Veličković<sup>5</sup>, Nataša Knežević<sup>4</sup>, Božidar Najdanović<sup>2</sup>, Aleksandar Marinković<sup>2</sup>

<sup>1</sup>University of Belgrade, Institute of Chemistry, Technology and Metallurgy – National Institute of the Republic of Serbia, Njegoševa 12, 11000 Belgrade, SERBIA

<sup>2</sup>University of Belgrade, Faculty of Technology and Metallurgy, Karnegijeva 4, 11000 Belgrade, SERBIA

<sup>3</sup>University of Sabratha, Sabratha, Faculty of Science, QF5G+6FV, Sabratha, LIBYA

<sup>4</sup>University of Belgrade, “VINČA” Institute of Nuclear Sciences – National Institute of the Republic of Serbia, Mike Petrovića Alasa 12–14, 11351 Belgrade, SERBIA

<sup>5</sup>University of Defence, Military Academy, Veljka Lukića Kurjaka 33, 11000 Belgrade, SERBIA

\*milena.milosevic@ihm.bg.ac.rs

### Abstract

*This study focuses on the removal of cation and cationic dye from wastewater by adsorption on a bio-based adsorbent. Cellulose bio-based membrane, CMTA, was obtained by cross-linking of amino-modified cellulose fiber (CF-A) and tartaric acid (TA) using L-lysine as a cross-linker. The properties of the prepared membrane were examined through FTIR and SEM techniques, and pH<sub>pzc</sub> and porosity determination. The effect of pH, initial concentration, temperature, and contact time on the adsorption efficiency was studied in a batch system. Results from the adsorption study proved CMTA adsorbs of Crystal violet (CV) dye and Ni<sup>2+</sup> cation ion with high adsorption capacities of 285.01 mg g<sup>-1</sup> and 54.35 mg g<sup>-1</sup>, respectively, fitted to the Langmuir isotherm. The kinetic study and thermodynamic parameters determination indicate spontaneous and diffusion-controlled processes.*

**Keywords:** bio-based membrane, batch adsorption study, cation and cationic dye, environmental protection.

### INTRODUCTION

Pollution from various industrial sectors (waste water, soil, air), influence sharp increase and disturbs human health and the environmental [1]. Heavy metals, textile dyes, plastics, cosmetics, and rubber are widely used and belong to the group of the most dominant pollutants. Crystal violet (CV) dye has been widely used as a dye in textiles, veterinary medicine, and medical solutions as a mutagenic and bacteriostatic agent, but it has harmful effects due to its carcinogenic and mutagenic nature. They influence the cell division process and cause long-lasting damage to the eyes [2,3]. The heavy metals are toxic, carcinogenic, and not biodegradable. Nickel causes brain and spinal cord damage, and its presence in water and soil has an impact on crop yields and aquatic resources [4].

Among many technologies as filtration, coagulation, oxidation, and sedimentation, adsorption is the most commonly used and effective method. Bio-based adsorbents as membranes are mostly used because they are environmentally acceptable, renewable, and harmless to nature and the living world [3]. Cellulose as a material is a natural, renewable, biodegradable, and non-toxic polymer. Hydroxyl groups in the structure are easily functionalized with other given functional groups, increasing their hydrophilicity, physical stability, and adsorption efficiency.

In the present study, bio-based membrane (CMTA) was prepared, characterized and their examine for effectiveness in the removal of CV and Ni<sup>2+</sup> ions from water solutions. The isotherms, thermodynamics, and kinetics of pollutants removal onto the CMTA were studied.

## MATERIALS AND METHODS

### Materials

All chemicals: Tartaric acid (TA), L-Lysine, *N*'-diisopropylcarbodiimide (DPCA), 4-dimethylaminopyridine (DMAP), dimethyl sulfoxide (DMSO), lithium chloride (LiCl) dimethylformamide (DMF), nickel standard 1000 mg dm<sup>-3</sup> and crystal violet (CV) are of *p.a.* quality, and supplied from Sigma Aldrich. The synthesis of ethyl 4-chloro-4-oxobutanoate (CPC) was performed according to the procedure described previously [5]. Cellulosic material from waste tobacco boxes was provided by Naša Kuća (Belgrade, Serbia). Adjustment of pH was accomplished with 0.1M NaOH and 0.1M HNO<sub>3</sub> (Sigma Aldrich).

### Preparation of membrane

The cellulose based membrane preparation (Figure 1a) was performed by cross-linking of amino functionalized cellulosic fibers with tartaric acid similarly to the procedure given in recent literature [6]. The cellulose fibers (CF) from waste paper was prepared by swelling, using DMSO/LiCl system, and after performing functionalization with CPC and L-Lysine to obtain amino-modified cellulose fiber (CF-A) [7]. In a subsequent step 10 g of CF-A were soaked in 30 mL of tartaric acid (TA) solution (0.2 mol in 20 mL of DMF) and mixed using a planetary stirrer (at 60 rpm) for 5 min. After that 2.5 g of DPCA (0.0156 mol) and 0.25 g of DMAP (10 mol.% with respect to DPCA) were added and continued with mixing for 20 min and then continuously heated at 100°C for 3 h. The obtained material was filtered (to remove excess of DMF), washed with ethanol, and pressed at room temperature between two porous plates (90 μm pore) with a load of 20–30 kN to obtain a membrane CMTA (thickness 4 mm).

### Characterization and adsorption method

The structural and morphological characterization, pHPZC, and porosity were performed using Fourier transform infrared spectroscopy (FTIR) (Nicolet iS10 spectrometer, Thermo Scientific, Sweden, in the transmission mode and range 4000–500 cm<sup>-1</sup>), Scanning Electron Microscopy (SEM) (Tescan Mira3 XMU Field, operated at 20 kV, Czech Republic), pH meter (HI-2210-02 Bench Top, HANNA instruments, Hungary) according to procedure described [7], image analysis (Image-Pro Plus software), and dry-wet weight method [7], respectively. Adsorption of CV dye and Ni<sup>2+</sup> ions was done in a batch system at different temperatures (25°C, 35°C, and 45°C), mixing of 1, 2, 3, 4, 5, 7.5, and 10 mg of CMTA with 10 cm<sup>-3</sup> of solution CV dye (C<sub>i</sub>=20.0 mg dm<sup>-3</sup> and pH 7) and 10 cm<sup>-3</sup> of Ni<sup>2+</sup> ions solution

( $C_i=7.55 \text{ mg dm}^{-3}$  and pH 7). The process of attaining of adsorption equilibrium for dye removal was monitored for 120 min at a wavelength of 590 nm, using the UV-Vis Spectrophotometer 1800 (Shimadzu, Japan). The concentrations of ions  $\text{Ni}^{2+}$  were measured by atomic absorption spectrometry (AAS) using a Perkin Elmer AAnalyst 300 (United States). The adsorption capacity was calculated using the equation given in the work of Muna *et al.* [7].

## RESULTS AND DISCUSSION

The result of the dry-wet weight method and the image analysis (Image-Pro Plus software, Media Cybernetics) revealed that the porosity of the membranes was about 54.8% and had an average pore diameter of about  $4.2 \mu\text{m}$ .

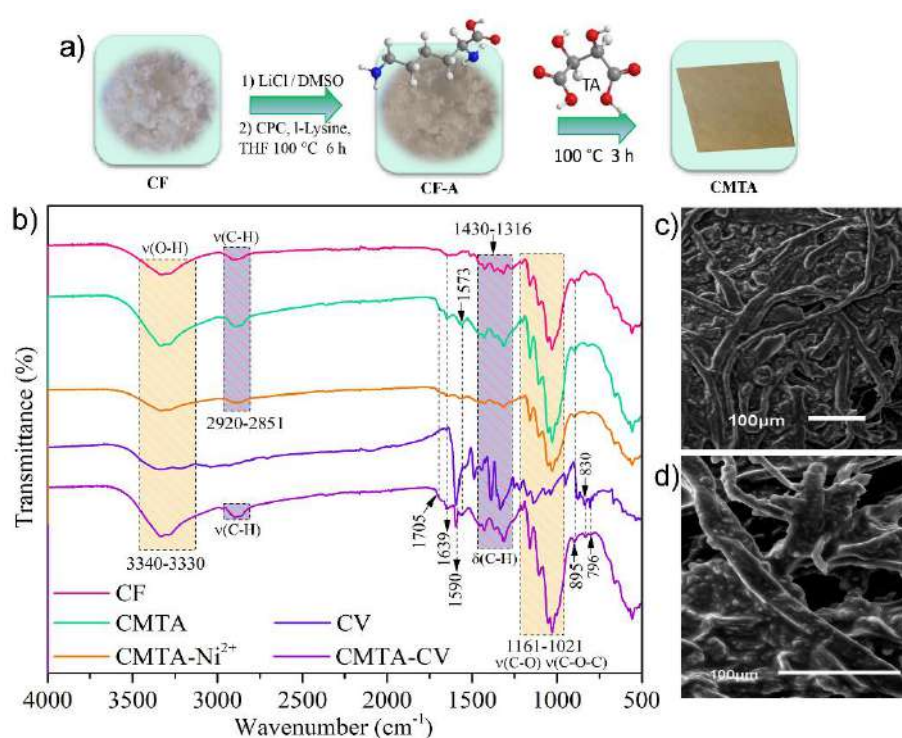


**Figure 1** a) Preparation of CMTA; b) FTIR spectra of membrane before and after adsorption with CV and  $\text{Ni}^{2+}$ ; c) SEM image of CF; d) CMTA

The FTIR spectra, presented in Figure 1b, confirmed successfulness of CMTA membrane preparation. FTIR spectra of CF show characteristic bonds for cellulose. The peaks at  $3340\text{--}3330 \text{ cm}^{-1}$ ,  $1639 \text{ cm}^{-1}$  refer to the stretching vibration and bending vibration of O-H group, respectively, and ones in the range from  $1161$  to  $1021 \text{ cm}^{-1}$  were assigned to asymmetric/symmetric vibrations of C-O, C-O-C groups of polysaccharide structure. Stretching and bending vibration of C-H groups are observed in  $2920\text{--}2851 \text{ cm}^{-1}$  and  $1430\text{--}1316 \text{ cm}^{-1}$  regions. After amino modification with lysine and cross-linking with tartaric acid, obtained CMTA show peaks from cellulose and small peaks at  $1705 \text{ cm}^{-1}$  and  $1573 \text{ cm}^{-1}$  corresponding to overlapped ester, carboxylic and the amide group, respectively, which confirmed successful modification. A new peaks at  $1592$ ,  $830$  and  $796 \text{ cm}^{-1}$  in the spectra

CMTA-CV corresponding to N-H and =CH out-of-plane deformation vibration of the aromatic ring from CV dye. In the spectrum of CMTA-Ni<sup>2+</sup> the decrease of peak intensity, due to electrostatic interaction of Ni<sup>2+</sup> with negative charges at the adsorbent surface, was observed.

SEM images (Figures 1c and 1d) indicate the change of cellulose surface after modification and the surface of obtained membranes gives the adsorbents with a highly porous morphology in relation to unmodified CF.

The determined pHPzc value of CMTA of 6.3 indicate that CMTA has a negative surface at pH > pHPzc which is beneficial condition for effective removal of cationic pollutants. The results of adsorption data fitting, determined using Langmuir adsorption models as described in the recently published work Muna *et al.* [7], are given in Table 1.

**Table 1** Results of Langmuir isotherm models for CV and Ni<sup>2+</sup> ions adsorption onto CMTA

Pollutant	t (°C)	q <sub>m</sub> (mg g <sup>-1</sup> )	K <sub>L</sub> (dm <sup>3</sup> mg <sup>-1</sup> )	R <sup>2</sup>
CV	25	285.01	20.557	0.999
	35	291.90	32.149	0.999
	45	298.84	57.205	0.999
Ni <sup>2+</sup>	25	54.35	7.6984	0.998
	35	56.36	9.5170	0.998
	45	58.39	12.061	0.999

The data from Table 1 show that adsorption capacity (q<sub>e</sub>) and Langmuir constant (K<sub>L</sub>) increases with increasing temperature, indicating a high affinity of CMTA surface sites for cationic pollutants removal.

Results of the adsorption study at 25, 35, and 45°C, fitted using Van't Hoff Equations [7], have been used for calculation of thermodynamic parameters presented in Table 2.

**Table 2** Calculated Gibbs free energy ΔG<sup>⊖</sup>, enthalpy (ΔH<sup>⊖</sup>), and entropy (ΔS<sup>⊖</sup>) for CV and Ni<sup>2+</sup> adsorption onto CMTA

Pollutant	ΔG <sup>⊖</sup> (kJ mol <sup>-1</sup> )			ΔH <sup>⊖</sup> (kJ mol <sup>-1</sup> )	ΔS <sup>⊖</sup> (J mol <sup>-1</sup> K <sup>-1</sup> )	R <sup>2</sup>
	25°C	35°C	45°C			
CV	-49.47	-52.28	-55.50	40.29	300.84	0.99
Ni <sup>2+</sup>	-42.23	-44.19	-46.25	17.69	200.92	0.99

Thermodynamic data indicate feasible and spontaneous adsorption processes with the participation of both physisorption and chemisorption [8], as well as an endothermic nature of the adsorption processes.

Additionally, the results in Table 3 show that the best correlation of experimental data was obtained using the PSO model of the equation. This result indicates that the rate depends on both adsorbate and surface functionalities concentration and diffusion-controlled processes (Table 4).

**Table 3** Pseudo-first, PSO and second-order model parameters for the adsorption of CV and Ni<sup>2+</sup> on CMTA

Pollutant	Model parameters	Pseudo-first	PSO	Second order	$E_a$ (KJ mol <sup>-1</sup> )
CV	$q_e$	76.92	189.98	189.98	9.60
	$k$ ( $k_1, k_2$ )	0.06086	0.00160	0.00568	
	$R^2$	0.994	0.999	0.950	
Ni <sup>2+</sup>	$q_e$	54.11	79.61	79.61	16.37
	$k$ ( $k_1, k_2$ )	0.04823	0.00080	0.00574	
	$R^2$	0.974	0.993	0.949	

**Table 4** Kinetic parameters of the Weber-Morris (W-M), Dunwald-Wagner (D-W), and Homogenous Solid Diffusion Model (HSDM) models for the adsorption of CV and Ni<sup>2+</sup> onto CMTA

Model	Model parameters	CV	Ni <sup>2+</sup>
Weber-Morris (W-M) (Step 1)	$k_{p1}$ (mg g <sup>-1</sup> min <sup>-0.5</sup> )	13.272	12.166
	$C$ (mg g <sup>-1</sup> )	97.89	8.89
	$R^2$	0.995	0.979
Weber-Morris (W-M) (Step 2)	$k_{p2}$ (mg g <sup>-1</sup> min <sup>-0.5</sup> )	0.59651	0.47721
	$C$ (mg g <sup>-1</sup> )	177.06	61.65
	$R^2$	0.997	0.997
Dunwald-Wagner (D-W)	$K \times 10^{-2}$	2.4972	1.3937
	$R^2$	0.938	0.921
Homogenous Solid Diffusion Model (HSDM)	$Ds \times 10^{-11}$	2.71	1.83
	$R^2$	0.933	0.894

## CONCLUSION

The aim of the present study was focused on development of a new bio-based membrane (CMTA), characterization and investigation of its adsorption efficiency. The adsorptive potential was studied concerning Ni<sup>2+</sup> and CV dye removal in the batch system. Thermodynamic parameters indicate the spontaneous and endothermic character, while kinetic data confirmed participation of both adsorbate and membrane surface functionalities in an adsorption step. Diffusional models indicate that intra-particle diffusion govern overall process.

## ACKNOWLEDGEMENT

This work was supported by the Ministry of Science, Technological Development and Innovation of the Republic of Serbia (Contract No. 451-03-66/2024-03/200026, 451-03-65/2024-03/200135, and 451-03-66/2024-03/200017) and the University of Defense, Project No. VA TT/1/22-24.

## REFERENCES

- [1] Sahnoun S., Boutahala M., *et al.*, CR CHIM 21 (2018) 391–398.
- [2] Sultana S., Islam K., *et al.*, Environ. Nanotechnol. Monit. Manag. 17 (2022) 100651.
- [3] Sen N., Shefa N.R., *et al.*, Sci. Rep.14 (2024) 5349.
- [4] Lan J., Ren Y., *et al.*, J. Chem. Eng. 359 (2019) 1139–1149.

- [5] Liu S., Yu C., *et al.*, J. Plant Growth Regul. 37 (2018) 166–173.
- [6] Knežević N., Milanovic J., *et al.*, J. Ind. Eng. Chem. 126 (2023) 520–536.
- [7] Abdurahman M.A., Vuksanović M.M., Milošević M., *et al.*, J Polym Environ. (2024)  
*Available on the following link:* <https://doi.org/10.1007/s10924-024-03192-x>.
- [8] Vuković G.D., Marinković A.D., *et al.*, J. Chem. Eng. 157 (2010) 238–248.





## HEMP MODIFIED WITH BETAINE AS A GREEN AND EFFICIENT ADSORBENT FOR REMOVAL OF ANIONIC DYES FROM WATER

Milena Milošević<sup>1\*</sup>, Aleksandar Marinković<sup>2</sup>, Marija M. Vuksanović<sup>3</sup>, Zlate Veličković<sup>4</sup>,  
Ivan Đuričković<sup>2</sup>, Božidar Najdanović<sup>2</sup>, Nataša Knežević<sup>3</sup>

<sup>1</sup>University of Belgrade, Institute of Chemistry, Technology and Metallurgy - National Institute of the Republic of Serbia, Njegoševa 12, 11000 Belgrade, SERBIA

<sup>2</sup>University of Belgrade, Faculty of Technology and Metallurgy, Karnegijeva 4, 11000 Belgrade, SERBIA

<sup>3</sup>University of Belgrade, “VINČA” Institute of Nuclear Sciences - National Institute of the Republic of Serbia, Mike Petrovića Alasa 12–14, 11351 Belgrade, SERBIA

<sup>4</sup>University of Defence, Military Academy, Veljka Lukića Kurjaka 33, 11000 Belgrade, SERBIA

\*milena.milosevic@ihm.bg.ac.rs

### Abstract

*In this work, natural lignocellulosic material, hemp fiber (HF), was functionalized with betaine and then cross-linking with tartaric acid to produce membrane (MHB-TA) effective in a two anionic dyes removal, Acid Blue 92 (AB92) and Congo Red (CR), from water. The obtained MHB-TA was structurally and morphologically characterized using FTIR and SEM analysis. The effects of initial dye concentration, pH, contact time, and temperature of anionic dyes on adsorption were studied in adsorption experiments performed by batch systems. The calculated maximum adsorption capacities of 352.27 mg g<sup>-1</sup> and 382.63 mg g<sup>-1</sup> for AB92 and CR, respectively, were obtained from Langmuir model fitting at 25°C. The calculated thermodynamic parameters indicate that the process is spontaneous and endothermic with participation of both physisorption and chemisorption processes. The kinetic experimental parameters were fitted through a pseudo-second-order model and a Weber–Morris model. The results present the high applicability of MHB-TA for wastewater purification.*

**Keywords:** Hemp fiber, batch adsorption study, Acid blue 92, Congo red, green adsorbent.

### INTRODUCTION

Synthetic organic dyes are widely used in industries, textile, paper, printing, cosmetics, and plastics [1,2]. Dyes cause pollution from effluents which disturb human health and ecological equilibrium. The purification of wastewater containing organic dyes is necessary before its discharge into surface waters, considering both the environmental and health effects, as these dyes can be toxic and potentially carcinogenic [3].

There are different physicochemical processes for the removal of dyes from wastewater but adsorption is widely used as an attractive and promising method due to low cost, high efficiency, and ability of the adsorbent regeneration [4,5]. Interest for the development of

biopolymer-based adsorbents for the adsorption of synthetic organic dyes has been seen due to their abundance and eco-friendliness [4,5].

Lignocellulose material contains the cellulose, lignin and hemicellulose natural biodegradable polymers with a main renewable source of aromatic structures, polyphenol/hydroxyl, carboxyl and other chemical functionality it has a high capacity to adsorb organic/inorganic pollutants, e.g. dyes and pharmaceuticals and heavy metal ions [4,5].

In the present work, natural biodegradable hemp fibers were modified with betaine and then cross-linked with tartaric acid to obtain a membrane (MHB-TA). The MHB-TA was characterized and used as an adsorbent for the removal of anionic dyes from aqueous solutions. The isotherms, thermodynamics, and kinetics of pollutant adsorption onto the MHB-TA adsorbent were studied.

## MATERIALS AND METHODS

### Materials

Waste hemp fibers were obtained from ITES Odžaci, Serbia. Tartaric acid (TA), Betaine (BE), dimethylformamide (DMF), dimethyl sulfoxide (DMSO), tetrabutylammonium hydroxide (TBAOH), 2-pyrrolidone, Acid blue 92 (AB92) and Congo red (CR) were obtained from Sigma Aldrich. Adjustment of pH was accomplished with 0.1M NaOH and 0.1M HNO<sub>3</sub> (Sigma Aldrich). All used chemicals are of *p.a.* quality.

### Preparation of adsorbent

Before the cross-linking reaction with tartaric acid, the raw hemp fibers (HF) were subjected to defibrillation using DMSO/TBAOH system. After extensive washing 10 g of this sample was mixed with 2 g of betaine dissolved in 50 mL of 2-pyrrolidone, and heated at 80°C for 4 h to obtain cationic modified fibers (HFBE) [6]. After cooling to room temperature and washing with ethanol, obtained HFBE material is treated with 250 mL of tartaric acid solution (0.2 mol in 20 mL DMF) by cross-linking reaction according to the procedure given in recent literature [7]. The obtained material was filtered (to remove excess DMF), pressed at room temperature between porous plates (0.2 mm pore) with a load of 20–30 kN and then reheated at 100°C for 4 h to obtain a compact material MHB-TA (thickness 4 mm). The modification path applied for HF fibers production is shown in Figure 1.

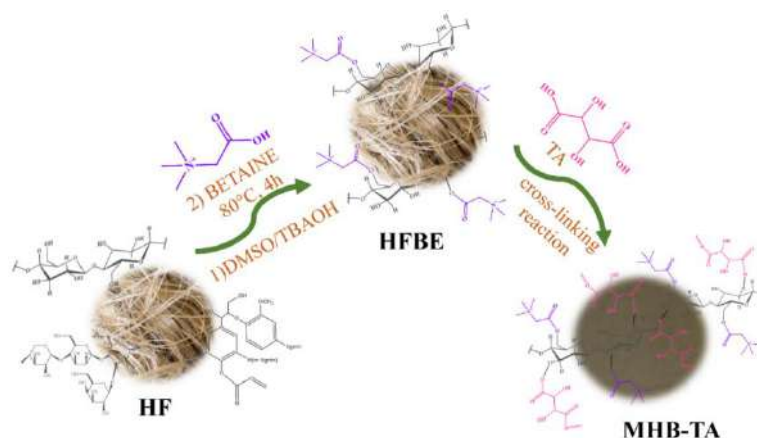


Figure 1 Preparation of MHB-TA adsorbent

### **Characterization of adsorbent**

Fourier-transform infrared (FTIR) (Nicolet iS10 spectrometer, Thermo Scientific, United States, in the transmission mode and range 4000–500  $\text{cm}^{-1}$ ), Scanning Electron Microscopy (SEM) (Tescan Mira3 XMU Field, operated at 20 kV, Czech Republic), used for determination of structural and morphological characterization, respectively.  $\text{pH}_{\text{PZC}}$  was performed using pH meter (HI-2210-02 Bench Top, HANNA instruments, Hungary) according to the procedure described [7], while image analysis (Image-Pro Plus software) and dry-wet weight method [7] were used for the determination of textural properties. The chloride group are the determination by titration with 0.02  $\text{mol L}^{-1}$   $\text{AgNO}_3$ , using 100  $\text{g L}^{-1}$   $\text{K}_2\text{CrO}_4$  as the indicator (Mohr's method). The nitrogen content (Nc) is determined by the Kjeldahl method in according to ASTM D3590-17. The standard test method for ester value (EV) covers the determination of the ester value of solvents and thinners in lacquers and other coatings. The EV was evaluated according to ASTM D1617-07 (Reapproved in 2012).

### **Batch adsorption methods**

Adsorption experiments were performed at different temperatures (25°C, 35°C, and 45°C), mixing 1, 2, 3, 4, 5, 7.5 or 10 mg of adsorbents with 15  $\text{cm}^3$  of AB92 and CR dyes solution ( $C_i=20.0 \text{ mg dm}^{-3}$ ) at  $\text{pH}=7$ . Thermodynamic parameters were evaluated from adsorption data at three temperatures (25°C, 35°C and 45°C). The adsorption kinetics were studied by varying the contact time in the range 5–60 minutes at  $C_i=20.0 \text{ mg dm}^{-3}$  of both dyes and 25°C, 35°C, and 45°C. The concentrations of AB92 and CR dyes were determined at a wavelength of 498 and 575 nm, using UV-Vis Spectrophotometer (1800 Shimadzu, Japan). The methodology applied for calculation adsorption performances is given in recently published work [7].

## **RESULTS AND DISCUSSION**

The result of the textural properties of MHB-TA revealed that the membrane porosity was 67.9% and an average pore diameter of 5.1  $\mu\text{m}$ , determined using image analysis and dry-wet weight method [7]. The  $\text{pH}_{\text{pzc}}$  value of MHB-TA is 7.6, indicate that surface of the obtained membrane is positive at  $\text{pH}<\text{pH}_{\text{pzc}}$ . Nitrogen and ester groups content in the unmodified HF, determined using volumetric methods [7], are as follow: 0.89  $\text{mg g}^{-1}$  and 12.1  $\text{mg KOH g}^{-1}$ , respectively. After modification with betaine and tartaric acid significant increase of these parameters, due to performed modification, was observed: 45.7  $\text{mg g}^{-1}$  of chloride ions, 17.7  $\text{mg g}^{-1}$  of nitrogen and 106.1  $\text{mg KOH g}^{-1}$  of ester groups.

SEM micrographs (Figures 2a and 2b) show the change of active fibers surface and porous morphology with larger number active sites available for pollutant binding in relation to unmodified HF, as presented by determination nitrogen and chloride content.

FTIR technique (Figure 2c) was used for analysis of the surface functionalities before and after adsorption. Spectra of HF and MHB-TA before and after dye adsorption show a broad absorption band in region 3463–3275 $\text{cm}^{-1}$  due to OH-groups. Other peaks are assigned to ester stretching vibration (1715  $\text{cm}^{-1}$ ), O-H bending (1635  $\text{cm}^{-1}$ ), C–H stretching and bending (2917–2850  $\text{cm}^{-1}$  and 1470–1317  $\text{cm}^{-1}$ , respectively), C-O/C-O-C stretching (1250–1024  $\text{cm}^{-1}$ ) in both HF and MHB-TA material. From the spectra of MHB-TA after dyes adsorption, significant amount of both dyes adsorbed, which are deduced from =CH out-of-plane deformations vibration observed in 830–500  $\text{cm}^{-1}$  region (Figure 2c).

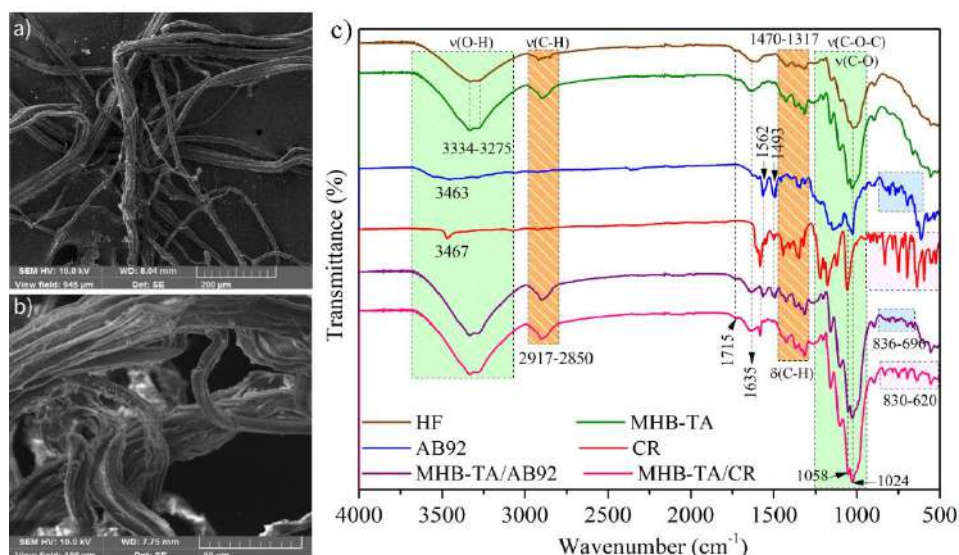


**Figure 2** SEM image of a) HF; b) MHB-TA; c) FTIR spectra of MHB-TA before and after adsorption with AB92 and CR

### Adsorption, kinetic and thermodynamic study

The adsorption experiment was used for calculation of adsorption isotherm data, i.e., capacity determination using the Langmuir equation, as described in the recent work [7]. The results are given in Table 1, at three temperatures.

**Table 1** Results of Langmuir isotherm models for AB92 and CR dyes adsorption onto MHB-TA

Pollutant	t (°C)	$q_m$ (mg g <sup>-1</sup> )	$K_L$ (dm <sup>3</sup> mg <sup>-1</sup> )	$R^2$
AB92	25	352.3	2.027	0.969
	35	354.6	2.169	0.972
	45	358.1	2.322	0.975
CR	25	382.6	1.915	0.957
	35	387.1	1.997	0.949
	45	390.7	2.096	0.938

Results in Table 1 show the high adsorptive capacity of the MHB-TA membrane. Maximum adsorption capacity slightly increases with temperature increase, changing from 352.3 mg g<sup>-1</sup> to 358.1 mg g<sup>-1</sup> and from 382.6 mg g<sup>-1</sup> to 390.7 mg g<sup>-1</sup> for AB92 and CR dyes, respectively.

Gibbs free energy ( $\Delta G^\ominus$ ), enthalpy ( $\Delta H^\ominus$ ), and entropy ( $\Delta S^\ominus$ ), fitted using Van't Hoff Equations [7], were used for the analysis of a thermodynamic aspect of the adsorption process. The calculated thermodynamic parameters are given in Table 2.

The negative values of Gibbs free energy indicate spontaneous adsorption processes with the participation of both physisorption and chemisorption [8], and the enthalpy values reflect an endothermic process.

**Table 2** Calculated Gibbs free energy, enthalpy and entropy for AB92 and CR adsorption onto MHB-TA

Pollutant	$\Delta G^\ominus$ (kJ mol <sup>-1</sup> )			$\Delta H^\ominus$ (kJ mol <sup>-1</sup> )	$\Delta S^\ominus$ (J mol <sup>-1</sup> K <sup>-1</sup> )	$R^2$
	25 °C	35 °C	45 °C			
AB92	-44.90	-46.57	-48.27	5.35	168.52	0.999
CR	-44.92	-46.53	-48.17	3.55	162.55	0.996

For determination of the adsorption rates of AB92 and CR dye removal onto MHB-TA, the experimental data were modelled using pseudo-first-order (Lagergren), pseudo-second-order (PSO), and second-order kinetic equations, as presented in the work by Knežević *et al.* [7]. The obtained results, shown in Table 3, indicate that the best correlation was obtained using a non-linear fitting with the PSO equation. The evaluation of the rate-limiting step of overall process was based on the results of kinetic data modelling using Weber–Morris (W–M), Dunwald–Wagner (D–W), and Homogenous Solid Diffusion (HSDM) evaluation, described in recent work [7]. This result indicates that the rate depends on both adsorbate and surface functionalities concentrations with a diffusional process as a rate control step.

**Table 3** Pseudo-first, PSO, and second order model parameters for the adsorption of AB92 and CR adsorption onto MHB-TA

Pollutant	Model parameter	Pseudo-first	PSO	Second order	$E_a$ (KJ mol <sup>-1</sup> )
AB92	$q_e$	66.11	157.14	157.14	6.39
	$k$ ( $k_1, k_2$ )	0.10318	0.00191	0.00984	
	$R^2$	0.874	0.998	0.796	
CR	$q_e$	81.52	157.94	157.94	2.79
	$k$ ( $k_1, k_2$ )	0.12107	0.00231	0.01256	
	$R^2$	0.959	0.999	0.819	

**Table 4** Kinetic parameters of the W-M, D-W, and HSDM models for the adsorption of AB92 and CR adsorption onto MHB-TA

Model	Model parameters	AB92	CR
Weber-Morris (W-M) (Step 1)	$k_{p1}$ (mg g <sup>-1</sup> min <sup>-0.5</sup> )	19.7496	17.1628
	$C$ (mg g <sup>-1</sup> )	47.48	62.57
	$R^2$	0.968	0.974
Weber-Morris (W-M) (Step 2)	$k_{p2}$ (mg g <sup>-1</sup> min <sup>-0.5</sup> )	0.14071	0.28141
	$C$ (mg g <sup>-1</sup> )	145.78	147.33
	$R^2$	0.997	0.998
Dunwald-Wagner (D-W)	$K \cdot 10^{-2}$	3.1012	3.265
	$R^2$	0.754	0.769
Homogenous Solid Diffusion Model (HSDM)	$D_s \cdot 10^{-11}$	3.47	3.59
	$R^2$	0.744	0.760

## CONCLUSION

In this work, the prepared MHB-TA membrane proved to be an effective adsorbent in the removal of anionic dyes from water. The high adsorption capacities, obtained using Langmuir model fitting and kinetic data, indicate the high performance of MHB-TA. The experimental

data fitted using the W-M, D-W, and HSDM models show that intra-particle diffusion is a rate-controlling process. Finally, the obtained results showed that the prepared bio-based MHB-TA membrane represent a good candidate to be considered for application in a real system for the water purification process.

### **ACKNOWLEDGEMENT**

*This work was supported by the Ministry of Science, Technological Development and Innovation of the Republic of Serbia (Contract Nos. 451-03-66/2024-03/200017, 451-03-65/2024-03/200135, and 451-03-66/2024-03/200026,) and the University of Defence, Project No. VA TT/1/22-24.*

### **REFERENCES**

- [1] Alothman Z.A., *et al.*, Food Chem. Toxicol. 50 (2012) 2709–2713.
- [2] Sahnoun S., Boutahala M., *et al.*, C. R. Chim. 21 (3–4) (2018) 391–398.
- [3] Wawrzekiewicz M., Podko B., *et al.*, Ind. Crops. Prod. 180 (2022) 114785.
- [4] Popovic A.L., Rusmirovic J. D., *et al.*, Int. J. Biol. Macromol. 156 (2020) 1160–1173.
- [5] Taleb K.A., Rusmirović J. D., *et al.*, J. Serb. Chem. Soc. 81 (2016) 1199–1213.
- [6] Liang Y., Duan W., *et al.*, Bioresour. Technol. 310 (2020) 123389.
- [7] Knežević N., Milanovic J., *et al.*, J. Ind. Eng. Chem. 126 (2023) 520–536.
- [8] Vuković G.D., Marinković A.D., *et al.*, J. Chem. Eng. 157 (2010) 238–248.





## PHENOL REMOVAL FROM WASTEWATER WITH HORSERADISH PEROXIDASE IMMOBILIZED BY PERIODATE METHOD ONTO NOVEL MACROPOROUS POLY(GMA-CO-EGDMA) CARRIERS

Nevena Surudžić<sup>1\*</sup>, Milica Spasojević<sup>2</sup>, Milica Crnoglavac Popović<sup>3</sup>, Marija Stanišić<sup>3</sup>,  
Radivoje Prodanović<sup>3</sup>, Olivera Prodanović<sup>1</sup>

<sup>1</sup>University of Belgrade-Institute for Multidisciplinary Research, Kneza Viseslava 1,  
11030 Belgrade, SERBIA

<sup>2</sup>University of Belgrade-Innovative Centre of the Faculty of Chemistry, Studentski trg 12–16,  
11000 Belgrade, SERBIA

<sup>3</sup>University of Belgrade-Faculty of Chemistry, Studentski trg 12–16,  
11000 Belgrade, SERBIA

\*nevena.pantic@imsi.rs

### Abstract

*One of the most important environmental problems that need to be addressed is wastewater contamination. Numerous researches have focused on solving the aforementioned problem by applying immobilized enzymes. When horseradish peroxidase, the most commonly used enzyme, is immobilized by one of many available methods on a suitable support, a biocatalyst with improved properties in terms of increased stability and reusability, is obtained. Dispersion polymerization was used for the synthesis of macroporous poly(GMA-co-EGDMA) copolymers with different pore size diameters. Prior to immobilization of HRP onto these carriers, their amination with ethylenediamine was performed. Periodate method was applied for the formation of covalent bond between the enzyme and used copolymer. Increase in specific activity of immobilized peroxidase was noticed. The copolymer with the pore size diameter of 297 nm showed the highest activity.*

**Keywords:** peroxidase, macroporous copolymer, periodate, immobilization.

### INTRODUCTION

Continuous industrialization and urbanization lead to the appearance of new and increasement of already existing environmental problems. Unfortunately, different forms of pollution have the greatest impact on water courses worldwide.

Removal of phenol and phenolic compounds [1,2] and decolorization of textile dyes [3] from waste streams are two greatest environmental problems the broad scientific community is aiming to address.

Wide range of enzymes immobilized on various carriers are frequently used for these purposes. By attaching the enzyme to a solid support, its increased stability was first noticed, and as a result good reusability and recovery also stood out [4]. Among widely available plant enzymes, horseradish peroxidase (HRP) occupied a special place and became one of the most commonly used peroxidases for these purposes [1]. Many methods can be applied for its immobilization, and just some of them are: adsorption, covalent binding, cross-linking and

entrapment. Strong linkage between the enzyme and carrier is achieved by applying one of the most used methods, covalent binding. This prevents enzyme leakage from carrier's surface, but at the same time increases the enzyme stability and improves its stereospecificity [5].

Natural polymers such as alginate, pectin, chitosan, magnetic-beads [1,2,6–8], polyacrylamide gels [9] and silica [10] are just some of the carriers that can be used for immobilization. However, synthetic polymers can be placed at the very top of a long list of different supports. By carefully choosing the reaction parameters their properties can easily be tailored during the synthesis process. Macroporous copolymers composed of glycidyl methacrylate (GMA) and ethylene glycol dimethacrylate (EGDMA) can be applied for enzyme immobilization [11]. These polymers have an allyl glycidyl (epoxide) groups that can be easily transformed into amino, keto, carboxyl or hydroxyl groups, thus facilitating the interaction with enzymes. One of the most important parameters that directly affects the activity and stability of immobilized enzyme is the porosity of macroporous carriers. It is, therefore, of utmost importance to control parameters that affect it. This will ultimately result in carriers with satisfactory properties that can be further applied in immobilization reactions, and subsequently in phenolic compounds removal.

## **MATERIALS AND METHODS**

### **Materials**

Chemicals used for copolymer synthesis and immobilization: glycidyl methacrylate (GMA), ethylene glycol dimethacrylate (EGDMA), 1-dodecanol, cyclohexanol, horseradish peroxidase (150–250 U/mg), pyrogallol used as a substrate for peroxidase oxidation reaction, and sodium periodate, were purchased from Sigma Aldrich (St. Louise, Mo, USA). Ethylenediamine, used for amination of copolymer samples, was obtained from Merck (Kenilworth, New Jersey, USA), while hydrogen peroxide was purchased from AppliChem GmbH (Darmstadt, Germany).

### **Copolymer Preparation and Amination**

A continuous phase consisting of 2.78 wt% PVP ( $M_w=24\ 000$  g/mol) in ethanol was heated to 70°C. A monomer phase (5.0 g of both the monomer GMA and cross-linking agent EGDMA (GMA/EGDMA = 60/40)), initiator (0.05 g of AIBN) and inert phase (2.25 g of 1-dodecanol and 2.25 g of cyclohexanol) was added to the continuous phase and stirred for 6 h. Ethanol was used for the rinsing of obtained copolymer (5 times), which was afterwards dried at room temperature. Epoxide groups presented on the surface of copolymer samples were aminated with ethylenediamine, washed first with ethanol and subsequently with water until the pH value of the filtrate was 6. The samples were dried in the oven at 50°C. Concentration of amino groups was calculated by using acidic-basic titration reaction.

### **Copolymer Characterization**

The pore size distributions of the synthesized copolymers poly(GMA-co-EGDMA) were determined by a mercury porosimetry (Carlo Erba 2000, software Milestone 200). Scanning electron microscope (Tescan FE-SEM Mira 3 XMU) was employed to characterize the morphology of poly(GMA-co-EGDMA).

### Horseradish Peroxidase Immobilization by Periodate Method

For the oxidation of horseradish peroxidase sodium periodate solution (50 mmol/L) in sodium acetate buffer pH 5 was used. Oxidized HRP was dialyzed overnight against sodium acetate buffer pH 5. In order for better interaction between enzyme and aminated copolymer, particles were first deaerated in sodium phosphate buffer pH 7 (0.1 mol/L), rinsed with the same buffer and subsequently, incubated with different amounts of oxidized HRP (1, 5, 15 and 25 mg/g) for 48 h. Sodium phosphate buffer pH 7 (0.1 mol/L) was used for the rinsing of copolymers with immobilized enzyme, which were, afterwards, stored in the same buffer at 4°C until further use.

### Enzyme Activity Studies

Pyrogallol and hydrogen peroxide (H<sub>2</sub>O<sub>2</sub>) were used as substrates for the determination of peroxidase activity. In the most common assay, 10 µL of the enzyme dilution from the washings and 10 µL of H<sub>2</sub>O<sub>2</sub> (9.7 mmol/L) were introduced into 1 mL of the pyrogallol solution (13 mmol/L) in sodium phosphate buffer pH 7. Absorbance was measured for 3 min at 420 nm using UV–VIS spectrophotometer (Shimadzu Corporation UV-2501PC, Japan). Nine mg of the copolymer with immobilized HRP and 30 µL of H<sub>2</sub>O<sub>2</sub> were introduced into 3 mL of pyrogallol for measurements of immobilized peroxidase activity. Every 60 s aliquots were taken out from the mixture, filtrated and the absorbance at 420 nm was measured. One unit of enzyme activity was defined as the amount of enzyme that produces 1 mg of purpurogallin in 20 s at 20°C.

## RESULTS AND DISCUSSION

Macroporous poly(GMA-co-EGDMA) copolymers were synthesized by dispersion polymerization reaction which, unlike the frequently used suspension polymerization, leads to the formation of smaller spherical particles (around 1.5 nm in diameter) (Figure 1).

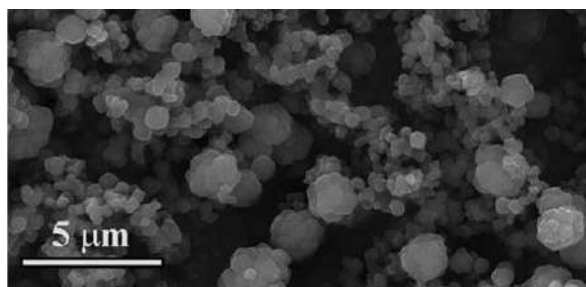


*Figure 1 SEM image of poly(GMA-co-EGDMA) prepared by dispersion polymerization*

Polymers with different average pore size diameters (ZP2, ZP5 and ZP12; 460, 297 and 235 nm) were subjected to amination prior to immobilization reaction. Epoxide groups on the surface of each copolymer was treated with ethylenediamine, which lead to the introduction of amino groups and thus easier immobilization. Concentrations of introduced amino groups were calculated and presented (Figure 2).

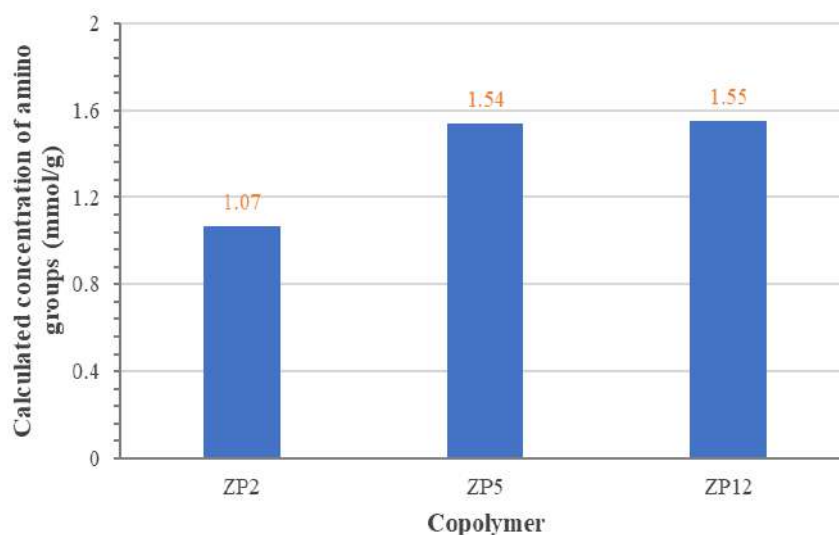


**Figure 2** Concentrations of introduced amino groups on the copolymer samples

Periodate method was used for the immobilization of horseradish peroxidase (HRP). This method leads to the oxidation of multiple carbohydrate moiety on the enzyme, by forming aldehyde groups with higher potential of interaction with macroporous copolymer.

Covalent binding of enzyme to the copolymer surface through carbohydrate moiety is schematically presented in Figure 3.

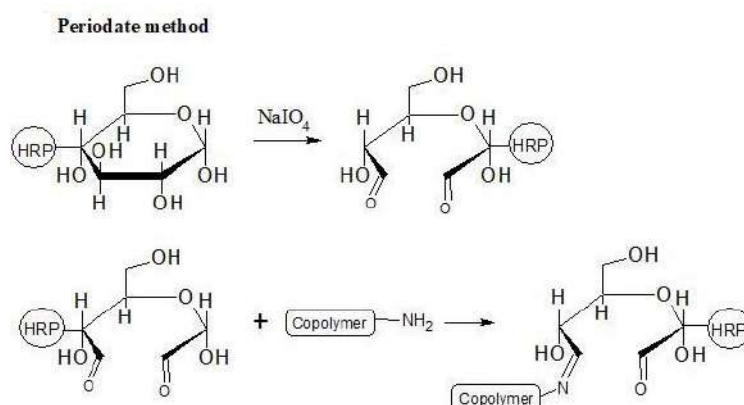


**Figure 3** Schematic presentation of periodate method for enzyme immobilization

When different amounts of HRP were introduced during immobilization and added per gram of copolymer (1, 5, 15 and 25 mg/g), increase in specific activity of immobilized enzyme can be observed (Figure 4).

For each of the copolymer samples used, the rule of increasing specific activity with the amount of added enzyme per gram applies. However, if you look at the values of only one enzyme concentration (e.g. 25 mg/g) for all copolymers, it can be seen that the polymer labeled as ZP5 with the pore size diameter of 297 nm, stands out (Figure 5).

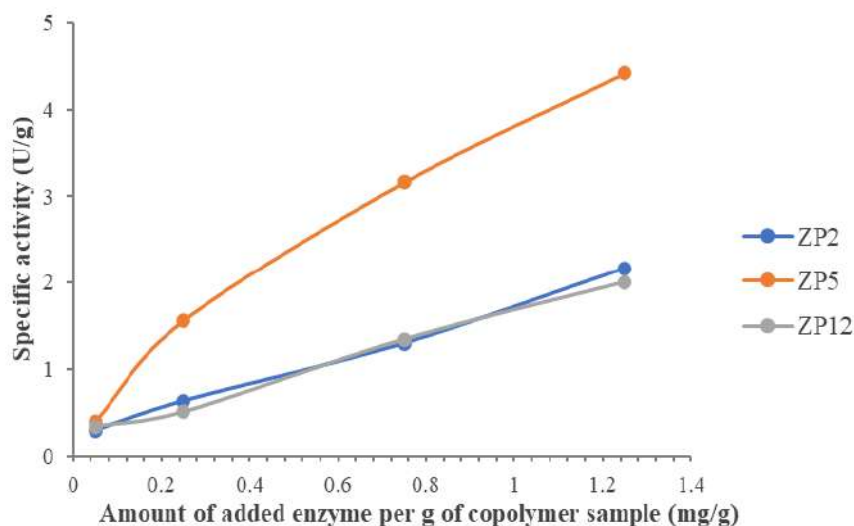


**Figure 4** Effect of the amount of added enzyme on the specific activity of immobilized horseradish peroxidase

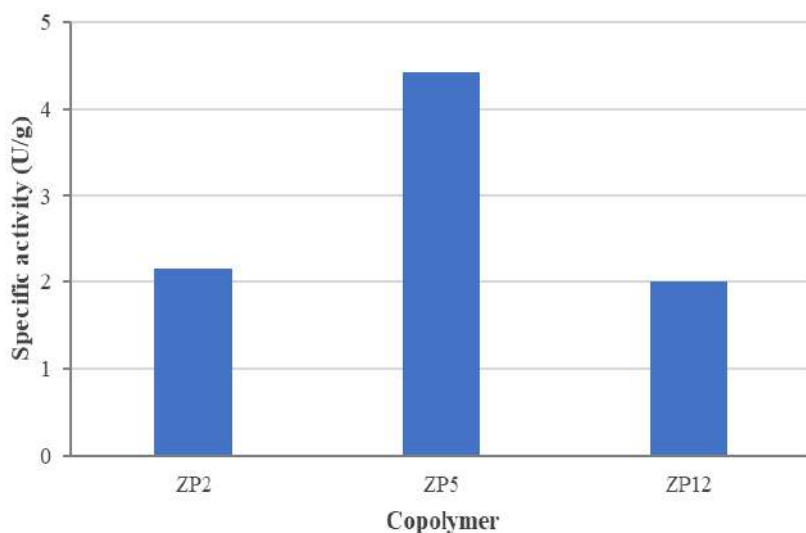


**Figure 5** Specific activities of copolymers with different pore size diameters

Enzyme immobilized on ZP5 copolymer (with pore size diameter of 297 nm) showed specific activity of 4.42 U/g, which is almost two times higher than specific activity of enzymes immobilized on two other copolymer samples (ZP2 and ZP12). From everything presented, the connection between the amount of amino groups on the copolymer with pore size diameter of 297 nm and the specific activity can be observed. The greater the amount of amino groups on the surface of the polymer is, the greater is the activity of the enzyme immobilized on it.

Horseradish peroxidase immobilized onto novel macroporous poly(GMA-co-EGDMA) copolymers with different surface characteristics could be applied for the removal of phenol and phenolic compounds from waste effluents.

## CONCLUSION

Dispersion polymerization was used for the synthesis of macroporous copolymers of glycidyl methacrylate (GMA) and ethylene ethylene glycol dimethacrylate (EGDMA). By involving covalent binding for the immobilization of horseradish peroxidase, periodate method was applied. Increasing the amount of immobilized HRP per gram of the copolymer leads to increase in specific activity. Copolymer with the pore size diameter of 297 nm showed the most promising results. Obtained biocatalyst can be successfully applied in phenol removal studies.

## ACKNOWLEDGEMENT

*This work was supported by the Ministry of Education, Science and Technological Development of the Republic of Serbia (Grant No. 451-03-66/2024-03/200053, University of Belgrade, Institute for Multidisciplinary Research; Grant No. 451-03-47/2023-01/200168, University of Belgrade-Faculty of Chemistry).*

## REFERENCES

- [1] Alemzadeh I.S., Nejati J., Hazard. Mater. 166 (2009) 1082–1086.
- [2] Bayramoglu G., Arica M.Y., J. Hazard. Mater. 156 (2008) 148–155.
- [3] Gholami-Borujeni F., Mahvi A.H., Naseri S., *et al.*, Res. J. Chem. Environ. 15 (2011) 217–222.
- [4] Magnin D., Dumitriu S., Chornet E., J. Bioact. Compat. Polym. 18 (2003) 355–373.
- [5] Fernández-Lorente G., Terreni M., Mateo C., *et al.*, Enzyme Microb. Technol. 28 (2001) 389–396.
- [6] Monier M., Ayad D.M., Wei Y., Sarhan A.A., Int. J. Biol. Macromol. 46 (2010) 324–330.
- [7] Bindhu L.V., Abraham E.T., J. Appl. Polym. Sci. 88 (2003) 1456–1464.
- [8] Prokopijevic M., Prodanovic O., Spasojevic D., *et al.*, Bioprocess Biosyst. Eng. 37 (2014) 799–804.
- [9] Temoçin Z., İnal M., Gökgöz M., *et al.*, Polym. Bull. 75 (2018) 1843–1865.
- [10] Voss R., Brook M.A., Thompson J., *et al.*, J. Mater. Chem. 17 (2007) 4854–4863.
- [11] Pramparo L., Stüber F., Font J., *et al.*, J. Hazard. Mater. 177 (2010) 990–1000.





## MODIFIED ACTIVATED WOOD SAWDUST AS GREEN ENVIRONMENTAL-FRIENDLY CATALYST FOR TREATMENT OF PHARMACEUTICAL EFFLUENT

Miljana Radović Vučić<sup>1</sup>, Nena Velinov<sup>1\*</sup>, Jelena Mitrović<sup>1</sup>, Slobodan Najdanović<sup>1</sup>,  
Milica Petrović<sup>1</sup>, Miloš Kostić<sup>1</sup>, Aleksandar Bojić<sup>1</sup>

<sup>1</sup>The University of Niš, Department of Chemistry, Faculty of Science and Mathematics,  
Višegradska 33, 18 000 Niš, SERBIA

\*[nena.velinov@yahoo.com](mailto:nena.velinov@yahoo.com)

### Abstract

*Photo-Fenton oxidation of Atenolol was carried out using iron(III) impregnated on activated wood sawdust as a heterogeneous catalyst. The catalyst was prepared by the wet impregnation method and characterized. The effectiveness of this catalyst in the degradation of the pharmaceutical, as well as the influence of reaction parameters on the catalytic activity, was discussed. The effects of pH, the initial hydrogen peroxide concentration and the catalyst loading on the oxidative degradation of Atenolol have been assessed. The best degradation efficiency (99.71%) was obtained at temperature = 25°C, pH=3, [H<sub>2</sub>O<sub>2</sub>]<sub>0</sub>=10 mM, catalyst loading = 0.5 g/dm<sup>3</sup> for initial Atenolol concentration of 10 mg/dm<sup>3</sup>.*

**Keywords:** AOPs, photo-Fenton, heterogeneous catalyst, wood sawdust, pharmaceuticals, Atenolol.

### INTRODUCTION

The past two decades have witnessed extensive scientific and public attention towards the presence of pharmaceuticals in the environment, as one of the most important groups of aquatic emerging contaminants (ECs) [1]. Global population growth and urbanization lead to a rise in resource consumption and chemical use, including pharmaceuticals [2]. Pharmaceuticals are continuously entering the environment and show negative impacts due to their persistence and adverse effects on aquatic organisms [3].

The failure of conventional methods to remove pharmaceuticals demonstrates the urgent need to develop suitable innovative technologies for the treatment of hospital effluents and urban wastewater in order to effectively deal with these compounds and minimize undesirable effects in the environment [4,5]. Therefore, advanced oxidation processes (AOPs) have been suggested as tertiary treatment in effluent wastewaters due to their versatility and ability to remove pollutants that are known to be non-biodegradable or have low biodegradability, persistence and possess high chemical stability [4]. AOPs are considered environmental-friendly methods and are based on physicochemical processes that induce decomposition, simplification of the chemical structure of the organic molecules and finally mineralization. These processes involve the generation of reactive transient species such as the hydroxyl (HO<sup>•</sup>), superoxide (O<sub>2</sub><sup>•-</sup>), hydroperoxyl (HO<sub>2</sub><sup>•</sup>), alkoxy (RO<sup>•</sup>), sulfate (SO<sub>4</sub><sup>•-</sup>) and chlorine

(Cl<sup>•</sup>) radicals (depending on the catalyst or the oxidant used), with the HO<sup>•</sup> having attracted the most attention [4]. Hydroxy radicals (HO<sup>•</sup>) are usually generated from reactions involving oxidants such as hydrogen peroxide, ozone or catalysts including metal ions and semiconductors under UV–vis irradiation or other sources of energy [5]. These species present high oxidation potential with a non-selective nature and high reaction rate, achieving the complete mineralization of the pollutants to CO<sub>2</sub>, water, and mineral acids or under selected conditions, transforming them into more biodegradable molecules. Different AOP methods include heterogeneous and homogenous photocatalysis, depending on the catalyst phase.

In view of the above, the objectives of this study were to evaluate the effectiveness of the oxidative degradation and mineralization of Atenolol in aqueous solutions using wood sawdust, as a catalytic material in a modified heterogeneous Fenton process, and to evaluate the influence of operative conditions on pharmaceuticals degradation.

## **MATERIALS AND METHODS**

### **Reagents**

Atenolol was obtained from Sigma-Aldrich (USA) and used without any purification. The hydrogen peroxide (H<sub>2</sub>O<sub>2</sub>) solution (30.0%), Fe(NO<sub>3</sub>)<sub>3</sub>·9H<sub>2</sub>O were of analytical grade and purchased from Merck (Germany).

### **Catalyst preparation**

As the basic lignocellulose raw material for obtaining the catalyst, wood sawdust was used, which was taken from the local furniture industry. The catalyst was prepared by impregnating the metal on activated wood sawdust. A certain amount of material was added to an aqueous solution of Fe(NO<sub>3</sub>)<sub>3</sub>·9H<sub>2</sub>O with stirring and maintaining the temperature at 100°C until the water evaporated. After washing the material with deionized water and drying at 100 degrees, the material used in the experiments was obtained and named wood sawdust-iron catalyst (WS-Fe).

### **Photoreactor**

Photochemical experiments were carried out in a batch photoreactor handmade in our laboratory. The UV lamps were turned on 10 min before performing each experiment. The intensity of UV radiation was measured by UV radiometer Solarmeter model 8.0 UVC (Solartech, USA). The total UV intensity was controlled by turning on different numbers of UV lamps and the maximum intensity was 1950 μW cm<sup>-2</sup> (with all ten UV lamps on) at a distance of 220 mm, from the working solution surface.

### **Procedures**

A stock solution of Atenolol was made by dissolving 0.5 g pharmaceutical in 1000.0 cm<sup>3</sup> of deionized water. Working solutions were prepared freshly, before irradiation, by diluting the stock to the desired concentration with deionized water. The pH of solutions was adjusted by the addition of NaOH and HNO<sub>3</sub> (0.1/0.01 mol dm<sup>-3</sup>) with a pH/ISE meter (Orion Star A214, Thermo Scientific, USA). The suspensions of Atenolol and WS-Fe were magnetically

stirred in the dark for 30 min to attain adsorption-desorption equilibrium, and then the solutions were treated in the UV reactor.

During irradiation, the solution was magnetically stirred (Are, Velp Scientifica, Italy) at a constant rate and temperature was maintained at  $25\pm 0.5^\circ\text{C}$  by thermostating. At required time intervals,  $4.0\text{ cm}^3$  of samples were withdrawn, centrifuged ( $3000\text{ rpm}^{-1}$ , 15 min) and filtered through a  $0.20\text{ }\mu\text{m}$  regenerated cellulose membrane filter (Agilent Technologies, Germany) to separate the catalyst. Absorbance was measured using a UV-vis spectrophotometer Shimadzu UV-1800 PC (Shimadzu, Japan) to determine the degree of degradation. To ensure the accuracy, reliability, and reproducibility of the collected data, all experiments were carried out in triplicate, and mean values were recorded. OriginPro 2016 (OriginLab Corporation) software was used for statistical analysis and calculation of the data.

## RESULTS AND DISCUSSION

### Effect of hydrogen peroxide concentration

The effect of  $\text{H}_2\text{O}_2$  concentration was investigated in an  $\text{H}_2\text{O}_2$  concentration range between 1 and 100 mM; while keeping the temperature, the catalyst loading and pH constant at  $25\pm 0.5^\circ\text{C}$ ,  $0.5\text{ g/dm}^3$  and 3, respectively. In addition to these, an experimental set without the addition of  $\text{H}_2\text{O}_2$  was performed. The results obtained are presented graphically in Figure 1. At very low concentrations of  $\text{H}_2\text{O}_2$  in the solution, approximately no degradation was observed. At higher concentrations (10–50 mM), the degradation efficiency was high. The increase in the degradation was due to the increase in hydroxyl radical concentration by the addition of  $\text{H}_2\text{O}_2$ . However, there was no considerable effect in using a concentration of 10, 30 or 50 mM. At very high concentrations (100 mM), because  $\text{H}_2\text{O}_2$  generates enough  $\cdot\text{OH}$  radicals, the degradation proceeded very fast. The results indicate that the degradation efficiency and rates increase with increasing  $\text{H}_2\text{O}_2$  concentration. Even though  $\text{H}_2\text{O}_2$  plays an important role, it is recommended to select an optimum  $\text{H}_2\text{O}_2$  concentration due to the environmental aspects and the cost of  $\text{H}_2\text{O}_2$  [6].

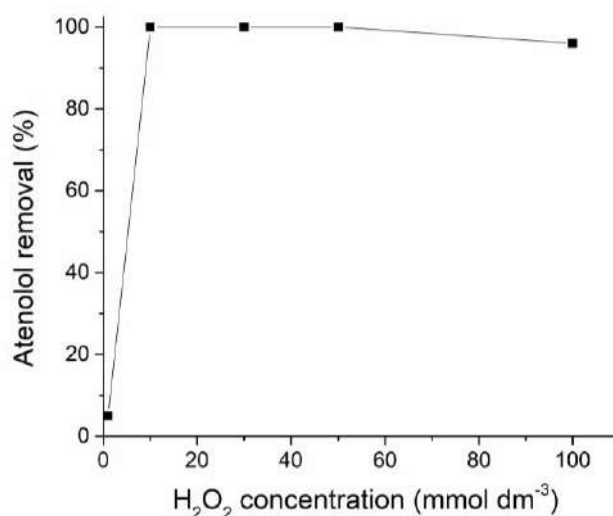


**Figure 1** Effect of  $\text{H}_2\text{O}_2$  concentration on degradation;  
Reaction conditions: catalyst loading =  $0.5\text{ g/dm}^3$ , temperature =  $25^\circ\text{C}$ ,  $\text{pH}=3$

The reason for being an optimum value can be explained as follows: At moderate concentrations, the  $\cdot\text{OH}$  radicals attack the molecules, whereas at high  $\text{H}_2\text{O}_2$  concentrations, the scavenging of  $\cdot\text{OH}$  radicals may occur and hence the degradation may decrease [6]. Therefore, for the effective degradation, 10 mM of  $\text{H}_2\text{O}_2$  concentration was selected as an optimum concentration.

### Effect of catalyst loading

In order to clarify the role of catalyst loading on the degradation of Atenolol by photo-Fenton oxidation, a series of experiments were performed with different catalyst loading values from 0.1 to 2  $\text{g}/\text{dm}^3$  at the fixed concentration of  $\text{H}_2\text{O}_2$ , the temperature and pH at 10 mM,  $25\pm 0.5^\circ\text{C}$  and 3, respectively. Figure 2 shows the effect of catalyst loading on the degradation. The results indicated that the degradation of the Atenolol is remarkably dependent on the catalyst loading parameter.

The low loading value ( $0.1 \text{ g}/\text{dm}^3$ ) had a minor effect on degradation efficiency. Generally, it can be concluded that degradation efficiency and the initial rate increase with increasing catalyst loading but approach a plateau at higher values. In other words, increasing the catalyst loading above  $0.5 \text{ g}/\text{dm}^3$  did not have a considerable effect. Moreover, many studies have revealed that the use of high catalyst loading ( $\text{Fe}^{2+}$  concentrations) favours the formation of the  $\cdot\text{OH}$  radicals, but too high a concentration will consume part of the  $\cdot\text{OH}$  radicals (could lead to the self-scavenging of  $\cdot\text{OH}$  radical by  $\text{Fe}^{2+}$ ) and thus decreases the dye degradation rate [7]. Hence,  $0.5 \text{ g}/\text{dm}^3$  catalyst loading was determined to be the optimum value.

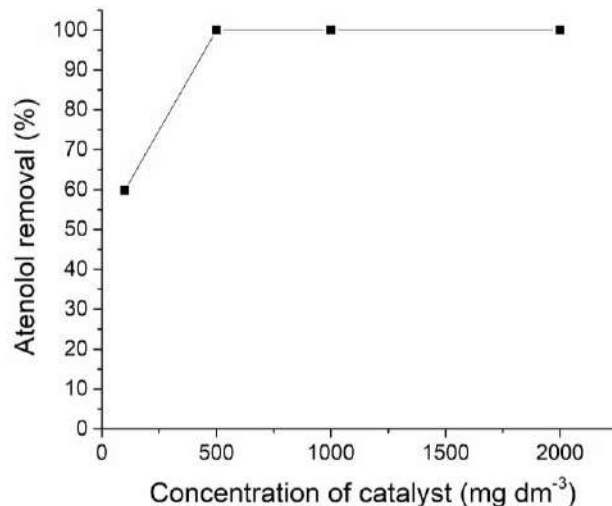


**Figure 2** Effect of catalyst loading on degradation;  
Reaction conditions:  $[\text{H}_2\text{O}_2]=10 \text{ mM}$ , temperature =  $25^\circ\text{C}$ ,  $\text{pH}=3$

### Effect of initial pH

To investigate the effect of initial pH, solutions of Atenolol were treated at various initial pHs (3, 4, 5, 7 and 10) at constant concentrations of  $\text{H}_2\text{O}_2$ , the temperature and catalyst loading at 10 mM,  $25\pm 0.5^\circ\text{C}$  and  $0.5 \text{ g}/\text{dm}^3$ , respectively. The results in Figure 3 indicate that the degradation efficiency at the constant operating conditions under both alkaline and weakly acidic conditions were very similar and appeared to be independent of the initial pH. On the

other hand, under strongly acidic conditions (pH=3) there was high degradation. This result is in agreement with previous studies in the literature [8]. Above the optimum pH value, there may be a possible decomposition of  $\text{H}_2\text{O}_2$  into water and oxygen and also the possible deactivation of the catalyst with the formation of the other complexes leading to a reduction of  $\cdot\text{OH}$  radicals [9].

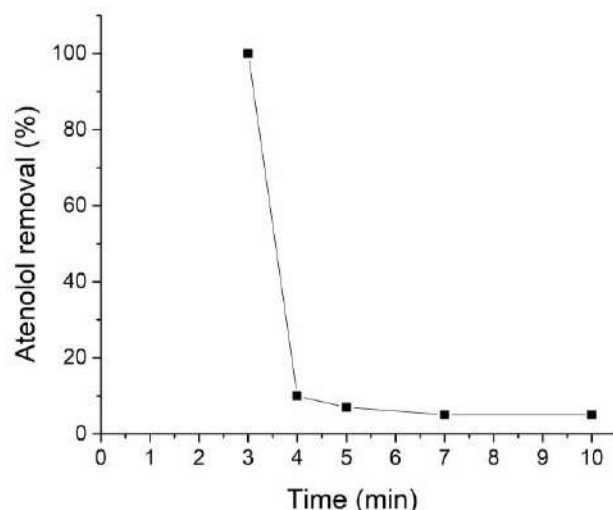


**Figure 3** Effect of initial pH on degradation;  
Reaction conditions:  $[\text{H}_2\text{O}_2]=10$  mM, catalyst loading =  $0.5$  g/dm<sup>3</sup>, temperature =  $25^\circ\text{C}$

## CONCLUSION

The degradation of reactive Atenolol in aqueous solutions by photo-Fenton oxidation using a wood sawdust-based catalyst (iron(III) impregnated) has been studied. Based on the results the following conclusions can be drawn:

The results showed that with a heterogeneous photo-Fenton process, 99.71% degradation can be achieved at the optimized conditions for Atenolol, which are 10 mM  $\text{H}_2\text{O}_2$ , pH=3,  $25\pm 0.5^\circ\text{C}$ ,  $0.5$  g/dm<sup>3</sup> catalyst loading and 15 min reaction time.

Generally, it can be concluded that the experimental data demonstrated that the photo-Fenton process is a promising technique for the degradation of Atenolol from aqueous solution.

## ACKNOWLEDGEMENT

*The authors would like to acknowledge financial support from the Ministry of Science, Technological Development and Innovation of the Republic of Serbia (Agreement No 451-03-66/2024-03/200124 and Agreement No 451-03-65/2024-03/200124).*

## REFERENCES

- [1] Zhou S., Di Paolo C., Wu X., *et al.*, Environ. Int. 128 (2019) 1–10.
- [2] Mole R.A., Brooks B.W., Environ. Pollut. 250 (2019) 1019–1031.
- [3] Kosma C.I., Nannou C.I., Boti V.I., *et al.*, Sci. Total Environ. 659 (2019) 1473–1483.

- [4] Kanakaraju D., Glass B.D., Oelgemöller M., *Environ. Chem. Lett.* 12 (2014) 27–47.
- [5] Perini J.A.L., Tonetti A.L., Vidal C., *et al.*, *Appl. Catal. B Environ.* 224 (2014) 761–771.
- [6] Dutta K., Mukhopadhyay S., Bhattacharjee S., *et al.*, *J. Hazard. Mater.* 84 (2001) 57–71.
- [7] Sun J.H., Sun S.P., Wang G.L., *et al.*, *Dyes Pigm.* 74 (2007) 647–652.
- [8] Meric S., Kaptan D., Ölmez T., *Chemosphere* 54 (2004) 435–441.
- [9] Daud N.K., Hameed B.H., *J. Hazard. Mater.* 176 (2010) 938–944.





## ADVANCE OXIDATION OF TEXTILE DYE BY ACTIVATED HYDROGEN PEROXIDE WITH UV-C LIGHT

Jelena Mitrović<sup>1</sup>, Miljana Radović Vučić<sup>1</sup>, Nena Velinov<sup>1\*</sup>, Slobodan Najdanović<sup>1</sup>,  
Miloš Kostić<sup>1</sup>, Milica Petrović<sup>1</sup>, Aleksandar Bojić<sup>1</sup>

<sup>1</sup>University of Niš, Faculty of Sciences and Mathematics, Višegradska 33, 18000 Niš,  
SERBIA

\*[nenavelinov@yahoo.com](mailto:nenavelinov@yahoo.com)

### Abstract

*The application of advanced oxidation processes in water and wastewater treatment has gained interest over the last decade. The degradation kinetics and mechanisms of the textile dye Reactive Orange 4 by advanced oxidation processes based on generation of hydroxyl radicals were investigated. The hydroxyl radicals were generated by UV photolysis of hydrogen peroxide. The effects of the initial pH of the solution, the concentration of the textile dye and the dosage of the oxidising agent were investigated. The results show that neutral conditions were favourable for the degradation of the investigated textile dye. An increase in the oxidising agent dosage or a reduction in the pollutant concentration was able to improve the degradation of the textile dye Reactive Orange 4.*

**Keywords:** hydroxyl radicals, wastewater treatment, irradiation.

### INTRODUCTION

The textile industry produces large quantities of liquid waste containing organic and inorganic compounds. During the dyeing processes, not all the dyes that are applied to the textiles are fixed to them, and there is always some of dyes that do not remain fixed to the textiles and are washed out. These unfixed dyes are found in high concentrations in textile wastewater [1]. The different types of synthetic dyes used in the textile industry are categorised into acid, base, direct, azo, disperse, sulphur and vat dyes [2]. Among these types of dyes, azo dyes are the most widely produced and used worldwide. These organic pollutants can interfere with photosynthesis, inhibit the growth of aquatic organisms, and pose a significant health risk to the skin, eyes, gastrointestinal tract, and respiratory tract of humans [3]. Consequently, dye-containing wastewater discharged into the environment without proper treatment can have a significant negative impact on both aquatic ecosystems and human health. Furthermore, due to their complex structures, dyes are generally resistant to light, aerobic digestion, and other conventional treatment processes [3].

In recent years, the use of advanced oxidation processes (AOPs) has become increasingly important in wastewater treatment. Advanced oxidation processes include a range of methods such as ozonation, photocatalysis, electrochemical oxidation, Fenton, and Fenton-like processes. Although these processes use different reaction systems, they are all characterised by a similar chemical feature, namely the use of highly reactive oxidants such as hydroxyl radicals (HO<sup>•</sup>) with a redox potential of 2.80 V [4]. These methods are successfully used to

remove and degrade organic pollutants, such as pharmaceuticals, pesticides, hormones, UV filters, surfactants, and textile dyes [5]. The most advanced and modern developments in water treatment technologies relate to the oxidation of organic components that are difficult to break down. The application of advanced oxidation processes produces highly reactive free radicals that can break down the most difficult molecules into small, biodegradable species or into inorganic compounds such as CO<sub>2</sub> and water.

Photolysis of hydrogen peroxide by ultraviolet light is one of the most effective AOPs. This process involves the homolytic cleavage of H<sub>2</sub>O<sub>2</sub> into hydroxide radicals using ultraviolet radiation (reaction 1). Hydrogen peroxide is a flexible oxidant that is powerful over the entire pH range (0–14) with high oxidation potential (E<sub>0</sub>=1.763 V at pH=0, E<sub>0</sub>=0.878 V at pH=14).



The mode of action of generated hydroxyl radicals on organic molecules is dependent on the nature and properties of the respective molecule. To generalise, there are three probable mechanisms of action associated with the activities of hydroxyl radicals: a reaction in which hydrogen is removed; a reaction in which an electron is transferred; and a reaction in which electrophilic material is added [6].

In the present research, the oxidation efficiency of the UV-activated hydrogen peroxide process for removal Reactive Orange 4 dye was investigated. This study systematically explored the effects of different crucial parameters on textile removal kinetics of textile dye Reactive Orange 4.

## **MATERIALS AND METHODS**

### **Chemicals**

Textile dye Reactive Orange 4 (RO 4, dye content about 50%) was purchased from Sigma-Aldrich (St. Louis, MO, USA) and used without further purification. The hydrogen peroxide solution (30%), analytical grade, was purchased from Merck (Germany). All other used chemicals were analytical grade and supplied from Merck (Germany). All solutions were prepared with ultrapure water from the Smart2Pure system with a conductivity of 0.055 μSm<sup>-1</sup> (Thermo Scientific, USA).

### **Irradiation experiment**

The degradation experiments were carried out in a laboratory-scale batch photoreactor equipped with ten low-pressure mercury lamps (Philips, Holland) emitting at 253.7 nm and mounted in parallel on the top of the photoreactor. The distance between the surface of the solution and the UV lamps was kept constant at 220 mm. The light intensity on the surface of the solution was measured with a UV radiometer Solarmeter model 8.0 UVC (Solartech, USA). The schematic of the photoreactor used for the irradiation experiments can be found elsewhere [7].

## Procedures

All experiments were performed with 100 cm<sup>3</sup> working solution, with the desired initial peroxide (10, 20, 40, 80 and 100 mmol dm<sup>-3</sup>) and textile dye concentration (50 mg/dm<sup>3</sup>) and at the corresponding pH values (2.0, 3.0, 7.0, 9.0 and 10.0) in glass Petri dishes. Samples were taken at specific time intervals (0, 1, 2, 4, 6, 10 and 15 minutes) and the residual concentration of RO 4 dye was determined by means of UV/Vis spectrophotometry. The efficiency of degradation was defined by the following equation (2):

$$\text{Removal efficiency (\%)} = \left(1 - \frac{c_t}{c_0}\right) \times 100 \quad (2)$$

where  $c_0$  is the initial RO 4 concentration,  $c_t$  is RO 4 concentration at irradiation time  $t$ .

The pseudo-first-order kinetic model, which can be described by equation (3), was used to follow the kinetics of the disappearance of textile dye RO 4.

$$\ln \frac{c_t}{c_0} = -k_{\text{app}} t \quad (3)$$

where  $c_0$  is the initial RO 4 dye concentration,  $c_t$  is RO 4 dye concentration at time  $t$ ,  $k_{\text{app}}$  is the apparent rate constant,  $t$  is the irradiation time. From the linear plot of  $\ln(c_t/c_0)$  versus time, the values of  $k_{\text{app}}$  can be calculated from experimentally obtained data. The values of  $R^2$  are greater than 0.9 in most experiments, indicating that the model used is in good agreement with the laboratory data. All tests were performed in triplicate and the average of the three values is shown with standard deviation error bars.

## RESULTS AND DISCUSSION

The first experiments were carried out only in the presence of hydrogen peroxide, only under UV irradiation and with a combination of oxidising agent and UV light. The results shown in Figure 1a indicated that the initial dye concentration did not change with UV irradiation only, probably because the RO 4 dye is stable in aqueous solution under direct UV-C photolysis. The presence of hydrogen peroxide only also did not have impact on removal of the RO 4 dye, while application of hydrogen peroxide in combination with UV irradiation lead to the drastic reduction of dye concentration.

The changes in the UV/Vis absorption spectra of the RO 4 dye during UV/H<sub>2</sub>O<sub>2</sub> treatment are shown in Figure 1b. The peak observed in the visible region corresponds to the orange colour, while the peaks observed in the UV region are due to the aromatic structure of the dye. It is evident that the intensity of a peak in the visible region of the spectrum decreased as the irradiation time increased and disappeared completely after 15 minutes of treatment. At the same time, the decrease in the intensity of a peak in the ultraviolet region of the spectrum was taken as evidence of the degradation of the aromatic part of the dye. It was found that under UV-activated hydrogen peroxide, both colour removal and a certain degree of degradation of RO 4 molecules was achieved.

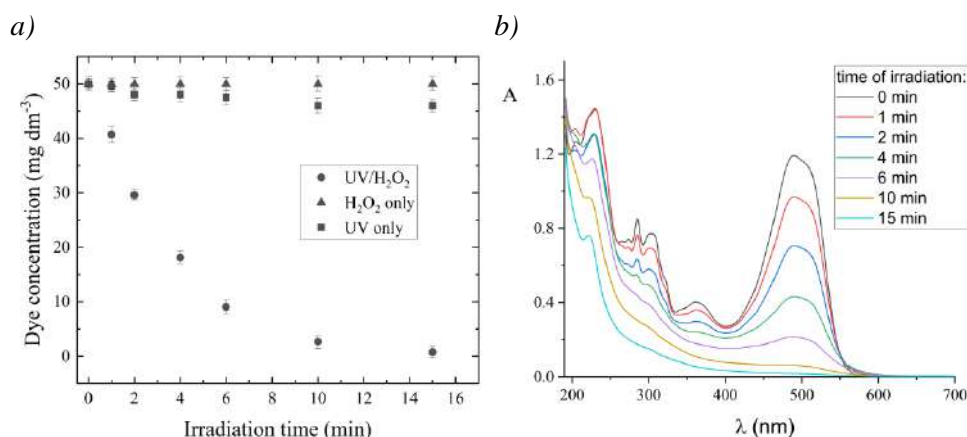


**Figure 1** a) RO 4 residual dye concentrations after treatment with UV irradiation, H<sub>2</sub>O<sub>2</sub> and UV/H<sub>2</sub>O<sub>2</sub>; b) UV/Visible spectral changes during UV/H<sub>2</sub>O<sub>2</sub> treatment of RO 4 dye.  $c_0(\text{RO } 4)=50 \text{ mg dm}^{-3}$ ,  $c_0(\text{H}_2\text{O}_2)=20.0 \text{ mmol dm}^{-3}$ ,  $\text{pH } 7 \pm 0.5$ , UV light intensity =  $1950 \mu\text{W cm}^{-2}$ , temperature =  $25 \pm 0.5^\circ\text{C}$ .

The efficiency of RO 4 dye removal by UV/H<sub>2</sub>O<sub>2</sub> at different concentration of oxidants was illustrated in Figure 2, where the removal efficiencies were increased with increase of oxidants concentration due to the formation of  $\cdot\text{OH}$ . The reaction rate has been greatly increased with the addition of H<sub>2</sub>O<sub>2</sub> due to the formation of  $\cdot\text{OH}$  under UV irradiation (reaction 1). Experimentally obtained reaction rate constant were 0.127, 0.287, 0.36, 0.324, 0.252 min<sup>-1</sup> for initial oxidant concentrations 10, 20, 40, 80 and 100 mmol dm<sup>-3</sup>, respectively. The reaction rate constant increase with increasing in oxidant concentration up to 40 mmol dm<sup>-3</sup>, while with further increase in oxidant concentration, removal rate of the investigated dye slightly decreases. This phenomenon is probably associated with scavenging effect of high doses of hydrogen peroxide [8].

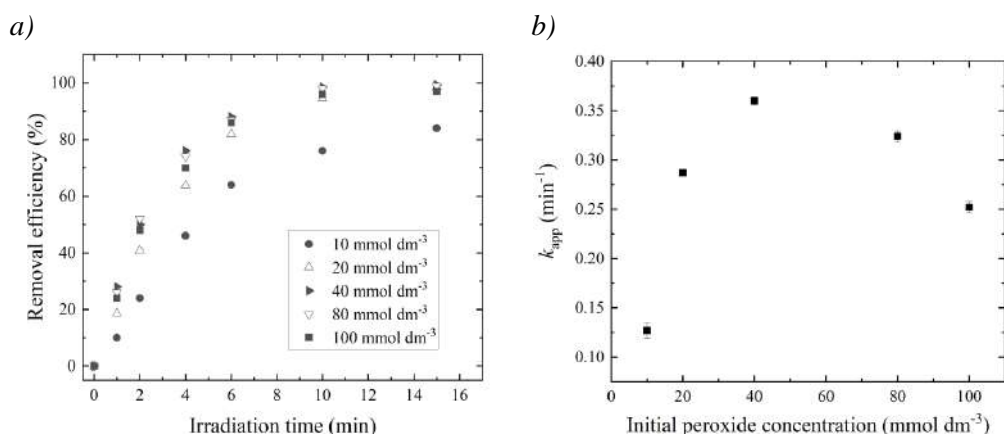


**Figure 2** The influence of different initial oxidant concentration on: a) removal efficiency of RO 4 dye; b) rate constant of RO 4 dye removal.  $c_0(\text{RO } 4)=50 \text{ mg dm}^{-3}$ ,  $\text{pH } 7 \pm 0.5$ , UV light intensity =  $1950 \mu\text{W cm}^{-2}$ , temperature =  $25 \pm 0.5^\circ\text{C}$ .

The influence of initial solution pH ranging from 2.0 to 10.0 on RO 4 dye degradation in UV/H<sub>2</sub>O<sub>2</sub> system was investigated (Figure 3a). For all pH conditions, the reaction follows pseudo-first-order kinetics ( $R^2 > 0.98$ ). The experimental rate constants  $k_{\text{app}}$  derived from the

slope of  $\ln(c/c_0)$  versus time were 0.221, 0.245, 0.287, 0.231 and 0.216  $\text{min}^{-1}$  for pH 2, 3, 7, 9 and 10, respectively. The best performances of investigated process were achieved at neutral conditions, while  $k_{\text{app}}$  values decreased slightly at basic and acidic conditions. The inhibition of degradation at higher pH values can be the result of several reasons: the reduction of oxidation power of  $\text{HO}^\bullet$  at this pHs, the scavenging of  $\text{HO}^\bullet$  by  $\text{OH}^-$  ions is also expressive under basic conditions, and  $\text{H}_2\text{O}_2$  self-decomposition is high at high pH values [9].

The investigation of the influence of the initial RO 4 dye loading in the reaction system is illustrated in Figure 3b. Experimental results exhibited an increasing difficulty in the degradation of the investigated dye as its initial concentration increased. According to Figure 3b, the fastest elimination of RO 4 dye was for the case where the initial concentration was 20  $\text{mg dm}^{-3}$  with a reaction rate constant of 0.33  $\text{min}^{-1}$ . The removal rate constants decreased with further increasing in initial dye concentration and reached values 0.291, 0.271, 0.255, 0.231  $\text{min}^{-1}$  for initial dye concentrations 40, 60, 80 and 100  $\text{mg dm}^{-3}$ , respectively. This behavior was expected since similar trends have been reported as common phenomena for various AOPs [10].

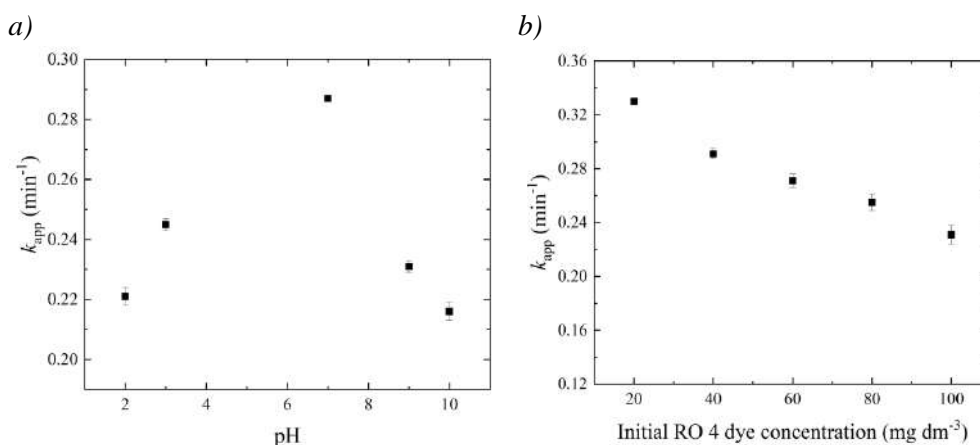


**Figure 3** a) The influence of different initial pH on the removal efficiency of RO 4 dye;

b) The influence of different initial RO 4 concentration on its degradation.

$c_0(\text{RO 4})=50 \text{ mg dm}^{-3}$ ,  $c_0(\text{H}_2\text{O}_2)=20.0 \text{ mmol dm}^{-3}$ ,  $\text{pH } 7 \pm 0.5$ ,  $\text{UV light intensity} = 1950 \mu\text{W cm}^{-2}$ ,  
 $\text{temperature} = 25 \pm 0.5^\circ\text{C}$ .

## CONCLUSION

The present work investigated the degradation of textile azo dye RO 4 by activated hydrogen peroxide with UV-C irradiation. Various parameters were studied to evaluate their impact on process efficiency. The studied system achieved the elimination of 50  $\text{mg dm}^{-3}$  of RO 4 dye in 15 min using 20  $\text{mmol dm}^{-3}$  of hydrogen peroxide. The RO 4 removal followed pseudo-first-order kinetics under all investigated conditions. Increasing in oxidant concentration significantly accelerated RO 4 degradation. Retarding phenomena were observed for increased RO 4 loading as well as at alkaline and acidic conditions.

## ACKNOWLEDGEMENT

The authors are grateful to the Ministry of Science, Technological Development and Innovation of the Republic of Serbia for financial support according to the contract with the registration number 451-03-66/2024-03/200124 and 451-03-65/2024-03/200124.

## REFERENCES

- [1] Ghaly A.E., Ananthashankar R., Alhattab M. *et al.*, J. Chem. Eng. Process Technol. (5:182) (2014) 1–18.
- [2] Maleki S., Samira Ghorbani S., Monajemi P., Biochem. Eng. J. 199 (2023) 109057.
- [3] Ding X., Gutierrez L., Croue J. P. *et al.*, Chemosphere 253 (2020) 126655.
- [4] Asghar A., Raman A.A.A., Daud W.M.A.W., J. Clean. Prod. 87 (2015) 826–838.
- [5] Zia U., Khan Z.U.H., Gul N.S., *et al.*, Ecotoxicol. Environ. Saf. (267) (2023) 115564.
- [6] Legrini O., Oliveros E., Braun A.M., Chemical Reviews. 93 (2) (1993) 671–698.
- [7] Mitrović J., Radović M., Bojić D., *et al.*, J. Serb. Chem. Soc., 77 (4) (2012) 465–481.
- [8] Xina X., Shaohua Suna S., Zhou A.J., *et al.*, Water Proc. Engineering 36 (2020) 101293.
- [9] Alberto E.A, Santos G.M., Marson E.O., *et al.*, Environ. Chem. Eng. 11 (2023) 110698.
- [10] L alas K., Arvaniti O.S., Zkeri E., *et al.*, Sci. Total Environ. 846 (2022) 157378.





## QUANTIFYING SOIL EROSION OF THE TOM'S BROOK CATCHMENT (WESTERN SERBIA)

Gordana Šekularac<sup>1\*</sup>, Miroljub Aksić<sup>2</sup>, Tatjana Dimitrijević<sup>3</sup>, Mihailo Ratknić<sup>4</sup>,  
Nebojša Gudžić<sup>2</sup>

<sup>1</sup>University of Kragujevac, Faculty of Agronomy, Cara Dušana 34, 32000 Čačak, SERBIA

<sup>2</sup>University of Priština, Kosovska Mitrovica, Faculty of Agriculture, Kopaonička nn,  
38219 Lešak, SERBIA

<sup>3</sup>Institute of Forestry, Kneza Višeslava 3, 11000 Belgrade, SERBIA

<sup>4</sup>Earth Climate Change Team (ECC Team), New Jersey, USA

\*gordasek@kg.ac.rs

### Abstract

*Soil erosion is one of the highly significant forms of the soil degradation in Serbia. In this sense, this paper may help consider better the erosion process exhibited to a greater or lesser extent on all the soil types with a slope more than 1%, which denotes to the necessity of taking anti-erosion measures towards protecting the soil as a nonrenewable natural resource. Due to a range of natural factors and human impact on the erosion process in the part of the Western Serbia as well as based on the overall condition of the torrent catchment Tom's Brook, the soil loss due to erosion could be predicted through Erosion Potential Model (EPM). As regards the torrential flow type, Tom's Brook is a landslide (E), with annual mean amount of erosion drift ( $W_{year}$ ) from  $539.11 \text{ m}^3 \text{ year}^{-1}$ . The specific annual amount of total erosion deposit ( $G_{year \text{ sp}}^{-1}$ ) reaching the confluence point of Tom's Brook from the right-hand side into the river Tinja (the left tributary of the river Kamenica within the Western Morava basin in the Western Serbia) amounted to  $120.92 \text{ m}^3 \text{ km}^{-2} \text{ year}^{-1}$ .*

**Keywords:** soil losses to erosion, catchment, erosion factors, erosion potential method (EPM).

### INTRODUCTION

The water soil erosion of various intensity conditioned by natural and antropogenous factors, is widespread in the whole world. Global climatic changes have shown that both, the time and the amount of precipitations have become lasting and disturbed, which means that even the coventional foresting technologies use will prove to be additionally ineffective [1]. Thus, soil erosion imposes a huge problem worldwide affecting the soil productivity, causing nutritional matters loss from the soil, mudding within the catchment and water quality deterioration [2].

Compared to geomorphological and climatic characteristics of the territory of Serbia, the most widespread is pluvial erosion accounting for 86% of the entire area, of which 90% accounts for the eroded soil of Central Serbia [3].

Understanding the soil erosion driving forces may detect the areas prone to erosion within the landscape, help soil management and other strategies to be used for efficient problem handling, with the most commonly used soil erosion model being the Universal Soil Loss Equation (USLE) as well as its model family [2]. Accordingly, we believe that it would be important to have knowledge based on the multiple soil erosion models, rather than rely only on the USLE-type ones. Hence, the Erosion Potential Model (EPM) accounting for other erosion processes (e.g. gully erosion or soil slumps) and not just for sheet and rill ones (e.g., USLE-type models) can be an interesting option to estimate the global and large-scale soil erosion rates especially because these processes can be important for the large-scale erosion-sediment balance [4].

Protective measures against water soil erosion can be a significant mission, not only for the environmental conservation, but also for agricultural production capacities as a fundamental food source. The basic prerequisite for putting the protective measures to use is to study thoroughly and define accurately the catchment characteristics, being the goal of this paper.

The extent to which the water erosion process is expressed due to different agents, and the amount of the sediment produced due to erosion under the natural conditions of the Kamenica catchment resource (the part of the Western Morava's river basin), on the part of its left side tributary (Tinja), is presented for the catchment of Tom's Brook, flowing into Tinja from its right side.

## **MATERIALS AND METHODS**

A group of methods, in the first place, a terrain analysis of the Tom's Brook entire catchment elements configuration, was utilized. The brook's natural characters were investigated using the mapping analysis records (hydrology, relief, geological substrate and soil). The maps scales were, as follows: topographic (1:25,000) (Figure 1) [5], geological (1:500,000) [6] and pedological map (1:50,000) [7]. Interpolation was used to determine how natural agents, climatic elements, rainfalls and air temperatures [8] affected erosion [9,10]. In addition, the erosion classification modules, according to which, the torrent classification was also made, were utilized, whereas the mean annual sediment amounts reaching the confluence point of Tom's Brook into the Tinja were calculated through the erosion potential module (EPM) [11].

## **RESULTS AND DISCUSSION**

Within the Kamenica torrent land catchment, on the slopes of the Mountain Maljen's southern part, Tom's Brook, springing in the Great Field (718 m of altitude), flows into the Tinja from the right side (the left tributary of the first order of the river Kamenica), into its middle part, being of a mildly winding course, with a narrow valley near the village Kneževići (624 m of the altitude; 44°3'39" N; 20°6'8" E), the settlements of Bogdanica, Gornji Milanovac, Moravički District (Figure 1).

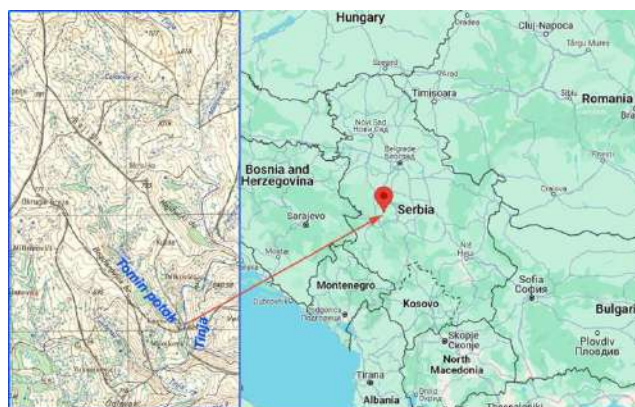


Figure 1 Tom's Brook catchment (mouth in the river Tinja)

The Tom's brook basin area amounts to  $1.07 \text{ km}^2$ , extent 5.50 km, length 2.12 km. The possibility of a sudden concentration of flood water reaching from the entire area depends on the basin's shape, which affects the development of the accelerated process of soil erosion in the basin, and the total amount of runoff water on the basin's size. By their shape, the basins may be categorized into four types [12]. By its surficial shape, the Tom's brook catchment belongs to the type four (IV). This basin's shape is featured by a uniformly bifurcated hydrographic network through the upper, middle and lower course, meaning that the soil and geological substrate material are also uniformly taken away from the entire basin.

Drift production from the Tom's Brook shares the entire annual substrate magnitude, both of the Tinja and the Kamenica. Thus, the whole substrate production of the Tom's Brook basin depends on the soil erosion natural factors and on the human influence if any. The extent to which the erosion natural factors exhibit their impact is conditioned by the basic catchment relief parameters, areal geological substrate, soil features, climate, and none the less by land cultures in which the humans play an essential part.

The relief parameters of the Tom's Brook are shown in the Table 1.

Table 1 The basic parameters of the Tom's Brook catchment relief

<b>Catchment Name: The Tom's Brook</b>	
The lowest point of the main watercourse and catchment (B), m	624
The highest point of the main watercourse (C), m	766
The highest point of the catchment (E), m	781
Average slope of the main watercourse in the catchment ( $I_a$ ), %	6.0
Mean catchment altitude ( $A_m$ ), m	725.41
Mean catchment altitudinal difference (D), m	101.41
Mean catchment slope ( $I_m$ ), %	17.9
Coefficient of catchment relief erosion energy ( $E_r$ ), $\text{m km}^{-1/2}$	49.22

The lowest point of the Tom's Brook (the confluence point into the Tinja) is at 624 m of altitude and the highest at 766 m of the altitude. The highest point of the Tom's Brook catchment is 781 m. The average riverbed slope of the major basin amounts to 6.0%. The mean basin's altitude ( $A_m$ ) amounts to 725.41 m with the mean catchment height difference (D) being 101.41 m. The Tom's Brook basin was found to have the mean slope ( $I_m=17.9\%$ ).

The already mentioned values along with the relief parameters magnitudes were found to contribute to the relief erosion energy coefficient ( $E_r$ ) being  $49.22 \text{ m km}^{-1/2}$  (Table 1).

The presence of a particular geological substrate is denoted by the soils of the areas formed on that substrate. Thus, the soils were formed within the Tom's Brook catchment basin on a serpentine of a poor water permeability spread on  $1.07 \text{ km}^2$ , Table 2. Water permeability coefficient ( $S_1$ ) for the basin underway amounts to 1.00, due to which the humus silicate soil is present in the basin, with the profile of  $A_h$ -C type and prone to erosion (Table 2).

The climatic elements are considered to be a significant factor imparting the soil erosion, with water runoff leading to it. The sum of the mean annual precipitations ( $P$ ) of the Tom's Brook basin amounts to 804.3 mm and the mean annual air temperature of the area underway to  $8.0^\circ\text{C}$ .

**Table 2** Geological substrate of the Tom's Brook catchment, coefficient of water permeability ( $S_1$ ) and erosion resistance

Catchment name: The Tom's Brook	$\text{km}^2$	%
$F_{\text{ppr}}$ – Poorly permeable rocks	1.07	100
• Serpentine	1.07	100
Coefficient of geological substrate water permeability ( $S_1$ )	1.00	
Resistance of geological substrate to erosion	Non-resistant	

The vegetation canopy coefficient ( $S_2$ ) depends on the presence of land cultures on the soil of the area considered. Through calculation, the canopy coefficient ( $S_2$ ) of the Tom's Brook catchment was found to amount to 0.80, which means that there are more bare earth grasses, i.e. pastures and devastated forests and bushes (84.11%), further the forests and bushes of a good pattern (6.54%), and meadows (3.74%), orchards (0.94%) with barren land with 4.67% (Table 3). Overall, this shows that the area of Tom's Brook basin is protected from the soil erosion from the aspect of land cultures.

**Table 3** The structure of the Tom's Brook catchment according to type of land use and vegetative cover coefficient ( $S_2$ )

Type of land use		Surface area	
		$\text{km}^2$	%
$\Sigma F_f$	Forests and coppice of good spacing	0.07	6.54
	Orchards	0.01	0.94
$F_g$	Meadows	0.04	3.74
	Pastures and devastated forests and coppices	0.90	84.11
$\Sigma f_g$		0.95	88.79
$F_b$	Arable land	0.00	0.00
	Infertile soil	0.05	4.67
$\Sigma f_b$		0.05	4.67
Vegetation cover coefficient ( $S_2$ )		0.80	

The soil erosion coefficient value of the basin surveyed, pointed to the type of the prevalent erosion related to the particular erosion strength, i.e. to its destructiveness category.

The erosion coefficient ( $Z$ ) of the Tom's Brook basin amounted to 0.35, inhering to the fourth (IV) destructiveness category, being of a poor strength and of a deep type of erosion process.

The established index of the hydrographic class ( $H_c$ ) of the torrential flows, can further determine their types against the classes. Tom's Brook pertains to the class E, i.e. to the landslide flows.

So featured factors of the Tom's Brook, gave rise to the particular sediment amounts produced along with the particular erosion intensity exhibited.

The erosion magnitude of the Tom's Brook catchment, is shown through the mean annual amount (produced) of the erosion process ( $W_{\text{year}}$ ) of  $539.11 \text{ m}^3 \text{ year}^{-1}$ .

The calculated mean annual volume of the total sediment ( $G_{\text{year}}$ ), reaching the mouth of the Tom's Brook into the river Tinja, amounted to  $129.38 \text{ m}^3 \text{ year}^{-1}$ , with the specific annual amount of the entire erosion sediment reaching the mouth into the Tinja ( $G_{\text{year sp}}^{-1}$ ), quantitatively expressed erosion intensity, amounting to  $120.92 \text{ m}^3 \text{ km}^{-2} \text{ year}^{-1}$ .

Therefore, the given data clearly show that Tom's Brook catchment erosion caused 0.27 ha land area the power of up to 0.20 m to disappear annually, and the average catchment soil to disappear by 0.05 mm, annually, too.

Given that the mean volume mass value is  $1.5 \text{ g cm}^{-3}$ ,  $0.40 \text{ t ha}^{-1}$  of the soil is lost annually. Although any soil loss of more than  $1 \text{ t ha}^{-1} \text{ yr}^{-1}$  can be considered to cause irreversible damages within the time span of 50–100 years, it is commonly accepted that agricultural soil can tolerate a certain amount of erosion, which typically ranges from  $1 \text{ t ha}^{-1} \text{ yr}^{-1}$  on shallow sandy soils to  $5 \text{ t ha}^{-1} \text{ yr}^{-1}$  on deeper soils [13].

## **CONCLUSION**

Based on the natural features of the Tom's Brook catchment, it may be inferred that the fundamental relief parameters are expressed, further, that geological substrate (serpentine) nonresistant to erosion, humus silicate soil prone to erosion favoured by the basic climatic elements (annual precipitation sums) and the mean air temperature, are exhibited, as well as the soil saturation by the existing vegetation. Therefore, such analysis suggests that the landslide Tom's Brook be featured as follows: IV class of destructiveness, with the erosion coefficient ( $Z$ ) of 0.35, being of poor strength, deep type of erosion process. These and other factors of the basin erosion studied, contributed to the mean annual erosion sediment to amount to  $129.38 \text{ m}^3 \text{ year}^{-1}$ , and erosion intensity to  $120.92 \text{ m}^3 \text{ km}^{-2} \text{ year}^{-1}$ .

## **ACKNOWLEDGEMENT**

*The authors are grateful to the Ministry of Science, Technological Development and Innovation of the Republic of Serbia for financial support (451–03–66/2024–03/200088; 451-03-65/2024-03/200189 and 451-03-66/2024-03/200027).*

## REFERENCES

- [1] Ministarstvo poljoprivrede i zaštite životne sredine, Nacionalni akcioni plan ublažavanja posledica suše i degradacije zemljišta, *Available on the following link:* [https://rsjp.gov.rs/upload/UNCCD\\_NAP\\_SRBIJA\\_NACRT.pdf](https://rsjp.gov.rs/upload/UNCCD_NAP_SRBIJA_NACRT.pdf).
- [2] Benavidez R., Jackson B., Maxwell D., *et al.*, Hydrol. Earth Syst. Sci. Discuss., Manuscript under review for journal Hydrol. Earth Syst. Sci., Discussion started: 23 February 2018, © Author(s) 2018. CC BY 4.0 License. *Available on the following link:* <https://doi.org/10.5194/hess-2018-68>.
- [3] Srbijašume, Plan upravljanja Predelom izuzetnih odlika „Maljen“ za period 2022–2031. godine, *Available on the following link:* <https://srbijasume.rs/ssume/wp-content/uploads/2022/01/Plan-upravljanja-PIO-Maljen-za-period-2022-do-2031.godine.pdf>.
- [4] Tadić E., Šljuka A., Res. Rev. DGTH, 47 (1) (2018) 32–43.
- [5] Vojnogeografski Institut, Beograd, Topografska karta (1:25.000), 1971.
- [6] Institut za zemljište, Beograd–Topčider, Geološka karta Zapadne i Severozapadne Srbije (1:500.000), 1966.
- [7] Institut za zemljište, Beograd–Topčider, Pedološka karta teritorije sreza Kraljevo (1:50.000), 1964.
- [8] PSSS, Čačak, Visina padavina i temperature vazduha (1949–1995).
- [9] Bonacci O., Priručnik za hidrotehničke melioracije, Društvo za navodnjavanje i odvodnjavanje Hrvatske, Zagreb (1984), p.66.
- [10] Dukić D., Hidrologija kopna, Naučna knjiga, Beograd (1984), p.185.
- [11] Gavrilović S., Inženjering o bujičnim tokovima i eroziji, Izgradnja, Beograd (1972), p.268.
- [12] Orlov T., Šćukin S., Voprosi Eroziiji i Stoka, 1962.
- [13] OECD. Environmental Indicators for Agriculture, OECD Publications Service, Paris (2001), p.198. *Available on the following link:* <https://www.oecd.org/greengrowth/sustainable-agriculture/40680869.pdf>.





## EFFECT OF IRRIGATION RATE ON THE ONSET INTENSITY OF GREY MOULD AND LATE BLIGHT IN GREEN HOUSE TOMATOES

Gordana Šekularac<sup>1\*</sup>, Miroljub Aksić<sup>2</sup>, Tatjana Dimitrijević<sup>3</sup>, Slaviša Gudžić<sup>2</sup>,  
Nebojša Gudžić<sup>2</sup>, Dragan Grčak<sup>2</sup>, Milosav Grčak<sup>2</sup>, Mihailo Ratknić<sup>4</sup>

<sup>1</sup>University of Kragujevac, Faculty of Agronomy, Cara Dušana 34, 32000 Čačak, SERBIA

<sup>2</sup>University of Priština, Kosovska Mitrovica, Faculty of Agriculture,  
Kopaonička nn, 38219 Lešak, SERBIA

<sup>3</sup>Institute of Forestry, Kneza Višeslava 3, 11000 Belgrade, SERBIA

<sup>4</sup>Earthe Climate Change Team (ECCTeam), New Jersey, USA

\*[gordasek@kg.ac.rs](mailto:gordasek@kg.ac.rs)

### Abstract

*When controlling tomato grey mould and late blight in dependance of irrigation rate, the experiment on fungicide efficiency was made in the greenhouses in 2022. The greenhouses are situated in the village of Batušinac, the municipality of Merošina (south-east Serbia) (43°26'11" N 21°82'28" E). Irrigation rates of 15 mm, 25 mm and 35 mm used for the greenhouse tomato were studied to find out the effect they had exhibited on grey mould and late blight onset intensity. Higher soil moisture at 25 and 35 mm irrigation rates favoured late blight and grey mould, affecting the tomato plants more intensively than being using 15 mm rate. Therefore, lower irrigation rates may efficiently be used as an integral measure of tomato protection from infestation intensity of *Phytophthora infestans* and *Botrytis cinerea*.*

**Keywords:** tomato, irrigation, grey mould, late blight.

### INTRODUCTION

Considering that tomato is commercially significant, widespread and usable, no doubt that it ranks among the first vegetable cultures worldwide, particularly in the regions with more suitable soil and climatic conditions for their cultivation, to which Serbia belongs, too [1].

The basic task of watering is to provide sufficient moisture for the agricultural land, which enables normal plant nutrition and growth [1]. In irrigation practice, tensiometer is most commonly used to determine soil moisture. Numerous researchers have confirmed the efficiency of this method when determining irrigation dates of vegetable crops [2,3,4].

When growing tomato under the intensive growing conditions, a whole array of diseases may arise, with an outbreak of *Phytophthora infestans* causing late blight with potato and tomato everywhere in the world where these vegetable crops are grown [5]. This disease is assumed to be one of the most detrimental tomato diseases. It can badly and often utterly damage its plants under suitable growing conditions. Thus, due to the partly or totally destroyed the above-ground plant mass, which looks as if it were burnt by fire, the tomato yield may drastically drop [6].

*Botrytis cinerea* causes grey mould in plants, thereby inflicting serious damages to the production of more than 200 plant varieties, mostly dicotyledon ones [7]. The gravest damages are incurred to grapevine, vegetables, flowers and soft fruits [8,9]. *Botrytis cinerea* may cause huge losses in plants during vegetation, both in fields and greenhouses as well as in the earlier developmental stages of some host plants [10–12]. Thus, the stem rot around the wounds due to sepal breaking is most commonly observed in the tomato grown in plastic and greenhouses whereas the fruits rot accompanied by an extensive pathogen sporulation is mainly detected after the harvest [13].

In essence, the current study was aimed at finding out the way in which a watering rate may cause the outbreak intensity of late blight and grey mould in tomato under the natural infestation conditions as well as at establishing the efficiency level to which the chemicals were used to protect this vegetable from late blight and grey mould.

## MATERIALS AND METHODS

When controlling tomato grey mould and late blight in dependence of watering rate, the experiment on fungicide efficiency was made in the greenhouses in 2022. The greenhouses are situated in the village of Batušinac, the municipality of Merošina (south-east Serbia) (43°26'11" N 21°82'28" E).

Tomato was sown using the hybrid Amati F1 on the 20<sup>th</sup> of January in the plastic containers placed in the warm garden bed. The transplants were picked in February, the 25<sup>th</sup> in the pots. Planting in a permanent place in the greenhouse was done on 23<sup>rd</sup> of March, in the previously marked rows, covered with black polyethylene film, 0.05 mm thick, with irrigation strips placed underneath. Irrigation in the greenhouse was done using a drop-by-drop system.

The effect of irrigation rates on the onset intensity of grey mould and late blight in tomato was studied with the three variants of irrigation rates being: 15 mm, 25 mm and 35 mm. The irrigation moment was determined by tensiometers. Irrigation started at pre-irrigation soil moisture of 30 kPa and stopped at the soil moisture potential of 10 kPa.

The disease onset intensity and fungicide efficiency in controlling tomato late blight and grey rot, was monitored in 600 plants, of which 100 plants pertained to the control variant without chemical protection. The onset intensity of *B. cinerea* was assessed through the division into five classes from 0 to 4 [14], defined as follows:

- 0 - healthy plants;
- 1 - up to 25% diseased plants;
- 2 - from 26% to 50% diseased plants;
- 3 - from 51% to 75% diseased plants;
- 4 - from 76% to 100% diseased plants.

After the infestation intensity of *B. cinerea* had been classified, the disease index calculated by the formula of Mc Kinney supposed to indicate the mean value of the disease attacking a particular area (Equation 1),

$$I = \frac{\sum(n \times k)}{N \times K} \times 100 \quad (1)$$

was put forth: I – disease index in %, n – plant number within a category, k – number of single categories, N – total plant number and, K – total number of the categories.

Observations for measuring the intensity of *Phytophthora infestans* attacks were carried out by a scoring system 1–9 [15] in Table 1.

The efficiency of fungicides (Table 2) was calculated using the formula of Abbott (Equation 2) being,

$$E = \frac{C-T}{C} \times 100 \quad (2)$$

was put forth: E – efficiency of the fungicide studied, C – plant number on the untreated variant and, T – plant number on the treated variant.

**Table 1** Scoring intensity of *Phytophthora infestans* attacks

Score	Percentage of leaves attacked	Description
0	0	No symptoms of an attack
1	<10	Attack spots are less than 10% in leaves
2	11–25	Spots of damage began to appear and reached 25%
3	26–40	Spots of damage to all leaves reach 40% but the plants are still green
4	41–60	Maximum damage has reached 60%
5	61–70	Maximum damage has reached 70% and the plants changed colour into brown
6	71–80	Maximum damage has reached 80%, the base of the stem and shoots are attacked and the symptoms of wither and death
7	81–90	Maximum damage reaches 90%, the green part is only the top of the leaf
8	>90	The green area is low
9	100	There are no more green leaves, the damage is complete

**Table 2** Overview of the fungicides tested

Fungicide	Formulation	Active substance	Dose
Nordox 75	WG	Copper oxide	2 kg/ha
Antracol 70	WP	Propineb	2.5 kg/ha
Quadris	SC	Azoksistrobin	0.75 L/ha
FolioGold 537.5	SC	Metalaksil-m (37.5 g/L) + Hlorotalonil (500 g/L)	2.5–3 L/ha
Switch 62.5	WG	Ciprodinil (375 g/kg) + Fludioksonil (250 g/kg)	0.6–0.8 kg/ha
Dional 500	SC	Iprodion	1.5 L/ha

## RESULTS AND DISCUSSION

Upon visual inspection of the experimental plot, the plants on the control variant without chemical protection were observed to have been infected with late blight. The plants on the variant treated with fungicides were successfully protected from *Phytophthora infestans* and the consequences of late blight largely reduced. On the variant treated with Nordox, <10% of the spots appeared on the leaves at 25 and 35 mm irrigation rates whereas no infestation did at 15 mm (Table 3).

On the variant treated with Antracol, infestation was <10% at 25 mm irrigation rate and *Phytophthora infestans* 11–25% at 35 mm (Table 4).

**Table 3** Intensity of *Phytophthora infestans* attacks on the variant treated with Nordox

Irrigation rate (mm)	Percentage of leaves attacked									
	0	<10	11–25	26–40	41–60	61–70	71–80	81–90	>90	100
15	-	-	-	-	-	-	-	-	-	-
25	-	+	-	-	-	-	-	-	-	-
35	-	+	-	-	-	-	-	-	-	-

**Table 4** Intensity of *Phytophthora infestans* attacks on the variant treated with Antracol

Irrigation rate (mm)	Percentage of leaves attacked									
	0	<10	11–25	26–40	41–60	61–70	71–80	81–90	>90	100
15	-	-	-	-	-	-	-	-	-	-
25	-	+	-	-	-	-	-	-	-	-
35	-	-	+	-	-	-	-	-	-	-

The variant treated with Quadris was infected with <10% late blight only at irrigation rate of 35 mm (Table 5).

**Table 5** Intensity of *Phytophthora infestans* attacks on the variant treated with Quadris

Irrigation rate (mm)	Percentage of the leaves attacked									
	0	<10	11–25	26–40	41–60	61–70	71–80	81–90	>90	100
15	-	-	-	-	-	-	-	-	-	-
25	-	-	-	-	-	-	-	-	-	-
35	-	+	-	-	-	-	-	-	-	-

On the control variant with no fungicides, the tomato plants appeared to have been much more infected with *Phytophthora infestans* than those in the variant treated with fungicides. Also, rather a high disease onset intensity of 41–60% was recorded at 25 and 35 mm irrigation rates whereas a much lower infestation of 11–25% with *Phytophthora infestans*, was manifested at 15 mm (Table 6).

**Table 6** Intensity of *Phytophthora infestans* attack on the control variant without chemical protection

Irrigation rate (mm)	Percentage of leaves attacked									
	0	<10	11–25	26–40	41–60	61–70	71–80	81–90	>90	100
15	-	-	+	-	-	-	-	-	-	-
25	-	-	-	-	+	-	-	-	-	-
35	-	-	-	-	+	-	-	-	-	-

The higher irrigation rates of 25 and 35 mm and, therefore, a higher soil moisture suited the onset and spreading of late blight, but did not at 15 mm rate. The high moisture level in the greenhouse could suit the disease onset, stimulating spore germination [16,17]. Either an excessive or deficient water use may result in developing many fungal and bacterial plant diseases, which threatens the produce yield and quality [18].

Upon regular visual monitoring of the experimental plot, the symptoms of grey mould appeared on the tomato fruits and on the stem ground part. The tomato preventive and chemical protection was successful in grey mould control. Thus, when irrigated with 15 mm rate, the variants treated with fungicides did not manifest being infested with grey mould whereas those on the control variant with no chemical protection did (8% of the infested plants) (Table 7).

On the variant with 25 mm irrigation rate, 3% accounted for the infected plants treated with Folio Gold whereas the other variants treated with fungicides were not infected with grey rot at all. As for the control variant without chemical protection, 14% accounted for the infected tomato plants.

Further, on the variant with irrigation rate of 35 mm, 5% accounted for the infected plants treated with Folio Gold. The plants on the variants treated with fungicides were not infected whereas 17% of those on the control variant without chemical protection were.

**Table 7** Intensity of *Botrytis cinerea* infection on tomato and efficiency of fungicides

Irrigation rate (mm)	Fungicide	Infected plants (%)	Efficiency of fungicides (%)
15	Folio Gold 537.5	-	100
	Switch 62.5	-	100
	Dional 500	-	100
	Control	8	-
25	Folio Gold 537.5	3	78.6
	Switch 62.5	-	100
	Dional 500	-	100
	Control	14	-
35	Folio Gold 537.5	5	70.6
	Switch 62.5	-	100
	Dional 500	-	100
	Control	17	-

The higher irrigation rates (25 and 35 mm), favoured a more serious tomato infection with grey rot in the experimental greenhouse than the lower irrigation rate of 15 mm did. There is a close relationship between the incidence of some diseases and insect pests and the way in which the water is supplied to the tomato plants. The conditions, favouring the majority of diseases are the existence of free water on the leaves and high water content in the soil [19].

The fungicides used to protect tomato from grey rot expressed a high level of efficiency. Thus, Switch and Dional exhibited 100% efficiency on all the irrigation variants. Folio Gold was also 100% efficient on the variants with 15 mm irrigation rate but less efficient (78.6% and 70.6%) on those with 25 mm and 35 mm irrigation rates.

## CONCLUSION

Investigating the onset and infesting intensity of *Phytophthora infestans* and *Botrytis cinerea* in tomato as well as the fungicides efficiency in its protection from all these phytopathogens, resulted in the following conclusions:

- higher soil moisture at 25 and 35 mm irrigation rates favoured a higher outbreak intensity of late blight and grey rot in tomato plants than 15 mm rate did. Therefore, the lower irrigation rates may efficiently be utilized as an integral tomato plants protection measure against the infestation intensity of *Phytophthora infestans* and *Botrytis cinerea*, and

- the successfully performed tomato chemical protection from the *Phytophthora infestans* and *Botrytis cinerea* largely reduced the consequences the infection had on the variants treated with the fungicides compared to the control variant without chemical protection.

## ACKNOWLEDGEMENT

The authors are grateful to the Ministry of Science, Technological Development and Innovation of the Republic of Serbia for financial support (451-03-66/2024-03/200088; 451-03-65/2024-03/200189 and 451-03-66/2024-03/200027).

## REFERENCES

- [1] Popović M., Povrtarstvo, Nolit, Beograd (1991), p.423, ISBN: 86-19-01891-4.
- [2] Smajstrla A.G., Locascio S.J., Appl. Eng. Agr. 12 (1996) 315–319.
- [3] Li Y., Rao R., Bryan H., *et al.*, Proc. Fla. State Hort. Soc. 111 (1998) 58–61.
- [4] Muñoz-Carpena R., Dukes M.D., Li Y.C., *et al.*, Proc. Fla. State Hort. Soc. 116 (2004) 80–85.
- [5] Stojanović S., Poljoprivredna fitopatologija, Srpsko biološko društvo „Stevan Jakovljević”, Kragujevac (2004), p.290, ISBN: 86-905643-0-6.
- [6] Mijatović M., Obradović A., Ivanović M., Zaštita povrća od bolesti, štetočina i korova, AgroMivas, Smederevska Palanka (2007), p.264, ISBN: 978-86-910485-0-1.
- [7] Williamson B., Tudzynski B., Tudzynski P., *et al.*, Mol. Plant Pathol. 8 (2007) 561–580.
- [8] Droby S., Lichter A., Botrytis: Biology, Pathology and Control, Published by Springer, Dordrecht (2004), p.349–367, ISBN: 978-1-4020-6586-6 (PB), ISBN: 978-1-4020-2624-9 (HB), ISBN: 978-1-4020-2626-3 (e-book).
- [9] Tanović B., Pesticidi 18(4) (2003) 223–235.
- [10] Giraud T., Fortini D., Levis C., *et al.*, Phytopathology 89 (1999) 967–973.
- [11] Chardonnet C.O., Sams C.E., Trigiano R.N., *et al.*, Phytopathology 90 (7) (2000) 769–774.
- [12] Staats M., Van Barlen P., Van Kan J.A.L., Mol. Biol. Evol. 22 (2005) 333–336.
- [13] Charabany G., Shtienberg D., Plant Dis. 83 (1999) 554–560.
- [14] Gudžić S., Praktikum iz fitopatologije, Poljoprivredni fakultet, Univerzitet u Prištini, Kosovska Mitrovica-Lešak (2006), p.160, ISBN: 86-80737-07-0.
- [15] Halterman D., Kramer A.L.C., Wielgus S., *et al.*, Plant Dis. 92 (2008) 339–343.
- [16] Shtienberg D., Elad Y., Bornstein S., *et al.*, Phytopathology 100 (1) (2010) 97–104.
- [17] Beckett M.C., Daughtrey M.L., Fry W.E., Plant Dis. 89(9) (2005) 975–979.



- [18] Café-Filho A.C., Lopes C.A., Rossato M., Irrigation in Agroecosystems, IntechOpen, Zagreb (2019), p.184, ISBN: 978-1-78984-924-0, Print ISBN: 978-1-78984-923-3, eBook (PDF) ISBN: 978-1-83881-743-5.
- [19] Peerzada S.H., Najjar A.G., Mushtaq A., *et al.*, Int. J. Curr. Microbiol. App. Sci. 2(9) (2013) 125–132.



## INFLUENCE OF SOIL TYPE ON MEAN TREE HEIGHTS OF FIR TREES IN A 40-YEAR PROVENANCE TRIAL

Tatjana Dimitrijević<sup>1\*</sup>, Mihailo Ratknić<sup>2</sup>, Gordana Šekularac<sup>3</sup>, Miroljub Aksić<sup>4</sup>

<sup>1</sup>Institute of Forestry, Kneza Višeslava 3, 11000 Belgrade, SERBIA

<sup>2</sup>Earthe Climate Change Team (ECCTeam), Lake Oswego, Oregon, USA

<sup>3</sup>University of Kragujevac, Faculty of Agronomy, Cara Dušana 34, 32000 Čačak, SERBIA

<sup>4</sup>University of Priština, Kosovska Mitrovica, Faculty of Agriculture, Kopaonička nn,  
38219 Lešak, SERBIA

\*taca0526@gmail.com

### Abstract

*The study analyzed the heights of dominant fir trees from different regions. It was found that even when the trees were growing in the same type of soil, there were significant variations in their heights depending on their origin. Additionally, within the same region, the dominant heights of trees were significantly lower in the ranker compared to the district cambisol, except in the Olovo-Palež region.*

**Keywords:** dominant tree height, provenance, soil characteristics.

### INTRODUCTION

Over the past five decades, Serbia has undergone extensive reforestation initiatives, primarily focusing on conifer species to reclaim barren lands and rehabilitate degraded sites and stands. These reforestation efforts have predominantly involved Austrian pine, Scots pine, and spruce, with the notably limited participation of fir. Consequently, the growth characteristics of fir in artificially established stands, especially in stands established outside of the current fir habitats, are still insufficiently studied [1,2]. One of the primary objectives of provenance research is experimentally determining important hereditary traits, primarily growth patterns and tree vitality of a given species. This is particularly significant for fir, which exhibits a broad distribution across various habitats, giving rise to a wide variety of subspecies and ecotypes. By studying fir cultures in southwestern Serbia, where different fir provenances are planted side by side in the same site, a quantitative assessment of the success of their development was conducted.

### MATERIALS AND METHODS

This study entailed a comparative analysis of dominant fir tree heights within artificially established stands, comprising nine provenances planted in the *Fagetum montanum* site of southwestern Serbia, specifically at the Reštevo site. The fir provenance trial was established at an elevation of 1,000 m, with a slope of 10° and a northwestern aspect. The trial was set up in a degraded beech stand that had undergone clear-cutting. Following the felling of beech trees, the stumps were treated with oyster mushroom mycelium to suppress their sprouting

ability. Fir seedlings were propagated from seeds sourced from diverse locations within the natural fir range [3]. The sowing took place in 1988. After they had been nurtured in the nursery for three years, the seedlings underwent a two-year training period (3+2), meaning that they were five years old at the time of planting in the trial. After the research conducted in the nursery, a field trial was established, comprising the following nine provenances: Prozor (PR), Bugojno (BU), Olovo-Klis (OK), Sokolac (SO), Olovo-Palež (OP), Pale (PA), Fojnica (FO), Konjic (KO), and Petrovac (BP). The trial was organized using a block system (two blocks, each containing nine replications). Fir seedlings were planted at a spacing of 2 m between seedlings, while the spacing between blocks with different provenances was 4 m. Within each block, 64 seedlings of the same provenance were planted in a single plot. Thorough soil investigations were conducted within each block. The results were analyzed using analysis of variance (ANOVA), and the post hoc procedure was conducted using the Bonferroni and Holm multiple comparison method. Data processing utilized the R programming language. Table 1 presents fundamental data regarding the stands from which the seeds were sourced to establish the trial.

**Table 1** Fir Provenances – Site Characteristics of Parent Stands

Provenance	Soil	Site	Elevation (m)	Aspect	Slope (%)
Prozor (PR)	Calcomelanosol, Luvisol	<i>Piceo-Abietum Fagetum</i>	1.300	N-E	5–10
Bugojno (BU)	Calcocambisol	<i>Piceo-Abietum</i>	1.090	N-W	10–25
Olovo-Klis (OK)	Luvisol-calcocambisol	<i>Abieto-Picetum Illyricum</i>	850	N-W	13
Sokolac (SO)	Calcomelanosol	<i>Abietum Piceetum Syllicicolum</i>	940	S-W	13
Olovo-Palež (OP)	Calcocambisol, Luvisol	<i>Galio-Abietetum</i>	960	N-E	12
Pale (PA)	Dystric Cambisol, Calcomelanosol	<i>Abieto-Picetum Illyricum</i>	1.200	N-E	20
Fojnica (FO)	Dystric Cambisol	<i>Piceo-Abietum Syllicicolum</i>	1.010	-	-
Konjic (KO)	Calcocambisol, Calcomelanosol	<i>Abietum-Fagetum Illyricum</i>	1.030	E-NE	10–22
Petrovac (BP)	Calcocambisol, Pseudogley	<i>Abieto-Picetum Illyricum</i>	900	N	2

Source: [3].

## RESULTS AND DISCUSSION

### Soil characteristics

Table 2 displays the results regarding soil physical properties, while Table 3 outlines the chemical characteristics of the soil across different blocks.

#### Block A:

The terrain exhibits a slope of approximately 10° with a northwestern aspect. The depth of the topsoil layer exceeds 1m. Bedrock comprises sandstone, shale, and clay. The soil corresponds to a strongly acidic brown soil – dystric cambisol. Within the 0–32 cm depth, the humus-accumulative A horizon is dark brown with a black shade. Granulometric analysis reveals this horizon to be sandy clay loam containing 34.10% physical clay and

approximately 15% coarse sand. The entire horizon is permeated with plant root systems and contains 30% skeletal material. The structure is well-defined with a crumbly to fine-grained texture. The soil is moist and humus-rich (4.29%), characterised by a mull-moder humus. Environmental pH is highly acidic, with active acidity at 4.8 pH units, potential acidity at 4.8 pH units, and hydrolytic acidity at 80.50 ccm. Base saturation is notably low, at 13.9%, with a base sum of 8.46% mil/eq. Assimilable phosphorus levels are high, while nitrogen and potassium are at moderate levels. The transition to the middle horizon is distinctly defined. This (B) horizon, found at a depth of 33–65 cm, is brown in colour with pronounced coarse redoximorphic mottles. Regarding its granulometry, the soil is notably heavier, characterised as sandy clay loam with 52.50% physical clay and 40% skeletal content. Humus content (1.33) and nutrient levels exhibit a sharp decline. Environmental pH is slightly less acidic. Beneath lies the C horizon, spanning from 65 to 100 cm. It is of the same colour but with a slightly lighter shade. The share of large skeletal fragments ranges up to 70%. The soil quality surpasses that of previously described trial fields, particularly in terms of the depth of the topsoil and granulometric composition, as the (B) horizon comprises more clay, contributing to better soil moisture retention. Chemical properties mirror those of prior trial fields, with the environmental pH even more acidic.

*Table 2 Physical properties of soil*

Block	Soil Type	Depth	Coarse	Fine	Silt	Clay	Total	Total	Texture Class	
		(cm)	Sand	Sand			Sand	Clay		
		cm	%	%	%	%	%	%		
A	Dystric	0–32	15.00	50.90	22.70	11.40	65.90	34.10	Sandy Clay Loam	
	Cambisol	32–65	14.00	33.50	24.80	27.70	47.50	52.50	Sandy Clay Loam	
D	Ranker	0–36	7.50	65.10	18.50	8.90	72.60	27.40	Sandy Clay Loam	

*Table 3 Chemical properties of soil*

Profile number	Depth cm	Adsorptive complex				pH			Total		Available		
		T	S	T-S	V	Y1	H <sub>2</sub> O	KCl	Humus	N	P <sub>2</sub> O <sub>5</sub>	K <sub>2</sub> O	C/N
		eq. m.mol NaOH		%		ccm			%	%	mg/100g		
A	0–32	60.81	8.46	52.35	13.91	80.50	4.8	3.7	4.29	0.16	20.0	9.5	15.5
	32–65	46.33	9.95	36.38	21.48	56.00	5.0	3.7	1.33		4.2	8.2	
D	0–36	37.76	8.48	29.27	22.46	45.00	5.3	4.2	4.56	0.20	20.0	7.0	13.2

#### *Block D:*

The terrain has a slope of 35° and faces northwest. Surface rocks are absent. The depth of the topsoil layer is approximately 50 cm. Bedrock includes sandstone, shale, and clay. The soil type is brown ranker. The A (humus-accumulative) horizon ranges from 0 to 36 cm and exhibits a dark brown colour. Granulometrically, it is composed of sandy clay loam, with 27.40% physical clay and 7.50% coarse sand. The horizon is permeated with skeletal material, constituting 40%. The fine soil displays a stable, crumbly structure. Root systems extend to a depth of 26 cm, with some individual roots reaching depths of 50 cm. Compared to Profile 1, the soil in Block D is notably drier. It is porous, permeable, and penetrable. The mature mull humus content (C/N – 13.22) measures at 4.56%, while the environmental pH registers as acidic at 5.3 pH units in water. The degree of base saturation is around 20%. The soil is well-supplied with nitrogen (0.20%) and phosphorus (exceeding 20 mg P<sub>2</sub>O<sub>5</sub>/100g of

soil), though potassium levels barely reach the lower limit of moderate availability. The A-C/C horizon is 36–50 cm thick and exhibits a light brown coloration. This horizon has slightly higher moisture levels, with skeletal material constituting 90% of its volume, mixed with fine soil of similar physical and chemical properties. However, its productivity is constrained by a relatively shallow topsoil (approximately 5 cm) and the steep terrain, leading to intense erosion processes and significant forest damage caused by pruning.

### Height of dominant trees

In natural stands, fir trees undergo a notably slow growth in their youth, while in artificially established stands, they grow significantly faster, nearly matching the growth rate of spruce, Scots pine, and Austrian pine. For instance, fir trees on Mount Goč within a natural stand regenerated through seed cutting reach a height of only three meters by the age of 30 [4]. In the majority of the utilized provenances, fir trees demonstrate relatively rapid height growth, indicating their vitality and successful development. Variations in height among them stem from their natural characteristics and the ability of provenance to adapt to new site conditions.

The average heights of dominant trees for the two analyzed blocks and provenances are presented in Table 4. After forty years of growth, notable differences were observed in the total dominant tree height attained by specific provenances (Table 5).

**Table 4** Basic statistical indicators of dominant heights by provenance

Block	Height	Provenance								
		PR-1	BU-1	OK-1	SO-1	OP-1	PA-1	FO-1	KO-1	BP-1
Block A	Xmean	19.3	22.7	20.8	22.9	21.8	23.2	21.7	21.7	23.4
	Sd	1.8	1.0	1.9	1.7	1.6	2.1	1.4	1.1	1.0
	Kv%	9.3	4.3	9.3	7.4	7.2	9.2	6.5	5.3	4.2
Block D	Xmean	15.5	17.3	18.8	16.4	20.4	18.4	16.7	15.1	14.3
	Sd	0.9	2.1	1.3	1.0	2.1	1.2	1.2	2.4	1.9
	Kv%	6.0	11.9	7.1	6.1	10.1	6.3	7.4	16.1	13.3

Analysis of the provenance F-test showed significant differences between provenances within each analyzed block. The F-test value for Block A amounts to 6.02 (DF 9 and 72), whereas for Block D, it is 12.05 (DF 9 and 72).

In Block A, on dystric cambisol, significantly lowest dominant tree heights were observed in the Prozor (PR1) provenance (19.3 m), with notably lower values compared to the Bugojno (BU1), Sokolac (SO1), Olovo-Palež (OP1), Pale (PA1), and Petrovac (BP1) provenances. Additionally, significantly lower dominant heights were recorded for the Olovo-Klis (OK1) provenance compared to the Petrovac (BP1) provenance (Table 5).

On ranker soil, the Prozor (PR1) provenance in Block D exhibited significantly lowest dominant tree heights (19.3 m). These values were notably lower compared to the Olovo-Klis (OK4), Olovo-Palež (OP4), and Pale (PA4) provenances. Significantly lower values of dominant heights were observed for the Bugojno (BU4) provenance compared to the Olovo-Palež (OP4) and Petrovac (BP4) provenances. The Olovo-Klis (OK4) provenance demonstrated significantly higher dominant tree heights compared to the Konjic (KO4) and

Petrovac (BP4) provenances. The Sokolac (SO4) provenance displayed significantly lower heights of dominant trees than the Olovo-Palež (OP4) provenance. Moreover, the Olovo-Palež (OP4) provenance showed significantly higher growth of dominant trees compared to the Fojnica (FO4), Konjic (KO4), and Petrovac (BP4) provenances. Additionally, the Pale (PA4) provenance exhibited significantly greater heights of dominant trees compared to the Konjic (KO4) and Petrovac (BP4) provenances (Table 6).

**Table 5** Bonferroni and Holm multiple comparison method values between provenances in Block A

Provenience	PR-1	BU-1	OK-1	SO-1	OP-1	PA-1	FO-1	KO-1	BP-1
PR-1	-								
BU-1	4.68**	-							
OK-1	2.01	2.64	-						
SO-1	4.86**	0.18	2.81	-					
OP-1	3.38**	1.30	1.33	1.48	-				
PA-1	5.35**	0.66	3.30	0.49	1.96	-			
FO-1	3.29	1.40	1.23	1.58	0.09	2.06	-		
KO-1	3.23	1.45	1.18	1.63	0.15	2.11	0.05	-	
BP-1	5.58**	0.89	3.53**	0.72	2.06	0.23	2.29	2.35	-

**Table 6** Bonferroni and Holm multiple comparison method values between provenances in Block D

	PR-1	BU-1	OK-1	SO-1	OP-1	PA-1	FO-1	KO-1	BP-1
PR-1	-								
BU-1	2.30	-							
OK-1	4.12**	1.82	-						
SO-1	1.07	1.23	3.05	-					
OP-1	6.18**	3.88**	2.06	5.10**	-				
PA-1	3.68**	1.39	0.43	2.61	2.49	-			
FO-1	1.52	0.78	2.59	0.45	4.66**	2.16	-		
KO-1	0.56	2.87	4.68**	1.63	6.74**	4.25**	2.09	-	
BP-1	1.54	3.85**	5.67**	2.62	7.73**	5.23**	3.07	0.98	-

Through the application of Bonferroni and Holm t-statistic and conducting tests on the same provenances growing on different soil types, it was observed that provenances planted on dystric cambisol (Block A) exhibited significantly greater heights of dominant trees compared to those planted on ranker soil (Block D). The exception to this trend was the Olovo-Palež provenance, for which the difference was not statistically confirmed (Table 7).

**Table 7** Bonferroni and Holm multiple comparison method values of the same provenance between blocks

Provenience	Bonferroni and Holm t-statistic	Bonferoni inference	Holm inference
PR1 vs PR2	5.61	<0.01	<0.01
BU1 vs BU2	7.08	<0.01	<0.01
OK1 vs OK2	2.59	<0.05	<0.05
SO1 vs SO2	9.93	<0.01	<0.01
OP1 vs OP2	1.63	insignificant	insignificant
PA1 vs PA2	5.92	<0.01	<0.01
FO1 vs FO2	7.96	<0.01	<0.01
KO1 vs KO2	7.32	<0.01	<0.01
BP1 vs BP2	12.62	<0.01	<0.01



## **CONCLUSIONS**

Our research has revealed significant differences in the heights of dominant trees from different provenances. Testing these heights on different soil types showed that, for all provenances (except Olovo-Palež), heights were notably greater on dystric cambisol compared to ranker soil. This underscores the importance of soil type as a significant factor influencing the height of dominant fir trees. In forest management practices, it is crucial to recognise soil type as an indicator of site fertility for fir trees. Additionally, dominant heights play a pivotal role in determining Site Index or productivity classes, which should be carefully considered in future afforestation or reforestation initiatives aimed at rehabilitating degraded forests.

## **ACKNOWLEDGEMENTS**

*The authors are grateful to the Ministry of Science, Technological Development and Innovation of the Republic of Serbia for financial support (451-03-66/2024-03/200027; 451-03-66/2024-03/200088 and 451-03-65/2024-03/200189).*

## **REFERENCES**

- [1] Gagov V., Ergebnisse des 8. Tannen-Symposiums: Schriften aus der IUFRO und der Forsttechnischen Universität Sofia, Sofia, Bulgarien (1997) 89–108.
- [2] Ratknic M., Vuckovic M., Stamenkovic V. *et al.*, Mitteilungen aus der Forschungsanstalt für Waldökologie und Forstwirtschaft, Rheinland – Pfalz. 50/3 (2002) 59–67.
- [3] Ballian D., Halilović V., Varijabilnost obične jele (*Abies alba* Mill.) u Bosni i Hercegovini (Variability of the Silver Fir (*Abies alba* Mill.) in Bosnia and Herzegovina), Udruženje inženjera i tehničara Federacije Bosne i Hercegovine (UŠIT FBiH, Silva Slovenica – izdavački centar Šumarskog instituta Slovenije, Ljubljana (2016), p.350, ISBN: 978-9926-8071-0-8.
- [4] Stamenković V., Vučković M., Ratknić M., Ergebnisse des 8. Tannen-Symposiums: Schriften aus der IUFRO und der Forsttechnischen Universität Sofia, Sofia, Bulgarien (1997) 185–192.



## AGITATION LEACHING OF FLOTATION TAILINGS AT THE PILOT PLANT

Dragana Božić<sup>1\*</sup>, Ljiljana Avramović<sup>1</sup>, Vanja Trifunović<sup>1</sup>, Radmila Marković<sup>1</sup>,  
Zoran Stevanović<sup>1</sup>, Vesna Marjanović<sup>1</sup>, Emina Požega<sup>1</sup>

<sup>1</sup>Mining and Metallurgy Institute Bor, Albert Einstein 1, 19210 Bor, SERBIA

\*dragana.bozic@irmbor.co.rs

### Abstract

*Flotation waste, which was produced through seventy years of copper ore processing in RTB Bor, Serbia, is deposited in a flotation tailings pond. In total, almost 22.3 Mt could be considered as available for eventual reprocessing and reuse. Chemical analysis had shown that an average concentration of targeted metals in the tailings is: 0.23% Cu, 0.53 g/t Au and 2.83 g/t Ag. Physical characteristics of representative sample of flotation tailings composites include determination of sample density, bulk density and sample pH. Based on the obtained results of the granulometric analysis, it can be concluded that in the sample 66.50% of the particles are smaller than 75 µm in size. The leaching degrees of the analyzed elements, based on the results of chemical analyzes of the solid residue, achieved after leaching of the composite sample of flotation tailings at the pilot plant were recalculated and are: 75.67% Cu, 16.48% Fe, 4.76% Ag and 5.6% Au.*

**Keywords:** leaching, flotation tailings, pilot plant.

### INTRODUCTION

In the process of flotation of copper ore, flotation tailings containing metal sulfides are separated and represent a special challenge for the topic of mining waste management. Due to the formation of acid mine waters (AMD) and the exposure of tailings to atmospheric oxygen, bacteria and water, metals from tailings are dispersed into the environment, which directly affects the degradation of the quality of surface and underground water as well as the surrounding soil [1,2].

Due to the increased exploitation of copper ores and the discovery of low-quality deposits, it can be expected that more tailings will be present in the coming years, which could cause more environmental problems and challenges to solve them.

Considering the fact that the recovery of copper from the ore through the flotation process is about 56%, this indicates that the flotation tailings contain valuable copper components. In addition, old flotation tailings sometimes have higher copper content (0.2–0.4% Cu) than low-grade ores (0.2–0.3% Cu). The copper content of old flotation tailings is similar to the world average content of about 0.4% Cu for copper in mined ore. Considering the current price of copper and predictions that demand for copper will increase, flotation tailings and low-grade copper ores represent a potential future source of copper.

Compared to pyrometallurgical processes, hydrometallurgical treatment has greater potential for treating complex low-grade sulphide ores and concentrates, resulting in increased metal recovery and reduced air pollution hazards. In recent years, research and development

of hydrometallurgical processes has intensified as an alternative to pyrometallurgical treatment.

The calculated mean contents of the deposit of man-made mineral raw materials in the area of the Old Flotation Tailings, calculated on the basis of data obtained during the entire research period (1961/62, 2007, 2015/16, 2016/17, and 2017/18), amount to: 0.530 g/t Au ; 2.826 g/t Ag and 0.230% Cu. It should be noted that during the research period, 1961/62 and during 2007, taken samples were not analyzed for gold and silver, but only for Cu [3].

The calculated reserves of the technogenic deposit amount to 22.3 Mt of mineral raw material, with about 12 t of Au, 63 t of Ag and 51,303 t of Cu metal. On the basis of the above, it can be concluded that significant amounts of gold, copper and silver are present in the flotation tailings, and that a significant profit would be achieved by valorizing them. Over the years, experience has taught us that flotation tailings ponds, containing many hazardous components, negatively affect the environment [4–6].

The aim of this paper was to confirm the leaching of Cu as an adequate process for hydrometallurgical extraction of copper from flotation tailings at the pilot plant after the laboratory tests were completed. And also to consider adequate treatment of the solid residue that is formed in the acid leaching process of copper and in which precious metals are concentrated: gold and silver.

The paper contains a systematized review of physical characteristics and granulometric analysis of representative sample of flotation tailings composite which is acid leached at atmospheric pressure on an enlarged scale – at a pilot plant.

## **MATERIALS AND METHODS**

In this paper, composite samples of flotation tailings with the following designations were used for the planned experimental tests of the leaching process of copper, gold and silver from the tailings of the Old Flotation Tailings:

Composite I + III was formed from samples from the part of the tailings that includes the Old French tailings and Field 1 with an estimated total amount of tailings of 14,862,708 t, which represents about 60% of the total amount of tailings. The estimated metal content is: 37,157 t Cu + 6.7 t Au + 20.0 t Ag.

## **RESULTS AND DISCUSSION**

### **Physical-chemical characterization of the samples**

Physical characteristics of representative samples of flotation tailings composites include determination of sample density, bulk density and sample pH. The results of physical characterization of representative samples of flotation tailings composites are shown in Table 1.

**Table 1** Physical characterization of representative composite samples of flotation tailings

Sample	Density (g/cm <sup>3</sup> )	Bulk mass (kg/m <sup>3</sup> )	pH
COMPOSITE I+III	2.765	1176.0	2.82

In Table 2 the chemical characterization of representative sample of flotation tailings composites is presented.

**Table 2** Chemical composition of representative sample of flotation tailings composite I + III

Element	Unit	Content	Analytical method*
Cu <sub>uk</sub>	%	0.25	AAS
Cu <sub>ox</sub>	%	0.18	AAS
Fe	%	7.62	ICP-AES
Ca	%	0.78	ICP-AES
K	%	0.54	ICP-AES
Na	%	0.23	ICP-AES
S	%	9.34	ACS
SiO <sub>2</sub>	%	52.88	G
Al <sub>2</sub> O <sub>3</sub>	%	10.76	ICP-AES
Au	ppm	0.45	FA/AAS
Ag	ppm	1.40	FA/AAS
Sr	ppm	648	ICP-AES
As	ppm	122	ICP-AES
Zn	ppm	23.6	ICP-AES

\* AAS - Atomic Absorption Spectrophotometer

ICP-AES - Inductively Coupled Plasma Atomic Emission Spectrometry

ACS - Carbon and Sulfur Analyzer

G - Gravimetry

FA - flame analysis of precious metals (cupellation)

Based on the copper analysis shown in Table 2, it can be stated that the share of oxide copper in relation to total copper for the examined composite samples is as follows:

$$\text{COMPOSITE I + III: Cu oxide/Cu total} = 0.18/0.25 = 0.72 \text{ (72\%)}$$

### Granulometric composition of the sample

The granulometric composition of sample of the flotation tailings composite was determined by the sieving method on laboratory sieves made of fine mesh, wire and perforated metal plate (SRPS ISO 2591-1:992).

Based on the obtained results of the granulometric analysis, it can be concluded that in the sample COMPOSITE I+III, 66.50% of the particles are smaller than 75 µm in size (Table 3).

**Table 3** The granulometric composition of the flotation tailings composite sample COMPOSITE I+III

d (mm)	m (%)	R (%)	D (%)
-4+2.36	7.60	7.60	100.0
-2.36+1.70	0.20	7.80	92.40
-1.70+0.850	0.40	8.20	92.20
-0.850+0.600	0.40	8.60	91.80
-0.600+0.425	0.30	8.90	91.40
-0.425+0.300	6.70	15.60	91.10
-0.300+0.212	1.10	16.70	84.40
-0.212+0.150	4.40	21.10	83.30
-0.150+0.106	6.30	27.40	78.90
-0.106+0.075	6.10	33.50	72.60
-0,075+0.053	5.50	39.00	66.50
-0.053+0.038	5.50	44.50	61.00
-0.038+0.00	55.50	100.00	55.50

### Copper leaching from the sample composite I+III

In a reactor made of poly-propylene, with a volume of 100 L, the leaching experiment of a composite sample of flotation tailings COMPOSIT I+III in an amount of 15 kg was carried out, under optimal conditions previously defined by laboratory tests (particle size:  $-75 \mu\text{m}$ , without the addition of oxidants, temperature: ambient, ratio of solid and liquid phase: 1:4, time: 4h, pH of the suspension:  $\text{pH}=1$ . To correct the pH value from  $\text{pH} 2.9$  to  $\text{pH} 1$ , it was added 600 ml of concentrated  $\text{H}_2\text{SO}_4$ , which represents the consumption of concentrated sulfuric acid of 70 kg per ton of tailings.

Apparatus for performing enlarged experimental testing of the copper agitation leaching process at the pilot plant is shown in Figure 1.

After the leaching process was completed, the suspension was filtered on a plan filter (Figure 1), and the solid residue was washed with water that was mixed with the alkaline solution. The volume of alkaline solution and rinse water was 87 L.



**Figure 1** Leaching and filtering of the composite sample of flotation tailings COMPOSITE I+III at the pilot plant

The solid residue was dried in a dryer to a constant mass of 12.5 kg, sampled, its physico-chemical characterization was performed (Table 4 and Table 5), and its granulometric composition was determined, the results of which are shown in Table 6.

**Table 4** Results of physical characterization of the solid residue (T-SFJ-PILOT)

Sample	Unit	Value	
T-SFJ-PILOT	Sample mass	kg	13.2
	Moisture	%	0.90
	Bulk mass	kg/m <sup>3</sup>	1120
	Density	kg/m <sup>3</sup>	2840
	pH	/	2.72

**Table 5** Results of the chemical analysis of the solid residue after copper leaching from the composite sample COMPOSIT I+III

Element	Cu (%)	Fe (%)	Ag (g/t)	Au (g/t)
Content	0.073	6.15	1.6	0.51

Based on the results of chemical analyzes of the solid residue, the leaching degrees of the analyzed elements achieved after leaching of the composite sample of flotation tailings I+III at the pilot plant were recalculated and are: 75.67% Cu, 16.48% Fe, 4.76% Ag and 5.6 % Au, which is in agreement with the results obtained at the laboratory level. Given that the content of oxide copper in the composite sample of flotation tailings I+III is 72% (based on the data shown in Table 2), we can state that the copper present in the oxide form was completely leached in the sulfuric acid solution without heating, in a time of 4h and at the ratio of solid and liquid phase 1:4.

**Table 6** Granulometric composition of the solid residue after leaching of the composite sample COMPOSIT I+III

d (mm)	m (%)	R (%)	D (%)
-0.300+0.212	1.00	1.00	100.00
-0.212+0.150	3.00	4.00	99.00
-0.150+0.106	6.00	10.00	96.00
-0.106+0.075	5.50	15.50	90.00
-0.075+0.053	4.50	20.00	84.50
-0.053+0.038	6.00	26.00	80.00
-0.038+0.020	10.50	36.50	74.00
-0.020+0.00	63.50	100.00	63.50

Based on the obtained results of granulometric analysis, it can be concluded that 90% of the sample of solid residue obtained after agitation leaching of the composite sample of flotation tailings COMPOSIT I+III at the pilot plant consists of particles smaller than -75  $\mu\text{m}$ .

## CONCLUSION

This paper presents the results of copper agitation acid leaching at atmospheric pressure for 4 hours, with a ratio of solid to liquid phase 1:4, and a concentration of sulfuric acid of 1.7% H<sub>2</sub>SO<sub>4</sub> at ambient temperature. Leaching was carried out at the pilot plant, during which



15 kg of flotation tailings were leached. The results showed that under these conditions the percentage of Cu leaching was over 75%.

#### **ACKNOWLEDGEMENT**

*This work was financially supported by the Ministry of Science, Technological Development and Innovation of the Republic of Serbia, Contract on realization and financing of the scientific research work of the Mining and Metallurgy Institute Bor in 2024, contract number: 451-03-66/2024-03/200052.*

#### **REFERENCES**

- [1] Hansen H.K., Lamas V., Gutierrez C., *et al.*, Miner. Eng. 41 (2013) 1–8.
- [2] Hansen H.K., Yianatos J.B., Ottosen L.M., Chemosphere 60 (2005) 1497–1503.
- [3] Mitrović Z., Jovanović R., Seventy Five Years of the RTB Flotation Concentrators, RTB Bor and Megatrend University, Bor, (2007), p. 266 (in Serbian).
- [4] Andrade S., Moffett J., J.A. Correa. Mar. Chem. 101 (2006) 203–212.
- [5] Schoenberger E., Resour. Policy 49 (2016) 119–128.
- [6] Lutandula M.S., Maloba B., J. Environ. Chem. Eng. 1 (2013) 1085–109.



## FOREST FRUIT SPECIES OF URBAN FOREST “KOŠUTNJAK” (SERBIA) – GENEPOOL ASSESSMENT AND CONSERVATION

Ivona Kerkez Janković<sup>1\*</sup>, Dragica Vilotić<sup>1</sup>, Marina Nonić<sup>1</sup>, Jovana Devetaković<sup>1</sup>,  
Mirjana Šijačić-Nikolić<sup>1</sup>

<sup>1</sup>University of Belgrade – Faculty of Forestry, Kneza Višeslava 1, 11030 Belgrade, SERBIA

\*ivona.kerkez@sfb.bg.ac.rs

### Abstract

Forest fruit species are important components of forest ecosystems in many aspects, as a food source for birds and small mammals; they attract and keep pollinators, and have an esthetic role in urban forests, especially during the flowering season. The potential impact of urbanization and pollution on their health and survival can significantly damage the balance of the ecosystem and represent a biodiversity loss. Aim of this paper was to identify individuals and groups of forest fruit species in the urban forest “Košutnjak” and to establish foundational knowledge about locally available gene pool recourses for further in situ and ex situ conservation. The protected area “Košutnjak Forest” is located in Belgrade, the capital of Serbia, with 1.6 million inhabitants. The entire area (330 ha) of the urban forest is under the strong anthropopressure. A significant number of species were found, 21 wild woody fruit species belonging to 7 families and 11 genera. Eight species in the shrub form: *Cornus mas*, *Cornus sanguinea*, *Corylus avellana*, *Crataegus monogyna*, *Rosa arvensis*, *Rosa canina*, *Rubus hirtus*, and *Sambucus nigra*, and 13 in the tree form, 9 native: *Prunus cerasifera*, *Prunus domestica*, *Prunus avium*, *Pyrus pyraster*, *Malus sylvestris*, *Sorbus domestica*, *Sorbus torminalis*, *Corylus colurna*, *Juglans regia*, *Castanea sativa*, and 4 non-native: *Juglans nigra*, *Morus alba*, *Morus nigra* and *Prunus serotina*, were found. The database of forest fruit species gene pool is deposited in the Center for Monitoring and Conservation of Forest Genetic Resources at the University of Belgrade - Faculty of Forestry.

**Keywords:** anthropopressure, forest ecosystem stability, biodiversity, dynamic conservation.

### INTRODUCTION

Forest ecosystems are under the strong pressure concerning climate change and a variety of human activities [1]. Evolution and adaptation of most European species have been done under variety of natural changes, but nowadays human disturbances and management practices have an enormous impact on biodiversity conservation and ecosystem functions [2], due to the continuous process of pollution, fragmentation and implementation of other forms of land use [3]. Among all forest ecosystems, urban forests are the one most exposed to significantly higher level of anthropopressure [4]. However, urban park forests have a high biodiversity value as they improve urban environment. They serve as biofilters that reduce the level of air and acoustic pollution [4], as a refuge habitat of flora and fauna and as areas of importance for species recovery and nature conservation [5]. The conservation and promotion of urban forest ecosystems should begin with gathering knowledge about the biodiversity they harbor.

According to the EUFORGEN Noble Hardwood Network Report [6], European long-term gene conservation strategy for noble hardwoods is necessary to gain knowledge about populations, on local and European level. The first step in that direction is identification of species and the *in situ* conservation of the local gene [7].

Many of forest wild fruit species in tree form belong to the group of noble hardwoods, such as *Sorbus* spp., *Prunus avium* L., *Pyrus pyraster* (L.) Burgsd., etc. They also attract and keep pollinators, and have an aesthetic function, especially during the flowering season. Forest wild fruit species play a key role in protecting biodiversity as they represent a source of food and shelter for birds, small mammals and insects. According to Wolf *et al.* [8] identification of individuals, groups or stands of wild fruit tree species is the first step for *in situ* and *ex situ* conservation and for the further utilization of available gene pool.

This research aimed to identify individuals and groups of forest fruit species in the urban forest “Košutnjak” and to establish foundational knowledge about locally available gene pool recourses for further *in situ* and *ex situ* conservation. Additionally, to consider possibilities and perspectives for direct utilization of the available gene pools in the future.

## MATERIALS AND METHODS

### Study site

The Natural monument “Košutnjak” Forest is one of the only two remnants of indigenous forest vegetation in the densely populated urban structure [9]. It is located above the left bank of the Topčiderska River in capital of Serbia – Belgrade. Altitude ranges from 75 to 216.9 masl with a dynamic landscape with very steep slopes sometimes exceeding 70% [10]. In Košutnjak, forest ecosystems are predominantly deciduous, with a small proportion of the conifers. The occurrence of 521 plant species has been recorded in this area [4]. Given that 3730 species grow in Serbia, this number indicates a high floristic diversity according to the criteria of vascular plants diversity [11]. It is declared protected due to significant spatial functions and bioecological values of the complex under forest vegetation and to preserve the habitat of diverse fauna of mammals, birds, insects, reptiles and amphibians, as well as signs of geological discovery [10]. There are two protection regimes. The largest part of forest (265 ha) is under the third (III) degree protection regime and the smaller part under the second degree protection regime – Natural reserve Forest of oak and hornbeam at Hajdučka fountain that has been protected since 1981 (3.5 ha) [9].

### Data collection and analysis

The research methodology is described in previously published researches [12–14], as an integrative methodological framework for conservation of genetic resources in urban park forests. After the field survey and identification of woody plant species we carried out an assessment of the degree of endangerment of woody plant species and focused on forest fruit species due to their rarity and endangerment. Both, the tree and shrub forms of the forest fruit species were examined. The species in tree form considered for the *ex situ* conservation were georeferenced. Coordinates for each tree were exported from the UTM Geo Map application to the Google Earth software. As a basis, a vector representation of the boundaries of the compartment and sub-compartment NM “Košutnjak” was used. In this way, the position of

the trees within the NM was additionally checked. The database of selected individuals is deposited in the Center for Monitoring and Conservation of Forest Genetic Resources at the University of Belgrade - Faculty of Forestry.

## RESULTS AND DISCUSSION

After the field survey and identification of woody plant species which included site reconnaissance and species identification, a considerable number of forest fruit species were found – 21 wild woody fruit species belonging to 7 families and 11 genera (Table 1). Eight species in the shrub form: *Cornus mas*, *Cornus sanguinea*, *Corylus avellana*, *Crataegus monogyna*, *Rosa arvensis*, *Rosa canina*, *Rubus hirtus*, and *Sambucus nigra*, and 13 in the tree form. Nine of them were native: *Prunus cerasifera*, *Prunus domestica*, *Prunus avium*, *Pyrus pyraster*, *Malus sylvestris*, *Sorbus domestica*, *Sorbus torminalis*, *Corylus colurna*, *Juglans regia*, *Castanea sativa*, and four non-native: *Juglans nigra*, *Morus alba*, *Morus nigra* and *Prunus serotina*. According to the IUCN [15] categorization, most species are in the “last concern” category, except apple and plums which are “data deficient”. Common dogwood, field rose and blackberry are not evaluated (NE). On the national level, according to Banković *et al.* [16] many of identified species are not evaluated (NE). However, European wild pear and wild service tree are in the category “at risk”; European wild apple and Persian walnut are considered as “rare/endangered” and Turkish hazel as “tertiary relict” (Table 1).

Based on the field survey and species identification considering both, national and IUCN [15] categories, evaluation of species status in NM “Košutnjak” Forest was done (Table 1). All the species in shrub form were abundantly present and considered as “last concern”. The only threat to these species in future could be negative human activities (eg. fire, over-consumption of fruits, destroying of habitat by urbanization). The most critical (CR) is true service tree genepool, represented by very few individuals (Figure 1). Wild service tree was categorized as “endangered” since it only occurs in a limited distribution range, as well as wild apple and wild pear. Common plum, sweet cherry and sweet chestnut were considered as “vulnerable” as the health status of the most individuals is very poor. Considering all factors, Turkish hazel and cherry plum were considered as “near treated”.

Despite the antropopressure, urban forests are biodiversity refugee in city limited space. Conservation of forest biodiversity, have great influence on the sustainable management of forest ecosystems [17]. The implementation of the genetic conservation framework [12], considering both *in situ* and *ex situ* conservation model, could ensure the long-term monitoring, protection and dynamic conservation of the woody forest fruit species in NM “Košutnjak Forest”. All the species, except ones categorized as “last concern” should be conserved *in situ*. *Ex situ* conservation is considered for *Sorbus torminalis*, *Sorbus domestica*, *Pyrus pyraster* and *Prunus avium*, and individuals of these species were georeferenced (Figure 1).



**Table 1** Identified wild forest woody fruit species in NM “Košutnjak Forest”

Species name		Protection status		Evaluated status in NM “Košutnjak Forest”
lat.	engl.	national category <sup>a</sup>	IUCN category <sup>b</sup>	
<i>Castanea sativa</i> Mill.	Sweet Chestnut	NE	LC	VU
<i>Cornus mas</i> L.	Cornelian Cherry	NE	LC	LC
<i>Cornus sanguinea</i> L.	Common Dogwood	NE	NE	LC
<i>Corylus avellana</i> L.	Hazel	NE	LC	LC
<i>Corylus colurna</i> L.	Turkish Hazel	tertiary relict	LC	NT
<i>Crataegus monogyna</i> Jacq.	Common Hawthorn	NE	LC	LC
<i>Juglans nigra</i> L.	Black Walnut	NE	LC	LC
<i>Juglans regia</i> L.	Persian Walnut	rare/endangered	LC	LC
<i>Malus sylvestris</i> (L.) Mill.	European Wild Apple	rare/endangered	DD	EN
<i>Morus alba</i> L.	White Mulberry	NE	LC	LC
<i>Morus nigra</i> L.	Black Mulberry	NE	LC	LC
<i>Prunus avium</i> L.	Sweet Cherry	at risk	LC	VU
<i>Prunus cerasifera</i> Ehrh.	Cherry Plum	NE	DD	NT
<i>Prunus domestica</i> L.	Common Plum	NE	DD	VU
<i>Prunus serotina</i> Ehrh.	Black Cherry	NE	LC	LC
<i>Pyrus pyraster</i> (L.) Burgsd.	European Wild Pear	at risk	LC	EN
<i>Rosa arvensis</i> Huds.	Field Rose	NE	NE	LC
<i>Rosa canina</i> L.	Dog Rose	NE	LC	LC
<i>Rubus hirtus</i> Waldst. & Kit.	Blackberry	NE	NE	LC
<i>Sambucus nigra</i> L.	European Elder	NE	LC	LC
<i>Sorbus domestica</i> (L.) Spach	True Service Tree	NE	LC	CR
<i>Sorbus torminalis</i> (L.) Crantz	Wild Service Tree	at risk	LC	EN

\* <sup>a</sup> according to Banković *et al.* [16]; <sup>b</sup> IUCN [15] category: NE- not evaluated; DD – data deficient; LC – last concern; NT – near threaten; VU – vulnerable; EN – endangered; CR – critically endangered

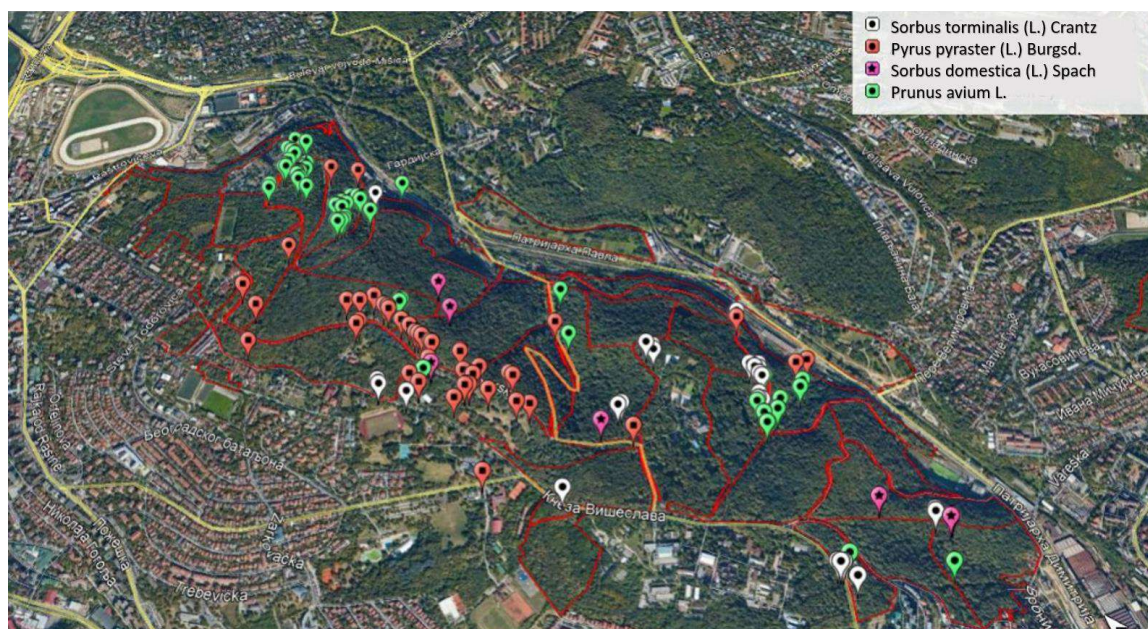


**Figure 1** Individuals representing genepool of wild service tree, true service tree, wild pear and sweet cherry

Considering the importance of urban park forests and their vulnerability due to many factors, the implementation of the concept of genetic conservation is one of the most important ways to preserve and improve these ecosystems. Many of these species have been considered for conservation at the European level for many years [6,18–21], but despite that not many conservation units of these species have been found in Europe [22]. Since, every urban forest could be considered as unique city area and a refuge for wildlife and all species found play an important role in biodiversity enrichment, the establishment of conservation programs for specific species or habitats would lead to the better protection of the entire ecosystem.

## CONCLUSION

Conservation of forest fruit species using metodological framework and both *in situ* and *ex situ* conservation model in urban forest such as Košutnjak would lead to benefit both human and flora and fauna of the urban area. All of the found forest fruit species should be considered for *in situ* conservation method. *In situ* conservation could be applied to a single species or to an entire habitat. At least nine native forest fruit species should be considered for *ex situ* conservation method in future. The overall conclusion of this study is that the NM “Košutnjak” Forest is home to 21 forest fruit species and that this urban forest should be considered as unique habitat that needs further effort on implementation of the concept of *in situ* and *ex situ* genetic conservation.

## ACKNOWLEDGEMENT

*This work was supported by the Secretariat for Environmental Protection of the City of Belgrade, project: Identification and monitoring of the gene pool of rare, vulnerable and endangered plant species in NM “Kosutnjak Forest”.*

## REFERENCES

- [1] Bengtsson J., Nilsson S.G., Franc A., *et al.*, For. Ecol. Manag. 132 (1) (2000) 39–50.
- [2] Perez-Espona S., ConGRESS Consortium, Biol. Conserv. 209 (2017) 130–136.
- [3] Tyrväinen L., Miettinen A., JEEM 39(2) (2000) 205–223.
- [4] Rašković D., Bull. Serb. Geog. Soc. 95 (4) (2015) 195–214.
- [5] Milovanović B., Trikić M., Jovanović B., *et al.*, Study of the Protection of the Natural Monument 'Miljakovačka Šuma'. Institute for Nature Conservation of Serbia, Belgrade (2012).
- [6] Turok J., Eriksson G., Kleinschmit J., Canger S., compilers. 1996. Noble Hardwoods Network. Report of the first meeting, 24–27 March 1996, Escherode, Germany. International Plant Genetic Resources Institute, Rome (1996), p.172, ISBN 92-9043-291-8.
- [7] Šijačić-Nikolić M., Milovanović J., Conservation of Plant Species *in Life on Land*, Editor: Leal Filho W., Azul A., Brandli L., Özuyar P., Wall T., Springer, Berlin (2019), ISBN: 978-3-319-71065-5.
- [8] Wolf H., Arenhövel W., Behm A., *et al.*, Acta Hort. 538 (2000) 57–62.



- [9] Lukić D., Andonović M., Zatezalo A., *et al.*, Study of the Protection of the Natural Monument 'Košutnjak Forest' – Proposal for Protection. Institute for Nature Conservation of Serbia, Belgrade (2012).
- [10] Proposed management plan of NM “Košutnjak Forest” (2025–2034). Public Enterprise for Forest Management “Srbijašume”, Forest management “Belgrade”, 2024, 1–55.
- [11] Jovanović S., Stojanović V., Lazarević P., *et al.*, Bot. Ser. 38 (2) (2014) 201–207.
- [12] Šijačić-Nikolić M., Nonić M., Perović M., *et al.*, IOP Conference Series: Earth and Environmental Science 1 (1). IOP Publishing. (2021) p.012002.
- [13] Šijačić-Nikolić M., Nonić M., Kerkez Janković I., *et al.*, Proceedings of the International Scientific Conference „Forestry science for sustainable development – FORS<sup>2</sup>D: Perspectives of forestry and related sectors as drivers of sustainable development in the post-Covid era“, 29–30 September, Banja Luka, Bosnia and Herzegovina (2022) 143.
- [14] Šijačić-Nikolić M., Nonić M., Gene pool of woody species of the Natural Monument 'Košutnjak Forest' – conservation and sustainable use, University of Belgrade, Faculty of Forestry, Belgrade (2023), p.200, ISBN: 978-86-7299-363-9.
- [15] IUCN. Available on the following link: <https://www.iucnredlist.org/>.
- [16] Banković S., Medarević M., Pantić D., *et al.*, Bull. Fac. For. 100 (2009) 7–29.
- [17] Šijačić-Nikolić M., Milovanović J., Bull. Fac. For. 95 (2007) 7–21.
- [18] Demesure-Musch B., Oddou-Muratorio S., 2004. EUFORGEN Technical Guidelines for genetic conservation and use for wild service tree (*Sorbus torminalis*). International Plant Genetic Resources Institute, Rome, Italy. 6 pages.
- [19] Rotach P., 2003. EUFORGEN Technical Guidelines for genetic conservation and use for service tree (*Sorbus domestica*). International Plant Genetic Resources Institute, Rome.
- [20] Russell K., 2003. EUFORGEN Technical Guidelines for genetic conservation and use for wild cherry (*Prunus avium*). International Plant Genetic Resources Institute, Rome, Italy.
- [21] Stephan B.R., I.Wagner, Kleinschmit J., 2003. EUFORGEN Technical Guidelines for genetic conservation and use for wild apple and pear (*Malus sylvestris* and *Pyrus pyraeaster*). International Plant Genetic Resources Institute, Rome, Italy. 6 pages.
- [22] EUFGIS. Available on the following link: <http://portal.eufgis.org/data/>.



## NEW DATA ON THE DISTRIBUTION OF AQUATIC BEETLES IN SERBIA

**Boris Novaković<sup>1\*</sup>, Nikola Paskaš<sup>1</sup>, Marko Raković<sup>2</sup>**

<sup>1</sup>Serbian Environmental Protection Agency, Ministry of Environmental Protection,  
Žabljačka 10A, 11160 Belgrade, SERBIA

<sup>2</sup>University of Belgrade-Institute for Multidisciplinary Research, Kneza Višeslava 1,  
11030 Belgrade, SERBIA

\*boris.novakovic@sepa.gov.rs

### Abstract

*New distributional data on 43 aquatic beetle species of Serbia from 17 sampling sites, mainly for Vojvodina (the part of Pannonian Plain) are provided. The field research was carried out in 2013–2023 (one decade). The rarity of findings particularly expressed in small lowland streams, such as those for Vojvodina revealed some aquatic beetle species are tolerant to water pollution. The study's main goal is to contribute to aquatic beetle taxa distribution in Serbia since the aquatic beetle fauna of Serbia is poorly explored in general. Further research should focus on habitat preference of aquatic beetle species and better conservation of small aquatic habitats.*

**Keywords:** aquatic beetles, new findings, distribution, Serbia.

### INTRODUCTION

With more than 13,000 described species water beetles are one of the most globally abundant groups of aquatic insects. Among insect orders, only Diptera has more aquatic taxa (though just as larvae) than Coleoptera, and the two largest water beetle families, Dytiscidae and Hydrophilidae, each have more species than either Ephemeroptera or Plecoptera [1]. Counting the presently described species, the Palearctic Region houses the highest number of water beetle species. Although comprehensive water beetle surveys are still lacking for large parts of the Neotropical and Afrotropical Realms, it is estimated (after including the undescribed species) that the Palearctic (ca. 3,350 described species/ca. 3,900 estimated total), the Neotropical (2,510/3,900), and the Afrotropical Region (2,700/3,750) harbor more or less the same number of water beetle species, followed by the Oriental (2,200/3,580) and the Australian/Pacific Realm (1,340/2,100). Undoubtedly, the Nearctic (1,420/1,550) is by far the poorest region in terms of water beetle diversity [2].

Within the Palearctic Region, the Mediterranean countries and Anatolia are regarded as biodiversity hot spots, at least for certain families [2]. However, the aquatic beetle fauna of Serbia and the Balkan Peninsula is insufficiently known. Therefore, this paper aims to present new data on the distribution of the aquatic beetle species of Serbia during ten years (2013–2023).

## MATERIAL AND METHODS

Aquatic beetle samples were taken using a hand net (25x25 cm, 500 µm mesh size) or specimens were manually collected using a tweezer. The samples were collected in the period 2013–2023 (one decade). Most aquatic beetle specimens are collected with other benthic invertebrate samples during the Regular Annual Water Monitoring programmes conducted by the Serbian Environmental Protection Agency (SEPA). The multi-habitat sampling procedure [3] and AQEM protocol [4] were applied. The samples were preserved using 70–90% ethyl-alcohol. The number of collected imago specimens is expressed by using the abbreviation ex. (exemplar) while larval specimens as Lv. Containers were labeled with all necessary information, and transported to the laboratory for sorting, counting, and identification. For identification, we used the stereomicroscope Carl Zeiss StereoDiscovery V.8 with Axio Cam ICc5 and ZEN2 imaging software by using appropriate taxonomic keys [5–8].

A map of aquatic beetle sampling sites in Serbia is provided (Figure 1).

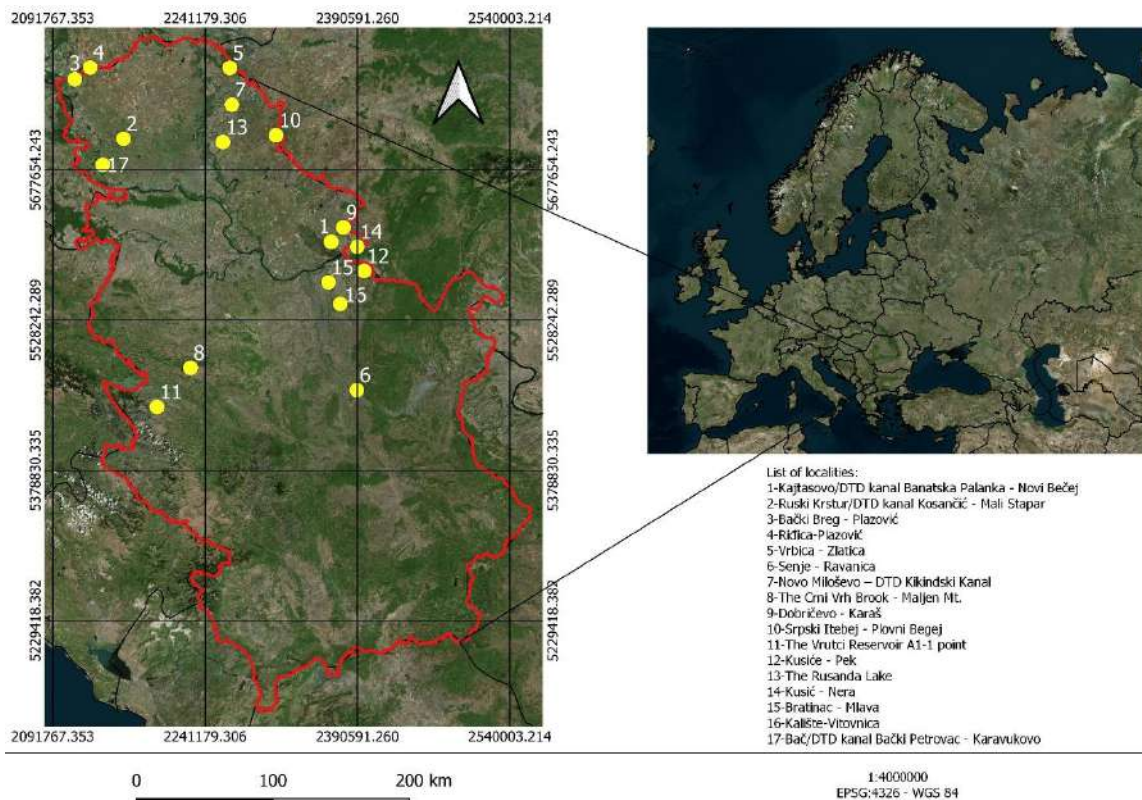


**Figure 1** Map of aquatic beetle sampling sites in Serbia (2013–2023 period)

## RESULTS AND DISCUSSION

New distributional records with related data on 43 aquatic beetle species from Serbia belonging to 27 genera and six families are provided in Table 1 while from other regions of Serbia in Table 2.

Table 1 Material examined - Vojvodina

Locality No.	Latitude	Longitude	Canal	River	Lake	Date - Species/No. of specimens
1	44.902635	21.245424	+			09.07.2015 – <i>Noterus clavicornis</i> /1 ex.
2	45.551866	19.413821	+			06.07.2015 – <i>Noterus clavicornis</i> /2 ex., <i>Noterus crassicornis</i> /1 ex., <i>Hydroglyphus geminus</i> /5 ex., <i>Hygrotus impressopunctatus</i> /1 ex., <i>Limnoxenus niger</i> /1 ex., <i>Helochaeres lividus</i> /1 ex., <i>Helophorus flavipes</i> /1 ex.
3	45.922801	18.985350			+	10.09.2014 – <i>Haliphus heydeni</i> /60 ex., <i>Agabus bipulstulatus</i> /6 ex., <i>Ilybius fenestratus</i> /4 ex.; 05.08.2015 - <i>Graptodytes bilineatus</i> /1 ex., <i>Hydroglyphus geminus</i> /1 ex., <i>Hydroporus angustatus</i> /1 ex., <i>Hydroporus palustris</i> /1 ex., <i>Hygrotus inaequalis</i> /1 ex., <i>Porhydrus obliquesignatus</i> /1 ex., <i>Helochaeres lividus</i> /1 ex., <i>Hydrochara flavipes</i> /1 ex., <i>Limnoxenus niger</i> /1 ex., <i>Hydrochus crenatus</i> /1 ex.; 02.09.2015 – <i>Haliphus immaculatus</i> /6 ex., <i>Agabus bipulstulatus</i> /3 ex., <i>Ilybius fenestratus</i> /3 ex., <i>Ilybius fuliginosus</i> /2 ex., <i>Hygrotus impressopunctatus</i> /1 ex.; 07.09.2016 - <i>Haliphus heydeni</i> /5 ex., <i>Haliphus lineatocollis</i> /3 ex., <i>Ilybius fenestratus</i> /5 ex.; 06.09.2017 – <i>Peltodytes caesus</i> /2 ex., <i>Graptodytes bilineatus</i> /1 ex., <i>Hydroglyphus geminus</i> /1 ex., <i>Limnoxenus niger</i> /1 ex.; 12.09.2018 – <i>Haliphus heydeni</i> /4 ex., <i>Helochaeres lividus</i> /1 ex.; 11.09.2019 – <i>Noterus clavicornis</i> /2 ex., <i>Noterus crassicornis</i> /1 ex., <i>Haliphus flavicollis</i> /4 ex., <i>Haliphus ruficollis</i> /4 ex., <i>Hydaticus transversalis</i> /2 ex., <i>Hygrotus decoratus</i> /1 ex., <i>Anacaena limbata</i> /1 ex., <i>Coelostoma orbiculare</i> /1 ex.
4	45.995828	19.120612			+	14.10.2019 – <i>Acilius canaliculatus</i> /4 ex., <i>Colymbetes fuscus</i> /1 ex., <i>Graphoderus austriacus</i> /1 ex., <i>Hydroglyphus geminus</i> /2 ex., <i>Hygrotus inaequalis</i> /4 ex., <i>Porhydrus lineatus</i> /1 ex.; 11.08.2021 – <i>Noterus crassicornis</i> /1 ex., <i>Acilius sulcatus</i> /3 ex., <i>Agabus guttatus</i> /2 ex., <i>Hydroglyphus geminus</i> /1 ex., <i>Enochrus affinis</i> /1 ex.
5	45.993935	20.350071			+	21.10.2013 – <i>Cybister lateralimarginalis</i> /2 ex.; 20.07.2015 – <i>Peltodytes caesus</i> /1 ex., <i>Porhydrus obliquesignatus</i> /1 ex., <i>Limnoxenus niger</i> /3 ex.
7	45.763721	20.369458	+			15.09.2014 – <i>Agabus bipulstulatus</i> /1 ex., <i>Hydroglyphus geminus</i> /1 ex., <i>Limnoxenus niger</i> /1 ex.
9	44.993907	21.350377			+	09.07.2015 – <i>Colymbetes fuscus</i> /22 ex.; 25.07.2016 – <i>Colymbetes fuscus</i> /16 ex.
10	45.573680	20.759129			+	03.08.2021 – <i>Cybister lateralimarginalis</i> /2 ex.
13	45.529609	20.289680			+	27.03.2017 – <i>Hygrotus confluens</i> /1 ex., <i>Enochrus halophilus</i> /1 ex.
14	44.871429	21.473503			+	10.08.2021 – <i>Potamophilus acuminatus</i> /1 Lv.; 17.08.2023 – <i>Macronychus quadrituberculatus</i> /4 ex.
17	45.388033	19.232140	+			16.09.2014 – <i>Helochaeres lividus</i> /1 ex.; 06.07.2015 – <i>Helochaeres lividus</i> /1 ex.

Table 2 Material examined - other regions of Serbia

Locality No.	Latitude	Longitude	Stream	River	Reservoir	Date - Species/No. of specimens
6	43.956512	21.469463	+			12.08.2015 – <i>Gyrinus colymbus</i> /20 ex.
8	44.099737	20.005220	+			04.10.2021 – <i>Agabus bipulstulatus</i> /1 ex., <i>Agabus nebulosus</i> /1 ex., <i>Hydroporus discretus</i> /1 ex.
11	43.848432	19.710379			+	07.08.2018 – <i>Graptodytes pictus</i> /1 ex.
12	44.717364	21.534722	+			11.08.2022 – <i>Hydroglyphus geminus</i> /1 ex.
15	44.646056	21.220032		+		11.08.2022 – <i>Potamophilus acuminatus</i> /1 Lv.; 15.08.2023 – <i>Potamophilus acuminatus</i> /1 Lv.
16	44.508243	21.323635	+			24.10.2019 – <i>Riolus subviolaceus</i> /2 ex.

The forty-three aquatic beetle species identified in this study represent an important contribution to their distribution in Serbia. This number of species reflects a high aquatic habitat heterogeneity in the study area, in a wide variety of water bodies, including lotic and lentic waters. Unfortunately, these habitats are currently not only endangered due to climate change, but also due to the drying up of several streams, deforestation, and urbanization by an intensification of agriculture, infrastructure development, water pollution by fertilizers for agriculture, mosquito control, and especially, by wastewaters [9–12]. Some of the found species inhabit waters characterized by higher organic pollution regarding total benthic invertebrate community composition and structure, representing a somewhat wider ecological tolerance of these aquatic beetle species to water pollution. Also, over time probably some species gradually became more tolerant to different environmental stress increasing their regional range. The small rivers with some aquatic beetle species are near the human settlements, particularly in Vojvodina. Bearing in mind some species are restricted to unpolluted and unregulated watercourses, the confirmed presence of larval specimens in moderately polluted and regulated watercourses, also with HYMO alterations, such those from the Bačka and Banat District (the DTD canal system) are situated nearby the human settlements could indicate the species wider ecological valence as well as its higher potential to colonize still inhabitable habitats in Serbia.

Aquatic beetle fauna of Serbia, and the Balkan Peninsula, is poorly known due to scarce data coverage and probably disjuncted ranges of some species. Also, the morphological approach in aquatic beetle taxa identification can lead to misidentification due to highly expressed aquatic beetle ecophenotypic variability in some aquatic beetle genera.

The scarcity of aquatic beetle species in Serbia can be primarily explained by habitat degradation and water pollution, particularly in water bodies close to human settlements. Considering the low dispersal potential of some aquatic beetle species, habitat fragmentation and deterioration are particularly dangerous [13,14].

Anthropogenic pressures are particularly expressed in small lowland streams, such as those for Vojvodina, primarily communal wastewater and agricultural runoff pollution.



## CONCLUSION

The present study adds considerably to the previous knowledge about aquatic beetles of Serbia, with new taxa distributional records for 43 species from 27 genera of the entire study area, particularly for Vojvodina. The Pannonian part of Serbia is characterized by the high diversity of aquatic beetle fauna due to lots of stagnant water habitats with shallow water, (canals, wetlands, swamps, ponds, etc.) where primarily predaceous aquatic beetles are abundant, and which is corroborated by the present study.

Conservation of natural resources and biodiversity has become an urgent issue in recent years for attaining an environmentally sustainable future. The impact of anthropogenic activities on freshwater systems is so adverse that the diversity of species inhabiting them is decreasing at alarming rate. The handling of this situation is becoming more difficult due to a lack of knowledge regarding their habitat selection.

The presence of wood debris in water, as a specific microhabitat for xylobiont species is necessary for development of larval instars. Also, the presence of aquatic and riparian vegetation is necessary for imagos' foraging. Due to the scarcity of the species findings, their disjuncted ranges, and specific ecological requirements, some aquatic beetle species nowadays become more vulnerable to pronounced anthropogenic pressures. Thus, adequate aquatic habitat conservation is necessary to improve the protection of rare aquatic beetle species in Serbia.

Bearing in mind some aquatic beetle taxa are restricted to unpolluted and unregulated watercourses, the confirmed presence of larval specimens in moderately polluted and regulated watercourses covered in the present study, also with HYMO alterations, such are those from the Bačka and Banat District (the DTD canal system), are situated nearby the human settlements could indicate the species wider ecological valence as well as its higher potential to colonize still inhabitable habitats in lowland regions of Serbia.

## REFERENCES

- [1] Short A.E., *Z. Syst. Entomol.* 43 (2018) 1–18.
- [2] Jäch M.A., Balke M., *Hydrobiologia* 595 (2008) 419–442.
- [3] Hering D., Verdonschot P.F.M., Moog O., *et al.*, *Hydrobiologia* 516 (2004) 1–20.
- [4] AQEM Consortium Manual for the application of the AQEM system, Version 1.0 (2002), p.202.
- [5] Olmi M., *Coleoptera, Dryopidae, Elminthidae. Fauna d'Italia.* 12<sup>th</sup> ed., Bologna, Calderini, (1976), p.280, ISBN: 978-8870191547.
- [6] Friday L.E., *A key to the adults of British water beetles*, Field Studies Council, Cambridge, Darwin College (1988), p.151, ISBN: 978-1851531899.
- [7] Nilsson A.N., Holmen M., *The Aquatic Adephaga (Coleoptera) of the Fennoscandia and Denmark, Vol. 2, Dytiscidea*, Brill (1995), p.192, ISBN: 978-9004104563.
- [8] Miller K.B., Bergsten J., *Diving beetles of the world: Systematics and biology of the Dytiscidae*, JHU Press (2016), p.320, ISBN: 978-1421420547.



- [9] Bensaad H., Mabrouki Y., Taybi A.F., *et al.*, J. Mater. Environ. Sci. 8 (7) (2017) 2365–2371.
- [10] Mabrouki Y., Taybi A.F., Bensaad H., *et al.*, J. Mater. Environ. Sci. 7 (1) (2016) 231–243.
- [11] Taybi A.F., Mabrouki Y., Berrahou A., *et al.*, J. Mater. Environ. Sci. 7 (1) (2016) 272–284.
- [12] Yahya H.S.A., Taybi A.F., Mabrouki Y., *et al.*, J. Mater. Environ. Sci. 8 (9) (2017) 3372–3381.
- [13] Ribera I., Biol. Conserv. 92 (2) (2000) 131–135.
- [14] Boukal D.S., Boukal M., Fikáček M., *et al.*, Klapalekiana 43 (Suppl.) (2007) 1–289.



## COMPARING FROST PROTECTION STRATEGIES FOR SUSTAINABLE AGRICULTURE IN SLOVENIA

Matej Fike<sup>1\*</sup>, Marko Pezdevšek<sup>1</sup>, Andraž Roger<sup>1</sup>

<sup>1</sup>University of Maribor, Faculty of Energy Technology, Hočevarjev trg 1, 8270 Krško,  
SLOVENIA

\*[matej.fike@um.si](mailto:matej.fike@um.si)

### Abstract

*This study investigates the economic and practical aspects of various frost protection methods employed in Slovenia's agricultural sector, focusing on their financial viability over a projected period. Utilizing a combination of empirical data and the Net Present Value (NPV) method, the research analyses the cost-effectiveness of traditional and advanced frost protection technologies. The findings demonstrate a significant difference in initial investments and ongoing costs between methods such as solid fuel heaters, wind machines, and sprinklers. With a special focus on their application in a typical Slovenian orchard, this study provides critical insights into how different frost protection strategies can be optimized to enhance economic outcomes and sustainability in agriculture.*

**Keywords:** frost protection, economic analysis, Net Present Value (NPV), Slovenian agriculture.

### INTRODUCTION

Frost events pose a critical threat to agriculture with the capacity to severely impact crop yields and economic stability. In Slovenia, the recurrence and intensity of these events have escalated, pressing the need for efficient and effective frost protection strategies. Agricultural practices in Slovenia are highly susceptible to frost damage due to the region's climatic conditions, which have become increasingly erratic in recent years. As frost events become more frequent and severe, they pose significant challenges to farmers, threatening not only immediate crop yields but also long-term agricultural sustainability.

The economic ramifications of frost damage extend beyond the immediate loss of crops. Farmers face substantial financial burdens from decreased yields, reduced quality of produce, and the increased costs of recovery efforts. These challenges are compounded by the cyclical nature of agricultural production, where a single frost event can have repercussions for multiple growing seasons. Consequently, there is an urgent need for effective frost protection measures that are both economically viable and capable of protecting crops from frost damage.

This paper examines various frost protection methods through detailed economic analysis and empirical data collection from local orchards, assessing both the immediate and long-term financial impacts. By comparing traditional practices like wood burning with more technologically advanced methods such as sprinklers and wind machines, the study seeks to identify the most cost-effective solutions that can protect crops against frost damage while

considering the economic constraints faced by farmers. The study employs the Net Present Value (NPV) method to evaluate the cost-effectiveness of different frost protection technologies, providing a comprehensive financial overview that can aid farmers and agricultural stakeholders in making informed decisions.

Additionally, this research aims to bridge the information gap that often hinders the adoption of effective frost protection methods. By presenting empirical data and economic analyses, the study offers valuable insights into the practical and financial aspects of various frost protection strategies. The goal is to equip farmers with the knowledge needed to invest in the most suitable technologies, thereby enhancing their resilience against frost events and contributing to the overall sustainability of Slovenian agriculture. Through this comparative study, the paper highlights the importance of strategic investments in frost protection, advocating for a balanced approach that considers both economic efficiency and the effectiveness of protecting crops from frost damage.

## DATA AND METHODS

Frost can cause devastating damage to crops, affecting not only the current season's yield but also the long-term viability of agricultural operations. In Slovenia, the frequency and severity of frost events have shown a worrying increase in recent decades, making effective management strategies essential [1]. As seen on Figure 1, according to survey data, frost occurs on average every other year, and when it does, it can destroy up to 50% of the crop yield. This high incidence rate underscores the critical need for robust frost protection measures [2].

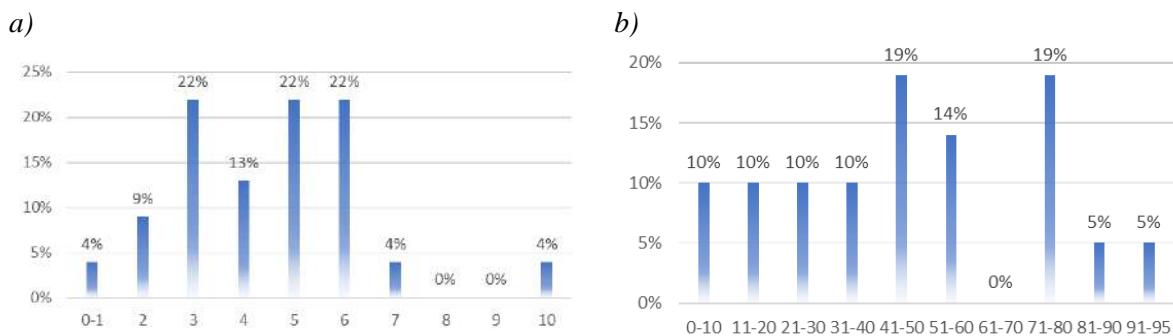


**Figure 1** a) How many frosty years have you had in the last ten years? ( $n=23$ ); b) On average, what percentage of your crop was destroyed by frost [%]? ( $n=21$ )

Moreover, the economic impact extends beyond the immediate crop loss. The cost includes lost future sales, reduced quality of surviving produce, and increased labor and material costs for recovery efforts. In some cases, farmers face a cycle of debt and recovery that can last several seasons. The survey highlighted that despite the clear risks, many farmers in Slovenia have not adopted adequate frost protection strategies, primarily due to cost and a lack of information on effective methods.

Our study focuses on a typical Slovenian orchard, spanning 5 hectares, as modeled by the Agricultural Institute of Slovenia [3]. This orchard produces 40 tons of fruit per hectare

annually, with apples priced at €0.49 per kilogram. The annual production costs for this orchard amount to approximately €17,423 per hectare. From the data we gathered, it's evident that a significant frost event is likely to occur once every two years, each lasting about 8 hours, and potentially damaging up to 50% of the fruit crop.

To evaluate the economic viability of frost protection methods, we applied the Net Present Value (NPV) method, a crucial financial metric [4].

For our analysis, the initial investment encompasses all upfront costs associated with any frost protection equipment needed before the first frost event. We've assumed that the net cash flows represent potential savings derived from the protection measures, presuming a 100% effectiveness rate to optimize economic outcomes.

The insights drawn from this economic analysis, detailing the cost-effectiveness of various frost protection strategies, are shown in Table 2. The assumed project lifetime for this analysis spans 6 years, allowing us to project the long-term benefits and costs of implementing these protective measures in the orchard.

Table 1 provides a detailed breakdown of the annual costs and investment requirements for various frost protection methods, offering essential insights into the economic aspects of implementing these technologies in agricultural practices. The table shows the initial investment costs against the ongoing annual expenses associated with each method, such as solid fuel heaters, liquid fuel heaters, sprinklers, wind machines, and helicopters.

Key points to note include:

- **Initial Investment:** This column reveals the upfront costs required to purchase and install each frost protection method. For example, wind machines and sprinklers require a higher initial investment, reflecting their more complex installation and infrastructure requirements.

- **Annual Cost:** This section details the recurring expenses associated with each method, covering maintenance, fuel, labor, and other operational costs. It highlights the economic sustainability of each method over time, crucial for long-term budget planning.

The data provided in Table 1 is critical for farmers and agricultural stakeholders to make informed decisions about which frost protection methods are most economically viable for their specific contexts. By comparing the costs associated with each method, stakeholders can assess the balance between initial costs and long-term benefits, leading to more strategic investment in technologies that offer optimal protection against frost damage while aligning with financial capabilities and goals.

**Table 1** Annual cost and investment data for each protection method

<b>Protection method</b>	<b>Annual cost</b>	<b>Investment</b>
Solid fuel heaters	€12,750	€1,200
Liquid fuel heaters	€2,460	€25,000
Sprinklers	€1,015	€37,250
Wind machines	€2,362	€35,000
Helicopters	€8,000	/
Wood burning	€4,680	€1,200

## RESULTS AND DISCUSSION

Our economic analysis, detailed in Table 2, confirms the efficacy of various frost protection methods within the projected lifetime of the systems. The analysis reveals a clear distinction in the financial outlay required by different technologies. High-end solutions like sprinklers, wind machines, and liquid fuel heaters entail significant initial investments but benefit from lower ongoing operational costs. In contrast, methods such as solid fuel heaters, helicopters, and traditional wood-burning involve minimal initial capital outlay but are associated with higher variable costs over time.

*Table 2 Net present value of different active protection methods*

Protection method	Annual cash flow (with frost)	Annual cash flow (no frost)	NPV (6 years)
Solid fuel heaters	€36,350	€0,00	€61,870.10
Liquid fuel heaters	€46,640	€0,00	€93,069.37
Sprinklers	€48,085	€0,00	€88,542.78
Wind machines	€46,738	€0,00	€83,593.17
Helicopters	€41,100	€0,00	€88,458.49
Wood burning	€44,420	€0,00	€105,003.64

Among the methods analyzed, wood burning stands out as the most cost-effective option. With the highest net present value of €105,003.64 at the end of the designated project lifetime, wood burning offers a compelling balance of cost and efficiency, affirming its viability for farmers prioritizing low upfront investment.

Below, in Figure 2, the NPV of the protection methods is shown. It is clear that most of the protection methods give positive cost-benefit results (in this case, the NPV value is greater than zero for all analysed protection methods in just one year) after the initial capital investment, if calculating using the specified input data.

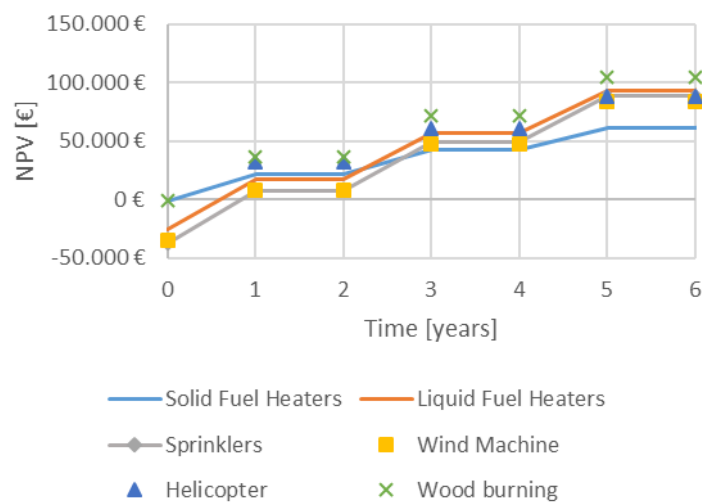


*Figure 2 Net Present Value of various active frost protection methods*

Additionally, the financial implications of maintaining these systems during periods without frost events are minimal to none. Given the short duration of the project analysis, the

maintenance requirements for these systems are considered negligible, further enhancing the appeal of investing in these frost protection technologies.

## **CONCLUSION**

The analysis presented in this study highlights the economic disparity between different frost protection technologies. While advanced methods like sprinklers and wind machines entail higher initial costs, they offer significant long-term savings on operational expenses, presenting a viable option for those who can afford the upfront investment. Conversely, traditional methods such as wood burning provide a cost-effective alternative with lower initial investment but higher ongoing costs. Ultimately, the choice of frost protection strategy should align with both the financial capabilities and specific needs of the agricultural stakeholders. This study underscores the importance of strategic investments in frost protection technologies, advocating for a balanced approach that considers both economic efficiency and effectiveness in protecting crops from frost damage.

## **REFERENCES**

- [1] Kodrič I., Lukačič M., Prošek J., *Zaščita pred spomladansko pozebo*, Ministry of Agriculture, Forestry and Food of Slovenia, Ljubljana, Slovenia (2006).
- [2] Fike M., Smrekar M., Fekonja M., *Journal of energy technology* 14(4) (2021) 69–78.
- [3] Agricultural Institute of Slovenia: Model calculations for standard yield crops [Online], 2020. *Available on the following link:* [https://www.kis.si/Standardni\\_nabor\\_1/](https://www.kis.si/Standardni_nabor_1/) (13.5.2024).
- [4] Fike M., Fekonja M., Smrekar M., *Journal of energy technology* 13(4) (2020) 39–49.





## GENE POOL OF FOREST FRUIT TREES IN THE PROTECTED AREA OF THE NATURAL MONUMENT “KOŠUTNJAK FOREST” – THEN AND NOW

Filip Maksimović<sup>1</sup>, Marina Nonić<sup>2</sup>, Dragica Vilotić<sup>2</sup>, Ivona Kerkez Janković<sup>2\*</sup>,  
Mirjana Šijačić-Nikolić<sup>2</sup>

<sup>1</sup>University of Belgrade, Institute for Multidisciplinary Research, Kneza Višeslava 1,  
11030 Belgrade, SERBIA

<sup>2</sup>University of Belgrade, Faculty of Forestry, Kneza Višeslava 1, 11030 Belgrade, SERBIA

\*ivona.kerkez@sfb.bg.ac.rs

### Abstract

*The Natural Monument “Košutnjak Forest” is a protected area on the territory of the city of Belgrade (Serbia). It is located in the immediate vicinity of the city center and covers 265.26 ha of protected area, of which 1.31% of the area is under the second degree of protection, and 98.69% is under the third degree of protection. The Košutnjak area is home to a large number of different woody species, making it exceptionally rich in biodiversity. Among the species that occur in this area, forest fruit trees occupy a significant percentage, and their value is reflected in their significant ecological impact, but also in their medicinal properties, importance for animal nutrition and landscape beautification. Forest fruit trees are less and less present in natural habitats due to anthropogenic influence, biotic factors, invasive species, and climate change which emphasize the need for their conservation. Within this research, an overview of forest fruit trees in the area of the Natural Monument “Košutnjak Forest” during 1952, 1972 and 2022 was presented. In this area, in the research that was conducted in the period from 2019 to 2022, 18 species of forest fruit trees were recorded, 12 of which are native, and five belong to the category of rare and endangered, relict or species at risk in the forest fund of the Republic of Serbia, which indicates the importance and necessity for their conservation.*

**Keywords:** Košutnjak, gene pool, forest fruit species, forest genetic resources.

### INTRODUCTION

The Natural Monument (NM) “Košutnjak Forest” is a protected area located on the territory of the city of Belgrade (Serbia). This urban forest, located about 6 km from the city centre, consists of 265.26 ha of protected area, of which 1.31% is under the second degree of protection, and 98.69% is under the third degree of protection.

A large number of different woody species, with their gene pool, make this area exceptionally valuable. They are exposed to the influence of various threatening factors, such as anthropogenic impact, the presence of invasive species, biotic factors, pollution, climate change, etc., and it is necessary to conserve them now, but also for future generations. Among the recorded woody species present in this area, the gene pool of forest fruit trees, which occur in smaller groups or as individual trees, has a significant share and ecological impact [1].

Forest fruit trees are important for human and animal nutrition, due to their medicinal properties and beautifying the landscape [2–4]. Their gene pool is threatened due to excessive logging, management activities mainly aimed at economic gain, climate change and other impacts, which has resulted in forest fruit trees becoming increasingly rare in their natural habitat [5]. For this reason, there is a need to conserve them in natural habitats such as NM “Košutnjak Forest”, which is in accordance with the conservation of the biodiversity of forest fruit trees of Serbia [1].

The aim of this research was to provide an overview of the recorded species of forest fruit trees in the area of the Natural Monument “Košutnjak Forest” then and now, i.e. their occurrence in 1952, 1972 and 2022.

## MATERIALS AND METHODS

The review of recorded species of forest fruit trees was made based on the results of research conducted in 1952, 1972 and 2022 [6–8].

For the identification of the gene pool of woody species in the area of Košutnjak, a research methodology has been defined [1,8], which includes terrain reconnaissance and recording of all species that occur in tree, shrub and ground flora layer, which represents the basis for future monitoring, conservation and sustainable use of forest fruit trees on the territory of NM “Košutnjak Forest”. The results of a detailed reconnaissance of the terrain and the identification of the gene pool of forest fruit trees in the area of NM “Košutnjak Forest”, carried out as part of the research study *“Identification and monitoring of the gene pool of rare, vulnerable and endangered plant species in NM “Košutnjak Forest”* and the monograph *“The gene pool of woody species of NM “Košutnjak Forest”- conservation and sustainable use”* served as the basis for a comparative review of recorded species of forest fruit trees in the area of Košutnjak (2022). The data were compared with the results of previous research conducted in Košutnjak in 1952 [6] and 1972 [7]. A tabular review of the recorded species of forest fruit trees was prepared, showing the family and genus to which they belong, the origin (native or non-native species), as well as the number of sections of MU “Košutnjak” in which the species was recorded in 2022. Also, the conservation status according to the IUCN categorization is listed for each species. The status in the Red list represents the probability that a certain taxon will disappear in the future, and it can be: NE – Not evaluated, DD – Data deficient, LC – Least concern, NT – Near threatened, VU – Vulnerable, EN – Endangered, CR – Critically endangered, EW – Extinct in the wild, EX – Extinct.

## RESULTS AND DISCUSSION

A comparative overview of recorded species of forest fruit trees in the tree layer in the area of Košutnjak, based on research conducted in 1952, 1972 and 2022, is shown in Table 1.

**Table 1** Overview of recorded species of forest fruit trees in the area of Košutnjak, according to the research conducted in 1952, 1972 and 2022

Family	Genus	Species	Origin	IUCN status	Species recorded (year)			Total number of sections in which the species was recorded in 2022
					1952	1972	2022	
Cornaceae	<i>Cornus</i>	<i>C. mas</i> L. – Cornel	Native	LC	+	+	+	44
		<i>C. sanguinea</i> L. – Dogwood	Native	-	+	+	+	12
Corylaceae	<i>Corylus</i>	<i>C. avellana</i> L. – Common hazel	Native	LC	-	-	+	1
		<i>C. colurna</i> L. – Turkish hazel	Native	LC	-	-	+	9
Fagaceae	<i>Castanea</i>	<i>C. sativa</i> Mill. – Sweet chestnut	Native	LC	-	-	+	1
Hippocastanaceae	<i>Aesculus</i>	<i>A. hippocastanum</i> L. – Horse chestnut	Non-native	VU	-	-	+	23
Juglandaceae	<i>Juglans</i>	<i>J. nigra</i> L. – Black walnut	Non-native	LC	-	-	+	12
		<i>J. regia</i> L. – Walnut	Native	LC	-	-	+	41
Moraceae	<i>Morus</i>	<i>M. alba</i> L. – White mulberry	Non-native	LC	-	-	+	16
		<i>M. nigra</i> L. – Black mulberry	Non-native	-	-	-	+	2
Rosaceae	<i>Crataegus</i>	<i>C. monogyna</i> Jacq. – Common hawthorn	Native	LC	+	+	+	52
	<i>Pyrus</i>	<i>P. pyraster</i> (L.) Burgsd. – Wild pear	Native	LC	+	+	+	26
		<i>P. avium</i> L. – Wild cherry	Native	LC	-	-	+	62
	<i>Prunus</i>	<i>P. cerasifera</i> Ehrh. – Cherry plum	Native	DD	-	-	+	36
		<i>P. serotina</i> Ehrh. – Black cherry	Non-native	LC	-	-	+	2
		<i>P. domestica</i> L. – Plum	Non-native	DD	-	+	+	10
	<i>Sorbus</i>	<i>S. domestica</i> L. – Service tree	Native	LC	-	-	+	3
<i>S. torminalis</i> (L.) Crantz – Wild service tree		Native	LC	+	+	+	14	
<b>Total species:</b>					<b>5</b>	<b>6</b>	<b>18</b>	

Based on the overview shown in Table 1, it can be stated that during 1952, five native forest fruit trees were recorded: cornel, dogwood, common hawthorn, wild pear and wild service tree [6]. After 20 years, in 1972, another native species was recorded – plum [7]. In the research conducted in the period from 2019 to 2022, 18 species of forest fruit trees were recorded, 12 native and 6 non-native. At that time, the following species were recorded: cornel, dogwood, common hazel, Turkish hazel, sweet chestnut, horse chestnut, black walnut, walnut, white mulberry, black mulberry, common hawthorn, wild pear, wild cherry, cherry plum, black cherry, plum, service tree, wild service tree [8].

According to the IUCN Red List of Threatened species, cornel, common hazel, Turkish hazel, sweet chestnut, black walnut, walnut, white mulberry, common hawthorn, wild pear, wild cherry, black cherry, service tree and wild service tree are classified in the category LC – Least concern. There is not enough data for the cherry plum and plum (DD – Data deficient), and dogwood and black mulberry are not listed in the IUCN Red List of Threatened Species.

Of the 12 native species of forest fruit trees that were recorded in research conducted from 2019 to 2022 [1,8], five are classified as rare and endangered, relict or species at risk in the forest fund of the Republic of Serbia [9]. These are the following species: walnut – rare/endangered species, wild cherry – rare/endangered species, wild pear – at risk, wild service tree – at risk, Turkish hazel – tertiary relict. Their status indicates the importance and necessity of their conservation, in order to preserve the genetic diversity of vulnerable species, and therefore their presence in natural habitats.

In the research from 2022, based on the criteria of endangerment, the criterion of representativeness (charismaticity) and scientific criteria, the following target species of forest fruit trees, that significantly contribute to the biodiversity of Košutnjak, and are included in the process of conservation strategic planning, were selected: wild cherry, wild pear, service tree and wild service tree [1,8,10]. Natural regeneration is difficult for all the species mentioned, except for the wild cherry, which rejuvenates well. The conservation of these species was started using *in situ* and *ex situ* methods [11]. Activities on the *in situ* conservation of these species included the proposal of setting conservation units (with georeferencing, mapping and evaluation of representative specimens). *Ex situ* conservation of wild cherry and wild pear was started with the establishment of generative progeny tests in the nursery of the Faculty of Forestry, University of Belgrade. A certain number of the wild pear and wild cherry seedlings from the generative progeny tests was planted in Košutnjak, thus expanding the available gene pool in this area.

## CONCLUSION

Based on the presented overview of recorded species of forest fruit species in NM “Košutnjak Forest”, based on the research conducted in 1952, 1972 and 2022, a significant increase in their number in this protected area was recorded (from 5 or 6 to 18 species in the tree layer, of which 12 are native). Of the 12 native species, almost half are classified as rare and endangered, relict or species at risk in the forest fund of the Republic of Serbia. This

information indicates the valuable biodiversity of the researched area, but also the necessity for the conservation of available genepool of forest fruit trees in NM “Košutnjak Forest”.

The increase in the number of forest fruit trees in the area of Košutnjak in the past may indicate an increased anthropogenic influence, i.e. that a large number of tree species were brought to this area by human, which is additionally emphasized by the location of Košutnjak. In addition, a considerable number of non-native invasive species have been introduced, which also disturb the natural rejuvenation of native forest fruit trees, which may also be influenced by other threatening factors that should be taken into consideration. However, the fact that the methodology applied in the conducted research was not the completely same should be also taken into account, which could also partially affect the evident large differences in the number of species.

The recorded gene pool of forest fruit trees in the area of NM “Košutnjak Forest”, in the period from 2019 to 2022, has been georeferenced and mapped, which enables future monitoring, conservation and sustainable use, and concrete activities have been started with the application of *in situ* and *ex situ* conservation methods [1].

Particular attention should be paid to forest fruit trees, as a large number of new species were recorded for the first time during the research carried out from 2019 to 2022. These species have a significant gene pool and contribute to the biodiversity of the entire area, and it is necessary to continue conservation measures.

## ACKNOWLEDGEMENT

*The research is financially supported by the funds of the Secretariat for Environmental Protection - City of Belgrade, within the project “Identification and monitoring of the gene pool of rare, vulnerable and endangered species of plants NM “Košutnjak Forest” under contract number V-01 401.1-56, dated 12.6.2019.*

## REFERENCES

- [1] Šijačić-Nikolić M., Nonić M., Genofond drvenastih vrsta SP “Šuma Košutnjak” - konzervacija i održivo korišćenje, Univerzitet u Beogradu, Šumarski fakultet, Beograd (2023), p.196, ISBN: 978-86-7299-363-9.
- [2] Orešković Ž., Dokuš A., Harapin M., *i sar.*, Istraživanja tehnologije proizvodnje voćkarica, Izvanredno izdanje 9, Hrvatski šumarski institute, (2006) 65–73.
- [3] Noćajević S., Ovčina J., Imširović E., *et al.*, Proceedings of the Sixth international scientific conference “June 5<sup>th</sup> - World environment day”, 18–19 June, Bihać, Bosnia and Herzegovina (2018) 36–50.
- [4] Bošnjaković D., Ognjanov V., Ljubojević M., *i sar.*, Genetika 44, (1) (2012) 81–90.
- [5] Čurović M., Jovančević M., Balijagić J., Wild Fruit Tree Species of Montenegrin Forests *in* Forests of Southeast Europe Under a Changing Climate - Conservation of Genetic Resources, Editors: Šijačić-Nikolić M., Milovanović J., Nonić M., Springer Cham, (2019), p.486, ISBN: 978-3-319-95266-6.

- [6] Gajić M., O vegetaciji Košutnjaka, Glasnik Šumarskog fakulteta 5, Univerzitet u Beogradu, Šumarski fakultet (1952) 283–301.
- [7] Ilić R., Cerović O., Gajić M., Flora Košutnjaka, Osnovna škola “Josif Pančić”, Beograd (1972) p.208.
- [8] Šijačić-Nikolić M., Vilotić D., Ivetić V., *i sar.*, Identifikacija i monitoring genofonda retkih, ranjivih i ugroženih vrsta biljaka SP „Šuma Košutnjak” – studija. Univerzitet u Beogradu, Šumarski fakultet, Sekretarijat za zaštitu životne sredine grada Beograda, Beograd (2021), p.317.
- [9] Banković S., Medarević M., Pantić D., *i sar.*, Glasnik Šumarskog fakulteta 100 (2009) 7–30
- [10] Šijačić-Nikolić M., Nonić M., Kerkez Janković I., Proceedings of the International scientific conference: “Better Forestry, for Better Forests, for a Better Planet”, 15–16 June, Skopje, North Macedonia (2022) 78.
- [11] Šijačić-Nikolić M., Nonić M., Kerkez Janković I., *et al.*, Proceedings of the International Scientific Conference “Forestry Science for Sustainable Development - FORS2D”, Perspectives of forestry and related sectors as drivers of sustainable development in the post-Covid era, 29–30 September, Banja Luka, Bosnia and Herzegovina (2022) 143.





## APPLICATION OF THE SHRINKING CORE MODEL IN THE LEACHING PROCESS OF $\text{LiNiMnCoO}_2$

Dragana Medić<sup>1\*</sup>, Snežana Milić<sup>1</sup>, Nemanja Milošević<sup>2</sup>, Maja Nujkić<sup>1</sup>, Marina Pešić<sup>3</sup>,  
Vladan Nedelkovski<sup>1</sup>, Sonja Stanković<sup>1</sup>

<sup>1</sup>University of Belgrade, Technical Faculty in Bor, V.J. 12, 19210 Bor, SERBIA

<sup>2</sup>Elixir Prahovo, Braće Jugovića br.2, 19330 Prahovo, SERBIA

<sup>3</sup>Public Utility Enterprise “Water supply” Bor, R.J: Čoče 16, 19210 Bor, SERBIA

\**dmedic@tfbor.bg.ac.rs*

### Abstract

*Lithium-ion batteries (LIBs) are electrochemical systems consisting of cathodes, anodes, separators and electrolytes. Improper treatment of LIBs waste can affect the quality of the environment. On the other hand, LIBs waste is a valuable source of many metals. In recent years, intensive efforts have been made to develop a hydrometallurgical recycling process for cathode materials, paying particular attention to the leaching process. The leaching of cathode material from spent LIBs is a heterogeneous reaction occurring at the solid-liquid interface. Various kinetic equations are used to process experimental results and determine the kinetic parameters of the leaching process. In this study, an overview of systems in which a shrinking core model is applied to describe the leaching process of nickel-, manganese- and cobalt-based cathode materials ( $\text{LiNi}_x\text{Mn}_y\text{Co}_z\text{O}_2$ ) is given.*

**Keywords:** LIBs, cathode material, kinetics, heterogeneous reactions.

### INTRODUCTION

Lithium-ion batteries (LIBs) are one of the most significant sources of electrical energy due to their favorable properties such as high current density, high specific capacity, wide temperature range, low self-discharge rate, and low cost [1]. The advantage of LIBs over older generation batteries, such as lead-acid and/or nickel-cadmium batteries, lies in the lithium itself. Lithium has the lowest reduction potential of all elements (the redox potential of the  $\text{Li}^+/\text{Li}$  pair is -3.01 V), which means that lithium-based batteries have a high cell potential [2].

Commercial LIBs consist of cathodes, anodes, separators, and electrolytes. Lithium ions diffuse between the cathode and anode, facilitating the movement of electrons. The cathode materials of LIBs contain different concentrations of valuable metals depending on their structure. The most commonly used cathode materials are lithium cobalt oxide ( $\text{LiCoO}_2$ ), lithium iron phosphate ( $\text{LiFePO}_4$ ), lithium manganese oxide ( $\text{LiMn}_2\text{O}_4$ ), and nickel, cobalt, and manganese-based cathode materials ( $\text{LiNi}_x\text{Mn}_y\text{Co}_z\text{O}_2$ ) [3]. In recent years, nickel, cobalt, and manganese-based cathode materials (NCM) have gained increasing significance and usage in the electronics industry.

Improper handling of spent LIBs can lead to contamination of soil, water, and air. On the other hand, spent LIBs represent valuable waste material for the recovery of valuable metals such as lithium, cobalt, nickel, manganese, and/or their compounds [4].

The recycling technologies used for the processing of cathode materials from spent LIBs can be divided into pyrometallurgical, hydrometallurgical and bio-hydrometallurgical processes [5–7]. Pyrometallurgical processes release toxic gases and a large amount of energy, and the percentage of material loss is high because the process is carried out at temperatures above 1400°C [8]. Biohydrometallurgical processes require a considerable amount of time and the presence of microorganisms for efficient incubation [9]. The application of hydrometallurgical treatment requires high metal purity, minimal gas emissions and low energy consumption. The most important step in the entire hydrometallurgical process is acid leaching [4].

During the hydrometallurgical process, especially in the leaching of metals from cathode material, it is necessary to understand the kinetics of heterogeneous chemical reactions, which enables the identification and definition of the appropriate reaction mechanism. The most commonly used kinetic models to represent heterogeneous chemical reactions during the metal leaching process from cathode material are the shrinking core model, the logarithmic model and the Avrami model [10,11].

This paper provides an overview of leaching systems in which the shrinking core model was used to determine the kinetic parameters of the cathode material leaching process.

## KINETICS AND MECHANISM OF LEACHING NICKEL, COBALT, AND MANGANESE-BASED CATHODE MATERIAL

The kinetic equations used to describe the leaching process of cathode material can be classified into four models: a model controlled by a chemical reaction (reaction 1), a model controlled by a diffusion process (reaction 2), the logarithmic model (reaction 3), and the Avrami model (reaction 4) [11].

$$1-(1-x)^{1/3} = k_1 t \quad (1)$$

$$1 - 2/3x - (1-x)^{2/3} = k_2 t \quad (2)$$

$$(-\ln(1-x))^2 = k_3 t \quad (3)$$

$$-\ln(1-x) = k_4 t^n \quad (4)$$

where:  $x$  - conversion degree;  $t$  - leaching time (min);  $k_1$ ,  $k_2$ ,  $k_3$ , and  $k_4$  - rate constants (1–4) ( $\text{min}^{-1}$ ).

In order to determine the control level of the process rate, the experimental data must be adapted to the existing kinetic equations. A high value for the correlation coefficient ( $R^2$ ) indicates the level that determines the reaction rate in the process under consideration. The value of the activation energy is calculated using the Arrhenius equation.

Numerous factors affect the kinetics of heterogeneous chemical reactions during the decomposition of cathode material, in particular the concentration of the leaching agent,

concentration of the reducing agent, temperature, time, and solid-liquid ratio. In addition, the pretreatment of the cathode material and the state of battery decomposition can significantly influence the metal leaching rate and activation energy values [12].

Table 1 contains literature data on the decomposition system of nickel, cobalt and manganese-based cathode materials as well as the kinetic equations used to determine the activation energy values. The data listed in Table 1 show that the shrinking core model is generally used to describe the kinetics and mechanism of leaching of LiNiMnCoO<sub>2</sub>.

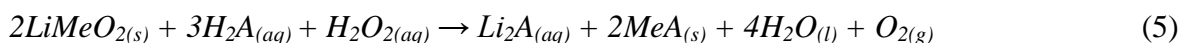
**Table 1** Kinetic equations for the leaching process of cathode material

Cathode Material	Leaching System	Kinetic equation	Activation energy (kJ/mol)	References
LiNi <sub>x</sub> Co <sub>x</sub> Mn <sub>x</sub> O <sub>2</sub>	C <sub>4</sub> H <sub>6</sub> O <sub>6</sub> + H <sub>2</sub> SO <sub>4</sub> + H <sub>2</sub> O <sub>2</sub>	$1 - (1 - x)^{1/3} = kt$	Li:49.7 Ni:48.5 Co:50.0 Mn:47.6	[12]
LiNi <sub>x</sub> Co <sub>x</sub> Mn <sub>x</sub> O <sub>2</sub>	NH <sub>3</sub> + (NH <sub>4</sub> ) <sub>2</sub> SO <sub>4</sub> + NaSO <sub>3</sub>	$1 - (1 - x)^{1/3} = kt$	Li:62.0 Ni:76.3 Co:81.5	[11]
LiNi <sub>x</sub> Co <sub>x</sub> Mn <sub>x</sub> O <sub>2</sub>	subcritical water + PVDF	$1 - (1 - x)^{1/3} = kt$	Li:63.7 Ni:73.5 Co:74.9 Mn:71.8	[13]
LiNi <sub>x</sub> Co <sub>x</sub> Mn <sub>x</sub> O <sub>2</sub>	H <sub>2</sub> SO <sub>4</sub> + H <sub>2</sub> S	$1 - 2/3x - (1 - x)^{2/3} = kt$	Li:23.3 Ni:28.7 Co:27.6 Mn:26.0	[14]
LiNi <sub>x</sub> Co <sub>x</sub> Mn <sub>x</sub> O <sub>2</sub>	H <sub>2</sub> SO <sub>4</sub> + H <sub>2</sub> O <sub>2</sub>	$1 - 2/3x - (1 - x)^{2/3} = kt$	Li:20.1 Ni:34.3 Co:29.9 Mn:20.8	[15]
LiNi <sub>x</sub> Co <sub>x</sub> Mn <sub>x</sub> O <sub>2</sub>	C <sub>2</sub> H <sub>2</sub> O <sub>4</sub> + H <sub>2</sub> O <sub>2</sub>	$(-\ln(1 - x))^2 = k_3t$	Li:9.7 Ni:11.2 Co:9.5 Mn:6.2	[16]
LiNi <sub>x</sub> Co <sub>x</sub> Mn <sub>x</sub> O <sub>2</sub>	H <sub>2</sub> SO <sub>4</sub> + ginkgo biloba	$1 - (1 - x)^{1/3} = kt$ $1 - 2/3x - (1 - x)^{2/3} = kt$	Li:23.4 Ni:74.6 Co:79.3 Mn:73.1	[17]

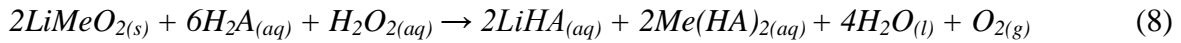
### SHRINKING CORE MODEL

Chen *et al.* [12] used the shrinking core model to investigate the dissolution kinetics of LiNi<sub>x</sub>Mn<sub>y</sub>Co<sub>z</sub>O<sub>2</sub> using sulfuric acid and tartaric acid and with the addition of hydrogen peroxide as a reducing agent.

The leaching mechanism of LiNi<sub>x</sub>Mn<sub>y</sub>Co<sub>z</sub>O<sub>2</sub> with tartaric acid can be illustrated by the reactions (5–8). If the ratio of cathode material (LiMeO<sub>2</sub>, where Me represents Ni, Co, and Mn) to tartaric acid (H<sub>2</sub>A) is 2:3, the soluble complex Li<sub>2</sub>A and the insoluble complexes MeA are formed according to reaction 5.



The soluble complex  $\text{Li}_2\text{A}$  and the insoluble complexes  $\text{MeA}$  can be dissolved by adding tartaric acid so that the ratio of cathode material to tartaric acid is 1:3.

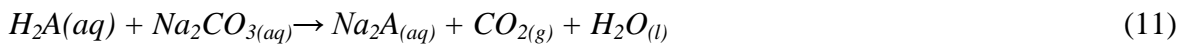
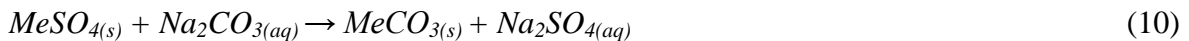


In the leaching of cathode material with tartaric acid, hydrogen peroxide is used to convert cobalt and manganese from higher oxidation states ( $\text{Co}^{3+}$  i  $\text{Mn}^{4+}$ ) to lower oxidation states ( $\text{Co}^{2+}$  i  $\text{Mn}^{3+}/\text{Mn}^{2+}$ ).

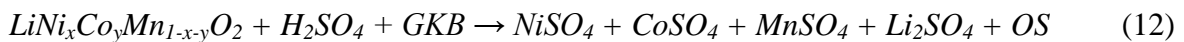
When  $\text{LiNi}_x\text{Mn}_y\text{Co}_z\text{O}_2$  is leached with tartaric acid, complexes are formed from which valuable metals cannot be extracted directly due to the disturbed crystal structure. However, the tartaric acid complexes can be easily dissolved by adding sulfuric acid to the leaching solution, whereby transition metal sulphates ( $\text{MeSO}_4$ ) are formed after the following reaction:



In order to ensure complete precipitation of the  $\text{Me}^{2+}$  ions, sodium carbonate is added to the resulting sulphates, resulting in transition metal carbonates:



Zhu *et al.* [17] used the shrinking core model to study the leaching kinetics of  $\text{LiNi}_x\text{Co}_y\text{Mn}_{1-x-y}\text{O}_2$  in the  $\text{H}_2\text{SO}_4$  + Ginkgo biloba system. The leaching mechanism of  $\text{LiNi}_x\text{Co}_y\text{Mn}_{1-x-y}\text{O}_2$  cathode material, under the influence of sulfuric acid and Ginkgo biloba can be represented by the following reaction:



where: GKB - Ginkgo biloba, reducing agent; OS - oxidation product.

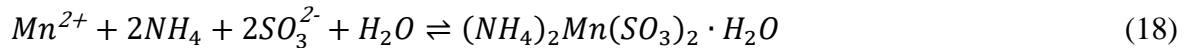
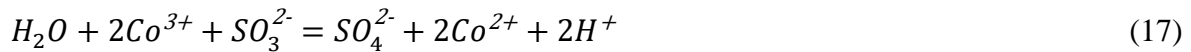
The dissolution mechanism of  $\text{LiNi}_x\text{Co}_y\text{Mn}_{1-x-y}\text{O}_2$  cathode material under the influence of sulfuric acid and Ginkgo biloba consists of three main stages [17]:

- Diffusion of sulfuric acid and Ginkgo biloba molecules to the surface of the cathode material by liquid flow,
- Penetration and diffusion of sulfuric acid and Ginkgo biloba molecules through the product layer to the surface of the unreacted core, and
- Chemical reaction of sulfuric acid and Ginkgo biloba with  $\text{LiNi}_x\text{Co}_y\text{Mn}_{1-x-y}\text{O}_2$  at the reaction surface.

Wang *et al.* [11] determined the kinetics and mechanism of leaching of transition metals from  $\text{LiNi}_x\text{Co}_x\text{Mn}_x\text{O}_2$  using the shrinking core model in the  $\text{NH}_3\text{-(NH}_4)_2\text{SO}_4\text{-Na}_2\text{SO}_3$  system. During the leaching process,  $\text{Ni}^{2+}$ ,  $\text{Co}^{2+}$ , and  $\text{Mn}^{2+}$  ions react with free ammonia to form stable amino complexes, corresponding to the following reactions:



Ammonium sulfate sulphate is used to facilitate the transition of cobalt from a higher oxidation state to a lower oxidation state. At temperatures above  $70^\circ\text{C}$ , the reduction of ammonium sulfate to ammonium sulfite takes place, which facilitates the easier separation of manganese compounds [11].



In addition to the formation of amino complexes, sulfates, carbonates, and oxides can also be formed, e.g.  $\text{Li}_2\text{CO}_3$ ,  $\text{CoSO}_4$ ,  $\text{NiSO}_4$ , and/or  $\text{Co}_3\text{O}_4$ . Manganese-amino complexes are unstable, and  $\text{Mn}^{2+}$  ions can react with  $\text{CO}_3^{2-}$  ions to form stable manganese carbonate complexes, according to the following reaction:



At operating temperatures above  $70^\circ\text{C}$ , manganese ions change from the  $\text{Mn}^{4+}$  oxidation state to the  $\text{Mn}^{2+}$  oxidation state and form unstable complexes, clathrates, manganese-ammonium-sulfite hydrates,  $(\text{NH}_4)_2\text{Mn}(\text{SO}_3)_2 \cdot \text{H}_2\text{O}$ , which leads to reduced manganese leaching [11].

Nshizirungu *et al.* [13] investigated the dissolution mechanism of  $\text{LiNi}_x\text{Co}_x\text{Mn}_x\text{O}_2$  in a polyvinylidene fluoride (PVDF) solution. Based on the shrinking core model, the authors assumed that the leaching of the transition metals occurs in two stages. In the first stage, the decomposition of PVDF takes place in the aqueous solution in the temperature range of  $270^\circ\text{C}$ – $350^\circ\text{C}$ . In the second stage, with an increase in the temperature range ( $350^\circ\text{C}$ – $370^\circ\text{C}$ ), secondary reactions take place between fluoride and hydroxyl ions. As a result, transition metal hydroxides and hydrofluoric acid are formed according to the following reactions:





## CONCLUSION

Spent lithium-ion batteries are a valuable waste material for the recovery of lithium, cobalt, nickel, manganese, and/or their compounds. However, if not handled properly, this type of electronic waste can pose a risk to the environment and human health. However, if not treated properly, this type of electronic waste can endanger the environment and human health. Numerous studies conducted to better understand the systems involved in the recycling process of cathode material show that the shrinking core model is often used to describe the leaching process. Various systems of organic and inorganic origin and their combinations are used as leaching agents. The calculated activation energy values for Li, Ni, Mn, and Co indicate that for most systems the process is determined by the chemical reaction between the leaching agent and the unreacted particles of LiNiMnCoO<sub>2</sub>.

## ACKNOWLEDGEMENT

*The research presented in this paper was performed with the financial support of the Ministry of Science, Technological Development, and Innovation of the Republic of Serbia, within the funding of the scientific research work at the University of Belgrade, Technical Faculty in Bor, according to the contract number (451-03-65/2024-03/200131).*

## REFERENCES

- [1] Wang T.W., Liu T., Sun H., Mater. Today Energy 38 (2023) 101434.
- [2] Piątek J., Afyon S., Budnyak T.M., *et al.*, Adv. energy mater. 11 (2021) 2003456.
- [3] Wang Y., An N., Wen L., *et al.*, J. Energy Chem. 55 (2021) 391–419.
- [4] Wang C., Wang S., Yan F., *et al.*, Waste Manage. 114 (2020) 253–262.
- [5] Ma Y., Liu X., Zhou X., *et al.*, J. Clean. Prod. 331 (2022) 129902.
- [6] Wu W., Liu X., Zhang X., *et al.*, J. Biosci. Bioeng. 128 (2019) 344–354.
- [7] Liu Z., Liu G., Cheng L., *et al.*, Green Energy & Environ. 9 (2024) 802–830.
- [8] Liu C., Lin J., Cao H., *et al.*, J. Clean. Prod. 228 (2019) 801–813.
- [9] Ghassa S., Farzanegan A., Gharabaghi M., *et al.*, Hydrometallurgy 197 (2020) 105465.
- [10] Zhuang L., Sun C., Zhou T., *et al.*, Waste Manage. 85 (2019) 175–185.
- [11] Wang H., Li Z., Meng Q., *et al.*, Hydrometallurgy 208 (2022) 105809.
- [12] Chen X., Kang D., Li J., *et al.*, J. Haz. Mat. 389 (2020) 121887.
- [13] Nshizirungu T., Rana M., Khan I.M.H., *et al.*, J. Environ. Chem. Eng. 11 (2023) 109160.
- [14] Su F., Zhou X., Liu X., *et al.*, Chem. Eng. J. 455 (2023) 140914.
- [15] Li C., Dai G., Liu R., *et al.*, Sep. Purif. Technol. 306 (2023) 122559.



- [16] Chabhadiya K., Srivastava R.R., Pathak P.J., Environ. Chem. Eng. 9 (2021) 105232.
- [17] Zhu B., Zhang Y., Zou Y., *et al.*, J. Environ. Manage. 300 (2021) 113710.



## IMMOBILIZATION OF LEAD USING CERIA CRYSTAL STRUCTURE

Branko Matovic<sup>1\*</sup>, Jelena Maletaskic<sup>1</sup>, Svetlana Butulija<sup>1</sup>, Sanja Petrovic<sup>2</sup>,  
Bratislav Todorovic<sup>2</sup>

<sup>1</sup>Vinča Institute of Nuclear Sciences - National Institute of the Republic of Serbia,  
University of Belgrade, Mike Petrovića Alasa 12–14, 11000 Belgrade, SERBIA

<sup>2</sup>Faculty of Technology University of Nis, Bulevar Oslobođenja 124, 16000 Leskovac,  
SERBIA

\*mato@vinca.rs

### Abstract

*Lead is a very useful element that has found application in batteries, construction, bullets and hunting ammunition, it is part of solder and various alloys. It is especially used in piezoelectrics and as a shield against radiation. Unfortunately, lead is a potent neurotoxin that accumulates in soft tissues and bones over time. Therefore, it is of great interest to control Pb mobility and bio-accessibility by its immobilization in a suitable crystal structure. Ceria with fluorite structure could play essential roles in lead immobilization. Nanosized Pb-doped ceria ( $Ce_{1-x}Pb_xO_2$ ) powders ( $0.1 \leq x \leq 0.3$ ) were obtained by self-propagating room temperature reaction. X-ray diffraction analysis and field emission scanning microscopy results showed that the doped samples are single phase solid solutions with fluorite-type structure and all prepared powders were nanometric in size. The thermal stability of solid solution was followed by XRD. The mass of Pb [ppm] in the solution with different concentration of Pb in the doped ceria after its dissolution in different time intervals at different pH values was measured by means of Inductively coupled plasma (ICP) spectroscopy. The TEM investigation showed that pattern of  $CeO_2$  before and after leaching confirms that samples are single phase  $CeO_2$ .*

**Keywords:** lead, immobilization, fluorite structure, stability of solid solution.

### INTRODUCTION

Enhanced industrial activities and human actions in recent times have led to increased release of toxic heavy metals into the environment, particularly agricultural lands [1]. Lead (Pb) is commonly found in polluted soils, and its elevated levels can diminish environmental quality, causing reduced crop yields and groundwater contamination, thus posing significant risks to human and animal health [2]. Consequently, the remediation of contaminated soils is a pressing concern for ensuring safe water and food production.

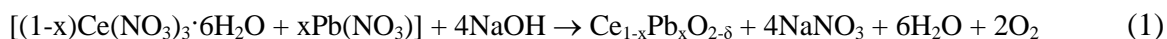
Various conventional techniques such as excavation, landfilling, and soil washing are commonly employed to remediate soils contaminated with heavy metals. However, these methods are often time-consuming, expensive, and sometimes not feasible. In contrast, the in situ immobilization technique has been anticipated as more environmentally friendly and effective for remediating heavy metals from contaminated soils [3,4]. One successful technique is immobilization, which has been primarily used for nuclear waste. Immobilization of heavy metals is the process of converting hazardous waste into a solid form to prevent its

release into the environment. This is done to reduce the risk of contamination and facilitate safe long-term storage or disposal. The most common method of immobilizing heavy metals is the use of suitable crystal lattice structures that can encapsulate and retain these elements.

In this work the powders were prepared by the self-propagating room temperature reaction (SPRT) [5]. This technique gives the possibility of producing very fine powders with very precise stoichiometry in accordance with the tailored compositions [6]. In addition, it is the first time that the results are shown, which evidence formation of solid solution between ceria and Pb. These solid solutions were obtained in a form of nanometric powders by applying SPRT. The effect of Pb concentration on the thermal and chemical stability of ceria solid solution was examined.

## **MATERIALS AND METHODS**

Nanocrystalline  $\text{Ce}_{1-x}\text{Pb}_x\text{O}_{2-\delta}$  ( $x = 0.0\text{--}0.3$ ) powders were synthesized by SPRT method [7]. The starting materials for the preparation of Pb immobilization by ceria crystal lattice were cerium nitrate hexahydrate, lead nitrate and sodium hydroxide. Used chemicals were 99.9% pure as stated by the manufacturer (OLDRICH). The compositions of the starting reacting mixtures were calculated according to the nominal composition of the final reaction product, according to the equation (1):



Synthesis procedure was carried out in an alumina mortar by mechanical activation (by hand mixing instead by heating) of reactants for 3–5 min, that allowed rapid progress of the reaction at room temperature in the air. After being exposed to air for 2 h, obtained mixtures of reaction products according to equation (1) was dissolved in water and subjected to centrifugation at Centurion 1020D centrifuge at 4000 rpm, for 10 min. Rinsing procedure was repeated four times with distilled water and twice with ethanol, in order to eliminate  $\text{NaNO}_3$  from the synthesized powder mixture. Finally, material was dried out at 70°C in ambient atmosphere. It should be outlined that this is the first time that solid solution powders were prepared directly after synthesis procedure was terminated.

The composition of the Ag-doped ceria was identified by means of powder XRD on a Rigaku IV, XRD diffractometer with Cu  $K\alpha$  radiation at room temperature. The present phases were identified with the help of the PDXL2 software (version 2.0.3.0) [8], with reference to the patterns of the International Centre for Diffraction Data (ICDD) [9], version 2012.

Morphology of obtained powders as well as their evolution during calcination was studied by the Field emission electron microscope model FE-SEM JEOL-5200F (Japan). The mass of Pb [ppm] in the solution with different percentage of Pb in the doped ceria after its dissolution in different time intervals at pH 3, pH 7 and pH 11 was measured by means of inductively coupled plasma optical emission spectrometry instrument (ICP-OES, ARCOS FHE12, SPECTRO, Germany), according to the manufacturer's instructions.

The conventional and high-resolution (HR) transmission electron microscopy (TEM/HRTEM) analyses were carried out using the FEI Talos F200X microscope (Thermo Fisher Scientific, Waltham, MA, United States) operating at 200 kV. The elemental composition and change of Pb content before and after leaching is investigated by an energy-dispersive X-ray spectroscopy (EDXS) system.

## RESULTS AND DISCUSSION

As-synthesized Pb immobilized in CeO<sub>2</sub> matrices, presented in Figure 1, revealed low intensity diffraction reflections in each sample and their significant broadening indicating small crystallite size. The obtained materials depicted explicit features of cubic fluorite crystal structure (space group 225), known as cerianite phase (JSPDS-ICDD 34-0394). The ceria peak shape of the plane reflections in the obtained samples broadened, with increasing Pb doping, respectively.

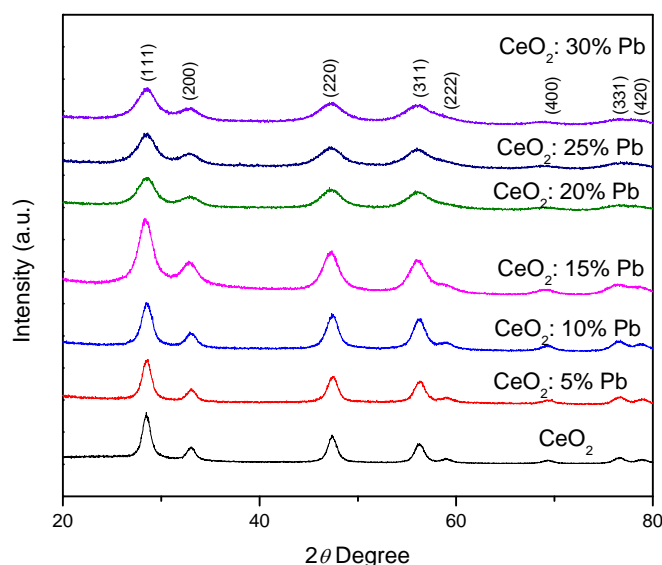


**Figure 1** X-ray diffraction patterns of synthesized  $Ce_{1-x}Pb_xO_{2-\delta}$  nanopowders at room temperature

The typical morphology of obtained solid solution is shown at Figure 2. As synthesized powders depict very small isometric particles which are agglomerated in the form of spheres. Roughly measured, the size of individual particles was about 5 nm, while the agglomerated spheres were about 100–150 nm.

In order to examine the stability of Pb immobilized in CeO<sub>2</sub> matrices (solid solutions), the samples  $Ce_{1-x}Pb_xO_{2-\delta}$  ( $x = 0.0-0.3$ ) were heat treated at the temperature of 600 and 900 °C for 1 h (Figure 3). All solid solutions throughout the entire range of Pb concentrations show stability at 600 °C. With further temperature increase to 900 °C, solid solutions with 15% Pb are also stable; however, at higher concentrations exceeding 15% of Pb (20 and 30%), the separation of PbO phase occurs at 900 °C. This confirms that the thermal stability of such a solid solution decreases with temperature.

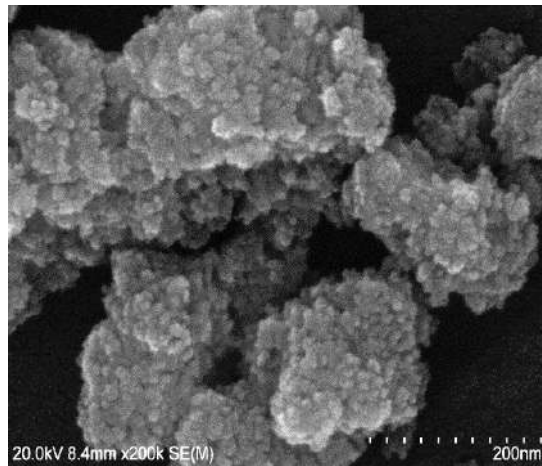


**Figure 2** Typical FE SEM of obtained of  $Ce_{1-x}Pb_xO_{2-\delta}$  nanopowders at room temperature

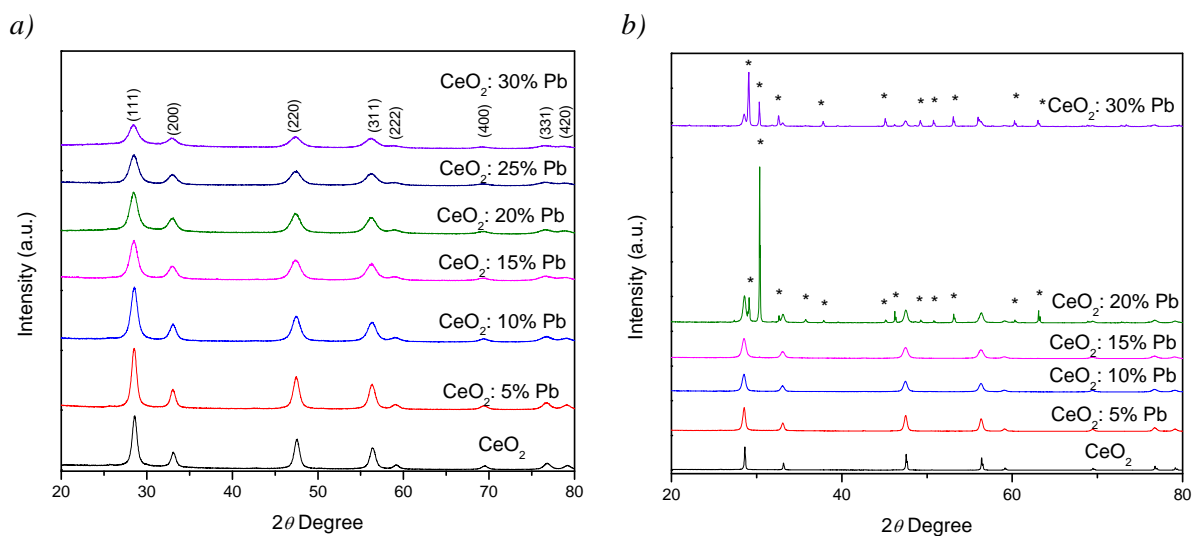


**Figure 3** X-ray diffraction pattern of  $Ce_{1-x}Pb_xO_{2-\delta}$  nanopowders calcined at a) 600; b) 900 °C:  $-(PbO)$ . Unmarked peaks belong to the fluorite structure

The chemical stability of immobilized lead in the matrix of cerium fluorite lattice was monitored at various time intervals at 3 different pH levels (3, 7, and 11), which is given in the Figure 4.

It is evident that under basic conditions, immobilized Pb is stable, while in neutral medium, it is partially soluble and highly soluble (around 20%) in acidic conditions. In the case of higher concentrations of Pb in the cerium matrix, this trend is even more pronounced. Specifically, in acidic conditions, almost 90% of Pb is dissolved after 30 hours, while in basic conditions, only 1.6% is dissolved in the same period (Table 1).

Considering that the highest concentration was 30% Pb, that sample was examined using TEM before and after Pb dissolution.

The TEM investigation of  $CeO_2$  showed agglomerated nanoparticles (Figure 5a and b) with particle size of only few nanometers. The particle size observed with HRTEM matches the calculated particle size of 2.98 nm from XRD patterns. The HRTEM image (inset of Figure 5a) reveals the lattice fringes corresponding to (1 1 1) plane of  $CeO_2$  with d spacing of 0.331 nm before leaching of Pb. The selected area electron diffraction (SEAD) pattern of  $CeO_2$

before and after leaching confirms that samples are single phase  $\text{CeO}_2$  and they are presented as insets of Figure 5 a,b. The SEAD pattern exhibits series of rings corresponding to the respective (1 1 1), (2 0 0), (2 2 0) and (3 1 1) planes of  $\text{CeO}_2$  nanoparticles. The elemental composition and change of Pb content before and after leaching is investigated by EDS. EDS shows that the content of Pb is 15 at% before leaching and dropping to 4 at% after leaching. Beside the change of Pb content observed in EDS spectrum of the sample, the change of interplanar distance of (111) plane from 0.331 to 0.327 nm is also observed, confirming that the Pb cations are leached out from  $\text{CeO}_2$  structure.

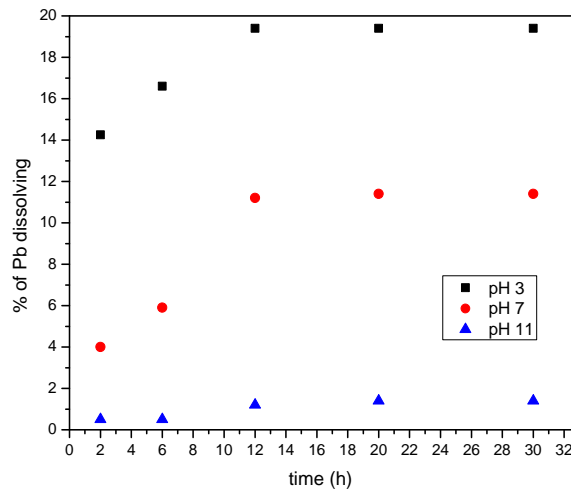


**Figure 4** Dissolved Pb in mass percentages in the solution of the sample with 10% Pb after its dissolution at various time intervals at pH 3, pH 7, and pH 11

**Table 1** Pb dissolution (mas.%) in the sample solution with 30% Pb after its dissolution at different time intervals at pH 3, pH 7 and pH 11

Time (h)	pH 3	pH 7	pH 11
2	62	18	1.6
6	69	32	1.6
12	77	34	1.6
20	85	42	1.6
30	90	46	1.6

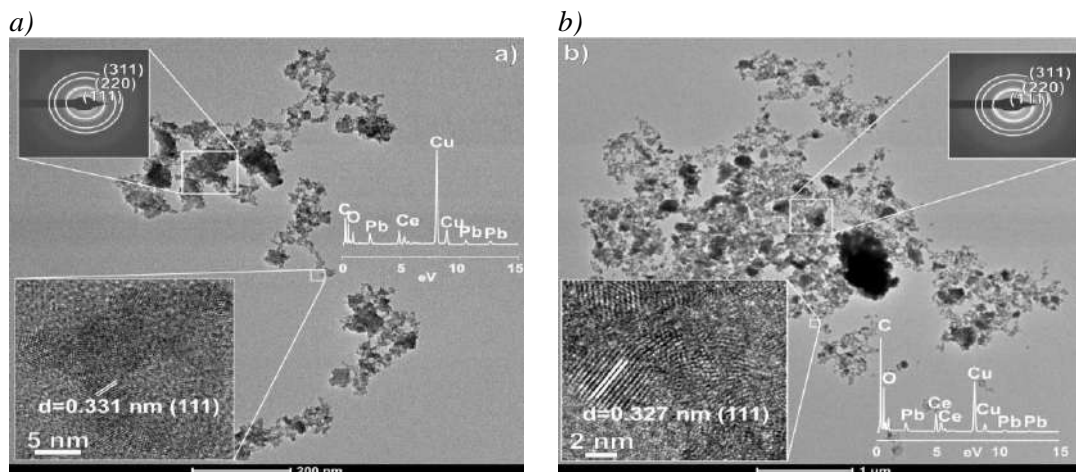


**Figure 5** TEM spectra of  $\text{Ce}_{0.7}\text{Pb}_{0.3}\text{O}_{2-\delta}$  solid solution a) before; b) after leaching (pH 3)



## CONCLUSION

Single Pb-ceria solid solutions were synthesized by self-propagating room temperature method (SPRT). XRD and TEM spectroscopy confirmed the pure solid solutions.

The solid solubility of Pb into ceria lattice was the topmost reported so far. Average crystallite size of the powders was less than 5 nm.

The thermal stability of solid solutions are stable till 600°C, after that it decreases with increasing the amount of Pb concentration at 900°C

These results demonstrate the highly effective room temperature immobilization of Pb in the form of ceria solid solutions using the SPRT method.

## ACKNOWLEDGEMENT

*The authors are grateful to the Ministry of Science, Technological development and Innovation of the Republic of Serbia for financial support according to the contract with the registration number (e.g. 451-03-68/2024-14/200017).*

## REFERENCES

- [1] Bian R., Chen D., Liu X., *et al.*, Ecol. Eng. 58 (2013) 378–383.
- [2] Houben D., Evrard L., Sonnet P., Biomass Bioener. 57 (2013) 196–204.
- [3] Al Chami Z., Cavoski I., Mondelli D., *et al.*, Environ. Sci. Pollut. Res. 20 (2013) 4766–4776.
- [4] Liang Y., Cao X., Zhao L., *et al.*, Environ. Sci. Pollut. Res. 22 (2014) 4665–4674.
- [5] Boskovic S., Matovic B., Nanostructured Solid Solutions of the Fluorite Type Crystal Structure *in* Fluorite: Structure, Chemistry and Applications, Editor: van Asten M., Nova Science, New York (2019), p.1–111, ISBN: 978-1-53615-204-3.
- [6] Matovic B., Dohcevic-Mitrovic Z, Radovic Z., *et al.*, J. Power Sources 139 (1) (2009) 146–149.
- [7] Boskovic S., Djurovic D., Dohcevic-Mitrovic Z., *et al.*, J Power Sources 145 (2) (2005) 237–242.
- [8] PDXLVersion 2.0.3.0 Integrated X-ray Powder Diffraction Software, Rigaku Corporation, Tokyo, Japan, 2011, pp. 196–8666.
- [9] Powder Diffraction File, PDF-2 Database, announcement of new database release 2012, International Centre for Diffraction Data (ICDD).



## CAUSES AND POSSIBLE CONSEQUENCES OF THERMAL RUNAWAY IN LITHIUM-ION BATTERIES

Dragana Medić<sup>1\*</sup>, Snežana Milić<sup>1</sup>, Nemanja Milošević<sup>2</sup>, Maja Nujkić<sup>1</sup>, Slađana Alagić<sup>1</sup>, Aleksandar Cvetković<sup>1</sup>, Aleksandra Papludis<sup>1</sup>

<sup>1</sup>University of Belgrade, Technical Faculty in Bor, V.J. 12, 19210 Bor, SERBIA

<sup>2</sup>Elixir Prahovo Ltd, Radujevački put bb, 19300 Prahovo, SERBIA

\**dmedic@tfbor.bg.ac.rs*

### Abstract

*Advances in lithium-ion battery (LIB) technology have facilitated its widespread use, including in electric vehicles and electronic devices. However, with the increasing use of LIBs, the risk of thermal runaway is also increasing. This article explains the causes and mechanisms of thermal runaway in LIBs and the possible consequences of this process. One way to mitigate the risk of thermal runaway is to improve battery design to minimise internal defects and increase thermal stability. In addition, the development of advanced thermal management systems capable of detecting and controlling thermal anomalies can be crucial. Understanding the causes and consequences of thermal runaway in LIBs is essential for their further development and safe application in various fields.*

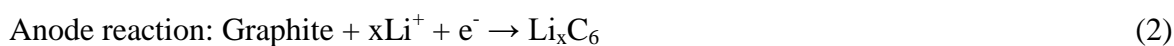
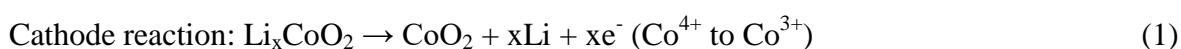
**Keywords:** LIBs, thermal runaway, mechanism.

### INTRODUCTION

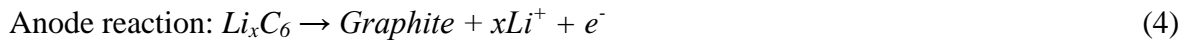
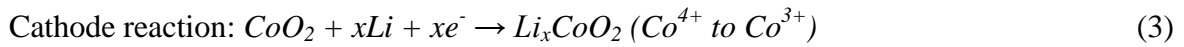
Lithium-ion batteries (LIBs) have become a key power source for a wide range of electronic devices and electric vehicles due to their high energy density, long lifespan, and low greenhouse gas emissions [1–3]. Over time, lithium-ion batteries have gradually replaced lead-acid batteries, nickel-metal hydride batteries, and nickel-cadmium batteries [4,5]. However, as the use of LIBs expands, awareness of their potential safety risks also grows.

Lithium-ion batteries usually consist of two intercalation materials that form the cathode and the anode in the electrochemical cell. To avoid short circuits, the cathode and anode are separated by a porous membrane, the separator. The separator is impregnated with an electrolyte that facilitates the diffusion of lithium ions between the electrodes [6].

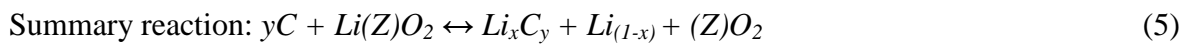
During the battery charging process, oxidation and reduction occur at the cathode and anode, respectively.  $\text{Li}^+$  ions are released from the cathode structure, move through the electrolyte, receive energy from the source, and are inserted into the anode structure, according to the following reactions [7,8]:



During the battery discharge process,  $\text{Li}^+$  ions are released from the anode structure, move through the electrolyte, generate energy, and are inserted into the cathode structure, as shown in reactions 3 and 4 [7,8]:



The overall reaction that take place in the battery during the charging and discharging process can be represented by the following reaction [7,8]:



where:  $x \sim 0.5$ ;  $y = 6$ ; Z can be cobalt, manganese or nickel.

Thermal runaway is a serious safety issue in LIBs where an irreversible process occurs within the battery that is accompanied by an increase in temperature that can lead to a fire or explosion. Understanding the causes and consequences of thermal runaway is critical to improving the safety of LIBs and minimising potential risks to users and the environment.

This paper aims to provide an overview of the main factors that contribute to thermal runaway in LIBs and the possible consequences of this process. By analysing relevant literature and research, the focus will be on the mechanisms by which thermal runaway occurs, factors that influence the likelihood of this process, and strategies to prevent and overcome this challenge.

## THERMAL RUNAWAY IN LITHIUM-ION BATTERIES

Thermal runaway is a process of uncontrolled temperature increase. In the context of batteries, thermal runaway can occur when the battery generates more heat than it can dissipate. The excess heat can accelerate chemical reactions within the battery, causing the temperature to increase, which can lead to a fire or even an explosion [9–11].

In practise, improper handling of LIBs often leads to the triggering of thermal chain reactions within the cell, resulting in the decomposition of battery components, the emission of toxic gases and even an explosion. Figure 1 shows the most common causes and possible consequences of thermal reactions within the battery.

Figure 1 shows numerous causes that can lead to thermal runaway in LIBs. The first cause can be physical damage to the battery, overload, overcharge/discharge or other factors that cause a localised temperature increase. As the battery heats up, the rate of chemical reactions within the battery can increase. The intense chemical reactions within the battery release gases that can increase the internal pressure and cause the battery to expand or even explode. If the battery explodes or ignites, it can react with the oxygen in the air, resulting in a more intense fire [12].

The improper use of LIBs not only leads to economic losses, but can also have a negative impact on human health and lives. Careful handling of LIBs is required at all times, as incorrect handling can lead to numerous side reactions and the formation of various chemical compounds. Thermal decomposition of chemical compounds releases toxic gases that can lead to health problems such as chronic damage, paralysis and even death.

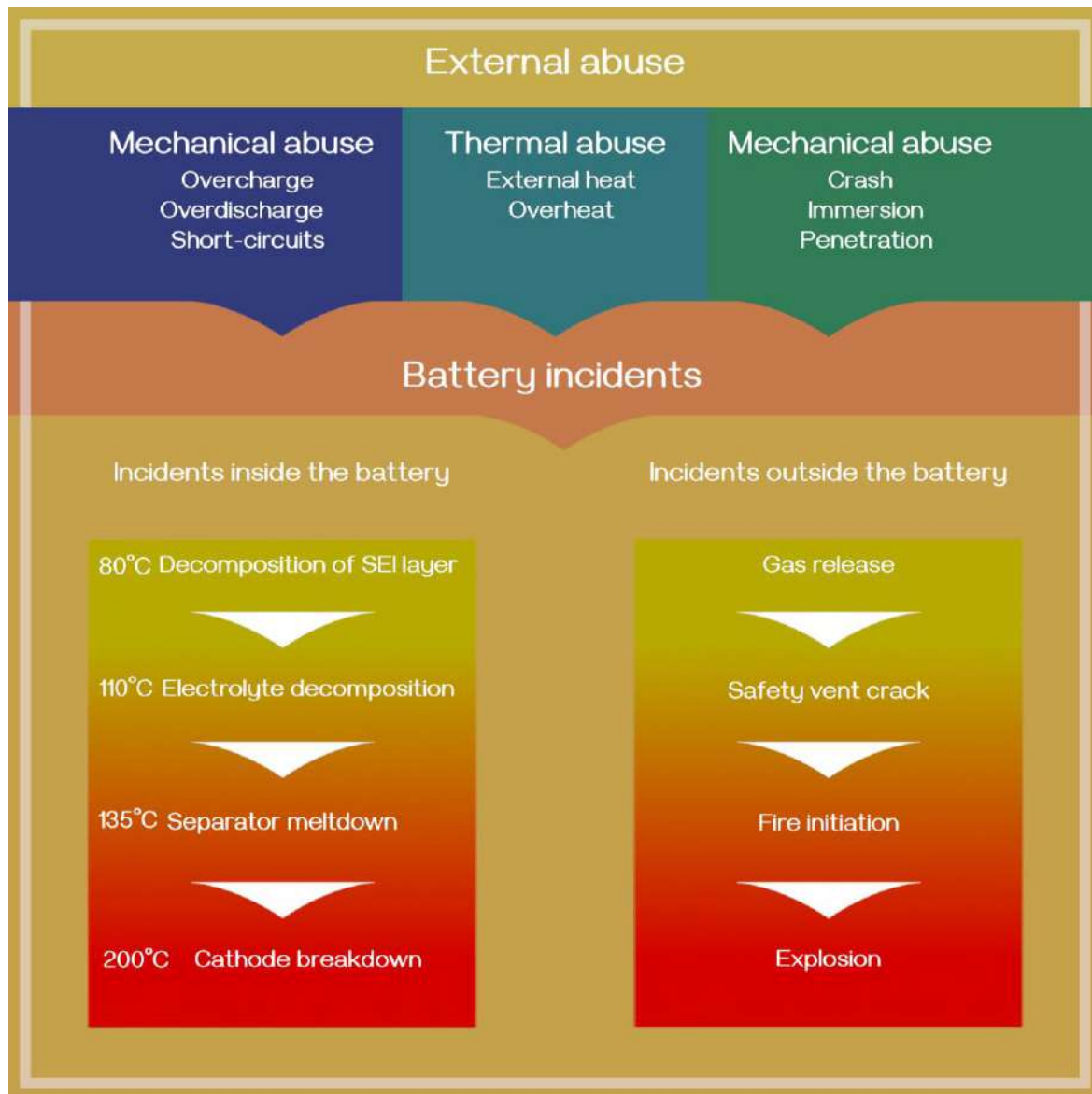


**Figure 1** Causes and possible consequences of thermal runaway in LIBs

Different types of lithium-ion batteries release different concentrations of gases when the electrolyte ignites and the cell decomposes. Table 1 shows the concentrations of gases emitted during the thermal decomposition of LIBs consisting of different types of cathode materials [12].

**Table 1** Gas composition resulting from thermal runaway in commercial LIBs [12]

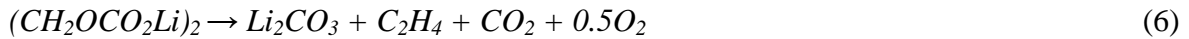
Gas	Unit	Cathode material		
		<sup>a</sup> LCO/NMC	<sup>b</sup> NMC	<sup>c</sup> LFP
H <sub>2</sub>	mol %	30.0	30.8	30.9
CO <sub>2</sub>	mol %	24.9	41.2	53.0
CO	mol %	27.6	13.0	4.8
CH <sub>4</sub>	mol %	8.6	6.8	4.1
C <sub>2</sub> H <sub>4</sub>	mol %	7.7	8.2	6.8
C <sub>2</sub> H <sub>6</sub>	mol %	1.2	/	0.3

<sup>a</sup>lithium cobalt oxide/lithium nickel cobalt manganese oxide; <sup>b</sup>lithium nickel cobalt manganese oxide; <sup>c</sup>lithium iron phosphate.

## MECHANISM OF THE THERMAL RUNAWAY OF THE LITHIUM-ION BATTERIES

The thermal runaway of LIBs consists of several phases. In each phase, exothermic reactions take place, not necessarily one after the other, but often simultaneously. Understanding the mechanisms of thermal runaway not only helps to identify key problems in the operation of LIBs, but also enables the development of preventive measures and technologies that can minimise the risk of such an incident.

In the first phase, when the temperature inside the battery rises to 70–90°C, the film at the solid electrolyte interface (SEI) decomposes and the following reactions can take place [12–15]:

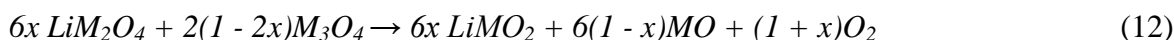
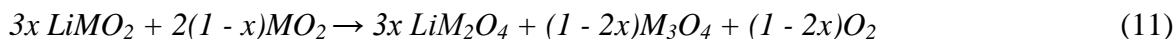


In the second phase, a reaction occurs between the electrolyte and the anode. From the anode, the intercalated lithium reacts with organic electrolytes, and the process is accompanied by the formation of flammable gases and a further temperature increase [14,15]:



In the third phase, at temperatures above 130°C, the separator melts because it is made of polyethylene (PE)/polypropylene (PP). As a result, a series of internal short circuits occur between the electrodes (and the voltage at the battery terminals drops to zero volts), and the energy accumulated in the battery through charging is released. This leads to a further increase in temperature in the battery [15].

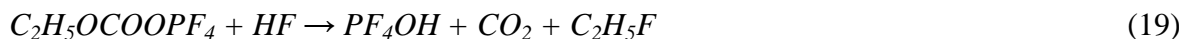
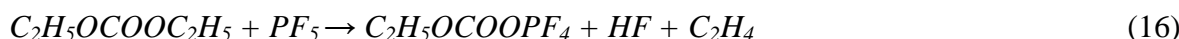
In the fourth phase, with a further increase in temperature, the active cathode materials begin to decompose, and oxygen is released. With a cathode made of LiMeO<sub>2</sub> where M stands for the composition of Ni, Co, and Mn, for example, the following reactions occur [16]:



The oxygen released during the reactions (11–13) can react with electrolytes in LIBs. For example, the combustion of ethylene carbonate (EC) can be represented by the following reaction [15]:



In the fifth phase, the electrolyte not only reacts with the electrodes, but is also degraded at temperatures of 200–300°C. In the case of diethyl carbonate (DEC), for example, the following reactions occur [15,17]:



In addition to the reactions already mentioned, reactions between the binder and the battery components can also occur during thermal runaway in LIBs. Polyvinylidene fluoride (PVDF) and carboxymethyl cellulose (CMC) are most commonly used as binders in lithium-ion batteries [14]:



Other mechanisms by which thermal runaway occurs can also be found in the scientific literature; however, only the most frequently investigated chemical reactions are presented in this paper.

## CONCLUSION

Thermal runaway is a serious challenge in the operation of LIBs, and its causes and potential consequences are topics of great interest to researchers and industry. In this review paper, several key causes of thermal runaway were identified, including overcharge/discharge, short circuits, mechanical damage, and high temperatures. In addition, the potential consequences of thermal runaway were analysed, including physical damage to LIBs and the emission of flammable gases that can cause fires and explosions.



To effectively manage the risks of thermal runaway, advanced detection and control technologies must be developed and battery designs improved to increase resilience to these challenges. In addition, continuous research and development of new materials and technologies are crucial to reduce the risk of thermal runaway and increase the safety of LIBs.

Studying and understanding the mechanisms of thermal runaway in LIBs plays a crucial role in ensuring the safe and reliable use of this technology in various applications, from mobile devices to electric vehicles and renewable energy sources.

## **ACKNOWLEDGEMENT**

*The research presented in this paper was performed with the financial support of the Ministry of Science, Technological Development, and Innovation of the Republic of Serbia, within the funding of the scientific research work at the University of Belgrade, Technical Faculty in Bor, according to the contract number (451-03-65/2024-03/200131).*

## **REFERENCES**

- [1] Xu J., Cai X., Cai S., *et al.*, *Energy Environ. Mater.* 6 (2023) e12450.
- [2] Zubi G., López R.D., Carvalho M., *et al.*, *Renew. Sust. Energ. Rev.* 89 (2018) 292–308.
- [3] Lai X., Gu H., Chen Q., *et al.*, *J. Clean. Prod.* 372 (2022) 133756.
- [4] Liu W., Placke T., Chau K.T., *Energy Rep.* 8 (2022) 4058–4084.
- [5] Sun Y., Zhu M., Yao Y., *Sep. Purif. Technol.* 237 (2020) 116325.
- [6] Liu C., Neale Z.G., Cao G., *Mater. Today* 19 (2016) 109–123.
- [7] Choudhari V.G., Dhoble, A.S., Sathe T.M., *J. Energy Storage* 32 (2020) 101729.
- [8] Manfo T.A., Şahin M.E., *TIJMET* 6(2) (2023) 70–78.
- [9] Escobar-Hernandez H.U., Gustafson R.M., Papadaki M.I., *J. The Electrochem. Soc.* 163(13) (2016) A2691–A2701.
- [10] Qiu M., Liu J., Cong B., *et al.*, *Batteries* 9(8) (2023) 411.
- [11] Zhou T., Sun J., Li J., *et al.*, *Batteries* 9(6) (2023) 308.
- [12] Sun J., Mao B., Wang, Q., *Fire Safety J.* 120 (2021) 103119.
- [13] Lyu P., Liu X., Qu J., *Energy Storage Mater.* 31 (2020) 195–220.
- [14] Huang Z., Zhao C., Li H., *Energy* 205 (2020) 117906.
- [15] Galushkin N.E., Yazvinskaya N.N., Galushkin D.N., *J. Energy Storage* 86 (2024) 111372.
- [16] Pastor J.V., García A., Monsalve-Serrano J., *et al.*, *Appl. Therm. Eng.* 230 (2023) 120685.
- [17] Golubkov A.W., Fuchs D., Wagner J., *RSC Adv.* 4 (2014) 3633.



## KINETIC AND EQUILIBRIUM STUDIES OF CHROMIUM SORPTION USING ULTRASONICALLY MODIFIED WOOD SAWDUST BY ALUMINA

Nena Velinov<sup>1\*</sup>, Miljana Radović Vučić<sup>1</sup>, Jelena Mitrović<sup>1</sup>, Milica Petrović<sup>1</sup>,  
Slobodan Najdanović<sup>1</sup>, Danijela Bojić<sup>1</sup>, Aleksandar Bojić<sup>1</sup>

<sup>1</sup>University of Niš, Department of Chemistry, Faculty of Science and Mathematics,  
Višegradska 33, 18000 Niš, SERBIA

\*[vena.velinov@yahoo.com](mailto:vena.velinov@yahoo.com)

### Abstract

*An oak tree sawdust was modified by a simple ultrasonically assisted synthesis method with alumina. Wood-alumina sorbent was used for chromium (VI) ions removal from water. The kinetics and equilibrium study of sorption process was studied in detail. The sorption mechanism was best described by Langmuir isotherm followed pseudo-second order kinetics and the maximal sorption capacity was 104.2 mg/g. The application of obtained sorbent presents very fast sorption with high removal efficiency of chromium.*

**Keywords:** wood sawdust, ultrasound modification, alumina, chromium removal.

### INTRODUCTION

In the past few decades, the removal of chromium (VI) from water and wastewaters has been a technological and scientific problem due to its toxicity [1]. Chromium (VI) wastewaters are mainly generated from a variety of industries including: leather tanning and pigment manufacturing, metal finishing, electroplating [2].

Various treatment methods and techniques, such as: precipitation, membrane separation, ion exchange, coagulation, solvent extraction, electroplating, photocatalytic reduction, have been used for chromium (VI) ions removal [3]. However, these methods and techniques have limitations including high demand energy and chemicals, high cost, low efficiency, and generation of toxic sludge [4].

Sorption processes could be used as alternative for removal of chromium (VI) from wastewater due to its simplicity, low cost, high efficiency, and eco-friendliness [5]. Novel sorbents synthesized using sawdust, which is a typical waste product from wood processing and furniture industry, have become widely used materials, because it is abundant and biodegradable waste and displays a unique porous microstructure [6].

The main idea of this study was the application of the kinetics and isotherm models for the determination of the sorption mechanism, equilibrium, and sorbent capacity of chromium (VI) sorption from water using novel sorbent synthesized using ultrasonic assisted modification of the oak tree sawdust with alumina.

## MATERIALS AND METHODS

### Reagents

$K_2Cr_2O_7$  was obtained from Sigma-Aldrich (USA) and used without any purification.  $Al(NO_3)_3 \cdot 9H_2O$  and NaOH were of analytical grade and purchased from Merck (Germany).

### Sorbent preparation

The oak tree sawdust was collected from furniture manufacturing in Eastern Serbia. Firstly, sawdust was separated by size and the 0.4–0.8 mm fraction was washed with deionized water several times. Then the sawdust was alkali-treated by 0.5M NaOH for 90 min and after that washed with deionized water several times to remove the excess of NaOH until the filtrate had a pH near 7. The 10 g of sawdust was added to the solution prepared by dissolving 1.0 g of  $Al(NO_3)_3 \cdot 9H_2O$  in 100.0 cm<sup>3</sup> of water, stirred for 30 min at room temperature and sonicated in the ultrasonic bath for 30 min, then washed with ultrapure water four times and dried for 120 min at 55.0°C.

### Procedure

Daily prepared chromium (VI) ions solutions were obtained by diluting of the stock (1.00 g dm<sup>-3</sup>). Solutions of chromium (VI) ions were mixed with 2.0 g dm<sup>-3</sup> sorbent at pH 2.0. pH adjustment was done using NaOH and HNO<sub>3</sub> solutions. The aliquots of the chromium (VI) ions solution were taken before the sorption started (0 min), and after periods of time (1, 5, 10, 20, 40, 60, 90, 120 and 180 min). The diphenyl carbazide method was used for determination of residual chromium (VI) concentration [7] at 540 nm on a UV-Vis spectrophotometer (UV-1800, Shimadzu, Japan). The sorbed amount  $q_t$  (mg g<sup>-1</sup>) of chromium (VI) was calculated using equation:

$$q_t = \frac{(c_0 - c_t) \cdot V}{m} \quad (1)$$

where  $c_0$  and  $c_t$  are the starting and final concentrations of the chromium (VI) ions (mg dm<sup>-3</sup>), respectively,  $V$  is volume of the solution (dm<sup>3</sup>) and  $m$  is mass of the sorbent (g).

### Sorption modelling

The kinetic and isotherm studies were carried out in the range of initial chromium (VI) ions concentration from 10.0 to 500.0 mg dm<sup>-3</sup> with 2.0 g dm<sup>-3</sup> sorbent dose. Two kinetic models: pseudo-first order kinetic model [8] and the pseudo-second order kinetic model [9] and three isotherm models: Langmuir isotherm model [10], Freundlich isotherm model [11] and Sips isotherm model [12], were applied for kinetic and equilibrium studies of chromium (VI) ions removal using wood-alumina sorbent. The nonlinear equations (Table 1) of the kinetics and isotherms models were used for determination of the sorption process parameters, since the nonlinear forms are more suitable than their linear forms for the modelling [13].

**Table 1** Kinetics and isotherms model equation

Model	Equation	Description and units
Pseudo-first order	$q_t = q_e(1 - e^{-k_1 t})$	$k_1$ – pseudo-first order rate constants (1 min <sup>-1</sup> )
Pseudo-second order	$q_t = \frac{q_e^2 k_2 t}{1 + q_e k_2 t}$	$k_2$ – pseudo-first order rate constants (g mg <sup>-1</sup> min <sup>-1</sup> )
Langmuir isotherm	$q_e = \frac{q_m K_L C_e}{1 + K_L C_e}$	$q_m$ – maximal sorbent capacity (mg g <sup>-1</sup> ) $K_L$ – Langmuir constant (dm <sup>3</sup> mg <sup>-1</sup> )
Freundlich isotherm	$q_e = K_F C_e^{\frac{1}{n_F}}$	$K_F$ – Freundlich constant (dm <sup>3</sup> mg <sup>-1</sup> ) $1/n_F$ – Freundlich exponent
Sips isotherm	$q_e = \frac{q_m K_S C_e^{1/n_S}}{1 + K_S C_e^{1/n_S}}$	$q_m$ – maximal sorbent capacity (mg g <sup>-1</sup> ) $K_S$ – Sips constant (dm <sup>3</sup> mg <sup>-1</sup> ) $1/n_S$ – Sips exponent

## RESULTS AND DISCUSSION

### Kinetic study

The obtained results and determined values of the application of the pseudo-first order model and the pseudo-second order model are presented in Table 2 and Figure 1.

**Table 2** Kinetic parameters for chromium (VI) sorption onto wood-alumina sorbent

Model	Parameter	Value						
Experimental	$c_0$	10.0	25.0	50.0	100.0	250.0	500.0	
	$q_{e, \text{exp}}$	4.99	12.49	24.95	49.89	102.8	104.59	
Pseudo-first order	$q_{e, \text{cal}}$	5.04	12.37	23.83	47.48	96.03	96.15	
	$k_1$	0.179	0.136	0.110	0.089	0.050	0.062	
	$r_2$	0.993	0.982	0.973	0.955	0.935	0.919	
	$q_{e, \text{cal}}$	5.00	12.50	25.00	50.00	105.06	107.91	
Pseudo-second order	$k_1$	0.281	0.221	0.159	0.119	0.066	0.053	
	$r_2$	0.999	0.998	0.998	0.995	0.994	0.994	

The  $q_e$  values for chromium (VI) ions sorption onto wood-alumina sorbent obtained by the pseudo-first order model and the pseudo-second order model are similar to the experimentally obtained values. The  $q_e$  values for the pseudo-second order kinetic model are closer to the experimental  $q_e$  values and the  $r^2$  values for the pseudo-second order model (0.999–0.994) are relatively higher than the  $r^2$  for the pseudo-first order model (0.993–0.919). The pseudo-first order model describes well experimental results obtained at lower ions concentrations because of the plenty free active sites on the sorbent surface, but at higher chromium (VI) ions concentrations the pseudo-first order model cannot be applied due to the saturation effect.

The results showed that the pseudo-second order model fits better obtained results than the pseudo-first order model for chromium (VI) ions sorption onto wood-alumina sorbent because the pseudo-second order model has a higher  $r^2$  and  $q_e$  values are closer to the experimentally obtained in all cases, so this model is preferable for the investigation of chromium (VI) ions sorption. This means that the sorption of chromium (VI) onto wood-alumina sorbent is dependent on the amounts of chromium (VI) ions in the solution and sorbed on the sorbent surface at equilibrium. The rate-limiting step of chromium (VI) sorption onto wood-alumina

sorbent was probably occurs by electrons sharing or exchanging between sorbent and chromium (VI) ions [14].

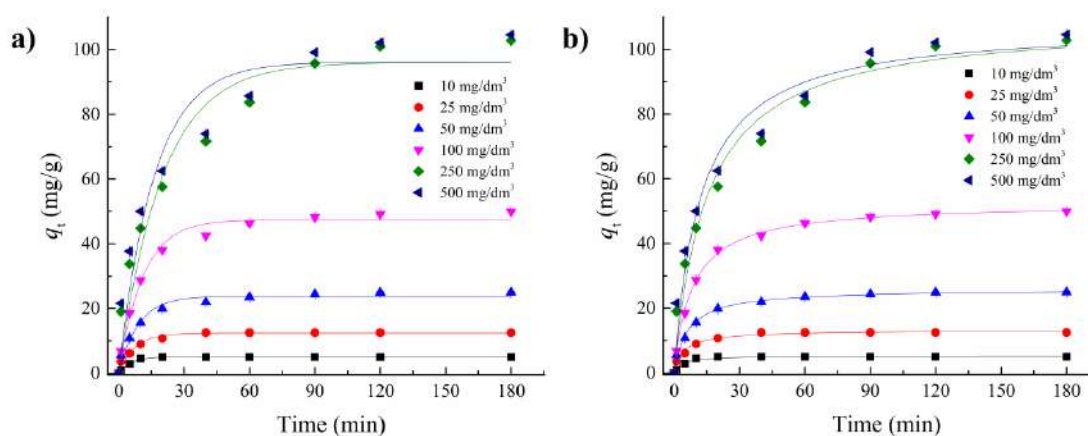


**Figure 1** Kinetic study for chromium (VI) onto wood-alumina sorbent: a) Pseudo-first order model; b) Pseudo-second order model

### Equilibrium study

The obtained results and determined values of the application of the Langmuir, Freundlich and Sips models are presented in Table 3 and Figure 2.

**Table 3** Isotherm parameters for chromium (VI) sorption onto wood-alumina sorbent

Model	Parameter	Value
Langmuir	$q_m$	104.2
	$K_L$	3.598
	$r_2$	0.996
Freundlich	$K_F$	45.06
	$n_F$	6.296
	$r_2$	0.867
Sips	$q_m$	103.9
	$K_S$	3.865
	$n_S$	0.99
	$r_2$	0.995

The highest  $r^2$  was for the Langmuir model ( $>0.99$ ) which indicates that the Langmuir model can better define chromium (VI) sorption onto wood-alumina sorbent than the Freundlich model which has lower values of  $r^2$  (0.867). This means that the chromium (VI) sorption took place in monolayer and after saturation of the layers no further sorption occurs. The obtained sorbent capacity of the Langmuir model was  $104.2 \text{ mg g}^{-1}$  (Table 2).

The  $r^2$  of the Freundlich model was 0.867, so this model does not describe well the experimental results (Table 3), but the value of the exponent  $n_F$  (6.296) in the Freundlich model, which is associated to the distribution of the sorption energy, lies between 1 and 10 meaning that the sorption process is favourable (Table 3) [15].

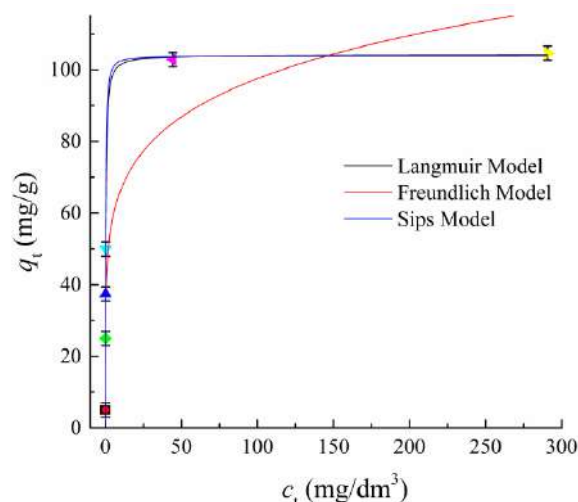


**Figure 2** Isotherm study for chromium (VI) onto wood-alumina sorbent

The Sips model has also very high  $r^2$  values (0.995) and almost the same  $q_e$  values ( $103.9 \text{ mg g}^{-1}$ ) for chromium (VI) ions sorption onto wood-alumina sorbent compared to experimental  $q_e$  values (Table 3), meaning that the Sips model also well describes the experimental results. The Sips model present a combination form of the Langmuir and Freundlich model, whereby at lower sorbate concentration the Sips model is reduced to the Freundlich model, while at higher sorbate concentration the Sips model overcomes the limitation of the Freundlich model and is reduced to the Langmuir model which refers to properties of monolayer sorption. The value of heterogeneity factor of the Sips model  $n_s$  (0.99) was close to 1, meaning that wood-alumina sorbent has approximately homogenous binding sites. This practically means that if  $n_s$  is close to 1, then the Langmuir model will be favoured, and the Sips model is successfully reduced to the Langmuir model, so the obtained equilibrium results for the chromium (VI) sorption onto wood-alumina sorbent can be effectively fitted by the Langmuir model [3].

## CONCLUSION

A novel wood-alumina sorbent was obtained via ultrasonically assisted synthesis method using oak tree sawdust and alumina. The sorption process of chromium (VI) onto wood-alumina sorbent followed the pseudo-second order model, meaning that the sorption of chromium (VI) onto wood-alumina sorbent is dependent on the amounts of chromium (VI) ions in the solution and sorbed on the sorbent surface at equilibrium. The Langmuir model best describes the experimental results and the maximal sorption capacities of the wood-alumina sorbent for chromium (VI) sorption is  $104.2 \text{ mg g}^{-1}$ , which presents potential material for chromium (VI) from water.

## ACKNOWLEDGEMENT

*The authors would like to acknowledge financial support from the Ministry of Science, Technological Development and Innovation of the Republic of Serbia (Agreement No 451-03-66/2024-03/200124 and Agreement No 451-03-65/2024-03/200124).*



## REFERENCES

- [1] Zeleke M.A., Kuo D.H., *Environ. Res.* 172 (2019) 279–288.
- [2] Zare E.N., Motahari A., Sillanpää M., *Environ. Res.* 162 (2018) 173–195.
- [3] Wang Q., Zhou C., Kuang Y-J., *et al.*, *Water Sci. Eng.* 13 (2020) 65–73.
- [4] da Rocha Ferreira G.L., Vendruscolo F., Antoniosi Filho N.R., *Heliyon* 5 (2019) e01450.
- [5] Wang J., Chen N., Li M., *et al.*, *J. Environ. Polym. Degrad.* 26 (2018) 1559–1572.
- [6] Adegoke K.A., Adesina O.O., Okon-Akan O.A., *et al.*, *Curr. Res. Green Sustain. Chem.* 5 (2022) 100274.
- [7] Gilcreas F.W., *Am. J. Public Health Nation's Health* 56 (1966) 387–388.
- [8] Lagergren S., *Kongl. Vetensk. Acad. Handl.* 24 (1898) 1–39.
- [9] Ho Y.S., McKay G., *Process Saf. Environ. Prot.* 76 (1998) 183–191.
- [10] Langmuir I., *J. Am. Chem. Soc.* 40 (1918) 1361–1403.
- [11] Freundlich H.Z., *Phys. Chem.* 57A (1906) 385–470.
- [12] Sips R., *J. Chem. Phys.* 16 (1948) 490–495.
- [13] Moussout H., Ahlafi H., Aazza M., *et al.*, *Karbala Int. J. Mod. Sci.* 4 (2018) 244–254.
- [14] Rambabu K., Bharath G., Banat F., *et al.*, *Environ. Res.* 187 (2020) 109694.
- [15] Bazzazzadeh R., Soudi M.R., Valinassab T., *et al.*, *Algal Res.* 48 (2020) 101896.



## THE INFLUENCE OF AGEING PARAMETERS ON MICROHARDNESS, ELECTRICAL CONDUCTIVITY AND MICROSTRUCTURE OF SOME Al-Mg-Si ALLOYS

Uroš Stamenković<sup>1\*</sup>, Ivana Marković<sup>1</sup>, Vladan Čosović<sup>2</sup>, Boštjan Markoli<sup>3</sup>

<sup>1</sup>University of Belgrade, Technical Faculty in Bor, Vojske Jugoslavije 12,  
19210 Bor, SERBIA

<sup>2</sup>University of Belgrade, Institute of Chemistry, Technology and Metallurgy, Njegoševa 12,  
11000 Belgrade, SERBIA

<sup>3</sup>University of Ljubljana, Faculty of Natural Sciences and Engineering, Aškerčeva cesta 12,  
1000 Ljubljana, SLOVENIA

\*ustamenkovic@tfbor.bg.ac.rs

### Abstract

*This paper investigates the influence of ageing parameters (temperature and time) on the microhardness, electrical conductivity and structural properties of two Al-Mg-Si aluminium alloys. After the applied heat treatment, both microhardness and electrical conductivity were measured. Optical microscopy was used to investigate the microstructures after ageing. The heat treatment began by solutionizing the samples at 550°C for 1 hour, followed by quenching in ice water. Samples were then aged at two separate temperatures, 180°C and 200°C, for 1–8 hours. The results indicate that with the increase in ageing time, the microhardness gradually increases up to a maximum and then decreases, while the electrical conductivity continuously increases. Analysis on the optical microscope shows that with longer ageing, there is precipitation of a larger amount of the strengthening phases due to more intense diffusion of alloying elements from the solid solution.*

**Keywords:** Al-Mg-Si, microhardness, electrical conductivity, ageing, microstructure.

### INTRODUCTION

The EN AW-6082 and EN AW-6060 aluminium alloys are two of the several alloys that make up the Al-Mg-Si alloy system. These alloys have garnered the interest of researchers because of their technical significance and observable increase in hardness as a result of precipitation hardening [1–3]. Ageing (precipitation) can improve mechanical and structural properties as well as properties such as electrical conductivity [4,5]. Samples have to be solutionized, quenched, and then aged in order to cause precipitation hardening. During the ageing process, precipitates form in accordance with the previously established precipitation sequence, which may be written as:  $\alpha_{\text{ssss}}$  (supersaturated solid solution)  $\rightarrow$  Mg:Si clusters  $\rightarrow$  GP zones (pre- $\beta''$ )  $\rightarrow$   $\beta''$   $\rightarrow$   $\beta'$   $\rightarrow$   $\beta$  ( $\text{Mg}_2\text{Si}$ ) [6–9]. The change in mechanical, electrical, and structural properties is caused by the precipitation of different metastable phases, mainly  $\beta''$  precipitates [9]. Because of their incoherency with the matrix, formed precipitates cause significant lattice deformation, which reduces dislocation mobility and enhances the alloy's hardness [7]. Al-Mg-Si alloys are often aged for an extended period of time at temperatures

below 200°C in order to achieve proper hardening. Numerous investigations focused on the impact of ageing time on mechanical, structural, and other properties, as demonstrated by numerous works [2,3,8–11]. Both investigated alloys can become excellent candidates for the manufacturing of overhead electrical wires that require high strength in addition to good electrical properties. Consequently, several researchers have investigated the impact of precipitation on the electrical properties of the Al-Mg-Si alloys [4,5,12]. It can be inferred from the analyzed literature that electrical and mechanical properties are significantly affected by ageing parameters, which emphasizes the importance of continuing research in this area. Consequently, we concentrated our attention on studying the ageing characteristics, which comprised two ageing temperatures: one conventional (180°C) and one greater than the conventional (200°C). Microhardness, electrical conductivity and microstructure were examined after the samples were aged for one to eight hours at each of the two ageing temperatures.

## MATERIALS AND METHODS

The aluminium alloys EN AW-6060 and EN AW-6082 were selected for this study. The alloys were delivered in T6 (aged) condition in the form of extruded rectangular bars. The "Belec Compact Port" optical emission spectrometer was used to determine the chemical composition of the investigated alloys. Table 1 reveals the results of the chemical analysis. All samples were annealed at 550°C for 6 hours in the electric resistance furnace Heraeus K-1150/2 and cooled in air to eliminate the as-received (aged) condition. In order to produce a supersaturated solid solution ( $\alpha_{\text{SSSS}}$ ), the samples were heated to 550°C for an hour and then quenched in icy water. This was done in order to prepare the samples for the ageing process. Samples were isothermally aged at 180°C and 200°C for one to eight hours post-quenching.

The properties of the aged samples were compared with those of the as-quenched samples (in the Figures marked as quenched state). Following the heat treatment, the samples underwent several analyses. Vickers microhardness values were measured using a 0.1 kg force and a 15-second dwell duration on a PMT 3 microhardness tester. The Sigmatest type 2.063 conductivity tester was used to measure the electrical conductivity values. Every measurement that is given was done at room temperature. All sample surfaces were ground to eliminate oxides before measurements. The samples have been analysed metallographically using the Carl-Zeiss Jena Epytip 2 optical microscope. The samples were prepared by wet grinding on an assortment of SiC papers and polishing with two different alumina suspensions containing different Al<sub>2</sub>O<sub>3</sub> granulations (0.3 µm and 0.05 µm). The samples were etched by immersion in Dix-Keller solution in order to reveal the microstructure.

**Table 1** Chemical compositions of the investigated alloys (wt. %)

EN AW-6060							EN AW-6082						
Si	Fe	Cu	Mn	Mg	Cr	Ni	Si	Fe	Cu	Mn	Mg	Cr	Ni
0.49	0.182	0.012	0.06	0.594	<0.03	0.028	0.807	0.354	0.042	0.453	0.696	<0.012	0.012
Zn	Ti	V	Co	Sn	Zr	Al	Zn	Ti	V	Co	Sn	Zr	Al
0.01	0.05	0.014	<0.003	<0.003	<0.003	98.62	0.115	0.25	<0.003	0.006	<0.003	<0.003	97.45

## RESULTS AND DISCUSSION

The microhardness values of the investigated alloys during isothermal ageing are shown in Figure 1. It is evident from the graphs in Figure 1 that the microhardness values are significantly influenced by ageing. The microhardness of the aged samples gradually increases to a maximum and subsequently decreases with an increase in ageing time. The samples reached maximal microhardness values after ageing for five hours at 180 °C for the EN AW-6060 and for six hours for the EN AW-6082 alloy.

For the EN AW-6060 alloy, the highest obtained microhardness value was 110 HV<sub>0.1</sub>, which is 42.8% higher than the microhardness value of the quenched sample (77 HV<sub>0.1</sub>;  $\alpha_1$  on Figure 1). For the EN AW-6082 alloy, the highest obtained microhardness value was 146 HV<sub>0.1</sub>, which is a 55.3% increase in comparison to the quenched state (94 HV<sub>0.1</sub>;  $\alpha_2$  on Figure 1).

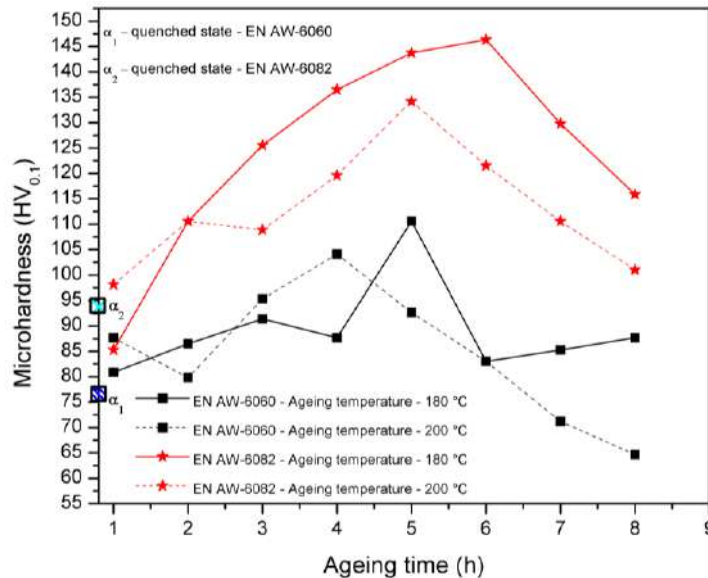


**Figure 1** Change in microhardness values of the investigated alloys as a function of ageing time at two different ageing temperatures

It is assumed that the formation of multiple vacancies upon quenching, which encourages nucleation of the pre- $\beta''$  phase, causes this phase to precipitate during the first four hours of ageing. As ageing continues, the Si and Mg atoms migrate from the solid solution and towards the pre- $\beta''$  phase, trading places with the Al atoms. Precipitates that already exist, transform and grow in numbers overall, which eventually causes coherence with the Al lattice to be reduced. Phase changes proceed in accordance with the precipitation sequence as ageing progresses, together with the exchange of alloying element atoms with Al atoms [9]. Consequently, the maximum microhardness values displayed in Figure 1 are achieved due to the creation of the  $\beta''$  metastable phase and have been observed by multiple investigators [1–3,8–13]. Marioara *et al.* [3] stated that even though the precipitate density is low during the precipitation of the  $\beta''$  phase, there is an increase in incoherency with the lattice, leading to peak hardness values. After ageing for 6–8 hours, precipitates of the  $\beta''$  phase grow and coagulate, causing a decrease in microhardness values. A deeper look at the graphs in

Figure 1 reveals that maximum microhardness values can be obtained faster as a result of higher ageing temperatures. However, after ageing at higher temperatures, the highest microhardness values obtained are not as high as those achieved at lower ageing temperatures. Diffusion rate increases with rising ageing temperature, which leads to faster precipitation of the pre- $\beta''$  phase and a faster loss of coherency, so the microhardness values are higher after an hour of isothermal ageing at 200°C as opposed to 180°C. However, the use of lower ageing temperatures with longer ageing times is essential for achieving a true peak-aged state.

The change in electrical conductivity values of the investigated alloys as a function of ageing time at two different ageing temperatures can be seen in Figure 2. In age-hardenable alloys, there is a strong relationship between electrical conductivity and precipitation [4]. Analysis of Figure 2 shows that with the increase in ageing time, the electrical conductivity gradually increases, reaching maximum values at the longest ageing times. When ageing for 1 hour, the electrical conductivity values are slightly lower than those obtained for the  $\alpha_{\text{SSSS}}$  (quenched state). At these ageing parameters, the pre- $\beta''$  phase (GP-zone) is formed. These precipitates have the effect of scattering electrons, which leads to a decrease in electrical conductivity values [5,12,14]. After the initial decrease, there is a gradual increase in electrical conductivity values until the maximum is obtained. As the ageing time increases, an increasing amount of precipitates are formed due to the reduction of alloying elements in the saturated solid solution ( $\alpha_{\text{SSSS}}$  becomes less saturated). As a result of this phenomenon, electrical conductivity increases due to the easier movement of electrons through the matrix. Electrical conductivity is highest when the saturation of the  $\alpha_{\text{SSSS}}$  is the lowest, and in this case, this was achieved first by the precipitation of the pre- $\beta''$  phase, and with prolonged ageing, by the  $\beta''$  phase [4,5].

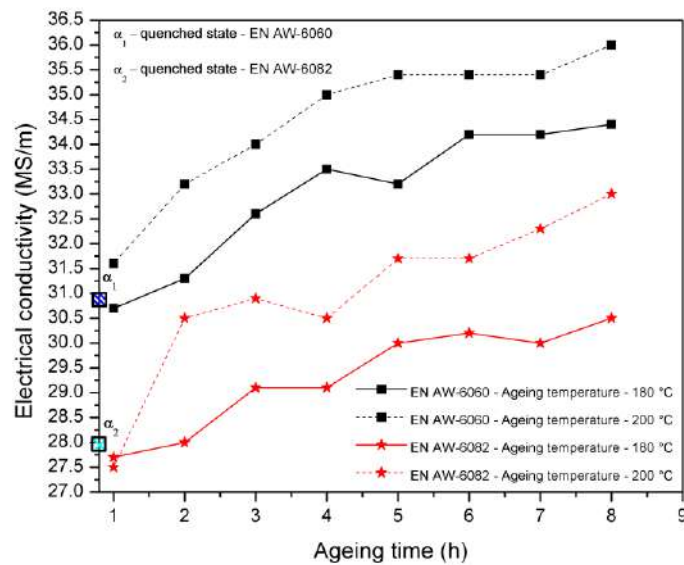


**Figure 2** Change in electrical conductivity values of the investigated alloys as a function of ageing time at two different ageing temperatures

Unlike mechanical properties, a higher ageing temperature (200°C) leads to higher values of electrical conductivity. At higher ageing temperatures, diffusion is accelerated and



precipitation is intensified, which leads to a faster desaturation of the  $\alpha_{\text{SSSS}}$  with alloying elements, as a result of which the electrical conductivity increases.

The maximum values of electrical conductivity for both alloys were achieved when ageing at 200°C for 8 hours. For the EN AW-6060 alloy, electrical conductivity increased from 30.8 MS/m in the quenched state ( $\alpha_1$  in Fig. 2) to 36 MS/m after isothermal ageing at 200°C for 8 h, so the relative increase in electrical conductivity compared to the quenched state was 16.89%. The relative increase in electrical conductivity for the alloy EN AW-6082 was slightly higher and amounted to 17.86%. For this alloy, electrical conductivity increased from 28 MS/m in the quenched state ( $\alpha_2$  in Fig. 2) to 33 MS/m after isothermal ageing at 200°C for 8 h.

For microstructural analysis, four different samples were chosen based on the microhardness measurements: underaged samples (aged for 1 hour at 180°C) as well as peak aged samples (aged for 5 or 6 hours at 180°C, depending on the alloy).

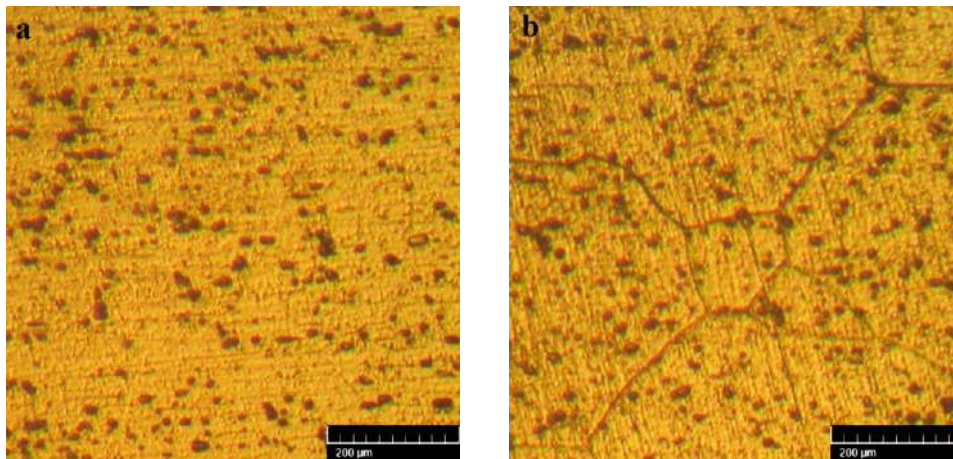


**Figure 3** Influence of ageing temperature on the microstructure of the EN AW-6060 aluminium alloy: a) after ageing for 1 hour at 180°C (underaged sample); b) after ageing for 5 hours at 180°C (peak-aged sample)

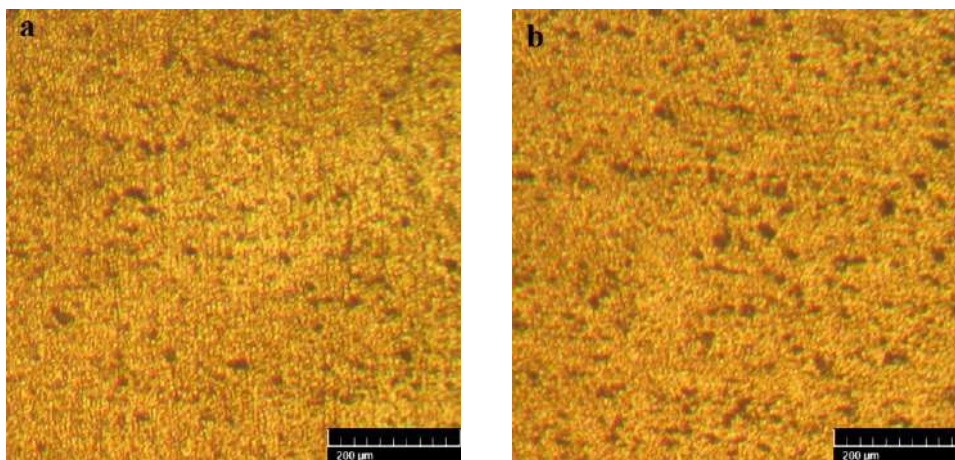


**Figure 4** Influence of ageing temperature on the microstructure of the EN AW-6082 aluminium alloy: a) after ageing for 1 hour at 180°C (underaged sample); b) after ageing for 6 hours at 180°C (peak-aged sample)



Figures 3(a–b) and 4(a–b) show optical microphotographs of underaged and peak-aged samples of the EN AW-6060 and EN AW-6082 alloys after ageing at 180°C, respectively. From the presented microphotographs, it can be concluded that with longer ageing, there is precipitation of a larger amount of the strengthening phase, which further leads to an increase in the microhardness values, confirming the comments given in regards to the microhardness results [1,13,15].

## CONCLUSIONS

Isothermal ageing led to an evident rise in mechanical and electrical properties. After ageing at 180°C for five or six hours, depending on the alloy, the highest values of microhardness were achieved. After ageing for eight hours at 200°C, the electrical conductivity values peaked for both investigated alloys due to the highest level of precipitation from the solid solution. Microstructural analysis showed the presence of finely distributed metastable phases, which caused a change in mechanical and electrical properties. The  $\beta''$  phase is thought to be primarily responsible for this improvement.

## ACKNOWLEDGEMENT

*The research presented in this paper was done with the financial support of the Ministry of Science, Technological Development and Innovation of the Republic of Serbia, within the funding of the scientific research work at the University of Belgrade, Technical Faculty in Bor, according to the contract with registration number 451-03-65/2024-03/200131.*

## REFERENCES

- [1] Tan C.F., Said M.R., Chiang Mai J. Sci. 36 (3) (2009) 276–286.
- [2] Abid T., Boubertakh A., Hamamda S., J. Alloys Compd. 490 (2010) 166–169.
- [3] Marioara C.D., Andersen S.J., Jansen J., *et al.*, Acta Mater. 51 (2003) 789–796.
- [4] Karabay S., Mater. Des. 27 (2006) 821–832.
- [5] Cui L., Liu Z., Zhao X., *et al.*, T. Nonferr. Metal. Soc. 24 (2014) 2266–2274.
- [6] Birol Y., T. Nonferr. Metal. Soc. 23 (2013) 1875–1881.
- [7] Zheng Y.Y., Luo B-H., Xie W., *et al.*, China Foundry 20 (2023) 57–62.
- [8] Birol Y., J. Mater. Process. Technol. 173 (2006) 84–91.
- [9] Gupta A.K., Lloyd D.J., Court S.A., Mater. Sci. Eng. A 316 (2001) 11–17.
- [10] Marioara C.D., Andersen S.J., Jansen J., *et al.*, Acta Mater. 49 (2001) 321–328.
- [11] Chang C.S.T., Wieler I., Wanderka N., *et al.*, Ultramicroscopy 109 (2009) 585–592.
- [12] Prabhu T.R., Eng. Sci. Technol. an Int. 20 (1) (2017) 133–142.
- [13] Masoud I.M., Abu Mansour T., Al-Jarrah J.A., J. Appl. Sci. Res. 8 (10) (2012) 5106–5113.
- [14] Edwards G.A., Stiller K., Dunlop G.L., *et al.*, Acta Mater. 46 (11) (1998) 3893–3904.
- [15] Mrówka-Nowotnik G., Arch. Mater. Sci. Eng. 46 (2) (2010) 98–107.



## KINETIC STUDY OF DEGRADATION BISPHENOL A BY FENTON PROCESS

Marija Simić<sup>1\*</sup>, Danka Aćimović<sup>1</sup>, Branislava Savić Rosić<sup>1</sup>, Marija Ječmenica Dučić<sup>1</sup>,  
Katarina Stojanović<sup>1</sup>, Danijela Maksin<sup>2</sup>, Tanja Brdarić<sup>1</sup>

<sup>1</sup>University of Belgrade, VINČA Institute of Nuclear Sciences-National Institute of the  
Republic of Serbia, Department of Physical Chemistry, Mike Petrovića Alasa 12–14,  
11000 Belgrade, SERBIA

<sup>2</sup>University of Belgrade, VINČA Institute of Nuclear Sciences-National Institute of the  
Republic of Serbia, Department of Chemical Dynamics and Permanent Education,  
Mike Petrovića Alasa 12–14, 11000 Belgrade, SERBIA

\**marija.simic@vin.bg.ac.rs*

### Abstract

*The degradation of bisphenol A in aqueous solutions using the Fenton reagents ( $H_2O_2$  and  $Fe^{2+}$ ) was investigated. The molar ratio of the catalyst has been 1:50 ( $H_2O_2:Fe^{2+}$ ). The treatment experiment was performed for 300 min to evaluate the kinetics of this process. The kinetics data showed the best fit with the second-order kinetics model.*

**Keywords:** bisphenol A, Fenton process, kinetic analysis.

### INTRODUCTION

Bisphenol A (BPA) (4,4'-isopropylidenediphenol) has been frequently applied in the industries of polycarbonate plastics, epoxy, and phenolic resins. It belongs to the group of chemicals that disrupt the endocrine system and therefore negatively affect the hormonal status of aquatic organisms and humans. To reduce its concentration in wastewater, various chemical and biological treatment techniques [1–3] have been applied.

During the last decade, advanced oxidation processes (AOPs) have emerged as promising options for wastewater treatment, due to their capability to oxidize a broad spectrum of compounds that are typically challenging to degrade. Among these processes, oxidation using Fenton's reagent stands out as an appealing treatment method for effectively degrading organic pollutants. This is primarily attributed to its cost-effectiveness, the non-toxic nature of its reagents ( $Fe^{2+}$  and  $H_2O_2$ ), the absence of mass transfer limitations owing to its homogeneous catalytic nature, and the simplicity of the technology involved.

The Fenton process employs the Fenton reaction (Eq. 1) to produce hydroxyl radicals ( $\bullet OH$ ) by mixing ferrous ions ( $Fe^{2+}$ ) with hydrogen peroxide ( $H_2O_2$ ) under acidic pH conditions, serving as a technique for wastewater purification.



The hydroxyl radical ( $\bullet\text{OH}$ ) initiates the breakdown of organic pollutants by cleaving chemical bonds and oxidizing the targeted compounds.

Numerous scientific articles [4,5] concentrate on investigating and applying the Fenton treatment for the removal of organic molecules. It has been established that factors such as pH, temperature, and particularly the molar ratio of hydrogen peroxide to iron influence the removal efficiency of organic pollutants from wastewater through the Fenton process. However, to the best of the author's knowledge, there is no available literature about the removal of BPA via the Fenton process.

This paper presents the investigation of the Fenton oxidation of BPA under acidic conditions, with a hydrogen peroxide to iron molar ratio of 1:50. The removal efficiency of BPA concerning treatment time was studied, as well as degradation kinetics.

## **MATERIALS AND METHODS**

### **Chemicals**

For presented experiments following chemicals were used: BPA (Sigma-Aldrich, St. Louis, Missouri, USA), sodium sulfate (Sigma-Aldrich, St. Louis, Missouri, USA), hydrogen peroxide (ZORKA Pharma, Šabac, Serbia), iron (II) sulfate heptahydrate (Sigma-Aldrich, St. Louis, Missouri, USA), dichloromethane (Sigma-Aldrich, St. Louis, Missouri, USA).

### **Method of Fenton oxidation process**

A reagent consisting of hydrogen peroxide and iron (II) ions in 1:50 mass ratios is used for BPA oxidation using the Fenton process. The experiments were performed by adding the Fenton reagent to a 0.1M  $\text{Na}_2\text{SO}_4$  model solution in which the BPA concentration was 30 mg  $\text{L}^{-1}$ . The BPA oxidation process lasted 5 hours, with aliquots taken for 1 hour. The Fenton process was stopped by the addition of 5M NaOH solution.

### **Analysis method**

The preparation of BPA degradation aliquots for GC-MS analysis and the GC-MS analysis program was performed in accordance with our previous work [6].

The obtained data were treated with kinetic models of zero-order, first-order and second-order kinetics models.

## **RESULTS AND DISCUSSION**

The Figure 1 illustrates the removal efficiency during the treatment process of BPA. It is evident (Figure 1) that as treatment time progresses, the efficiency of BPA removal also rises. Initially, BPA degradation occurs rapidly within the first 120 minutes, achieving an efficiency of approximately 41%. Subsequent treatment stages show a gradual increase in BPA removal efficiency, likely attributed to the consumption of Fenton reagents.

The oxidative degradation process of BPA by Fenton was kinetically modelled using zero-order, first-order and second-order kinetic models. The parameters of applied kinetic models, such as rate constants,  $k$  and coefficient of determination were calculated from the linear plots. They are pre-sented in Table 1.

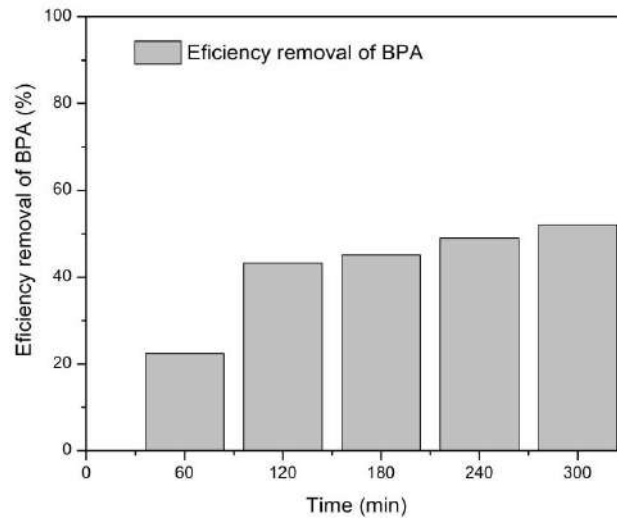


**Figure 1** Efficiency removal of BPA

**Table 1** Kinetic model equations and parameters for the Fenton oxidation of BPA

Kinetics model	Equation	Rate constants, k	Coefficient of determination
Zero order	$[A] = [A]_0 - kt$	$-2.194 \cdot 10^{-7} \text{ (M min}^{-1}\text{)}$	0.868
First order	$\ln[A] = \ln[A]_0 - kt$	$-0.00243 \text{ (min}^{-1}\text{)}$	0.930
Second order	$1/[A] = 1/[A]_0 + kt$	$28.045 \text{ (M}^{-1} \text{min}^{-1}\text{)}$	0.970

The coefficient of determination for the second-order model was relatively satisfactory and close to 1. This confirms that the degradation of BPA by the Fenton process most closely follows second-order kinetics. It is opposite to the earlier study by Wang *et al.* [7].

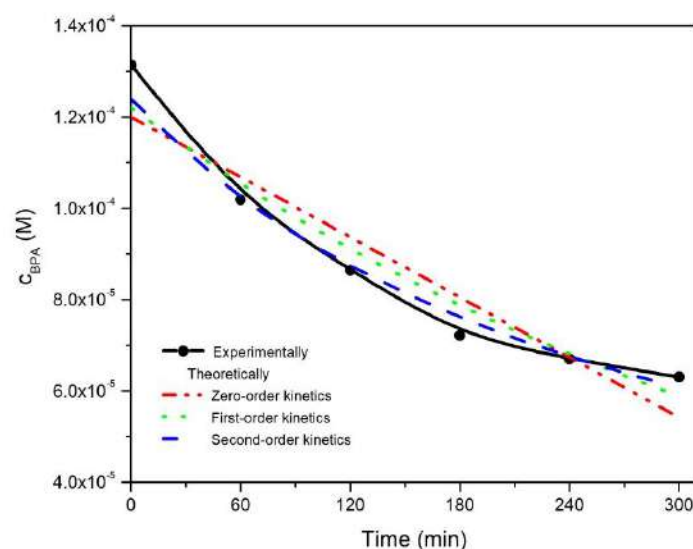


**Figure 2** Comparison of experimentally and kinetic simulation of Fenton oxidation for BPA

The constructed BPA degradation kinetics model can be applied to evaluate the degradation level of BPA and predict its concentration during the treatment time. Based on kinetics parameters of  $k$  for the BPA obtained based on the method mentioned above, the

equations presented in Table 2 can be used to calculate the  $c$  values under different treatment times.

Figure 2 shows the plots of the degradation profile from the theoretical model for the degradation of the BPA in 0.1M Na<sub>2</sub>SO<sub>4</sub> solutions. The data of concentration at degradation time from experimental findings are also presented, which match well with the theoretical curve for the second-order reaction.

## **CONCLUSION**

In summary, our proof-of-concept study has established a Fenton treatment for the degradation of BPA in sulphate-rich wastewater. The rate equations of the Fenton processes in BPA degradation follow second-order kinetics. The construction of the BPA degradation kinetics model in this work would provide better insight in prediction of BPA degradation time and facilitate the optimization of process for practical applications.

## **ACKNOWLEDGEMENT**

*The authors are grateful to the Ministry of Science, Technological development and Innovation of the Republic of Serbia for financial support according to the contract with the registration number (grant number 451-03-66/2024-03/ 200017).*

## **REFERENCES**

- [1] Tang Y., Li Y., Zhan L., *et al.*, *Sci. Total Environ.* 805 (2022) 150158.
- [2] Dudziak M., Kudlek E., Laskawiec E., *et al.*, *Ecol. Eng.* 19 (2018) 69–74.
- [3] Zhao Z., Yang H., Feng Z., *et al.*, *Chemosphere* 307 (2022) 135829.
- [4] Sajiki J., Yonekubo J., *Environ. Int.* 30 (2004) 145–150.
- [5] Babuponnusami A., Muthukumar K., *J. Environ. Chem. Eng.* 2 (2014) 557–572.
- [6] Simić M.D., Savić B.G., Ognjanović M.R., *et al.*, *J. Water Process Eng.* 51 (2023) 103416.
- [7] Wang S., *Dye. Pigment.* 76 (2008) 714–720.



## DETECTION OF BISPHENOL A INTERMEDIATES DURING FENTON PROCESS AND PREDICTION OF REACTION PATHWAYS

**Danka Aćimović<sup>1\*</sup>, Katarina Stojanović<sup>1</sup>, Marija Simić<sup>1</sup>, Branislava Savić Rosić<sup>1</sup>,  
Zdravko Vranješ<sup>2</sup>, Marija Ječmenica Dučić<sup>1</sup>, Tanja Brdarić<sup>1</sup>**

<sup>1</sup>University of Belgrade, VINČA Institute of Nuclear Sciences-National Institute of the  
Republic of Serbia, Department of Physical Chemistry, Mike Petrovića Alasa 12–14,  
11000 Belgrade, SERBIA

<sup>2</sup>Public Company Nuclear Facilities of Serbia, Mike Petrovića Alasa 12–14,  
11000 Belgrade, SERBIA

\*[dankavla@vin.bg.ac.rs](mailto:dankavla@vin.bg.ac.rs)

### Abstract

*Bisphenol A (BPA), extensively used in the production of polycarbonate plastic and epoxy resin, poses significant threats to aquatic ecosystems and human health. Advanced oxidation processes (AOPs), which generate reactive species in situ, offer promising alternatives for wastewater treatment. Among these, the Fenton process, generating OH radicals, stands out. This study aims to explore the oxidative degradation of BPA by detecting its intermediates and elucidating its degradation pathway. Our findings reveal the existence of two interconnected degradation pathways. This study underscores the importance of advanced oxidation processes in mitigating the detrimental effects of BPA contamination, emphasizing the need for further research to optimize wastewater treatment methods and safeguard both ecosystems and human health.*

**Keywords:** BPA intermediates, Fenton process, hydroxyl radical.

### INTRODUCTION

Bisphenol A (BPA), a widely used in polycarbonate plastic and epoxy resin production, is notorious for its adverse effects on both aquatic life and humans. With its ability to mimic and oppose hormone effects, BPA is classified as an endocrine disrupting compound, and poses significant health risks to living organisms [1,2]. Conventional wastewater treatment methods struggle to efficiently eliminate BPA. Consequently, advanced oxidation processes (AOPs), comprising techniques that generate highly reactive species in situ, present an alternative for wastewater treatment. The Fenton process is also classified among AOP methods. In the classic Fenton chemistry, the reaction between hydrogen peroxide and Fe<sup>2+</sup> ions in an acidic aqueous solution is commonly understood to generate hydroxyl radicals [3].

The main objective of this study is to analyze the oxidative degradation of BPA by detecting BPA intermediates and predicting the degradation pathway of BPA.



## **MATERIALS AND METHODS**

### **Fenton reaction**

Fenton's reagent (14.66 mM Fe<sup>2+</sup> and 3.66 mM H<sub>2</sub>O<sub>2</sub>) at pH 4 was used for oxidative degradation of BPA. The initial concentration of BPA in the solution was 30 mg L<sup>-1</sup>. The Fenton reaction was stopped with 5 M sodium hydroxide. Model wastewater solution for Fenton reaction was 0.1M Na<sub>2</sub>SO<sub>4</sub>, pH~4. The Fenton reaction was stopped with 5M sodium hydroxide.

### **Isolation and detection of BPA intermediates**

Intermediates resulting from the degradation of BPA by Fenton's reagent were isolated using liquid-liquid extraction (starting solution/diethyl ether) every hour from the beginning of the Fenton reaction. Isolated intermediates were subjected to BSTFA (N,O-Bis (trimethylsilyl)trifluoroacetamide) derivatization. BSTFA was employed for the specific derivatization of BPA and its intermediates (trimethylsilyl (TMS) ethers/esters), followed by targeted fragmentation to facilitate the successful structural identification using GC-MS.

BPA intermediates underwent analysis using gas chromatography/mass spectrometry, GC-MS (Agilent Technologies 7890B GC System, Agilent Technologies 5977 MSD, Santa Clara, California, USA). This system was outfitted with a fused silica GC capillary column Agilent J&W (HP-5 ms 30 m × 0.25 mm i.d., film thicknesses 0.25 μm) and employed helium, grade 5.0, as a carrier gas at a constant flow rate of 1.0 mL min<sup>-1</sup>. The gas chromatograph settings were as follows: the splitless injector operated at 250°C, with an injection volume of 1 μL; the transfer line temperature was set to 300°C, and the oven temperature was programmed from 50°C (held for 2 min) at a rate of 9°C min<sup>-1</sup> up to 320°C (held for 5 min), then at 9°C min<sup>-1</sup> up to 320°C (held for 1 min). Data acquisition was conducted in full scan mode within the m/z range of 33–800 amu (atomic mass unit) for identification purposes. Analysis and processing of the GC-MS data were performed using Agilent GC-MS MassHunter software in conjunction with the NIST 14 mass spectral library.

## **RESULTS AND DISCUSSION**

Eight BPA intermediates were detected during the Fenton reaction. The use of silanization and the obtained trisilyl esters and ethers facilitated the identification and structural elucidation of intermediates through mass-to-charge ratio (m/z) measurements and characteristic ion spectra obtained via GC-MS [4]. Furthermore, the instrument software suggested pseudo-molecular formulas by utilizing the NIST library (see Table 1). In Table 1, as well as in Figure 1, BPA intermediates with molecular weights smaller than BPA, such as benzoic acid, hydroxyquinone, 4-hydroxybenzoic acid, 4-hydroxyacetophenone and 4-isopropenylphenol can be observed. Since BPA intermediates appear at the beginning of the Fenton reaction, it indicates that their formation arises directly from the cleavage of BPA's isopropyl chain.

This finding is in line with previous studies and represents an important pathway for BPA degradation facilitated by OH radicals [5,6]. Later, due to the action of hydroxyl radicals, the

single-ring intermediate is opened and carboxylic acids are formed, which eventually leads to the complete mineralization of BPA to carbon dioxide and water.

**Table 1** BPA intermediates detected on GC/MS

Name	Retention time (min)	Pseudo-molecular formula	m/z <sup>a</sup>
Bisphenol A	23.47	C <sub>15</sub> H <sub>16</sub> O <sub>2</sub>	228.29 (372.66)
Product 1	25.49	C <sub>15</sub> H <sub>14</sub> O <sub>4</sub>	258.27 (474.21)
Product 2	24.64	C <sub>14</sub> H <sub>12</sub> O <sub>4</sub>	244.07 (460.19)
Product 3	24.23	C <sub>14</sub> H <sub>12</sub> O <sub>4</sub>	244.07 (388.15)
Hydroxyquinone	13.74	C <sub>6</sub> H <sub>6</sub> O <sub>2</sub>	110.04 (254.12)
4-isopropenylphenol	13.17	C <sub>9</sub> H <sub>10</sub> O	134.18 (206.36)
4-hydroxyacetophenone	14.72	C <sub>8</sub> H <sub>8</sub> O <sub>2</sub>	136.15 (208.09)
4-hydroxybenzoic acid	16.74	C <sub>7</sub> H <sub>6</sub> O <sub>3</sub>	138.12 (282.11)
Benzoic Acid	11.36	C <sub>7</sub> H <sub>6</sub> O <sub>2</sub>	122.12 (194.31)

<sup>a</sup> m/z of the non-derivatized analyte and its trimethylsilyl ether/ester, in Da.

During the reaction of the OH radical with the BPA molecule, modifications can occur either on the isopropyl chain or on the aromatic ring of BPA. Although the OH radical is unselective, the favoring of certain sites on the aromatic ring is present. Hydroxylated BPA can be generated through the addition of OH groups at the *ortho* and *para* positions on the aromatic ring, as depicted in Figure 1 [5]. This degradation pathway is marked as “Degradation pathway 1” and its main products are catechols and quinones. Under the additional influence of OH radicals, “Degradation pathway 1” will transit into “Degradation pathway 2”.

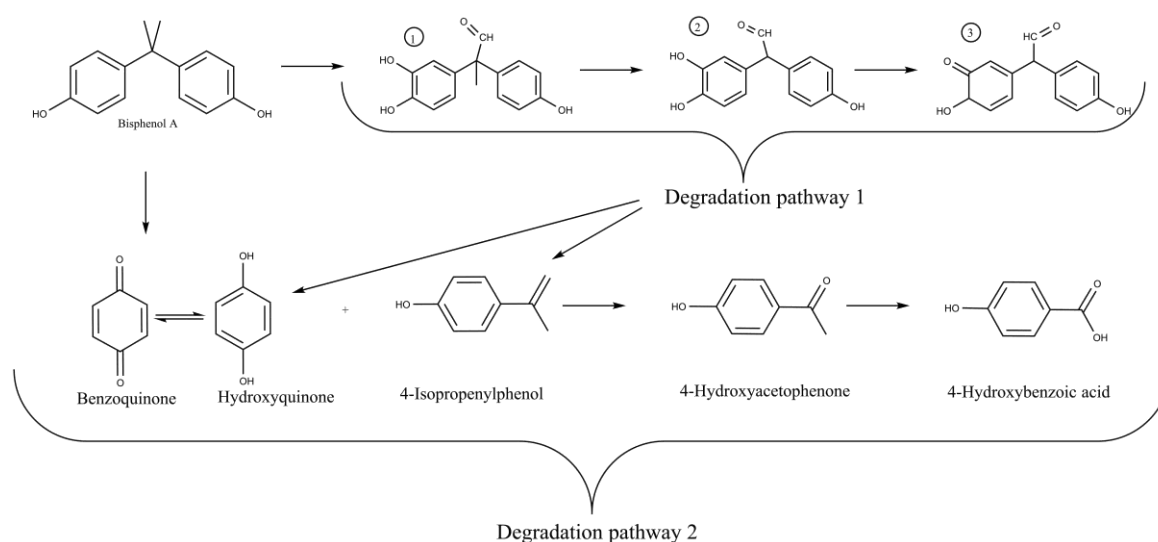


**Figure 1** Proposed reaction pathways

## **CONCLUSION**

GC-MS methods are commonly employed for acquiring structural information about products formed during Fenton oxidation processes. The modified analytical approach enable us do to isolate and identify eight BPA intermediates and to clarify the pathways of BPA oxidative degradation. In this study, two interconnected degradation pathways are found. In future experiments, based on proposed degradation pathways along with detected intermediates, toxicity estimation of Fenton process on BPA could be done.

## **ACKNOWLEDGEMENT**

*This work was supported by Ministry of Science, Technological Development, and Innovation of the Republic of Serbia [grant number 451-03-66/2024-03/ 200017].*

## **REFERENCES**

- [1] Pollard S.H., Cox K.J., Blackburn B.E., *et al.*, *Reprod. Toxicol.* 90 (2019) 82–87.
- [2] Usman A., Ahmad M., *Chemosphere* 158 (2016) 131–142.
- [3] Babuponnusami A., Muthukumar K., *J. Environ. Chem. Eng.* 2 (2014) 557–572.
- [4] Poerschmann J., Trommler U., Górecki T., *Chemosphere* 79 (2010) 975–986.
- [5] Darsinou B., Frontistis Z., Antonopoulou M., *et al.*, *Chem. Eng. J.* 280 (2015) 623–633.
- [6] Han Q., Wang M., Sun F., *et al.*, *Environ. Res.* 216 (2023).



## ADVANCED OXIDATION PROCESSES (AOPs) FOR WASTEWATER TREATMENT: BIBLIOMETRIC STUDY

Tanja Brdarić<sup>1\*</sup>, Danka Aćimović<sup>1</sup>, Branislava Savić Rosić<sup>1</sup>, Katarina Stojanović<sup>1</sup>,  
Marija Simić<sup>1</sup>, Zdravko Vranješ<sup>2</sup>, Marija Ječmenica Dučić<sup>1</sup>

<sup>1</sup>University of Belgrade, VINČA Institute of Nuclear Sciences-National Institute of the  
Republic of Serbia, Department of Physical Chemistry, Mike Petrovića Alasa 12–14,  
11000 Belgrade, SERBIA

<sup>2</sup>Public Company Nuclear Facilities of Serbia, Mike Petrovića Alasa 12–14,  
11000 Belgrade, SERBIA

\*[tanja.brdaric@vin.bg.ac.rs](mailto:tanja.brdaric@vin.bg.ac.rs)

### Abstract

*Advanced oxidation processes (AOPs) represent promising technologies for solving complex challenges in wastewater treatment, using powerful oxidants to degrade a wide range of pollutants. However, achieving a comprehensive understanding of the research landscape in this area is crucial. This paper presents a bibliometric analysis of publications related to AOPs for wastewater treatment, in order to map research trends, identify key contributors and highlight new areas of research. By analyzing data obtained from the Web of Science Core Collection using CiteSpace software, significant insights into publication trends and collaboration are revealed. Key results include the dominance of chemical engineering and environmental sciences as primary research categories. In addition, institutional contributions and author co-citations highlight the significant role of specific subjects and researchers. Furthermore, keyword analysis sheds light on prominent research topics, with degradation and wastewater treatment emerging as central themes. Cluster mapping identifies the main research points, highlighting wastewater treatment as a primary focus, followed by the development and application of photocatalytic methods and graphene oxide. This study provides valuable insights to guide future research directions and collaborative efforts to advance AOP-based wastewater treatment technologies.*

**Keywords:** AOPs, bibliometric analysis, wastewater treatment.

### INTRODUCTION

AOPs represent innovative approaches in wastewater treatment, offering solutions to the complex challenges associated with pollutant degradation. These processes utilize powerful oxidants, such as hydroxyl radicals ( $\bullet\text{OH}$ ), to degrade a wide range of organic and inorganic pollutants present in wastewater. Despite the growing interest and significant advancements in AOPs, there remains a need for a comprehensive understanding of the research landscape in this field.

Bibliometric analysis is a mathematical and statistical technique used to trace the evolution of research topics, elucidate trends, advancements, and emerging scientific interests [1]. Several researchers have applied bibliometric methods to analyze wastewater treatment technologies. Some studies have focused on industrial wastewater treatment [2], while others

have explored technologies for controlling pollution in sulfate-rich wastewater [3]. Additionally, Macías-Quiroga *et al.* [4] applied bibliometric analysis to examine the research trends of AOPs techniques from 1980 to 2018. Considering the large number of scientific publications, it is interesting to analyze the publication trend within a single year.

This paper aims to conduct a bibliometric analysis of the scientific literature about AOPs in wastewater treatment published over one year (2023–2024). The primary goal is to systematically review and analyze existing research publications to map out research trends, identify key contributors, and highlight emerging research areas of interest. Additionally, this analysis aims to uncover potential knowledge gaps and interesting areas for future exploration within AOP-based wastewater treatment. This scientific research is expected to promote collaboration, innovation, and knowledge exchange within the scientific community to achieve improvements in wastewater treatment efficacy and environmental quality.

## MATERIALS AND METHODS

The Web of Science Core Collection (WoSCC), renowned as the world's most comprehensive scientific database, served as the primary resource for data retrieval. The search criteria, keywords and Boolean operators were: (“Advanced Oxidation Process” OR “Advanced Oxidation Technologies” OR “AOPs” OR “Fenton” OR “Fenton-like” OR “photo-Fenton” OR “electro Fenton” OR “ultrasound Fenton” OR “heterogeneous Fenton” OR “homogeneous Fenton” OR “photocatalysis\*” OR “electrooxidation” OR “electrochemical oxidation” OR “anodic oxidation” OR “ozonization” OR “UV peroxide” OR “TiO<sub>2</sub>/UV” OR “TiO<sub>2</sub>/H<sub>2</sub>O<sub>2</sub>”). (Topic) AND (“wastewater treat\*” or “water pollution control” or “polluted water control” or “sewage treat\*” or “effluent treat\*”) (Topic). Applying language restrictions exclusively to English and filtering for article types, including only articles and reviews, yielded a comprehensive dataset comprising 1420 documents. These documents were sourced from the Web of Science Core Collection (WoSCC), covering the period from January 1, 2023, to January 1, 2024. To maintain data integrity and mitigate the potential for document alterations during WoSCC database updates, all data exports were completed within a single day.

Statistical data extracted from an extensive array of academic literature was processed using bibliometric software, notably CiteSpace (version 6.3.R1). Visual representations, in the form of figures, were employed to illustrate data concerning institutes, authors, and keywords. In these visualizations, each node represented institutes, authors, or keywords, with node size proportional to the number of publications associated. Interconnections among nodes were depicted by lines, with line thickness reflecting the frequency of connections.

## RESULTS AND DISCUSSION

According to data from the WoSCC databases, a total of 1420 papers in the English language were published within one year (2023–2024). Among these, 1166 were articles and 254 were review articles. These contributions were distributed across various research categories, with Engineering Chemical (29.8%), Environmental Sciences (29.8%), Engineering Environmental (26.8%), Chemistry Physical (15.2%), Water Resources (12.6%),

Materials Science Multidisciplinary (11.8%), and Chemistry Multidisciplinary (11.3%) emerging as key areas of publication. The most cited journal is Chemosphere (see Figure 1A).

Figure 1B illustrates a co-authorship network map showing countries actively involved in researching the use of AOPs for wastewater treatment. The network comprises 10 nodes and 27 links, representing countries and connections between them. Node sizes correspond to the number of publications from each country. The People's Republic of China has the largest node size, indicating leadership in productivity with 675 papers, followed by India with 198, Saudi Arabia with 84, Spain with 64, the USA with 58, South Korea with 54, Pakistan and Brazil with 48. The purple ring surrounding each node signifies the centrality of the respective country. A higher centrality, denoted by the thickness of the purple ring, indicates increased collaboration with other countries and, consequently, greater influence in the academic sphere. Notably, India and the People's Republic of China exhibit the highest centrality (0.45 and 0.25 respectively), indicating extensive collaboration with authors from various countries in research on AOP technology. Following closely is South Korea (0.20).

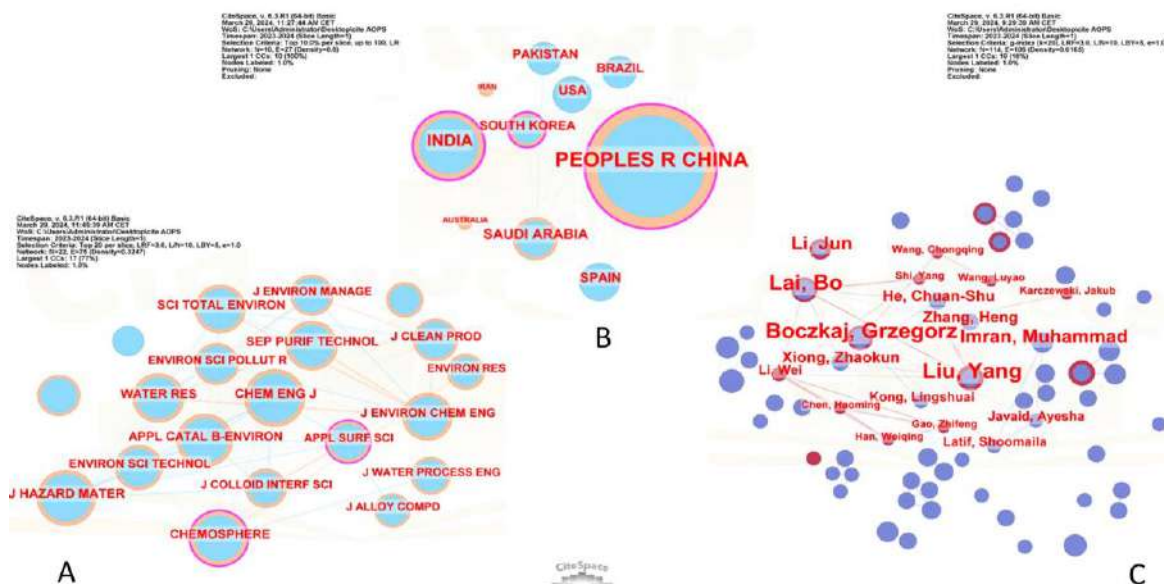


**Figure 1** CiteSpace network of A) journals; B) countries; and C) The co-citation network map of author which research AOPs

To identify authors with two or more articles cited simultaneously by another article, a co-citation analysis was conducted. The co-citation network map (Figure 1C) illustrates the size of nodes and their centrality. Liu Yang, Lai Bo, Boczka Grzegorz and Li Jun, emerges with the highest number of co-citations (9) and centrality (0.03), indicating their significant influence on the research topic.

Institutional contributions were also analysed, extracting information regarding institutions and their collaborative efforts through published articles. The mapping results (see Figure 2) highlight institutions that frequently appear in scientific publications within the research area. The size of each node indicates the productivity of the institutions. The Chinese Academy of



Sciences, Egyptian Knowledge Bank (EKB), and King Saud University exhibit significant centrality, underscoring their pivotal roles in investigating AOPs for wastewater treatment.

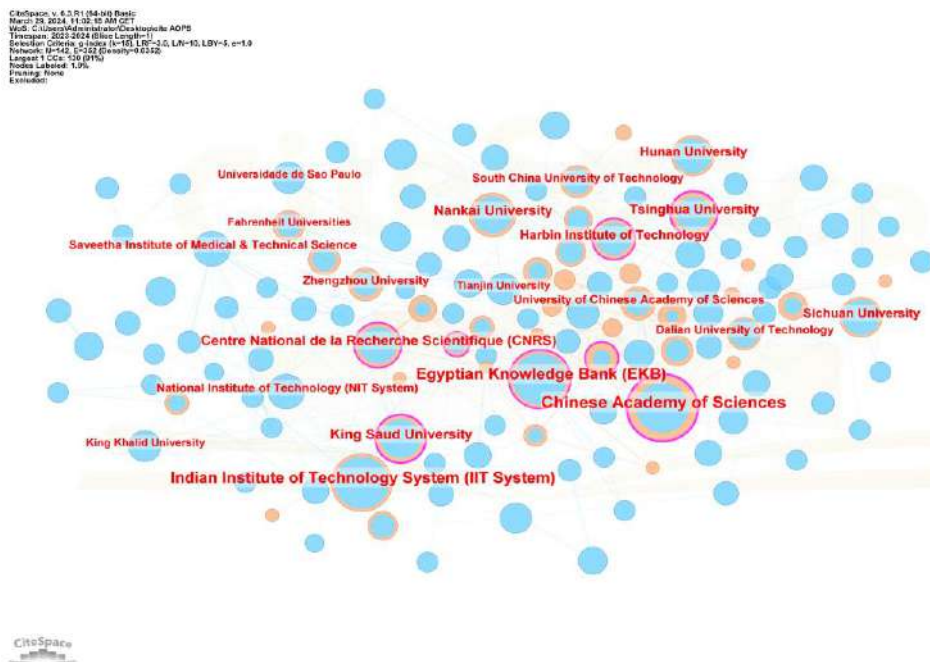


*Figure 2* The institutions network which research AOPs

### Keywords and cluster analysis

The keywords of an article serve to elucidate its research themes and focal points within a specific field. They offer essential insights into the content, guiding both readers and the scientific community towards areas of interest. Employing CiteSpace software, a comprehensive analysis was conducted on keyword occurrence, including author keywords, keywords plus, and abstracts from publications over the last year.

The resulting network co-occurrence map of keywords, depicted in Figure 3A, comprises 176 nodes representing different keywords. The size of each node correlates with the frequency of co-occurrences of its respective keywords. Notably, the nodes with the highest frequencies include degradation (471), removal (348), wastewater treatment (323), oxidation (232), performance (200), advanced oxidation processes (193), nanoparticles (158), photocatalytic degradation (147), adsorption (141). Certain nodes, marked with a purple ring in Figure 3A, exhibit good centrality (0.22 to 0.1), indicating significance of keywords in the research field. The cluster map analysis, aims to identify primary hotspots. The modularity (K) and silhouette (S) values serve as key criteria, with Q values near 1 (0.4 to 0.8 being acceptable) indicating clearly defined clusters, and S values near 1 (above 0.6 being reasonable) indicating a high level of confidence in node grouping.

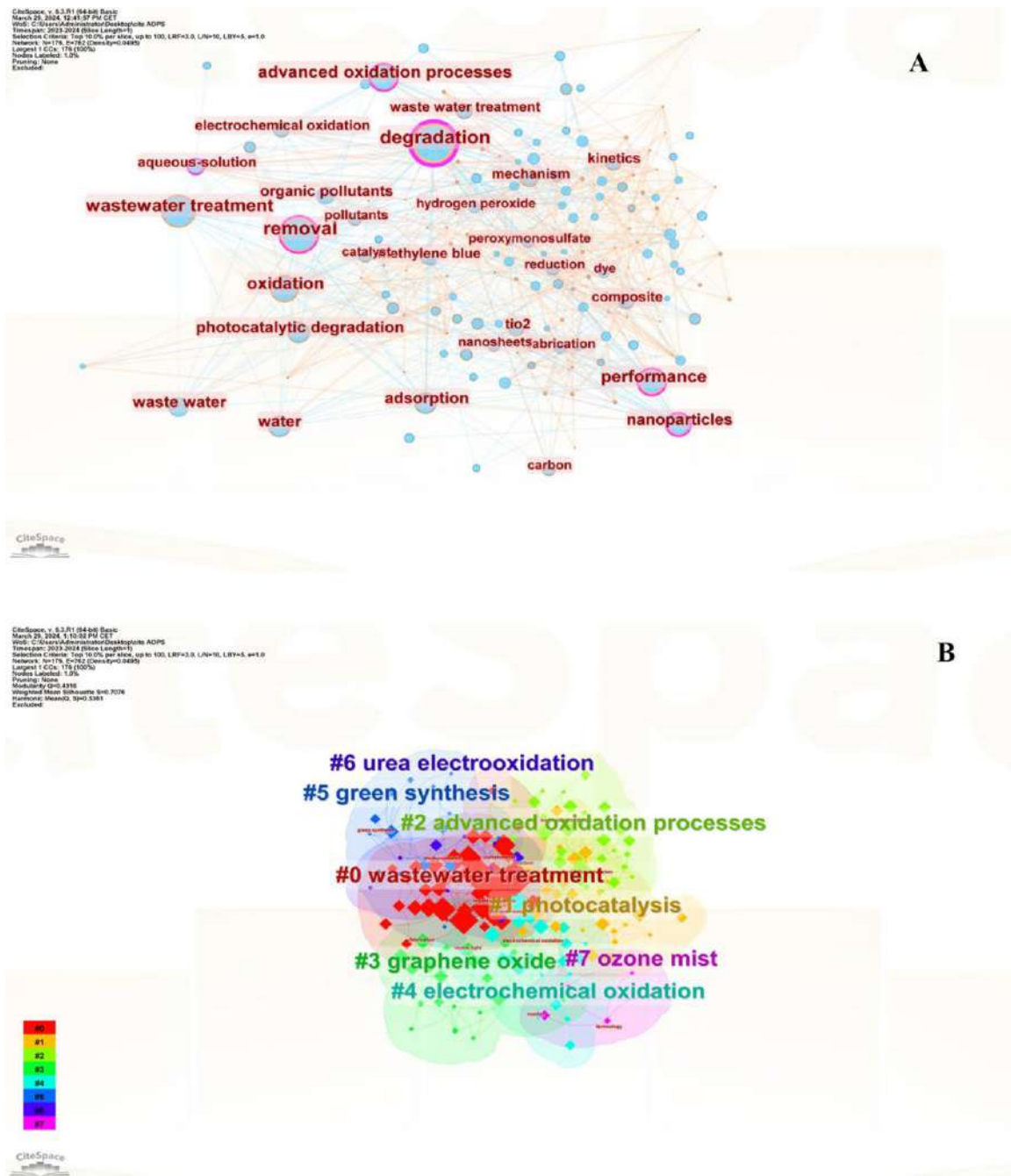


**Figure 3** A) The network co-occurrence map of keywords; and B) cluster map analysis

The principal research topics concerning the application of AOPs for wastewater treatment are delineated by cluster titles, as illustrated in Figure 3B. The largest cluster, is the main hotspot, denoted as #0, pertains to wastewater treatment research, comprising 36 members and boasting a silhouette value of 0.85. Following cluster #1 is related to photocatalysis (30 members), cluster #2 advanced oxidation processes, #3 graphene oxide, #4 electrochemical oxidation, #5 green synthesis, #6 urea electrooxidation and # 7 ozone mist.

## **CONCLUSION**

This bibliometric analysis elucidates the multifaceted landscape of research on AOPs in wastewater treatment. By systematically examining publication trends, key contributors, and emerging research areas, significant insights are gained into the evolving research domain. The dominance of Engineering Chemical and Environmental Sciences underscores the interdisciplinary nature of AOP research. Notable institutions and authors, such as the Chinese Academy of Sciences and Liu Yang, Lai Bo, Boczkaj Grzegorz and Li Yun, emerged as an influential contributors. Keyword analysis highlights key research themes, with degradation and wastewater treatment being central. Cluster mapping identifies major research hotspots, emphasizing wastewater treatment as a primary focus, followed by emerging areas like photocatalysis and graphene oxide applications. This comprehensive analysis serves as a valuable resource for researchers, and engineers, facilitating informed decision-making and collaboration efforts to address pressing environmental challenges in wastewater treatment.

## **ACKNOWLEDGEMENT**

*The authors are grateful to the Ministry of Science, Technological development and Innovation of the Republic of Serbia for financial support according to the contract with the registration number (grant number 451-03-66/2024-03/ 200017).*

## **REFERENCES**

- [1] Donthu N., Kumar S., Mukherjee D., *et al.*, J. Bus. Res. 133 (2021) 285–296.
- [2] Mao G., Hu H., Liu X., *et al.*, Environ. Pollut. 275 (2021) 115785.
- [3] Ding M., Zeng H., Ecotoxicol. Environ. Saf. 238 (2022) 113626.
- [4] Macías-Quiroga I.F., Henao-Aguirre P.A., Marín-Flórez A., *et al.*, Environ. Sci. Pollut. Res. 28 (2021) 23791–23811.



## POSSIBILITY OF ZINC AND CADMIUM RECOVERY FROM HAZARDOUS INDUSTRIAL WASTE – EAF DUST

Vanja Trifunović<sup>1\*</sup>, Snežana Milić<sup>2</sup>, Ljiljana Avramović<sup>1</sup>

<sup>1</sup>Mining and Metallurgy Institute Bor, Albert Ajnštajn 1, 19210 Bor, SERBIA

<sup>2</sup>University of Belgrade, Technical Faculty in Bor, V.J. 12, 19210 Bor, SERBIA

\*vanja.trifunovic@irmbor.co.rs

### Abstract

*Electric arc furnace dust (EAF dust) is a hazardous solid industrial waste that needs to be disposed of in an adequate manner primarily for environmental protection. However, due to the high content of zinc and other useful components found in it, EAF dust can also be considered as a secondary raw material for their recovery. In this paper, experimental investigations of the application of hydrometallurgical treatment of the EAF dust to zinc and cadmium recovery were carried out. The treatment was carried out in two phases: 1<sup>st</sup> phase - pretreatment, 2<sup>nd</sup> phase - leaching with sulfuric acid. The leaching rate of monitored elements in the second stage of treatment was examined depending on the concentration of H<sub>2</sub>SO<sub>4</sub> and the duration of the process. The highest Zn leaching rate of 65% and Cd of 80% were achieved at a concentration of H<sub>2</sub>SO<sub>4</sub> of 1.50 M in a time of 20 min, at ambient temperature, and a S:L ratio=1:4.*

**Keywords:** EAF dust, hydrometallurgy, treatment.

### INTRODUCTION

As a result of the melting of waste iron at high temperatures in an electric arc furnace, in the steel production process, an intermediate product of the process occurs, *i.e.* electric arc furnace dust (EAF dust) [1–4]. This intermediate product is considered a hazardous solid industrial waste in many countries of the world since it contains heavy metals. The potential pollution of this type of waste consists in the possibility of self-leaching of the elements found in its composition, the most represented of which are: Zn, Fe, and Pb, while in smaller quantities can be found Cu, Ni, Cd, Pb, Mn, Ca, F, K, Cl and others [1,5–11]. If this type of waste is inadequately disposed of, surface and underground water pollution, or environmental pollution with heavy metals, may occur due to atmospheric influences. Considering that it is hazardous waste, it is necessary to carry out its treatment in an adequate way for environmental protection. EAF dust has a high zinc content in its composition (in the form of zincite - ZnO and zinc-ferrite - ZnFe<sub>2</sub>O<sub>4</sub>), and as such it can be seen as a source of secondary raw material for obtaining zinc, but also other useful components, such as cadmium for example. By applying adequate treatment, a double effect can be achieved - both environmental protection and profit-making [1,8,12,13]. Treatment of the EAF dust can be achieved using hydrometallurgical, pyrometallurgical, and combined processes. The problem in choosing an effective treatment procedure is that the chemical and mineralogical composition of each EAF dust from steel production is individual. For this reason, it is

necessary to define optimal treatment conditions for each generated dust individually [1,2,5–7,13–15].

In this work, the characterization of a representative sample of the EAF dust was performed, and the possibility of zinc and cadmium recovery from the EAF dust was investigated using a hydrometallurgical procedure that includes two technological phases: pretreatment and acid leaching. The pretreatment of the initial sample of the EAF dust is carried out to selectively remove water-soluble components and involves a simple and inexpensive process of water leaching. The next phase involves acid leaching of the solid residue formed after pretreatment to zinc and cadmium recovery. The influence of the concentration of sulfuric acid and the duration of the leaching process on the zinc and cadmium leaching rate in the acid leaching process was investigated.

## MATERIALS AND METHODS

### Characterization of the initial EAF dust sample

The initial sample of the EAF dust was homogenized, and then the representative sample shown in Figure 1 was separated for chemical characterization using the quartering method.



*Figure 1* A representative sample of the EAF dust

The chemical composition of a representative sample of the EAF dust is presented in Table 1.

*Table 1* Chemical composition of the initial EAF dust sample

Element	Content, %	Element	Content, %
Zn	36.40	Cd	0.05
Fe	21.58	Ca	3.02
Na	1.18	Mg	0.76
Cl	2.90	K	0.99
Pb	1.86	Na	1.18
Si	1.69	Mn	2.12
Cu	0.19	Mg	0.76
Al	0.70	F	0.05

The greater number of elements present in the EAF dust occurs in the form of oxides, which is confirmed by the XRF analysis of the investigated EAF dust sample presented in Table 2. In the case of zinc, this element is present as zinc oxide (ZnO, zincite) with a share of about 50%, and as zinc-ferrite ( $ZnFe_2O_4$ , franklinite).

*Table 2 XRF analysis of the initial EAF dust sample*

Oxides	Content, %	Oxides	Content, %
ZnO	47.92	K <sub>2</sub> O	1.409
Fe <sub>2</sub> O <sub>3</sub>	30.897	CaO	3.94
MgO	0.9288	TiO <sub>2</sub>	0.155
Al <sub>2</sub> O <sub>3</sub>	0.6860	Cr <sub>2</sub> O <sub>3</sub>	0.519
SiO <sub>2</sub>	3.619	Mn	3.334
P <sub>2</sub> O <sub>5</sub>	0.259	Cu	0.331
Cl	3.582	PbO	2.319

### Experimental part

The hydrometallurgical treatment of the EAF dust applied in this paper, with the aim of zinc and cadmium recovery, was carried out in two phases: applying pretreatment, and then leaching with sulfuric acid.

#### *Pretreatment*

As the first technological phase of the hydrometallurgical treatment of the EAF dust, a simple and inexpensive leaching process of an initial representative sample of the EAF dust with distilled water was applied. The pretreatment was carried out to selectively remove water-soluble components from the initial sample of the EAF dust, with the following process parameters: water as a leaching reagent, temperature - ambient, ratio S:L=1:10, stirring speed - 500 rpm, time - 30 min.

#### *Acid leaching*

In the second technological phase of the EAF dust treatment, the effects of different concentrations of sulfuric acid and time on the zinc and cadmium leaching rate from the solid residue formed after the applied pretreatment were investigated. The following concentrations of sulfuric acid were investigated: 0.10 M, 0.25 M, 0.50 M, 0.75 M, 1.00 M, and 1.50 M. The time of the leaching process was investigated in the range of 5 to 60 min, while the temperature of 25°C, the ratio S:L=1:4, and the stirring speed of 500 rpm were constant in all experiments.

## RESULTS AND DISCUSSION

By applying pretreatment, selective removal of water-soluble components (Cl, K, Na, and Ca compounds) was achieved, which is convenient for the acid leaching process that follows, because in this way the consumption of leaching reagent (H<sub>2</sub>SO<sub>4</sub>) in the next phase, the acid leaching phase, is reduced. Also, the application of pretreatment avoids contamination of the resulting pregnant leaching solution with chlorides and other water-soluble components. Palimaka *et al.* [12], and Ruiz *et al.* [6] came to the same conclusion in their research.



Zinc and cadmium leaching rates depending on the concentration of sulfuric acid and the time of the acid leaching process are presented in Figure 2 (2a and 2b).

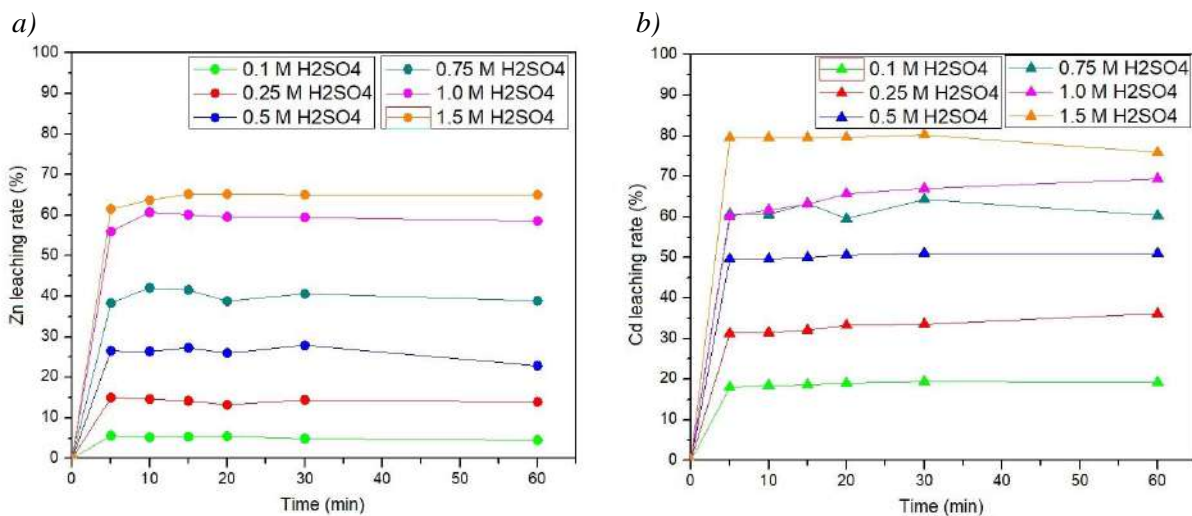


**Figure 2** Zinc and cadmium leaching rates depending on H<sub>2</sub>SO<sub>4</sub> concentration and time: a) Zn; b) Cd

Based on the obtained results, it can be concluded that the highest zinc leaching rates are achieved after 15–20 minutes, at all investigated concentrations of H<sub>2</sub>SO<sub>4</sub>, and then remain almost unchanged. During 20 min, the zinc leaching rate increases from 5.50% at an acid concentration of 0.10 M to 65.21% at a concentration of 1.50 M H<sub>2</sub>SO<sub>4</sub>. The highest cadmium leaching rates were reached in 20 min, after which the time parameter had no significant effect on the Cd leaching rate. Increasing the concentration of H<sub>2</sub>SO<sub>4</sub>, as well as the zinc leaching rate, has a favorable effect on the cadmium leaching rate so that the cadmium leaching rate ranges from 19% to 80% in a time of 20 min. The obtained results are in agreement with the research of Montenegro *et al.* [16], who also at ambient temperature, with a ratio S:L=1:5, in 20 min, with 1.00 M H<sub>2</sub>SO<sub>4</sub>, achieved a zinc leaching rate of 74% and cadmium of 87%. Hazaveh *et al.* [10] investigated the effect of H<sub>2</sub>SO<sub>4</sub> concentration from 1.00 M to 3.00 M and concluded that the zinc leaching rate from the EAF dust sample increases with increasing H<sub>2</sub>SO<sub>4</sub> concentration.

Further investigations will be carried out with the aim of zinc and cadmium recovery from the obtained pregnant leaching solution and obtaining commercial quality products.

## CONCLUSION

Based on the investigation results obtained in this paper, it can be concluded that the EAF dust can be used as a secondary raw material for zinc and cadmium recovery. Hydrometallurgical treatment aimed at recovering these metals from the investigated EAF dust sample is applicable and achieved a relatively high leaching rate of both monitored elements. After the applied pretreatment aimed at the selective removal of water-soluble components from the initial sample of the EAF dust, in the acid leaching phase, at ambient temperature, at a concentration of H<sub>2</sub>SO<sub>4</sub> of 1.50 M, the ratio S:L=1:4, in a time of 20 min, it was achieved zinc leaching rate of 65%. With the same parameters of the leaching process, a

cadmium leaching rate of 80% was achieved. Our future investigations will be directed towards the zinc and cadmium recovery from the obtained pregnant leaching solution.

## **ACKNOWLEDGEMENT**

*The authors are grateful to the Ministry of Education, Science and Technological Development of the Republic of Serbia for financial support according to the contract with the registration number 451-03-66/2024-03/200052 and number 451-03-65/2024-03/200131.*

## **REFERENCES**

- [1] Kukurugya F., Vindt T., Havlík T., *Hydrometallurgy* (154) (2015) 20–32.
- [2] Oustadakis P., Tsakiridis P.E., Katsiapi A., *et al.*, *J. Hazard. Mater.* (179) (2020) 1–7.
- [3] Chen W.S., Shen Y.H., Tsai M.S., *et al.*, *J. Hazard. Mater.* (190) (2011) 639–644.
- [4] Hamann C., Piehl P., Weingart E., *et al.*, *J. Hazard. Mater.* (465) (2024) 133421.
- [5] Wang J., Zhang Y., Cui K., *et al.*, *J. Clean. Prod.* (298) (2021) 126788.
- [6] Ruiz O., Clemente C., Alonso M., *et al.*, *J. Hazard. Mater.* (141) (2007) 33–36.
- [7] Havlik T., Turzakova M., Stopic S., *et al.*, *Hydrometallurgy* (77) (2005) 41–50.
- [8] Trifunović V., Milić S., Avramović Lj., *et al.*, *Hem. Ind.* 76(4) (2022) 237–249.
- [9] Almeida M.M., Saczk A.A., Felix F.S., *et al.*, *J. Photochem. Photobiol. A.* (438) (2023) 114585.
- [10] Hazaveh P.K., Karimi S., Rashchi F., *et al.*, *Ecotoxicol. Environ. Saf.* (202) (2020) 110893.
- [11] Terrones-Saeta J.M., Suárez-Macías J., Moreno-López E.R., *et al.*, *Metals* (11) (2021) 1603.
- [12] Palimąka P., Pietrzyk S., Stępień M., *et al.*, *Metals* (8) (2018) 547.
- [13] Gamutan J., Koide S., Sasaki Y., *et al.*, *J. Environ. Chem. Eng.* (12) (2024) 111789.
- [14] Trifunović V., Milić S., Avramović Lj., *et al.*, *Metals* (14) (2024) 426.
- [15] Rudnik E., *Miner. Eng.* (139) (2019) 105871.
- [16] Montenegro V., Agatzini-Leonardou S., Oustadakis P., *et al.*, *Waste Biomass Valorization* (7) (2016) 1531–1548.



## MAGNETIC BIOSORBENT BASED ON THE *Ambrosia arthemisiifolia* FOR ADSORPTION OF MALACHITE GREEN FROM WATER

Sandra Bulatović<sup>1\*</sup>, Natalija Nedić<sup>1</sup>, Tamara Tadić<sup>1</sup>, Bojana Marković<sup>1</sup>,  
Aleksandra Nastasović<sup>1</sup>

<sup>1</sup>University of Belgrade, Institute of Chemistry, Technology and Metallurgy (ICTM),  
Njegoševa 12, 11000 Belgrade, SERBIA

\*sandra.bulatovic@ihm.bg.ac.rs

### Abstract

*The modification of widespread plant and their use as low-cost and efficient biosorbents is a prospective way for dissolving environmental problems. In this research, the adsorption capacity of biosorbent based on the *Ambrosia arthemisiifolia* was improved by modification with magnetite. The adsorption capacity of the modified magnetic biosorbent was determined with the help of cationic dye Malachite Green (MG). The maximum of MG adsorption capacity, after 20 min, was 7.65 mg/g, with removal efficiency of 100%. The adsorption kinetic of the MG was described by the pseudo-second-order model. FTIR analyses also confirmed biosorption of MG on magnetic biosorbent. The present study verified that magnetic biosorbent can be used as an economic and effective adsorbent for removal of MG from aqueous solutions.*

**Keywords:** magnetic biosorbent, *Ambrosia arthemisiifolia*, malachite green.

### INTRODUCTION

*Ambrosia artemisiifolia* is the most widespread plant of the *Ambrosia* genus in Europe, including Serbia [1,2]. This invasive weed plant causes environmental, agronomical, and medical problems [3]. Pollen of *A. artemisiifolia* is the most represented seasonal allergen in Europe that triggers rhinitis, conjunctivitis, and asthma [4,5]. According to the latest Report of the Environment Quality (2022), the concentration of *Ambrosia* pollen in Serbia was 9476 grain/m<sup>3</sup>, and it was dominant compared to the other allergens during the pollination period [6]. The objective of this study was investigation of biomass potential and its conversion into more valuable product, such as biosorbent for sorption of organic pollutants, like synthetic organic dyes.

This study was focused on the design of the novel magnetic hybrid biosorbent, based on the biomass of the *A. artemisiifolia* for sorption of synthetic organic dye, Malachite Green (MG), from aqueous solution, using UV-Vis spectrophotometer for dye detection. MG is a cationic dye, widely used in textile industry, as an antimicrobial agent in aquaculture, etc. This dye is toxic, with teratogenic, carcinogenic, and mutagenic effects on organisms [7]. The advantages of magnetic biosorbent for MG biosorption are multiple, with focus on green sustainability, eco-friendly approaches, easy separation using an external magnetic field, and as an economic method with potential for the future implementation in wastewater treatments.

## MATERIALS AND METHODS

### Preparation of magnetic biosorbent

The plant *Ambrosia artemisiifolia* was sampled on the periphery area of Belgrade (capital of Serbia), by cutting off plants parts above the ground. After sampling, the plant material was washed with water, and dried naturally, on the sun light and wind, for a one week. After drying, the plants were cut into small pieces with scissors, and ground in an electric mill. After the milling, the resulting particles were sieved to obtain particles with a size range <300  $\mu\text{m}$ . The obtained particles were then washed with distillate water, to remove possible impurities, after which they were dried overnight in an oven, at 50°C. The synthesis of magnetic biosorbent was performed following coprecipitation method with some modifications, proposed by Medina-Zazueta *et al.* [8]. The method consists of mixing a 0.39 g of  $\text{FeCl}_3 \cdot \text{H}_2\text{O}$  and 0.17 g of  $\text{FeCl}_2 \cdot \text{H}_2\text{O}$  in 190  $\text{cm}^3$  deionized water, in a  $\text{N}_2$  atmosphere, at 80°C, with magnetic stirring (450 rpm, 20 min). After that, 10M NaOH was added, and stirring was continued under the same conditions (30 min). At the end, 0.2 g of biosorbent was added to the reaction mixture, and stirring was continued under the same conditions (30 min). Finally, prepared magnetic biosorbent was filtered and washed, until the pH neutral, and dried in an oven, overnight, at 50°C.

### Biosorption of MG

Magnetic biosorbent (0.1 g) was added to the 20  $\text{cm}^3$  of 50 ppm MG solution. Subsequently, magnetic biosorbent samples with adsorbed dye were separated from the mixture via external magnet. The adsorption time was monitored from 1 to 20 min, at room temperature (25°C). The residual amounts of dye in the water solution were determined spectrophotometrically (NOVEL-102S UV-Vis Double Beam Spectrophotometer, COLO Lab Experts, Slovenia). The adsorption capacity ( $Q_t$ ) and removal efficiency of the magnetic biosorbent at equilibrium ( $E$  (%)) were determined using Equations (1) and (2) [9]:

$$Q_t = \frac{(C_0 - C_t) \times V}{m} \quad (1)$$

Where:  $C_0$  ( $\text{mg}/\text{dm}^3$ ) and  $C_t$  ( $\text{mg}/\text{dm}^3$ ) are the initial concentration and concentration at time  $t$  of MG in the solution,  $V$  ( $\text{dm}^3$ ) is the volume of the solution, and  $m$  (g) is the mass of the magnetic biosorbent.

$$E(\%) = \frac{(C_0 - C_t)}{C_0} \times 100\% \quad (2)$$

Where:  $C_0$  ( $\text{mg}/\text{dm}^3$ ) and  $C_t$  ( $\text{mg}/\text{dm}^3$ ) are the initial concentration and concentration at time  $t$  of MG in solution.

### The Kinetic Study of the Adsorption of MG

MG adsorption rates were analysed using pseudo-first-order and pseudo-second-order kinetic model, according to the Equations (3) and (4) [10]:

$$\log(q_e - q_t) = \log q_e - \frac{k_1}{2.303} t \quad (3)$$

$$\frac{i}{q_e} = \frac{1}{k_2 q_e^2} + \frac{t}{q_e} \quad (4)$$

Where:  $q_t$  is the equilibrium sorption capacity in time  $t$  (mg/g),  $q_e$  is the adsorption capacity in equilibrium (mg/g),  $k_1$  is the pseudo-first-order rate constant (1/min),  $k_2$  is the pseudo-second-order rate constant (g/mg 1/min).

### Fourier Transform Infrared Spectroscopy (FTIR)

FTIR spectra of biosorbent, before and after magnetisation and biosorption of MG, were taken in ATR mode using a Nicolet SUMMIT FTIR Spectrometer (Thermo Fisher Scientific, Waltham, MA, USA).

## RESULTS AND DISCUSSION

The concentration of MG in the aqueous solution was monitored by UV-Vis spectroscopy, based on the standard curve for MG (Figure 1).

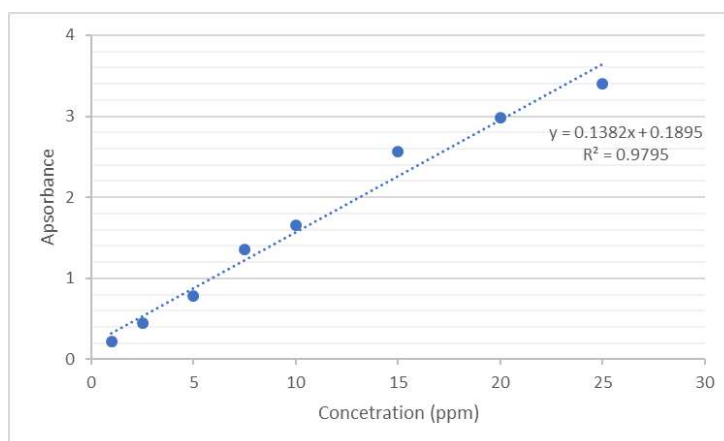


**Figure 1** Standard curve for MG determination

Biosorption of MG was monitored at room temperature (25°C), with shaking on a shaker. Aliquots were taken in the range of 1-20 min, and concentrations of MG were measured with UV-Vis spectroscopy, at 618 nm (Table 1). As can be seen from the obtained results (Table 1, Figure 2), the MG biosorption was occurred in two stages. In the first stage, the uptake was rapid within 7 min, and then in the second stage, it was slow from 7 to 20 min and reached equilibrium at 10 min. The maximum of MG adsorption capacity after 20 min was 7.65 mg/g, with exceptionally high removal efficiency of almost 100 %. The fast removal of the MG at the first stage may be attributed to the rapid attachment of dye ions on the biosorbent surface, and the number of available binding sites. The following slower adsorption process with increasing contact time may be due to the unavailability of free binding sites. The kinetics of the MG adsorption was analysed by the two kinetics models, pseudo-first-order and pseudo-second-order kinetic model. The values of the kinetics parameters are shown in **Table 2**. The experimental data confirmed the pseudo-second-order model, with  $R^2$  (correlation coefficient) close to 1, and the calculated  $q_e$  ( $q_{e, cal}$ ) value essentially matched the experimental  $q_e$  ( $q_{e, exp}$ )

value. The obtained results are in accordance with the studies that dealt with similar topics [11–13].

**Table 1** Biosorption efficiency

t (min)	E (%)
0	0.0
1	16.7
3	65.4
5	86.0
7	92.3
10	97.4
13	99.2
16	99.7
20	100.0

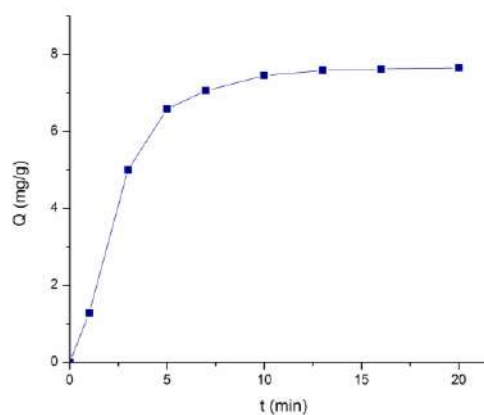


**Figure 2** Effect of contact time on MG adsorption capacity ( $C_0$ : 50 ppm, adsorbent dose: 5 g/dm<sup>3</sup>,  $T$ : 25°C, pH 4.2)

**Table 2** Kinetic parameters for the adsorption of MG onto biosorbent, at 25°C.

Kinetic model	Parameter	Magnetic biosorbent-MG
Pseudo-first-order	$q_{e,exp}$ (mg/g)	7.65
	$q_{e,cal}$ (mg/g)	6.85
	$k_1$ (1/min)	0.35
	$R^2$	0.9976
Pseudo-second-order	$q_{e,cal}$ (mg/g)	8.33
	$k_2$ (1/min)	0.08
	$R^2$	0.9976

The FTIR technique is a useful tool for identification of characteristic functional groups on the surface of the biosorbent material. A comparison of the FTIR spectra of biosorbent before and after magnetisation, and biosorption of MG is shown in Figure 3. FTIR spectra showed the characteristic broad bands around 3400 and 3300 cm<sup>-1</sup>, due to the stretching vibration of –OH from macromolecules: cellulose, hemicellulose, and lignin [14,15]. The peaks at 2920 and 2840 cm<sup>-1</sup> represent the –CH stretching and vibration of –CH<sub>3</sub> and –CH<sub>2</sub> groups in cellulose and hemicellulose [16]. The peaks associated with the stretch vibration of aromatics were about 1600 cm<sup>-1</sup>. A characteristic stretching vibration absorption band of the (–C(=O)–OH) is at 1730 cm<sup>-1</sup>. Peak at about 1030 cm<sup>-1</sup> is due to C–O bending [17]. Peak about 570 cm<sup>-1</sup> corresponds to the magnetite [18], and it is obvious difference between biosorbent and magnetic biosorbent. Based on the FTIR spectra each of the functional group have an affinity for MG adsorption. Some peaks shifted or disappeared after adsorption, which was a clear indication that adsorption of MG onto Ambrosia magnetic biosorbent had happened.



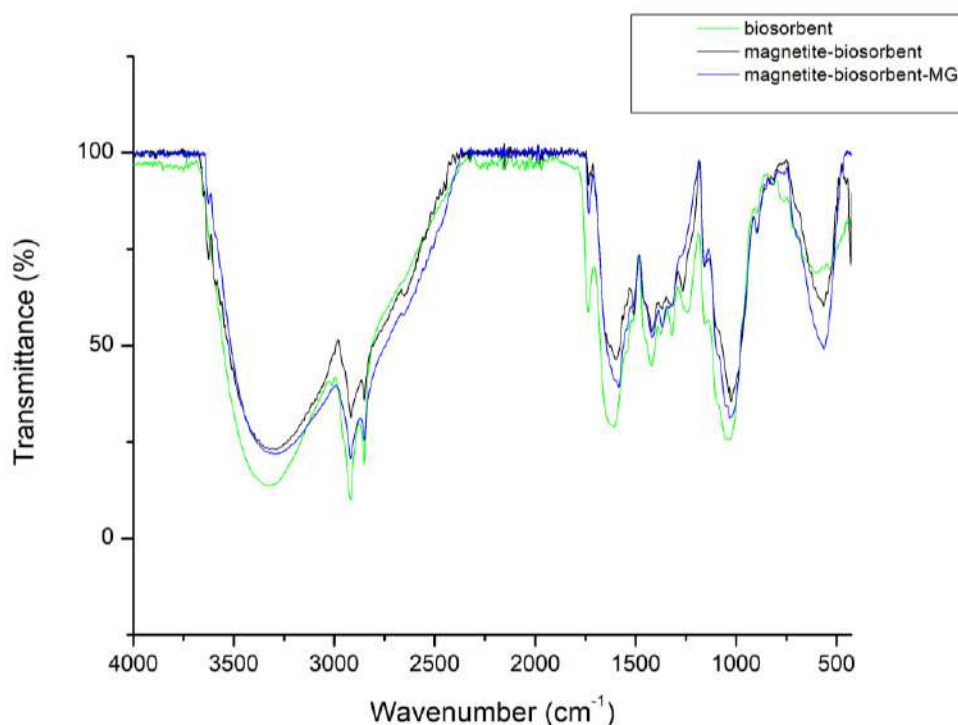


Figure 3 FTIR spectra of biosorbent, magnetic biosorbent, and magnetic biosorbent-MG.

## CONCLUSION

Experimental results showed that magnetic biosorbent based on the *A. arthemisiifolia* can be used successfully in the removal of MG from aqueous solutions. The maximum of MG adsorption capacity of magnetic biosorbent was 7.65 mg/g, and removal efficiency of almost 100 %. Pseudo-second-order kinetic model could be used for prediction of the adsorption kinetics of this adsorption process. FTIR analysis also confirmed adsorption of MG on magnetic biosorbent. This green approach has potential to be implemented in the future, as very economic method, for the treatments of industry wastewater.

Further research should focus on the optimization parameters for the adsorption of MG and other synthetic organic dyes on magnetic biosorbent, including its implementation on real wastewater samples.

## ACKNOWLEDGEMENT

This research has been financially supported by the Ministry of Science, Technological Development and Innovation of Republic of Serbia (Contract No: 451-03-66/2024-03/200026).

## REFERENCES

- [1] Albertini R., Veronesi L., Colucciet M. E., *et al.*, *Acta. Biomed.* 93 (2022) 2022324.
- [2] Kovacs B., Hohmann J., Csupor-Loffler B., *et al.*, *Heliyon* 8 (2022) e09884.
- [3] Hrabovský M., Ščevková J., Mičieta K., *et al.*, *Ann. Agric. Environ. Med.* 23 (2016) 64–70.
- [4] Mihajlovic L., Radosavljevic J., Burazer L., *et al.*, *Phytochemistry* 109 (2015) 125–132.

- [5] Skjøth C. A., Sun Y., Karrer G., *et al.*, *Sci. Total. Environ.* 686 (2019) 212–222.
- [6] Ministarstvo zaštite životne sredine Republike Srbije, Agencija za zaštitu životne sredine: Izveštaj o stanju životne sredine u Republici Srbiji, Beograd (2022), *Available on the following link*: [http://www.sepa.gov.rs/download/Izvestaj\\_2022\\_usvojen.pdf](http://www.sepa.gov.rs/download/Izvestaj_2022_usvojen.pdf).
- [7] Chen Z., Deng H., Chen, C., *et al.*, *J. Environ. Health Sci. Eng.* 12 (2014) 63.
- [8] Medina-Zazueta L., Miranda-Castro F.C., Romo-Garcia F., *et al.*, *Sustainability* 15 (2023) 4586.
- [9] Şenol Z.M., *Int. J. Environ. Anal. Chem.* 102 (2020) 4550–4564.
- [10] Isik B., Cakar F., Cankurtaran O., *Mater. Sci. Eng. B.* 293 (2023) 116451.
- [11] Escudero L.B., Agostini E., Dotto G.L., *Chem. Eng. Commun.* 205 (2018) 122–133.
- [12] Soldatkina L., Yanar M., *Colloids Interfaces* 5 (2021) 52.
- [13] Soldatkina L.M., Yanar M.A., *Himia, Fizika ta Tehnologija Poverhni* 13 (2022) 197–208.
- [14] Li S., Tao M., *Desalin. Water Treat.* 57 (2016) 5193–5199.
- [15] Farias K.C.S., Guimarães R.C.A., Oliveira K.R.W., *et al.*, *Toxics* 11 (2023) 664.
- [16] Abate G.Y., Alene A.N., Habte A.T., *et al.*, *Environ. Syst. Res.* 9 (2020) 29.
- [17] Bayramoğlu G., Çelik G., Arica M.Y., *J. Hazard. Mater.* 137 (2006) 1689–1697.
- [18] Muinde V.M., Onyari J.M., Wamalwa B., *et al.*, *J. Environ. Prot.* 8 (2017) 215–230.
- [19] Stoia M., Istrate R., Pacurariu C., *J. Therm. Anal. Calorim.* 125 (2016) 1185–1198.



## STUDIES OF THE INFLUENCE OF GRAPHENE NANOSHEETS ON THE WETTABILITY OF ECO-FRIENDLY SOLDER ALLOYS

Milan Nedeljković<sup>1\*</sup>, Srba Mladenović<sup>1</sup>, Jasmina Petrović<sup>1</sup>, Milijana Mitrović<sup>1</sup>

<sup>1</sup>University of Belgrade, Technical Faculty in Bor, V.J. 12, 19210 Bor, SERBIA

\*mnedeljkovic@tfbor.bg.ac.rs

### Abstract

*Lead-based solders are harmful to the environment and human health, so they must be replaced. Numerous studies have focused on the production of “eco-friendly” solder alloys. Recently, there has been an increasing number of researches dealing with lead-free composite solder alloys. This paper presents a review of research on the influence of graphene nanosheets (GNS) on the wettability of tin-based solder alloys. GNSs have been used to improve the physical and mechanical properties of solder. The variable mass content of GNS particles was successfully pressed into lead-free solder using a high-planetary ball mill. This method enabled better homogeneous mixing and consolidation of the mixed powder. After that, the powder that was obtained was sintered, and the effect of GNS on wettability was investigated. Increasing the mass content of GNS reduces the surface tension between the substrate and the composite solder, resulting in a lower contact angle and improved wettability.*

**Keywords:** lead-free solders, graphene nanosheets, high-planetary ball mill, sintering.

### INTRODUCTION

In the electrical industry, soldering is the most crucial connection method. The solders were heated to the melting point before soldering. The molten solder wet the substrate, creating connections between the liquid (solder) and the solid (substrate). The solder then solidifies as the joints cool, creating solder joints. Solders are often made of low melting point alloys since melting is a need for the soldering procedures. The most common solders are Pb-Sn alloys, and research into their characteristics is significant [1–4]. Lead is toxic and poses a danger to the environment and human health, therefore its elimination is necessary. Recognizing these facts, several nations have begun to take necessary safety measures, such as establishing rules limiting or prohibiting the use of lead in electronics. In this regard, the European Union (EU) adopted two directives: WEEE (Waste Electrical and Electronic Equipment) and RoHS (Restriction of the Use of Certain Hazardous Substances) [5,6].

There is no lead-free solder that can entirely outperform lead solder characteristics. It has been challenging to substitute lead-based solder, and research is ongoing. The new solder alloys must meet specific requirements in terms of melting temperature, wettability, mechanical, and electrical properties. Additionally, it must exhibit the right corrosion resistance in various conditions and at various temperatures. The lead-free solders that are used most frequently today are Sn-Cu, Sn-Ag, and Sn-Ag-Cu [7].

Reinforcements can be added to standard alloys to create a composite lead-free solder. There are many methods for reinforcing these solders, including powder metallurgy (PM),

melting and casting (MC), physical vapor deposition, precipitation, and others. PM includes mixing powders, compressing them at a certain pressure, and then sintering. The PM process is the most often used way of producing composite solder. Many researchers have chosen nano-sized particles for the reinforcements. As reinforcement, the following particles can be used:  $\text{Si}_3\text{N}_4$ ,  $\text{Al}_2\text{O}_3$ ,  $\text{SiC}$ ,  $\text{TiB}_2$ ,  $\text{TiO}_2$ ,  $\text{ZrO}_2$ ,  $\text{SnO}_2$ , and  $\text{ZnO}$ . Due to its remarkable properties, graphene has recently captured considerable attention from researchers. With superior mechanical properties, and electrical and thermal conductivity, graphene nanosheets (GNS) are expected to outperform carbon nanotubes (CNTs) and hold significant promise in the field of electronics [8]. To achieve better wettability and mechanical properties than the pure solder, Nai *et al.* [9] investigated the wettability of Sn-3.5Ag-0.5Cu solder reinforced with multi-wall carbon nanotubes (MWCNTs), produced by the PM method. The research results showed that with 0.07 mass.% MWCNTs in the matrix, the contact angle decreased from  $29^\circ$  to  $24^\circ$ , indicating an improvement in the wettability of the composite solder. The results corresponded with previous studies.

Solder wettability is a critical factor in determining the quality of the solder to substrate bond. Strong bonds between the solder and the substrate were promoted by good wetting. Wettability is the ability of a liquid to diffuse onto a solid surface in a specific environment, such as the atmosphere, temperature, and so on [10]. Wettability is defined by the contact angle ( $\theta$ ). Figure 1 illustrates the relationship between surface tension and contact angle, which can be described using the Young-Laplace equation (1):

$$\cos \theta = \frac{\gamma_{sa} - \gamma_{sl}}{\gamma_{la}} \quad (1)$$

The contact angle is the angle between the tangent drawn from point A to the circular line representing the contour of the solder drop and the surface of the substrate.

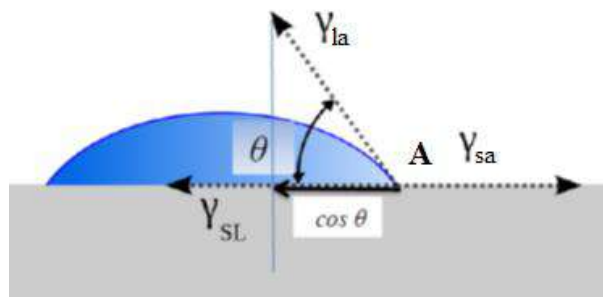


**Figure 1** Schematic of contact angle ( $\theta$ ) of liquid metal on a solid surface [11,12]

When the contact angle ( $\theta$ ) is between  $0^\circ$  and  $90^\circ$ , the solder is considered to wet the substrate well. Better wettability is achieved with less contact angle, greater surface area, and spreading speed. Generally, a solder alloy with a smaller contact angle to the substrate provides a much more reliable interconnection during the soldering process [11,12].

This paper presents an overview of the research on the influence of GNS particles on the wettability of different tin-based composite solder alloys. The variable mass content of GNS

has been successfully integrated into lead-free solder using a high-planetary ball mill. This technique provided significantly greater homogenous mixing and consolidation of the mixed powder. Following that, the powder was sintered and the wettability was determined. The contact angle was measured using the sessile drop technique. The droplet was photographed and analyzed, and the contact angle between the solid surface, air, and the droplet was determined.

## OVERVIEW OF RECENT RESEARCH

Yin *et al.* [13] used the contact angle method to measure the wettability of the Sn-0.3Ag-0.7Cu composite solder depending on the mass content of GNS. The result of the test shows that adding GNS increased solder wettability significantly. Figure 2 shows the influence of different mass content of GNS on the contact angle of the composite solder. The figure presents that the contact angle of the Sn-0.3Ag-0.7Cu solder decreased by approximately 29% with the addition of 0.01% GNS. With a further increase in the mass content of the reinforcement, the contact angle continued to decrease.

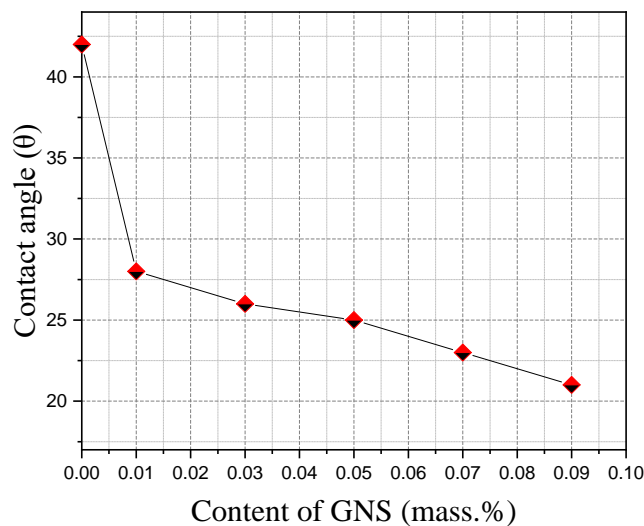


**Figure 2** Contact angle of Sn-0.3Ag-0.7Cu-x GNS solder on the copper substrate [13]

After analyzing the results and reviewing previous research, they come to the following explanation. GNS are non-polar molecules with a hexagonal honeycomb lattice composed of carbon-carbon covalent bonds. When the GNS in the molten composite solder comes into contact with the non-polar organic acids in the rosin (solder paste) during soldering, the dispersion between the non-polar molecules of these substances can occur. The interphase tension between the composite solder and the rosin was reduced. When the interphase tension was reduced, the contact angle decreased, and the solder wettability was improved.

Liu *et al.* [14] studied the influence of GNS particles on the Sn-3Ag-0.5Cu composite solder and arrived at the following conclusions. As shown in Figure 3, the contact angle decreased as GNS content increased.

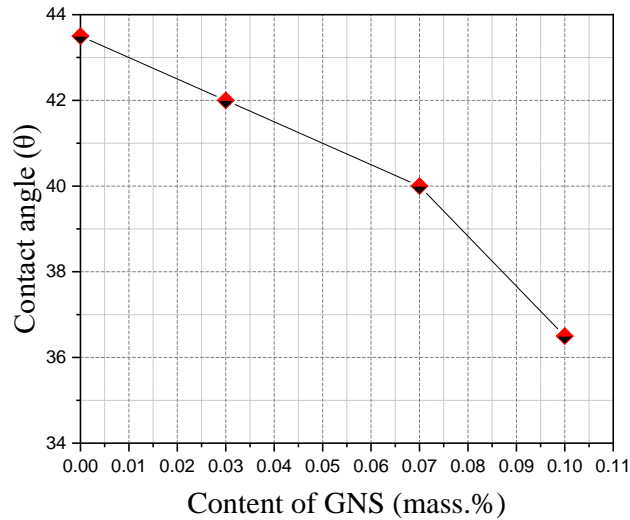


**Figure 3** Contact angle of Sn-3Ag-0.5Cu-x GNS solder on copper substrate [14]

The composite solder with a mass content of GNS of 0.1% shows the smallest contact angle, which is 15.5% smaller than the starting solder. Analyzing the obtained results they came to the following conclusion. This improved wettability can be explained based on the effect of GNS particles on the interfacial tension between the composite solder and rosin during the soldering process. Through the soldering process, GNS should be dispersed at the solder/rosin interface. The presence of GNS can reduce the surface tension of the interface. Reduced interphase tension between the solder and the rosin causes a decrease in the contact angle. That improved the wettability of the composite solder.

Yin *et al.* [15] also studied the effect of different mass content of GNS on Sn-0.3Ag-0.7Cu composite solder and reached the following conclusions. In Figure 4, it can be seen that the contact angle decreases with the increasing mass content of GNS. The contact angle of Sn-0.3Ag-0.7Cu solder decreased by 31% by adding only 0.01% GNS particles. A further increase in the mass content of GNS up to 0.09% leads to a decrease in the contact angle. It follows that the wettability of the composite solder increases.

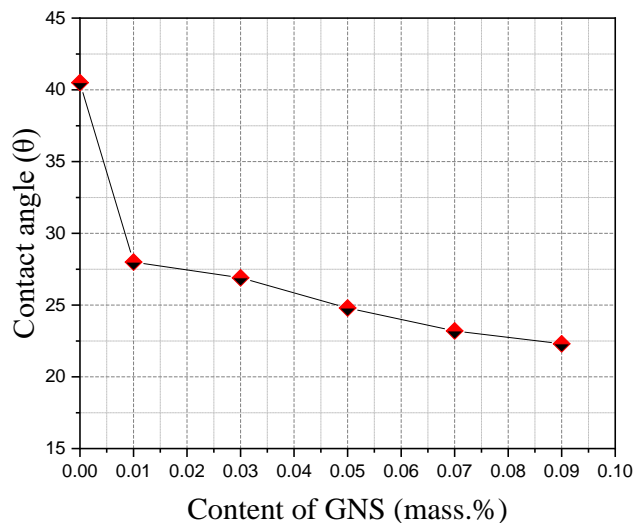


**Figure 4** Contact angle of Sn-0.3Ag-0.7Cu-x GNS solder on the copper substrate [15]



According to the results, they reached the same conclusions as previous researchers. When the GNS particles present in the solder come into contact with the rosin, dispersion occurs between these compounds. The interfacial tension was reduced. Based on equation 1, reducing the interfacial tension between the composite solder and the rosin reduces the contact angle, which increases the wettability of the composite solder.

## CONCLUSION

Solderability is the ability of solder alloys to wet and bond with a surface, forming a reliable and durable joint. Wettability tests were performed on several tin alloys reinforced with GNS particles, and the results were practically similar. The presence of GNS reduces the interfacial tension between the solder and the surface. As a result of the decreased contact angle, the wettability of the composite solder improved. By reviewing the literature and analyzing previous studies, it can be determined that the wettability of tin-based solder alloys reinforced with GNS increases.

## ACKNOWLEDGMENT

*The research presented in this paper was done with the financial support of the Ministry of Science, Technological Development and Innovation of the Republic of Serbia, within the funding of the scientific research work at the University of Belgrade, Technical Faculty in Bor, according to the contract with registration number 451-03-65/2024-03/200131.*

## REFERENCES

- [1] Islam R., Wu B., Alam M., *et al.*, J. Alloys Compd. 392(1–2) (2005) 149–158.
- [2] Salleh M., Hazizi M., Ahmad M., *et al.*, Adv. Mater. Res. 277 (2011) 106–111.
- [3] Shen J., Chan Y., Microelectron. Reliab. 49(3) (2009) 223–234.
- [4] Puttlitz K., Stalter K., Handbook of lead-free solder technology for microelectronic assemblies, CRC Press, New York, (2004), p.8–14, ISBN: 9780824748708.
- [5] Hongtao M., Jeffrey C., J. Mater. Sci. 44(5) (2009) 1141–1158.
- [6] Chiang W., Chen Y., Chen M., *et al.*, J. Electron. Mater. 35 (2006) 1032–1040.
- [7] Hsi C., Lin C., Chang T., *et al.*, Metall. Mater. Trans. A, 41(2) (2010) 275–284.
- [8] Liu X., Han Y., Jing H., *et al.*, Mater. Sci. Eng. A. 562 (2013) 25–32.
- [9] Nai S., Wei J., Gupta M., J. Electron. Mater. 35(7) (2006) 1518–1522.
- [10] Ryu B., Choi Y., Park H., *et al.*, Colloids and Surfaces A: Physicochemical and Engineering Aspects 270 (2005) 345–351.
- [11] Nai S., Wei J., Gupta M., Thin Solid Films 504(1–2) (2006) 401–404.
- [12] Yoon S., Choi W., Lee H., Scripta Mater. 40(3) (1999) 327–332.
- [13] Yin L., Zhang Z., Zuo C., *et al.*, J. Mater. Sci-Mater. El. 31(3) (2020) 1861–1867.
- [14] Liu X., Han Y., Jing H., *et al.*, Mater. Sci. Eng. A. 562 (2013) 25–32.
- [15] Yin L., Zhang Z., Su Z., *et al.*, J. Electron. Mater. 49(12) (2020) 7394–7399.



## ELECTROCHEMICAL SENSORS FOR DETERMINATION OF ANTIBIOTICS

Ana Simonović<sup>1\*</sup>, Marija Petrović Mihajlović<sup>1</sup>, Milan Radovanović<sup>1</sup>, Žaklina Tasić<sup>1</sup>,  
Milan Antonijević<sup>1</sup>

<sup>1</sup>University of Belgrade, Technical Faculty in Bor, V.J. 12, 19210 Bor, SERBIA

\*[asimonovic@tfbor.ac.bg.rs](mailto:asimonovic@tfbor.ac.bg.rs)

### Abstract

*In today's pharmaceutical practise, antibiotics are used to treat bacterial infections because they are easy to use, inexpensive and effective. For this reason, they are very often prescribed for the treatment of humans and animals. However, the continuous and long-term use of antibiotics has led to the need to detect and determine their presence in a large number of different samples using appropriate sensors. However, electrodes used for electrochemical analysis can perform poorly as their surface can be easily contaminated by analytes or intermediates of electrochemical reactions. To solve these problems, many researchers have focused on modifying the relevant electrodes to achieve better performance.*

**Keywords:** electrochemical sensor, electrodes, antibiotic.

### INTRODUCTION

Since their discovery until today, antibiotics have played a very important role in reducing bacterial growth or suppressing bacteria. Due to the uncontrolled use of antibiotics, they can be found in canned food, milk, meat and waste water. The antibiotic residues in wastewater from pharmaceutical waste cause side effects, even a low concentration leads to serious consequences for the environment and human health [1]. Therefore, there is a need to find simple, precise and economical methods for their detection in various samples. Recently, the methods investigated, as fast and accurate, are electrochemical methods and the use of suitable electrodes as electrochemical sensors. Electrochemical methods are characterised by high sensitivity, high accuracy and trace detection. Great attention of researchers is paid to the search for new electrodes that have a large surface area, good electrical conductivity and high electronic transport, which has been demonstrated by carbon-based electrodes such as carbon nanomaterials, carbon nanotubes, graphene (and its derivatives) [2–5]. Metal-based electrodes also showed good results as electrochemical sensors for the detection of antibiotics [1,6]. The paper presented research in which very efficient electrochemical sensors for the detection and determination of some types of antibiotics were found.

### RESULTS AND DISCUSSION

#### Carbon based electrochemical sensors for detection of antibiotics -composites

Dehdashtian and her team [7] investigated sensitive and selective sensor based on carbon paste electrode which was modified by Sodium Montmorillonite nanoclay. This composite was developed as an electrochemical sensor for antibiotic Cefotaxime. The researchers used

the composite to study the electrooxidation of Cefotaxime using cyclic voltammetry and differential pulse voltammetry. The morphology of the modified and unmodified electrode was characterized by scanning electron microscopy. Results of the investigation that current oxidation peak on the modified carbon paste electrode was significantly improved compared to unmodified carbon paste electrode. Modified carbon electrode exhibited linear response over two linear concentration ranges from 0.5 to 40nM and 40 to 2400nM Cefotaxime. Detection limit of modified carbon electrode was 0.1nM. Investigation confirmed that this sensor can be applied for monitoring of Cefotaxime in urine and serum samples.

Iron cation exchanged montmorillonite modified glassy carbon electrode (Fe-Mt/GCE) via a direct voltametric method was used as electrochemical sensor for detection of antibiotic Tetracycline hydrochloride [8]. Modified electrode showed sensitivity of 27.1  $\mu\text{A}/\text{Mcm}^2$ . The Fe-Mt/GCE exhibits higher response current intensity in the rapid scanning process in regard to traditional electrode, which should be contributed to the larger surface area and more active sites of the modified electrode for the oxidation reaction of Tetracycline hydrochloride.

Yu and his colleges developed ultra-sensitive graphene and copper sensor, Gr/Cu, supported on glassy carbon (GCE/Gr/Cu) [9] for the determination of Levofloxacin. The composite give very good conducting properties and impressive sensitivity of 19.7  $\mu\text{A}/\mu\text{Mcm}^2$ . The achieved detection limit of Levofloxacin was 11.86nM. Good selectivity was proved in the presence of various ions typically found in water and other drug molecules. Recovery values were between 97.7 and 103.8% in tap water.

The presence of  $\beta$ -lactam antibiotics in milk samples is of particular concern and represents an unavoidable contaminant of milk. Therefore, it was necessary to develop a sufficiently precise and sensitive method for rapid  $\beta$ -lactam antibiotics detection. Specific electrochemical receptor sensor based on the graphene/thionine (GO/TH) composite was established. The mechanism of the electrochemical receptor sensor was a direct competitive inhibition of the binding of horseradish peroxidase-labeled ampicillin (HRP-AMP) to the mutant BlaR-CTD protein by free-lactam antibiotics. Then, horseradish peroxidase (HRP) catalyzed the hydrolysis of the substrate hydrogen peroxide ( $\text{H}_2\text{O}_2$ ), which produced an electrochemical signal. Experimental data showed that this method gives possibility for quantitative detection of Cefquinome from 0.1 to 8  $\mu\text{g}/\text{L}$  and the limit detection was 0.16  $\mu\text{g}/\text{L}$ , which represents a much smaller value than the maximum residue limit of 5 $\mu\text{g}/\text{L}$  set by the European Union. The limit of detection of spiked milk samples with cefalexin, cefquinome, cefotafur, penicillin G and ampicillin were 14.88  $\mu\text{g}/\text{L}$ , 2.46  $\mu\text{g}/\text{L}$ , 17.16  $\mu\text{g}/\text{L}$ , 0.06  $\mu\text{g}/\text{L}$ , 0.21  $\mu\text{g}/\text{L}$  and the limits of quantitation (LOQ) were 36.09  $\mu\text{g}/\text{L}$ , 5.40  $\mu\text{g}/\text{L}$ , 41.45  $\mu\text{g}/\text{L}$ , 0.13  $\mu\text{g}/\text{L}$ , 0.42  $\mu\text{g}/\text{L}$ , respectively. Investigated electrochemical sensor showed that it can be successfully applied for the assessment of  $\beta$ -lactam antibiotics in milk, and the obtained results were confirmed by the application of chromatography-tandem mass spectrometry. The obtained results point to conclusion that electrochemical receptor sensor had a favourable recovery of 84.89–102.44% [10].

### **Carbon based electrochemical sensors for detection of antibiotics -nanocomposites**

Due to their great potential in sensitivity and selectivity in the determination of pharmaceutical products, among other things, and antibiotics in different samples, electrochemical sensors play an increasingly important role, especially electrochemical

sensors produced with different electrode modifications. Guo *et al.* [11] synthesized three-dimensional porous MXene-carbon nanofiber (CNF) nanocomposites by assembling environmentally friendly and inexpensive bacterial cellulose gel sheets as a carbon source with novel two-dimensional MXenes nanoplate clusters and pyrolyzing the composite for determination of Chloramphenicol. The presented research results show that MXene/CNF nanocomposites give excellent electrical conductivity, large specific surface area, abundant active sites, and excellent electrochemical properties. New synthesized electrochemical sensor MXene/CNF for determination Chloramphenicol achieved a good liner response in concentration range of Chloramphenicol from 0.03–25 $\mu$ M and with a low detection limit of 9nM. These investigators confirmed that the sensor demonstrated good repeatability and reproducibility with relative standard deviations of 2.94 and 3.29%, respectively. This sensor was successfully applied for detection of Chloramphenicol in real samples as milk and jasmine tea beverage. Roushani *et al.* [12] also develop an electrochemical sensor for the selective determination of Chloramphenicol. This group of scientist prepared an electrochemical sensor by modifying GCE with nanocomposite of (3-Aminopropyl) triethoxysilane, graphene oxide and silver nanoparticles. The method used during research was differential pulse voltammetry. The prepared sensor showed good electrochemical performances: linear response in concentration range of 10 pM/L to 0.2  $\mu$ M/L; detection limit of 3.3 pM/L. Electrochemical sensor for determination of Chloramphenicol developed by fabricating CGE with a nanocomposite of graphene oxide and zinc oxide showed excellent analytical performance with detection limit of 0.01 $\mu$ mol/L and linearity over a concentration range of 0.2 to 7.2  $\mu$ M/L. Electrochemical method using during the research was differential pulse voltammetry [12,13].

In order to increase the sensitivity of Levofloxacin detection nanocomposite-modified glassy carbon electrode ( $\text{Ti}_3\text{AlC}_{2\text{max}}$  AND/GCE) featured in as sensor [14]. Great electrocatalytic activity for the oxidation of Levofloxacin is exhibited by the Activated Nanodiamond (AND) and  $\text{Ti}_3\text{AlC}_2$  max phase ( $\text{Ti}_3\text{AlC}_{2\text{max}}$ ) nanocomposite-modified glassy carbon electrode ( $\text{Ti}_3\text{AlC}_{2\text{max}}$  AND/GCE). This modified electrode performed high selectivity and sensitivity with limits of detection of Levofloxacin 20.47nM. Research confirms the fact that the novel sensor can be used as a content monitoring sensor of Levofloxacin in milk yogurt and cheese samples with high reliability and accuracy.

The highly sensitive electrode was fabricated based on cobalt oxide nanorods integrated hexagonal boron nitride-modified glassy carbon electrode ( $\text{CoCo}_2\text{O}_4$  NRs/h-BN/GCE) for the determination of veterinary antibiotic drug ronidazole (RNZ) [1]. The  $\text{CoCo}_2\text{O}_4$  nanorods were prepared by cetyl trimethyl ammonium bromide (CTAB) assisted hydrothermal method and the  $\text{CoCo}_2\text{O}_4$  NRs/h-BN composite was prepared using an ultra-sonication/stirring process. Modified electrode nanocomposite  $\text{CoCo}_2\text{O}_4$  NRs/h-BN showed lower LOD of 3nM and highest sensitivity of 5.845  $\mu\text{A}/\mu\text{Mcm}^2$  for RNZ determination.

Babulal [15] and co-workers were successfully synthesized ytterbium molybdate nano petals (YbMO) with porous carbon (PC) nanocomposite (NC) using ultrasonication method for monitoring the levels of Metronidazole [15]. Obtained modified electrode YbMO/PC NC/GCE exhibited larger reduction peak current and lower potential compared to other modified electrodes. The YbMO/PC NC/GCE performed following results: exceptional

sensitivity of  $3.28 \mu\text{A}/\mu\text{Mcm}^2$ ; wide linear range 0.01–10.61 and 20.61–1630.61  $\mu\text{M}$ ; and low detection limit (LOD) of 0.006  $\mu\text{M}$ . Modified YbMO/PC NC/GCE was used for detection of Metronidazole in serum (101%), urine (97.9%), tablets (99.15%), lake (99.1%), and river water (99.8%).

The antibiotic Oxytetracycline (OTC) has a significant role in increasing food production because it is effectively and efficiently used in the fight against bacterial infections in crops and livestock. That's why antibiotics Oxytetracycline entered in wide application in agriculture and animal husbandry. However, their wide application results in a bad impact on people's health and the environment in general. So the goal is to identify the appropriate agent for the detection of these antibiotics, which are also environmentally friendly. Therefore, Mliki *et al.* [16] report the fabrication of cobalt-doped ZnO/GO nanocomposites for OTC sensors using a simple and environmentally friendly method that does not require toxic solvents. The successful preparation of cobalt-doped ZnO/GO nanocomposites and the determination of the surface area, structure, morphological features, chemical composition and purity of the nanocomposites were demonstrated by contact angle measurements, X-ray diffraction (XRD), Fourier transform infrared spectroscopy (FTIR), scanning electron microscopy (SEM), X-ray photoelectron spectroscopy (XPS) and UV–Vis. The electrochemical methods used were cyclic voltammetry (CV), electrochemical impedance spectroscopy and differential pulse voltammetry. The ZnO/GO nanocomposites showed a line response in concentration ranges from  $10^{-12}$  M to  $10^{-7}$  M, and an impressive detection limit of  $1.6 \cdot 10^{-13}$  M was achieved. Among others, this sensor showed very good performances and remarkable selectivity, proving its usefulness for the detection of OTC traces in real milk samples.

Due to the increasing use of the antibiotic Ciprofloxacin, which leads to an increase in endogenous resistance and numerous health risks, Jiwanti *et al.* [17] present a novel electrochemical sensor in the form of a screen-printed electrode (SPE) reinforced with a novel rGO-SnO<sub>2</sub> nanocomposite. The electrochemical method used to investigate the behaviour of the electrochemical sensor was square-wave voltammetry. The investigated electrochemical sensor showed unparalleled sensitivity and accuracy in the determination of Ciprofloxacin content. The results obtained indicate the superior performance of the SPE/rGO-SnO<sub>2</sub> electrode. The SPE/rGO-SnO<sub>2</sub> electrode exhibited the largest active surface area ( $0.0252 \text{ cm}^2$ ), which enabled faster electron transfer. In addition, the SPE/rGO-SnO<sub>2</sub> electrode showed an impressively low detection limit of  $2.03 \mu\text{M}$  in a concentration range of  $30\text{--}100 \mu\text{M}$  for Ciprofloxacin, setting a new benchmark for the sensitivity of  $9.348 \mu\text{A}/\mu\text{M}$  in the detection of Ciprofloxacin. The investigated electrode also showed its good properties in real samples such as river water and milk with remarkable recovery rates of 101.2 and 97.7%, respectively. In view of the research results, the SPE/rGO-SnO<sub>2</sub> electrode proved to be a promising and effective tool for ciprofloxacin detection and determination [17].

Metronidazole is an antibiotic which has a highly harmful impact on human health and domestic animals that's why it's very important to avoid environmental pollution [18]. The hydrothermal technique has been utilized to prepare Nickel Tungsten oxide (NiWO<sub>4</sub>) nanosheets which were anchored with the carbon nanofiber (CNF) to produce CNF/NiWO<sub>4</sub> nanocomposite, the nanocomposite was coated on the glassy carbon electrode (GCE) and



applied to the electrochemical detection of MTD. For detection of electrochemical behavior of the GCE/CNF/NiWO<sub>4</sub> electrochemical impedance spectroscopy (EIS), cyclic voltammetry studies (CV), and differential pulse voltammetry (DPV) were used. The investigated electrode performed following results: a low detection limit of 0.4 μM, a wide linear response range of 0.01–650 μM, and a higher sensitivity of 0.274 μA/μMcm<sup>2</sup>. Prepared electrode was applied for detection of Metronidazole in tap water and urine samples with acceptable recoveries [18].

## CONCLUSION

Antibiotics are very useful drugs for the treatment of bacterial infections, but recently their use has been intensified so that they can be found in samples of milk, meat, water, pharmaceutical waters, etc. In addition, prolonged exposure to antibiotics through the consumption of products containing antibiotics or exposure to untreated waste containing antibiotics can lead to various health problems. Therefore, it is very important to find suitable sensors for the detection of antibiotics in different samples. Electrochemical sensors for the detection of antibiotics in various samples provided particularly good results, showing good selectivity and sensitivity, and their performance was particularly improved by suitable modifications.

## ACKNOWLEDGEMENT

*The research presented in this paper was done with the financial support of the Ministry of Science, Technological Development and Innovation of the Republic of Serbia, within the funding of the scientific research work at the University of Belgrade, Technical Faculty in Bor, according to the contract with registration number 451-03-65/2024-03/200131.*

## REFERENCES

- [1] Karupppaiah B., Jeyaraman A., Chen S. M., *et al.*, *Electrochim. Acta.* 446 (2023) 142008.
- [2] Simioni N.B., Silva T.A., Oliveira G. G., *et al.*, *Sens. Actuators. B* 250 (2017) 315–323.
- [3] Wang L., Zhang L., Wang Y., *et al.*, *Int. J. Mol. Sci.* 21 (2021) 3306.
- [4] Aihaiti A., Li Z., Qin Y., *et al.*, *Nanomaterials* 12 (2022) 2789.
- [5] Lochab A., Baxi S., Tiwari P., *et al.*, *Microchem. J.* 199 (2024) 109923.
- [6] Chunli W., Qu A., Li M., *et al.*, *Anal. Chem.* 94 (2022) 732–739.
- [7] Dehdshatian S., Behbahani M., Noghrehabadi A., *J. Electroanal. Chem.* 801 (2017) 450–458.
- [8] Guo H., Xu F., Li L., *et al.*, *J. Electrochem. Soc.* 171 (2024) 047511.
- [9] Yu Y., Kasturi P. R., Breslin C.B., *Talanta* 275 (2024) 126132.
- [10] Wang L., Zhang L., Wang Y., *et al.*, *Int. J. Mol. Sci.* 21 (2020) 3306.
- [11] Guo Q., Yang X., Chen Z., *et al.*, *J Mater Sci: Mater Electron* 33 (2022) 427–442.
- [12] Roushani M., Rahmati Z., Farokhi S., *et al.*, *Mater. Sci. Eng. C* 108 (2020) 110388.
- [13] Sebastian N., Yu W.C., Balram D., *et al.*, *Inorg. Chem. Front.* 6(1) (2019) 82–93.
- [14] Kholafazadehastamal G., Khan M., Soylak M. *et al.*, *Carbon Lett.* 34 (2024) 929–940.



- [15] Babulal S.M., Alagumalai K., Sivakumar M., *et al.*, J. Environ. Chem. Eng. 12 (2024) 112331.
- [16] Mliki H., Echabaane M., Rouis A., *et al.*, Heliyon 10 (2024) e30265.
- [17] Jiwanti P.K., Sukardi D.K.A., Sari A.P., *et al.*, Sens. Int. 5 (2024) 100276.
- [18] Mariappan K., Sakthianathan S., Chen T.W., *et al.*, J. Electrochem. Soc. 171 (2024) 037524.



## INFLUENCE OF CALCINATION TEMPERATURE ON THE MORPHOLOGY, CHEMICAL COMPOSITION, AND STRUCTURE OF ZnO NANOPARTICLES

Sonja Stanković<sup>1\*</sup>, Vladan Nedelkovski<sup>1</sup>, Dragos Buzdugan<sup>2</sup>, Iosif Hulka<sup>3</sup>,  
Milan Gorgievski<sup>1</sup>, Snežana Milić<sup>1</sup>, Milan Radovanović<sup>1</sup>

<sup>1</sup>University of Belgrade, Technical Faculty in Bor, V.J. 12, 19210 Bor, SERBIA

<sup>2</sup>Politehnica University of Timișoara, Faculty of Mechanics, M.V.S. 1,  
300222 Timișoara, ROMANIA

<sup>3</sup>University Politehnica Timișoara, Research Institute for Renewable Energies, S.M.G. 138,  
300501 Timișoara, ROMANIA

\*sstankovic@tfbor.bg.ac.rs

### Abstract

*In this study, the influence of calcination temperature on the morphology, chemical composition, and structure of ZnO nanoparticles (ZnO–NP) was investigated. The ZnO nanoparticles were synthesized by a co–precipitation method. Zinc acetate dihydrate was used for the synthesis of zinc oxide nanoparticles. Thermogravimetric analysis (TGA) of the precursor was performed to determine the calcination temperature. The results of the TG analysis indicate high stability of ZnO at temperatures above 325°C. Therefore the prepared samples were calcined at temperatures of 400°C, 500°C, 600°C, or 700°C. The ZnO nanoparticles were morphologically and structurally characterized by X–ray diffraction (XRD), scanning electron microscopy (SEM), and energy dispersion spectroscopy (EDS). The results of the XRD analysis show that pure ZnO is obtained by the co–precipitation method and that the ZnO nanoparticles have a wurtzite structure. The average crystallite sizes of the materials calcined at 400°C, 500°C, 600°C and 700°C were 32.07 nm, 32.89 nm, 35.63 nm and 38.48 nm, respectively. As the calcination temperature increases, the crystallite size also increases. The results of SEM analysis show that the nano–sized particles were obtained by the co–precipitation method and that the calcination temperature significantly affects the size and morphology of the particles. The results of the EDS analysis show that pure ZnO was synthesized, which is consistent with the results of the XRD analysis.*

**Keywords:** ZnO, nanoparticles, coprecipitation method.

### INTRODUCTION

Urbanization and industrialization have contributed to the generation of large quantities of wastewater [1,2]. Eighty percent of wastewater is discharged into the environment without prior treatment. The discharge of wastewater into aquatic ecosystems without prior treatment is harmful to the environment and human health and is a growing problem worldwide [3–5]. For this reason, wastewater treatment is important for the protection of the environment and the preservation of human health.

There are a variety of traditional and non–conventional methods for wastewater treatment. However, the application of these methods is limited [6,7]. Photocatalysis is an efficient and

environmentally friendly process that can achieve complete mineralization of organic matter with low investment and operating costs, making it a promising method for wastewater treatment [5,8–10]. In recent years, researchers have focused on the synthesis of nano-sized photocatalysts for wastewater treatment. The nanomaterial that has attracted the most attention is zinc oxide, due to its stability, favorable photophysical properties, and antibacterial activity [7,11,12]. ZnO nanomaterials can be synthesized by various methods, including the sol-gel method, hydrothermal method, co-precipitation method, thermal decomposition method, and spray pyrolysis [7]. One of the simplest and most commonly used methods for the synthesis of ZnO nanoparticles is the co-precipitation method. In addition to the synthesis method, the size and morphology of ZnO nanoparticles, and thus their photocatalytic activity, are largely influenced by the calcination temperature.

In this paper, the influence of calcination temperature on the morphology, chemical composition, and crystallite size of ZnO nanoparticles synthesized by the co-precipitation method is investigated.

## **EXPERIMENTAL PART**

### **Synthesis of ZnO nanoparticles**

22 g of  $\text{Zn}(\text{CH}_3\text{COO})_2$  was dissolved in 100 ml of 80% ethanol. 0.05M NaOH was used to adjust the pH of the solution. The resulting solution (pH 12.86) was heated to 80°C and kept at a constant temperature until the clarified liquid separated from the precipitate. The suspension is filtered through filter paper (black tape). The resulting sediment is dried in a laboratory dryer at 80°C until it is dry. The dried sediment is transferred to a porcelain crucible and calcined at temperatures of 400°C, 500°C, 600°C or 700°C and labelled with the following markers: ZnO-400, ZnO-500, ZnO-600, or ZnO-700.

### **Characterization methods**

The characterization of ZnO nanoparticles is essential to determine their structure and properties, as these can influence their photocatalytic activity in wastewater treatment. Various analytical techniques have been used to characterize zinc oxide (ZnO) nanoparticles, including thermogravimetric analysis (TGA), X-ray diffraction (XRD), scanning electron microscopy (SEM), and energy dispersion spectroscopy (EDS).

The thermogravimetric (TG) curve of zinc acetate dihydrate was recorded using the SDT Q600 simultaneous thermal analyzer from room temperature to 800°C at a heating rate of 10°C/min. X-ray diffraction (XRD) analysis was performed using an X'Pert<sup>3</sup> powder diffractometer at a heating rate of 10°/min and an opening angle of 20–90°. SEM-EDS analyses were performed with the QUANTA FEG 250 SEM microscope.

## **RESULTS AND DISCUSSION**

### **TGA**

Thermogravimetric analysis was carried out to determine the calcination temperature. By analyzing the differential thermogravimetric curves shown in Figure 1, a two-stage mass loss was observed. In the first stage, in the temperature range from 56 to 104°C, about 16.53% of

the initial mass of the sample is lost due to the dehydration of the zinc acetate dihydrate. Similar results and observations were obtained by Ghule *et al.* [13], Horzum *et al.* [14], and Nguyen and Nguyen [15]. In the second phase in the temperature interval from 156°C to 325°C, a mass loss of 67.73% was observed due to the decomposition of zinc acetate to zinc oxide [14,15]. The thermogravimetric curves in the temperature range from 325 to 800°C revealed no weight loss, indicating complete decomposition of the precursor and the formation of highly stable ZnO nanoparticles [15].

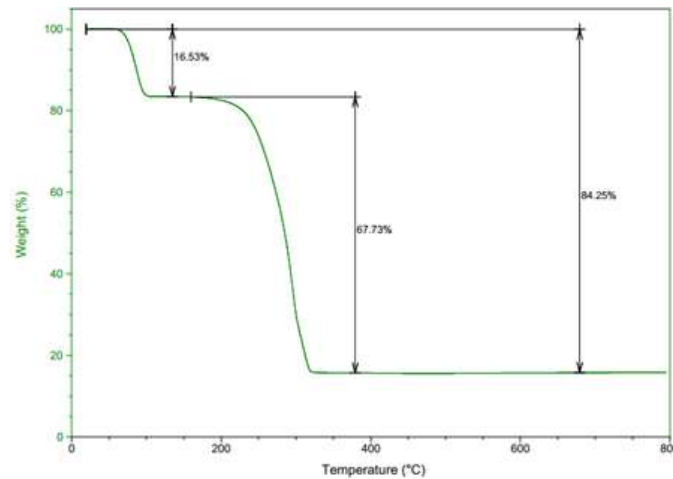


Figure 1 Thermogravimetric analysis of  $\text{Zn}(\text{CH}_3\text{COO})_2 \cdot 2\text{H}_2\text{O}$

## XRD

The structure of the prepared ZnO samples was investigated using X-ray powder diffraction, and the diffractograms of the samples are shown in Figure 2. The diffraction peaks corresponding to (100), (002), (101), (102), (110), (103), (112), and (201) planes of ZnO are identical to those from the JCPDS database (JCPDS No. 036–1451) and indicate the characteristic wurtzite structure of ZnO [15–18]. Zincite was the only crystalline phase identified in all four samples analyzed. Not a single peak indicating the presence of impurities, Zn or  $\text{Zn}(\text{OH})_2$ , was detected. This indicates that high-purity ZnO was synthesized by the coprecipitation method. Similar results and observations were obtained by Saravanan *et al.* [19], Baharudin *et al.* [20], Akpomie *et al.* [21], and Talam *et al.* [22]. The Debye–Scherrer equation (1) was used to determine the average crystallite size of ZnO nanoparticles:

$$D = \frac{k \cdot \lambda}{\beta \cdot \cos\theta} \quad (1)$$

where:  $D$  – crystallite size (nm),  $k$  – constant (0.89),  $\lambda$  – wavelength of X-ray radiation (0.154 nm),  $\beta$  – full width at half maximum of the most intense diffraction peak (FWHM) (rad),  $\theta$  – Bragg's angle (°) [23]. The average crystallite size of the ZnO–400, ZnO–500, ZnO–600 and ZnO–700 samples was 32.07 nm, 32.89 nm, 35.63 nm and 38.48 nm, respectively. It can be concluded that the crystallite size of the ZnO–NP calcined at 400°C was the smallest and that the crystallite size increases with increasing calcination temperature.

This is probably due to the fusion of smaller crystallites into larger ones caused by high calcination temperatures [24].

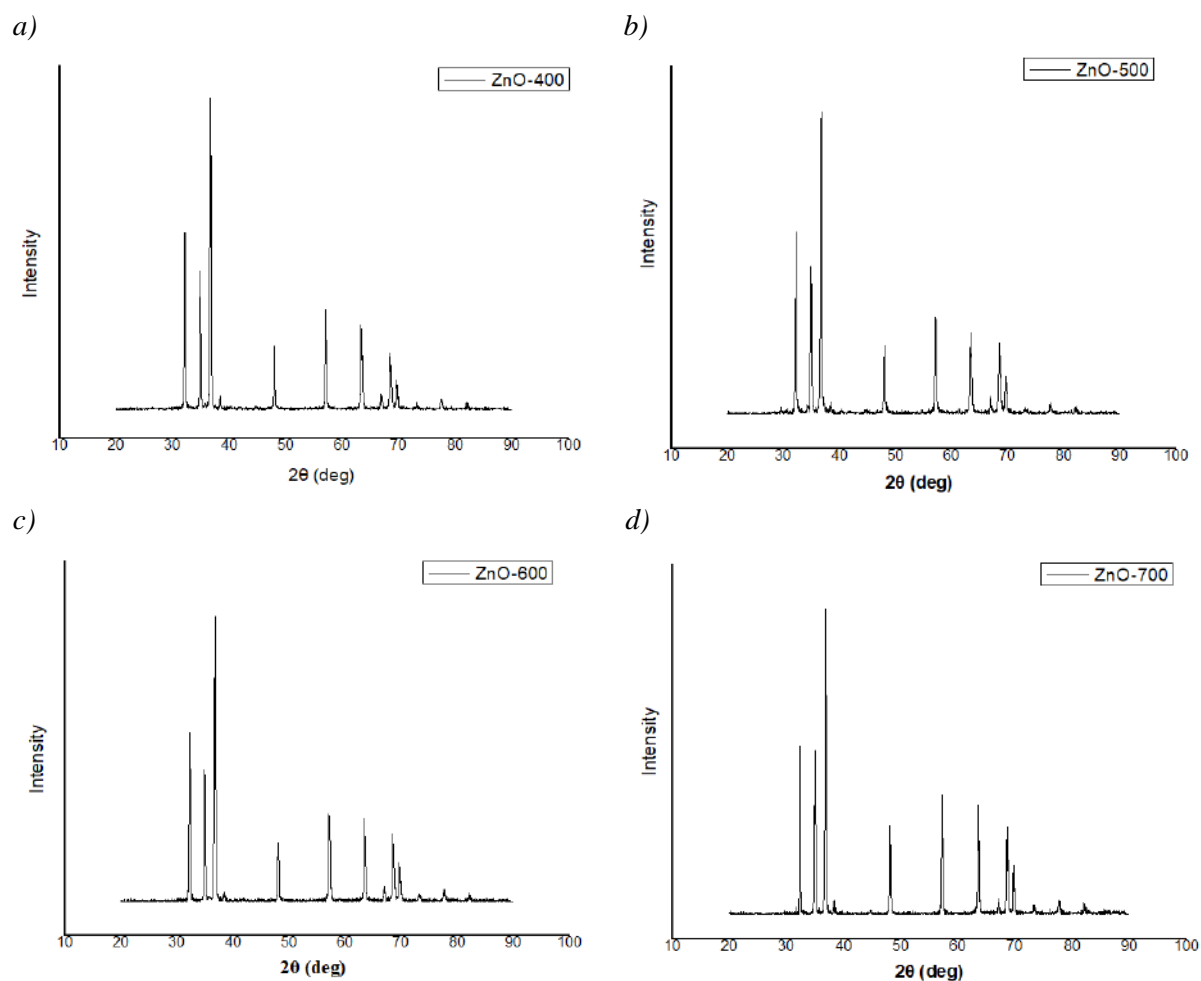


**Figure 2** Diffractograms of ZnO–NP calcined at: a) 400°C; b) 500°C; c) 600°C; and d) 700°C

### SEM–EDS

Scanning Electron Microscopy (SEM) was used to investigate the morphology and size of the ZnO nanoparticles. The results of the SEM analysis are shown in Figure 3 and indicate that the ZnO nanoparticles are heterogeneous in nature and agglomerate under certain conditions. The calcination temperature affects the morphology of the ZnO nanoparticles. Increasing the calcination temperature leads to a lower uniformity of the particles [20]. In samples calcined at temperatures of 400–600°C, spherical and nanorod-shaped particles dominate, while in the sample calcined at 700°C, hexagonal-shaped particles can be observed in addition to spherical and nanorod-shaped particles.

There is a correlation between the particle size and the crystallite size: as the calcination temperature increases, the size of the crystallites and particles increases [18]. In addition, as the calcination temperature increases, the pore volume increases, which can consequently have a positive effect on increasing the photocatalytic activity of the ZnO particles.

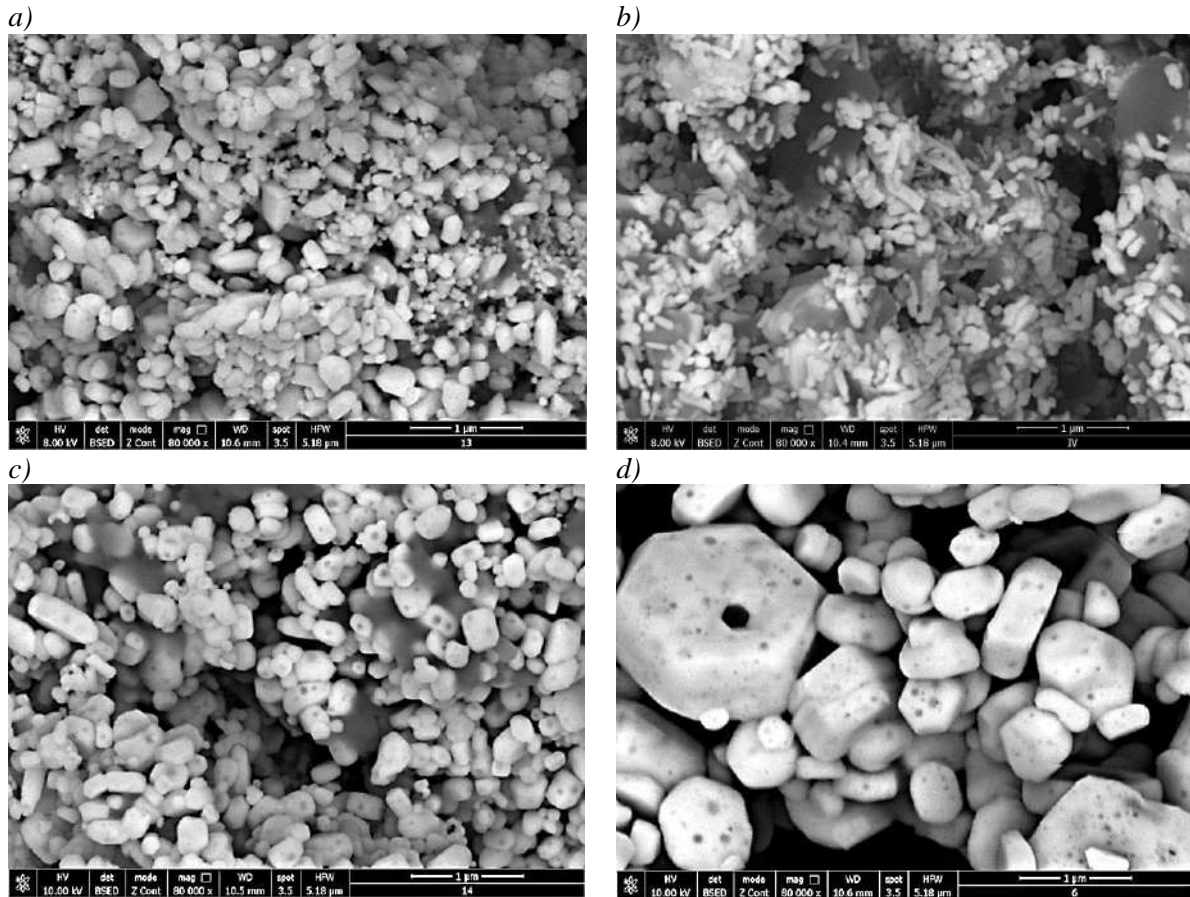


**Figure 3** SEM images of the ZnO nanoparticles thermally decomposed at a) 400°C; b) 500°C; c) 600°C; d) 700°C

Energy dispersion spectroscopy (EDS) was used to determine the elemental composition. The results of the analysis (Figure 4) clearly show the strong peaks of the elements zinc (Zn) and oxygen (O). The absence of peaks of other elements indicates that pure ZnO was synthesized by the co-precipitation method, which is consistent with the results of XRD analysis. Similar results were obtained by Lad *et al.* [16], and Akpomie *et al.* [21]. The absence of impurities is very important for the further application of the synthesized ZnO NPs for wastewater treatment.

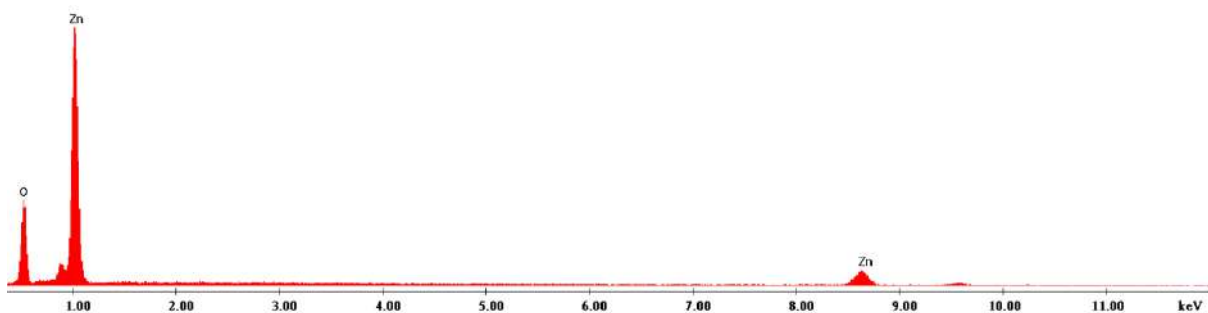


**Figure 4** Energy dispersive spectroscopy spectra of ZnO-NPs



## CONCLUSION

ZnO nanomaterials were successfully prepared by the co-precipitation method. The comprehensive characterization of the ZnO nanoparticles using SEM, EDS, and XRD techniques has provided valuable insights into the influence of calcination temperature in the range of 400–700°C on their structure, morphology, and chemical composition. The results show a wurtzite hexagonal structure of ZnO-400, ZnO-500, ZnO-600, and ZnO-700 with crystal sizes of 32.07 nm, 32.89 nm, 35.63 nm and 38.48 nm, respectively. The particles are heterogeneous in nature and the calcination temperature has a significant effect on the morphology of the particles. In samples calcined at temperatures of 400–600°C, spherical and nanorod-shaped particles dominate, while in the sample calcined at 700°C, hexagonal-shaped particles can be found in addition to spherical and nanorod-shaped particles. The particle size also increases with increasing calcination temperature. The results of the EDS analysis agree with the results of the XRD analysis and indicate that pure ZnO was synthesized by the coprecipitation method. From the presented results, it can be concluded that the calcination temperature significantly influences the morphology and size of the particles.

## ACKNOWLEDGEMENT

*The authors are grateful to the Ministry of Science, Technological development and Innovation of the Republic of Serbia for financial support according to the contract with the registration number 451-03-65/2024-03/200131.*

## REFERENCES

- [1] Nujkić M., Tasić Ž., Medić D., *et al.*, APTEFF 54 (2023) 187–196.
- [2] Dutta D., Arya S., Kumar S., Chemosphere 285 (2021) 131245.
- [3] Mao G., Han Y., Liu X., *et al.*, Chemosphere 288 (2022) 132483.
- [4] Jiang Y., Zhao H., Liang J., *et al.*, Electrochem. commun. 123 (2021) 106912.
- [5] Mohamed A., Yousef S., Nasser W., *et al.*, Environ. Sci. Eur. 32 (1) (2020) 1–8.
- [6] Rathod S., Preetam S., Pandez C., *et al.*, Biotechnol. Rep. 41 (2024) e00830.
- [7] Spoiala A., Ilie C.I., Trusca R.D., *et al.*, Materials 14 (2021) 1–15.
- [8] Nguyen T.H., Vu A.T., Dang V.H., *et al.*, Top. Catal. 63 (2020) 1215–1226.
- [9] Sin J.C., Lama S.M., Satoshib I., *et al.*, Appl. Catal. B: Environ. 148–149 (2014) 258–268.
- [10] Parida K.M., Parija S., Solar Energy 80 (2006) 1048–1054.
- [11] Puri N., Gupta A., Environ. Res. 227 (2023) 115786.
- [12] Abdul Mutalib A.A., Jaafar N.F., Total Environment Research Themes 3–4 (2022) 100013.
- [13] Ghule A.V., Ghule K., Chen C.Y., *et al.*, J. Mass Spectrom. 39 (2004) 1202–1208.
- [14] Horzum N., Hilal M.E.H., Isik T., New J. Chem. (2018) 1–9.
- [15] Nguyen N.T., Nguyen V.A., J. Nanomater. (2020) 1–8.
- [16] Lad P., Pathak V., Thakkar A.B., *et al.*, Braz. J. Phys. 53 (2023) 1–14.

- [17] Adam R.E., Pozina G., Willander M., *et al.*, *Photonic. Nanostruct.* 32 (2018) 11–18.
- [18] Uribe–Lopez M.G., Hidalgo–Lopez M.C. Lopez–Gonzalez R., *et al.*, *J. Photochem. Photobiol. A* 404 (2021) 112866.
- [19] Saravanan R., Gupta V.K., Narayanan V., *et al.*, *J. Mol. Liq.* 181 (2013) 133–141.
- [20] Baharudin K.B., Abdullah N., Derawi D., *Mater. Res. Express* 5 (2018) 125018.
- [21] Akpomie K.G., Ghosh S., Gryzenhout M., *et al.*, *Sci. Rep.* 11 (2021) 8305.
- [22] Talam S., Karumuri S.R., Gunnam N., *ISRN Nanomater.* (2012) 1–6.
- [23] Boppudi H.B., Subba Rao Y., Kuchi C., *et al.*, *Results Chem.* 6 (2023) 101227.
- [24] Sharma V., Sharma J.K., Kansay V., *et al.*, *Chem. Phys. Impact.* 6 (2023) 100196.



## CHILDREN HEALTH RISK ASSESSMENT OF TRIHALOMETHANES CONTENT IN HOTEL'S SWIMMING POOL WATER IN MONTENEGRO

Milena Tadić<sup>1</sup>, Irena Nikolić<sup>1</sup>, Dijana Đurović<sup>2,3\*</sup>, Jelka Vuković<sup>2</sup>, Nevena Cupara<sup>2</sup>

<sup>1</sup>University of Montenegro, Faculty of Metallurgy and Technology, Džordža Vašingtona bb,  
81000 Podgorica, MONTENEGRO

<sup>2</sup>Institute of Public Health of Montenegro, Džona Džeksona bb, 81000 Podgorica,  
MONTENEGRO

<sup>3</sup>Faculty of Food Technology, Food Safety and Ecology, University Donja Gorica, Oktoih 1,  
81000 Podgorica, MONTENEGRO

\**dijana.djurovic@ijzcg.me*

### Abstract

*The aim of this paper was to investigate the quality of indoor and outdoor swimming pool water with respect to trihalomethanes (THMs) content and health risk assessment of children THMs exposure via two exposure rout, ingestion and dermal contact. The water samples were collected during the summer touristic season in coastal area of Montenegro. The obtained results have shown that THMs content in swimming pool water was not of concern. The values of lifetime cancer risk (CR) exceeded  $10^{-6}$ , for both, indoor and outdoor swimming pool water, while values of hazard index (HI) were less than 1, indicating that children population was faced with carcinogenic health risk of THMs exposure, while noncarcinogenic risk is not of concern.*

**Keywords:** trihalomethanes, health risk, ingestion, dermal contact.

### INTRODUCTION

Disinfection of water in swimming pools is extremely important from the aspect of health safety of swimmers and chlorination is the most common type of disinfection of pool water. The chlorine that remains after the chlorination process additionally protects the pool water from further contamination, but also causes the formation of disinfection by-products in the water. About 30–60% of the total disinfection by-products in water are results of chlorination, and the most abundant are trihalomethanes (THMs) and haloacetic acids [1,2]. THMs are formed by the reaction of residual chlorine with organic compounds present in the water. THMs, which can expose a potential danger to swimmer's health, include: chloroform ( $\text{CHCl}_3$ ), bromodichloromethane (BDCM)-( $\text{CHBrCl}_2$ ), dibromochloromethane (DBCM) ( $\text{CHBr}_2\text{Cl}$ ) and tribromomethane (bromoform- $\text{CHBr}_3$ ). These compounds have carcinogenic properties and other toxic effects on human health. The toxicological effect of THMs on human health is reflected through their adsorption during water use and their bioaccumulation in liver, kidneys and lungs, which can lead to serious health problems [3–5]. Thus, this paper aimed to assess health risk of THMs exposure of children population in swimming pools in a coastal area of Montenegro.

## MATERIALS AND METHODS

### Sampling and analysis

For the purposes of this work, a total of 23 water samples from indoor and 74 water samples from outdoor hotel pools from 6 municipalities in the southern part of Montenegro (Herceg Novi, Kotor, Tivat, Budva, Bar and Ulcinj) were analysed in the period from June to September 2022.

Sampling of pool water was done using glass bottles with a capacity of 1 L, and for THMs testing, glass vessels with a cap (Winkler bottles/vessels) with a capacity of 100 to 150 ml, were used. For the purposes of sampling, the Winkler vessel was immersed in a pool to a depth of about 30 cm. The vessel was filled to the top, then removed from the pool and closed tightly with a stopper, so that the water was forced out to remove air bubbles. The samples were stored at room temperature. THMs in water samples were analysed by GC/ECD with Head Space (Agilent 7890).

### Health risk assessment

Human health risk was calculated for the children population aged from 11 to 14 years. Exposure assessment was conducted to evaluate the potential THMs uptake via oral ingestion and dermal absorption using the methodology proposed by USEPA [6]. The next equations were used for this purpose:

$$CDI_{ing} = \frac{C \cdot IR \cdot ET \cdot EF \cdot ED}{BW \cdot AT} \cdot CF \quad (1)$$

$$CDI_{der} = \frac{C \cdot SA \cdot Kp \cdot ET \cdot EF \cdot ED}{BW \cdot AT} \cdot CF \quad (2)$$

where, CDI is the chronic daily dose through ingestion of swimming pool water (mg/kg/day); C is THM concentration in swimming pool water ( $\mu\text{g/L}$ ), IR: ingestion rate of swimming pool water (0.05 L/event); ET is exposure time (1 h/event), EF is exposure frequency (120 event/year); ED: exposure duration, (4 years); BW is body weight (48.17 kg), AT: averaging lifetime (30 years), CF is conversion factor from micrograms to milligrams (0.001). SA is the skin surface area exposed to THMs and Kp is the dermal permeability coefficient.

Carcinogenic and non-carcinogenic health risks of each individual compound were assessed as lifetime cancer risk (CR) and hazard index (HI), respectively according to the Eq. (3) and (4).

Based on the multi-exposure routes the total lifetime cancer risk and the total hazard index were estimated using the Eq. (3) and (4), respectively:

$$CR = \sum_{i=1}^m \sum_{j=1}^n CDI_{ij} \cdot S_{fi} \quad (3)$$

$$HI = \sum_{i=1}^m \sum_{i=1}^m CDI_i / RfDi \quad (4)$$

where  $m$  presents each one of the three considered THMs;  $n$  is a specific exposure route;  $RfDi$  and  $Sf_i$  are the reference daily dose and cancer slope factor for each individual compound. Factors used in the health risk assessment equations are given in Table 1. Values of  $Kp$ ,  $RfD$  and  $Sf$  are obtained from Integrated Risk Information system (IRIS) and Risk Assessment Information System (RAIS) [7,8]. If the HI ratio is observed to be less than 1, the risk exposure is considered to be controlled at the given exposure scenario. If the observed HI ratio is more than 1, significant concern exists on human health and certain risk management actions have to be taken. Cancer risk is defined in four classes: negligible risk ( $CR < 10^{-6}$ ), acceptable low risk ( $1 \cdot 10^{-6} \leq CR < 5.1 \cdot 10^{-5}$ ), acceptable high risk ( $5.1 \cdot 10^{-5} \leq CR < 10^{-4}$ ), and unacceptable risk ( $CR \geq 10^{-4}$ ) [9,10].

**Table 1** Factors used in the risk assessment equations

Factor	Value
$Kp$ (chloroform), (cm/h)	8.9E-03
$Kp$ (BDCM), (cm/h)	5.8E-03
$Kp$ (DBCM), (cm/h)	3.9E-03
$RfD$ (chloroform) (mg/kg/day)	0.01
$RfD$ (BDCM) <sub>ingestion</sub> , (mg/kg/day)	0.02
$RfD$ (DBCM) <sub>ingestion</sub> , (mg/kg/day)	0.02
$Sf$ (chloroform) <sub>ingestion</sub> , (mg/kg/day)	6.1E-03
$Sf$ (BDCM) <sub>ingestion</sub> , (mg/kg/day)	6.2E-02
$Sf$ (DBCM) <sub>ingestion</sub> , (mg/kg/day)	8.4E-02
$Sf$ (chloroform) <sub>dermal</sub> , (mg/kg/day)	3.1E-02
$Sf$ (BDCM) <sub>dermal</sub> , (mg/kg/day)	6.33E-02
$Sf$ (DBCM) <sub>dermal</sub> , (mg/kg/day)	1.40E-01

## RESULTS AND DISCUSSION

Concentration of THMs in indoor and outdoor swimming pool water samples collected from different sampling site in coastal area of Montenegro are given in Table 2. Concentrations of bromoform were below the limits of detection or were very low, so in further analysis has not been included in risk calculation. Concentrations of total THMs were 39.31  $\mu\text{g/L}$  and 67.96  $\mu\text{g/L}$  for indoor and outdoor swimming pools water, respectively, and chloroform mainly contribute to the total THMs concentration. Average concentrations of total THMs are in accordance to Montenegrin regulations (100  $\mu\text{g/L}$ ) [11].

The results of health risk assessment of THMs exposure are given in Table 3 and 4. The results obtained indicated there is no non-carcinogenic health risk of individual and total THMs, since obtained values of hazard index (HI) were less than one (Table 3). However, the results obtained for carcinogenic health risk were of concern. It is evident that for indoor swimming pools water, values of lifetime cancer risk (CR) were higher than  $10^{-6}$  for both exposure routs, ingestion and dermal contact, which indicates that children population is faced with a certain carcinogenic health risk of THMs exposure (Table 4).

**Table 2** Descriptive statistic of THMs ( $\mu\text{g/L}$ ) content outdoor swimming pool water (Coastal area of Montenegro 2022)

Pool	Parameter	Chloroform	BDCM	DBCM	Bromoform	Total THMs
Indoor	Average	34.18	3.93	1.10	0.10	39.31
	Minimum	0.44	0.26	0.22	ND	0.91
	Maximum	87.35	11.08	4.87	1.94	93.80
	Median	29.76	2.98	0.54	1.11	35.18
	SD*	26.68	2.73	1.28	1.17	27.61
Outdoor	Average	58.69	6.95	2.40	0.19	67.96
	Minimum	1.13	1.01	0.18	ND	2.19
	Maximum	217.16	29.43	16.19	3.97	237.18
	Median	36.29	3.84	1.00	0.72	43.18
	SD*	55.19	7.11	3.51	1.45	61.11

\* - standard deviation

**Table 3** Non-carcinogenic health risk of THMs exposure

Pool	Exposure pathway	Chloroform	BDCM	DBCM	Total THMs
Indoor	Ingestion	$5.68 \cdot 10^{-2}$	$3.26 \cdot 10^{-3}$	$9.14 \cdot 10^{-4}$	$6.09 \cdot 10^{-2}$
	Dermal	$1.43 \cdot 10^{-1}$	$5.37 \cdot 10^{-3}$	$1.01 \cdot 10^{-3}$	$2.58 \cdot 10^{-1}$
Outdoor	Ingestion	$9.75 \cdot 10^{-2}$	$5.77 \cdot 10^{-3}$	$1.99 \cdot 10^{-3}$	$1.05 \cdot 10^{-1}$
	Dermal	$2.46 \cdot 10^{-1}$	$9.51 \cdot 10^{-3}$	$2.21 \cdot 10^{-3}$	$2.58 \cdot 10^{-1}$

**Table 4** Carcinogenic health risk of THMs exposure

Pool	Exposure pathway	Chloroform	BDCM	DBCM	Total THMs
Indoor	Ingestion	$3.46 \cdot 10^{-6}$	$4.04 \cdot 10^{-6}$	$1.54 \cdot 10^{-6}$	$9.04 \cdot 10^{-6}$
	Dermal	$4.45 \cdot 10^{-5}$	$6.80 \cdot 10^{-6}$	$2.83 \cdot 10^{-7}$	$5.46 \cdot 10^{-5}$
Outdoor	Ingestion	$5.95 \cdot 10^{-6}$	$7.16 \cdot 10^{-6}$	$3.35 \cdot 10^{-6}$	$1.65 \cdot 10^{-5}$
	Dermal	$7.64 \cdot 10^{-5}$	$1.20 \cdot 10^{-5}$	$6.18 \cdot 10^{-7}$	$8.90 \cdot 10^{-5}$

The values of CR for ingestion, for each THMs and total THMs as well, were in the range of acceptable low risk ( $1 \cdot 10^{-6} \leq \text{CR} < 5.1 \cdot 10^{-5}$ ). On the other hand, children population was faced with acceptable high risk of chloroform exposure, acceptable low risk of BDCM and negligible risk of DBCM exposure via dermal contact. Risk of exposure to the total THMs characterised as acceptable high risk.

As for carcinogenic risk of THMs exposure for outdoor swimming pools, CR values of chloroform, BDCM and DBCM exposure were in the range of acceptable low risk, but acceptable high risk of total THMs exposure was obtained for the ingestion pathway. As in case of indoor swimming pools water, dermal contact presents the higher carcinogenic risk for children population in outdoor swimming pools, and it is characterised as acceptable high risk of total THMs and individual THMs, chloroform and BDCM. The risk of DBCM exposure via dermal contact was at negligible risk.



## CONCLUSION

The results of water quality testing sampled from indoor and outdoor swimming pools on the Montenegrin coast during the summer season (June–September) in 2022 showed that content of total THMs is in accordance to Montenegrin regulations, i.e. the content of total THMs was below the maximum allowed concentration of 100 µg/L prescribed by Montenegrin legislation.

The health risk associated with THMs exposure in swimming pools water indicated that children population was not faced with noncarcinogenic health risk but there is certain carcinogenic health risk which was characterised as acceptable low for ingestion pathway and acceptable high for the exposure via dermal contact. It is necessary to include analysis of THMs in swimming pools water in monitoring programmes on regular basis.

## REFERENCES

- [1] de Castro Medeiros L., de Alencar F.S., Navoni J.A., *et al.*, Environ. Sci. Pollut. Res. 26(6) (2019) 5316–5332.
- [2] Petronijević M., Uticaj oksidacionih procesa na bazi ozona, vodonik-peroksida i UV zračenja na sadržaj i reaktivnost prirodnih organskih materija u vodi, doktorska disertacija, Univerzitet u Novom Sadu, Prirodno-matematički fakultet, Departman za hemiju, biohemiju i zaštitu životne sredine, 2019.
- [3] WHO (2000). Disinfectants and disinfectants by products. Geneva: United Nations Environment, Programme 36–37.
- [4] Silva Z.I., Rebelo M.H., Silva M.M., *et al.*, J. Toxicol. Environ. Health A 75 (2012) 878–892.
- [5] Wang X., Dong S.J., Water Health 18(4) (2020) 533–544.
- [6] United States Environmental Protection Agency – USEPA (1989). Risk Assessment Guidance for Superfund, Vol. I. Human Health Evaluation Manual, EPA/540/1-89/002. December.
- [7] IRIS. Integrated Risk Information system. 2017. Available on the following link [http://cfpub.epa.gov/ncea/iris/search/index.cfm?first\\_letter=C](http://cfpub.epa.gov/ncea/iris/search/index.cfm?first_letter=C).
- [8] RAIS, 2005. Risk Assessment Information System [EB/OL]. (2005-12-30). Available on the following link: [http://rais.ornl.gov/homepage/rap\\_docs.shtml](http://rais.ornl.gov/homepage/rap_docs.shtml).
- [9] Raheleh K., Mahdavianpour M., Ghanbari F., Environ. Sci. & Pollut. Res. 27 (2020) 42621–42630.
- [10] Legay C., Rodriguez M.J., Sadiq R., *et al.*, Environ. Manag. 92 (2011) 892–901.
- [11] Pravilnik o sanitarno-tehničkim i higijenskim uslovima, kao i uslovima za zdravstvenu ispravnost vode za rekreativne potrebe i druge vode od javno zdravstvenog interesa, (SL.Crne Gore", br. 57/2018 i 112/2020).



## HEALTH RISK ASSESSMENT OF ACRYLAMIDE IN POTATO CHIPS FROM MONTENEGRIN MARKET

Miljan Bigović<sup>1</sup>, Dijana Đurović<sup>2,3\*</sup>, Ljubica Ivanović<sup>2</sup>, Maja Blagojević<sup>4</sup>,  
Amil Orahovac<sup>3</sup>

<sup>1</sup>University of Montenegro, Faculty of Science of Mathematics, Džordža Vašingtona bb,  
81000 Podgorica, MONTENEGRO

<sup>2</sup>Institute of Public Health of Montenegro, Džona Džeksona bb, 81000 Podgorica,  
MONTENEGRO

<sup>3</sup>Faculty of Food Technology, Food Safety and Ecology, University Donja Gorica, Oktoih 1,  
81000 Podgorica, MONTENEGRO

<sup>4</sup>University of Montenegro, Biotechnical Faculty, Mihaila Lalića 15, 81000 Podgorica,  
MONTENEGRO

\*[dijana.djurovic@ijzcg.me](mailto:dijana.djurovic@ijzcg.me)

### Abstract

*Acrylamide is a chemical, often present in potato chips, classified as carcinogen and toxicant. Since potato chips is consumed widely in Montenegro, especially in young population, determination of acrylamide in potato chips is of high interest. In this study, acrylamide was monitored in 51 samples of chips sampled from Montenegrin market. Its concentration was determined using liquid chromatography-mass spectrometry, LCMS. Moreover, carcinogenic health risk was assessed for the four population groups aged 10–14 years and 15–17 years, 18–24 years and 25–44 years. The results have shown that quality of chips samples were in accordance with the EU directive (EU 2017/2158) in 98% of tested samples i.e. the acrylamide content was below 750 µg/kg. Moreover, there is an acceptable low risk of acrylamide exposure for investigated population groups and the youngest population (10–11 years) was under the highest risk.*

**Keywords:** health risk, acrylamide, potato chips.

### INTRODUCTION

Acrylamide is at room temperature an odorless and colorless crystalline solid which is readily soluble in water and polar solvent such as acetone, methanol and ethanol and almost insoluble in non-polar solvents with a molecular formula  $\text{CH}_2=\text{CH}-\text{CO}-\text{NH}_2$ , molecular weight of 71.08, boiling point of 125°C, melting point of 84.5°C and density of 1.27 g/ml (25°C) [1]. It is chemical agent that is used for producing of polymers and copolymers. Also, it has been shown that acrylamide is formed in carbohydrate foods when prepares at high-temperature (>120°C) processing such as cooking, frying, toasting, roasting or baking. It happens when amino acid asparagine reacts with sugars especially glucose and fructose as a result of the Maillard reaction [2] and is mainly identified in potato chips, coffee and bread [3].

Acrylamide is classified as “probably carcinogenic to humans” according the International Agency on Research on Cancer (IARC) due to their toxic properties such as neurotoxicity, genotoxicity in both somatic and germ cells, carcinogenicity, and reproductive toxicity [4].

Considering the carcinogenic effects of acrylamide on one hand and the high consumption of chips in young Montenegrin population on the other hand, determination of this contaminant in potato chips consumed in Montenegro and the respective health risk characterization and finally assessment becomes necessary. Thus, the aim of this study was to investigate the content of acrylamide in potato chips sampled from Montenegrin market and to assess the carcinogenic health risk of acrylamide exposure for different population groups.

## MATERIALS AND METHODS

### Sampling and analysis

Experimental methods included methods of sample preparation for analysis and determination of arylamide content. In this study 51 sample of potato chips sampled from Montenegrin market were analysed by liquid chromatography-mass spectrometry, LCMS using an Agilent 1260 Infinity LC system coupled to an Agilent 6465B triple quadrupole LCMS system. Samples were prepared by homogenization, extraction (using deionized water, acetonitrile and a mixture of salts and buffers according to the QuEChERS EN method (EN15662)) and purification.

### Health risk assessment

Carcinogenic health risk assessment of acrylamide content in potato chips was evaluated through the target coefficient carcinogenic risk (CR). The health risk was assessed for four populations of aged 10–14 years and 15–17 years, 18–24 years and 25–44 years. Next equations were used for the evaluation of carcinogenic health risk of acrylamide exposure:

$$CDI = \frac{C_i \cdot IR_i \cdot ED_i \cdot EF_i}{BW \cdot AT} \quad (1)$$

$$CR = CDI_i \cdot CSF \quad (2)$$

$$TCR = \sum CR_i \quad (3)$$

where:  $CDI$  is the daily intake (mg/kg/day),  $IR_i$  is the intake of the (g/day),  $ED_i$  is the duration of exposure (year),  $EF_i$  is the frequency of exposure (year/day),  $BW$  is the average body weight (kg),  $AT$  is the mean time of action of acrylamide ( $AT=EF_i \cdot ED_i$ ) and  $CSF$  is a cancer slope factor for acrylamide.

Factors used in the health risk assessment equations are given in Table 1. Cancer risk is defined in four classes: negligible risk ( $CR < 10^{-6}$ ), acceptable low risk ( $1 \cdot 10^{-6} \leq CR < 5.1 \cdot 10^{-5}$ ), acceptable high risk ( $5.1 \cdot 10^{-5} \leq CR < 10^{-4}$ ), and unacceptable risk ( $CR \geq 10^{-4}$ ) [5,6].

**Table 1** Factors used in the risk assessment equations

Parameter	Population				Ref.
	10–14 years	15–17 year	18–24 year	25–44 year	
$IR_i$ (g/day)	5.28	4.59	5.96	2.51	[7]
$ED_i$ (year)	6	6	70	70	[8]
$EF_i$ (year/day)	365	365	365	365	[8]
$BW$ (kg)	51.74	69.34	75.52	78.96	[7]
$AT$ (day)	2190	2190	25550	25550	[8]
$CSF$ (mg/kg/day) <sup>-1</sup>	0.5	0.5	0.5	0.5	[9]

## RESULTS AND DISCUSSION

Descriptive statistic of acrylamide content in the tested samples of potato chips is given in Table 2. The values of acrylamide content were ranged from 49.3 µg/kg to 1089.30 µg/kg with an average value of 238.38 µg/kg. The average value of acrylamide content in potato chips sampled from Montenegrin market was below the maximally allowed concentration of 750 µg/kg prescribed by the EU directive ((EU) 2017/2158) [10]. Only one of 51 tested samples was not in accordance with the EU legislative, i.e. 2% of tested sample. The average value of acrylamide content in chips obtained in this study (238.38 µg/kg) was significantly lower than the value of acrylamide content in chips obtained in studies conducted by the European Agency for Food Safety (EFSA) of 758 µg/kg [11].

**Table 2** Descriptive statistic of acrylamide content (µg/kg) in potato chips

Average	Minimum	Maximum	SD*
238.38	49.30	1089.30	21.36

\*Standard deviation.

The results of the assessment of the carcinogenic health risk due to the effect of acrylamide through the consumption of chips for the studied population are shown in Table 3.

**Table 3** CR values of acrylamide exposure through the potato chips consumption

Parameter	Population			
	(10–14 years)	(15–17 years)	(18–24 years)	(25–44 years)
<b>Average</b>	$1.21 \cdot 10^{-5}$	$7.89 \cdot 10^{-6}$	$9.41 \cdot 10^{-6}$	$3.79 \cdot 10^{-6}$
<b>Minimum</b>	$2.50 \cdot 10^{-6}$	$1.63 \cdot 10^{-6}$	$1.95 \cdot 10^{-6}$	$7.83 \cdot 10^{-6}$
<b>Maximum</b>	$5.03 \cdot 10^{-5}$	$3.61 \cdot 10^{-6}$	$4.30 \cdot 10^{-6}$	$1.73 \cdot 10^{-6}$
<b>SD*</b>	$9.72 \cdot 10^{-6}$	$6.33 \cdot 10^{-6}$	$7.55 \cdot 10^{-6}$	$3.04 \cdot 10^{-6}$

\*Standard deviation.

The obtained values ranged from  $10^{-6}$  to  $10^{-5}$ . The mean values of the carcinogenic risk (CR) due to the consumption of potato chips ranged from  $3.79 \cdot 10^{-6}$  to  $1.21 \cdot 10^{-5}$ . The values of CR from the consumption of chips for the studied populations can be arranged in order CR (10–14 years) > CR (18–24 years) > CR (15–17 years) > CR (25–44 years). The highest carcinogenic risk from the consumption of chips ( $1.21 \cdot 10^{-5}$ ) was obtained for the youngest population aged 10–14 years. The values of the carcinogenic risk for other populations were

calculated to be 9.41E-06, 7.89E-06 and 3.71E-06, for the populations of 18–24 years, 15–47 years and 25–44 years, respectively. The values of cancer risk (CR) obtained in this study were in the range of acceptable low risk ( $1 \cdot 10^{-6} \leq CR \leq 5.1 \cdot 10^{-5}$ ).

## CONCLUSION

The results of investigation of acrylamide content in potato chips from Montenegrin markets showed that 98% of the tested samples met the criteria prescribed by the European Union directive ((EU) 2017/2158). However, there is a potential carcinogenic risk from the effects of acrylamide for all the investigated populations through the consumption of potato chips. The highest carcinogenic risk from the consumption of chips was recorded for the youngest population aged 10–14 years.

## REFERENCES

- [1] Zamani E., Shokrzadeh M., Fallah M., *et al.*, Pharm. Biomed. Res. 3 (1) (2017) 1–7.
- [2] Claus A., Carle R., Schieber A., J. Cereal. Sci. 47 (2008) 118–33.
- [3] Fang J., Liang C. L., Jia X. D., *et al.*, Biomed. Environ. Sci. 27 (2014) 401–9.
- [4] Keramat J., Le Bail A., Prost C., *et al.*, Food Bioprocess Technol. 4 (2011) 530–43.
- [5] Raheleh K., Mahdavianpour M., Ghanbari F., Environ. Sci. & Pollut. Res. 27 (2020) 42621–42630.
- [6] Legay C., Rodriguez M. J., Sadiq R. S., *et al.*, Environ. Manag. 92 (2011) 892–901.
- [7] Martinovic A., Barjaktarovic Labovic S., Orahovac A., *et al.*, (2022). National Dietary Survey on Adolescents, Adults, Elderly and Pregnant Women in Montenegro. EFSA Supporting Publications, 19(2), 7196E.
- [8] Eslamizad S., Kobarfard F., Tsitsimpikou C., *et al.*, Food. Chem. Toxicol. 126 (2019) 162–168.
- [9] US EPA, 2010. Toxicological review of acrylamide (CAS no. 79-06-1) in support of summary Information on the Integrated Risk Information System (IRIS). EPA/635/R-07/009F, US EPA Washington, DC.
- [10] EC, 2017. Commission Regulation (EU) 2017/2158 of 20 November 2017 establishing mitigation measures and benchmark levels for the reduction of the presence of acrylamide in food. Available on the following link: <https://eur-lex.europa.eu/eli/reg/2017/2158/oj>.
- [11] EFSA, 2011. European Food Safety Authority. Results on acrylamide levels in food from monitoring years 2007–2009. EFSA J. 4, 2133.



## ACCUMULATION OF HEAVY METALS AND HUMAN HEALTH RISK ASSESSMENT *via* THE CONSUMPTION OF FRESHWATER FISH *Esox lucius*

Vesna Djikanović<sup>1\*</sup>, Katarina Jovičić<sup>1</sup>, Jelena S. Vranković<sup>1</sup>, Milena Dimitrijević<sup>2</sup>,  
Snežana Kovačević<sup>2</sup>, Nemanja Pankov<sup>3</sup>, Branko Miljanović<sup>3</sup>

<sup>1</sup>University of Belgrade, Institute for Biological Research “Siniša Stanković” - National  
Institute of the Republic of Serbia, Bulevar despota Stefana 142, 11108 Belgrade, SERBIA

<sup>2</sup>University of Belgrade, Institute for Multidisciplinary Research, Kneza Višeslava 1,  
11030 Belgrade, SERBIA

<sup>3</sup>University of Novi Sad, Faculty of Science, Dositeja Obradovića 1,  
21000 Novi Sad, SERBIA

\*[djiki@ibiss.bg.ac.rs](mailto:djiki@ibiss.bg.ac.rs)

### Abstract

*The aim of this work was to evaluate the impact of anthropogenic pollution on the bioaccumulation of heavy metals in the muscle of the northern pike (Esox lucius L.1758). The specimens were caught at the four sites of the Belocrkvan lakes. The heavy metal concentration was analysed and based on this, the estimated daily intake (EDI), target hazard quotient (THQ) and carcinogenic risk (CR) were calculated to assess the risk to human health. The results showed that the values of the calculated indices were acceptable, so that the consumption of northern pike muscle from the Belocrkvan Lakes should not pose a health risk.*

**Keywords:** heavy metals, risk assessment, northern pike, artificial lakes.

### INTRODUCTION

Pollution of the aquatic environment remains a serious problem despite years of research and monitoring [1]. Heavy metal pollution is a consequence of increasing urbanisation and industrialisation. Metals and metalloids are considered dangerous pollutants because they can enter the food chain and accumulate there, which is harmful to human health [2]. The pollution of aquatic ecosystems by heavy metals is a burning issue worldwide, mainly due to the toxicity of these elements, their long persistence, their bioaccumulation and their biomagnification in the food web [3]. Heavy metals in aquatic ecosystems originate from two sources: from the natural geological background and from anthropogenic activities, such as industrial and agricultural emissions and atmospheric deposition [4].

Since aquatic organisms, including fish, can accumulate high levels of contaminants such as metals that can enter the human body through food, strict monitoring of metal contamination in fish flesh is advisable [5]. In the case of the northern pike, it is important to note that it is a carnivorous fish [6] and a common top predator [7] and is therefore exposed to metal contamination from various sources originating from the entire aquatic food web.



The northern pike (*Esox lucius* Linnaeus, 1758) is a typical sit-and-wait and a common top predator in many temperate freshwaters [8–10]. The northern pike is a piscivorous and photophilic species strongly dependent on backwaters and vegetated river areas for spawning and recruitment. It is thought to be a good bioindicator for ecotoxicological studies of aquatic ecosystems for several reasons: abundance, trophic position (top predator), feeding characteristics, small size of activity centre and great importance for commercial, recreational and sport fisheries [8,10].

Heavy metal concentrations are usually measured in fish muscle (the main food product) and only sometimes in whole fish and individual metabolic organs such as gonads, gills and liver. However, lower concentrations of metals generally accumulate in the muscle.

The Bela Crkva Lakes are a group of six larger and several smaller artificial lakes near the town of Bela Crkva in the province of Vojvodina. The Bela Crkva Lakes differ in size, depth, time of formation and morphological characteristics. They are artificial, crystal-clear lakes with a total surface area of 150 hectares, created by the extraction of gravel from the soil of the Pannonian Basin for industrial purposes. The water from the lakes is used for water supply and irrigation of agricultural land. They have a consistent water quality and a similar fish population, which is due to the artificial colonisation of fish in the lakes.

In this study, we analysed the concentrations of elements (As, Cd, Co, Cr, Cu, Hg, Mn, Ni, Pb and Zn) in the muscles of northern pike to assess the potential risk to humans from consuming pike meat as part of the diet by calculating appropriate target hazard ratios and hazard indices for the elements studied.

## MATERIALS AND METHODS

### Sampling

The 20 specimens of northern pike (*E. lucius*) were caught in four sampling locations/lakes (15<sup>th</sup>/16<sup>th</sup> November 2023) (Figure 1). Electrofishing device PER-MB (2.0 KW, 1300/600 V max.) was applied for fish sampling. Collection of fish samples was performed using a set of standing gillnets with a mesh diameter of 10–60 mm. Fish weight and total length were measured *in situ*.



*Figure 1* Sample localities and collected fish specimens

### Sample analysis

In the laboratory, the samples were dried using a GAMMA 1-16 LSCplus Freeze Dryers Rotational-Vacuum-Concentrator (Germany), and sample portions between 0.2 and 0.4 g dry weight were subsequently processed in a microwave digester (SpeedWave XPERT, Berghof) using 6 ml of 65% HNO<sub>3</sub> and 2 ml of 30% H<sub>2</sub>O<sub>2</sub> (Merck Suprapur). The following temperature program was used (default food program): 10+10 min–160°C; 5+20 min–190°C; and 1+10 min–50°C.

After cooling, digested samples were quantitatively transferred into polypropylene volumetric flasks and diluted to volume of 10 ml with ultrapure water (Milli Q water, Thermo Scientific, UK). In order to assess the possible presence of trace elements in reagents or carry-over effect of digestion vessels, two reagent blank samples were prepared during sample preparation, one per each session, according to the described procedure. These samples were analyzed in each analytical batch. The prepared samples were analysed with an ICP-MS instrument (ICP-MS, iCAP Qc, Thermo Scientific, UK) to determine the mercury concentration. The standard Mercury Standard, Merck, whose initial concentration is 1000 mg/L, was prepared, from which a corresponding standard solution series was prepared by dilution. The results obtained are given as the mean of three repeated measurements of each sample.

Inductively-coupled plasma optical spectrometry (ICP-OES, Avio 200, Perkin Elmer) was used to measure the concentration of nine elements in the fish muscle samples. The detection limit of each sample was verified based on the instrumental detection limit, sample mass (g), and volume to which the sample had been diluted. The average detection limits for each of the assessed elements were (mg kg<sup>-1</sup> dw): As (0.223), Cd (0.010), Co (0.019), Cr (0.029), Cu (0.046), Mn (0.032), Ni (0.090), Pb (0.271) and Zn (0.031).

Comparison of trace element concentrations in muscle samples with the maximum allowed concentrations (MAC) in fish meat for the utilization in human diet, established by the European Union (EU) [11] and the national legislation of Serbia [12], was conducted by recalculating concentrations to wet tissue weight (ww), as ratio between dry weight and wet weight of the sample, multiplied by element concentration measured in dry weight.

### Health risk analysis

#### *Estimated daily intake*

The assessment of risk associated with consumption of heavy metals contained in fish muscle was performed using following indices.

The estimated daily intake (EDI; in mg kg<sup>-1</sup> day<sup>-1</sup>) of heavy metals through the consumption of fish muscle was calculated using the following equation [13,14]:

$$EDI = (C_i \cdot IR) / BW$$

where: C<sub>i</sub> is the element concentration in the fish muscle (mg kg<sup>-1</sup> wet weight); IR is the fish muscle ingestion rate (0.03 kg day<sup>-1</sup>); and BW is the average body weight (70 kg for

adults). The resulting EDI values were compared with the reference (safe) oral dose of the element (RfD) [15,16].

#### *Human health risk assessment*

The non-carcinogenic target hazard quotient (THQ) was calculated by the equation:

$$\text{THQ} = [(\text{EF} \cdot \text{ED} \cdot \text{IR} \cdot \text{Ci})/(\text{RfD} \cdot \text{BW} \cdot \text{AT})] \cdot 10^{-3}$$

where: EF is the exposure frequency (365 days year<sup>-1</sup>); ED is the exposure duration equivalent to the average human lifetime (70 years); IR is the fish muscle ingestion rate (30 g day<sup>-1</sup>); Ci is the element concentration in the fish muscle (mg kg<sup>-1</sup>); RfD is the oral reference dose for contaminant (mg kg<sup>-1</sup> day<sup>-1</sup>); BW is the average body weight (70 kg for adults); and AT is the exposure time for non-carcinogens (365 days year<sup>-1</sup> ED). To evaluate the potential risk of adverse health effects from a mixture of elements the hazard index (HI) was calculated as the sum of THQ for each element:

$$\text{HI} = \sum \text{THQ}_i$$

The carcinogenic risk (CR) was calculated for Cr, Ni, and Pb, using the formula:

$$\text{CR} = [(\text{EF} \cdot \text{ED} \cdot \text{IR} \cdot \text{Ci} \cdot \text{CSF})/(\text{BW} \cdot \text{AT})] \cdot 10^{-3}$$

CSF, is the cancer slope factor set by the US EPA [16].

## **RESULTS AND DISCUSSION**

The age of sampled northern pike individuals was from 1<sup>+</sup> to 2<sup>+</sup>, with equally distributed male and female individuals. The biometric analyses of sampled fish specimens are presented in the Table 1.

*Table 1* Body length and weight of sampled northern pikes specimens

<b>length ± SD (mm)</b>	<b>weight ± SD (g)</b>
31.42±9.20	232.79±332.98

The concentration of various heavy metals (Cd, Co, Cr, Mn, Ni, Pb, Zn) in the edible part (muscle) of fish from the Belocrkvan Lakes is shown in Table 2.

The concentrations of As and Cu in the fish muscle were below the detection limit. Furthermore, the concentrations of Cu, Hg and Zn in the muscle did not exceed the MACs, with the exception of the one muscle sample for Hg (1.102 mg/kg), prescribed by the EU [11] and/or the national legislation [12] meaning that there was no human health risk due to consumption of northern pike meat.

**Table 2** Concentrations of measured elements

Elements	Cd	Co	Cr	Hg	Mn	Ni	Pb	Zn
Average	0.005	0.138	0.282	1.989	1.369	0.531	0.407	24.637
SD	0.007	0.033	0.064	1.701	0.806	0.152	0.128	18.516

In the current study, the muscle in particular was selected for analysis, as it is the only edible tissue and therefore the concentration of toxicants in it is important. Fish muscle is considered a target tissue for Hg accumulation [17–19], which could explain the higher Hg concentrations in this study.

According to the Environmental Protection Agency (EPA), human health risk assessment is defined as the process of estimating the nature and likelihood of adverse health effects in humans exposed to chemicals in contaminated environmental media. In our study, risk assessment is estimated using parameters: EDI, THQ, HI and target cancer risk TR.

The values for the above-mentioned indices for metals from the consumption of fish *Esox lucius* are listed in Table 3.

**Table 3** Estimated daily intake (EDI), Target hazard quotient (THQ), Hazard index (HI) and carcinogenic risk (CR), values as represented as mean

Elements	EDI	THQ	HI	CR
Cd	2.202E-05	8.806E-05	4.403E-06	2.934E-10
Co	5.915E-05	3.93E-04	1.972E-04	-
Cr	1.207E-05	8.00E-04	4.025E-05	6.049E-08
Hg	8.52E-04	-	-	-
Mn	1.9E-05	8.383E-05	4.19168E-06	-
Ni	2.276E-04	2.30E-04	1.138E-05	3.869E-07
Pb	1.743E-04	9.60E-04	4.842E-05	1.481E-09
Zn	0.0106	7.00E-04	3.52E-05	-

The estimated daily intake (EDI, in  $\text{mg kg}^{-1} \text{ day}^{-1}$ ) of heavy metals from the consumption of 30 g of fish muscle ranged from 1.207E-05 (for Cr) to 0.0106 (for Zn) (Table 3). According to the NYS DOH [20], if the ratio between the EDI value of an element and the RfD value is equal to or less than the RfD value, the risk is minimal; if it is 1–5 times higher than the RfD value, the risk is low; if it is 5–10 times higher than the RfD value, the risk is low; if it is 10 times higher than the RfD value, the risk is high. In the present study, the EDI values were below the RfD, which means that the risk was minimal.

The target hazard quotient ranged from 8.383E-05 (for Mn) to 9.6E-04 (for Pb) (Table 3). This parameter deals with individual heavy metal, but food usually contains more than one heavy metal, as can be seen in the case of fish muscle, in which six heavy metals were detected. So it becomes mandatory to calculate the hazard Index (HI). Like the THQ, the HI should not exceed 1. Lower HI values were observed in our study.

According to the US EPA [21], a lifetime CR below 1E-06 is negligible, a risk above 1E-04 is unacceptable, and a range of 1E-06–1E-04 is acceptable. In this study, the CR was

calculated for Cd, Cr, Ni and Pb and the values obtained showed that the cancer risk is negligible (Table 3).

## **CONCLUSION**

Since the values for EDI of heavy metals, THQ and CR were within acceptable ranges, the consumption of northern pike muscle meat from the Belocrkvan lakes should not pose a health risk. It can be concluded that the northern pike muscle in the study conducted is acceptable for human consumption.

## **ACKNOWLEDGEMENT**

*This research was funded by the Ministry of Science, Technological Development and Innovation of the Republic of Serbia, Contract Nos. 451-03-66/2024-03/200007, 451-03-66/2024-03/200125 and 451-03-65/2024-03/200125.*

## **REFERENCES**

- [1] Singh A., Sharma A., Verma R.K., *et al.*, Heavy Metal Contamination of Water and Their Toxic Effect on Living Organisms *in* The Toxicity of Environmental Pollutants, Editor: Dorta D.J., IntechOpen, Sao Paolo (2022), p.302, ISBN: 978-1-80355-580-5.
- [2] Jarić I., Višnjić-Jeftić Ž., Cvijanović G., *et al.*, *Microchem. J.* 98 (2011) 77–81.
- [3] Carneiro M.F.H., Grotto D., Barbosa F., *J. Toxicol. Environ. Health. Part A* 77(1–3) (2014) 69–79.
- [4] Carrasco L., Barata C., García-Berthou E., *Chemosphere* 84(11) (2011) 1642–1649.
- [5] Arroyo-Abad U., Pfeifer M., Mothes S., *et al.*, *Environ. Pollut.* 208 (2016) 458–466.
- [6] Jovičić K., Janković S., Nikolić D.M., *et al.*, *Knowl. Manag. Aquat. Ecosyst.* 424(4) (2023) 1–9.
- [7] Nikolić D., Skorić S., Janković S., *et al.*, *Environ. Monit. Assess.* 193 (2021) 229.
- [8] Simonović P. *Ribe Srbije [Fish of Serbia]*, NNK International, Belgrade (2006), p.247, ISBN: 86-83635-60-0.
- [9] Nilsson P.A., *Oikos* 113 (2006) 251–258.
- [10] Craig J.F., A short review of pike ecology, *Hydrobiologia* 601 (2008) 5–16.
- [11] EU Commission Regulation (EC) No. 2023/915 of 25 April 2023 on maximum levels for certain contaminants in food and repealing Regulation (EC) No 1881/2006 (Text with EEA relevance) Official Journal of the European Union, 119.
- [12] Official Gazette of the Republic of Serbia Nos 22/2018 & 90/2018, 2018. Regulation on the maximum allowed quantities of residues of plant protection products in food and feed and on food and feed for which the maximum permitted quantities of residues of plant protection product.
- [13] Zhou M., Wu Q., Wu H., *et al.*, *Aquaculture* 535 (2021) 736366.
- [14] Nędzarek A., Czerniejewski P., *Sci. Total Environ.* 828 (2022) 154435.

- [15] Li Z., Ma Z., van der Kuijp T.J., *et al.*, *Sci. Total Environ.* 468–469 (2014) 843–853.
- [16] U.S. E.P.A. United States Environmental Protection Agency, 2023. Regional Screening Level (RSL) summary table (TR=1E-06, HQ=1).
- [17] Amundsen P.A., Staldvik F.J., Lukin A.A., *et al.*, *Sci. Total Environ.* 201(3) (1997) 211–224.
- [18] Jovičić K., Nikolić D.M., Višnjić-Jeftić Ž., *et al.*, *Sci. Pollut. Res.* 22(5) (2015) 3820–3827.
- [19] Nikolić D., Skorić S., Rašković B., *et al.*, *Chemosphere* 244 (2020) 125503.
- [20] N.Y.S. D.O.H. New York State Department of Health, 2007. Hopewell precision area contamination: Appendix C – NYS DOH, In: Procedure for evaluating potential health risk for contaminants of concern.
- [21] U.S. E.P.A. United States Environmental Protection Agency, 2000. Guidance for Assessing Chemical Contaminant Data For Use In Fish Advisories, vol 2. Risk Assessment and Fish Consumption Limits, 3<sup>rd</sup> edit.





## OPTIMIZATION OF PREPARATION PROCEDURES FOR FUNGAL INFECTED PLANTS BY FTIR ANALYSES

Vitaly Erukhimovitch<sup>1\*</sup>, Mahmoud Huleihel<sup>1</sup>

<sup>1</sup>Ben-Gurion University of the Negev, Faculty of Health Sciences, 84105 Beer-Sheva, ISRAEL

\*[evitaly@bgu.ac.il](mailto:evitaly@bgu.ac.il)

### Abstract

*Efficient and swift identification of phytopathogens responsible for plant diseases plays a crucial role in devising effective control strategies. Currently available methods for identifying fungi are often time-consuming and lack specificity. Fourier-transform infrared (FTIR) microscopy has emerged as a comprehensive and sensitive analytical tool for detecting molecular changes in cells. Given the similarity in spectra among different fungal pathogen species, selecting the most suitable sample preparation procedure becomes paramount to enhance species discrimination. In this study, we evaluated three potential procedures for preparing pathogen samples for examination using FTIR microscopy. Our findings indicate that directly preparing fungal samples from liquid growth media is the optimal method for FTIR microscopy examinations, offering improved results in the discrimination of fungal species.*

**Keywords:** FTIR microscopy, fungi, spectral characteristics, fungal detection, agar.

### INTRODUCTION

Fungal pathogens are recognized as a prevalent cause of severe diseases in various plants, often resulting in substantial economic damage [1]. One example is *Colletotrichum coccodes*, a significant pathogen affecting potato and tomato crops [2]. Early identification is crucial for precisely targeting pathogens with the most effective treatments, thereby preventing significant economic losses. However, the currently available commercially-based identification systems, relying on the physiological and nutritional characteristics of fungi, are often time-consuming, taking 2–4 weeks, and lack specificity.

Spectroscopic techniques offer promising avenues for the detection and identification of microorganisms due to their sensitivity, speed, cost-effectiveness, and simplicity. Additionally, these techniques provide rich qualitative and quantitative information about a given sample, with each compound's spectrum acting as a unique "fingerprint" [3,4]. Leveraging the extensive knowledge about spectral peaks from FTIR spectra of living cells [5,6], these spectroscopic methods become attractive for detecting and identifying intact biomolecules and living cells, including pathogens. These techniques have previously been employed in the detection and characterization of cancer cells [7,8], cells infected with viruses [9,10], and various microorganisms, including certain fungi [4,6,11–13].

In the present study, we assessed the reliability of three different procedures for preparing fungal slides suitable for examination by FTIR microscopy.

## MATERIALS AND METHODS

### Fungi

Two distinct isolates (112 and 136) from the *Colletotrichum coccodes* genus, a prominent pathogen affecting potato and tomato crops, were employed in this study. Cultures of the fungi were nurtured at 27°C for 3–4 days, either on solid Potato Dextrose Agar (Difco) or in liquid Czapek Dox Broth (Difco) with continuous shaking at 500 rpm.

### Procedures used for the purification of fungi samples

In the present investigation, we compared between three possible procedures of pathogen sample preparation for their examination by FTIR microscopy. Fungi suspension was prepared by three different procedures:

1. Picking up from the growing fungi on the agar,
2. Same by adding of distilled water,
3. The fungi growth in appropriate liquid media.

The obtained samples were examined by FTIR microscopy.

### Sample preparation for FTIR microscopy

A 1 µl droplet of the obtained fungal suspension was deposited onto a specific area on a zinc selenide crystal, air-dried for 15 minutes at room temperature (or 5 minutes with air drying in a laminar flow), and subsequently analyzed using FTIR microscopy.

### FTIR spectra measurement

FTIR measurements were performed in the transmission mode with a liquid-nitrogen-cooled MCT detector of the FTIR microscope (Bruker IRScope II) coupled to an FTIR spectrometer (BRUKER EQUINOX model 55/S, OPUS software). The spectra were obtained in the wave number range of 600–1800 cm<sup>-1</sup>. Spectral resolution was set at 4 cm<sup>-1</sup>. Baseline correction using the rubber band method and vector normalization were obtained for all spectra by OPUS software. Peak positions were determined by means of a second derivation method by OPUS software. Since the samples to be analyzed were often heterogeneous, appropriate regions were chosen by FTIR microscopy so as to eliminate different impurities (salts, medium residuals, etc.). For each sample, the spectrum was taken as the average of five different measurements at various sites of the sample. Each experiment with each sample was repeated five times and average of obtained results was determined.

## RESULTS

### FTIR spectra of fungi strains prepared by the different preparation procedures

Fungal strains 112 and 136 were prepared using the aforementioned methods and subjected to FTIR microscopy analysis. The average FTIR spectra of fungi species 112 and 136 are depicted in Figures 1A and 2A, respectively, as acquired through the examined procedures. While the spectra exhibit a general similarity, notable differences attributable to the specific procedures employed are evident. Notably, the spectral outcomes appear susceptible to interference from agar remnants, as indicated by pronounced absorbance peaks in the 1000–1100 cm<sup>-1</sup> range corresponding to carbohydrate bands of pure agar (Figures 1A, 2A).

The substantial absorbance peaks of agar have the potential to significantly impact the fungal spectra if the samples are not thoroughly purified from any residual agar.

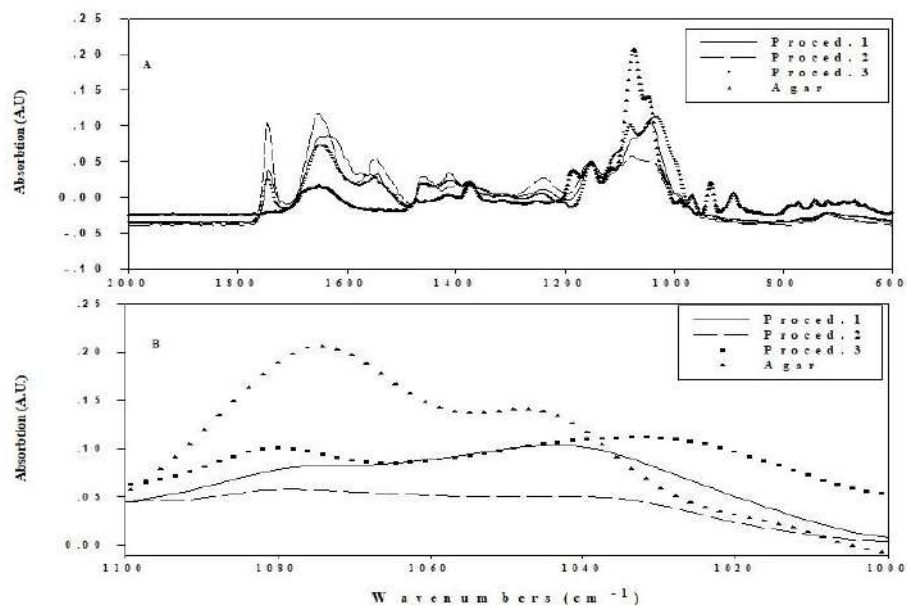


**Figure 1** FTIR spectra of fungi isolate 112 prepared by three different procedures and of pure agar. (A) at the region 600–2000  $\text{cm}^{-1}$ ; (B) at the region 1000–1100  $\text{cm}^{-1}$ . Results are means of 5 different members of this species and separate experiments for each sample. The SD for these means was  $\leq 0.01$

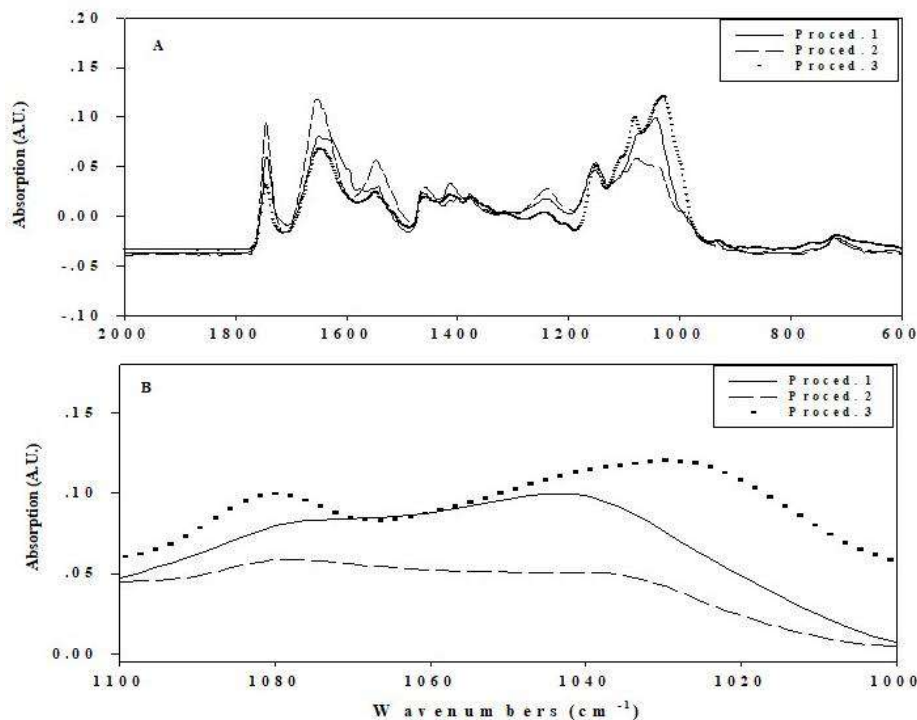


**Figure 2** FTIR spectra of fungi isolate 136 prepared by three different procedures. (A) at the region 600–2000  $\text{cm}^{-1}$ ; (B) at the region 1000–1100  $\text{cm}^{-1}$ . Results are means of 5 different members of this species and separate experiments for each sample. The SD for these means was  $\leq 0.01$

### **Comparison of IR spectra in the 1000–1100 cm<sup>-1</sup> region**

As illustrated in Figures 1B, distinct and intense absorbance peaks of agar emerge prominently at 1044 and 1075 cm<sup>-1</sup>. The spectrum of the fungi examined using procedure 1 exhibits two discernible peaks in this region, aligning closely with the positions of the peaks observed in pure agar, as depicted in Figures 1B and 2B. Conversely, the results obtained through procedure 2 also display two peaks in this region, but with a noticeable shift compared to both the agar peaks and the peaks obtained in procedure 1 (Figures 1B, 2B). Notably, procedure 3 yields two peaks in this region, demonstrating a remarkable deviation from the agar peaks (Figures 1B, 2B).

### **DISCUSSION**

Plants face a myriad of threats from various fungal pathogens belonging to different genera, posing a significant risk to crops and directly impacting the economy. The severity of fungal infections underscores the importance of early identification of the specific fungal pathogen, a crucial factor in determining the most effective treatment strategy. Spectroscopy has gained increasing prominence in discriminating and identifying microorganisms [11]. The challenges of reproducibility encountered by scientists [13] appear to have been overcome by establishing standardized conditions for cell growth and sample preparation [11]. Through these precautions, several scientists have markedly enhanced their capacity to identify diverse microorganisms using spectroscopic methods [12,14–16]. This study focuses on assessing the potential of FTIR microscopy for identifying fungal pathogens. In the initial phase, we explored and evaluated various methods for preparing fungal slides, aiming to identify the most reliable approach for subsequent analyses. Our findings indicate that Procedure 1, involving direct extraction of fungi from agar, is unsuitable for fungal identification due to significant contamination with agar remnants. FTIR microscopy results (Figures 1, 2) reveal that pure agar exhibits robust spectral peaks in the 1000–1100 cm<sup>-1</sup> region, completely obscuring the authentic spectral peaks of the fungi in this range. Conversely, Procedure 3, which involves growing fungi in liquid media without agar, yielded the best results, free from any agar-related interference. Procedure 2, wherein fungi are suspended in distilled water from agar, also produced satisfactory results.

### **CONCLUSIONS**

1. Our results showed that procedure 3, based on growing the fungi in liquid media without agar, provided the best results for identification of fungi without any effect of agar.
2. Procedure 1, which based on picking up the fungi directly from the agar, is the worst and cannot be used for identification of fungi due to a serious contamination with agar leftovers.

### **REFERENCES**

- [1] Agrios G.N., Plant Pathology, Academic Press Inc., New York (1997), ISBN: 9780120445646.

- [2] Tsrer L. (Lahkim), Erlich O., Hazanovsky M., *Plant Dis.* 83 (1999) 566–569.
- [3] Naumann D., Helm H., Labischinski H., *Nature* 351 (1991) 81–82.
- [4] Valentine N., Wahl J., Kingsley M., *et al.*, *RCM* 16 (2002) 1352–1357.
- [5] Diem M., Boydston-White S., Chiriboga L., *Appl. Spectrosc.* 53 (1999) 148–151.
- [6] Amiri-Eliasi B., Fenselau C., *Anal. Chem.* 73 (2001) 5228–5231.
- [7] Huleihel M., Erukhimovitch V., Talyshinsky M., *et al.*, *Appl. Spectroscopy* 56 (2002) 640–645.
- [8] KH Y., Rustgi A.K., Blair I.A., *J. Proteome. Res.* 4 (2005) 1742–51.
- [9] Salman A., Erukhimovitch V., Talyshinsky M., *et al.*, *Biopolymers* 67 (2002) 406–412.
- [10] Fang C., Yi Z., Liu F., *et al.* *Proteomics* 6 (2006) 519–27.
- [11] Naumann D., Helm D., Labischinski H., *et al.*, *Modern Techniques for Rapid Microbiological Analysis*, VCH, New York p. 43–54, ISBN: 9781560810018.
- [12] Gordon S.H., Jones R.W., McClell J.F., *et al.*, *J. Agric. Food Chem.* 47 (1999) 5267–5272.
- [13] Lipkus A.H., Chittur K.K., Vesper S.J., *et al.*, *J. Ind. Microbiol.* 6 (1990) 71–75.
- [14] Schmalreck A.F., Trankle P., Vanca E., *et al.*, *Mycoses* 41 (1998) 71–75.
- [15] Maquelin K., Choo-Smith L.P., Endtz H.P., *et al.*, *J. Clin. Microbiol.* 40 (2002) 594–600.
- [16] Erukhimovitch V., Tsrer L., Hazanovsky M., *et al.*, *J. of Agricul. Technol.* 1 (2005) 145–152.



## POSSIBLE USE OF FOURIER-TRANSFORM INFRARED (FTIR) MICROSCOPY FOR IDENTIFICATION OF FUNGAL PHYTO-PATHOGENS

Mahmoud Huleihel<sup>1\*</sup>, Vitaly Erukhimovitch<sup>1</sup>

<sup>1</sup>Department of Microbiology, Immunology and Genetics, Faculty of Health Sciences,  
Ben-Gurion University of the Negev, Beer-Sheva 84105, ISRAEL

\*mahmoudh@bgu.ac.il

### Abstract

*Fungi pose a significant threat to numerous plants, leading to considerable economic damage. Detecting and identifying these pathogens early on is crucial and can be pivotal for effective control measures. Current methods for fungi identification are often time-consuming and lack specificity. In our study, we employed Fourier-transform infrared (FTIR) microscopy, a proven reliable and sensitive technique for detecting molecular changes in cells. Our research demonstrated the efficacy of FTIR microscopy as a sensitive and effective assay for detecting and distinguishing between various fungal genera. The results revealed notable spectral differences among the different examined fungal genera.*

**Keywords:** fungal pathogens, FTIR microscopy, spectral characteristics.

### INTRODUCTION

Fungal pathogens inflict significant damage on a wide range of crops, causing substantial negative impacts on the economy. Early identification is crucial for precisely targeting the pathogen and implementing the most effective treatment strategies. Currently, fungal identification relies on classic microbiological, biochemical, immunological, and molecular methods. However, these approaches prove ineffective for screening a large number of samples. For instance, classic microbiological methods involve time-consuming visual and microscopic observations of the fungus after cultivation in selective media, taking weeks and exhibiting low specificity. Biochemical methods lack efficacy at the isolate level. Immunological methods depend on the availability of specific monoclonal antibodies tailored to the tested fungi, while molecular techniques, although highly specific, are costly and not universally applicable to different isolates [1–8].

Infrared spectroscopy is gaining increasing attention as a diagnostic tool for biological samples, offering a reagent-free and rapid alternative. Numerous studies have demonstrated that FTIR spectroscopy, coupled with multivariate analysis, is an excellent method with significant potential for identifying and studying microorganisms, even at the isolate level. Infrared spectroscopy can detect biochemical changes at the cellular and sub-cellular levels in various phytopathogens. The infrared absorption spectra, reflecting molecular vibrational modes, provide characteristic insights into the biochemistry of cells and their sub-cellular components [9–15].



## MATERIALS AND METHODS

### Fungi

In the present study, we used the following fungal pathogens:

1. *Pythium* spp. – the cause of Damping-off disease on vegetables and flowers.
2. *Fusarium* spp. – the causal of wilt diseases in various crops.

From each genus 40 different species were examined. All fungi were supplied by L. Tsrer from the Department of Plant Pathology at Gilat Experiment Station, ARO, Israel. These fungi were grown on Potato Dextrose Agar (PDA) (Difco) for several days in 27°C.

### Sample preparation

To overcome the strong absorption exhibited by regular glass slides in the wavelength range relevant to our study, we opted for zinc selenide crystals known for their high transparency to IR radiation. Fungal samples were collected from 3-day-old fungal colonies using a bacteriological loop, suspended in 100 µl of saline, and then centrifuged at 1000 rpm for 2 minutes to form pellets. Each pellet was re-suspended in 20 µl of saline, and a 1 µl drop of the resulting suspension was carefully placed in a specific area on the zinc selenide crystal. The samples were air-dried for 15 minutes at room temperature (or for 5 minutes in a laminar flow) before being examined using FTIR microscopy.

### FTIR spectra measurement

FTIR measurements were conducted in the transmission mode using a liquid-nitrogen-cooled MCT detector on the FTIR microscope (Bruker IR Scope II). This microscope was coupled to an FTIR spectrometer (BRUKER EQUINOX model 55/S, OPUS software). Spectra were acquired within the wavenumber range of 600–800 cm<sup>-1</sup> with a spectral resolution set at 4 cm<sup>-1</sup>. Baseline correction using the rubber band method and vector normalization were applied to all spectra using the OPUS software.

Given the heterogeneous nature of the analyzed samples, specific regions were selected using FTIR microscopy to eliminate various impurities such as salts and medium residuals. The chosen aperture for this study was 100 µm, as it provided the optimal signal-to-noise ratio. Lower apertures resulted in poor spectrum quality due to increased noise levels. Each sample's spectrum was obtained as the average of five measurements at different sites on the sample. Each experiment for each sample was replicated five times, and it is noteworthy that there were no significant differences observed in the spectra across various sites (standard deviation did not exceed 0.005).

### Principal component analysis (PCA)

PCA is an algebraic technique used to analyze the variance within a dataset. It accomplishes this by identifying a set of orthonormal vectors, which are the eigen-vectors of the covariance matrix, known as principal components (PCs), ordering them in descending order due to their eigen-values capturing the maximum variance in the data. These PCs are linear combinations of the original vectors. Finally, the original vector is projected on the subspace spanned by the first eigen-vectors, and the resulting coefficients are the new data representation. While PCA is commonly used for dimensionality reduction, it also serves purposes such as data visualization, feature extraction, and noise reduction [16]. This study

utilized PCA for data visualization, employing three PCs. The resulting output is a three-dimensional plot that visualizes the data.

## RESULTS AND DISCUSSION

FTIR microscopy was employed to identify specific spectroscopic biomarkers for distinguishing between fungal genera, particularly *Pythium* spp. and *Fusarium* spp. Results, depicted in Figure 1, revealed unique spectra for each genus despite general similarities. This preliminary insight suggests potential spectral parameters for fungal genus identification. The dominant bands at  $1655\text{ cm}^{-1}$  and  $1546\text{ cm}^{-1}$  in all examined fungal spectra were linked to protein amide I and II bands, while the shoulder at  $1750\text{ cm}^{-1}$  was associated with lipid C=O stretching vibrations. These findings align with previous research on bacterial strains, supporting the development of reliable detection methods for these pathogens using FTIR microscopy.

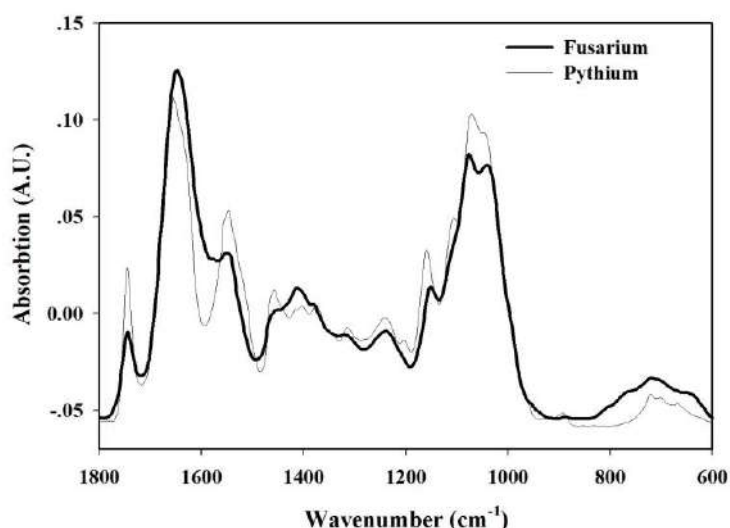


**Figure 1** FTIR spectra at the region  $600\text{--}1800\text{ cm}^{-1}$  of the different examined fungal genera (*Pythium* spp.; *Fusarium* spp.). Results are means of 20 different species of each genus and separate experiments for each sample. The SD for these means was  $\leq 0.01$

The band at  $1465\text{ cm}^{-1}$  was assigned to the  $\text{CH}_2$  bending mode of the cell lipids. The band at  $1460\text{ cm}^{-1}$  represents asymmetric  $\text{CH}_3$  bending modes of end ethyl groups of proteins [17]. The band at  $1402\text{ cm}^{-1}$  represents the C=O symmetric stretching of  $\text{COO}^-$  [13] and is assigned to lipids [13], and the band at  $1377\text{ cm}^{-1}$  represents the C-H bending mode of  $\text{CH}_2$  [13]. From information obtained from previous studies [13] we assigned the remaining IR bands as follows: The peaks at  $1237\text{ cm}^{-1}$  and  $1082\text{ cm}^{-1}$  were attributed to asymmetric and symmetric stretching vibrations and phospholipids. The peak at  $1064\text{ cm}^{-1}$  resulted from the overlap of several bands, including absorption due to the vibration modes of  $\text{CH}_2\text{OH}$  and the C–O stretching vibration coupled to the C–O bending mode of cell carbohydrates [18].

### Discrimination between the examined fungi genera

In order to differentiate between the two fungus genera, we applied PCA. Figure 2 shows a 3D plot for the examined fungi.

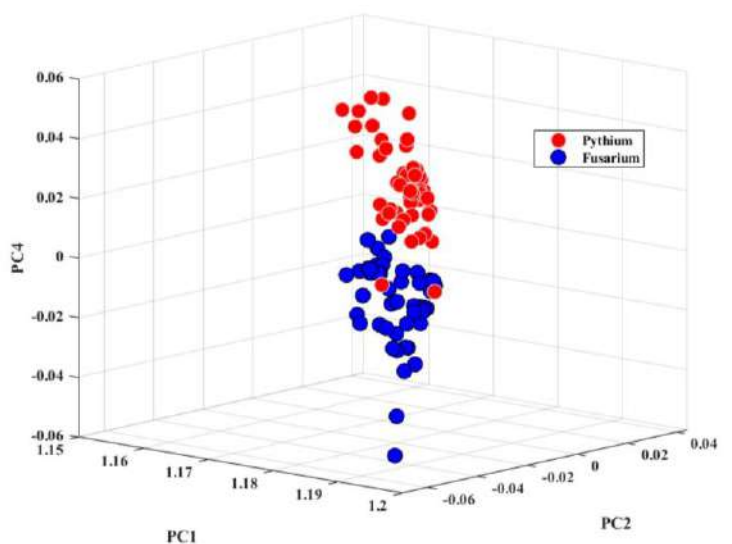


**Figure 2** 3D plot of the scores of different PCs for the classification between the different fungi (*Pythium* spp. and *Fusarium* spp.). Each spectrum is represented as one point in this plot. The coordinates of each single point are the coefficients of the used PCs that represent each spectrum

As can be seen from Figure 2, although there are some overlapping points, there is still a clear separation between the two categories (*Pythium* spp. and *Fusarium* spp.) with 96.3% success, as can be seen in Table 1.

**Table 1** Confusion matrix of the Linear discriminant analysis (LDA) using the first 15 PCs for the classification of the fungi samples

		Predicted	
		<i>Pythium</i>	<i>Fusarium</i>
True	<i>Pythium</i>	39 (97.5%)	1 (2.5%)
	<i>Fusarium</i>	2 (5.0%)	38 (95.0%)

Success rate is calculated as the sum of truly predicted samples of both *Pythium* spp. and *Fusarium* spp. divided by the total number of samples. In this case  $(39+38)/80=0.963$ .

### CONCLUSION

In the present study, we examined the potential of FTIR microscopy for easy and rapid discrimination and identification of various fungi genera, which are responsible for serious damage to agriculture. The results obtained in this study:

1. Provide a unique and consistent spectral marker/s for each of the examined fungi genera.

2. Show that the spectral area ranging between 1000 and 1800  $\text{cm}^{-1}$  can be considered as an important region for easy and reliable discrimination between the various examined fungi genera with a 96.3% accuracy.

Additionally, the fact that the final results could be obtained during a very short time (approximately 1 hour) from a small amount of sample supports the possibility of developing FTIR spectroscopy as a reliable method for rapid identification of fungal infections in plants.

## REFERENCES

- [1] Barkdoll A.W., Davis J.R., *Plant Dis.* 76 (1992) 131–135.
- [2] Lees A.K., Hilton A.J., *Plant Pathol.* 52(1) (2003) 3–12.
- [3] Tsrer L., *Plant Pathol.* 53(3) (2004) 288–293.
- [4] Kim G.-H., Kim J.-J., Lim Y.W., *et al.*, *Can. J. Bot.* 83(3) (2005) 272–278.
- [5] Moreth U., Schmidt O., *Holzforschung* 59(1) (2005) 90–93.
- [6] Nikkari S., Relman D.A., *Curr. Opin. Rheumatol.* 11(1) (1999) 11–16.
- [7] Clark N.C., Olsvik O., Swenson J.M., *et al.*, *Antimicrob. Agents Chemother.* 43(1) (1999) 157–160.
- [8] Vaneechoutte M., Van Eldere J., *J. Med. Microbiol.* 46(3) (1997) 188–194.
- [9] Maquelin K., Kirschner C., Choo-Smith L. P., *et al.*, *J. Microbiol. Methods* 51(3) (2002) 255–271.
- [10] Salman A., Shufan E., Tsrer L., *et al.*, *Methods* 68(2) (2014) 325–330.
- [11] Salman A., Pomerantz A., Tsrer L., *et al.*, *Analyst* 136(5) (2011) 988–995.
- [12] Salman A., Pomerantz A., Tsrer L., *et al.*, *Analyst* 137(15) (2012) 3558–3564.
- [13] Salman A., Lapidot I., Pomerantz A., *et al.*, *J. Biomed. Opt.* 17(1) (2012) 017002.
- [14] Naumann D. Infrared and NIR Raman spectroscopy in medical microbiology. *Proceedings of SPIE*, (1998) 245–257.
- [15] Naumann D., Helm D., Labischinski H., *Nature* 351(6321) (1991) 81–82.
- [16] Bishop C.M., *Pattern Recognition and Machine Learning*. Springer (2006).
- [17] Wong P., Goldstein S., Grekin R., *et al.*, *Cancer Res.* 53 (1993) 762–765.
- [18] Yang D., Castro D., El-Sayed I., *et al.*, *SPIE* 2389 (1995) 543–550.



## RADIOACTIVITY IN SAMPLES OF IMPORTED MINERAL FERTILIZER ANALYZED IN THE PERIOD 2020–2022

Ana Čučulović<sup>1\*</sup>, Jelena Stanojković<sup>1\*</sup>, Rodoljub Čučulović<sup>2</sup>

<sup>1</sup>University of Belgrade, Institute for the Application of Nuclear Energy – INEP,  
Banatska 31b, 11080 Zemun, SERBIA

<sup>2</sup>University of MB, Faculty of Business and Law, Teodora Dražera 27,  
11000 Belgrade, SERBIA

\*[anas@inep.co.rs](mailto:anas@inep.co.rs), [jelenas@inep.co.rs](mailto:jelenas@inep.co.rs)

### Abstract

*In the period 2020–2022 the Institute for the Application of Nuclear Energy – INEP received 677 samples of mineral fertilizer for gamma spectroscopic investigation of various compositions. In all investigated samples different activity levels of natural (<sup>40</sup>K, <sup>232</sup>Th, <sup>226</sup>Ra, <sup>238</sup>U) and artificially produced (<sup>137</sup>Cs) radionuclides were determined. The activity levels of <sup>137</sup>Cs in all samples were very low. Depending on the type and composition of the fertilizer, different levels of natural radionuclides were registered. All analyzed samples were in accordance with activity levels prescribed by the Regulations and were imported into Serbia.*

**Keywords:** mineral fertilizer, radionuclides, gamma-spectrometry.

### INTRODUCTION

In the XXI century the human population faces the issue of hunger and lack of food. In 1840 Justus von Liebig presented the results of his research on the significance of nutrients for plant growth in the British Royal Society and set the basis of modern agriculture and production of mineral fertilizers. In the last 100 years the use of mineral fertilizers is constantly increasing [1].

According to their origin, fertilizers can be organic and inorganic (mineral). Inorganic are composed of artificially obtained materials and minerals. They can be solid, water-soluble and with controlled release of chemical elements; simple (nitrogen, phosphorus and potassium, less often calcium) and complex (produced by mixing simple ones) that can be mixed and complex [2]. Inorganic fertilizers contain macro and micronutrients. Nitrogen, phosphorous and potassium are primary macronutrients, consumed in large quantities and are present in plant tissue. Calcium, sulfur and magnesium are secondary macronutrients, while boron, chlorine, manganese, iron, zinc, copper, molybdenum and selenium are micronutrients (trace elements) [3]. Excessive or too little amount of fertilizer can be harmful. Excessive amounts of fertilizer can lead to the burning of plant crops (drying of the roots, damage or even the death of the plant).

Phosphorus fertilizers are the most interesting for our research and they are used in plant production in different quantities depending on the supply of phosphorus to the soil and the needs of plant species. Phosphorus fertilizers are produced from phosphorus ores: apatite and

phosphorite [4]. Depending on the geographical origin of the ores from which they are produced and the chemical composition of fertilizers in them, the level of activity of natural radionuclides varies [5,6]. When producing phosphorus mineral products from phosphorus ores, over 90% of uranium remains in the final products. In countries producing phosphoric acid, the problem of extracting uranium from it is being worked on, either for economic and technical or environmental reasons. Three extraction procedures for uranium extraction are known in the World. The procedure known as DENTRA-TORO has been applied in Serbia in the semi-industrial installation located close to the IHP Prahovo factory. The efficiency of uranium extraction from phosphorous acid was 90 to 95% [7].

Radioactive substances from mineral fertilizers that are deposited on the soil can be adopted by grown plants, both the above-ground parts of the plant and the root system. The adoption of natural radionuclides from phosphorus fertilizers by plants depends on many factors [8]. The use of phosphorus mineral fertilizers in agriculture constitutes the largest anthropogenic source of  $^{226}\text{Ra}$ ,  $^{232}\text{Th}$  and  $^{238}\text{U}$  in soil [9]. Studies have shown that radionuclides that are introduced into the soil through mineral fertilizers that contain phosphorous can lead to an increase in basic radiation levels in certain regions and can represent significant local risks of exposing the population to ionizing radiation [10–12].

The mineral fertilizer factories in each country are one of the pillars of the overall economy and part of the national strategy of each country, as this production is in the function of food the Chemical Products Industry in Prahovo (IHP-Prahovo) was founded by the Bor Mining and Smelting Basin on September 19, 1960. In 2008, the factory was privatized by the Greek company Neochimiki-Athens, but in 2011 IHP Prahovo was introduced into bankruptcy. The Elixir Group Šabac, created from the family company Narcis Popovići (1998), on 02.08.2012 purchased the bankrupted factory and on 01.02.2013 became its formal owner. In 2011 the Elixir Group bought Zorka Šabac. With the purchase of two chemical companies, the Elixir Group has become a major producer of chemical components based on phosphorus, primarily phosphoric acid, complex mineral fertilizers and feed additives. Investment in capacities for the production of mineral fertilizers, as a development potential of this branch of the chemical industry, already in 2015 made the Elixir Group the undisputed leader in the region. By purchasing two large chemical companies the Elixir Group took over a great responsibility of protecting the environment [13]. The Elixir group in 2023 was the only producer of artificial NPK fertilizer. Serbia has moved from being a serious producer of fertilizers to a serious importer, as many factories producing mineral fertilizers have stopped working.

NP and NPK fertilizers with different formulations are most often imported into Serbia. When importing into the Republic of Serbia, gamma spectrometric analysis of mineral and organic fertilizers that have the macronutrient element phosphorus in their composition is mandatory. Fertilizers that are produced in our country are not subject to mandatory control before [14]. According to the Regulations on the limits of the content of natural radionuclides in mineral phosphate fertilizers containing the macronutrient element phosphorus, placed on the market, the permitted level of activity for  $^{238}\text{U}$  is  $1600 \text{ Bq kg}^{-1}$  for mineral fertilizers and  $3200 \text{ Bq/kg}$  for raw materials for the production of mineral fertilizers, and for  $^{226}\text{Ra}$   $1000 \text{ Bq kg}^{-1}$ . The permitted activity level for  $^{40}\text{K}$  is  $27000 \text{ Bq kg}^{-1}$  for mineral



fertilizers containing the macronutrient elements K and/or P, placed on the market and applied as raw materials for their production. According to the Regulations fertilizer samples in which the measured levels of natural radionuclides are higher than these stated values cannot be imported into country [14]. The purpose of this work is to show the activity levels of natural ( $^{40}\text{K}$ ,  $^{232}\text{Th}$ ,  $^{226}\text{Ra}$ ,  $^{238}\text{U}$ ) and artificially created ( $^{137}\text{Cs}$ ) radionuclides in imported mineral fertilizers.

## **MATERIALS AND METHODS**

In the period 2020–2022 the Institute for the Application of Nuclear Energy – INEP followed activity levels of the artificial ( $^{137}\text{Cs}$ ) and natural ( $^{40}\text{K}$ ,  $^{232}\text{Th}$ ,  $^{226}\text{Ra}$ ,  $^{238}\text{U}$ ) radionuclides in fertilizer samples containing the phosphorous macronutrient element and imported from; Russian Federation, Spain, Greece, France, Italy and other countries.

Fertilizer samples (677) were taken by the phytosanitary inspection and sent to be analyzed in INEP, where they were homogenized, put in 1 L Marinelli containers and measured. Gamma spectrometric measurements of fertilizer samples were performed according to the standard method of the International Agency for Atomic Energy [15]. The semiconducting high purity germanium detector of the n-type, produced by ORTEC-AMETEK, USA was used. The 8192 channel detector has a resolution of 1.65 keV and relative efficiency of 34% at 1.33 MeV for  $^{60}\text{Co}$ . The samples were measured for 60000 seconds and spectral analysis was performed using the Gamma Vision 32 software. The activity level of  $^{238}\text{U}$  on the lines:  $^{234}\text{Th}$  (63 and 93 keV) and  $^{234}\text{Pa}$  (1000 keV),  $^{226}\text{Ra}$  on the lines:  $^{214}\text{Bi}$  (609, 1120 and 1764 keV) and  $^{214}\text{Pb}$  (295 and 352 keV), while  $^{232}\text{Th}$  on the lines  $^{228}\text{Ac}$  (338, 911 and 969 keV). The activity level of  $^{40}\text{K}$  was determined based on the gamma line at 1460.8 keV, while for  $^{137}\text{Cs}$  it was at 661.6 keV [16]. Detector calibration was performed using two different radioactive reference materials in Marinelli geometry. The total measurement uncertainty that includes many elements was lower than 20%. Quality control of gamma spectrometric measurements used for the analysis was performed using a calibration standard and reference materials and also by yearly participation in comparisons organized by the International Atomic Radiation Agency.

## **RESULTS AND DISCUSSION**

This work presents the activity levels of radionuclides in imported fertilizer samples (677). All samples contained natural radionuclides ( $^{40}\text{K}$ ,  $^{232}\text{Th}$ ,  $^{226}\text{Ra}$ ,  $^{238}\text{U}$ ) and the artificial radionuclide ( $^{137}\text{Cs}$ ). During 2020–2022 INEP received 384 samples of NPK fertilizer (75 formulations 15-15-15, 171 formulations 16-16-16, 30 formulations 20-20-20, 41 formulation 16-16-8, 67 different formulations). Low levels of activity of  $^{226}\text{Ra}$  and  $^{238}\text{U}$  were measured in 104 samples of NPK fertilizer and 36 NPK fertilizer samples had a low  $^{40}\text{K}$  content. Imports also included 69 samples of NP fertilizer and 84 samples of MAP.

Table 1 shows the type of investigated fertilizer, import year, average radionuclide activity levels ( $\text{Bq kg}^{-1}$ ), minimal and maximal values for fertilizers imported between 2020 and 2022. The activity levels of  $^{137}\text{Cs}$  in all samples were low and can be ignored ( $<4.0 \text{ Bq kg}^{-1}$ ). The

activity levels of  $^{232}\text{Th}$  in fertilizers were up to  $43.0 \text{ Bq kg}^{-1}$ , and the average activity levels are higher than the values shown in previous research [17].

**Table 1** Fertilizer type, investigation year, average radionuclide activity levels ( $\text{Bq kg}^{-1}$ ), minimal and maximal values of radionuclide activity levels ( $\text{Bq kg}^{-1}$ )

Fertilizer type	Year	$^{137}\text{Cs}$	$^{40}\text{K}$	$^{226}\text{Ra}$	$^{232}\text{Th}$	$^{238}\text{U}$
		$\text{Bq kg}^{-1}$				
15-15-15 (75)	2020 (12)	1.3	3683	20.5	9.1	39.9
	2021 (21)	0.8	3685	32.9	7.6	93.0
	2022 (42)	0.7	2812	70.0	8.0	125
	Min-max	0.3–2.3	1256–4147	7.0–409	4.0–29.0	10.0–510
16-16-16 (171)	2020 (83)	1.2	4096	23.1	20.8	49.4
	2021 (65)	0.9	3800	66.6	23.0	107
	2022 (23)	0.7	2951	19.9	20.7	33.2
	Min-max	0.4–1.8	1390–4622	10.0–674	2.0–41.0	4.0–826
20-20-20 (30)	2020 (6)	1.3	4292	17.3	6.3	25.7
	2021 (9)	1.0	4823	16.8	9.1	32.1
	2022 (15)	0.9	3833	17.9	6.5	29.9
	Min-max	0.3–2.5	587–6248	6.0–40.0	4.0–13.0	2.0–66.0
16-16-8 (41)	2020 (0)	---	---	---	---	---
	2021 (26)	0.6	1625	15.7	23.5	33.0
	2022 (15)	0.6	1944	19.6	24.9	39.9
	Min-max	0.3–1.1	848–2571	5.0–29.0	11.0–36.0	8.0–76.0
MAP (84)	2020 (32)	0.5	44.3	43.7	4.2	125
	2021 (21)	0.4	33.6	14.5	5.7	79.2
	2022 (31)	0.3	39.6	64.5	4.2	143
	Min-max	0.1–0.8	6.0–143	5.0–300	1.0–22.0	1.0–685
NP (69)	2020 (5)	0.5	17.4	25.0	4.2	31.6
	2021 (10)	0.4	59.1	113	7.4	305
	2022 (56)	0.4	142	157	7.0	303
	Min-max	0.1–0.9	13.0–763	7.0–542	1.6–27.0	5.0–991
NPK (67)	2020 (8)	1.3	5217	128	19.3	209
	2021 (19)	0.9	4356	106	11.5	231
	2022 (40)	0.7	3420	170	14.0	341
	Min-max	0.3–1.6	23.0–10927	8.0–578	2.0–33.0	20.0–944
NPK small participation of $^{226}\text{Ra}$ and $^{238}\text{U}$ (104)	2020 (31)	1.3	5680	15.5	8.3	35.8
	2021 (52)	0.9	4798	16.6	7.3	31.0
	2022 (21)	0.8	4064	17.8	8.7	30.5
	Min-max	0.2–3.1	1038–11175	3.0–57.0	1.0–25.0	4.0–82.0
NPK small participation of $^{40}\text{K}$ (36)	2020 (0)	---	---	---	---	---
	2021 (15)	0.9	420	11.5	3.3	21.9
	2022 (21)	0.6	423	124	12.9	164
	Min-max	0.2–1.6	5.0–954	1.0–637	1.0–43.0	3.0–930

The NPK fertilizers with the formulation: 15-15-15, 16-16-16, 20-20-20 and 16-16-8, are the most significant for this research, as they are used the most for fertilizing soil. The average activity level of  $^{40}\text{K}$  in these fertilizers was in the range  $1625\text{--}4823 \text{ Bq kg}^{-1}$ . The maximal level of activity of  $^{40}\text{K}$  ( $6248 \text{ Bq kg}^{-1}$ ) was determined in a fertilizer with a 20-20-20 formulation imported in 2021. This value is still much lower than the maximal allowed value determined by the Regulations [14]. Maximal activity levels of  $^{226}\text{Ra}$  and  $^{238}\text{U}$  were measured in a fertilizer with a formulation 16-16-16 imported in 2021 (674, and 826  $\text{Bq kg}^{-1}$ , respectively). In our research from 2014 the maximal activity level of  $^{226}\text{Ra}$  was measured in

a NPK fertilizer sample 15-15-15 ( $775 \text{ Bq kg}^{-1}$ ) [18]. Table 1 also gives the activity levels of radionuclides in NPK fertilizers (67 samples) with different formulations. The maximal activity level of  $^{40}\text{K}$  in fertilizers was  $11175 \text{ Bq kg}^{-1}$ . In our research from 2014 the maximal activity level of  $^{40}\text{K}$  was  $12965 \text{ Bq kg}^{-1}$  [18]. The maximal activity levels of  $^{226}\text{Ra}$  and  $^{238}\text{U}$  were 578 and  $944 \text{ Bq kg}^{-1}$ , respectively. The Table 1 also shows activity levels of radionuclides in NPK fertilizers with a small participation of  $^{226}\text{Ra}$  and  $^{238}\text{U}$ , and also a small participation of  $^{40}\text{K}$  (140 samples in total 140). Maximal activity levels of  $^{226}\text{Ra}$ ,  $^{238}\text{U}$  and  $^{40}\text{K}$  in fertilizers with a small participation of potassium was 637, 930 and  $954 \text{ Bq kg}^{-1}$ , respectively. It can be concluded that the activity levels of  $^{226}\text{Ra}$  and  $^{238}\text{U}$  in this type of fertilizer are high. Activity levels of radionuclides in mono-ammonium phosphate were also monitored (MAP) and NP fertilizers. The maximal activity levels of  $^{226}\text{Ra}$  and  $^{238}\text{U}$  in MAP were  $300 \text{ Bq kg}^{-1}$  and  $685 \text{ Bq kg}^{-1}$ , respectively and this is lower than in our previous research ( $745$  and  $1450 \text{ Bq kg}^{-1}$ ). A high average activity level of  $^{238}\text{U}$  was measured in MAP samples in 2001 ( $1348 \text{ Bq kg}^{-1}$ ) [17]. The maximal activity levels of  $^{226}\text{Ra}$  and  $^{238}\text{U}$  in NP fertilizers were 542 and  $991 \text{ Bq kg}^{-1}$ , respectively. These results are higher than previous results obtained for the same fertilizer type ( $450$  and  $750 \text{ Bq kg}^{-1}$ ) [18]. The average activity level of  $^{238}\text{U}$  in MAP is significantly lower in this work than in previous research [18].

## CONCLUSION

The following radionuclides:  $^{40}\text{K}$ ,  $^{232}\text{Th}$ ,  $^{226}\text{Ra}$ ,  $^{238}\text{U}$  and  $^{137}\text{Cs}$  were determined in all measured fertilizer samples (677) sent to INEP for gamma spectrometric analysis by the phyto-sanitary inspection. The activity level of  $^{137}\text{Cs}$  in all measured fertilizer samples was negligible. The maximum activity level of  $^{40}\text{K}$  was measured in NPK fertilizer with a small proportion of  $^{226}\text{Ra}$  and  $^{238}\text{U}$  ( $11175 \text{ Bq kg}^{-1}$ ). The maximum activity level of  $^{226}\text{Ra}$  was measured in a sample of fertilizer with the formulation 16-16-16 ( $674 \text{ Bq kg}^{-1}$ ), and  $^{238}\text{U}$  in a sample of NP fertilizer ( $991 \text{ Bq kg}^{-1}$ ). All fertilizer samples had activity levels that are allowed by the Regulations and allowed to be imported into our country. In order to observe the cumulative effect due to the increasing content of uranium arable land due to fertilization and the possibility of establishing a food chain, constant but systematic measurements of the radioactivity of mineral fertilizers are necessary. These measurements should allow a long-term forecast of the content of uranium in the soil, due to the constant and necessary application of fertilizers.

## ACKNOWLEDGMENTS

*The authors are grateful to the Ministry of Science, Technological Development and Innovation of the Republic of Serbia, as part of financing scientific research at the Institute for the Application of Nuclear Energy-INEP, contract number 451-03-66/2024-03/200019.*

## REFERENCES

- [1] Janković V., Hemija i hemijska industrija u Srbiji, Srpsko hemijsko društvo, Beograd (1997), 302–308 (*in Serbian*).
- [2] Kastori R., Fiziologija biljaka, Naučna knjiga, Beograd (1989) (*in Serbian*).

- [3] Sarić M., Jocić B., Belić J., Biološki potencijal gajenih biljaka u agrofitocenozi u zavisnosti od mineralne ishrane, SANU, Beograd (1993) (*in Serbian*).
- [4] Gržetić I., Jelenković R., Prirodni radioaktivni elementi, geološko poreklo i oblici pojavljivanja i migracije, Jonizujuća zračenja iz prirode, JDZZ, INN Vinča, Beograd, (1995) 3–9 (*in Serbian*).
- [5] Ajdačić N., Gnjatović S., Vujović V., X Simpozijum Jugoslovenskog društva za zaštitu od zračenja (JDZZ), Date 29.5-1.6. 1979., Aranđelovac, Srbija, (1979) 437–441 (*in Serbian*).
- [6] Mitrović B., Vitorović G., Stojanović M., *i sar.*, Veterinarski glasnik, 65 (1–2) (2011) 123–140 (*in Serbian*).
- [7] Babić M., Spasić A., Marinko M., *i sar.*, Zbornik radova: Uticaj upotrebe fosfornih đubriva na kontaminaciju uranom, SANU, Beograd, Srbija, LXXII-5 (1993) 41–55 (*in Serbian*).
- [8] Stojanović M., Radosavljević S., Martinović Lj., Zbornik radova: Uticaj upotrebe fosfornih đubriva na kontaminaciju uranom, SANU, Beograd, Srbija, LXXII-5 (1993) 1–17 (*in Serbian*).
- [9] Mitrović B., Vitorović G., Andrić V., *i sar.*, Veterinarski glasnik, 67 (5–6) (2013) 359–367 (*in Serbian*).
- [10] Hamamo H., Landsberger S., Harbotile G., *et al.*, J. Radioan. Chem. 194 (1995) 331–336.
- [11] Abbady A., Uosif M., El-Taher A., J. Environ. Radioact. 84(1) (2005) 65–78.
- [12] Bolca M., Sac M., Cokuysal B., *et al.*, Radiat. Meas. 42 (2007) 263–270.
- [13] Trišić M., Hemijska industrija u Prahovu juče, danas, sutra, Elixir Prahovo, Industrija hemijskih proizvoda, (2018) (*in Serbian*).
- [14] Pravilnik o granicama sadržaja radionuklida u vodi za piće, životnim namirnicama, stočnoj hrani, lekovima, predmetima opšte upotrebe, građevinskom materijalu i drugoj robi koja se stavlja u promet Službeni glasnik RS 36/11 od 10.05.2018. godine (2018) (*in Serbian*).
- [15] Measurement of radionuclides in food and the environment. A Guide Book, Technical Reports Series No.295. International Atomic Energy Agency, Vienna (1989).
- [16] Boukhenfouf W., Boucenna A., J. Environ. Radioact. 102(4) (2011) 336–339.
- [17] Čučulović A., Dragović S., Stanković S., *i sar.*, Prirodni i veštački proizvedeni radionuklidi u mineralnim đubrivima, Eko-KONFERENCIJA 2002, Ekološki pokret grada novog Sada, ZDRAVSTVENO BEZBEDNA HRANA, SAFE FOOD I, Monografija, Novi Sad, (2002) 275–280.
- [18] Čučulović A., Čučulović R., Veselinović D., Ecologica 23(83) (2016) 492–496.



## METAL CONTENTS IN VEGETABLES ORIGINATING FROM COAL FIRED THERMAL POWER PLANTS REGION

Nenad Zarić<sup>1,2\*</sup>, Milana Zarić<sup>3</sup>

<sup>1</sup>Faculty of Biology, University of Belgrade, Studentski trg 12–16, 11000 Belgrade, SERBIA

<sup>2</sup>Department of Agrobiotechnology IFA-Tulln, Institute of Bioanalytics and Agro-Metabolomics, University of Natural Resources and Life Sciences Vienna (BOKU), Konrad-Lorenz-Straße 20, 3430 Tulln, AUSTRIA

<sup>3</sup>Institute for chemistry, technology and metallurgy, University of Belgrade, Njegoševa 12, 11000 Belgrade, SERBIA

\* [nenad.zaric@bio.bg.ac.rs](mailto:nenad.zaric@bio.bg.ac.rs)

### Abstract

*Coal-fired thermal power plants make an important contribution to the global energy supply, but pose a significant environmental and health risk due to pollutant emissions, including heavy metals. These pollutants can contaminate soil and water, leading to bioaccumulation of toxic elements in plants. In this study, the elemental composition of vegetables (carrots, peppers, potatoes and tomatoes) grown near the Kostolac A and B coal-fired power plants in Serbia is investigated. Samples were taken from four locations (Požarevac, Petka, Kostolac and Drmno), processed and analyzed using inductively coupled plasma mass spectrometry (ICP-MS). The results showed that carrots had the highest accumulation of elements, including both essential nutrients and toxic heavy metals, although none of them exceeded the safety thresholds set by local, EU or FAO/WHO standards. The results underline the need for continuous monitoring of vegetable safety in the vicinity of coal-fired power plants to mitigate potential health risks. Further studies, including soil analysis, are recommended to identify the sources of these elements and to fully understand their impact on the environment.*

**Keywords:** ICPMS, vegetables, metals, power plant.

### INTRODUCTION

Coal-fired thermal power plants play a crucial role in meeting the world's energy needs, but their operation comes at a significant environmental cost. These power plants are known to emit large amounts of pollutants, including particulate matter, sulphur dioxide, nitrogen oxides and a range of heavy metals, which can have harmful effects on the environment and human health [1,2]. The deposition of these pollutants on the surrounding soils and water bodies can lead to the contamination of agricultural land, posing a risks to the quality and safety of food grown in these areas [3,4]. Heavy metals such as lead (Pb), cadmium (Cd), mercury (Hg) and arsenic (As) are of particular concern due to their persistence in the environment and their ability to bioaccumulate in the food chain [5,6]. These elements can be taken up by plants through their roots from contaminated soil or water and then enter the human diet through the consumption of contaminated vegetables. The accumulation of heavy

metals in vegetables not only compromises food safety, but also poses serious health risks such as neurotoxicity, carcinogenicity and various other chronic diseases [7].

Previous research has documented the elevated levels of heavy metals in crops grown near industrial areas, including coal-fired power plants, highlighting the potential health risks associated with these pollutants [8,9]. For example, vegetables grown near industrial areas in India have been found to contain high concentrations of heavy metals exceeding the permissible limits of international standards [10]. This underlines the need for rigorous monitoring and regulation to ensure food safety.

The elemental composition of vegetables is influenced by several factors, including soil characteristics, crop type, irrigation practices and the extent of atmospheric deposition from nearby industrial sources [11]. The type of soil and its pH can significantly affect the availability and uptake of heavy metals by plants. Similarly, different plant species can accumulate heavy metals differently, with leafy vegetables often having higher concentrations than root vegetables [12].

In this study, we aim to analyze the elemental composition of vegetables grown in the vicinity of coal-fired thermal power plants. The results of this research will contribute to a better understanding of the environmental impact of coal-fired power plants on agricultural products and provide insights to policy makers and stakeholders in the field of environmental and food safety management.

## **MATERIALS AND METHODS**

### **Sampling locations**

Samples were taken from four locations in the vicinity of two coal fired thermal power plants, Kostolac A and B. The locations are also characterized by an open pit coal mine and an ash disposal site. Sampling locations with pollution sources can be seen in Figure 1.

*Požarevac* – A city of just above 40 000 inhabitants. It is located about 10 km to the south of the two power plants, open pit coal mine and ash disposal site.

*Petka* – Small village located about 4 km south-west of Kostolac A power plant, 6 km from the ash disposal site and Kostolac B power plants and 10 km to the west of the open pit coal mine.

*Kostolac* – A town on whose outskirts Kostolac A power plant is located. It is 2 km to the south of the ash disposal site, 4 km to the west of the power plant Kostolac B and 7 km from the coal mine.

*Drmno* – Small village less than 1 km south from thermal power plant Kostolac B, 4 km west from the open pit coal mine, 4 km east from thermal power plant Kostolac B and 4 km south-east of the ash disposal site.



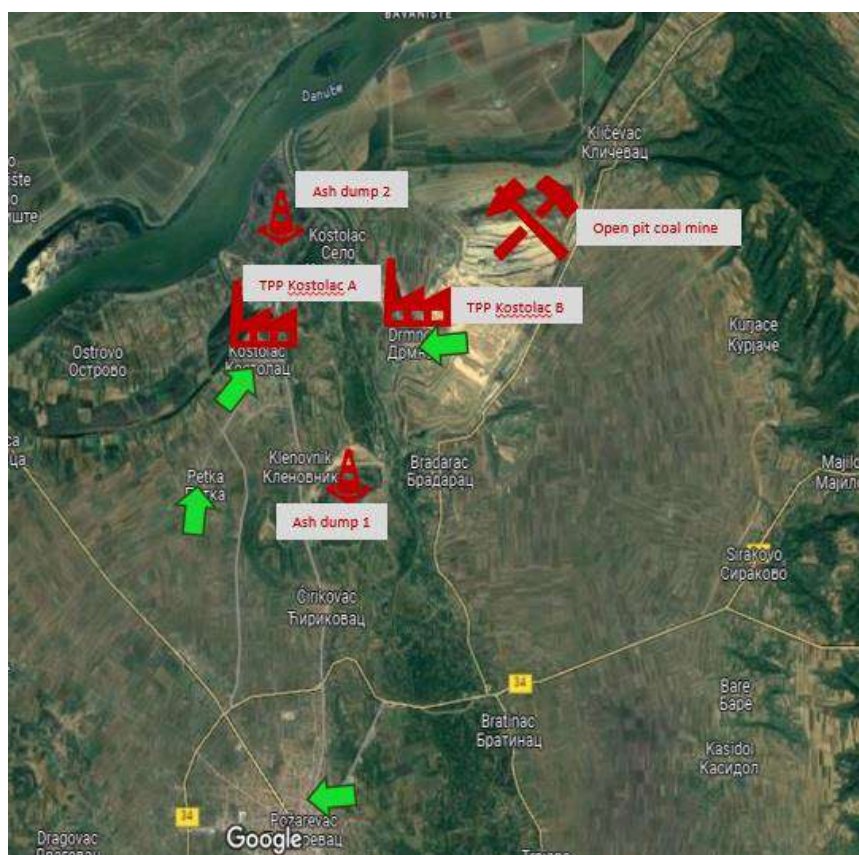


Figure 1 Sampling locations (green arrows) and pollution sources (red)

### Sample collection, preparation and analyses

Four vegetables were chosen to be sampled. Two root vegetables: carrot and potato and two above ground vegetables: pepper and tomato. Each sample was collected and frozen at  $-80^{\circ}\text{C}$ . Samples were then freeze dried for 72 hours. They were homogenized in an ultra-centrifugal mill with a final fineness size of  $<1$  mm (ZM 200, 1 mm titanium sieve, Retch GmbH, Haan, Germany). About 100 mg of homogenized vegetables were weighted into 10 mL pre-cleaned quartz vessels, in triplicate, and digested with concentrated, subboiled  $\text{HNO}_3$  using an ultraCLAVE IV microwave digestion system (MLS GmbH, Leutkirch, Germany). All the samples were diluted to a final volume of 10% v/v  $\text{HNO}_3$ . In addition, blanks and the certified reference material (CRM) BOVM-1 Bovine muscle powder (previously SRM 8414, NRC, Canada) were prepared using the same procedure.

Element concentrations were determined with an inductively coupled plasma mass spectrometer (ICPMS, ICP-MS 7700x, Agilent Technologies, Waldbronn, Germany). For thirty-one elements an external calibration curve in four different concentration ranges and with six points each, was made in 10%  $\text{HNO}_3$ .

#### Quality control

Continuous addition of internal standard solution using standard tubings was used for instrument stability control. The solution contained  $200 \mu\text{g L}^{-1}$  of Be, Ge, In and Lu in a matrix of 1% v/v  $\text{HNO}_3$ . In addition, drift standards were measured every ten samples. The accuracy was evaluated using two reference materials: SRM 1640a Trace elements in natural

water (National Institute of Standards & Technology, Gaithersburg, USA) and CRM 8414 Bovine muscle powder (NRC, Canada).

## **RESULTS AND DISCUSSION**

Almost all of the analysed elements were detected in the vegetable's samples, except for Hg which was detected only in Carrots.

Looking at all samples' locations combined, the sum of all analysed elements was the highest in carrots, followed by tomatoes, potatoes and pepper. Elements with the highest concentrations in carrots were B, Na, Mg, Al, P, K, Ca, Cr, Fe, Zn, As, Se, Sr, Cd, Sn, Cs, Ba, Gd, Tl, Pb, Bi and U. Highest concentrations in peppers were observed for Li, S, Co and Ni; in potatoes for V, Mo, Ag and in tomatoes for Mn, Cu and Rb. From this data we can conclude that carrots are the best vegetable to be used as a mineral source. However, caution should be taken as they also accumulate the most toxic elements such as As, Pb, Cd, U, etc. None of the analysed elements was above the safety thresholds established by local and EU legislation or by FAO/WHO. Usually, they were a few magnitudes lower. The only exception is Pb in carrots where the concentration was  $0.16 \text{ mg kg}^{-1}$  with the FOA/WHO level set at  $0.3 \text{ mg kg}^{-1}$ ; and Cd with measured concentration of  $0.14 \text{ mg kg}^{-1}$  in carrots, while safe levels were determined at  $0.2 \text{ mg kg}^{-1}$ . Although none of the samples exceeded these limits these vegetables should be closely monitored.

Considering that carrots accumulated the most elements we used them to look at differences between sampling locations. The sum of all elements was the highest in Petka, followed by Drmno, Kostolac and Požarevac. However, this was expected as in Petka some of the most abundant elements had the highest concentrations (Mg, P, K). Other elements that had the highest concentrations in Petka were Li, V, Mn, Co, Ni, Ba and Pb. Elements with the highest concentrations in Drmno were Na, S, Ca, Se, Sr, Cd and Bi. Carrots from Kostolac were characterized with the highest concentrations of Al, Cr, Fe, Cu, As, Rb, Mo, Sn, Cs, Gd and Hg. The least number of elements showed highest concentrations in carrots from Požarevac (B, Zn, Ag, Tl and U). Element accumulation in plants does not depend only on pollution sources in the region, but also on the soil origin and its physio-chemical properties. To determine the exact sources of the analysed elements, further study is needed that including soil analyses.

## **CONCLUSION**

Four vegetable types were analyzed for elemental composition: carrots, peppers, potatoes and tomatoes. The highest concentrations of 22 out of 32 analyzed elements were found in carrots, followed by tomatoes, with significantly lower concentrations in peppers and potatoes. Different locations had different element distributions. In carrots Požarevac had only five elements with the highest concentrations followed by Drmno, Petka and Kostolac in which 11 elements had highest values. None of the analyzed elements had concentrations that were above the allowed limits.

## ACKNOWLEDGEMENT

We would like to acknowledge the help of the University of Graz, Graz, Austria and prof. Walter Goessler and his group for making the analyses possible. We acknowledge the support of BOKU university and FWF. The authors are grateful to the Ministry of Science, Technological development and Innovation of the Republic of Serbia for financial support according to the contract with the registration number (451-03-66/2024-03/200178 and 451-03-66/2024-03/200026).

## REFERENCES

- [1] Guttikunda S.K., Jawahar P., Atmos. Environ. 92 (2014) 449–460.
- [2] Wang G., Deng J., Zhang Y., *et al.*, Sci. Total Environ. 741 (2020) 140326.
- [3] Hariram M., Sahu R., Kumar A., *et al.*, Impact of Emissions from Coal-Based Thermal Power Plants on Surrounding Vegetation and Air Quality over Bokaro Thermal Power Plant *in* Asian Atmospheric Pollution: Sources, Characteristics and Impacts, Editor Singh R.P. Elsevier, Orange (2022), p. 255, ISBN 978-0-12-816693-2.
- [4] Hossain M.N., Paul S.K., Hasan M.M., Environ. Monit. Assess. 187 (2015) 202.
- [5] Sridhara Chary N., Kamala C.T., Samuel Suman Raj D., Ecotoxicol. Environ. Saf. 69 (2008) 513–524.
- [6] Järup L., Br. Med. Bull. 68 (2003) 167–182.
- [7] Tchounwou P.B., Yedjou C.G., Patlolla A.K., *et al.* Heavy Metal Toxicity and the Environment *in* Molecular, Clinical and Environmental Toxicology: Volume 3: Environmental Toxicology, Editor Luch, A., Springer Basel, Basel (2012), p.133, ISBN: 978-3-7643-8340-4.
- [8] Khan S., Cao Q., Zheng Y.M., *et al.*, Environ. Pollut. 152 (2008) 686–692.
- [9] Kumar Sharma R., Agrawal M., Marshall F., Ecotoxicol. Environ. Saf. 66 (2007) 258–266.
- [10] Gupta N., Khan D.K., Santra S.C., Environ. Monit. Assess. 184 (2012) 6673–6682.
- [11] Smolders E., Mertens J., Heavy Met. soils-Trace Met. Met. soils thier Bioavailab (2013) 283–312.
- [12] Sultana R., Tanvir R.U., Hussain K.A., *et al.*, Environ. Syst. Res. 11 (2022) 15.
- [13] Liu X., Song Q., Tang Y., *et al.*, Sci. Total Environ. 463 (2013) 530–540.



## ENHANCING OXYGEN EVOLUTION: THE ELECTROCATALYTIC POWER OF Ag-DOPED BISMUTH FERRITE

Snežana Brković<sup>1</sup>, Nikola Zdolšek<sup>1</sup>, Ivana Perović<sup>1\*</sup>, Mina Seović<sup>1</sup>, Petar Laušević<sup>1</sup>,  
Jelena Georgijević<sup>1</sup>, Maria Čebela<sup>1</sup>

<sup>1</sup>University of Belgrade, Vinča Institute of Nuclear Sciences, National Institute of the  
Republic of Serbia, Mike Petrovića Alasa 12–14, 11351 Vinča, SERBIA

\*ivanaperovic@vin.bg.ac.rs

### Abstract

*This study explores the electrochemical performance of Ag-doped bismuth ferrite (BFO+Ag) as a novel electrocatalyst for the oxygen evolution reaction (OER). Utilizing a cost-effective hydrothermal method, BFO+Ag nanopowders were synthesized and characterized for their electrocatalytic properties. The incorporation of silver was found to significantly enhance the activity and reduce the overpotential in OER applications. Electrochemical evaluations demonstrated that BFO+Ag electrodes achieve a current density of 10 mA cm<sup>-2</sup> at a reduced overpotential of 1.52 V and display improved Tafel slopes, particularly at elevated temperatures. This work positions BFO+Ag as a promising and economically viable alternative to traditional precious metal-based catalysts for energy conversion and storage solutions, emphasizing the potential for future research to optimize performance and explore practical applications.*

**Keywords:** OER, bismuth ferrite, hydrothermal synthesis.

### INTRODUCTION

The increasing global demand for renewable and eco-friendly energy conversion and storage solutions is driven by energy shortages and environmental concerns stemming from fossil fuel usage [1]. At the core of these renewable energy technologies lie two crucial oxygen electrochemical processes: the oxygen reduction reaction (ORR) and the oxygen evolution reaction (OER) [2,3]. The ORR significantly influences the overall performance of fuel cells and metal-air batteries, both recognized as promising systems for energy conversion and storage. Conversely, the OER serves as the anode reaction in water electrolyzers for electrochemical water splitting and in unitized regenerative fuel cells [4]. Given the sluggish kinetics of these reactions, research efforts in the field have been directed towards the development of highly efficient and stable electrocatalysts aimed at minimizing overpotential and enhancing the kinetics of the OER [5].

As of now, Pt-based electrocatalysts stand out as the most effective for ORR, whereas IrO<sub>2</sub> and RuO<sub>2</sub> demonstrate the highest activity for OER [3]. Despite their efficiency, the widespread adoption of these electrocatalysts is hindered by their prohibitive costs. Consequently, numerous research teams have shifted their attention towards the exploration of novel non-precious and cost-effective materials, aiming to create an ideal reversible oxygen electrode capable of accelerating both ORR and OER [3,6]. Magnetoelectric multiferroics,

due to simultaneous ferroelectric and ferromagnetic ordering, have attracted wide attention in recent years, offering a wide range of potential applications in data storage media, spintronics, and multi-state memories. One of the well-known materials exhibiting such properties is bismuth ferrite (BFO)  $\text{BiFeO}_3$  [7].

In our study, we investigate the influence of silver (Ag) doped bismuth ferrite (BFO) nanopowders on electrocatalytic performance in relation to OER. Utilizing a simple, low-cost, and energy-efficient hydrothermal method, which offers advantages over conventional methods, we synthesized the materials and conducted a series of electrochemical measurements to investigate its catalytic properties for the oxygen evolution reaction (OER). Furthermore, we assessed the energy consumption of an alkaline electrolyzer with electrodes coated with this Ag-doped BFO material.

## **MATERIALS AND METHODS**

### **Synthesis of $\text{BiFeO}_3$ 33%Ag and Materials characterization**

Nano-crystalline powders of  $\text{Bi}_{1-x}\text{Ag}_x\text{FeO}_3$  ( $x=0.33$ ) were synthesized using the hydrothermal method. This approach is simple, low-cost, and energy-saving, offering advantages over conventional methods. The chemical compounds used included bismuth nitrate ( $\text{Bi}(\text{NO}_3)_3 \times 5\text{H}_2\text{O}$ ), silver nitrate ( $\text{AgNO}_3$ ), iron nitrate ( $\text{Fe}(\text{NO}_3)_3 \times 9\text{H}_2\text{O}$ ), and potassium hydroxide (KOH), all of analytical grade from Sigma-Aldrich. The bismuth nitrate, silver nitrate, and iron nitrate were dissolved in 40 mL of 8M KOH, stirred vigorously for 30 minutes, and then transferred into an autoclave. Hydrothermal treatments were conducted under autogenous pressure at 200°C for six hours. After cooling to room temperature, the produced powders were collected at the bottom of the autoclave. The products were washed at least five times through repeated cycles of centrifugation in distilled water and then dispersed in ethanol, followed by sonication for 60 minutes. The final powders were obtained by evaporating ethanol in a mortar heated to 60°C.

Elemental composition of obtained sample was determined by XRF measurements, performed by Thermo Scientific Niton XL3t XRF analyzer, at room temperature.

### **Electrochemical measurements**

The working electrodes were fabricated by dispersing 5 mg of the synthesized BFO+Ag materials in 980  $\mu\text{l}$  of deionized water and 20  $\mu\text{l}$  of 5% Nafion solution (Sigma Aldrich). This mixture was sonicated for 30 minutes at room temperature to form a homogeneous catalytic ink. Subsequently, 10 ml of this ink was applied to a glassy carbon electrode (GCE) and allowed to dry at room temperature. Electrochemical measurements were performed using a Gamry PCI4/750 potentiostat/galvanostat within both three-electrode and two-electrode cells under varying temperatures. In the three-electrode setup, the modified GCE served as the working electrode, platinum as the counter electrode, and a saturated calomel electrode (SCE) as the reference electrode, with 1M KOH as the electrolyte. In the two-electrode configuration, the modified Ni electrode acted as the working electrode, and a pure Ni electrode served as the counter electrode, utilizing 6M KOH as the electrolyte. Throughout this study, all potentials are reported relative to the reversible hydrogen electrode (RHE), and all current densities ( $j$ ) were calculated based on the geometric area of the electrodes (1  $\text{cm}^2$ ).



## RESULTS AND DISCUSSION

The obtained material ( $\text{BiFeO}_3+\text{Ag}$ ) was analyzed using X-ray fluorescence method in order to determine the elemental composition. Results are given in Table 1.

To demonstrate the oxygen evolution activity of the studied materials, two critical parameters were examined to facilitate the comparison of electrocatalysts; the overpotential required to achieve a current density of  $10 \text{ mA cm}^{-2}$  (Figure 1) and the Tafel slope, depicted in Figure 2. Notably, the samples subjected to the highest test temperature of  $80^\circ\text{C}$  displayed the most favorable results. Specifically, BFO doped with Ag at  $80^\circ\text{C}$  achieved a current density of  $10 \text{ mA cm}^{-2}$  at an overpotential of  $1.52 \text{ V}$ .

**Table 1** Amounts of most abundant elements (Bi, Fe, Ag) found by XRF analysis in BFO+Ag sample

Element	Bi	Fe	Ag
(%)	76.04	14.43	9.31

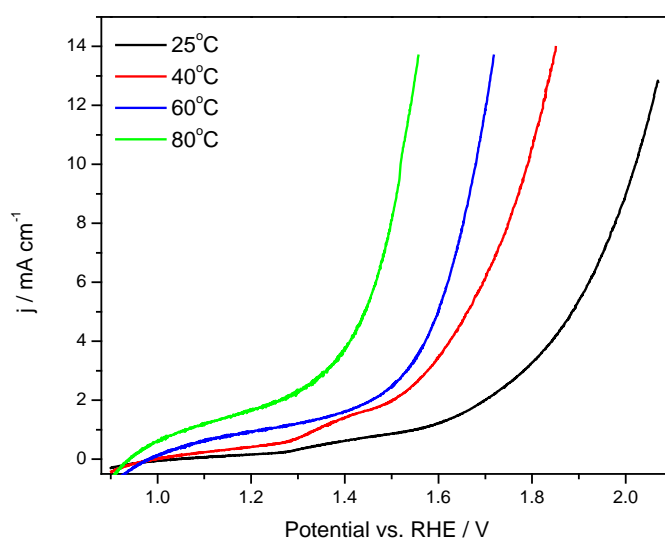


**Figure 1** Comparison of electrochemical activity for OER - LSV curves at different temperatures

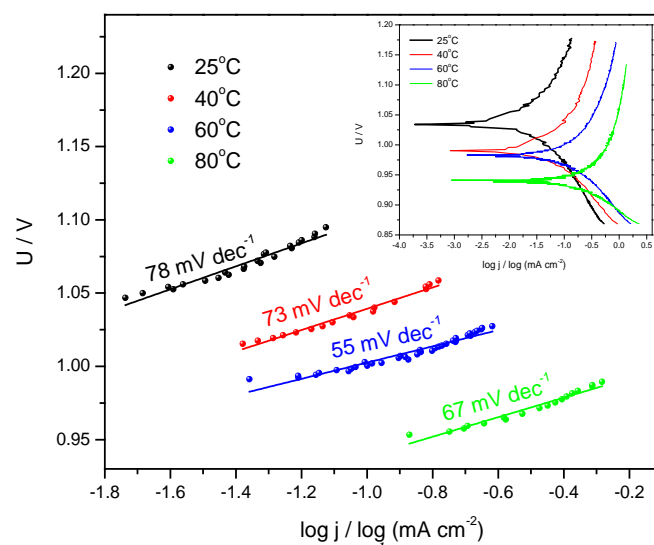


**Figure 2** Comparison of Tafel slopes ( $b / \text{mV dec}^{-1}$ ) at different temperatures; Polarization curves (inset)



The Tafel slopes, indicative of the kinetics of the electrochemical reaction, were lowest at higher temperatures (60°C and 80°C), measuring approximately 60 mV dec<sup>-1</sup>, as listed in Table 2. This observation underscores that the OER activity improves significantly with increased temperature, particularly at 80°C, where the catalytic efficiency was observed to be the highest.

**Table 2** Parameters obtained from Tafel polarization curves and LSV curves, at different temperatures

T / K	b / mV dec <sup>-1</sup>	j <sub>0</sub> / mA cm <sup>-2</sup>	OER / V
298	78.4	0.03	2.02
313	72.7	0.08	1.79
333	55.4	0.18	1.68
353	66.8	0.45	1.52

The study also investigated the relationship between energy consumption, temperature, and current densities comparing the electrolyzer system with pure nickel electrodes and with BFO + Ag electrode. The energy balance of electrolysis is represented by the energy consumed per mole of oxygen produced, calculated on the basis of formula (1):

$$Q = \frac{I \cdot U \cdot t}{0,084 \text{ mmol}} = [\text{kJ mol}^{-1}] \quad (1)$$

where Q is the energy consumption in kJ mol<sup>-1</sup>, U is the total voltage of electrolysis in V, i.e. the potential difference of the cathodic and anodic reactions and the voltage drop through the electrolyte, I is the total current in A, t is the time in seconds for which 1 mol of oxygen is developed. The results obtained from the analysis of this system are represented by a three-dimensional diagram in the Figure 2, and numerically in Table 3.

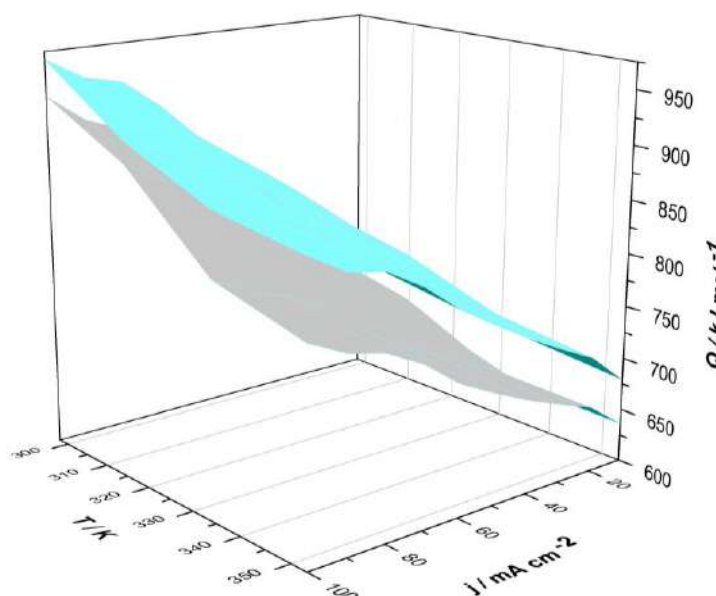


**Figure 3** Comparative 3D representation of energy consumption as a function of current density and temperature, Ni electrode in 6M KOH (upper surface) and BFO+Ag electrode (lower surface)

**Table 3** Alkaline electrolyzer energy consumption at different current densities and electrolysis temperatures in 6M KOH

$Q / \text{kJ mol}^{-1}$								
$j / \text{mA cm}^{-2}$	Ni electrode				BFO + Ag electrode			
	298 K	303 K	333 K	353 K	298 K	303 K	333 K	353 K
<b>10</b>	722.7	720.0	691.0	679.0	689.9	672.2	640.1	636.3
<b>20</b>	771.2	757.6	723.4	709.1	727.1	712.5	666.9	662.0
<b>30</b>	801.2	779.9	743.1	726.4	750.2	740.1	685.1	674.6
<b>40</b>	826.9	799.6	763.8	744.94	774.5	763.8	702.4	688.4
<b>50</b>	851.0	820.7	784.2	765.8	799.4	790.1	721.5	704.6
<b>60</b>	876.1	842.5	804.8	787.8	825.5	814.4	742.3	722.7
<b>70</b>	910.5	871.6	833.0	815.4	863.4	846.5	772.3	749.1
<b>80</b>	937.8	894.9	854.3	836.6	892.6	872.7	791.8	767.8
<b>90</b>	946.7	900.9	862.2	843.6	906.8	884.9	802.6	776.6
<b>100</b>	968.1	921.5	879.4	864.8	934.2	906.2	821.6	794.3

The presented diagram indicates that higher temperatures result in greater energy savings, both for the with pure nickel electrodes and with BFO+Ag electrode. The improvement of the electrolytic process is affected by both the elevated temperature and the BFO+Ag catalyst.

The results obtained indicate an enhanced OER performance with electrodes coated with BFO+Ag. This improvement can likely be attributed to the dual characteristics of our synthesized material. As a ferroelectric material, our BFO+Ag exhibits spontaneous polarization that can be reoriented by an external electric field. This reorientation affects the electronic structure and can significantly enhance the charge transfer processes that are crucial for electrocatalysis. Additionally, as a ferromagnetic material, it displays ordered magnetic moments that can alter the spin states of electrons. In the realm of catalysis, such spin-polarized electrons can modify reaction pathways and potentially reduce the activation energy required for key steps in the OER process. These properties make our synthesized material particularly valuable for practical applications in energy conversion and storage technologies, where efficient and cost-effective catalysts are essential.

## CONCLUSION

This study highlights the effectiveness of Ag-doped bismuth ferrite (BFO+Ag) as an electrocatalyst for the oxygen evolution reaction (OER). The addition of silver enhances the electrochemical performance of BFO, benefiting from the synergistic ferroelectric and ferromagnetic properties that improve charge transfer and lower activation energies. The hydrothermal synthesis of BFO+Ag proves to be a cost-effective and scalable method, offering a viable alternative to traditional, more expensive catalysts like iridium or ruthenium oxides. Future work should focus on optimizing doping levels and evaluating long-term stability to further advance the application of BFO+Ag in sustainable energy technologies.

## **ACKNOWLEDGEMENT**

*The authors are grateful to the Ministry of Science, Technological development and Innovation of the Republic of Serbia for financial support according to the contract with the registration number 451-03-66/2024-03/ 200017.*

## **REFERENCES**

- [1] Fujimoto K., Ueda Y., Inohara D., *et al.*, *Electrochim. Acta* 354 (2020) 136592.
- [2] Lingappan N., Li B., Lee T.H., *et al.*, *Electrochim. Acta* 313 (2019) 41–7.
- [3] Jiang H., Gu J., Zheng X., *et al.*, *Energy Environ. Sci.* 12 (2019) 322–33.
- [4] Hu L., Hu Y., Liu R., *et al.*, *Int. J. Hydrogen Energy* 44 (2019) 11402.
- [5] Suermann M., Schmidt T.J., Buchi F.N., *Electrochim. Acta* 281 (2018) 466–71.
- [6] Zhang H., Wang Z., Zhou J., *et al.*, *J. Int. J. Hydrogen E.* 47 (2022) 11224–35.
- [7] Neogi S., Ghosh R., *Appl. Mater. Today* 29 (2022) 101611.



## NONLINERA PHENOMENA DURING VOLTAMMETRIC MEASUREMENT OF COPPER CORROSION

Nebojša Potkonjak<sup>1\*</sup>, Đuro Čokeša<sup>1</sup>, Mirjana Marković<sup>1</sup>

<sup>1</sup>Institute of Nuclear Sciences, National Institute of the Republic of Serbia,  
University of Belgrade, Mike Petrovica Alasa 12–14, 11000 Belgrade, SERBIA

\*[npotkonjak@vin.bg.ac.rs](mailto:npotkonjak@vin.bg.ac.rs)

### Abstract

*Bifurcation analysis of the Cu|1 M TFA electrochemical oscillatory system was done by using voltammetric data, obtained under quasi-potentiostatic polarization conditions. A super-critical Hopf bifurcation and a saddle-loop bifurcation were identified at following bifurcation potentials  $E_{BIF1}=0.5446$  V and  $E_{BIF2}=0.7536$  V, respectively.*

**Keywords:** copper, anodic dissolution, trifluoroacetic acid, electrochemical oscillations.

### INTRODUCTION

The multivalent nature of transition metals introduces a rich array of nonlinear dynamics to electrode reactions [1]. This propensity can lead to nonlinear phenomena like electrochemical oscillations and the formation of metal fractals. Being far-from-equilibrium, the electrochemical systems can spontaneously form a wide spectrum of spatio-temporal patterns [2]. Spontaneous emergence of such patterns implies that the dynamical systems, such as electrochemical, undergo self-organization [2]. Appearance of oscillations implies that the electrochemical system can not longer achieve stable steady states, and that its existence is only possible through oscillatory states [1]. Transition from a stable steady state to an oscillatory state goes via bifurcation point. In order to be identified, evolution of the system has to be monitored through phase space diagram; constructed from a series of coordinates characterized by a parameter (controlled quantity) and a variable (quantity which is an appropriate representative of the systems state) [3]. Looking from this perspective, linear sweep voltammetry can be observed as instrumental technique which dynamically drives the system throughout a series of variable-to-parameter points [4].

### MATERIALS AND METHODS

Experiments were carried out in a three-electrode electrolytic cell, at 293 K, with a copper rod (Goodfellow, 99.99%) as the working electrode, Pt foil as the counter electrode, and a saturated calomel electrode (SCE) as the reference one. The working electrode was embedded in a plastic capillary, leaving only the rod cross-section ( $0.0314\text{ cm}^2$ ) exposed to the electrolyte solution. Prior to each experiment the working electrode was abraded by a series of wet sanding paper with different grit size (320, 600, 800, 1000, 1200 and 2000). Thereupon, the working electrode was rinsed with deionized water in an ultrasonic bath for 2 min. Electrolyte solution was 1 M TFA. Experiments were carried under natural convection

of electrolyte in the electrolytic cell, without any external resistance applied in the circuit. Linear sweep voltammetry was performed using anodic scan, starting from 0.5 V<sub>SCE</sub>, at a rate of 1 mV s<sup>-1</sup>. All applied circuit potentials ( $E$ ) are given with the respect to the SCE.

## RESULTS AND DISCUSSION

By carefully selection of initial conditions, we were able to locate an oscillatory state (OsS) region of investigated system at the current-potential ( $I$ - $E$ ) polarization curve (Figure 1). The first bifurcation point occurs at  $E_{\text{BIF1}}=0.5446$  V (looking from the direction of polarization). This bifurcation point can be observed as an entering one, marking a discontinuity in evolution of the system from the steady stable state (SSS1) to OsS; it is a characteristic of the SSS1→OsS transient. With respect to above mention perspective, the second bifurcation point, located at  $E_{\text{BIF2}}=0.7536$  VSCE, can be taken as the exit point; it is a feature of the OsS→SSS2 transient (Figure 1).

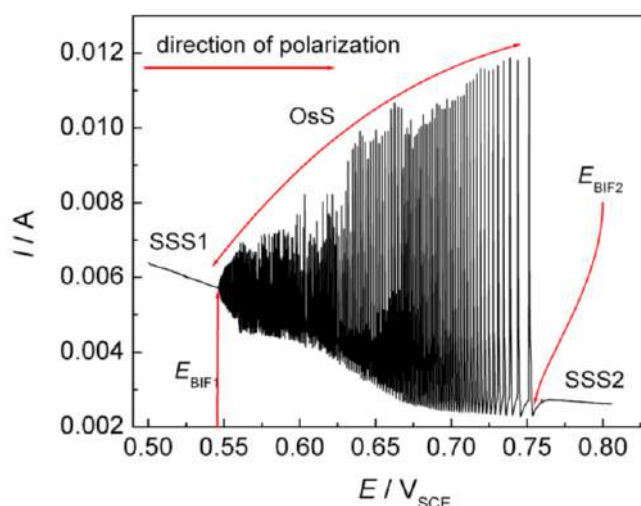


**Figure 1**  $I$ - $E$  polarization curve of Cu electrode in 1M TFA

Smooth increase of current oscillation amplitudes observed near on the SSS1→OsS transient is shown in Figure 2.

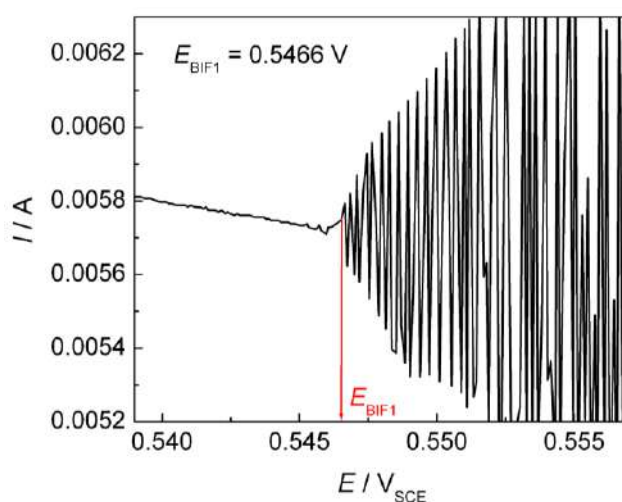


**Figure 2** Detail from  $I$ - $E$  polarization curve, Figure 1, in the vicinity of the SSS1→OsS transient

Linear dependence between the square amplitude of current oscillations ( $A^2$ ) and increase of the distance of controllable parameter from EBIF1 ( $|E_{OSC}-E_{BIF1}|$ ) was found (Figure 3).

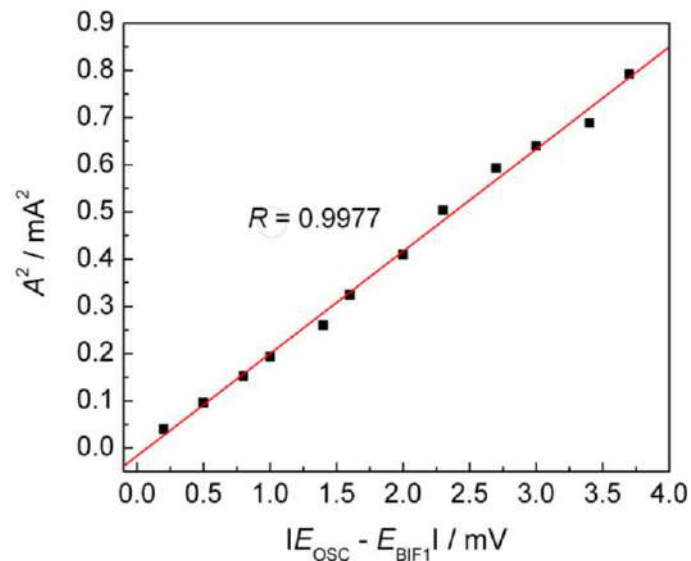


**Figure 3** Dependence of the square amplitude of current oscillations ( $A^2$ ) vs. distance of controllable parameter from EBIF1 ( $|E_{OSC}-E_{BIF1}|$ )

On the other hand, the period of current oscillations ( $\tau$ ) increases as the system approaches the OsS→SSS2 transient, ending with sudden termination of oscillatory behavior (Figure 4). Linear dependence between  $\tau$  and logarithmic value of the distance from  $E_{BIF2}$  ( $\ln |E_{OSC}-E_{BIF2}|$ ) is shown in Figure 5. Combined with an existence of hysteresis [5] (not shown in abstract), it implies that the OsS→SSS2 transient goes via the saddle-loop bifurcation [3,5,6]. Correlation coefficients ( $R$ ), shown in Figures 3 and 5, were found to be considerably high. Hence, we can say that the procedure for bifurcation analysis was verified.

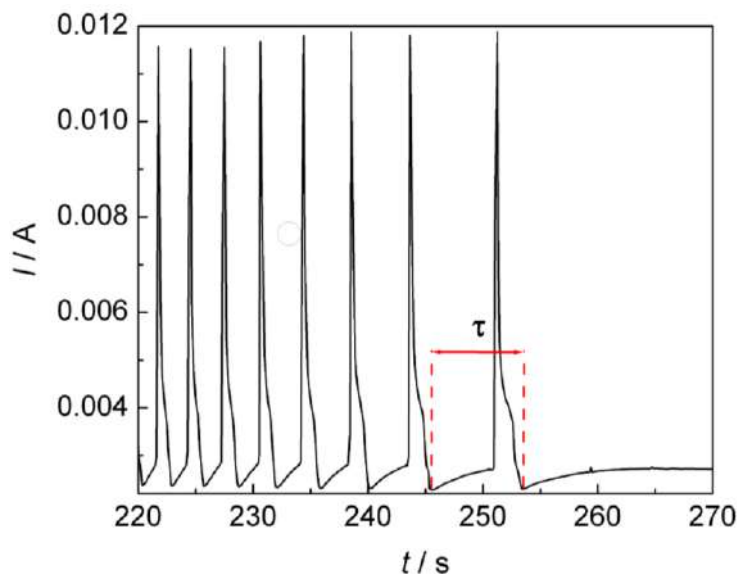


**Figure 4** Detail from  $I$ - $E$  polarization curve, Figure 1, in the vicinity of the OsS→SSS2 transient (units of x-axis are converted from potential to time)



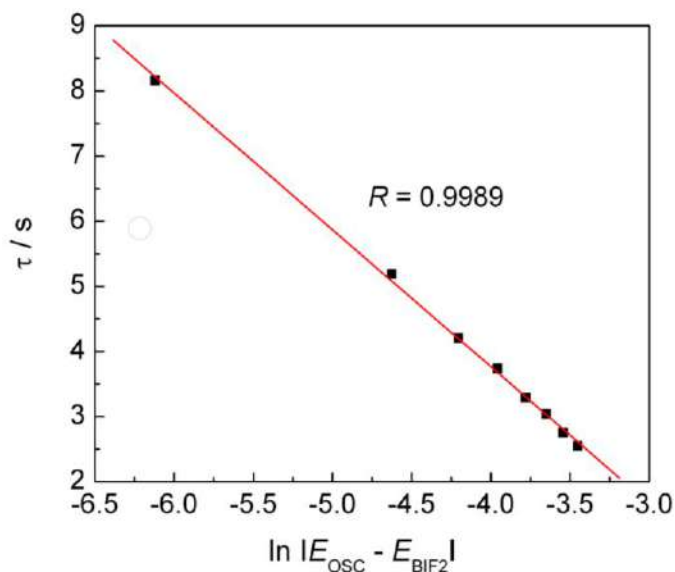


**Figure 5** Semilogarithmic plot of the period current oscillations ( $\tau$ ) vs. the distance of controllable parameter from  $E_{BIF2}$  ( $\ln |E_{OSC} - E_{BIF2}|$ )

## CONCLUSION

In this study, a voltammetric data, obtained from quasi-potentiostatic polarization curve of the Cu | 1M TFA electrochemical oscillatory system, were used for bifurcation analysis. This was based on the presumption that voltammogram can be considered as a phase space diagram. Results presented have showed that bifurcation scenario can be built from voltammetric data with a high accuracy.

## ACKNOWLEDGEMENT

*This research was funded by the Ministry of Science, Technological Development and Innovation of the Republic of Serbia [grant number: 451-03-66/2024-03/200017].*

## REFERENCES

- [1] Zinan X., Zuohua L., Changyuan T., *et al.*, J. Mater. Res. Technol. 18 (2022) 4804–4815.
- [2] Krischer K., Mazouz N., Grauel P., Angew. Chem. 40 (2001) 850–869.
- [3] Koper M.T.M, J. Chem. Soc. Faraday Trans. 94 (1998) 1369–1378.
- [4] Sazou D., Pagitsas M., J. Electroanal. Chem. 451 (1998) 77–87.
- [5] Potkonjak N., React. Kinet. Mech. Catal. 123 (2018) 155–163.
- [6] Pagitsas M., Diamantopoulou A., Sazou D., Electrochim. Acta 47 (2002) 4163–4179.



## EVALUATION OF THE HYDROGEN DIFFUSION COEFFICIENT IN METAL HYDRIDE BATTERIES

Mirjana Marković<sup>1</sup>, Đuro Čokeša<sup>1</sup>, Nebojša Potkonjak<sup>1\*</sup>

<sup>1</sup>Institute of Nuclear Sciences, National Institute of the Republic of Serbia,  
University of Belgrade, Mike Petrovica Alasa 12–14, 11000 Belgrade, SERBIA

\*[npotkonjak@vin.bg.ac.rs](mailto:npotkonjak@vin.bg.ac.rs)

### Abstract

*In this study, the hydrogen diffusion coefficient in the metal hydride electrode having composition of  $LmNi_{3.55}Co_{0.75}Mn_{0.4}Al_{0.3}$  was determined by using cyclic voltammetry. Results are presented to show that the hydrogen diffusion coefficient increases with increasing of the depth of discharge.*

**Keywords:** hydrogen, diffusion, metal hydride, batteries.

### INTRODUCTION

The rechargeable nickel-metal hydride (Ni-MH) batteries operating with hydrogen storage alloys as a negative electrode material have been broadly investigated, developed and commercialized [1]. Several families of thermodynamically stable intermetallic compounds, such as AB, AB<sub>2</sub> and AB<sub>5</sub> (A, rare-earth or transition element; B, transition element) have been intensively places in focus of research and industrial application [1]. During the charge process of MH electrode, electrolytically generated hydrogen atom at the electrode/electrolyte interface diffuses into a bulk of alloy, where it is stored in the metallic lattice in the form of hydride [2]. Discharge process includes diffusion of hydrogen from the bulk of alloy back to the surface, where it will be oxidized. The performance of the MH electrode is determined by both: the charge transfer kinetics of hydrogen at the electrode/electrolyte interface and the rate of hydrogen diffusion within the bulk of electrode [1–3]. The hydrogen diffusion coefficient is an important parameter to understand the diffusion process within the MH electrode. Generally, the large is the hydrogen diffusion coefficient, the faster is the hydrogen diffusion and the better is the electrode performance. Aim of present study is to use cyclic voltammetry for determination of the hydrogen diffusion coefficient in an AB<sub>5</sub> type hydrogen storage alloy as a function of the depth of discharge (DOD).

### MATERIALS AND METHODS

The intermetallic compound,  $LmNi_{3.55}Co_{0.75}Mn_{0.4}Al_{0.3}$  (Lm - 51 wt.% La, 33 wt.% Ce, 12 wt.% Nd and 4 wt.% Pr), was prepared from constituent metals by the arc-melting method. Resulting ingot was inverted and remelted, followed by an annealing treatment. The ingot was mechanically pulverized and ground into a fine powder (275–325 mesh). The alloy electrode was prepared by mixing the intermetallic powder with carbonyl nickel. Polytetrafluoroethylene (PTFE) dispersion was used as a binder. The mixture was filled into a

double nickel mesh and cold-pressed into pellets. The working electrode was placed in the main compartment of the cell together with a Hg/HgO, 6M reference electrode. Ni(OH)<sub>2</sub>/NiOOH was used as the counter electrode. The electrolyte was a 6M KOH aqueous solution. The metal hydride electrode was activated by galvanostatic charge/discharge at  $\pm 60 \text{ mA g}^{-1}$  at 293 K. The electrode was fully charged at  $-60 \text{ mA g}^{-1}$  for 5 h (corresponding to 0 % of DOD). Thereupon, the MH was discharged at  $60 \text{ mA g}^{-1}$  for a certain period of time to reach a specified DOD. After that, the electrode was kept under the open-circuit conditions until the equilibrium potential was reached. After that, cyclic voltammetry measurements were performed at various scan rates: 10, 15, 20, 35 and  $50 \text{ mV s}^{-1}$ . All electrochemical experiments were performed using a Solartron SI 1286 electrochemical interface, supported with corrosion measurement software (CorrWare®).

## RESULTS AND DISCUSSION

The cyclic voltammograms of the  $\text{LaNi}_{3.55}\text{Co}_{0.75}\text{Mn}_{0.4}\text{Al}_{0.3}$  metal hydride electrode were recorded at various DOD (0, 5, 10, 20, 50, 80, 90, 95, 98 and 99%) and scan rates. In Figure 1 are presented the cyclic voltammograms of the MH electrode at 0% of DOD. The broad peak which can be observe between  $-0.6 \text{ V}$  and  $-0.4 \text{ V}$  is attributed to the mass transfer and charge transfer of adsorbed hydrogen in the bulk of the investigated MH alloy. The shift of the peak towards less negative values with the increase of a scan rate can be observed. Also, it was noticed that the peak current density ( $j_p$ ) increases with the scan rate. When the diffusion process is the rate determining step, the peak current density observed is proportional to: the hydrogen concentration ( $C_H$ ), square root of the scan rate ( $v^{0.5}$ ), the hydrogen diffusion coefficient ( $D_H$ ), the surface area of the MH electrode ( $S$ ), the charge transfer number ( $n$ ), the number of electrons transferred up to and including the rate determining step ( $n_\alpha$ ), the transfer coefficient ( $\alpha$ ).

Generally, values of all variables, except for  $D_H$ , are known or can be determined by some other technique. So, the slope of the linear dependence of  $j_p$  versus  $v^{0.5}$  can be used for determination of  $D_H$  (Figure 2).

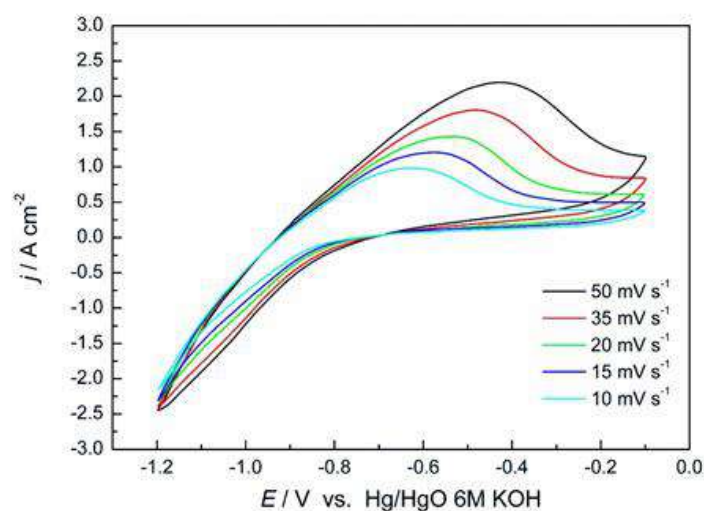


**Figure 1** Cyclic voltammograms of MH electrode at 0% DOD

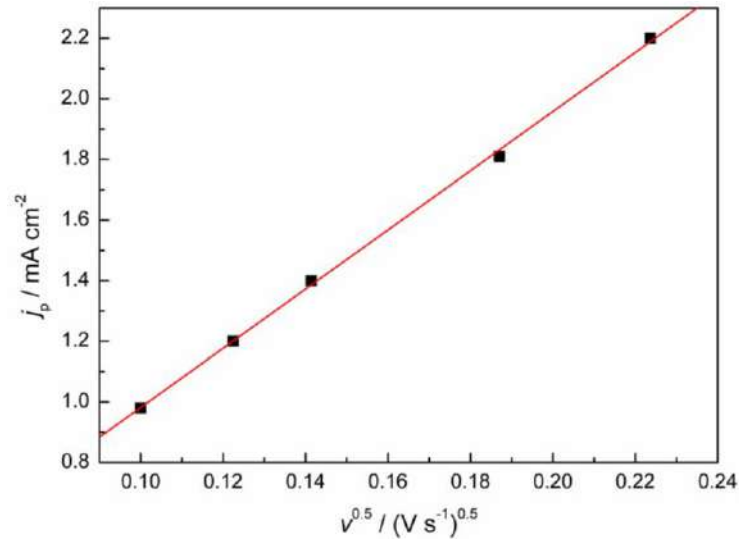


**Figure 2** Detail from I-E polarization curve, Figure 1, in the vicinity of the SSSI→OsS transient

It was found that the hydrogen diffusion coefficient increases with increasing DOD (Figure 3). The existence of two slopes in DH vs. DOD dependence has suggested that hydrogen diffusion is strongly related with the type of hydride phase existing in the metal hydride electrode. Namely, at low or medium DOD hydrogen has to overcome structural transformation from  $\beta$  to  $\alpha$  hydride phase but also the existence of hydrogen–hydrogen and hydrogen–intermetallic interactions before diffusion. Consequently, the hydrogen diffusion will be affected. At high DOD ( $\geq 90\%$ ) hydrogen exists absorbed into MH alloy only through  $\alpha$  solid solution phase. So, the diffusion is not affected by hydride phase structural transformation or hydrogen–hydrogen interactions, which results in noticeable increase of the hydrogen diffusion coefficient.

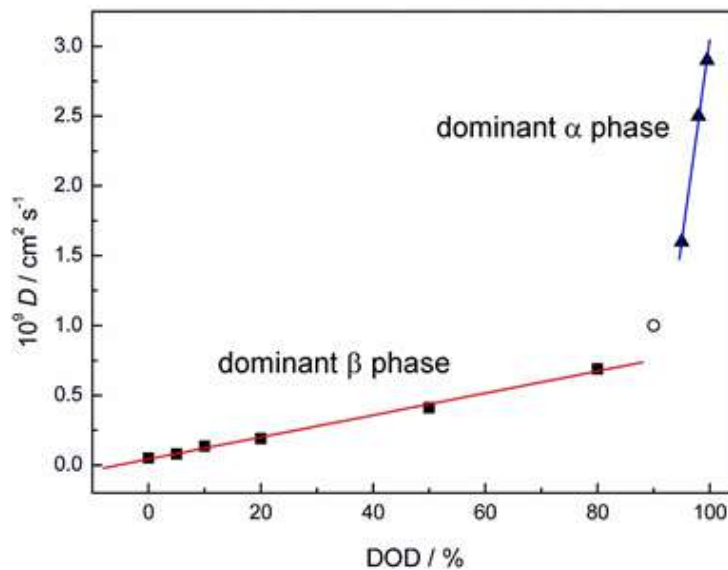


**Figure 3** Hydrogen diffusion coefficient in MH electrode as a function of DOD at 293 K

## CONCLUSION

The hydrogen diffusion coefficient in  $\text{LmNi}_{3.55}\text{Co}_{0.75}\text{Mn}_{0.4}\text{Al}_{0.3}$  was found to be in the range from  $4.72 \cdot 10^{-11} \text{ cm}^2\text{s}^{-1}$  to  $2.91 \cdot 10^{-9} \text{ cm}^2\text{s}^{-1}$ . The diffusion coefficient of hydrogen was found to increase with increasing depth of discharge, with the significant increase at the depth of discharge  $\text{DOD} > 90\%$ . This behaviour can explain in following direction: at low DOD the diffusion of hydrogen is under strong influence of hydride phase structural transformation or hydrogen–hydrogen interactions, these influences are absent at high DOD.

## ACKNOWLEDGEMENT

*This research was funded by the Ministry of Science, Technological Development and Innovation of the Republic of Serbia [grant number: 451-03-66/2024-03/200017].*

## REFERENCES

- [1] Raju M., Anath M.V., Vijayaraghavan L., *Electrochim. Acta* 54 (2009) 1368–1374.
- [2] Potkonjak N.I., Blagojevic B.N., Suznjevic D.Z., *J. Alloys Compd.* 484 (2009) 689–692.
- [3] Ben Moussa M., Abdellaoui M., Mathlouthi H., *et al.*, *J. Alloys Compd.* 407 (2006) 256–262.



## FORESTS UNDER THREAT: IMPLICATIONS OF CLIMATE CHANGE ON SERBIAN WOODLANDS

Slobodan Milutinović<sup>1\*</sup>, Tamara Rađenović<sup>1</sup>, Snežana Živković<sup>1</sup>

<sup>1</sup>University of Niš, Faculty of Occupational Safety, Čarnojevića 10a, 18000 Niš, SERBIA

\*slobodan.milutinovic@zrfak.ni.ac.rs

### Abstract

*Climate change and human activities jeopardize the sustainability and resilience of forest ecosystems in Serbia, impacting biodiversity, forest resources, and the economy. Climate change poses significant threats to forest ecosystems in Serbia, including shifts in forest boundaries, changes in tree species distribution, and modifications in plant communities. The projected effects have direct implications for biodiversity conservation and the need for sustainable forest management practices. Various tree species in Serbia, such as oak, beech, fir, spruce, and pine, are vulnerable to climate change. Their habitats are expected to decrease, leading to potential habitat loss and reduced growth. Drought periods and extreme weather events contribute to the vulnerability of forest ecosystems, causing drying, loss of vitality, and increased incidence of pests and diseases. Deforestation, clear-cutting, and excessive wood use for fuel and timber industries pose additional threats to forest cover and genetic resources. Soil erosion, influenced by climate factors and irrational land use, is a concern, particularly in areas with low rainfall. Forest fires are also a growing concern, with the number of incidents increasing since 2000. The length of the fire season and the occurrence of extreme events are expected to rise, posing a significant risk to temperate forests. Regions such as Zapadnobački, Severnobački, Severnobanatski, Srednjebanatski, Podunavski, Šumadijski, Rasinski, Nišavski, Toplički, Jablanički, and Pčinjski districts are identified as the most vulnerable to climate change impacts due to their natural characteristics, infrastructure, forest resources, and economic development. Mitigation and adaptation measures, including afforestation, improved forest management, and conservation efforts, are necessary to mitigate the adverse effects of climate change on forests.*

**Keywords:** forests, climate change, Serbia.

### INTRODUCTION

Forests play an indispensable role in the realm of climate change adaptation and mitigation strategies, encompassing several pivotal dimensions that underscore their significance. This paper delves into the multifaceted contributions of forests in addressing the challenges posed by climate change. Firstly, through the process of carbon sequestration, forests emerge as crucial carbon sinks on Earth, actively absorbing carbon dioxide via photosynthesis and storing carbon within their biomass and soils, thereby mitigating the detrimental effects of greenhouse gases and the greenhouse effect [1,2]. Additionally, forests offer a diverse array of ecosystem services that bolster climate change adaptation efforts [3], including the regulation of water flows, prevention of soil erosion, and preservation of ecosystem stability. Moreover, by serving as natural shields against extreme weather occurrences like floods and storms,



forests play a pivotal role in reducing the impacts of such events and safeguarding communities. Furthermore, the conservation of biodiversity within forest ecosystems is paramount, given their role as habitats for a substantial portion of terrestrial biodiversity. Preserving these ecosystems ensures the protection of a myriad of plant and animal species critical for fostering ecosystem resilience and facilitating adaptation to evolving climatic conditions [4,5]. Sustainable land management practices within forests are integral to enhancing their resilience and sustainability. Techniques such as afforestation, reforestation, and agroforestry empower strategic management approaches that augment carbon sequestration, preserve soil fertility, and promote sustainable land utilization practices [6,7]. Notably, forests also play a pivotal role in nurturing climate-resilient communities, particularly in rural settings, by providing livelihoods, fostering sustainable resource utilization, and encouraging local engagement in decision-making processes. Moreover, in urban environments, forests aid in mitigating the urban heat island effect by offering shade, reducing heat absorption by structures, and enhancing air quality through the absorption of pollutants. Lastly, the significance of forest conservation and sustainable management is underscored by international agreements such as the United Nations Framework Convention on Climate Change (UNFCCC) and the Paris Agreement, which highlight the pivotal role of forests in climate change mitigation and adaptation strategies, thereby fostering international collaboration and support for sustainable forest management practices. In essence, this paper elucidates the critical importance of forests in the realm of climate change adaptation and mitigation, emphasizing their multifaceted contributions to ecosystem health and human well-being, and advocating for their preservation and sustainable management on a global scale.

Based on the data derived from the 2018 CORINE Land Cover dataset, the forested area within the Republic of Serbia (excluding the region of AP Kosovo and Metohija) is officially documented at 2,380,917 hectares, constituting approximately 30% of the nation's total land area [8]. Conversely, analysis utilizing SPOT5 satellite imagery suggests a larger forested expanse of around 2,654,000 hectares, representing a proportion of roughly 35% of the territorial extent [8]. Within this delineated forested region, deciduous forests encompass the majority at 92%, followed by coniferous forests at 6%, with mixed forests contributing 2% to the total coverage.

Detailed assessments conducted by the Forest Inventory in conjunction with the Ministry of Agriculture, Forestry, and Water Management - Forestry Directorate reveal that boreal forests, encompassing broad-leaved and mixed forests typical of temperate zones, emerge as the dominant forest type, constituting a substantial 91.27% of the overall forested landscapes. Notably, oak forests and beech forests are identified as the primary constituents within this classification, representing 32% and 29.3%, respectively.

Serbia's ecological classification aligns with forest biomes, signifying that the inherent environmental conditions facilitate the proliferation of primary climate forest vegetation across a significant 85% of its land surface. Over the temporal span from 1953 to 2012, the forested area witnessed a notable expansion exceeding one million hectares or a remarkable 75% surge. In stark contrast, the subsequent period from 2000 to 2013 recorded a marginal increment of merely 6,000 hectares, translating to a nominal growth rate of 0.001% [9]. Recent trends underscore a discernible reduction in forest coverage within specific regions of

Serbia, notably observed in locales such as Srem, Peć, West Bačka, and Kosovo-Pomoravlje districts [10]. Recognizing the pivotal role of forest ecosystems in environmental preservation, strategic initiatives involving afforestation with resilient species, enhancement of forest conditions, and the adoption of adaptive forest management practices hold promise in ameliorating the adverse repercussions of climate change within these landscapes.

### IMPACT OF CLIMATE CHANGE ON FORESTS AND FORESTRY IN SERBIA

Significant forested areas in Serbia have faced threats in recent years. Oak trees in Vojvodina have experienced drying and loss of vitality due to prolonged drought periods, while forested areas have been devastated by ice storms in eastern Serbia and spruce trees have dried out in coniferous areas after particularly warm and dry years. Monitoring and analysis results indicate the vulnerability of the most significant forest species: pedunculate oak (*Quercus robur*) (the most affected as it also depends on groundwater levels that are increasingly declining), beech, sessile oak (*Quercus petraea* (Matt.) Liebl.), hornbeam (*Carpinus betulus*), fir (*Abies Alba* Mill.), and spruce (*Picea abies*). These tree species, given their economic and ecological importance, as well as their spatial distribution, represent the most significant segment of forestry in the Republic of Serbia. Similar to most forests in Europe, the area covered by beech forests in Serbia is expected to decrease from 56% to 58% by 2100 [11]. Likewise, a reduction in the area covered by Turkey oak (*Quercus cerris*), pedunculate oak, and sessile oak is expected. The decrease in the distribution of Turkey oak could reach one-third of its current habitat or even 48% by the end of the 21<sup>st</sup> century. The area covered by pedunculate oak could potentially decrease by 61% to 70%, while the decrease for sessile oak is projected to be 50% to 63% [12]. Increasing drought periods will be one of the reasons for the reduction in the area covered by sessile oak due to its sensitivity to drought. In contrast to the mentioned species, potential expansion of habitat for Hungarian oak (*Quercus frainetto* Ten.) by as much as 66% is expected due to its ability to thrive in dry conditions [13]. Significant reductions in distribution are also expected for silver fir. The distribution of fir, spruce, and pine (black pine - *Pinus nigra* JF Arnold; Scots pine - *Pinus sylvestris*) forests is also expected to decrease [12]. The projected reduction in the distribution of fir forests by the end of the century ranges from one-fifth to one-third of their current habitat, while spruce forests are projected to decrease by 70% to 77%, and pine forests are likely to decrease by 22% to 31%. The area covered by Scots pine is expected to decrease, while black pine would remain in most of its current range. Studies on the potential impact of climate change on forests in Serbia using climate indices (FAI drought index and Elenberg index) indicate that from the middle (2041–2070) to the end of the 21<sup>st</sup> century (2071–2100), assuming the realization of the RCP4.5 climate model, the rate of habitat loss for fir and spruce populations will be relatively small (up to 25%) and constant [14]. These changes are expected to occur along the eastern and southern “boundaries” of their distribution at lower altitudes. On the other hand, slightly higher rates of reduction (up to 35%) are expected for beech and black and Scots pine forests in the south and southeast of Serbia, to a lesser extent, and for beech forests only in the east and west. A slight expansion of suitable habitats for Scots and black pine can be expected in eastern Serbia. According to the RSP8.5 climate model, by 2070, 55% (based on the FAI drought index) or 75% (based on the Elenberg index)

of the total area covered by beech, fir, spruce, and black and Scots pine forests is projected to remain unaffected by altered climatic conditions [14], with coniferous forests in southeastern and eastern Serbia being the most vulnerable. From 2070 to the end of the century, a decrease in habitat for fir, spruce, black and Scots pine, and beech forests is expected, ranging from 75–85% (based on the Elenberg index) to 90–100% (based on the FAI index).

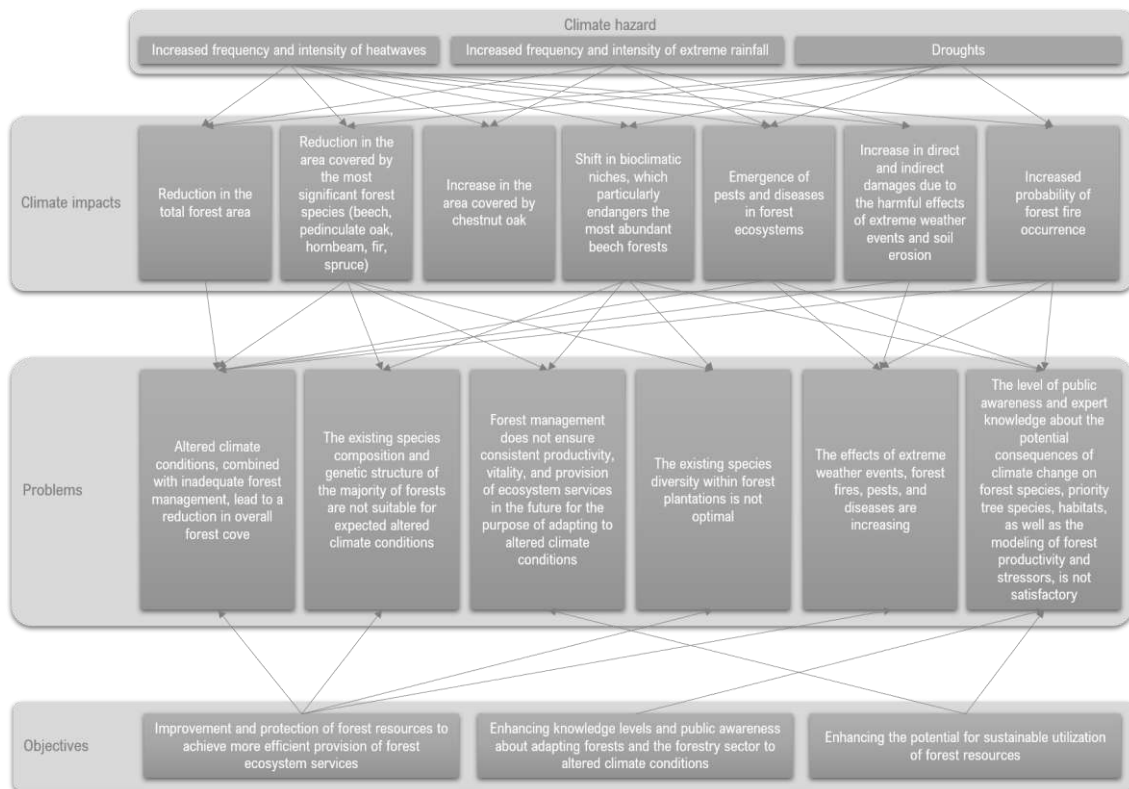


**Figure 1** Interdependence of climate hazards, impacts of climate change, issues they bring to forests and forest management, and potential adaptation goals in Serbia

By the end of the century, the bioclimatic conditions will be significantly altered across the entire territory of Serbia. Research indicates that the values of the FAI (Drought Index) will increase to above 15 in some parts of the country, compared to its value of below 10 during the reference period of 1961–1990. In the period from 2011 to 2040, the bioclimatic conditions in most of Vojvodina will be equivalent to the conditions in most arid parts of North Banat. The increased aridity resulting from changes in precipitation patterns and temperature rise will have pronounced negative effects on the changes in bioclimatic niches. This will undoubtedly lead to significant changes in the bioclimatic niches of most tree species. The most vulnerable will be the pedunculate oak due to the extreme habitat change, while drought-resistant species (such as pine and turkey oak) will be less threatened. The sessile oak, hornbeam, fir, spruce, and beech will be outside their 20<sup>th</sup>-century bioclimatic niches before the end of the 21<sup>st</sup> century [15]. It can be expected that by the end of the 21<sup>st</sup> century, around 90% of today's beech forests will be outside their bioclimatic niche of the 20<sup>th</sup> century, with around 50% being in the zone where mass mortality is expected. Considering that beech forests are predominantly found at elevations ranging from 500 to 1000 meters above sea level, where the conditions for beech growth were most favorable during the period

from 1961 to 1991, and that the optimal habitats are likely to shift to elevations of 750 to 1250 meters above sea level during the period from 2041 to 2070 due to the altered climate conditions [16], given that beech cannot migrate to higher elevations within such a short time span, a decrease in growth, drying, and habitat loss of beech at lower elevations can be expected.

Climate change is anticipated to have substantial repercussions on forest ecosystems, particularly regarding the occurrence of pests and diseases. Although there's no clear-cut evidence linking pests and diseases directly to climate change, the warming of temperate forests and the intensification and prolongation of droughts are expected to play pivotal roles. Climate change influences various aspects of tree disease development, including host susceptibility, pathogen virulence, and environmental conditions conducive to disease propagation. For instance, higher temperatures accelerate the development rates of herbivorous insects like the oak lace bug (caused enormous ecological damage, mainly negatively impacting natural forest regeneration in Serbia in 2013), and bark beetles, leading to increased ecological damage and tree mortality. Serbia has experienced significant losses due to outbreaks of pests like the spruce bark beetle and the six-toothed spruce bark beetle, contributing to ecological and economic setbacks. Furthermore, altered climate conditions may indirectly affect disease vectors and biological control agents, potentially amplifying the abundance of pathogens and their transmission vectors (such as scale insects, certain bark beetles, fungi from the genus *Neonectria* spp. and *O. ulmi*, phytopathogenic viruses, phytoplasmas, phytopathogenic nematodes, etc.).

Increasingly frequent and prolonged droughts and extreme weather will heighten soil erosion damage. Pluvial erosion, prevalent in Serbia due to its rugged terrain and reduced forest cover, primarily affects sloping areas. Despite rainfall being a key factor in erosion, regions most impacted by erosion, like the South Morava River basin, don't necessarily have the highest rainfall. These areas suffer from various negative climate effects and poor land management practices. Climate-vulnerable regions, already struggling with forestation and the benefits forests offer, will face amplified challenges. This decline in forest health will detrimentally affect forestry sectors and related rural economies.

Certain regions in Serbia face heightened pressure due to a combination of altered climatic conditions, natural characteristics, infrastructure, forest resources, and economic development. Vulnerability analyses highlight the following districts: Zapadnobački, Severnobački, Severnobański, Srednjebański, Podunavski, Šumadijski, Rasinski, Nišavski, Toplički, Jablanički, and Pčinjski [10]. These areas, already at risk in terms of forestation and benefiting from ecosystem services provided by forests, are expected to bear the brunt of climate change impacts.

The vulnerability of forests to altered climatic conditions is increasing due to the increased likelihood of forest fires. The influence of weather conditions on the behavior and spread of forest fires is well documented [17]. Key climatic factors influencing forest fire danger include air temperature, precipitation, humidity, wind, and drought. Larger fires can devastate ecosystems, prompting species migrations. Soil moisture, particularly organic matter, can hinder fire spread and ignition. Since 2000, Serbia has seen a rise in forest fires, with longer seasons and more extreme events expected. By the century's end, temperate forests may face

escalating fire risks due to decreased summer rainfall, rising temperatures, and drought. The most severe wood loss from fires occurred in 2012 (63,000 m<sup>3</sup>), 2003 (48,000 m<sup>3</sup>), and 2016 (47,000 m<sup>3</sup>). Disturbances caused by fires facilitate the spread of invasive species (boxelder maple - *Acer negundo*), false indigo (*Amorpha fruticosa*), tree of heaven (*Ailanthus altissima* /Mill./ Swingle), and black locust (*Robinia pseudoacacia*) in central Serbia, along with hackberry (*Celtis occidentalis*), green ash (*Fraxinus pennsylvanica* Marsh.), honey locust (*Gleditsia triachantos*), black cherry (*Prunus serotina* Ehrh.), and Siberian elm (*Ulmus pumila*) in Vojvodina), outcompeting native plants and destabilizing ecosystems. Forest management strategies like thinning, vegetation removal, and diverse tree planting can mitigate fire risks. Forest fires also impact air quality and the environment locally and beyond.

Climate change and global warming also significantly affect forestry sector production. This industry contributes 0.3% to Serbia's GDP. Scenarios indicate a clear impact of climate change on forest production. With a 3°C temperature rise, the forestry industry's additional gross value is projected to decrease annually by 0.020% by 2027, 0.300% by 2037, 0.608% by 2067, and 1.645% thereafter [18]. Adhering to the Paris Agreement's temperature limits (up to 2°C), it's anticipated that production losses in the forestry industry will reach \$10.674 billion from 2020 to 2040, escalating to \$216.247 billion by the century's close. Doubling the global temperature would triple these losses.

## CONCLUSION

Forests are essential for climate change adaptation and mitigation efforts. They contribute to carbon sequestration, provide crucial ecosystem services, conserve biodiversity, support sustainable land management, empower communities, mitigate the urban heat island effect, and align with global climate change agreements. Protecting and sustainably managing forests are key components of comprehensive climate action plans.

The influence of climate change on forest ecosystems can trigger notable alterations in their composition, structure, and spatial distribution. Within the context of Serbia, the foreseen adverse effects of climate change on forests encompass a spectrum of dimensions. These encompass anticipated transformations such as potential shifts in the geographic latitude and altitude boundaries of specific forest types, modifications in the light requirements of select tree species, changes in the natural distribution patterns of forest types in correlation to each other, potential retreat and extinction of distinct communities, and adjustments in the makeup of plant communities spanning vegetation strata and social hierarchies, among other factors. Significant forested areas in Serbia are under threat, with various tree species experiencing drying, loss of vitality, and habitat reduction due to climate change-induced factors such as prolonged drought periods, ice storms, and warmer, drier conditions. The vulnerability of key species like pedunculate oak, beech, sessile oak, hornbeam, fir, and spruce poses significant challenges to forest ecosystems and the forestry sector. Vulnerable species such as pedunculate oak are particularly at risk due to extreme habitat changes. Furthermore, climate change is expected to exacerbate pest and disease outbreaks, increase soil erosion, and heighten the risk of forest fires, further impacting forest health and ecosystem stability. Zapadnobački, Severnobački, Severnbanatski,



Srednjobanatski, Podunavski, Šumadijski, Rasinski, Nišavski, Toplički, Jablanički, and Pčinjski districts, characterized by a combination of altered climatic conditions, natural characteristics, and economic development, are particularly vulnerable to the impacts of climate change on forests. Envisaged impacts carry direct implications for biodiversity preservation and underscore the imperative of embracing informed forest resource management practices. Furthermore, they intricately shape the viability and intensity of implementing sustainable forest management strategies.

Production losses in the forestry industry are projected to escalate under different climate scenarios, highlighting the importance of implementing adaptive measures and policies to sustainably manage forest resources and mitigate economic losses.

Overall, the findings underscore the urgent need for comprehensive strategies to mitigate the impacts of climate change on Serbian woodlands, including conservation efforts, sustainable forest management practices, and adaptation measures to safeguard forest ecosystems and the associated socio-economic benefits they provide.

## ACKNOWLEDGEMENT

*This paper is a part of the research funded by the Ministry of Science, Technological Development and Innovation of the Republic of Serbia pursuant to the agreement No. 451-03-66/2024-03/ 200148. Part of this paper is based upon work from the COST Action “CA20138: Network on water-energy-food nexus for a low-carbon economy in Europe and beyond – NEXUSNET”, supported by COST (European Cooperation in Science and Technology).*

## REFERENCES

- [1] Pan Y.B., Birdsey R.A., Fang J., *et al.*, *Science* 333 (6045) (2011) 988–993.
- [2] Poorter L., Bongers F., Aide T.M., *et al.*, *Nature* 530 (7589) (2016) 211–214.
- [3] Lohbeck M., Poorter L., Martinez-Ramos M., *et al.*, *Ecology* 96(10) (2015) 2626–2639.
- [4] Lindenmayer D.B., Franklin J.F., Fischer J., *et al.*, *Biol. Conserv.* 14(9) (2008) 1871–1884.
- [5] Barlow J., Lennox G.D., Ferreira J., *et al.*, *Nature* 535 (7610) (2016) 144–147.
- [6] FAO, *Global Forest Resources Assessment 2015: How are forests changing?*, Food and Agriculture Organization of the United Nations, Rome (2018).
- [7] Reed M.S., Buenemann M., Althopheng J., *et al.*, *Land Degrad. Dev.* 27(3) (2016) 814–826.
- [8] Agencija za zaštitu životne sredine, *Privredni potencijali i aktivnosti od značaja za životnu sredinu Republike Srbije 1019. godine: Indikatorski prikaz*, Ministarstvo zaštite životne sredine Republike Srbije, Beograd (2021).
- [9] Agencija za zaštitu životne sredine, *Indikatori životne sredine, 2024. Available on the following link: <http://indicator.sepa.gov.rs/pretrazivanje-indikatora/indikatorilat/svefind/5cd5fd0a8a944df482165e2f246e9e98>*.
- [10] Stojanović D., Orlović S., *Izveštaj o uticaju klimatskih promena na sektor šumarstva, sa predlogom mera adaptacije, 2022, Available on the following link:*



<https://adaptacije.klimatskepromene.rs/wp-content/uploads/2022/03/Sumarstvo-Uticaj-klimatskih-promena-na-sektor-sumarstva.pdf>

- [11] Pavlović L., Stojanović D., Mladenović E., *et al.*, *Front. Plant. Sci.* 10(849) (2019) 1–8.
- [12] Stojanović D., *Topla 208* (2021) 39–56.
- [13] Apostol E.N., Stuparu E., Scarlatescu V., *et al.*, *iForest - Biogeosciences and Forestr.* 13(1) (2020) 9–15.
- [14] Miletić B., Orlović S., Lalić B., *et al.*, *Austrian J. For. Sci.* 138(3) (2021) 183–208.
- [15] Stojanović D.B., Matović B., Orlović S., *et al.*, *SE Eur For.* 5(2) (2014) 117–124.
- [16] Pavlović L., Stojanović D., Mladenović E., *et al.*, *Front. Plant Sci.* 10 (2019) 849.
- [17] Flannigan M.D., Wotton B., *Climate, weather, and area burned in Forest Fires: Behavior and Ecological Effects*, Editors: Johnson E.A., Miyjanishi K., Academic Press, San Deigo (2001), p.351–373, ISBN: 9780080506746.
- [18] UNDP, *Study on the Socio-economic Aspects of Climate Change in the Republic of Serbia*, UNDP Serbia, Belgrade (2019).



## GLOBAL WARMING – TREND ANALYSIS IN THE REPUBLIC OF SERBIA

Danijela Nikolić<sup>1</sup>, Saša Jovanović<sup>1\*</sup>, Zorica Đorđević<sup>1</sup>, Davor Končalović<sup>1</sup>,  
Vladimir Vukašinić<sup>1</sup>

<sup>1</sup>Faculty of Engineering, University of Kragujevac, Sestre Janjić 6, 34000 Kragujevac,  
SERBIA

\*dviks@kg.ac.rs

### Abstract

*Global warming, as part of general climate change, has certainly become an undeniable fact. An increasingly small part of the scientific and professional population denies this dramatic change in one of the most important parameters of the Earth's climate system, as well as the causes that encourage this process. The trend of temperature increase, as expected, varies to a certain extent in different parts of our planet. In this paper, an appropriate analysis of the temperature increase in the territory of the Republic of Serbia from the middle of the last century until today was performed. At the same time, as part of the analysis, a comparison was made with the global change. In the end, the city of Kragujevac was taken as a representative of the change in climate parameters in the Republic of Serbia and an analysis of the changes in the mentioned period was carried out. All the presented data indicate that climate change, and primarily Global Warming, is accelerating. This process already has serious, and with intensification can have catastrophic consequences for the living world on the planet, including humans.*

**Keywords:** climate change, Republic of Serbia, global warming, changes in climate parameters.

### INTRODUCTION

The Earth's climate system is a complex dynamic system made up of five most important components, namely the atmosphere, hydrosphere, cryosphere, lithosphere and biosphere. Part of the climate system, in addition to these components, are also the constant reactions between them. The Earth's climate, as a product of the functioning of the climate system, has experienced a number of smaller or larger, as well as faster and slower changes in the history of the planet. All these changes, until recently, were always under the influence of natural mechanisms and certain internal and external factors. If we define the influence of man on the climate, since the middle of the twentieth century, as “unnatural” (although man himself is a part of nature, his influence and activities over the last few decades have exceeded the defense mechanisms of the climate system), then this is the first period in the history of the Earth in which “unnatural” changes. The greenhouse effect is one of the natural climate regulatory mechanisms available to the Earth's atmosphere. This mechanism raises the average temperature on our planet by more than thirty degrees Celsius (compared to a hypothetical state without an atmosphere) and allows life conditions to exist in the largest part of it.

The sudden increase in the number of human population, accelerated industrialization, way of life and high energy needs cause huge emissions of gases with the greenhouse effect. These emissions exceed the natural abilities of the system to absorb them and keep them within acceptable limits. By comparing the corresponding diagrams, a clear coincidence is observed between the increase in CO<sub>2</sub> concentration and the increase in global temperature [1]. Global warming is the most significant part of overall climate change. The trend of temperature increase varies in intensity in different regions of the Earth, but the change is certainly of a general, planetary character.

### TREND OF CHANGE IN AVERAGE ANNUAL TEMPERATURES IN THE WORLD

An increase in global temperatures has been observed since the middle of the 20<sup>th</sup> century, but in recent decades, and especially in the last one, there has been an acceleration of changes. Figure 1 shows the increase in average annual temperatures by world region in the last two decades (2002–2011 and 2012–2021) measured above the land surface of the planet [2]. It is observed that the regions of Asia, Africa and North America record temperature increases at the level of the global average. Below that average, with a slightly slower rate of warming so far, are the regions of Australia and Latin America. The most significant increase in average annual temperatures is recorded on the European continent, and it is almost 50% higher than the world average, and twice as high as the Australian region.

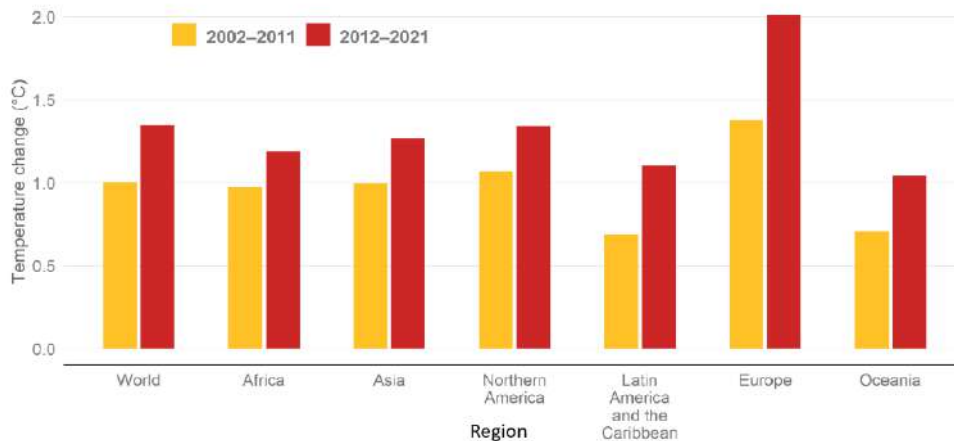


**Figure 1** Temperature changes by world regions in the last two decades  
(Source: FAO, 2022. FAOSTAT: Temperature change)

Figure 2 shows a diagram that compares the annual deviations of Tan values (average annual air temperatures), i.e. the values of GLaOATA (Global Land and Ocean Average Temperature Anomalies) and GLATA (Global Land Average Temperature Anomalies) for the period from 1850–2023. and in relation to the reference period 1901–2000 [3,8]. Due to the significantly higher inertia and heat capacity, it can be seen that the curve of global air temperature change over land including sea and ocean surfaces (GLaOATA) is significantly more stable (with a smaller amplitude of variation, as well as a smaller overall change) than

the curve that corresponds only to land areas (GLATA). In colder periods, especially in the first half century of the observed time range, the change in air temperatures over the land had a larger negative deviation compared to the global one. Similarly, in the warm period, and especially in the last few decades, the difference between the increase in air temperatures over the land compared to the ocean surfaces is rapidly increasing. A huge problem and great potential for future warming of the planet is the enormous accumulated heat in the ocean waters, especially in the surface layer (up to 700 meters deep). That new accumulated energy (period 1950–2023) is estimated (for a depth of up to 2000 meters) at about 500 Zettajoules (1 Zettajoules = 1 billion trillion joules) [4].

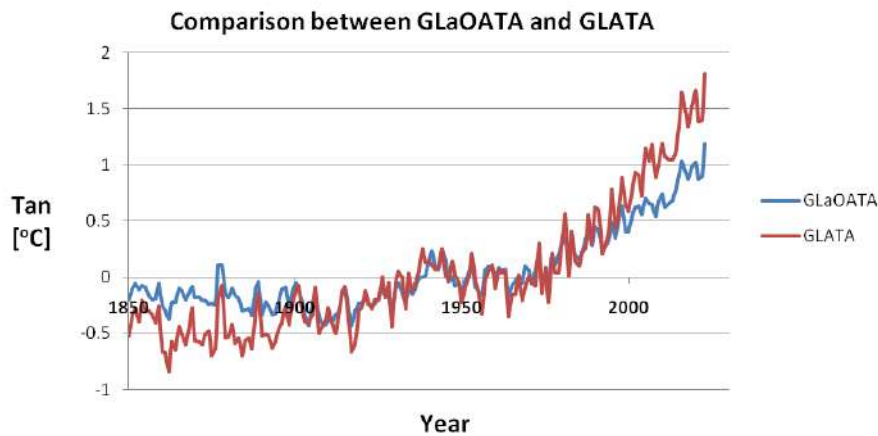


Figure 2 Comparison between values GLaOATA and GLATA

Figure 3 shows the deviations of annual mean air temperatures, namely NHLaOATA (Northern Hemisphere Land and Ocean Average Temperature Anomalies), NHLATA (Northern Hemisphere Land Average Temperature Anomalies) and EATA (European Average Temperature Anomalies). Values for NHLaOATA and NHLATA [3,8] are given for the interval 1850–2023, and the period 1901–2000 was taken as reference. For the size of EATA, data are presented for the period 1910–2023, with the reference period 1910–2000 (due to lack of earlier data).

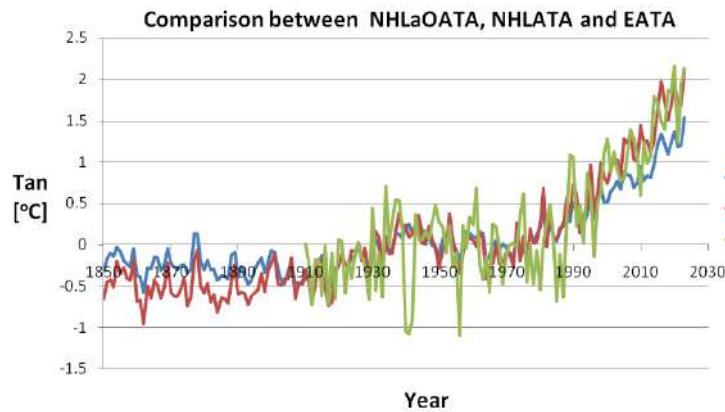
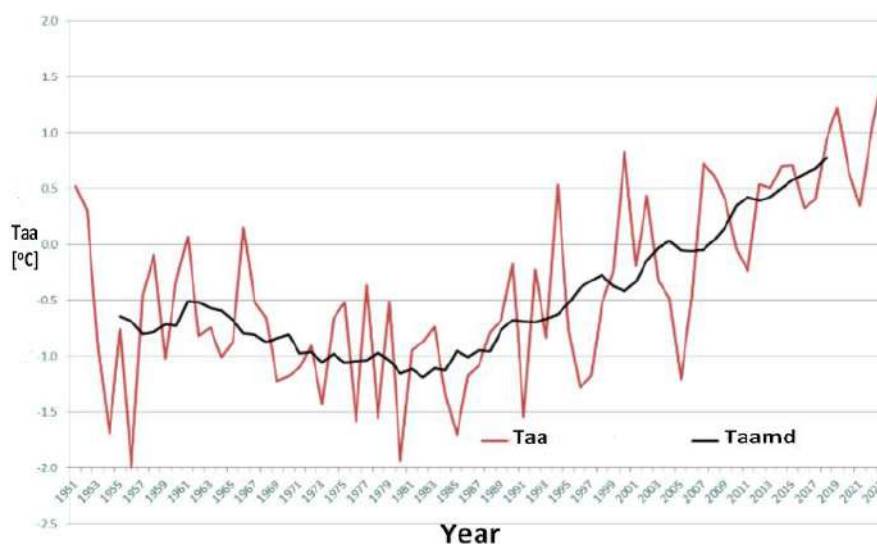


Figure 3 Comparison between values NHLaOATA, NHLATA and EATA

The relationship between the magnitudes of NHLoOATA and NHLATA roughly corresponds to the relationship already described for Figure 2 (magnitudes of GLaOATA and GLATA) When it comes to the magnitude of EATA, a significantly greater instability of mean temperatures can be observed. The reason for this probably lies in the fact that the land area is significantly smaller. And based on this diagram, it can be concluded that, especially in the last few decades, the European continent is warming at a faster rate than the rest of the Northern Hemisphere.

## CHANGES IN AVERAGE ANNUAL TEMPERATURES IN THE REPUBLIC OF SERBIA

The Republic of Serbia is located in the southeastern part of the European continent, which, according to decades of observations, has one of the highest rates of increase in average annual temperatures. The Republic of Serbia is landlocked and, until recently, most of it had a typical moderate-continental climate. The diagram shown in Figure 4 shows the deviations of the average annual temperature (Taa) calculated for the territory of the entire republic in the period 1951–2023 from the norm for the reference period 1991–2020 [5,6,7]. As in the previous diagrams, a significant increase in the displayed size can be observed here, especially in the last two decades. In the last year (2023), a deviation of 1.5°C was reached, noting that already in the reference period (1991–2020) there was an increase compared to the previous one (1961–1990) by about 1°C. This means that the total increase in average annual temperatures for the territory of the Republic of Serbia in recent years has already reached an extremely serious 2.5°C. As part of the further analysis, the city of Kragujevac was chosen, which is located in the central part of the Republic of Serbia and is located at an average altitude of about 180 meters.



**Figure 4** Deviation of the average annual temperature in Serbia in the period 1951–2023 (compared to the reference period 1991-2020; Taamd – average anomaly for the decade)

The diagram in Figure 5 shows the average annual temperatures for the city of Kragujevac (Tak) in the period 1961–2023. Here too, a very similar increase can be observed from an

average of about 11°C during the period 1961–1990, to a value of 13.6°C in 2023. Perhaps an even more obvious presentation of the trend is given in Figure 6, where the values of average annual temperatures by decade (T<sub>adk</sub>) are given, noting that the last interval refers to the last three-year period (2021–2023). To the possible remark that the three-year period is relatively short to reflect the character of the trend for the whole decade, comes the pessimistic statement that the average value of the future period of the rest of that decade (until 2030) will increase that value even more.

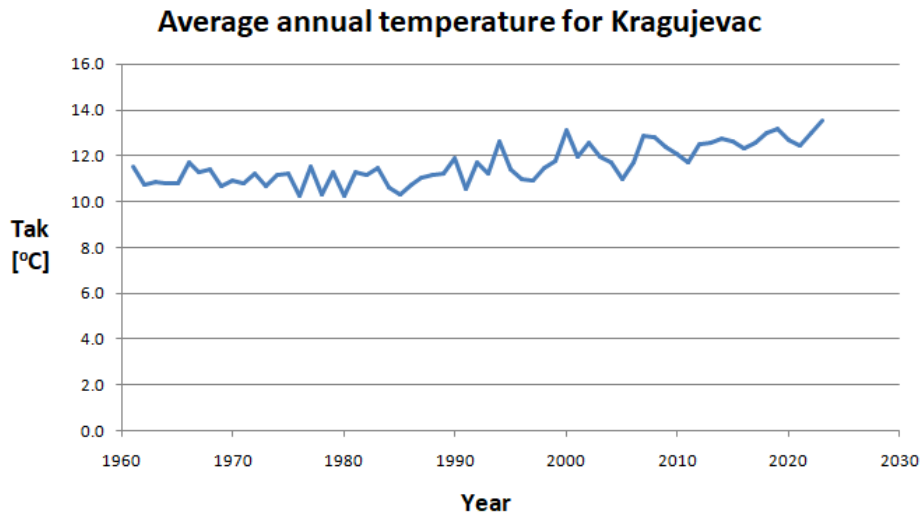


Figure 5 Average annual temperatures for Kragujevac (in the period 1961–2023)

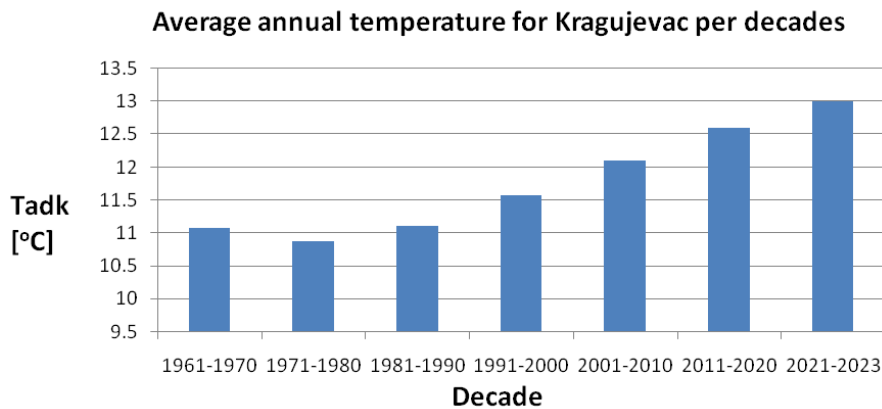


Figure 6 Average annual temperatures for Kragujevac per decades (in the period 1961–2023)

Table 1 shows the values of average summer temperatures (T<sub>asm</sub>) for three summer months (June, July and August) by decades of the observed period. The summer part of the year, both for the territory of the Republic of Serbia and for the city of Kragujevac, showed the highest degree of increase in average temperatures compared to other parts of the year [9].



**Table 1** Average temperatures for Kragujevac in the summer months (June, July and August) by decades

Decade	1961–1970	1971–1980	1981–1990	1991–2000	2001–2010	2011–2020	2021–2023
Tasm	20.2	19.6	20.1	21.4	21.9	22.3	22.9

## CONCLUSION

The climate system of the Earth as a product of its functioning forms the climate of our planet. Excessive human influence causes various disturbances in the functioning of that system, and thus leads to climate changes. Global warming is the main representative of climate change and currently the most pronounced change in one of the climate parameters. The increase in average temperatures is not uniform in all parts of the planet and in this sense there are significant differences by region. Land areas are warming faster than ocean surfaces, but the oceans have been storing enormous amounts of additional heat during recent decades that will certainly affect the future temperature regime of the planet. The European continent shows one of the fastest rates of warming, and this fact is especially true for its southeastern part, to which the Republic of Serbia belongs. The presented values of the increase in average annual temperatures for the Republic of Serbia and the city of Kragujevac indicate that in relation to the reference period 1961–1990, there was a warming of 2 to 2.5 degrees Celsius in these areas. This level of increase in average annual temperatures to an extremely serious extent can affect many aspects of human life, as well as the entire flora and fauna. What is particularly worrying is that the trend of warming the planet, and especially some of its parts, is accelerating.

## REFERENCES

- [1] Available on the following link: <https://www.co2.earth/>.
- [2] Available on the following link: <https://www.fao.org/3/cb9051en/cb9051en.pdf>.
- [3] Available on the following link: [https://www.ncei.noaa.gov/access/monitoring/climate-at-a-glance/global/time-series/globe/land\\_ocean/ytd/12/1850-2023](https://www.ncei.noaa.gov/access/monitoring/climate-at-a-glance/global/time-series/globe/land_ocean/ytd/12/1850-2023).
- [4] Available on the following link: <https://www.carbonbrief.org/state-of-the-climate-2023-smashes-records-for-surface-temperature-and-ocean-heat/>.
- [5] Available on the following link: <https://www.hidmet.gov.rs/data/klimatologija/ciril/2023.pdf>.
- [6] Available on the following link: <https://atlas-klime.eko.gov.rs/>.
- [7] Available on the following link: [https://www.hidmet.gov.rs/ciril/meteorologija/klimatologija\\_srbije.php](https://www.hidmet.gov.rs/ciril/meteorologija/klimatologija_srbije.php).
- [8] Available on the following link: <https://www.ncei.noaa.gov/access/monitoring/monthly-report/global/202213>.
- [9] Jovanovic S., Petrovic J., Nikolic D., *et al.*, Climate Changes – Trends and perspectives in the Republic of Serbia, 14. International Quality Conference, 24–27 May, Kragujevac, Serbia (2023) 1753–1760.



## CONTRIBUTION OF THE INSTITUTE FOR TECHNOLOGY OF NUCLEAR AND OTHER MINERAL RAW MATERIALS TO THE SDGS – TOWARDS INTERNATIONAL DECADE OF SCIENCE FOR SUSTAINABLE DEVELOPMENT

**Dragana Randelović<sup>1\*</sup>, Aleksandar Jovanović<sup>1</sup>, Branislav Marković<sup>1</sup>, Miroslav Sokić<sup>1</sup>**

<sup>1</sup>Institute for Technology of Nuclear and Other Mineral Raw Materials,  
Boulevard Franchet d'Esperey 86, 11000 Belgrade, SERBIA

\*[d.randjelovic@itnms.ac.rs](mailto:d.randjelovic@itnms.ac.rs)

### Abstract

*Scientific institutions could play a prominent role in solving global problems and attaining Sustainable development goals (SDG). International Decade of Science for Sustainable Development stipulates an opportunity to align research priorities and knowledge generation more effectively towards sustainability. Institute for Technology of Nuclear and Other Mineral Raw Materials (ITNMS) contributes to various SDGs through its project activities, concentrating on those that cover a range of socio-technical systems or the areas of application as well as those that promote transversal directions for system change. This paper aimed to comprehensively present Institutes' scientific projects in coordination with the set of 17 officially ratified goals of sustainable development. Obtained results are categorized according to several parameters: project realization period, institution position in the project (leader or participant), and type of the project (international or national). The Institute scientific activities possesses' good alignment with several SDGs, particularly: SDG 12 (Responsible consumption and production) and SDG 9 (Industry, innovation, and infrastructure), but also directly or indirectly with SDG 2 (Zero hunger) and SDG 3 (Good health and well-being). Additionally, ITNMS project activities contribute to the Planet, Prosperity, People and Partnership UN pillars of sustainable development. With consideration of the guidelines of International Decade of Science for Sustainable Development and Strategy for scientific and technological development of the Republic of Serbia, ITNMS may effectively contribute to the solutions for current scientific and technological problems in a way that promotes sustainable development and various SDGs in future.*

**Keywords:** ITNMS, sustainable development goals, scientific projects.

### INTRODUCTION

The paradigm of sustainable development is marking contemporary world's efforts for meeting various development targets by enabling and balancing social, economic and environmental issues. The 17 Sustainable Development Goals (SDG) presents a set of goals, targets and indicators aimed at achieving worldwide sustainability. They were adopted by the United Nations General Assembly in 2015 as part of Agenda for Sustainable Development 2030, and represent a substitute for Millennium Development Goals, taking into account the broader economic, environmental and social scope. SDGs are considered and important global transformative tool for achieving a better and more sustainable future for the planet, referring to: No poverty (SDG 1), Zero Hunger (SDG 2), Good health and well-being

(SDG 3), Quality education (SDG 4), Gender equality (SDG 5), Clean water and sanitation (SDG 6), Affordable and clean energy (SDG 7), Decent work and economic growth (SDG 8), Industry, innovation and infrastructure (SDG 9), Reduced inequality (SDG 10), Sustainable cities and communities (SDG 11), Responsible consumption and production (SDG 12), Climate action (SDG 13), Life below water (SDG 14), Life on land (SDG 15), Peace and justice strong institutions (SDG 16) and Partnership for the goals (SDG 17). Those goals are accompanied by 169 specific targets and 232 measurable indicators.

World countries are called to incorporate Agenda 2030 and SDGs into their national policies, planning instruments, strategies and finances, and provide annual Progress reports on the Implementation of SDGs. Role of government, business, research, non-profit organizations and other key stakeholders is recognized for the successful implementation of SDGs. The international science system currently produces fragmented and compartmentalized knowledge and there is a strong need to align research and development with society's urgent needs (International Science Council, 2023). Research institutions could play an important role in achieving SDGs, providing new knowledge, solutions and innovations, particularly through inter- multi- and transdisciplinary approaches, and serving as generators of ideas and solutions for complex global problems. An advance of science, technology and innovation (STI) has been observed as one of the key features guiding the society's progress. Therefore, the utilization of STI in developing the SDG roadmaps has been perceived as an advancing approach for global sustainability.

The Republic of Serbia has been committed to the attainment of the SDGs, developing a strategic framework for successful monitoring and improvement of this process within the frame of Agenda 2030. Serbia has taken the pioneering role by becoming one of the first countries in the world that use a Smart specialization approach for developing the STI for SDGs Roadmap within the UN Global Pilot Programme. Recognizing the key role of science in solving global problems and attaining SDGs, at the initiative of Serbia, the United Nations General Assembly adopted the Resolution on the International Decade of Science for Sustainable Development (IDSSD) 2024–2033. One of the imperatives of this Resolution is to set bridges across the scientific disciplines for addressing complex global problems by using a transformative multidimensional approach that provides policymakers with evidence-based analyses. Strategy for scientific and technological development of the Republic of Serbia for the period from 2021 to 2025 “The power of knowledge” [1] additionally focuses researches on social challenges and priorities that are aligned with the SDGs through mechanism of competitive financing the science, technology and innovation system, primarily through the programs of the Science Fund and the Innovation Fund of the Republic of Serbia. Scientific institutions in Serbia should align their strategies and development plans with these priorities.

The aim of this paper is to assess the contribution of the Institute for Technology of Nuclear and Other Mineral Raw Materials (ITNMS) to the SDGs and to identify the basic sustainable development goals important for the work and strategic development of the ITNMS, that, with an adequate transformative approach to STI, may contribute to more effectively solving of contemporary complex problems and achieving sustainability on national and international level.

## MATERIALS AND METHODS

Analysis and mapping of the project's direct and indirect contributions to the 17 SDG targets was done for the research projects that were implemented at ITNMS starting from 2015 forward [2,3]. The direct or indirect representation of SDGs in a total number of 33 projects was analysed, followed by several sub-criteria: projects in which the institution is the leader as opposed to those in which it is a participant; project categories (national or international). Moreover, level of representation of 17 SDGs in ITNMSs projects was identified and classified according to the frequency of occurrence.

## RESULTS AND DISCUSSION

The level of representation of SDGs in ITNMS projects was identified and classified by the frequency of occurrence in the period 2015–2024 (Table 1).

*Table 1 Level of representation of 17 SDGs in ITNMS projects in period 2015–2024*

Representation in ITNMS projects	Sustainable development goal	Criteria
Well represented	2, 3, 9, 12	>25%
Moderately represented	6, 7, 14, 15	10–20%
Low represented	4, 8, 13, 17	0–10%
Not represented	1, 5, 10, 11, 16	0%

As visible from Table 1, SDGs 2, 3, 9 and 12 are particularly well represented, confirming the prevailing institution's orientation towards enhancing scientific research to increase resource-use efficiency and promote the adoption of clean and environmentally sound technologies in industrial processes, encourage environmentally sensitive management of chemicals and wastes throughout their life cycles, significantly reduce the generation of waste through prevention, reduction, reusing and recycling. ITNMS projects outputs could also be employed for the purpose of enhancing sustainable food production and resilient agricultural practices, and, indirectly, to reduce illnesses and deaths from hazardous chemicals and pollution.

The following grouping and categorization of projects was made according to the ITNMS position in the implemented projects. Namely, the matching of projects with the SDGs was monitored, depending on whether the ITNMS had a leading role or was participating as a partner in project. Findings are presented in Figure 1. Figures a) and b) generally show similar trends. SDG 9 and SDG 12 are the most dominant in both groups, being in line with main research and development areas of ITNMSs work.

Next separation was done by the type of project (national or international), with results presented in Figure 2. Lower number of SDGs is represented in national projects (8) in comparison to the international projects (12), revealing the increased consideration of SDGs issues by projects of broader scope.

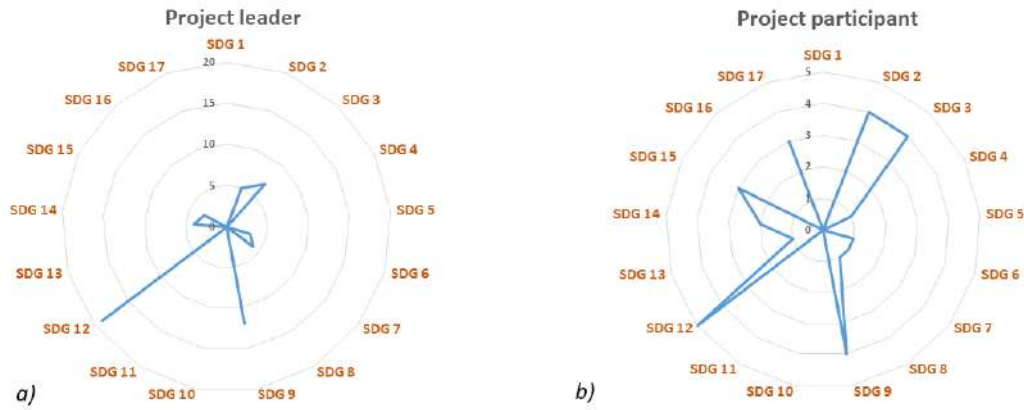


**Figure 1** Mapping of projects matching with SDGs depending on ITNMS role as a) project leader; or b) project participant

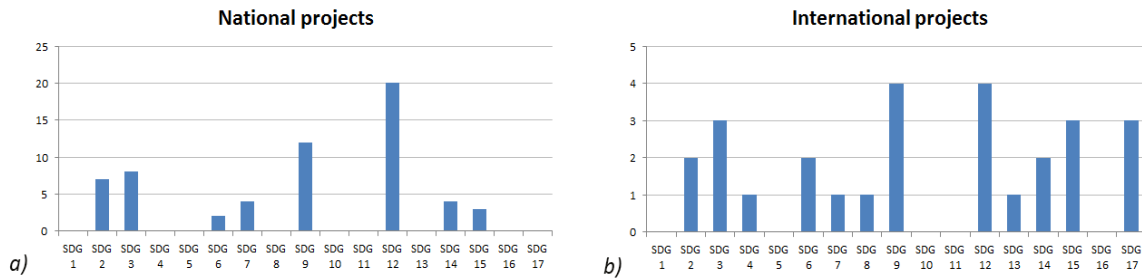


**Figure 2** Classification of SDGs by type of projects from 2015 to 2024: a) national projects; b) international projects

Lack of representation of goals 1, 5, 10, 11, and 16 in both groups from Figure 2 is justified by the fact that the work of ITNMS is concentrated on technical-technological area and that sociological aspects as well as the aspects of inequalities are not being part of the current institution's work. The inclusion of SDG 8 (Decent work and economic growth), Quality education (SDG 4), as well as the inclusion of SDG 17 (Partnership for the goals) in international projects is other notable distinction between the two groups, reflecting the specific focus areas of these two project categories. According to the national Agenda 2030, SDG 8 should be more strongly linked to the areas of science and innovation, emphasizing way the Serbia's research system may be strengthened by enhancing its ties to the economy, thus supporting economic expansion. Moreover, Strategy for scientific and technological development encourages association and cooperation at the international level for achieving the SDG's 17 target, particularly within the European Research Area.

On a global level, SDGs are categorized through addressing the UN 5 pillars of sustainable development: People, Prosperity, Planet, Peace, and Partnership. Work of [4] proposed three additional categories of SDG's from an STI point, namely: 1) ones that cover a range of socio-technical systems or the areas of application, 2) ones that promote transversal directions for system change, 3) goals that focus on framing conditions focusing on governmental transformation. The transformative potential of generated scientific knowledge could be enhanced and integrated if the links among socio-technical system change, directionality, and framework conditions become established and gradually stronger [5]. Moreover, such STI



transformation calls for fundamental shifts in system paradigm and goals, as well as their acceleration by involved collaborators [6]. Figures 3 and 4 present two SDG categorizations with accented SDGs tackled by ITNMS projects.

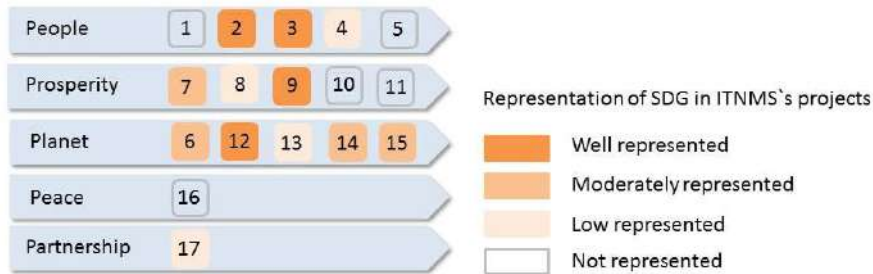


Figure 3 Representation of SDGs in ITNMS projects across categories according to UN 5 pillars of sustainable development

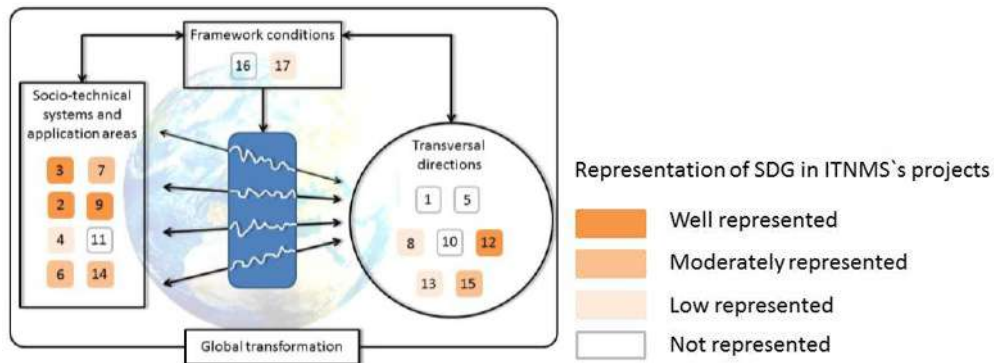


Figure 4 SDGs from transformative science, technology and innovation (STI) point of view, modified from [4]

## CONCLUSION

Mapping the overall contribution of the scientific projects realized in ITNMS during 2015–2024 to the 17 UN SDGs resulted in identification of sustainable development goals primarily important for the work and strategic development of the ITNMS, as well as those that are moderately represented in current scientific activities, but may become more important in the future as the scope of the scientific work and projects expands in accordance with actual needs and resource use patterns and demands.

Strategic development of the ITNMS is in line with the Strategy for scientific and technological development of the Republic of Serbia, aiming to ensure sustainable functioning of ITNMS as a multidisciplinary institute which is recognizable by its modern approach to science and research. Competitiveness should be built through focusing the researches on defined challenges and priorities on national and international level that are aligned with the SDGs, including those already well represented in the ITNMSs projects (SDGs 2, 3, 9, 12), as well as straightening those defined as important by national strategies and international programs (SDGs 8 and 17). With an adequate transformative, collaborative and multidisciplinary approach to STI, ITNMS may more efficiently contribute to the solving of contemporary scientific and technical challenges in a sustainable development manner,



particularly taking into account the guidelines of International Decade of Science for Sustainable Development.

### **ACKNOWLEDGEMENT**

*The authors are grateful to the Ministry of Science, Technological development and Innovation of the Republic of Serbia for financial support according to the contract with the registration number (451-03-66/2024-03/200023).*

### **REFERENCES**

- [1] Strategy for scientific and technological development of the Republic of Serbia for the period from 2021 to 2025 “The power of knowledge”, Official Gazette RS, no. 10/21.
- [2] Godišnji izveštaji o radu Instituta za tehnologiju nuklearnih i drugih mineralnih sirovina (ITNMS) za period 2015–2023 godine, Arhiva ITNMS.
- [3] Plan rada Instituta za tehnologiju nuklearnih i drugih mineralnih sirovina (ITNMS) za 2024. godinu, *Available on the following link:* <https://planrada.nitra.gov.rs/enginez.php>.
- [4] Schot J., Boni A., Ramirez M., *et al.*, (2018): Addressing SDGs through transformative innovation policy, *Available on the following link:* [https://tipconsortium.net/wp-content/uploads/2019/04/4198\\_TIPC\\_research\\_brief\\_web-FINAL.pdf](https://tipconsortium.net/wp-content/uploads/2019/04/4198_TIPC_research_brief_web-FINAL.pdf).
- [5] Goyeneche O.Y.R., Ramirez M., Schot J., *et al.*, Res. Policy 51(10) (2022) 104589.
- [6] Malekpour S., Sustain. Sci. 18 (2023) 1939–1960.



## CHEMICAL DURABILITY EVALUATION OF SINTERED FLY ASH BASED GLASS

Veljko V. Savić<sup>1</sup>, Jelena D. Nikolić<sup>1\*</sup>, Vladimir S. Topalović<sup>1</sup>, Marija S. Djošić<sup>1</sup>,  
Marija A. Marković<sup>1</sup>, Srdjan D. Matijašević<sup>1</sup>, Snežana R. Grujić<sup>2</sup>

<sup>1</sup>Institute for the Technology of Nuclear and other Mineral Raw Materials-Belgrade,  
Franchet d'Esperey 86, 11000 Belgrade, SERBIA

<sup>2</sup>University of Belgrade, Faculty of Technology and Metallurgy, Karnegijeva 4,  
11000 Belgrade, SERBIA

\*j.nikolic@itnms.ac.rs

### Abstract

*In order to preserve the environment, the strategy of economic development in the world is based on the use of waste as a raw material for obtaining new products. Waste can be used in the same industry in which it was produced or in other industries. This paper presents an examination of the chemical durability of glass-ceramics obtained by sintering fly ash glass at characteristic temperatures (850 and 900°C). The chemical stability of the glass-ceramics was tested in three solvents, distilled water, HCl (0.01 mol/dm<sup>3</sup>) and NaOH (0.01 mol/dm<sup>3</sup>). The results indicate that the chemical durability of glass sintered at 900°C is slightly lower than glass-ceramic sintered at 850°C. The higher chemical durability of the glass-ceramic sintered at 850°C can be attributed to the presence of wollastonite, which was not detected in the glass-ceramic sintered at 900°C. The obtained glass-ceramics has a high chemical durability, with mass changes below 1%. FTIR and SEM analysis of the samples after dissolution revealed that there was no disruption of the structure.*

**Keywords:** fly ash, glass-ceramic, sintering, chemical durability.

### INTRODUCTION

The Europe 2020 strategy aims to increase the share of energy from renewable resources to 20%, to reduce the primary energy consumption up to 20% by improving energy efficiency, to reduce the use of virgin raw materials and to reduce the greenhouse gas emissions by 20%, compared to the 1990 levels [1]. The linear economy model was based on the “take-make-consume-dispose” pattern. The circular economy advocates for keeping resources in circulation for extended periods through practices like resource sharing, leasing, reusing, repairing, refurbishing, and recycling. The number of research studies aimed at using waste as a raw material for obtaining new materials as well as new usable products is growing. Waste can be turned into a valuable resource for the manufacturing industries, avoiding disposal and the use of virgin raw material. Waste from one industry should become raw material for another [2,3].

Fly ash is a mineral residue after burning coal in thermal power plants that leaves the combustion furnace together with flue gases. Fly ash is separated from the flue gas stream in electrostatic filters. The Nikola Tesla thermal power plant annually uses about 29 million tons

of lignite to produce electricity. Between 14 and 30% of ash is produced by burning Kolubara lignite [4]. Lignites have a high content of volatile substances, mineral substances, moisture and sulfur. In the world, there is a noticeable trend of increase in use of fly ash as a secondary raw material, but there is still a huge difference between developed countries, where the degree of utilization of fly ash is high, and developing countries, where the degree of utilization of fly ash is only a few percent or does not exist. The usage of different waste materials, like fly ash for commercial purposes, in addition to economic growth, also contributes to the improvement of the quality of the environment [5–7]. The use of waste materials generated in thermal power plants in Serbia is very low. In recent years, an initiative has been launched to use fly ash, slag and gypsum as raw materials, and also to export them to countries where these wastes are used as useful raw materials [4].

The goal of the research was to use a fly ash as a raw material and to obtaining fly ash glasses and glass-ceramics with good mechanical properties and good chemical durability that could be used in the construction industry. The environmental impact of the obtained glass-ceramic materials was examined according to the TCLP (Toxicity Characteristic Leaching Procedure) method by leaching toxic metals. All solutions after testing had heavy metal content below the US EPA limits, which confirms that the synthesized materials are safe for the environment [5]. In the current paper, the chemical durability of glass-ceramics obtained by sintered fly ash glass is presented.

## **MATERIALS AND METHODS**

### **Glass-ceramics synthesis**

The glass batch composition was prepared from fly ash (75 wt.%), CaO (15 wt.%) and Na<sub>2</sub>O (10 wt.%). CaCO<sub>3</sub> and Na<sub>2</sub>CO<sub>3</sub> are added in order to add CaO and Na<sub>2</sub>O to the glass batch. Modifying oxides are added to achieve the optimal viscosity of the glass melt. The melting was performed in an electric furnace Elektron at T=1500°C for one hour in 200 ml open Zr/Si crucible. The glass was obtained by quenching the melt on a steel plate. The glass was ground in a TENCAN planetary mill at 400 rpm for 60 minutes. After grinding, the glass was sieved through a sieve and glass powder with a grain size of <0.063 mm was used. The glass powder was uniaxially pressed in a laboratory hydraulic press Manfredi C 95 at 20 MPa for 30 s, with the addition of 5% water as a binder. The obtained pellets, weighing 1 g each and measuring 15 mm in diameter and 3 mm in thickness. The pellets were heated at a rate of 10°C/min and sintered at temperatures of 850 and 900°C for 1 hour in an electric furnace Carbolite CWF 13/13. The sintering temperatures were determined based on the HSM (Hot Stage Microscopy) results [5].

### **Leaching tests**

The sintered pellets (glass-ceramics) are crushed in an agate mortar. Sintered glass-ceramics powders with a grain size of 0.3–0.5 mm were used in the leaching tests. 2 g of glass-ceramic powders were placed in a flask with a lid and 70 ml of one of the solvents was added. The influence of distilled water, 0.01 mol/dm<sup>3</sup> HCl and 0.01 mol/dm<sup>3</sup> NaOH was tested. Closed flasks were placed in a water bath and kept for 2 h at 95°C at 90 rpm. After 2 h, the glass-ceramic powders were separated from the solution by filtration. The sample was

dried to a constant mass at 110°C and the change in mass was determined. The structural characteristics of the sintered samples before and after dissolution were examined by the FTIR-ATR method. The glass-ceramic surface in contact with solvents was examined by SEM analysis. The concentration of present ions in the solutions was determined.

### Characterization of glass-ceramics and solution

The chemical composition of glass and solutions was determined by gravimetric and spectroscopic methods, i.e., by AAS using a PERKIN ELMER 703 instrument and UV/VIS spectroscopy using a PHILIPS 8610 spectrophotometer. The Fourier transform infrared spectroscopy (FTIR) studies were performed using a PERKIN ELMER 2000 FTIR spectrometer in the 4000–400 cm<sup>-1</sup> range.

## RESULTS AND DISCUSSION

Powder X-ray diffraction (XRD) analysis confirmed the quenched melts to be amorphous (data not shown). Chemical analysis determined that the glass has a composition: 49.9SiO<sub>2</sub>·12.0Al<sub>2</sub>O<sub>3</sub>·21.9CaO·2.2MgO·10.7Na<sub>2</sub>O·0.6K<sub>2</sub>O·0.7TiO<sub>2</sub>·2.0Fe<sub>2</sub>O<sub>3</sub> (mol%).

The chemical durability of sintered glasses was tested in neutral, acidic and basic environments. Dissolving the glass network is a complex process consisting of several steps. In a neutral and acidic environment at the beginning of dissolution, the process of ion exchange between protons (or hydronium ions) from the solution and cations of the glass network modifier is characteristic, creating a hydrated layer through which diffusion takes place. In the initial phase, alkali ions diffuse through the glass network over the hydrated layer into the solution. The next stage is the hydrolysis of the glass network, during which the covalent bonds of the network builder with oxygen are broken [8,9]. In the base environment, the glass network former is directly dissolved into the solution. SiO<sub>4</sub>-tetrahedra in the glass network are susceptible to nucleophilic attack by OH<sup>-</sup> ions, resulting in the formation of a reactive five-coordinated intermediate that disintegrates, breaking the Si-O-Si bond [10,11].

Table 1 shows the mass change and concentration of elements in the solution after testing the chemical durability of glass sintered at 850°C.

**Table 1** The mass change ( $\Delta m$ ) and concentration of elements in the solution after testing the chemical durability of glass sintered at 850°C

Leaching solution	$\Delta m$ , %	Concentration of element in solution, mg/l							
		Si	Al	Ca	Mg	Na	K	Ti	Fe
H <sub>2</sub> O	0.22	1.94	<0.1	0.6	0.05	0.49	0.14	<1	0.17
HCl	0.32	3.21	<0.1	3.8	0.35	0.85	0.16	<1	0.10
NaOH	0.28	6.26	1.20	0.6	0.01	/	0.36	<1	0.34

The concentration of Si in the solution after the leaching test in the 0.01 mol/dm<sup>3</sup> NaOH solution is significantly higher than the concentration of Si in the solution after the chemical stability test in water and the 0.01 mol/dm<sup>3</sup> HCl solutions. It is clear that the destructive nucleophilic attack of OH<sup>-</sup> ions on the silicate network is the dominant dissolution mechanism. Ion exchange is more dominant in an acidic environment compared to a neutral

environment due to the higher concentration of  $H^+$  ( $H_3O^+$ ) ions in the solution, which results in higher concentrations of alkaline and alkaline earth elements in the solution. The mass change of the sample after dissolution in all three environments is approximately the same and was below 0.5%. Figure 1 shows the FTIR analysis before and after testing the chemical durability of glass sintered at  $850^\circ\text{C}$ .

The FTIR spectrum of sintered glass differs from the FTIR spectrum of the parent glass (data not shown) because bands characteristic of crystalline phases formed during sintering can be observed [5]. In the FTIR spectra of the samples after dissolution in all three media, no shifts in bands are observed, indicating that the material structure has not been disrupted. In the FTIR spectrum of glass sintered at  $850^\circ\text{C}$ , bands in the range of  $850\text{--}1000\text{ cm}^{-1}$  ( $969$  and  $897\text{ cm}^{-1}$  – shoulder) can be attributed to the asymmetric stretching vibrations of Si-O-Si and asymmetric and symmetric stretching vibrations of O-Si-O bonds in wollastonite.

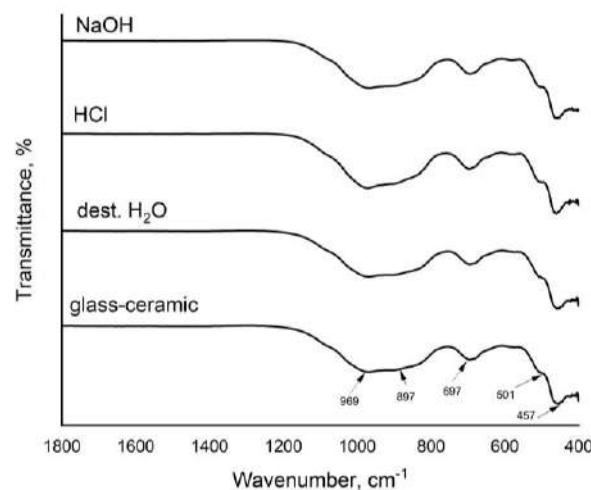


**Figure 1** FTIR spectra: original glass-ceramic sintered at  $850^\circ\text{C}$ , glass-ceramic after immersion in: distilled water (dest.  $H_2O$ ),  $0.01\text{ mol/dm}^3$  HCl (HCl) and  $0.01\text{ mol/dm}^3$  NaOH (NaOH)

A band detected at  $697\text{ cm}^{-1}$  can be attributed to bending vibrations of the Si-O-Si bond and confirms the presence of nepheline. Bands corresponding to bending vibrations of Si-O and stretching vibrations of Ca-O bonds in wollastonite can be detected at  $501$  and  $457\text{ cm}^{-1}$ . On the other hand, according to the literature, bands for bending vibrations of Si-O-Al bonds in nepheline can be detected in the range of  $510\text{--}470\text{ cm}^{-1}$  [12,13].

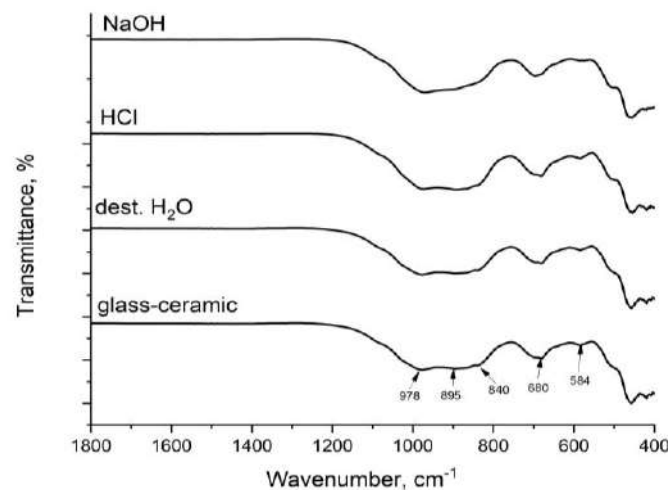
Table 2 shows the mass change and concentration of elements in the solution after testing the chemical durability of glass sintered at  $900^\circ\text{C}$ .

The results shown in Table 2 indicate that the chemical durability of glass sintered at  $900^\circ\text{C}$  is slightly lower than glass sintered at  $850^\circ\text{C}$ . The higher chemical durability of the glass sintered at  $850^\circ\text{C}$  can be attributed to the presence of wollastonite, which was not detected in the glass, sintered at  $900^\circ\text{C}$ .

**Table 2** The mass change ( $\Delta m$ ) and concentration of elements in the solution after testing the chemical durability of glass sintered at 900°C

Leaching solution	$\Delta m$ , %	Concentration of element in solution, mg/l							
		Si	Al	Ca	Mg	Na	K	Ti	Fe
H <sub>2</sub> O	0.17	1.52	0.5	0.6	0.13	0.72	0.23	<1	0.12
HCl	0.74	2.57	<0.1	2.80	0.37	1.34	0.36	<1	0.23
NaOH	0.65	6.76	1.2	0.6	0.1	/	0.98	<1	0.33

Figure 2 shows the FTIR analysis before and after testing the chemical durability of glass sintered at 900°C. In the FTIR spectrum of the sintered glass sample, bands characteristic of crystalline phases formed during sintering can be observed. As in the previous case, the structure remains intact after chemical durability tests.

**Figure 2** FTIR spectra: original glass-ceramic sintered at 900°C, glass-ceramic after immersion in: distilled water (dest. H<sub>2</sub>O), 0.01 mol/dm<sup>3</sup> HCl (HCl) and 0.01 mol/dm<sup>3</sup> NaOH (NaOH)

In the analyzed sample, an FTIR band at 978 cm<sup>-1</sup> can be identified, corresponding to the symmetric stretching of Si-O-Si and Si-O-Al bonds, bands at 680 and 584 cm<sup>-1</sup> attributed to bending vibrations of the Si-O-Si bond, and a band at 457 cm<sup>-1</sup> corresponding to bending vibrations of the Si-O-Al bond, confirming the presence of nepheline in the sample. Kushiorite, which is structurally similar to pyroxenes, is also present in the sample. For pyroxene samples, bands in the range of 1100–800 cm<sup>-1</sup> can be attributed to symmetric and asymmetric stretching vibrations of bonds in the SiO<sub>4</sub>-tetrahedron, so in the analyzed sample, the presence of kushiorite can be confirmed by bands at 895 and 840 cm<sup>-1</sup> (shoulder). The results of the FTIR analysis are consistent with the results obtained by XRD analysis [13,14].

SEM analysis of the glass-ceramic samples showed that no changes occurred on the surface after immersion in distilled water, HCl or NaOH. The SEM micrographs of the surfaces of glass-ceramic sintered at 900°C and the surface of glass-ceramic sintered at 900°C after immersion in 0.01 mol/dm<sup>3</sup> HCl are presented in Figure 3.



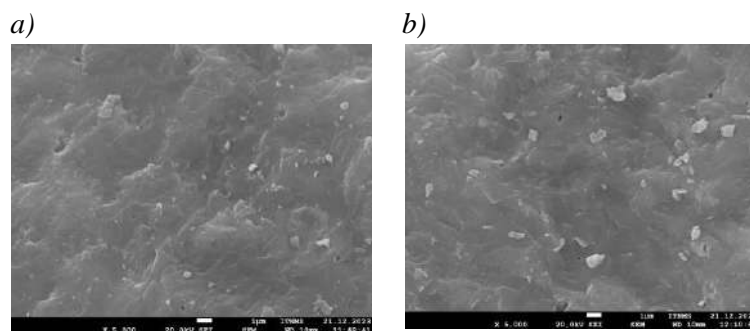


**Figure 3** SEM micrographs of the surface of: a) glass-ceramic sintered at 900°C; b) glass-ceramic sintered at 900°C after immersion in 0.01 mol/dm<sup>3</sup> HCl

## CONCLUSION

Using waste materials as raw materials for new products is one of the basic principles of the circular economy. This paper presents an examination of the chemical durability of glass-ceramic materials obtained by sintering fly ash-based glass. The obtained glass-ceramics has a high chemical durability, with mass changes below 1%. The results indicate that the chemical durability of glass sintered at 900°C is slightly lower than glass-ceramic sintered at 850°C. The higher chemical durability of the glass sintered at 850°C can be attributed to the presence of wollastonite, which was not detected in the glass-ceramic sintered at 900°C. Both glass-ceramics have the lowest durability in 0.01 mol/dm<sup>3</sup> HCl. Tests showed that chemically stable materials were obtained that can be used as construction materials.

## ACKNOWLEDGEMENT

*This research is supported by The Ministry of Science, Technological Development and Innovation, Republic of Serbia, (Contracts No. 451-03-66/2024-03/200023 and 451-03-65/2024-03/200135).*

## REFERENCES

- [1] Landia D., Germania M., Marconib M., Proceedings of 26<sup>th</sup> CIRP Life Cycle Engineering (LCE) Conference, May 7–9, West Lafayette, USA (2019) 399–404.
- [2] Zhang J., Bhuiyan M., Zhang G., *et al.*, J. Cleaner Production 434 (2024) 139991.
- [3] Deschamps J., Simon B., Tagnit-Hamou A., *et al.*, J. Cleaner Production 185 (2018) 14–22.
- [4] Šljivić-Ivanović M., Pepeo, šljaka i gips-otpad ili resurs. Available on the following link: <https://energijabalkana.net/pokrenut-dijalog-eps-a-i-korisnika-pepela-sljake-i-gipsa/>.
- [5] Savić V., Dojčinović M., Topalović V., *et al.*, Int. J. Environ. Sci. Technol. 21 (2024) 6065–6074.
- [6] Robl T., Oberlink A., Jones R., Coal Combustion Products (CCPs): Characteristics, Utilization and Beneficiation, Woodhead Publishing, Kidlington (2017), 99–118, ISBN: 9780081009451.
- [7] Savić V., Topalović V., Nikolić J., *et al.*, Heliyon 9 (2023) e17664.
- [8] Gin S., Jégou C., Frugier P., *et al.*, Chem. Geol. 255 (2008) 14–24.

- [9] Savić V., Topalović V., Matijašević S., *et al.*, Proceedings of Adv. Ceram. Appl. VIII New Front. Multifunct. Mater. Sci. Process., 23–29 September, Belgrade, Serbia (2019) 59.
- [10] Bunker B.C., Tallant D.R., Headley T.J., *et al.*, Phys. Chem. Glas. 29 (1988) 106–120.
- [11] Savić V., Topalović V., Matijašević S., *et al.*, Metall. Mater. Eng. 27 (2021) 105–113.
- [12] Chen W., Liang Y., Hou X., *et al.*, Materials (Basel). 11 (2018) 593.
- [13] Zosin A.P., Priimak T.I., Koshkina L.B., *et al.*, Russ. J. Appl. Chem. 78 (2005) 1077–1083.
- [14] Tian M., Liu B.S., Hammonds M., *et al.*, Philos. Trans. R. Soc. A Math. Phys. Eng. Sci. 371 (2013).



## RECYCLING ELECTRONIC WASTE CPUs FOR ENHANCED HYDROGEN AND OXYGEN EVOLUTION: AN ECO-FRIENDLY LEACHING APPROACH

**Stefan Mitrović<sup>1</sup>, Snežana Brković<sup>1</sup>, Mina Seović<sup>1</sup>, Nikola Zdolšek<sup>1</sup>, Petar Laušević<sup>1</sup>,  
Jelena Georgijević<sup>1</sup>, Ivana Perović<sup>1\*</sup>**

University of Belgrade, Vinča Institute of Nuclear Sciences, National Institute of the Republic  
of Serbia, Mike Alasa 12–14, 11351 Vinča, SERBIA

\*ivanaperovic@vin.bg.ac.rs

### Abstract

*This study delves into the recycling potential of electronic waste, specifically focusing on CPUs, for the facilitation of hydrogen and oxygen evolution reactions. Through the implementation of eco-friendly leaching methodologies, valuable metals were extracted from discarded electronic components, paving the way for their utilization in sustainable energy applications. A multi-step leaching protocol was employed to obtain a solution directly applicable as an electrolyte for electrochemical analysis. Results from cyclic voltammetry and Tafel analysis unveiled a notable enhancement in electrocatalytic activity for hydrogen evolution compared to oxygen production, indicating the intricate behavior of the electrolyte. While the electrolyte demonstrates promise in promoting hydrogen evolution, further optimization may be necessary to maximize its efficiency for oxygen evolution reactions. Overall, this research contributes to advancing eco-friendly recycling strategies and underscores the potential of electronic waste recycling for renewable energy generation.*

**Keywords:** e-waste, hydrogen evolution reaction, oxygen evolution reaction, CPU recycling.

### INTRODUCTION

In the digital age, electronic waste (e-waste) has emerged as a pressing environmental concern, with discarded CPUs (Central Processing Units) representing a significant portion. As technology advances and consumer demand escalates, the proliferation of e-waste continues to surge year after year. Addressing this challenge is paramount, not only to mitigate environmental hazards but also to harness valuable resources embedded within these electronic components [1].

This paper explores the critical need to recycle e-waste CPUs, highlighting the growing trend of electronic waste accumulation. While conventional methods of disposal often lead to detrimental environmental consequences, this study proposes a transformative approach centred around the utilization of eco-friendly chemicals and methodologies. Specifically, the focus is directed towards the leaching of precious metals like gold, alongside other valuable metals, from discarded CPUs.

By harnessing the extracted metals, particularly gold, in conjunction with environmentally friendly leaching techniques, this study aims to facilitate the production of hydrogen and oxygen through electrochemical processes. The synthesis of hydrogen and oxygen via

electrolysis holds promise as a clean and renewable energy source, contributing to the global transition towards a low-carbon economy.

## **MATERIALS AND METHODS**

### **Sample collection and Pre-treatment**

All CPUs utilized in this study were sourced from the same brand and generation. The computers underwent disassembly, and the processors were meticulously removed from their sockets and motherboards. Subsequently, a thorough cleaning process was employed to eliminate any contaminants such as dirt, plastic residues, and thermal paste, ensuring uniformity across all samples.

The processing of these CPUs involved the utilization of a basic electrical mill and the resulting powder exhibited some variance in particle size, which was subsequently assessed using a lab sieve. Following this characterization, the powder underwent the leaching procedure [2].

### **Leaching procedure**

The leaching process employed in this study was a multi-step method utilizing various chemicals, offering the possibility of effectively separating different metals present in CPU powder.

The initial step involved dissolution in 1M HCl at ambient temperature and under an inert gas atmosphere for a duration of 5 hours. This step aimed to dissolve and segregate Fe and Ni from the other metals present in the powder.

Following dissolution, the solution underwent filtration, and the sediment was subsequently separated, washed, and dried until complete dryness was achieved. Subsequently, the dry powder was immersed in a solution comprising  $\text{NH}_3/(\text{NH}_4)_2\text{SO}_4 + \text{H}_2\text{O}_2$  at room temperature for 2 hours. This step facilitated the dissolution and removal of Cu and Ag from the sample.

Upon completion of this leaching step, the powder underwent another round of filtration, washing, and complete drying, preparing it for the final leaching phase. In this last procedure, the dried powder was dissolved in a mixture of 4-PSH + DMF +  $\text{H}_2\text{O}_2$  at 60°C for 25 minutes. Here, the metallic Au dissolved from the powder and formed a complex with 4-PSH. Finally, the solution underwent filtration once more, and the resultant solution was reserved for subsequent testing [3].

### **Electrochemical testing**

Electrochemical assessments were conducted within a three-electrode glass cell setup. The working electrode comprised a pure metallic nickel electrode with a surface area of 1 cm<sup>2</sup>, while high-surface-area nickel foam served as the counter electrode. An Ag/AgCl electrode functioned as the reference electrode.

Electrochemical characterization involved the recording and analysis of polarization curves to ascertain the kinetics of hydrogen and oxygen evolution reactions within the electrolyte. The electrolyte employed was a solution prepared from the aforementioned powder.

## RESULTS AND DISCUSSION

The primary focus of this investigation was to explore the feasibility of employing recycled metals sourced from electronic waste, particularly CPUs, in hydrogen and oxygen evolution reactions. The three-step protocol for metal leaching yielded a solution utilized directly as an electrolyte for this analysis.

Recorded cyclic voltammogram (Figure 1) offers valuable insights into the oxidation and reduction processes occurring at the electrode surface. While the oxidation peak at approximately 0.5 V vs Ag/AgCl suggests nickel oxidation, the absence of a corresponding reduction peak, expected around 0.1 V vs Ag/AgCl, indicates the involvement of additional processes at the electrode surface [4].

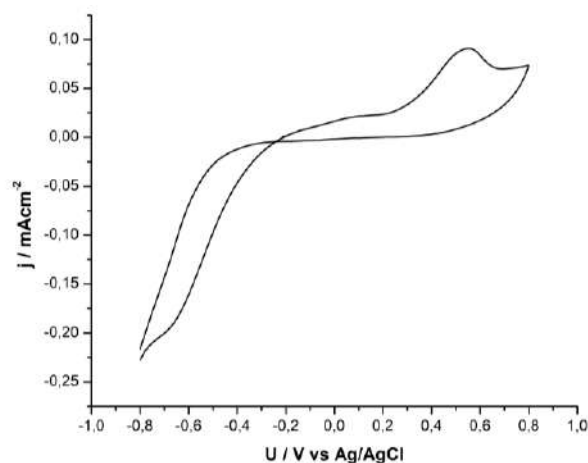


**Figure 1** Cyclic voltammogram of a pure nickel electrode in prepared solution

As evidenced by recorded polarization curve (Figure 2), the metal complex, likely the Au-PSH complex, exhibited relatively favorable electrochemical activity for the hydrogen evolution reaction. Conversely, its performance in oxygen production was comparatively less promising.

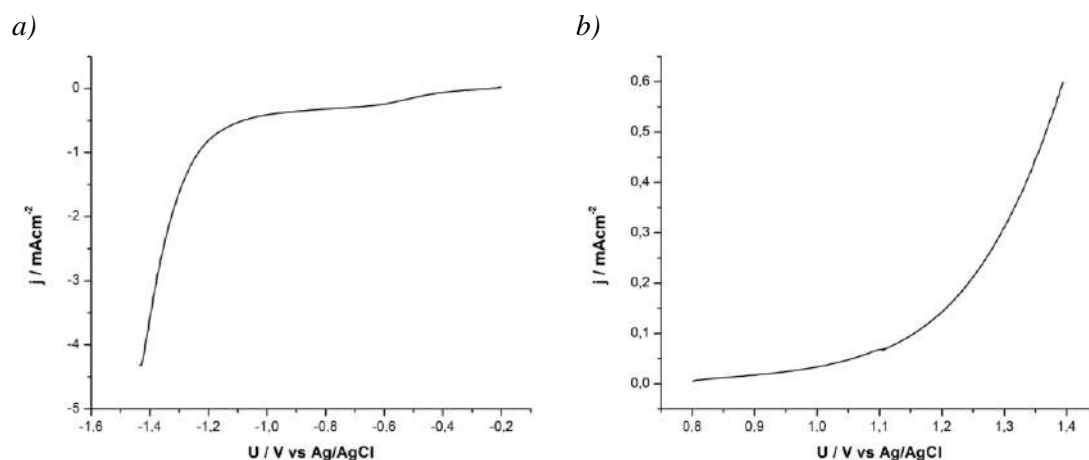


**Figure 2** Polarization curves for a) hydrogen; b) oxygen evolution reactions

A subsequent Tafel analysis was conducted on the recorded polarization curves, and the resulting plots are depicted in Figure 3. In the Tafel plot, a linear correlation emerges between the logarithm of the current and the overpotential. The slope of these curves, referred to as the Tafel slope, offers insights into the reaction mechanism and activation energy. Tafel slope values categorize reactions into three mechanisms: activation-controlled, diffusion-controlled, and mixed-controlled.

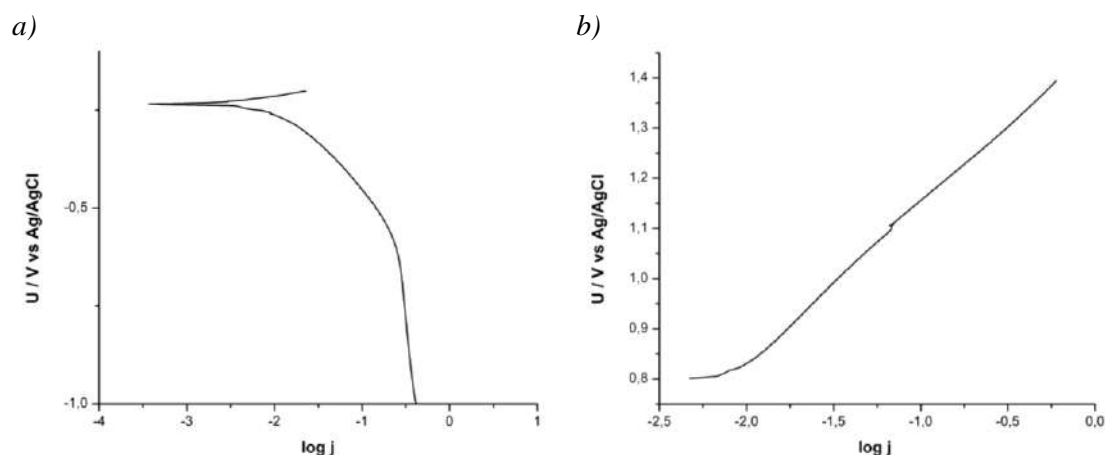


**Figure 3** Tafel plots for a) hydrogen; b) oxygen evolution reaction

The Tafel slope values obtained from the analysis and presented in the Table 1 provides further confirmation of the initial hypothesis, indicating that the electrolyte prepared using this protocol exhibits a superior electrocatalytic capacity for hydrogen production compared to the oxygen evolution reaction. This disparity in electrocatalytic performance between the two reactions underscores the nuanced behavior of the electrolyte and highlights its selective enhancement towards hydrogen evolution.

**Table 1** Kinetic parameters for Ni electrode in prepared solution

Reaction	Tafel slope (mV/dec)
Hydrogen evolution reaction	$-266.8 \pm 0.8$
Oxygen evolution reaction	$318.8 \pm 0.5$

The discrepancy in Tafel slope values between hydrogen and oxygen evolution reactions suggests that the activation energy barrier for hydrogen production is comparatively lower, facilitating a more efficient electrochemical process. Conversely, the higher activation energy barrier associated with the oxygen evolution reaction indicates a more sluggish kinetics, impeding the rate of oxygen generation [5].

## CONCLUSION

The exploration into the recycling of electronic waste, particularly CPUs, for the purpose of hydrogen and oxygen evolution reactions presents a multifaceted endeavour with profound implications for sustainability and clean energy generation. Multi-step leaching protocol



showcased in this research offers a promising avenue for reclaiming metals from e-waste CPUs, with the resultant solution serving as a direct electrolyte for electrochemical analysis. Through cyclic voltammetry and Tafel analysis, insights into the electrochemical behaviour of the recycled metals have been gleaned, revealing a preferential enhancement towards hydrogen evolution over oxygen production.

The complex interaction between electrolyte composition and electrochemical processes underscores the need for tailored strategies to use recycled materials for energy production. While the electrolyte exhibits promising electrocatalytic capabilities for hydrogen evolution, further optimization may be necessary to improve its effectiveness in oxygen evolution reactions.

Overall, this study underscores the potential of recycling e-waste for resource recovery and renewable energy generation. By advancing eco-friendly leaching methodologies and elucidating electrochemical mechanisms, this research contributes to the ongoing efforts towards a circular economy model and the transition to a greener, more sustainable future.

## **ACKNOWLEDGEMENT**

*The authors are grateful to the Ministry of Science, Technological development and Innovation of the Republic of Serbia for financial support according to the contract with the registration number 451-03-66/2024-03/200017.*

## **REFERENCES**

- [1] Robinson B.H., *Sci. Total Environ.* 408 (2009) 183–191.
- [2] Mitrović S., Brković S., Živković S., *et al.*, *Materials* 20 (2023) 6795.
- [3] Räsänen M., Heliövaara E., Al-Qaisi F., *et al.*, *Angew. Chemie Int. Ed.* 52 (2018) 17104–17109.
- [4] Ghosh S., Bagchi D., Mondal I., *et al.*, *Adv. Energy Mater.* 2400696 (2024).
- [5] Shinagawa T., Garcia-Esparza A.T., Takanabe K., *Sci. Reports* 1 (2015) 1–21.



## BRAND MANAGEMENT AND SOCIO-ECONOMIC ASPECTS OF ADAPTATION TO CLIMATE CHANGES

Adrijana Jevtić<sup>1</sup>, Dejan Riznić<sup>1\*</sup>, Milovan Vuković<sup>1</sup>

<sup>1</sup>University of Belgrade, Technical Faculty in Bor, V.J. 12, 19210 Bor, SERBIA

\*driznic@tfbor.bg.ac.rs

### Abstract

*International business requires a special commitment of the company's management, due to cultural differences. Globalization has imposed an imperative to accept cultural diversity in the world, so diversity becomes a source of competitiveness. Companies that form strategic partnerships based on cultural differences face numerous problems. However, well-formed strategic partnerships can greatly contribute to positive business results. A company's brand can be a significant source of competitive advantage. The aim of this work is to indicate the existence of diversity in the management processes of Brand management within the intercultural area at the global level and in the part of adaptation to climate change. As a solution to this problem, the necessity of understanding cultural differences is proposed, because differences in management style do not have to be obstacles but should complement each other. It is a unique position that cultural diversity is a source of creativity and original ideas in adaptation to climate change.*

**Keywords:** brand, globalization, climate changes, cultural differences, business.

### INTRODUCTION

Climate change is increasingly affecting the environment and the economy. Until the beginning of the industrial revolution, the climate was changing because of modifications in natural circumstances. However, today, global warming does not happen by itself, it is a consequence of increasing anthropogenic influence [1]. Based on all the social, ecological, economic, and other consequences brought by climate change, the importance of studying the effects of climate change on the economy and society is necessarily imposed, all with the aim of increasing the nation's awareness [2]. Doing business outside the home country has become a common form of development for an increasing number of companies. When implementing their strategy, managers should consider the unique culture of each country in which they operate, because the culture of each country represents the generally accepted values, traditions and ways of behaviour of social groups.

Every brand manager is faced with the challenge of finding the right solution that would represent the best incentive for employees while respecting cultural diversity. Successful business is possible if the cultural differences and rules of participants from different parts of the world are understood. A good knowledge of intercultural management helps to understand business in another market, and neglecting the influence of culture on the company's business in another country today definitely leads to failed business negotiations, which is reflected in unfavourable business results. Only those companies that understand and respect cultural

differences in brand management can achieve successful business. Today's business management requires efficiency, flexibility, innovation, stability and, based on that, productivity improvement in all aspects of business.

### **CULTURE AND INTERCULTURALITY**

A discussion of intercultural sensitivity, intercultural competence or intercultural intelligence should begin with a discussion of the term culture itself. Culture is usually defined as a system of shared values, attitudes, communication patterns, beliefs, behaviours, norms, material objects, and symbolic resources that distinguish members of one group of people from others. Theorists define culture as the rules of living and functioning in society. Since the rules differ from culture to culture, one should know how to play by the rules. Rules make it possible to design the environment and reduce uncertainty about the social environment.

A culturally diverse society must understand that interculturality is a key prerequisite for effective communication. It represents a challenge, the creation of a fairer one, to “learn to live together” [3]. The increasing cultural complexity of contemporary social and business environments requires an understanding of the importance of managing cultural differences in such a way that they become opportunities. Interculturality implies openness, interest, curiosity and empathy towards people from other cultures. It enables people to function effectively and achieve interactional and transactional goals. Interculturality is based on a series of basic cognitive and affective competences, combined and known as intercultural competence.

Skills developed from intercultural sensitivity are intercultural competencies. Intercultural sensitivity is “a person's response to intercultural differences”. Scientists define intercultural sensitivity as an active desire to understand, appreciate and accept differences between cultures, even in relation to climate change [4]. The business phenomenon itself is based on collecting or adopting the values of other cultures or even the culture of the people to which the user-customer belongs. Namely, it is necessary to know a lot, and not only to be familiar with climate change and the possibilities for adaptation to climate change within different cultures.

International management, as a “translation” of the term “international management”, can also be related to the international political events that marked the nineties of this century. The conception of the new world order, which is dictated by the United States of America, has, in its basis, many elements of the so-called of international management. If the geoeconomic aspects of this American concept are added to that, then one can talk about its significant impact on the macroeconomics of individual countries, as well as on their microeconomic structures [5]. Instead of the so-called international management, it is better to use the term intercultural management, since its content is more appropriate to contemporary trends in the global economy. Likewise, governance among nations should be replaced by governance among different cultures.

The elements of the international lose their importance through the usual divisional organizational structure of multinational companies. Therefore, the international operations

and facilities of the parent company retain their national characteristics and take on the cultural characteristics of the country in which they are located. This is confirmed by the multitude of so-called transplant companies, which large Japanese corporations – from the beginning of the eighties until today – established in America and Europe [6].

The purpose of intercultural management is to assess the impact of culture on the perceptions, interpretations and actions of brand management. In the field of management, the cultural system gives individuals cognitive abilities and a specific approach to solving problems. Therefore, collaborators from other countries are likely to find different solutions when faced with the same problems. One of the interesting assumptions of intercultural management concerns the study of the interaction of managers from different cultural systems. The problem arises in the process of coordinating managers over teams that come from different cultures. Due to the formation of strategic partnerships, companies from different cultural areas are forced to cooperate, and the occurrence of intercultural conflict is common.

Intercultural management plays an important role in international business activities, where we place business partners from several countries in a teamwork situation. Nevertheless, today a team approach is expected in the implementation of business activities regardless of the cultural background of the manager, where because of misinterpretation, verbal and non-verbal communication can lead to conflicts and misunderstandings. This underestimation of cultural factors is present on the world business scene because the merger of companies also means the merger of their intellectual capital.

The manager's recommendation is to implement a human resources policy aimed at building a common business spirit. English is mostly adopted as the official language and the corporate culture is based on the spirit of teamwork. It is advisable to separate many people who should work on the harmonization and integration of human resources. Recruiting a new workforce contributes to building a new corporate culture. Managers working in strategic partnerships of different cultural climates consider cultural diversity as a special advantage. It is a unique position that cultural diversity is a source of creativity and original ideas in brand management.

## **INTELLECTUAL CAPITAL AND ADAPTATION TO CLIMATE CHANGE**

Diffusion of knowledge and technology should enable strong cultural and regional cooperation that will meet the needs not only of the most developed, but also of other European countries, and diversity is considered the main catalyst of scientific, technological and innovative development [3]. New forms of human resource education and training are considered strategic goals in the process of developing “learning organizations”. Intellectual capital is a condition for the survival and growth and development of a company. The company's competitive position depends on it. It affects business decision-making and adaptation to climate change. Companies that own intellectual capital are superior in every way.

Human resources are the carriers of human capital, and they include information and knowledge that everyone has and that allows him to be more productive in performing his

activities. Seen from the company's point of view, human capital represents the cumulant of knowledge, skills, inventions, energy and enthusiasm that people are willing to invest in the business. The importance of intellectual capital is growing for companies operating in different cultural areas. Contemporary research shows that there are different values between different cultures, which every international corporation should be aware of.

The development of information technology faces numerous challenges, such as cultural diversity and intercultural brand management. Cultural diversity is inseparable in global development as team members have different national, organizational and professional cultures. Diversity itself can have a beneficial effect on promoting creativity, but it can also be a barrier to communication and knowledge exchange. The basic vision of managers around the world is to attract, develop and retain talent. The development of companies in the global economy implies investment in human resources. Contemporary trends in human resource management are projected through demographic changes, an aging workforce and increased global mobility. The problem that companies face in the process of human resource management is how to retain them. It is necessary to provide awards, create an atmosphere of togetherness and teamwork and create conditions for their further development and improvement, and a good reputation can attract human resources.

The Boston Consulting Group and the European Association for Personnel Management conducted a survey of 1,350 managers from 27 European Union countries. The research showed that all European companies will face the problem of labor shortage, especially talented labor. Managers of large companies also note that demographic changes are a problem. To fully utilize the sources of talented workforce and ensure the development of companies, a global approach is necessary, to ensure recruitment from all over the world [3].

Corporations need to prepare their employees to cope with the complex and accelerated pace of the global economy. Simply investing in training programs alone will not automatically improve productivity. Instead, managers must clearly define, and measure return on investment. To attract and retain highly talented individuals from around the world who will be required to be able to enter new markets, manage corporate and cultural change, companies will also need to offer flexible arrangements for work and socioeconomic aspects of adaptation to climate change.

Employees working in these companies should be interculturally competent. Being interculturally competent means that a person from one culture can interact effectively with people from different cultures. For intercultural contact to be constructive, it is necessary: (1) intercultural way of thinking (cognitive characteristics) – recognition of cultural differences and maintaining a positive attitude towards them; (2) intercultural skills (behavioral characteristics); and (3) intercultural sensitivity (affective characteristics), i.e. the ability to experience cultural differences in a sophisticated way [4].

The business of many companies is based on service. The purchase of services is based on intangible experiences and subsequent perceptions of customers. Customers evaluate the service in accordance with the behavior and treatment of employees towards them. Globalization has changed the demands and expectations of service users, which companies must be aware of, employees should possess specific qualities: interpersonal skills, multilingualism, real interest in their needs and enjoyment in meeting them, creative problem-

solving skills, action-oriented abilities, as well as motivation for attracting new users and retaining existing ones. All those who are aware of their culture and its values, traditions and norms can become aware and understand the culture and values of others. Awareness leads to deeper knowledge, skills, attitudes and emotions and should be expressed in company managers so that they can successfully balance cultural differences.

### **ANALYSIS OF COMPETITIVENESS ON THE EXAMPLE OF A TOURIST PRODUCT-BRAND AND ADAPTATION TO CLIMATE CHANGE**

The best example for moving forward is tourist services. Created in the era of “old” mass tourism and confirmed in the era of “new” tourism, the tourist destination represents much more than a specific territory. The variety of products, services, natural resources, anthropogenic elements and information, which attract tourists, shape spaces where tourist needs and demands of different market segments are met. An attractive, attractive and, in terms of activities, recognizable destination – brand, on the tourist market represents the goal of organized tourist trips and the basic resource of the “leisure industry”. The original elements of a tourist destination include geographical location and climate, with adaptation to climate change.

Climate is not only important for agriculture, as some think, but also for other activities, such as tourism. If you are planning where to go on vacation, it would be wise to compare the average weather during the period you are going, as well as the weather in recent years, to reduce the chance of bad and unsuitable weather spoiling your vacation. Climate change has been one of the most important world topics in the last few years. From huge fires to increasingly powerful storms and floods, which destroy everything in front of them, as well as hot summers and mild winters without snow, the climate on our planet is changing. Climate change is a long-term change in the climatic conditions on our planet Earth.

In the last 140 years, our planet has warmed by about 1°C, which causes numerous changes in the climate. This is a topic about which it is important to be informed, that is why in this work we clarified the place and role of climate change in tourism, to better understand climate change and its impact on popular tourist destinations – brands, as well as how society can cope with this challenge.

In addition to numerous changes in the way tourism entities do business, the modern development of tourism has also brought new forms of management of the tourist destination – the brand. As a tourist destination represents a complex whole, an integral approach to management at all its levels is necessary. Management of tourism, i.e. a tourist destination at the level of a town, region or country through brand management implies the coordination of all factors and the systematicity of activities, all with the aim of defining an appropriate management strategy and tourism policy that will contribute to the achievement of set goals.

The choice of way of management of the destination is adapted to the nature of the destination, the level of development and numerous other elements, of which the attractiveness of the destination and the quality of the tourist offer are particularly important, but also natural ones, including climate changes. By forming modern organizational forms of destination brand management, such as management organizations and management



companies, the development of tourism in the destination can be improved and the quality of tourist products can be improved.

In tourism, competitiveness analysis refers to the comparison of tourist values or parameters and indicators of tourist development of a certain destination. As part of this analysis, values related to the number and attractiveness of natural and cultural motifs, tourist traffic, capacities, traffic infrastructure, dispersive and contractive tourist zone and many other values should be taken. Since tourism is a service sector, quantitative indicators are more precise, but it is certainly advisable to pay more attention to qualitative ones, namely those related to guest satisfaction, which are subject to a high level of subjectivity.

All tourist destinations in their essence possess certain constitutive elements that motivate tourists to satisfy their tourist needs in each destination. There are different opinions regarding the key elements that make a tourist destination a brand, and enable the development of tourist traffic, forming an integral product of the destination. Most authors agree that it is a combination of different material and immaterial, i.e. natural and social elements. Even Krippendorf [7] distinguishes between original and derived elements of the offer of tourist destinations, where he classifies as original elements: geographic location, climate, language, culture, hospitality, folklore, traffic situation, communal facilities, etc., while he observes derived elements through tourist capacity, infrastructural facilities for the needs of tourism development, organizational activities, information, entertainment and sports-recreational facilities.

This resource base and motives need to be designed into a tourism product of the destination through special forms of tourism as individual, but at the same time as a unique integrated product of the destination. A diversification strategy would develop new products – brands and new markets. Actors in tourism will have to focus their activity primarily on more and more educated and sophisticated tourists by creating new tourist products – brands, where special attention should be paid to individual existing and new integrated tourist products.

Development trends show an increasing need for specialized adaptations of tourist services for certain demand segments. Differentiation strategy, creating a clear identity. By forming a brand, every new tourism product should contain many characteristics of the local indigenous environment. Identity, brand, image and visibility are the keys to competitive advantage. The marketing of a tourist destination must be based on the most creative and unique approaches, combining the use of traditional and new approaches to the market, certainly considering new tools of communication and promotion with the support of modern technologies.

Development of tourism development strategy, clear identity, differentiation of tourist products, destination image, brand building, way of organizing tourism management in the destination, coordination and harmonization of interests of stakeholders involved in tourism and compatible activities, implementation and creation of marketing studies, market research, improvement of service quality, training of professional staff and animating potential investors to invest in infrastructure projects (primarily in the form of hotel facilities more affordable for middle-income clientele, as well as other attractions in the form of swimming pools, sports fields, etc.). These are just some of the guidelines for the future of the destination to achieve a sustainable competitive advantage.

Being able to link specific cases to climate change is very important. Scientists can already say with great certainty how the global climate will change in the future and what weather extremes await us, and as we have noticed in recent years, their forecasts are unfortunately coming true. Although this is the case, many people still believe that climate change is not happening and attribute extreme events to natural variability. When we are able to see together with the weather forecast in real time and the assessment of the impact of climate change on that specific event, it will be much easier to convince decision makers and the public of the necessity of quick and decisive action in order to stop climate change.

## **CONCLUSION**

The strategy of cooperation and brand management should, to the greatest extent possible, be harmonized with the strategy of developing economic relations with foreign countries and the strategy of technological development, and of course with adaptation to climate change. One should keep in mind the new tendencies in the international business environment that have an impact on the company's operations: globalization, regionalization, economic integration, multiculturalism, etc. As a result of globalization, many companies are created and connected around the world. Strategic partnerships are a very flexible and attractive form for realizing the company's development goals. The development behavior of the company relies more and more on a larger number of partners and special forms of cooperation, to preserve the vitality of the company, that is, to increase its resistance to shocks from the market and climate change.

The company's development behavior, internal configuration and brand management are correlated with relativized independence, self-sufficiency and external growth limits. Therefore, strategic partnerships appear more and more as a rational form of development behavior of a modern company in its effort to adapt to changed market, technological and social trends. By starting strategic partnerships, companies gain the opportunity to expand their business to many markets, because globalization sees the whole world as one market. By starting partnerships, companies more easily articulate environmental challenges, such as climate change.

The business and technological environment in which companies operate will become more and more complex, changes are fast and unpredictable. Management processes in the intercultural area differ from country to country. Understanding cultural differences is the first and important step towards creative leadership in a global environment. Differences in style do not have to be obstacles but should complement each other. There are different values between cultures that every international corporation must be aware of. The different needs and expectations of employees in different countries require brand managers in particular to implement a policy that is flexible enough to respond to local specificities and to meet personal expectations at a higher level.

## **ACKNOWLEDGEMENT**

*The research presented in this paper was done with the financial support of the Ministry of Science, Technological Development, and Innovation of the Republic of Serbia, within the funding of*

*the scientific research work at the University of Belgrade, Technical Faculty in Bor, according to the contract with registration number 451-03-65/2024-03/200131.*

## **REFERENCES**

- [1] Riznić D., Jevtić A., Dukić A., *Ecologica* 27 (9) (2020) 544–552.
- [2] Durkalić D., Kostić M., Riznić D., *Ecologica* 22 (79) (2015) 528–532.
- [3] Langović-Milićević A., *Strategijski menadžment i interkulturalnost. Fakultet za hotelijerstvo i turizam, Vrnjačka Banja* (2014).
- [4] Moore-J P.J., *JEC* 2 (2) (2018), DOI:10.22158/jecs.v2n2p75.
- [5] Ineta L., *Policy Futures Educ.* 9 (1) (2011) 114–122.
- [6] Babaita C., Istodor D., Ispas A., *Annals of Faculty of Economics* 2 (1) (2009) 23–28.
- [7] Krippendorf J. *The Holiday Makers*. London: Heinemann (1987).



## PROSPECTS OF SUSTAINABLE UTILIZATION OF FOOD WASTE

Ana Radojević<sup>1\*</sup>, Jelena Jordanović<sup>1</sup>, Tanja Kalinović<sup>1</sup>, Jelena Kalinović<sup>1</sup>,  
Snežana Šerbula<sup>1</sup>

<sup>1</sup>University of Belgrade, Technical Faculty in Bor, V.J. 12, 19210 Bor, SERBIA

\*aradojevic@tfbor.bg.ac.rs

### Abstract

*Food waste is a global problem associated with environmental, economic and social impacts. Since the food waste amount to one third of generated municipal solid waste, it represents one of the most unutilized waste streams. Therefore, it is crucial to reduce food waste generation and implement strategies to minimize its impacts on the environment, mostly reflected through greenhouse emissions, water and land use. However, diverse and highly variable nature and composition of food waste is significantly affecting its valorisation and pose main challenge of the food waste management. In order to meet sustainability goals, food waste should be managed in an environmentally and economically viable manner.*

**Keywords:** food waste utilization, valorisation, biogas production, sustainability.

### INTRODUCTION

In recent years increasing concern has arisen regarding food waste as one of the global problems which have a huge economic, social and environmental impact.

‘Food waste’ is generally referred as food losses (i) within the food supply chain, including inedible parts (such as bones, rinds, pits, eggshells etc.) and (ii) after its expiration date [1]. Food waste occurs at all stages of the food supply chain, from the production step to the consumption. However, the largest share of food waste is generated during consumption (i.e. household waste). Only in the European Union (EU) during 2021 household food waste represented 54% of total share, followed by the food processing and manufacturing (21%), while wholesale and retail (7%), restaurants and food services (9%), and primary production (9%) account for the rest of the generated waste [2]. In the EU, nearly 30 million tonnes of inedible parts of food from the production are left per year [3].

Food waste accounts for a substantial portion of municipal solid waste, representing up to 33% of all waste generated [4]. Around 931 million tonnes of food waste were generated during 2019 globally, 61% of which originated from households, 26% from food service and 13% from retail [5]. However, the degree of food loss and waste fluctuates significantly throughout the regions [6]. In the EU, more than 58 million tonnes of fresh mass of food waste was generated during 2021 (131 kg per inhabitant) [2], which represented an estimated loss of 132 billion euros [7]. At the same time, over 37 million people in the EU cannot afford a quality meal every second day [7], in addition to an almost 770 million of people in the world that were undernourished during 2021 [8]. Therefore, food waste has very important

social aspect. Donation of fresh food cannot be commercialised due to logistic or marketing reasons, however it could be facilitated by “food banks” [9].

Other than economical lost, food waste has a huge environmental impact. Food waste is highly biodegradable compared to other types of waste due to high content of degradable nutrients such as proteins, carbohydrates, and lipids which are degraded to methane (CH<sub>4</sub>). Methane is gas more detrimental for the environment than carbon dioxide (CO<sub>2</sub>). According to the data, about 16% of the total greenhouse gas (GHG) emissions from the EU food system accounts for 254 million tonnes of CO<sub>2eq</sub>, representing the fifth largest emitter of GHG [7]. Diverting food waste from landfills and converting it into a useful resource, such as biofuels and other by-products, it could reduce its negative impact on the environment and diminish climate change effects [4,10]. Regarding food industries, the beverage industry is major contributor accounting for 26% of all food wastes, followed by the dairy industry (21%), the fruit and vegetable production (14.8%), and the cereal industry (12.8%) [3]. It should be noted that, wasting food puts unnecessary burden on already limited natural resources – land and water use [2,11]. Also labour, effort and investment during producing food are wasted, as well as the resources used in the transport [12]. Moreover, in the last 20 years, primary crop production, vegetable oil and meat production has globally risen for around 52%, 125% and 45%, respectively, and it is estimated that will rise in the future [8].

This paper aims to emphasize the global problem of food waste generation and discuss some value addition processes for sustainable utilization of food waste.

## FOOD WASTE

In order to prevent conventional landfilling, several strategies can be employed to diminish the adverse environmental impacts of food waste generation, including source reduction, composting, anaerobic digestion, biogas and energy production. In Figure 1, the proposed food waste hierarchy is given, which consists of descending waste management practices, from more to less preferable and sustainable.

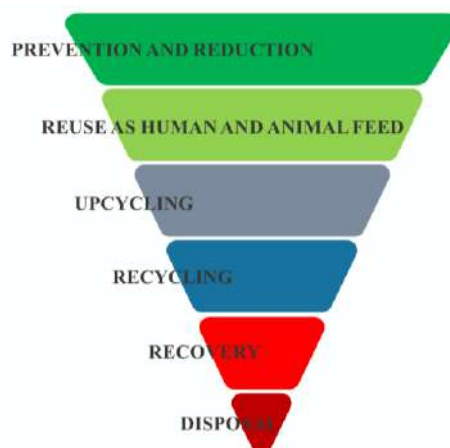


*Figure 1 Food waste hierarchy (adopted from Rakesh and Mahendran [13])*

In the value addition processes (i.e. “upcycling”), wide range of products can be gained by utilizing food waste such as biogases (hydrogen and methane), biodiesel, biopolymers,

bioplastics, enzymes, biochar, organic acids, biofertilizers, etc. [4,10,11,13]. Numerous sectors of the food industry generate by-products that can be re-used as animal feed such as sunflower seed expeller, wheat germ from flour milling, sugar beet molasses from sugar production, starch hydrolysates cake from starch production, as well as various by-products from the bakery and pasta industry [14].

Efficient food waste management requires careful consideration of energy consumption, environmental and economic factors. Lifecycle analysis (LCA) as a method for measuring the environmental effects of products throughout its stages from the beginning to its end (including production, consumption, and final disposal), and can be used in order to evaluate the impacts of the food waste technologies in order to minimize its effects and enhance sustainability [1]. Batool *et al.* [1] used the LCA for evaluating today's most used technologies in food waste management to assess its environmental impacts. The results of the LCA showed that among landfilling, composting, anaerobic digestion, incineration, pyrolysis, hydrothermal carbonization, gasification and esterification, landfilling and composting had the highest overall LCA impact value (Figure 2), while anaerobic digestion, gasification and esterification had the lowest. Compared to pyrolysis, incineration and hydrothermal carbonization had higher impact and overall medium LCA impact.

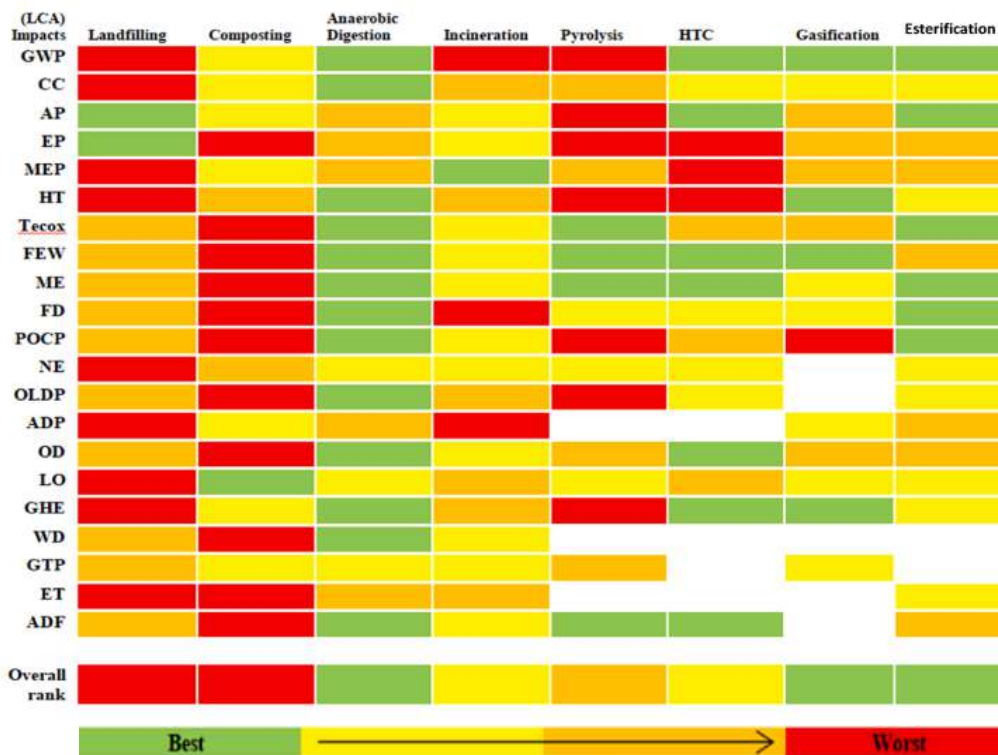


Figure 2 Life cycle analysis (LCA) environmental impacts comparison of most used technologies in food waste management [1]

(GWP – global warming potential, CC – climate change, AP – acidification potential, EP – eutrophication potential, MEP – marine eutrophication, HT – human toxicity, Tecox – terrestrial ecotoxicity, FEW – freshwater ecotoxicity, ME – marine ecotoxicity, FD – fossil depletion, POCP – photochemical ozone creation potential, NE – nutrient enrichment, OLDP – ozone layer depletion potential, ADP – abiotic depletion potential, OD – ozone depletion, LO – land occupation, GHE – greenhouse emissions, WD – water depletion, GTP – global temperature potential, ET – ecotoxicity, ADF – abiotic depletion fossil fuel)



Preferred method in the waste management is related to the level of the development of certain country [15]. Similarly, food waste generation in households per capita is found to be high in the developed countries (Table 1).

**Table 1** Average food waste (kg/capita/year) depending on the income of the country [5]

Income group	Average food waste (kg/capita/year)		
	Household	Food service	Retail
High-income	79	26	13
Upper middle-income	76	/	/
Lower middle-income	91	/	/

“/” Insufficient data.

It is obvious that a focus area for food waste prevention programmes must be household waste. For example, a 4-person household could save on average about 400 €/year if food waste is reduced in line with various proposals [2]. The Food and Agriculture Organization (FAO) of the United Nations is strongly dedicated to raise public awareness of this global problem by publishing guides explaining how to reduce environmental footprint from household food waste in simple and effective way [12,16]. The “motivation-opportunity-ability” framework has recently been promoted as a theoretical tool for reduction of household food waste by using tools such as stickers, leaflets, measuring cups, recipe cards etc. [17]. By analysing several household food management behaviours, van Herpen *et al.* [18] has provided initial evidence that self-reported survey measurements can be used to assess the effects of household food waste interventions and to effectively decrease the amount of food waste.

Comprehensive understanding of the factors contributing to food waste in various facilities such as healthcare, is crucial to develop effective strategies to minimize waste generation in complex surroundings [19]. Arriz-Jorquiera *et al.* [19] proposed mathematical framework for reducing food waste by approximately 22.5% in a 1000-bed hospital in Florida (USA) which could lead to weekly reduction of more than 113 kg of food waste.

### Prevention of food waste generation under legislative framework

The European Commission (EC) has established an action plan to reduce food waste as integral part of the Circular Economy [14]. Generally, the legislative proposals on waste in the Circular Economy include long-term targets to reduce landfilling of waste while increasing reuse and recycling of key waste streams, such as municipal and packaging waste [9]. The EU's Horizon research programme (2021–2027), will target actions in six clusters under ‘Global challenges and European industrial competitiveness’, in which one cluster represent food, bioeconomy, natural resources, agriculture and environment [20]. The EU and its Member States are also committed to achieving the global Sustainable Development Goal (SDG) of the United Nations, to reduce food waste per capita at the retail and consumer level by 2030, and to reduce food losses along the food production and supply chains within SDG Target 12.3. The focus is on two indexes: *the Food Loss Index* (measures losses for key commodities in a country across the supply chain, up to and not including retail), and *the Food Waste Index* (measures food and inedible parts wasted at the retail and consumer levels in food retail, households and food service sector) [5]. The EC also supports awareness rising

at national, regional and local levels and the dissemination of good practices in food waste prevention which are urgently needed in order to reach sustainability targets [9].

### **Value addition processes for biogas production**

Food waste as a stream of municipal solid waste is particularly hard to quantify because absence of harmonised and reliable method, which makes more difficult to assess its scale, origins, and trends of this kind of waste over time [9].

Prior to the production of valuable products, pretreatments of waste food are needed due to variable composition influenced by factors such as seasonal effect, cooking methods, consumption patterns and geographical variations. The percentage of biodegradable substances in food waste vary in the terms of carbohydrate (6–54%), protein (2.4–28%) and lipid (1.5–30%) contents. Kitchen waste, fruit and vegetable waste were found to contain the highest content of water, amounting to 60–90% [11]. According to Kannah *et al.* [10], food waste contains 39–65wt.% of carbon and 5.8–7.5wt.% of hydrogen, and regarding component analysis, it contains 35.1–67wt.% of carbohydrates. In addition, the food waste from beverage, dairy, fruit/vegetable, and cereal industries are rich in protein, fat, carbohydrates, which provides good possibility for production of fermentative products [3].

The pretreatment of food waste includes physical, chemical and biological methods, which can be used to enhance the hydrolysis rate of food digestion. The physical pretreatment methods, such as freezing, sonication, microwave and hydrothermal/thermal treatments, can disrupt the matrix structure of food waste resulting in enhancement of liquefaction of bio-substances, similar to chemical methods including ozonation, acid and alkaline reactions, which are used for disintegration. During biological methods, proteins, macromolecular starches, lipids, long chain fatty acids and free amino acids are converted by hydrolytic enzymes (protease, amylase, and lipase) into glucose and free ammoniacal nitrogen. This disintegration is favourable for biomethane production, and it does not cause secondary pollution of the environment [11].

Hydrogen is considered as one of the most promising clean and renewable fuels. Currently, prevalent processes for hydrogen production are unsustainable due to their dependence on fossil fuels or non-renewable energy sources [21]. Food waste can be converted to hydrogen through gasification of biomass *via* partial oxidation under high temperatures with suitable catalyst. However, the economic feasibility of this promising method needs further investigation [22]. The cost of hydrogen production from food waste is in the wide range, from 2.05 \$/kg up to 13.55 \$/kg [21]. Hossain *et al.* [21] showed that hydrogen fuel generated from food waste in Bangladesh during the course of 2023 was 0.46 million tons. The benefits from hydrogen production from food waste are numerous, apart from solving the problem of landfill sites, hydrogen used for energy production could have positive impact on the environment by reducing CO<sub>2</sub> emitted from fossil fuels, thus diminishing global warming potential, since a significantly smaller mass of hydrogen can displace much larger mass of fossil fuels, thus emphasizing its economic justification. The quantity of 0.46 million tons of hydrogen can substitute 1.9 million tons of coal, or 1.3 million tons of diesel or 1.19 million tons of natural gas. The quantity of saved diesel fuel could cut CO<sub>2</sub> emissions by 3.85 million tons [21,22].

Valorisation of food waste to biomethane is promising solution, which align with the growing global focus on sustainability, renewable energy, and waste reduction. Biomethane recovery from the organic biomass is the most successful by the anaerobic digestion. Process based on microorganisms or bacteria digestion can be operated at temperatures within mesophilic (at 37 °C) and thermophilic (at 55 °C) conditions. The recovered biogas comprises of 50–75% of biomethane and 25–50% of carbon dioxide [10], as well as hydrogen sulfide, ammonia gas, siloxanes, water vapour, and other volatile organic compounds. Therefore, biomethane need to be purified to a level above 95% [11]. According to data from the study by Ahire *et al.* [4], the highest quality biomethane was observed for fruit pulp, whereas the lowest quality was observed for vegetable waste. As previously said, anaerobic digestion is one of the technologies with the lowest LCA impact value [1].

## CONCLUSION

The main challenge of food waste management is highly variable and diverse nature and composition of food waste, which could be solved by central separation or by separation at the source. The improvements of the determination of feedstock composition are needed for efficient food valorisation. In the future, innovations in pretreatment methods would result in higher efficiency of the various bio-products from the food waste (e.g. food waste could be sustainable source of hydrogen-based energy). Probably the most cost-effective design regarding household food waste, as the dominant portion of the municipal waste, is to prioritize food waste reduction at the source. Multidisciplinary approach to this complex problem is surely needed, as well as greater engagement of all structures in resolving inappropriate disposal of food waste and cutting food losses.

## ACKNOWLEDGEMENT

*The authors are grateful to the Ministry of Science, Technological Development and Innovation of the Republic of Serbia for financial support, within the funding of the scientific research at the University of Belgrade, Technical Faculty in Bor (No. 451-03-65/2024-03/200131).*

## REFERENCES

- [1] Batool F., Kurniawan T.A., Mohyuddin A., *et al.*, Trends Food Sci. Technol. 143 (2024) 104287.
- [2] Eurostat, Food waste and food waste prevention – Estimates, Available on the following link: [https://ec.europa.eu/eurostat/statistics-explained/index.php?title=Food\\_waste\\_and\\_food\\_waste\\_prevention\\_-\\_estimates#Amounts\\_of\\_food\\_waste\\_at\\_EU\\_level](https://ec.europa.eu/eurostat/statistics-explained/index.php?title=Food_waste_and_food_waste_prevention_-_estimates#Amounts_of_food_waste_at_EU_level).
- [3] Sarangi P.K., Singh A.K., Sonkar S., *et al.*, Ind. Crops Prod. 205 (2023) 117488.
- [4] Ahire P.D., Upadhyay A., Talwar P., *et al.*, Biomass Bioenergy 182 (2024) 107107.
- [5] United Nations Environment Programme (UNEP) 2021, Food Waste Index Report 2021. Nairobi, ISBN: 978-92-807-3868-1.
- [6] Rifna E.J., Dwivedi M., Seth D., *et al.*, Sus. Chem. Pharm. 38 (2024) 101515.

- [7] European Commission, EU Food Loss and Waste Prevention Hub, *Available on the following link:* [https://ec.europa.eu/food/safety/food\\_waste/eu-food-loss-waste-prevention-hub/about](https://ec.europa.eu/food/safety/food_waste/eu-food-loss-waste-prevention-hub/about).
- [8] Food and Agriculture Organization (FAO), World Food and Agriculture – Statistical Yearbook 2022. Rome, ISBN: 978-92-5-136930-2.
- [9] European Commission, EC 2015, Closing the loop – An EU action plan for the Circular Economy, Brussels, 2.12.2015.
- [10] Kannah R.Y., Merrylin J., Devi T.P., *et al.*, Bior. Technol. Rep. 11 (2020) 100524.
- [11] Sethupathy A., Arun C., Vigneswaran V.S., *et al.*, Fuel 366 (2024) 131388.
- [12] Food and Agriculture Organization (FAO), Five quick tips for reducing food waste and becoming a Food hero, *Available on the following link:* [www.fao.org/newsroom/story/15-quick-tips-for-reducing-food-waste-and-becoming-a-Food-hero/en](http://www.fao.org/newsroom/story/15-quick-tips-for-reducing-food-waste-and-becoming-a-Food-hero/en).
- [13] Rakesh B., Mahendran R., Trends Food Sci. Technol. 143 (2024) 104274.
- [14] Official Journal of the European Union, Commission Notice, Guidelines for the feed use of food no longer intended for human consumption, 2018/C 133/02, 16.4.2018.
- [15] Khan A.H., Lopez-Maldonado E.A., Khan N.A., *et al.*, Chemosphere 291 (2022) 133088.
- [16] Food and Agriculture Organization (FAO) of the United Nations, Say NO to FOOD WASTE! – A guide to reduce household food waste, Cairo, 2020, ISBN: 978-92-5-131917-8.
- [17] Soma T., Li B., Maclaren V., Res. Conser. Rec. 168 (2021) 105313.
- [18] van Herpen E., Wijnen T., Quested T., *et al.*, J. Clean. Prod. 429 (2023) 139604.
- [19] Arriz-Jorquiera M., Acuna J.A., M. Rodríguez-Carbó, *et al.*, Waste Manag. 175 (2024) 12–21.
- [20] European Commission (EC) 2021, Horizon Europe, The EU Research & Innovation Programme 2021–2027, Investing to shape our future, *Available on the following link:* [https://research-and-innovation.ec.europa.eu/system/files/2022-06/ec\\_rtd\\_he-investing-to-shape-our-future\\_0.pdf](https://research-and-innovation.ec.europa.eu/system/files/2022-06/ec_rtd_he-investing-to-shape-our-future_0.pdf).
- [21] Hossain M.S., Wasima F., Shawon M.S.I.K., *et al.*, Energy Rep. 11 (2024) 3367–3382.
- [22] Elgazar Y.G., Khalifeh H.A., Alkhedher M., *et al.*, Int. J. Hydrogen Energy, *Article in press* (<https://doi.org/10.1016/j.ijhydene.2024.03.070>).



## DECENTRALIZATION OF THE URBAN TOURIST ZONE OF ZLATIBOR

Maja Bogdanović<sup>1\*</sup>, Irena Blagajac<sup>1</sup>

<sup>1</sup>University of Belgrade, Faculty of Geography, Studentski trg 3/3, 11000 Belgrade, SERBIA

\*[bogdanovic.maja97@gmail.com](mailto:bogdanovic.maja97@gmail.com)

### Abstract

*Tourism cannot be imagined without preserved natural and cultural values, and it is important to raise awareness about the responsible business of the carriers of the tourist offer and the conscientious behavior of tourists. They should be directed towards insufficiently valorized potentials and thereby enable more even tourism development. The urban area of Zlatibor and the surrounding tourist values are an example of the necessary decentralization in order to prevent environmental degradation. The goal of scientific paper is twofold. The authors aim to point out the aggressive urbanization of Zlatibor, which greatly affects the once-preserved natural values and which directly conflicts with the application of the principles of sustainable development. Also, the goal is to present opportunities for the responsible development of tourism and complementary activities, which will undoubtedly encourage the conscientious construction of residential buildings and other facilities, important for the quality of life of the resident population. Establishing sustainability in mountains is of multiple importance, which can be observed at the local, regional, national and even global level. The analysis of planning documentation, available literature and satellite images determined the criteria on the basis of which the main analysis in the paper, SWOT analysis, was applied. Using Geographical Information Systems, the program QGIS 3.16. the analyzed data are shown cartographically.*

**Keywords:** decentralization, Zlatibor, sustainable tourism, urban area.

### INTRODUCTION

Environmental degradation, caused as a result of anthropogenic activities, is one of the more serious problems of today [1,2]. The authors Hoffmann *et al.* [3], in addition to climate change, population growth and intensive exploitation of natural resources, identify urbanization, with all its effects on the environment, as a leading problem of society, and the consequences of urbanization are deforestation, loss of habitat and biodiversity, pollution water, air and soil [4].

Mountain ecosystems represent an important source of water, energy and biological diversity, and are key to maintaining the global ecosystem [5]. Deforestation, intensive agriculture, pollution and accelerated infrastructure construction have caused more than 50% of mountain areas worldwide to be under strong pressure from human activities, especially at lower altitudes and mountain bases [6–8]. Zlatibor is the oldest mountain tourist destination in Serbia. It developed as a sports and recreation center on gentle slopes, at an altitude between 950 and 1,000 m. According to the data of the Statistical Office of the Republic of Serbia, Zlatibor has been the most visited mountain destination in Serbia for a long time, both in terms of arrivals and overnight stays of domestic tourists, as well as in terms of arrivals and

overnight stays of foreign tourists [9]. The growing interest of domestic and foreign tourists has encouraged the construction of accommodation facilities and additional facilities, complementary to tourism. The development of infrastructure was particularly favored by the accelerated issuance of building permits, which was shortened from more than a year to at least a month. Such conditions in Zlatibor led to urban disorder, caused by the expansion of tall buildings in a short time [10]. The urban center of the Zlatibor mountain is located in the municipality of Čajetina. Also, on the territory of the municipality of Čajetina, there are natural and cultural-historical values which are recognized as a potential for the decentralization of the urban tourist zone of Zlatibor. Nature Park “Zlatibor” includes the municipalities of Nova Varoš, Užice and Čajetina.

## **MATERIALS AND METHODS**

The method of analysis and synthesis, the method of comparison, the statistical method and the method of classification were used. The main analysis used in the paper is SWOT, which was conceived by a research team consisting of A. Humphrey, M. Doshier, O. Benepe, B. Lien in the period 1960–1970. The SWOT analysis matrix is composed of weaknesses and strengths related to the internal environment of the observed territory, and opportunities and threats as external factors. The advantage of SWOT analysis is setting a clear development strategy and defining concrete goals. It should be kept in mind that, if the data is not analyzed in a proper way, it is possible to identify the current situation poorly and set goals inadequately [11]. The SWOT analysis was done with the aim of assessing the strengths, weaknesses, opportunities and threats for the decentralization of the touristic urban zone of Zlatibor. The analysis of the planning documentation, available literature and satellite images determined the criteria on the basis of which the SWOT analysis was performed.

The program used to process cartographic data is QGIS 3.16. SRTM (Shuttle Radar Topography Mission) DEM (Digital Elevation Model) was used to create the terrain slope and hypsometry Figure, which was recorded in 2000, and the resolution of the image was reduced to 100 m [12]. The land use Figure was made based on Corine Land Cover 2018 [13]. Geospatial data were digitized using Google Satellite.

## **RESULTS AND DISCUSSION**

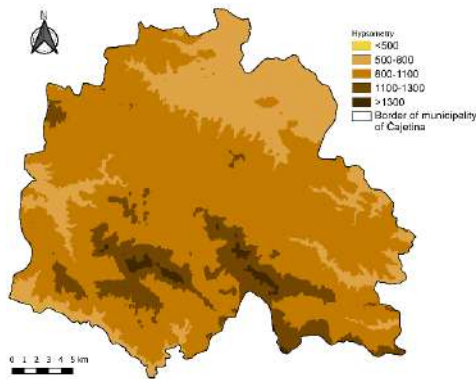
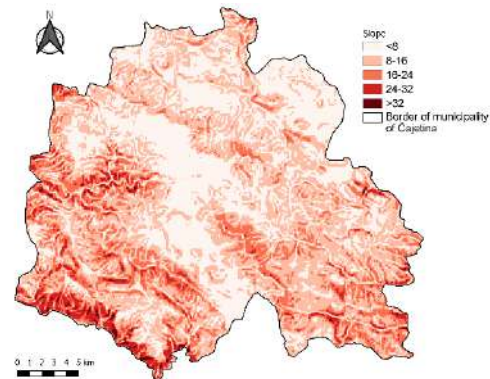
### **Physical-geographic characteristics**

The following mountain peaks stand out: Tornik (1,496 m asl), Čigota (1,422 m asl), Borkovac (1,260 m asl). By dividing Crni Rzav, lakes Kraljeve Voda and Ribničko Lake were formed. The climate is moderate-continental, mountain climate [14]. The areas (km<sup>2</sup>) and share in the total area (%) of all hypsometric zones and terrain slope zones are shown in Table 1. Figure 1 shows the hypsometry of the terrain, the zone 800–1,100 m above sea level is the most represented (417.58 km<sup>2</sup>, 64.74% of the total area). The slope of the terrain is shown on Figure 2, the most common slopes are from 8° to 16° (268.22 km<sup>2</sup>, 41.58% of the total area).



**Table 1** Area (km<sup>2</sup>) and share in the total area (%) of classes of hypsometry and terrain slope [12]

<b>Hypsometry</b>				<b>Slope</b>			
<i>m asl</i>	<i>class</i>	<i>km<sup>2</sup></i>	<i>%</i>	<i>Slope (°)</i>	<i>class</i>	<i>km<sup>2</sup></i>	<i>%</i>
<500	1	0,63	0,10%	<8	1	241,8	37,49%
500–800	2	144,3	22,37%	8–16	2	268,22	41,58%
800–1100	3	417,58	64,74%	16–24	3	103,3	16,02%
1100–1300	4	75,53	11,71%	24–32	4	28,76	4,46%
>1300	5	6,97	1,08%	>32	5	2,93	0,45%

**Figure 1** Hypsometry [12]**Figure 2** Slope of the terrain [12]

### Analysis of natural and cultural-historical values recognized as the potential of urban zone decentralization

Zlatibor Mountain has an exceptional natural potential, which, together with anthropogenic values, forms a good basis for the development of various forms of tourism [10]. However, according to the Spatial Plan of the Republic of Serbia, this area is assessed as an area of endangered environment with minor impacts on biodiversity, people and quality of life [15]. That is why it is important to look at the natural and cultural values which favour the decentralization of the urban zone and the development of sustainable forms of tourism.

Figure 3 shows the natural and cultural-historical values which are recognized as potential for the decentralization of the urban zone. The ski center “Tornik”, named after the highest peak of Zlatibor, stands out. There are five trails with a total length of 10 km, and the capacity of the ski resort is 5,400 skiers per hour. Especially attractive is the Gold gondola which goes over the mountain scenery and the Ribnica lake. The ski center is also open to visitors during the summer months, and offers: a panoramic cable car ride, bobsled, tubing track, adventure park, mini golf course, zip line and multifunctional sports fields [16].

The observed area is also characterized by geoheritage, which is reflected in the terrain made of limestone with dolomites, with the presence of ultrabasic rocks (periodite) and serpentine. The speleological object Nature Monument “Stopića cave” stands out [17]. Stopića cave is located on the left bank of the river Prištevica, on the eastern slopes of Zlatibor. Big green tubs are attractive, which are also the emblem of the cave and the main reason for the arrangement of the cave system [18].

Near Zlatibor is the village of Gostilje, known for its waterfall, which represents one of the most attractive hydrological values of this region. Harmoniously arranged rocks covered with moss and water breaking through them attract the attention of domestic and foreign tourists.

The area around the waterfall is completed with marked footpaths, benches and a children's playground [19]. Of the natural values, the Prerast in Dobroselica, Jokino spring, Sušičko spring, viewpoints of Gradina and Obadovo brdo, as well as Skakavac waterfall are also significant. The municipality of Čajetina partly includes the area of the “Zlatibor” Nature Park. It was declared as a natural asset of exceptional importance due to the geomorphological and hydrological phenomena of distinctly dissected terrain, striking valleys of canyon and gorge type, preserved ecosystems, as well as exceptionally preserved monumental and ethnic heritage [20].

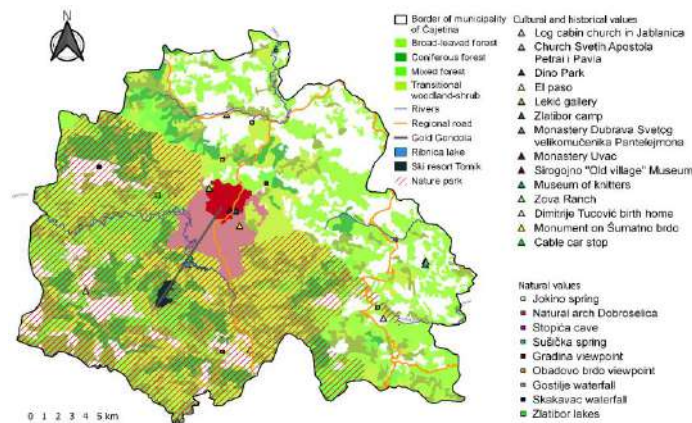


Figure 3 Natural and cultural-historical values [13]

Among the cultural values, the village of Sirogojno, which houses the National Architecture Museum “Old village”, is a unique example of a traditional Serbian village in the mountainous areas of the Dinaric region. The museum complex also includes the Church of the Holy Apostles Peter and Paul and together they form a category I protected cultural property of exceptional importance [14]. In the village of Sirogojno there is also the Museum of Knitters, which preserves the memory of the handicrafts of Zlatibor knitters. At the place where the municipalities of Čajetina and Priboj meet, there is the Uvac monastery, which, thanks to the research of the National Museum from Užice, was renovated and placed under the protection of the state [16]. On one of the meanders of the Uvac river, on a hill which surrounds the impressive canyon of the river on three sides, the Dubrava monastery is located. Tourist attractions such as the “El Paso City” theme park, Dino Park, Dimitrije Tucović's birthplace, etc. contribute to the development of tourism in this region.

### SWOT analysis

Directing tourists and developing the tourist offer towards natural and cultural values which are outside the strict urban center of Zlatibor is key to preserving the environment of this area. The excessive pressure of tourists towards the center of Zlatibor encourages uncontrolled construction, which leads to inevitable devastation, not only of the mentioned urban zone, but also threatens the ecological sustainability of protected areas. In order to accurately present the possibilities for the decentralization of the tourist offer, but also to define the perspectives of future, sustainable development, a SWOT analysis was used.

In order to talk about the possibilities for further development, it is necessary to refer to the identified weaknesses and risks. If the competent institutions and bodies do not look at these problems, the key values of this area may lose their importance and thereby endanger the development of tourism and future economic development. In the Report [21], it is stated that tourist facilities and households are the main source of pollution, and that the cause is a partially constructed sewage system. Due to the planned increase in tourist capacities, greater pressure on the quality of water and soil is expected. The more intensive development of the tourist offer, among other things, affects the increase in the amount of waste that is disposed of in illegal landfills, the occupation of free land in order to build tourist facilities and the increase of waste water. It is also emphasized that natural and cultural assets may be exposed to greater risk due to construction pressure.

**Table 2** SWOT analysis of tourism development in the territory of the municipality of Čajetina

STRENGTHS	WEAKNESSES
<ul style="list-style-type: none"> <li>• favorable traffic-geographical position</li> <li>• favorable tourist-geographic position</li> <li>• favorable climatic conditions</li> <li>• medicinal and recreational importance</li> <li>• recognition on the tourist market</li> <li>• attractive natural values</li> <li>• rich cultural and historical heritage</li> <li>• diverse tourist offer</li> <li>• Tornik ski resort</li> <li>• preservation of ethnic heritage</li> <li>• recognizable gastronomic specialties</li> </ul>	<ul style="list-style-type: none"> <li>• inadequate protection of natural values in the zone of more intensive tourist use</li> <li>• inadequate presentation of cultural and historical heritage</li> <li>• excessive unplanned construction</li> <li>• monocentric tourist offer</li> <li>• large concentration of tourists in the urban area</li> <li>• noise emission</li> <li>• inadequate regulation of waste water</li> <li>• abandonment of villages and rural activities</li> <li>• environmental pollution</li> </ul>
OPPORTUNITIES	THREATS
<ul style="list-style-type: none"> <li>• creation of attractive tourist arrangements aimed at areas outside the urban area</li> <li>• ecotourism</li> <li>• creative tourism</li> <li>• rural tourism</li> <li>• cycle tourism</li> <li>• adventure tourism</li> <li>• sustainable tourism</li> <li>• gastronomic tourism</li> <li>• educational tourism</li> <li>• raising environmental awareness</li> <li>• cooperation of the local community and local authorities</li> <li>• greater commitment of local self-government and competent institutions</li> <li>• marketing activities aimed at sustainable tourism</li> </ul>	<ul style="list-style-type: none"> <li>• permanently degraded surfaces</li> <li>• deforestation</li> <li>• environmental devastation</li> <li>• natural disasters</li> <li>• soil erosion</li> <li>• disruption of the natural balance, especially in the area of the “Zlatibor” Nature Park</li> <li>• climate changes</li> <li>• threatened biodiversity and habitats</li> <li>• competitiveness of destinations in the area in the field of winter tourism</li> <li>• the disappearance of the winter season</li> <li>• departure of young people from rural areas of Zlatibor</li> <li>• construction pressure</li> <li>• economic crisis and inflation</li> <li>• market instability</li> </ul>

Source: SWOT analysis was created based on available data from relevant documents [21,14,22]

Jeftić *et al.* [9] warn that climate change directly affects mountain tourism in the winter season. Zlatibor cannot redirect the winter tourism offer to higher altitudes because all facilities are already located at the highest altitudes. They propose to improve the offer in the off-season, as well as in the summer period of the year. The authors particularly point to the importance of ecotourism, which significantly contributes to sustainable development at the

local level, nurtures natural values, educates tourists about the importance of environmental protection and is a source of income for the local population [23]. The potential for the development of cycle tourism contributes to the preservation of the environment and the relief of the urban zone of Zlatibor. In the Spatial Plan [22] trails suitable for mountain biking are highlighted: “Ozone trails of Zlatibor” for excursions (health trails on Čigota, “Avantura Mokra Gora”, “Zlatibor Bogaze” and “Sirogojno”), as well as excursion sites and bathing areas such as Jokino spring, which is located on the way to Mokra Gora. These forms of tourism can attract domestic and foreign tourists who are looking for active rest and recreation. Raising the environmental awareness of the local community and tourists, greater efforts by competent institutions and adequate promotion of sustainable forms of tourism can greatly contribute to reducing the pressure on the urban area of Zlatibor, adequate valorization of tourist values in the immediate vicinity, higher tourist traffic and more even occupancy of accommodation capacities.

Mountains are attractive tourist destinations, so the competent authorities adapt them to the needs of modern tourist demand, investors and the local community. On the one hand, the development of tourism in the mountains can have a positive impact on the implementation of sustainability principles, economic benefits for the local population and the valorization of the natural beauty of the mountain area [24], however, large-scale construction projects, noise and a large number of tourists threaten natural habitats and the quality of life of the resident population [25]. Natural values should be used for the development of tourism, but with an emphasis on environmental protection. This would encourage the construction of new accommodation capacities, the modernization and reconstruction of roads, while it is necessary to respect the principles of ecological capacity of the territory [26].

## **CONCLUSION**

In order to prevent the devastation of natural and cultural values, and at the same time preserve the authenticity of the destination, it is necessary to use the available potential evenly. Also, investments should be directed towards values that are not sufficiently utilized so that the tourist offer outside the urban zone of Zlatibor attracts the attention of domestic and foreign visitors. At the same time, educational workshops should be organized so that the local population and tourists are aware of the consequences of inadequate use of space and resources.

If the trend of increasing anthropogenic influence in the urban part of Zlatibor continues, it will threaten the natural values of the “Zlatibor” nature park. The anthropogenic pressure exerted on the physical-geographical characteristics of the observed territory exceeds the ecological capacities. Biodiversity, habitats, forest landscapes, geological and pedological base, terrain hydrology and geomorphological values are threatened. Therefore, it is necessary for the local government to point out the problem of increasing intensity of anthropogenic influence in the urban center of Zlatibor and to propose a measure of environmental protection by decentralizing the center to the peripheral zone. A stay in the strict center of Zlatibor gives the impression of a classic city, where noise, crowds, high prices and air pollution are inevitable. Control of protective measures due to illegal construction should be increased and the time for issuing building permits should be increased. Stricter punitive

measures are necessary for unscrupulous behavior of tourists who endanger natural and cultural-historical values.

## **ACKNOWLEDGEMENT**

*The study was supported by the Ministry of Science, Technological Development and Innovation of the Republic of Serbia (Contract number 451/03/65/2024-03/200091). Maja Bodanović, Scholarship recipient, is grateful to the Ministry of Science, Technological Development and Innovation of the Republic of Serbia for the support provided in research work.*

## **REFERENCES**

- [1] Raj, A., Jhariya, M. K., Banerjee, A., *et al.*, Land and Environ. Manage. through Forestry, 66 (2023) 1–21.
- [2] Zhang, J., Chen, Y., Li, Z., *et al.*, Sustain. Cities and Soc., 51 (2019).
- [3] Hoffmann, E.M., Schareika, N., Dittrich, C. *et al.*, Sustain Sci, 18 (2023) 1739–1753.
- [4] Understanding global change. Urbanization, Available on the following link: <https://ugc.berkeley.edu/background-content/urbanization/>.
- [5] Kuščer, K., Mihalič, T. Acta Turistica 26(2) (2014) 103–129.
- [6] Bohara, M., Yadav, R.K.P., Dong, W., *et al.*, Sustainability, 11(6) (2019).
- [7] Elsen, P.R., Monahan, W.B., Merenlender, A.M. Nature Commun., 11(1974) (2020).
- [8] He, X., Ziegler, A.D., Elsen, P.R., *et al.*, One Earth, 6(3) (2023) 303–315.
- [9] Jeftić, M. R., Šećerov, V., Nikolić, T., *et al.*, Fresen. Environ. Bullet. Parlar Scient. Public., 31(3) (2022) 2862-2870.
- [10] Filipović, M., Hadžić, M., Vujošević, M. 6<sup>th</sup> International Thematic Monograph - Modern Management Tools and Economy of Tourism Sector in Present Era, Editors: Bevanda, V., Štetić, S., Association of Economists and Managers of the Balkans in cooperation with the Faculty of Tourism and Hospitality, Ohrid (2022), p. 501, ISBN: 978-86-80194-49-3.
- [11] Božac, M. G. Economic research, 21 (1) (2008) 19–34.
- [12] USGS, USGS EROS Archive - Digital Elevation - SRTM, Available on the following link: <https://www.usgs.gov/centers/eros/science/usgs-eros-archive-digital-elevation-shuttle-radar-topography-mission-srtm-1>.
- [13] Copernicus, Corine Land Cover, CLC 2018 (vector 100 m), Europe, Available on the following link: <https://land.copernicus.eu/en/products/corine-land-cover/clc2018>.
- [14] Government, Territorial Unit of the Republic of Serbia. Spatial plan of the Municipality of Cajetina (“Official Gazette of the City of Belgrade”, no. 10/10) Belgrade, Serbia, (2010).
- [15] Đorđević, S., Đorđević-Milošević, S., Vujović, Z., *et al.*, Svarog, 12 (2016) 249-266.
- [16] Tourist association of Zlatibor. Skiing, Available on the following link: <https://www.zlatibor.org.rs/sr/o-zlatiboru/sportski-turizam/skijanje/>.
- [17] Denda, S. Hotel and Tourism Manage., 2(2) (2014) 95–105.



- [18] Stupar, M., Savković, Ž., Popović, S., *et al.*, *Microb Ecol*, 86 (2023) 2021–2031.
- [19] Tourist association of Gostilje. Gostilje waterfall near Zlatibor, *Available on the following link*: <http://www.gostiljevodopad.rs/vodopad.html>
- [20] Šljukić, B., Miletić, D., Jančić, G. *et al.*, *Bullet. of the Faculty of Forestry*, (2023) 119–134.
- [21] Government, Territorial Unit of the RS. Report on the strategic assessment of the impact of the Spatial Plan of the Special Purpose Area of the “Zlatibor” Nature Park on the environment (“Official Gazette of the City of Belgrade”, no. 92/17) Belgrade, Serbia, (2017).
- [22] Government, Territorial Unit of the RS. Spatial plan of the special purpose area of the Zlatibor Nature Park (“Official Gazette of the City of Belgrade”, no. 2/20) Belgrade, Serbia, (2020).
- [23] Muntlak Ivanović, O., Nadić, P.D., Vujić, M.M. *Ecologica*, 30(110) (2023) 189–194.
- [24] Firoiu, D., Ionescu, H.G., Bădîrcea, R., *et al.* *Sustainability*, 11(22) (2019) 6487.
- [25] Bogdanović, M., Đukić, M. *Environmental Sustainability and Climate Changes: scientific monograph*, Editors: Šarović, R., Bigović, M., Kasalica, S., University of Montenegro. Environmental Protection Agency of Montenegro. Wild Beauty Art Festival (2023), p.576, ISBN: 978-86-7664-252.6.
- [26] Blagajac, I., Djuric, M. *Collec. of papers of young resear.: “Local self-govern. in plan. and arrange. of space and settle.”*, Belgrade, Serbia (2022) 53–61.





## ISOLATION AND CULTIVATION OF CHROOCOCCUS (CYANOBACTERIA) FROM AEROPHYTIC BIOFILM IN STOPIĆ CAVE

Sladana Popović<sup>1\*</sup>, Nataša Nikolić<sup>1</sup>, Željko Savković<sup>1</sup>, Miloš Stupar<sup>1</sup>,  
Dragana Predojević<sup>1</sup>, Ana Anđelković<sup>2</sup>, Olga Jakovljević<sup>1</sup>

<sup>1</sup>University of Belgrade, Faculty of Biology, Institute of Botany and Botanical Garden  
“Jevremovac”, Department of Algology and Mycology, Takovska 43,  
11000 Belgrade, SERBIA

<sup>2</sup>Department of Weed Research, Institute for Plant Protection and Environment,  
Teodora Drajzera 9, 11040 Belgrade, SERBIA

\*spopovic.bio@gmail.com, sladjana.popovic@bio.bg.ac.rs

### Abstract

*Cyanobacteria, characterized by unique physiological and biochemical mechanisms to withstand harsh conditions in different habitats, can thrive in a variety of environments, including extreme ones such as illuminated parts of caves. The information on diversity, biology and ecology of aerophytic Cyanobacteria, especially those from cave habitats, is very limited, which is especially true for the coccoid forms. Phototrophic biofilm was collected from the entrance zone of Stopić Cave to isolate coccoid Cyanobacteria. The biofilm was inoculated in situ into test tubes containing solid BG11 growth medium, after which the test tubes were kept in a growth chamber under controlled conditions. From the initial culture, which contained multiple cyanobacterial species, subsamples were extracted and transferred to Petri dishes. These were kept under optimal conditions until a pure cultures were obtained. The representative of the coccoid Cyanobacteria, Chroococcus, was isolated and its characteristics best matched the original description of Chroococcus turgidus.*

**Keywords:** phototrophic biofilms, cave habitats, algal cultures, Cyanobacteria, *Chroococcus*.

### INTRODUCTION

Cyanobacteria are known to thrive in a variety of environments, including extreme ones. Their ability to colonize extreme environments reflects their versatility and adaptability, and it is known that they have usually evolved unique physiological and biochemical mechanisms to withstand the harsh conditions in different habitats. Many of them inhabit caves, which often harbour unique and interesting organisms that have adapted to the particular conditions in these subterranean spaces. In caves, Cyanobacteria are found in a variety of locations, often associated with specific microhabitats where light, water and nutrients are available. Light in caves is available through entrances, cave holes or cracks in the cave ceiling, but also through the installed artificial light in show caves. The diversity and abundance of Cyanobacteria in caves can depend on various factors, e.g. light, the presence of water, the availability of nutrients, microclimatic conditions, the morphology of the cave, etc. However, cave Cyanobacteria are often adapted to low light conditions and may have unique characteristics compared to their surface-dwelling relatives [1,2].

Although aerophytic Cyanobacteria are found in a wide range of environments, detailed information on their diversity, biology, and ecology remains limited [3]. Many cyanobacterial species, especially in aerophytic habitats, are still considered unknown and the morphology of coccoid Cyanobacteria is particularly poorly characterized [4]. In recent years, considerable efforts have been made to improve the knowledge on coccoid Cyanobacteria by adopting a polyphasic approach based on morphology, ecology, physiology, systematics, and molecular biology [5]. Although morphological analyses are becoming less common, they remain crucial for studying Cyanobacteria and can be the key to linking all findings when studying certain taxa [6]. Additionally, correct identification often requires the isolation of Cyanobacteria and their cultivation on defined growth media prior to any other analysis [3].

The aim of the study was to isolate and cultivate coccoid Cyanobacteria from a biofilm at the cave entrance in order to characterize it based on morphological and ecological criteria.

## **MATERIALS AND METHODS**

### **Locality and sampling procedure**

The aerophytic biofilm sample from which the Cyanobacterium was isolated was collected in the entrance zone of the Stopić Cave (43°42'12.0"N 19°51'12.4"E), a famous show cave in western Serbia. The biofilm was sampled in two ways: the algal material was scraped directly with a sterile scalpel into the test tubes with solid growth medium [3,7] and was collected in sterile polyethylene bags and transported to the laboratory [8,9], where it was optically observed using a Zeiss Axio Imager M1 light microscope connected to camera and photographs we got were analysed by Axio Vision 4.8 software. The predominant phototrophs of the biofilm were identified using the standard identification keys.

### **Medium preparation for algal cultivation**

The BG11 medium was prepared according to the recipe given in Rippka *et al.* [10]. The further steps were carried out as described in Nikolić *et al.* [7]. The medium was poured into test tubes and Erlenmeyer flasks in which agar was added at a concentration of 1.3 % to 1.5 % to solidify the BG-11 medium and autoclaved at 121°C for 15 minutes after sealing the glassware. After autoclaving, the agar slants were allowed to cool completely in an inclined position, while the slightly cooled medium in the Erlenmeyer flasks was poured into sterile plastic Petri dishes and then allowed to solidify completely. The agar slants with solid BG11 medium were used to collect the biofilm as described above, while the Petri dishes with solid BG11 medium were used to cultivate and subcultivate the phototrophs of interest.

### **Cultivation process and observing the taxa developed in culture**

The test tubes in which the biofilm was sampled were kept in a growth chamber at a temperature between 19°C and 22°C and a 12-hour light: 12-hour dark cycle. After the Cyanobacteria had developed on agar slants, small parts of the developed colonies were transferred to Petri dishes where they could continue to grow. The Petri dishes were regularly sub-cultured until a uni-culture was obtained and everything was optically examined using a light microscope.

## RESULTS AND DISCUSSION

The cave walls in the entrance zone of the Stopić Cave are covered with diverse phototrophic biofilms, varying from weak to well developed, non-gelatinous or gelatinous, green to different colours. The sampled biofilm was well developed, dark coloured and gelatinous, indicating the dominance of Cyanobacteria, more specifically coccoid forms [11]. Microscopical analyses showed the presence of Cyanobacteria, Chlorophyta and Bacillariophyta, with Cyanobacteria dominating. More precisely, coccoid cyanobacterial forms dominated, and the following taxa were prevalent in the biofilm: *Aphanocapsa muscicola*, *Chroococcus ercegovicii*, *Chroococcus tenax*, *Chroococcus turgidus*, *Gloeocapsa alpina*, *Gloeocapsa compacta*, *Gloeocapsa nigrescens*. Simple trichal forms were characterized by the presence of *Leptolyngbya* representatives, with *Leptolyngbya foveolarum* being the most conspicuous, while *Nostoc punctiforme* and *Scytonema mirabile* represented heterocytous forms. The dominance of coccoid forms in the biofilms of the cave entrance zone has been noted in many studies of cave environments in Serbia and abroad [8,12,13].

After inoculation of the biofilm into the growth medium *in situ*, the agar slants were placed in the algal growth chamber, where the growth of algal colonies of different algal and cyanobacterial taxa on the solidified BG11 medium was observed after three weeks. They were all transferred to separate Petri dishes to form different cyanobacterial cultures. After several subculturing steps at three-week intervals, pure uni-cyanobacterial cultures were obtained, and some coccoid cyanobacterial forms were isolated. One colony transferred to Petri dishes led to the establishment of a culture of a coccoid Cyanobacterium of the genus *Chroococcus*.

*Chroococcus* Nägeli is one of the most common genera of coccoid Cyanobacteria [6]. According to Komárek and Anagnostidis [14], the genus *Chroococcus* is characterized by the following features: the cells are rarely solitary (only initial stages) and often aggregate into colonies with a small number of cells (2-16-32), rarely forming compound and multicellular agglomerations; within multicellular colonies, the cells sometimes form packet-like groups of 2–8 cells; the cells or groups of cells are surrounded by mucilaginous sheaths, which may vary in thickness, lamellation (simple – single-layered or strongly lamellated), colour and whether they are delimited or not, depending on the species; narrow individual sheaths following the cell outline surround the cells; the cells are initially subspherical, widely oval or spherical, later hemispherical or in the form of a segment of sphere; cell content is highly variable depending on the species and may be differently coloured, homogeneous or granular [14]. *Chroococcus* is found in terrestrial environments, where it inhabits the soil and various substrates exposed to the air (aerophytic), and in aquatic environments (freshwater ecosystems, marine and thermal waters), as well as in many extreme habitats [6,14].

The isolated taxon was characterized by 2-4-8 (-16-32) celled colonies, while solitary cells were rarely seen. The mucilaginous envelope is lamellate (in many cases a slight lamellation is visible), colourless and usually copies the outline of single cell or groups of cells. Cells are spherical, oval, later hemispherical or in the form of a segment of a sphere, blue-green, olive-green, yellowish to brownish, 13.5–28.5 µm in diameter without sheaths. The cell contents are finely granular (Figure 1). This isolated Cyanobacterium has characteristics that are most consistent with the original description of *Chroococcus turgidus*.

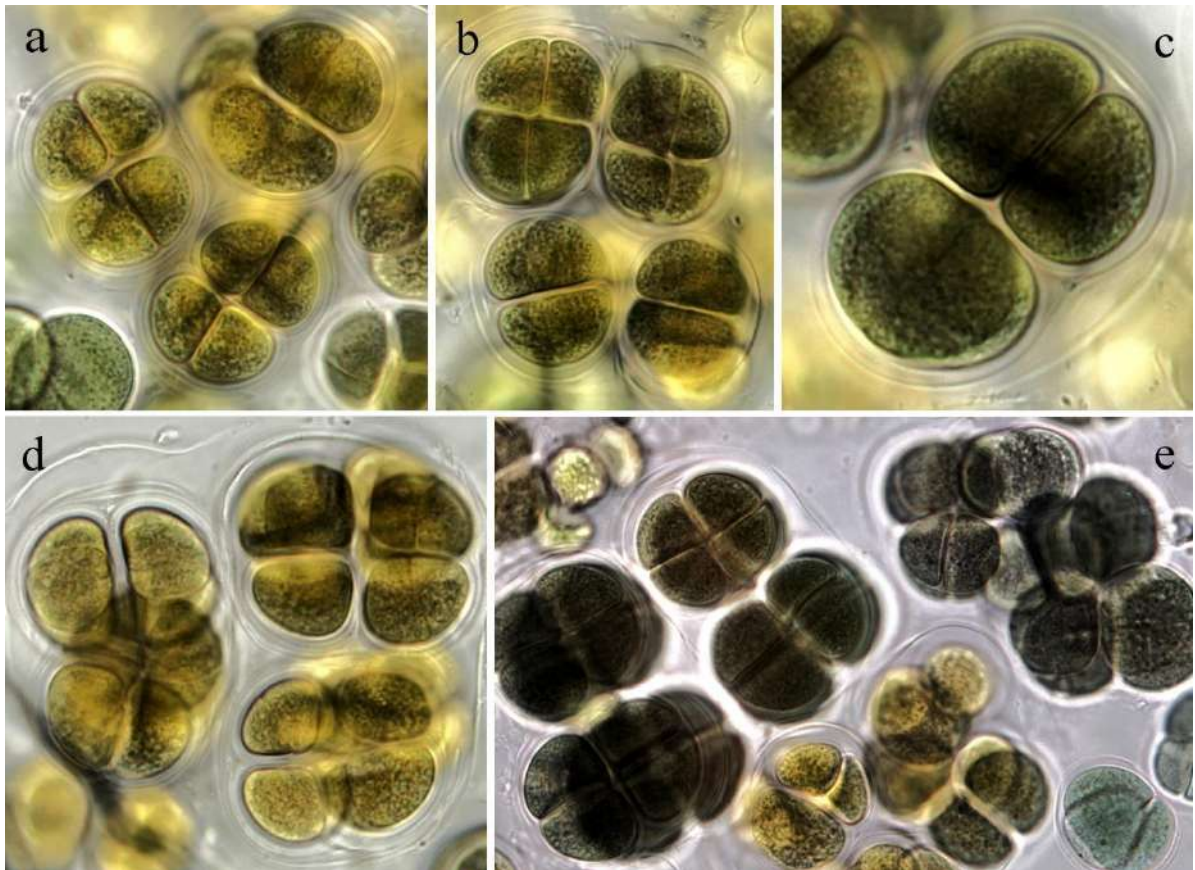


**Figure 1** a)–e): The isolated coccoid Cyanobacteria (genus *Chroococcus*) from cave entrance zone aerophytic phototrophic biofilm in Stopić Cave

According to many studies, *Chroococcus turgidus* inhabits diverse environments and shows significant morphological variations [6,14], suggesting a generalist habitat and a wide distribution [6]. As can be seen in Figure 1, variable cell sizes, cell arrangements and colours are observed. This is to be expected and is also confirmed by phylogenetic studies, according to which some morphological features of *Chroococcus* species, such as the presence and morphology of mucilage and the size of cells, are generally environment dependent [15]. Nevertheless, we should not exclude the phenomenon of possible slight differences between the phenotype in laboratory culture and the phenotype in its natural habitat [16,17].

## CONCLUSION

The representative of coccoid Cyanobacteria was isolated from an aerophytic phototrophic biofilm that had developed in the entrance zone of the Stopić Cave. In terms of its characteristics, it was the most consistent with the original description of *Chroococcus turgidus*. Coccoid cyanobacterial species are generally poorly studied, especially from aerophytic habitats and caves, so this study should serve as a basis for many similar future researches. The study of extremophilic Cyanobacteria not only improves our understanding of the diversity of life, but also provides insights into the mechanisms of adaptation to extreme conditions that can be utilised in various scientific and industrial fields.



## ACKNOWLEDGEMENT

The authors are grateful to the Ministry of Science, Technological Development and Innovation of the Republic of Serbia for the financial support according to the contract with the registration number (451-03-66/2024-03/ 200178, 451-03-65/2024-03/ 200178, 451-03-66/2024-03/200010).

## REFERENCES

- [1] Albertano P., Cyanobacterial biofilms in monuments and caves in *Ecology of Cyanobacteria II: their diversity in space and time*, Editor: Whitton B.A., Springer, Netherlands (2012), pp. 317–343.
- [2] Pentecost A., Whitton B.A., Subaerial Cyanobacteria in *Ecology of Cyanobacteria II: their diversity in space and time*, Editor: Whitton B.A., Springer, Netherlands (2012), pp. 291–316.
- [3] Gärtner G., Stoyneva P.M., Mancheva D.A., *et al.*, Ber. Nat. Med. Verein Innsbruck. 96 (2010) 27–34.
- [4] Luz R., Cordeiro R., Kaštovský J., *et al.*, Diversity 15 (12) (2023) 1157.
- [5] Komárek J., Kaštovský J., Mareš J., *et al.*, Preslia. 86 (2014) 295–335.
- [6] Gama W.A., Rigonato J., Fiore M.F., *et al.*, Eur. J. Phycol. 54 (3) (2019) 315–325.
- [7] Nikolić N., Subakov Simić G., Golić I., *et al.*, Arch. Biol. Sci. 73 (3) (2021) 341–351.
- [8] Popović S., Subakov Simić G., Stupar M., *et al.*, J. Cave. Karst Stud. 79 (1) (2017) 10–23.
- [9] Popović S.S., Nikolić N.V., Pečić M.N., *et al.*, Geoheritage 15 (2023) 14.
- [10] Rippka R., Deruelles J., Waterbury J., *et al.*, J. Gen. Microbiology 111 (1) (1979) 1–61.
- [11] Popović S., Krizmanić J., Vidaković D., *et al.*, Environ. Monit. Assess. 192 (11) (2020) 720.
- [12] Martinez A., Asencio A.D., J. Cave. Karst Stud. 72 (2010) 11–20.
- [13] Mulec J., Kosi G., Vrhovšek D., J. Cave. Karst Stud. 70 (1) (2008) 3–12.
- [14] Komárek J., Anagnostidis K., Cyanoprokariota. 1. Teil: Chroococcales in *Süßwasserflora von Mitteleuropa*, Editors: Ettl H., Gärtner G., Heynig H., Mollenhauer D., Spektrum Akademischer Verlag, Heidelberg, Berlin (1998).
- [15] Komárková J., Jezberová J., Komárek O., *et al.*, Hydrobiologia 639 (2010) 69–83.
- [16] Palinska K.A., Krumbein W.E., Ann. Bot. Fenn. 35 (1998) 219–227.
- [17] Morales E.A., Trainor F.R., Korean J. Phycol. 12 (3) (1997) 147–157.



## MORPHOMETRIC STUDY OF EUROPEAN BULLHEAD *Cottus gobio* FROM DIFFERENT DRAINAGE POPULATIONS

Tamara Mitić<sup>1\*</sup>, Jelena Čanak Atlagić<sup>1</sup>, Jelena Tomović<sup>1</sup>, Jelena Stanković<sup>1</sup>,  
Danilo Mrdak<sup>3</sup>, Dubravka Škraba Jurlina<sup>2</sup>, Ana Marić<sup>2</sup>

<sup>1</sup>Department of Hydroecology and Water Protection, National Institute for Biological  
Research “Siniša Stanković”, University of Belgrade, Bulevar despota Stefana, 142,  
11108 Belgrade, SERBIA

<sup>2</sup>University of Belgrade, Faculty of Biology, Studentski trg 16, 11000 Belgrade, SERBIA

<sup>3</sup>University of Montenegro, Faculty of Science and Mathematics, Džordža Vašingtona bb,  
81000 Podgorica, MONTENEGRO

\*tamara.mitic@ibiss.bg.ac.rs

### Abstract

The European bullhead, *Cottus gobio* Linnaeus, 1758, is widespread across European freshwaters, but strictly protected in Serbia due to habitat degradation. The complex geomorphology of the Balkan Peninsula and its role as an ancient refugium are reflected in many species distributions, including European bullhead. This species is known for its complex phylogenetic background with several lineages. Populations from different drainages should vary in external morphology due to geographical isolation. The aim of this study was to determine whether there is a considerable difference in morphological traits among the analysed populations belonging to two drainage systems: the Adriatic and the Black Sea drainage. Two populations from the Gradac and Nožica Rivers were tested for differences in 18 morphometric and 6 meristic traits. The test for independent samples and the Mann-Whitney U test showed the populations to be different in 12 out of 18 morphometric traits, 3 out of 6 meristic traits, and two traits were shown to have distinguishing weight according to discriminant analysis: prepelvic and postorbital length. These findings could be useful in the fieldwork assessment.

**Keywords:** linear morphometry, Balkans, Adriatic drainage, Black Sea drainage, protected species.

### INTRODUCTION

The rivers in Serbia belong to three major basins: the Adriatic, the Aegean, and the Black Sea basin, with the majority of rivers draining to the Black Sea via the Danube. The Danube used to represent one of the most important dispersal corridors during Pleistocene glacial cycles (and earlier) for many fish species, including *Cottus gobio*, Linnaeus 1758 [1,2]. This event shaped the distribution of numerous organisms. The European bullhead is the most widespread European member of the genus *Cottus*, and the possible explanation for its' successful expansion (and the expansion of numerous other species) throughout Europe can be attributed to ancient orogenic movements during the Cenozoic era, which, together with glaciation cycles, shaped the land of Europe [3]. These changes in the geomorphology of Europe comprised the emergence of mountain massifs, the splitting of the big water masses,



the drying up of the landlocked water bodies, etc., which were reflected in the distribution of myriad species. In addition to that, more recent secondary contact between the Danube's tributaries during the Pleistocene was an important factor in "fine-tuning" the current wide distribution of plenty of species [3], including European bullhead.

The European bullhead is a small, cold-adapted benthic fish inhabiting clear and fast-flowing freshwaters of Europe, and it mainly feeds on macroinvertebrates, such as larvae of Chironomidae, Simuliidae, and Hydropsychidae, plant parts, and detritus to a lesser extent [4]. According to the IUCN Red List of Threatened Species [5], European bullhead is assessed as the Least Concern (LC) category, however, many European populations are locally endangered [6]. This is due to ever-increasing anthropogenic river pollution, industrialization, and habitat degradation. According to the Habitats Directive [7], this species is listed in Annex II, requiring a designation for special areas of conservation. European bullhead populations in Serbia are found in small, so-called "salmonid" rivers and streams coexisting with populations of fish, such as *Salmo trutta* Linnaeus, 1758, and *Thymallus thymallus* Linnaeus, 1758. These species are under protection by the Serbian Ministry of Environmental Protection, with European bullhead being strictly protected in Serbia [8].

The European bullhead has its fair share of taxonomic complications. In the literature, its taxonomic status is still debated, whether it is a distinct species or if it is a species complex [6]. Its phylogenetic background is complex and characterised by the existence of several allopatric lineages throughout its vast range, which are hard to discern using only morphological data. Given that, many authors use molecular data as a significant tool in distinguishing different phylogenetic lineages of this species [9,10]. However, it's to be expected for populations belonging to different drainages to show a degree of differing morphology due to geographical isolation.

The aim of this study was to determine whether there are noticeable differences in the morphological traits in analysed populations belonging to two drainage systems (and most likely different phylogenetic lineages), which of the morphological traits account for the greatest differences, and to conclude if they can be used as a way of distinguishing populations belonging to different drainages.

## MATERIALS AND METHODS

European bullhead specimens were sampled by electrofishing from two sites: 14 specimens from the Gradac River situated in a gorge belonging to the Black Sea basin in October of 2023 and 12 specimens from the Nožica River located at the karst plateau belonging to the Adriatic Sea basin in July of 2012. Juvenile specimens were excluded from the analysis. The specimens were preserved in 96% ethanol until further examination. Based on the morphometric distances provided by Rowsey and Egge [11], 18 morphometric measures were used and modified for the purpose of this study (Figure 1). All specimens were measured manually using an electronic digital calliper with an accuracy of 0.1 mm. Morphometric traits were measured three times, and a mean value was used for further analyses. Also, 6 meristic traits, i.e., the number of first dorsal fin rays, the number of second dorsal fin rays, the number of anal fin rays, the number of pectoral fin rays, the number of pelvic fin rays, and the number of caudal fin rays, were counted. The test for independent

samples and discriminant analysis were performed for morphometric traits, while the Mann-Whitney U-test was conducted for the non-normally distributed meristic traits. The analyses were performed for meristic data and for proportionally scaled morphometric data expressed as a percentage of standard body length. A size correction was implemented to ensure that morphological variability between populations was not present due to differences in body size [12]. Statistical analyses were performed in the software Statistica, Statsoft Inc. (2013), Version 12, with a statistical significance value of  $p < 0.05$ .

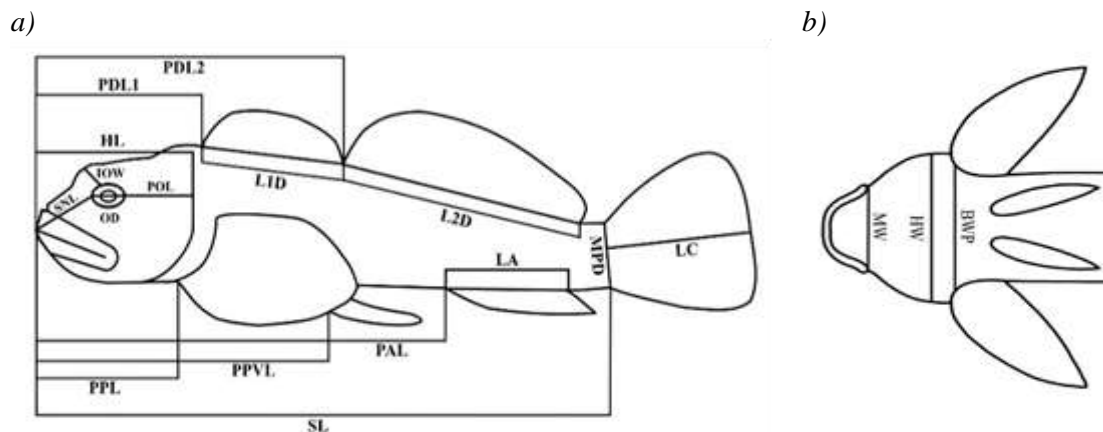


**Figure 1** Graphical representation of measured morphometric distances a) (sideways view): HL – head length from the tip of the snout to the posteriormost point of the operculum, SNL – snout length (from the tip of the snout to the anteriormost point of the orbit, POL – postorbital length from the posteriormost point of the orbit to the posteriormost point of the operculum, OD – orbit diameter, IOW – interorbital width, PDL1 – 1<sup>st</sup> predorsal length from the tip of the snout to the origin of the 1<sup>st</sup> dorsal fin base, PDL2 – 2<sup>nd</sup> predorsal length from the tip of the snout to the origin of the 2<sup>nd</sup> dorsal fin base, PPL – prepectoral length from the tip of the snout to the origins of the pectoral fins, PPVL – prepelvic length from the tip of the snout to the origin of the pelvic fins base, PAL – preanal length from the tip of the snout to the origin of the anal fin base, L1D – length of the 1<sup>st</sup> dorsal fin base, L2D – length of the 2<sup>nd</sup> dorsal fin base, LA – length of the anal fin base, LC – length of the caudal fin, MPD – minimal caudal peduncle depth, SL – standard length from the tip of the snout to the origin of the caudal fin; b) (ventral view): MW – mouth width, HW – maximum head width, BWP – body width between the origins of pectoral fins

## RESULTS AND DISCUSSION

The mean value expressed as the percentage and standard deviation of all morphometric traits' are shown in Table 1. Based on the results of the test for independent samples on morphometric data, 12 out of 18 morphometric traits were found to be statistically different between the two populations. The results of discriminant analysis showed two traits to be important in discriminating tested populations: prepelvic and postorbital length.

The range values of counted meristic traits are shown in Table 2. The nonparametric Mann-Whitney U-test used for meristic traits showed statistical differences between two populations in 3 out of 6 traits: the number of first dorsal fin rays, the number of second dorsal fin rays, and the number of anal fin rays. The number of pectoral fin rays wasn't shown to be statistically significant, whereas the number of pelvic fin and caudal fin rays showed no

differences between the two populations – the number of rays in the mentioned fins was quite uniform.

**Table 1** Mean values and standard deviation of measured morphometric traits

Morphometric traits (Abbr.)	Gradac	Nožica	Morphometric traits (Abbr.)	Gradac	Nožica
	Mean±SD (%)	Mean±SD (%)		Mean±SD (%)	Mean±SD (%)
HL	30.78±0.97	28.31±0.82	L2D	39.24±1.36	39.07±2.44
SNL	9.07±0.61	8.14±0.94	LA	28.64±1.17	29.07±1.80
OD	6.64±0.40	5.37±0.64	LC	20.24±1.30	20.75±2.64
IOW	4.74±0.68	3.96±0.70	MPD	8.05±0.47	8.38±0.50
POL	15.80±0.83	14.57±0.73	PPL	24.99±1.05	23.77±1.20
HW	31.54±1.63	26.85±2.32	PDL1	35.63±1.14	32.88±1.80
MW	20.11±1.64	18.06±2.34	PDL2	52.53±1.00	49.65±3.07
BWP	16.94±1.25	17.65±1.43	PPVL	28.77±0.93	26.79±1.24
L1D	18.31±0.98	15.21±2.34	PAL	55.27±1.25	54.58±1.71

**Table 2** Range values of counted meristic traits

Meristic traits	Gradac	Nožica
No. of 1 <sup>st</sup> dorsal fin rays	6–8	6–7
No. of 2 <sup>nd</sup> dorsal fin rays	16–19	15–17
No. of anal fin rays	12–13	10–14
No. of pectoral fin rays	14–15	13–15
No. of pelvic fin rays	4	4
No. of caudal fin rays	14	14

The late Pleistocene cycles of ice sheet advancements and regressions are known to be crucial in shaping the natural distribution of myriad organisms [13]. During the southward advancement of ice sheets from northern parts of Europe, many organisms retreated to the three major southern refugia, corresponding to the three European Peninsulas – the Balkans, the Iberian, and the Apennine Peninsula. Those refugia are known as biodiversity and endemism hotspots, because of the insurmountable barriers, such as mountain massifs. That's a very suitable terrain for prolonged isolation of populations and, consequently, for allopatric speciation. When the global temperatures rose and the ice sheets regressed up north, the surviving organisms recolonized the rest of Europe from those regions. However, besides three major southern refugia, there could be a number of previously unknown, cryptic sites. Scarce populations outside of refugia sites were known to exist in Central Europe [14], changing dramatically what we believed to be established colonisation routes.

The European bullhead is a cold-adapted fish that could resist harsh conditions in the course of the glaciation period [13]. Large scale geological changes that affected the Balkans pre- and during the Pleistocene, moulded its' relief and, consequently, led to the lineage divergence of various fish species, as displayed on the brown trout [3], with whom the European bullhead shares a similar habitat. All of the above points out a complex phylogeography and a deep allopatric division in the distribution of this species. As expected, tested populations were subjected to a long period of independent evolution caused by the existence of natural barriers and showed an overall presence of morphological differences in many tested traits. However, according to discriminant analysis, only two of those traits have

a distinguishing weight. Since the study was done on a small sample size, a low number of discriminating traits is to be expected. In addition to that, those two traits overlap longitudinally, meaning only a small part of the body has actual discriminating weight. The main disadvantage of using fine morphometric traits is that they might be impractical in the fieldwork, because they require more time and precision for measurement. Countable, meristic traits could be more convenient in the fieldwork, since the specimens could be distinguished by the number of 1<sup>st</sup>, 2<sup>nd</sup> dorsal and anal fin rays. On the other hand, the number of fin rays in European bullhead shows a degree of variability, which is an inherent characteristic of this species [9,15].

## **CONCLUSION**

Since tested specimens belong to different drainage systems, it is reasonable to expect that they belong to different phylogenetic lineages, as well. The conducted statistical analyses of morphometric and meristic traits showed that the populations from the Adriatic and Black Sea drainages differed in external morphology.

This initial indicator of allopatric differentiation should be further validated by molecular data, both mitochondrial and nuclear. Should these morphological differences, also, be detected at the molecular level, they could be used in the field for identification and could be a good way to avoid specimen sacrifice, which, in most cases, is necessary for further assessment.

Morphological and molecular data should be integrated to create a more comprehensive study on larger samples and more populations from different drainage systems across Europe. If the molecular data detects certain genetic distinctiveness of Serbian populations compared to the rest of the Balkans and wider (e.g., novel haplotypes), additional efforts should be made to avoid further endangerment of this strictly protected species and its habitat in Serbia.

## **ACKNOWLEDGEMENT**

*This research was funded by the Ministry of Science, Technological Development and Innovation (451-03-66/2024-03/200007).*

## **REFERENCES**

- [1] Economidis P.S., Banarescu P.M., *Int. Rev. Ges. Hydrobiol. Hydrogr.* 76 (2) (1991) 257–284.
- [2] Kontula T., Dissertation. Department of Ecology and Systematics, Division of Population Biology and Finnish Museum of Natural History, University of Helsinki (2003) 1–22.
- [3] Marić A., Batoćanin D.S., Jurlina D.Š., *et al.*, *Acta Ichthyol. Piscat.* 53 (2023) 1–18.
- [4] Števo B., Babel'ová M., Haruštiaková D., *et al.*, *Sci. Total Environ.* 651 (2019) 1903–1912.
- [5] IUCN, 2023. The IUCN Red List of Threatened Species Version 2023-1.
- [6] Freyhof J., Maurice K., *Handbook of European freshwater fishes*. Publications Kottelat, Cornol and Freyhof, Berlin (2007), p.646, ISBN 978-2-8399-0298-4.

- [7] Habitats Directive – Council Directive 92/43/EEC of 21 May 1992 on the conservation of natural habitats and of wild fauna and flora.
- [8] Official Gazette of the Republic of Serbia (2016). The Regulation on Proclamation of Strictly Protected and Protected Wild Species of Plants, Animals and Fungi. “Official Gazette RS” No. 98/2016.
- [9] McLeish J., Briers R. A., Dodd J. A., *et al.*, *J. Fish Biol.* 96 (3) (2020) 617–630.
- [10] Englbrecht C.C., Freyhof J., Nolte A., *et al.*, *Mol. Ecol.* 9 (6) (2000) 709–722.
- [11] Rowsey D. M., Egge J.J.D., *Northwest. Nat.* 98 (3) (2017) 190–202.
- [12] Berner D., *Oecologia* 166 (4) (2011) 961–971.
- [13] Hänfling B., Hellemans B., Volckaert F.A.M., *et al.*, *Mol. Ecol.* 11(9) (2002) 1717–1729.
- [14] Provan J., Bennett K.D., *Trends Ecol. Evol.* 23 (10) (2008) 564–571.
- [15] Simonović P., *Ribe Srbije*. NNK International, University of Belgrade, Agency for Nature Conservation of Serbia, Belgrade (2001), p.247, ISBN 86-7078-025-9.



## ECOLOGICAL POTENTIAL OF THE DANUBE RIVER THROUGH SERBIA BASED ON BIOLOGICAL QUALITY ELEMENTS

**Jelena Đuknić<sup>1\*</sup>, Nataša Popović<sup>1</sup>, Božica Vasiljević<sup>1</sup>, Bojana Tubić<sup>1</sup>, Stefan Andjus<sup>1</sup>,  
Marija Ilić<sup>1</sup>, Momir Paunović<sup>1</sup>**

<sup>1</sup>Department for Hydroecology and Water Protection, Institute for biological research  
“Siniša Stanković”, National Institute of the Republic of Serbia, University of Belgrade,  
Bulevar despota Stefana 142, 11000 Belgrade, SERBIA

\*[jelena.djuknic@ibiss.bg.ac.rs](mailto:jelena.djuknic@ibiss.bg.ac.rs)

### Abstract

*The Danube as the second longest river in Europe passes through many densely populated cities with high developed industry, traffic and agriculture, why it suffer a huge anthropogenic pressure. Serbian part of the Danube River belongs to its middle course that is under great influence of the Iron Gate. This study is aimed to assess the ecological potential of the Danube through Serbia using macroinvertebrate communities. The research was carried out on 16 localities on the Danube River and its main tributaries in year 2023. Samples were collected in May and September. To assess the ecological potential, following indices were calculated: Total number of taxa, Saprobic Index (SI), Biological Monitoring Working Party (BMWP), Average Score Per Taxon (ASPT), Diversity Index (H'), participation of Oligochaeta (Tubificidae) in total community and the number of Gastropoda and Bivalvia (Mollusca) taxa. Total of 102 taxa, from 18 groups, were identified. Diptera, Crustacea, Gastropoda and Oligochaeta were the dominant taxa with the high abundance. Study of macroinvertebrate community during high water regime (May) showed presence of 55 taxa, while 80 taxa were recorded during low water regime (September). Based on available data and employed indices, ecological potential of the Danube in investigated stretch could be assessed as “moderate” to “very poor” (III-V class). The researched stretch of the Danube River is primarily under the influence of hydromorphological degradation and organic pollution.*

**Keywords:** Danube, macroinvertebrate communities, ecological potential.

### INTRODUCTION

The Danube is the second longest river in Europe that flows through 10 countries from Germany to the Black Sea. Along its course it passes through many densely populated cities with high developed industry, traffic and agriculture, why it suffer a huge anthropogenic pressure that reflects on the morphology, hydrology, chemistry, as well as flora and fauna of the Danube's aquatic habitats [1–3]. Serbian part of the Danube River belongs to its middle course that is under great influence of the Iron Gate.

For the ecological assessment of waterbodies, the Water Framework Directive (WFD) requires five obligatory biological quality elements (BQE), among which are macroinvertebrates. The long life cycles and limited mobility makes them suitable for monitoring since these feature unable theme to escape anthropogenic pressure. Thus, the structure of their communities is strongly influenced by numerous anthropogenic impacts [4].



Also, macroinvertebrates have a significant influence on nutrient cycles, primary productivity, decomposition, and translocation of materials [5].

This study aimed to assess the ecological potential of the Danube River through Serbia based on macroinvertebrate communities.

## MATERIAL AND METHODS

The research was carried out on 16 localities on the Danube River and its main tributaries (Sava, Tisa, Velika Morava and Pek) through Serbia in year 2023 (Figure 1). Samples were collected twice: in the period of high water level in May, and during low water level in September. Macroinvertebrate samples were collected with bentological hand nets (mesh size 500  $\mu\text{m}$ ) applying the multihabitat sampling method [6]. Ethanol (70%) was used in the field to preserve samples that were later transported to the laboratory of the Institute for Biological Research “Siniša Stanković”, National Institute of the Republic of Serbia (IBISS), for the further analysis.

Identification of the organisms to the lowest taxonomic level was done at IBISS using a stereomicroscope (ZEISS, Stemi 508) and a microscope (ZEISS, AXIO Lab.A1), and adequate identification keys.

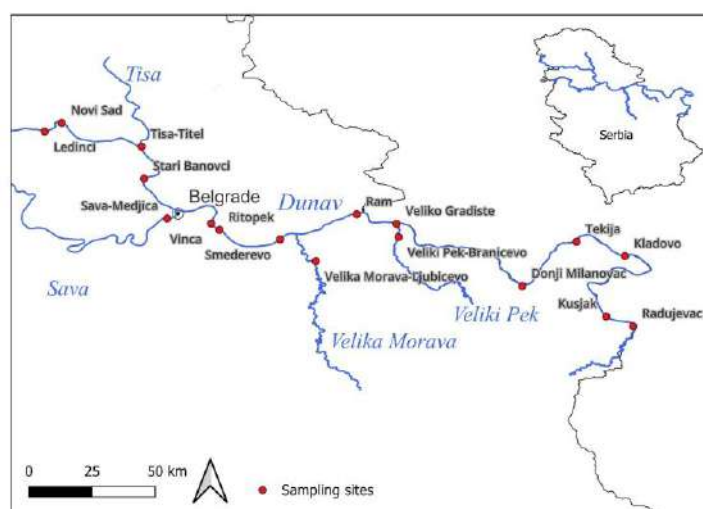


Figure 1 Map of localities

In order to analyse the quantitative and qualitative community composition, following biological indices were calculated: total number of taxa, Diversity Index ( $H'$ ) [7], Saprobic Index (SI) [8], Biological Monitoring Working Party score (BMWP), proportion of the Tubificinae family in the macroinvertebrate community (% Tubificinae), and the number of Gastropoda and Bivalvia (Mollusca) taxa present in the community. To calculate the biological indices, the ASTERIX software package (AQEM, 2002) was used. The indicator list for the identified taxa that was used was according to Moog [9]. Based on the threshold values established by national legislation, the obtained index values were used to assess the ecological potential [10]. The overall potential is determined by the index, which had the worst grade.

SHE analysis were performed in order to follow the changes in diversity (species richness, the Shannon-Wiener diversity index and species evenness) with increasing sampling effort.

## RESULTS AND DISCUSSION

Total of 102 taxa, from 18 groups, were identified. Study of macroinvertebrate community during high water regime (May) showed presence of 55 taxa, while 80 taxa were recorded during low water regime (September). The smallest number of taxa (3) was recorded at the locality Sari Banovci in September, while the locality at the Pek River was one with the highest taxa richness (Figure 2).

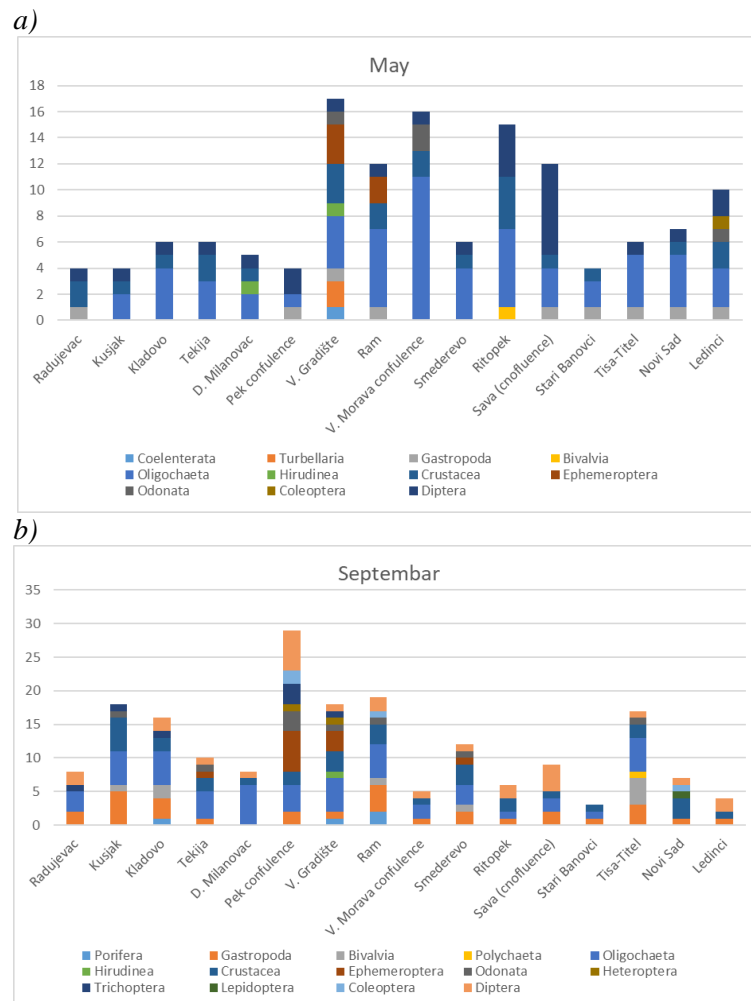


**Figure 2** Number of collected taxa in a) May; b) September at each locality

During high water regime Diptera was the most dominant taxa with the highest abundance (average 53.83%) in macroinvertebrate community, while Crustacea (23.58%) and Oligochaeta (17.48%) were subdominant. The exceptions were Ram, Donji Milanovac, Tekija and Kladovo with domination of Crustacean species. During low water regime the Crustacea (33.72%), Oligochaeta (25.79%), Diptera (19.22%) and Gastropoda (12.44%) were the dominant taxa with the high abundance in macroinvertebrate community.

In the Danube through Serbia the crustacean species *Limnomysis benedeni* Czerniavsky, 1882 and *Dikerogammarus villosus* (Sowinsky, 1894) were to be most abundant, followed by oligochaete species *Limnodrilus hoffmeisteri* Claparede, 1862. Other ubiquitous taxa were the chironomid *Chironomus* spp. and *Cricotopus* gr. *sylvestris*.

Diversity of the macroinvertebrate communities were shown through SHE analysis to define the role of each diversity components: species richness S, the Shannon-Wiener diversity index H' and species evenness E. Both models (for May and September) showed a different response in equitability and species richness with increased sampling effort. The increase of S and H, and a decline of E were observed in both models suggesting present of log series distributions in relation to increase number of species (Figure 3).

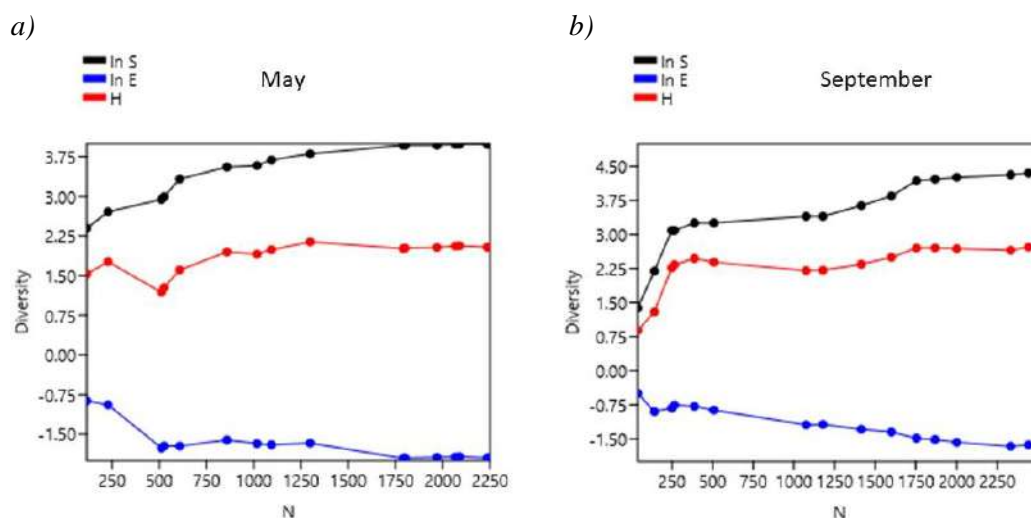


**Figure 3** The SHE analysis (diversity analysis S – Species richness, H – Shannon-Weiner diversity index, E – Evenness component of Shannon-Weiner diversity index) of the macroinvertebrates communities observed in the investigated sites in a) May; b) September

The ecological potential of the Danube was assessed using biological indices. The number of taxa was high at Ram and Veliko Gradište both seasons and achieved a good ecological potential (class II). Localities downstream Novi Sad, Stari Banovci and Radujevac were characterised by low number of taxa in both seasons, where the ecological potential was poor and very poor (class IV and V).

Saprobic index (SI) most of the localities were classified as class II. The highest values of the saprobic index were determined for the Tisa near Titel in May (3.31 – V class), an in September at Sava confluence (3.24 – V class), Ritopek (3.02 – IV class) and the Kusjak (2.94 – IV class).

According to the BMWP index, all samples collected in May had the quality class IV and V, except Veliko Gradište that achieved good ecological potential (class II). In September ecological status according to BMWP score at most localities improved reaching III and IV classes.

The lowest diversity index value (0.29) was determined for the Tisa near Titel in May, which was classified as class V. All other localities were classified as class II, III and IV.

The percentage of tubificids was low in all samples collected during high water regime achieving good ecological potential (class II). During low water regime at the Sava confluence, Ritopek and Smederevo the percentage of tubificids was higher reaching poor ecological potential (class IV) and Velika Morava and Kusjak reaching moderate potential (class III). At all other sites was good reaching II class.

According to the number of Gastropoda and Bivalvia (Mollusca) all localities in both seasons, had not achieved good ecological potential. The exception was samples of Bivalvia from Tisa near Titel in September, and Gastropoda from Ram and Kusjak, also in September, which had achieved good ecological potential.

Biological indices based on aquatic macroinvertebrates (Table 1) indicate that the ecological potential of the entire studied sector of the Danube and its main tributaries was poor to very poor (class IV and V) in May. In September ecological potential was good (class II) at Veliko Gradište and Pek confluence, while at Tisa near Titel and Ram it was moderate (class III).

**Table 1** Biological potential based on aquatic macroinvertebrates

Locality number	River	Locality	Ecological potencial MAY	Ecological potencial SEPTEMBER
1	Danube	Ledinci	IV	V
2	Danube	downstream Novi Sad	V	IV
3	Tisa	Titel, confluence	V	III
4	Danube	Stari Banovci	V	V
5	Sava	Confluence	V	V
6	Danube	Ritopek	IV	IV
7	Danube	Smederevo	V	IV
8	Velika Morava	Confluence	IV	IV
9	Danube	Ram	IV	III
10	Danube	Veliko Gradište	IV	II
11	Pek	Confluence	V	II
12	Danube	Donji Milanovac	IV	V
13	Danube	Tekija	IV	IV
14	Danube	Kladovo	V	IV
15	Danube	Kusjak	V	IV
16	Danube	Radujevac	V	IV

## CONCLUSION

This study shows that macroinvertebrate community in Danube and its main tributaries were taxa reach with 102 taxa identified. The most dominant taxa were Diptera, while crustacean species *Limnomysis benedeni* and *Dikerogammarus villosus* were to be most abundant.

Based on available data and employed indices, ecological potential of the Danube in investigated stretch could be assessed as “poor” to “very poor” (IV–V class). The researched stretch of the Danube River is under the impact of the Djerdap I and Djerdap II (Iron Gate) dams and large reservoirs constructed in the area. It is primarily under the influence of hydromorphological degradation and organic pollution.

## **ACKNOWLEDGEMENT**

*This research was funded by the Ministry of Science, Technological Development and Innovation of the Republic of Serbia, Contract No. 451-03-66/2024-03/ 200007.*

## **REFERENCES**

- [1] Liška I., Wagner F., Slobodnik J. Joint Danube survey 2, Final scientific report. ICPDR, (2008).
- [2] Kolarević S., Knežević-Vukčević J., Paunović M., *et al.*, Arch. Biol. Sci. 63(4) (2011) 1209–1217.
- [3] Liška I., Wagner F., Sengl M., *et al.*, Joint Danube Survey 3, Final Scientific Report ICPDR, (2015).
- [4] Dorn L., Multi-habitat macroinvertebrate sampling in wadeable freshwater streams, U.S. Environmental Protection Agency, (2007)
- [5] Wallace J. B., Webster, J.R., Annu. Rev. Entomol. 41(1) (1996) 115–139.
- [6] Consortium A., Manual for the Application of the AQEM System. A Compr. method to assess Eur. streams using benthic macroinvertebrates, Dev. Purp. Water Framew. Dir. Version (2002).
- [7] Shannon C.E., Weaver W., The Mathematical Theory of Communication. Univ. Illinois Press (1949) 1–117. ISBN: 0252725484.
- [8] Zelinka M., Marvan P., Arch. fur Hydrobiol. 57 (1961) 389–407.
- [9] Moog O., Fauna Aquatica Austriaca Katalog Zur Autökologischen Einstufung Aquatischer Organismen Österreichs, (2002) 670, ISBN: 3-85 174-0440-0.
- [10] Regulative on Parameters of Ecological and Chemical Status of Surface Waters and Parameters of Chemical and Quantitative Status of Groundwaters). Off. Gaz. RS No. 74/2011.



## *Chlorella vulgaris* GROWTH IN SMALL OPEN CULTIVATION SYSTEMS

Sladana Popović<sup>1\*</sup>, Gordana Subakov Simić<sup>1</sup>, Srđan Stanković<sup>1</sup>, Dejan Lazić<sup>2</sup>

<sup>1</sup>University of Belgrade, Faculty of Biology, Institute of Botany and Botanical Garden  
„Jevremovac“, Department of Algology and Mycology, Takovska 43,  
11000 Belgrade, SERBIA

<sup>2</sup>University of Belgrade, Innovation Center of the Faculty of Biology, Studentski trg 16,  
11000 Belgrade, SERBIA

\*spopovic.bio@gmail.com, sladjana.popovic@bio.bg.ac.rs

### Abstract

*Phototrophs are a diverse group of microorganisms that include many representatives with unique properties. They can be used for various purposes and offer a wide range of applications, making their use in the field of biotechnology increasingly important. One of the most commonly cultivated algae is Chlorella. There are numerous experiments dedicated to the cultivation of Chlorella, studying different and altered conditions under which this algae develops, all with the aim of obtaining the best possible product and achieving the highest possible production. In this experiment, Chlorella vulgaris was cultivated in two small open systems with built-in light and two types of aeration, where the main parameters affecting algae growth were monitored regularly until the biomass was harvested.*

**Keywords:** *Chlorella vulgaris*, cultivation system, biomass.

### INTRODUCTION

Phototrophic microorganisms are very diverse and include many representatives with their own unique characteristics and properties, ranging from unicellular representatives to more complex ones and from prokaryotic cyanobacteria to eukaryotic algae [1]. They occur in a variety of different environments, from aquatic to terrestrial and even in extreme ones.

Phototrophs are very valuable and can be used for various purposes; they are extensively studied in biotechnology and offer a wide range of potential applications. They contain many bioactive compounds, including proteins, lipids, carbohydrates, carotenoids and vitamins, which can be used for commercial applications [1,2,3]. However, not many phototrophs have been studied in this way, especially those from extreme habitats, and the methods that utilize them are still not fully understood.

*Chlorella vulgaris* is a microscopic green algae characterized by a defined spherical shape with a size of 2 to 10 µm and a cell wall of varying thickness, occurring in nature as a single or microorganism that can form colonies/clusters. It is characterized by high resistance and adaptability, good growth rates under different conditions and metabolic diversity (autotrophic, mixotrophic and heterotrophic) [4,5]. Interest in this algae is growing in the field of biotechnology, as some of the primary and secondary metabolites synthesized are proteins, lipids and carbohydrates, as well as some pigments, vitamins and minerals [4]. *C. vulgaris* has



a high protein content (~56.8%), which means that it has a high nutritional value and contains about ~5.9% carbohydrates and ~16.9% lipids (calculated as % of dry matter) [4,5,6].

Cultivation of algae can be carried out under laboratory conditions and in systems that can be divided into open, closed (depending on whether material exchange between the culture and the environment is possible or not) and hybrid [3]. Open systems are a widely used cultivation method worldwide and are cost-efficient, but are influenced by external factors and are susceptible to contamination. Closed systems are more expensive, but algae growth can be better controlled under certain conditions. Hybrid systems are a mixture of the two cultivation systems mentioned above and overcome the limitations of open systems and the high initial operating costs of closed systems [3].

The aim of the study was to cultivate a commercial *Chlorella vulgaris* strain in two small open systems to obtain algal biomass.

## MATERIALS AND METHODS

### Algal strain and growth in laboratory conditions

The algae strain selected for cultivation was a commercially purchased *Chlorella vulgaris*, which was kept in BG11 medium. The medium was prepared according to the recipe given in Rippka *et al.* [7], poured into 250 ml Erlenmeyer flasks and autoclaved at 121°C for 15 minutes. After autoclaving and cooling the medium, *Chlorella vulgaris* was inoculated and then subcultured regularly to maintain a pure culture and gain more biomass before the open culture systems were inoculated. The cultures were kept in a growth chamber at a temperature between 19°C and 22°C and a 12:12 light:dark cycle.

### Algal culturing in small open cultivation systems

Erlenmeyer flasks containing *Chlorella vulgaris* cultures were used to inoculate two small open systems for algae cultivation – System 1 (S1) and System 2 (S2) (volume of 30 l each), to which growth medium was also added for the corresponding volume. Both culture systems consisted of a glass tank, a built-in light source and an aeration mechanism that supplied the systems with CO<sub>2</sub>-rich air, which, however, came from different sources for each system. The aeration mechanism (consisting of a source of CO<sub>2</sub>-rich air, a pump, a tube and an air stone blister) was used simultaneously to constantly mix the contents of the systems (Figure 1).

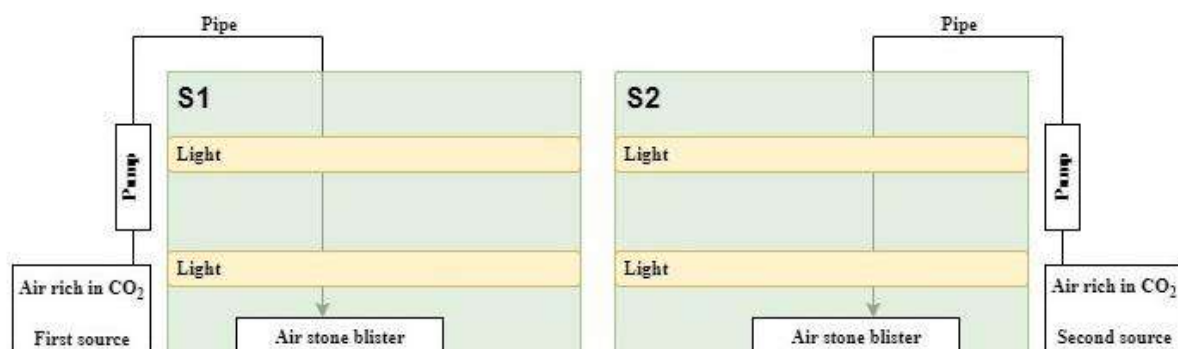


Figure 1 Schematic view of the algae cultivation systems S1 and S2

As both systems are open systems, the surface was covered with a foil to prevent contamination to a certain degree. The systems were kept in a closed room to avoid strong temperature fluctuations.

The algae were cultivated for one month and pH, T and EC were measured daily. Biomass production was assessed at the end of the experiment.

## RESULTS AND DISCUSSION

In order to study phototrophs in their applicability, they need to be cultivated, and consequently biomass must be harvested for further investigation. Their growth and cultivation depend on a number of different factors, but an ideal cultivation system should have the following features, among others: a suitable light source, effective material transfer across the liquid-gas barrier, ease of operating, minimal contamination rate, favorable overall design, and production costs [1].

Many factors affect algal growth and can influence the dynamics in culture and biomass productivity; among the most important are light (light intensity and illumination cycle), carbon source (for autotrophic metabolism), media type (presence of macro- and micronutrients) and nutrient strength, abiotic factors such as pH and temperature, and some biotic ones such as the concentration of algal inoculum or the presence of microfauna in the growth medium [3,8].

There are many individual studies on different growth-controlling factors in algal technology, but the joint effect of different abiotic parameters is the least studied for *C. vulgaris*. To optimally adjust the algal growth system, basic abiotic parameters such as light intensity, temperature and pH should be optimized [8].

Micrograph of *Chlorella vulgaris* used for cultivation in our S1 and S2 is shown in Figure 2.

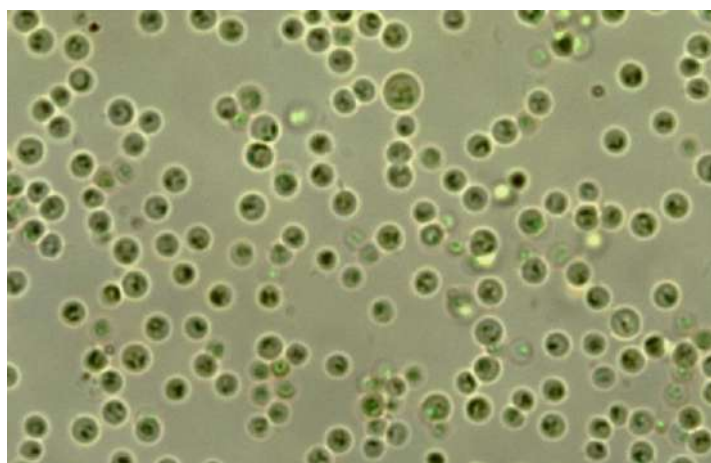


**Figure 2** *Chlorella vulgaris*

Both of our cultivation systems had a built-in light source with a 12:12 light/dark photoperiod. Light is an important factor for the growth of photosynthetic microorganisms, and as the intensity increases, the products generated by photosynthesis also increase, but

only up to a certain point, known as the maximum point; after that, the excessive radiation causes stress and has a negative effect on the algae, leading to the phenomenon known as photoinhibition. In contrast, in culture systems, “self-shading” can occur, which affects the algae in the medium further away from the light source and impairs their growth because there is not enough light. For this reason, it is necessary that the contents of the systems are mixed [4], and as mentioned earlier, we achieved this with built-in aeration mechanisms that allowed constant mixing of the contents in addition to the air supply. The photoperiod is also a crucial factor in the cultivation of algae and should be optimized for optimal growth. Experiments with *Chlorella vulgaris* are carried out with different photoperiods, which usually include 16:8 and 18:6 in addition to the 12:12 light/dark regime [8,9,10].

Although our culture systems were housed in a closed room, the water temperature fluctuated between 18–25°C (S1) and 18–24°C (S2). The average water temperature was 21.72°C (S1) and 21.47°C (S2). Suthar and Verma [8] reported that temperatures between 20 and 30°C promote maximum growth of *Chlorella*. It should be noted that temperatures below 16°C slow down the metabolic system and growth, while temperatures above 35°C are lethal for many species [11].

The pH of the culture system is an important limiting factor for the physiology of algal strains and the yield of algal biomass. The pH affects nutrient uptake and thus leads to different growth patterns [8]. Different optimal pH values for the growth of *C. vulgaris* have been reported: according to Sakarika and Kornaros [12], a value of 7.5 is the optimal pH for achieving maximum biomass, He *et al.* [13] reported that the optimal pH values are in the range of 5–9, while Suthar and Verma [8] found that the highest biomass is achieved at pH values between 7 and 9. The pH is considered to be the easiest factor to control, which is usually achieved by introducing CO<sub>2</sub> into the system [14]. In our experiment, the pH for S1 had its lowest value of 7.3, while the highest value measured was 9.54 at the end of the experiment. Similar results were obtained for S2, where the pH ranged from 7.3 to 9.59. The average pH was 8.33 and 8.32, for S1 and S2, respectively. The increase in pH was also reported by many researchers, and according to He *et al.* [13], the pH of the solution reached a maximum of 10.7 within a week.

The values of EC were higher towards the end of the experiment, when they reached 3.84 mS (S1) and 4.05 mS (S2).

In both systems, S1 and S2, air containing CO<sub>2</sub> was continuously supplied. Algal production requires a large amount of inorganic carbon, and up to 1.8 kg of CO<sub>2</sub> is needed to produce 1 kg of microalgal biomass. For this reason, Cardias *et al.* [14] concluded that the best option is to supply the cultivation systems with pure CO<sub>2</sub>.

The biomass produced by *Chlorella vulgaris* in S1 was 59 mg L<sup>-1</sup> d<sup>-1</sup> and in S2 40 mg L<sup>-1</sup> d<sup>-1</sup>. Similar results as for S1 were reported by El-Fayoumy *et al.* [15], but the algae was cultivated under different stressors. The production of biomass and the sustainability of this process depend on the design of the cultivation system as well as on all the factors mentioned above. The differences in biomass production in our systems S1 and S2 are probably due to the use of different air sources where the CO<sub>2</sub> concentration varied, as well as the outcome of biomass harvesting in the systems. In general, different values for the biomass obtained were reported by the researchers. It should also be mentioned that most studies

address the problem of processing algal biomass and not the fact how to produce it in sufficient quantities [16].

## CONCLUSION

*Chlorella vulgaris* was cultivated in two small open culture systems (S1 and S2), which were housed in a closed room to avoid strong fluctuations in environmental parameters. Culture systems S1 and S2 were aerated with CO<sub>2</sub>-rich air, which came from different sources for each system, and were equipped with a built-in light source (12:12 light/dark). Parameters such as pH, T and EC were monitored regularly. Biomass was harvested at the end of the experiment and was higher in S1.

## ACKNOWLEDGEMENT

*The authors are grateful to the Ministry of Science, Technological Development and Innovation of the Republic of Serbia for the financial support according to the contract with the registration number (451-03-66/2024-03/200178, 451-03-65/2024-03/200178).*

## REFERENCES

- [1] Tan J.S., Lee S.Y., Chew K.W., *et al.*, *Bioengineered*. 11(1) (2020) 116–129.
- [2] Chew K.W., Yap J.Y., Show P.L., *et al.*, *Bioresour. Technol.* 229 (2017) 52–63.
- [3] Tiwari A., Kiran T., Pandey A., *Algal cultivation for biofuel production in Second and Third Generation of Feedstocks*, Editors: Basile A., Dalena F., Elsevier (2019), p.383–403, ISBN: 9780081026564.
- [4] Coronado-Reyes J.A., Salazar-Torres J.A., Juárez-Campos B., *et al.*, *Food Sci. Technol.* 42 (2022).
- [5] Silva D.A., Cardoso L.G., de Jesus Silva J.S., *et al.*, *Environ. Technol. Inno.* 25 (2022) 102204.
- [6] Spolaore P., Joannis-Cassan C., Duran E., *et al.*, *J. Biosci. Bioeng.* 101 (2006) 87–96.
- [7] Rippka R., Deruelles J., Waterbury J., *et al.*, *J. Gen. Microbiol.* 111 (1) (1979) 1–61.
- [8] Suthar S., Verma R., *Process Saf. Environ. Prot.* 113 (2018) 141–148.
- [9] Kendirlioğlu G., Agirman N., Cetin A.K., *Turk. J. Sci. Technol.* 10 (2015) 7–10.
- [10] Nwankwo U.N., Agwa O.K., *Int. J. Sci. Res. Arch.* 11 (01) (2024) 2469–2476.
- [11] Barsanti L., Gualtieri P., (2014). *Algae: Anatomy, Biochemistry, and Biotechnology*, Second Edition, CRC Press, p.361, ISBN: 9780429107184.
- [12] Sakarika M., Kornaros M., *Bioresour. Technol.* 219 (2016) 694–701.
- [13] He L., Chen Y., Wu X., *et al.*, *Water*. 12(1) (2020) 34.
- [14] Cardias B.B., Barceló-Villalobos M., Lafarga T., *et al.*, *Algal Res.* 74 (2023) 103197.
- [15] El-Fayoumy E.A., Ali H.E.A., Elsaid K., *et al.*, *Biomass Conv. Bioref.* (2023).
- [16] Borowitzka M.A., Vonshak A., *Eur. J. Phycol.* 52 (4) (2017) 407–418.



## EPIPHYTIC DIATOMS AS TOOL IN BIOINDICATION OF LAKE PALIĆ

Olga Jakovljević<sup>1</sup>, Slađana Popović<sup>1\*</sup>, Dragana Predojević<sup>1</sup>

<sup>1</sup>University of Belgrade, Faculty of Biology, Institute of Botany and Botanical Garden „Jevremovac“, Department of Algology and Mycology, Takovska 43, 11000 Belgrade, SERBIA

\*[spopovic.bio@gmail.com](mailto:spopovic.bio@gmail.com), [sladjana.popovic@bio.bg.ac.rs](mailto:sladjana.popovic@bio.bg.ac.rs)

### Abstract

*The main objectives of this study are to reveal diversity of diatoms (Bacillariophyta), to analyze their community temporally and spatially and to assess the ecological status of Lake Palić based on the phytobenthos. High diatom taxa richness was found –105 taxa in total. In general, the dominant species are pollution-resistant and mostly tolerate high levels of organic pollution and nutrients. Two dominant taxa (Amphora pediculus and Gomphonema parvulum) were also the most frequent diatom taxa, recorded in all samples. Ecological status based on diatom indices values can be defined in a range from good (class II) to bad (class V) depending on the season and sampling site. The worst quality class (V – bad ecological status) is indicated by two indices (TID and TDI) created with the aim of determining the amount of nutrients. According to national legislation, the ecological status of Lake Palić can be characterized as good (class II) on the basis of phytobenthos. Only at second site in summer indicated a moderate status.*

**Keywords:** Bacillariophyta, biomonitoring, WFD, ecological status, Palić.

### INTRODUCTION

Bioindicator organisms are beneficial tools for reflecting environmental conditions. Diatoms (Bacillariophyta) are among the most significant aquatic bioindicator groups. This group of organisms has long been recognised as an effective bioindicator of water pollution in rivers and lakes [1]. While invertebrates respond to environmental changes primarily through changes in taxonomic richness, diatoms respond through changes in community structure [2]. Therefore, diatom indices are calculated by analysing composition and structure of diatoms community. Based on their values, we can draw conclusions that are very useful in monitoring of lakes, but also in determining vulnerabilities due to excessive recreational activities and other anthropogenic pressures [3].

The European Union's Water Framework Directive (WFD) is the most important document for the management of surface waters with the aim of achieving good ecological status. According to the WFD, fish, invertebrates, macrophytes, phytobenthos and phytoplankton are defined as Biological Quality Elements that are used to determine ecological status [4]. Within the phytobenthos, diatoms are the most important component.

Lake Palić is a natural lake in northern Serbia which, together with the surrounding area, is protected as the Palić Nature Park. According to the IUCN classification, it belongs to category IV (Habitat and species management area). It is an important ecological corridor that



enables the survival of numerous protected and strictly protected species of birds, reptiles, amphibians and mammals [5].

The aim of this study was to reveal diversity of diatoms, to analyze their community temporally and spatially and to assess the ecological status of Lake Palić based on this group of organisms as a member of the phytobenthos.

## MATERIALS AND METHODS

### Sampling and laboratory procedures

Epiphytic samples were collected from three sites during three seasons (spring (May), summer (July) and autumn (September)) in 2022 according to the standard [6]. The samples were then treated with the hot acid method using HCl and KMnO<sub>4</sub> to remove the organic content from diatom cells [6]. They were then mounted in Naphrax<sup>®</sup> medium and permanent slides were made.

### Microscopic analyses and identification

The Carl Zeiss AxioImagerM.1 light microscope with the AxioCam MRc5 camera was used to observe and photograph the diatom taxa. Taxa identification was based on standard taxonomic literature and quantitative analysis by counting 400 diatom valves on each slide [7].

### Ecological status assessment

Diatom indices values were calculated using OMNIDIA software [8]. The ecological status of Lake Palić was assessed based on phytobenthos, taking into account the class boundaries given in Prigyel and Coste [9], as well as based on the class boundaries given in the Rulebook of the Republic of Serbia, based on which only IPS index values are considered [10].

## RESULTS AND DISCUSSION

During the study period, a total of 105 diatom taxa were recorded from Lake Palić. The lowest number of taxa was recorded at the second site in spring and the highest at the third site in summer (Figure 1), which is characterized by the strongest anthropogenic influence. Diatoms diversity is not proportional to the impact of anthropogenic activities based on our results, which is consistent with other studies. Corrêa da Rosa and Copertino [11] pointed out that a higher diversity and lower dominance was found at the non-impacted sites.

*Achnantheidium minutissimum* (Kützing) Czarnecki, *Amphora pediculus* (Kützing) Grunow, *Aulacoseira granulata* var. *angustissima* (O.Müller) Simonsen, *Epithemia sorex* Kützing, *Gomphonema exilissimum* (Grun.) Lange-Bertalot & Reichardt, *Gomphonema parvulum* (Kützing) Kützing, *Gomphonella olivacea* (Hornemann) Rabenhorst and *Ulnaria ulna* (Nitzsch.) Compere were recorded as the most dominant species in Lake Palić (Figure 2). The highest relative abundance (45%) of some taxon was recorded at the first site in summer (*E. sorex*) and at the second site in spring (*G. olivacea*) (Figure 2). *E. sorex* is commonly found as an epiphyte taxon on aquatic plants and coarse filamentous algae in rivers and lakes, which often tolerate moderate organic pollution; generally in environments with an alkaline pH, moderately to highly mineralized or even slightly brackish [12]. Two dominant taxa (*A.*



*pediculus* and *G. parvulum*) were also the most frequent diatom taxa, recorded in all samples from Lake Palić, but also *Nitzschia amphibia* Grunow. All these dominant species are pollution-resistant, mostly tolerate high levels of organic pollution and nutrients.

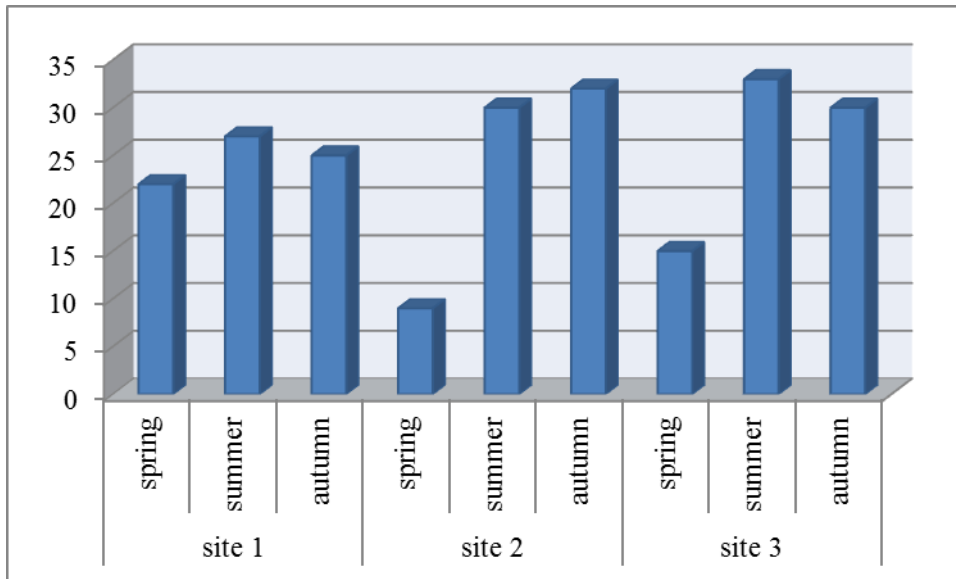


**Figure 1** The number of recorded diatom taxa by sites in three seasons (spring, summer and autumn)

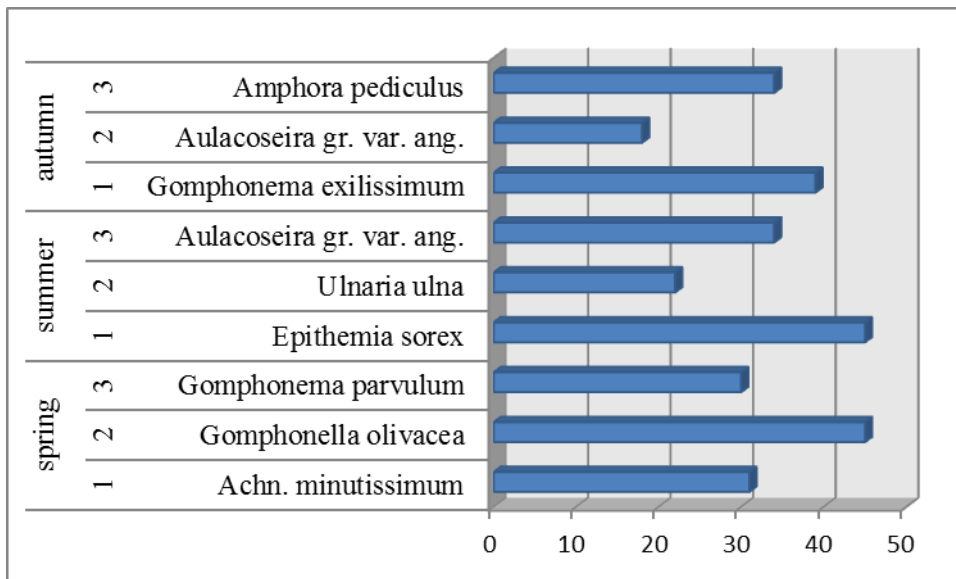


**Figure 2** The highest relative abundance (%) of dominant diatom taxa by sites (1-3) in three seasons (spring, summer and autumn)

Ecological status based on diatom indices values can be defined in a range from good (class II) to bad (class V) depending on the season and sampling site (Table 1). Only Descy and Lobo indicated high ecological status (class I) at one site each. However, it should be borne in mind that the LOBO index [13] was created on the basis of data and research in South America, so the degree of reliability is low. The TDIL index developed specifically for lakes indicated a moderate (III) and poor (IV) status of Lake Palić, but also the reliability is

low as the percentage of species included in the calculation did not exceed 70% at the studied sites during the study period; the exception is the second and third sites in spring. Nevertheless, most indices indicated a moderate ecological status at most sites during the study period. The worst quality class (V – bad ecological status) is indicated by two indices (TID and TDI), which were created with the aim of determining the amount of nutrients [14]. The degree of their reliability is high, considering the percentage of species included in their calculation.

**Table 1** Ecological status classes of Lake Palić based on the values of diatom indices at the investigated sites (1–3) during three seasons (spring, summer and autumn); class boundaries according to Prygiel and Coste (2000)

Diatom index	spring			summer			autumn		
	1	2	3	1	2	3	1	2	3
IBD	13.6	13	12	10.4	10	10.6	15.7	11.5	13.8
IPS	12.2	12.7	10.9	11.9	9.6	10.6	12.9	11.4	13.8
IDG	12.6	14.8	11.5	12.7	11	10.9	11.3	8.5	10
Descy	11.4	12.7	11.7	7.7	9.6	14.1	10	14	17.9
Sla.	12.9	10.7	11.5	12.3	10.3	11.6	11.7	12	12.8
IDSE	13.6	10.5	11.5	10.5	10.3	12.1	12.1	12.5	13.4
IDAP	11.6	8.4	8.5	5.7	9.3	10.2	6.7	9.2	12.8
EPID	13.6	14.2	12.9	11.3	9.4	10.8	9.8	10.5	12.2
Lobo	18.6	6.7	11.4	16.4	14.8	10.6	16.6	12.9	11.9
Hurl.	10.1	14.1	11.1	8.1	6.8	9.4	13.3	7.8	9.9
TID	5.6	4.5	4.5	4.9	4.5	6.7	9.7	6.7	7.2
SID	12.5	12.6	12.5	14.9	11.5	12.4	12.7	12.2	13.3
TDIL	10.9	10.1	8.5	9.5	10.1	9.1	6.4	8.9	9.6
CEE	13.8	11.3	10.1	8.6	9.5	10.4	8.2	12.3	14.6
WAT	14.8	11.5	12.7	11.2	10.3	12.5	10.7	11.9	14.2
TDI	8	1.3	1.1	3.9	4.2	3.7	2.2	2.6	2.3
IDP	11.4	5.1	7.4	10.5	10.3	11.3	7.9	10.1	10.8
SHE	13.5	9	9.4	12.3	12.7	13.8	13.7	13.2	13.3

According to national legislation [10], ecological status based on phyto-benthos for shallow lakes (up to 10 m deep) is determined based on the IPS values. The boundaries between ecological status classes differ from those in Prygiel and Coste [9]. The IPS values indicated a good (class II) ecological status in accordance with the legislation of the Republic of Serbia [10]. Only at the second site in summer indicated a moderate status.

## CONCLUSION

Diatoms are a group of microorganisms that are very important and useful for the bioindication of aquatic ecosystems. A total of 105 diatom taxa from Lake Palić were recorded at three sampling sites during 2022. Diatom indices are widely used in Europe and around the world to assess the ecological quality of rivers and are part of national legislation in many European countries. The ecological status based on diatom indices values can be

defined in a range from good (class II) to bad (class V) depending on the season and sampling site. According to Serbian legislation, the ecological status of Lake Palić can be characterized as good (class II) during spring, summer and autumn in 2022. An exception is the second site in summer, where the water of the lake can be characterized as moderate (class III). This study shows that continuous biomonitoring is necessary, especially considering the touristic importance of Lake Palić.

## **ACKNOWLEDGEMENT**

*The authors are grateful to the Ministry of Science, Technological development and Innovation of the Republic of Serbia for financial support according to the contract with the registration number 451-03-66/2024-03/200178.*

## **REFERENCES**

- [1] Tokatli C., Solak C., Islam A., *et al.*, Acta Sci. Pol-Form. C. 22 (3) (2023) 73–81.
- [2] Della Bella V., Mancini L., Hydrobiologia 634 (2009) 25–41.
- [3] Barinova S., Krupa E., Khitrova Y., Ecologies 4 (2023) 242–268.
- [4] Marchetto A., Sforzi T., Adv. Oceanogr. Limnol. 9 (1) (2018).
- [5] Available on the following link: <https://www.ekourbapv.vojvodina.gov.rs>.
- [6] SRPS EN 13946:2015. Kvalitet vode – Uputstvo za rutinsko uzimanje uzoraka i pripremu preparata bentosnih silikatnih algi reka i jezera.
- [7] SRPS EN 14407:2015. Kvalitet vode – Uputstvo za identifikaciju i utvrđivanje brojnosti bentosnih silikatnih algi iz reka i jezera.
- [8] Lecointe C., Coste M., Prygiel J., Hydrobiologia 269/270 (1993) 509–513.
- [9] Prigyl J., Coste M., Guide méthodologique pour la mise en oeuvre de l'Indice Biologique Diatomées, Agence de l'eau Artois Picardie, Douai (2000), p.134.
- [10] Službeni glasnik Republike Srbije 74/2011. Pravilnik o parametrima ekološkog i hemijskog statusa površinskih voda i parametrima hemijskog i kvantitativnog statusa podzemnih voda.
- [11] Corrêa da Rosa V., Copertino Margareth., Diversity 14 787 (2022).
- [12] Bey M.-Y., Ector L., Atlas des diatomées des cours d'eau de la région Rhône-Alpes, Tome 6: Les PENNÉES, Direction régionale de l'Environnement, de l'Aménagement et du Logement Rhône-Alpes, Lyon (2013), ISBN: 978-2-11-129817-0.
- [13] Lobo E.A., Callegaro V.L.M., Bender E.P., Utilização de algas diatomáceas epilíticas como indicadoras da qualidade da água em rios e arroios da Região Hidrográfica do Guaíba, RS, Brasil, EDUNISC, Santa Cruz do Sul (2002), p.127. ISBN: 85-85869-90-9.
- [14] Kelly M.G., Whitton B.A., J. Appl. Phycol. 7 (4) (1995) 433–444.



## IMPROVING PALEOENVIRONMENTAL RECONSTRUCTIONS BASED ON SMALL VERTEBRATES IN THE BALKANS

Mihailo Jovanović<sup>1\*</sup>, Jane Paunković<sup>2</sup>

<sup>1</sup>University Rovira i Virgili, The Catalan Institute of Human Paleocology and Social Evolution, Edificio W3, Campus Sescelades URV, Zona Educacional, 4, 43007 Tarragona, SPAIN

<sup>2</sup>LUM Jean Monnet, Libera Università Mediterranea di Bari, Strada Statale 100 km 18, 70010 Casamassima BA, ITALY

\*mjovanovic@iphes.cat

### Abstract

*Paleoenvironmental research in the Balkans offers an extraordinary approach into the region's past climates and environments. To improve our knowledge of the events that shaped natural systems and human evolution over the past 120 thousand years, it is important to focus on two major climatic events that occurred during this time globally and affected the territory of Balkan Peninsula. The first climatic event that's important is the gradual global cooling after the last major interglacial period (Marine isotope stage MIS 5) before the Holocene. The second event is the eruption of the Campanian Ignimbrite, one of the largest known volcanic eruptions of the Quaternary. Paleoecologists are able to calculate climatic parameters such as: Mean annual temperature, mean annual precipitation, temperature of the coldest month, temperature of the warmest month, number of dry months etc. To make paleoreconstructions based on archeological small vertebrate remains paleoecologists use data from living ecosystems. Among microvertebrates, rodents are known to be the best tools for biochronological, biostratigraphic, and paleoecological reconstructions. Amphibians and reptiles are also becoming better known in the context of paleoclimatic and paleoecological analyses. During preliminary results of field surveys conducted in Serbia in 2019, researchers encountered hundreds of animals and positively identified 14 species of amphibians and 15 species of reptiles in their natural habitats.*

**Keywords:** Paleoenvironment, biodiversity, herpetofauna.

### INTRODUCTION

The Balkan Peninsula has already been identified as a confirmed route for animal migrations in the early Pleistocene [1]. For the Middle and Late Pleistocene, it would be very important to establish a pattern of emergence and disappearance of small vertebrates. Such an attempt is an ongoing process that will be strengthened by future research. Because of their small size, small habitats, and generally low mobility, small vertebrates are known to be more susceptible to regional change than large mammals and plants, especially in Europe where mountain ranges and marine barriers block their retreat southward.

To make paleoreconstructions based on archeological small vertebrate remains paleoecologists use data from living ecosystems. Among microvertebrates, rodents are known to be the best tools for biochronological, biostratigraphic, and paleoecological

reconstructions. Amphibians and reptiles are also becoming better known in the context of paleoclimatic and paleoecological analyses [2]. According to Musil [3], a relatively warm climate was recognized in Central Europe in 31500, 30000, 27500, 26000, and 21000 years ago, while there were relatively cold periods in 32000, 31000, 29000–27500, 25000–21500 years ago (all data are in calibrated years BP). These climatic fluctuations can be assigned to specific climatic phases for the purpose of establishing typical herpetofaunal assemblages for Balkans. This concept is introduced by Böhme [4,5], and phases include: late glacial, early interglacial, interglacial climate optima, late interglacial and interstadial. Latest interglacial to Early glacial, and Glacial periods. Paleoecologists are able to calculate climatic parameters such as: Mean annual temperature, mean annual precipitation, temperature of the coldest month, temperature of the warmest month, number of dry months etc. These parameters can be compared with present ones and correlated with habitat distribution, there are also many other analyses applicable for past and present comparisons and possibly future predictions. For the future research it is necessary to make data collections to unite known data about species distribution together with data about habitat distribution. Additional advantages will be presented by totaling with climatological data, as these way researchers will be able to fully use modern technological advancement in GIS software.

## **MATERIALS AND METHODS**

The methods for paleoenvironmental research include: Bioclimatic analysis [6–9]; Mutual Ecogeographic Range [10,11]; Habitat types [12]; Statistical analyses of the small vertebrates distribution using Paleontological statistical program PAST3, in particularly Hierarchical clustering in addition with the Jaccard similarity index can be applied, since this is recommended for clustering binary data as it gives more importance to joint concurrences in the assemblages [13]. Correspondence Analysis can be used to support the results of the hierarchical clustering. Correspondence Analysis is the recommended method for comparing associations (assigned to columns) with the total count of taxa or identifying taxa (assigned to rows) through associations [14].

Field surveys are one of the most common methods used to assess biodiversity. Researchers conduct systematic surveys of different habitats, including forests, wetlands, grasslands, and urban areas, to document the presence of amphibians and reptiles. Surveys may involve visual encounters, where researchers search for animals directly or use techniques like pitfall traps, funnel traps, drift fences, or cover boards to capture and record species. Animals are released unharmed without exceptions. In addition, comparative methods for gathering information about natural habitat distribution will be used to correlate species with their natural habitats.

## **RESULTS**

Assessing the distribution of herpetofauna involves gathering information about where different species of amphibians and reptiles are found within a particular geographic area. This process typically involves a combination of field surveys, literature reviews, and data analysis. Researchers reviewed existing scientific literature, including published papers,



reports, and species distribution maps, to gather information about the distribution of herpetofauna. This supplemented field data and provided a more comprehensive understanding of species distributions over time and across different regions. In particular, field research was conducted in areas with insufficient data. Field surveys were used to assess the distribution of herpetofauna. Researchers conducted systematic surveys of different habitats, including forests, wetlands, grasslands, and urban areas, to document the presence of amphibians and reptiles. Surveys involved visual encounters, where researchers search for animals directly. Animals were released unharmed without exceptions. In addition, information about natural habitat distribution was gathered to correlate species with their natural habitats (Figure 1).



**Figure 1** Field research map of areas and distance covered: 1 Starting point – Belgrade – searching for herpetofauna at the Avala mountain; 2,3,4,5,6,7,8 – searching for herpetofauna; - documenting the environment and associated herpetofauna

During the field surveys researchers encountered hundreds of animals and positively identified 11 species of amphibians and 13 species of reptiles (Table 1). Most notable absence on the list is snake *Vipera berus* due to this species decreasing numbers.



**Table 1** Field list of species encountered and identified during the field surveys

Lizards	Snakes	Slow worms	Tortoises	Frogs	Toads	Salamanders and newts
<i>Lacerta viridis</i>	<i>Natrix tessellata</i>	<i>Anguis fragilis</i>	<i>Testudo hermanni</i>	<i>Pelophylax ridibundus</i>	<i>Bombina variegata</i>	<i>Salamandra salamandra</i>
<i>Podarcis tauricus</i>	<i>Zamenis longissimus</i>			<i>Pelophylax kl. exculantus</i>	<i>Bufo bufo</i>	<i>Triturus vulgaris</i>
<i>Podarcis muralis</i>	<i>Vipera ammodytes</i>			<i>Rana dalmatina</i>	<i>Bufo viridis</i>	<i>Ichthyosaura alpestris</i>
<i>Darevskia praticola</i>	<i>Dolichopis caspius</i>			<i>Rana graeca</i>		
<i>ablepharus kitaibelii</i>	<i>Natrix natrix</i>			<i>Hyla arborea</i>		
	<i>Coronella austriaca</i>					

As an additional research task, an assessment will have to be made about the current distribution ranges for each herpetofaunal and rodent species living in the Balkans. From the preliminary research, there are strong indications of inaccuracies and approximations on existing distribution maps. Assessing the distribution of herpetofauna involves gathering information about where different species of amphibians and reptiles are found within a particular geographic area. This process typically involves a combination of field surveys, literature reviews, and data analysis. This data has to be published in various publications, but often unavailable to a broad public, and in some cases can be found only in libraries. Researchers will review existing scientific literature, including published papers, reports, and species distribution maps, to gather information about the distribution of herpetofauna. This helps to supplement field data and provide a more comprehensive understanding of species distributions over time and across different regions.

To present all available data an interactive map has to be created in ArcGIS software. The map would unite, combine, and present archaeological, ecological, and climatological data gathered by the proposed research. The user would be able to zoom in on any area in the territory of Serbia, Croatia, Montenegro, Bosnia and Hercegovina, and Albania. Users will be able to select any of the following options: Habitat distribution, species distribution, and climate parameters. The selected items will be graphically shown on the map, together with a reference (if available) as proof of the reliability of the information. The map will be extra detailed in areas archeological sites: Baranica, Hadzi Prodanova, Pesturina, Smolucka, Vindija, Krapina, Mujina, and Crvena Stijena caves. These sites are of particular interest as archaeologically excavated layers within will be dated and eligible for paleoreconstructions. Acquiring data from caves will allow the software to show climate change through time in the vicinity of the sites.

## DISCUSSION

Crossing national borders and accessing equivalent material in neighbouring countries has always been a challenge for researchers in the Balkans. In comparison, the Iberian Peninsula and the Apennine Peninsula have much better-filled data on biodiversity and climate changes in the late Pleistocene, as their researchers have no such problem. We have to build collaboration among researchers in the region that can be beneficial to all, and to complete the

missing data. When sorted and united, ecological, climatological and archaeological data will be put in context, creating an interactive map easily accessible and available to various researchers from different scientific communities that might be interested in Balkans. The aim of this approach is to assemble relevant, available information and create new data regarding the climate and environmental changes in the Balkan Peninsula in the last 120 thousand years using FAIR principles. In the final stages, the results will be used for comparison of past ecosystems with the present, to predict future events. It will require the conception of multidisciplinary teams working on similar topics across borders and collaboration between researchers from neighbouring countries resulting in new knowledge and completing the gaps in missing data.

## CONCLUSION

It is important for paleoenvironmental studies in Balkans to disseminate contemporary methods for paleoenvironmental and paleoclimatic reconstructions, using FAIR principles, at the territory of Balkans. Multidisciplinary approach to the complex problem of climate change has to be used in order to understand past, present and future events and improve the resilience of society and nature. It will also promote public understanding of the scientific facts in a field of environmental protection and sustainability. The realization of this research approach will have a positive impact on the local communities as well as the general public on the Balkans. Local people are usually very interested in scientific research, and friendly to the researchers despite political and national disputes. Using the popularity of the subject we hope to build strong relationships with local communities and researches that will continue in the future. The interactive map will be of particular impact for educational purposes as it will be completely free to use. It will also be of significant use to the scientific community as it will offer a large amount of data for scientific purposes.

## REFERENCES

- [1] O'Regan H.J., Turner A., Bishop L.C., *et al.*, Climatic influence on the late Quaternary mammalian fauna of Southwestern Europe. *Journal of Biogeography*, 38(1) (2011) 91–102.
- [2] López-García J.M., Blain H.A., *Quat. Sci. Rev.* 233 (2020) 106242.
- [3] Musil R., Palaeoenvironment at Gravettian Sites in Central Europe with emphasis on Moravia (Czech Republic): Die Paläoumwelt mitteleuropäischer Gravettien-Fundstellen mit Schwerpunkt auf Mähren (Tschechische Republik). *Quartär–Internationales Jahrbuch zur Erforschung des Eiszeitalters und der Steinzeit* 57 (2010) 95–123.
- [4] Böhme G., Zur historischen Entwicklung der Herpetofaunen Mitteleuropas im Eiszeitalter (Quartär). *Die Amphibien und Reptilien Deutschlands*. Gustav Fischer, Stuttgart (1996) 30–39.
- [5] Böhme G., Fossile Amphibien und Reptilien im Quartär Thüringens. *Veröffentlichungen Naturkundemuseum Erfurt* 19.2000 (2000) 79–97.

- [6] Fernández M.H., Bioclimatic discriminant capacity of terrestrial mammal faunas. *Glob. Ecol. Biogeogr.* 10.2 (2001) 189–204.
- [7] Fernández M.H., and Peláez-Campomanes P., Quantitative palaeoclimatic inference based on terrestrial mammal faunas. *Quantitative palaeoclimatic inference based on terrestrial mammal faunas* 14.1 (2005) 39–56.
- [8] Fernández M.H., Álvarez Sierra M.A., Peláez-Campomanes P., Bioclimatic analysis of rodent palaeofaunas reveals severe climatic changes in Southwestern Europe during the Plio-Pleistocene. *Palaeogeogr. Palaeoclimatol. Palaeoecol.* 251.3–4 (2007) 500–526.
- [9] Royer A., et al., New bioclimatic models for the quaternary palaeartic based on insectivore and rodent communities. *Palaeogeogr. Palaeoclimatol. Palaeoecol.* 560 (2020) 110040.
- [10] Blain, H.A., et al., Long-term climate record inferred from early-middle Pleistocene amphibian and squamate reptile assemblages at the Gran Dolina Cave, Atapuerca, Spain. *J. Hum. Evol.* 56.1 (2009) 55–65.
- [11] Blain H.A., Bailon S., Agustí., *Comptes Rendus Palevol* 15.6 (2016) 731–744.
- [12] Popov V.V., Quaternary small mammals from deposits in Temnata-Prohodna Cave system. *Temnata Cave. Excavations in Karlukovo Karst Area, Bulgaria* 1.2 (1994) 11–53.
- [13] Hammer Ø., Harper D.A., Ryan P. D., PAST: Paleontological statistics software package for education and data analysis. *Palaeontol. Electron.* 4(1) (2001) 9.
- [14] Greenacre M.J., Correspondence analysis. *WIREs Comput. Stat.* 2(5) (2010) 613–619.



## SUPPLEMENT TO THE LIST OF ENTOMOFAUNA FROM THE RESEARCH ACTIONS AND CAMPS OF SRSBE “JOSIF PANČIĆ” AT SRN ZASAVICA

**Jovana Damjanović<sup>1</sup>, Matija Milković<sup>1</sup>, Aleksandra Mišćević<sup>1</sup>, Marko Šćiban<sup>1</sup>,  
Vidak Lakušić<sup>1</sup>, Mihajlo Stanković<sup>2\*</sup>**

<sup>1</sup>Scientific Research Society of Biology and Ecology Students “Josif Pančić”,  
Trg Dositeja Obradovića 2, 21000 Novi Sad, SERBIA

<sup>2</sup>Nature Conservation Movement of Sremska Mitrovica – Special Nature Reserve of Zasavica,  
Svetog Save 19, 22000 Sremska Mitrovica, SERBIA

\*[trogloxen@gmail.com](mailto:trogloxen@gmail.com)

### Abstract

*During the research actions carried out by the members of NIDSBE “Josif Pančić” in cooperation with the manager, new taxa were recorded for the list of entomofauna of the reserve. For the past 20 years of research activities, a total of 67 taxa from 5 orders and 33 families have been recorded. Where one strictly protected taxon (*Necrophorus litoralis*) and two protected taxons (*Distoleon tetragranicus*, *Mantispa stiriaca*) were recorded in Serbia. Out of a total of 33 families, 12 of them are listed for the first time for the entomofauna of the reserve and Mačva. According to the Alcifron electronic database, for the taxa *Cantharis pardona*, *Tribolium confusum*, *Oedemera annulate*, *Anacaena globulus*, *Ctenophora guttata* and *Dichlostigma flavipes*, there are no data for the Vojvodina area in the database, and for the orders *Raphidoptera* and *Neuroptera* in the Alcifron database, there are no data for the area of Srem and Mačva. The significance of the research actions carried out by the members of NIDSBE “Josif Pančić” or any other student association for protected areas is very great because it contributes to better research of the protected area and is a significant help to managers in inventorying the species and ecosystem diversity of the area.*

**Keywords:** NIDSBE “Josif Pančić”, reserve Zasavica, research, 20 years.

### INTRODUCTION

A significant form of student engagement and satisfaction of their interest is made possible through the activities of the “Josif Pančić” Scientific Research Society of Biology and Ecology Students. NIDSBE “Josif Pančić” [1] was founded in 1973, on the basis of many years of work by students and staff of the then Institute of Biology. The society officially began working in 1983, and gathers students of biology, ecology, dual-subject courses and all others who want to engage in scientific research, protection and improvement of the environment or education in the same fields. Within this Society, especially interested students are given the opportunity, with the help of professors, assistants and senior colleagues, to become more concretely acquainted with the principles and methods of scientific and research work, to actively participate in the production of scientific papers, to realize their ideas and present the results at student and other gatherings, satisfying in this way, needs and interests that are not covered in such detail during regular studies. Through the implementation of the Society's regular activities - scientific and popular lectures,

educational walks, motivational weekends, research camps, organization of student seminars and scientific gatherings - but also by participating in various manifestations and events, students are enabled to engage in additional activities during their studies, fulfill their interests and realizing their own ideas. Every year NIDSBE “Josif Pančić” organizes several scientific and research camps in Serbia. By participating in the camps, students gain the necessary experience in field and research work, orient themselves and acquire practical knowledge in the areas that interest them. Also an important aspect of such camps are the results that become available to the public through scientific papers that participants can write based on the results and observations from the field. One of the oldest camps that is continuously held is the “Research Camp Zasavica”, which has been running since 2003 until today. Over the past 20 years, more than 1,500 students from the University of Novi Sad or as guests from various other universities from the country and abroad (Europe, Asia, America) have passed through the “Zasavica” research camps, among whom we now have recognized experts in the country and abroad. It is a ten-day field work according to a pre-prepared plan and program of field trips. After returning from the field, the collected material is sorted and prepared for further processing (herbarization, preparation - entomological material), which follows after returning from the field with its professors and assistants at the faculty. After processing, the material is deposited either in the reserve natural history collection or in the collection at the university. The obtained results, depending on their importance, are published at domestic or international scientific and professional gatherings, congresses, etc. The aim of this work is to show the importance of such research camps for a protected area in its valorization of natural values using the example of entomofauna and to publish hitherto unpublished findings.

## **MATERIALS AND WORKING METHODS**

Research camps in Zasavica are organized during the month of August and are ten days of fieldwork conducted according to a pre-prepared plan and program of field trips. In addition to large actions from spring to autumn, the reserve also conducts occasional weekend actions and individual (single) research. During fieldwork, entomological material is collected by hand, with a catcher, various traps, mercury (Hg) lamp, examination of rotten stumps and trees, under stones, in water, vegetation (coastal, macrophyte-aquatic, forest, ...) and others.

Species determination was done according to: Reitter [2], Harde and Severa [3], Bechyně [4], Tanasijević and Sinova-Tošić [5], Garms and Borm [6], Chinery [7], Mikšić [8], Yoshihiko and Hamano [9], Mihajlović [10].

## **RESULTS WITH DISCUSSION**

For the past twenty years of research camps on Zasavica, a good part of the material has already been published, with the fact that part of the entomological material has remained undetermined until now or unpublished from field notebooks. By reviewing the material from the collection and its subsequent determination, as well as by collecting data from field diaries, a list of new species of insects for the entomofauna checklist of the reserve was obtained, and it looks as follows:

Red. COLEOPTERA:

**Fam. Scarabaeidae**

- Aphodius fimetarius*: 04.04.2021., Zasavica II, Valjevac, in the pasture, in the dung; 29.05.2009., Zasavica II, Turske livade, meadow,
- Bolboceras armiger*: 01.08.2022., Zasavica II, Turske livade, on the road at night; 04.08.2022., Zasavica II, Valjevac, in the pasture at night,
- Caccobius schreberi*: 04.08.2020., Banovo Polje, Trebljevine, meadow; 02.08.2020., Ravnje, Zovik, meadow,
- Onthophagus ovatus*: 11.06.2023., Zasavica II, Valjevac, meadow,
- Onthophagus taurus*: 02.08.2017., Ravnje, Zovik, meadow; 10.05.2006., Zasavica II, Valjevac, in the meadow, in the dung.

**Fam. Cantharidae**

- Cantharis pardona*: 15.06.2019., Zasavica II, Turske livade, meadow.

**Fam. Melyridae**

- Clanoptilus marginellus*: 15.06.2019., Zasavica II, Turske livade, meadow,
- *Clanoptilus geniculatus*: 02.05.2021., Zasavica II, Lađine, meadow,

**Fam. Silphidae**

- Nicrophorus humator*: 29.07.2008., Glušci, Bitva, animal carcass; 02.08.2021., Zasavica II, Turske livade, at night,
- *Nicrophorus littoralis*: 22.06.2020., Zasavica II, Turske livade, on an animal carcass,
- Nicrophorus interruptus*: 05.08.2012., Radenković, Vrbovac, on an animal carcass,

**Fam. Trogidae**

- Trox hispidus*: 29.05.2006., Crna bara, Jovača b., meadow; 02.08.2020., Ravnje, Zovik, meadow,
- Trox sabulosus*: 02.08.2006., Noćaj, Lug, meadow; 07.08.2011., Crna bara, Drenova greda, meadow; 08.08.2022., Glušci, Češljuška bara, meadow.

**Fam. Staphyllionidae**

- Creophilus maxillosus*: 08.08.2020., Banovo Polje, Duge njive, goat carcass,
- Scaphisoma sp.*: 02.08.2022., Banovo Polje, Duge njive, animal carcass,
- Oxyporus rufus*: 08.08.2008., Glušci, Bitva, meadow.

**Fam. Tenebrionidae**

- Crypticus quisquilius*: 10.04.2006., Zasavica II, Valjevac, meadow,
- Diaperis boleti*: 04.08.2020., Banovo Polje, Trebljevine, the forest,
- Podonta nigrita*: 05.08.2021., Radenković, Batar, the forest,
- Stenomax aeneus*: 15.04.2006., Salaš Noćajski, the edge of the forest,
- Tribolium confusum*: 04.08.2020., Banovo Polje, Trebljevine, forest, tree stump.

**Fam. Lampyridae**

- Lampyris noctiluca*: 21.06.2012., Banovo Polje, Trebljevine, the forest,
- Luciola lusitanica*: 05.03.2014., Zasavica I, Šumareva ćuprija, the forest,

**Fam. Oedemeridae**

- Oedemera annulate*: 08.05.2007., Crna bara, Drenova greda, meadow,
- Oedemera femorata*: 11.06.2006., Zasavica I, Valjevac, meadow; 04.08.2008., Radenković, Batar, meadow; 20.06.2007., Ravnje, Zelena bara, meadow.

**Fam. Cetonidae**



-*Potetia metallica*:21.06.2012., Banovo Polje, Trebljevine, meadow,

-*Trichis sexualis*:05.08.2011., Radenković, Vrbovac, meadow.

**Fam. Chrysomelidae**

-*Althica oleracea*:03.08.2023., Zasavica II, Vizitorski centar, Hg (mercury) lamp,

-*Cryptocephalus connexus*:04.08.2019, Zasavica I, Valjevac, meadow,

-*Diabrotica virgifera*:02.08.2019., Ravnje, Zovik, meadow,

**Fam. Scirtidae**

-*Cyphon variabilis*:03.08.2023., Zasavica II, Vizitorski centar, Hg (mercury) lamp.

**Fam. Hydrophilidae**

-*Anacaena globulus*:27.10.2014., Radenković, Pačija bara, peatland.

**Fam. Dytiscidae**

-*Rhantus sp.*:03.12.2014., Radenković, Pačija bara, peatland; 27.10.2014., Radenković, Pačija bara, peatland.

**Fam. Heterocerhidae**

-*Heterocerus fenestratus*:05.07.2023., Glušci, Češljuška bara, the forest.

**Fam. Nitidulidae**

-*Glischrochilus hortensis*:04.08.2020., Banovo Polje, Trebljevine, the forest.

**Fam. Carabidae**

-*Calistus lunatus*:08.08.2019, Ravnje, Bostanište, the forest; 29.04.2023., Zasavica II, Valjevac, meadow,

-*Philochthus biguttatus*:02.08.2022., Radenković, Batar, the forest.

Ordo NEUROPTERA:

**Fam. Myrmeleontidae**

-*Distoleon tetragranicus*:01.08.2021., Zasavica II, Vizitorski centar, meadow; 01.08.2022., Zasavica II, Vizitorski centar, meadow; 01.08.2022., Zasavica II, Turske livade, the edge of the forest,

-*Euroleon nostrans*: 02.08.2017., Crna bara, Jovača b., meadow,

-*Osmylus filvicephalus*:07.07.2007., Zasavica II, Valjevac, meadow,

-*Palpares libelluloides*:08.07.2007.,Zasavica I, Valjevac, meadow,

**Fam. Mantispidae**

-*Mantispa stiriaca*: 04.08.2022, Lađine, meadow.

Ordo DIPTERA:

**Fam. Tabanidae**

-*Tabanus svedicus*: 06.07.2007., Ravnje, Bostanište, the forest; 04.08.2021., Banovo Polje, Trebljevine, the forest; 08.08.2021., Banovo Polje, Duge Njive, the forest,

-*Theriopectes gigas*:02.06.2019., Zasavica II, Vizitorski centar.

**Fam. Asilidae**

-*Dysmachus bifurcus*: 02.08.2022., Banovo Polje, Batar, the forest,

-*Laphria flava*: 03.07.2014., Banovo Polje, Batar, the forest.

**Fam. Bibionidae**

-*Dilophus sp.*:22.04.2022., Radenković, Pačija bara, peatland.

**Fam. Tipulidae**

- Ctenophora flaveolata*:04.08.2020., Banovo Polje, Trebljevine, reed beds,
- Ctenophora ornate*:02.08.2020., Ravnje, Zovik, meadow,
- Ctenophora guttata*:23.05.2009., Zasavica II, Turske livade, the forest,
- Nephrotoma appendiculata*:02.08.2018., Ravnje, Zovik, meadow; 04.08.2020., Banovo Polje, Trebljevine, reed beds; 09.09.2018., Banovo Polje, Batar, the forest,
- Tipula balcanica*: 03.08.2020., Radenković, Batar, the forest,
- Ptychoptera contaminate*:02.08.2020., Radenković, Gajića ćup., meadow.

Ordo RAPHIDIIDAE:

**Fam. Raphidiidae**

- Dichlostigma flavipes*:22.04.2022., Radenković, Pačija bara, peatland,
- Phaeostigma notata*:01.08.2022., Zasavica II, Turske livade, the edge of the forest; 02.06.2019., Zasavica II, Vizitorski centar,
- Raphidia ophiopsis*: 18.04.2013., Radenković, Pačija bara peatland.

Ordo HYMENOPTERA:

**Fam. Sphecidae**

- Sceliphron caementarium*: 03.08.2020., Radenković, Batar, meadow,
- Sceliphron destillatorium*: 01.08.2021., Zasavica II, Vizitorski centar, meadow,
- Isodontia mexicana*:01.08.2022., Zasavica II, Vizitorski centar, meadow.

**Fam. Vespidae**

- Delta unguiculatum*:07.08.2021., Glušci, Bitva, on the forest road.

**Fam. Pompilidae**

- Anoplus viaticus*:09.08.2021., Banovo Polje, Banov brod, embankment.

**Fam. Ichneumomidae**

- Enicospilus merdarius*:14.04.2023., Zasavica II, Turske livade, the forest.

**Fam. Melittidae**

- Melitta sp.*:04.08.2020., Banovo Polje, Trebljevine, reed beds.

**Fam. Stephanidae**

- Stephanus serrator*:04.08.2020., Banovo Polje, Trebljevine, reed beds.

**Fam. Gasteruptionidae**

- Gasteruption jaculator*:02.08.2018., Ravnje, Zovik, meadow.

**Fam. Formicidae**

- Myrmica ruginosis*:06.08.2019., Zasavica II, Turske livade, the forest.

**Fam. Braconidae**

- Doryctes leucogaster*:05.08.2020., Zasavica II, Turske livade, the edge of the forest.

A total of 67 taxa from 5 orders and 33 families were recorded. Out of a total of 67 taxa, one taxon (*Necrophorus litoralis*) is strictly protected and two taxa (*Distoleon tetragranicus*, *Mantispa stiriaca*) are protected in Serbia. Out of a total of 33 families, 12 families (Fam. Melyridae; Trogidae; Oedemeridae; Scirtidae; Heterocerhidae; Nitidulidae; Myrmeleontidae; Raphidiidae; Pompilidae; Melittidae; Stephanidae, Silphidae, Lampyridae and Gasteruptionidae) are listed for the first time as entomofauna of the reserve. From the order Coleoptera the following families Scarabaeidae, Cantharidae, Staphyllionidae, Tenebrionidae,

Cetonidae, Chrysomelidae, Hydrophilidae, Dytiscidae and Carabidae are included in the research so far. According to the data of Stanković [11] the Scarabaeidae fauna has a total of 6 taxa, the Cantharidae fauna 3 taxa, the Staphyllionidae fauna 3 taxa, Tenebrionidae fauna 4 taxa and Cetonidae fauna 5 taxa. According to Stanković [12] the Chrysomelidae fauna in the reserve has a total of 75 taxa, this research found three new taxa for the list, which increases the total diversity of leaf beetles to 78 taxa. The aquatic Coleoptera fauna has a total of 81 taxa, of which 47 taxa are from the suborder Adepnaga [13] and 34 taxa from the family Hydrophilidae [14]. The survey found two new taxa for the list, which increases the total diversity of paddlefish and grebes to 83 taxa. According to Ćurčić [15], the Carabidae fauna in the reserve has a total of 72 taxa, this research found three new taxa for the list, which increases the total diversity of the carabidae to 75 taxa. The order Neuroptera has not been recorded so far, so the recorded Fam. Myrmeleontidae with 4 taxa and Fam. Mantispidae with one taxon are new to the fauna of the reserve. The order Hymenoptera is represented by three taxa from Fam. Sphecidae, while the remaining families Vespidae, Pompilidae, Ichneumonidae, Melittidae, Stephanidae, Gasteruptionidae, Formicidae and Braconidae are represented by one taxon each. Species of the genus *Sceliphron*, *Isodontia*, *Delta*, *Anoplius*, *Enicospilus*, *Doryctes*, *Gasteruption*, *Stephanus* represent a parasitic group of wasps that regulate the number of so-called wasps “harmful insects” in agriculture and forestry. Myrmecofauna (Formicidae) from the order Hymenoptera has been investigated in detail so far, where a total of 31 taxa of ants were recorded [16], with this finding the number of taxa has increased on 32 taxa. According to the Alciphron electronic database [17] for the taxa *Cantharis pardona*, *Tribolium confusum*, *Oedemera annulate*, *Anacaena globulus*, *Ctenophora guttata* and *Dichlostigma flavipes*, there are no data in the database for the area of Vojvodina. For the order Raphidioptera and Neuroptera, according to the Alciphron electronic database, there are no data for the area of Srem and Mačva. For the Mačva area in the Alciphron electronic database there are three UTM fields with data for taxa; *Diabrotica virgifera* and *Calistus lunatus*, then for two UTM data fields for taxa; *Oedemera femorata* and *Tabanus suedicus*, while for the taxa *Nicrophorus interruptus*, *Creophilus maxillosus*, *Oxyporus rufus*, *Crypticus quisquilius*, *Stenomax aeneus*, *Lampyris noctiluca*, *Trichis sexualis*, *Cryptocephalus connexus*, *Theriopectes gigas*, *Ctenophora ornate*, *Isodontia mexicana* and *Stephanus serrator* there is one UTM data field in the Alciphron database.

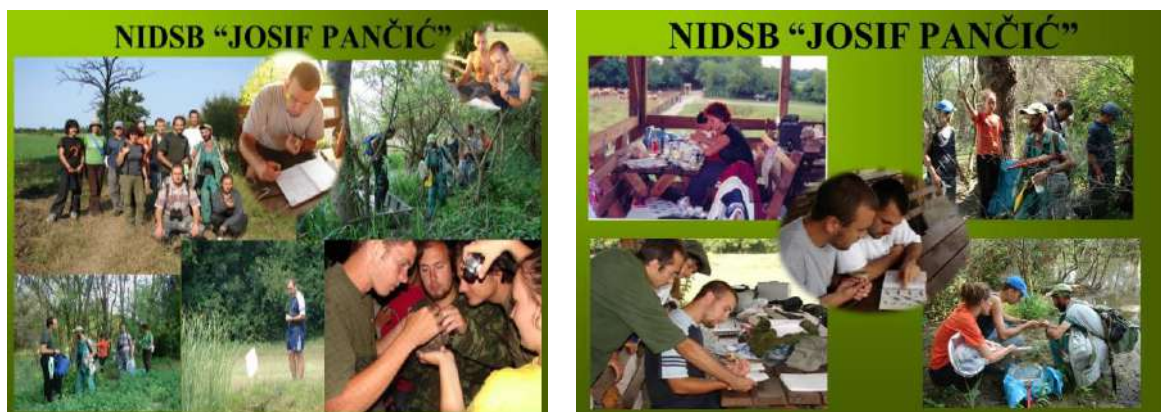


Figure 1 Photos from the field of NIDSB members “Josif Pančić” from Novi Sad

## CONCLUSION

During the research actions carried out by the members of NIDSBE “Josif Pančić” in cooperation with the manager, new taxa were recorded for the list of entomofauna of the reserve. For the past 20 years of research activities, a total of 67 taxa from 5 orders and 33 families have been recorded. Where one strictly protected taxon (*Necrophorus litoralis*) and two protected taxons (*Distoleon tetragranicus*, *Mantispa stiriaca*) were recorded in Serbia. Out of a total of 33 families, 12 of them are listed for the first time for the entomofauna of the reserve and Mačva. According to the Alcifron electronic database, for the taxa *Cantharis pardona*, *Tribolium confusum*, *Oedemera annulate*, *Anacaena globulus*, *Ctenophora guttata* and *Dichlostigma flavipes*, there are no data for the Vojvodina area in the database, and for the orders Raphidoptera and Neuroptera in the Alcifron database, there are no data for the area of Srem and Mačva. So far, the research includes the Coleoptera families Scarabaeidae, Cantharidae, Silphidae, Staphyllionidae, Tenebrioidae, Lampyridae, Cetonidae, Chrysomelidae, Hydrophilidae, Dytiscidae and Carabidae [10–14], and the myrmecofauna (Formicidae) from the Hymenoptera order was investigated [15]. The significance of the research actions carried out by the members of NIDSBE “Josif Pančić” or any other student association for protected areas is very great because it contributes to better research of the protected area and is a significant help to managers in inventorying the species and ecosystem diversity of the area.

## THANK-YOU NOTE

*We would like to thank our colleague Dr. Gabor Mesaroš for his help in determining certain groups of insects.*

## REFERENCES

- [1] Available on the following links: [www.dbe.uns.ac.rs/o-nama/nidsb-josif-pancic/](http://www.dbe.uns.ac.rs/o-nama/nidsb-josif-pancic/); [www.nidsbejosifpancic.com](http://www.nidsbejosifpancic.com)
- [2] Reitter E., Fauna Germanica – Die Käfer des Deutschen Reiches. Band III, Stuttgart, Lutz Verlag, Aschersleben, (1911).
- [3] Harde W.K., Severa B. Beetles - a field guide in colour, Printed in the Czech Republic, Prague, (2000).
- [4] Bechyne J., Welcher kafer ist das?, Kosmos, Stuttgart (1988).
- [5] Tanasijević N., Sinova-Tošić D., Posebna entomologija, Naučna knjiga, Beograd (1987).
- [6] Garms H., Borm L., Fauna Evrope, Mladinska knjiga, Ljubljana (1981).
- [7] Chinery M., Insects, Harper collins Publishers, Glasgow (1997).
- [8] Mikšić R., Scarabaeidae Jugoslavije, SANU, Posebna izdanja, knjiga CCCXLVIII, odeljenje Prirodno-Matematičkih nauka, knjiga 28, Naučno delo, Beograd (1962).
- [9] Yoshihiko K., Hamano E., Insekti, Izdavački zavod, Beograd (1980).
- [10] Mihajlović Lj., Šumarska entomologija drugo izdanje, Univerzitet u Beogradu, Šumarski fakultet, Beograd (2015).

- [11] Stanković M., Vodič kroz prirodu u Specijalnom rezervatu prirode Zasavica (drugo izmenjeno i dopunjeno izdanje), Pokret gorana Sremska Mitrovica, Sremska Mitrovica (2014).
- [12] Stanković M., Fauna Chrysomelidae Zasavice i severne Mačve, Zbornik rezimea XIV Simpoziuma entomologa Srbije, Novi Sad (2023).
- [13] Mesaroš G., Stanković M., Prilog poznavanju grabljivih vodenih tvrdokrilaca (Coleoptera, Adephaga) SRP Zasavica, Zbornik radova Naučno stručnog skupa Zasavica 2012, Pokret gorana Sremska Mitrovica, Sremska Mitrovica (2012).
- [14] Mesaroš G., Stanković M., Prilog poznavanju faune veslara (Coleoptera - Hydrophilidae) Specijalnog rezervata prirode Zasavica, Zbornik radova Naučno-stručnog skupa o biodiverzitetu i drugim vrednostima rezervata Zasavica „Zasavica 2022.” (2022).
- [15] Ćurčić S., Stanković M., The ground beetles (Coleoptera: Carabidae) of the Zasavica Special Nature Reserve (Serbia). *Acta entomologica Serbica*, 16(1/2), 61–79 (2011).
- [16] Karaman G.M., Karaman S.G., Prilog poznavanju mrava (Hymenoptera, Formicidae) Specijalnog rezervata prirode Zasavica, Srbija, Zbornik Naučno-stručni skup Zasavica 2007 sa međunarodnim učešćem, (2007).
- [17] Elektronska baza podataka Alciphron ([www.habiprot.org.rs](http://www.habiprot.org.rs)) HabiProt – Udruženje za održivi razvoj i očuvanje prirodnih staništa Srbije.





## “LIVING FOSSILS” IN THE CRASH FAUNA OF THE ZASAVICA SPECIAL NATURE RESERVE

Mihajlo Stanković<sup>1\*</sup>

<sup>1</sup>Nature Conservation Movement of Sremska Mitrovica – Special Nature Reserve of Zasavica, Svetog Save 19, 22000 Sremska Mitrovica, SERBIA

\*trogloxen@gmail.com

### Abstract

*In the fauna of the Zasavica reserve, a total of 21 species of Macrocrustacea were recorded, and the status of “living fossils” belongs to organisms from the class Branchipoda, order Anostraca, and from the class Ostracoda, because they have not changed in evolutionary terms for hundreds of millions of years. Anostraca species Chirocephalus brevivalpis has the status of a “living fossil” and from the order Notostraca there are two species Lepidurus apus and Triops cancriformis. The species Chirocephalus brevivalpis is a rare species, whose find in Zasavica is the westernmost of this species and the only one south of Sava and Danube. The finding of the species Lepidurus apus in the Batar tributary is unique because the individuals were found in running water. While the discovery of the species Triops cancriformis in Zasavica is new for Serbia and a new species for the reserve. So far, nine species of ostracods have been discovered in the Reserve, and the discovery of Candona aff. candida in Zasavica is the first in Serbia.*

**Keywords:** living fossils, Zasavica, Serbia.

### INTRODUCTION

Few of us know that we share today's planet Earth with organisms that have not changed evolutionarily for hundreds of millions of years. We call such organisms “living fossils” – which are almost unchanged from the time of their extinct ancestors and usually have no closer living relatives. Their characteristic development has led to the fact that today such organisms often differ in appearance, way of life and reproduction, and still resist today's conditions on Earth. Unlike other species that have evolved, or are even still evolving, living fossils are those species whose anatomy and behavior have not changed over millions of years. “Living fossils” are organisms that have survived meteor bombardments, ice ages, floods, fires, earthquakes, gigantic volcanic eruptions, etc. The best-known living fossils of plants are ginkgo (*Ginkgo biloba*) and the genus *Cycas*, which grew in the times when dinosaurs still walked the Earth [1]. We discovered some of the living fossils only recently, while they have been under our noses for years. Thus, the metasequoia (*Metasequoia glyptostroboides*) was thought to be extinct long ago, until the Chinese forester Tsou Kan came across several specimens of this unusual deciduous tree in the southwest of China in 1947 [1,2]. Among the five most famous living fossils in animals are *Coelacanth pronunciation* (Coelacanth), *Acipenser ruthenus* (Kechiga), *Macrochelys temminckii* (Alligator turtle), *Dicerorhinus sumatrensis* (Sumatran rhinoceros), *Okapia johnstoni* (Okapi) and



*Nautilus sp.* (Indian ship) that have not changed at all or little in the past almost 500 million years [3].

Crayfish in Serbia live wherever there is surface water, as well as underground water. Many live hidden, secretive lives, and to see them you need to be at the right time, in the right place. Numerous adaptations of the body structure and their great diversity enable them to survive in the most diverse habitats. A small number of species have adapted to life on land in extremely humid environments or humus. The Balkan Peninsula, and especially Serbia, is known as the center of crab diversity, some of which live only here. Many crustaceans play an important role in food chains. Although it is a common belief among people that crabs live in clean waters, this is not always the case because some crabs feed on decaying organic particles.

The Zasavica Reserve is located on the border of two very important areas of the Balkan Peninsula in terms of diversity, characterized by an extremely rich and specific fauna, many of which are endemic to the area and the Pannonian Plain. Taube [4], Josif Pančić [5] and the Dombrowski brothers [6] provided the first data on the flora and fauna of Northern Mačva (Peripannonian Serbia), and thus the area of today's Special Nature Reserve (SNR) "Zasavica". A period of over half a century of sporadic research by small groups and individual researchers followed. In 1995, an initiative for the protection of Zasavica was launched and the Decree on preliminary protection was adopted [7]. At the proposal of the Institute for Nature Protection of Serbia, in 1997 the Government declared the Special Nature Reserve "Zasavica" [8] with an area of 1,850 ha, then in 2019 the boundaries of the Reserve were expanded to a total of 3,400 ha [9].

This paper aims to show organisms from the distant past, the so-called "living fossils" present in the crustacean fauna of the SNR "Zasavica".

## MATERIALS AND WORKING METHODS

The material for this work was collected from published works and submitted research reports in the period 1997–2023.

## RESULTS WITH DISCUSSION

A total of 21 species of Macrocrustacea were recorded in the fauna of the Zasavica Reserve [10]. Even if crabs are an ancient group of organisms, not all of them are "living fossils". The status of "living fossils" belongs to organisms from the class Branchipoda, order Anostraca, and from the class Ostracoda, because they have not changed in evolutionary terms for hundreds of millions of years. Within the Arthropoda phylum, which also includes Crustacea, in the Branchipoda class, three orders with the following species are present in the Reserve: Ordo: Anostraca; Species: *Chirocephalus brevipalpis* (Orhgidan, 1953); Ordo: Notostraca, Species: *Lepidurus apus* (Linnaeus, 1758), *Triops cancriformis* (Bose, 1801); Superorder: Diplostraca, Ordo: Spinicaudata, Species: *Cyzicus tetracerus* (Krynicky, 1830). Of the four branchipod species present, the status of "living fossils" is in the order Anostraca species *Chirocephalus brevipalpis* (Orhgidan, 1953) and in the order Notostraca *Lepidurus apus* (Linnaeus, 1758) and *Triops cancriformis* (Bose, 1801); Superordo: Diplostraca, Ordo:

Spinicaudata, Species: *Cyzicus tetracerus* (Krynicky, 1830). Of the four branchipod species present, the status of “living fossils” is in the order Anostraca species *Chirocephalus brevivalpis* (Orhgidan, 1953) and in the order Notostraca *Lepidurus apus* (Linnaeus, 1758) and *Triops cancriformis* (Bose, 1801).

#### **Anostraca**

*Chirocephalus brevivalpis* is a rare species (Figure 1), known only from a few localities in Romania and two areas in Serbia, and the find in Zasavica is the westernmost of this species and the only one south of the Sava and Danube rivers. *Ch. brevivalpis* is an early spring lowland species found from late February to mid-May. It inhabits shallow ephemeral waters with or without vegetation and floodplain forests [11]. Within the Reserve, it was found in several locations (depressions with water in the Valjevac pasture and in the forests of Valjevac, Jovača bara, ephemeral water in Sadžak, Prekopac, Zovik and Vrbovac), and the location where it is recorded regularly every year is the Valjevac pasture in depressions with water.



*Figure 1 Chirocephalus brevivalpis*

*Lepidurus apus* is a species with a very limited distribution in Serbia (Figure 2), found only in two localities in central Banat [12]. It inhabits clear waters with submerged vegetation, but also flooded forests. This is an early spring species and is found from February to April [13]. Within the Reserve, the species was found in a total of three localities (Crkvine, Neškovine and Jovača), of which two localities (Crkvine and Neškovine) are on the Batar tributary, of which the Crkvine locality is found in a riverbed with running water, and the other (Neškovine) in occasional the active part of the stream where ephemeral waters appear.



*Figure 2 Lepidurus apus*

The finding of the species in the Batar tributary is unique because the individuals were found in running water [11]. Generally, *L. apus* is present in the western part of the Reserve, where it is found both in floodplain forests along the Batar tributary and in the ephemeral Jovača pond. Unlike other sites in Serbia where only females were found, bisexual populations were found here in Zasavica in all three habitats [14].

*Triops cancriformis* is a “living fossil” (Figure 3) originating from the Upper Cambrian over 500 million years ago (Dragana, M., 2014). It lives in shallow intermittent water habitats and has developed two characteristic features, the ability to reach sexual maturity in a short time and produce offspring and to survive in the period without water in the habitat in the form of resistant forms (in the form of dormant fertilized egg cells, so-called cysts). The species was found in 2020 at the Batar locality in a small puddle on a forest road in the mud, with ten individuals for the first time in Yugoslavia, Marinček (1961) registered the presence of the species *Triops cancriformis* (Bosc, 1801) near the village of Ečka near Zrenjanin (Banat, Vojvodina). Later, this species was discovered in many other localities, mostly in the Pannonian Plain in Serbia (e.g. Ritovi donje Potisje, etc.) and now neighboring countries, but also in Serbia south of the Danube (e.g. Stara planina). Only females were present in that collected material (Marinček, Petrov, 1994). Only in 1991 in the vicinity of the village Melenci, males of this species were found for the first time in Yugoslavia (Petrov, Cvetković, 1996). The finding of this crayfish in Zasavica is new for Serbia and a new species for the Reserve.

These species belong to an old development line of crustaceans originating from the Cambrian, when there was an explosion of the appearance of numerous organisms, which are considered the ancestors of the species that live on Earth today. The species *Triops cancriformis* was found in a place where hardly anyone even looks for life, i.e. it was found in a pond ten centimeters deep, with a layer of mud of a few centimeters, on a forest road, which was made by tractors when passing by.



**Figure 3** *Triops cancriformis*

The species *Lepidurus apus* and *Triops cancriformis* are characterized by their complete development – emergence, mating, egg-laying and death, in a few days. It is interesting that in the period when there is no water in the habitat, these crabs survive in the form of resistant dormant embryos (cysts), which can survive in the substrate for several decades, even hundreds of years. The eggs that are there now and are very small are literally standing there

waiting for the right moment to emerge again. It could be next year, it could be in 50 years, it all depends on when all the optimal conditions for their appearance will coincide.

### Classes: Ostracoda

Ostracods are “by far the most common arthropods in the fossil record” [15] with fossils found from the Early Ordovician to the present. Although they are usually small in size, we have an example of a large ostracod from the genus *Herrmannina* up to 3 cm long from Silurian deposits found on the eastern island of Saaremaa in Estonia. In addition to marine and freshwater sediments, ostracods have also been found in Baltic amber of Eocene age, where they arrived as they were probably deposited on trees during floods [16]. Ostracods are particularly useful for local or regional biozonation of marine strata, and they are invaluable paleoenvironmental indicators because of their widespread, small size, easily preserved, generally moulted, calcified shells, and valves are a common microfossil.

So far, nine species of ostracods from eight genera have been discovered in the Reserve, namely: *Candona aff. candida* (O. F. Muller, 1776), *Cypria ophthalmica* (Jurine, 1820), *Cyclopris laevis* (O. F. Muller, 1776), *Cyclopris ovum* (Jurine, 1820), *Eucypris virens* (Jurine, 1820), *Bradleystrandesia reticulata* (Zaddach, 1844), *Heterocypris incongruens* (Ramdorh, 1808), *Cypris pubera* (O. F. Muller, 1776) and *Ilyocypris sp.* [10]. Although a widespread and common species on the Eurasian continent, with exceptional tolerance to different habitat conditions, the finding of *Candona aff. candida* in Zasavica is the first in Serbia [11]. In Central Europe, the species *C. aff. candida* appears in spring (March-April) and develops rapidly. The authors Hartmann and Hiller [17] consider it a permanent form in waters whose temperature does not exceed 18°C during the summer. In the Reserve, ostracods are mostly found in ephemeral waters in meadows or parched fields and ruts in a total of four localities (Batar, Sadžak, Valjevac and Jovača) and have drought-resistant eggs. They have mixed copulatory and parthenogenetic reproduction and newly born individuals, the ability to swim immediately. These biological attributes allow them to survive as successfully as possible in these habitats [18]. Among the recorded ostracods, the most common species in the Reserve is *Cypris pubera* [11]. The closest localities to Zasavica where these ostracods were found are in Srem on Fruška Gora [19]. According to Menković *et al.*, the found ostracods from the genera *Ilyocypris* and *Cyclopris* in the Reserve belong to the oldest early Holocene fauna.

### CONCLUSION

In the fauna of the Zasavica Reserve, a total of 21 species of Macrocrustacea were recorded, and the status of “living fossils” belongs to organisms from the class Branchipoda, order Anostraca, and from the class Ostracoda, because they have not changed in evolutionary terms for hundreds of millions of years. Anostraca species *Chirocephalus brevivalpis* has the status of a “living fossil” and from the order Notostraca there are two species *Lepidurus apus* and *Triops cancriformis*. The species *Chirocephalus brevivalpis* is a rare species, whose find in Zasavica is the westernmost of this species and the only one south of Sava and Danube. The finding of the species *Lepidurus apus* in the Batar tributary is unique because the individuals were found in running water. The discovery of the species *Triops cancriformis* in

Zasavica is new for Serbia and a new species for the Reserve. So far, nine species of ostracods have been discovered in the Reserve, and the discovery of *Candona aff. candida* in Zasavica is the first in Serbia.

## REFERENCES

- [1] Juretić B., Kovačić S., Mihelj D., *et al.*, Pedeset znamenitosti botaničkoga vrta obilazak za prolaznika, šetača i ljubitelja – Vodič kroz botanički vrt Prirodoslovno-Matematičkoga fakulteta Sveučilišta u Zagrebu – prigodom 125. obljetnice Sveučilište u Zagrebu Prirodoslovno-matematički fakultet, Biološki odsjek Botanički vrt, (2014).
- [2] Available on the following link:  
[www.monumentaltrees.com/en/trees/dawnredwood/dawnredwood](http://www.monumentaltrees.com/en/trees/dawnredwood/dawnredwood)
- [3] Available on the following link: <https://pixelizam.com/5-najpoznatijih-zivih-fosila-na-svijetu/>
- [4] Taube W.F., Historische und geografische Beschreibung des königreiches Slavonien und das Herzogthumes Syrmien, Leipzig (1776).
- [5] Pančić J., Ptice u Srbiji, Državna štamparija, Beograd (1867).
- [6] Dombrowski E., Osnovi ornitologije sjeverozapadne Srbije, Glasnik Zemaljskog muzeja, Sarajevo (1895).
- [7] Official Gazette RS, No. 51/95, Decision on the prior protection of the Zasavica natural property (1995).
- [8] Official Gazette RS, No. 19/97, Decision on the protection of the natural asset of Zasavica (1997).
- [9] Official Gazette RS, No. 54/19, Decree on the proclamation of the Special Nature Reserve “Zasavica” (2019).
- [10] Stanković M., 29<sup>th</sup> International Conference Ecological Truth & Environmental Research – EcoTER'22, 21–24 June 2022, Sokobanja, Srbija (2022).
- [11] Petrov B., Miličić D., Karan-Žnidaršič T., Zbornik radova Naučno-stručnog skupa Zasavica 2007 sa međunarodnim učešćem, Sremska Mitrovica, Srbija (2007).
- [12] Petrov B., Petrov I., The status of Anostraca, Notostraca and Conchostraca in Yugoslavia, Hydrobiologia, (1997).
- [13] Petrov B., Cvetković D., Community structure of Brachiopods (Anostraca, Notostraca and Conchostraca) in the Banat province in Yugoslavia, Hydrobiologia, (1997).
- [14] Petrov B., Zbornik naučno-stručnog skupa “Zasavica 2012”, Sremska Mitrovica, Srbija (2012).
- [15] Siveter D.J., Briggs D.E.G., Siveter D.J., *et al.*, Proceedings of the Royal Society B, 277(1687) (2010) 1539–1544.
- [16] Ikeya N., Tsukagoshi A., Horne J.D., The phylogeny, fossil record and ecological diversity of ostracod crustaceans, Hydrobiologia 538(1–3) (2005) VII–XIII.

- [17] Hartmann G., Hiller D., Beitrag zur Kenntnis der Ostracoden fauna des Harzes und seines nördlichen Vorlandes (unter besonderer Berücksichtigung des Männchens von *Candona candona*), 125. Jahre Naturwissenschaftlicher Verein Goslar, (1977).
- [18] Horne D.J., Koen M., An assessment of the importance of resting eggs for the evolutionary success of non-marine Ostracoda (Crustacea) In Brendonck L., De Meester L., Hairston N.: Evolutionary and ecological aspects of crustacean diapause, 52. Advances in Limnology, (1998).
- [19] Karanović I., Fauna ostrakoda (Ostracoda, Crustacea) Fruške gore (Vojvodina, Jugoslavija), Magistarska teza, Novi Sad, (1996).





## DEGRADATION OF DYE CRYSTAL VIOLET RELEASED FROM THE TEXTILE INDUSTRY

Nataša Knežević<sup>1\*</sup>, Aleksandar Jovanović<sup>2</sup>, Marija Vuksanović<sup>1</sup>, Marjetka Savić<sup>1</sup>,  
Milena Milošević<sup>3</sup>, Aleksandar Marinković<sup>4</sup>

<sup>1</sup>University of Belgrade, “VINČA” Institute of Nuclear Sciences – National Institute of the Republic of Serbia, Mike Petrovića Alasa 12–14, 11351 Belgrade, SERBIA

<sup>2</sup>Institute for Technology of Nuclear and Other Mineral Raw Materials, Bulevar Franše d'Eperea 86, 11000 Belgrade, SERBIA

<sup>3</sup>University of Belgrade, Institute of Chemistry, Technology and Metallurgy, National Institute of the Republic of Serbia, Njegoševa 12, 11000 Belgrade, SERBIA

<sup>4</sup>University of Belgrade, Faculty of Technology and Metallurgy, Karnegijeva 4, 11000 Belgrade, SERBIA

\* [natasa.knezevic@vin.bg.ac.rs](mailto:natasa.knezevic@vin.bg.ac.rs)

### Abstract

*Textile industry wastewater is a significant source of pollution, often containing hazardous organic dyes like Crystal Violet (CV). Photocatalytic degradation using semiconductor materials such as titanium dioxide (TiO<sub>2</sub>) presents a promising solution for wastewater treatment due to its effectiveness in breaking down organic pollutants under UV irradiation. This study investigates the efficiency of TiO<sub>2</sub> as a catalyst for the photodegradation of CV removed from textile wastewater. Experimental trials were conducted in a batch reactor under UV irradiation, with CV (20 ppm) and varying concentrations of TiO<sub>2</sub> catalyst. Results revealed a significant reduction in CV concentration with increasing catalyst dosage (to 0.1 g/L) and irradiation time. The optimal conditions for maximum degradation efficiency were determined, highlighting the potential of TiO<sub>2</sub> photocatalysis for textile wastewater treatment. Furthermore, the kinetics of CV degradation were analyzed to understand the reaction mechanism and rate. The degradation of the dye (20 ppm) was 98% for 95 min with 0.1 mg/L TiO<sub>2</sub>. This research contributes to developing sustainable and efficient methods for treating textile wastewater, addressing environmental concerns associated with dye pollution.*

**Keywords:** photocatalytic degradation, TiO<sub>2</sub> catalyst, crystal violet, environmental remediation, UV-Vis.

### INTRODUCTION

In the enormous panorama of environmental conservation, battling the persistence of CV dye in water systems, particularly those originating in the textile sector, appears as a major necessity. The textile industry is one of the major water users and pollutants, emitting effluents containing a variety of chemical elements, including bright dyes such as crystal violet [1]. These contaminants not only affect water quality, but also pose serious environmental and human health threats. This work conducts analysis, diving into the kinetics

of photodegradation to uncover the various routes of CV elimination post-purification techniques customized to textile industry wastewater.

By studying photodegradation dynamics, we want to explain the underlying processes that influence dye removal efficiency and rate, which is critical for developing optimal purifying procedures. The use of sophisticated degrading methods, particularly photocatalysis using titanium dioxide ( $\text{TiO}_2$ ) catalysts, appears to be a potential approach to tackling the persistence of CV contaminants.  $\text{TiO}_2$  promotes the breakdown of organic molecules by combining light energy with catalytic activity, resulting in benign byproducts. Understanding photodegradation kinetics not only improves our understanding of purification processes, but also influences the development of novel solutions for effective pollution remediation.

In summary, this work seeks to traverse the complex relationship between textile industry wastewater and crystal violet dye persistence, offering information on the kinetics of photodegradation as a critical component of environmental rehabilitation.

## MATERIALS AND METHODS

### Materials

The following materials were used in photodegradation processes: catalyst  $\text{TiO}_2$  (Sigma-Aldrich, Germany), hydrochloric acid (HCl, Alkaloid, Macedonia), The crystal violet solution (20 ppm; 20 mg/L) was made using a standard manufactured by Merck, Germany. Double distilled water was used for all studies.

### Crystal violet (CV)

Crystal violet (C.I. Basic Violet 3,  $\text{C}_{25}\text{H}_{30}\text{ClN}_3$ ) is a synthetic azo dye that is used mostly in the textile industry, as a dyeing agent (Figure 1) [2].



**Figure 1** Structure of cationic dye crystal violet

Despite its widespread use, crystal violet threatens human health and the environment. Prolonged exposure to crystal violet, especially through skin contact or inhalation of its vapors in work environments such as textile factories, can lead to dermatitis, allergic reactions, and respiratory problems. Some studies have suggested potential carcinogenic effects of crystal violet, although further research is needed to confirm these findings [3,4].

However, it is important to note that while crystal violet is effective for dyeing textiles, it can also pose environmental concerns when wastewater containing the dye is discharged

untreated [5]. Crystal violet is not readily biodegradable and can persist in aquatic ecosystems, potentially causing harm to aquatic organisms and disrupting the balance of aquatic ecosystems.

Therefore, proper wastewater treatment methods should be implemented to remove crystal violet and other dye pollutants before discharge to minimize environmental impact.

### Photocatalytic process

The photocatalytic degradation of organic dyes using commercial  $\text{TiO}_2$  as a catalyst has emerged as a powerful technique for environmental remediation. Harnessing the unique properties of  $\text{TiO}_2$  and the energy of sunlight, the photocatalytic process offers a sustainable and effective method for the removal of CV from wastewater.

The photocatalytic degradation of CV with  $\text{TiO}_2$  involves a series of steps driven by the interaction between the catalyst, the dye molecules, and light. When  $\text{TiO}_2$  is exposed to UV irradiation, it absorbs photons with energy equal to or greater than its bandgap, generating electron-hole pairs [6,7]. These energetic charge carriers migrate to the surface of  $\text{TiO}_2$ , where they participate in redox reactions with adsorbed species, including oxygen and water molecules.

Several factors influence the efficiency of the photocatalytic degradation of CV, including the characteristics of the catalyst, such as crystalline phase, surface area, and particle size. Additionally, parameters such as pH, temperature, catalyst and dye concentration, and light intensity play crucial roles in determining the rate and extent of CV degradation. Optimization of these parameters is essential to maximizing the efficiency of the photocatalytic process.

The photocatalytic tests in this study with a dye concentration of 20 mg/L were conducted. For initial experiments, 0.05 g/L and 0.1 g/L of catalyst were added to the photocatalytic reactor together with 150 mL of pollutant solution (pH=6.2). The mixed dye and catalyst were allowed to stir in the dark for 30 min to homogenize the suspension (150 rpm), after which the solutions were exposed to 588 nm radiation for the time required for complete degradation. After every 15–20 min 2.0 mL of the solution was taken, passed through PVDF 0.22  $\mu\text{m}$  pore syringe filters, and measured using UV-Vis spectrometry (Shimadzu UV-1800, Japan). Photocatalytic experiments were performed in a doubled-wall quartz glass reactor (Figure 2). For irradiation of pesticide solutions, an Osram Ultra Vitalux lamp nominal wattage of 300 W (UVA:UVB=13.6:3), was used.

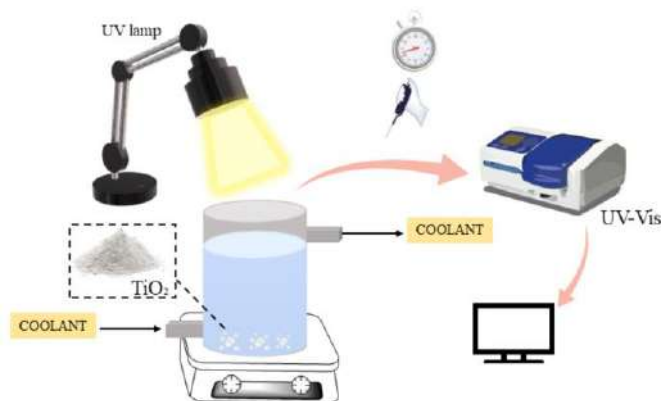


**Figure 2** Reactor system used for experiments

## RESULTS AND DISCUSSION

The removal of textile crystal violet (Figure 1) from wastewater using a commercial  $\text{TiO}_2$  catalyst (Figure 3) and UVA/UVB lamp was studied as simulated sunlight radiation. In the absence of UV-Vis radiation and the catalyst, the degradation process was not observed. The efficiency of the photocatalytic process will decrease if the initial concentration of the substrate increases because the number of adsorbed CV molecules on the surface of the catalyst increases [8].

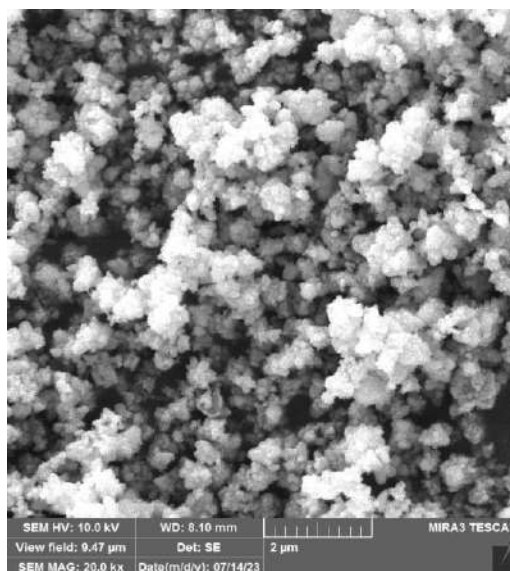


Figure 3 SEM image of  $\text{TiO}_2$  catalyst

After reaching the adsorption equilibrium, in the presence of UV, the rate of CV dye degradation was higher (98%) using a higher catalyst concentration (0.1 g/L) after 95 min, which is attributed to the large surface area of the catalyst and high absorbability (Figure 4). By using half the  $\text{TiO}_2$  concentration, the maximum degradation was 10 min later, after 105 min.

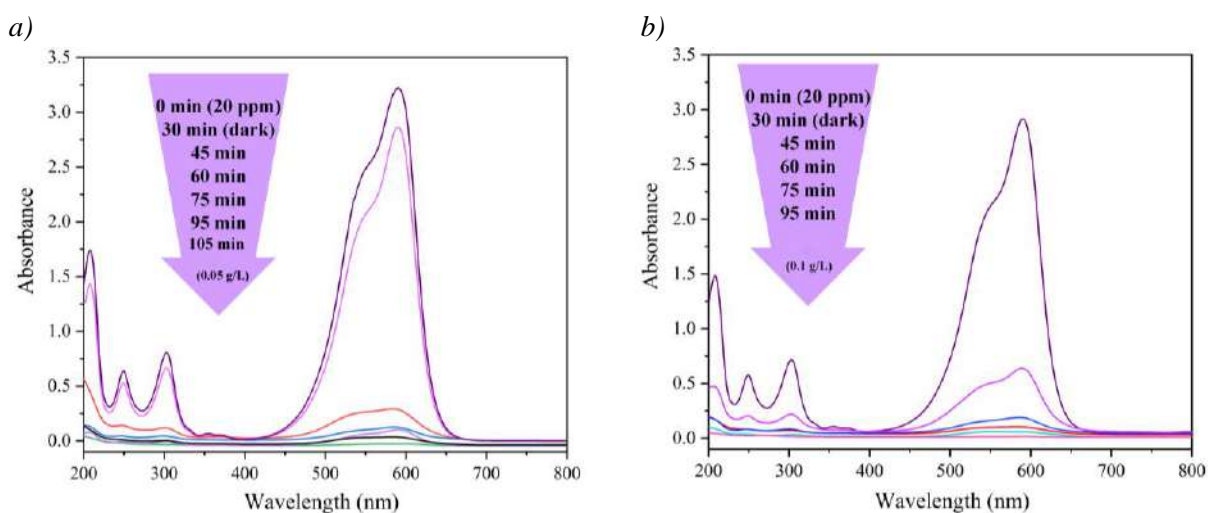


Figure 4 Kinetics of photocatalytic CV degradation using: a) 0.05 g/L; b) 0.1 g/L  $\text{TiO}_2$

The mechanism of TiO<sub>2</sub> activation by UV light and photosensitized oxidation for CV, as well as the identification of intermediate products, is presented in the work of Sugashini *et al.* [9].

## CONCLUSION

The photocatalytic degradation of crystal violet dye using TiO<sub>2</sub> catalysts was investigated. This method holds immense potential for various environmental and industrial applications, including wastewater treatment, pollutant remediation, and the development of sustainable technologies. Continued research efforts are focused on designing advanced photocatalytic materials, reactor configurations, and optimizing processes to enhance efficiency, selectivity, and scalability for the removal of organic dyes and other contaminants from water resources. In conclusion, the photocatalytic degradation of crystal violet with TiO<sub>2</sub> represents a promising approach for addressing dye pollution challenges and advancing towards a cleaner and healthier environment. By harnessing the power of sunlight and the catalytic properties of TiO<sub>2</sub>, this process offers a sustainable and effective solution for remediating dye-contaminated wastewater streams.

## ACKNOWLEDGEMENT

*This work was supported by the Ministry of Science, Technological Development and Innovation of the Republic of Serbia (Contract No. 451-03-66/2024-03/200017, 451-03-66/2024-03/200023, 451-03-66/2024-03/200026, 451-03-65/2024-03/200135).*

## REFERENCES

- [1] Dodevski V., Kaluđerović B., Krstić S., *et al.*, J. Eng. Process. Manag. 8 (2017).
- [2] Sahoo C., Gupta A., Pal A., Dye. Pigment 66 (2005) 189–196.
- [3] Mani S., Bharagava R. N., Rev. Environ. Contam. Toxicol. 237 (2016) 71–104.
- [4] Au W., Pathak S., Collie C.J., *et al.*, Mutat. Res. Toxicol. 58 (1978) 269–276.
- [5] Dilaver M., Hocaoglu S.M., Soydemir G., *et al.*, J. Clean. Prod. 171 (2018) 220–233.
- [6] Madkhali N., Prasad C., Malkappa K., *et al.*, Results Eng. 17 (2023) 100920.
- [7] Rehman R., Tahir N., Samin G., *et al.*, J. Dispers. Sci. Technol. (2023) 1–10.
- [8] Šojić D.V., Orčić D.Z., Četojević-Simin D.D., *et al.*, J. Mol. Catal. A Chem. 392 (2014) 67–75.
- [9] Sugashini S., Gomathi T., Devi A.R., *et al.*, Environ. Res. 204 (2022) 112047.



## APPLICATION AND ENVIRONMENTAL SUITABILITY OF HYBRID GEOGRIDS

Milenko Jovanović<sup>1\*</sup>, Daniel Kržanović<sup>1</sup>, Emina Požega<sup>1</sup>, Vladan Marinković<sup>1</sup>,  
Miomir Mikić<sup>1</sup>

<sup>1</sup>Institute for Mining and Metallurgy Bor, Albert Ajnštajn 1, 19210 Bor, SERBIA

\*milenko.jovanovic@irmbor.co.rs

### Abstract

*Geogrids, with all their specificities and type of purpose, differ primarily in the type of material they are made of and the way they are made. There are geogrids that are made of synthetic materials, geogrids made of natural materials, and a hybrid type of geogrid, which combines the materials and characteristics of the first two types.*

*A special part of this scientific field that deals with the use of new materials, the possibility of combining them, the type of production and the value of use refers to geogrids and geotextiles made of combined building materials. This type of geogrid would be obtained by crossing bundles of natural materials (organic) and bundles of synthetic fibers (used in geosynthetics).*

*By combining these types (types of materials) of geogrids (and geotextiles) in the form of a kind of hybrid technology for the production of these products, we obtain useful parameters suitable in the field of environmental protection and the required mechanical and temporal usability.*

*In this paper, we will call such type of geogrids hybrid geogrids.*

*Seemingly contradictory requirements, by applying these “hybrid geomaterials”, can be effectively fulfilled.*

**Keywords:** geogrids, geotextile, geosynthetics, hybrid geogrids, hybrid materials and natural vegetation.

### INTRODUCTION

A special part of the field of application of geomaterials is represented by geogrids and geotextiles, made of organic material (from nature), which, with some variations in the use of construction material, is the main topic of this paper. Organic geogrids have unique characteristics consisting of biologically and chemically degradable natural fibers. They are designed to hold the soil in place until natural vegetation is established. On the other hand, geogrids and geotextiles made of synthetic materials have much greater strength, elasticity and durability [1–4].

Geogrids provide tensioning for: various types of landfills, foundations and foundations of railway lines and roads, steep sided earth embankments, earth reinforcement of earth embankments, transfer of loads on extreme mass terrain, arrangement of deep holes and areas of irregular profiles, covering of trenches and lathes, etc...

With their tensile strength, geogrids are suitable for many different demanding projects. This type of geo-grids are excellent reinforcement elements, as they withstand high tensile



loads with very little elongation. This results in immediate connection and coupling of the forces that the geogrid develops on the embankment without basic deformation.

The flat monolithic polymer sheets used to make geogrids are extremely strong and have excellent chemical resistance. Engineering solutions that include the use of geogrids can preserve natural mineral resources by reducing the thickness of the roadbed and the need for large amounts of soil to stabilize steep slopes.

Geogrids are relatively easy to manage, large quantities of this material can be installed quickly with minimal labor and lower installation costs. The geogrid can be installed in all weather conditions without demanding equipment or special construction techniques.

By crossing (combining) these types (materials) of geogrids (geotextiles) in the form of a certain hybrid technology for the production of these products, we obtain usable parameters suitable in the field of environmental protection and the necessary mechanical and temporal usability (durability).

These contradictory requirements, using hybrid geomaterials, can be effectively fulfilled [3,4].

## **TYPES OF GEOGRIDS**

### **Geogrids - materials, differences and types**

Geosynthetics are synthetic products used to stabilize terrain (Figure 1). They are mainly polymer products that are used to solve construction or mining problems (there are also various, other uses). These include eight main product categories: geotextiles, geogrids, geonets, geomembranes, geosynthetic clays, geofabric, geocells and geocomposites. The polymer nature of the products makes them suitable for use in the country where high levels of durability are required. They can also be used in exposed applications. Geosynthetics are available in a wide range of shapes and materials. These products have a wide range of applications and are currently used in many civil, geotechnical, transportation, geoenvironmental, hydraulic and private development applications, including roads, airports, railways, embankments, retaining structures, reservoirs, canals, dams, erosion control, landfills, landfills, mining and agriculture.



*Figure 1 Setting up the geogrid*

Geosynthetic products are usually divided according to the type and purpose, as well as the materials from which they are made. According to the type of product, geosynthetics are available in the form of: geogrid, geotextile, geomembranes, geocomb, geosynthetic clay and other types (type and subtype) of products.

The basic division that interests us here is, according to the material of manufacture, into synthetic and natural (organic).

In addition to stabilizing and strengthening weakly load-bearing soil, geogrids are also used to reinforce asphalt by placing them between layers of asphalt or between soil and asphalt. The geogrid absorbs the forces and prevents the creation of cracks on the newly laid asphalt layer. A third important purpose of geogrids is protection against soil erosion. For this purpose, there are two-dimensional geogrids that have small mesh openings and three-dimensional geogrids.

The use of anti-erosion geotextiles can increase and support the effect of erosion control in areas with particularly steep slopes or in substrates subject to erosion [1,3,5,7].

### **Organic geogrids**

Organic geogrids are more flexible than most types of synthetic geogrids. This allows them to easily follow the contour of the soil surface. The ability to make direct contact between the fibers and the soil and allow the bond between them to develop allows for a reduction in soil loss by 90% or more.

In addition to the above, organic geogrids act as "mulch" and thereby improve the establishment of vegetation. After degradation, they do not leave any toxic material.

Geo-grid made of jute - annual plant that requires a very warm climate and a lot of moisture. Jute material geogrids is used to cover slopes and protect against erosion (Figure 2). Jute yarn is thick with pronounced 3D characteristics and provides numerous obstacles, thus reducing the speed of water runoff. Jute netting stops movement of soil clearings. Jute netting has an excellent ability to shape and follow the contours of the soil on which it is placed. It absorbs water up to almost 4–5 times its dry weight, keeping water from rain and preventing soil separation. In wet conditions, its flexibility increases due to water absorption. Jute grids provides surface stability on steep slopes and slopes at an angle of about 45 degrees. When the vegetation starts to grow, it takes over the role of the jute net. It takes about 2 years for jute netting to biodegrade [4,6,7].

Coconut – Geogrids, geotextil, geocomposites, etc., made of organic material – coconut is a natural and 100% biodegradable solution for landslide control using a geomaterial base made of coconut fibers. The permeable geotextile provides a natural support system (improvement of characteristics) to the soil and vegetation. Coconut fiber is obtained from the husk of the coconut. They are naturally strong, durable and biodegradable.



*Figure 2 Geogrid made of jute*

Coconut fibers are very strong and form a very strong and durable network. The open weave allows seed and vegetation to be planted both before and after the mat is laid and offers strong support to the vegetation. The lifespan of a coir mat is four to six years. A period sufficient for consolidation by consolidation. After that time, the mat slowly biodegrades. This geogrid has high tensile strength (35 kN/m) and elasticity and can be installed even on very steep slopes of around 70 degrees. On steep slopes, which are more prone to erosion, an organic geogrid can be installed in combination with metal grids. Once vegetation is established, organic geogrids no longer serve as protection. The metal mesh remains permanently as active or passive tilt protection. The geogrid can be placed up to 60 degrees, with the support of a metal grid, while the coconut geogrid combined with metal can also be placed on vertical slopes [4,6,7].

#### *Synthetic geogrids*

The polymeric nature of geosynthetics makes them suitable for use in earth where high levels of durability are required.

Plastics represent a group of materials of organic origin that are made of a binder polymer component and various additives, such as: hardeners, plasticizers, stabilizers, pigments... For the strength and resistance of polymers, the molecular weight is the most important. As molecular weight increases, strength, elongation, impact resistance, thermal stability, tear resistance increase, and rheological properties and workability decrease. Thermoplastics are most often used for the production of geotextiles: polyethylene (PE), polypropylene (PP), polyester (PES) and polyamide (PA). Thermoplastics are used for the production of geomembranes: polyethylene (PE and HDPE), polypropylene (PP), polyvinyl chloride (PVC) and elastomers. Elastomeric geosynthetics include artificial rubber geomembranes. at the basis of its name. When talking about the durability or stability of geosynthetics in the long term, it should be taken into account that increasing the thickness of threads, fibers or products automatically increases resistance [2,3].

## MATERIALS AND MANUFACTURING OF GEOGRIDS

### Types of materials - fibers

#### *Primary fiber properties*

In order for the fibers to be further processed into more complex textiles (materials) and for the final products to meet their intended purpose, the fibers must meet certain requirements. Some characteristics reflect the behavior of fibers under the influence of external forces and influences. Mechanical properties (characteristics) describe the behavior of fibers under the influence of different types of forces and loads. In order to find out the strength of the fibers, the maximum force that the fiber can withstand is measured - breaking force [cN]. Different types of fibers vary significantly in strength. Table 1 shows the strength values of fibers - building material (geogrid) under normal conditions (environmental influence).

*Table 1 Fiber strength under normal conditions [3,7]*

<b>Fiber</b>	<b>Strength [cN/dtex]</b>	<b>Fiber</b>	<b>Strength [cN/dtex]</b>
Raw cotton	3.0–4.9	Viscose – standard type	0.7–3.2
Linen	2.6–7.7	Viscose – HWM type	2.5–5.0
Hemp	5.8–6.8	Polyester (PES)	4.6–9.5
Jute	3.0–5.8	Polyamide (PA)	2.5–8.3
Ramya	5.5	Acrylic (PAN)	2.0–4.5
Silk	2.4–5.1	Modacrylic (MAC)	2.5–3.5
Wool	1.0–1.7	Polypropylene (PP)	3.0–7.5

Physical properties represent the response of fibers to various external physical influences, such as the effect of heat, various types of radiation, atmosphere, etc. Another type of characteristics is related to the appearance of the fiber, its dimensions and surface characteristics. These properties are very specific to fibers - as a form of material, but also different and characteristic of certain types of fibers. The characteristics of this group are also important for workability and based on them numerous differences in the behavior of textile products in application arise. Behavior during the action of chemical agents is important for the implementation of various physicochemical processes, and resistance to certain chemicals is an important characteristic. It is usual for numerous characteristics of fibers, which depend on the possibility of their processing and suitability for a certain purpose, to be classified into two groups: primary and secondary properties [4,6,7].

#### *Origin of fibers*

According to the origin, all fibers can be classified into two groups - the group of natural and the group of artificial fibers. Within their group, natural fibers are divided according to the type of natural source in which the fiber is formed, and in the group of artificial fibers we distinguish fibers from organic polymers and fibers made from inorganic material. Organic polymer fibers are usually further classified according to the origin of the polymer, where it is important to distinguish man-made fibers from natural polymers and man-made fibers from synthetic polymers [4,7]:

- Natural fibers: - Plant fibers: fibers from seeds, fruits, bark and leaves; - animal: hair, wool and silk and - mineral: asbestos. The main component of plant fibers is cellulose;
- Artificial fibers: artificial silk: viscous copper nitrate and nitrate, copper, acetate; - cellulose wool and - protein fibers: animal and vegetable;
- Synthetic fibers: polymerization and polycondensation.

### **Application and durability of hybrid types of geogrids**

Surface erosion can cause damage and instability that can lead to failure/sliding of the landfill cover. Erosion can occur due to atmospheric and wind action. For situations where there is less risk of erosion, even the vegetative cover is sufficient in itself as protection. Geosynthetics can be used to support the development of vegetation of this type, in the form of synthetic or natural materials that are placed on or below the surface of (mining) waste disposal sites. The natural (organic) type of usable fiber allows for the planting of seeds and vegetation both before and after the installation of the geogrid and offers strong support to the vegetation.

Once vegetation is established, organic geogrids no longer serve as protection. This is where synthetic materials in geogrids come in, which significantly improve tensile strength and permanent active and passive protection - strengthening the slope of the landfill.

The lifetime of organic - plant fibers in the geogrid varies, mostly, in the range of 3–4 to 10 years. The lifespan of synthetic fibers is very long and generally exceeds 100 years.

To some extent, this makes a compromise, but very applicable (efficient) and environmentally friendly solution for the creation of protective geogrids (hybrid type of geomaterial) [4,6,7].

### **CONCLUSION**

Geosynthetics has proven to be the most effective material for wide application. Its building elements provide multi-purpose use in civil engineering, construction, mining and environmental protection.

Organic geogrids are a non-polluting biodegradable solution for erosion control using natural geomaterials. Hybrid type of geogrids provide a natural support system to soil and vegetation.

The installation of these efficient systems (geogrids, geotextiles, geomembranes...) in various branches of application in mining, construction and various types of industry, makes an inseparable connection with ecological parameters and their usefulness directly depends of the building materials used.

An acceptable solution for savings in cases where an efficient result is needed, both ecologically and in terms of safety, protection on the ground, is a hybrid approach to the use of geomaterials (geogrid, geotextile, etc.). By using different materials, by crossing organic and synthetic materials, in the production of geogrids or geotextiles, we can solve seemingly contradictory requirements in their application [4].

A special review is directed towards the use of new natural materials and the application of hybrid technology for the production of geomaterials.

## **ACKNOWLEDGMENT**

*This work is financially supported by the Ministry of Science, Technological Development and Innovation of the Republic of Serbia, agreement on the implementation and financing of scientific research work of the Institute of Mining and Metallurgy Bor in 2024, registration number 451-03-66/2024-03/200052.*

## **REFERENCES**

- [1] Bogićević Mladen (03.12.2008): “Civil Engineering”; Belgrade, Serbia.
- [2] Lukavečki Iva (2010/2011): “On geosynthetics and their application in landfill rehabilitation”; Final work; (p.1821).
- [3] Jovanović Milenko (June, 2019), Study research II (doctoral dissertation): “Geosynthetics - purpose and application (in mining)”; University of Belgrade, Technical Faculty in Bor.
- [4] Jovanović Milenko (July, 2019), Study research III (doctoral dissertation): “Organic geonetworks”; University of Belgrade, Faculty of Technology in Bor.
- [5] Nonweiler E. (1987): “Slope sliding and stabilization”; School book [Školska knjiga], Zagreb, (p.197–201) .
- [6] Veinović Ž. , Kvasnička P. (2007): “Surface landfills”; Internal script, Faculty of Mining, Geology and Petroleum, RGN University of Zagreb.
- [7] Web Material – Rejda: Coconut and jute grids, Slovenia; *Available on the following link:* <https://rejda.si/produkti/mreze-kokos-juta>.





## MODERN APPROACH TO SUPPLY CHAIN BASED ON CIRCULAR ECONOMY PRINCIPLES

Miroslav Drljača<sup>1\*</sup>

<sup>1</sup>University North, Trg dr. Žarka Dolinara 1, 48000 Koprivnica, CROATIA  
Zračna luka Zagreb d.o.o., Velika Gorica, CROATIA & Croatian Quality Managers Society,  
Cimermanova 36a, 10000 Zagreb, CROATIA

\*[mdrljaca@zagreb-airport.hr](mailto:mdrljaca@zagreb-airport.hr)

### Abstract

*The traditional approach to supply chains is based on the principles of linear economy and is depicted as a one-way flow of materials and information. Given the change in the global and European context and the need to contribute to mitigating the adverse effects of climate change, this approach to supply chains is not acceptable. All the more so as waste and harmful emissions into the environment occur at every stage of the supply chain and all logistics processes. For this reason, a modern approach to supply chains based on the principles of the circular economy is necessary. The scope of the paper is the process of transition from a traditional to a modern approach of supply chains based on the principles of circular economy. The author researches this complex process using the methods of scientific cognition. The result of this transition are supply chains that are based on: the feedback of materials and information, the principles of the circular economy and the life cycle of products, that contributes to sustainable development through continuous improvement of processes and products.*

**Keywords:** modern approach to the supply chain, circular economy, product life cycle.

### INTRODUCTION

The importance of the normal development of the supply chain (SC) is best understood in situations where circumstances occur that cause disruption or interruption in the development of the SC. There have been more such circumstances in recent times. The terrorist attack in New York in 2001, the emergence of the SARS disease, the war in Iraq in 2003, the economic crisis starts in 2008, the eruption of the Ejaflajökull volcano in Iceland, the corona virus pandemic (COVID-19) in 2019/2020 marked as a new respiratory disease [1,2]

The change of context in recent times was also influenced by other circumstances, which caused significant disruptions in the development of global SCs, namely the blockade of the Suez Canal due to the stranding of the ship Ever Given in 2021 [3] and the war in Ukraine, [4,5] the war in the Middle East that began in 2023, terrorist attacks on merchant ships in the Red Sea in 2024. The change in context caused a completely new view of the development of SCs, reversed processes in relation to the period 40 or 50 years ago, the need for a more flexible interpretation of some quality concepts. The changes are significant and have led to a new paradigm in the development of global SCs [6].

## **MATERIALS AND METHODS**

The scope of the paper is the process of transition from a traditional to a modern approach of SCs based on the principles of circular economy. The author researches this complex process using the methods of scientific cognition. In particular, this refers to the method of analysis when presenting the SC structure, the method of comparison when researching the differences between the traditional approach to SC based on the principles of the linear economy, on the one hand, and the modern approach to the SC based on the principles of the circular economy, on the other hand. The definition method was applied in detail in defining SC in accordance with international ISO norms, etc. The synthesis method was applied when formulating the final research results and drawing conclusions. The hypothesis with which the research was started reads: The transition from the traditional SC approach to the modern SC approach implies the application of the principles of the circular economy.

## **RESULTS AND DISCUSSION**

Definitions of SC are numerous. Only a few will be listed here. But, regardless of the nuances in the definitions of SC, it is evident that all the definitions contain common elements such as: 1) two or more organizations that are participants in SC, 2) linked set of resources, 3) raw material purchasing, production, storage, distribution, retail to the end users, 4) logistic processes, 5) sourcing of raw material and extends through the delivery of products to the end users, 6) modes of transportation.

### **Definition of supply chains**

According to ISO 28001:2007: “The SC is linked set of resources and processes that upon placement of a purchase order begins with the sourcing of raw material and extends through the manufacturing, processing, handling and delivery of goods and related services to the purchaser. The SC may include vendors, manufacturing facilities, logistics providers, internal distribution centers, distributors, wholesalers and other entities involved in the manufacturing, processing, handling and delivery of the goods and their related services” [7].

World ISO standards provide several more definitions of SC. According to ISO 22095:2020: “The SC is series of processes or activities involved in the production and distribution of a material or product through which it passes from the source. A SC is typically composed of a series of different organizations” [8].

Furthermore, ISO/PAS 5112:2022 states: “The SC is set of organizations with a linked set of resources and processes, each of which acts as a customer, supplier, or both to form successive supplier relationships established upon placement of a purchase order, agreement, or other formal sourcing agreement” [9].

“The SC is a system of organizations, people, activities, information and resources involved in transforming materials and knowledge in a product or a service for the customer”, according to ISO/TS 22163:2017 [10]. Furthermore, ISO 10377:2013 states: “SC is a network that designs, manufacturers, imports, distributes and sells a product” [11].

In some definitions of SC, logistics processes are explicitly mentioned. Thus ISO 13065:2015 stated: “The SC is a linked set of resources and processes that begins with the sourcing of raw material and extends through transport and storage of products to the end

user. The SC may include raw material producers, vendors, manufacturing facilities, logistics providers, internal distribution centers, distributors, wholesalers and other entities that lead to the end user” [12].

In some definitions of SC, transport is explicitly mentioned, such as in ISO 28002:2011: “The SC is a linked set of resources and processes that begins with the sourcing of raw material and extends through the delivery of products or services to the end user across the modes of transport” [13]. ISO 20333:2017 provides a definition that says: “The SC is a linked set of resources and processes that begins with the sourcing of raw material and extends through the delivery of products or services to the end user across the modes of transport” [14]. Finally, “The SC is a flow of goods, services and information from suppliers, through transportation, producers, distributors, and retailers to the final customer” [15].

Despite changes in the context and disruptions in SCs, customers, as well as other interested parties, find it difficult to give up their usual demands for the quality of products and services. This is a significant problem that many participants in SCs should try to solve. The normal development of SCs is important to maintain the balance between global supply and demand. If there is a significant disruption of this balance, numerous consequences arise for participants in the global economy, such as: 1) shortages of vital products, 2) strengthening of the black market, 3) rising prices, 4) crime, 5) conflicts, 6) in extreme cases wars, when it comes to strategic products like food, energy, medicines, etc.

### Traditional approach to supply chain

The traditional SC approach is characterized by the one-way movement of materials and products, from the procurement of raw materials and materials for production, production, storage, transportation, distribution to the final consumer. The vehicle transports the products from the manufacturing stock to the purchasing warehouse [15]. In the representation in Figure 1, in addition to the one-way movement of materials and products, there is also a one-way movement of information, from the end user, back to the suppliers of raw materials. Also in Figure 1, it is not visible that transport connects all phases of SC from beginning to end, and within the framework of the production phase and the storage phase, we can also talk about the so-called internal transport.

The following significant shortcoming of this presentation is the fact that it does not show the creation and management of waste, which is characteristic of all stages in SC, not only those used by the end user.

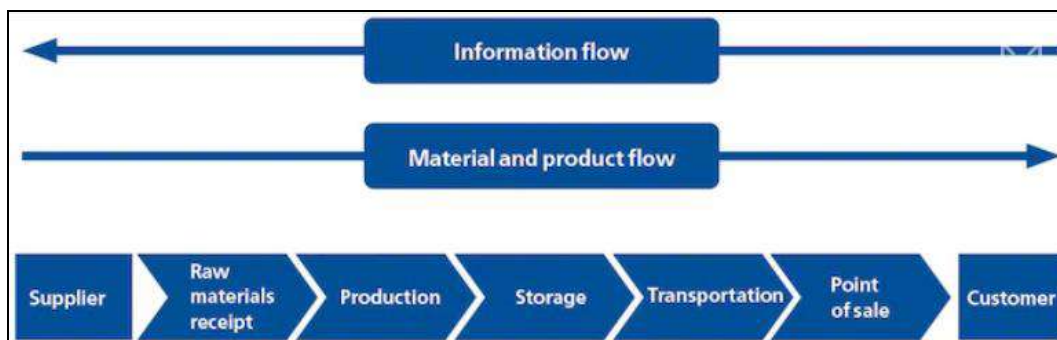


*Figure 1 Traditional approach to supply chain*

This representation of SC is based on a linear economy characterized by one-way movement of materials and information. The need and requirements of sustainable development are not taken into account. Such an approach is not sustainable in the modern economy, which, among other things, should be based on the principles of sustainability and social responsibility.

For this reason, the SC approach should undergo a radical transformation and transition and should take into account the principles of sustainable development and social responsibility, as well as the increasingly strong requirements and institutional framework that advocates for environmental protection.

### Modern approach to supply chain

“For a modern approach to the interpretation of SC, it is necessary to understand the need for the existence of a feedback. Namely, the traditional SC approach is characterized by one-way movement from raw materials, procurement of raw materials, production, storage and distribution to the end users. SC was considered to end with delivery to the end user. However, practice teaches that the modern SC approach also implies the existence of a feedback, because the consumption of the product by the end user creates waste. Also, waste is produced in all stages of SC, from the exploitation of raw materials to delivery to the end user. This waste must not be dumped into the environment, as has been the case throughout most of human history.

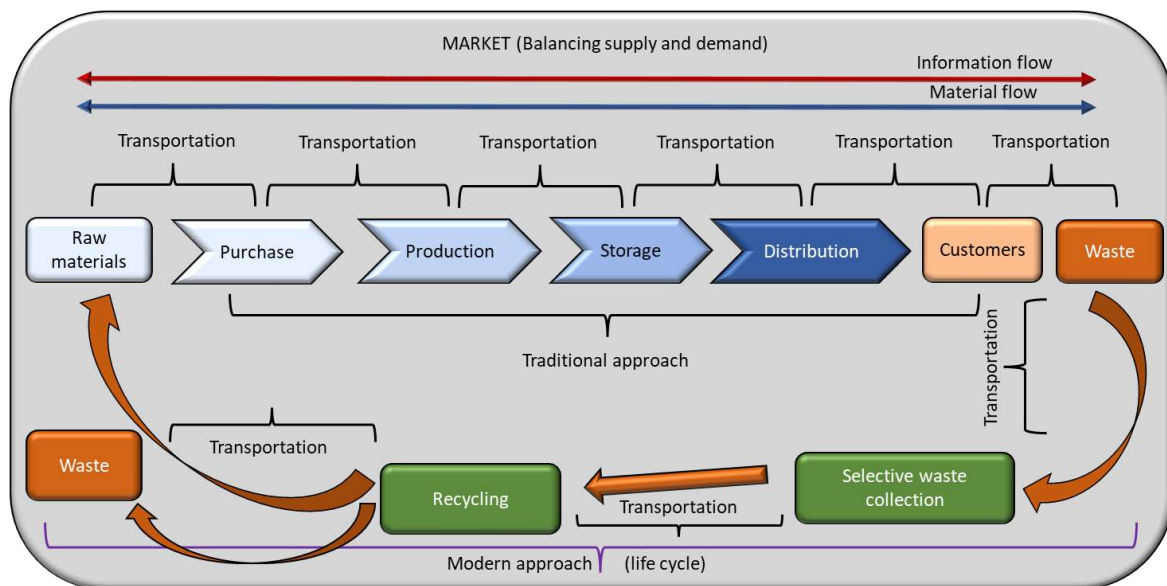


**Figure 2** Modern approach to supply chain

According to the principles of the circular economy, waste should be selectively collected, recycled and partially reused as raw material in a new production cycle. In this way, the need to exploit natural resources is reduced. Part of the waste that cannot be recycled for technological reasons must be permanently disposed of in a harmless manner, in accordance with the law” [16]. The modern approach to SC is shown in Figure 2.

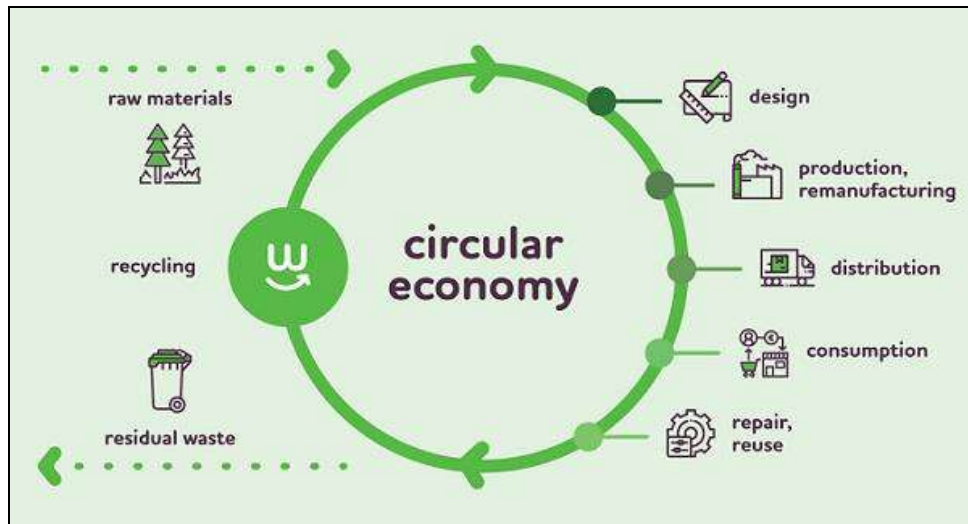


*Figure 2 Circular economy flow*

For the transition from a traditional to a modern SC approach, it is necessary to apply the principles of circular economy: 1) product designing without waste and pollution, as possible, 2) using products and materials in use as much as possible, 3) repair and reuse products and materials, 4) rational consumption of resources, 5) permanent disposal of material that cannot be recycled, in a legal and harmless way. Applying the principles of the circular economy in the development of SCs ensures: 1) feedback of materials, 2) feedback of information. The modern approach to SC is based on another important concept, which is to look at the product through its entire life cycle.

## CONCLUSION

The smooth running of the SC is important for the stability of the economy of the society at all levels: 1) the micro level of the organization, 2) the level of the national economy, 3) the global level. In everyday life, a numerous circumstances arise that change the context of the development of SC and may affect disruptions in the development of SC or their interruption, which will cause an imbalance between supply and demand occurs with all the negative consequences for the economy and consequently the quality of life of people. SC is a complex phenomenon, and it is not possible to understand it and manage it well if it is viewed as a one-way movement of materials and products, independent of the impact on the environment. For this reason, it is necessary to make a transition from the traditional SC approach to a modern SC approach, where it is necessary to apply the principles of the circular economy. For this complex process of transition to the SC approach, it is necessary to look at the product through its life cycle. Based on the research results presented in the paper, the hypothesis set at the beginning of the paper, can be accepted.

## REFERENCES

- [1] Ceylan R., Ozkan B., Mulazimogullari E., EJHE (21) (2020) 817–823.

- [2] Cleveland Clinic, Health essentials, *Available on the following link:* <https://health.clevelandclinic.org/heres-how-thecoronavirus-pandemic-has-changed-our-lives/>.
- [3] Blockage of the Suez Canal, Blockage of the Suez Canal, March 2021 | Port Economics, Management and Policy, *Available on the following link:* [porteconomicsmanagement.org](http://porteconomicsmanagement.org).
- [4] Gao Y., Feng Z., Zhang S. FEM (3) (2021) 465.
- [5] Bennett N., Lemoine G., What VUCA Really Means for You, Harvard Business Review. pdf. Harvard Business Review, *Available on the following link:* <https://hbr.org/2014/01/what-vuca-really-means-for-you>.
- [6] Drljača M., PEA (22) (2019) 30–35.
- [7] ISO 28001:2007 – Security management systems for the supply chain – Best practices for implementing supply chain security, assessments and plans – Requirements and guidance, Clause 3.24.
- [8] ISO 22095:2020 – Chain of custody – General terminology and models, Clause 3.2.1.
- [9] ISO/PAS 5112:2022 – Road vehicles – Guidelines for auditing cybersecurity engineering, Clause 3.4.
- [10] ISO/TS 22163:2017 – Railway applications – Quality management system – Business management system requirements for rail organizations: ISO 9001:2015 and particular requirements for application in the rail sector, Clause 3.1.41.
- [11] ISO 10377:2013 – Consumer product safety – Guidelines for suppliers.
- [12] ISO 13065:2015 – Sustainability criteria for bioenergy, Clause 3.47.
- [13] ISO 20333:2017 – Traditional Chinese medicine – Coding rules for Chinese medicines in supply chain management, Clause 3.2.
- [14] ISO 28002:2011 – Security management systems for the supply chain – Development of resilience in the supply chain – Requirements with guidance for use, Clause 3.64.
- [15] Sadv T. *et al.*, Sustainability 9(4) (2017) 561.
- [16] Drljača M., Sesar V. JP (74) (2023) 338–345.





## ASSESSMENT OF THE MUNICIPAL SOLID WASTE MANAGEMENT – CASE STUDY: NOVI SAD (SERBIA)

Isidora Berežni<sup>1\*</sup>, Tijana Marinković<sup>1</sup>, Nemanja Stanisavljević<sup>1</sup>, Marko Muhadinović<sup>2</sup>,  
Bojan Batinić<sup>1</sup>

<sup>1</sup>Department of Environmental Engineering, Faculty of Technical Sciences,  
University of Novi Sad, 21000 Novi Sad, SERBIA

<sup>2</sup>Lafarge BFC Srbija d.o.o. Beočin, Trg Beočinske fabrike cementa 1, 21300 Beočin, SERBIA

\*isidoraberezni@uns.ac.rs

### Abstract

*Municipal solid waste (MSW) management represent important environmental issue, especially in countries in transition and developing countries. While developed countries made progress and achieved good results with different MSW practices, countries in transition still struggle to be effective. The aim of this paper is to analyze and present the situation of MSW management in Serbia, with case study of Novi Sad, and to understand what weakness needs to be overcome as a prerequisite for improvement. The methodology integrates literature data with material flow analysis (MFA) to analyse and evaluate the current scenario. Additionally, recommendations for future actions to improve current waste management system in Novi Sad are discussed.*

**Keywords:** municipal solid waste, waste management, MFA, transition country.

### INTRODUCTION

The rapid expansion of urban areas, together with population growth and economic progress, has led to a significant increase in production of municipal solid waste (MSW). Currently, more than half of the global population lives in cities, contributing to the generation of approximately 2.01 billion tons of municipal waste in 2016, with projections suggesting a staggering 3.40 billion tons by 2050 [1].

The predominant method of MSW disposal remains landfilling, accounting for 37% of waste globally. Of this, 8% is directed to sanitary landfills equipped with gas collection systems. Open dumping constitutes approximately 33% of waste disposal, while 19% undergoes recycling and composting, and 11% is incinerated for final disposal [2]. The handling of MSW comes with environmental consequences, with an estimated 1.6 billion tonnes of carbon dioxide (CO<sub>2</sub>) equivalent greenhouse gas emissions attributed to solid waste treatment and disposal in 2016. These emissions, largely driven by open dumping and landfilling without gas capture systems; represent around 5% of global emissions. Without intervention, these emissions are forecasted to escalate to 2.6 billion tonnes of CO<sub>2</sub>-equivalent annually by 2050 [2].

Past research has pinpointed key factors influencing waste management systems. Hazra and Goel [3] highlighted issues like improper bin collection systems, aged vehicles, and inadequate infrastructure, which hinder collection and transport practices. Tadesse *et al.* [4]

found that limited waste containers and distant recycling bins contribute to open dumping. Conversely, Gonzalez-Torre and Adenso-Diaz [5] noted that proximity to recycling bins encourages household separation of waste fractions. Regulatory support, financial backing for recycling initiatives, and organizing the informal sector are factors that influence municipalities' recycling habits [6]. However, Burntley [7] has pointed out that municipalities often struggle with organizational, financial, and logistical challenges in implementing efficient waste management systems.

In countries transitioning, challenges persist due to outdated technologies, insufficient resources, and lax enforcement of regulations [8]. Support from local authorities, coupled with robust legal frameworks and strategic planning, as well as accurate waste management data, can enhance waste management systems [9].

## **MATERIALS AND METHODS**

The existing waste management system is described in terms of government laws and regulations, waste generation and composition, waste collection methods, and waste treatment and disposal. This is done through available research studies, reports, statistical data, legislation and other public documents. Additionally, material flow analysis (MFA) was used to model mass balance within MSW management systems in Nov Sad, where 2019 is taken as the reference year based on available data. The method used to estimate the uncertainty of the data is presented and modified by Lanner *et al.* [10] and based on the approach of Hedbrant and Sorne [11]. The data sources are divided into five levels of uncertainty and the corresponding coefficients are assigned variations. Coefficients of variation depend on the data source: 15% for data from national official statistics for the year for which the research is carried out, 30% for data from national official statistics with a deviation of 1–5 years from the selected year, 45% for data from scientific literature that are not related to observed country, 60% for information obtained from the plant operator and 75% for expert assessment.

## **RESULTS AND DISCUSSION**

### **Legal and institutional framework**

The EU directives provide a comprehensive framework for member states to implement measures promoting reuse, industrial symbiosis, and sustainable waste management practices. By defining targets and obligations, these directives guide Serbia and other EU candidate countries in achieving environmental sustainability and resource efficiency. Key provisions within the directives include the establishment of extended producer responsibility programs for packaging waste, limiting landfill disposal of municipal waste to 10% by 2035, and prioritizing waste prevention, particularly food waste reduction. Additionally, the directives emphasize the importance of improving the quality of secondary raw materials, separate collection of hazardous waste, and promoting reuse of construction and demolition waste [12].

In the Republic of Serbia, key regulations governing waste management include the Waste Management Program in the Republic of Serbia for the period of 2022–2031 (2022), The Law

on Waste Management (2018), the Decree on Waste Landfilling (2010), and the Law on Packaging and Packaging Waste (2018). Responsibilities in waste management are divided between the National and local self-government. While the Republic is tasked with legislative frameworks and fostering public awareness, local authorities oversee enforcement and provision of waste management conditions. However, municipalities often struggle due to financial constraints and regulatory inconsistencies [12].

The Law on Waste Management comprehensively covers waste types, classification, planning, responsibilities, permits, financing, and supervision. Municipalities must develop local and regional waste management plans to address their specific needs and objectives. For instance, within the Regional plan for Novi Sad, goals include establishing sanitary landfills, incinerating organic waste, treating hazardous waste, and promoting recycling. Supplementing the Law are decrees like the Decree on Waste Landfilling, which sets standards for landfill selection, operation, and waste acceptance. Despite alignment with EU directives, Serbia's targets for landfilling biodegradable waste are on a delayed timeline. The Law on Packaging and Packaging Waste introduces extended producer responsibility, aiming to reduce packaging waste and promote recyclable materials. Its enactment marks a significant step forward in modern waste management practices [12].

### **Waste generation and composition**

In Serbia, data on municipal waste are submitted by public utility companies or other companies that have a contract with the local self-government to perform these activities. In accordance with the Rulebook on the methodology for collecting data on composition and quantities municipal waste on the territory of the local self-government unit (Official Gazette of RS, No. 61/2010, 14/2020) local governments are obliged to perform quantity analyses four times a year and composition of municipal waste on its territory. In 2019 total amount of generated MSW in Serbia was 2.35 million tons with the average of 0.92 kg/inhab/day. Based on data provided by the companies responsible for waste collection in region of Novi Sad, amount of municipal solid waste that ended up at the landfill in 2019 was 198,035 tonnes, or 543 t/day. From this amount, 135,700 tonnes (372 t/day) were collected in the city of Novi Sad. Most of this waste is mixed municipal domestic and commercial waste, while smaller part makes waste from cleaning the public spaces and bulky waste [13].

The composition of household waste in the city of Novi Sad is given in Table 1.

*Table 1 Waste composition in Novi Sad*

<b>Waste component</b>	<b>Garden waste</b>	<b>Bio-degradable</b>	<b>Paper and cardboard</b>	<b>Glass</b>	<b>Metal</b>	<b>Plastic</b>	<b>Textile</b>	<b>Leather</b>	<b>Other</b>
(%)	12.14	37.62	11.47	5.44	1.38	12.73	5.25	0.4	13.57

Most of the generated waste in Novi Sad makes biodegradable (37.62%) followed by plastic (12.79%) and paper and cardboard (11.47%). High percentage of garden, as well as total biodegradable waste indicate the need to consider recovery options or treatments of that kind of waste to reduce the disposal of biodegradable waste in landfills. The relatively large amount, as well as the expected increase in waste production will have a negative impact.

## MSW collection system

The collection of MSW in Novi Sad is based on the collection of mixed waste. In the inner city core, where underground containers were implemented, a two-stream separation system was introduced (mixed recyclable and residual waste) (Figure 1).

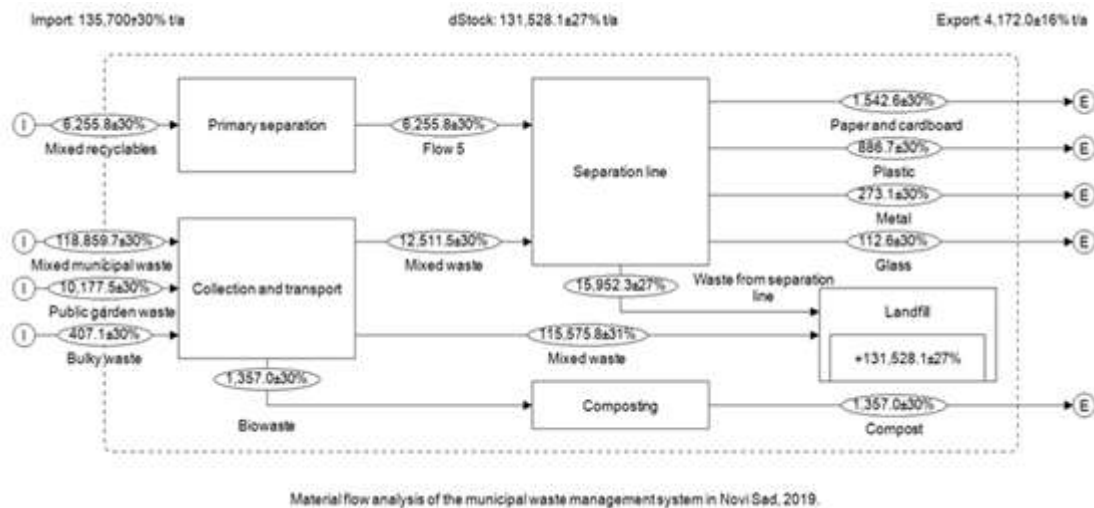


**Figure 1** MFA of the municipal waste management in Novi Sad, 2019

Collection is performed by a public municipal company (PUC) “Čistoća”. According to latest data, service coverage is 100% (the population covered by waste collection services is 341,625 and number of covered households is 128,876). For the collection of municipal waste, PUC “Čistoća” uses standard plastic bins with a volume of 120 l (51,176 pieces), containers with a volume of 10 m<sup>3</sup> (7 pieces), 5 m<sup>3</sup> (97 pieces), 1,100 m<sup>3</sup> (4,342 pieces), roll containers (17 pieces) and underground containers (882 pieces). Municipal waste in the territory of the City of Novi Sad is collected 7 days a week, in three shifts [13]. Although the current collection is mostly based on a collection of mixed waste, company in November 2016 implemented a pilot project for the introduction of primary waste separation for about 15,000 households. This is done in wider city centre and for this purpose 75 underground containers for collection of the dry recyclable fraction were installed. According to the data of PUC “Čistoća”, currently around 2,910 t of waste is collected annually through the primary separation system.

The fees that citizens pay for waste management are different between the municipalities and there is no uniform method for charging among the MSW collection companies. In Novi Sad, fee is defined by the number of inhabitants per household. For economic entities, payment is in most cases performed per square meter, and the fee can vary depending on the type of industry or business sector or based on the type of collection activities performed. According to available data, fee for each inhabitant is around 10 € per year, while for private business and industry fee varies from 40 € to 250 € per year. Data for Novi Sad shows that chargeability for households is around 85% and 70% for private business. This price primarily reflects the costs of waste collection and transport, while managing controlled waste landfill sites is usually financed by city governments or, less frequently, by municipal companies that

operate these disposal locations and even if chargeability were to increase to 100%, at current prices, the system would still be difficult to sustain.

### **Waste treatment and disposal**

All waste, except hazardous and industrial waste, collected on the territory of Novi Sad and surrounding settlements, except for waste that is separated at the separation plant, is disposed of in the city landfill. Next to the main landfill, there is about 20 illegal landfills located throughout the municipality. Many illegal landfills are a consequence of a lower degree of coverage by waste collection services in the previous period but to a greater extent due to human negligence and poor work of inspection services. Although small illegal landfills are regularly removed, municipalities often missing funds for the removal of larger landfills located in suburban settlements. Also, individuals often use illegal landfills to dispose of bulky, construction and other types of waste.

Other treatments of municipal solid waste are not widely implemented. For instance, incineration of municipal solid waste is carried out in cement kilns, but only on a negligible scale. Other waste management options, such as biological treatments, are primarily applied only on a household level (e.g., home composting) and mostly in rural areas [12].

According to the Regional waste management plan for the city of Novi Sad and the surrounding municipalities, it is predicted that by 2026, a Regional center for waste management will operate at the site of the current landfill. According to this plan, three recycling yards will be built in the Novi Sad, two transfer stations in the municipalities of Bačka Palanka and Vrbas, while the regional landfill itself, in addition to the line for secondary separation of waste and composting site for green waste, will also have mechanical-biological treatment and bio drying, as well as a recycling yard for construction waste.

### **CONCLUSION**

Based on the analysis of the systems, certain measures can be proposed for further improvement:

- Analyse current waste management plans and make changes if necessary. Plans should be made in accordance with the quantities and characteristics of the waste being managed, therefore it is necessary to establish a system for regular and transparent data collection. Also, the plan should include all participants in the waste management system, from public companies to operators dealing with recycling and collection, so that mutual cooperation can be established and common goals can be met;

- Improve the model of calculation of fees for services in the MSWM in the direction of transparent and realistic models based on responsibility and respect for the “polluter pays” principle. Within this, it is important to educate citizens about the health hazards and environmental risks of inadequate management of municipal waste, in order to motivate them to pay fees for MSWM services;

- With the participation of all stakeholders at the local self-government level, work on strengthening the implementation of alternative solutions for waste management, primarily aimed at its reduction, repurposing and reuse of resources and materials;

- Continuously carry out information and education at all levels about proper MSWM through interactive workshops, seminars, expert meetings and another. Also provide the public with constantly available information about waste flows, methods of treatment and disposal, which they can access at any time.

## **REFERENCES**

- [1] World Bank, 2018, Solid Waste Management (published on 20<sup>th</sup> Sept 2018). [www.worldbank.org/en/topic/urbandevelopment/brief/solid-waste-management](http://www.worldbank.org/en/topic/urbandevelopment/brief/solid-waste-management) (Accessed on 10<sup>th</sup> Apr 2024).
- [2] Kaza S., Yao L.C., Bhada-Tata P., Van Woerden F., What a Waste 2.0: A Global Snapshot of Solid Waste Management to 2050; 2018, Urban Development, World Bank, Washington, DC. Available on the following link: <https://openknowledge.worldbank.org/handle/10986/30317> (Accessed on 10<sup>th</sup> Apr 2024).
- [3] Hazra T., Goel S., J. Waste Manag. 29 (2009) 470–478.
- [4] Tadesse T., Ruijs A., Hagos F., J. Waste Manag. 28 (2008) 2003–2012.
- [5] Gonzalez-Torre P.L., Adenso-Diaz., J. Waste Manag. 25 (2005) 15–23.
- [6] Sharholly M., Ahmad K., Vaishya R.C., Gupta R.D., J. Waste Manag. 27 (2007) 490–496.
- [7] Burntley S.J., J. Waste Manag. 27 (10) (2007) 1274–1285.
- [8] Chen X.D., Geng Y., Fujita T., J. Waste Manag. 30 (4) (2010) 716–724.
- [9] Asase M., Yanful E.K., Mensah M., *et al.*, J. Waste Manag. 29 (2009) 2779–2786
- [10] Laner D., Rechberger H., Astrup F.T., J. Ind. Ecol. 19 (6) (2015) 1055–1069.
- [11] Hedbrant J., Sörme L., Water Air Soil Pollut. 1 (3) (2001) 43–53.
- [12] Vujić G., Stanisavljevic N., Batinić B., *et al.*, J. Mater. Cycles Waste Manag. 19 (2015) 55–69.
- [13] Draft of the Regional waste management plan for The city of Novi Sad and the municipalities of Bačka Palanka, Backi Petrovac, Beocin, Žabalj, Srbobran, Temerin and Vrbas for the period 2019–2028. Available on the following link: <https://skupstina.novisad.rs/wp-content/uploads/2020/07/sl-29-2020.pdf> (Accessed on 10<sup>th</sup> Apr 2024).





## CALCULATION OF THERMODYNAMIC PROPERTIES Al-Ga-Sn TERNARY ALLOY USING GENERAL SOLUTION MODEL

Ljubiša Balanović<sup>1\*</sup>, Dragan Manasijević<sup>1</sup>, Ivana Marković<sup>1</sup>, Uroš Stamenković<sup>1</sup>,  
Kristina Božinović<sup>1</sup>

<sup>1</sup>University of Belgrade, Technical Faculty in Bor, V.J. 12, 19210 Bor, SERBIA

\*ljbalanovic@tfbor.bg.ac.rs

### Abstract

*The paper presents the calculated results of the thermodynamic properties of Al-Ga-Sn liquid alloys using the General Solution Model – GSM. The calculations were conducted in nine cross-sections from all three corners within the temperature range of 800–1600 K. Integral molar excess Gibbs energies, partial molar Gibbs energies, activity coefficients, and activities for all components were determined. The activities of Al and Sn deviate negatively from Raoult's law in all investigated sections. In contrast, the activity of Ga is close to ideal conditions and even coincides with the line for high Ga content in the alloy. The predicted values are compared with the experimental data found in the literature. The results indicate that the model is reliable as well as convenient.*

**Keywords:** GSM, Al-Ga-Sn alloys, thermodynamic properties, activity.

### INTRODUCTION

Due to its adverse effects on human health and the environment, the use of lead in solders was banned in Europe by July 2006 when the RoHS directive was adopted [1–4]. Consequently, extensive research is underway to identify suitable lead-free solder alternatives [5–14].

The miniaturization of electronic devices, along with the transition to lead-free RoHS standards, is a challenge due to the higher temperatures of the reflow process, which can damage printed circuit boards and components [1,15]. Low-temperature solders are advantageous because they reduce thermal damage [6,10,16]. Defects such as delamination or “pop-corning” in moisture-sensitive devices can be minimized using solders with lower melting temperatures [8,12]. The search for lead-free solder alternatives has led to various alloys with properties comparable to traditional lead-based solders. Tin-based alloys, such as tin-silver-copper (Sn-Ag-Cu) and tin-silver (Sn-Ag), have emerged as popular choices for lead-free solder due to their desirable mechanical and thermal properties. Tin melts at 232°C, and alloying elements such as Ga, In, and Bi can lower this temperature. Tin is the primary component in mostly new solder alloys, with Ag, Cu, Ga, In, Zn, Bi, and Al, given its widespread use in electronic equipment soldering [10,12,15,17–20]. Established tin-based solder alloys such as SAC305, SAC387, SAC405, and Sn0.7Cu have gained recognition in the electronic industry because of their favorable mechanical and thermal properties, positioning them as viable alternatives to lead-based solders [10,12,16]. These alloys exhibit good solderability, thermal conductivity, and reliability, making them suitable for the

demanding requirements of semiconductor manufacturing. In addition to these formulations, ternary alloys such as Al-Sn-Zn [21–23] and Ag-Sn-Zn [21,24–27] show promising characteristics for soldering applications. Additionally, Al-Ga-Sn alloys have emerged as another area of interest, demonstrating the potential to enhance soldering performance and address environmental concerns.

A systematic exploration of new solder materials requires understanding phase diagrams, phase equilibria, and melting behaviors. Thermodynamic calculations and modelling are essential for determining a coherent dataset and predicting thermodynamic behavior [11,12,14,17–19,28].

Integral molar excess Gibbs energies, partial molar Gibbs energies, activity coefficients, and activities are essential for predicting the behavior of solder materials during manufacturing and throughout their service life. This knowledge aids in developing more reliable and environmentally friendly soldering solutions for modern electronics [10,12,15,17–20]. Numerous methods enable the calculation of the thermodynamic properties of a ternary system based on the known thermodynamic properties of the constituent binary systems. The GSM [29–31] has proven to be the most efficient among the existing models. Therefore, this model was utilized to calculate the thermodynamic properties of the investigated ternary systems. In this study, the calculation of thermodynamic properties of Al-Ga-Sn ternary alloy using a GSM is compared with the experimental data [14].

## THEORETICAL BASIS

Chou's GSM [29–31] is considered the most reasonable method for calculating the thermodynamic properties of a ternary system using information about the constituent binary systems. It overcomes the inherent defects of traditional symmetrical and asymmetrical geometric models in all aspects. This model has already been proven in practical examples [32–35] to be correct and accurate, making it suitable for this type of calculation. Therefore, this General Solution Model - GSM version is used to calculate the thermodynamic properties of the Al-Ga-Sn ternary system. The basic equation of GSM for the ternary system is:

$$\Delta G^E = x_1 x_2 \Delta G_{12}^E + x_2 x_3 \Delta G_{23}^E + x_1 x_3 \Delta G_{31}^E + x_1 x_2 x_3 f_{123} \quad (1)$$

$$\Delta G_{ij}^E = x_i x_j (A_{ij}^0 + A_{ij}^1 (x_i - x_j) + A_{ij}^2 (x_i + x_j)^2 + \dots + A_{ij}^n (x_i - x_j)^n) \quad (2)$$

where  $A_{ij}^0$ ,  $A_{ij}^1$ , and  $A_{ij}^2$  are parameters of two-component systems “ $ij$ ” (the Redlich-Kister parameters), which can depend on temperature.  $x_i$  and  $x_j$  are the mole fractions of components “ $i$ ” and “ $j$ ” in “ $ij$ ” binary system.  $f_{123}$  is the three-component interaction coefficient expressed as:

$$\begin{aligned} f_{123} = & (2\xi_{12} - 1) \{ A_{12}^2 ((2\xi_{12} - 1)x_3 + 2(x_1 - x_2)) + A_{12}^1 \} + \\ & + (2\xi_{23} - 1) \{ A_{23}^2 ((2\xi_{23} - 1)x_1 + 2(x_2 - x_3)) + A_{23}^1 \} + \\ & + (2\xi_{31} - 1) \{ A_{31}^2 ((2\xi_{31} - 1)x_2 + 2(x_3 - x_1)) + A_{31}^1 \} \end{aligned} \quad (3)$$

$\xi_{ij}$  are the similarity coefficients defined by  $\eta_i$  (deviation of the sum of squares):

$$\xi_{ij} = \eta_i / (\eta_i + \eta_j) \quad (4)$$

$$\xi_{12} = \eta_I / (\eta_I + \eta_{II}); \quad \xi_{23} = \eta_{II} / (\eta_{II} + \eta_{III}); \quad \xi_{31} = \eta_{III} / (\eta_I + \eta_{III}); \quad (5)$$

where are:

$$\eta_I = \int_0^1 (\Delta G_{12}^E - \Delta G_{13}^E)^2 dX_1; \quad \eta_{II} = \int_0^1 (\Delta G_{21}^E - \Delta G_{23}^E)^2 dX_2; \quad \eta_{III} = \int_0^1 (\Delta G_{31}^E - \Delta G_{32}^E)^2 dX_3 \quad (6)$$

$\Delta G^E$  is integral molar excess Gibbs energy for the ternary system, and  $x_i$  is mole fraction of the component  $i$ . Number  $n$  equals the maximum number of components in the system, and coefficients  $i, j$ , and  $k$  are always numbers between zero and  $n$ .

Partial thermodynamic quantities are calculated according to the equations:

$$G_i^E = G^E + (1 - x_i) \left( \partial G^E / \partial x_i \right) = RT \ln \gamma_i \quad (7)$$

$$a_i = x_i \gamma_i \quad (8)$$

where  $G_i^E$  is partial molar excess Gibbs energy,  $a_i$  is the activity of component  $i$ ,  $\gamma_i$  is the activity coefficient of component  $i$ ,  $T$  is temperature,  $R$  is gas constant ( $8.314 \text{ J K}^{-1} \text{ mol}^{-1}$ ), and  $G^E$  is Gibbs energy for the whole system, dependent on composition. Integral molar excess Gibbs energy ( $\Delta G^E$ ) corresponds to the whole system, while partial molar excess Gibbs energy ( $G_i^E$ ) corresponds to the individual component.

## RESULTS AND DISCUSSION

### Calculation of thermodynamic properties by GSM

Table 1 presents the thermodynamic data for the constituent binary subsystems of Al-Ga [36], Al-Sn [37], and Ga-Sn [38] needed for the calculation of thermodynamic properties in the investigated Al-Ga-Sn system.

**Table 1** Redlich-Kister parameters for constitutive binary systems

System $ij$	$A^0_{ij}(T)^*$			$A^1_{ij}(T)^*$			$A^2_{ij}(T)^*$			Ref.
	A	B	C	A	B	C	A	B	C	
Al-Ga	2613.3	-	/	692.4	-	/	319.5	/	/	[36]
Al-Sn	16329.85	-	/	4111.97	-	/	1765.43	-	/	[37]
Ga-Sn	3369.7	0.03854	/	528.9	-0.1145	/	/	/	/	[38]

\*  $L=A+B \cdot T+C \cdot T \cdot \ln T$

The thermodynamic properties of the ternary Al-Ga-Sn system were investigated in nine sections, taken from the Al, Ga, and Sn corners, respectively, with mole ratios of 1:3, 1:1, and 3:1, with molar content ranging from 0 to 0.9 for the third component. The calculated integral molar Gibbs excess energies ( $\Delta G^E$ ) and activities ( $a_i$ ) of the investigated system Al-Ga-Sn, along selected sections and at given temperatures, are presented in Figure 1 and 2.

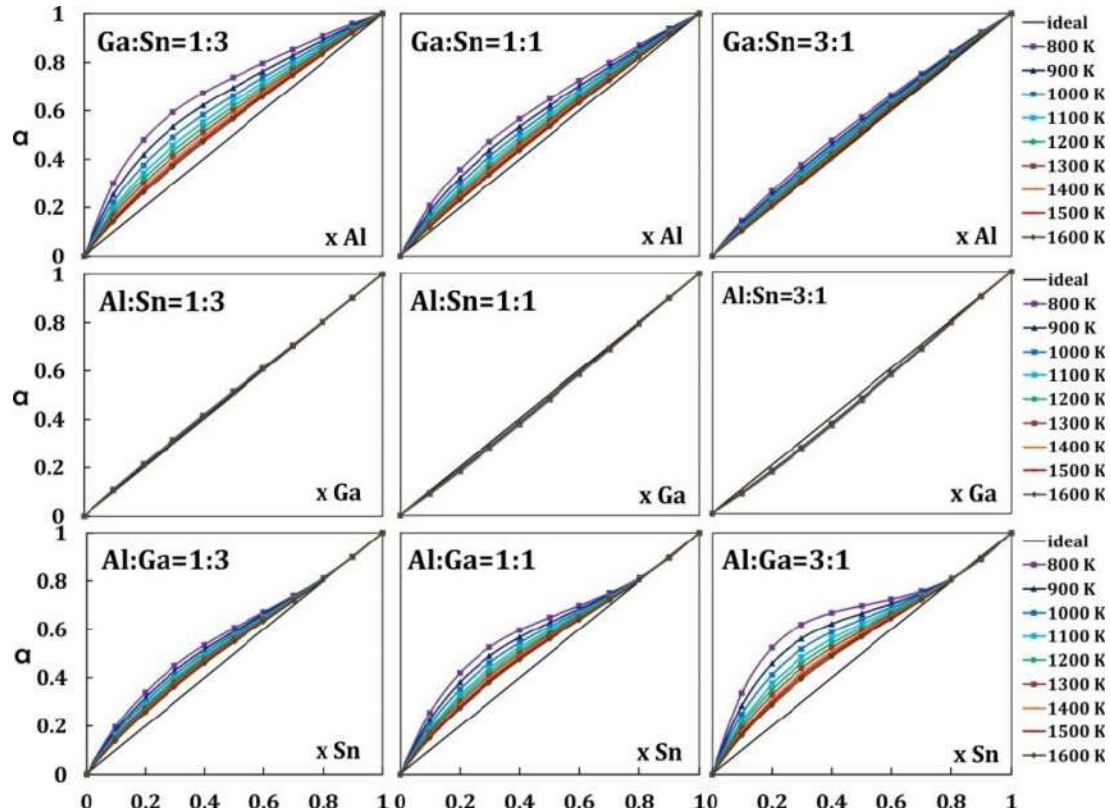


**Figure 1** Activity of Al, Ga, and Sn in the Al-Ga-Sn system by GSM in the temperature range of 800–1600 K for cross sections from Al, Ga, and Sn corner

All thermodynamic properties calculated in this work are related to the liquid phase. The values for the activity of aluminum and tin in the temperature range of 800–1600 K (Figure 1) for all examined sections, obtained through thermodynamic prediction by the GSM, exhibit a positive deviation from Raoult's law. As the gallium content increases, the deviation from the line of ideal behavior decreases. The activity of gallium aligns with the line of ideal behavior. The integral molar excess Gibbs energy values for the ternary system Al-Ga-Sn in the temperature range of 800–1600 K (Figure 2) for all examined sections range from 0 to 3 kJ/mol.

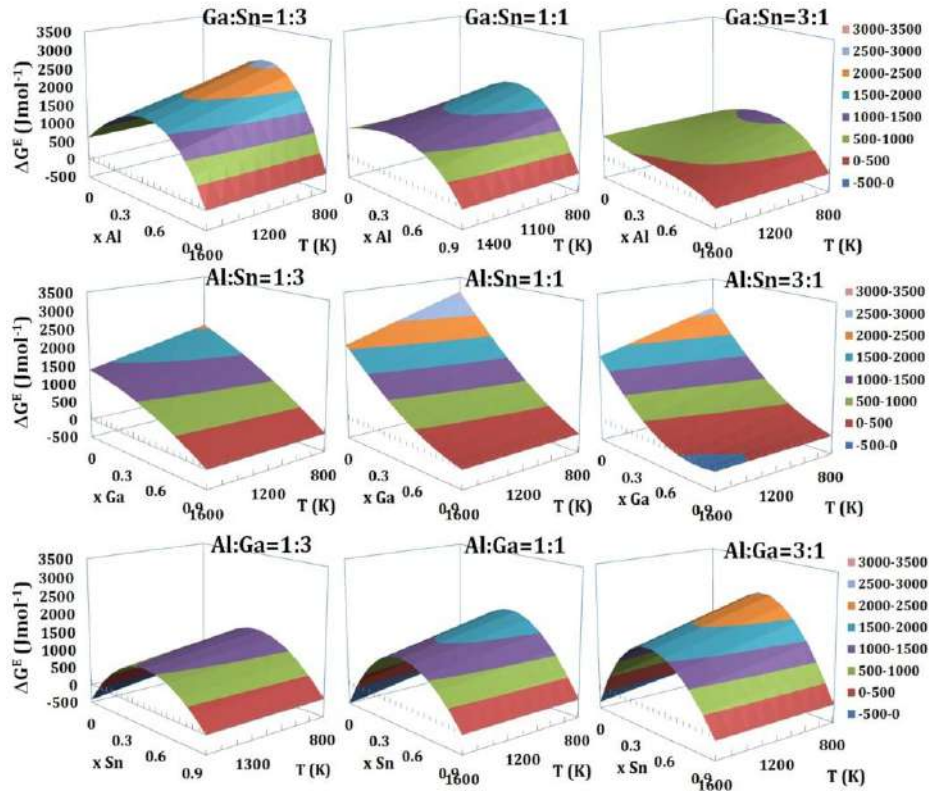


**Figure 2** Integral molar excess Gibbs energy in the AlGa-Sn system according to GSM in the temperature range of 800–1600 K for cross sections from Al, Ga, and Sn corner

The values for gallium activity in the three-component Al-Ga-Sn system at 800, 900, and 1000 K, obtained by the GSM, were compared with experimentally determined values using Oelsen calorimetry and using two other different prediction methods – model Muggianu [39], and model Toop [40], available in Balanović [14]. Comparison shows good agreement, where experimental values for gallium activity show a more negative trend at all temperatures compared to activities obtained by prediction (Figure 3, Figure 4).

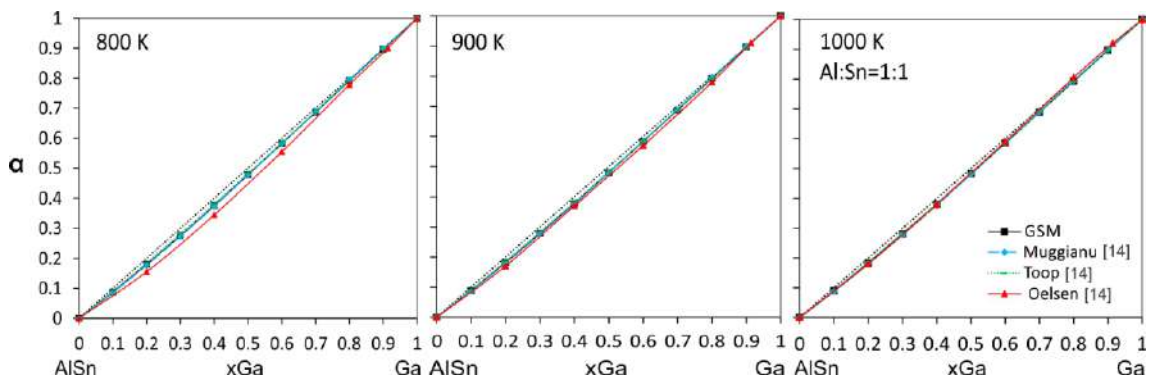


**Figure 3** Activity dependences of gallium in Al-Sn-Ga section at 800, 900, and 1000 K obtained by GSM and experimentally determined by Oelsen calorimetry and other prediction methods [14]



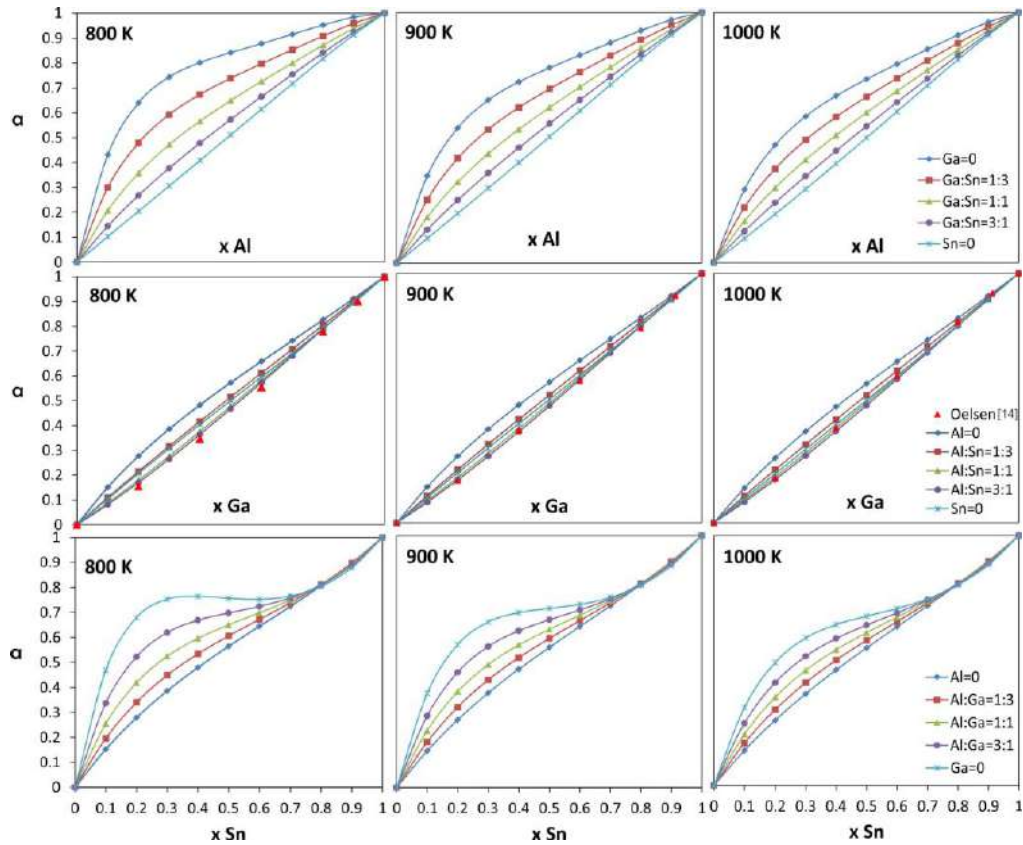


**Figure 4** Dependence of component activity on composition for characteristic sections at 800, 900, and 1000 K from Al, Ga, and Sn corner calculated by GSM and comparison with the results of Oelsen's calorimetry [14]

The iso-activity lines of aluminum, gallium, and tin in the Al-Ga-Sn system at 1000 K (Figure 5), obtained by thermodynamic prediction according to the general solution model, were compared with the activity values of gallium obtained experimentally using Oelsen's calorimetry [14]. Agreement between experimentally obtained and thermodynamically predicted values for gallium activity was observed.

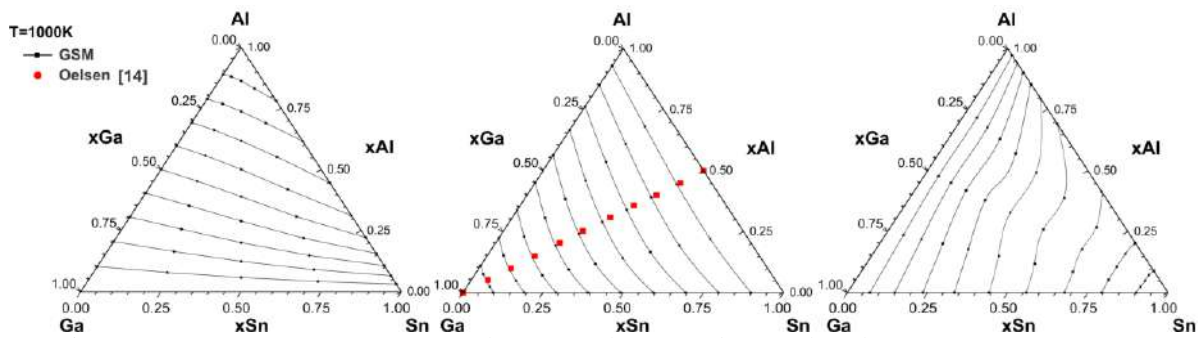


**Figure 5** Comparison of iso-activity lines for Al, Ga, and Sn in the Al-Ga-Sn system at 1000 K determined using GSM with Ga activities obtained by Oelsen calorimetry [14]



## CONCLUSION

The Al-Ga-Sn system's thermodynamic properties were calculated using the GSM in the temperature interval from 800 to 1600 K. Based on this, all components' excess molar Gibbs energies and activities were calculated. The calculated excess integral Gibbs energies for investigated sections are positive, with values up to 3 kJ/mol. The activity of aluminum and tin shows a positive deviation from Raoult's law for all investigated sections. Still, deviation aligns with the line of ideal behavior for alloys with a high gallium content. Gallium activity is close to the line of ideal conditions and coincides with the line for high content of gallium in the alloy. The presented thermodynamic data for the Al-Ga-Sn alloys could be helpful for the further assessment of this system and its phase diagram, as well as for completing the thermodynamic description of these alloys.

## ACKNOWLEDGEMENT

*The authors are grateful to the Ministry of Science, Technological Development and Innovation of the Republic of Serbia for financial support according to the contract with the registration number (e.g., 451-03-65/2024-03/200131).*

## REFERENCES

- [1] Directive 2002/95/EC of the European Parliament and of the council on the restriction of the use of certain hazardous substances in electrical and electronic equipment (RoHS), OJEU. L 37 (2003) 19–23.
- [2] Puttlitz K., Galyon G., *J. Mater. Sci. Mater. Electron.* 18 (1) (2007) 347–365.
- [3] Puttlitz K., Galyon G., *J. Mater. Sci. Mater. Electron.* 18 (1) (2007) 331–346.
- [4] Menon S., George E., Osterman M., *et al.*, *J. Mater. Sci. Mater. Electron.* 26 (6) (2015) 4021–4030.
- [5] Živković D., Mitovski A., Novaković S., *et al.*, *Prakt Metallogr-Pr M.* 50 (3) (2013) 177–195.
- [6] Zeng G., McDonald S., Nogita K., *Microelectron Reliab.* 52(7) (2012) 1306–1322.
- [7] Kroupa A., Dinsdale A.T., Watson A., *et al.*, *J Min Metall B.* 43(2) (2007) 113–123.
- [8] Suganuma K., *Curr. Opin. Solid State Mater. Sci.* 5(1) (2001) 55–64.
- [9] Homma H., Yamamoto K., Kitajima M., *et al.*, *Proceedings of the 38<sup>th</sup> International Symposium on Microelectronics*, 25–29 September 2005, Philadelphia, PA (2005) 433–440.
- [10] Cheng S., Huang C.M., Pecht M., *Microelectron Reliab.* 75 (2017) 77–95.
- [11] Kroupa A., Dinsdale A., Watson A., *et al.*, *J. Min. Metall. B.* 48 (3) (2012) 339–346.
- [12] Arfaei B., *JOM* 66(11) (2014) 2309–2310.
- [13] Kotadia H.R., Howes P.D., Mannan S.H., *Microelectron Reliab.* 54(6–7) (2014) 1253–1273.

- [14] Balanović Lj.T., Doctoral Dissertation: Comparative thermodynamic analysis and characterization of alloys in Ga-Zn-Me (Me=Al, Sn) system, University of Belgrade, Technical Faculty Bor, 2013.
- [15] Abteu M., Selvaduray G., *Mater. Sci. Eng. R Rep.* 27(5) (2000) 95–141.
- [16] Zhang L., Han J.G., He C.W., *et al.*, *J. Mater. Sci. Mater. Electron.* 24(1) (2013) 172–190.
- [17] Dinsdale A.T., Kroupa A., Vízdal J., *et al.*, COST531 – Database for Lead-free Solders, 2.1 ver., 2007.
- [18] Dinsdale A.T., Watson A., Kroupa A., *et al.*, COST 531, Lead Free Solders – Atlas of Phase Diagrams for Lead-free Solders (2008).
- [19] Kroupa A., Dinsdale A.T., Watson A., *et al.*, *JOM.* 59(7) (2007) 20–25.
- [20] McCormack M., Jin S., *J. Electron.* 23(7) (1994) 635–640.
- [21] Mikula A., Proceedings of the Yazawa International Symposium: Metallurgical and Materials Processing: Principles and Technologies; Materials Processing Fundamentals and New Technologies, March 2–6, San Diego, CA (2003) 395–403.
- [22] Prasad L.C., Mikula A., *Physica B Condens. Matter.* 373(1) (2006) 64–71.
- [23] Knott S., Mikula A., *Mater. Trans. JIM.* 43(8) (2002) 1868–1872.
- [24] Karlhuber S., Komarek K.L., Mikula A., *Z. Met.kd.* 85(5) (1994) 307–311.
- [25] Peng M., Qiao Z., Mikula A., *Calphad.* 22(4) (1998) 459–468.
- [26] Knott S., Mikula A., Proceedings of the Yazawa International Symposium: Metallurgical and Materials Processing: Principles and Technologies; Materials Processing Fundamentals and New Technologies, March 2–6, San Diego, CA (2003) 441–449.
- [27] Knott S., Flandorfer H., Mikula A., *Z. Met.kd.* 96(1) (2005) 38–44.
- [28] Chidambaram V., Hald J., Hattel J., *Arch. Metall. Mater.* 53(4) (2008) 1111–1118.
- [29] Chou K.C., *Calphad.* 19(3) (1995) 315–325.
- [30] Chou K.C., Li W.C., Li F., *et al.*, *Calphad.* 20(4) (1996) 395–406.
- [31] Zhang G.H., Chou K.C., *J Solution Chem.* 39(8) (2010) 1200–1212.
- [32] Gomidželović L., Živković D., *J Therm Anal Calorim.* 98(3) (2009) 743–748.
- [33] Gomidzelovic L., Zivkovic D., Mihajlovic I., *et al.*, *Arch. Metall. Mater.* 51(3) (2006) 355–364.
- [34] Gandova V., Vassilev G., *J Min Metall B.* 49(3) (2013) 347–352.
- [35] L., Zivkovic D., Balanovic L., *et al.*, *Rare Met.* (2015) 262–268.
- [36] Watson A., *Calphad.* 16(2) (1992) 207–217.
- [37] Fries S.G., Lukas H.L., Kuang S., *et al.*, Proceedings of the International Conference, 25–27 June 1990, Petten, Netherlands (1990) 280–286.
- [38] Anderson T.J., Ansara I., *J. Phase Equilibria.* 13(2) (1992) 181–189.
- [39] Muggianu Y.M., Gambino M., Bros J.P., *J. Chim. Phys.* 72(1) (1975) 83–88.
- [40] Toop G.W., *Trans. Am. Inst. Min. Eng.* 233(5) (1965) 850–855.



## LIFE CYCLE ASSESMENT OF THE HAIR DRYER WITH ECO-it SOFTWARE

Danijela Nikolić<sup>1\*</sup>, Saša Jovanović<sup>1</sup>, Dajana Mikić<sup>1</sup>, Zorica Đorđević<sup>1</sup>

<sup>1</sup>University of Kragujevac, Faculty of Engineering, Sestre Janjić 6, 34000 Kragujevac,  
SERBIA

\*danijela1.nikolic@gmail.com

### Abstract

*The key step towards achieving sustainable development is the assessment of the impact on the environment due to the consumption of goods and services. Life Cycle Assessment (LCA) is a process of collecting and evaluating data on inputs, outputs, and possible impacts of a product system on the environment, throughout its entire life cycle. Household appliances play an important role and should be thoroughly assessed, i.e. all phases of the life cycle should be taken into account. This paper presents the assessment of the hair dryer's environmental impact using the Eco-it software and the potential reduction of the environmental impact at different scales. With LCA analysis and Eco-it software, it will be presented the technical evaluation of the product, as well as its redesign, due to better performance and decreasing environmental impact.*

**Keywords:** Life Cycle Assessment, hair dryer, ECO-it software, environmental impact.

### INTRODUCTION

Since the middle of the last century, there has been constant population growth in the world, and therefore the need for material resources is increasing. The industrial way of production became necessary, and the improvement of living standards came about due to the availability of natural resources, along with the development of technology [1]. Traditionally, products were designed and developed without considering their harmful impact on the environment. Conventional regulation focuses only on the emissions from the manufacturing processes. However, harmful impacts on the environment occur from the other life cycle stages such as use, disposal, distribution, and raw material acquisition [2].

In recent decades, many corporations recognized the importance of the product's environmental impacts and began to include environmental aspects in product design and development processes. This includes the activities, processes, and materials starting from raw materials acquisition, manufacturing, distribution, use, and to disposal, i.e. during the entire life cycle. Thus, there was a need for systematic analytical tool for the product environmental assessment during the entire life cycle. This tool is a Life Cycle Assessment, which is a quantitative analysis of the environmental aspects of a product over its entire life cycle. It offers a “cradle to grave” look at a product or process, considering environmental aspects and potential impacts on ecosystems, human health, and natural resources [3,4].

Home appliances are currently a key area of energy consumption in developed and developing countries, and projections related to the population growth predict that more and more people will use these appliances in the future [5]. A recent study showed that household

appliances account for 70% of China's carbon dioxide emissions and that air conditioners, refrigerators and televisions are responsible for 50% of these emissions [6]. These devices should be evaluated taking into account all phases of the life cycle, as well as their technological efficiency, and based on this, a plan for potential reduction of impacts at different scales should be developed.

This paper presents an LCA analysis of the hair dryer impact on the environment, using the eco-indicator methodology and software ECO-it 1.4. A comparative analysis was made for the hair dryer and its redesigned version, and the possibility of reducing the harmful impact on the environment was shown through the improvement of the hair dryer design.

## MATERIALS AND METHODS

### Life Cycle Assessment

Life cycle assessment (LCA) is a tool for decision-making on the production or quality of a certain product while identifying its impact on the environment, throughout the entire life cycle, starting from resources and material exploitation to final disposal. LCA is actually an analytical instrument in the environmental field that provides an understanding and comparison of different products or services through a “cradle to grave” approach [7]. This method can analyze all and/or more stages of the life cycle and thus helps companies to decide to what level it is necessary to “incorporate” environmental issues into the process of deciding on the characteristics of a certain product or on the types of services.

The Life Cycle Assessment includes four phases and key considerations (Figure 1):

1. Goal and scope definition.
2. The life cycle inventory (LCI).
3. The life cycle impact assessment (LCIA).
4. Life cycle interpretation.

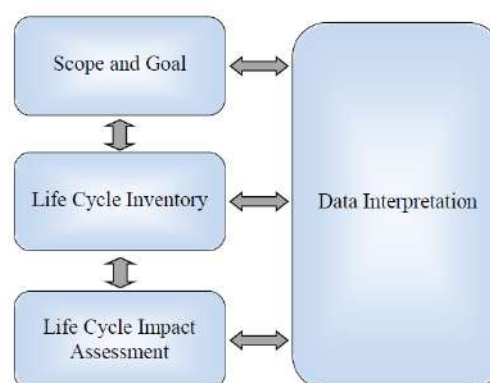


**Figure 1** Phases of an LCA

The methodological structure of the Life Cycle Assessment is given in the ISO 14040 series of standards: ISO 14040:2008 - LifeCycle Assessment - Principles and Framework and ISO 14044:2008 - Life Cycle Assessment – Requirements and Guidelines.

## Eco-indicator Method

The eco-indicator method (implemented in ECO-it 1.4 software) is one of the most developed methods for life cycle impact assessment. With the aim of presenting the LCA results at all levels, this model was developed to link the LCI results with the procedures for determining the weighting coefficients. This included the processes of characterization and normalization. The results can be presented as one quantified result - eco-indicator, which can facilitate the work of designers and production managers in the decision-making process related to the harmfulness of products to the environment [8].

The idea of the emergence of ecological indicators was initiated in the late 1990s by the Dutch Ministry of Construction, Spatial Planning and the Environment with the intention of encouraging care for the environment. The main idea of eco indicators is to compare two products or two variants of the same product from the aspect of environmental impact, and the values of eco indicators point to possible directions for product improvement [8]. The eco indicator calculation method has a modular structure. In order to ensure the correct use of eco-indicators, there are several steps that must be followed: determining the purpose of calculating eco-indicators, defining the lifetime of the analysed product, quantifying materials and processes, filling out the form for calculating eco indicators and results interpretation

### Model of analyzed hair dryer

In this analysis, a hair dryer Solride 2-Professional (Figure 2) of low power and small dimensions, intended for home use, will be analyzed. The hair dryer has a power of 800 W and three speed levels. The purpose of the hair-dryer analysis is to determine the overall eco-indicator of the hair dryer's life cycle and then to determine which processes have the most significant impact on the environment. In this case, there will be no comparison of two products of the same purpose, but an analysis of the impact of one product on the environment, with the aim of its improving.

According to the estimates, the average life-cycle of a hair dryer is from 70 to 1000 working hours. Also, in an average household on a weekly basis, a hair dryer is used about 1.5 hours, so the life-cycle of this device is estimated at 10 to 12 years.



*Figure 2 Analyzed hair-dryer Solride 21-Professional*

The components of the hair dryer are shown in Table 1.

*Table 1* Constituent parts of hair dryer

Name	Mass (g)	Material	Quantity
Front housing	120	Plastic	1
Rear housing	114	Plastic	1
Motor holder	47	Plastic	1
Coil	12	Aluminum	1
Back net	8	Stainless steel/plastic	2
Front neck	6	Stainless steel	1
Heater	13	NiCr alloy	4
Engine	30	-	1
Heater housing	64	Aluminum	2
Propeller	25	Plastic	1
Cable	126	Copper/rubber	1
Screw	9	Steel	11

Using the ECO-it 1.4 software, the eco-indicator for the observed individual process can be calculated, by multiplying the tabular eco-indicator, which is expressed in points per kilogram of some raw material, with the amount of raw material (or energy) that is characteristic of the observed process [9]:

$$EI_n = ei_n \cdot m_n \quad (1)$$

where:

$EI_n$  - eco-indicator for the observed process;

$ei_n$  - tabular eco indicator (expressed by characteristic size for a process);

$m_n$  - mass of raw material in the observed process;

$e_n$  - amount of energy in the observed process.

Entering data into the ECO-it 1.4 software is performed in three phases: the production phase, the use phase and the disposal phase. Then, software calculates eco-indicator for each process. These value is expressed in millipoints (mPt) and can be presented graphically.

## RESULTS AND DISCUSSION

### Results for analyzed hair dryer Solride 2-Professional

After defining the life cycle, classifying materials and processes in the 3 mentioned phases, points are calculated for each phase, as well as the eco-indicator. In Figure 3a), it can be seen that the total eco-indicator of the analyzed hair dryer is 1100 Pt. Since the largest share of points is in the use phase (it cannot be influenced in the calculation and consideration phase of the product), the points for this part of the analysis are ignored. Figure 3b) shows the eco-indicator for the hair dryers without the use phase (362 mPt).

Hair dryer has the greatest impact on the environment in the production phase, while waste disposal is significantly less in case without consideration of use phase. Waste disposal and



waste sorting in Serbia is still not fully defined, so, in this part of the analysis all hair dryer waste goes to the landfill. In the further part of the work, changes will be proposed in order to reduce energy consumption and the environmental impact of hair dryer.

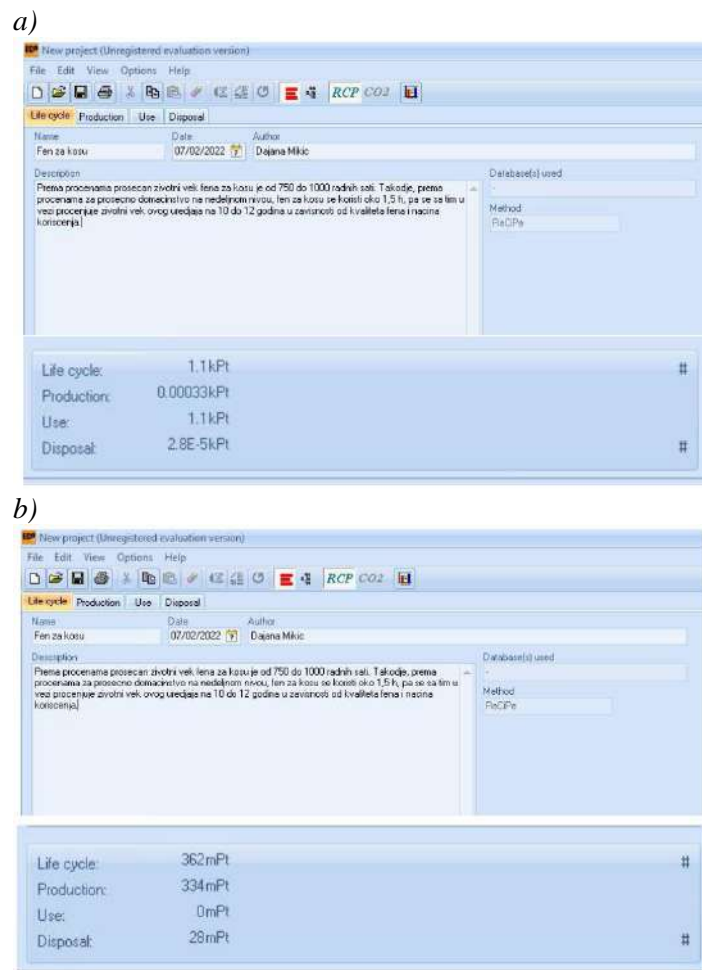


Figure 3 Results of hair dryer LCA analysys a) with use phase; b) without use phase

### Results for redesigned hair dryer

In the production phase, it is possible to redesign the hair-dryer housing, as well as all the parts that go with it, by reducing their volume of 10%. This would not affect the function of the product, and there would be a reduction in the production of plastic materials. With such a redesign, it is possible to reduce the number of required connecting elements.

The use phase consumes a certain amount of energy, which depends on the way of use. It is possible to reduce this consumption by introducing IC heaters. By installing IR heaters, energy savings of 20% are achieved. Energy consumption in this case amounts to 6400 kWh, while in the previous phase this amount was 8000 kWh during the entire life of the product.

And at the very end, the phase of waste disposal, which has a great impact on the environment, can be reduced by recycling individual parts of the hair dryer.

By redesigning the case and the parts that go with it, that is, by reducing the volume by 10% and installing an IR heater, the overall eco-indicator of the observed product is

significantly reduced, which is now 896 Pt (in the previous case it was 1100 Pt). By comparing the original and the redesigned hair dryer, it can be seen that the redesigned hair dryer is less harmful to the environment.

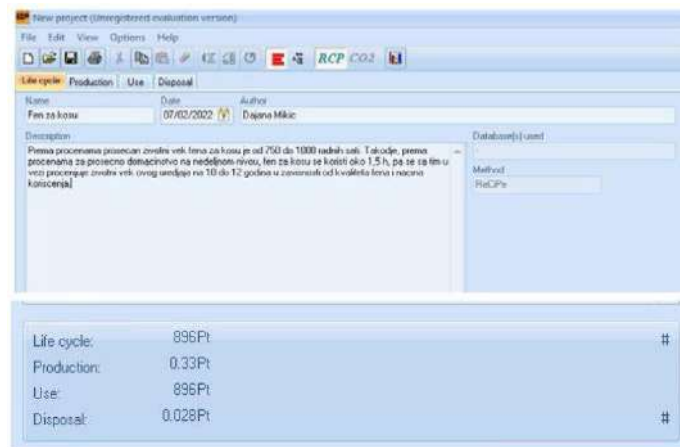


**Figure 4** Results of LCA analysis for redesigned hair dryer with use phase

## CONCLUSION

The Life Cycle Assessment method is a tool that can be used to assess the impact of a product on the environment throughout its entire life cycle. In this paper, the method of evaluating the product's harmfulness to the environment. The methodology Eco-it 99 and software ECO-it 1.4 were chosen, which was applied to the LCA of hair dryers. The LCA of the hair dryer was carried out in three phases: the production phase, the use phase, and the disposal phase. The production phase has the greatest impact on the environment.

An analysis of the redesigned hair dryer was also done - the housing material was changed and IC heater was implemented.

The recycling of certain materials after the hair dryer use is also foreseen. The entire redesign process was aimed at reducing the harmful impact of hair dryer on the environment. Analysis of the redesigned hair dryer has shown that its impact on the environment has decreased. If such changes were be introduced in other devices, they would lead to a big move and more visible results related to harmful impact on the environment.

## ACKNOWLEDGEMENT

*This investigation is a part of the project TR 33015. The authors would like to thank the Ministry of Education of the Republic of Serbia for their financial support during this investigation.*

## REFERENCES

- [1] Glumpak I., Utjecaj sustava za upravljanje okolišem na životni ciklus proizvoda, Fakultet strojarstva i brodogradnje, Zagreb (2009).
- [2] Golsteijn L., Life Cycle Assessment (LCA) explained, Available on the following link: <https://pre-sustainability.com/articles/life-cycle-assessment-lca-basics/>.

- [3] Feng C., Ma, X.Q., *J. Clean. Prod.* 17 (1) (2009) 13–25.
- [4] Štrbac N., Vuković M., Voza D. *et al.*, *Održivi razvoj i zaštita životne sredine*, Univerzitet u Beogradu, Tehnički fakultet u Boru, Bor (2012), ISSN 1820-7480.
- [5] Hischier R., Reale F., Castellani V. *et al.*, *J. Clean. Prod.* 267 (2020) 121952.
- [6] Bhutto M.Y., Liu X., Soomro Y.A. *et al.*, *Sustainability* 13 (1) (2021) 1–25.
- [7] Carapina H., Jovovic A., Stepanov J., *Ocena životnog ciklusa LCA (Lyfe Cycle Assessment) kao instrument u strateškom upravljanju otpadom*, Univerzitet Educons, Sremska Kamenica (2010), ISBN 978-86-877785-26-7.
- [8] Jönbrink A.K., Wolf-Wats C., Erixon M., *et al.*, *LCA Software Survey - report*, Stockholm (2000).
- [9] Zrnić N., *Dizajn i ekologija održivog razvoja proizvoda*, Mašinski fakultet Univerziteta u Beogradu, Beograd (2012), ISBN: 978-86-7083-772-0.

**6<sup>th</sup> Student section**



## SOME ASPECTS OF THE APPLICATION OF METAL-ORGANIC FRAMEWORKS

### NEKI ASPEKTI PRIMENE METALNIH ORGANSKIH OKVIRA

Students: Sofija Kostić<sup>1\*</sup>, Aleksa Marjanović<sup>1</sup>

Mentor: Maja Nujkić<sup>1</sup>

<sup>1</sup>University of Belgrade, Technical Faculty in Bor, V.J. 12, 19210 Bor, SERBIA

\*[ksofija94@gmail.com](mailto:ksofija94@gmail.com)

#### Abstract

Nanomaterials, such as metal-organic frameworks (MOFs), are key materials in many areas of science and technology due to their unique properties and wide range of applications. This review focuses on the synthesis and applications of MOFs in various fields, including gas storage, catalysis, photocatalysis and biomedicine. The synthesis of MOFs is a fundamental process that enables the production of materials with desired properties. There are several methods for synthesizing MOFs, the most commonly used of which are hydrothermal, sonochemical and microemulsion methods. In hydrothermal synthesis, metal ions are reacted with organic ligands in an aqueous solution at elevated temperature and pressure. Sonochemical synthesis uses ultrasonic waves for a rapid reaction between metal salts and organic ligands. The microemulsion method uses microscopic emulsions for a controlled reaction between the reagents. The application of MOFs is extremely diverse and covers different areas. In gas storage, MOFs show great potential for the adsorption and storage of various gasses such as hydrogen, carbon dioxide and methane. The catalytic properties of MOFs make them useful materials for various reactions, including reduction, oxidation and acylation reactions. The photocatalytic activities of MOFs are utilized in the degradation of organic pollutants and in the production of hydrogen from water. In biomedicine, MOFs are being researched as potential drug carriers, contrast agents for imaging and antibacterial agents. Despite their many advantages, MOFs also face challenges such as their stability under aqueous conditions, which can limit their application in certain areas. However, researchers continue to work on improving the stability and functionality of MOFs to expand their potential applications. To summarize, this review provides a deeper insight into the properties and applications of MOFs in various fields of science and engineering. Their unique properties make them important materials in many ways. At the same time, there is still room for further research and improvement to increase their usefulness and practical application.

**Keywords:** metal-organic frameworks, synthesis, toxicity, biomedicine, gas storage

## **ACKNOWLEDGEMENT**

*The authors are grateful to the Ministry of Science, Technological development and Innovation of the Republic of Serbia for financial support according to the contract with the registration number (451-03-65/2024-03/200131).*

## **REFERENCES**

- [1] Zheng S.S., Li Q. Xue, H.G., *et al.*, *Natl. Sci. Rev.* 7 (2020) 305–314.
- [2] Stock N., Biswas S., *Chem. Rev.* 112 (2012) 933–969.
- [3] Lawrence M.J., Rees G.D., *Adv. Drug Deliv. Rev.* 64 (2012) 175–193.
- [4] Raptopoulou C.P., *Materials* 14 (2021) 310.
- [5] Xue, Y.P., Zhao, G.C., Yang, R.Y., *et al.*, *Nanoscale* 13 (2021) 3911–3936.





## MECHANISMS OF CADMIUM UPTAKE INTO THE PLANT

### MEHANIZMI USVAJANJA KADMIJUMA OD STRANE BILJAKA

**Student: Jelena Janković<sup>1\*</sup>**

**Mentor: Maja Nujkić<sup>1</sup>**

<sup>1</sup>University of Belgrade, Technical Faculty in Bor, V.J. 12, 19210 Bor, SERBIA

\*[jankoviceva81@gmail.com](mailto:jankoviceva81@gmail.com)

#### Abstract

The growth of the world's population and the increasing demand for natural resources are leading to significant environmental problems such as air, water, and soil pollution, habitat destruction, biodiversity loss, and climate change. These problems have a negative impact on ecosystems, human health, the economy, and society. In particular, problems related to pollution from heavy metals such as cadmium are highlighted, emphasizing the importance of exploring the mechanisms by which plants take up these harmful substances.

Cadmium is a heavy metal present in the environment as a result of industrial activities and its accumulation in plants poses a serious problem for human health and the ecosystem. For this reason, the focus of this work is precisely on the mechanisms of cadmium uptake in plants. Through a review of the relevant literature, the processes and pathways of cadmium uptake in plants and the mechanisms that influence this process were investigated. The accumulation of cadmium poses a serious threat to the environment, food safety and public health and exceeds the natural ability of the soil ecosystem to regenerate and cleanse itself. Plants growing on cadmium-contaminated soils are directly affected, which can lead to serious changes in their development, metabolism and physiological functions, compromising their quality and safety for consumption.

Particular attention is paid to the physiological and molecular mechanisms that regulate the uptake of cadmium from the soil into the plant roots, the transport through the roots to the aerial parts and the accumulation in the plant tissue. Understanding these mechanisms is crucial for the development of strategies to reduce cadmium accumulation in crops and to protect the health of humans and animals that consume these plants. The ideal long-term solution to the problem of cadmium toxicity is the remediation of soils contaminated with this heavy metal and preventive measures against further anthropogenic cadmium inputs. However, this approach requires time and coordinated efforts from various sectors of society and is considered a strategic goal. For the current situation, a biological, i.e. genetic, approach has been proposed, which includes the development of plant varieties with a lower capacity to accumulate cadmium. This is to be achieved through an in-depth study of the genetic mechanisms that regulate the uptake and distribution of cadmium in plants, with the aim of reducing its presence. It is particularly important to reduce the accumulation of cadmium in

the grains of the three main cereals - rice, wheat, and maize - as these account for more than half of the calorie intake in the human diet. Selection and breeding programs aim to understand and genetically modify the process of cadmium transport from the roots to the aerial parts of the plant to reduce the transfer of cadmium to the grains, which directly contributes to food safety and protects public health from the negative effects of cadmium.

The availability of cadmium in soil depends primarily on pH, with other factors such as root exudates, organic matter, plant age, and plant genotype also playing a role. A low pH value means a higher uptake of cadmium by the plants. Controlling soil pH is the key to controlling cadmium uptake.

The application of sustainable plant nutrition and advanced bioremediation technologies are key strategies in the fight against cadmium pollution. These techniques include innovative methods such as phytovolatilization, phytodegradation, phytoremediation, and microbial remediation, which are used for the ecological and economical remediation of cadmium-contaminated soils. In addition, the use of biochar, organic fertilizers, and growth hormones can contribute significantly to reducing the negative effects of cadmium in soil. Effective remediation and proper management of contaminated soils are key to reducing the risks that cadmium poses to agricultural soils, crops, and ultimately human health.

**Keywords:** cadmium, land remediation, bioremediation, pollution, toxicity

#### **ACKNOWLEDGEMENT**

*The authors are grateful to the Ministry of Science, Technological development and Innovation of the Republic of Serbia for financial support according to the contract with the registration number (451-03-65/2024-03/200131).*

#### **REFERENCES**

- [1] Guo J., Xie S., Huang Y., *et al.*, *Ecotoxicol. Environ. Saf.* 226 (2021) 112813.
- [2] Haider F. U., Liqun C., Coulter J. A., *et al.*, *Ecotoxicol. Environ. Saf.* 211 (2021) 111887.
- [3] Huang X., Duan S., Wu Q., *et al.*, *Plants* 9 (2020) 223.
- [4] Ismael M. A., Elyamine A., Moussa M. G., *et al.*, *Metallomics* 11 (2019) 2.
- [5] Li W., Chen K., Li Q., *et al.*, *Plants* 12 (2023) 1–15.



## COAGULATION PROCESS AND APPLICATION OF NEW ECOLOGICAL COAGULANTS

### PROCES KOAGULACIJE I PRIMENA NOVIH EKOLOŠKIH KOAGULANATA

**Student: Jovana Kumbrijanović<sup>1\*</sup>**

**Mentors: Maja Nujkić<sup>1</sup>, Sonja Stanković<sup>1</sup>**

<sup>1</sup>University of Belgrade, Technical Faculty in Bor, V.J. 12, 19210 Bor, SERBIA

*\*[jkumbrijanovic@gmail.com](mailto:jkumbrijanovic@gmail.com)*

#### **Abstract**

Industrialization is unstoppable and is advancing every day, which brings advantages and disadvantages. The disadvantages of industrialization are mainly to be seen in environmental pollution. For this reason, it is very important to consider and improve processes that can help reduce the damage caused by industrial production processes, and among these processes, coagulation stands out as one of the safe, efficient, and economically profitable methods. The aim of this work is to define the process of coagulation and flocculation as well as their purpose and application in chemical technology for the purpose of treatment and purification of wastewater. Various mechanisms in the coagulation process were considered, starting with the compaction of the bilayer, the electrostatic mechanism of coloration, bridging, and flocculent purification, but also methods that can influence the optimization of the process itself, such as the method of microsand addition. Since coagulation stands out as part of the technological process and is an indispensable part of the water treatment process, research has focused on optimization, i.e. on improving the coagulation process itself. Optimization was originally proposed and applied in the USA for drinking water treatment. It proved to be a method that provided satisfactory results, so its application has been continued and extended. The work includes studies and analyses of the different types of coagulants and their application, as well as their advantages and disadvantages. The production of chemical coagulants is described, from iron-, aluminum- and titanium-based coagulants to organic hybrid coagulants and their effect in the removal of heavy metals, certain by-products, microalgae, and nitrogen. The work also includes a detailed analysis of the production and effect of natural coagulants obtained by extraction processes from fruit shells, walnut kernels, and pine seeds, while synthetically turbid water produced by the addition of kaolin was used for the analysis. Studies have been carried out on the treatment of water coming from different environments and containing different types of wastewater, including colored colloids, which are waste from the textile industry, comparing the quality of the coagulation carried out depending on the application of the corresponding natural or chemical coagulant, but also the efficiency of the combination of these agents. Microplastics are a widespread pollutant that poses a major threat to the environment. Microplastic particles originate from

synthetic polymer products, can have different shapes and dimensions, and their surface is coated with negatively charged functional groups (e.g. polystyrene particles with carboxyl groups), which is why the effect of a coagulant based on amyloid fibers on water contaminated with microplastic particles is being investigated. The extent to which industrial waste resulting from the production of aluminum from bauxite can be used for the production of coagulants was investigated, and a comparison of their potential with conventional coagulants was made.

**Keywords:** chemical coagulants, natural coagulants, turbidity, decolorization, microplastics

### **ACKNOWLEDGEMENT**

*The authors are grateful to the Ministry of Science, Technological development and Innovation of the Republic of Serbia for financial support according to the contract with the registration number (451-03-65/2024-03/200131).*

### **REFERENCES**

- [1] Sun Y., Zhou S., Shah K. J. MRF 91 (2021) 219-252.
- [2] Wang P., Ding S., An G., *et al.*, J. Haz. Mat. 420 (2021) 126558.
- [3] Zedan T., Mossad M., Fouad M., *et al.*, Water Pract. Technol. 17 (2022) 684-698.
- [4] Hadadi A., Imessaoudene A., Bollinger J. C., *et al.*, J. Environ. Manage. 331 (2023) 117286.
- [5] Peydayesh M., Suta T., Usulli M *et al.*, Environ. Sci. Technol. 55 (2021) 8848-8858.



## SOME APPLICATION ASPECTS OF THE MATERIALS BASED ON THE GREEN MAGNESIUM OXIDE

### NEKI ASPEKTI PRIMENE MATERIJALA NA BAZI MAGNEZIJUM-OKSIDA

**Student: Lazar Cvetković<sup>1\*</sup>**

**Mentors: Maja Nujkić<sup>1</sup>, Tanja Kalinović<sup>1</sup>, Jelena Kalinović<sup>1</sup>**

<sup>1</sup>University of Belgrade, Technical Faculty in Bor, V.J. 12, 19210 Bor, SERBIA

\*[Cvele94@outlook.com](mailto:Cvele94@outlook.com)

#### Abstract

The ecological production of materials is becoming increasingly important in today's world. The production of materials based on traditional methods leads to heavy environmental pollution, so there is a tendency to obtain materials in an ecological way. Due to its good properties, the demand for magnesium oxide is increasing in the world, and the possibility of obtaining it by green synthesis is also important. This study provides general explanations of the most common extracting methods of magnesium oxide from natural materials such as different types of plant material. It also gives an overview of the application of green magnesium oxide or magnesium oxide nanoparticles (MgONP) in various industries.

For the green synthesis of magnesium oxide nanoparticles, extracts of organisms such as algae, bacteria and fungi or extracts of plant parts rich in various biomolecules such as polyphenols, as well as extracts of mixtures of several plants or their parts can be used.

Under the particular conditions of green synthesis, attention must also be paid to the parameters that influence the formation of MgONP sizes. For example, Mg(OH)<sub>2</sub> can precipitate in an alkaline solution with a pH above 9 and be a precursor for formation of nanoparticles. The effect of pH on the morphology of MgONP obtained with an extract of Tricolor amaranth leaves was investigated in a pH range of 3 to 11. The authors concluded that in an acidic environment, smaller nanoparticles are formed, while in a basic environment, larger particle agglomerates are formed, which become smaller after calcination and loss of phytochemicals.

The green synthesis of MgONP particles is illustrated by the following example. The washed samples of *C. crinita* were dried in an oven at 70°C for 24 hours and then ground to a fine powder using an electric mixer. About 10 g of *C. crinita* powder was added to 100 ml of distilled water, which was heated to 60°C and stirring with a magnetic stirrer at 120 rpm. The mixture was then centrifuged at 1500 rpm for about 10 minutes, the precipitate was collected and used as a reducing and stabilizing agent for MgONP as follows: 51.3 mg of the metal oxide precursor [Mg(NO<sub>3</sub>)<sub>2</sub>·6H<sub>2</sub>O] was dissolved in 10 ml of distilled H<sub>2</sub>O and added to 90 ml of the resulting aqueous algal extract to obtain a final concentration of 2 mM. After 24

hours of incubation, a color change from pale yellow to yellowish-brown occurs, indicating the formation of MgONPs. Finally, the obtained nanoparticles were calcined at 400°C for 4 hours.

The MgONP material obtained by synthesis with leaf extracts of *Sesbania bispinosa* was used to germinate seeds of *Cicer arietinum* (chickpea) and *Solanum lycopersicum* (tomato). The total chlorophyll and carotenoid content was higher in *Cicer arietinum* than in *Solanum lycopersicum*, and accordingly the chickpea seeds germinated better than the tomato seeds. Therefore, the synthesized MgONP increased the chlorophyll content and showed favorable growth of the examined plants, proving the effectiveness of MgONP in regulating plant growth with promising application in agriculture.

In addition, MgONP leads to the death of the larvae, whereby the mortality is directly related to the dose. The mortality of the first-stage larvae was 40 and 99% at concentrations of 2 and 10 mg mL<sup>-1</sup>, respectively. In contrast, the mortality of the second-stage larvae was between 36.6 and 95% when treated with 2 and 10 mg mL<sup>-1</sup> MgONP, respectively. The mortality of third-stage larvae was 30.8 and 92.2% when treated with concentrations of 2 and 10 mg mL<sup>-1</sup> MgONP, respectively.

The value and importance of materials obtained through green synthesis will only increase with the development of science, and further research in this area is recommended.

**Keywords:** magnesium oxide, nanoparticles, ecology, green synthesis

## ACKNOWLEDGEMENT

*The authors are grateful to the Ministry of Science, Technological development and Innovation of the Republic of Serbia for financial support according to the contract with the registration number (451-03-65/2024-03/200131).*

## REFERENCES

- [1] Marouzi S., Sabouri Z., Darroudi M., *Ceram. Int.* 47 (14) (2021) 19632–19650.
- [2] Abinaya S., Kavitha H.P., Prakash M., *et al.*, *Sustain. Chem. Pharm.* 19 (2021) 100368.
- [3] Moorthy S.K., Ashok C.H., Rao K.V., *et al.*, *Mater. Today: Proc.* 2 (2015) 4360–4368.
- [4] Pugazhendhi A., Prabhu R., Muruganatham K., *et al.*, *J. Photochem. Photobiol. B Biol.* 190 (2019) 86–97.
- [5] Silva A.A., Sousa A.M.F., Furtado C.R.G., *et al.*, *Mater. Today Sustain.* 20 (2022) 100203.





## RECYCLING OF USED LITHIUM-ION BATTERIES

### RECIKLAŽA ISKORIŠĆENIH LITIJUM-JONSKIH BATERIJA

**Students: Milena Radivojević<sup>1\*</sup>, Kristina Konstadinović<sup>1</sup>**

**Mentors: Maja Nujkić<sup>1</sup>, Dragana Medić<sup>1</sup>**

<sup>1</sup>University of Belgrade, Technical Faculty in Bor, V.J. 12, 19210 Bor, SERBIA

\*[milenamimaradivojevic@gmail.com](mailto:milenamimaradivojevic@gmail.com)

#### Abstract

Lithium-ion batteries have become an integral part of modern life. Their application extends to all areas of our daily lives, from cell phones to electric cars. One of the main advantages of these batteries is their ease of use, but at the same time, we face a serious problem - the disposal of used batteries. Most of these batteries end up in landfill, which has serious negative consequences for the environment. Given the enormous quantities of batteries that are used and thrown away every day, the recycling process is becoming increasingly important to reduce the negative impact on the environment and lower the cost of new batteries.

To better understand the recycling process of lithium-ion batteries, we need to look at their structure and manufacturing process. These batteries consist of a cathode, an anode, an electrolyte, and a separator, which together ensure that the lithium flows between the electrodes during charging and discharging. The production of these batteries requires the use of various materials, including lithium, cobalt, nickel, aluminum, and other metals. However, it is precisely because of these valuable materials that recycling is an economically and environmentally viable option.

Recycling lithium-ion batteries involves processes such as collecting, separating, shredding, separating, and regenerating materials. Lithium, cobalt, nickel, and other valuable materials are separated and can be reused for the production of new batteries. The benefits of recycling are obvious: it reduces the need to extract new raw materials, reduces energy consumption and CO<sub>2</sub> emissions, and prevents pollution from hazardous substances from batteries.

However, the recycling process also presents some challenges and shortcomings. For example, the complex structure of batteries makes the recycling process itself very complicated. The high recycling costs and low prices for secondary materials also pose a major challenge for the battery recycling industry. The cost of transporting, processing, and storing waste can also be high, making recycling less economical.

Despite these challenges, the recycling of lithium-ion batteries is crucial for environmental protection and a sustainable future. Developing effective technologies and policies to promote

battery recycling can help reduce the environmental impact and create a cleaner and healthier environment for us all.

**Keywords:** lithium-ion batteries, recycling techniques, challenges of recycling, advantages of recycling

### **ACKNOWLEDGEMENT**

*The authors are grateful to the Ministry of Science, Technological development and Innovation of the Republic of Serbia for financial support according to the contract with the registration number (451-03-65/2024-03/200131).*

### **REFERENCES**

- [1] Hu Y., Yu Y., Huang K., *et al.* J. Energy Storage 27 (2020) 101111.
- [2] Larouche F., Tedjar F., Amouzegar K., *et al.*, Materials 13 (2020) 801.
- [3] Medić D., Valorizacija kobalta iz katodnog materijala istrošenih litijum-jonskih baterija (2021), Available on the following link: <https://nardus.mpn.gov.rs/handle/123456789/18854>.
- [4] Milović M., Sinteza, strukturna i elektrohemijska svojstva  $\text{LiFePO}_4$  i  $\text{Li}_2\text{FeSiO}_4$  kao katodnih materijala za litijum-jonske baterije (2016), Available on the following link: <https://dais.sanu.ac.rs/handle/123456789/815?locale-attribute=en>.
- [5] Radić N., Radić V., 6. Konferencija studenata industrijskog inženjerstva i menadžmenta, June 4-th, Kragujevac, Serbia (2015) 137-139.



## MEDICAL WASTE ISSUES RELATED TO COVID-19 PANDEMIC

### PROBLEMI MEDICINSKOG OTPADA VEZANI ZA PANDEMIJU COVID-19

**Student: Milica Denić<sup>1\*</sup>**

**Mentor: Ana Radojević<sup>1</sup>**

<sup>1</sup>University of Belgrade, Technical Faculty in Bor, V.J. 12, 19210 Bor, SERBIA

*\*[milicaddenic@gmail.com](mailto:milicaddenic@gmail.com)*

#### Abstract

Waste management is a fundamental and continuous responsibility of society, and it turned out to be a substantial challenge encountered by authorities worldwide during the COVID-19 pandemic crisis. Challenges can be attributed to the presence of a diverse variety of hazardous materials including used needles and syringes, personal protective equipment (PPE), contaminated dressings, heavy metals, biological substances, pathogens, diagnostic samples, blood, toxic chemicals, pharmaceuticals, medical devices, radioactive materials, etc. Medical waste primarily originates from hospitals, clinics, and healthcare centres, as well as from home quarantines. Since the medical waste contains traces of infectious agents it is classified as hazardous waste. However, around 75–90% of medical solid waste has a similar composition to household waste, wherefore it is categorized as 'non-hazardous' or 'general medical' waste. The remaining 10–25% is labelled as 'hazardous waste', related to environmental and health hazards.

Throughout the COVID-19 pandemic, there has been a significant increase in the generation of medical waste, ranging from 3 to 6 times more than the typical generated volume of municipal solid waste. In addition to other medical waste, a consequence of the COVID-19 pandemic is the substantial increase in plastic waste. This includes items such as surgical drapes, disposable gowns, syringes, personal protective equipment (face masks and shields), disposable gloves, and testing kits.

In Hubei province (China), medical waste generation has increased by 600%, from 40 to 240 tons, overloading the existing transport and disposal infrastructure. Other countries are facing similar challenges in dealing with the substantial volume of waste. This trend has been observed in France, Italy, and the Netherlands. Medical solid waste in France and the Netherlands has increased from 40% to 50% and 45% to 50%, respectively.

Common disinfection methods used for COVID-19 medical waste treatment include incineration, as well as physical and chemical approaches. Pyrolysis, a thermochemical process, involves disintegrating organic compounds, present in solid and liquid waste, at elevated temperatures within anaerobic or low-oxygen environments. The macromolecular compounds contained in COVID-19 medical waste are consequently decomposed into compounds such as solid or liquid fuels, raw synthetic gases, and carbonaceous materials (e.g.

coke, char). The products resulting from pyrolysis have significant commercial value and can be used as an alternative energy source to supplement decreased fossil fuel reserves. However, technologies such as plastic waste incineration can result in the release of harmful pollutants in the atmosphere, like dioxins and furans, requiring the use of additional flue-gas treatments.

Throughout the COVID-19 pandemic, various nations have implemented different approaches for managing medical solid waste, while the World Health Organization (WHO) has developed specific guidelines for its management. In general, waste management represents a significant and challenging sector for the society which was further strained by the recent COVID-19 pandemic, introduced new mandatory practices. The measures taken to fight the COVID-19 virus might have had a positive impact on the environment by enhancing air quality and lowering carbon footprint, but they also led to an unrivalled increase in the amount of waste being produced.

**Keywords:** medical waste management, COVID-19 pandemic, pollution

### **ACKNOWLEDGEMENT**

*The authors are grateful to the Ministry of Education, Technological development and Innovation of the Republic of Serbia for financial support, within the funding of the scientific research at the University of Belgrade, Technical Faculty in Bor (No. 451-03-65/2024-03/200131).*

### **REFERENCES**

- [1] Olawade D., Wada O., Ore O., *et al.*, WMB, 1 (2024) 93–103.
- [2] Manupati V.K., Ramkumar M., Baba V., Agarwal A., J. Clean. Prod. 281 (2021) 125175.
- [3] Dharmaraj S., Veeramuthu A., Pandiyan R., *et al.*, Chemosphere 275 (2021) 130092.
- [4] Das A.K., Islam N., Billah M., Sarker A., Sci. Total Environ. 778 (2021) 146220.
- [5] Asian Development Bank (ADB), Managing Infectious Medical Waste during the COVID-19 Pandemic, 2020, Available on the following link: <https://www.adb.org/publications/managing-medical-waste-covid19>.
- [6] World Health Organization (WHO), Water, sanitation, hygiene, and waste management for SARS-CoV-2, the virus that causes COVID-19, Interim guidance, 2020, Available on the following link: <https://www.who.int/publications/i/item/WHO-2019-nCoV-IPC-WASH-2020.4>.



## PRESENCE OF TOXIC AND POTENTIALLY TOXIC ELEMENTS IN SOME DOMESTIC FRUIT FROM THE PEŠTER PLATEAU, SJENICA, SERBIA

## PRISUSTVO TOKSIČNIH I POTENCIJALNO TOKSIČNIH ELEMENATA U DOMAĆEM VOĆU SA PEŠTERSKE VISORAVNI, SJENICA, SRBIJA

**Student: Sara M. Pantović<sup>1\*</sup>**

**Mentor: Enisa S. Selimović<sup>1</sup>**

<sup>1</sup>State University in Novi Pazar, Department of Natural Sciences and Mathematics,  
Vuka Karadžića 9, Novi Pazar, SERBIA

\* [spantovic@np.ac.rs](mailto:spantovic@np.ac.rs)

### Abstract

The aim of this work was to determine the content of toxic and potentially toxic elements in selected samples of domestic fruits from the Pešter Plateau, Serbia. Berries and stone fruits were analysed. The domestic fruit is traditionally used as food and in folk medicine. Seven samples of different types of domestic fruit trees were collected from one location in Sjenica, at an altitude of 1020 m. Given that berries and stone fruits are very rich in bioactive compounds and phytochemicals that are associated with multiple healthy properties and are used in nutrition, it is important to determine the content of toxic elements.

The samples examined in this work are: raspberry (*Rubus idaeus L.*), cherry (*Prunus cerasus L.*), red plum (*Prunus cerasifera L.*), grape (*Vitis vinifera L.*), chokeberry (*Aronia arbutifolia L.*), red currant (*Ribes rubrum L.*), and black currant (*Ribes nigrum L.*).

Using the inductively coupled plasma optical emission spectrometry (ICP OES) method, the content of 5 elements was determined in samples of domestic fruits from the Pešter Plateau, Serbia.

In this work, the content of five toxic and potentially toxic elements (Al, Pb, Cd, As, and Ba) was determined. Our red plum samples contained less toxic elements such as Al, Ba (about 8 times), Cd (about 10 times), Pb (about 4 times), and As (about 400 times) compared to the results of the content in the wild red plum grown in Düzce Province, Turkey. According to the literature data, the content of Pb and Cd in grapes from Lagos, Nigeria, is significantly lower. The results obtained in this work showed a lower content of the toxic elements Pb (about 5 times), As (about 30 times), and Cd (about 8 times) compared to the data obtained for grapes from eastern Serbia. Of the toxic elements in chokeberry, only arsenic was detected in a lower concentration than stated in the literature. Domestic currants on the Pešter plateau contained less toxic elements such as As (about 95 times), Cd, and Ba, while they contained higher amounts of Al and Pb than samples in the Düzce Province, Turkey.

Red plum contains the smallest amount of all toxic elements. The most lead is in domestic sour cherries, while the most aluminium is in aronia.

In general, the content of toxic elements was lower than the data from the literature. This shows that domestic fruits from Pešter Plateau can be safely consumed by humans without risk. It would be interesting to investigate the soils on which the fruits grew. By comparing the content results in berry and stone fruit, we conclude that there are no significant deviations. The obtained data on the content of toxic and potentially toxic elements on the Pešter Plateau can supplement and clarify the available data in the literature and the database on the chemical composition of foods.

**Keywords:** domestic fruit, elements, ICP OES, Sjenica, Pešter Plateau

### **ACKNOWLEDGEMENT**

*The authors are grateful to the State University of Novi Pazar, Novi Pazar, of the Republic of Serbia for financial support.*

### **REFERENCES**

- [1] Al-Juhaimi, F., Kulluk, D.A., Ahmed, I.A.M., *et al.*, *Environ. Monit. Assess.*, 195 (2023) 1370.
- [2] Sobukola, O.P., Adeniran, O.M., Odedairo, A.A., *et al.*, *Afr. J. Food Sci.*, 4 (2010) 389–393.
- [3] Alagić, S.Č., Tošić, S.B., Dimitrijević, M.D., *et al.*, *Commun. Soil Sci. Plant Anal.*, 47 (2016) 2034–2045.
- [4] Pavlović A.N., Brčanović J.M., Veljković J.N., *et al.*, *Fruits* 70 (2015) 385–393.





## CHEMICAL COMPOSITION OF ESSENTIAL OIL ISOLATED FROM FRESH AND DRY LEAVES OF *Geranium robertianum* L.

### HEMIJSKI SASTAV ETERIČNOG ULJA IZOLOVANOG IZ SVEŽIH I SUVIH LISTOVA *Geranium robertianum* L.

**Student: Milena Stanković<sup>1\*</sup>**

**Mentor: Ljiljana Stanojević<sup>1</sup>**

<sup>1</sup>University of Niš, Faculty of Technology, Bulevar Oslobođenja 124, 16000 Leskovac, SERBIA

\*[milenna.stankovic@gmail.com](mailto:milenna.stankovic@gmail.com)

#### Abstract

*Geranium robertianum* L., commonly known as Herb Robert or Red Robin, has long been used in the folk medicine of several countries and in herbalism's practice for a number of different therapeutic purposes. *G. robertianum* has been used for a long time in the folk medicine of several countries in different preparations, for a multitude of therapeutic purposes. Its anti-inflammatory, haemostatic, antidiabetic, antibacterial, antidiarrhoeic, antiallergic, anti-cancer, antihepatotoxic, diuretic, and tonic properties, as well as its suitability for the treatment of digestive system ailments, have made this species very appreciated in herbal medicine.

The chemistry of the *Geranium* genus is reasonably well-known and clearly dominated by phenolic constituents, the most studied classes of compounds being tannins, flavonoids, and phenolic acids. The phytochemical characterization of *G. robertianum* has been focused mostly on the investigation of extracts of the plant, with special emphasis on phenolic compounds, particularly flavonoids. Studies concerning the essential oils of this species are still scarce.

The aim of this study was a comparative analysis of the chemical composition of the essential oil isolated from fresh and dry leaves of *Geranium robertianum* L. grown in south Serbia. The essential oil was obtained by Clevenger-type hydrodistillation with hydromodule 1:10 m/V. The qualitative and quantitative composition of essential oil was determined by GC/MS and GC/FID analyses.

The yield of essential oil obtained was 0.078 and 0.066 g/100 g of fresh and dry plant material, respectively. Twenty-three compounds were identified from fresh leaves essential oil, mainly oxygen-containing sesquiterpenes (84.1%), sesquiterpene hydrocarbons (5.9%), monoterpene hydrocarbons (3.5%), oxygen-containing monoterpenes (3.4%), and others, where the most abundant compounds were germacrene (76.2%). Twenty compounds were identified from dry leaves essential oil, mainly oxygen-containing sesquiterpenes (39.4%), monoterpene hydrocarbons (38.5%), oxygen-containing monoterpenes (17%), sesquiterpene

hydrocarbons (4.2%), and others, where the most abundant compounds were germacrene (39.4%), limonene (29.4%) and  $\beta$ -pinene (6.1%).

Based on the obtained results, it can be concluded that the chemical composition of *G. robertianum* essential oil differs depending on the plant material used (dry or fresh leaves). Further research should focus on more detailed research of the chemical composition and determination of biological activities of *G. robertianum* that would expand its application in Serbia.

**Keywords:** *geranium robertianum* L., essential oil, chemical composition

### **ACKNOWLEDGMENT**

*This work was supported by the Ministry of Science, Technological Development and Innovation of the Republic of Serbia under the program of financing scientific research work, 451-03-65/2024-03/200133 and 451-03-66/2024-03/200133.*

### **REFERENCES**

- [1] Graça V.C., Ferreira I.C.F.R., Santos P.F., *Ind. Crop. and Prod.* 87 (2016) 363–378.
- [2] Pedro L.G., Pais M.S.S., Schetter J.J.C., *Flavour Frag. J.* 7 (1992) 223–226.
- [3] Harborne, J.B., Williams, C.A., *Phytochemistry of the genus Geranium in Geranium and Pelargonium - The genera Geranium and Pelargonium*, Lis-Balchin, M., Taylor & Francis, London, 2002., pp. 20–29, ISBN: 9780429218606.



## TOXIC EFFECTS OF PETROLEUM DERIVATIVES ON LIVING ORGANISMS FROM CONTAMINATED SOILS

### TOKSIČNI EFEKAT NAFTNIH DERIVATA NA ŽIVE ORGANIZME IZ ZAGAĐENOG ZEMLJIŠTA

**Student: Nikola Petrović<sup>1\*</sup>**

**Mentor: Ana Simonović<sup>1</sup>**

<sup>1</sup>University of Belgrade, Technical Faculty in Bor, V.J. 12, 19210 Bor, SERBIA

\*[nikola.petrovic9700@gmail.com](mailto:nikola.petrovic9700@gmail.com)

#### Abstract

Soil is a dynamic resource formed from abiotic components (sand, silt, clay, and organic matter) and biotic components (living organisms). Soil degradation can directly impact water and air quality, biodiversity, and climate change. Additionally, it can jeopardize human health and food security, both for humans and animals.

The processes of petroleum extraction, processing, and transportation can contribute to the entry of this harmful material into the surrounding soil. One of the main causes of soil contamination is petroleum spills. In soil contaminated with petroleum pollutants, the primary pollutants are mainly aliphatic, cycloaliphatic, and aromatic hydrocarbons. Gasoline, kerosene, diesel fuels, mineral motor oils, hexane, benzene, toluene, xylenes, and polycyclic aromatic hydrocarbons (PAHs) are important chemicals comprising the total petroleum hydrocarbons. It is estimated that globally, natural petroleum seepage amounts to 600,000 metric tons annually. According to reports, petroleum pollution has affected about 3.5 million sites in Europe.

Petroleum pollutants have the ability to penetrate plant tissues and move through the intracellular space and vascular system. Plant roots can uptake petroleum pollutants from the soil, transport them to leaves and fruits, store them, and transfer pollutants from leaves to roots. Plant growth is slowed, stem length and diameter are shortened, aboveground tissue length is decreased, and root length and leaf surface area are altered due to the lack of oxygen and nutrients in contaminated soil (depending on the plant species). Hussain et al. investigated the physiological impact on the growth of two plant species (*Lolium multiflorum* and *Lotus corniculatus*) tolerant to diesel and concluded that both the physical and chemical effects of oil have negative impacts on plant growth and root development.

Exposure to petroleum and petroleum derivatives, whether directly (breathing polluted air and direct skin contact) or indirectly (bathing in contaminated water and consuming contaminated food), can cause significant health problems in humans. Some aromatics negatively impact human liver and kidney functions and even induce cancer. Moreover, since PAHs are highly lipophilic, animals readily absorb them through the digestive tract.

Prolonged exposure to contaminated areas can lead to fatigue, respiratory problems, eye irritation, and headaches, with a higher likelihood of women experiencing spontaneous abortion. Hawrot-Paw *et al.* conducted a study in which they added conventional diesel fuel and two types of biodiesel to the soil, and monitored the reactions of invertebrates, specifically earthworms. They concluded that fuels have a negative impact on earthworms.

Biological methods for removing petroleum hydrocarbons are grouped into two main categories: bioremediation and phytoremediation. Bioremediation utilizes microorganisms, particularly bacteria and fungi, to remove petroleum hydrocarbons from contaminated environments. Phytoremediation, on the other hand, employs plants and various types of symbionts to remove polycyclic aromatic hydrocarbons from polluted soil. This method is facilitated by changes in the soil and the application of appropriate agricultural practices.

Phytoremediation stands out as an extremely effective strategy for reducing the presence of organic compounds and has recently garnered significant attention due to its ability to degrade pollutants over a wider area, its broad applicability, environmental friendliness, and economic viability.

**Keywords:** soil pollution, petroleum derivatives, toxic effect, bioremediation, phytoremediation

## **ACKNOWLEDGEMENT**

*The authors are grateful to the Ministry of Education, Technological development and Innovation of the Republic of Serbia for financial support, within the funding of the scientific research at the University of Belgrade, Technical Faculty in Bor (No. 451-03-65/2024-03/200131).*

## **REFERENCES**

- [1] Ambaye T.G., Gomez F.H., Chebbi A., *et al.*, Chemosphere 293 (2022) 133572.
- [2] Cachada A., Rocha-Santos T., Duarte A.C., Soil Pollut., Academic Press (2018) pp. 1–28, ISBN 9780128498736.
- [3] Haider F.U., Ejaz M., Cheema S.A., *et al.*, Environ. Res. 197 (2021) 111031.
- [4] Hawrot Paw M., Koniuszy A., Zając G., *et al.*, Sci. Rep. 10 (2020) 16436.
- [5] Hussain I., Puschenreiter M., Gerhard S., *et al.*, Environ. Sci. Pollut. Res. 26 (2019) 18451–18464.
- [6] Kuppusamy S., Maddela N.R., Megharaj M., *et al.*, Total Petroleum Hydrocarbons, Environmental Fate, Toxicity and Remediation, Springer Nature Switzerland AG (2020), ISBN 978-3-030-24034-9.
- [7] Sui X., Wang X., Li Y., Ji H., Sustainability 13 (2021) 9267.



## ENZYME IMMOBILIZATION ON MODIFIED BIOMASS: OPTIMIZATION AND CHARACTERIZATION

### IMOBILIZACIJA ENZIMA NA MODIFIKOVANOJ BIOMASI: OPTIMIZACIJA I KARAKTERIZACIJA

**Students: Anja Antanasković<sup>1\*</sup>, Nevena Ilić<sup>3</sup>**

**Mentors: Milan Milivojević<sup>2</sup>, Suzana Dimitrijević-Branković<sup>2</sup>, Zorica Lopičić<sup>1</sup>, Nikola Vuković<sup>1</sup>**

<sup>1</sup>Institute for Technology of Nuclear and Other Mineral Raw Materials, Franchet d'Esperey Boulevard 86, Belgrade, SERBIA

<sup>2</sup>Faculty of Technology and Metallurgy, University of Belgrade, Karnegijeva 4, Belgrade, SERBIA

<sup>3</sup>Innovation Center of Faculty of Technology and Metallurgy, Karnegijeva 4, Belgrade, SERBIA

\*[a.antanaskovic@itnms.ac.rs](mailto:a.antanaskovic@itnms.ac.rs)

#### Abstract

The rise in global food production and consumption has resulted in waste biomass accumulation at the local landfills, which represents economic and environmental challenges. This biomass, rich with lignocellulosic components, is recognized as valuable resources that align with the principles of zero waste and circular economy. Recently, these materials have garnered growing interest as a promising renewable resource with multifunctional properties as energy fuel, adsorbents, green chemical sources, etc. In this study, waste lignocellulosic biomasses were used as a support material for enzyme immobilization, attributed to their accessibility, surface functional groups, and porosity. In this study, food waste (peach stone (PS), sour cherry stone (CS), and plum stone (PLS)) were thermally treated (pyrolysis) to obtain biochar, a material rich in carbon content, with a high specific surface area, porosity and significant presence of aromatic functional groups, appropriate for organic materials binding. Biochars were further chemically modified (acid treatment) to produce: peach stone biochar (PSB), sour cherry stone biochar (CSB), and plum stone biochar (PLSB) for potential application for laccase immobilization. All biochars were characterized by pH suspension ( $\text{pH}_{\text{SUS}}$ ), Fourier transform infra-red (FTIR-ATR) technique, and scanning electron microscopy with energy-dispersive X-ray spectroscopy (SEM-EDX). The successful immobilization of commercial laccase from *T. versicolor* (0.274 U/ml) on obtained biochars was performed by the adsorption process. The findings showed that the optimal parameters for laccase immobilization were the following: pH=5, temperature 40°C, and contact time 24 hours. Immobilization efficiency (IE) and residual activity (RA) were determined for all types of biochars. Cherrystone biochar showed the highest IE (91%) and RA (77%), compared to PSB

(IE of 36%, RA of 16%) and PLSB (IE of 86%, RA of 44%). These findings are in accordance with SEM results, confirming that CSB has a highly developed porous structure with deepest pores and cracks. This study demonstrates the potential of utilizing modified food waste biomass, particularly cherry stone, as an effective and sustainable enzyme carrier, with future research aimed at exploring its application for the removal of various contaminants from wastewater, contributing to reducing environmental risks.

**Keywords:** food waste, biochar, immobilization, laccase

### **ACKNOWLEDGEMENT**

*This work is supported by the Ministry of Education, Science and Technology Development of the Republic of Serbia (Contract number: 451-03-66/2024-03/200023).*

### **REFERENCES**

- [1] Al-sareji O.J., Meiczinger M., Somogyi V., *et al.*, Environ. Chem. Eng. 11 (2023) 109803.
- [2] Li N., Xia Q., Niu M., *et al.*, Sci. Rep. 8 (2018) 13947.
- [3] Al-sareji O.J., Abdulzahra M.A., Hussein T.S., *et al.*, Water. 15 (2023) 3437.





## BIOLOGICAL TREATMENT OF THE BIODEGRADABLE WASTE

### BIOLOŠKI TRETMAN BIODEGRADABILNOG OTPADA

**Student: Milena Balabanović<sup>1\*</sup>**

**Mentor: Ana Radojević<sup>1</sup>**

<sup>1</sup>University of Belgrade, Technical Faculty in Bor, V.J. 12, 19210 Bor, SERBIA

\* [milena14b997@hotmail.com](mailto:milena14b997@hotmail.com)

#### Abstract

According to the World Bank report, approximately 2.01 billion tons of solid municipal waste are generated annually in the world. However, the amount will drastically rise by 2050, and the world is expected to generate 3.40 billion tons of waste annually. The largest component of municipal waste is organic waste i.e. biodegradable waste which refers to the waste that can undergo decomposition, including food, paper/cardboard, garden waste, etc.

Due to aging, components of the organic waste fraction chemically and mechanically degrade by present microorganisms such as bacteria, algae, fungi, and molds. Certain conditions are required for the growth and reproduction of microbial communities: moisture, temperature, suitable carbon, oxygen, and nitrogen content, specific pH values, etc. However, during its decomposition, biodegradable waste can release large amounts of nutrients (N, P, K) that can exceed normal levels in soils and aquatic environments, as well as contribute to greenhouse gases (GHG) emission (CO<sub>2</sub>, CH<sub>4</sub>, and N<sub>2</sub>O), in addition to the release of pathogenic microorganisms and heavy metals into the environment.

The biological treatments today include composting and anaerobic digestion, while biodrying and biostabilization, are still in development. The efficiency of the biological treatments is increased by mechanical procedures, where inorganic components are separated from the organic. Inorganic components are further treated with specific processes according to the type of waste.

Digestion of biological waste can occur anaerobically, without the presence of oxygen, or aerobically, in the presence of oxygen. The composting process represents a biological aerobic process in which easily degradable organic waste is converted into CO<sub>2</sub> and stable organic matter which is the final product of this process called compost. Compost can be used to improve soil quality or as fertilizer. The composting process depends on factors such as the composition of biodegradable waste added to the composting reservoir, moisture content, particle size, additive content, temperature, and microorganisms.

Anaerobic digestion is a biochemical process that involves the microbiological degradation of organic matter in the absence of oxygen resulting in the production of biogas and digestate. The obtained digestate can be in solid form or as slurry. Biogas is a mixture of different gases,

with CO<sub>2</sub> and CH<sub>4</sub> constituting about 90% of the total gas composition. Biogas could be used for the production of heat and electricity, while digestate, after composting, is used as fertilizer for agricultural land due to high content of beneficial components (N, P, K), necessary for plant growth. Anaerobic digestion has advantages over composting due to the production of biogas and the absence of odour. As part of an integrated waste management system, it could reduce emissions of GHG gases into the atmosphere.

**Keywords:** biodegradable waste, treatment, composting, anaerobic digestion

## **ACKNOWLEDGEMENT**

*The authors are grateful to the Ministry of Education, Technological development and Innovation of the Republic of Serbia for financial support, within the funding of the scientific research at the University of Belgrade, Technical Faculty in Bor (No. 451-03-65/2024-03/200131).*

## **REFERENCES**

- [1] Lopes I.G., Yong J.W., Lalander C., *Waste Manag.*, 142 (2022) 65–76.
- [2] Pešević D., *Upravljanje otpadom*, Univerzitet u Banja Luci, Prirodno-matematički fakultet, Banja Luka (2022), p. 388, ISBN 978-99976-86-08-4.
- [3] SEPA, Serbian Agency for Environmental Protection, Report on waste management in the Republic of Serbia for the period 2011–2022, *Available on the following link:* [www.sepa.gov.rs/download/Upravljanje\\_otpadom\\_2011-2022.pdf](http://www.sepa.gov.rs/download/Upravljanje_otpadom_2011-2022.pdf).
- [4] Sridhar A., Kapoor A., Kumar P.S., *et al.*, *Fuel* 302 (2021) 121069.
- [5] The World Bank, What a Waste 2.0: A Global Snapshot of Solid Waste Management to 2050, *Available on the following link:* <https://openknowledge.worldbank.org/server/api/core/bitstreams/92a50475-3878-5984-829e-0a09a6a9badc/content>.
- [6] Tun M.M., Juchelková D., Raclavská H., Sassmanová V., *Energies* 11 (2018) 3183.
- [7] Kaza S., Yao L.C., Bhada-Tata P., Van Woerden F., What a Waste 2.0: A Global Snapshot of Solid Waste Management to 2050, World Bank (2018), *Available on the following link:* <http://hdl.handle.net/10986/30317>.



## ADSORPTION MATERIALS BASED ON NANOPARTICLES FOR THE REMOVAL OF ARSENIC FROM WASTEWATER

### ADSORPCIONI MATERIJALI NA BAZI NANOČESTICA ZA UKLANJANJE ARSENA IZ OTPADNIH VODA

**Student: Natalija Stojanović<sup>1\*</sup>**

**Mentors: Maja Nujkić<sup>1</sup>, Vladan Nedelkovski<sup>1</sup>**

<sup>1</sup>University of Belgrade, Technical Faculty in Bor, V.J. 12, 19210 Bor, SERBIA

*\*snatalija48@gmail.com*

#### **Abstract**

In the modern world, with its rapid scientific and technological development, environmental problems arise in all areas of the economy. One of the biggest problems is the wastewater produced during the extraction and processing of metallic raw materials such as copper, lead, zinc, cadmium, manganese, molybdenum, tin, etc. Wastewater management is very demanding and complicated due to its toxic content. Various methods are therefore being developed to purify the wastewater as much as possible and remove heavy metals or various pollutants. The presence of arsenic or its compounds in wastewater, which are very toxic, leads to severe pollution of the environment and thus endangers human health. The most effective way to solve the problem of industrial wastewater is to purify the wastewater, regardless of whether the purified water is discharged into natural water bodies or used as return water in technological processes. Wastewater treatment technology should be efficient, environmentally friendly and economically viable. Adsorption is one of the optimal removal methods, efficient and affordable without the need to add chemicals, and easily applicable in developing countries with unstable power supply and labor shortage. It is also noteworthy that the elimination rate of arsenate and arsenite adsorption is over 95%. According to Panat and Varanasi, this process is mainly based on the van der Waals method of repulsion and electrostatic attraction between adsorbed molecules. Adsorbents for arsenic removal include bioadsorbents such as hydrochar, certain silicas, resins, gels and hydrothermal carbonization processes. Carbonization converts biomass into useful carbon materials that produce hydrocarbons for a variety of adsorption applications. Hydrochar-based adsorption in combination with nanoparticles has proven to be a good choice for the treatment of wastewater containing organic and inorganic pollutants, which is why special attention is being paid to the removal of arsenic with hydrochar and nanoparticles. The porous structure of hydrochar provides a sufficient surface area for the adsorption of arsenic. Through reduction, we therefore convert toxic arsenic species into less harmful forms. Nanoparticles and hydrochar complement each other in the regeneration process. The nanoparticles can be easily regenerated, while the hydrocarbon forms a stable matrix for its immobility. In this

paper, we will mention iron-based nanoparticles such as magnetite and maghemite, which are capable of adsorbing and removing As(III) and As(V) from wastewater. TiO<sub>2</sub> nanoparticles also show the ability to adsorb arsenic and can be modified to improve efficiency. There are also metal-based particles, such as manganese oxide (MnO<sub>2</sub>), aluminum oxide (Al<sub>2</sub>O<sub>3</sub>) and zirconium oxide (ZrO<sub>2</sub>). It has been proven that aluminum oxide impregnated with iron oxide, for example, has a much higher capacity than aluminum oxide alone. Manganese oxide impregnated with aluminum oxide is also more effective at removing As(III) and As(V). Modification with titanium and zirconium increased the adsorption capacity for arsenic after activation with acid. This structure enables multiple adsorption-desorption cycles. The aim of these studies is to investigate the potential of hydrochar as an effective adsorbent for the removal of arsenic from wastewater together with other adsorbents and biomass-based hydrochar preparations. In particular, hydrochar with metal nanoparticles represents a promising economic solution for the removal of arsenic from wastewater, achieving an efficiency of over 99%. The aim is to promote green chemistry and environmental remediation. If research continues to progress, this process could become the key to access to clean water around the world.

**Keywords:** wastewater, arsenic, adsorption, nanoparticles, environmental protection

#### **ACKNOWLEDGEMENT**

*The authors are grateful to the Ministry of Science, Technological development and Innovation of the Republic of Serbia for financial support according to the contract with the registration number (451-03-65/2024-03/200131).*

#### **REFERENCES**

- [1] Manning B.A., Fendorf S., Bostick B. *ES&T* 36 (2002) 976–981.
- [2] Singh T.S., Pant K.K., *Sep. Purif. Technol.* 48 (2006) 288–296.
- [3] Pena M., Meng X., Konfiatis G.P., *Sci. Technol.* 40 (2006) 1257–1262.
- [4] Duta P.K., Ray A.K., *J. Colloid Interface Sci.* 278 (2004) 270–275.
- [5] Kumar R., Patel M., Singh P. *Sci. Total Environ.* 694 (2019) 133427.



## HEALTH RISK ASSESSMENT OF RARE EARTH ELEMENTS IN GROUNDWATER NEAR A THERMAL POWER PLANT

### PROCENA ZDRAVSTVENOG RIZIKA OD ELEMENATA RETKIH ZEMALJA U PODZEMNOJ VODI U BLIZINI TERMOELEKTRANE

**Student: Jelena Vesković<sup>1\*</sup>**

**Mentor: Antonije Onjia<sup>1</sup>**

<sup>1</sup>University of Belgrade, Faculty of Technology and Metallurgy, Karnegijeva 4,  
11120 Belgrade, SERBIA

\*[jelena.veskovic.12@gmail.com](mailto:jelena.veskovic.12@gmail.com)

#### Abstract

Groundwater serves as the primary source of drinking and agricultural water. Therefore, it is vital to ensure clean water supply to people. However, recently, anthropogenic activities led to groundwater degradation worldwide. Activities related to thermal power plants, including coal fly ash and wastewater disposal, are one of them. Coal fly ash is known to contain significant amounts of contaminants, such as rare earth elements (REEs). Inadequate management of coal fly ash landfills may lead to the leaching of REEs from ash into groundwater, which can have a harmful effect on human health.

This study investigated both non-carcinogenic and carcinogenic health risk posed by REEs in groundwater near the largest thermal power plant in Serbia, namely Nikola Tesla power plant. A total number of sixteen samples were collected and analysed for sixteen REEs, including lanthanum (La), cerium (Ce), praseodymium (Pr), neodymium (Nd), samarium (Sm), europium (Eu), gadolinium (Gd), terbium (Tb), dysprosium (Dy), holmium (Ho), erbium (Er), thulium (Tm), ytterbium (Yb), lutetium (Lu), scandium (Sc), and yttrium (Y). The study encompassed both adults and children as population groups, examining ingestion and dermal pathways as primary exposure routes.

Non-carcinogenic risk for adults (*HIA*) was in the range of  $1.1 \times 10^{-4} - 1.4 \times 10^{-4}$ , averaging  $5.2 \times 10^{-4}$ . Moreover, non-carcinogenic risk for children (*HIC*) ranged from  $1.6 \times 10^{-4}$  to  $2.0 \times 10^{-3}$ , with an average value of  $7.6 \times 10^{-4}$ . Children were more susceptible to non-carcinogenic risk compared to adults. Such results can be explained by the lower body weight of the children. None of the samples exceeded the threshold of 1 regarding both groups, suggesting negligible non-carcinogenic risk. Carcinogenic risks for adults (*ILCRA*) and children (*ILCRc*) were in the range of  $2.0 \times 10^{-18} - 2.7 \times 10^{-17}$  and  $8.1 \times 10^{-18} - 1.0 \times 10^{-17}$ , with average values of  $9.8 \times 10^{-18}$  and  $3.9 \times 10^{-18}$ , respectively. Adults were more prone to carcinogenic risk, as evidenced by the results. Both population groups had *ILCR* values within the threshold of  $1.0 \times 10^{-6}$ , implying insignificant carcinogenic risk. In addition, ingestion through drinking water was identified as the main

exposure route for both risk, while Sc showed the greatest contribution to both risk assessments.

Although REEs in groundwater do not pose a risk to human health, ongoing ash disposal may lead to an increase in health risk, therefore continuous monitoring of the area under study is advised.

**Keywords:** non-carcinogenic risk, carcinogenic risk, REE

## **ACKNOWLEDGEMENT**

*The authors are grateful to the Ministry of Science, Technological development and Innovation of the Republic of Serbia for financial support according to the contract with the registration number 451-03-65/2024-03/200135.*

## **REFERENCES**

- [1] Vesković J., Deršek-Timotić I., Lučić M., *et al.*, Mar. Pollut. Bull. 201 (2024) 116277–116294.
- [2] Vesković J., Bulatović S., Miletić A., *et al.*, Stoch. Environ. Res. Risk Assess. 38 (2024) 1597–1612.
- [3] Franus W., Wiatros-Motyka M., Wdowin M., Environ. Sci. Pollut. Res. 22 (2015) 9464–9474.
- [4] Vesković J., Lučić M., Ristić M., *et al.*, Toxics 12 (2024) 62–78.





## EFFECT OF PHOSPHATE GLASS AND BIOCHAR ON ROSE GROWTH

### UTICAJ FOSFATNOG STAKLA I BIOČADJI NA RAST RUŽA

**Students:** Vladimir S. Topalović<sup>1</sup>, Anja V. Antanasković<sup>1</sup>, Veljko V. Savić<sup>1</sup>,

**Mentors:** Marija S. Djošić<sup>1</sup>, Zorica R. Lopičić<sup>1</sup>, Ana M. Vujošević<sup>2</sup>, Jelena D. Nikolić<sup>1</sup>

<sup>1</sup>Institute for the Technology of Nuclear and other Mineral Raw Materials-Belgrade,  
Franchet d'Esperey 86, 11000 Belgrade, SERBIA

<sup>2</sup>University of Belgrade, Faculty of Agriculture, Nemanjina 6, 11080 Zemun, SERBIA

*\*j.nikolic@itnms.ac.rs*

#### Abstract

Fertilizers with controlled release (CRF) are materials that have nutrients for the plant and can be dissolved after a certain time from the moment they are introduced into the soil. They are available to the plant much longer than conventional fertilizers. Phosphate glasses (PG) are quite interesting for controlled release systems due to their low chemical durability. Although pure PG have highly hygroscopic nature, their chemical durability can be compositionally controlled. Biochar is the product of biomass pyrolysis, a process where organic substances are broken down at temperatures ranging from 350°C to 900°C in a reduced oxygen thermal process. Biochar applications have an effect on soil improvement, waste management, climate change mitigation and energy, and consequently might have social and economic benefits. Biochar improves soil physiology and increases productivity, assisting with crop residue management.

This paper presents the results of testing the effect of PG and biochar from plum stones (PSB) on rose plantings (sort *Lavaglut*). The control sample were rose plantings without fertilizer addition.

The phosphate glass ( $45.4\text{P}_2\text{O}_5 \cdot 25.6\text{K}_2\text{O} \cdot 14.5\text{CaO} \cdot 3.1\text{SiO}_2 \cdot 9.3\text{MgO} \cdot 1.2\text{ZnO} \cdot 0.9\text{MnO}_2$ ) was prepared from reagent grade raw materials. The glass mixture was melted at  $T = 1230^\circ\text{C}$  for  $t = 1\text{h}$  in an open porcelaine crucible in an electric furnace and the melt was quenched on a steel plate. Phosphate glass and biochar were added in a variety of dosages. The application of 1 g of phosphate glass and the application of 10 g of PSB had the greatest effect on increasing the average height of plants. The application of PG and biochar had no significant effect on the average number of formed branches in the crown, as well as on the average number of newly formed branches. Higher doses of PG (3 g) and PSB (10 g) have a favorable effect on increasing the average number of formed flowers. The chemical analysis of the plant material at the end of the vegetative cycle determined: increase in phosphorus and manganese content in all tested varieties; the highest content of zinc was determined in the variant where 2 g of PG was used; the calcium content was increased in all tested varieties. The data obtained

within the scope of this study indicates that PG and PSB fertilizers have a positive effect on rose plant growth.

**Keywords:** phosphate glass, biochar, CR fertilizers

### **ACKNOWLEDGEMENT**

*This research is supported by The Ministry of Science, Technological Development and Innovation, Republic of Serbia, (Contracts No. 451-03-66/2024–03/200023 and 451-03-66/2024–03/200116).*

### **REFERENCES**

- [1] Ersundu M. Ç., Kuzu B., Ersundu A. E., *J. Non-Cryst. Solids* 576 (2022) 121239.
- [2] Vujošević A, Matijašević S., Smiljanić S. *et al.*, *Zaštita Materijala*, 60(1) (2019) 96–104.
- [3] Lopičić Z., Antanasković A., Šoštarić T. *et al.*, *Proceedings of XIV Conference of Chemists, Technologists and Environmentalists of Republic of Srpska*, October 21–22, Banjaluka, Republic of Srpska, BiH (2022) 252–257.
- [4] Ahmad M., Rajapaksha A.U., Lim J.E. *et al.*, *Chemosphere* 99 (2014) 19–33.



## THE REDUCING POWER OF BLACK PEPPER (*Piper nigrum* L.) ESSENTIAL OIL HYDRODISTILLATION FRACTIONS

### REDUKCIONA MOĆ FRAKCIJA DOBIJENIH HIDRODESTILACIJOM ETARSKOG ULJA CRNOG BIBERA (*Piper nigrum* L.)

**Student: Aleksandra Milenković<sup>1\*</sup>**

**Mentor: Ljiljana Stanojević<sup>1</sup>**

<sup>1</sup>University of Niš, Faculty of Technology, Bulevar Oslobođenja 124, Leskovac, SERBIA

\*[aleksandram@tf.ni.ac.rs](mailto:aleksandram@tf.ni.ac.rs)

#### Abstract

Black pepper (*Piper nigrum* L.), perennial climbing vine of the family Piperaceae, is a very rich source of a wide range of chemical ingredients, most of which are biologically active. Black pepper essential oil (BPEO) rich in mono- and sesquiterpenes, shows numerous biological activities such as antioxidant, antimicrobial, anti-inflammatory, hepatoprotective activity, etc. Considering that the antioxidant activity of BPEO based on its reducing ability of Fe<sup>3+</sup> to Fe<sup>2+</sup> has not been thoroughly investigated, the aim of this study is to examine the reduction power of BPEO's fractions.

The essential oil was obtained by Clevenger-type hydrodistillation (CHD), and each fraction was separated through a measuring tube after a certain period of time (five hydrodistillation periods: I (0-15 min), II (15-30 min), III (30-60 min), IV (60-90 min) and V (90-120 min). The quali- and quantitative composition of the collected BPEOs' fractions was determined by GC/MS and GC/FID analysis. The reducing power of BPEOs fractions was determined according to the method of Oyaize known as a „Prussian blue“ method, with certain modifications. The reducing power of BPEOs' fractions was expressed as gallic acid equivalents per gram of essential oil (mg GAE/g).

It was determined that compounds of BPEOs' fractions with a lower molecular weight emerged early, while their contents were high at the beginning and decreased towards higher distillation intervals. The most abundant compounds of BPEOs' fractions were (*E*)-caryophyllene, (*E*)-nerolidol, sabinene, and limonene. Results indicated that all collected BPEOs' fractions showed reducing ability: (I – 2.36 mgGAE/g, II – 4.64 mgGAE/g, III – 7.71 mgGAE/g, IV – 8.64 mgGAE/g, V – 9.63 mgGAE/g, where fraction V showed clearly the highest activity. Ascorbic acid was the reference standard for the assay, with the best reduction power (176.93 mgGAE/g) compared to all examined samples.

This study showed that the fractionation of the essential oil affected the reduction ability of iron ions. Although the reduction power of the BPEOs' fractions increases with hydrodistillation time, these changes are insignificant when the activity of ascorbic acid is taken into account. Further investigation will focus on examining the reducing ability of

individual components of the BPEOs' fractions, especially (*E*)-caryophyllene, (*E*)-nerolidol, sabinene, and limonene. Also, determining other biological activities will be of great importance for future research.

**Keywords:** black pepper, essential oil fractions, Clevenger-type hydrodistillation, reducing power assay

### **ACKNOWLEDGEMENT**

*This work was supported by the Ministry of Science, Technological Development and Innovation of the Republic of Serbia under the program of financing scientific research work, 451-03-65/2024-03/200133 and 451-03-66/2024-03/200133.*

### **REFERENCES**

- [1] Milenković A.N., Stanojević L.P., *Advanced Technologies* 10 (2021) 40–50.
- [2] Oyaizu M., *Jpn. J. Nutr. Diet.* 44 (1986) 307–315.



## ENVIRONMENTAL METHOD OF GOLD NANOPARTICLES SYNTHESIS AND THEIR CHARACTERIZATION

### METODA SINTEZE NANOČESTICA ZLATA NA EKOLOŠKI NAČIN I NJIHOVA KARAKTERIZACIJA

**Student: Marija Tasić<sup>1\*</sup>**

**Mentor: Dragan Cvetković<sup>2</sup>**

<sup>1</sup>Innovation Centre University of Niš, Niš, SERBIA

<sup>2</sup>University of Niš, Faculty of Technology, Leskovac, SERBIA

\* [marijast190@gmail.com](mailto:marijast190@gmail.com)

#### Abstract

The environment is crying out for help more and more because industrialization greatly affects our environment. Therefore, natural raw materials and materials should be resorted to, in order to start reducing pollution. As far as synthesis is concerned, the biological method, i.e. green synthesis, is an alternative method for preserving the human environment. The green synthesis method involves the use of plants, bacteria, yeasts, molds, algae, etc. Therefore, this method implies the use of a cheaper, less harmful, and toxic chemical.

Aqueous extract of *Rubus spp.* leaves obtained by reflux extraction at boiling temperature were used as a stabilizing agent in the synthesis of gold nanoparticles (AuNPs-E). Synthesis was performed at a temperature of 80°C. The synthesized nanoparticles were further characterized using scanning electron microscopy (SEM), energy dispersive X-ray (EDX) spectroscopy, X-ray diffraction (XRD), dynamic light scattering (DLS), and zeta potential.

SEM analysis showed that cubic, triangular, and rod-shaped nanoparticles are present in the sample. Based on the EDS spectrum, it can be seen that the signal originating from carbon dominates, while the signal originating from gold is somewhat lower in intensity and shows its intensity at around 2.2 keV. The percentage of atomic content of carbon in this sample confirmed its highest presence at 68.8%, while the percentage of mass content showed the highest presence of elemental gold at 75.6%. Elemental mapping analysis of gold nanoparticles showed the distribution of element chlorine in this sample probably originating from the chloroauric acid used in the synthesis. The XRD peaks of synthesized nanoparticles with  $2\theta$  at about 38.2°, 44.4°, 64.6, 77.5° and 81.8° correspond to the reflection planes (111), (200), (220), (311) and (222), respectively, with the (111) plane as the most intense. The obtained average crystallite size of green synthesized nanoparticles was 15.7±2 nm. The average value of z-potential was -17.7 mV, while the measured average size of nanoparticles was 61.55 nm. This difference can be explained by the fact that XRD detects the size of crystallites, while DLS provides information about the size of whole nanoparticles, i.e. the dimension of a capping or stabilizing agent enveloping the particles along with the size of the

metallic core. The average value of mobility and conductivity was  $-1.389 \mu\text{mcm/Vs}$  and  $0.0964 \text{ mS/cm}$ , respectively.

Synthesized AuNPs-E stabilized with an aqueous extract of blackberry leaves will be subjected to further tests to be applied in some cosmetic preparations.

**Keywords:** green synthesis, gold nanoparticles, SEM, EDX, XRD, DLS, blackberry leaves

### **ACKNOWLEDGEMENT**

*This research is a part of Projects 451-03-65/2024-03/200133 and AG082 supported by the Ministry of Science, Technological Development and Innovation of the Republic of Serbia.*

### **REFERENCES**

- [1] Ying S., Guan Z., Ofoegbu P.C., *et al.*, Environ. Technol. Inno. 26 (2022) 102336.
- [2] Yilmaz M., Turkdemir H., Kilic M.A., *et al.*, Mater. Chem. Phys. 130 (2011) 1195–1202.
- [3] Nadaroğlu H., Güngör A.A., İnce S., Inter. J. Inno. Res. Rev. 1 (2017) 6–9.
- [4] Patil T.P., Vibhute A.A., Patil S.L., *et al.*, Appl. Surf. Sci. Adv. 13 (2023) 100372.
- [5] Sujitha M.V., Kannan S., Spectrochim. Acta A Mol. Biomol. Spectrosc. 102 (2013) 15.





## PURIFICATION METHODS FOR POLLUTED AIR

### METODE PREČIŠĆAVANJA ZAGAĐENOG VAZDUHA

**Student: Marija Stanković<sup>1\*</sup>**

**Mentor: Jelena Kalinović<sup>1</sup>**

<sup>1</sup>University of Belgrade, Technical Faculty in Bor, V.J. 12, 19210 Bor, SERBIA

\*[stankovicmarija829@gmail.com](mailto:stankovicmarija829@gmail.com)

#### Abstract

Air pollution has serious consequences for human health and the environment, causing millions of deaths. Methods such as filtration, catalysis, and emission reduction technologies can improve air quality. High concentrations of pollution increase the risk of respiratory infections, heart diseases, and lung cancer. PM particles, such as PM<sub>10</sub> and PM<sub>2.5</sub>, are particularly dangerous as they can penetrate deep into the lungs, increasing the risk of premature death. Air pollution is also associated with diabetes, obesity, inflammatory reactions, and neurological disorders. Children are especially vulnerable due to underdeveloped organs.

Airborne pollutants can harm plant life, and emissions of CO<sub>2</sub>, methane, and black carbon contribute to climate change. Filtration, adsorption, and disinfection technologies are effective in air purification, but they have limitations. Many countries are in the process of establishing air quality standards and developing detection and purification devices.

Photocatalysis stands out as a promising method for air purification. This technology uses semiconductor materials to absorb certain radiation, generating reactive oxygen species that degrade pollutants. Photocatalysis is a simple and effective method for removing pollutants, making it superior to other techniques.

Combustion is highlighted as an efficient method for reducing pollutant emissions. In the combustion process, substances are completely burned or degraded into less harmful forms, which is especially useful for controlling emissions of toxic organic substances from industrial plants.

Absorption is a technique that uses liquid or solid materials to absorb gas components. This operation can be physical or chemical, depending on the presence of a chemical reaction between the gas and the liquid. Absorption enables efficient removal of gas components from the air.

Adsorption is a process of removing gas or liquid components using porous solid materials. This technique is used to remove particles from gas streams, such as smoke and dust, using electrostatic attraction. Electrostatic filters are effective in removing various particles from gases but require regular maintenance.

Bag filters are used to remove suspended particles from gases. These filters consist of a frame onto which a bag made of filtration material is attached. The filtration material is selected according to the properties of the gas being filtered. Bag filters are effective in removing particles of various sizes from gas streams.

There are various policies and approaches in sectors that can reduce air pollution and improve environmental quality. In industry, the use of clean technologies and improved waste management systems can significantly reduce exhaust emissions. In the energy sector, transitioning to renewable energy sources and low-emission technologies can reduce the usage of fossil fuels and emissions of harmful gases. Urban planning that promotes energy efficiency and sustainable transportation systems can reduce emissions from construction and transportation. Managing municipal and agricultural waste, along with recycling and waste treatment, can reduce waste emissions. Providing support to experts to assess the health effects of air pollution can support the implementation of pollution reduction measures. All these actions require a cross-sectoral approach and collaboration among different sectors to integrate them into a comprehensive framework for environmental monitoring.

**Keywords:** polluted air, air filtration, adsorption, catalysis, air purification.

## **ACKNOWLEDGEMENT**

*The authors are grateful to the Ministry of Science, Technological Development and Innovation of the Republic of Serbia for financial support, within the funding of the scientific research at the University of Belgrade, Technical Faculty in Bor (No. 451-03-65/2024-03/200131).*

## **REFERENCES**

- [1] Ren H., Koshy P., Chen W.F., *et al.*, J. Haz. Mat. 325 (2017) 340–366.
- [2] Roy A., Mishra C., Jain S., *et al.*, J. Ther. Eng. 5(2) (2019) 22–28.
- [3] Wan Z., Zhang Q., Xu L., Proceedings of the 5<sup>th</sup> International Symposium on Resource Exploration and Environmental Science, University of Technology, Phnom Penh, Cambodia, 24–25 April 2021, 1–10.
- [4] Šećerov-Sokolović R., Sokolović S., Inženjerstvo u zaštiti okoline, Tehnološki fakultet, Novi Sad (2002), p.135–146., ISBN: 628.316.12(0.75).
- [5] Šerbula M.S., Grbavčić B.Ž., Zagađenje i zaštita vazduha, Tehnički fakultet u Boru, Univerzitet u Beogradu, Bor (2011), ISBN: 978-86-80987-89-7.
- [6] DAERA, Effects of Air Pollution on Natural Ecosystems, *Available on the following link:* <https://www.daera-ni.gov.uk/topics/protect-environment/effects-air-pollution-natural-ecosystems>
- [7] WHO, Climate impacts of air pollution, *Available on the following link:* <https://www.who.int/teams/environment-climate-change-and-health/air-quality-energy-and%20health/health-impacts/climate-impacts-of-air-pollution>



## PURIFICATION OF INDUSTRIAL WASTEWATER

### PREČIŠĆAVANJE INDUSTRIJSKIH OTPADNIH VODA

**Student: Marija Stanković<sup>1\*</sup>**

**Mentor: Jelena Kalinović<sup>1</sup>**

<sup>1</sup>University of Belgrade, Technical Faculty in Bor, V.J. 12, 19210 Bor, SERBIA

\*[stankovicmarija829@gmail.com](mailto:stankovicmarija829@gmail.com)

#### Abstract

Water pollution by contaminants such as dyes, pesticides, drugs, phenols, and heavy metals has global consequences on ecosystems. Although mining industries significantly contribute to this pollution, they are crucial for the economy of both local communities and nations. Wastewater from mining industries and chemical plants requires proper treatment before discharge into watercourses. Over time, numerous processes have been developed to reduce the toxic impact of these wastewaters on human health and the environment, including physical, chemical, and biological methods, as well as hybrid approaches.

Wastewater can be contaminated with various pollutants, especially with heavy metals such as copper, zinc, and manganese, as well as suspended particles. Sedimentation is a process in which suspended particles and sludge are gradually separated from water by settling at the bottom. This method is used for pretreatment of water. Adsorption is an increasingly popular and effective method for purification, followed by neutralization and precipitation for effective results. Adsorption is defined as the removal of a substance from a liquid or gas using a solid phase, resulting in a higher concentration (or accumulation) of removed molecules on the surface of the adsorbent compared to the mass of the solution.

Adsorbents for heavy metals removal can be divided into few categories. Carbon-based adsorbents include activated carbon, activated carbon cloth, and activated carbon fibre. Nanomaterial adsorbents include nanoparticles, nanotubes, nanowires, and nanorods. Low-cost sorbents refer to agricultural materials (agricultural solid waste) or industry by-products, natural materials (clays, zeolites, and siliceous materials), and biosorbents (biomass, biopolymers, and peat).

Industrial wastewaters may have different pH values, whether alkaline or acidic. To be discharged into the environment, such as rivers and lakes, neutrality needs to be achieved, meaning the pH value should be in the range of 6.5 to 8.5. Achieving neutrality can be done through neutralization processes in several ways: mutual neutralization, neutralization with reagents, and neutralization through neutralizing materials. Precipitation aims to bind metal ions into low-solubility compounds, thereby assisting in water purification. Through the application of precipitating reagents, low-solubility compounds with metal ions are formed.

These insoluble precipitates are then removed from the water, improving its purity. In the case of heavy metal ions such as zinc, chromium, lead, copper, cadmium, etc., the process occurs by forming their low-solubility hydroxides. Filtration is the process by which a suspension is separated using a porous barrier, retaining the solid phase (sludge) while allowing the liquid phase (filtrate) to pass through. Filtration is used at the end of the treatment process.

Literature data indicate that the methods for water purification are chosen based on the type and amount of impurities present in the water, as well as the economic feasibility, efficiency, and sustainability of using the selected chemicals required for the process.

**Keywords:** wastewater, adsorption, copper, manganese, suspended particles.

## **ACKNOWLEDGEMENT**

*The authors are grateful to the Ministry of Education, Technological development and Innovation of the Republic of Serbia for financial support, within the funding of the scientific research at the University of Belgrade, Technical Faculty in Bor (No. 451-03-65/2024-03/200131).*

## **REFERENCES**

- [1] Dutta D., Arya S., Kumar S., Chemosphere 285 (2021) 1–10.
- [2] Aćić R., Magdalinović N., Trumić M., *et al.*, Odvodnjavanje i jalovišta, IP “NAUKA”, Beograd (2001) 106–146.
- [3] Soliman N.K., Moustafa A.F., J. Mater. Res. Technol. 9 (2020) 10235–10253.
- [4] Rukavina S.V., Damnjanović D., Tehnologija vode i tehnologija napojne vode, Savez energetičara SR Srbije, Beograd (1984).
- [5] Zahoor A., Mao G., Jia X., *et al.*, ESA 1 (2022) 92–109.
- [6] Zaimee M.Z.A., Sarjadi M.S., Rahman M.L., Water 2659 (2021) 14.



## RISKS OF CHLORINE EXPOSURE IN HOUSEHOLD CLEANING: A CALL FOR AWARENESS AND PREVENTION

### RIZICI OD IZLAGANJA HLORU TOKOM ČIŠĆENJA U DOMAĆINSTVU: POZIV NA OPREZ I PREVENCIJU

**Students: Željka Nikolić<sup>1\*</sup>, Nebojša Radović<sup>2</sup>**

**Mentor: Olga Tešović<sup>3</sup>**

<sup>1</sup>Institute of General and Physical Chemistry, Studentski trg 12-16, Belgrade, SERBIA

<sup>2</sup>University of Belgrade - Faculty of Chemistry, Studentski trg 12-16, Belgrade, SERBIA

<sup>3</sup>Institute of Criminological and Sociological Research, Gračanička 18, Belgrade, SERBIA

\*[zeljkanikolic79@gmail.com](mailto:zeljkanikolic79@gmail.com)

#### Abstract

Cleaning agents play a crucial role in maintaining cleanliness and hygiene in households. However, the improper use or inadvertent mixing of these products can lead to serious health hazards. One such risk arises from the combination of sodium hypochlorite-based cleaners with acidic products, resulting in the formation of hazardous chlorine gas. This article aims to provide an overview of the dangers posed by the chemical reactions of chlorine generation in household cleaning and propose measures to prevent its occurrence.

This study has a twofold objective: firstly, to underscore the critical importance of preventing the formation of hazardous chlorine gas by the mixing of household cleaning agents; secondly, to advocate for comprehensive legal regulations mandating clear warning messages on cleaning product labels, thereby educating and safeguarding consumers from potential risks.

To achieve these objectives, we conducted an analysis of data spanning from 2011 to 2023, sourced from the Annual Reports of the National Poison Control Centre of the Military Medical Academy in Belgrade, Serbia (NPCC MMA) to assess the prevalence of chlorine poisoning cases. Additionally, during May 2024, a pilot screening examination of labelling practices among cleaning agent manufacturers was conducted to evaluate the adequacy of warning messages and pictogram symbols on product containers (n=15) in Belgrade, Serbia markets.

Analysis of patient data from the NPCC MMA reports revealed a concerning prevalence of chlorine poisoning cases, with an average annual number of medical examinations of patients being 42.8, representing 24.0% of all patients examined for intoxication by gases and vapors. Furthermore, in comparison to intoxications by all gases and vapors, the occurrence of chlorine poisoning annually ranged from zero to 33.8%, with an average annual number of hospitalized patients due to chlorine intoxication being 4.1. However, it is crucial to acknowledge the potential underestimation of the number of chlorine poisoning cases annually, given the limitations of data sourced from a single healthcare facility, although it is

a tertiary institution specialized in treating poisoned patients. Evaluation of labeling practices indicated significant shortcomings in communicating the risks associated with mixing cleaning agents. Although analyzed containers of household cleaning products mostly contain an adequate pictogram symbols (such as "Corrosive", "Hazardous to the environment", and "Health hazard"), manufacturers largely failed to provide appropriate textual messages that would unambiguously and visually warn end-users about the prohibited mixing of different cleaning agents. The findings of this study underscore the urgent need for preventive measures to mitigate the risks associated with chlorine gas formation from household cleaning agents mixing. Regulatory bodies must enforce stringent guidelines requiring manufacturers to provide clear and unambiguous warnings on product labels. Additionally, consumer education campaigns are essential to raise awareness and prevent future incidents of chlorine poisoning during household cleaning activities.

In conclusion, the formation of chlorine gas from the mixing of household cleaning agents poses a significant risk to public health. Immediate action is required from regulatory bodies, such as government agencies, to implement stricter labeling regulations and to educate consumers about the associated risks.

**Keywords:** chlorine gas, household cleaners, health risks, public awareness, legislative regulation

## **ACKNOWLEDGEMENT**

*The Ministry of Science, Technological Development and Innovation of the Republic of Serbia supported this study (Contracts numbers: 451-03-66/2024-03/200168, 451-03-66/2024-03/200039, and 451-03-66/2024-03/200051).*

## **REFERENCES**

- [1] Lin G. D., Wu J. Y., Peng X. B., *et al.*, World J Clin Cases 10 (25) (2022) 8872–8879.
- [2] Carlisle M., Lam A., Svendsen E., *et al.*, Ann. N. Y. Acad. Sci. 1374 (1) (2016) 159–167.
- [3] Annual Reports of the NPCC MMA, Available on the following link: <http://www.vma.mod.gov.rs/sr/specijalnosti/centri/nacionalni-centar-za-kontrolu-trovanja/godisnjak-NCKT> (Serbian).
- [4] Boelhouwe E., Davis J., Franco-Watkins A., *et al.*, J. Saf. Res. 46 (2013) 145-155.
- [5] Law on Chemicals ("Official Gazette of Republic of Serbia", No. 36/2009-33, 88/2010-158, 92/2011-26, 93/2012-26, 25/2015-3).
- [6] Law on Biocidal Products ("Official Gazette of the Republic of Serbia", No. 109, November 19, 2021).
- [7] Cleaning Product Labeling Act of 2017, Available on the following link: <https://www.congress.gov/115/bills/hr2728/BILLS-115hr2728ih.xml>.
- [8] Guidance on labelling and packaging in accordance with Regulation (EC) No 1272/2008, Available on the following link: [https://echa.europa.eu/documents/10162/2324906/clp\\_labelling\\_en.pdf/89628d94-573a-4024-86cc-0b4052a74d65?t=1614699079965](https://echa.europa.eu/documents/10162/2324906/clp_labelling_en.pdf/89628d94-573a-4024-86cc-0b4052a74d65?t=1614699079965).





## IS THERE A NEED TO INFORM CITIZENS MORE DIRECTLY ABOUT THE HANDLING OF HOUSEHOLD HAZARDOUS WASTE?

### DA LI POSTOJI POTREBA DA SE GRAĐANI DIREKTNIJE INFORMIŠU O NAČINU POSTUPANJA SA OPASNIM OTPADOM IZ DOMAĆINSTVA?

**Students:** Željka Nikolić<sup>1\*</sup>, Nebojša Radović<sup>2</sup>

**Mentor:** Olga Tešović<sup>3</sup>

<sup>1</sup>Institute of General and Physical Chemistry, Studentski trg 12–16, Belgrade, SERBIA

<sup>2</sup>University of Belgrade - Faculty of Chemistry, Studentski trg 12–16, Belgrade, SERBIA

<sup>3</sup>Institute of Criminological and Sociological Research, Gračanička 18, Belgrade, SERBIA

\*[zeljkanikolic79@gmail.com](mailto:zeljkanikolic79@gmail.com)

#### Abstract

Municipal solid waste (MSW) is a part of overall solid waste which is generated in human society, besides commercial and industrial waste. Depending on the dangerous characteristics affecting human health and the environment, it can be inert, non-hazardous and hazardous. Subcategory of waste, which represents over 66% of MSW is household waste, generated from domestic source. Around 1% of household waste is defined as household hazardous waste (HHW).

There are several definitions of household hazardous waste, depending on legislation of different countries. A comprehensive definition is given by the UK National Household Hazardous Waste Forum (NHHWF): “any material discarded by a household, which is difficult to dispose of, or which puts human health or the environment at risk because of its chemical or biological nature”. HHW is a heterogeneous waste group with flammable, corrosive, reactive, caustic, and toxic characteristics. Quantity and type of HHW generating on source depends on average standard of living. Citizens in everyday life are not completely and directly informed about the handling of their waste. The aim of this study is to emphasize the need to inform citizens more closely about the characteristics of HHW and how improper waste management can affect their health, habitation, and wider environment.

A review of the legislation in the field of solid and hazardous waste management in Republic of Serbia (RS) was carried out, as well as local waste management plans for major cities in RS. These are public documents available online at Environmental Protection Agency (Serbia) website. Local waste management plans for city of Belgrade, Novi Sad and Nis for period from 2011 to 2020 were used. Attention was focused on HHW in which manner it was accorded to overall municipal solid waste.

Local waste management plan for city of Belgrade laid out the most precise selection of special waste streams whose some components are and household hazardous wastes. Recycling yards are in the plan for HHW collection sites besides bulky waste, construction

waste from households (<1m<sup>3</sup>) and useful components of municipal waste (paper, glass, plastic, metal waste). Mainly components of HHW are: paints (latex and oil-based), flammable liquids and solids (ex. gasoline, paint thinner), automotive oil, filters, and antifreeze, poisonous materials (insecticides, herbicides), corrosive materials (ex. household cleaners), mercury containing materials (fluorescent lights, thermometers), compressed gases (ex. propane), batteries (lead-acid, cadmium, lithium and alkaline), oxidizing substances (ex. household cleaners, polishes), aerosols in line with its mass share in HHW stream. Local waste management plan for city of Novi Sad and Nis also rely on special waste streams when point to HHW. Waste is classified according to the waste catalog in which within number 20 is listed municipal solid waste including HHW.

Unambiguous identification for HHW is required so that the citizens could adequately manage with the aforementioned waste. Considering that HHW can cause health issues to citizens according to its nature and can cause local environmental damage, it would be of great importance to publish a manual referred to HHW handling and identification, designed for domestic use.

**Keywords:** household hazardous waste, hazardous waste management, domestic waste handling

## **ACKNOWLEDGEMENT**

*The Ministry of Science, Technological Development and Innovation of the Republic of Serbia supported this study (Contracts numbers: 451-03-66/2024-03/200168, 451-03-66/2024-03/200039, and 451-03-66/2024-03/200051).*

## **REFERENCES**

- [1] Law on Waste Management ("Official Gazette of the Republic of Serbia" No. 36/2009, 88/2010, 14/2016, 95/2018 and 35/2023) (Serbian).
- [2] Inglezakis V. J., Moustakas K., J. Environ. Manage. 150 (2015) 310-321.
- [3] Binxian G., Weimo Z., Haikun W. *et al.*, Waste Management 34 (2014) 2414–2423.
- [4] Lim-Wavdea K., Kauffman R. J., Dawson G. S., Resour. Conserv. Recy. 120 (2017) 88–107.
- [5] Available on the following link: <http://www.sepa.gov.rs/>.
- [6] Local waste management plan, City of Belgrade 2011-2020, City Administration of the City of Belgrade, Secretariat for Environmental Protection, Belgrade, July 2011.
- [7] Household hazardous waste, Technical resource guide for local governments, The Carolina Recycling Association Household Hazardous Waste Council, November 2020.
- [8] Waste catalog, Instructions for determining the index number, Republic of Serbia, Ministry of Environment and Spatial Planning, Environmental Protection Agency, Belgrade, December 2010.



**SOLID WASTE FROM HYDRODISTILLATION OF *HERNIARIAE HERBA*  
(*Herniaria glabra* L.) AS A POTENTIAL SOURCE OF ANTIOXIDANTS**

**ČVRSTI OTPAD NAKON HIDRODESTILACIJE NADZEMNOG DELA SITNICE  
(*Herniaria glabra* L.) KAO POTENCIJALNI IZVOR ANTIOKSIDANASA**

**Students: Nataša Simonović<sup>1\*</sup>, Tamara Milosavljević<sup>1</sup>**

**Mentors: Jelena Stanojević<sup>1</sup>, Ljiljana Stanojević<sup>1</sup>, Jelena Zvezdanović<sup>1</sup>,  
Dragan Cvetković<sup>1</sup>**

<sup>1</sup>University of Niš, Faculty of Technology, Bulevar Oslobođenja 124, Leskovac, SERBIA

\* [simonovicnattasa@gmail.com](mailto:simonovicnattasa@gmail.com)

**Abstract**

Rupturewort (*Herniaria glabra* L.) is a herbaceous medicinal plant belonging to the family Caryophyllaceae. Plants from the genus *Herniaria* are primarily used as diuretics for the treatment of kidney and gallstones, gout, urinary tract infections, hypertension, and diabetes. The aerial parts of the rupturewort (*Herniariae herba*), used as a medicinal part of the plant, contain approximately 3% of triterpenic saponosides, coumarin, and its derivatives, flavonoid heterosides, up to 0.6% essential oil and a few alkaloids of unknown structure.

The aim of the present paper was to analyze the effect of hydrodistillation on the content of residual antioxidants from *Herniariae herba* by comparing the chemical composition and antioxidant activity of ethanolic extracts (EE) obtained from plant material (PM) used for essential oil (EO) isolation and waste plant material (WPM) obtained after EO isolation.

The plant material was purchased from the Institute for Medicinal Plants Research, "Dr. Josif Pancic". The essential oil was isolated by Clevenger hydrodistillation for 2 hours using a hydromodulus of 1:10 m/V. The ethanolic extracts were obtained by Soxhlet extraction for 4 h (PM) and 3.5 h (WPM) using a solvomodule of 1:10 m/V. The chemical composition of the extracts obtained was determined by the UHPLC-DAD-ESI-MS method. The contents of total phenols (TPC) and total flavonoids (TFC) were determined by the Folin-Ciocalteu method and the AlCl<sub>3</sub> method, respectively, while the antioxidant activity was determined by the DPPH assay.

According to the results obtained, ethanolic extracts were rich in phenolic acids (e.g., 4-*O*-caffeoyl-quinic acid) and flavonoids (e.g., oxytroflavoside A). The TPC and TFC for ethanolic extracts obtained from PM and WPM were 87.9 mg GAE/g of dry extract and 78.2 mg GAE/g of dry extract; and 36.2 mg QE/g of dry extract and 58.0 mg QE/g of dry extract, respectively. According to the EC<sub>50</sub> values obtained, both the EEWPM (0.10 mg/cm<sup>3</sup>) and the EEPM showed better (0.14 mg/cm<sup>3</sup>) antioxidant activity in comparison to the synthetic antioxidant butylated hydroxy toluene (0.43 mg/cm<sup>3</sup>) after 20 minutes of incubation

with DPPH radical. Ethanolic extract of the WPM showed higher TFC and a better antioxidant activity in comparison to the EEPM.

It could be concluded that solid waste from hydrodistillation of *Hernariae herba* could be used as a potential source of antioxidants and should be treated as a hydrodistillation co-product and not as its by-product

**Keywords:** waste plant material, rupturewort, hydrodistillation by-product

### **ACKNOWLEDGEMENT**

*This work was supported by the Ministry of Science, Technological Development and Innovation of the Republic of Serbia under the Program of financing scientific research work, number 451-03-65/2024-03/200133. Nataša Simonović is a Scholar of the Ministry of Science, Technological Development and Innovation of the Republic of Serbia.*

### **REFERENCES**

- [1] Kozachok S., Marchyshyn S., Ostapchuk A., et al., *Curr. Issues Pharm. Med. Sci.* 29 (3) (2016) 142–144.
- [2] Tucakov J., *Healing with plants New*, revised and updated edition, Vulkan, Belgrade (2014), p. 501, ISBN: 978-86-10-01124-1 (In Serbian).



## SUSTAINABLE SOLUTIONS IN ANALYTICAL CHEMISTRY: COMBINING OF INSTRUMENTAL TECHNIQUES AND ENVIRONMENTAL-FRIENDLY NATURAL INDICATORS FOR CLASSICAL VOLUMETRY

### ODRŽIVA REŠENJA U ANALITIČKOJ HEMIJI: KOMBINACIJA INSTRUMENTALNIH TEHNIKA I EKOLOŠKI PRIHVATLJIVIH PRIRODNIH INDIKATORA ZA KLASIČNU VOLUMETRIJU

**Students:** Aleksa Vizi<sup>1\*</sup>, Nebojša Radović<sup>2</sup>, Željka Nikolić<sup>3</sup>, Stefan Lekić<sup>4</sup>

**Mentors:** Goran Roglić<sup>2</sup>, Ksenija Stojanović<sup>2</sup>, Vele Tešević<sup>2</sup>

<sup>1</sup>University of Belgrade, Innovative Centre of the Faculty of Chemistry, Ltd.,  
Studentski trg 12–16, Belgrade, SERBIA;

<sup>2</sup>University of Belgrade - Faculty of Chemistry, Studentski trg 12–16, Belgrade, SERBIA;

<sup>3</sup>Institute of General and Physical Chemistry, Studentski trg 12–16, Belgrade, SERBIA;

<sup>4</sup>Institute of Chemistry, Technology and Metallurgy, National Institute of the Republic of Serbia, University of Belgrade, Njegoševa 12, Belgrade, SERBIA

\* [vizialeksa@gmail.com](mailto:vizialeksa@gmail.com)

#### Abstract

Dimethyl fumarate (DMF) serves as the active ingredient in medications designed to treat relapsing forms of multiple sclerosis, yet there is a notable absence of specific monographs for this compound in available pharmacopeia's. Nevertheless, various instrumental chromatographic techniques are employed to determine the concentration of DMF across diverse matrices.

This study endeavours to highlight the viability of merging structural instrumental analytical methods with a simple classical volumetric approach utilizing a cost-effective, non-toxic, and natural indicator - the ethanol extract of *Curcuma longa* powder. The primary aim is to accurately determine DMF assay in commercial samples without utilizing certified reference materials (CRM).

Samples of DMF procured from a commercial supplier underwent analysis employing instrumental techniques including GC/MS, IR, and NMR. An innovative titrimetric method for determining DMF content involved ultrasonically assisted alkaline hydrolysis by sodium hydroxide solution at 70°C for 15 minutes, followed by back titration of excess alkali using a standard hydrochloric acid solution and the ethanol extract of *Curcuma longa* powder as an indicator. To evaluate the analytical validity of this innovative method, a modified standard method for ester content determination served as a comparative benchmark. This standard method entails alkaline hydrolysis of the DMF sample by sodium hydroxide solution, boiling for 30 min, and subsequent back titration of excess alkali with a standard hydrochloric acid solution, employing phenolphthalein as indicator.

GC/MS analysis revealed a significant DMF content in the sample (99.9%), with the detection of a 0.1% cyclic dimer of dimethyl fumarate, specifically the tetramethyl ester of

1,2,3,4-cyclobutanetetracarboxylic acid (TMCBA). However, these findings necessitate careful interpretation as they exclusively relate to the compound's gaseous phase. The IR spectrum exhibited characteristic absorption bands for DMF, alongside a broad absorption band at 3400 to 3000  $\text{cm}^{-1}$  region, indicative of fumaric acid (FA). Proton NMR analysis highlighted dominant peaks for DMF protons (6.7 and 3.7 ppm) and low-intensity peaks around 6.6 ppm, potentially arising from protons attached to  $\alpha$ -C atoms of FA carboxyl groups. Regarding volumetric techniques for DMF assay determination, it is important to emphasize that during the alkaline hydrolysis procedures, all detected fumarate compounds present in the commercial material (DMF, TMCBA, and FA) were successfully converted to sodium fumarate, with their total content expressed as DMF. Finally, the result of the DMF assay obtained using the innovative volumetric method (99.4%,  $n=5$ ) did not show a statistically significant difference compared to the DMF content determined using the standard volumetric method (99.3%,  $n=5$ ).

Instrumental analyses suggest that the investigated DMF sample exhibits high purity (>95%) with low-level impurities (TMCBA and FA), a conclusion supported by DMF content results obtained through both standard and innovative volumetric methods (>99%). Ultimately, the combining of described instrumental techniques with the innovative method for DMF assay determination, using environmental friendly ethanol extract of *Curcuma longa* powder as indicator, represents a successful analytical tool for quantifying DMF content without CRM.

**Keywords:** dimethyl fumarate analysis, instrumental techniques, environmental-friendly indicator, *Curcuma longa*, volumetric analysis.

## ACKNOWLEDGEMENT

*The support from the Ministry of Science, Technological Development and Innovation of Republic of Serbia (Contracts numbers: 451-03-66/2024-03/200168, 451-03-66/2024-03/200288, 451-03-66/2024-03/200026, and 451-03-66/2024-03/200051) is greatly appreciated.*

## REFERENCES

- [1] Gold R., Barnett M., Chan A. *et al.*, Ther. Adv. Neurol. Disord. 16 (2023) 1–24.
- [2] Lu Y., Zhu Y., Talanta 119 (2014) 430–434.
- [3] Narizzano R., Risso F., Venturelli G., *et al.*, J. Chromatogr. 1216 (39) (2009) 6762–6766.
- [4] Habib A., Hammad S., Amer M., *et al.*, J. Sep. Sci. 44 (3) (2021) 726–734.
- [5] Juárez S., Carrión F., Carrión J., *et al.*, Sensors 23 (12) (2023) 5602.
- [6] Olivares I.R.B., Souza G.B., Nogueira A.R.A., *et al.*, TrAC, Trends Anal. Chem. 100 (2018) 53–64.
- [7] ISO 7660:1983 Essential oils - Determination of ester value of oils containing difficult-to-saponify esters, Available on the following link: <https://www.iso.org/standard/14479.html>.





## EFFICIENT DETERMINATION OF UNDECYLENIC ACID CONTENT IN PHARMACEUTICAL PRODUCTS: A NOVEL SIMPLE APPROACH

### EFIKASNO ODREĐIVANJE SADRŽAJA UNDECILENSKE KISELINE U FARMACEUTSKIM PREPARATIMA: NOVI, JEDNOSTAVAN PRISTUP

**Students:** Aleksa Vizi<sup>1\*</sup>, Nebojša Radović<sup>2</sup>, Željka Nikolić<sup>3</sup>

**Mentor:** Ivan Kojić<sup>1</sup>, Ksenija Stojanović<sup>2</sup>

<sup>1</sup>University of Belgrade, Innovative Centre of the Faculty of Chemistry, Ltd.,  
Studentski trg 12–16, Belgrade, SERBIA

<sup>2</sup>University of Belgrade - Faculty of Chemistry, Studentski trg 12–16, Belgrade, SERBIA

<sup>3</sup>Institute of General and Physical Chemistry, Studentski trg 12–16, Belgrade, SERBIA

\* [vizialeksa@gmail.com](mailto:vizialeksa@gmail.com)

#### Abstract

Undecylenic acid (UDA), a medium-chain fatty acid industrially derived from castor oil, naturally occurs in black elderberry. UDA has attracted significant attention due to diverse applications in pharmaceutical formulations, particularly as a topical antifungal agent. Recent research has even hinted potential role of UDA in inducing apoptosis in tumor cells, further elevating its importance in therapeutic contexts.

The primary objective of this study was to design a rapid and straightforward analytical method for determining UDA content in commercially available preparations. The presence of a terminal double bond in UDA enables it to undergo addition reactions, rendering it an invaluable tool for quantifying UDA concentration in commercial products.

In pursuit of this objective, a commercially available liquid preparation, sourced from a U.S.A. manufacturer (AS), was employed as the UDA test sample. This preparation represented a binary mixture of UDA and isopropyl palmitate. Its precise qualitative composition was confirmed by GC-MS analysis subsequent to sample derivatization, in accordance with the ISO 12966-2:2017 procedure. A novel approach for determining UDA content in pharmaceutical preparations was established, drawing upon the ISO 3961:2018 standard method for determining the iodine value of fats and oils. Initially, the density of the AS sample was determined using the pycnometer method. Then, the prescribed AS mass was dissolved in *n*-hexane, and a reaction mixture was prepared by introducing 25.00 mL of iodine monochloride (ICI) solution in glacial acetic acid. Ultrasonic sonication facilitated the reaction at room temperature for 10 minutes. Subsequently, a 10% potassium iodide solution was introduced, and the liberated iodine was titrated using a standard solution of sodium thiosulfate. A blank test (without AS) was concurrently conducted applying the same procedure.

The results of this innovative method showcased a calculated mass/volume concentration of UDA in the tested sample at 25.1% (n=5). This finding closely aligned with results obtained utilizing the European Pharmacopoeia method for UDA assay determination, which yielded a UDA concentration in AS of 25.2% (n=5). This robust correlation underscores the efficacy of the new method for rapid and uncomplicated determination of UDA content in commercial pharmaceutical products devoid of auxiliary substances, which chemically react with the halogenating reagent, ICl [7]. The novel advantage of this method (over conventional chromatographic techniques) lies in its economic accessibility. Eschewing the necessity for analytical instruments, complex sample derivatization, or the procurement of expensive certified reference materials, this method offers a cost-effective solution without compromising accuracy.

In conclusion, the rapidity and simplicity of this innovative method render it as viable option for routine UDA content determination in pharmaceutical preparations. However further research, involving a broader spectrum of pharmaceutical products containing UDA, is mandatory to fully explore the applicability of this technique in routine analytical practice.

**Keywords:** undecylenic acid, antifungal agent, pharmaceutical analysis, volumetric technique, rapid determination

## **ACKNOWLEDGEMENT**

*The support from the Ministry of Science, Technological Development and Innovation of Republic of Serbia (Contracts numbers: 451-03-66/2024-03/200168, 451-03-66/2024-03/200288, and 451-03-66/2024-03/200051) is greatly appreciated.*

## **REFERENCES**

- [1] Vanderlei C., Marcele C., Vanderleia B. *et al.*, Chem. Ind. Chem. Eng. Q. 29 (4) (2023) 263–271.
- [2] Shi D., Zhao Y., Yan H., *et al.*, Int. J. Clin. Pharmacol. Ther. 54 (5) (2016) 343–353.
- [3] Day Z.I., Mayfosh A.J., Giel M.C., *et al.*, Int. J. Mol. Sci. 23 (22) (2022) 14170.
- [4] ISO 3961:2018, Animal and vegetable fats and oils - Determination of iodine value, Available on the following link: <https://www.iso.org/standard/71868.html>
- [5] ISO 12966-2:2017, Animal and vegetable fats and oils - Gas chromatography of fatty acid methyl esters, Part 2: Preparation of methyl esters of fatty acids, Available on the following link: <https://www.iso.org/standard/72142.html>
- [6] European Pharmacopoeia Tenth Edition Volume I, European Directorate for the Quality of Medicines & Health Care of the Council of Europe, Strasbourg Cedex (2019), p. 4148, ISBN: 978-92-871-8912-7.
- [7] Day D., Alsenani N., Alsimaree A., Eur. J. Org. Chem. 2021 (30) (2021) 4299–4307.
- [8] Olivares I.R.B., Souza G.B., Nogueira A.R.A., *et al.*, TrAC, Trends Anal. Chem. 100 (2018) 53–64.



## HEALTH RISK ASSESSMENT OF POTENTIALLY TOXIC ELEMENTS IN AGRICULTURAL SOIL OF BRANIČEVO DISTRICT

### PROCENA ZDRAVSTVENOG RIZIKA OD POTENCIJALNO TOKSIČNIH ELEMENTATA U POLJOPRIVREDNOM ZEMLJIŠTU BRANIČEVSKOG OKRUGA

**Student: Andrijana Miletic<sup>1\*</sup>**

**Mentor: Antonije Onjia<sup>1</sup>**

<sup>1</sup>University of Belgrade, Faculty of Technology and Metallurgy, Karnegijeva 4,  
11120 Belgrade, SERBIA

\* [amiletic@tmf.bg.ac.rs](mailto:amiletic@tmf.bg.ac.rs)

#### Abstract

The presence of potentially toxic elements (PTEs) in the soil ecosystem is a worldwide problem of great concern. As a significant part of the environment, soil represents a source of nutrients and habitat for many living beings. A large number of human activities, such as industrialization, urbanization, and agriculture have led to PTE pollution of soil. Among these activities, agricultural practices can cause significant soil contamination with PTEs due to excessive use of pesticides and other chemicals. Because of PTE toxicity and bioaccumulation, they are a threat to both environment and human health. A high concentration of PTEs can reduce the quality of soil, water, and plants, and also lead to the entry of PTEs into the food chain. PTEs from soil can enter the human body through three exposure routes: ingestion, inhalation, and dermal contact. The health risk assessment method is widely used for the determination of possible non-carcinogenic and carcinogenic effects that PTEs cause to human health.

This research investigated PTE contamination of soil through health risk assessment posed by As, Cd, Cr, Cu, Ni, Pb, and Zn. The study was carried out on selected agricultural soil in Braničevo district where 200 samples were collected. The non-carcinogenic risk was estimated through HQ (hazard quotient) and HI (hazard index), while carcinogenic was represented by CR (carcinogenic risk) and TCR (total carcinogenic risk).

The greatest contribution to non-carcinogenic risk was from As and Cr, while Zn had the smallest impact on HI values. The mean value of HI for adults was 0.077, and for children 0.55, which was far below the threshold limit of 1. In all samples, HI for adults was below 1, while regarding children, 7.5% of the samples exceeded the limit value. Carcinogenic risk assessment was carried out for potentially carcinogenic elements: As, Cd, Cr, and Pb. The highest TCR values for adults were within the acceptable range ( $1 \cdot 10^{-6}$  -  $1 \cdot 10^{-4}$ ), while the maximum TCR value for children was  $1.29 \cdot 10^{-4}$ , which is above the permissible limit of  $1 \cdot 10^{-4}$ . Regarding adults, all samples showed acceptable or insignificant carcinogenic risk, while a TCR value greater than  $1 \cdot 10^{-4}$  was recorded only in 0.5% of the samples for children.

The majority of the investigated agricultural soil samples were categorized by extremely low non-carcinogenic and carcinogenic risks. Compared to adults, children were more exposed to both non-carcinogenic and carcinogenic risks. The health risks posed by ingestion and dermal contact were the highest. Only a small number of samples showed elevated TCR and HI values. Therefore, it can be concluded that for both populations, the health risk results were within the permissible limits.

**Keywords:** agriculture, soil pollution, non-carcinogenic risk, carcinogenic risk

### **ACKNOWLEDGEMENT**

*The authors are grateful to the Ministry of Science, Technological development and Innovation of the Republic of Serbia for financial support according to the contract with the registration number 451-03-65/2024-03/200135.*

### **REFERENCES**

- [1] Ke W., Zeng J., Zhu F. *et al.*, Environ. Pollut. 307 (2022) 119486.
- [2] Baltas H., Sirin M., Gökbayrak E. *et al.*, Chemosphere 241 (2020) 125015.
- [3] Yang J., Sun Y., Wang Z. *et al.*, Chemosphere 304 (2022) 135340.
- [4] Vesković J., Bulatović S., Miletić A. *et al.*, Stoch. Environ. Res. Risk. Assess. 38 (2024) 1597–1612.
- [5] Miletić A., Savić A., Slavković-Beškoski L., *et al.*, Serbian. J. Geosci. 6 (2020) 1–7.
- [6] Miletić A., Lučić M., Onjia A., Metals 13 (2023) 1266.



## DISTRIBUTION OF PM<sub>2.5</sub>, CO<sub>2</sub>, HCHO, AND TVOC IN AIR IN A HIGH SCHOOL CLASSROOM

### DISTRIBUCIJA PM<sub>2.5</sub>, CO<sub>2</sub>, HCHO I TVOC U VAZDUHU U UČIONICI U SREDNJOJ ŠKOLI

**Student: Jelena Obradovic<sup>1\*</sup>**

**Mentor: Antonije Onjia<sup>2</sup>**

<sup>1</sup>College of Applied Studies Aviation Academy, Belgrade, SERBIA

<sup>2</sup>University of Belgrade, Faculty of Technology and Metallurgy, Belgrade, SERBIA

\* [obradovic.j@vakademija.edu.rs](mailto:obradovic.j@vakademija.edu.rs)

#### Abstract

Indoor and outdoor air exchange has an important role in indoor air quality in schools. This is particularly important for urban areas where increased concentrations of outdoor air pollutants impact indoor air quality and adversely affect student health. The aim of this study was to assess the relationship between fine particulate matter (PM<sub>2.5</sub>), carbon dioxide (CO<sub>2</sub>), formaldehyde (HCHO), and total volatile organic compound (TVOC) concentrations in indoor and outdoor air of school environment when classrooms are occupied and unoccupied.

The research was conducted from 16 February to 01 March 2024 at a high school located in the center of Belgrade. Low-cost sensors (BRAMC BR-SMART-128SE 5-in-1 Air Quality Monitor) were used for measuring concentrations of PM<sub>2.5</sub>, CO<sub>2</sub>, HCHO, and TVOC. The sensors were fixed indoors in a classroom located on the first floor of the main building and outdoors on the ground in front of the school to determine air pollution concentrations. The classroom has natural ventilation and is occupied by students from 8:00 a.m. to 8:20 p.m. on weekdays.

The results found that average indoor concentrations of PM<sub>2.5</sub> during weekdays ( $16.1 \pm 10.2$  vs  $36.3 \pm 35.2$   $\mu\text{g}/\text{m}^3$ ) were higher compared with indoor concentrations during weekends ( $14.3 \pm 10.2$  vs  $35.3 \pm 28.1$   $\mu\text{g}/\text{m}^3$ ). When the classroom was occupied with students the average outdoor concentrations of PM<sub>2.5</sub> ( $15.8 \pm 11.9$  vs  $27.7 \pm 26.1$   $\mu\text{g}/\text{m}^3$ ) were higher than outdoor concentrations in the period when the classroom was unoccupied ( $16.4 \pm 9.3$  vs  $45.6 \pm 40.9$   $\mu\text{g}/\text{m}^3$ ). The average indoor and outdoor concentrations of CO<sub>2</sub> during weekdays ( $630 \pm 217$  vs  $446 \pm 24$  ppm) were different for indoor concentrations of CO<sub>2</sub> compared to the concentrations during weekends ( $475 \pm 74$  vs  $463 \pm 55$  ppm). Similarly, the average indoor and outdoor concentrations of CO<sub>2</sub> during weekdays when the classroom was occupied with students ( $689 \pm 239$  vs  $446 \pm 24$  ppm) were higher only for indoor concentrations when the classroom was unoccupied ( $566 \pm 169$  vs  $446 \pm 23$  ppm). The average indoor and outdoor concentrations of HCHO during weekdays ( $27.5 \pm 19.8$  vs  $7.4 \pm 5.5$   $\mu\text{g}/\text{m}^3$ ) were similar for both indoor and outdoor concentrations during weekends

( $25.2 \pm 6.5$  vs  $8.6 \pm 5.8$   $\mu\text{g}/\text{m}^{-3}$ ). The distribution pattern for HCHO concentrations was found to be similar during weekdays when the classroom was occupied with students for outdoor concentrations ( $28.5 \pm 26.5$  vs  $8.4 \pm 7.3$   $\mu\text{g}/\text{m}^{-3}$ ), but slightly decreased indoor concentrations for the period when the classroom was unoccupied ( $26.5 \pm 7.6$  vs  $6.3 \pm 1.7$   $\mu\text{g}/\text{m}^{-3}$ ). The average indoor and outdoor concentrations of TVOC during weekdays ( $11.6 \pm 30.8$  vs  $26.5 \pm 41.5$   $\mu\text{g}/\text{m}^{-3}$ ) were different for both indoor and outdoor concentrations during weekends ( $0.3 \pm 1.5$  vs  $33.9 \pm 51.5$   $\mu\text{g}/\text{m}^{-3}$ ). When the classroom was occupied with students the average indoor and outdoor concentrations of TVOC ( $15.2 \pm 38.5$  vs  $38.1 \pm 50.9$   $\mu\text{g}/\text{m}^{-3}$ ) were higher compared to indoor and lower for outdoor concentrations when the classroom was unoccupied ( $7.8 \pm 18.8$  vs  $13.9 \pm 21.9$   $\mu\text{g}/\text{m}^{-3}$ ).

The results indicate that the average indoor concentrations of  $\text{PM}_{2.5}$ ,  $\text{CO}_2$ , HCHO, and TVOC were higher during weekdays compared to the concentrations during weekends, despite variations in outdoor concentrations. During weekdays, the average indoor concentrations of  $\text{CO}_2$ , HCHO, and TVOC were higher when the classroom was occupied with students. These findings indicate that the presence of students in the classroom influence the distribution of indoor air pollution concentrations.

**Keywords:** school, particulate matter, carbon dioxide, formaldehyde and volatile organic compound

## REFERENCES

- [1] Sadrizadeh S., Yao R., Yuan F. *et al.*, JOBE. 57 (2022) 104908.
- [2] Baloch R.M., Maesano C.N., Christoffersen J. *et al.*, Sci. Total. Environ. 739 (2020) 139870.
- [3] Ćirović Ž., Ćujić M., Radenković M. *et al.*, Thermal Science. 27 (3) (2023) 2321–31.





## TOXICOLOGICAL EFFECTS OF MICRO- AND NANO-PLASTICS ON HUMAN HEALTH

### TOKSIKOLOŠKO DEJSTVO MIKRO- I NANO-PLASTIKE NA LJUDSKO ZDRAVLJE

**Student: Gordan Mišić<sup>1\*</sup>**

**Mentors: Ana Radojević<sup>1</sup>, Jelena Jordanović<sup>1</sup>**

<sup>1</sup>University of Belgrade, Technical Faculty in Bor, V.J. 12, 19210 Bor, SERBIA

\*[ggmisic@gmail.com](mailto:ggmisic@gmail.com)

#### Abstract

Evidence of the harmful effects of micro- and nanoparticles of plastic (MPs and NPs, respectively) on all living organisms is drawn from numerous studies conducted on animal models, as well as *in vitro* conditions on human cells. The considered micro- and nanoparticles have dimensions of 1–5000  $\mu\text{m}$  and 1–1000 nm, respectively. Regarding their origin, plastic particles could be classified as *primary* (intentionally made to those dimensions) or *secondary* (formed by degradation of larger pieces).

The health risks of MPs/NPs depend on the hazardous characteristics of the particles and the level of exposure. Plastic poses two main categories of negative effects to humans. *Physical effects* are related to their presence in organisms and primarily are determined by their size, shape, and concentration. *Chemical effects* are associated with the polymer composition, release of chemical additives, and the presence of toxic compounds adsorbed on the external surface of particles. Exposure to MPs/NPs occurs primarily *via* ingestion, respiration, and/or dermal absorption. The primary route of plastic particle exposure is through ingestion, mainly by food and water consumption. Sea salt is recognized as a microplastic carrier, the annual consumption is from 37 up to 1000 MPs. One of the hazards is that humans can potentially accumulate MPs in their bodies by consuming seafood that has already accumulated MPs. Humans also exhibit the phenomenon of “casual ingestion” of plastics. For example, humans inhale on average from 26 to 130 airborne plastic particles a day. Many of the inhaled particles are subjected to clearance mechanisms, such as sneezing, the mucociliary escalator, phagocytosis by macrophages, and lymphatic transport. The dermal exposure to MPs/NPs is still the subject of ongoing research. Current findings indicate that MPs absorbed through the skin could potentially cause skin irritation, inflammation, and possible systemic effects. The most common way of dermal exposure to MPs is through microbeads added to personal care products. The spherical or irregularly shaped microbeads added to facial cleansers, bath gels, toothpaste, and makeup are used as cleansers or exfoliators.

In general, exposure to MPs and NPs could lead to gastrointestinal blockages, mental disorders, asthma, allergies, and chronic lung inflammation. Moreover, the release of harmful substances, such as antimony and heavy metals (arsenic, cadmium, chromium, lead, mercury) from MPs/NPs can increase health risks, including the development of cancer. Recycled plastic materials pose additional hazards due to the presence of catalysts, added because of reduced stability compared to virgin plastic. The leaching of various chemicals from plastic (plasticizers, antioxidants, phthalates, bisphenol A-based polycarbonates, polybrominated diphenyl ethers, bisphenols, clarifiers, flame retardants, colorants, etc.) can lead to a series of health problems because they can act as endocrine disruptors, which can result in diabetes, obesity, and problems in reproductive health.

The importance of addressing the problem of micro- and nanoparticle pollution of the environment and their adverse effects on human health requires further research for a better understanding of the involved mechanisms and for developing strategies to reduce the exposure of humans to these harmful pollutants.

**Keywords:** waste, microplastic, neoplastic, exposure, health risks

### **ACKNOWLEDGEMENT**

*The authors are grateful to the Ministry of Education, Technological development and Innovation of the Republic of Serbia for financial support, within the funding of the scientific research at the University of Belgrade, Technical Faculty in Bor (No. 451-03-65/2024-03/200131).*

### **REFERENCES**

- [1] Dhaka V., Singh S., Anil G. A., *et al.* Environ. Chem. Lett. 20 (2022) 1777–1800.
- [2] Gambino I., Bagordo F., Grassi T., *et al.* IJERPH 19 (9) (2022) 5283.
- [3] Le V-G., Nguyen K-M., Nguyen L-H., *et al.* Sci. Total Environ. 904 (2023) 166649.
- [4] Wang Y., Fu Z., Guan D., *et al.* Appl. Biochem. Biotechnol. (2023), Available on the following link: <https://doi.org/10.1007/s12010-023-04832-z>.
- [5] Haleem N., Kumar P., Zhang C., *et al.* Sci. Total Environ. 912 (2024) 169594.
- [6] Pironti C., Ricciardi M., Motta O., *et al.* Toxics 9 (2021) 224.
- [7] Chen G., Feng Q., Wang J. Sci. Total Environ. 703 (2020) 135504.
- [8] Anbumani S., Kakkar P. Environ. Sci. Pollut. Res. 25 (2018) 14373–14396.
- [9] Wang Y., Zhao J., Fu Z., *et al.* Environ. Pollut. 346 (2024) 123623.



## MAGNESIUM AND ITS ALLOYS

### MAGNEZIJUM I NJEGOVE LEGURE

**Student: Andela Bogdanović<sup>1\*</sup>**

**Mentor: Marija Petrović Mihajlović<sup>1</sup>**

<sup>1</sup>University of Belgrade, Technical Faculty in Bor, V.J. 12, 19210 Bor, SERBIA

<sup>\*</sup>[andjela030@gmail.com](mailto:andjela030@gmail.com)

#### **Abstract**

As various branches of industry have progressed and adapted to the demands of modern society, there has been a rapid increase in demand for materials capable of meeting increasingly complex performance requirements and standards. In this context, magnesium and its alloys have emerged as key materials that have found application in various sectors, from aerospace and automotive industries to electronics, sports, and even the medical industry. Their unique combination of lightweight, high strength and good corrosion resistance makes them indispensable in many applications. The use of magnesium and its alloys in aerospace brings advantages such as reducing the weight of aircraft, contributing to improved performance and fuel efficiency. In the automotive industry, these materials are used to produce lightweight and environmentally friendly vehicle components, leading to reduced fuel consumption and emissions of harmful gases. The electronics industry also utilizes magnesium and its alloys for their high electrical conductivity and ability to absorb electromagnetic waves. In sports, particularly in the production of sports equipment such as bicycles, tennis rackets, and golf clubs, magnesium is used for its exceptional strength and lightness. However, despite their many advantages, such as high specific strength and good thermal and electrical conductivity, magnesium and its alloys face challenges such as sensitivity to high temperatures and susceptibility to corrosion in certain environments. Corrosion can be a particular issue, especially in industries requiring long-term and reliable material protection. This paper provides a deeper insight into the characteristics of magnesium and its alloys, explores various manufacturing processes and applications, and identifies areas for improvement to better meet the requirements of future applications. For example, the extrusion process is often used to shape magnesium alloys into various forms and parts, enabling improved control over the material's structure and properties. Given their significance in various sectors, further research and innovation are crucial to realizing the full potential of magnesium and its alloys in modern industry. Additionally, it is important to develop advanced methods for corrosion protection and improve the thermal stability of these materials to expand their application possibilities and ensure their long-term use in various operating conditions.

**Keywords:** magnesium, alloys, corrosion, extrusion, anisotropy.

## **ACKNOWLEDGEMENT**

*The research presented in this paper was performed with the financial support of the Ministry of Science, Technological Development, and Innovation of the Republic of Serbia, within the funding of the scientific research work at the University of Belgrade, Technical Faculty in Bor, according to the contract number (451-03-65/2024-03/200131).*

## **REFERENCES**

- [1] Qi Li Y., Li F., Kang F.W., *et al.*, J. Alloy Compd. 953 (1) (2023) 1–10.
- [2] Arul Kumar M., Beyerlein I.J., Tome C.N., J. Alloy Compd. 695 (1) (2017) 1488–1497.
- [3] Shi R., J. Magnes. Alloys 10 (9) (2021) 2421–2432.
- [4] Kang JH., Park J., Song K., J. Magnes. Alloys 10 (6) (2022) 1672–1679.
- [5] Xu B., Song Y., Yang K., *et al.* J. Magnes. Alloys 11 (3) (2023) 763–775.

## **Author index**



## A

Abdualatif Abdurahman, M. 363  
Aćimović, D. 472,476,480  
Adamović, D. 206  
Aksić, M. 393, 399, 406  
Alagić, S. 38, 454  
Anđelković, A. 621  
Anđelković, D. 43, 49, 55  
Anđelković, T. 132, 138, 144  
Andjus, S. 632  
Antanasković, A. 727, 735  
Antonijević, D. 200  
Antonijević, M. 502  
Apostolovski-Trujić, T. 251  
Avramović, Lj. 412, 486

## B

Balabanović, M. 729  
Balanović, Lj. 693  
Barbov, B. 358  
Bartolić, D. 30, 299  
Bartonova, A. 14  
Batinić, B. 687  
Berbecea, A. 160  
Berežni, I. 687  
Bigović, M. 520  
Blagajac, I. 231, 613  
Blagojević, M. 520  
Bogdanović, A. 761  
Bogdanović, D. 132, 138, 144  
Bogdanović, M. 613  
Bojić, A. 381, 387, 460  
Bojić, D. 460  
Božić, D. 287, 412  
Božinović, K. 282, 693  
Branković, G. 329  
Branković, M. 43, 49, 55  
Brdarić, T. 472, 476, 480  
Brković, S. 323, 552, 593  
Budzakoska Gjoreska, B. 169  
Bugarčić, M. 265  
Bugarski, B. 1  
Bulatović, S. 491  
Butulija, S. 329, 448  
Buzdugan, D. 335, 508

## C

Carbajal Ccoyllo, M. D. 8  
Chaves e Silva, J. F. 8  
Correia de Siqueira, R. N. 8  
Crista, F. 156,160  
Crista, L. 160  
Crnoglavac Popović, M. 375  
Cupara, N. 61, 515  
Cvetković, A. 454  
Cvetković, D. 739  
Cvetković, L. 715

## Č

Čanak Atlagić, J. 95, 626  
Čebela, M. 552

Čokeša, Đ. 558, 562  
Čučulović, A. 541  
Čučulović, R. 541  
Čukanović, J. 106, 113, 119

## Ć

Ćosović, V. 466  
Ćurčić, M. 200

## D

Damjanović, J. 654  
Damjanović, Z. 251  
Del Grande, M. R. 8  
Denić, M. 719  
Devetaković, J. 418  
Dimitrijević, J. 317  
Dimitrijević, M. 524  
Dimitrijević, T. 393, 399, 406  
Dimitrijević-Branković, S. 727  
Dimitrov, O. 276  
Dimova, S. 276  
Dimović, S. 200  
Djošić, M.S. 586, 735  
Drljača, M. 681  
Dumenčić, D. 246

## Đ

Đikanović, V. 66, 95, 524  
Đorđević, Z. 574, 701  
Đorđević, S. 206  
Đukić, M. 206  
Đuknić, J. 126, 632  
Đuretanić, S. 212  
Đuričković, I. 369  
Đurović, D. 61, 515, 520

## E

Ercegović, M. 317  
Erukhimovitch, V. 531, 536

## F

Fike, M. 430

## G

Galečić, N. 106, 113, 119  
Georgijević, J. 323, 552, 593  
Ghosh, A. 8  
Gois de Oliveira, V.C. 8  
Gojić, M. 246  
Gorgievski, M. 282, 294, 508  
Grčak, D. 399  
Grčak, M. 399  
Grekulović, V. 282, 294  
Grujić, S. 586  
Gudžić, N. 393, 399  
Gudžić, S. 399

## H

Hotea, I. 156, 160  
Huleihel, M. 531, 536  
Hulka, I. 335, 508

## I

Ilić, M. 632  
Ilić, N. 727  
Ivanić, I. 246



Ivanović, Lj. 520

## J

Jakovljević, M. 212

Jakovljević, O. 621, 643

Janković, J. 711

Janković, M. 200

Ječmenica Dučić, M. 472, 476, 480

Jelić, I. 200

Jevtić, A. 598

Jevtović, S. 38

Jordanović, J. 225, 606

Jovanović Mihailo 648

Jovanović Milenko 71, 77, 101, 674

Jovanović, A. 265, 580, 669

Jovanović, D. 282, 294

Jovanović, S. 574, 701

Jovičić, K. 66, 95, 524

## K

Kalinović, J. 225, 606, 715, 741, 743

Kalinović, T. 225, 606, 715

Kamenović, V. 251

Kanjuh, T. 194

Karan Žnidaršič, T. 194

Kerkez Janković, I. 418, 435

Knežević, A. 258

Knežević, G. 311

Knežević, N. 265, 363, 369, 669

Kojadinović, N. 212

Kojić, I. 753

Končalović, D. 574

Konstadinović, K. 717

Koprivica, M. 317

Korać Jačić, J. 30, 299

Kostić Kokić, I. 132, 138, 144

Kostić, M. 381, 387

Kostić, S. 709

Kovačević, S. 524

Kožuh, S. 246

Kričak, L. 216

Krnjajić, S. 311

Krstić, A. 329

Kržanović, D. 674

Kumbrijanović, J. 713

## L

Lakušić, V. 654

Lato, A. 156

Laušević, P. 323, 552, 593

Lazić, D. 638

Lekić, J. 89

Lekić, Lj. 206

Lekić, S. 751

Leshoski, J. 176

Letichevsky, S. 8

Lopičić, Z. 727, 735

## M

Majstorović, J. 216

Maksimović, F. 435

Maksimović, M. 101

Maksin, D. 472

Maletaškić, J. 329, 448

Manasijević, D. 693

Marić, A. 95, 194, 626

Marinković, A. 265, 363, 369, 669

Marinković, N. 126

Marinković, T. 687

Marinković, V. 101, 674

Marjanović, A. 709

Marjanović, V. 71, 77, 287, 412

Markoli, B. 466

Marković Nikolić, D. 341, 348, 354

Marković, Bojana 491

Marković, Branislav 580

Marković, I. 466, 693

Marković, Marija 586

Marković, Marina 282, 294

Marković, Miljan 282, 294

Marković, Mirjana 558, 562

Marković, R. 71, 77, 287, 412

Matijašević, S. 586

Matović, B. 329, 448

Medić, D. 335, 441, 454, 717

Mihailović, R. 329

Mikić, D. 701

Mikić, M. 71, 77, 674

Milanović, S. 216

Milenković, A. 737

Milenković, M.R. 30, 299

Miletić, A. 755

Milić, S. 38, 335, 441, 454, 486, 508

Miličić, D. 194

Milivojević, M. 727

Miljanović, B. 524

Miljojić, T. 200

Milković, M. 654

Milosavljević, T. 749

Milošević, M. 363, 369, 669

Milošević, N. 441, 454

Milošković, A. 212

Milovanović, M. 132, 138, 144

Milutinović, S. 566

Miščević, A. 654

Mišić, G. 759

Mitić, T. 95, 626

Mitrović, J. 381, 387, 460

Mitrović, M. 497

Mitrović, S. 593

Mladenović, S. 497

Mrdak, D. 626

Muhadinović, M. 687

## N

Najdanović, B. 363, 369

Najdanović, S. 381, 387, 460

Nastasović, A. 491

Nedeljković, M. 497

Nedelkovski, V. 335, 441, 508, 731

Nedić, N. 491

Negovanović, M. 216

Nikolić, Danijela 574, 701

Nikolić, Dušan 24  
Nikolić, I. 38, 515  
Nikolić, J. 735  
Nikolić, J.D. 586  
Nikolić, Marijana 212  
Nikolić, Milena 341, 348, 354  
Nikolić, N. 621  
Nikolić, T. 341, 348, 354  
Nikolić, V. 194  
Nikolić, Ž. 745, 747, 751, 753  
Nonić, M. 418, 435  
Novaković, B. 183, 189, 424  
Nujkić, M. 441, 454, 709, 711, 713, 715, 717, 731

## O

Obradović, J. 757  
Obradović, V. 83, 89, 270  
Očokoljić, M. 106, 113, 119  
Onjia, A. 733, 755, 757  
Orahovac, A. 220

## P

Pajić, P. 270  
Pankov, N. 524  
Pantović, S. M. 721  
Papludis, A. 38, 454  
Paskaš, N. 424  
Patcheva, S. 176  
Paunković, J. 648  
Paunović, M. 126, 632  
Pavlović, A. 354  
Pavlović, J. 17  
Penchev, H. 276  
Perović, I. 323, 552, 593  
Perović, M. 83, 89, 270  
Pešić, M. 441  
Petković, G. 341, 354  
Petrov, Dj. 106, 113, 119  
Petrov, P. D. 276  
Petrović, S. 448  
Petrović, A. 206  
Petrović, J. 206  
Petrović, J. T. 265, 317  
Petrović, Jasmina 497  
Petrović, M. 381, 387, 460  
Petrović, Mihajlović, M. 502, 761  
Petrović, N. 725  
Pezdevšek, M. 430  
Pijović Radovanović, M. 323  
Popović, N. 126, 632  
Popović, S. 621, 638, 643  
Potkonjak, N. 558, 562  
Požega, E. 412, 674  
Predojević, D. 621, 643  
Prodanović, O. 375  
Prodanović, R. 375

## R

Radenković, M. 212  
Rađenović, T. 566  
Radivojević, M. 717  
Radojević, A. 225, 606, 719, 729, 759

Radovanović, M. 335, 502, 508  
Radović Vučić, M. 381, 387 460  
Radović, B. 251  
Radović, N. 745, 747, 751, 753  
Radović, V. 311  
Radović, Ž. 240, 258  
Rajić, N. 17  
Rajković, D. Z. 150  
Rajković, M. 200  
Rajković, R. 71, 77  
Raković, Maja 95, 126  
Raković, Marko 150, 183, 189, 424  
Randelović, D. 580  
Ratknić, M. 393, 399, 406  
Ristić, I. 348  
Ristić, N. 251  
Riznić, D. 598  
Roger, A. 430  
Roglić, G. 751

## S

Samardžić, I. 231  
Sarap, N. 200  
Savić Rosić, B. 472, 476, 580  
Savić, A. 200  
Savić, M. 669  
Savić, V.V. 586, 735  
Savković, Ž. 621  
Sejdinović, B. 305  
Selimović, E.S. 721  
Senna, C. A. 8  
Seović, M. 323, 552, 593  
Simić, M. D. 472, 476, 480  
Simić, M. S. 317  
Simić, N. 216  
Simić, V. 212  
Simonović, A. 502, 725  
Simonović, N. 749  
Simonović, P. 194  
Simović, I. 106, 113, 119  
Skočajić, D. 106, 113, 119  
Skorić, S. 150  
Sokić, M. 265, 580  
Sokolović, V. 194  
Spasojević, M. 375  
Stamenković, U. 466, 693  
Stanić, V. 200  
Stanisavljević, N. 687  
Stanišić, M. 375  
Stankov Jovanović, V. 38  
Stanković, D. 150  
Stanković, J. 95, 626  
Stanković, Marija 741, 743  
Stanković, Mihajlo 654, 662  
Stanković, Milena 723  
Stanković, Slađan 311  
Stanković, Sonja 335, 441, 508, 713  
Stanković, Srđan 638  
Stanojević, J. 749  
Stanojević, Lj. 723, 737, 749

Stanojković, J. 541  
Stevanović, M. 265  
Stevanović, Z. 412  
Stojadinović, D. 341, 348  
Stojanović, Katarina 472, 476, 480  
Stojanović, Ksenija 751, 753  
Stojanović, N. 731  
Stupar, M. 621  
Subakov Simić, G. 638  
Surudžić, N. 375

## Š

Šćiban, M. 654  
Šekularac, G. 393, 399, 406  
Šerbula, S. 225, 606  
Šijačić-Nikolić, M. 418, 435  
Škraba Jurlina, D. 194, 626  
Šljivić-Ivanović, M. 200  
Štrbac, N. 282, 294

## T

Tadić, M. 61, 515  
Tadić, N. 240, 258  
Tadić, T. 491  
Tasić, A. 24  
Tasić, M. 739  
Tasić, V. 251  
Tasić, Ž. 502  
Teixeira, L. T. 8  
Tešević, V. 751  
Tešović, O. 745, 747  
Todorović, B. 329, 448  
Tomić, V. 311  
Tomović, J. 626  
Topalović, V. 586, 735  
Trajanovski, S. 169  
Trifunović, V. 412, 486  
Trujić, S. 101  
Tubić, B. 126, 632

## V

Vasiljević, B. 632  
Veličković, M. 164  
Veličković, T. 212  
Veličković, Z. 363, 369  
Velinov, N. 381, 387, 460  
Veljanoska Sarafiloska, E. 176  
Vesković, J. 733  
Vilotić, D. 418, 435  
Vizi, A. 751, 753  
Voza, D. 164  
Vranješ, Z. 476, 480  
Vranković, J. S. 66, 524  
Vučković, T. 83  
Vujičić, D. 106, 113, 119  
Vujošević, A. M. 735  
Vukašinović, V. 574  
Vuković, J. 61, 515  
Vuković, M. 598  
Vuković, N. 727  
Vuksanović, M. M. 363, 369, 669

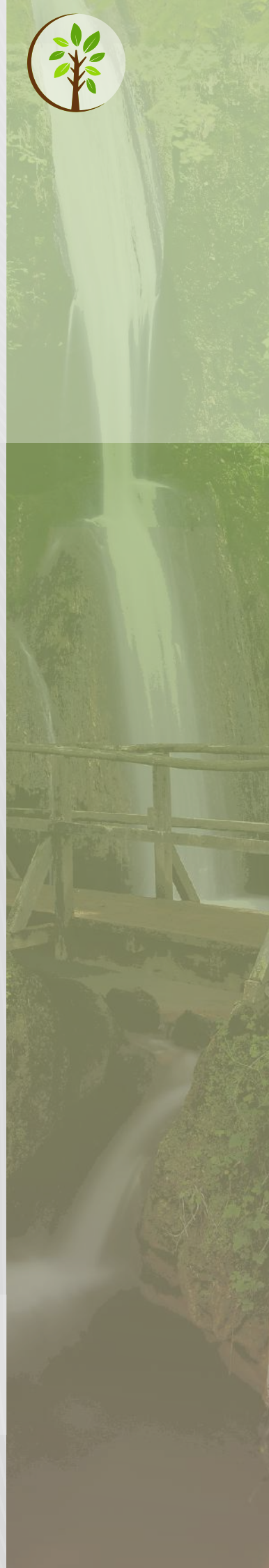
## Z

Zaharieva, K. 276, 358  
Zarić, M. 156, 160, 547  
Zarić, N. 156, 160, 547  
Zdolšek, N. 323, 552, 593  
Zdravković, A. 341, 348, 354  
Zdravković, M. 294  
Zlatanović, I. 38  
Zlatković, I. 251  
Zorić, K. 126  
Zvezdanović, J. 749

## Ž

Živković, S. 566

**Authors are responsible  
for the content of their papers.**



**ISBN 978-86-6305-152-2**